CHEMOENZYMATIC SYNTHESIS OF POLYKETIDE NATURAL PRODUCTS

by

TAYLOR P. A. HARI

**A dissertation submitted to the Faculty of Science
at the University of Ottawa in partial fulfillment
of the requirements for the degree of**

Doctor of Philosophy

University of Ottawa
Department of Chemistry
& Biomolecular Sciences
Ottawa, ON, Canada
K1N 6N5

© Taylor Patrick Allan Hari
Ottawa, Canada, 2018
ALL RIGHTS RESERVED

Parts of this dissertation have been published in the following journal articles:

An Evolutionary Model Encompassing Substrate Specificity and Reactivity of Type I Polyketide Synthase Thioesterases

Taylor P. A. Hari, Puneet Labana, Meaghan Boileau, and Christopher N. Boddy

ChemBioChem, **2014**, *15*, 2656-2661; DOI: 10.1002/bcic.201402475

Diastereoselective Transannular Oxa-Conjugate Addition Generates the 2,6-cis-Disubstituted Tetrahydropyran of Neopeltolide

Taylor P. A. Hari, Burkhardt I. Wilke, James A. Davey, and Christopher N. Boddy

J. Org. Chem., **2016**, *81*, 415-423; DOI: 10.1021/acs.joc.5b02014

Polyketide synthase and non-ribosomal peptide synthetase thioesterase selectivity: logic gate or victim of fate?

Mark E. Horsman, **Taylor P. A. Hari**, and Christopher N. Boddy

Nat. Prod. Rep., **2016**, *33*, 182-202; DOI: 10.1039/c4np00148f

Abstract

Polyketide secondary metabolites constitute a structurally-diverse and clinically-important family of natural products. The wide range of biological activities represented by these substrates have contributed to therapeutic agents with annual sales exceeding $20B USD. Large multi-domain proteins called polyketide synthases (PKSs) use simple building blocks to generate highly-oxygenated and stereochemically-rich frameworks with astonishing selectivity. These substrates often feature rigidifying biases imposed by macrocyclic lactones and substituted heterocycles, which can impact their bioactive conformation. The work of this dissertation combines synthetic chemistry and biochemistry to investigate chemoenzymatic production of macrocyclic polyketide natural products. Research focused on validating a transannular oxa-conjugate addition strategy to assembly 2,6-*cis*-tetrahydropyran (THP) ring systems, as demonstrated by synthesis of the macrocyclic core to neopeltolide. Ultimately, we wish to apply this chemistry to *de novo* PKS pathways for rapid, reliable, and sustainable production of THP-bearing products like neopeltolide, and toward building SAR libraries.

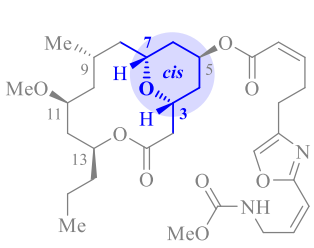

neopeltolide
(*anticancer / antifungal*)

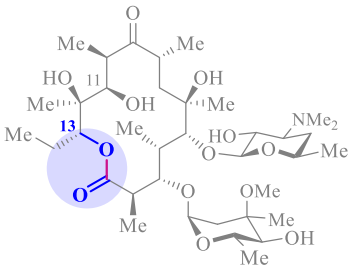

erythromycin
(*antibiotic*)

Additionally, a second study probed the specificity of the macrolactonizing thioesterase (TE) domain from the 6-deoxyerythronolide B (DEBS) biosynthetic pathway. This pathway is the paradigm for type-I PKS systems, and is responsible for producing the macrolide core of erythromycin. Our on-going research evaluates the limits of promiscuity within this specific catalytic domain, to characterize the structural elements required to accurately predict macrolactonization. The long-term goal of this study is to assess the potential applicability of DEBS TE as a generalized cyclization biocatalyst for combinatorial biochemistry and chemoenzymatic research.

CHEMOENZYMATIC SYNTHESIS OF NATURAL PRODUCTS

This dissertation was presented by

TAYLOR P. A. HARI

It was defended on

12/19/2017

Table of Contents

1 Accessing Polyketide Natural Products *via* Interdisciplinary Methods 1

1.1 Natural Products for Drug-Development 2

1.1.1 What Are Polyketides? 2

1.2 The Biosynthesis of Polyketide Natural Products 4

1.2.1 The General Biosynthetic Machinery of a Type-I Polyketide Synthase 4

1.2.2 An In Vitro Total Synthesis of Enterocin using Purified Enzymes 5

1.2.3 PKS Biosynthesis Is Not as Tolerant as Chemical Synthesis 6

1.3 The Chemical Synthesis of Polyketide Natural Products 6

1.3.1 Total Synthesis of Neopeltolide as a Platform for New Methodology & Capability 7

1.3.2 A Re-Emergence of Total Synthesis for Clinical Development 7

1.3.3 Chemical Synthesis Is Not as Efficient as PKS Biosynthesis 8

1.4 Where Biology Meets Chemistry: Chemoenzymatic Syntheses & Biocatalysts 8

1.4.1 Semi-Synthesis as a Solution to Natural Product Drug-Development 8

1.4.2 A Chemo-Biosynthetic-Chemosynthesis of Spinosyn A 9

1.4.3 The Potential of Enzymes as Catalysts in Organic Synthesis 10

1.4.3 A Notable Gap Between Promise and Reality of Chemoenzymatic Strategies 11

1.5 Dissertation Outline 11

1.5.1 Development of a Chemoenzymatic Synthesis for Neopeltolide 11

1.5.2 Development of a Macrocyclizing Biocatalyst 13

1.6 Conclusions 14

1.7 References 15

STUDY I: *EFFORTS TOWARD DEVELOPMENT OF A DE NOVO CHEMOENZYMATIC SYNTHESIS FOR NEOPELTOLIDE*

2 *cis*-Tetrahydropyran Assembly Strategies in Neopeltolide Synthesis 19

2.1 The Marine Habitat as a Source for Bioactive Natural Products 20

2.1.1 Neopeltolide: A Promising New Antiproliferative Compound 21

2.2 Early Synthetic Efforts Determine Absolute Configuration 22
2.2.1 *First Synthesis & Partial Reassignment by the Panek Group* 23
2.2.2 *Absolute Stereochemistry Confirmed by the Scheidt Group* 25
2.2.3 *Scope & Focus of Review Chapter* 26
2.3 THP Assembly *via* Prins-Type Oxocarbenium Ion Cyclization 28
2.3.1 *Total Synthesis by the Maier Group* (Intermolecular Prins) 28
2.3.2 *Total Synthesis by the Lee Group* (Intramolecular Prins) 29
2.3.3 *Total Synthesis by the Kozmin Group* (Desymmetrizing Prins) 30
2.3.4 *Total Synthesis by the Floreancig Group* (Oxidative Prins) 32
2.3.5 *Synthesis of (+)-Macrocycle by the Yadav Group* (Intramolecular Prins) 33
2.3.6 *Synthesis of (–)-Neopeltolide by the Jennings Group* (Oxocarbenium Reduction) 34
2.3.7 *Fragment Synthesis by the Mineeva Group* (Oxocarbenium Reduction) 36
2.3.8 *Concluding Remarks on Prins-Type Cyclization Strategies* 36
2.4 THP Assembly *via* Hetero-Diels-Alder Cycloaddition 37
2.4.1 *Total Synthesis by the Paterson Group* 37
2.4.2 *Formal Synthesis by the Raghavan Group* 38
2.4.3 *Total Synthesis by the Arun K. Ghosh Group* 40
2.4.4 *Concluding Remarks on Hetero-Diels-Alder Cycloaddition Strategies* 41
2.5 THP Assembly *via* Ring-Closing Metathesis 42
2.5.1 *First-Generation Synthesis by the Fuwa Group* 42
2.6 THP Assembly *via* Intramolecular Radical Cyclization 44
2.6.1 *Formal Synthesis by the Taylor Group* 44
2.7 THP Assembly *via* Intramolecular Oxa-Conjugate Addition 46
2.7.1 *Formal Synthesis by the Hong Group* (*α*,*β*-unsaturated aldehyde) 46
2.7.2 *Total Synthesis by the Roulland Group* (*α*,*β*-unsaturated aldehyde) 48
2.7.3 *Second-Generation Synthesis by the Fuwa Group* (*α*,*β*-unsaturated ester) 49
2.7.4 *Formal Synthesis by the Subhash Ghosh Group* (*α*,*β*-unsaturated ketone) 52
2.7.5 *Fragment Synthesis by the Florence Group* (*α*,*β*-unsaturated ester) 54
2.7.5 *Concluding Remarks on Intramolecular Oxa-Conjugate Addition Strategies* 54
2.8 THP Assembly *via* Transition-Metal-Activated Alkene Additions 55
2.8.1 *Formal Synthesis by the She Group* (Pd-Alkoxycarbonylation) 55
2.8.2 *Formal Synthesis by the Sharma Group* (Hg-Oxymercuration) 57
2.8.3 *9-Desmethyl Synthesis by the Dai Group* (Pd-Alkoxycarbonyl Macrocyclization) 58
2.8.4 *Total Synthesis by the Hoveyda Group* (Mo-Ring-Opening/Cross-Metathesis) 60
2.8.5 *Concluding Remarks on Transition-Metal Catalyzed Strategies* 62
2.9 General Evaluation of Neopeltolide Synthesis 63
2.9.1 *C9-Methyl Installation* 64
2.9.2 *C11-C13 Anti-Selectivity* 64
2.9.3 *cis-THP Assembly* 64
2.9.4 *Macrocyclization* 65
2.9.5 *Side-Chain Incorporation* 65
2.10 Conclusions and Prospects 65
2.11 References 66

3 A Transannular Oxa-Conjugate Addition Model of Neopeltolide 73

3.1 2,6-*cis*-Tetrahydropyrans & Polyketide Natural Products 74

3.2 Neopeltolide: A Polyketide Natural Product 76

3.2.1 Research Milestones of Neopeltolide Study 77

3.3 Oxa-Conjugate Addition Assembly of Disubstituted THPs 78

3.3.1 Oxa-Conjugate THP Assembly in Neopeltolide Synthesis 79

3.3.2 Neopeltolide Models for Transannular Oxa-Conjugate THP Assembly 80

3.4 *α,β*-Unsaturated Ester Model for Neopeltolide 83

3.4.1 RCM Yields Dimerization 84

3.4.2 Oxa-Conjugate Assembly of THP Unsuccessful using Ester System 85

3.5 *α,β*-Unsaturated Ketone Model for Neopeltolide 87

3.5.1 Convergent Synthesis Designed Around Racemic C3-Alcohol 88

3.5.2 THP Assembly can be Thermodynamically-Controlled 90

3.6 Transannular Oxa-Conjugate Model System Conclusions 94

3.7 Experimental 95

3.7.1 General Procedures 95

3.7.2 Experimental Procedures & Physical Data of Compounds 95

3.8 References 112

4 Formal Synthesis of Neopeltolide by Transannular Oxa-Conjugate Addition 116

4.1 Applications of Semi-Synthesis for Natural Drug Development 117

4.1.1 De Novo Biosynthetic Pathways for Natural Product Semi-Synthesis 118

4.2 Designing a *De Novo* PKS Pathway for Semi-Synthesis of Neopeltolide 119

4.3 Assembly of Complex Natural Products *via* Macrocyclic Stereocontrol 121

4.3.1 Macrocyclic Stereocontrol in Neopeltolide Synthesis 122

4.3.2 Macrocyclic Stereocontrol for Transannular Systems 123

4.4 Toward a Transannular Oxa-Conjugate Precursor for Neopeltolide 124

4.4.1 Rapid Development of C1-C6 Framework 125

4.4.2 Bio-Inspired Development of C7-C16 Fragment is Abandoned 126

4.4.3 Tandem Hydrogenation/Hydrogenolysis Yields Complete C7-C16 Fragment 127

4.4.4 Model Olefination Conditions Fail with Neopeltolide Framework 129

4.4.5 Screening Conditions for HWE Coupling 132

4.5 A Second-Generation *α,β*-Unsaturated Ketone Model 135

4.5.1 Development of Ketone Model to Evaluate Native C13 Substitution 136

4.5.2 Thermodynamic Equilibration Achieves Exclusive Formation of cis-Pyranone 138

4.6 Transannular Oxa-Conjugate Addition Generates Neopeltolide Core 142

4.6.1 Optimized Conditions Furnish C3 Diastereomeric Oxa-Conjugate Precursors 142

4.6.2 Native cis-THP Configuration of Neopeltolide is Not Energetic Minimum 144

4.7 Conclusions & Future Direction: Advancing from Early Milestones 150

4.8 Experimental 153

4.8.1 General Procedures 153
4.8.2 Experimental Procedures & Physical Data of Compounds 153
4.9 References 200

STUDY II: *EFFORTS TOWARD DEVELOPMENT OF A GENERALIZED CHEMOENZYMATIC MACROCYCLIZATION TOOL*

5 Macrocyclization Strategies in Natural Product Synthesis 205
5.1 Macrolactones: A Privileged Scaffold in Natural Products 206
5.2 General Difficulties Associated with Chemical Synthesis of Macrolactones 207
5.3 Accessing Macrolactones *via* Carboxyl-Activation Strategies 209
5.3.1 PKS Biosynthesis: A Muse for Synthetic Chemistry 209
5.3.2 Macrolactonization via Activating Thioester Reagents 210
5.3.3 Macrolactonization via Activating Carbodiimide Reagents 211
5.3.4 Macrolactonization via Formation of Mixed-Anhydrides 212
5.4 Macrolactone Synthesis *via* Alternative Strategies 213
5.5 Thioesterase-Mediated Macrocyclization: A Potential Chemoenzymatic Tool 215
5.6 Conclusions 217
5.7 References 218

6 Probing the Specificity of the DEBS Thioesterase 220
6.1 Harnessing PKS for Chemoenzymatic Synthesis of Macrocyclic Products 221
6.1.1 Research Milestones of Biocatalytic Thioesterase Study 223
6.2 6-Deoxyerythronolide B Synthase as a Model of Study 224
6.3 Development of Second-Generation Acyl-Intermediate Models 227
6.3.1 Design & Convergent Synthesis of Second-Generation Analog Panel 228
6.3.2 Unprecedented Macrodiolide Observed by In Vitro Incubation with DEBS TE 230
6.3.3 Steady-State Kinetics Consistent with Catalytic Efficiencies of PKS TEs 234
6.3.4 Collision-Induced Dissociation Confirms Formation of Macrodiolide 235
6.3.5 DEBS TE Tolerable of Exogenous Nucleophilic Attack 238
6.3.6 A Fitness-Based Model for Evolution of Thioesterase Substrate Tolerance 241
6.4 Conclusions & Future Directions 242
6.5 Experimental 245
6.5.1 General Procedures 245
6.5.2 Experimental Procedures & Physical Data of Compounds 245
6.6 References 264

7 Future Directions: Combining Lessons from Both Doctoral Studies 267
7.1 Chemoenzymatic Synthesis of Polyketide Natural Products 268
7.2 Development of a *De Novo* PKS Pathway for Neopeltolide 269

7.2.1 *Current State of the Neopeltolide Study and Knowledge Acquired* 269
7.2.2 *Optimization of Oxa-Conjugate Addition for Selective Pyran Assembly (On-Going)* 271
Aim 1: Synthesis of Enantiopure C3 Hydroxy Phosphonate 272
Aim 2: Development of C7 *β'*-Hydroxy *α,β*-Unsaturated Ketone System 272
Aim 3: Investigation of Oxa-Conjugate Addition Reaction Conditions 273
Aim 4: Preparation of Pyranyl Analogues for Neopeltolide 274
7.2.3 *Toward a De Novo Synthesis of Neopeltolide (Long-Term)* 275
Aim 5: Evaluation of Enzyme-Mediated Cyclization with Neopeltolide 276
Aim 6: Rational Design of *De Novo* System for Production of Neopeltolide 277
7.3 Development of a Macrocyclizing Biocatalytic Thioesterase 278
7.3.1 *Current State of Biocatalytic TE Study & Knowledge Acquired using DEBS TE* 279
7.3.2 *Development of Precursor Library for Identification & Characterization of Suitable TE* 281
Aim 7: Design Synthetically-Tractable Complexity to Probe Substrate-Selectivity 282
Aim 8: Rapid Library Development for Continued Mapping of Substrate-Specificity 283
Aim 9: Identification of Macrocyclization Thioesterase with Broad Substrate-Tolerance 284
7.4 Concluding Remarks 288
7.5 References 289

Appendix I: Spectroscopic Data 293

S1.1 General Procedures 294
S1.2 A Transannular Oxa-Conjugate Addition Model of Neopeltolide (Chapter 3) 295
S1.2.1 *First-Generation α,β-Unsaturated Ketone Model v1.1* 295
S1.2.2 *First-Generation α,β-Unsaturated Ketone Model v1.2* 307
S1.2.3 *First-Generation α,β-Unsaturated Ketone Model v2.1* 316
S1.2.4 *First-Generation α,β-Unsaturated Ketone Model v2.2* 322
S1.2.5 *First-Generation α,β-Unsaturated Ketone Model v2.3* 324
S1.3 Formal Synthesis of Neopeltolide by Transannular Oxa-Conjugate Addition (Chapter 4) 343
S1.3.1 *Development of C7-C16 Framework* 343
S1.3.2 *Tandem Hydrogenation/Hydrogenolysis C13-Benzyl Ether Model* 365
S1.3.3 *Completed Carbon Framework for Macrocyclic Core v1* 377
S1.3.4 *Alternative C1-C6 Phosphonate Fragments & HWE Olefination Screening* 390
S1.3.5 *Second-Generation α,β-Unsaturated Ketone Model Fragment Development* 405
S1.3.6 *Completion of Second-Generation α,β-Unsaturated Ketone Model* 417
S1.3.7 *Accessing Key Oxa-Conjugate Addition Precursors for Neopeltolide* 434
S1.3.8 *Thermodynamic Transannular Oxa-Conjugate Assembly of cis-THP of Neopeltolide* 453
S1.4 Probing the Specificity of the DEBS Thioesterase (Chapter 6) 481
S1.4.1 *Second-Generation NAC-Thioesters: D-Configured Analog Design & Evaluation* 481
S1.4.2 *Second-Generation NAC-Thioesters: L-Configured Analog Design & Evaluation* 506
S1.4.3 *Second-Generation NAC-Thioesters: Racemic Methyl Derivative Design & Evaluation* 518
S1.4.4 *Preliminary Development of Precursors for In Vitro Generation of 12-Membered Rings* 527

Appendix II: Supplemental Information 535

S2.1 Chapter 2 536
S2.2 Chapter 3 537
S2.2.1 *Development of C1-C6 Fragment* 537

S2.2.2 *Alternative Ester Moieties Fail to Hydrolyze Cleanly (Ketone Model v2)* 538
S2.2.3 *Calculation Protocol & Computational Data for First-Generation Ketone Model* 538

S2.3 Chapter 4 548

S2.3.1 *Screening Conditions for HWE Coupling of Diprotic Phosphonate* 548
S2.3.2 *Secondary HWE Screening & Serendipitous Discovery* 556
S2.3.3 *Comparison of Energetic Profiles for Transannular Oxa-Conjugate Systems* 557
S2.3.4 *Calculation Protocol & Computational Data for Neopeltolide Core* 558

S2.4 Chapter 6 567

S2.4.1 *Tree Construction & Phylogenetic Analysis* 567
S2.4.2 *Expression & Purification of Thioesterase Proteins* 573

S2.5 Chapter 7 574

S2.5.1 *A Proposed Biosynthetic Pathway to Neopeltolide* 574
S2.5.2 *Chemoenzymatic Development of Diastereomeric Triketide Lactone Libraries* 576
S2.5.3 *Proposed Research Beyond the Scope of this Dissertation* 577
Aim S1: Controlled Re-Evaluation of Biological Activity 578
Aim S2: Determination of Protein Target *via* Activity-Based Proteomics 578

S2.6 References 580

S2.7 Re-Print of Publications 582

The role of transcription in heterologous expression of polyketides in bacterial hosts 583

An evolutionary model encompassing substrate specificity and reactivity of Type I polyketide synthase thioesterases 604

Diastereoselective transannular oxa-conjugate addition generates the 2,6-*cis*-disubstituted tetrahydropyran of neopeltolide 611

Polyketide synthase and non-ribosomal peptide synthetase thioesterase selectivity: logic gate or victim of fate? 620

List of Abbreviations

A-15	Amberlyst-15®
acac	Acetylacetonate
ACP	Acyl Carrier Protein
Ad	1-Adamantyl
AT	Acyltransferase
9-BBN	9-Borabicyclo[3.3.1]nonane
BINOL	1,1'-Bi-2-naphthol
Bn	Benzyl
Boc	*Tert*-Butoxycarbonyl
Bz	Benzoyl
CAM	Ceric Ammonium Molybdate Solution
^{13}CNMR	Carbon Nuclear Magnetic Resonance
COSY	Correlation (2D-NMR) Spectroscopy
CSA	Camphorsulfonic Acid
DCC	*N,N'*-dicyclohexylcarbodiimide
DCM	Dichloromethane
DDQ	2,3-Dichloro-5,6-dicyano-1,4-benzoquinone
DH	Dehydratase
DEAD	Diethyl Azodiacarboxylate
DET	Diethyl Tartrate
DIAD	Diisopropyl Azodicarboxylate
DIBAL-H	Diisobutylaluminum Hydride
DIPEA	*N,N*-diisopropylethylamine (also refered to as Hünig's Base)
DMAP	4-*N,N*-Dimethylaminopyridine
DMP	Dess-Martin Periodinane
DMF	*N,N*-Dimethylformamide
DMMP	Dimethylmethyl Phosphonate
DMSO	Dimethyl Sulfoxide
d.r.	Diastereomeric Ratio
DTBMP	2,6-Di-*tert*-butyl-4-methylpyridine
DVDS	1,3-Divinyl-1,1,3,3-tetramethyldisiloxane
EtOAc	Ethyl Acetate
ee	Enantiomeric Excess
EI	Electron Impact
equiv.	Equivalents
ESI+	Electrospray (Positive Mode)
Et_2O	Diethyl Ether
g	Gram
G-II	Second Generation Grubbs' Catalyst
h	Hour(s)
HCl	Hydrochloric Acid
HG-II	Second Generation Hoveyda-Grubbs' Catalyst
HMDS	Hexamethyldisilazane
HMPA	Hexamethylphophoramide
HMBC	Heteronuclear Multiple-Bond Correlation Spectroscopy
^{1}HNMR	Proton Nuclear Magnetic Resonance
HPLC	High Performance Liquid Chromatography
HRMS	High-Resolution Mass Spectrometry
HSQC	Heteronuclear Single-Quantum Correlation Spectroscopy
Hz	Hertz
IBX	2-Iodoxybenzoic Acid
IC_{50}	Half Maximal Inhibitory Concentration
Ipc	Isopinocamphenyl
IR	Infrared Spectrum
KR	Ketoreductase
KS	Ketosynthase
LD_{50}	Median Lethal Dose
LDA	Lithium Di-*tert*-butyl Amine
LiDBB	Lithium 4,4'-Di-*tert*-butylbiphenylide

LLS	Longest-Linear Sequence
M	Molar (mol · L^{-1})
Mes	Mesitylenyl
mg	Milligram
$MgSO_4$	Anhydrous Magnesium Sulphate
MIC	Minimum Inhibitory Concentration
min	Minute
mmol	Millimole
mmu	Milli Mass Unit
MNBA	2-Methyl-6-nitrobenzoic Anhydride
mL	Milliliter
mol	Mole
MOM	Methoxymethyl
4 Å ms	Four Ångström (4 x 10^{-10} m) Molecular Sieves
MTPA	(*S*)-(+)-α-Methoxy-α-(trifluoromethyl)-phenylacetyl Chloride
m/z	Mass-to-charge ratio
NAC	*N*-Acetyl cysteamine
$NaHCO_3$	Saturated Sodium Bicarbonate Solution
nM	Nanomolar (10^{-9} mol · L^{-1})
NOESY	Nuclear Overhauser Effect Spectroscopy
o-DPPB	*o*-Diphenylphosphinobenzoyl
PCC	Pyridinium Chlorochromate
Ph	Phenyl
pH	Power of Hydrogen
PKS	Polyketide Synthase
PLE	Pig Liver Esterase
PMB	*p*-Methoxybenzyl
ppm	Parts Per Million
PPTS	Pyridinium *p*-Toluenesulfonate
Pr	Propyl
Proton Sponge	1,8-bis(dimethylamino)naphthalene
RCM	Ring-Closing Metathesis
R_f	Retention Factor
rt	Ambient Temperature (~22 °C)
SEM	2-(Trimethylsilyl)ethoxymethyl
S_N2	Bimolecular Nucleophilic Substitution
TE	Thioesterase
TBAF	Tetrabutylammonium Fluoride
TBAI	Tetrabutylammonium Iodide
TBDPS	*tert*-Butyldiphenylsilyl
TBS	*tert*-Butyldimethylsilyl
TDP	Thymidine Diphosphate
TEMPO	(2,2,6,6-Tetramethylpiperidin-1yl)oxyl
TfOH	Triflic Acid
THF	Tetrahydrofuran
THP	Tetrahydropyran
TLC	Thin Layer Chromatography
TMS	Trimethylsilyl
TOF	Time-of-Flight
Ts	*p*-Toluenesulfonyl (Tosyl)
µ	Micro

· Chapter 1 ·

Accessing Polyketide Natural Products via Interdisciplinary Methods

1.1 Natural Products for Drug Development

After 3.8 billion years of research and development,[1] Mother Nature has generated an abundant library of bioactive compounds. Traditional medicines have relied on nature's pharmacy for millennia,[2] and not surprisingly, the commercial sector created natural product drug discovery programs. Of all new small-molecule drugs approved over the last four decades, it is estimated that 65% are natural products or are derived from/contain a natural product pharmacophore.[3] Interdisciplinary efforts have studied the ecological significance, biological roles, and therapeutic potential of these important molecules, determining that they are not integral to the central metabolism of the producing organism. Rather, these secondary metabolites offer complementary function as physiological responses during the interactions with their biotic and abiotic environments (for example, as defense strategies), which accounts for their extraordinary variation in structure and activity. Among them is the polyketide class of compounds, which is the focus of research in this thesis.

Unfortunately, source organisms produce these clinically-relevant metabolites only when they are needed, and in many cases harvesting the producing organism to isolate the active compounds is not possible or sustainable. This low natural abundance becomes of greater concern when factors like climate change and global population growth put increased stress on resources. Thus, researchers from fields of chemistry, biology, engineering, and medicine have been dedicated to designing innovative methods for drug development, and sustainable alternatives for generation of therapeutic natural products.

1.1.1 What Are Polyketides?

Polyketide secondary metabolites represent a structurally-diverse and clinically-important family of natural products that target a wide range of biological activities (Figure 1.1).[4] Like fatty acid synthesis (FAS), large polyketide synthase (PKS) multi-domain proteins biosynthetically-construct this family using simple building blocks. Based on the architecture and machinery (*vide infra*), PKSs can be classified into three different types.[5] Within the scope of this dissertation, emphasis is placed on modular type-I PKS systems.[6–10] Readers are encouraged to review the following excellent resources for details on type-II[11] and type-III[12] polyketide biosyntheses.

Unlike the highly-reduced products from FAS, PKS products remain highly-oxygenated and stereochemically-rich. These frameworks can undergo additional modifications that often include formation of macrocyclic lactones, cyclic five- and six-membered oxacycles or polyethers. Such features add significant conformational biases, which can play a role in controlling the bioactive conformation of the molecule. Within the Boddy Lab, our research uses synthetic chemistry, biochemistry, and molecular biology to determine how microorganisms build complex polyketide natural products. With this

knowledge, we then try to harness or mimic these biosynthetic pathways to produce biologically-active polyketides and their analogues.[13–18]

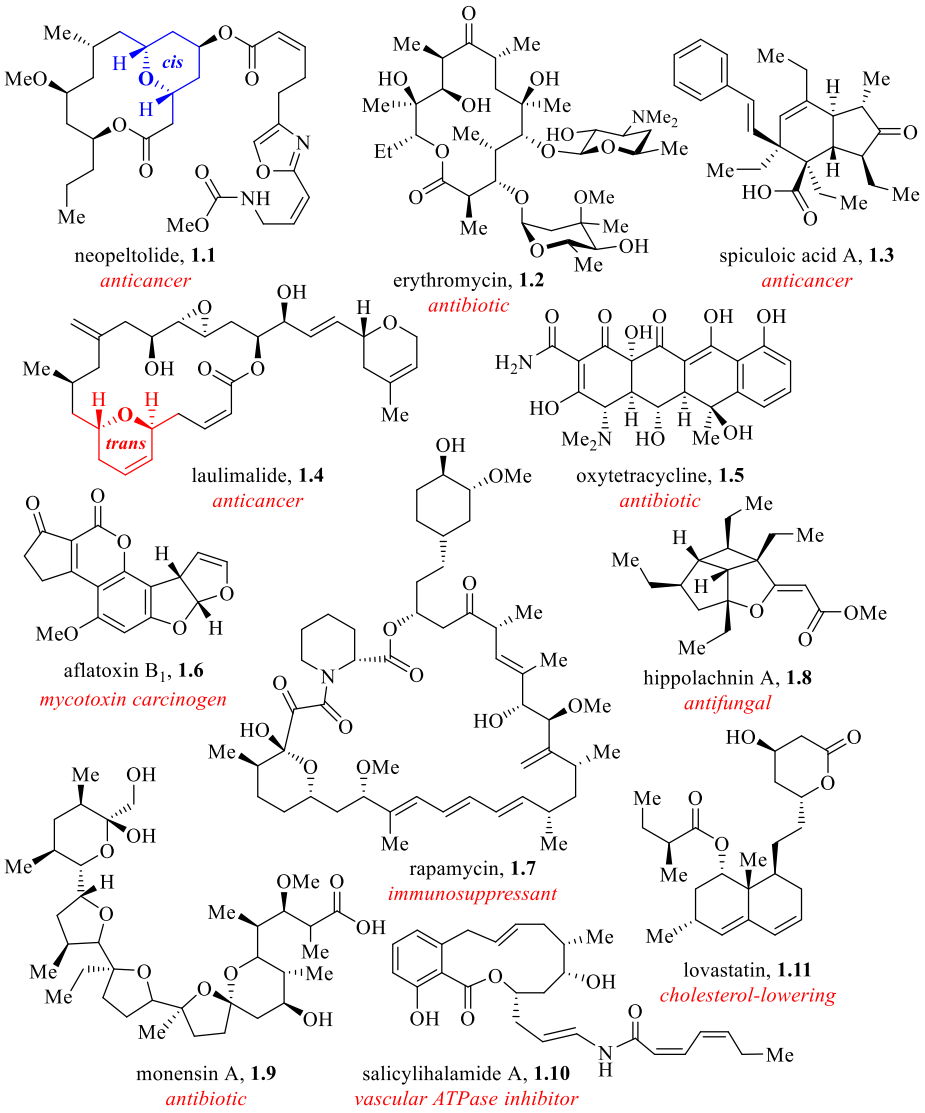

Figure 1.1 – Select examples of polyketide products that have been investigated by the Boddy Lab (**1.1 – 1.5**), as well as other well-known and clinical compounds. This selection demonstrates a small array of the chemical scaffolds represented by this class of compounds and assorted therapeutic applications.

A major limitation for development of many polyketide natural products is supply. Isolation from the natural source only furnishes minute amounts of active compound, and chemical synthesis of enough material for preclinical trials is extremely challenging due to their complex structures. Consequently, harnessing PKS biosynthesis as a method to produce such molecules could provide a solution to the supply problem of clinically-promising polyketides. This chapter introduces key methods of accessing polyketide natural products, which will be used to highlight the efforts of my doctoral research on the chemoenzymatic synthesis of polyketide natural products.

1.2 The Biosynthesis of Polyketide Natural Products

The modular assembly of polyketide biosynthesis was first determined in 1990,[19] and has seen considerable progress into understanding its mechanistic details. While elucidation of biosynthetic data requires substantial efforts and may sometimes never be determined,† sound knowledge of the general workings of PKS machinery can allow one to create reasonable hypotheses and predict putative pathways and intermediates based on the chemical framework.[20–25] The following section is written to provide a basic overview for the general assembly of polyketide products. Please refer to excellent reviews by field experts Fischbach and Walsh,[6] Cane,[7] Khosla,[8,26,27] Weissman,[10] Hertweck,[28,29] Keatinge-Clay,[30,31] Leadlay,[32] Sherman,[33] Staunton,[34] and any cited material for in-depth analysis of advanced type-I PKS details.

1.2.1 The General Biosynthetic Machinery of Type-I Polyketide Synthases (PKS)

The type-I PKS proteins are composed of groups (modules) of specific catalytically-active protein folds (domains), and these modular assembly lines are amongst the largest and most sophisticated enzymes known.[9] Using simple building blocks, PKSs generally catalyze two-carbon linear elongations *via* thio-Claisen condensation reactions (Figure 1.2).[28,29,34,35] To perform this chemistry, each module must house three core domains including a ketosynthase (**KS**) to initiate the process, acyltransferase (**AT**) for selection of an extender unit,[35] and an acyl carrier protein (**ACP**). The ACP possesses a phosphopantetheine arm that acts as a covalent tether within the module, holding the extender unit **1.13** and growing polyketide intermediate **1.12** prior to, during, and following chain elongation, respectively.

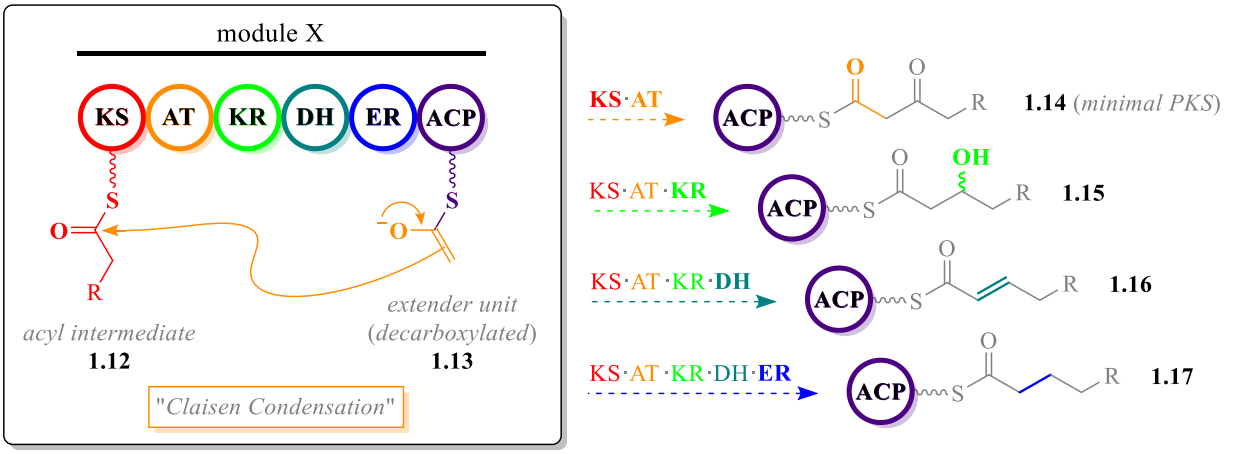

Figure 1.2 – The minimal PKS requires the acyl carrier protein (**ACP**), ketosynthase (**KS**), and acyl transferase (**AT**) domains to perform one round of chain elongation by decarboxylative Claisen condensation. The growing *β*-keto intermediate can undergo optional processing by ketoreductase (**KR**), dehydratase (**DH**), and enoyl reductase (**ER**) domains. A PKS megaenzyme does not require all three (or any) of these reductively-modifying domains; when present, they must operate in sequence (KR → DH → ER).

† Many isolated compounds harbor a symbiotic microorganism that is responsible for the biosynthesis of the active compound, making pathway elucidation, source re-isolation, or *in vitro* culturing difficult-to-impossible.[87–89]

The resulting acyl intermediate may undergo optional reductive modification at the *β*-carbonyl of the incorporated acyl unit **1.14**.[7,8,30,36] This processing may provide stereospecific[31] *β*-hydroxy- **1.15**, *α*,*β*-unsaturated **1.16**, or fully-reduced thioester **1.17** products by ketoreductase (**KR**), dehydratase (**DH**), and enoyl reductase (**ER**) domains, respectively (Figure 1.2). While these three modifying enzymes are optional, they must operate in sequence (partial, or complete). Once the enzymatically-programmed chain length is constructed, the presence of a thioesterase domain (**TE**) acts as the final enzymatic process (Figure 1.3).[37] At this site **1.18**, the growing chain is either cyclo-released *via* intramolecular macrocyclization by a nucleophilic hydroxyl group or is hydrolytically-cleaved from its covalent tether to the megaenzyme to yield cyclic lactone **1.19** or linear acid **1.20** products, respectively.

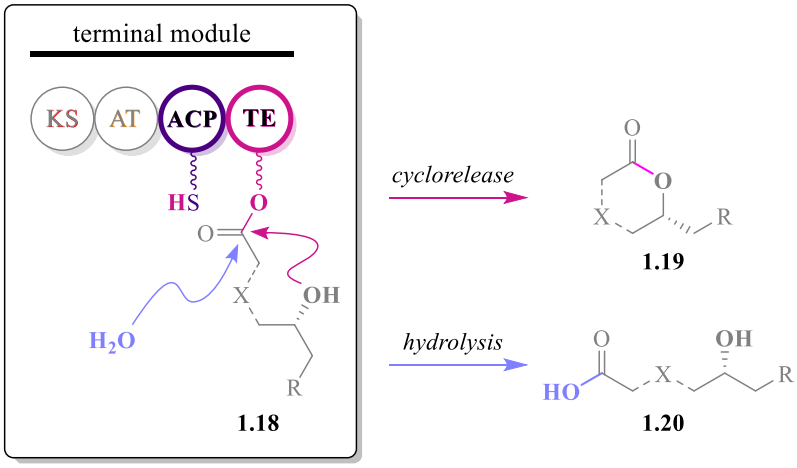

Figure 1.3 – A thioesterase (**TE**) domain is the final enzymatic site of the terminal module within PKS megaenzymes. This domain is responsible for release of the full-length polyketide by intramolecular lactonization, or by hydrolysis with exogenous water.

Frequently, off-loading from the PKS protein does not yield the final polyketide product and following release the immature product is subjected to additional site-specific tailoring modifications catalyzed by free-standing enzymes.[38–40] These post-PKS tailoring modifications are in many cases implicitly-required to establish the bioactivity of the synthase product, and include transformations such as glycosylation, halogenation, methylation, acylation, and hydroxylation, among various others.

1.2.2 An In Vitro Total Synthesis of Enterocin using Purified Enzymes

The incredible power of native PKS proteins was highlighted by Moore and coworkers with their *in vitro* total synthesis of the bacteriostatic natural product enterocin (Figure 1.4).[41] Relying on their understanding of the biosynthetic machinery and using purified (recombinant) PKS proteins as biocatalysts, they assembled the complex tricyclic framework of **1.23** from simple building blocks.

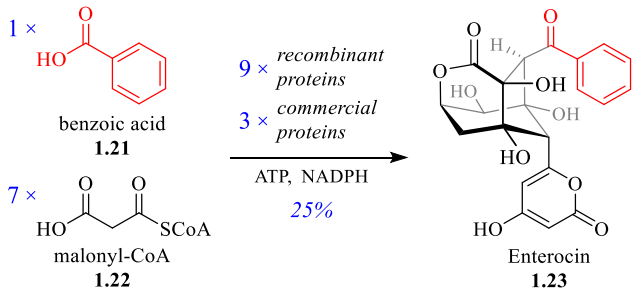

Figure 1.4 – The enterocin total synthesis by Moore and coworkers is the first *in vitro* assembly of a complete PKS biosynthetic pathway. They used 12 proteins in a cascade sequence to generate ten (10) C–C bonds and seven (7) stereogenic centers in 25% overall yield.

This synthesis highlights the incredible ability of enzymatic proteins for rapid and economical generation of complex scaffolds. In this novel strategy, Moore and coworkers installed ten carbon-carbon bonds, five carbon-oxygen bonds, and seven stereogenic centers (three quaternary) within a tricyclic system in a single enzymatic cascade. While this remains a monumental feat, it required extensive biosynthetic knowledge of PKS systems and the specific natural product. Moreover, this synthesis employed recombinant proteins to assemble their natively-programmed product, and would require the complete biosynthetic information of desired target compounds to generate them *via* this strategy.

1.2.3 PKS Biosynthesis Is Not as Tolerant as Chemical Synthesis

The biosynthesis of polyketide products is a natural accomplishment that has required extensive evolutionary optimization. Scientific advances have established an incredible understanding of PKS mechanistic details, and continues to report new discoveries. The work of Moore and coworkers highlights the power of nature's economical assembly of simple building blocks into complex scaffolds, but also illustrates its limitations. They required a fully-characterized biosynthetic pathway, which often is not available for most compounds. In addition, this work was confined to the pre-established transformations using pre-determined materials under physiological conditions, effectively eliminating the potential to easily generate structural analogues.

1.3 The Chemical Synthesis of Polyketide Natural Products

Chemical synthesis allows access to nearly-limitless structural diversity. Far-removed from Wöhler's synthesis of urea,[42] the chemical synthesis of secondary metabolites became an art where complex scaffolds posed intellectually-stimulating puzzles that challenged experimental capabilities.[43] The field has reached a point where, based on continuing achievements[44–50] and innovations,[51–53] organic chemists can synthesize *nearly* any structure drawn. This section illustrates the role of chemical synthesis in accessing polyketide natural products.

1.3.1 Total Synthesis of Neopeltolide as a Platform for New Methodology & Capability

Total synthesis of complex natural products remains the inspiration behind, and a vehicle used for testing new synthetic methodologies. In addition to highlighting innovative strategies developed in-house, it provides a stage for researchers to underscore proficiencies within specific fields and topics (Figure 1.5). An example is Hoveyda's recent synthesis of neopeltolide **1.1**, where his extensive experience in metal catalysis and olefin metathesis was used to selectively install each stereogenic center.[54]

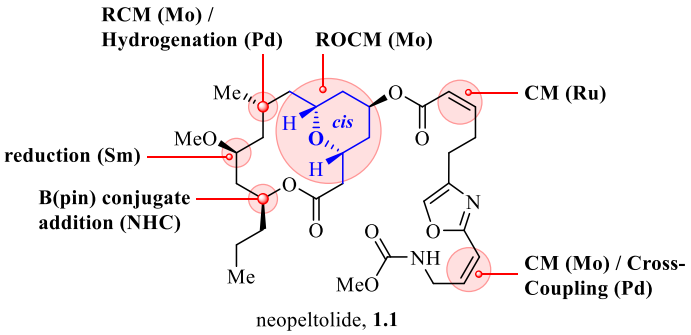

Figure 1.5 –Hoveyda and coworkers' synthesis of neopeltolide used olefin metathesis as a principal strategy. Catalysis was used for the selective installation of all six stereocenters.

The Hoveyda synthesis stands as the most efficient synthesis of neopeltolide to date, and highlighted novel sequences and reagents. However, use of intricate reagents and conditions limit these transformations, hampering their ability as economical or sustainable methods for commercial production.

1.3.2 A Re-Emergence of Total Synthesis for Clinical Development

Ongoing improvement for selectively accessing biosynthetically-available functional groups with incredible reliability and predictability preserves total synthesis as a cornerstone in drug development. This method allowed scalable-access to discodermolide **1.24**,[55] sagopilone **1.25**,[56,57] and Halaven® **1.26**.[44]

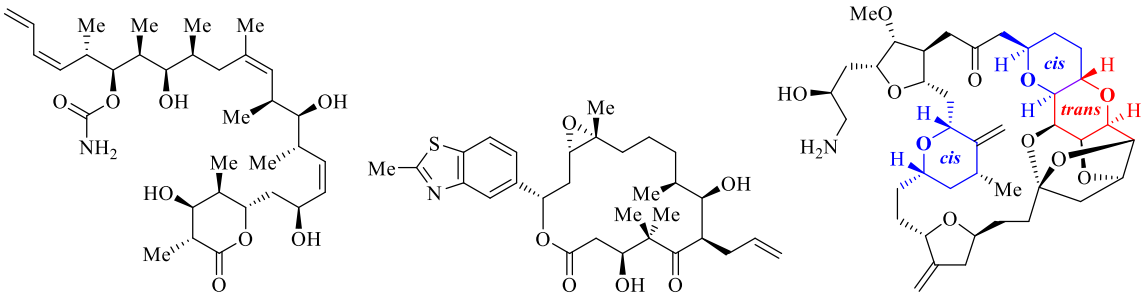

Figure 1.6 – Examples of anticancer polyketide natural products accessed by total synthesis on large scale for clinical evaluation (**1.24** & **1.25**), and for commercial production (**1.26**).[44,56–59]

These three compounds represent breakthroughs on the established-perception of what druggable chemical leads should look like for drug discovery. The extreme complexity of **1.26** marked a herculean achievement for the total synthesis when it was approved in 2010 for cancer therapy,[44] and is considered the most-complex molecular structure on the market prepared by this method.[60]

1.3.3 Chemical Synthesis Is Not as Efficient as PKS Biosynthesis

The development of polyketide natural products by chemical synthesis demonstrates the enormous diversity of reagents and transformations available, and the flexible substrate scope that is difficult to achieve by biological approaches. However, despite the examples presented, it remains a rarity to produce sufficient material for clinical applications by total synthesis. Structural complexity remains the limiting factor for PKS products, and generally results in poor overall yields, economy, scalability, and control of selectivity. Accordingly, syntheses are often designed as highly-convergent routes to minimize linear steps and improve efficiency, yet nature's linear multi-step biosynthesis remains the gold standard.

1.4 Where Biology Meets Chemistry: Chemoenzymatic Syntheses & Biocatalysts

The previous sections illustrate a small example of the many scientific achievements in accessing polyketide natural products. Though each entry is a deserved success story, there exist common limitations with both enzymatic and chemical syntheses. Biosynthetic methods are incredibly efficient and selective processes, but typically suffer from very-defined transformations and substrate tolerability. Conversely, chemical synthesis offers nearly limitless access to structural diversity, but often requires use of protecting groups to suppress unwanted side-reactions, regulated conditions to lower energetic barriers, or intricate catalytic reagents to improve enantio- or diastereoselectivity. These requirements rapidly increase the number of linear steps, and decrease overall yields and efficiency of the process.

Decades of interdisciplinary research has provided insights into merging the advantages of these methods for production of polyketide natural products. Within this dissertation, chemoenzymatic synthesis is a sweeping definition for accessing bioactive compounds through any combination of synthetic chemistry and biosynthetic proteins (enzymatic synthesis). In this section, select chemoenzymatic methods for polyketide products will be introduced.

1.4.1 Semi-Synthesis as a Solution to Natural Product Drug Development

In natural product drug development, semi-synthetic derivatives often represent the only practical means of obtaining sufficient material for clinical evaluation and exploration of structure-activity relationships (SAR) for low-producing or overly-complex metabolites. This strategy employs simpler and

more readily-available congeners (or naturally-sourced intermediates) as starting material. The epothilone family of anticancer compounds, and macrolide antibiotics have greatly-benefited from this advantageous strategy (Figure 1.7).[61]

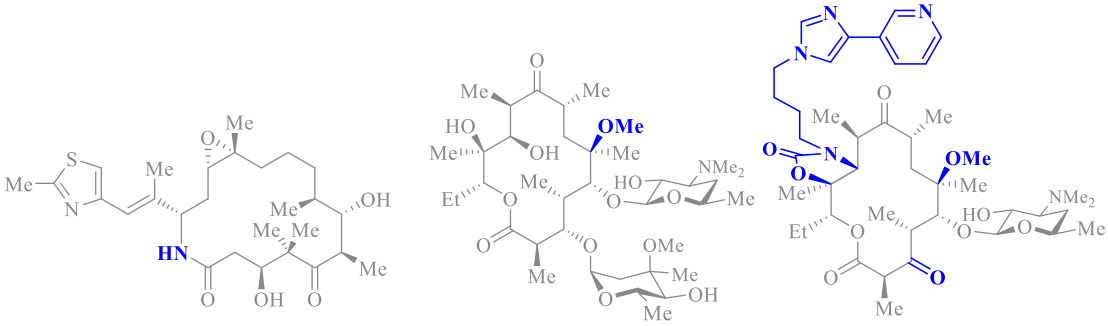

Figure 1.7 – Select polyketide clinical agents manufactured by semi-synthetic strategies. Steps required to access the analogue from, and alterations to the parent frameworks of epothilone B and erythromycin are highlighted in **blue**.

Macrolide antibiotics have heavily-relied on semi-synthesis due to the incredible complexity of their highly-functionalized macrocyclic framework (Figure 1.4). The lone chemical synthesis of erythromycin required 77 steps and illustrated dismal prospect of accessing this intricate framework synthetically.[48–50] Like the epothilones,[61] the semi-synthesis relies on fermentation of the parent framework. This allows chemical synthesis to efficiently generate new analogues such as telithromycin **1.29** of the ketolide family, which would certainly not exist without this method of manufacture.[62]

1.4.2 A Chemo-Biosynthetic-Chemosynthesis of Spinosyn A

The unique and complex structure of spinosyn A has proven a synthetic challenge (Figure 1.8).[63–66] In 2014, Liu published a chemoenzymatic total synthesis where classic chemical synthesis furnished the putative cyclo-released product **1.31** of modular PKS assembly. Treatment by corresponding post-PKS tailoring enzymes prepared **1.32** with stereo- and regiocontrol in a single enzymatic sequence.

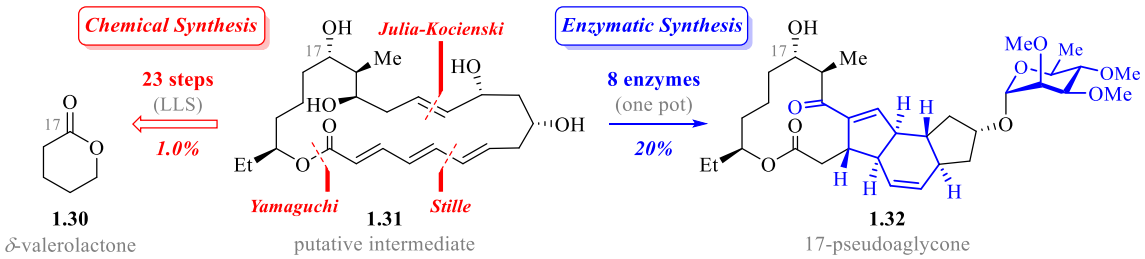

Figure 1.8 – In Liu's report, chemical synthesis furnished putative PKS intermediate for processing by treatment with recombinant PKS proteins. Completion of spinosyn A synthesis required chemical glycosylation at the C17 position.[67]

The process is a shining demonstration of alternating chemical and enzymatic synthesis to produce complex polyketides. Nevertheless, this strategy presents associated difficulties such as the long chemical preparation of the specific intermediate needed to initiate the enzymatic cascade, or the failed glycosyltransferase step due to an absence of requisite cofactors, yet to be elucidated.[67]

1.4.3 The Potential of Enzymes as Catalysts in Organic Synthesis

The use of isolated enzymes as catalysts (*biocatalysts*) in organic chemistry is a green technology capable of delivering highly stereo-, chemo- and regioselective transformations. Because of this, they are commonly used to produce building blocks for fine and commodity chemical manufacturing; hydrolytic biocatalysts have proven instrumental. Esterases are cofactor- and metal-free biocatalysts for broad chemical applications, including desymmetrization reactions of prochiral materials like **1.33** (Figure 1.9A).

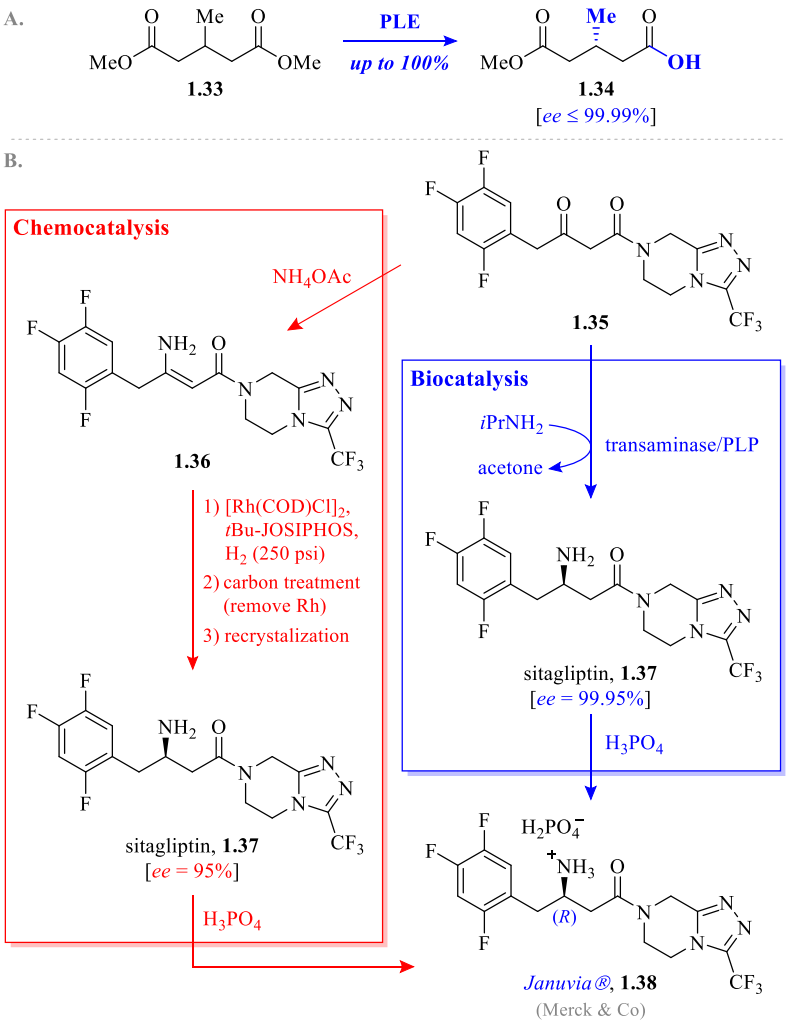

Figure 1.9 – A) Pig liver esterase (PLE) is commonly-used in organic synthesis. B) Comparison of second-generation chemical synthesis (79% overall) and chemoenzymatic (92%) methods of accessing sitagliptin **1.37**, the active ingredient of clinical anti-diabetic agent Januvia® by Merck & Co.[68,69]

Protein engineering has improved some biocatalytic transformations by expanding the substrate tolerability of a native enzyme. Merck's third-generation synthesis of sitagliptin **1.38** employed an engineered transaminase protein for production of chiral amine **1.37** as the only detectable enantiomer (Figure 1.9B).[68] This strategy provided 53% increase in productivity (kg/L per day), and 19% reduction in total waste compared to the second-generation chemical process.[69] More importantly, biocatalysis reduced total manufacturing costs with the elimination of heavy metals and specialized equipment.

1.4.2 A Notable Gap Between Promise and Reality of Chemoenzymatic Strategies

Chemoenzymatic synthesis provides the strengths of enzymatic and chemical synthesis, which has been shown to revolutionize process chemistry in the case of Januvia®.[68–70] Combined with fermentation strategies to epothilones and macrolide antibiotics, this work underscores the potential power of harnessing biosynthesis for efficient, economical, and environmentally-benign processes for pharmaceutical manufacturing. However, these highlight inherent difficulties such as the fact semi-synthetic epothilone analogues have largely been limited to two groups that possess both the producing organism and fermentation capabilities.[61] To fully-exploit the power of this method, continued research is required to advance protein engineering for modification of enzyme activity, or multienzyme systems for *in vitro* synthesis.

1.5 Dissertation Outline

The CRC Press dictionary of natural products estimates 90% of chemically-individual natural products contain a cyclic component.[71] Consequently, the ability to perform key bond-forming steps to generate cyclic products from acyclic scaffolds in a regio- and stereochemical manner has yielded a wealth of innovative strategies from the scientific community.[72–77] The work of the dissertation encompasses both chemical and biosynthetic studies, with an overall goal of developing chemoenzymatic strategies to access polyketide products more efficiently. In particular, this research is inspired by the numerous THP-bearing macrocyclic polyketides that have found clinical success.[3,44,61,78–81]

1.5.1 Development of De Novo PKS Pathway for Neopeltolide

The main study of my doctoral research was toward a chemoenzymatic synthesis for neopeltolide (Figure 1.11). Research milestones are divided into two distinct stages where *de novo* PKS design represents the final and long-term goal for this research, and presents an opportunity to modify this strategy for transannular THP assembly of neopeltolide analogues and other THP-bearing polyketides.[26,33,82,83] The immediate goal of this project has thus been to establish and evaluate the foundations of a transannular oxa-

conjugate addition strategy for the assembly of 2,6-*cis*-tetrahydropyran ring systems, and apply this chemistry to the synthesis of neopeltolide.

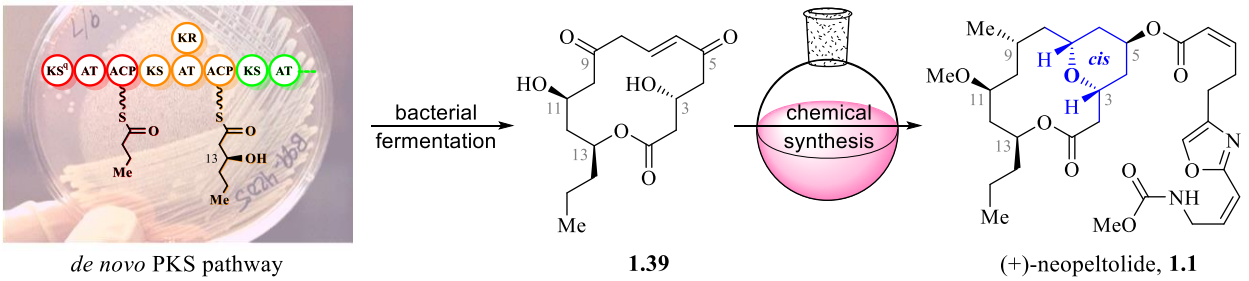

de novo PKS pathway **1.39** (+)-neopeltolide, **1.1**

Figure 1.10 – Summary of neopeltolide project, highlighting the long-term milestone of *de novo* PKS production of intermediates for transannular oxa-conjugate addition assembly of the *cis*-THP ring using synthetic chemistry.

A simplified model of the macrocyclic core of neopeltolide **1.40** afforded preliminary synthetic validation of this strategy (Scheme 1.1). Acid-mediated intramolecular attack of racemic *β'*-hydroxy nucleophile into an *α,β*-unsaturated ketone system proved superior to acid- or base-mediated addition into an *α,β*-unsaturated ester system.[17] Diastereoselectivity of the transformation was governed by reaction conditions, where thermodynamic control favors assembly of *cis*-pyranone product **1.41** (*d.r.* > 9:1). This published strategy[17] represented the first use of acid-mediated transannular oxa-conjugate assembly of *cis*-THP scaffolds, and is detailed in **Chapter 3** of this dissertation.

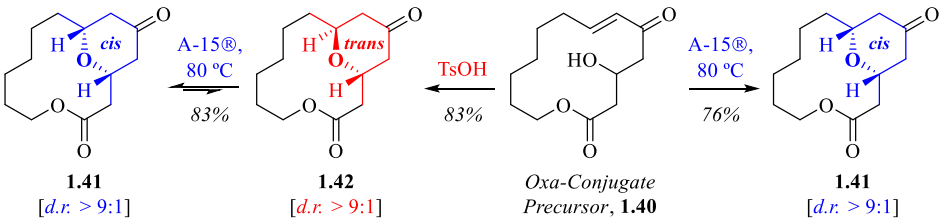

1.41 [*d.r.* > 9:1] **1.42** [*d.r.* > 9:1] *Oxa-Conjugate Precursor*, **1.40** **1.41** [*d.r.* > 9:1]

Scheme 1.1 – Summary of *α,β*-unsaturated ketone model for the transannular oxa-conjugate addition strategy for assembly of *cis*-THP; acid-mediated thermodynamic control selectively furnishes the *cis*-pyranone product.

The success of the model system inspired the total synthesis of the fully-elaborated macrocyclic core of neopeltolide **1.1** using the transannular oxa-conjugate addition strategy (Scheme 1.2). Using a 13-step asymmetric sequence, aldehyde **1.44** was prepared from commercial materials‡ and coupled with diprotic acid phosphonate **1.45** by Horner-Wadsworth-Emmons conditions.[84] Following macrocyclization, desilylation by treatment with HF spontaneously-afforded all four THP-stereoisomers, favoring the *trans*-product. Thermodynamic conditions promoted the acid-mediated interconversion, shifting the equilibrium

‡ Acid **1.43** is commercially available from Sigma-Aldrich or readily accessible in large scale over three steps (84%), including the PLE-catalyzed desymmetrization from § 1.4.3 (*ee* > 95%).[90]

to exclusive formation of *cis*-THP products. This work represents one of the higher-yielding syntheses of the macrocyclic core of neopeltolide, and is detailed in **Chapter 4** of this dissertation.

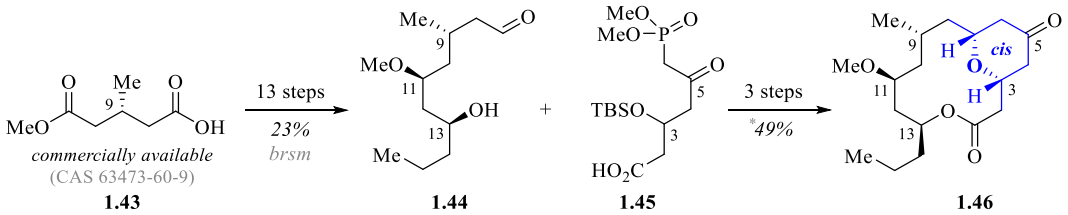

Scheme 1.2 – Summary of the total synthesis of the neopeltolide macrocyclic core by transannular oxa-conjugate addition for assembly of the *cis*-THP, highlighted by racemic hydroxy nucleophile. *The key formation of *cis*-**1.46** was performed on sub-milligram quantities, and conversion was estimated (75%).

Additional optimization is required to confidently predict diastereoselectivity based on molecular framework and reaction conditions, but these successes provide synthetic validation of a transannular oxa-conjugate addition to *cis*-THP rings. This work will facilitate the investigation into protein engineering of *de novo* PKS pathways to produce advanced intermediates using biosynthetically-available functional groups, namely alcohols (**KS**·**AT**·**KR**), olefins (**KS**·**AT**·**KR**·**DH**) and carbonyls (**KS**·**AT**), that can exploit this strategy. The long-term goal of this study is an improved production of natural, as well as unnatural, pyran-bearing PKS products. Fermentation processes would yield reliable and sustainable production of advanced molecular frameworks from simple materials, allowing synthetic chemistry to rapidly access lead compounds and SAR libraries, akin to the development of next-generation macrolide antibiotics.[62]

1.5.2 Development of a Thioesterase Macrocyclizing Biocatalyst

The paradigm model for PKS systems is the 6-deoxyerythronolide B synthase (DEBS) that produces the macrocyclic core of erythromycin (**1.2**, Figure 1.1).[85,86] The second study of my doctoral research probed specificities of the macrocyclizing thioesterase domain (§ 1.2.1) from the DEBS PKS pathway, using non-native linear substrates (Figure 1.11). The Boddy Lab has pioneered investigation into limits of promiscuity within this specific catalytic domain,[13,14,18,37] with the goal of developing it into a general macrocyclizing tool for organic synthesis. Rapid assembly of simplified analogues such as **1.48** were generated with *N*-acetyl cysteamine (SNAC) thioester handles that are mimics for the covalent tether of the acyl-carrier protein domain, which promotes enzyme binding. Our *in vitro* evaluation produced desired macrocyclic product **1.50**, in addition to an unexpected suite of related metabolites suggesting plasticity of available chemistries within this protein. This published work[18] demonstrated an evolutionary model where TEs selectively produce metabolites for improving fitness in a particular environment, and is detailed in **Chapter 6** of this dissertation.

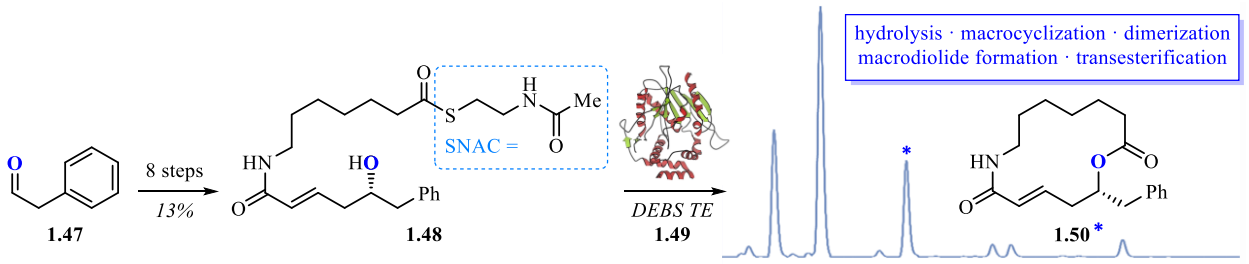

Figure 1.11 – The *in vitro* evaluation of DEBS thioesterase with simplified peptidyl analogues demonstrates that in addition to its native macrocyclizing chemistry, a variety of related metabolite products were isolated. This suggests the native DEBS TE is not suitable as a general biocatalyst for organic synthesis.

Although the native thioesterase from DEBS biosynthetic pathway is unlikely to be developed as a macrocyclizing tool for organic chemists, this work is part of ongoing efforts that evaluate its scope through *in vitro* testing. These details can provide significant data that can potentially be used to improve scope and function through protein engineering, or for alternative proteins to achieve our goal.

1.6 Conclusions

This chapter demonstrates that polyketides are an incredibly diverse and important family of secondary metabolites, and have produced many clinical successes. Unfortunately, their complex structures and extremely-limited natural supply have made these compounds historically difficult for drug development. Through two independent studies, the unifying goal of my presented research in this dissertation is to provide improved access to polyketide natural products using chemoenzymatic methods. Each study currently remains limited to specific targets, but their combined efforts provide a foundation for future work. These strategies present an opportunity to exploit the tremendous natural diversity of PKS systems, which would significantly expand the toolbox for next-generation scientists and expedite production of natural product leads. The ability to harness the power of biosynthetic assembly lines for *de novo* PKS pathways or to isolate enzymes as biocatalysts remains relatively new and unoptimized, though we hope our efforts require less R&D than that of nature.

1.7 References

(1) Wender, P. *Nat. Prod. Rep.* **2014**, *31*, 433–440.
(2) Yuan, H.; Ma, Q.; Ye, L.; Piao, G. *Molecules* **2016**, *21* (5), 1–18.
(3) Newman, D. J.; Cragg, G. M. *J. Nat. Prod.* **2016**, *79* (3), 629–661.
(4) Yuzawa, S.; Keasling, J. D.; Katz, L. *J. Antibiot.* **2016**, *69* (7), 494–499.
(5) Müller, R. *Chem. Biol.* **2004**, *11* (January), 4–6.
(6) Fischbach, M.; Walsh, C. T. *Chem. Rev.* **2006**, *106* (8), 3468–3496.
(7) Lowry, B.; Li, X.; Robbins, T.; Cane, D. E.; Khosla, C. *ACS Cent. Sci.* **2016**, *2* (1), 14–20.
(8) Robbins, T.; Liu, Y.-C.; Cane, D. E.; Khosla, C. *Curr. Opin. Struct. Biol.* **2016**, *41*, 10–18.
(9) Till, M.; Race, P. R. In *Nonribosomal Peptide and Polyketide Biosynthesis: Methods and Protocols*; Humana Press, 2016; pp 31–52.
(10) Weissman, K. J. *Beilstein J. Org. Chem.* **2017**, *13*, 348–371.
(11) Hertweck, C.; Luzhetskyy, A.; Rebets, Y.; Bechthold, A. *Nat. Prod. Rep.* **2007**, *24* (1), 162–190.
(12) Shimizu, Y.; Ogata, H.; Goto, S. *ChemBioChem* **2017**, *18*, 50–65.
(13) Wang, M.; Boddy, C. N. *Biochemistry* **2008**, *47* (45), 11793–11803.
(14) Pinto, A.; Wang, M.; Horsman, M.; Boddy, C. N. *Org. Lett.* **2012**, *14* (9), 2278–2281.
(15) Pinto, A.; Boddy, C. N. *Bioorg. Med. Chem. Lett.* **2012**, *22* (16), 5253–5256.
(16) Cole Stevens, D.; Henry, M. R.; Murphy, K. A.; Boddy, C. N. *Appl. Environ. Microbiol.* **2010**, *76* (8), 2681–2683.
(17) Hari, T. P. A.; Wilke, B. I.; Davey, J. A.; Boddy, C. N. *J. Org. Chem.* **2016**, *81*, 415–423.
(18) Hari, T. P. A.; Labana, P.; Boileau, M.; Boddy, C. N. *ChemBioChem* **2014**, *15* (18), 2656–2661.
(19) Cortes, J.; Haydock, S. F.; Roberts, G. A.; Bevitt, D. J.; Leadlay, P. F. *Nature* **1990**, *348*, 176–178.
(20) Müller, M.; Kusebauch, B.; Liang, G.; Beaudry, C. M.; Trauner, D.; Hertweck, C. *Angew. Chem. Int. Ed.* **2006**, *45* (46), 7835–7838.
(21) Moses, J. E.; Baldwin, J. E.; Marquez, R.; Adlington, R. M. *Org. Lett.* **2002**, *4* (21), 3731–3734.
(22) Aquino, C.; Sarkar, M.; Chalmers, M. J.; Mendes, K.; Kodadek, T.; Micalizio, G. C. *Nat. Chem.* **2012**, *4* (2), 99–104.
(23) Navarro, I.; Basset, J. F.; Hebbe, S.; Major, S. M.; Werner, T.; Howsham, C.; Bräckow, J.; Barrett, A. G. M. *J. Am. Chem. Soc.* **2008**, *130* (31), 10293–10298.
(24) Cookson, R.; Barrett, T. N.; Barrett, A. G. M. *Acc. Chem. Res.* **2015**, *48* (3), 628–642.
(25) Asai, T.; Luo, D.; Yamashita, K.; Oshima, Y. *Org. Lett.* **2013**, *15* (5), 1020–1023.
(26) Khosla, C.; Harbury, P. B. *Nature* **2001**, *409* (6817), 247–252.
(27) Khosla, C.; Herschlag, D.; Cane, D. E.; Walsh, C. T. *Biochemistry* **2014**, *53* (18), 2875–2883.
(28) Hertweck, C. *Angew. Chem. Int. Ed.* **2009**, *48* (26), 4688–4716.
(29) Hertweck, C. *Trends Biochem. Sci.* **2015**, *40* (4), 189–199.
(30) Keatinge-Clay, A. T. *Nat. Prod. Rep.* **2012**, *29* (10), 1050–1073.
(31) Keatinge-Clay, A. T. *Nat. Prod. Rep.* **2016**, *33* (2), 141–149.
(32) Weissman, K. J.; Leadlay, P. F. *Nat. Rev. Microbiol.* **2005**, *3* (12), 925–936.
(33) Sherman, D. H. *Nat. Biotechnol.* **2005**, *23* (9), 1083–1084.
(34) Staunton, J.; Weissman, K. J. *Nat. Prod. Rep.* **2001**, *18* (4), 380–416.
(35) Chan, Y.; Podevels, A. M.; Kevany, B. M.; Thomas, M. G. *Nat. Prod. Rep.* **2009**, *26* (1), 90–114.
(36) Caffrey, P. *Comput. Struct. Biotechnol. J.* **2012**, *3* (4), 1–8.
(37) Horsman, M. E.; Hari, T. P. A.; Boddy, C. N. *Nat. Prod. Rep.* **2016**, *33*, 183–202.
(38) Olano, C.; Carmen, M.; Méndez, C.; Salas, J. *Nat. Prod. Rep.* **2010**, *27* (4), 571–616.
(39) Lin, S.; Huang, T.; Shen, B. *Tailoring enzymes acting on carrier protein-tethered substrates in natural product biosynthesis*, 1st ed.; Elsevier Inc., 2012; Vol. 516.
(40) Rix, U.; Fischer, C.; Remsing, L. L.; Rohr, J. *Nat. Prod. Rep.* **2002**, *19* (5), 542–580.
(41) Cheng, Q.; Xiang, L.; Izumikawa, M.; Meluzzi, D.; Moore, B. S. *Nat. Chem. Biol.* **2007**, *3* (9), 557–558.
(42) Wöhler, F. *Ann. Phys.* **1828**, *88* (2), 253–256.
(43) Nicolaou, K. C.; Hale, C. R. H.; Nilewski, C.; Ioannidou, H. A. *Chem. Soc. Rev.* **2012**, *41* (15), 5185.
(44) Bauer, A. In *Topics in Heterocyclic Chemistry*; Cossy, J., Ed.; Springer, 2016; pp 209–270.
(45) Gao, X.; Woo, S. K.; Krische, M. J. *J. Am. Chem. Soc.* **2013**, *135*, 4223–4226.
(46) Baran, P. S.; Maimone, T. J.; Richter, J. M. *Nature* **2007**, *446*, 404–408.
(47) Nicolaou, K. C.; Li, H.; Boddy, C. N. C.; Ramanjulu, J. M.; Yue, T. Y.; Natarajan, S.; Chu, X. J.; Brase, S.;

Rubsam, F. *Chem.-Eur. J.* **1999**, *5* (9), 2584–2601.
(48) Woodward, R. B.; Logusch, E.; Nambiar, K. P.; Sakan, K.; Ward, D. E.; Auyeung, B. W.; Balaram, P.; Browne, L. J.; Card, P. J.; Chen, C. H.; Chenevert, R. B.; Fliri, A.; Frobel, K.; Gais, H. J.; Garratt, D. G.; Hayakawa, K.; Heggie, W.; Hesson, D. P.; Hoppe, D.; Hoppe, I.; Hyatt, J.; Ikeda, D.; Jacobi, P.; Kim, K. S.; Kobuke, Y.; Kojima, K.; Krowicki, K.; Lee, V. J.; Leutert, T.; Malchenko, S.; Martens, J.; Matthews, R. S.; Ong, B. S.; Press, J. B.; Rajanbabu, T. V; Rousseau, G.; Sauter, H. M.; Suzuki, M.; Tatsuta, K.; Tolbert, L. M.; Truesdale, E.; Uchida, I.; Ueda, Y.; Uyehara, T.; Vasella, T.; Vladuchick, W. C.; Wade, P.; Williams, R. M.; Wong, H. N. C. *J. Am. Chem. Soc.* **1981**, *103* (11), 3210–3213.
(49) Woodward, R. B.; Au-Yeung, B. W.; Balaram, P.; Browne, L. J.; Ward, D. E.; Card, P. J.; Chen, C. H. *J. Am. Chem. Soc.* **1981**, *103* (11), 3213–3215.
(50) Woodward, R. B.; Logusch, E.; Nambiar, K. P.; Sakan, K.; Ward, D. E.; Au-Yeung, B. W.; Balaram, P.; Browne, L. J.; Card, P. J.; Chen, C. H. *J. Am. Chem. Soc.* **1981**, *103* (11), 3215–3217.
(51) Doi, T.; Fuse, S.; Miyamoto, S.; Nakai, K.; Sasuga, D.; Takahashi, T. *Chem. Asian J.* **2006**, *1* (3), 370–383.
(52) Li, J.; Ballmer, S. G.; Gillis, E. P.; Fujii, S.; Schmidt, M. J.; Palazzolo, A. M. E.; Lehmann, J. W.; Morehouse, G. F.; Burke, M. D. *Science* **2015**, *347* (6227), 1221–1226.
(53) Snead, D. R.; Jamison, T. F. *Angew. Chem. Int. Ed.* **2015**, *54* (3), 983–987.
(54) Yu, M.; Schrock, R. R.; Hoveyda, A. H. *Angew. Chem. Int. Ed.* **2015**, *54* (1), 215–220.
(55) Mickel, S. J.; Niederer, D.; Daeffler, R.; Osmani, A.; Kuesters, E.; Schmid, E.; Schaer, K.; Gamboni, R.; Chen, W.; Loeser, E.; Kinder, F. R.; Konigsberger, K.; Prasad, K.; Ramsey, T. M.; Repič, O.; Wang, R.-M.; Florence, G.; Lyothier, I.; Paterson, I. *Org. Process Res. Dev.* **2004**, *8* (1), 122–130.
(56) Klar, U.; Platzek, J. *Synlett* **2012**, *23* (9), 1291–1299.
(57) Klar, U.; Buchmann, B.; Schwede, W.; Skuballa, W.; Hoffmann, J.; Lichtner, R. B. *Angew. Chem. Int. Ed.* **2006**, *45* (47), 7942–7948.
(58) Longley, R. E. In *Natural Products and Cancer Drug Discovery*; 2013; pp 213–237.
(59) Chamberlain, M. C.; Baik, C. S.; Gadi, V. K.; Bhatia, S.; Chow, L. Q. M. *Neuro. Oncol.* **2017**, *19* (1), i1–i24.
(60) Hunziker, J.; Koch, G. *Chem Cell Press* **2016**, *1* (3), 336–338.
(61) Altmann, K.-H.; Gaugaz, F. Z.; Schiess, R. *Mol. Divers.* **2011**, *15*, 383–399.
(62) Wright, P. M.; Seiple, I. B.; Myers, A. G. *Angew. Chem. Int. Ed.* **2014**, *53* (34), 8840–8869.
(63) Paquette, L. A.; Collado, I.; Purdie, M. *J. Am. Chem. Soc.* **1998**, *120* (11), 2553–2562.
(64) Mergott, D. J.; Frank, S.; Roush, W. R. *Proc. Natl. Acad. Sci.* **2004**, *101* (33), 11955–11959.
(65) Evans, D. A.; Black, W. C. *J. Am. Chem. Soc.* **1993**, *115* (11), 4497–4513.
(66) Paquette, L. A.; Gao, Z.; Ni, Z.; Smith, G. F. *J. Am. Chem. Soc.* **1998**, *120* (11), 2543–2552.
(67) Kim, H. J.; Choi, S. H.; Jeon, B. S.; Kim, N.; Pongdee, R.; Wu, Q.; Liu, H. W. *Angew. Chem. Int. Ed.* **2014**, *53* (49), 13553–13557.
(68) Jarvis, W. R.; Colbeck, J. C.; Krebber, A.; Fleitz, F. J.; Brands, J. *Science*, **2010**, *329*, 305–310.
(69) Hansen, K. B.; Hsiao, Y.; Xu, F.; Rivera, N.; Clausen, A.; Kubryk, M.; Krska, S.; Rosner, T.; Simmons, B.; Balsells, J.; Ikemoto, N.; Sun, Y.; Spindler, F.; Malan, C.; Grabowski, E. J. J.; Armstrong, J. D. *J. Am. Chem. Soc.* **2009**, *131* (25), 8798–8804.
(70) Hansen, K. B.; Balsells, J.; Dreher, S.; Hsiao, Y.; Kubryk, M.; Palucki, M.; Rivera, N.; Steinhuebel, D.; Armstrong, J. D.; Askin, D.; Grabowski, E. J. J. *Org. Process Res. Dev.* **2005**, *9* (5), 634–639.
(71) Bon, R. S.; Waldmann, H. *Acc. Chem. Res.* **2010**, *43* (8), 1103–1114.
(72) Parenty, A.; Moreau, X.; Niel, G.; Campagne, J.-M. *Chem. Rev.* **2013**, *113*, PR1-PR40.
(73) Kopp, F.; Marahiel, M. A. *Nat. Prod. Rep.* **2007**, *24*, 735–749.
(74) Perry, M. A.; Rychnovsky, S. D.; Sizemore, N. In *Synthesis of Saturated Oxygenated Heterocycles I*; Cossy, J., Ed.; Springer-Verlag, 2014; pp 43–95.
(75) Crane, E.; Scheidt, K. *Angew. Chem. Int. Ed.* **2010**, *49* (45), 8316–8326.
(76) Bai, Y.; Davis, D. C.; Dai, M. *Angew. Chem. Int. Ed.* **2014**, *53*, 6519–6522.
(77) Nasir, N. M.; Ermanis, K.; Clarke, P. A. *Org. Biomol. Chem.* **2014**, *12*, 3323–3335.
(78) Butler, M. S.; Robertson, A. A. B.; Cooper, M. A. *Nat. Prod. Rep.* **2014**, *31* (11), 1612–1661.
(79) Schwecke, T.; Aparicio, J. F.; Molnár, I.; König, A.; Khaw, L. E.; Haydock, S. F.; Oliynyk, M.; Caffrey, P.; Cortés, J.; Lester, J. B.; Böhm, G.; Staunton, J.; Leadlay, P. F. *Proc. Natl. Acad. Sci.* **1995**, *92* (17), 7839–7843.
(80) Denvir, J.; Neitch, S.; Fan, J.; Niles, R. M.; Boskovic, G.; Schreurs, B. G.; Primerano, D. A.; Alkon, D. L. *J. Alzheimers Dis.* **2015**, *46* (2), 483–490.
(81) Rothmeier, A. S.; Schneiders, U. M.; Wiedmann, R. M.; Ischenko, I.; Bruns, C. J.; Rudy, A.; Zahler, S.;

Vollmar, A. M. *Int. J. Cancer* **2010**, *127* (5), 1096–1105.
(82) Menzella, H. G.; Reid, R.; Carney, J. R.; Chandran, S. S.; Reisinger, S. J.; Patel, K. G.; Hopwood, D.; Santi, D. V. *Nat. Biotechnol.* **2005**, *23* (9), 1171–1176.
(83) Menzella, H. G.; Carney, J. R.; Santi, D. V. *Chem. Biol.* **2007**, *14* (2), 143–151.
(84) Wadsworth, W. S.; Emmons, W. D. *J. Am. Chem. Soc.* **1961**, *83* (7), 1733–1738.
(85) Rawlings, B. J. *Nat. Prod. Rep.* **2001**, *18* (3), 231–281.
(86) Cane, D. E. *J. Biol. Chem.* **2010**, *285* (36), 27517–27523.
(87) Xiong, Z.-Q.; Wang, J.-F.; Hao, Y.-Y.; Wang, Y. *Mar. Drugs* **2013**, *11* (3), 700–717.
(88) Gerwick, W. H.; Moore, B. S. *Chem. Biol.* **2012**, *19* (1), 85–98.
(89) Salomon, C. E.; Magarvey, N.; Sherman, D. H. *Nat. Prod. Rep.* **2004**, *21* (1), 105–121.
(90) Lam, L. K. P.; Hui, R. H. F.; Jones, J. B. *J. Org. Chem.* **1986**, *51* (11), 2047–2050.

EFFORTS TOWARD DEVELOPMENT OF A DE NOVO CHEMOENZYMATIC SYNTHESIS OF NEOPELTOLIDE

· Study I ·

Abstract

Neopeltolide is a highly potent marine polyketide natural product with activity against multiple cancer cell lines *in vitro*. Nanomolar cytotoxicities and limited natural supply has led to several syntheses of this tetrahydropyran (THP)-bearing polyketide (**Chapter 2**). In this study, the feasibility of a transannular oxa-conjugate addition strategy for assembly of *cis*-2,6-THP rings was established using cyclic *α,β*-unsaturated model systems (**Chapter 3**). This transformation was applied to the fully-elaborated macrocyclic core of neopeltolide, which highlights a highly-convergent olefination to prepare the full carbon framework (**Chapter 4**). Long-term milestones of this study include the development of a *de novo* chemoenzymatic synthesis of neopeltolide that relies of chemistry catalyzed by polyketide synthase (PKS) enzymes. Success of the study can lead to rapid, reliable, and sustainable production of neopeltolide, as well as other THP-bearing natural products and analogues.

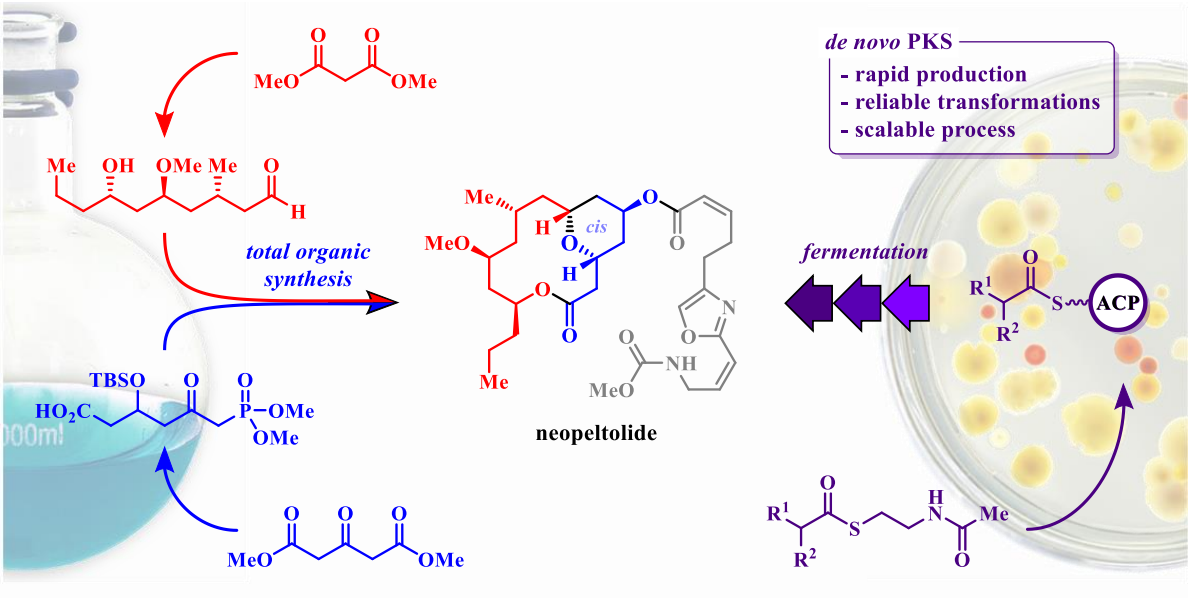

· Chapter 2 ·

cis-Tetrahydropyran Assembly Strategies in Neopeltolide Synthesis

2.1 The Marine Habitat as a Source for Bioactive Natural Products

The marine habitat is the largest and least-studied ecosystem on Earth. This ecosystem possesses a wealth of biodiversity, and many of the often-sessile and soft-bodied inhabitants produce or harbor[†] secondary metabolites with potent bioactivities.[1–5] In comparison to the terrestrial environment, the marine habitat is relatively new to bioprospecting and is virtually untapped.[6] Despite this, thousands of novel compounds and chemical scaffolds have been discovered. Several of these compounds have been developed as FDA-approved therapeutic agents, or are undergoing preclinical and clinical trials.[3,4,7,8]

As part of ongoing efforts to discover marine natural products with useful therapeutic properties, a Florida Atlantic University (Harbor Branch) research program led by Dr. Amy Wright reported the isolation of a novel macrolide with potent cancer inhibition.[9,10] Collection of a deep-water sponge of the family Neopeltidae furnished the novel polyketide product, neopeltolide (**2.1**, Figure 2.1). Key structural elements of **2.1** include a bicyclic 14-membered macrocyclic core embedded with a 2,6-*cis*-tetrahydropyran ring anchoring an oxazole- and carbamate-bearing side-chain. The side-chain is identical to that of structurally-homologous 18-membered leucascondrolide A **2.2**, which was previously-isolated from a marine sponge in 1996.[11]

Deep-water sponge collection
(Neopeltidae *Dædalopelta sp.*)

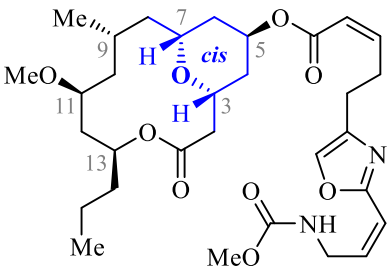

revised structure
neopeltolide, **2.1**

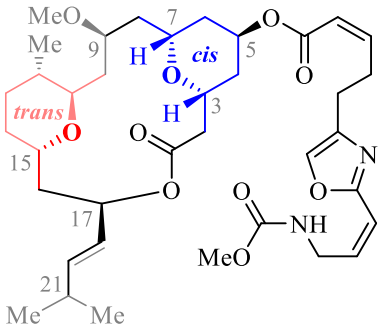

leucascandrolide A, **2.2**

Figure 2.1 – The deep-water sponge collected by Wright *et al*. that was used to isolate the cytotoxic new polyketide natural product neopeltolide **2.1**, which shares strong homology and an identical oxazole-bearing side-chain to the previously-reported 18-membered macrolide, leucascandrolide A **2.2**.

This chapter reviews synthetic efforts of neopeltolide (**2.1**) available up to December 2016, highlighting diastereoselective construction of the macrocyclic core, with emphasis on the assembly of the 2,6-***cis***-tetrahydropyran ring moiety.

[†] Many isolated compounds (mostly from mollusks, sponges, and tunicates)[7] harbor a symbiont that is responsible for the biosynthesis of the active compound; many of these are symbiotic bacteria, and can make re-isolation or *in vitro* culturing difficult to impossible.[2,4,283]

2.1.1 Neopeltolide: A Promising New Antiproliferative Compound

Neopeltolide is a 14-membered macrolide natural product that was isolated from a deep-water sponge collected off the northern coast of Jamaica by Wright and coworkers in 2007.[9] The sponge was not identified, but it most-closely matches the taxonomic description for the genus *Dædalopelta*, which is described as a close relative member of *Callipelta*.[12–14] The planar structure of neopeltolide was established from extensive one- and two-dimensional spectroscopic data, where one-dimensional double-pulsed field gradient spin echo (DPFGSE) NOE[15] was relied upon in regions of heavy peak overlap. Key structural elements include six stereogenic centers within a bicyclic 14-membered macrolactone core bearing a 2,4,6-trisubstituted tetrahydropyran ring that serves as an anchor for an oxazole-containing side-chain identical to that of leucascandrolide A.

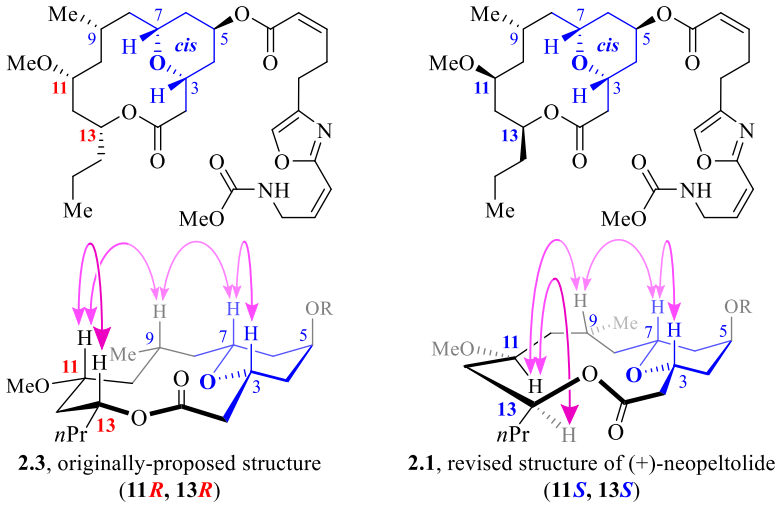

Figure 2.2 – Originally-proposed structure **2.3** was proposed by Wright, and the partially-revised **2.1** from independent syntheses by Panek and Scheidt. Key NOE correlations used for the relative and absolute stereochemical assignments are presented in **pink**; the oxazole-containing side-chain was not included for clarity.

The relative stereochemistry of neopeltolide was assigned by careful analysis of coupling constants, and 1D-DPFGSE NOE experiments.[9] As a result of being an oil, crystallographic studies were not a viable option to elucidate the structure of neopeltolide.[16] The configuration of the originally-proposed structure **2.3** was established as (3*R*,5*R*,7*R*,9*S*,11*R*,13*R*) based on observed NOE enhancements (Figure 2.2); however, the absolute and relative configurations were later established by total synthesis (*vide infra*), and required partial-reassignment by inversion of C11 and C13 to *S*-configurations.[17,18]

Initial biological testing of the isolated material revealed potent *in vitro* cytotoxicity toward various cancer cell lines including A549 human lung adenocarcinoma (IC_{50} = 1.2 nM), NCI/ADR-RES ovarian sarcoma (IC_{50} = 5.1 nM), and P388 murine leukemia (IC_{50} = 0.56 nM). It is interesting to note that the multibillion dollar[19] anticancer pharmaceutical Taxol® reported IC_{50} values of 3.10,[20] 3814,[21] and 7.7 nM[22] for these same cells lines, respectively, indicating great potential for neopeltolide. Additional activities

included strong inhibition of pancreatic and colorectal cell lines with p53 mutations,[23] and revealed potent growth-inhibition of fungal pathogen *Candida albicans* (minimum inhibitory concentration, MIC = 0.625 µg/mL).[9]

Preliminary investigation into identifying a putative cellular target for neopeltolide was performed by the Kozmin group, and was evaluated with a synthetic congener of leucascandrolide A.[24] Due to their strong structural-homology, it has been proposed that neopeltolide may be a shunt-product of leucascandrolide A, and that they may share biological targets.[25] Kozmin confirmed that neopeltolide does not act *via* interaction with tubulin or actin,[9,24] but induces apoptosis through inhibition of cytochrome bc_1 (complex III) of the electron transport chain. This transmembrane protein is critical to ATP synthesis and maintaining efflux of protons; cancerous cells are particularly vulnerable to disruption of ATP synthesis due to an increased dependency on glycolysis.[26] While it remains uncertain whether the inhibition of cytochrome bc_1 fully-accounts for the potent antiproliferative activity, this work provided a molecular basis for further biological investigation.

The bioactivities of neopeltolide and leucascandrolide A make them promising compounds. Their pharmacophoric elements could be used as a tool for the investigation of eukaryotic energy metabolism, and may benefit new discoveries and strategies for treatment of energy metabolism-directed cancer.[25] However, in order to address this potential, there must be a strategy for rapid, reliable, and sustainable production of the desired structural scaffold. Re-isolation of the active compound failed, which has led to suggestions that the producing organism may be symbiotic, and not the sponge itself.[9] Consequently, due to the combination of its appealing architecture, promising biological profile, and extremely-limited natural supply, neopeltolide has received considerable attention from the synthetic community.[17,18,24,27–44]

2.2 Early Synthetic Efforts Determine Absolute Configuration

Shortly following Wright's report,[9] synthetic efforts toward neopeltolide **2.1** were quickly initiated by groups that had previously-prepared homologous metabolites. The research groups of Panek[17] and Scheidt[18] independently-noted spectroscopic discrepancies between Wright's originally-proposed structure and the synthetic copy. In his dissertation,[45] Dr. Willmen Youngsaye‡ purported a heavily-overlapped aliphatic region of the ^{1}HNMR caused misinterpretation of NOE correlations, and designed four additional stereoisomers to test his hypothesis (Figure 2.4). The configuration of **2.1** was a perfect match with the isolated material, and was later confirmed by Scheidt.

‡ Former doctoral student of the Panek Group, and lead author of their neopeltolide publication.[17]

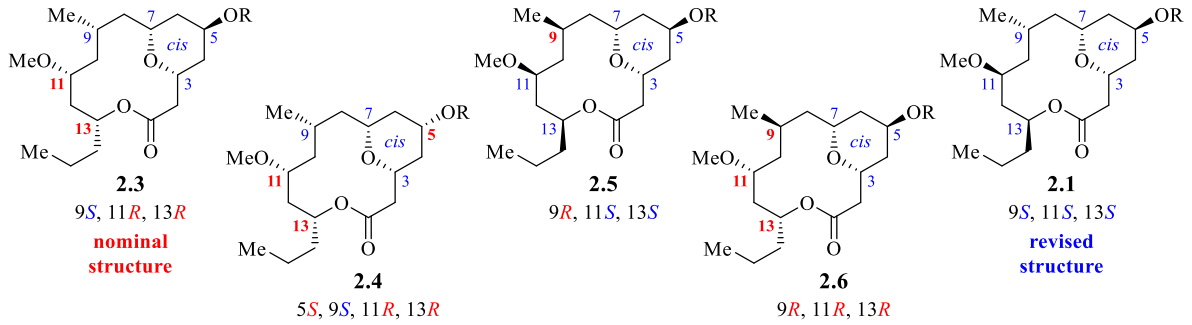

Figure 2.3 – Summary of diastereoisomers prepared by Youngsaye *en route* to his partial-reassignment of the originally-proposed structure proposed by Wright *et al.* in the seminal report. R = oxazole-bearing side-chain.

The efforts of this work resulted in the partial-reassignment of neopeltolide, and the first total synthesis of the novel polyketide. Herein, all reference to "neopeltolide" or structure "**2.1**" refers to the revised, native (3*R*,5*R*,7*R*,9*S*,11*S*,13*S*)-configuration, unless otherwise noted.

2.2.1 First Synthesis & Partial Reassignment by the Panek Group (Boston University, 2007)[17]

The Panek group has established itself as a leader in asymmetric additions of chiral crotyl- and allylsilanes.[46,47] In the early 2000s they extended their methodology to the diastereoselective assembly of *cis*- and *trans*-dihydropyrans *via* [4+2]-annulation.[48] This technique was first employed in their synthesis of leucascandrolide A (**2.2**, Figure 2.1),[49] and later for other natural products[50–53] including assembly of the *cis*-THP rings of phorboxazoles A/B,[54] herboxidiene,[55] and kendomycin.[56] This strategy has since been used to assemble furanyl-[57] and heptanyl-oxacylic products.[58]

Panek's synthesis of neopeltolide **2.1** promptly followed Wright's seminal report,[§] and can be credited to its similarities to **2.2**. Beginning with commercially available acid **2.7** (Scheme 2.1), derivatization to its silyl-protected dithioacetal allowed Umpolung coupling[59] with enantioenriched epoxide **2.8** to furnish the C7-C16 framework. A modified Evans-Tishchenko[60] reduction of ketone **2.9** furnished the requisite *anti*-diol with excellent diastereoselectivty, which was alkylated as **2.10** and converted to precursor aldehyde **2.11** over two steps. Treatment of **2.11** and chiral allylsilane *syn*-**2.12** with triflic acid promoted the generation of oxocarbenium transitions states **TS-1** and **TS-2**. The diastereoselectivity of this process is controlled by *syn*-**2.12**, whereby intramolecular cyclization is favored *via* boat-like **TS-2** due to the maximal *σ*-*p*-orbital overlap to afford *cis*-**2.13**, with concomitant desilylation; cyclization of disfavored chair-like **TS-1** proceeds slower than that of **TS-2** and furnishes the *trans*-isomer as the minor product. Advancement to its *seco*-acid over five steps allowed macrocyclization by Yamaguchi esterification,[61] providing macrolactone **2.14** in modest yield. Diastereoselective oxymercuration of the dihydropyran

[§] Wright's isolation paper was first published online February 20, 2007, and the Panek group had first-submitted their manuscript September 6, of the same year (197 days).

yielded *β*-trisubstituted pyran **2.15** as a single diastereomer following reductive demercuration of the resulting adduct, which completed the synthesis of the macrocyclic core of neopeltolide.

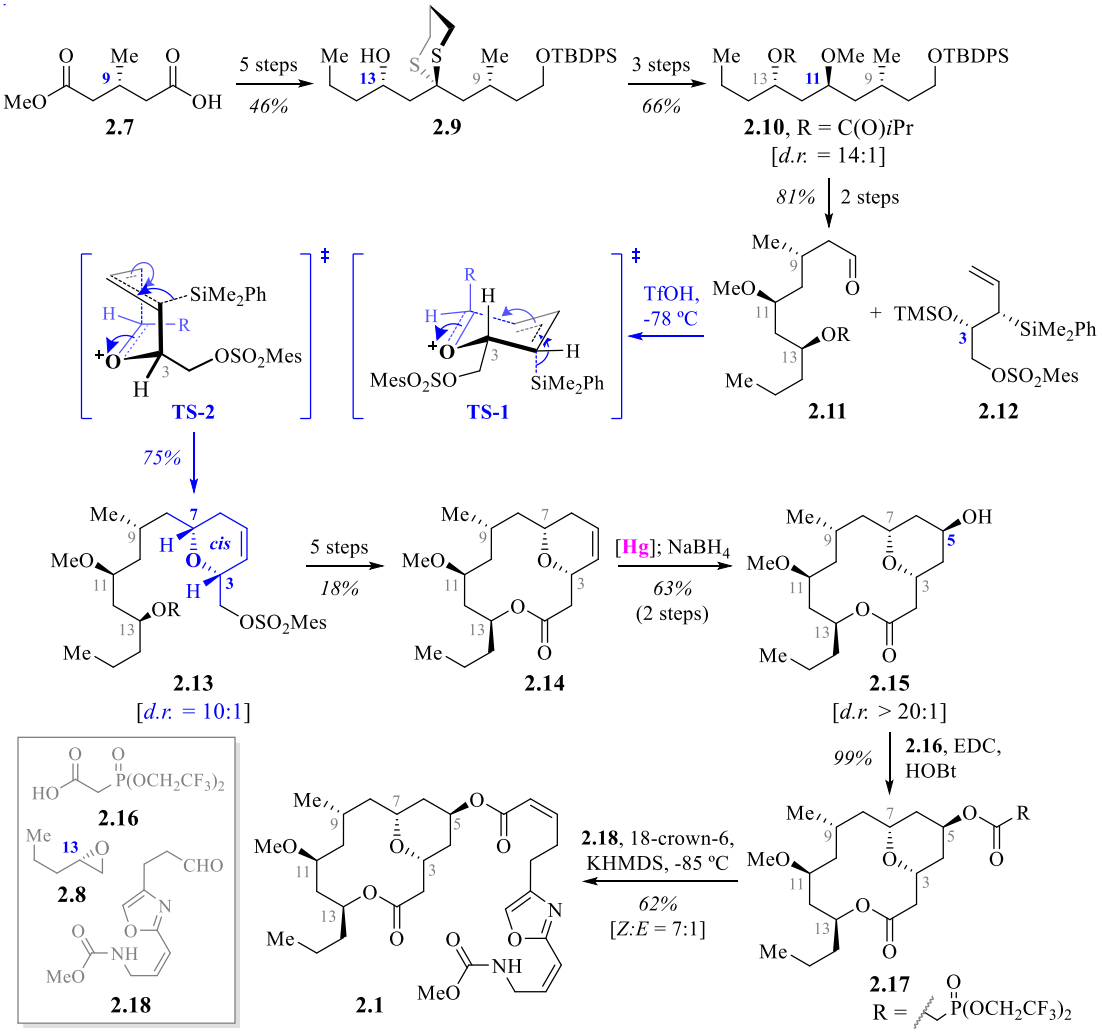

Scheme 2.1 – Summary of the first synthesis of neopeltolide, by Panek and coworkers. From this report, absolute stereochemistry was determined and revised the structure by a partial-reassignment. Key to their synthesis is the chiral allyl-silane-mediated [4+2]-annulation assembly of ***cis***-THP.

During completion of their leucascandrolide A synthesis, difficulty in direct coupling of the *Z*-*α*,*β*-unsaturated ester side chain to the *axially*-oriented C5-hydroxyl group of the tetrahydropyran was reported. Mitsunobu conditions[62] were successfully employed, but required an additional two-step inversion of the C5 stereocenter prior to coupling. To improve efficiency and complete the synthesis of neopeltolide, **2.15** was esterified as phophoacetate **2.16**, and coupled *via* Still-Gennari olefination[63] to selectively establish the *Z*-enoate of the oxazole side-chain.

Key Installation Strategies (*James S. Panek and coworkers*, 2007)	
C9 – Enzymatic desymmetrization (PLE)	**C11** – Evans-Tishchenko reduction
C13 – (2*S*)-Propyloxirane (epoxide-opening)	***cis*-THP** – [4+2]-Annulation
Macrocyclization – Yamaguchi esterification	

In the first synthesis of neopeltolide, Panek and coworkers identified spectroscopic discrepancies from the originally-proposed structure and reassigned the stereochemical and absolute configurations for the natural isomer. They required 20 linear steps to access neopeltolide, with a linear yield of 1.3% from commercially-available **2.7**.

2.2.2 Absolute Configuration Confirmed by the Scheidt Group (Northwestern University, 2008)[18]

The Scheidt research group is focused on the development of new catalytic reactions for application to therapeutic translational sciences. Specifically, they have exploited the use of small molecules as catalysts to assemble privileged-scaffolds of bioactive natural products and related analogues. Their interest in THP scaffolds inspired scandium-catalyzed Prins-like assembly of *cis*-pyranyl rings and concurrent macrocyclization,[64] similar to a method reported by Hoye.[65] They demonstrated the utility of this diastereoselective reaction in their synthesis of neopeltolide (Scheme 2.2), and the flexibility of their strategy in preparing three diastereoisomers.

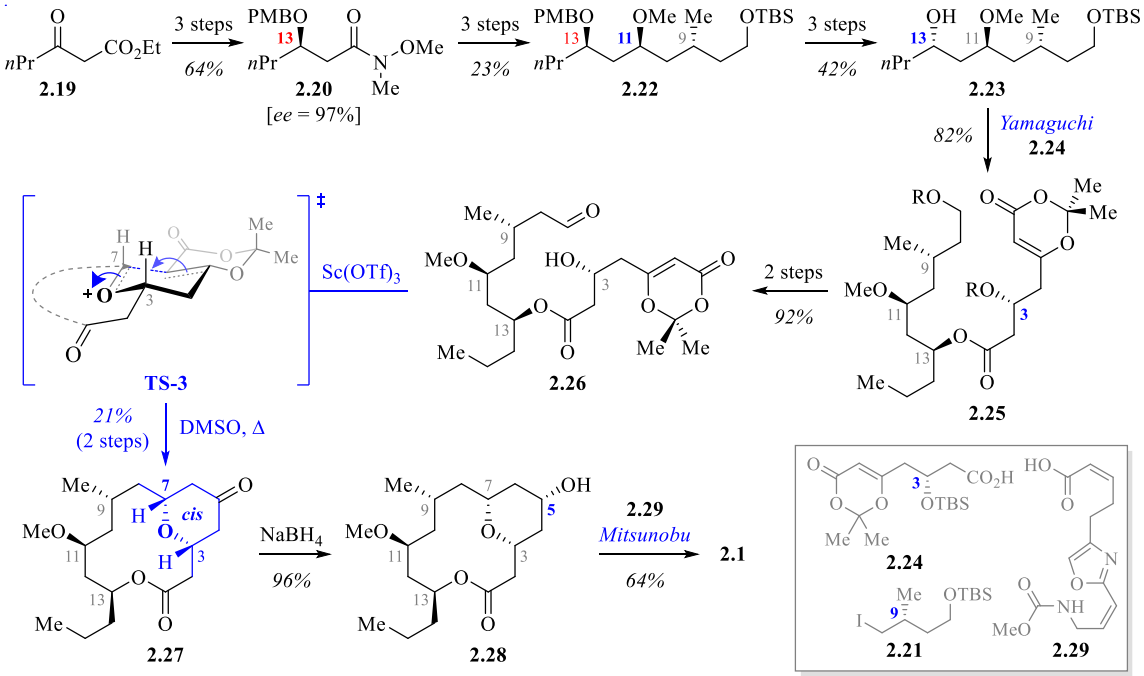

Scheme 2.2 – Summary of Scheidt and coworkers' synthesis of neopeltolide **2.1**, highlighted by intramolecular Prins-like assembly of the ***cis***-THP with concomitant macrocyclization. This route differs from their synthesis of the originally-proposed structure, which installed (11*R*) by Evans-Tishchenko reduction.

Synthesis of the revised structure **2.1** started with Noyori reduction[66] of *β*-keto ester **2.19**, and its conversion to PMB-protected Weinreb amide **2.20** over two steps, in an identical sequence to their generation of the originally-proposed **2.3** isomer.[18] This was reduced by DIBAL-H, and coupled to lithiated-**2.21**, which was prepared over a short alkylation sequence from pseudoephedrine.[67] Coupling

afforded a mixture (1:1) of diastereomers, that were *O*-methylated as **2.22** and purified in modest yield. Inversion of the (11*R*)-configuration by Mitsunobu esterification[68] and hydrolysis of the corresponding adduct furnished **2.23**, which was esterified under Yamaguchi conditions[61] with their known[64] dioxinone acid **2.24**. Protecting group manipulation provided key substrate **2.26**, which formed the oxocarbenium ion *via* the all-*equatorial* chair-like transition state **TS-3** under Lewis acid catalysis. Addition from the α-position of dioxinone afforded the bicyclic adduct, and was converted to *cis*-pyranone **2.27** by thermolysis with unreported selectivity. Substrate-controlled reduction produced α-**2.28**, which was coupled with known acid fragment **2.29**[69] *via* Yamaguchi esterification.

While the key transformation of their synthesis was modest in yield, it did install a great deal of complexity in a single step. Despite the low conversion, the Scheidt synthesis only required 16 linear steps from commercial **2.19**, with a linear yield of 0.6% overall. More importantly, this work confirmed the absolute configuration of neopeltolide required partial-reassignment. The Scheidt group followed this publication with preparation of two simple analogues that swapped the oxazole-bearing side-chain for benzoic- and *n*-octanoic acid.[70] This strategy was later used successfully to synthesize (–)-exiguolide,[71] and attempted with (–)-okilactomycin.[72]

Key Installation Strategies (*Karl A. Scheidt and coworkers*, 2008/2009)	
C9 – Asymmetric alkylation (pseudoephedrine)	**C11** – Evans-Tishenko reduction
C13 – Noyori reduction / Mitsunobu	***cis*-THP** – Prins cyclization
Macrocyclization – Prins	

2.2.3 Scope & Focus of this Review Chapter

From these first two syntheses, inconsistencies observed in spectral data prompted the generation of three diastereoisomers to identify the absolute configuration of the natural product.[17,18] This work served as the foundation for numerous syntheses to follow from the international synthetic community (Figure 2.4).[24,27-44] The oxocarbenium ion cyclizations employed by both Panek and Scheidt represent a common strategy to assemble the *cis*-THP of neopeltolide, particularly among the early reports (greater than 55% of the 2008 syntheses used this strategy, refer to § 2.3 of this chapter). However, the THP ring is a common structural feature of many bioactive natural products; as such, a wide array of strategies exists for their assembly. Though a detailed examination of these strategies and their limitations is beyond the scope of this document (please refer to the following resources[73–75]), neopeltolide serves as a notable compound to highlight many of the common methodologies.

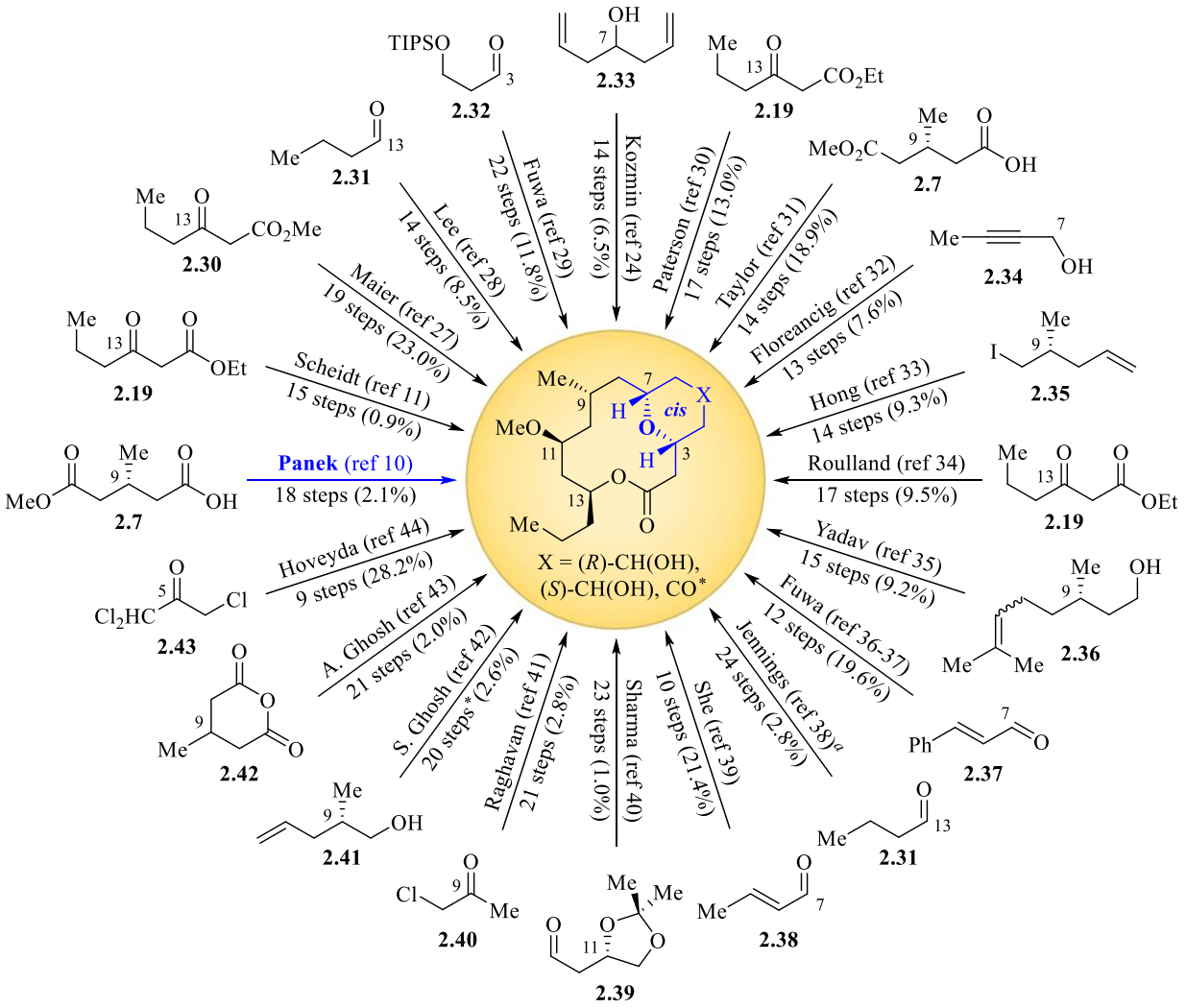

Figure 2.4 – The 20 successful syntheses to the macrocyclic core of neopeltolide (2007-2016), presented clockwise in order of publication from Panek's first total synthesis in 2007. Linear steps and yields are highlighted. *Indicates synthesis of pyranone product, and suggests an extra step is required for proper step-count comparison. [a] (–)-neopeltolide synthesis.

Herein reports a summary of published neopeltolide syntheses available through December 2016, which are grouped by THP-assembly strategies and presented in order of publication. Yields of accessing the macrocyclic core are reported from commercially-available starting materials when possible, to attempt the best and most-impartial comparison of syntheses. During the preparation of this chapter, Fuwa published similar material in *Marine Drugs*;[76] these works were prepared independently of each other and combine to serve as excellent resources for synthetic contributions toward, and study of neopeltolide.

2.3 Tetrahydropyran Assembly *via* Oxocarbenium Ion Cyclizations

The Prins reaction is a powerful synthetic tool that exists in many variations from that of its seminal report in 1919.[77] The Prins cyclization has emerged as a common strategy to generate oxacyclic

frameworks,[75,78,79] particularly the selective assembly of substituted *cis*-THP scaffolds.[80] The reaction is mechanistically-driven by the formation of an oxocarbenium intermediate, and subsequent ring-closure by addition of a π-nucleophile. In this section, six additional syntheses of neopeltolide are presented that assemble the *cis*-THP ring of the macrocyclic core by oxocarbenium ion cyclization strategies. Specifically, this includes intramolecular (Lee,[28] and Yadav[35]), intermolecular (Maier[27]), desymmetrizing (Kozmin[24]), and oxidative (Floreancig[32]) variations of the Prins reaction, as well as the stereoselective reduction of an oxocarbenium ion (Jennings[38]). Herein summarizes these works in chronological order.

2.3.1 Maier Group – Total Synthesis & Analogue Design (Universität Tübingen, 2008)[27,81]

In early 2008, the Maier group reported a synthesis of the macrocyclic core of neopeltolide, employing an intermolecular Prins cyclization for THP assembly (Scheme 2.3).[27] Synthesis began with Noyori asymmetric hydrogenation[66] of **2.30** to install C13-alcohol with excellent selectivity (*ee* = 98%). Following silylation and ester reduction, Leighton asymmetric allylation[82] of **2.46** using (*R*,*R*)-**2.47** afforded diol **2.48** with unreported selectivity.[83] Conversion to α,β-unsaturated thioester **2.49** allowed diastereoselective conjugate addition by Feringa-Minnaard conditions[84,85] to install C9-methyl of **2.51**,[83] and was subsequently reduced to its corresponding aldehyde **2.52** by Fukuyama conditions.[86]

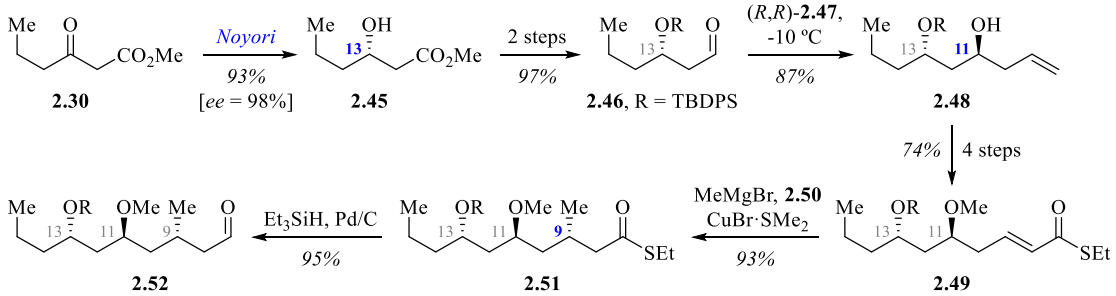

Scheme 2.3a – Generation of C7-C16 carbon framework **2.52** for the Maier *et al.* total synthesis of neopeltolide.

Aldehyde **2.52** was reacted with homoallylic alcohol **2.53** (Scheme 2.3b), which was generated by Leighton's conditions using (*S*,*S*)-**2.47**. The all-*equatorial*-orientation of the substituents in chair-like transition state of oxonium ion **TS-4** afforded pyran **2.54** with good diastereoselectivity (*d.r.* = 8:1). Over six steps, this was converted to *seco*-acid **2.55** for macrocyclization by Yamaguchi conditions[61] and unmasked to yield the macrocyclic core of neopeltolide **2.28**.

The Maier synthesis required 19 linear steps to access the macrocyclic core of neopeltolide, with excellent overall yield (23%). By extension of this strategy, they successfully completed the total synthesis of **2.1** *via* Mitsunobu esterification with known oxazole-bearing acid fragment **2.29**,[69] in addition to 5- and 11-*epi*-**2.1** analogues, and several side-chain analogues.[81]

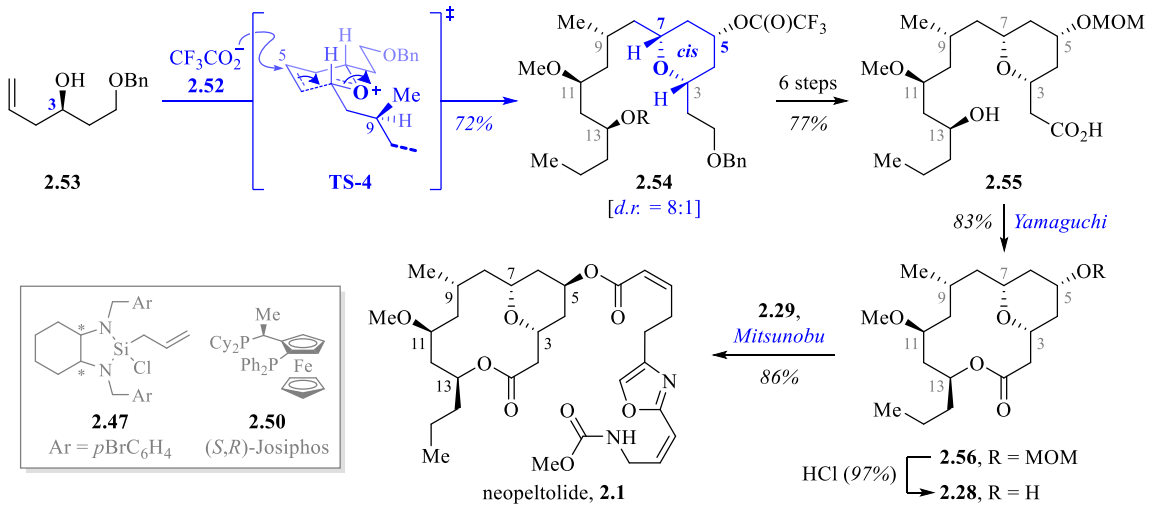

Scheme 2.3b – Completion of the Maier *et al*. total synthesis, highlighted by intermolecular Prins cyclization for ***cis***-THP assembly.

Key Installation Strategies (*Martin E. Maier and coworkers*, 2008)	
C9 – Feringa-Minnaard addition	**C11** – (*R*,*R*)-Leighton allylation
C13 – Noyori reduction	***cis*-THP** –Prins cyclization
Macrocyclization – Yamaguchi esterification	

2.3.2 Lee Group – Total Synthesis (Seoul National University, 2008)[28]

Like Scheidt, the Lee group reported a synthesis of neopeltolide that employed an intramolecular Prins macrocyclization for THP assembly (Scheme 2.4).[28] Synthesis began with asymmetric[83] Loh crotyl transfer[87] of butanal **2.31** using branched allylating reagent **2.57**. Conversion of **2.58** to its aldehyde for chelate-controlled methallylation under Sakurai conditions,[88] and subsequent protection with 2-diphenylphosphinobenzoic (*o*-DPPB) acid yielded diol **2.59**.[83] Substrate-directed hydroformylation provided aldehyde **2.60** (*d.r.* = 5:1 overall), and was converted to acetal **2.61** over a four-step sequence. This was esterified under Steglich conditions[89] with C1-C5 fragment **2.63**, that was generated by Brown's asymmetric allylation[90] of **2.62**, to provide the carbon framework of the neopeltolide core **2.64** in good yield. *Equatorial*-orientation of the C3/C5-substituents in the chair-like transition state of oxonium ion **TS-5** generated the *cis*-THP and macrocyclic core of neopeltolide **2.28** with complete stereocontrol, following hydrolysis of the Prins adduct. Completion of the synthesis was achieved by Mitsunobu esterification[68] with known acid **2.29**.[69]

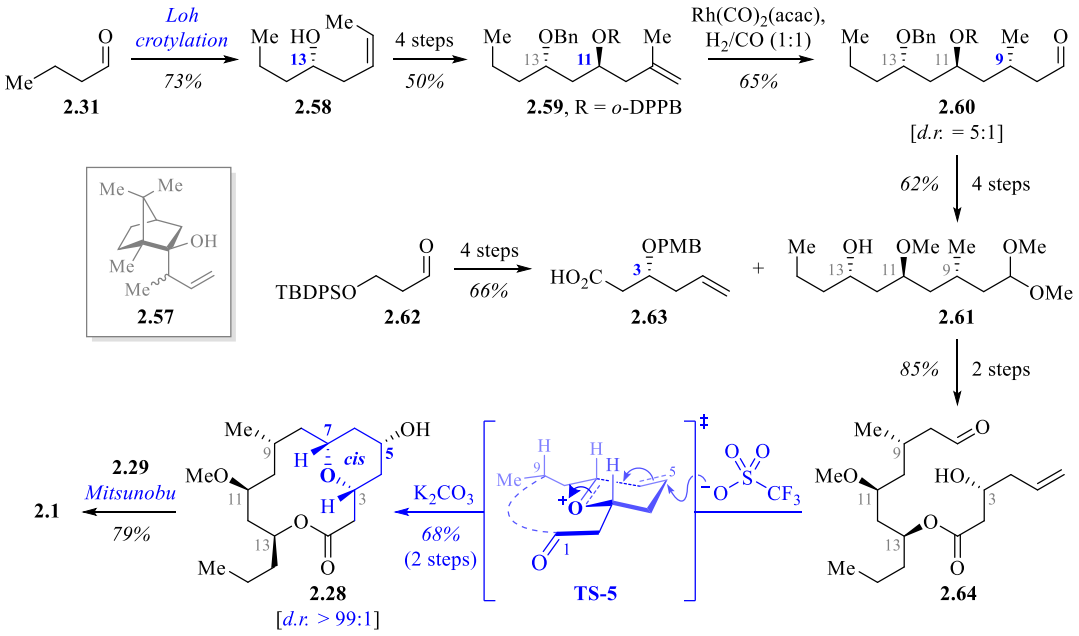

Scheme 2.4 – Summary of Lee and coworkers' total synthesis of neopeltolide **2.1**, highlighted by intramolecular Prins reaction for the assembly of ***cis***-THP and macrocyclization.

The Lee synthesis required 14 linear steps to access the macrocyclic core of neopeltolide, with an yield of 8.5% overall. Embedded in their publication was an alternative, first-generation single-sequence intramolecular Prins cyclization. This strategy completed the carbon framework by linear extension of **2.60** by Brown's asymmetric allylation to generate a Prins-precursor with a C5-homoallylic alcohol.

Key Installation Strategies (*Eun Lee and coworkers*, 2008)	
C9 – Hydroformylation (Rh)	**C11** – Sakurai methallylation
C13 – Loh crotylation	***cis*-THP** – Prins cyclization**
Macrocyclization – Prins cyclization**	** *single-sequence*

2.3.3 Kozmin Group – Total Synthesis (University of Chicago, 2008)[24]

Previous work[91–93] on leucascandrolide A by the Kozmin group directed their investigation of neopeltolide to provide an efficient total synthesis (Scheme 2.5). Synthesis began with the vinylogous transesterification of heptandienol **2.33** to generate Prins cyclization precursor **2.66**. Treatment by TFA successfully assembled the THP as a single diastereomer *via* a desymmetrizing Prins reaction[94] and the kinetically-favored *equatorial*-orientation of the acid-mediated chair-like oxocarbenium transition state **TS-6**. Subsequent benzylation and Wacker alkene oxidation[95] provided ketone **2.68**, which coupled with **2.69** to yield aldol product **2.70** with excellent selectivity (*d.r.* > 98:2).[96] Wittig methylenation (C9-Me) provided the full carbon framework for the macrocyclic core. Conversion to diol **2.71**[97] and cyclization by Yamaguchi esterification conditions[61] afforded energetically-preferred 14-membered macrocycle **2.72** with

complete regioselectivity. Completion of the synthesis was accomplished over 5 steps, including inversion of C11-alcohol and addition of requisite side-chain **2.29**[69] by Mitsunobu conditions.[68]

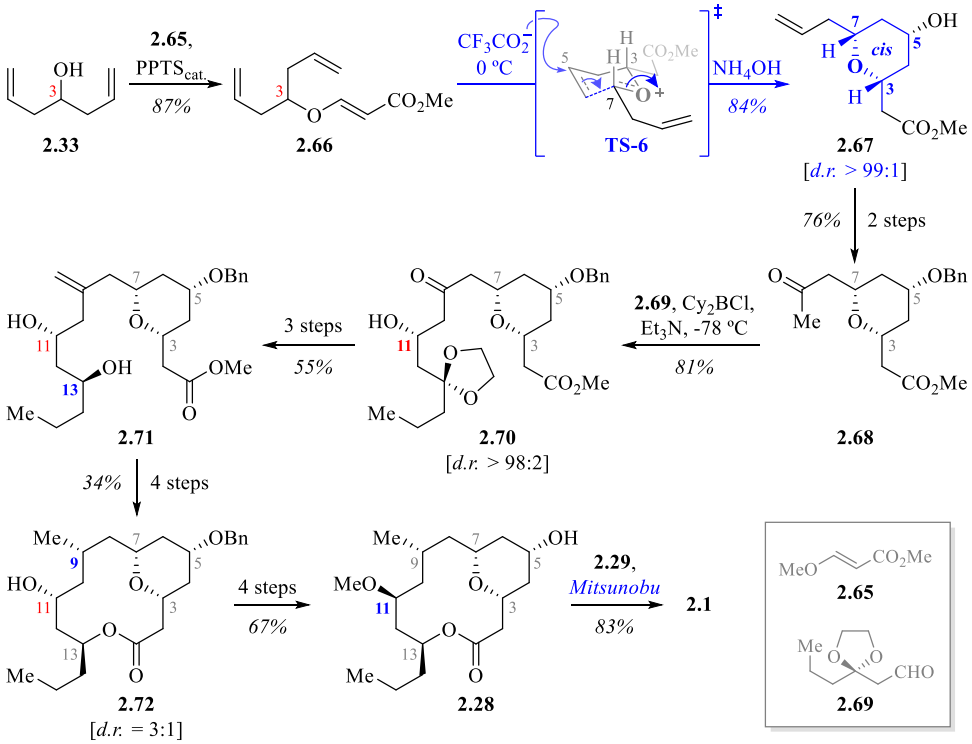

Scheme 2.5 – Summary of Kozmin and coworkers' total synthesis of neopeltolide **2.1**, highlighted by desymmetrizing intramolecular Prins reaction for the assembly of ***cis***-THP and macrocyclization.

The Kozmin synthesis required 14 linear steps to access the macrocyclic core of neopeltolide, with a 6.5% overall yield. Although modest, their synthesis illustrates the power of this strategy for the construction of polysubstituted *cis*-THP products *via* its highly-controlled construction of three stereogenic centers in a single desymmetrizing step. More importantly, this synthesis provided sufficient material to enable the determination of the putative cellular target for neopeltolide.

Key Installation Strategies (*Sergey A. Kozmin and coworkers*, 2008)	
C9 – Stereoselective hydrogenation (Pd)	**C11** – Asymmetric Aldol / Mitsunobu
C13 – 1,3-*syn*-Selective reduction	***cis*-THP** – Prins cyclization
Macrocyclization – Yamaguchi esterification	

2.3.4 Floreancig Group – Total Synthesis & Analogue Design (University of Pittsburgh, 2009)[98,99]

Over the past decade, the Floreancig group has published extensively on the use of single-electron oxidation as an alternative to Lewis acid activation for imparting electrophilic character to molecules.[100–110] They have used their electron transfer-initiated cyclization (ETIC) methodology for the assembly of *cis*-THP rings in syntheses of clavosolide A[111] and leucascandrolide A;[112] their synthesis of neopeltolide is another example of the capability for this strategy to selectively install 2,6-*cis*-THPs into complex natural

product scaffolds (Scheme 2.6).[32] Synthesis began with the conversion of alcohol **2.34** into its trichloroacetamidate **2.73**, and subsequent etherification with alcohol **2.74**. Sonogashira coupling[113] with alkyne **2.76** provided the full carbon framework for the neopeltolide core in good yield, and was converted to the β,γ-unsaturated ketone **2.78** with good selectivity. Asymmetric reduction *via* Evans-Tishchenko conditions[60] yielded the C11-alcohol in good yield (77%), which was alkylated and converted to its *seco*-acid for macrocyclization by Yamaguchi's esterification procedure.[61] Conversion to enol acetate **2.80** provided the precursor for the key ETIC reaction, which proceeded in modest yield to generate ***cis*-2.81** as a single diastereomer (65% based on pure **2.80**). The *equatorial*-orientation of oxocarbenium ion transition state **TS-7** is favored by an attractive electrostatic interaction between π-electrons of the axial C5-alcohol and the partial positive charge of H7 (**TS-8**, Scheme 2.6). The modest yield, and longer reaction time compared to previous examples, was suggested could result from conformational bias within the macrocycle. These effects either inhibit proper alignment for bond formation in **TS-8**, or result in inductive stabilization of a proximal C11-oxygen.[99] Completion of the macrocyclic core was accomplished by substrate-controlled hydrogenation and reduction reactions.[32]

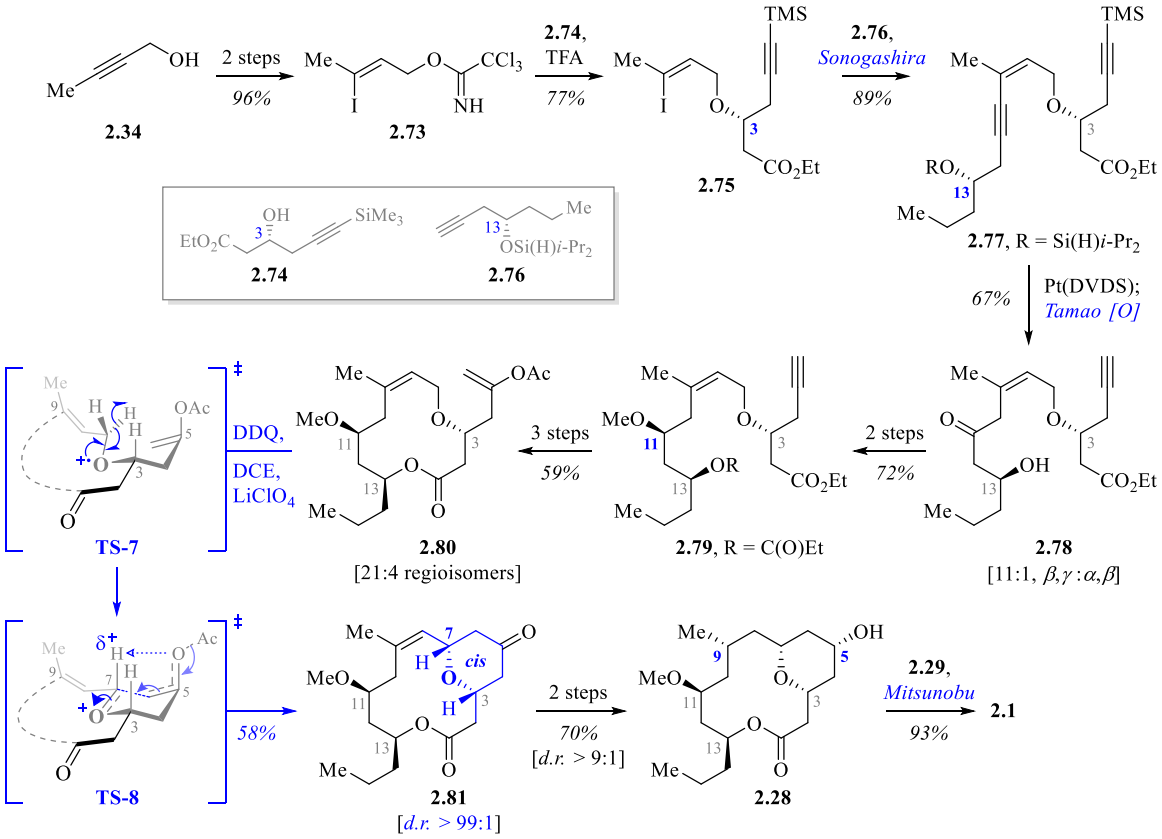

Scheme 2.6 – Summary of Floreancig and coworkers' total synthesis of neopeltolide **2.1**, highlighted by oxidative Prins reaction for the assembly of ***cis*-THP** and macrocyclization.

The Floreancig synthesis required 13 linear steps from 2-butyn-1-ol **2.34** to access the macrocyclic core of neopeltolide, with an overall yield of 7.6%. Within months of this report, they generated the natural product by coupling acid side-chain **2.29**[69] *via* Mitsunobu esterification, and designed novel analogues.[62] Late-stage alkene functionalization of *cis*-tetrahydropyranone **2.81** allowed rapid generation of six unique macrocyclic analogues,[98,99] as well as an amide-linked and side-chain analogues of the native core.[99]

Key Installation Strategies (*Paul E. Floreancig and coworkers*, 2009/2010)	
C9 – Stereoselective hydrogenation (Pd)	**C11** – Evans-Tishenko reduction
C13 – (2*S*)-Propyloxirane (epoxide-opening)	***cis*-THP** – ETIC Prins cyclization
Macrocyclization – Yamaguchi esterification	

2.3.5 *Yadav Group – Formal Synthesis* (Indian Institute of Chemical Technology, 2010)[35]

The high degree of selectivity for oxocarbenium ion cyclizations has resulted in their use to establish stereochemical relationships in downstream targets; the Yadav group has utilized this strategy effectively in natural product synthesis (Scheme 2.7).[114–119] Their synthesis of neopeltolide is an excellent example of this strategy, which employed two separate Prins cyclization reactions. Synthesis began with (*S*)-citronellol **2.36**, which was converted to Prins precursor aldehyde **2.82** over a three-step sequence. The intermolecular Prins cyclization with alcohol **2.76** in the presence of TFA provided 2,4,6-*syn*-trisubstituted pyran **2.84** *via* the all-*equatorial*-orientation of transition state **TS-9**, following hydrolysis of the Prins adduct. Selectivity was not reported for this process, though, it was suggested that the stereochemistry of *cis*-**2.84** can be assumed to "be in anticipated line" due to their experience with the reaction.[35] Functional group manipulation afforded iodide **2.85**, and the pyran was cleaved by treatment with unactivated zinc to deliver linear C7-C16 framework **2.86**. A four-step sequence generated acetal **2.61**, which is a common intermediate from the Lee synthesis.[28] The remainder of the Yadav synthesis was carried out in identical fashion to the Lee synthesis, including all reported yields.

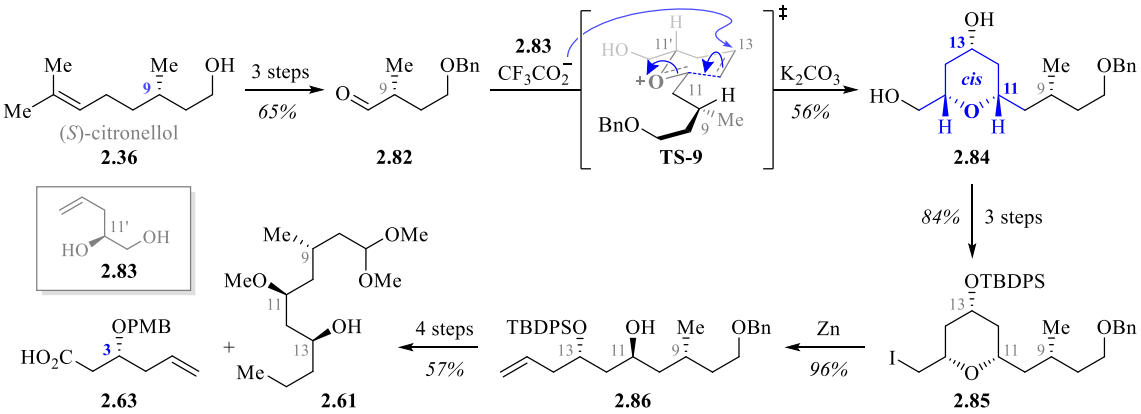

Scheme 2.7 – Highlights of the Yadav *et al.* synthesis of the macrocyclic core of neopeltolide **2.28**, which used Prins cyclization for installation of four stereocenters, ***cis*-THP** assembly and macrocyclization.

The Yadav synthesis required 15 linear steps to generate the macrocyclic core of neopeltolide with a reported overall yield of 9.2%. Although the synthesis bears significant resemblance to the previously-published work of Lee,[28] this work highlights the value of oxocarbenium ion cyclizations for the installation of pyran rings and their stereogenic centers.

Key Installation Strategies (*Jhillu Singh Yadav and coworkers*, 2010)	
C9 – (*S*)-citronellol	**C11** – Prins cyclization "A"
C13 – Prins cyclization "A"	***cis*-THP** – Prins cyclization "B"
Macrocyclization – Prins cyclization "B"	

2.3.6 Jennings Group – Enantiomeric Formal Synthesis (University of Alabama, 2010)[38]

The Jennings research group have demonstrated success in synthesis of pyran-bearing natural products using Kishi's method[120] of stereoselective reduction of six-membered hemiacetals *via* half-chair oxonium ion intermediates (Scheme 2.8).[121–126] Based on their synthesis of (–)-dactylolide and an increase of bioactivity in various cell lines compared to its enantiomer,[123] they were interested in evaluating the bioactivity for the antipode of neopeltolide's native macrocyclic core. Synthesis began with installation of the C13-alcohol by Brown's asymmetric allylation[90] of butyraldehyde **2.31**. Formation of aldehyde **2.87** allowed asymmetric methallylation by chelate-control to install the C11-alcohol.[88] This was esterified with acryloyl chloride **2.88**, and subsequently cyclized with Grubbs' second-generation (G-II) catalyst[127] **2.89** to afford *α*,*β*-unsaturated lactone **2.90** with good selectivity. Stereoselective hydrogenation set the C9-methyl stereocenter while simultaneously unmasking C13, requiring silylation prior to transamidation to afford amide **2.91**.[128] Alkylation, DIBAL reduction, and linear elongation by a second asymmetric allylation by Brown's conditions produced homoallylic alcohol **2.92** (*d.r.* = 6:1). Cross-metathesis with methyl acrylate **2.93** allowed selective conversion to *syn*-benzylidene **2.94** *via* intramolecular oxa-conjugate addition of the resulting *α*,*β*-unsaturated ester.[129] Key precursor **2.95** was converted to intermediate lactol by addition of excess Grignard reagent,[130] and subsequently generated oxocarbenium ions **TS-10** and **TS-11** by treatment with TFA. Stereoselective reduction occurred by axial hydride attack *via* the less-hindered, thermodynamically-preferred reactive half-chair conformer **TS-11**. This conformation favors attractive electrostatic interactions between the pseudo-axial C5-acetal and the partial positive charge of C3 in an analogous fashion to that seen by Floreancig.[32] Completion of the antipode formal synthesis was accomplished by conversion of *cis*-**2.96** to its *seco*-acid for macrocyclization by Yamaguchi esterification,[61] and subsequent cleavage of the C5-MOM protecting group.

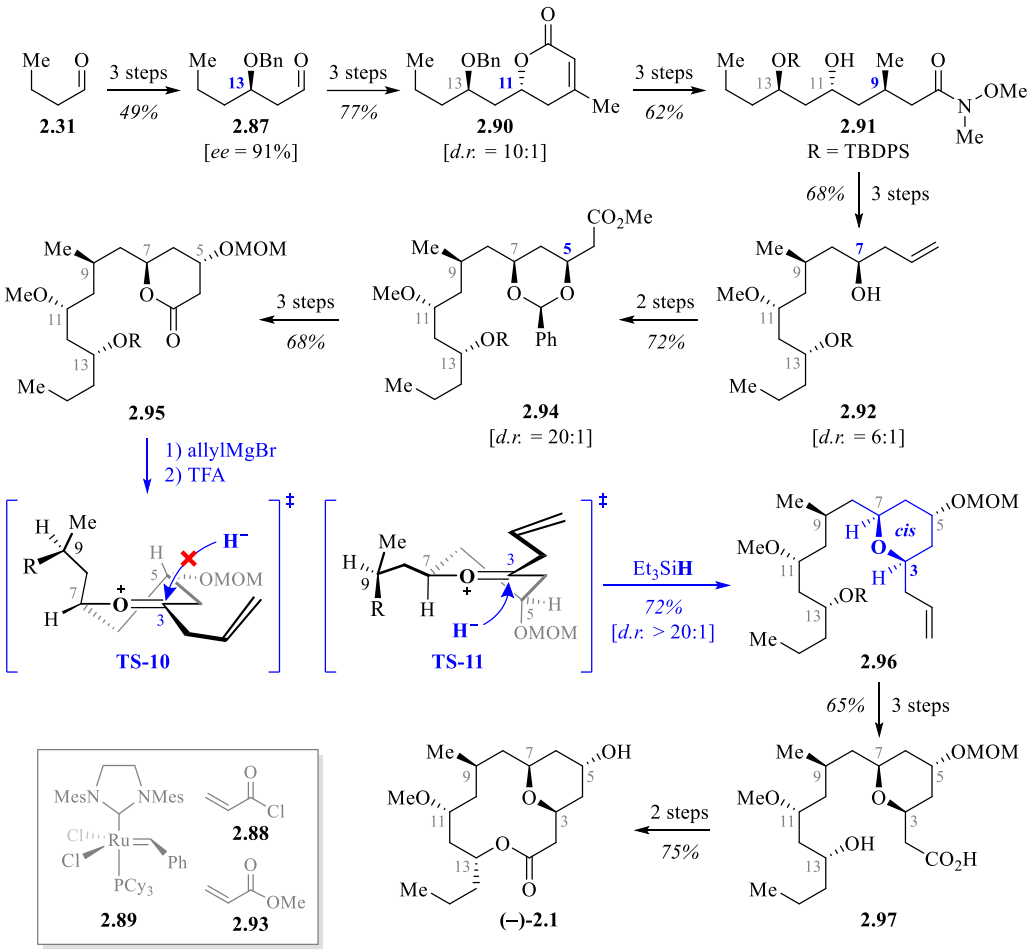

Scheme 2.8 – Summary of Martinez-Solorio and Jennings' synthesis of the unnatural macrocyclic core of the neopeltolide antipode **(–)-2.28**, highlighted by oxocarbenium reduction for ***cis***-THP assembly.

Synthesis of the enantiomeric core of (–)-neopeltolide by Martinez-Solorio and Jennings was accomplished in 24 linear steps from butyraldehyde **2.31**, with an overall yield of 2.8%. Unfortunately, extension of the synthesis to the unnatural antipode of neopeltolide was not attempted, nor were biological activities reported; however, based on analogue work by Fuwa (*vide infra*),[37] the closely-related (–)-8,9-dehydroneopeltolide exhibited activities two-fold less potent than the parent natural product.

Key Installation Strategies (*Dionicio Martinez-Solorio and Michael P. Jennings*, 2010)	
C9 – Stereoselective hydrogenation (Pd)	**C11** – Sakurai methallylation
C13 – (–)-Brown allylation	***cis*-THP** – Oxocarbenium reduction
Macrocyclization – Yamaguchi esterification	

2.3.7 Mineeva Group – Fragment Synthesis (Belorussian State University, 2015)[131]

The Mineeva group has demonstrated cyclopropanol methodology in the synthesis of methyl-branched carbon frameworks.[132] In their fragment synthesis of the C7-C16 framework of the neopeltolide macrocyclic core, this strategy is applied to install the C9-methyl of **2.99** (Scheme 2.9). Mineeva envisaged

Kishi's method[120] for stereoselective oxocarbenium reduction would provide the *cis*-THP from the lactol intermediate of **2.100**, in an approach mirroring Jennings' work.[38]

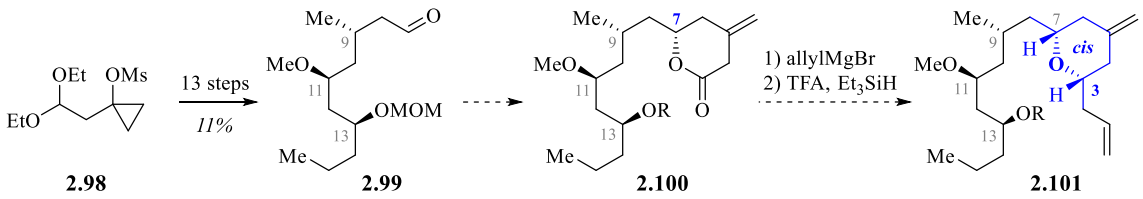

Scheme 2.9 – Summary of Mineeva's fragment synthesis, and proposed endgame for the assembly of the ***cis***-THP by means of Kishi's method[120] for stereoselective oxocarbenium reduction.

The macrocyclic core of neopeltolide was not completed *via* this strategy though; the authors do highlight the potential of their strategy for accessing chiral building blocks for natural product synthesis.

2.3.8 Oxocarbenium Ion Cyclization Conclusions

Prins-type oxocarbenium ion cyclizations have proven instrumental for generation of substituted pyranyl scaffolds within natural products. Neopeltolide has not been an exception; 40% of successful syntheses have employed this strategy to date. This strategy is highly diastereoselective because chirality is transferred from starting material *via* the preferred *E*-geometry of the oxocarbenium ion. Conformational preferences for *equatorial*-orientations in chair-like transition states readily afford *cis*-THP products, which combined with operational simplicity, has resulted in this being the most-employed strategy toward neopeltolide synthesis. Based on these reports (n = 8), generation of the neopeltolide macrocyclic core *via* this strategy averaged 7.4% overall yield across 17 linear steps, where the Prins-type oxocarbenium ion cyclization assembly of the *cis*-THP averaged 65% with excellent selectivity (*d.r.* ~ 20:1).

2.4 THP Assembly *via* Hetero-Diels-Alder (HDA) Cycloaddition

The Diels-Alder cycloaddition represents one of the most powerful tools in natural product synthesis, and the use of carbonyl reagents has become a common strategy to access dihydropyranyl products with excellent regio- and diastereoselectivity. The use of Danishefsky's dienes[133] and aldehyde dienophiles efficiently provides *cis*-tetrahydropyran-4-one products under Lewis acid catalysis. Jacobsen has pioneered asymmetric HDA reactions with chiral chromium complexes that enhance rates and influence selectivity. This section highlights three independent syntheses of neopeltolide that assembled the *cis*-THP ring by asymmetric hetero-Diels-Alder cycloaddition using chiral chromium$^{(III)}$-catalysts (Paterson,[30] and A. K. Ghosh[43]) or complexes (Raghavan[41]). Each of these works involved intermolecular reaction of *E*-dienes with unactivated carbonyl dienophiles of normal-electron demand. Herein summarizes these works in order of publication.

2.4.1 Paterson Group – Total Synthesis (University of Cambridge, 2008)[30]

The Paterson group is renowned for their efforts toward synthesis of biologically-active, complex natural products and structural analogues,[134,135] including many 14-membered macrocyclic polyketides.[136–138] They have previously demonstrated success installing pyranyl rings using HDA cycloaddition in syntheses of laulimalide,[139] phorboxazole,[140] and leucascandrolide A,[141] which heavily-influenced their work on neopeltolide (Scheme 2.10). Synthesis began with asymmetric Noyori hydrogenation[66] of ketoester **2.19** to install the C13-alcohol.[83] *β*-Hydroxy **2.102** was converted to **2.103** by a short sequence that included asymmetric Brown methallylation. Subsequent ozonolysis, followed by homologation *via* HWE conditions,[142] afforded an α,*β*-unsaturated ester that was adjusted to its corresponding enal **2.104**. The stereoselective reduction of **2.104** by MacMillan protocol[143] provided an inseparable 3:1 C9-mixture of desired dienophile product **2.107** in good yield (80% overall). Jacobsen's asymmetric HDA cycloaddition between **2.107** and diene **2.108** was promoted by chiral tridentate chromium$^{(III)}$ catalyst **2.109**[144] to provide the full carbon framework of the macrocyclic core. This key reaction furnished *cis*-tetrahydropyranone product **2.111** with complete stereocontrol *via endo*-transition **TS-12**, following acidic workup of the [4+2]-cycloadduct **2.110**. Completion of synthesis by conversion of **2.111** to its *seco*-acid for macrocyclization by Yamaguchi esterification,[61] and subsequent coupling of acid **2.29**[69] under Mitsunobu protocol.[68]

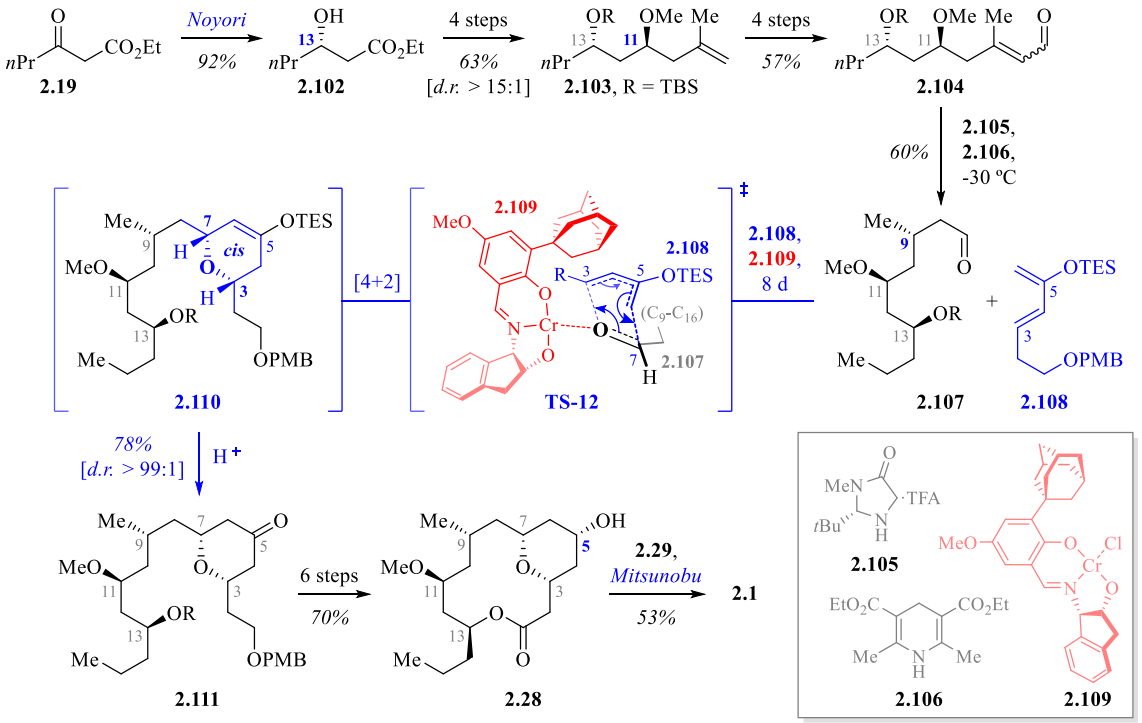

Scheme 2.10 – Summary of Paterson and Miller's synthesis of neopeltolide **2.1**, highlighted by hetero Diels-Alder ***cis***-THP assembly using Jacobsen's chiral tridentate chromium$^{(III)}$ catalyst **2.109**.

The Paterson publication came one year following Wright's first report[9] and represents the seventh successful synthesis of neopeltolide, illustrating the considerable attention this metabolite received in a short period of time. This route required 17 linear steps to access the macrocyclic core of the natural product from ketoester **2.19**, with a linear yield of 13% overall.

Key Installation Strategies (*Ian Paterson and Natalie A. Miller*, 2008)	
C9 – Asymmetric hydrogenation (MacMillan)	**C11** – (–)-Brown methallylation
C13 – Noyori hydrogenation	***cis*-THP** – HDA (Jacobsen Cr^{III} catalyst)
Macrocyclization – Yamaguchi esterification	

It should be noted that HDA precursor **2.107** was generated by Hartmann and Oestreich in their 2010 report on efforts toward neopeltolide using asymmetric conjugate silyl transfer in iterative catalytic sequences.[145] Their strategy employed modification of Feringa-Minnaard[84,85] diastereoselective conjugate-addition to iteratively install methyl or silyl groups in 1,3-substitution patterns. Oestreich's synthesis required 13 linear steps to access aldehyde **2.107** in 9.2% overall yield; the Paterson strategy accessed this material in 9 linear steps (21.8% overall), from a shared silylated *β*-hydroxy ester intermediate.

2.4.2 Raghavan Group – Formal Synthesis (Indian Institute of Chemical Technology, 2012)[41]

Several years would pass before another synthesis of neopeltolide utilized HDA to assemble the *cis*-THP (Scheme 2.11). Starting from 2-chloroacetone **2.40**, the Raghavan group prepared aldehydic dienophile **2.112** over a four-step sequence that employed MacMillan's asymmetric reduction with imidazolidinone catalyst **2.105**·TCA and Hantzch ester **2.106** to install the C9-methyl with excellent enantioselectivity. Jacobsen's asymmetric HDA cycloaddition between **2.112** and Danishefsky's diene **2.113**[133] was promoted by chiral (*S*,*S*)-chromium$^{(III)}$-salen complex **2.114**[146] *via endo*-transition state **TS-13** with complete stereocontrol. Acidic treatment of [4+2]-adduct **2.115** afforded dihydropryanone **2.116**, which was reduced and acetylated for conversion to ester **2.117** by Ireland-Claisen rearrangement[147]/esterification to re-establish the C3-stereochemistry. Following ester reduction and silylation, Rychnovsky's protocol[148] successfully appended enantiopure (Krische protocol[149]) **2.118** *via* reductive lithiation of the thiophenol with LiDBB. Oxidation and desilylation allowed Evans-Tishchenko reduction[60] of **2.120** to install the C11-alcohol with excellent diastereoselectivity, which was alkylated and converted to **2.14** *via* its corresponding *seco*-acid. Completion of the synthesis was accomplished by oxymercuration of the dihydropyran and reductive elimination of the adduct.

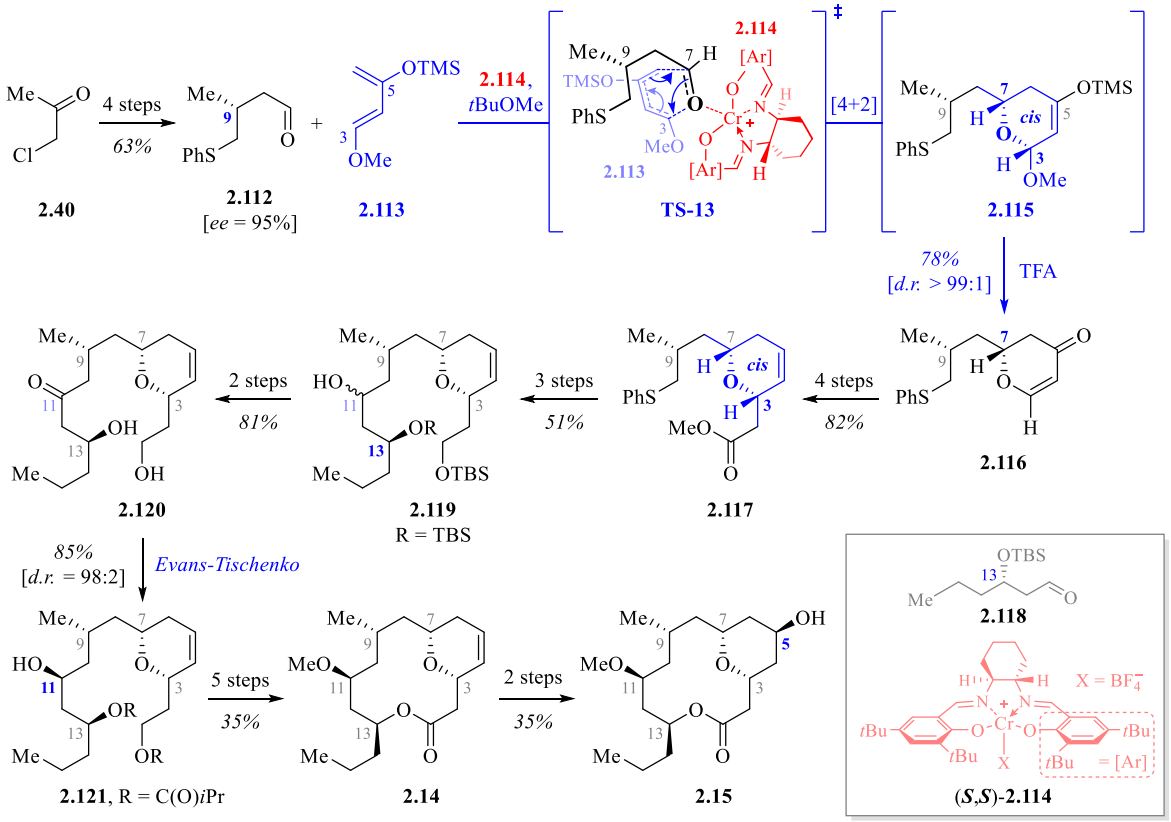

Scheme 2.11 – Summary of Raghavan and Samanta's synthesis of the macrocyclic core of neopeltolide **2.15**, highlighted by asymmetric HDA assembly of ***cis***-THP using Jacobsen's $Cr^{(III)}$-salen complex **2.114**.

Raghavan and Samanta's synthesis of the macrocyclic core[150] of neopeltolide required 21 linear steps, with an overall yield of 2.8%. Following this work, they have shown greater interest in polyketides with subsequent efforts toward complex macrocyclic compounds such as peloruside A,[151,152] and pyran-containing products laulimalide[153,154] and sorangicin A.[155] Their laulimalide report employed a similar HDA strategy to their neopeltolide synthesis.

Key Installation Strategies (*Sadagopan Raghavan and Pradip K. Samanta*, 2012)	
C9 – Asymmetric hydrogenation (MacMillan)	**C11** – Evans-Tishchenko reduction
C13 – Krische allylation ($[Ir(cod)Cl]_2$ & (*R*)-BINAP)	***cis*-THP** – HDA (*S,S*-Cr^{III}-salen complex)
Macrocyclization – Yamaguchi esterification	

2.4.3 A. K. Ghosh Group – Total Synthesis (Purdue University, 2013)[43]

The A. K. Ghosh research group publishes efficient syntheses of complex natural products and has helped emphasize the prevalence of THP ring moieties in bioactive compounds. They have assembled *cis*-THP frameworks relying on a variety of strategies, including Kishi's[120] diastereoselective oxocarbenium reduction,[156–158] oxidative Prins cyclization,[159,160] and both asymmetric intra- and intermolecular HDA.[161–165] Their synthesis of neopeltolide employed a late-stage intermolecular strategy (Scheme 2.12). Synthesis began with enzymatic desymmetrization of 3-methylglutaric anhydride **2.42** with PS-30 lipase[166] to afford

linear half-acid in good enantioselectivity, which was selectively reduced to deliver **2.122**. Conversion to **2.123** allowed Brown's asymmetric allylation[90] to install C11-alcohol, which was promptly alkylated. Following Lemieux-Johnson[167] oxidation of the terminal olefin, a second allylation by Brown's asymmetric conditions to install the C13-alcohol. Acetal cleavage unmasked the corresponding aldehyde, and was converted to siloxy diene **2.125** by olefination.[142] Jacobsen's asymmetric HDA cycloaddition between diene **2.125** and **2.126** was promoted by chiral tridentate chromium(III) catalyst ***ent*-2.109**[144] *via endo*-transition state **TS-14** with excellent selectivity (*d.r.* = 97:3). Subsequent acidic workup of [4+2]-adduct **2.127** afforded *cis*-pyranone **2.128** in good yield. Unfortunately, cycloaddition was sensitive to alkyl chain-length, and required a four-step homologation sequence to furnish the full-carbon framework of the macrocyclic core as *seco*-acid **2.129**. Yamaguchi[61] esterification conditions provided its macrolactone in modest yield (40%), which was hydrogenated and reduced to **2.28** with excellent yield and selectivity.

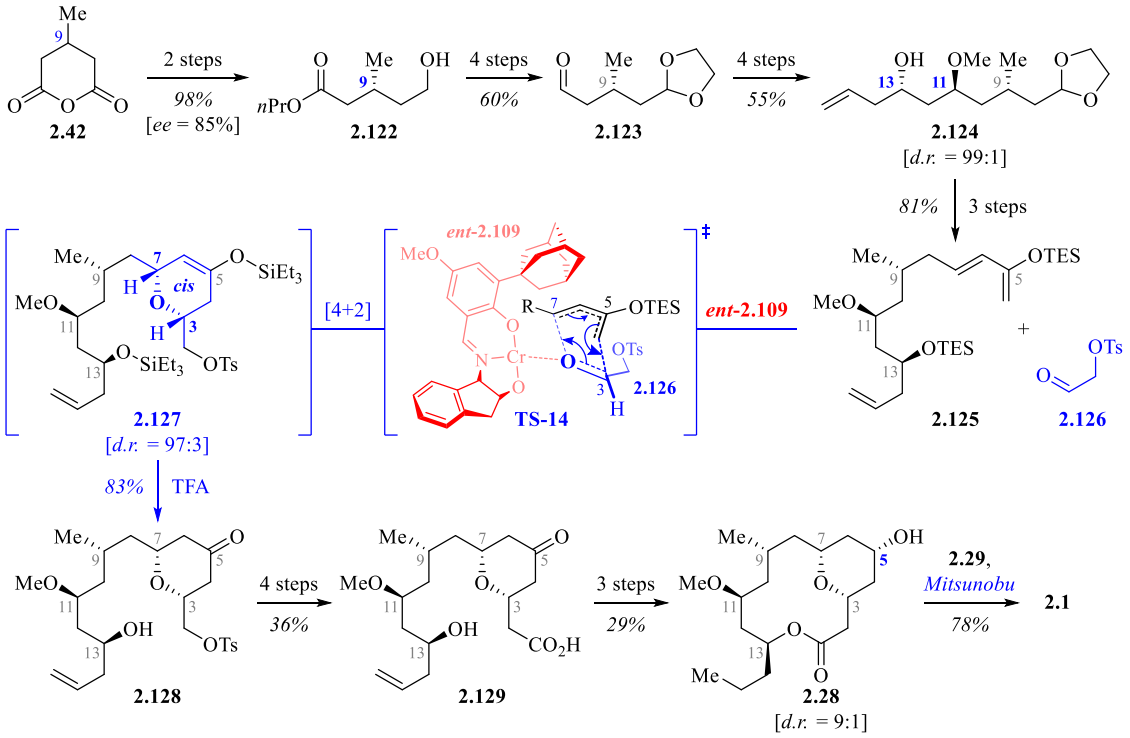

Scheme 2.12 – Summary of Arun K. Ghosh and coworkers' synthesis of neopeltolide, highlighted by asymmetric HDA assembly of the ***cis*-THP** using Jacobsen's chiral tridentate chromium(III) catalyst ***ent*-2.109**.

The A. K. Ghosh synthesis required 21 linear steps to access the macrocyclic core of neopeltolide, with an overall yield of 2.0% from anhydride **2.42**. Generation of the natural product was accomplished by Mitsunobu esterification[68] with the known acid fragment **2.29**.[69]

Key Installation Strategies (*Arun K. Ghosh and coworkers*, 2013)	
C9 – Enzymatic desymmetrization (lipase PS-30)	**C11** – (+)-Brown allylation
C13 – (–)-Brown allylation	***cis*-THP** – HDA (Jacobsen Cr^{III} catalyst)
Macrocyclization – Yamaguchi esterification	

2.4.4 Hetero-Diels-Alder Cycloaddition Conclusions

The HDA cycloaddition has become a staple in the generation of 2,6-disubstituted pyranyl elements in complex natural products. A variety of techniques exist, but these examples demonstrate the strength of asymmetric chromium catalysis to generate chiral products with high selectivity. These bulky Lewis acids lower the LUMO of the aldehyde dienophile to enhance reaction rate, while controlling *endo*-selectivity of the transition states. Based on the three reports, generation of the macrocyclic core *via* this strategy averaged 5.9% overall yield across 20 linear steps. The key *cis*-THP assembly averaged as impressive 80% yield (*d.r.* > 20:1), illustrating its synthetic prowess.

2.5 THP Assembly *via* Ring-Closing Metathesis (RCM)

Olefin metathesis is a fundamental strategy for formation of C–C bonds in linear and cyclic systems of complex natural products. The transformation shows remarkable tolerance of functional groups and a deep availability of commercial catalysts with a range of reactivity, which has seen assembly of pyranyl rings *via* this method. Ring-closure of C3-C4 atoms is preferable to the slower and more problematic C2-C3 metathesis.[75] The main limitation of this strategy is the requirement for stereochemistry to be installed prior to the reaction, and that asymmetric reduction is necessary to attain 2,6-*cis*-THP products.

2.5.1 Fuwa Group – First-Generation Synthesis (Tohoku University, 2008)[29]

The Fuwa group has provided significant synthetic contributions to the field of bioactive polyketide natural products. In particular, they have become instrumental to the global study of neopeltolide with a total of seven research articles[29,36,37,168–171] and one review.[76] In total, they have reported synthesis of the originally-proposed structure of neopeltolide, its revised structure, and 29 analogues consisting of macrocyclic core and side-chain derivations. Their work has identified pharmacophoric elements, and benefited preliminary biological testing. Fuwa's formal entry into the neopeltolide study came in 2008, with a first-generation synthesis that relied on RCM for assembly of the *cis*-THP (Scheme 2.13). Synthesis began with Brown's[90] asymmetric allylation of aldehyde **2.32** that was prepared over two-steps from commercial propanediol. Subsequent protection, homologation with methyl acrylate, and reduction, afforded **2.130** with excellent enantioselectivity. Sharpless' method[172] for asymmetric epoxidation furnished the requisite C5 stereogenic center as a single diastereomer. Conversion of **2.131** to its allylic alcohol by iodination and zinc reduction, and subsequent protecting group manipulation provided acetate **2.132**. Enolization in the presence of $(PhO)_2P(O)Cl$ furnished enol phosphonate **2.133** for *in situ* Suzuki-Miyaura coupling[173] with the alkylborate of iodo **2.136**. Chemoselectivity of this reaction over intramolecular Heck cyclization of **2.133** was not accounted for by the authors. Key precursor **2.137**

underwent metathesis in the presence of Grubbs' second-generation catalyst **2.89**, whereby substrate-controlled hydrogenation furnished *cis*-THP **2.138** as a single isomer. Oxidation state and protecting group manipulations afforded the linear *seco*-acid, which was cyclized by Yamaguchi esterification.[61] This strategy required 22 linear steps from aldehyde **2.32** (11.8%) to afford the macrocyclic core of neopeltolide **2.28**, which was subsequently converted to the natural product *via* Mitsunobu esterification with known acid fragment **2.29**.[69]

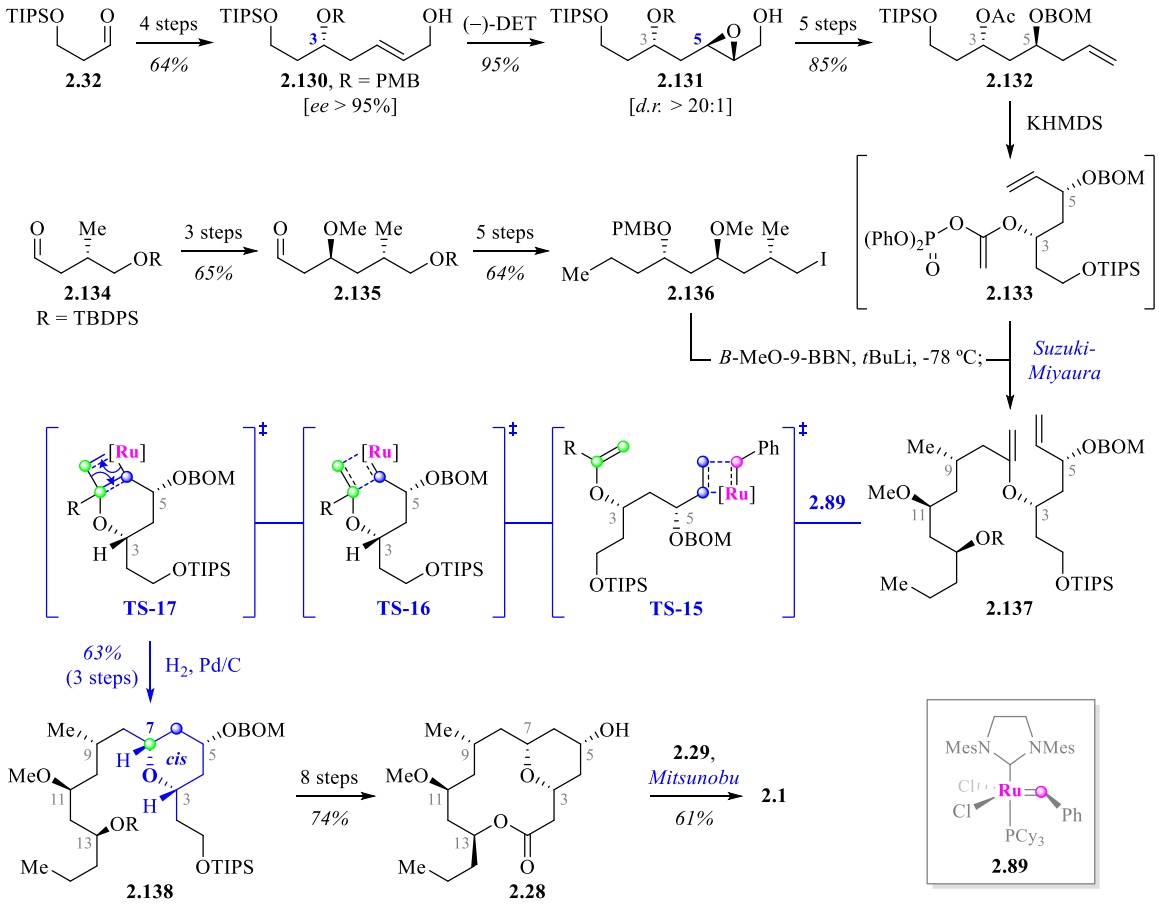

Scheme 2.13 – Summary of Fuwa and coworkers' first-generation synthesis of neopeltolide **2.1**, highlighted by RCM assembly of the ***cis***-THP.

In 2009, Fuwa published an alternative version of this strategy to prepare 11-demethoxy- and 9-*des*methylneopeltolide analogues (Scheme 2.14).[168] Preparation of enol phosphonate fragment **2.133** was unaltered, but accessing iodo coupling fragment **2.136** was greatly-improved. Synthesis began with the preparation of PMB-protected aldehyde **2.140** from the reported starting material diol **2.139** that was prepared over two steps[174] in unknown yield or selectivity. Chelate-controlled allylation by allyltrimethyl-silane in the presence of $MgBr_2 \cdot OEt_2$ provided homoallylic alcohol **2.141** in excellent yield and selectivity. Two-step hydroboration/oxidation delivered alcohol **2.142**, and was derivatized with (*S*)-oxazolidinone

auxiliary.[175] This directed the methylation to afford a single isomer,[176] for subsequent conversion to iodo species by cleavage of the auxiliary and iodination.

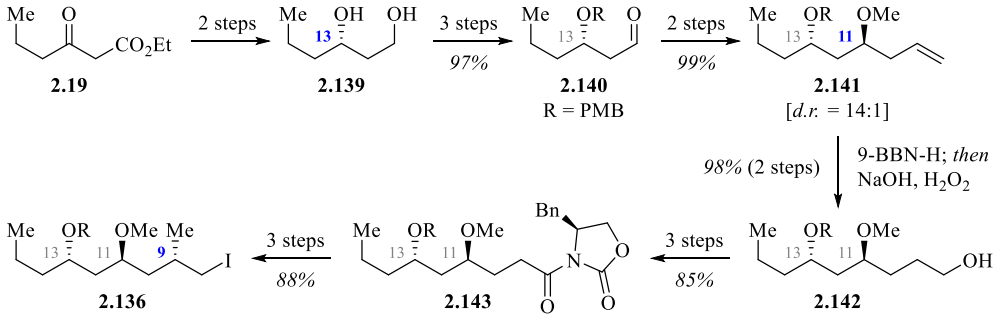

Scheme 2.14 – Summary of the modified synthesis of iodo-**2.127** from Fuwa's 2009 report on analogue design. This alternative route added 50% more steps, while reporting nearly two-fold increase in linear yield.

The first-generation neopeltolide synthesis by Fuwa allowed preparation of two novel analogues, and represented a starting point for further investigation of this natural product (*vide infra*). The updated 2009 route adjusted the linear step-count of 22 steps (from **2.32**) to 24 steps (from **2.19**); however, due to truly *unbelievable* reported yields in their generation of iodo-**2.136**, the overall yield nearly doubled despite the addition of over 50% more steps.

Key Installation Strategies (*Haruhiko Fuwa and coworkers*, First-Generation – 2008/2009)	
C9 – (*R*)-(–)-3-Bromo-2-methyl-1-propanol (2008) & diastereoselective alkylation (2009)	
C11 – (+)-Brown & chelate-controlled allylations	**C13** – (–)-Brown allylation
Macrocyclization – Yamaguchi esterification	***cis*-THP** – $RCM_{C6\text{-}C7}$ (Grubbs-II)

2.6 THP Assembly *via* Intramolecular Radical Cyclization

Radical cyclization reactions represent a powerful and versatile strategy for generation of small- and medium-sized ring systems due to broad functional group tolerance, mild conditions and excellent selectivity.[177–179] Selectivity is governed by Beckwith's guidelines,[180,181] serving as a radical-focused extension of Baldwin's rules;[182] these guidelines suggest that *exo*-cyclizations are favored to their *endo*-counterparts. Formation of oxacycles by this strategy has proven particularly attractive due to improved reactivity from shortened C–O bonds and smaller C–O–C angles, leading to better overlap in the transition state.[178] Lee and coworkers have reported that intramolecular radical cyclization (IRC) of *β*-alkoxyacrylates is an attractive strategy to selectively furnish *cis*-tetrahydrofuranyl[**] and pyranyl rings.[179,183,184]

[**] The generation of 5-membered rings by IRC is a more generalized strategy than that of its 6-membered counterpart, providing increased reactivity and selectivity. Competitive formation of reduced, linear by-products hinders 6-membered ring formation; however, can be circumvented by polarization of the olefin with neighboring activating-substituents.[284]

2.6.1 Taylor Group – Formal Synthesis (University of Notre Dame, 2008)[185]

The Taylor research group highlight their syntheses of complex bioactive polyketide natural products with analogue designs that focus on structural and conformational binding constraints.[186–191] Their synthesis of neopeltolide features ether transfer methodology that they developed and used in previous works,[192–196] and provided significant quantities (> 300 mg) of material that allowed rapid access to analogue production (Scheme 2.15). Similar to Panek,[17] their synthesis began with commercially-available **2.7**, which was furnished by enzymatic desymmetrization[197] to selectively install the C9-methyl. Amide **2.144** underwent mild asymmetric allylation with Soderquist's reagent[198] to generate **2.146**, protected, and coupled with LiDBB-lithiated-**2.147** by Rychnovsky's method.[148] Evans-Tishchenko reduction[60] and *O*-methylation generated ether-transfer precursor **2.149**, which upon treatment with iodine monochloride promoted direct-installation of the C5-alcohol with excellent diastereoselectivity *via* 1,2-chirality transfer in the all-*equatorial*-orientation chair-like transition state **TS-18** (*d.r.* > 20:1). Conjugate addition with ethyl propiolate **2.151** provided *β*-alkoxyacrylate **2.152** for IRC, which proceeded by *exo*-ring-closure with excellent yield and selectivity *via* the pseudo-*equatorial*-orientation of chair-like transition state **TS-19** in accordance with Beckwith's guidelines. The synthesis was completed by saponification of *cis*-**2.154**, macrocyclization by Yamaguchi esterification,[61] and hydrogenolysis of the C5-ether.

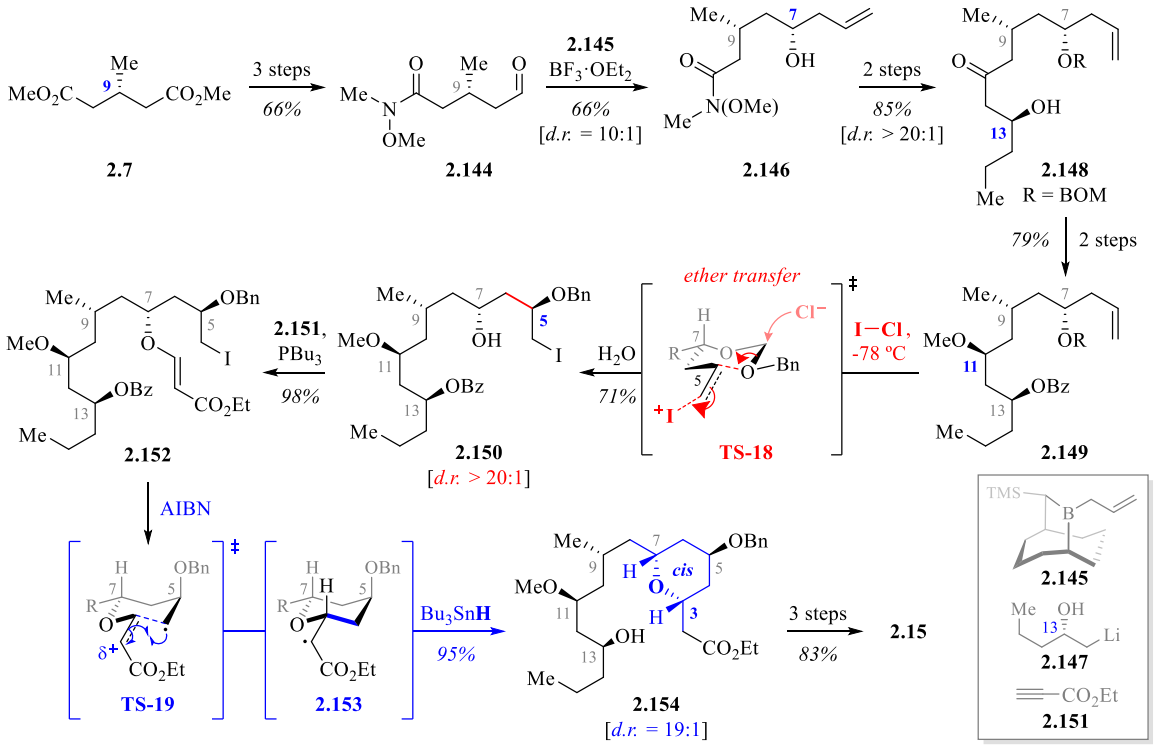

Scheme 2.15 – Summary of Taylor and coworkers' synthesis of macrocyclic core of neopeltolide **2.1**, highlighted by ether transfer methodology *en route* to ***cis***-THP assembly by intramolecular radical cyclization.

Intramolecular radical cyclization of *β*-alkoxyacrylates has proven to be an attractive approach for assembly of 2,6-*cis*-THPs in natural product synthesis. It is surprising that Taylor's study is the lone representative of this strategy for neopeltolide synthesis. Their route to the macrocyclic core of neopeltolide was accomplished in 14 linear steps from commercially-available (*R*)-(+)-3-methylglutarate with an excellent overall yield of 18.9%, representing one of the most efficient syntheses to date. Their route also limited use of protecting groups (2), whereby each installed concomitantly with setting of the stereocenter.

Key Installation Strategies (*Richard E. Taylor and coworkers*, 2008)	
C9 – Enzymatic desymmetrization (PLE)	**C11** – Evans-Tishchenko reduction
C13 – (2*S*)-Propyloxirane (epoxide-opening)	***cis*-THP** – Radical cyclization (AIBN)
Macrocyclization – Yamaguchi esterification	

2.7 THP Assembly *via* Oxa-Conjugate Addition

The intermolecular conjugate addition of alcohols represents an excellent strategy for assembly of linear *β*-hydroxy carbonyl products, while intramolecular variety yields oxacycles. In general, assembly of simple 2,6-THPs involves intramolecular 6-*exo*-trig cyclization[182] of a *ζ*-hydroxy into an *α*,*β*-conjugated system, furnishing *cis*-THP products under base-mediated thermodynamic conditions, or acid-mediated kinetic conditions.[75] Unfortunately, these reactions suffer from reversibility, limited stereocontrol, and modest nucleophilicity of the alcohol; alcohols must be deprotonated by strong bases, or the conjugate acceptor must be activated by Lewis/Brønsted acids or transition-metal complexes. The required conditions can be harsh and often incompatible with other functional groups of the substrate and as a result, addition of hetero-nucleophiles into conjugated systems has been historically less-explored in comparison to its carbon counterpart.[199–202]

In this section, four independent syntheses of neopeltolide are presented whose assembly of the *cis*-THP ring were achieved by the oxa-conjugate addition of a *ζ*-hydroxy alcohol into *α*,*β*-unsaturated aldehyde (Hong,[33] and Roulland[34]) and ester systems (Fuwa[36,37]), as well as the *β'*-hydroxy alcohol into an *α*,*β*-unsaturated ketone system (S. Ghosh[42]). The latter strategy serves as the central theme to the transannular assembly of the *cis*-THP ring system in the synthesis of the macrocyclic core of neopeltolide from my graduate research (for details, refer to **Chapters 3** & **4**).[202]

2.7.1 Hong Group – Formal Synthesis (Duke University, 2009)[33]

The Hong research group focuses on developing novel strategies to access molecular complexity by rapid construction, and apply these techniques to generate bioactive natural products (Scheme 2.16). In their synthesis of the macrocyclic core of neopeltolide, they developed a tandem allylic oxidation/oxa-conjugate addition sequence for intramolecular assembly of the *cis*-THP. Following a three-step conversion

of commercially-available (*S*)-(+)-3-bromo-2-methyl-1-propanol **1.155**,[203] known iodo-species **2.35** was transformed to **2.157** by dithioacetalization and subsequent alkylation with (*R*)-epichlorohydrin **2.156**. Cuprate-addition and dithioacetal cleavage afforded *β*-hydroxy ketone **2.158**. Evans-Tishchenko reduction conditions[60] installed the *anti*-1,3-diol, where subsequent dihydroxylation using Sharpless' asymmetric conditions (AD-mix-*β*)[204] and epoxide-formation modestly-yielded **2.159**. Umpolung[59] addition of dithiane **2.160** provided the key precursor for their cascade reaction. Mild allylic oxidation of **2.161** by treatment of MnO_2 generated the *α,β*-unsaturated oxa-conjugate precursor, promoting cyclization *via* the kinetically-favored pseudo-*equatorial*-orientation of chair-like transition state **TS-21**. The process was highly selective for *cis*-THP (*d.r.* > 20:1), as a result of Thorpe-Ingold effect;[205] minimized 1,3-diaxial interactions in **TS-21** effectively lowered entropic barriers compared to that of sterically-disfavored **TS-20**. *In situ* ester formation by Scheidt's **2.162**-catalyzed oxidation method[206] delivered **2.164** upon workup, with excellent overall yield and selectivity. This sequence proved highly chemoselective, and did not require use of protecting groups for any of the three free alcohols. Completion of synthesis was accomplished by conversion of **2.164** to its *seco*-acid for ring-closure *via* Shiina esterification conditions,[207] cleavage of dithioacetal **2.165**, and subsequent reduction of the pyranone product.

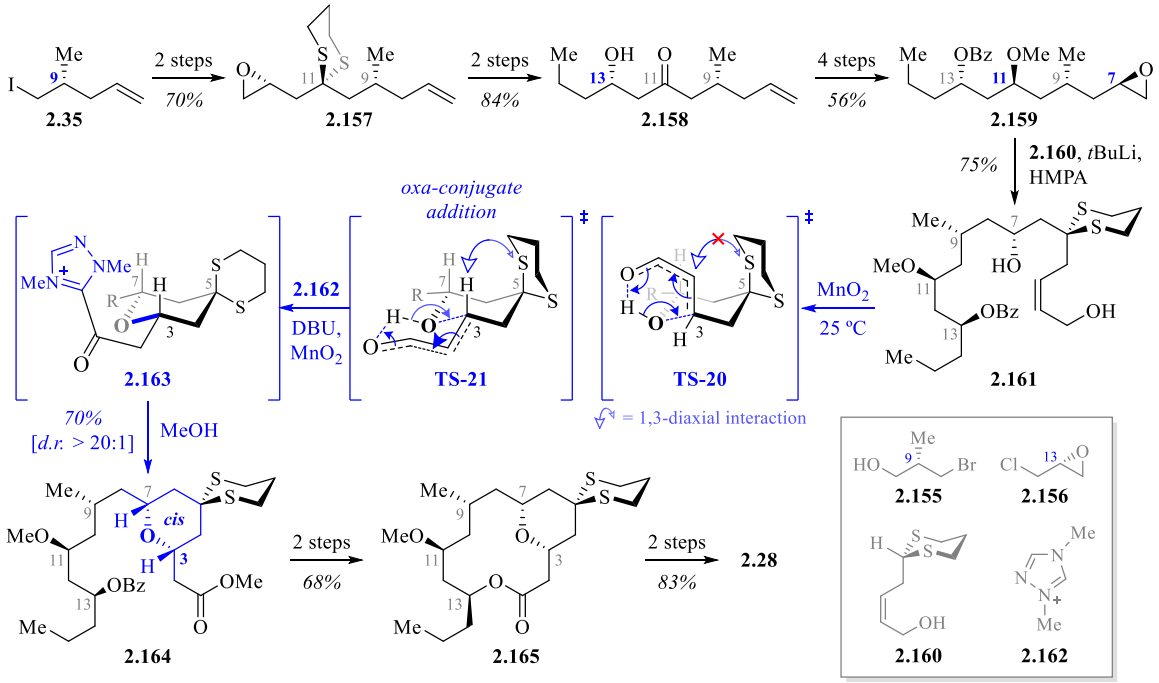

Scheme 2.16 – Summary of Hong and coworkers' synthesis of the macrocyclic core of neopeltolide **2.28**, highlighted by intramolecular oxa-conjugate addition of *α,β*-unsaturated aldehyde for ***cis***-THP assembly.

The Hong synthesis required 14 linear steps to access the macrocyclic core of neopeltolide from known iodo-species **2.35**,[203] in 9.3% overall yield.[††] This synthesis represents pioneering work in stereoselective synthesis of *cis*-THPs by *substrate*-controlled oxa-conjugate addition. The Hong group has since applied this methodology to the syntheses of leucascandrolide A,[208] (+)-dactylolide,[209] clavosolide A[210] and *ent*-sorangicin A.[211] Recently, they have reported the use of organocatalysts for *reagent*-controlled oxa-conjugate addition toward the synthesis of *cis*- and *trans*-heterocycles.[212,213]

Key Installation Strategies (*Jiyong Hong and coworkers*, 2008)	
C9 – (*S*)-(+)-3-Bromo-2-methyl-1-propanol	**C11** – Evans-Tishchenko reduction
C13 – (*R*)-(–)-Epichlorohydrin (epoxide-opening)	***cis*-THP** – Oxa-conjugate (Thorpe-Ingold)
Macrocyclization – Yamaguchi esterification	

2.7.2 *Roulland Group – Total Synthesis* (Institut de Chemie des Substances Naturelles, 2009)[34]

Despite being historically less-explored,[200] within three weeks of Hong's oxa-conjugate report, Guinchard and Roulland published their synthesis of a ruthenium-catalyzed alkyne-enal coupling/intramolecular oxa-conjugate addition cascade to selectively assemble the *cis*-THP ring system of neopeltolide (Scheme 2.17). This sequence was developed by Trost,[214,215] and elegantly used in syntheses of bryostatins 1[216] and 16.[217] The Roulland synthesis began with ruthenium-catalyzed asymmetric reduction[218] of β-keto ester **2.19** and subsequent conversion to its Weinreb amide.[128] Grignard addition of **2.167** provided a β,γ-unsaturated ketone, which was reduced by Evans-Tishchenko[60] protocol to install the C11-alcohol with complete stereocontrol and concomitant benzoyl-protection at C13. Acylation of C11 with acryloyl chloride **2.88**, and subsequent ring-closure by treatment with Grubbs' second-generation catalyst[127] **2.89** (refer to Scheme 2.8) furnished α,β-unsaturated lactone **2.169**. Substrate-controlled hydrogenation and acid-catalyzed solvolysis yielded a linear ester, and was converted to **2.170** in good yield. Loh's method of silicon-assisted propargylic transfer[219] promoted the fully stereoselective transfer of allenic alcohol **2.171** to aldheyde **2.170** installed C7-alcohol (with opposite configuration) *via* $In^{(III)}$-catalyzed oxonium [3,3]-sigmatropic rearrangement. Desilylation provided terminal alkyne **2.173**, which coupled with 4,4-diethoxybutene **2.174** in the presence of ruthenium complex **2.175**[220] and catalytic AcOH *via* thermodynamically-favored transition state **TS-22**.[215] *Syn*-β-Hydride elimination of ruthenacyclo-**2.176** delivered "branched" product **2.177**, which underwent reductive elimination and necessary *in situ* acetal cleavage to provide the oxa-conjugate precursor. Addition of the ζ-hydroxy occurred *via* favored chair-like transition state **TS-23**, stereoselectively affording *cis*-THP complete diastereocontrol. Completion of the macrocyclic core was achieved by oxidative cleavage of the *exo*-methylene, subsequent conversion to the *seco*-acid for cyclization by Yamaguchi esterification,[61] and substrate-controlled reduction of the pyranone.

[††] The authors report a 16-step (5.2% overall) sequence starting from commercially-available (*S*)-(+)-4-isopropyl-3-propionyl-2-oxazolidinone; it is unclear from their supporting information, or available theses,[285] how this was obtained.

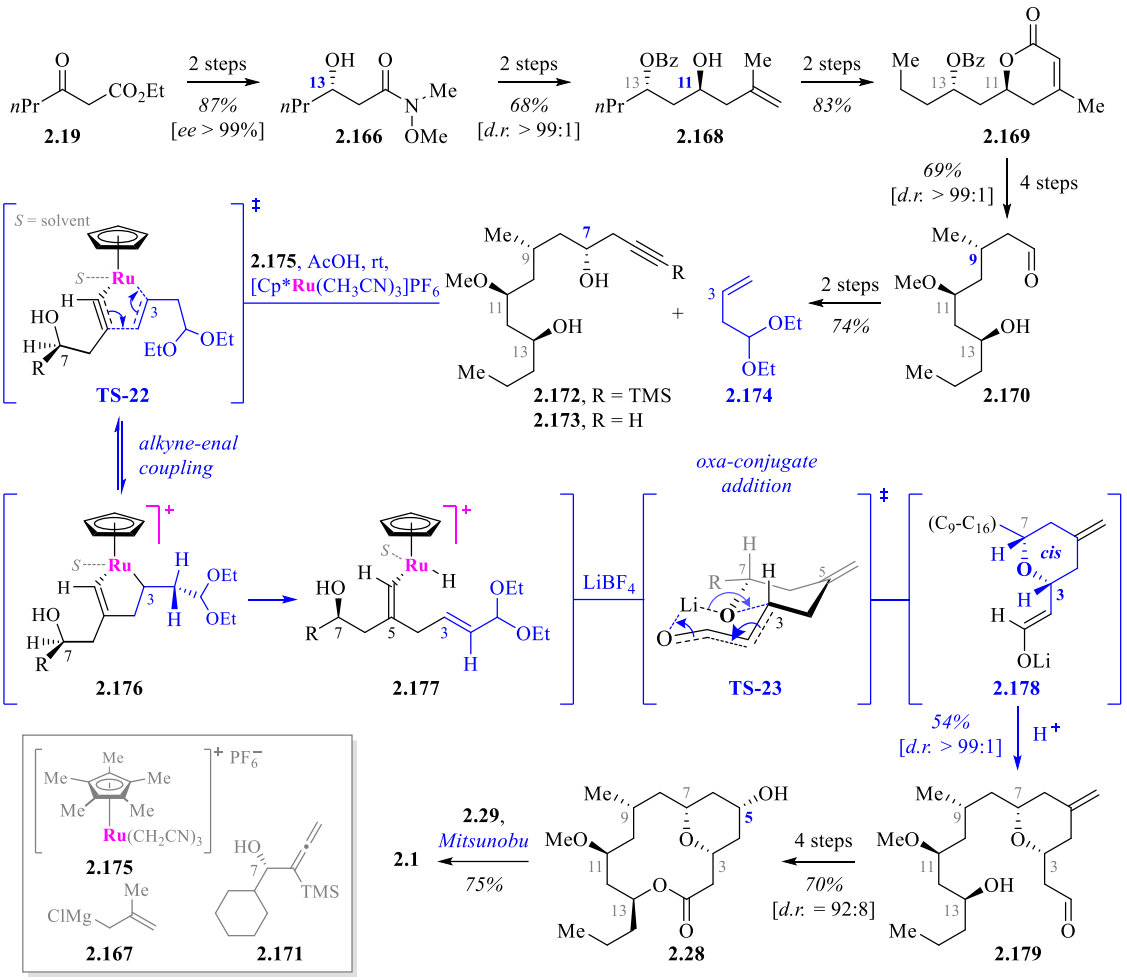

Scheme 2.17 – Summary of Guinchard and Roulland's synthesis of neopeltolide **2.1**, highlighted by tandem alkyne-enal/oxa-conjugate addition of *α*,*β*-unsaturated aldehyde for the generation of the ***cis***-THP. The methyl groups of ruthenium complex **2.175** were omitted from the reaction scheme for purposes of clarity.

Guinchard and Roulland accessed the macrocyclic core of neopeltolide in 17 linear steps from **2.19**, with an overall yield of 9.5% for the process. Their total synthesis by Mitsunobu esterification with known acid fragment,[69] which they prepared in a modified route.[34] Use of tandem alkyne-enal/oxa-conjugate addition strategy was subsequently applied to their synthesis of (–)-exiguolide.[221]

Key Installation Strategies (*Xavier Guinchard and Emmanuel Roulland*, 2009)	
C9 – Asymmetric hydrogenation (Pd)	**C11** – Evans-Tishchenko reduction
C13 – Asymmetric reduction (Ru)	***cis*-THP** – Intramolecular oxa-conjugate
Macrocyclization – Yamaguchi esterification	

2.7.3 Fuwa Group – Second-Generation Syntheses (Tohoku University, 2010 & 2013)[36,37]

To facilitate detailed investigations on the structure-activity relationship of neopeltolide, the Fuwa group required an improvement to their earlier work (Scheme 2.18). Their first-generation synthesis required 22 linear steps to access the macrocyclic core of neopeltolide (refer to § 2.5.1), and limited its use

for analogue design.[168] A second-generation synthesis began with the asymmetric allylation[‡‡] of *trans*-cinnamaldehyde **2.37** according to the procedure of Maruoka,[222] and subsequent silylation (98%) of the homoallylic alcohol yielded **2.180** (Scheme 2.18a). Chemoselective dihydroxylation and oxidative cleavage allowed asymmetric allylation by Brown's conditions[90] to afford **2.181**, which underwent cross-metathesis with methyl acrylate **2.88** in the presence of Grubbs' second-generation catalyst[127] **2.89**. Protecting group manipulation provided oxa-conjugate precursor **2.183**. Long reaction times at elevated-temperatures were required to selectively furnish the thermodynamically-favored *cis*-**2.184** *via* transition state **TS-24** with the pro-*equatorial* (*E*)-*α*,*β*-unsaturated ester. Under basic conditions, the forcing reaction conditions are required to cyclize the energetically-disfavored *s-trans* **TS-24** due to its decreased orbital overlap.[75,223] However, the desired product was yielded with excellent diastereoselectivity (*d.r.* > 20:1). Hydrolysis of the C5-ester completed the C1-C8 fragment of the macrocyclic core of neopeltolide **2.185**.

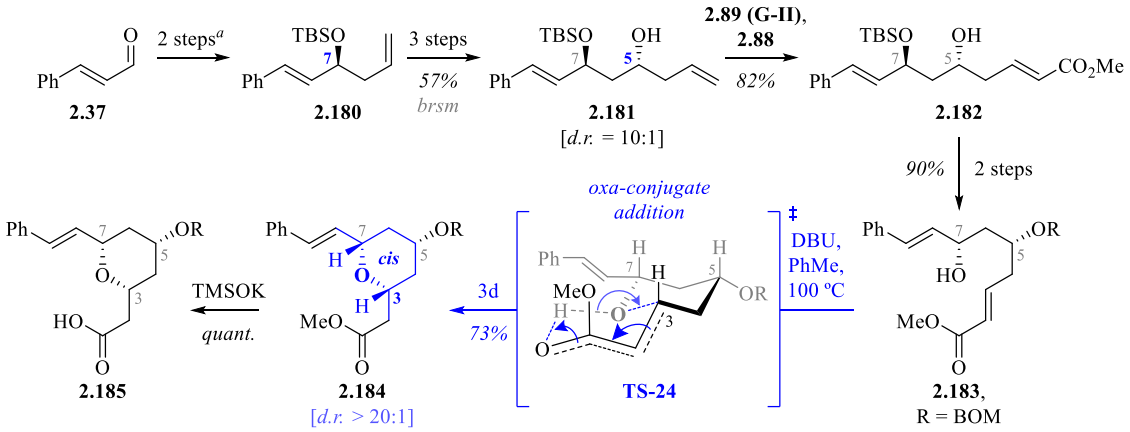

Scheme 2.18a – Synthesis of pyranyl fragment **2.185**, highlighted by intramolecular oxa-conjugate addition of *α*,*β*-unsaturated ester assembly of ***cis***-THP. [a] Unreported yield and selectivity for referenced *bis*-Ti^{IV}-catalyzed asymmetric allylation.[222]

The C9-C16 coupling fragment **2.187** was prepared in 8 linear steps from *β*-keto ester **2.30** (Scheme 2.18b), employing asymmetric Noyori reduction[66] and Brown allylation[90] procedures to install the *anti*-relationship of C11- and C13-alcohols, respectively. Yamaguchi esterification of acid **2.185** and alcohol **2.187** provided RCM-precursor **2.188**, which metathesized under the influence of GII-**2.89** to furnish macrocycle **2.189** in 80% over the two steps. Substrate-controlled hydrogenation proceeded with complete stereocontrol, and completed the synthesis of the macrocyclic core in 13 linear steps from *trans*-cinnamaldehyde.

‡‡ The authors did not report a yield or selectivity for this process, indicating in a footnote that "details will be reported in a full account of this study." No such account has been reported to date; overall yield is provided from **2.180**.

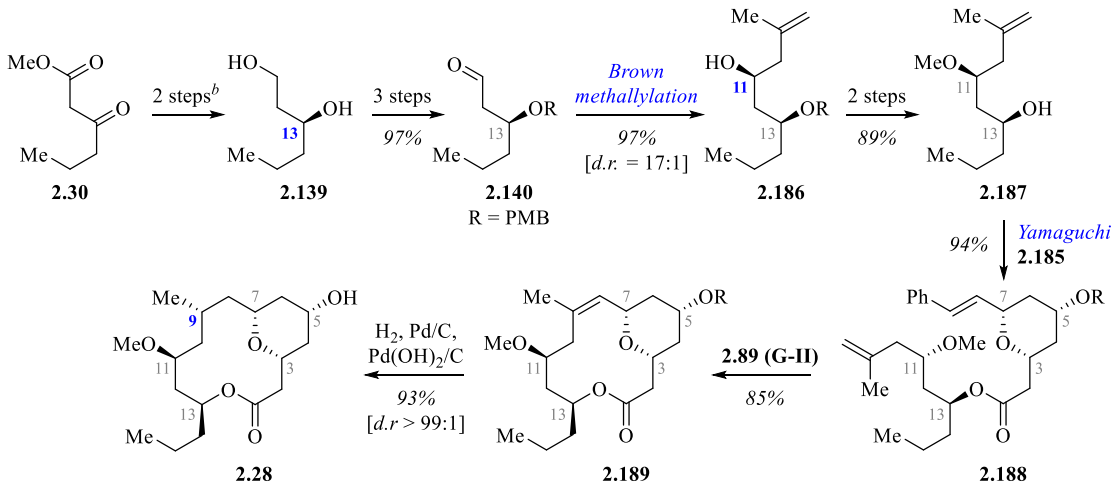

Scheme 2.18b – Completion of Fuwa and coworkers' second-generation synthesis of the macrocyclic core of neopeltolide. [b] Unreported yields and selectivity for two-step asymmetric-Noyori/$LiAl_4H$ reduction.[174]

An alternative route was presented in their 2013 publication that identified pharmacophoric elements of neopeltolide using a stereoisomeric library of $^{\Delta 8,9}$-dehydroneopeltolide analogues.[37] Synthesis of the C1-C8 fragment began with the asymmetric allylation of *trans*-cinnamaldehyde **2.37** using the titanium enolate of auxiliary **2.190** by Nagao aldol protocol (Scheme 2.19).[224] Subsequent generation of the Weinreb amide[128] cleaved the thiazolidinethione auxiliary, which was alkylated by allylmagnesium bromide and reduced by Evans-Tishchenko[60] asymmetric conditions to furnish the *anti*-**2.192** with excellent selectivity. A similar sequence including G-II cross-metathesis and intramolecular oxa-conjugate addition afforded *cis*-acid **2.185**, reducing the linear step count by a single transformation. Cyclization at room temperature furnished poor diastereoselectivity (*cis*-to-*trans*, 2:1), providing support for base-mediated oxa-conjugate additions into *α,β*-unsaturated esters require thermodynamic conditions to overcome unfavorable entropic barriers.[223] A modified generation of C9-C16 coupling fragment **2.187** employed (*R*)-epichlorohydrin **2.156** as starting material. Completion of synthesis was accomplished *via* the same sequence with identical yield and selectivity; installation of known acid **2.29**[69] by Mitsunobu esterification conditions[68] generated the natural product.

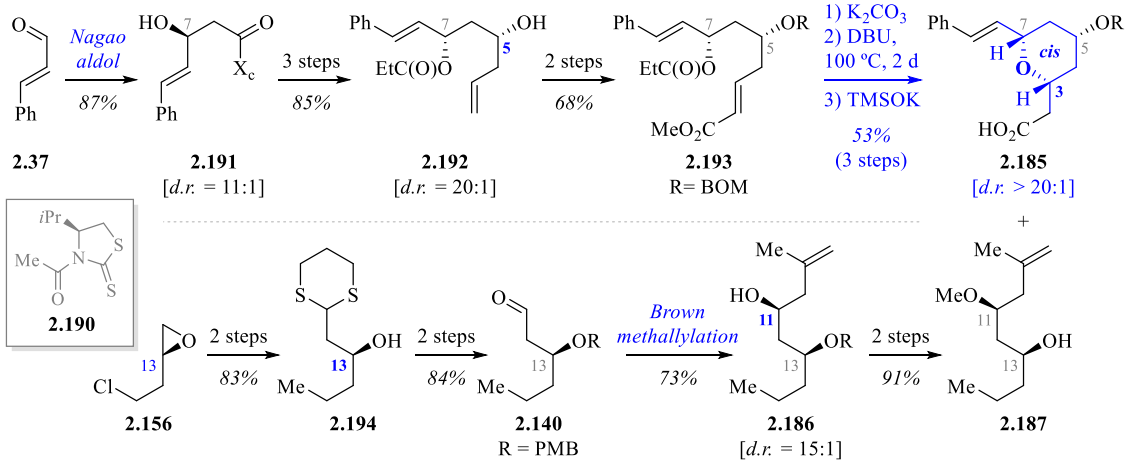

Scheme 2.19 – The 2013 update by Fuwa and coworkers fails to provide an obvious improvement to their 2010 report; however, demonstrated the flexibility of chemical transformation that can be used to access their coupling fragments. This flexibility is amenable to additional analogue design.

The second-generation synthesis of neopeltolide by the Fuwa group dramatically-improved overall efficiency compared to their RCM strategy. The oxa-conjugate addition strategy shortened the step-count by half, while doubling overall yield. This route remains one of the shortest, and highest-yielding syntheses of the natural product to date. It also supported extensive analogue design that determined the pharmacophoric elements of neopeltolide.[37,170,171] While step-count of the alternative 2013 synthesis was lowered, it should be noted that the route is less efficient. The 2010 synthesis reported the generation of the *cis*-**2.185** in 54% overall yield from the metathesis precursor (five linear-steps), and the updated route furnished the same material in 36% overall yield, over a similar five linear-steps. Additionally, the three-step conversion of **2.140**-to-**2.187** decreased in both yield and selectivity.

Key Installation Strategies (*Haruhiko Fuwa and coworkers,* Second-Generations 2010/2013)	
C9 – Asymmetric hydrogenation (Pd)	**C11** – (–)-Brown methalyllation
C13 – Noyori reduction[36] & (*R*)-epichlorohydrin[37]	***cis*-THP** – Intramolecular oxa-conjugate
Macrocyclization – Yamaguchi esterification	

Following this work, the Fuwa group has established itself as a leader in intramolecular oxa-conjugate addition synthesis,[223] whereby applying this strategy to the synthesis of pyranyl-containing (–)-exiguolide,[225,226] aspergillides A and B,[227,228] centrolobine.[229] They have also extended the strategy to oxa-conjugate addition into *α,β*-unsaturated ester surrogates including thioesters, oxazolidinone imides, and pyrrole amides,[230,231] and developed a palladium-catalyzed domino olefin cross-metathesis/intramolecular oxa-conjugate assembly of *cis*-THP derivatives.[232,233]

2.7.4 S. Ghosh Group – Formal Synthesis (Indian Institute of Chemical Technology, 2012)[42]

The Subhash Ghosh research group is the last of three colleagues (Yadav, § 2.3.5; Sharma, § 2.8.2) from the Indian Institute of Chemical Technology to publish a synthesis of neopeltolide (Scheme 2.20).

They focus on natural product synthesis with an emphasis on macrocyclic peptidyl and polyketide scaffolds.[234–236] Their synthesis of neopeltolide began with a two-step preparation of known[175] alcohol **2.41** by Evans asymmetric alkylation[176] with unreported yield or selectivity. Silylation and treatment with *m*CPBA afforded a diastereomeric mixture of epoxides, which were selectively converted to **2.197** by Jacobsen hydrolytic kinetic resolution[237] with **2.196**.[§§] Cuprate-addition of vinylmagnesium bromide furnished the homoallylic alcohol, which was alkylated as methyl ether **2.198**. A similar asymmetric epoxidation sequence with *ent*-**2.196** selectively installed the C13 stereogenic center (see footnote), and converted to **2.199**. Completion of the C7-C16 fragment was achieved by one-carbon-homologation *via* cyanohydrin, and reduced to aldehyde **2.200**.

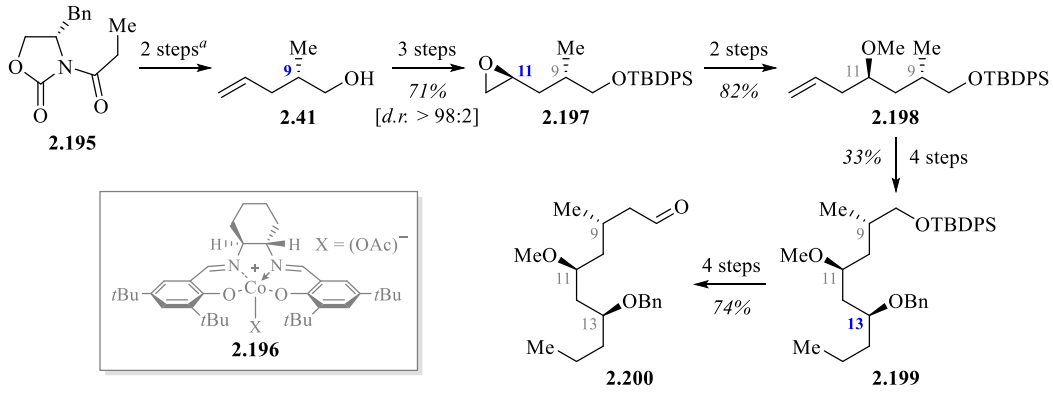

Scheme 2.20a – Synthesis of C7-C16 fragment from S. Ghosh and coworkers' synthesis of the macrocyclic core of neopeltolide. [a] Unreported yield or selectivity for two-step synthesis of **2.41**.

Under Masamune-Roush[238] conditions, aldehyde **2.200** was coupled with phosphonate **2.203** that was derived from known mono-protected diol **2.201**. With the complete carbon framework installed, treatment by HF furnished key precursor **2.205** for oxa-conjugate addition by unmasking the *β'*-hydroxy nucleophile. Activation of the *α,β*-unsaturated ketone C=O bond by $Pd^{(II)}$-catalyst **2.206**[239] promoted 6-*endo*-trig cyclization through a non-oxidative pathway *via* reversible formation of the transient carbonyl-metal complex of transition state **TS-25**. Protonolysis of the resulting metal enolate furnished a mixture of *cis*-to-*trans* products (*d.r.* = 4:1); no attempt at equilibration under thermodynamic conditions to improve their *cis*/*trans* ratio was reported. Ring-closure of *cis*-THP **2.207** was achieved over a four-step sequence to generate *cis*-pyranone product **2.27**.

[§§] The resulting diol from the HKR reaction was reportedly converted to its desired epoxide over a three-step sequence; however, this conversion was not differentiated between epoxidation processes for the installation of the C11- and C13-alcohols, and were reported as identical yields of 30% overall (from each respective diastereomeric mixture). This yield was only added to the generation of **2.197** due to a lack of supporting information for the second process.

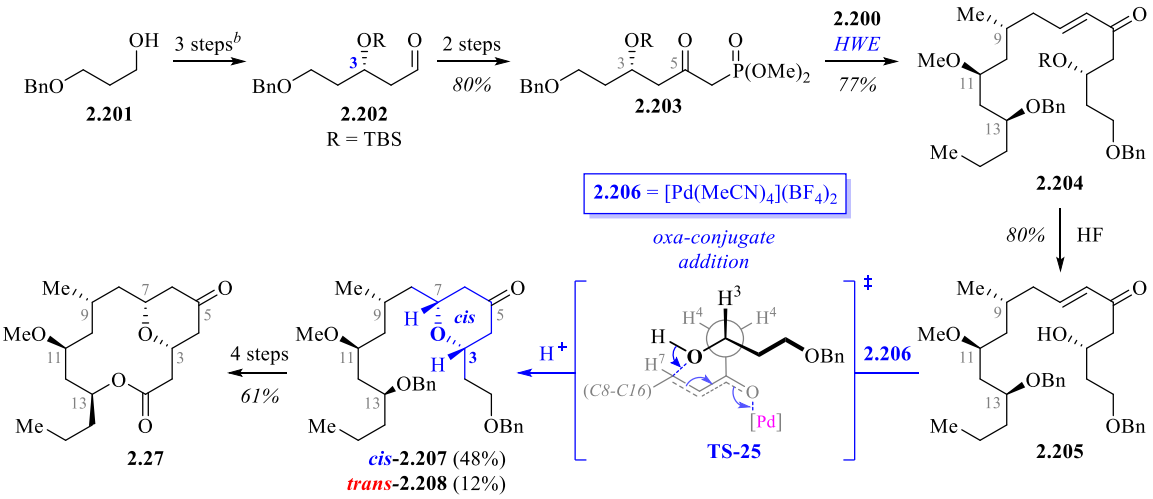

Scheme 2.20b – Completion of S. Ghosh and coworkers' synthesis, highlighted by Gouverneur's[239] $Pd^{(II)}$-catalyzed intramolecular oxa-conjugate addition of *α,β*-unsaturated aldehyde for assembly of ***cis***-THP. [b] Ambiguous citation does not indicate how **2.202** was accessed, though does not affect the LLS sequence.

The convergent synthesis of the macrocyclic core by the S. Ghosh group required 20 linear steps from known alcohol **2.41**, and was achieved in 2.6% overall yield (see footnote). The S. Ghosh group has applied this same strategy to the generation of the bicyclic lactone polyrhacitide A,[240] and most-recently to their alternative synthesis of a mandelalide A fragment.[241]

Key Installation Strategies (*Subhash Ghosh and coworkers*, 2012)	
C9 – Evans asymmetric alkylation	**C11** – Hydrolytic kinetic resolution (Co^{III})
C13 – Hydrolytic kinetic resolution (Co^{III})	***cis*-THP** – Intramolecular oxa-conjugate
Macrocyclization – Yamaguchi esterification	

2.7.5 Florence Group – Fragment Synthesis (University of St. Andrews, 2010)[242]

As part of their interest in cyclic ether formation in natural products, the Florence group published efforts towards synthesis of the macrocyclic core of neopeltolide (Scheme 2.21). In this work, they planned a transannular oxa-conjugate addition for assembly of the *cis*-THP, though were unsuccessful in accessing their requisite precursor **2.209**.

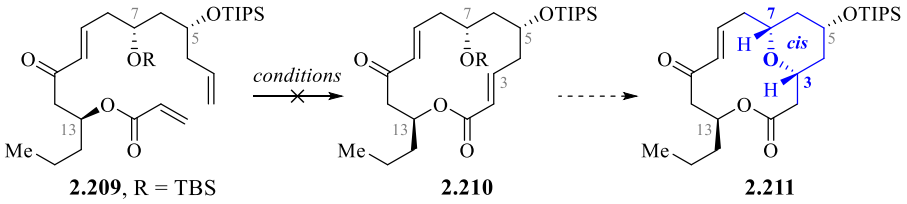

Scheme 2.21 – Florence and Cadou's proposed ***cis***-THP assembly by transannular oxa-conjugate addition of *ζ*-hydroxy into an *α,β*-unsaturated macrolactone.

The Florence group envisaged conformational biases of the macrocyclic core would control the installation of C3-, C9- and C11-stereocenters. Completion of the synthesis by this, or alternative strategies

have not been reported to date, and is believed the presented strategy would fail in accordance with preliminary research[202] of this dissertation (please refer to Chapter 3, § 3.4[243]).

2.7.6 Intramolecular Oxa-Conjugate Addition Conclusions

Intramolecular oxa-conjugate addition has become a valuable strategy for selective generation of pyranyl scaffolds of natural products like neopeltolide. These works demonstrated the need for controlling factors under kinetic conditions, such as the *gem*-dialkyl effect or the use of heavy metal catalysis in both acid- and base-mediated systems. Excluding S. Ghosh's synthesis, these factors proved sufficient for excellent selectivity. Only Fuwa reported thermodynamic conditions were required to overcome entropic barriers of base-mediated addition into an α,β-unsaturated ester system. Based on these four reports, generation of the macrocyclic core of neopeltolide by this strategy averaged 10.3% overall yield across 16 linear steps. The key intramolecular oxa-conjugate assembly of the *cis*-THP averaged 64% yield (*d.r.* ~ 12:1), which is significantly more selective (*d.r.* > 20:1) when excluding Ghosh's outlier result.

2.8 THP Assembly *via* Transition-Metal-Activated Alkene Additions

Electrophile-activated alkene additions are a common chemical transformation of carbon–carbon double bonds. Typically, THP formation occurs by 6-*exo*-trig cyclization of a δ-hydroxyl nucleophile into a metal-activated alkene π-system. The stereochemical outcome is dictated by nucleophilic attack occurring on the face opposite electrophilic π-complexation; facial discrimination is either substrate-controlled (chiral directing-group coordination) or reagent-controlled (chiral metal catalyst). Metal-activated alkene additions can be classified as stoichiometric or catalytic processes. Stoichiometric processes for THP synthesis typically involve the use of mercury salts for oxymercuration reactions. Catalytic variations generally involve palladium complexes, but other transition metals are becoming more common. In this section, four independent syntheses of neopeltolide are presented whose assembly of the *cis*-THP ring were mediated by transition-metals including palladium (She,[39] and Dai[244]), mercury (Sharma[40]), and molybdenum (Hoveyda[44]).

2.8.1 She Group – Formal Synthesis (Lanzhou University, 2011)

The She research program is focused on the synthesis of natural products,[245–250] with numerous publications representing a diverse set of metabolite families (Scheme 2.22). Often, they report syntheses that propose or support biosynthetic hypotheses, and have assembled pyranyl rings by Prins and oxa-conjugate addition strategies. Their synthesis of neopeltolide deviates from these methods, but demonstrates an incredibly efficient process.[39] Synthesis began with Krische's method[251] for iterative two-directional asymmetric allylation of 1,3-propanediol **2.212**, affording *bis*-homoallylic alcohol **2.213** as the

key substrate for their assembly of the *cis*-THP by intramolecular alkoxycarbonylation. Direct-coordination of the $Pd^{(II)}$-catalyst to the pseudo-*equatorial* olefinic double-bond promoted oxypalladation by 6-*exo*-trig Markovnikov addition of **TS-26**,[252–254] to furnish *σ*-alkyl metal intermediate **2.214**. It is uncertain whether the chlorine-ligand coordinates to the proximal C5-hydroxy with any directing-effect of the nucleophilic addition.[255] Concomitant chain-extension by migratory insertion of carbon monoxide into the metal-carbon bond *via* **TS-27** afforded the activated *σ*-acyl metal intermediate **2.215**, which is followed by terminating methanolysis to deliver *cis*-**2.216** in excellent yield and selectivity (83%, *d.r.* > 20:1).[256] Hanessian's conditions[257] were used for G-II-catalyzed allyl-to-propenyl transposition, where ester hydrolysis provided acid fragment **2.217**. This was coupled by Shiina's esterification conditions[207] with C9-C16 fragment **2.187** that was obtained in a similar sequence to Fuwa[37] using crotonaldehyde **2.38** for the asymmetric alkylation. Ring-closure was achieved in the presence of Grubbs-Hoveyda second-generation catalyst **2.223**, and was followed by substrate-controlled hydrogenation to complete the synthesis of the macrocyclic core of neopeltolide.

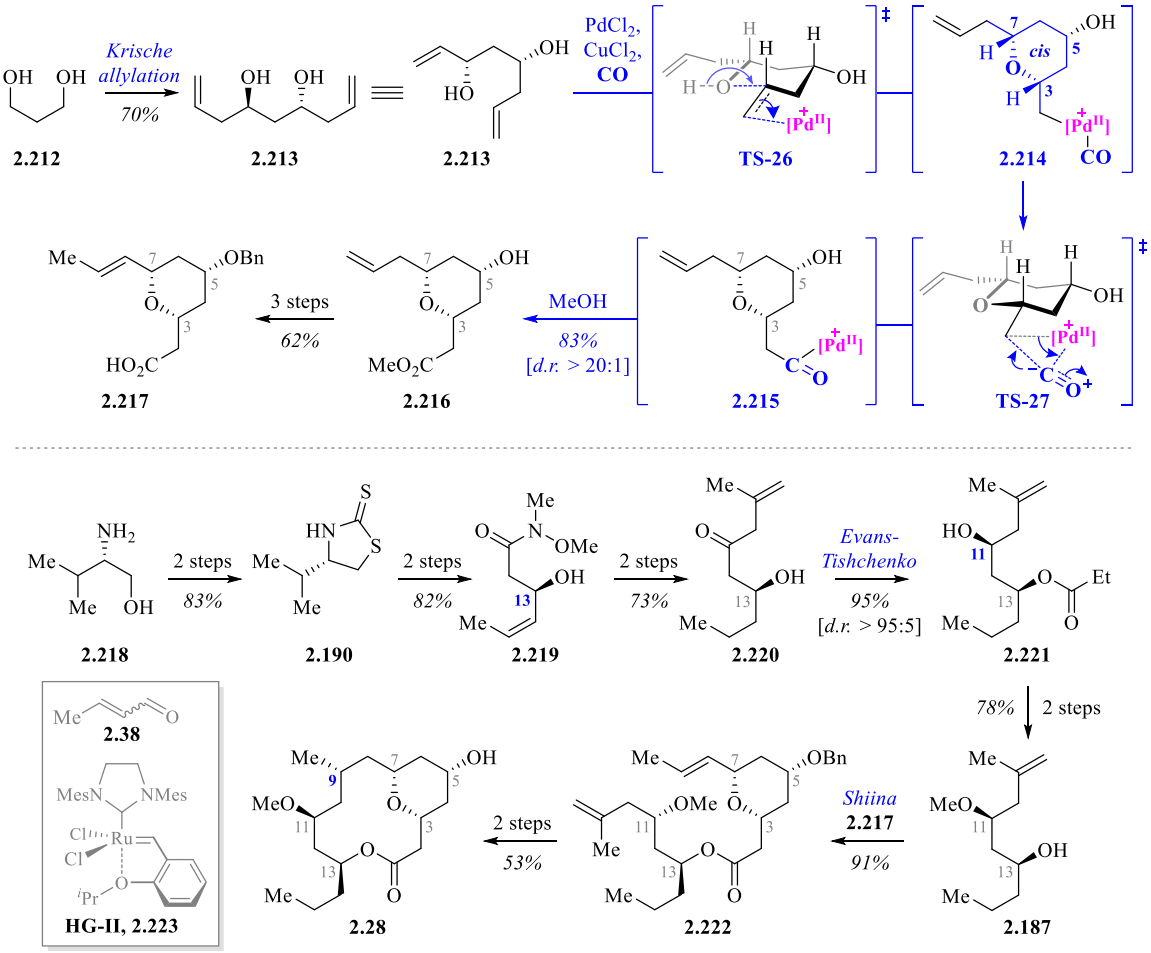

Scheme 2.22 – Summary of She and coworkers' synthesis of the macrocyclic core of neopeltolide **2.28**, highlighted by Pd-catalyzed intramolecular alkoxycarbonylation assembly of the ***cis***-THP.

The She synthesis demonstrated the power of transition-metal catalysis in stereoselective synthesis. Their route required 10 linear steps[***] to furnish the macrocyclic core of neopeltolide from commercially-available crotonaldehyde with excellent overall yield (21.4%), representing one of the most-efficient syntheses to date. The She group has since used this strategy for installing the *cis*-THP in their synthesis of cyanolide A.[258]

Key Installation Strategies (*Xuegong She and coworkers* 2011)	
C9 – Asymmetric hydrogenation (Pd)	**C11** – Evans-Tishchenko reduction
C13 – Nagao-Aldol (thiazolidinethione auxialiary)	***cis*-THP** – $Pd^{(II)}$-alkoxycarbonylation
Macrocyclization – $RCM_{C8\text{-}C9}$ (Grubbs-Hoveyda-II)	

2.8.2 Sharma Group – Formal Synthesis (Indian Institute of Chemical Technology, 2012)[40]

The Sharma group is one of three groups from the Indian Institute of Chemical Technology to report a synthesis of neopeltolide (Scheme 2.23). Their research focuses on synthesis of natural products, with an interest in macrolactone polyketide scaffolds and oxacyclic-bearing metabolites.[259–263] These works commonly employ their patented[264] epoxide-opening technique to access pyranyl structures and rely on malic acid as starting precursor; however, their synthesis of neopeltolide applied a transannular oxymercuration strategy. Synthesis of the C8-C16 fragment began with aldehyde **2.39** that was prepared over three steps[265] from (L)-malic acid with unreported yield. Grignard addition and Swern oxidation,[266] followed by chelate-controlled reduction furnished **2.225** with good selectivity reported as a diastereomeric excess.[267] Protecting group manipulation installed C11-stereocenter by base-mediated formation of epoxide **2.226**, which was subsequently opened with THP-protected propargyl alcohol **2.227**.[268] Sharpless' method[172] for asymmetric epoxidation prepared **2.229** from the deprotected/reduced alkyne, and was regioselectively-methylated to furnish diol **2.230** by Roush protocol.[269] Treatment of the diol with iodine and triphenylphosphine, with subsequent desilylation by TBAF, afforded alcohol **2.231** over 19 linear steps from (L)-malic acid.

Synthesis of the C1-C7 fragment began with diol **2.232** that was prepared from (L)-malic acid over 8 linear steps according to Tanner.[270] Following protecting group manipulation, **2.233** was converted to epoxide **2.234** *via* base-mediated attack of a terminal tosylate. Cuprate-addition furnished the homoallylic alcohol, and was transformed to carboxylic acid for coupling *via* Steglich esterification.[89] Ring-closing metathesis in the presence of Grubbs' second-generation catalyst[127] afforded the macrocyclic core of neopeltolide, which was prepared as key precursor **2.238** by DDQ-deprotection. The α-face configuration of the C9-methyl provided facial bias for attack of the incoming mercuric nucleophile from the less-

[***] The two-step preparation of Nagao auxiliary[224] **2.190** from L-valinol was not included in the linear step-count, as it was omitted from the step-count of Fuwa's second-generation synthesis due to unreported preparative details.

hindered β-face of the $^{\Delta 7,8}$-alkene to yield mercurinium ion of **TS-28** (Scheme 2.23). Nucleophilic attack by δ-hydroxy into C8 afforded the *cis*-THP with complete diastereomeric control *via* twist-boat configuration. In this transition state, the C5 acetal is placed in pseudo-*equatorial* orientation and was confirmed by their presented energy-minimized structure of the adduct.[40] Reductive demurcuration of adduct **2.239** with tin hydride and AIBN under reflux conditions, and acid-mediated deprotection completed the synthesis of the macrocyclic core of neopeltolide in 25 linear steps from (L)-malic acid.

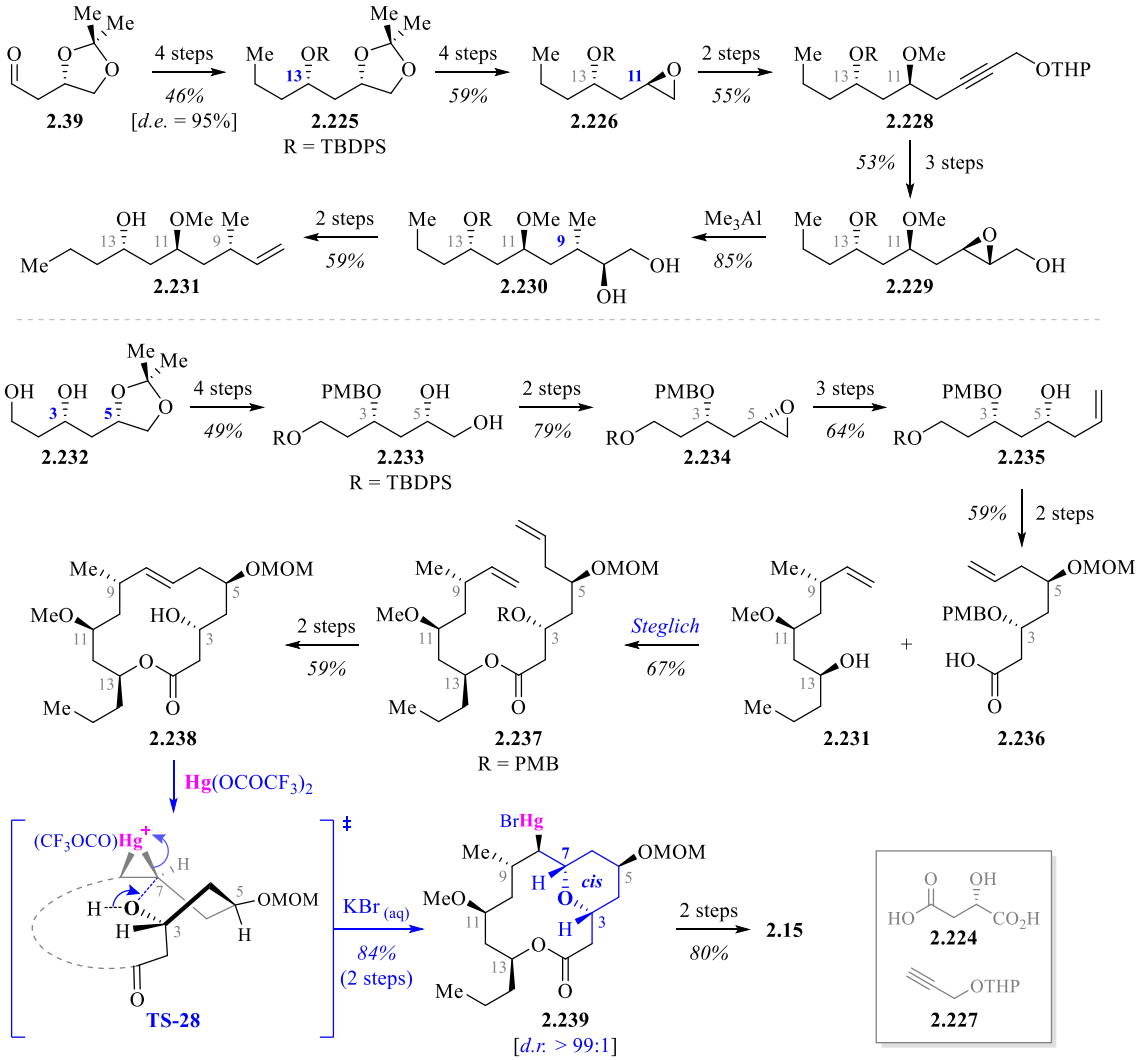

Scheme 2.23 – Summary of Sharma and coworkers' synthesis of the macrocyclic core of neopeltolide **2.15**, highlighted by transannular oxymercuration assembly of the ***cis***-THP, representing the lone report of THP-formation following construction of the 14-membered macrolactone.

The formal synthesis by the Sharma group does not represent the most efficient route, requiring 23 linear steps (1.0% overall) from aldehyde **2.39**, and a total of 45 steps to access the macrocyclic core. However, this represented the lone example of transannular assembly of the *cis*-THP, and highlights the

ability to rely on conformational bias of the macrocyclic backbone to promote diastereoselectivity. This provided support to the synthetic strategy in my doctoral research, which is presented in **Chapters 3** and **4**.

Key Installation Strategies (*Gangavaram V. M. Sharma and coworkers*, 2012)	
C9 – Regioselective epoxide-opening	**C11** – (L)-Malic Acid **2.223**
C13 – Chelation-controlled reduction (LiI)	***cis*-THP** – Transannular Oxymercuration
Macrocyclization – $RCM_{C7\text{-}C8}$ (Grubbs-II)	

2.8.3 Dai Group – 9-Desmethyl Total Synthesis (Purdue University, 2014)

The Dai group is interested in improving the synthesis of natural and unnatural products with innovative strategies and methodologies for a more efficient optimization of lead compounds (Scheme 2.24). Their work commonly employs transition-metal catalysis, and their synthesis of the unnatural 9-desmethylneopeltolide analogue was highlighted by a novel $Pd^{(II)}$-catalyzed cascade alkoxycarbonylative macrocyclization for assembly of the *cis*-THP ring. Synthesis began by iodination of alcohol **2.19**, which was prepared according to Fuwa's protocol from their 2009 manuscript (*vide supra*).[168] Lithiation of iodo-**2.242** by treatment with *t*-BuLi promoted addition to aldehyde **2.243**, and was unmasked with DDQ as an equal mixture of C7-diastereomers. Similar to She,[39] assembly of the *cis*-THP was accomplished by *trans*-oxypalladation of the C2-C3 olefin *via* 6-*exo*-trig cyclization of transition state **TS-27**. Chemoselectivity of this step was not reported. However, directing-effects may favor proximal attack over formation of the 12-membered oxacycle. The resultant *σ*-alkyl-metal intermediate undergoes migratory insertion of carbon monoxide *via* transition state **TS-28**, whereby terminating alcoholysis step is now intramolecular addition. Macrocyclization by intramolecular nucleophilic attack of C13-alcohol into the activated C=O bond of the *σ*-acyl-metal intermediate *via* **TS-29** provides both *cis*-diastereomers from their respective precursors with good yield and excellent selectivity[83] (58% from **7*S*-2.245**; 60% from **7*R*-2.246**). Analogue synthesis was completed by ketal hydrolysis, substrate-controlled reduction and Mitsunobu esterification with known acid;[271] formation of the derivatized analogue from ^{3R,7R}*cis*-**2.248** was not reported.

The Dai synthesis of 9-desmethylneopeltolide analogue **2.249** highlighted their novel cascade assembly of *cis*-THP rings and macrocyclic scaffolds. Including preparation of known alcohol **2.241**, this strategy required 14 linear steps to access the macrocyclic core of this analogue, from commercially-available **2.19**. Comparatively, this aligns well with the Paterson synthesis,[30] which shares the same starting material (refer to § 2.5.1). Recent modifications of this strategy by the Dai group have been reported in syntheses of spinosyn A[272] and *α*-levantenolide,[273] which employed $Pd^{(II)}$-catalyzed carbonylative Heck macrocyclization and spirolactonization cascades, respectively.

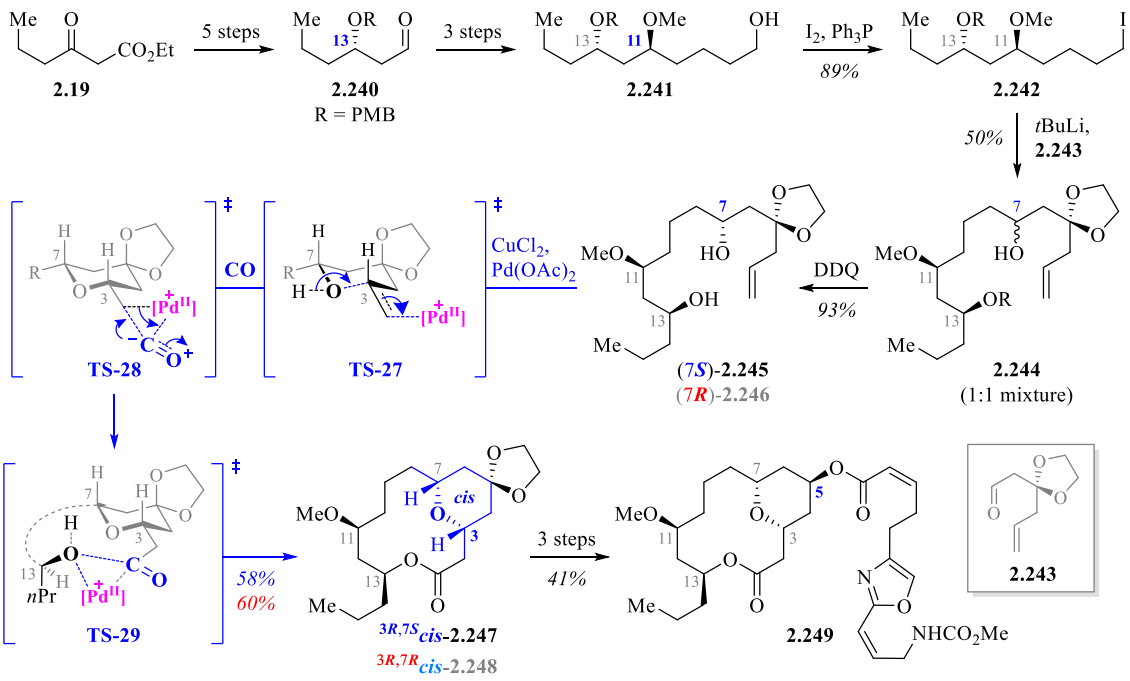

Scheme 2.24 – Summary of the Dai synthesis of 9-desmethylneopeltolide **2.249**, highlighted by their novel $Pd^{(II)}$-catalyzed cascade alkoxycarbonylative macrocyclization for assembly of the *cis*-THP. For purpose of space, only (**7*S***)-**2.245** is used to illustrate the key transformation; yields of each diastereomer are presented per color-coding.

2.8.4 Hoveyda Group – Total Synthesis (Massachusetts Institute of Technology, 2015)[44]

A major limitation of current metathesis catalysts is the inability to form *Z*-alkenes selectively and reliably, and was not until 2009 that a solution was disclosed.[274] Schrock and Hoveyda are synonymous with olefin metathesis, and their synthesis of neopeltolide (the last report, to date) exploited their extensive experience in this field and originally-developed catalysts to selectively address each key structural element (Scheme 2.25). Synthesis began with the three-step preparation[†††] of benzylated *endo*-oxabicycle-**2.251** from the cycloaddition of furan **2.250** and trichloroacetone **2.43**, according to the procedure of Hoffmann.[275] This *meso*-product is the key precursor for the desymmetrizing Mo-MAP-catalyzed ROCM strategy of *cis*-THP assembly. Following *in-situ* generation of chiral catalyst (***S***)-**2.254** by treatment of enol ether alkylidine **2.252** with butyl vinyl ether **2.253**, coordination to bicyclic **2.251** occurs *anti* to the pyrrolide ligand *via* transition state **TS-30** (Scheme 2.25). The freely-rotating aryloxide ligand directs substituents of the all-*syn*-metallacyclobutane intermediate **2.255** toward the smaller adamantylimido ligand, favoring formation of *Z*-alkene.[276,277] The high-energy all-*axial*-pyran **2.256** rapidly isomerizes to energetically-favored all-*equatorial* chair-like intermediate **2.257**, which is unlikely to participate in non-productive metathesis. Likewise, the stereogenic metal center undergoes an inversion during retro-[2+2]

[†††] The authors reported the preparation as a four-step sequence, which considered the reductive work-up of a non-isolated cycloaddition adduct; thus, was considered a single-step transformation for this review.

cycloaddition, sterically-limiting *inter*molecular metathesis and leading to the desired product **2.258** upon catalytic turnover. This efficient, enantio- and *Z*-selective process proved incredibly facile, furnishing gram-scale quantities of *Z*-*cis*-THP **2.258** in 88% yield, with nearly-exclusive selectivities, within 10 minutes at ambient temperature. The reagent-mediated selectivity controls the overall ROCM sequence akin to kinetic conditions, whereby use of *exo*-**2.251** or (***R***)-**2.252** facilitates erosion of enantiopurity[278] and formation of intermolecular metathesis by-products such as *meso*-*bis*-enol ether.

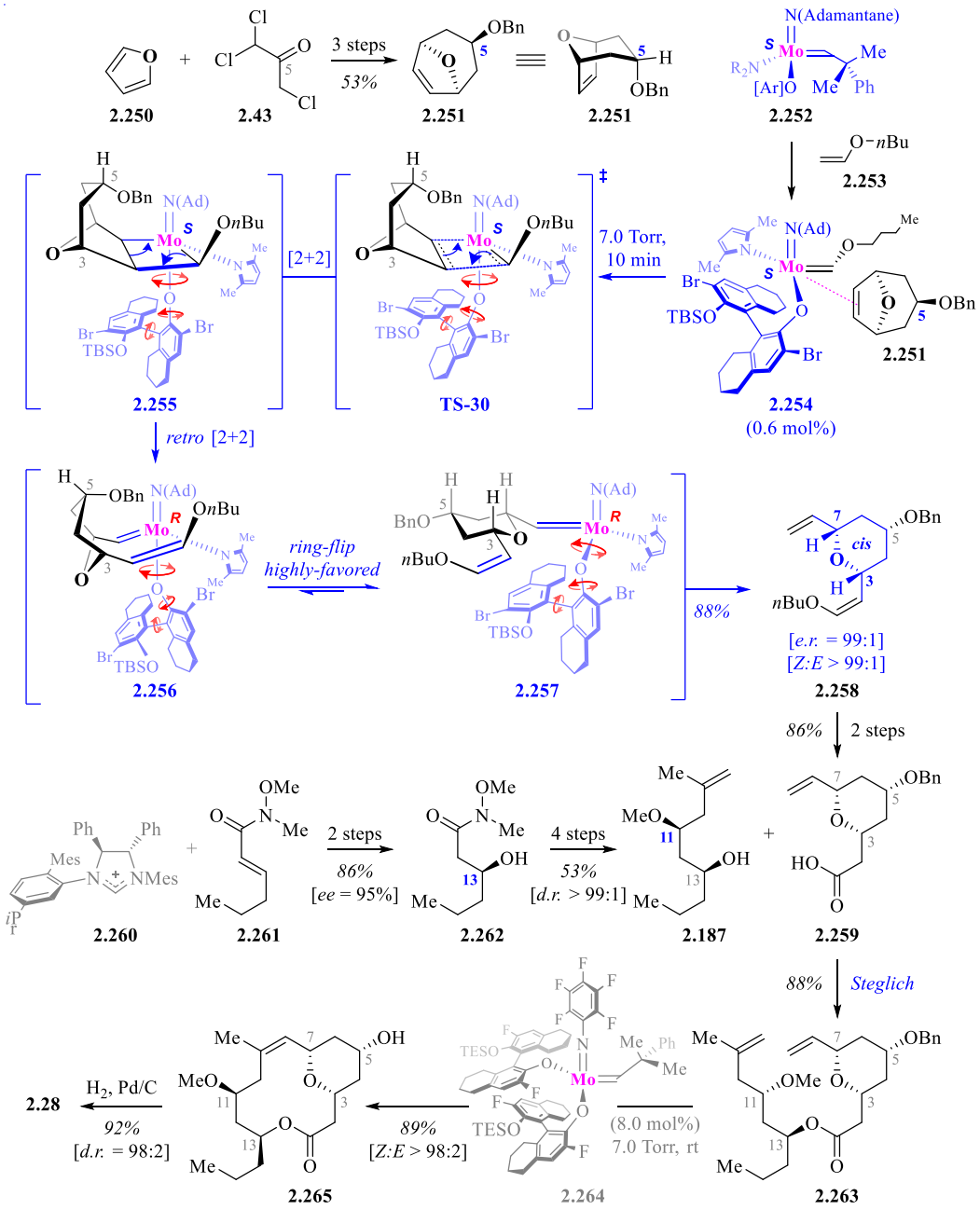

Scheme 2.25 – Summary of Hoveyda and coworkers' synthesis of the macrocyclic core of neopeltolide **2.28**, highlighted by enantiomeric ring-opening/cross-metathesis assembly of the ***cis***-THP using stereogenic-at-Mo catalysis. This route represents the most-efficient synthesis to date.

Conversion of **2.258** to acid **2.259** provided the coupling partner for alcohol **2.187** that was furnished by a short sequence including enantioselective conjugate borylation[279] of amide **2.261** and Evans-Tishchenko reduction.[60] Steglich esterification[280] furnished the full-carbon framework of the macrocyclic core, and was readily macrocyclized by RCM using chiral Mo-complex **2.264**.[281] Hydrogenation of **2.265** under substrate-control completed the formal synthesis of **2.28** with excellent *Z*- and diastereoselectivity.

Hoveyda and coworkers demonstrated the scope of their ability to catalytically install *Z*-olefins *via* preparation of the unsaturated oxazole-bearing side-chain using cross-metathesis (CM) and cross-coupling (CC) reactions (Scheme 2.26). Their *de novo* synthesis began with *Z*-selective CM of allylic carbamate **2.266** and **2.267**, using chiral Mo-MAP catalyst **2.252** from the ROCM reaction (Scheme 2.25) under modified conditions. Suzuki-coupling[173] with iodo-oxazole **2.269** maintained excellent *Z*-selectivity, and the alcohol was converted to alkene **2.270**. Ru-catechothiolate complex **2.272** catalyzed CM of **2.270** with commercial *Z*-diol **2.271** to afford **2.273**, which was oxidized to known acid **2.29** for Mitsunobu esterification with the macrocyclic core **2.28**.

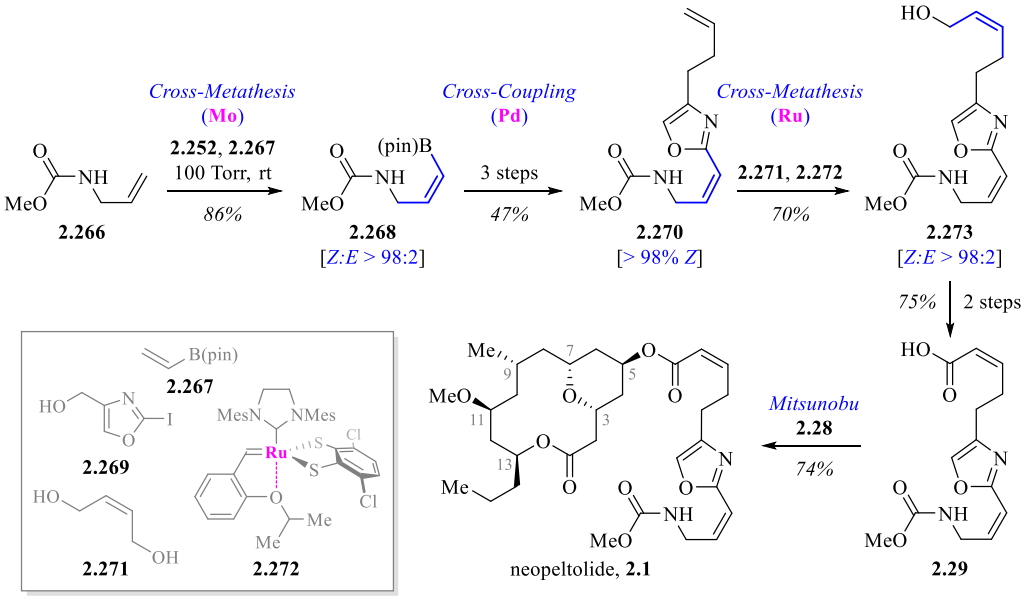

Scheme 2.26 – Completion of neopeltolide synthesis followed *de novo* synthesis of oxazole-bearing side-chain **2.29** *via* Mo-, Pd-, and Ru-catalyzed *Z*-selective CM/CC strategies.

Hoveyda and coworkers highlighted the immense potential of transition-metal catalysts in stereoselective olefin metathesis *via* originally-developed reagents. Their synthesis is the most-efficient to date, and required only 9 linear steps from readily-accessible furan and trichloroacetone, to access the macrocyclic core in 28.2% overall yield.

Key Installation Strategies (*Amir H. Hoveyda and coworkers*, 2014)	
C9 – Asymmetric hydrogenation (Pd)	**C11** – Evans-Tishchenko reduction
C13 – Asymmetric conjugate borylation	***cis*-THP** – Ring-opening/CM cascade (Mo)
Macrocyclization – $RCM_{C8\text{-}C9}$ (Mo)	

2.8.5 Transition-Metal-Activated Alkene Addition Conclusions

The use of transition-metals for the formation of *cis*-THP rings by nucleophilic addition into activated alkene systems has proven an incredibly efficient process. These reactions are usually high yielding with nearly-exclusive diastereoselective control under mild conditions and short reaction times. The molybdenum-based catalysts provided excellent *Z*-selectivity, but are incredibly water and air sensitive in comparison to the related ruthenium-based systems and restricted to vacuum atmospheres. Moreover, while the syntheses are generally very efficient, the overall simplicity of the strategy is hindered by the caveat of preparation and cost of the incredibly-intricate and non-commercial catalysts. Much like the abandoned use of rhodium-catalysis for commercial manufacture of sitagliptin (Chapter 1, § 1.4.3),[282] heavy metals make large-scale synthesis difficult due to cost, waste production, specialized equipment, and additional purification requirements. Lastly, chirality is transferred from the precursor substrates during assembly of the *cis*-THP rings, thus requiring the asymmetric installation of the hydroxy nucleophile into a scaffold that is designed to avoid *β*-elimination.[75]

Comparatively, the transition-metal-activated alkene addition represents an advantageous strategy for accessing the *cis*-THP of neopeltolide. Excluding Dai's novel synthesis,[‡‡‡] the generation of the macrocyclic core of neopeltolide *via* this strategy ($n = 3$) averaged 16.9% over 14 linear steps. Transition-metal methodologies for key assembly of the *cis*-THP averaged 85% with nearly-exclusive diastereoselectivity.

2.9 General Evaluation

It the decade since Wright isolated and identified neopeltolide as a novel natural product,[9,10] numerous groups have reported their work on the compound. To date, this work includes twelve total-,[17,18,24,28–30,34,37,43,44,81,98] eleven formal-,[27,31–33,35,36,38–42] seven analogue-,[70,99,168–170,202,244] and three fragment-syntheses.[131,145,242] Key structural elements of this natural product include a bicyclic 14-membered macrolactone core containing six stereogenic centers with defined configurations; three of these stereocenters exist within the embedded 2,4,6-trisubstituted tetrahydropryanyl ring system, with a *cis*-bridged ether and oxazole-bearing side-chain attached to the *β*-hydroxy. These publications highlight many common strategies for the assembly of *cis*-disubstituted THPs, and in some cases, have developed innovative modifications and cascading reaction sequences.

[‡‡‡] Synthesis is not considered due to unreported yields in accessing advanced intermediate substrate by Fuwa's method.

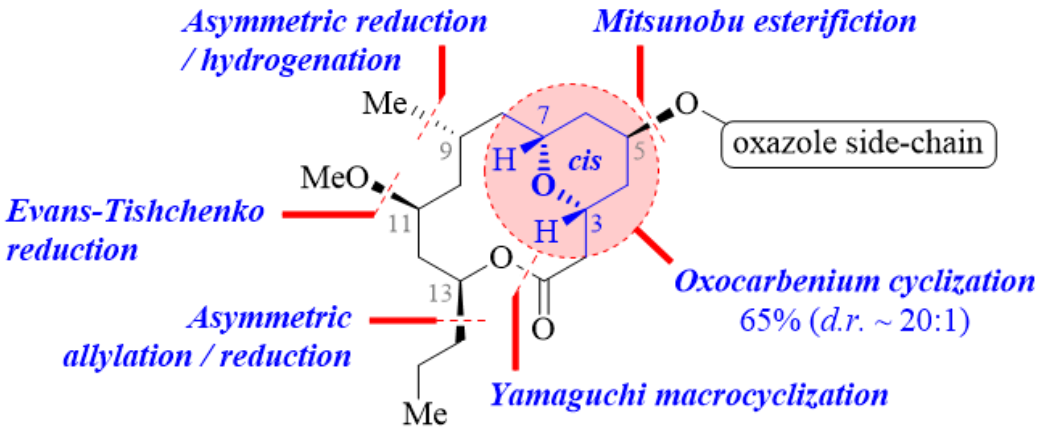

Figure 2.5 – Retrosynthetic evaluation of neopeltolide based on most commonly-employed strategies to access key structural elements of the macrocyclic core neopeltolide. Average yield and diastereoselectivity are presented based on ***cis***-THP assembly *via* oxocarbenium ion cyclization strategies (n = 8).

After presenting the complete synthetic work directed toward neopeltolide, the following short discussion underscores basic aspects of neopeltolide chemistry (Figure 2.5). Please refer to the supporting information for a table that lists and groups the strategies used to install key structural elements of the macrocyclic core of **2.1**, from the 22 unique and successful syntheses.

2.9.1 C9-Methyl Installation

Installation of the C9-methyl group relied on diastereoselective reduction, and proved to be dependent on the stage of its synthesis. Late-stage installation was substrate-controlled (for example, please see Scheme 2.6), and allowed mild hydrogenation to proceed selectively by treatment with catalytic metal (§ 2.8.2). Conversely, early-stage installation was reagent-controlled, and required specific conditions to prove selective (§ 2.5.2). Enzymatic desymmetrization (§ 2.5.3) and the use of commercially-available chiral building blocks represent the other strategies used for its incorporation.

2.9.2 C11-C13 Anti-Selectivity

Generation of the *anti*-diol presented great variation in synthetic strategy, but was most efficiently-installed by Evans-Tishchenko stereoselective reduction protocol (for example, please see Scheme 2.22). The clear benefit of this strategy is concomitant protection of the directing C13-β-hydroxy, while selectively reducing the C11-carbonyl. Accessing the requisite β-hydroxy substrate was accomplished under a variety of asymmetric reductive processes, or through asymmetric allylation conditions (§ 2.7.1); the latter represents the most-common alternative for installation of the C11-alcohol.

2.9.3 cis-THP Assembly

As the emphasis of this review chapter, it has been illustrated that many common strategies have been successfully-employed for assembly of the *cis*-THP ring system of neopeltolide. Use of a Prins-type oxocarbenium ion cyclization represents 40% of successful syntheses, and this propensity likely arises from operational simplicity and high-degree of stereocontrol (§ 2.2–2.3). Formation 2,6-*cis*-THPs by this strategy is typically diastereotopic however, and relies on the transfer of chirality from starting material. Scheidt (§ 2.2.2) and Lee (§ 2.3.2) use of Prins-type cyclization efficiently furnished the THP and macrolactone core in one step, which was also accomplished by Dai *via* his novel $Pd^{(II)}$-catalyzed alkoxycarbonylative macrocyclization cascade (§ 2.8.3). Of interest is the stage of pyran assembly precedes macrocyclization in every other synthesis; Sharma's transannular oxymercuration of the pre-assembled 14-membered lactone (§ 2.8.2) is the lone exception.

2.9.4 Macrocyclization

Like most macrolide natural products, the ester (lactone) bond of neopeltolide represents an attractive disconnection; similarly, the paradigm ring-closure strategy employed carboxyl-activation as a mixed-anhydride. Greater than 60% of publications used Yamaguchi's esterification conditions to access the macrocyclic core of neopeltolide, despite its attendant protecting group manipulations and oxidation state adjustments. In addition to single-step and cascade sequences used for ring-closure of both the *cis*-THP and macrolactone, metathesis represents the only alternative strategy used. Unfortunately, these conditions required forcing conditions that included high catalyst-loading and elevated temperatures, or proved to be an insurmountable obstacle (§ 2.7.5).

2.9.2 Oxazole-Bearing Side-Chain

Greater than 90% employ Mitsunobu esterification conditions to install the oxazole-bearing side-chain. The ubiquitous employment of the Mitsunobu reaction can be explained by the selectivity of substrate-controlled keto reduction favoring formation of the α-pyranyl product from the C5-*cis*-pyranone. Worth mention is Hoveyda's *de novo* synthesis of the side-chain acid fragment, highlighting his transition-metal-catalyzed *Z*-selective cross-metathesis in the most-efficient synthesis of both neopeltolide and its side-chain (§ 2.8.4). Panek's use of Still-Gennari olefination (§ 2.2.1) was established to circumvent an additional inversion of the proper C5-alcohol configuration obtained from oxymercuration.

2.10 Conclusions and Prospects

Neopeltolide is a polyketide natural product with unique and potent bioactivity, which holds great promise as an anticancer agent that rivals paclitaxel. The bioactive potential and combined structural complexity has led to 23 research groups from the international synthetic community that have published at least one synthetic effort on-or-toward this natural product. These studies have enabled the elucidation of its correct structure, prepared sufficient material for biological evaluation and identification of putative cellular targets, and have led to an extension into analogue design and establishment of SAR. More importantly, the sum of these efforts illustrated common synthetic strategies for the assembly of 2,6-*cis*-disubstituted tetrahydropyran rings, and included innovative modifications and cascades. These synthetic efforts have shown there exists a great interest in this structural feature, and to improve the efficiency of its assembly to minimize step-count and maximize yield and selectivity – the holy grail of chemical synthesis. Natural product total synthesis remains a cornerstone of organic chemistry; the study of neopeltolide is a reminder of the impetus for developing strategies to facilitate rapid, reliable, and sustainable production of bioactive compounds for drug discovery.

2.11 References

(1) Martins, A.; Vieira, H.; Gaspar, H.; Santos, S. *Mar. Drugs* **2014**, *12* (2), 1066–1101.
(2) Xiong, Z.-Q.; Wang, J.-F.; Hao, Y.-Y.; Wang, Y. *Mar. Drugs* **2013**, *11* (3), 700–717.
(3) Hu, Y.; Chen, J.; Hu, G.; Yu, J.; Zhu, X.; Lin, Y.; Chen, S.; Yuan, J. *Mar. Drugs* **2015**, *13* (1), 202–221.
(4) Gerwick, W. H.; Moore, B. S. *Chem. Biol.* **2012**, *19* (1), 85–98.
(5) Lindequist, U. *Biomol. Ther.* **2016**, *24* (6), 561–571.
(6) Leal, M. C.; Puga, J.; Serôdio, J.; Gomes, N. C. M.; Calado, R. *PLoS One* **2012**, *7* (1).
(7) Mayer, A. M. S. Marine Pharmaceuticals: The Clinical Pipeline http://marinepharmacology.midwestern.edu/clinPipeline.htm.
(8) Bauer, A. In *Topics in Heterocyclic Chemistry*; Cossy, J., Ed.; Springer, 2016; pp 209–270.
(9) Wright, A. E.; Botelho, J. C.; Guzmán, E.; Harmody, D.; Linley, P.; McCarthy, P. J.; Pitts, T. P.; Pomponi, S.; Reed, J. K. *J. Nat. Prod.* **2007**, *70* (3), 412–416.
(10) Wright, A. E.; Pomponi, S. A.; McCarthy, P. J. Biologically Active Neopeltolide Compounds. US 7,179,828 B2, 2007.
(11) D'Ambrosio, M.; Guerriero, A.; Pietra, F.; Debitus, C. *Helv. Chim. Acta* **1996**, *79* (1), 51–60.
(12) Sollas, W. J. In *Report on the Scientific Results of the Voyage of H.M.S. Challenger During the Years 1873-76*; 1888; Vol. 25, pp 284–346.
(13) Kelly, M. *ZooSystema* **2000**, *22* (2), 265–283.
(14) Winder, P. L.; Pomponi, S. A.; Wright, A. E. *Mar. Drugs* **2011**, *9* (12), 2643–2682.
(15) Stott, K.; Keeler, J.; Van, Q. N.; Shaka, A. J. *J. Magn. Reson.* **1997**, *125* (2), 302–324.
(16) Custar, D. W. I . Studies Toward the Total Synthesis of Chrolactomycin and Okilactomycin II . Total Synthesis , Structural Reassignment and Biological Evaluation of Neopeltolide, Northwestern University, 2009.
(17) Youngsaye, W.; Lowe, J. T.; Pohlki, F.; Ralifo, P.; Panek, J. S. *Angew. Chem. Int. Ed.* **2007**, *46* (48), 9211–9214.
(18) Custar, D. W.; Zabawa, T. P.; Scheidt, K. A. *J. Am. Chem. Soc.* **2008**, *130* (3), 804–805.
(19) Oberlies, N. H.; Kroll, D. J. *J. Nat. Prod.* **2004**, *67*, 129–135.
(20) Perez, E.; Buckwalter, C. *Cancer Chemoth. Pharm.* **1998**, *41* (6), 448–452.
(21) Dong, X.; Mattingly, C.; Tseng, M. T.; Cho, M. J.; Liu, Y.; Adams, V. R.; Mumper, R. J. *Cancer Res.* **2009**, *69* (9), 3918–3926.
(22) Gunasekera, S. P.; Wright, A. E. In *Anticancer Agents from Natural Products*; Kingston, D. G. I., Cragg, G. M., Newman, D. J., Eds.; CRC Press, 2005; pp 171–190.
(23) Wang, Z.; Sun, Y. *Transl. Oncol.* **2010**, *3* (1), 1–12.
(24) Ulanovskaya, O.; Janjic, J.; Suzuki, M.; Sabharwal, S. S.; Schumacker, P. T.; Kron, S. J.; Kozmin, S. *Nat. Chem. Biol.* **2008**, *4* (7), 418–424.
(25) Altmann, K.-H.; Carreira, E. M. *Nat. Chem. Biol.* **2008**, *4* (7), 388–389.
(26) Bertram, J. S. *Mol. Aspects Med.* **2000**, *21*, 167–223.
(27) Vintonyak, V. V; Maier, M. E. *Org. Lett.* **2008**, *10* (6), 1239–1242.
(28) Woo, S. K.; Kwon, M. S.; Lee, E. *Angew. Chem. Int. Ed.* **2008**, *47* (17), 3242–3244.
(29) Fuwa, H.; Naito, S.; Goto, T.; Sasaki, M. *Angew. Chem.* **2008**, *120* (25), 4815–4817.
(30) Paterson, I.; Miller, N. *Chem. Commun.* **2008**, No. 39, 4708–4710.
(31) Taylor, R. E.; Kartika, R.; Gruffi, T. R. *Org. Lett.* **2008**, *10* (21), 5047–5050.
(32) Tu, W.; Floreancig, P. E. *Angew. Chem. Int. Ed.* **2009**, *48* (25), 4567–4571.
(33) Kim, H.; Park, Y.; Hong, J. *Angew. Chem. Int. Ed.* **2009**, *48* (41), 7577–7581.
(34) Guinchard, X.; Roulland, E. *Org. Lett.* **2009**, *11* (20), 4700–4703.
(35) Yadav, J. S.; Krishana, G. G.; Kumar, S. N. *Tetrahedron* **2010**, *66* (2), 480–487.
(36) Fuwa, H.; Saito, A.; Sasaki, M. *Angew. Chem.* **2010**, *122* (17), 3105–3108.
(37) Fuwa, H.; Kawakami, M.; Noto, K.; Muto, T.; Suga, Y. *Chem. Eur. J.* **2013**, *19*, 8100–8110.
(38) Martinez-Solorio, D.; Jennings, M. P. *J. Org. Chem.* **2010**, *75* (12), 4095–4104.
(39) Yang, Z.; Zhang, B.; Zhao, G.; Yang, J.; Xie, X.; She, X. *Org. Lett.* **2011**, *13* (21), 5916–5919.
(40) Sharma, G. V. M.; Reddy, S. V.; Ramakrishna, K. V. S. *Org. Biomol. Chem.* **2012**, *10* (18), 3689–3695.
(41) Raghavan, S.; Samanta, P. K. *Org. Lett.* **2012**, *14* (9), 2346–2349.
(42) Athe, S.; Chandrasekhar, B.; Roy, S.; Pradhan, T. K.; Ghosh, S. *J. Org. Chem.* **2012**, *77*, 9840–9845.
(43) Ghosh, A. K.; Shurrush, K. A.; Dawson, Z. L. *Org. Biomol. Chem.* **2013**, *11* (44), 7768–7777.

(44) Yu, M.; Schrock, R. R.; Hoveyda, A. H. *Angew. Chem. Int. Ed.* **2015**, *54* (1), 215–220.
(45) Youngsaye, W. I. Total Synthesis, Stereochemical Reassignment, and Biological Evalution of (+)-Neopeltolide and Related Stereoisomers. II. Development of Chiral Benzylsilanes: Reagents For Stereoselective, Silicon-Mediated Oxa-Pictet-Spengler Reactions., Boston University, 2010.
(46) Masse, C. E.; Panek, J. S. *Chem. Rev.* **1995**, *95* (5), 1293–1316.
(47) Panek, J. S.; Yang, M. *J. Am. Chem. Soc.* **1991**, *113* (17), 6594–6600.
(48) Huang, H.; Panek, J. S. *J. Am. Chem. Soc.* **2000**, *122*, 9836–9837.
(49) Su, Q.; Dakin, L.; Panek, J. S. *J. Org. Chem.* **2007**, *72* (1), 2–24.
(50) Arefolov, A.; Panek, J. S. *J. Am. Chem. Soc.* **2005**, *127* (15), 5596–5603.
(51) Huang, H.; Panek, J. S. *Org. Lett.* **2004**, *6* (23), 4383–4385.
(52) Lowe, J. T.; Wrona, I. E.; Panek, J. S. *Org. Lett.* **2007**, *9* (2), 327–330.
(53) Su, Q.; Panek, J. S. *J. Am. Chem. Soc.* **2004**, *126*, 2425–2430.
(54) Huang, H.; Panek, J. S. *Org. Lett.* **2001**, *3* (11), 1693–1696.
(55) Yun, Z.; Panek, J. S. *Org. Lett.* **2007**, *9* (16), 3141–3143.
(56) Lowe, J. T.; Panek, J. S. *Org. Lett.* **2008**, *10* (17), 3813–3816.
(57) Lee, J.; Panek, J. S. *Org. Lett.* **2011**, *13* (3), 502–505.
(58) Zhang, Y.; Panek, J. S. *Org. Lett.* **2009**, *11* (15), 3366–3369.
(59) Gröbel, B. T.; Seebach, D. *Synthesis*, **1977**, *6*, 357–402.
(60) Evans, D. A.; Hoveyda, A. H. *J. Am. Chem. Soc.* **1990**, *112* (17), 6447–6449.
(61) Yamaguchi, M.; Inanaga, J.; Hirata, K.; Saeki, H.; Katsuki, T. *Bull. Chem. Soc. Jpn.* **1979**, *52* (7), 1989–1993.
(62) Mitsunobu, O. *Synthesis*, **1981**, 1–28.
(63) Still, W. C.; Gennari, C. *Tetrahedron Lett.* **1983**, *24* (41), 4405–4408.
(64) Morris, W. J.; Custar, D. W.; Scheidt, K. A. *Org. Lett.* **2005**, *7* (6), 1113–1116.
(65) Hoye, T. R.; Danielson, M. E.; May, A. E.; Zhao, H. *Angew. Chem. Int. Ed.* **2008**, *47* (50), 9743–9746.
(66) Tokunaga, M.; Ohkuma, T.; Noyori, R. *Org. Synth.* **1992**, *71*, 1.
(67) Myers, A. G.; Yang, B. H.; Chen, H.; McKinstry, L.; Kopecky, D. J.; Gleason, J. L. *J. Am. Chem. Soc.* **1997**, *119*, 6496–6511.
(68) Mitsunobu, O.; Yamada, M.; Mukaiyama, T. *Bull. Chem. Soc. Jpn.* **1967**, *40* (4), 935–939.
(69) Hornberger, K. R.; Hamblett, C. L.; Leighton, J. L. *J. Am. Chem. Soc.* **2000**, *122* (51), 12894–12895.
(70) Custar, D. W.; Zabawa, T. P.; Hines, J.; Crews, C. M.; Scheidt, K. A. *J. Am. Chem. Soc.* **2009**, *131* (34), 12406–12414.
(71) Crane, E. A.; Zabawa, T. P.; Farmer, R. L.; Scheidt, K. A. *Angew. Chem. Int. Ed.* **2011**, *50*, 9112–9115.
(72) Tenenbaum, J. M.; Morris, W. J.; Custar, D. W.; Scheidt, K. A. *Angew. Chem. Int. Ed.* **2011**, *50*, 5892–5895.
(73) Clarke, P. A.; Santos, S. *Eur. J. Org. Chem.* **2006**, No. 9, 2045–2053.
(74) Nasir, N. M.; Ermanis, K.; Clarke, P. A. *Org. Biomol. Chem.* **2014**, *12*, 3323–3335.
(75) Perry, M. A.; Rychnovsky, S. D.; Sizemore, N. In *Synthesis of Saturated Oxygenated Heterocycles I*; Cossy, J., Ed.; Springer-Verlag, 2014; pp 43–95.
(76) Fuwa, H. *Mar. Drugs* **2016**, *14* (65).
(77) Prins, H. J. *Chem. Weekbl.* **1919**, *16* (64), 1072, 1510.
(78) Crane, E.; Scheidt, K. *Angew. Chem. Int. Ed.* **2010**, *49* (45), 8316–8326.
(79) Han, X.; Peh, G.; Floreancig, P. E. *Eur. J. Org. Chem.* **2013**, No. 7, 1193–1208.
(80) Hanschke, E. *Chem. Ber.* **1955**, *88*, 1053–1061.
(81) Vintonyak, V. V; Kunze, B.; Sasse, F.; Maier, M. E. *Chemistry (Easton).* **2008**, *14* (35), 11132–11140.
(82) Kubota, K.; Leighton, J. L. *Angew. Chem. Int. Ed.* **2003**, *42* (8), 946–948.
(83) The selectivity of this transformation was not reported by the authors.
(84) ter Horst, B.; Feringa, B. L.; Minnaard, A. J. *Chem. Commun.* **2007**, *5* (5), 489–491.
(85) ter Horst, B.; Feringa, B. L.; Minnaard, A. J. *Org. Lett.* **2007**, *9* (16), 3013–3015.
(86) Fukuyama, T.; Lin, S. C.; Li, L. *J. Am. Chem. Soc.* **1990**, *112* (19), 7050–7051.
(87) Lee, C.-L. K.; Lee, C.-H. A.; Tan, K.-T.; Loh, T.-P. *Org. Lett.* **2004**, *6* (8), 1281–1283.
(88) Hosomi, A.; Sakurai, H. *Tetrahedron Lett.* **1976**, *17* (16), 1295–1298.
(89) Steglich, W.; Höfle, G. *Angew. Chem. Int. Ed.* **1969**, *8* (12), 981–981.
(90) Brown, H.; Jadhav, P. K. *J. Am. Chem. Soc.* **1983**, *105* (4), 2092–2093.
(91) Kozmin, S. *Org. Lett.* **2001**, *3* (5), 755–758.
(92) Wang, Y.; Janjic, J.; Kozmin, S. *J. Am. Chem. Soc.* **2002**, *124* (46), 13670–13671.

(93) Wang, Y.; Janjic, J.; Kozmin, S. *Pure Appl. Chem.* **2005**, *77* (7), 1161–1169.
(94) Nussbaumer, C. *Helv. Chim. Acta* **1987**, *70*, 396–401.
(95) Tsuji, J. *Synthesis*, **1984**, *1984* (5), 369–384.
(96) Paterson, I.; Gibson, K. R.; Oballa, R. M. *Tetrahedron Lett.* **1996**, *37* (47), 8585–8588.
(97) Chen, K. M.; Hardtmann, G. E.; Prasad, K.; Repič, O.; Shapiro, M. J. *Tetrahedron Lett.* **1987**, *28* (2), 155–158.
(98) Cui, Y.; Tu, W.; Floreancig, P. E. *Tetrahedron* **2010**, *66* (26), 4867–4873.
(99) Cui, Y.; Balachandran, R.; Day, B. W.; Floreancig, P. E. *J. Org. Chem.* **2012**, *77*, 2225–2235.
(100) Han, X.; Floreancig, P. E. *Org. Lett.* **2012**, *14* (14), 3808–3811.
(101) Clausen, D. J.; Floreancig, P. E. *J. Org. Chem.* **2012**, *77* (15), 6574–6582.
(102) Liu, L.; Floreancig, P. E. *Angew. Chem. Int. Ed.* **2010**, *49* (34), 5894–5897.
(103) Liu, L.; Floreancig, P. E. *Angew. Chem. Int. Ed.* **2010**, *49* (17), 3069–3072.
(104) Tu, W.; Liu, L.; Floreancig, P. E. *Angew. Chem. Int. Ed.* **2008**, *47* (22), 4184–4187.
(105) Floreancig, P. E. *Synlett* **2007**, *3* (2), 191–203.
(106) Seiders, J. R.; Wang, L.; Floreancig, P. E. *J. Am. Chem. Soc.* **2003**, *125* (9), 2406–2407.
(107) Wang, L.; Seiders, J. R.; Floreancig, P. E. *Electrochemistry* **2004**, No. 4, 12596–12603.
(108) Liu, L.; Floreancig, P. E. *Org. Lett.* **2009**, *11* (14), 3152–3155.
(109) Brizgys, G. J.; Jung, H. H.; Floreancig, P. E. *Chem. Sci.* **2012**, *3* (2), 438.
(110) Cui, Y.; Floreancig, P. E. *Org. Lett.* **2012**, *14* (7), 1720–1723.
(111) Peh, G.; Floreancig, P. E. *Org. Lett.* **2012**, *14* (21), 5614–5617.
(112) Jung, H. H.; Seiders, J. R.; Floreancig, P. E. *Angew. Chem. Int. Ed.* **2007**, *46* (44), 8464–8467.
(113) Sonogashira, K.; Tohda, Y. *Tetrahedron Lett.* **1975**, No. 50, 4467–4470.
(114) Rama Rao, A. V.; Reddy, E. R.; Joshi, B. V.; Yadav, J. S. *Tetrahedron Lett.* **1987**, *28* (51), 6497–6500.
(115) Yadav, J. S.; Reddy, M. S.; Prasad, A. R. *Tetrahedron Lett.* **2005**, *46* (12), 2133–2136.
(116) Yadav, J. S.; Reddy, M. S.; Prasad, A. R. *Tetrahedron Lett.* **2006**, *47* (29), 4995–4998.
(117) Yadav, J. S.; Rao, P. P.; Reddy, M. S.; Rao, N. V.; Prasad, A. R. *Tetrahedron Lett.* **2007**, *48* (8), 1469–1471.
(118) Yadav, J. S.; Reddy, M. S.; Rao, P. P.; Prasad, A. R. *Tetrahedron Lett.* **2006**, *47* (26), 4397–4401.
(119) Yadav, J. S.; Reddy, M. S.; Prasad, A. R. *Tetrahedron Lett.* **2006**, *47* (28), 4937–4941.
(120) Lewis, M. D.; Cha, J. K.; Kishi, Y. *J. Am. Chem. Soc.* **1982**, *104* (8), 4976–4978.
(121) Ding, F.; Jennings, M. P. *J. Org. Chem.* **2008**, *73* (15), 5965–5976.
(122) Jennings, M. P.; Clemens, R. T. *Tetrahedron Lett.* **2005**, *46* (12), 2021–2024.
(123) Ding, F.; Jennings, M. P. *Org. Lett.* **2005**, *7* (12), 2321–2324.
(124) Sawant, K. B.; Jennings, M. P. *J. Org. Chem.* **2006**, *71* (20), 7911–7914.
(125) Carrick, J. D.; Jennings, M. P. *Org. Lett.* **2009**, *11* (3), 769–772.
(126) Jennings, M. P.; Clemens, R. T. *Tetrahedron Lett.* **2005**, *46* (12), 2021–2024.
(127) Scholl, M.; Ding, S.; Lee, C. W.; Grubbs, R. H. *Org. Lett.* **1999**, *1* (6), 953–956.
(128) Nahm, S.; Weinreb, S. M. *Tetrahedron Lett.* **1981**, *160* (10), 26.
(129) Evans, D.; Gauchet-Prunet, J. *J. Org. Chem.* **1993**, *58* (9), 2446–2453.
(130) Ashby, E. C. *Q. Rev. Chem. Soc.* **1967**, *21* (2), 259.
(131) Mineeva, I. V. *Russ. J. Org. Chem.* **2015**, *51* (8), 1083–1092.
(132) Mineeva, I. V. *Russ. J. Org. Chem.* **2016**, *52* (3), 355–367, (and the references therein).
(133) Danishefsky, S.; Kitahara, T. *J. Am. Chem. Soc.* **1974**, *11*, 7807–7808.
(134) Norcross, R. D.; Paterson, I. *Chem. Rev.* **1995**, *95* (April), 2041–2114.
(135) Paterson, I.; Findlay, A. D. *Aust. J. Chem.* **2009**, *62* (7), 624–638.
(136) Paterson, I.; Findlay, A. D.; Florence, G. J. *Tetrahedron* **2007**, *63* (26), 5806–5819.
(137) Paterson, I.; Florence, G. J.; Heimann, A. C.; Mackay, A. C. *Angew. Chem. Int. Ed.* **2005**, *44* (7), 1130–1133.
(138) Paterson, I.; Davies, R. D. M.; Heimann, A. C.; Marquez, R.; Meyer, A. *Org. Lett.* **2003**, *5* (23), 4477–4480.
(139) Paterson, I.; De Savi, C.; Tudge, M. *Org. Lett.* **2001**, *3* (20), 3149–3152.
(140) Paterson, I.; Luckhurst, C. A. *Tetrahedron Lett.* **2003**, *44* (19), 3749–3754.
(141) Paterson, I. *Tetrahedron* **2003**, *59* (35), 6833–6849.
(142) Wadsworth, W. S.; Emmons, W. D. *J. Am. Chem. Soc.* **1961**, *83* (7), 1733–1738.
(143) Ouellet, S. G.; Tuttle, J. B.; MacMillan, D. W. C. *J. Am. Chem. Soc.* **2005**, *127* (1), 32–33.
(144) Dossetter, A. G.; Jamison, T. F.; Jacobsen, E. N. *Angew. Chem. Int. Ed.* **1999**, *38* (16), 2398–2400.
(145) Hartmann, E.; Oestreich, M. *Angew. Chem. Int. Ed.* **2010**, *49* (35), 6195–6198.
(146) Schaus, S. E.; Brånalt, J.; Jacobsen, E. N. *J. Org. Chem.* **1998**, *63* (2), 403–405.

(147) Ireland, R. E.; Mueller, R. H. *J. Am. Chem. Soc.* **1972**, *94* (16), 5897–5898.
(148) La Cruz, T. E.; Rychnovsky, S. D. *J. Org. Chem.* **2007**, *72* (7), 2602–2611.
(149) Kim, I. S.; Ngai, M.-Y.; Krische, M. J. *J. Am. Chem. Soc.* **2008**, *130* (44), 14891–14899.
(150) The *cis*-tetrahydropyranone form of neopeltolide's macrocyclic core represents a formal synthesis of the natural product; however, to accurately compare linear steps of each publication, one must consider the necessary addition of the C5-keto-reduction.
(151) Raghavan, S.; Rajendar, S. *Tetrahedron Lett.* **2013**, *69*, 4835–4844.
(152) Raghavan, S.; Vinoth Kumar, V. *Org. Biomol. Chem.* **2013**, *11*, 2847–2858.
(153) Raghavan, S.; Samanta, P. K. *Tetrahedron Lett.* **2014**, *55*, 913–915.
(154) Raghavan, S.; Samanta, P. K. *Synlett* **2013**, *24* (15), 1983–1987.
(155) Raghavan, S.; Nyalata, S. *J. Org. Chem.* **2016**, *81*, 10698–10706.
(156) Ghosh, A. K.; Chen, Z. H.; Effenberger, K. A.; Jurica, M. S. *J. Org. Chem.* **2014**, *79* (12), 5697–5709.
(157) Ghosh, A. K.; Chen, Z. H. *Org. Lett.* **2013**, *15* (19), 5088–5091.
(158) Ghosh, A. K.; Li, J. *Org. Lett.* **2011**, *13* (1), 1631–1634.
(159) Ghosh, A. K.; Cheng, X. *Org. Lett.* **2011**, *13* (15), 4108–4111.
(160) Ghosh, A. K.; Cheng, X.; Bai, R.; Hamel, E. *Eur. J. Org. Chem.* **2012**, No. 22, 4130–4139.
(161) Ghosh, A. K.; Li, J. *Org. Lett.* **2009**, *11* (18), 4164–4167.
(162) Ghosh, A. K.; Gong, G. *Chem. Asian J.* **2008**, *3* (10), 1811–1823.
(163) Ghosh, A. K.; Gong, G. *Org. Lett.* **2007**, *9* (8), 1437–1440.
(164) Ghosh, A. K.; Kai, X. *Org. Lett.* **2007**, *9* (20), 4013–4016.
(165) Ghosh, A. K.; Ren, G. B. *J. Org. Chem.* **2012**, *77* (5), 2559–2565.
(166) Oshima-Hirayama, N.; Yoshikawa, K.; Nishioka, T.; Oda, J. J. *Eur. J. Biochem.* **1993**, *215*, 239–246.
(167) Pappo, R.; Allen, Jr., D. S.; Lemieux, R. U.; Johnson, W. S. *J. Org. Chem.* **1956**, *21* (4), 478–479.
(168) Fuwa, H.; Saito, A.; Naito, S.; Konoki, K.; Yotsu-Yamashita, M.; Sasaki, M. *Chem. Eur. J.* **2009**, *15*, 12807–12818.
(169) Fuwa, H.; Noto, K.; Kawakami, M.; Sasaki, M. *Chem. Lett.* **2013**, *42* (9), 1020–1022.
(170) Fuwa, H.; Noguchi, T.; Kawakami, M.; Sasaki, M. *Bioorg. Med. Chem. Lett.* **2014**, *24*, 2415–2419.
(171) Fuwa, H.; Sato, M.; Sasaki, M. *Mar. Drugs* **2014**, *12*, 5576–5589.
(172) Katsuki, T.; Sharpless, K. B. *J. Am. Chem. Soc.* **1980**, *102* (18), 5974–5976.
(173) Miyaura, N.; Suzuki, A. *Chem. Rev.* **1995**, *95* (7), 2457–2483.
(174) Taber, D. F.; Deker, P. B.; Silverberg, L. J. *J. Org. Chem.* **1992**, *57*, 5990–5994.
(175) Chakraborty, T. K.; Suresh, V. R. *Chem. Lett.* **1997**, *6*, 565–566.
(176) Evans, D. A.; Ennis, M. D.; Mathre, D. J. *J. Am. Chem. Soc.* **1982**, *104*, 1737–1739.
(177) Giese, B.; Kopping, B.; Göbel, T.; Dickhaut, J.; Thoma, G.; Kulicke, K. J.; Trach, F. In *Organic Reactions, Vol. 48*; Paquette, L. A., Ed.; John Wiley & Sons, Inc., 1996; pp 301–856.
(178) Jasperse, C. P.; Curran, D. P.; Fevig, T. L. *Chem. Rev.* **1991**, *91*, 1237–1286.
(179) Lee, E. *Pure Appl. Chem.* **2005**, *77* (12), 2073–2081.
(180) Beckwith, A. L. J.; Easton, C. J.; Serelis, A. K. *J. Chem. Soc., Chem. Commun.* **1980**, 482–483.
(181) Beckwith, A. L. J.; Schiesser, C. H. *Tetrahedron* **1985**, *41* (19), 3925–3941.
(182) Baldwin, J. *J. Chem. Soc., Chem. Commun.* **1976**, 734–736.
(183) Lee, E.; Cho, Y. *Tetrahedron Lett.* **1997**, *38* (44), 7757–7758.
(184) Lee, E.; Tae, J. S. *Tetrahedron Lett.* **1993**, *34* (30), 4831–4834.
(185) Kartika, R.; Gruffi, T. R.; Taylor, R. E. *Org. Lett.* **2008**, *10* (21), 5047–5050.
(186) Taylor, R. E.; Chen, Y.; Beatty, A.; Myles, D. C.; Zhou, Y. *J. Am. Chem. Soc.* **2003**, *125*, 26–27.
(187) Chang, C. F.; Stefan, E.; Taylor, R. E. *Chem. Eur. J.* **2015**, *21* (30), 10681–10686.
(188) Anderl, T.; Nicolas, L.; Münkemer, J.; Muthukumar, Y.; Baro, A.; Frey, W.; Sasse, F.; Taylor, R. E.; Laschat, S. *Eur. J. Org. Chem.* **2011**, *4* (36), 7294–7307.
(189) Zhao, Z.; Taylor, R. E. *Org. Lett.* **2012**, *14* (3), 669–671.
(190) Larsen, E. M.; Wilson, M. R.; Zajicek, J.; Taylor, R. E. *Org. Lett.* **2013**, *15* (20), 5246–5249.
(191) Larsen, E. M.; Wilson, M. R.; Taylor, R. E. *Nat. Prod. Rep.* **2015**, *32* (8), 1183–1206.
(192) Kartika, R.; Frein, J. D.; Taylor, R. E. *J. Org. Chem.* **2008**, *73*, 5592–5594.
(193) Kartika, R.; Taylor, R. E. *Angew. Chem. Int. Ed.* **2007**, *46* (36), 6874–6877.
(194) Liu, K.; Arico, J. W.; Taylor, R. E. *J. Org. Chem.* **2010**, *75* (12), 3953–3957.
(195) Stefan, E.; Nalin, A. P.; Taylor, R. E. *Tetrahedron* **2013**, *69*, 7706–7712.
(196) Liu, K.; Taylor, R. E. R.; Kartika, R. *Org. Lett.* **2006**, *8* (23), 5393–5395.
(197) Lam, L. K. P.; Hui, R. H. F.; Jones, J. B. *J. Org. Chem.* **1986**, *51* (11), 2047–2050.

(198) Burgos, C. H.; Canales, E.; Matos, K.; Soderquist, J. *J. Am. Chem. Soc.* **2005**, *127* (22), 8044–8049.
(199) Nising, C. F.; Bräse, S. *Chem. Soc. Rev.* **2008**, *37*, 1218–1228.
(200) Nising, C. F.; Bräse, S. *Chem. Soc. Rev.* **2012**, *41*, 988–999.
(201) Hu, J.; Bian, M.; Ding, H. *Tetrahedron Lett.* **2016**, *57* (50), 5519–5539.
(202) Hari, T. P. A.; Wilke, B. I.; Davey, J. A.; Boddy, C. N. *J. Org. Chem.* **2016**, *81*, 415–423.
(203) El Hadrami, M.; Lavergne, J.-P.; Viallefont, P. *Tetrahedron Lett.* **1991**, *32* (32), 3985–3988.
(204) Hentges, S. G.; Sharpless, K. B. *J. Am. Chem. Soc.* **1980**, *102* (12), 4263–4265.
(205) Beesley, R. M.; Ingold, C. K.; Thorpe, J. F. *J. Chem. Soc. Trans.* **1915**, *107*, 1080–1106.
(206) Maki, B. E.; Scheidt, K. A. *Org. Lett.* **2008**, *10* (19), 4331–4334.
(207) Shiina, I.; Mukaiyama, T. *Chem. Lett.* **1994**, *23* (4), 677–680.
(208) Lee, K.; Kim, H.; Hong, J. *Org. Lett.* **2011**, *13* (10), 2722–2725.
(209) Lee, K.; Kim, H.; Hong, J. *Angew. Chem. Int. Ed.* **2012**, *51* (23), 5735–5738.
(210) Baker, J. B.; Kim, H.; Hong, J. *Tetrahedron Lett.* **2015**, *56* (23), 3120–3122.
(211) Lee, K.; Kim, H.; Hong, J. *Eur. J. Org. Chem.* **2012**, No. 5, 1025–1032.
(212) Byeon, S. R.; Park, H.; Kim, H.; Hong, J. *Org. Lett.* **2011**, *13* (21), 5816–5819.
(213) Lanier, M. L.; Kasper, A. C.; Kim, H.; Hong, J. *Org. Lett.* **2014**, *16*, 2406–2409.
(214) Trost, B. M.; Frontier, A. J. *J. Am. Chem. Soc.* **2000**, *122* (47), 11727–11728.
(215) Trost, B. M.; Frederiksen, M. U.; Rudd, M. T. *Angew. Chem. Int. Ed.* **2005**, *44* (41), 6630–6666.
(216) Trost, B. M.; Yang, H.; Thiel, O. R.; Frontier, A. J.; Brindle, C. S. *J. Am. Chem. Soc.* **2007**, *129* (8), 2206–2207.
(217) Trost, B. M.; Dong, G. *Nature* **2008**, *456*, 485–488.
(218) Paule, S. D. de; Jeulin, S.; Ratovelomanana-Vidal, V.; Genêt, J.-P.; Champion, N.; Dellis, P. *Eur. J. Org. Chem.* **2003**, *2003* (10), 1931–1941.
(219) Lee, K.-C.; Lin, M.-J.; Loh, T.-P. *Chem. Commun.* **2004**, No. 21, 2456–2457.
(220) Gill, T. P.; Mann, K. R. *Organometallics* **1982**, *1* (3), 485–488.
(221) Cook, C.; Guinchard, X.; Liron, F.; Roulland, E. *Org. Lett.* **2010**, *12* (4), 744–747.
(222) Hanawa, H.; Uraguchi, D.; Konishi, S.; Hashimoto, T.; Maruoka, K. *Chem. Eur. J.* **2003**, *9* (18), 4405–4413.
(223) Fuwa, H. *Heterocycles* **2012**, *85* (6), 1255–1298.
(224) Nagao, Y.; Dai, W.; Ochiai, M. *J. Org. Chem.* **1990**, No. 7, 1148–1156.
(225) Fuwa, H.; Suzuki, T.; Kubo, H.; Yamori, T.; Sasaki, M. *Chem. Eur. J.* **2011**, *17* (9), 2678–2688.
(226) Fuwa, H.; Sasaki, M. *Org. Lett.* **2010**, *12* (3), 584–587.
(227) Fuwa, H.; Yamaguchi, H.; Sasaki, M. *Tetrahedron* **2010**, *66*, 7492–7503.
(228) Fuwa, H.; Yamaguchi, H.; Sasaki, M. *Org. Lett.* **2010**, *12* (8), 1848–1851.
(229) Fuwa, H.; Noto, K.; Sasaki, M. *Heterocycles* **2010**, *82* (1), 641–647.
(230) Fuwa, H.; Ichinokawa, N.; Noto, K.; Sasaki, M. *J. Org. Chem.* **2012**, *77*, 2588–2607.
(231) Fuwa, H.; Noto, K.; Sasaki, M. *Org. Lett.* **2011**, *13* (7), 1820–1823.
(232) Fuwa, H.; Mizunuma, K.; Matsukida, S.; Sasaki, M. *Tetrahedron* **2011**, *67*, 4995–5010.
(233) Fuwa, H.; Noguchi, T.; Noto, K.; Sasaki, M. *Org. Biomol. Chem.* **2012**, *10*, 8108–8112.
(234) Ghosh, S.; Rao, R. V. *Tetrahedron Lett.* **2007**, *48* (39), 6937–6940.
(235) Athe, S.; Sharma, A.; Marumudi, K.; Ghosh, S. *Org. Biomol. Chem.Org. Biomol. Chem.* **2016**, *14*, 6769–6779.
(236) Pradhan, T. K.; Reddy, K. M.; Ghosh, S. *Tetrahedron Asymmetry* **2013**, *24* (17), 1042–1051.
(237) Schaus, S. E.; Brandes, B. D.; Larrow, J. F.; Tokunaga, M.; Hansen, K. B.; Gould, A. E.; Furrow, M. E.; Jacobsen, E. N. *J. Am. Chem. Soc.* **2002**, *124* (7), 1307–1315.
(238) Blanchette, M. A.; Choy, W.; Davis, J. T.; Essenfeld, A. P.; Masamune, S.; Roush, W. R. *Tetrahedron Lett.* **1984**, *25* (21), 2183–2186.
(239) Reiter, M.; Turner, H.; Gouverneur, V. *Chem. Eur. J.* **2006**, *12* (27), 7190–7203.
(240) Ghosh, S.; Nageswara Rao, C. *Tetrahedron Lett.* **2010**, *51*, 2052–2054.
(241) Athe, S.; Ghosh, S. *Synthesis*, **2016**, *48*, 917–923.
(242) Florence, G. J.; Cadou, R. F. *Tetrahedron Lett.* **2010**, *51* (44), 5761–5763.
(243) Wilke, B. I. Examining Polyketide Synthase Mechanisms Through Biomimetic Synthesis, Syracuse University, 2013.
(244) Bai, Y.; Davis, D. C.; Dai, M. *Angew. Chem. Int. Ed.* **2014**, *53*, 6519–6522.
(245) Li, J.; Zheng, H.; Su, Y.; Xie, X.; She, X. *Synlett* **2010**, No. 15, 2283–2284.
(246) Zhong, Z.; Zhao, G.; Xu, D.; Dong, B.; Song, D.; Xie, X.; She, X. *Chem. Asian J.* **2016**, *11* (10), 1542–1547.

(247) Fang, B.; Xie, X.; Zhao, C.; Jing, P.; Li, H.; Wang, Z.; Gu, J.; She, X. *J. Org. Chem.* **2013**, *18*, 2–7.
(248) Zhang, B.; Yang, Z.; Yang, J.; Zhao, G.; Ma, B.; Xie, X.; She, X. *Synlett* **2012**, *23* (14), 2129–2131.
(249) Li, H.; Zhang, Y.; Xie, X.; Ma, H.; Zhao, C.; Zhao, G.; She, X. *Org. Lett.* **2014**, *16* (17), 4440–4443.
(250) Li, H.; Zheng, J.; Xu, S.; Ma, D.; Zhao, C.; Fang, B.; Xie, X.; She, X. *Chem. Asian J.* **2012**, *7* (11), 2519–2522.
(251) Lu, Y.; Kim, I. S.; Hassan, A.; Del Valle, D. J.; Krische, M. J. *Angew. Chem. Int. Ed.* **2009**, *48* (27), 5018–5021.
(252) Semmelhack, M. F.; Bodurow, C. *J. Am. Chem. Soc.* **1984**, *106*, 1496–1498.
(253) McCormick, M.; Monahan Robert, I. I. I.; Soria, J.; Goldsmith, D.; Liotta, D. *J. Org. Chem.* **1989**, *54* (19), 4485–4487.
(254) Li, H.; Dong, K.; Jiao, H.; Neumann, H.; Jackstell, R.; Beller, M. *Nat. Chem.* **2016**, *8*, 1159–1166.
(255) Semmelhack, M. F.; Bodurow, C.; Baum, M. *Tetrahedron Lett.* **1984**, *25* (30), 3171–3174.
(256) Hutchins, R.; Learn, K. *J. Org. Chem.* **1982**, *47* (22), 4382–4384.
(257) Hanessian, S.; Giroux, S.; Larsson, A. *Org. Lett.* **2006**, *8* (24), 5481–5484.
(258) Yang, Z.; Xie, X.; Jing, P.; Zhao, G.; Zheng, J.; Zhao, C.; She, X. *Org. Biomol. Chem.* **2011**, *9*, 984–986.
(259) Sharma, G. V. M.; Srikanth, G.; Reddy, P. P. *Org. Biomol. Chem.* **2012**, *10* (40), 8119–8124.
(260) Sharma, G. V. M.; Chary, D. H.; Chandramouli, N.; Achrainer, F.; Patrudu, S.; Zipse, H. *Org. Biomol. Chem.* **2011**, *9*, 4079–4084.
(261) Veena, B.; Sharma, G. V. M. *Synlett* **2014**, *25* (14), 2039–2043.
(262) Sridhar, G.; Sharma, G. V. M. *Synth. Commun.* **2016**, *46* (4), 314–321.
(263) Babu, K. V.; Sharma, G. V. M. *Tetrahedron Asymmetry* **2008**, *19* (5), 577–583.
(264) Chorghade, M. S.; Lalitha, S. V. S.; Gurjar, M. K.; Hymavathi, L.; Murugaiah, A. M. S.; Sharma, G. V. M.; Reddy, B. S.; Prasad, T. R.; Reddy, V. G.; Adhikari, S. S.; Mhaskar, S. V.; Krishna, P. R.; Sreenivas, P.; Sadalapure, K. Substituted Oxygen Alicyclic Compounds, Including Methods for Synthesis Thereof. WO 00/01381, 1999.
(265) Guindon, Y.; Yoakim, C.; Bernstein, M. A.; Morton, H. E. *Tetrahedron Lett.* **1985**, *26* (9), 1185–1188.
(266) Omura, K.; Swern, D. *Tetrahedron* **1978**, *34* (11), 1651–1660.
(267) Gawley, R. E. *J. Org. Chem.* **2006**, *71* (6), 2411–2416.
(268) Yamaguchi, M.; Hirao, I. *Tetrahedron Lett.* **1983**, *24* (4), 391–394.
(269) Roush, R.; Adam, A.; Peseckis, S. M. *Tetrahedron Lett.* **1983**, *24* (13), 1377–1380.
(270) Tanner, D.; Somfai, P. *Tetrahedron Lett.* **1988**, *29* (19), 2373–2376.
(271) Hackman, B. M.; Lombardi, P. J.; Leighton, J. L. *Org. Lett.* **2004**, *6* (23), 4375–4377.
(272) Bai, Y.; Shen, X.; Li, Y.; Dai, M. *J. Am. Chem. Soc.* **2016**, *138* (34), 10838–10841.
(273) Davis, D. C.; Walker, K. L.; Hu, C.; Zare, R. N.; Waymouth, R. M.; Dai, M. *J. Am. Chem. Soc.* **2016**, *138* (33), 10693–10699.
(274) Hoveyda, A. H. *J. Org. Chem.* **2014**, *79* (11), 4763–4792.
(275) Kim, H.; Hoffmann, H. M. R. *Eur. J. Org. Chem.* **2000**, *2000* (12), 2195–2201.
(276) Ibrahem, I.; Yu, M.; Schrock, R. R.; Hoveyda, A. H. *J. Am. Chem. Soc.* **2009**, *131* (11), 3844–3845.
(277) Wang, C.; Haeffner, F.; Schrock, R. R.; Hoveyda, A. H. *Angew. Chem. Int. Ed.* **2013**, *52* (7), 1939–1943.
(278) Reversibility in a catalytic enantioselective reaction leads to erosion of enantiomeric purity, since the minor enantiomer undergoes the reverse process less readily than the major product isomer (larger activation barrier to minor isomer translates to a higher activation energy for the backward reaction as well). As a result, every time the major enantiomer is converted to the starting material and the enantioselective transformation takes place, a certain amount of the minor enantiomer is again formed. Repetition of this sequence leads to eventual generation of racemic product. Thus, a catalytic enantioselective reaction that is more highly selective (i.e., the barrier for formation and reversion of the minor isomer is higher) requires a longer time to achieve equilibration, since with every reverse/forward sequence, less of the minor enantiomer, which less readily participates in the reverse reaction, is generated. The larger the amount of the minor enantiomer generated with each cycle, the less time it takes to accumulate 50% of that isomer (i.e., reach complete equilibration between the two enantiomers).)
(279) Wu, H.; Radomkit, S.; O'Brien, J. M.; Hoveyda, A. H. *J. Am. Chem. Soc.* **2012**, *134* (19), 8277–8285.
(280) Neises, B.; Steglich, W. *Angew. Chem. Int. Ed.* **1978**, *17* (7), 522–524.
(281) Hoveyda also attempted RCM with G-II (59%) and HG-II (54%) catalysts. Based on their obtained yields and extensive experience, it calls into question previously-reported yields for G-II (85%) and to a lesser extent, HG-II (74%) by Fuwa and She, respectively. All substrates share high levels of structural homology, with key differences being choice of distal protecting groups.

(282) Jarvis, W. R.; Colbeck, J. C.; Krebber, A.; Fleitz, F. J.; Brands, J. *Science*, **2010**, *329*, 305–310.
(283) Salomon, C. E.; Magarvey, N.; Sherman, D. H. *Nat. Prod. Rep.* **2004**, *21* (1), 105–121.
(284) Hanessian, S.; Dhanoa, D. S.; Beaulieu, P. L. *Can. J. Chem.* **1986**, *65*, 1859–1866.
(285) Lee, K. Stereoselective syntheses of Tetrahydropyrans: Applications to the Synthesis of (+)-Leucascandrolide A, (+)-Dactylolide and (±)-Diospongin A, Duke University, 2014.

· Chapter 3 ·

A Transannular Oxa-Conjugate Addition Model of Neopeltolide

3.1 2,6-*cis*-Tetrahydropyrans & Polyketide Natural Products

2,6-Disubstituted pyrans are a common ring system found in polyketides; they add significant conformational bias (rigidity) to these natural products and can play a role in controlling the bioactive form of the molecule. While pyrans with varying oxidation states are observed in polyketides, a common and important motif is the tetrahydropyran (THP), as seen in neopeltolide[1] (**3.1**), the structurally-related leucascandrolide A[2] (**3.2**), and a wealth of other biologically-interesting natural products (Figure 3.1). As a direct result of the significant diversity of pharmacological activities within these metabolites (including antiproliferative, antibiotic, antiviral, and antifungal cytotoxicities),[3] synthesis of substituted THPs and their biosynthetic details have attracted significant attention from both the organic chemistry[4–9] and biosynthetic communities,[10–18] respectively.

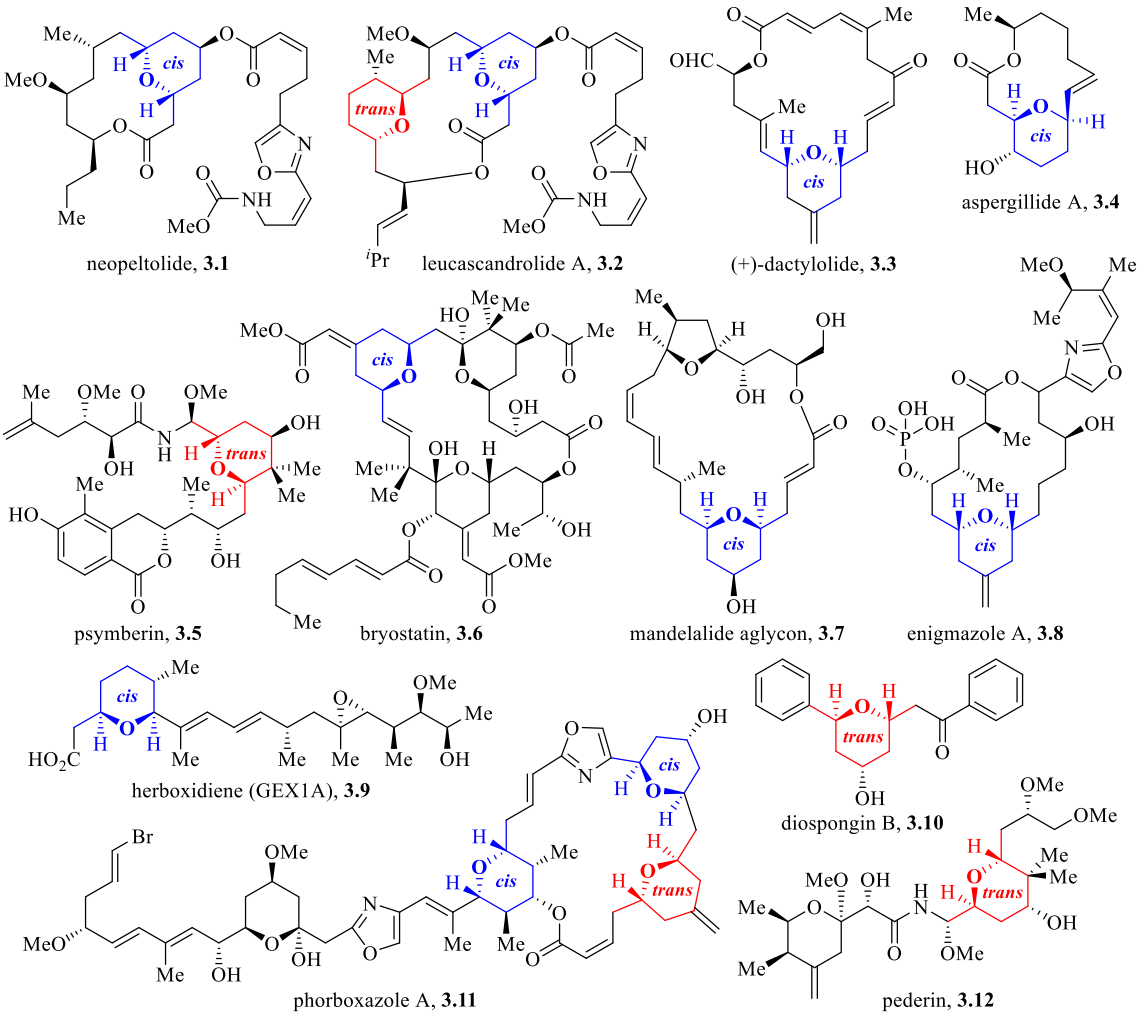

Figure 3.1 – Select examples of 2,6-disubstituted tetrahydropyrans within bioactive natural products.[1,2,19–30]

In **Chapter 2**, several common strategies for assembly of THPs were outlined in efforts toward the synthesis of **3.1** (§ 2.9.3), including Prins[31] and related oxocarbenium ion cyclizations,[32–43] hetero-Diels-

Alder cycloadditions,[44–46] ring-closing metathesis,[47] radical cyclization,[48] transition metal-mediated cyclizations,[49–52] as well as bio-inspired oxa-conjugate addition reactions.[53–56] Despite the array of these and other strategies for building THP ring systems,[57,58] each method has limitations that restrict the scope of its synthetic utility in ways analogous to the discussion in **Chapter 1**.

Conversely, biosynthetic details of THP formation are relatively new and encumbered by limited genomic information for most natural products bearing this motif. Within polyketide synthase (PKS) systems, a putative pyran synthase (**PS**) enzymatic domain catalyzes a diastereoselective 6-*exo*-trig[59] intramolecular nucleophilic addition of the *ζ*-hydroxy into the *α,β*-unsaturated thioester of the growing chain (**3.15**, Figure 3.2).[10,15,18†] Recently, the first example of a pyran synthase to follow canonical assembly-line enzymology[60] of *cis*-AT PKS systems was reported by Leadlay and coworkers in their elucidation of the salinomycin biosynthetic pathway.[17] All other PS-containing systems known to date belong to the class of *trans*-AT PKS within non-elongating modules,[13] which are known to provide great architectural diversity within polyketide metabolites. Piel and coworkers have successfully demonstrated *in vitro* assembly of THP products using a putative PS of the pederin biosynthetic pathway;[11,18] however, this work was limited to highly-simplified linear substrates, and provided low selectivity.

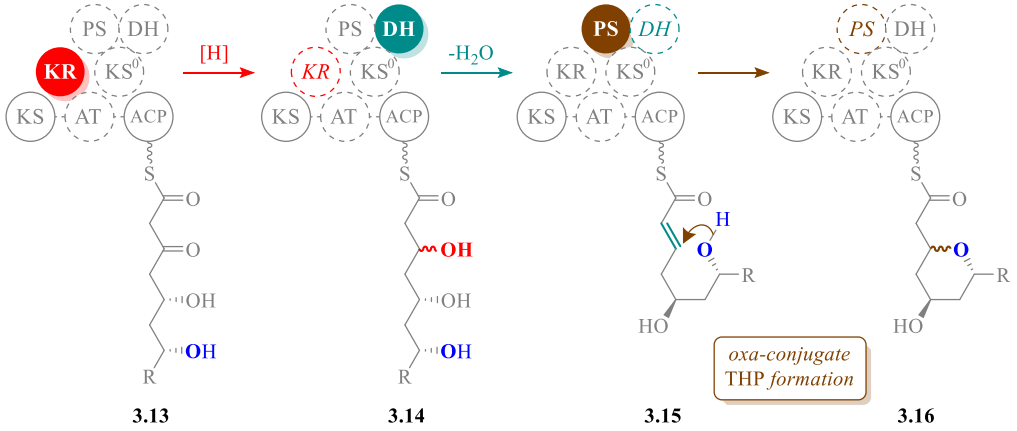

Figure 3.2 – Proposed mechanistic sequence of the biosynthetic oxa-conjugate assembly of THP motifs. Dashed catalytic domains represent non-canonical components of *trans*-AT PKSs.

The total synthesis of complex THP-bearing compounds of clinical-relevance is rarely a viable option for production at industrial scale; metabolic engineering for their over-production requires substantially more genetic information, and *in vitro* evaluation. Chemoenzymatic synthesis represents an attractive solution for development of complex THP-containing lead compounds. This chapter introduces efforts toward combining PKS biosynthesis and organic chemistry for *de novo* design of complex

† THP assembly within polyether ionophores occurs by flavin-linked oxidation of diene- or triene-containing substrates to epoxides. Epoxide hydrolases/cyclases of the monensin[144] and lasalocid[145,146] families catalyze subsequent epoxide-opening/pyran formation by 5-*exo*-tet and anti-Baldwin 6-*endo*-tet nucleophilic additions by the *ε*-hydroxy, respectively.

polyketide natural products bearing 2,6-disubstituted-tetrahydropryan ring motifs, as highlighted by the study of neopeltolide **3.1**.

3.2 Neopeltolide: A Polyketide Natural Product

Neopeltolide (**3.1**, Figure 3.1) is a 14-membered macrolide natural product that was isolated from a deep-water sponge of the family Neopeltidae, collected off the northern coast of Jamaica by Wright and coworkers in 2007.[1] They established the planar structure and relative configuration of **3.1** through extensive NMR spectroscopic data. Subsequent reassignment of the proposed stereochemistry and determination of the absolute configuration were independently reported by the Panek[32] and Scheidt[33] research groups through total syntheses. The key structural elements of **3.1** include a 14-membered macrocyclic backbone containing a 2,6-*cis*-disubstituted THP ring, with an oxazole-bearing side chain attached to the THP.

Initial biological evaluation revealed that neopeltolide exhibits potent cytotoxic activities against several cell lines with nanomolar IC_{50} values.[1] Kozmin and coworkers reported that neopeltolide targets cytochrome bc_1 complex and may inhibit mitochondrial ATP synthesis.[38] Substantial attention from the synthetic community has solved the acute supply problem for neopeltolide, and provided sufficient material for establishing the minimum structural requirements for activity (Figure 3.3). Like most natural product leads, total synthesis is unlikely to provide a permanent solution to the supply problem faced by neopeltolide if it were to be developed as a clinical therapeutic.

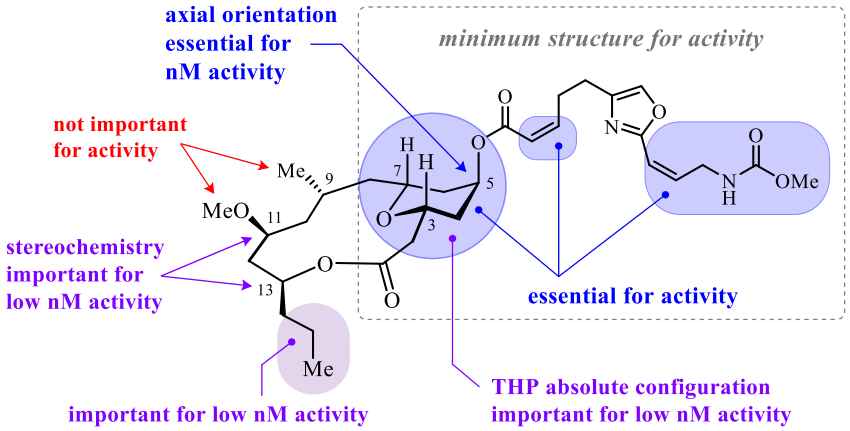

Figure 3.3 – Summary of structure-activity relationships (SAR) and identified pharmacophoric elements of neopeltolide, as adapted from the study of Fuwa and coworkers.[61] **Blue** labelling denotes essential structural elements, **purple** denotes non-critical importance, and **red** denotes elements that are superfluous.

To address supply needs for neopeltolide and to push the state-of-the-art in combining biosynthesis and synthetic chemistry, we have focused on the exploration of bioinspired transannular oxa-conjugate strategies for assembly of 2,6-*cis*-tetrahydropyran ring systems.

3.2.1 Research Milestones of Neopeltolide Study

Over the past two decades, it has become increasingly clear that modular polyketide synthase pathways are amenable to re-engineering.[62–65] Substantial work in literature has shown that genetic engineering of PKS genes allows groups of catalytic domains to be added or removed from biosynthetic pathways in ways akin to LEGO® bricks,[64] leading to predictable changes in the obtained "unnatural" polyketide product.[62,63,65] An outstanding example of this flexibility can be seen in work from Kosan Bioscience, where 14 different groups of PKS catalytic domains were shuffled and recombined in *de novo* fashion to generate more than 70 designer polyketide products.[62,63] The flexibility and amenability of these PKSs to *de novo* design enables researchers to make medically-relevant improvements to known polyketides, or to build new biosynthetic pathways to produce novel complex molecules through bacterial fermentation.

Because the genome for the producing organism of neopeltolide was not sequenced and re-isolation has not been realized, application of *de novo* pathway design is highly appealing, particularly due to the rapid and scalable production of PKS products *via* bacterial fermentation. However, due to poorly-characterized biosynthetic details for THP assembly, engineering *in vitro* production is not currently a reliable process. To overcome this limitation, this study investigates chemical synthesis for THP assembly from functional groups easily accessible through *de novo* PKS pathway design – namely alcohols, carbonyls, and olefins. For example, if a complex neopeltolide precursor such as **3.17** (Figure 3.4) can be chemically converted into neopeltolide **3.1**, then a fermentation route for reliable, sustainable production of this natural product can be established.

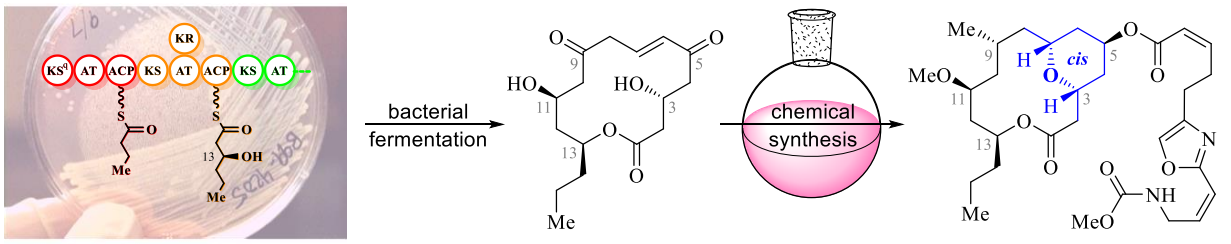

de novo PKS pathway **3.17** (+)-neopeltolide, **3.1**

Figure 3.4 – A combined *de novo* biosynthetic-synthetic approach for production of complex polyketide natural products, such as neopeltolide (**3.1**).

This study differs philosophically from both *de novo* PKS design and classic organic synthesis. While a retrosynthesis is clearly required to propose a route toward a target such as **3.1** and to consider a specific strategy for the THP assembly using biosynthetically-accessible functional groups, a "retro-biosynthesis" must also be considered for the advanced precursor structure. This retro-biosynthesis faces many challenges that are unique to the limitations of modern protein engineering, particularly the large

number of theoretical possibilities for bio-transformations and limited availability of desired enzymes to mediate such conversions *in vitro*. To illustrate one limitation, proposed precursor **3.17** lacks the 9-(*S*)-methyl group of neopeltolide, which is hypothesized to be biosynthetically-installed *via* a homologue of an 3-hydroxy-3-methyl-glutaryl-CoA (HMG-CoA) synthase found in *trans*-AT pathways.[13] However, such *β*-branching remains an incredible hurdle for protein engineering due to substrate specificity at the KS of the downstream module,[60,66] and use of an HMG-CoA synthase homologue has not been used in *de novo* design to date.

Research milestones of the neopeltolide study are divided into two distinct stages where *de novo* PKS design represents the final and long-term goal for this research, and presents an opportunity to modify this strategy for transannular THP assembly of neopeltolide analogues and other THP-bearing polyketides.[62–65] The immediate goal of this project has thus been to establish and evaluate foundations of the transannular oxa-conjugate assembly of 2,6-*cis*-tetrahydropyran ring systems, and apply this chemistry to the synthesis of neopeltolide.

3.3 Oxa-Conjugate Addition Assembly of Disubstituted-THPs

The chemistry that fulfills the requirement of synthesizing the THP of neopeltolide from functional groups easily-accessible by *de novo* engineered PKS systems is oxa-conjugate addition. While conjugate addition using carbon or nitrogen nucleophiles is common and typically facile, use of hard oxygen nucleophiles present a challenge due to being mismatched with the softer *β*-carbon of the *α*,*β*-unsaturated carbonyl.[5,67–69] Consequently, oxa-conjugate additions are readily reversible under both acidic and basic conditions. Because of this reversibility, it is often possible to obtain kinetic or thermodynamic selectivity; reaction conditions and stereoelectronics primarily govern the selectivity of addition. In general, assembly of simple 2,6-THPs involves intramolecular 6-*exo*-trig cyclization[59] of a *ζ*-hydroxy into an *α*,*β*-conjugated system, furnishing *cis*-THP products under base-mediated thermodynamic conditions, or acid-mediated kinetic conditions.[70] Under the more-commonly-employed base-mediated conditions, *cis*-THP formation is thermodynamically-controlled and enthalpically-unfavorable. Stereoselectivity is attributed to a higher energy state and decreased highest-occupied molecular orbital/lowest-unoccupied molecular orbital (HOMO/LUMO) orbital overlap in the s-*trans* olefin of chair-like transition states like **TS-1** (Figure 3.5). Conversely, *a priori* hypothesis predicted that under acid-mediated conditions the *cis*-THP is kinetically-favored due to increased stabilizing HOMO/LUMO interaction of the oxygen lone pair with the allylic cationic species of a transition state like **TS-2**.[5] These generalities validate the observed selectivity for simple 2,6-substituted THPs; the stereochemical outcome of more complex systems require detailed conformational analysis of the resultant heterocycle.

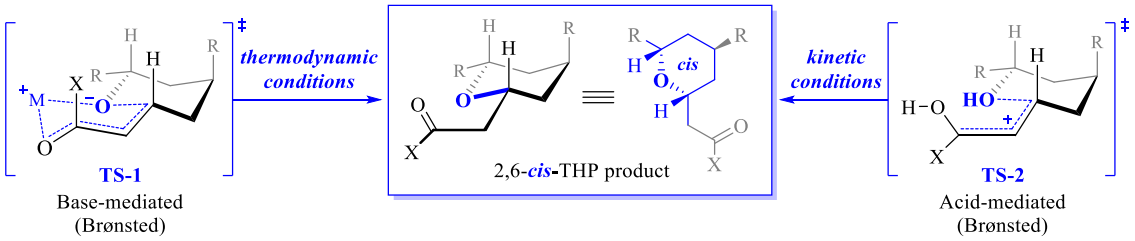

Figure 3.4 – Reaction conditions control formation of simple 2,6-*cis*-THP products by oxa-conjugate addition. Base-mediated reactions are typically under thermodynamic control and enthalpically-unfavorable due to decreased overlap in **TS-1**; it is proposed that acid-mediated reactions are kinetically-favored due to stabilizing orbital overlap in **TS-2**.

For in-depth discussion of this chemical transformation, its mechanistic details and application to natural product synthesis, please refer to the excellent reviews of Nising and Bräse,[67,68] Fuwa,[5] or the recently-published Ding and coworkers.[69]

3.3.1 Oxa-Conjugate THP Assembly in Neopeltolide Synthesis

In spite of inherent challenges, oxa-conjugate additions have proven useful for synthesis of various heterocycles.[67–69] Since this strategy provides direct and rapid access to THPs, it has been applied to the construction of neopeltolide (Scheme 3.1). The first reports of this strategy were in 2009 by Hong,[53] and Roulland,[54] which used addition of a ζ-hydroxy into a linear *α,β*-unsaturated aldehyde to generate the *cis*-THP found in neopeltolide (**3.18** & **3.20**, Scheme 3.1). The following year, Fuwa[55] used base-mediated thermodynamic control in his simplified linear *α,β*-unsaturated ester **3.23** to overcome the unfavorable LUMO energy compared to the corresponding *α,β*-unsaturated aldehyde or ketone systems, and facilitate the addition reaction. The final example was reported in 2012 by S. Ghosh,[56] who relied on cyclization of a *β*-hydroxy into an *α,β*-unsaturated ketone system **3.35** under mild conditions.

While these four strategies provided strong precedent for use of oxa-conjugate addition to generate the *cis*-THP of neopeltolide, they also highlight associated challenges with this transformation. In Hong's tandem allylic oxidation/oxa-conjugate addition system,[53] exploitation of the *gem*-dialkyl (Thorpe-Ingold)[71] effect was required to lower entropic barriers and accelerate kinetic addition. The successful oxa-conjugate addition into the ester system of Fuwa's second-generation synthesis required forcing conditions for THP assembly, and should be noted that a relatively small, unencumbered substrate was employed. Alternatively, the milder conditions of Roulland's aldehyde and S. Ghosh's ketone strategies suffer from lower yields and required use of transition metal catalysts, arguably a deviation from biomimetic conditions.

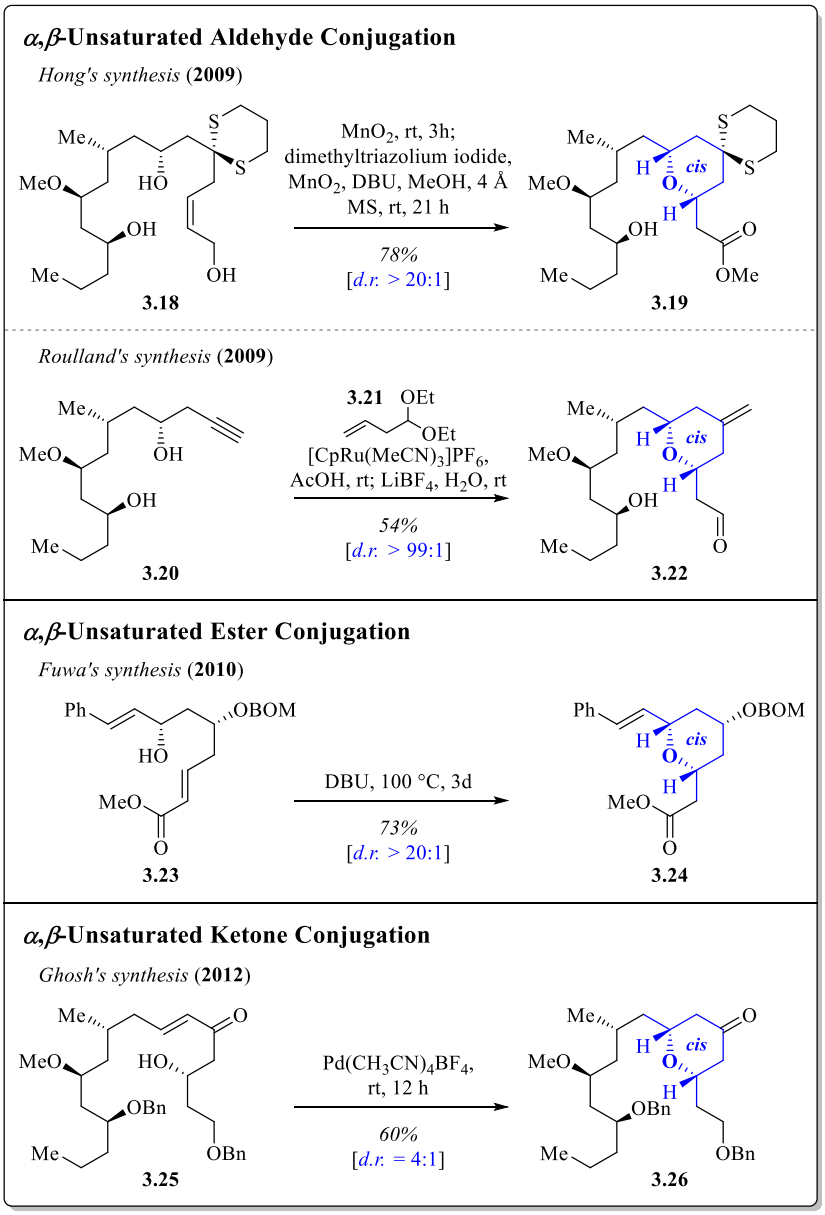

Scheme 3.1 – Literature examples of oxa-conjugate addition strategies using *α,β*-unsaturated aldehyde, ester and ketone systems to generate the 2,6-*cis*-THP ring of neopeltolide.

Oxa-conjugate strategies have proven effective for diastereoselective assembly of the 2,6-*cis*-disubstituted THP ring system of neopeltolide. However, it is important to note that all examples presented have been performed on linear substrates. The inherent conformational bias (rigidity) of the macrocyclic core of neopeltolide and its impact on this highly-reversible transformation have not been evaluated.

3.3.2 Neopeltolide Models for Transannular Oxa-Conjugate THP Assembly

In line with the first milestone in this study, the viability of transannular oxa-conjugate assembly of 2,6-*cis*-tetrahydropyran ring systems needed to be established. Transannular cyclization is an incredible

tool within organic chemistry, and has been applied to synthesis of many natural products with excellent selectivity (Scheme 3.2).[72,73] Transannular chemistry involves ring-closure reactions across macrocycles, forming polycyclic products. The basis of this strategy relies on intrinsic conformational biases and rigidifying elements (unsaturations, stereogenic centers, and substitutions), which provide entropic advantages to otherwise difficult transformations.[73]

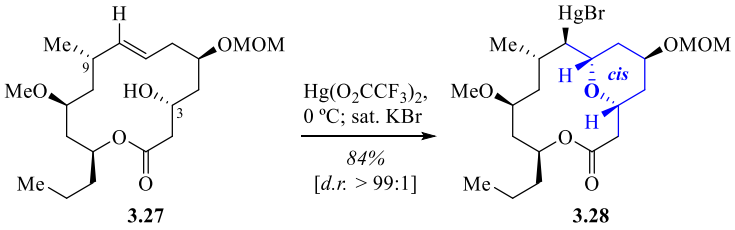

Scheme 3.2 – Transannular oxymercuration assembly of *cis*-THP **3.28** by Sharma and coworkers.[74]

Transannular strategy was employed by Sharma and coworkers to install the *cis*-THP of neopeltolide in their formal synthesis.[74] In their report, the C9-methyl acted as an auxiliary to direct formation of the mercurinium ion on the less-hindered β-face of the C7-C8 olefin. Subsequent THP assembly by 6-*exo*-trig cyclization of the δ-hydroxy alkene, and treatment with aqueous KBr solution yielded transannular product **3.28** in 84% yield with excellent selectivity. This is the only example of transannular THP formation within the neopeltolide system.

Transannular cyclization has effectively demonstrated its potential within natural product synthesis, and in the assembly of THP systems;[74–76] however, examples of transannular oxa-conjugate additions to this motif are exceedingly rare, being limited to two research groups.[77–82] Shishido and coworkers developed transannular oxa-conjugate addition strategies for synthesis of aspergillides A (**3.4**) and B (**3.30**),[77] as well as the $^{\Delta 5,6}$dihydropyran-**3.30** variant, aspergillide C.[75] Under a screen of basic conditions, formation of THP products was realized in high yield and selectivity. DBU afforded fully-diastereoselective conversion to *cis*-**3.4** both stoichiometrically and catalytically, under kinetic conditions; however, use of stronger bases generated *trans*-**3.30** with complete diastereoselectivity under similar reaction conditions.[77] Acidic conditions were not explicitly tested, but pyran formation was not reported by treatment of PPTS or HF in the preceding deprotection of **3.29**. Using a computational approach, the *cis*-THP (**3.4**) was calculated to be 1.8 kcal/mol higher in energy than the *trans*-THP (**3.30**), suggesting reversible oxa-conjugate addition under thermodynamic control would favor **3.30**. Importantly, they successfully demonstrated thermodynamic control through interconversion of *cis*-**3.4** to *trans*-**3.30**; the reverse process was not realized even at prolonged exposure to refluxing conditions. This study represented the only example of transannular oxa-conjugate addition into an α,β-unsaturated ester system.[77–79]

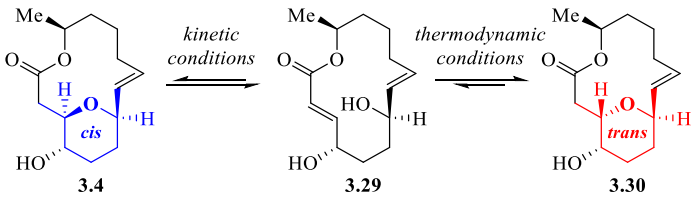

Figure 3.5 – The synthesis of aspergillides A and B by Shishido and coworkers demonstrates the success of a reversible base-mediated transannular addition of a *ζ*-hydroxy into an *α,β*-unsaturated ester system.

Pioneering work in transannular oxa-conjugate addition was reported by Rizzacasa and coworkers with their study of apicularen A.[80–82] Treatment of precursor **3.31** under basic conditions resulted in decomposition and isomerization of the double bond to the *β,γ*-position, with no observable pyran products.[80] Evaluation of acidic conditions‡ revealed Amberlyst-15® ion resin efficiently accessed kinetic *cis*-pyranone **3.32**, and that, *via* E1cB elimination/oxa-conjugate addition mechanisms, they were able to equilibrate the products to thermodynamically-favored *trans*-pyranone **3.33** with good diastereomeric ratio (*d.r.* > 9:1). More importantly, they demonstrated that use of 13-*epi*-**3.31** or *rac*-**3.31** generated the same *trans*-**3.33** under extended thermodynamic conditions in comparable yield.[81,82] Computational calculations indicated the *cis*-THP (**3.32**) is 2.6 kcal/mol higher in energy than the *trans*-THP (**3.33**), supporting epimerization of C13 and efficiency of thermodynamic equilibrium. This study represented the only example of transannular oxa-conjugate addition into an *α,β*-unsaturated ketone system.[80–82]

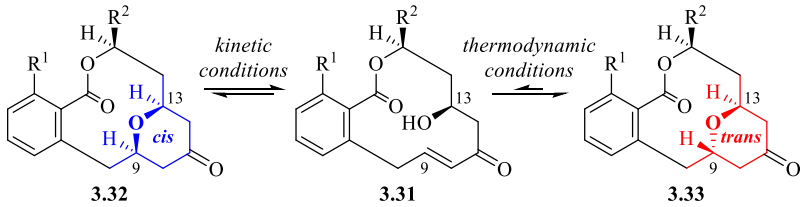

Figure 3.6 – The synthesis of apicularen A by Rizzacasa and coworkers demonstrates the success of a reversible acid-mediated transannular addition of a *β*'-hydroxy into an *α,β*-unsaturated ketone system.

Inspired by the independent successes of Shoshido[77,78] and Rizzacasa,[80,81] two conjugated model substrates were designed to address the impact of the macrocyclic framework of neopeltolide (**3.34**, Figure 3.6) on oxa-conjugate addition approaches toward THP formation. In the first model system, THP assembly relies on addition of a *ζ*-hydroxy group into an *α,β*-unsaturated ester (**3.35**). Ester **3.35** was envisioned as readily accessible through sequential allylations, with the macrocyclic core being synthesized *via* Yamaguchi esterification.[83] In the second system, assembly of the THP relies on addition of a *β*'-hydroxy into an *α,β*-unsaturated ketone (**3.36**), followed by selective reduction of the obtained pyranone product.

‡ TBAF conditions were used for the unmasking of *β*'-nucleophile, thus requiring explicit testing. CSA and TsOH did not induce cyclization; $BF_3{\cdot}Et_2O$ Lewis acid conditions also yielded *cis*-**3.32** but with poorer selectivity over isomerization.

Ketone **3.36** was designed to be accessed through a convergent route relying on a Horner-Wadsworth-Emmons[84–87] olefination and ring-closure *via* intramolecular S_N2 substitution.[§]

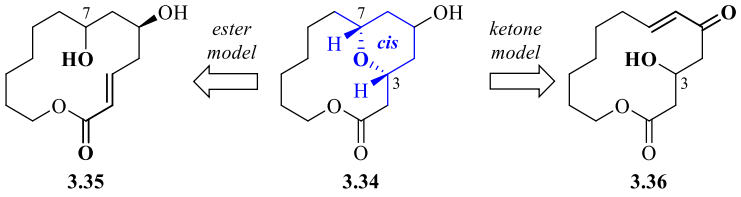

Figure 3.6 – Proposed *α,β*-unsaturated ester and ketone model systems for accessing the macrocyclic core of neopeltolide *via* transannular oxa-conjugate addition assembly of the 2,6-*cis*-THP rings.

With this study, we investigated the effect of pre-organizing the nucleophilic alcohol and electrophilic *α,β*-unsaturated carbonyl for oxa-conjugate addition by constraining it in a 14-membered macrocycle. Like Hong's[53] use of the Thorpe-Ingold effect,[71] this pre-organization is expected to lower the reaction energy barrier, thereby enabling milder reaction conditions.[73] The macrocycle is also expected to exacerbate energetic differences between the *cis*- and *trans*-THP, resulting in increased diastereoselectivity. Herein reports efforts toward the design and synthesis of *α,β*-unsaturated ester and ketone models for evaluation of a transannular oxa-conjugate assembly of the 2,6-*cis*-tetrahydropyan ring in neopeltolide.

Results & Discussion

3.4 *α,β*-Unsaturated Ester Model for Neopeltolide

Development of the *α,β*-unsaturated ester model (**3.35**) was retrosynthetically-designed to mimic assembly-line biosynthesis of PKS systems.[60] Homoallylic alcohol **3.39** diverged into two unique macrocyclizing substrates *via* linear elongation (Figure 3.7), which is analogous to PKS assembly.[60] It was proposed that the *ζ*-hydroxy of oxa-conjugate precursor **3.35** would generate the bicyclic core of neopeltolide **3.34** under mild conditions due to conformational bias of the pre-organized macrocycle. Ambitiously, this system was planned for use with heterologously-expressed[88] PKS mutants to evaluate mechanistic possibilities of THP biosynthesis; success of this design would readily provide synthetic intermediates for derivatization as NAC-thioesters. Such intermediates could be used as substrates for feeding experiments with individually-expressed modules or hybrid pathways.

[§] It should be noted that *β*'-hydroxy addition from the C7-position is also plausible, and should add additional credence to thermodynamic equilibration of isomers akin to the apicularen A synthesis[80–82]

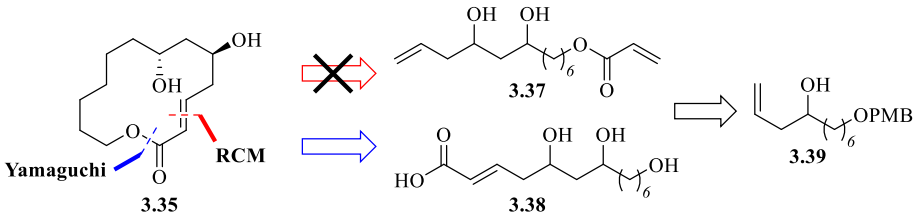

Figure 3.7 – Retrosynthetic analysis for oxa-conjugate precursor **3.35** of the *α,β*-unsaturated ester model. Although two distinct routes were evaluated, each diverge from common synthetic intermediate **3.39**.

This section provides a summary of efforts contributed by Dr. Burkhardt I. Wilke – a former doctoral student of the Boddy Lab – toward the synthesis of the *α,β*-unsaturated ester model **3.35**. Selected details of synthetic schemes are included, though a comprehensive discussion of the results can be found in his Ph.D. dissertation.[89]

3.4.1 RCM Yields Dimerization

The ring-closing metathesis strategy was evaluated under various conditions using two different metathesis catalysts (Scheme 3.3). Second-generation Grubbs catalyst **3.43** led exclusively to dimerization of precursor **3.40**, which is rationalized by greater activity of the electron-rich terminal alkene in comparison to the electron-deficient acrylate in cross metathesis reactions. Use of second-generation Hoveyda-Grubbs catalyst **3.44** resulted in the consumption of starting material into uncharacterized decomposition products, with no evidence of dimerization.

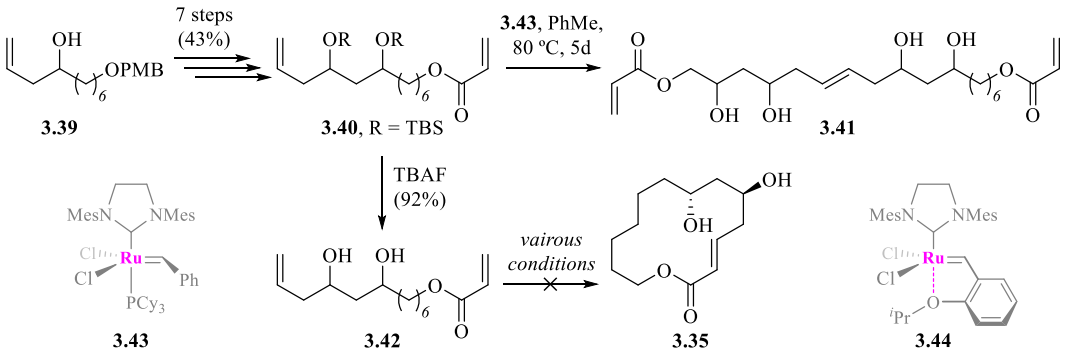

Scheme 3.3 – RCM strategies failed to provide oxa-conjugate precursor **3.35**. Grubbs second-generation catalyst (**3.43**) yielded dimer product **3.41**, while Grubbs-Hoveyda second-generation catalyst (**3.44**) consumed starting materials and gave no discernible dimer, or desired product.

Steric bulk near the catalytic center has been reported to dramatically affect the success of similar reactions.[90,91] Global desilylation with TBAF afforded diol **3.42** in excellent yield. Treatment with **3.43** catalyst again yielded the corresponding dimer product, albeit in very low yields. Use of **3.44** catalyst consumed the starting material and gave no discernible dimerization; however, it also failed to yield the expected macrolactone **3.35** (Scheme 3.3).

During review of our work, similar difficulties with the RCM strategy were independently-reported by Florence and Cadou in their study toward the synthesis of neopeltolide.[92] At reflux, Grubbs' second-generation catalyst efficiently generated cycloheptene **3.47** in 70% yield, under high-dilution conditions (Scheme 3.4). Likewise, use of Nolan's indenylidene complex **3.48** provided the undesired cyclic by-product in similar yields at room temperature. They suggested conformational flexibility of **3.45** leading to preferential C3-C7 metathesis, or transient formation of desired macrolactone is followed by transannular metathesis due to rigid conformational bias. Alternative strategies were not attempted for the synthesis of *α,β*-unsaturated ester **3.46**; successful completion – or modified follow-up – of this synthesis has not been reported to date.

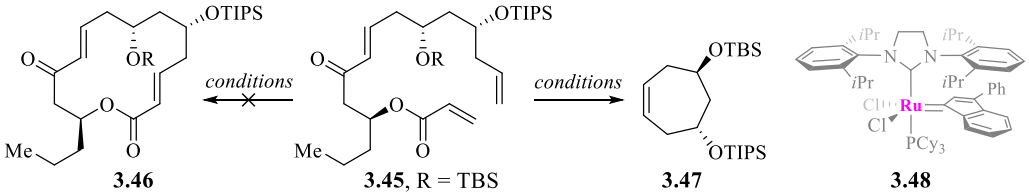

Scheme 3.3 – RCM strategies of Florence and Cadou similarly failed to provide oxa-conjugate precursor **3.45**. Both Grubbs second-generation catalyst (**3.43**) and Nolan's indenylidene (**3.48**) cleanly afforded cycloheptene **3.47** in yields of 70% and 65%, respectively.

The failure of this approach was disappointing due to a previous report that cited alkenes and acrylates as neighboring cross-metathesis classes.[93] Numerous examples of cross- and ring-closing metathesis reactions with acrylates have proven successful,[94] including the synthesis of 14-membered macrolactone narbonolide by Xuan *et al*.[95] Ultimately, RCM synthesis of our desired oxa-conjugate precursor **3.35** was abandoned in favor of a more traditional carboxyl-activating macrolactonization.[96]

3.4.2 Oxa-Conjugate Assembly of THP Unsuccessful using Ester System

Based on the failure of RCM, the *α,β*-unsaturated ester model **3.35** was re-designed for a lactonization strategy that was amenable to greater flexibility between the nucleophilic and electrophilic fragments.[96] Synthesis of *bis*-benzyl protected **3.49** was accomplished in low overall yield (< 1% over 8 steps) from the TBDPS-variant of intermediate **3.39**. Attempts of macrolactonization under Corey-Nicolaou conditions[97] proved unsuccessful. The low yields and failed lactonization prompted an investigation of alternative protecting group of **3.49**; *bis*-TBS protected **3.49** was accomplished in 24% overall yield (5 steps) from **3.39**. Yamaguchi esterification conditions successfully yielded macrocycle **3.50**, which subsequently underwent global desilylation to afford *syn* (**3.35**) and *anti* (**3.51**) oxa-conjugate precursors in equal ratio and good yield (Scheme 3.4). The diastereomers were separated, and the Rychnovsky acetal-based approach[98] was used to establish relative stereochemistry of the diols in each diastereomer.[99]

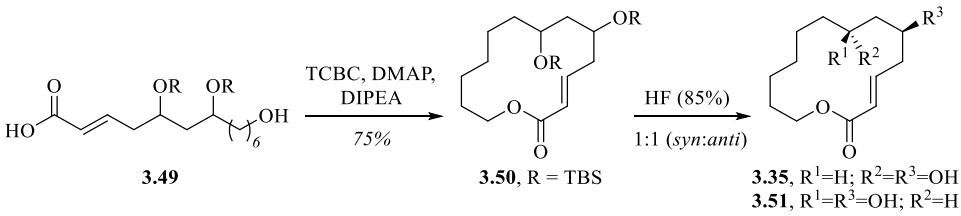

Scheme 3.4 – Synthesis of *α,β*-unsaturated conjugated ester model was successfully accomplished by Yamaguchi esterification conditions,[83] providing an equal ratio of **3.35** and **3.51** products. The Rychnovsky acetal-based method[98] was used to establish the relative stereochemistry of the diol diastereomers.

A stock solution of 0.1 M DBU in C_6D_6 was prepared and used as the reaction solvent for both diastereomers **3.35** and **3.51**. Contrary to the successful use of DBU in oxa-conjugate additions observed for both linear and transannular systems by Fuwa[55] and Shishido,[77,78] respectively, **3.35** and **3.51** were unreactive at room temperature and completely consumed at reflux without observable formation of any cyclization product ($^{\Delta 3}$*rac*-**3.34**). Elimination, leading to formation of sorbate-containing compounds predominated (Figure 3.8). Screening of a variety of alternative basic and acidic reaction conditions similarly failed to find conditions that accessed the 2,6-*cis*-THP from **3.35** or **3.51**.

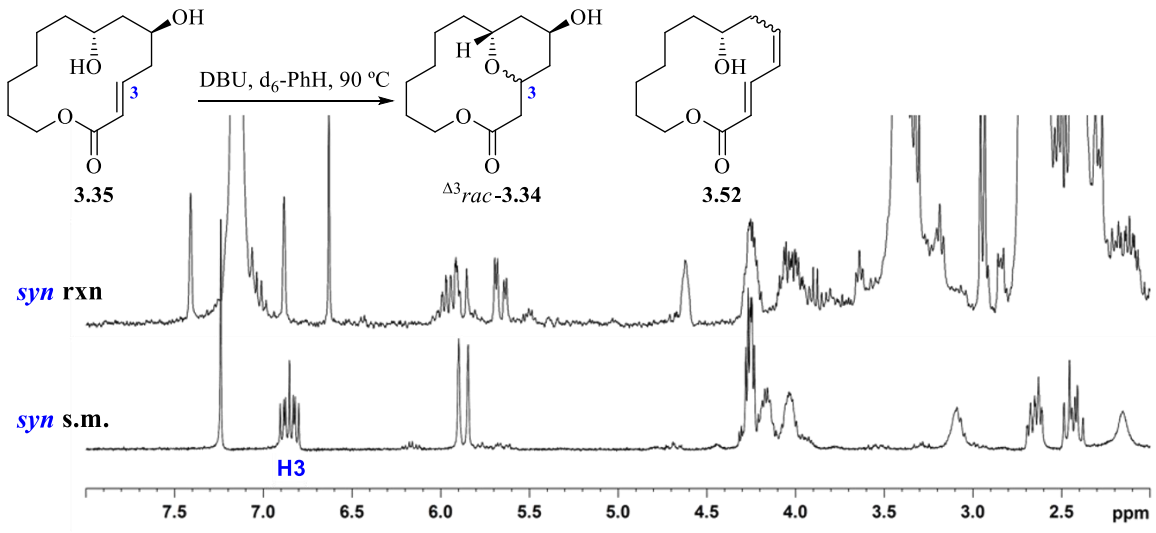

Figure 3.8 – ^{1}NMR comparison of attempted oxa-conjugate addition of *syn*-**3.35** (native configuration) using the basic conditions successfully employed by Fuwa and coworkers in their linear system.[55] Starting material is visualized by t = 0 for the observed reaction.

It is interesting to note the use of an *α,β*-unsaturated ester system for oxa-conjugate pyran assembly was evaluated by Ferrié *et al* in the formal synthesis of leucascandrolide A.[100] They similarly report the formation of undesired sorbate product **3.55** as the major product, when unmasking *ζ*-hydroxy **3.53** (Scheme 3.5). Furthermore, in the late-stages of an alternative route, the axial C5 alcohol induced retro-Michael cascade and eliminated to produce (*Z,E*)-dienoic acid as a major product under basic conditions.[100] It was noted that the epimeric C5 alcohol does not undergo elimination due to disfavored stereochemistry.

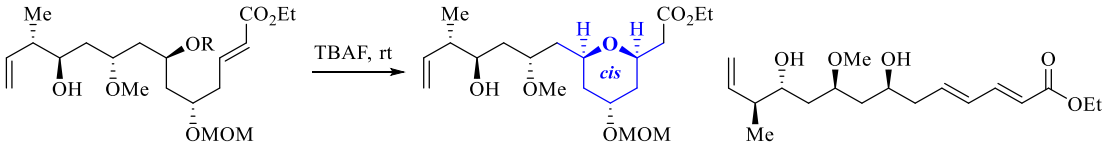

3.53, R = TBS **3.54**, (6%) **3.55**, (65%)

Scheme 3.5 – Ferrié *et al* reported that oxa-conjugate precursor **3.53** provides the expected 2,6-*cis*-THP of leucascandrolide A in poor yield, accompanied by sorbate product **3.55** as the major product.[100]

Previous investigation into transannular oxa-conjugate addition by the Boddy Lab also failed to provide desired 2,6-disubstituted pyran product.[101] The doctoral research of Dr. Stephen R. Houghton discovered unexpected formation of highly-strained *trans*-oxetane **3.56** from his model system of the polyketide natural product laulimalide (Scheme 3.6). Neither oxa-conjugate precursors were reactive under basic conditions, even at elevated temperatures; however, both products generated the oxetane as a single product under acidic conditions analogous to Rizzacasa's apicularen A synthesis.[80,81]

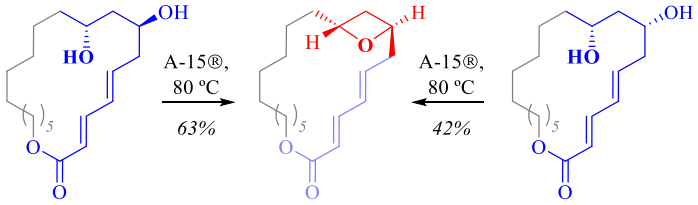

syn-**3.57** 5.8 kcal/mol *trans*-**3.56** 14.2 kcal/mol *anti*-**3.58** 7.1 kcal/mol

Scheme 3.6 – Previous difficulties experienced by the Boddy Lab using diol oxa-conjugate systems: Houghton reported the energetically-disfavored formation of *trans*-oxetane **3.56** by 1,8-elimination/oxa-conjugate addition cascade mechanism for both *syn*- and *anti*-diastereomers.

Despite reported success of base-mediated linear[53,55] and transannular[77,78] oxa-conjugate assembly of 2,6-*cis*-THP within *α,β*-unsaturated ester systems, cyclization products were not observed for neopeltolide models **3.35** and **3.51** (Figure 3.8).[89] In line with the rarity of literature examples, the expected conformational bias of a pre-configured macrocycle did not sufficiently lower energetic requirements of this bio-inspired transannular ester system. While energetic differences clearly do not guarantee success of transannular oxa-conjugate addition,[101] we believed the alternatively-conjugated ketone system possessed stronger electrophilic character and would improve reactivity.

3.5 *α,β*-Unsaturated Ketone Model for Neopeltolide

The presented difficulties of transannular pyran formation in conjugated ester systems supported concerns of low-reactivity and reversibility issues for this reaction;[67,68] accordingly, our focus shifted toward design of the alternative conjugated ketone system. We hypothesized that the failure of transannular oxa-conjugate addition within either of the diastereomeric *α,β*-unsaturated ester systems of our neopeltolide model was owing to the high energy of the ester LUMO. Because *α,β*-unsaturated ketones possess

markedly lower-energy LUMOs, as compared to their ester homologues,[81] we redesigned a model system to incorporate this functional group as oxa-conjugate precursor **3.36** (Figure 3.9)

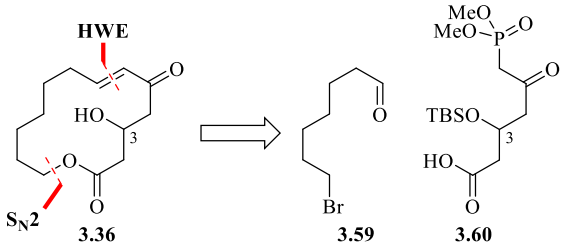

Figure 3.9 – Retrosynthetic analysis for oxa-conjugate precursor **3.36** of the *α,β*-unsaturated ketone model, highlighted by the racemic C3-hydroxy phosphonate fragment **3.60**.

A key precedent for our ketone model system **3.36** was the study of apicularen A by Rizzacasa and coworkers.[80,81] In their total synthesis of this *trans*-tetrahydropyranone polyketide natural product **3.33**, they relied on reversible acid-catalyzed intramolecular 6-*endo*-trig-type conjugate addition of a *β*'-hydroxy into the protonated ketone of an *α,β*-unsaturated system **3.31**, followed by ring-closure and protonolysis of the resulting enol (§ 3.3.2, Figure 3.6). Their studies showed that they could access the kinetic *cis*-pyranone **3.32**,[80] and reliably equilibrate the pyranone products to the thermodynamically-favored *trans*-diastereomer **3.33** with good diastereoselectivity (*d.r.* > 10:1).[81] Based on this precedent, we undertook the synthesis of an *α,β*-unsaturated ketone model system for the transannular oxa-conjugate assembly of the 2,6-*cis*-THP of neopeltolide.

3.5.1 Convergent Synthesis Designed Around Racemic C3-Alcohol

The development of the C1-C6 phosphonate fragment hinged upon interconvertible oxa-conjugate assembly of the THP – analogous to the Rizzacasa synthesis of apicularen A,[81] allowing the C3-alcohol to be racemic (Scheme 3.7). Synthesis was straightforward, and began with selective reduction of commercially available dimethyl-1,3-acetonedicarboxylate **3.61**. Subsequent silylation and conversion to half-acid **3.62** was accomplished in good yield. Phosphonylation of the **3.62** ester provided beta-keto-phosphonate **3.60** in high yield, which was then alkylated to provide known ester phosphonate **3.63**.[102–104]

Initial coupling attempts employed readily-prepared TBS-aldehyde **3.66** under previously-successful conditions of KOH in THF.[105,106] These conditions proved to be too basic, and resulted in decomposition products that were predominated by *β*-elimination of the C3-alcohol. Coupling was accomplished using modified Horner-Wadsworth-Emmons conditions;[84–87] use of the milder cesium carbonate promoted deprotonation *via* formation of the stabilized cesium salt of the 1,3-dicarbonyl.[107] Unfortunately, the obtained *α,β*-unsaturated full carbon framework of **3.67** remained base-sensitive, and exposure to traditional saponification conditions using hydroxide resulted in *β*-elimination of the C3-

alcohol (Scheme 3.7). Additional attempts to hydrolyze the methyl ester, including *in situ* formation of 3-hydroxypropionitrile alkoxide,[108] mild and anhydrous conversion to the corresponding acid salt using potassium trimethylsilanoate,[109] or use of silica-supported sodium hydrogen sulfate as a heterogeneous catalyst,[110] all failed to provide acid **3.68** and resulted in *β*-elimination.

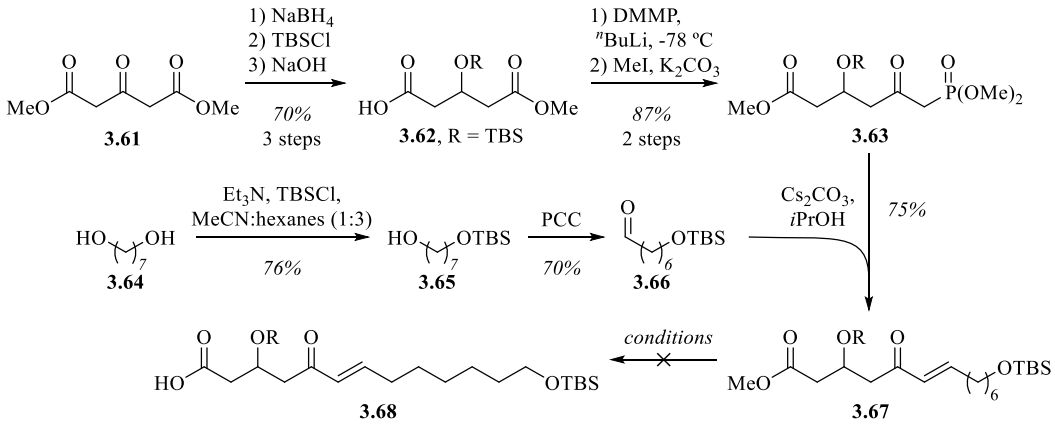

Scheme 3.7 – Base-sensitivity is apparent by the observed C3 silyl-protected alcohol *β*-elimination.

To prepare an alternative C1-C6 fragment that would readily be hydrolyzed to the acid following olefination, a benzyl variant (**S-3**) of the ester phosphonate was synthesized. Initially, the benzyl ester phosphonate was prepared based on reports of silica-supported sodium hydrogen sulfate being capable of selective debenzylation in the presence of double- and triple-bonds, including *α*,*β*-unsaturated esters.[111] However, based on the observed elimination in the methyl ester system, combined with an inability to cleave *via* hydrogenolysis due to the requisite unsaturation, an investigation into the effect of desilylation was performed. Reports show preference for chemoselective deprotection of secondary alcohols over primary alcohols within *bis*-silyl-protected systems,[112–114] prompting global desilylation of **3.69**.

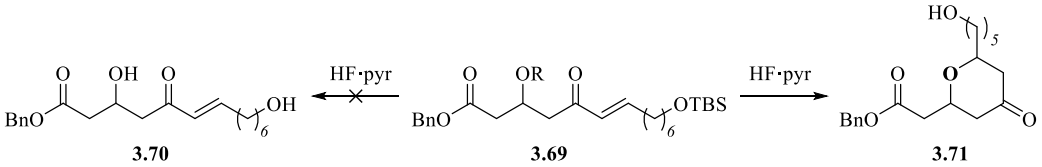

Scheme 3.8 – Global deprotection of *bis*-silyl **3.69** *via* acidic conditions spontaneously generates an equal mixture of *cis*- and *trans*-THP stereoisomers, without observation of oxa-conjugate precursor **3.70**.

Under HF conditions, isolation of diol **3.70** was not realized, but spontaneous formation of pyranone **3.71** was observed in an equal mixture of *cis*-to-*trans* isomers (Scheme 3.8), suggesting non-favored energies. Unfortunately, due to limited material, hydrogenation was not attempted to generate the esterification precursor. Ultimately, macrocyclization with this precursor would not provide details about the viability of transannular oxa-conjugate assembly, and was abandoned. Investigation into thermodynamically-controlled interconversion (*vide infra*) of linear THP diastereomers was not evaluated from this data, and remains a potential area for future exploration.

3.5.2 THP Assembly can be Thermodynamically-Controlled

Based on the difficulties experienced with our prepared ester moieties, olefination attempts using acid phosphonate **3.60** directly were attempted. Delightfully, previously-employed coupling conditions provided the full linear *seco*-acid **3.72** (Scheme 3.9). A small elevation in temperature (ambient-to-30 ºC) positively-affected initial yields of the reaction by nearly 30%. It is assumed that this increase in yield resulted from improved solubility of the cesium carbonate, mimicking hydration conditions of liquid-solid phase-transfer catalysis (LS-PTC).[115–117]

Under PTC conditions, rate and yield of olefinations using bases such as barium hydroxide, potassium carbonate, and cesium carbonate depend heavily on the quantity of water present in the reaction medium.[115] Aqueous media disrupt reticular energies (lattice formation) of bases and improves access to the basic sites, thus increasing the capability of carbonate or hydroxide anions for requisite deprotonation of the phosphonate. During coupling of acid phosphonate **3.60** and 7-bromoheptanal **3.59**, cesium carbonate failed to provide a heterogeneous reaction mixture, further decreasing the likelihood of anionic-activation of the weakly acidic phosphonate methylene. Through phase-transfer, disruption of the cesium carbonate crystal lattice promotes the requisite anionic-activation in three principle steps: (1) adsorption of phosphonate **3.60** onto basic sites, with formation and transformation of carbanionic species; (2) reaction between carbanion and the aldehydic carbonyl of **3.59**, and subsequent formation of *α,β*-unsaturated product **3.72**; (3) desorption of reaction products.[115]

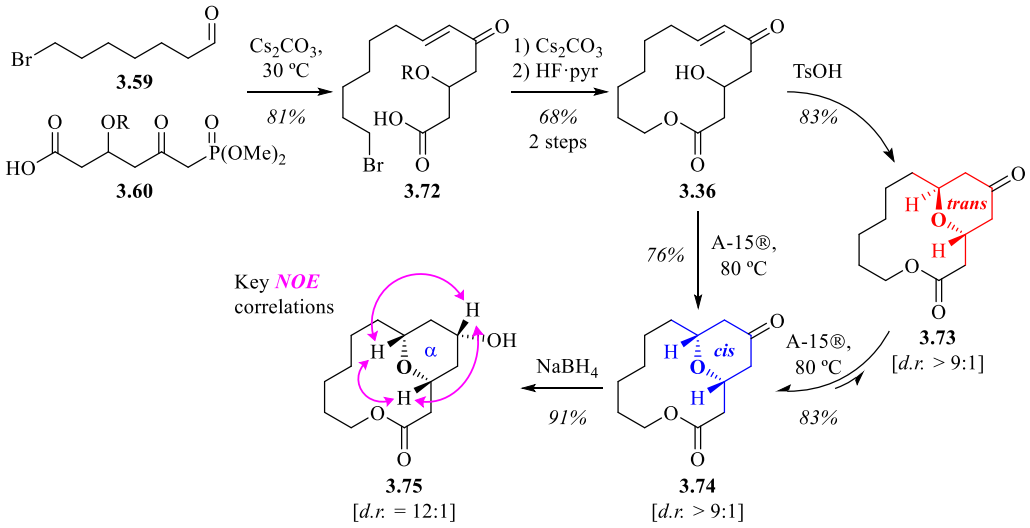

Scheme 3.9 – Synthesis of the *α,β*-unsaturated ketone model system successfully demonstrates transannular oxa-conjugate assembly of the 2,6-*cis*-THP is viable, and thermodynamically-controlled.[99]

With appreciable quantities of *α,β*-unsaturated product **3.72** synthesized, efforts toward macrocyclization and unmasking of the oxa-conjugate precursor were initiated. Whether due to a proposed

cesium effect,[107,118–120] or an increased reactivity due to cation size,[121] macrolactonization is known to proceed *via* nucleophilic displacement with cesium carboxylates. It is shown that these conditions require long-chain acids with a good leaving group at the ring-closing site, but not the typical high-dilution techniques used to minimize formation of diolide or oligomeric byproducts.[118,120] Long-chain *ω*-bromoalkanoic acid **3.72** readily underwent ring-closure with cesium carbonate in acetone, and was subsequently desilylated to afford oxa-conjugate precursor **3.36** in quantitative yield (Scheme 3.9). Attempts at telescoping olefination and ring-closure steps proved unsuccessful.

Under a wide variety of typical base-mediated conditions for oxa-conjugate addition, including DBU[55] and KO*t*Bu,[122–124] at ambient- and elevated-temperatures (up to 110 ºC), oxa-conjugate precursor **3.36** failed to produce any THP product. These basic conditions were predominantly unreactive, leading to re-isolation of starting material and trace amounts of uncharacterized elimination product (*vide infra*). Treatment with *p*-toluenesulfonic acid at room temperature led to instantaneous formation** of two higher-R_f compounds (Figure 3.10), which was later identified as desired THP-containing macrocycles with high diastereoselectivity for kinetic *trans*-pyranone (*d.r.* > 9:1).[125] Extensive 1D- and 2D-NMR analysis (HSQC, COSY, NOESY, TOCSY) confirmed that the major product was the 2,6-*trans*-THP, which was separable by column chromatography.

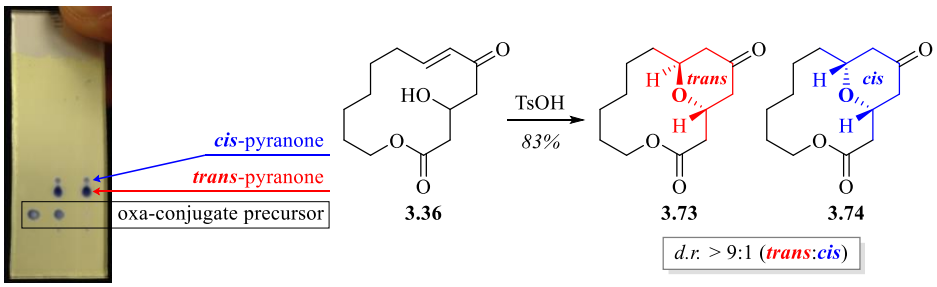

Figure 3.10 – TLC analysis shows instantaneous formation of two higher-R_f compounds from treatment of oxa-conjugate precursor **3.36** with *p*-toluenesulfonic acid in $CDCl_3$ at room temperature.

A computational approach was used to evaluate the relative energies of *cis*- and *trans*-diastereomers to determine if reversible oxa-conjugate addition under thermodynamic control could access the desired *cis*-product. The structures of *trans*-**3.73** and *cis*-**3.74** were subjected to an initial PM6[126] optimization prior to a B3LYP/6-31++G** energy minimization.[127–129] Potential energies of energy-minimized structures were computed. A vibrational analysis was performed and resulted in no imaginary frequencies, indicating the geometries of each compound occupied a local minimum. The *trans*-**3.73** was found to be in a twist-boat

** Upon addition of TsOH, conversion (< 6% starting material) had occurred by ^{1}HNMR of reaction mixture at t = 0.

conformation and was approximately 1.4 kcal/mol higher in energy than the *cis*-**3.74**, which was predicted to adopt a chair conformation.

Inspired by the initial results, isolated *trans*-**3.73** was re-subjected to *p*-toluenesulfonic acid and heated at 40 ºC for 60 minutes, 60 ºC for 120 minutes, and 70 ºC for 3 hours in deuterochloroform (Figure 3.11). These conditions were monitored hourly by TLC/^{1}HNMR and proved to be largely unreactive, indicating the thermodynamic requirements were not met. Pleasingly, an increase of temperature to a reported[80,81,101] 80 ºC promoted equilibration of pyranone products, as evidenced by a new diastereomeric ratio of 5:3 favoring the *trans*-product within 60 minutes. The thermodynamic interconversion plateaued near 5 hours at 80 ºC, with high diastereoselectivity that favored *cis*-pyranone product **3.74** (*d.r.* ~ 6:1, based on crude reaction mixture ^{1}HNMR). The previously uncharacterized elimination product predominated as by-product at elevated temperatures; elimination by-product represented greater than 30% of the overall yield at plateau. Although the scale at which these experiments were carried out did not allow publishable-characterization of the isolated material, it is believed the by-product was diene **3.76** (Figure 3.11), which is analogous to observations in Rizzacasa's study of apicularen A.[80,82] It is noteworthy to question whether the presence of the C9-methyl or C11-methoxy groups of neopeltolide are enough to reduce C8 acidity, and impede formation of elimination by-product. In any case, this study verified our approach and efforts toward optimization were carried out.

To suppress formation of by-product, it was found that substituting TsOH for use of acidic ion-exchange resin (Amberlyst-15®) led to efficient thermodynamic control for transannular oxa-conjugate addition.[130] Precursor **3.36** was converted in high diastereoselectivity (*d.r.* > 9:1) to the thermodynamic *cis*-product **3.74** by treatment with Amberlyst-15® within 5 hours at 80 ºC (Figure 3.11). The observed *cis*-to-*trans* product ratio of 90:10 is in good agreement with computationally-predicted equilibrium ratio at 80 ºC of 87.5:12.5 *cis*-to-*trans*.[99] To confirm that formation of desired *cis*-THP product occurred from the kinetic *trans*-THP product, spectroscopically-pure **3.73** was subjected to identical thermodynamic Amberlyst-15® conditions, and *cis*-**3.74** was isolated in comparable yield with identical diastereoselectivity (*d.r.* > 9:1).

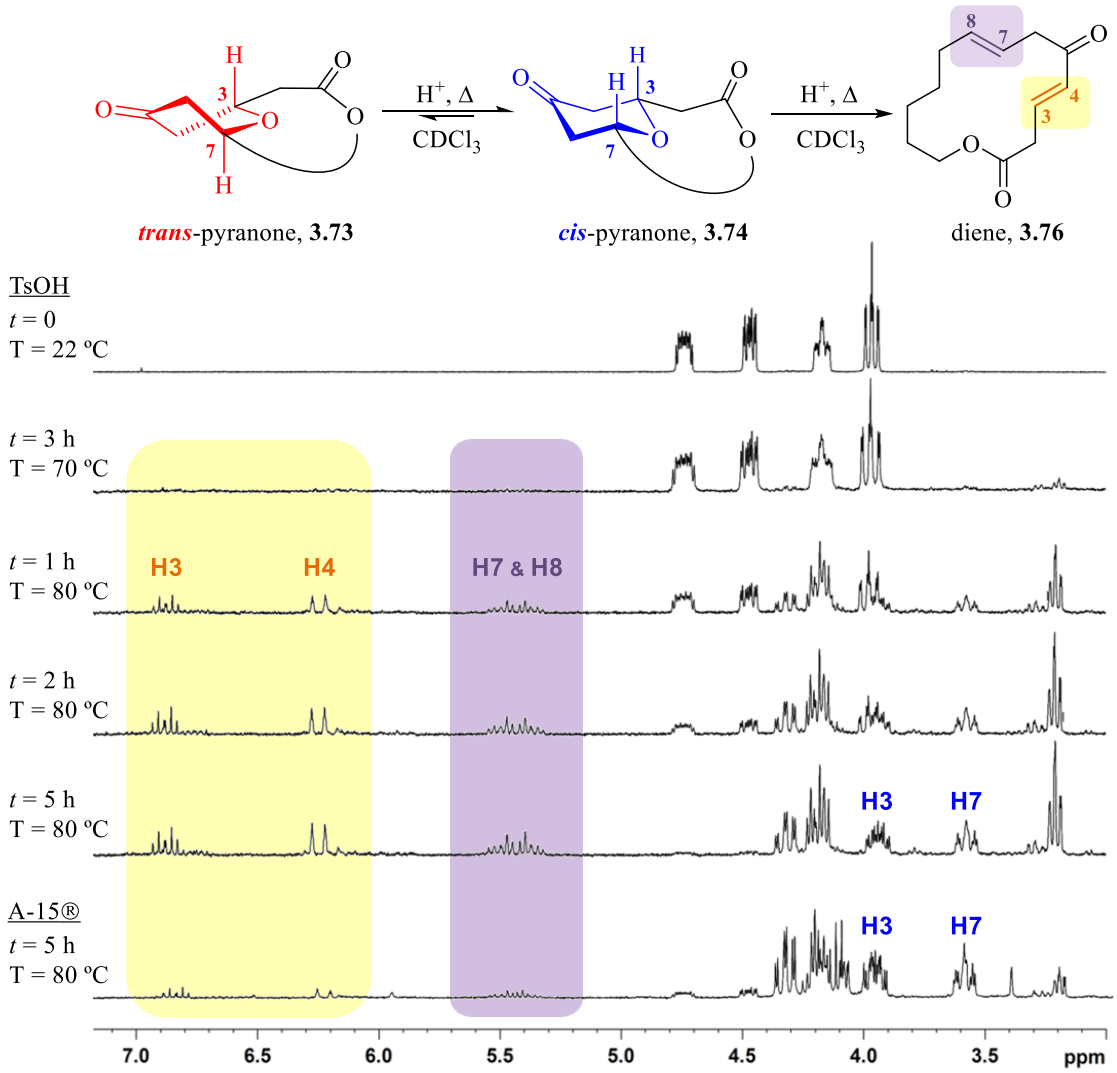

Figure 3.11 – Acid-mediated thermodynamic conditions facilitate interconversion of the *trans*-pyranone product at 80 °C. Extended reaction times lead to elimination by-product (30% overall), which are effectively-suppressed by use of Amberlyst-15® as the acid source (< 8% overall).

During thermodynamic-acid-mediated interconversion, THP ring-opening is expected to occur through elimination of the C3-*O* bond and C7-*O* bond, as seen for the thermodynamically-controlled oxa-conjugate additions of enantiopure linear *β*-hydroxy enones[131] and the transannular oxa-conjugate addition-based synthesis of apicularen A.[80] For enantiopure linear *β*-hydroxy enones, this dual elimination pathway is problematic as it leads to erosion of stereochemical integrity due to racemization of the stereogenic center.[131] However, in the context of transannular oxa-conjugate addition approaches, it enables remote stereochemical control of both stereogenic centers, as was shown in the synthesis of **3.33** from **3.32**, where configuration of the lactone stereocenter was sufficient to control both THP stereogenic centers (§ 3.3.2, Figure 3.6).[81] This remote stereocontrol is expected to prove useful in the total synthesis of the macrocyclic core of neopeltolide *via* transannular oxa-conjugate assembly of the 2,6-*cis*-THP.

Selective reduction of *cis*-pyranone **3.74** was accomplished with $NaBH_4$ into desired alcohol **3.75**[61,99] in high selectivity (*d.r.* = 12:1, *α*:*β*). Under Mitsunobu conditions,[132] Scheidt[33] and many others[35,37,38,40,41,46,47,51,52,54,61] have established that this configuration at C5 allows efficient coupling with the requisite oxazole-bearing side-chain from neopeltolide.

This work demonstrates that transannular oxa-conjugate addition is a viable strategy toward assembly of the 2,6-*cis*-THP of neopeltolide. Control of relative stereoisomer formation indicates that the reaction is reversible *via* E1cB elimination/oxa-conjugate addition mechanisms, where thermodynamically-favored *cis*-pyranone **3.74** was yielded with good diastereomeric ratio (*d.r.* > 9:1). This result was supported by a computational study that predicted a similar equilibrium ratio, and suggested that stereocontrol of the nucleophilic oxygen is not required for diastereoselective synthesis of THPs using this strategy.

The facile oxa-conjugate addition under acidic treatment represents great promise for this study. Acidic desilylation conditions did not result in any observable cyclization products in the systems of aspergillide A–C,[79] apicularen A,[82] or laulimalide;[101] however, formation of the kinetically-favored *trans*-THP was readily attained under similar conditions spontaneously in good diastereoselectivity (*d.r.* > 9:1). Moreover, the conformational bias of this system was represented by lower energetic differences than the aforementioned ones. Cautiously, one must question if the rigidifying elements of the native neopeltolide backbone will reinforce or negatively-alter this conformational bias.[73]

3.6 Transannular Oxa-Conjugate Model System Conclusions

As described above, transannular oxa-conjugate addition is a viable strategy toward assembly of the 2,6-*cis*-THP of neopeltolide, realizing our first milestone of the neopeltolide study. This work demonstrated that acid-mediated nucleophilic addition of a *β*'-hydroxy into an *α*,*β*-unsaturated ketone embedded in a 14-membered macrolactone is superior to acid- or base-mediated additions into an *α*,*β*-unsaturated ester system. The experimental and computational data clearly indicated that the reaction is reversible and can successfully be performed under kinetic control to access the *trans*-THP product or thermodynamic control to access the *cis*-THP. This work represents the first known example of transannular oxa-conjugate assembly of 2,6-*cis*-THPs under thermodynamic control.

The reversibility of this reaction demonstrated the potential applicability of racemic nucleophiles in diastereoselective synthesis of substituted THPs. We expect the results of our transannular oxa-conjugate ketone model will establish facile routes to stereoselective synthesis of 2,6-*cis*-substituted tetrahydropyrans

and be viable toward the total synthesis of the macrocyclic core of neopeltolide and other complex polyketides.

3.7 Experimental

3.7.1 General Procedures

All reactions were carried out using oven-dried glassware under an inert atmosphere (nitrogen, or argon gas) with dry solvents under anhydrous conditions, unless otherwise noted. Anhydrous solutions of THF, Et_2O, and CH_2Cl_2 were obtained from an anhydrous solvent delivery system;[133] other solvents were freshly distilled.[134] Yields refer to chromatographically and spectroscopically (^{1}HNMR) homogenous materials, unless otherwise stated. Reagents were commercially purchased at the highest quality and used without further purification, unless otherwise stated. Reactions were monitored by TLC carried out on 0.25 Mm Silicycle silica gel plates (60F-254) using either UV light as a visualizing agent, or an aqueous solution of CAM, *p*-anisaldehyde or iodine$_{(s)}$, and heat as a developing agent. Preparative thin-layer chromatography (PTLC) separations were carried out on 0.25 Mm Silicycle silica gel plates (60F-254). NMR spectra were recorded on Bruker Avance 300 or 400 MHz, Avance II 300 MHz, or Avance III 600 MHz instruments, and calibrated using residual undeuterated solvent ($CDCl_3$: δ H = 7.26 ppm, δ C = 77.0 ppm)[135] as internal references. Data is reported as follows: chemical shift (multiplicity abbreviations: s = singlet, d = doublet, t = triplet, q = quartet, p = pentet, m = multiplet, br = broad), *J* = coupling constant (Hz), integration, peak assignment. Infrared (IR) spectra were recorded on an ABB Bomen MB Series Arid-Zone™ Infrared Spectrometer. HRMS were recorded by positive ion electrospray on Kratos Analytical Concept 11A mass spectrometer with an electron beam of 70 eV (Ottawa-Carleton Mass Spectrometry Centre).

3.7.2 Experimental Procedures and Physical Data of Compounds

All the experimental procedures are representative, and arranged to reflect the synthetic procedures shown in the schemes.

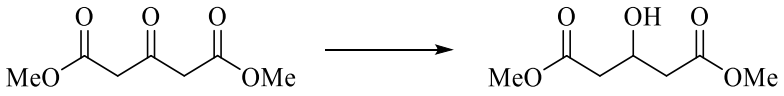

3.61 **S-1**

Dimethyl-3-hydroxypentanedioate (S-1). A stirred solution of diester **3.61** (10.0 g, 57.4 mmol, 1.0 equiv.) in methanol (60 mL), was cooled using an ice bath, and sodium borohydride (1.1 g, 28.7 mmol, 2.0 equiv.) was slowly added in small portions. The clear solution gradually turned clear and yellow in color. Upon completion, the reaction mixture was evaporated to dryness. The crude residue was diluted in EtOAc (50 mL) and washed with brine. The aqueous phase was separated and extracted with EtOAc (2 × 20 mL), and

the combined organic layers were dried over $MgSO_4$, filtered, and concentrated *in vacuo*. The crude residue was sufficiently pure for use in the following step, and yielded 8.60 g (48.8 mmol, 85%) as clear, colorless oil.

R_f = 0.28 (silica gel, 20% EtOAc in hexanes; CAM stain).

^{1}HNMR (400 MHz, $CDCl_3$): δ 4.44 (dp, J = 4.0, 6.1 Hz, 1H, -C*H*-), 3.70 (s, 6H, 2 × -OCH_3), 3.35 (d, J = 4.1 Hz, 1H, -O*H*), 2.54 (d, J = 6.0 Hz, 4H, 2 × -CH_2) ppm.

^{13}CNMR (100 MHz, $CDCl_3$): δ 172.2, 64.7, 51.9, 40.4 ppm.

Characterization data for **S-1** proved consistent with previously reported literature data.[136]

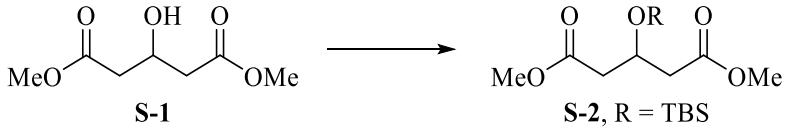

S-1 **S-2**, R = TBS

Dimethyl-3-(*tert*-butyldimethylsilyloxy)pentanedioate (S-2). To **S-1** (17.5 g, 99 mmol, 1.0 equiv.) dissolved in anhydrous DMF (75 mL, 0.8 M) under inert atmosphere, was added TBSCl (15 g, 138 mmol, 1.4 equiv.). Imidazole (20 g, 0.3 mol, 3.0 equiv.) was added to a rapidly stirring solution, and stirred for 12 h at ambient temperature. The reaction mixture was quenched with saturated ammonium chloride, and diluted in EtOAc. The organic layers were washed with water (2 × 50 mL) and brine (3 × 50 mL), dried ($MgSO_4$), filtered, and concentrated *in vacuo*. Purification of the crude residue (5% EtOAc in hexanes) yielded 23.0 g (80 mmol, 96% yield) of **S-2** as clear, colorless oil.

R_f = 0.27 (silica gel, 10% EtOAc in hexanes; CAM stain).

^{1}HNMR (300 MHz, $CDCl_3$): δ 4.53 (p, J = 6.2 Hz, 1H, C*H*), 3.65 (s, 6H, 2 × OCH_3), 2.54 (d, J = 6.2 Hz, 4H, 2 × CH_2), 0.82 (s, 9H, O-TBS *t*-Bu), 0.04 (s, 6H, O-TBS -CH_3), ppm.

^{13}CNMR (100 MHz, $CDCl_3$): δ 171.4, 66.3, 51.6, 42.4, 25.6, 17.9, -5.0 ppm.

Characterization data for **S-2** proved consistent with previously reported literature data.[137]

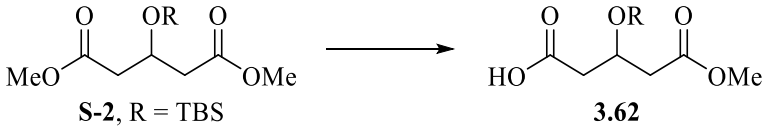

S-2, R = TBS **3.62**

3-(*tert*-Butyldimethylsilyloxy)-5-methoxy-5-oxopentanoic acid (3.62). To **S-2** (2.0 g, 6.89 mmol, 1.0 equiv.) in a 2:1 mixture of MeOH and H_2O (36 mL) was added NaOH (7.7 mL, 1.0 M). The reaction mixture was stirred at 30 ºC for 8 h. Upon completion, the mixture was quenched with saturated NH_4Cl, diluted in EtOAc (50 mL), and extracted (3 × 10 mL). The aqueous layer was acidified and re-extracted with EtOAc (30 mL). The combined organic layers were dried ($MgSO_4$), filtered, and concentrated to afford 1.63 g (5.91 mmol, 86%) of **3.62** as clear, colorless oil. Spectral analysis revealed a crude material of high purity;

however, it is advised to further purify by flash chromatography (silica gel, 10% EtOAc in hexanes) prior to use in the subsequent phosphonylation step.

R_f = 0.20 (silica gel, 20% EtOAc in hexanes; CAM stain).

^{1}HNMR (300 MHz, $CDCl_3$): δ 10.65 (br s, 1H, -CO_2H), 4.53 (p, J = 6.0 Hz, 1H, -C*H*-), 3.66 (s, 3H, -OCH_3), 2.65 – 2.53 (m, 4H, 2 × -CH_2-), 0.83 (s, 9H, O-TBS *t*-Bu), 0.06 (m, 6H, O-TBS -CH_3) ppm.

^{13}CNMR (100 MHz, $CDCl_3$): δ 175.5, 171.3, 66.1, 51.7, 42.1, 41.9, 25.6, 17.9, -5.0 ppm.

Characterization data for **3.62** proved consistent with previously reported literature data.[138]

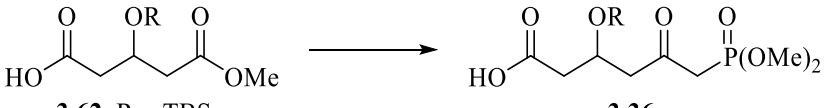

3.62, R = TBS **3.36**

3-(*tert*-butyldimethylsilyloxy)-6-(dimethoxyphosphoryl)-5-oxohexanoic acid (3.36). A stirring solution of freshly-distilled dimethyl methylphosphonate (750 μL, 6.70 mmol, 3.7 equiv.) in dry THF (8 mL) was cooled to -78 ºC under inert atmosphere. To this solution, 2.5 M ^{n}BuLi (2.5 mL, 6.25 mmol, 3.5 equiv.) was added dropwise to affect a yellow color, and stirred for 2 h. If the reaction mixture occasionally freezes, or appears thick and milky; allow the mixture to warm to the point that stirring is possible, and re-cool prior to next step. Addition of acid **3.62** (500 mg, 1.81 mmol, 1.0 equiv.) in THF (4 mL) *via* cannula yielded a clear, orange solution. The solution was brought to rt and product formation was observed *via* TLC (silica gel, 5% MeOH in CH_2Cl_2), where the product was bright red under visualization with *p*-anisaldehyde stain. Upon completion, the reaction was quenched with 1.0 M HCl solution (3 × 3 mL), diluted in EtOAc (3 × 20 mL), and separated. The combined organic layers were washed with brine, dried ($MgSO_4$), filtered, and concentrated to afford 645.6 mg of crude phosphonate **3.36** as pale-yellow oil.

R_f = 0.24 (silica gel, 5% MeOH in DCM; *p*-anisaldehyde stain).

^{1}HNMR (300 MHz, $CDCl_3$): δ 4.54 (p, J = 5.8 Hz, 1H, -C*H*-), 3.78 (d, J = 11.3 Hz, 3H, -OCH_3), 3.77 (d, J = 11.3 Hz, 3H, -OCH_3), 3.11 (d, J = 22.7 Hz, 2H, -CH_2-), 2.89 (d, J = 6.1 Hz, 2H, -CH_2-), 2.58 (dd, J = 5.9, 15.4 Hz, 1H, -C*H*H-), 2.49 (dd, J = 5.5, 15.4 Hz, 1H, -C*H*H-), 0.84 (s, 9H, O-TBS *t*-Bu), 0.09 (s, 3H, O-TBS -CH_3), 0.06 (s, 3H, O-TBS -CH_3) ppm.

^{13}CNMR (75 MHz, $CDCl_3$): 199.7, 173.2, 65.2, 53.1 (t, J = 6.2 Hz), 50.7, 43.1, 41.4, 25.6, 17.8, -4.9, -5.0 ppm.

^{31}PNMR (121 MHz, $CDCl_3$): δ 19.6 ppm.

HRMS (EI) *m/z*: calculated for $C_{10}H_{20}O_7PSi$ [M – *t*-Bu] 311.0716, observed 311.0705 (Δ = 1.1 mmu).

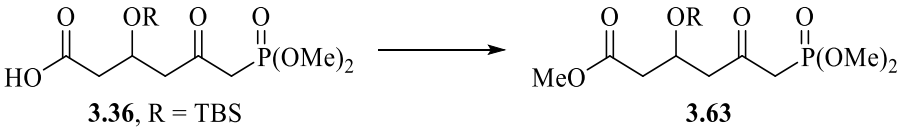

3.36, R = TBS **3.63**

Methyl 3-(*tert*-butyldimethylsilyloxy)-6-(dimethoxyphosphoryl)-5-oxohexanoate (3.63). According to the patented procedure by Harada and coworkers,[104] a solution of **3.36** (710 mg, 1.92 mmol, 1.0 equiv.) in acetone (13 mL, 0.15 M) was added potassium carbonate (286 mg, 2.11 mmol, 1.1 equiv.), and stirred for 10 min. Methyl iodide (600 μL, 9.64 mmol, 5.0 equiv.) was added to the solution and stirred overnight (8-12 h). The reaction mixture was quenched with water (15 mL), and diluted with EtOAc (30 mL). Layers were separated, and washed with EtOAc (3 × 10 mL). The combined organic layers were washed with brine, dried ($MgSO_4$), filtered, and concentrated. The crude product was purified *via* flash chromatography (30% EtOAc in hexanes) and yielded 653.5 mg (1.71 mmol, 89%) of **3.63** as clear, colorless oil.

R_f = 0.38 (silica gel, 40% acetone in hexanes; *p*-anisaldehyde stain).

^{1}HNMR (400 MHz, $CDCl_3$): δ 4.54 (p, *J* = 6.1 Hz, 1H, -C*H*-), 3.79 (d, *J* = 1.1 Hz, 3H, -OCH_3), 3.75 (d, *J* = 1.1 Hz, 3H, -OCH_3), 3.64 (s, 3H, -OCH_3), 3.09 (d, *J* = 22.8 Hz, 2H, -CH_2-), 2.86 (d, *J* = 6.1 Hz, 2H, -CH_2-), 2.53 (dd, *J* = 5.8, 14.8 Hz, 1H, -C*H*H-), 2.44 (dd, *J* = 6.4, 14.8 Hz, 1H, -C*H*H-), 0.82 (s, 9H, O-TBS *t*-Bu), 0.05 (s, 3H, O-TBS -CH_3), 0.04 (s, 3H, O-TBS -CH_3) ppm.

^{13}CNMR (100 MHz, $CDCl_3$): δ 200.1, 171.4, 65.5, 53.0, 52.9, 51.5, 51.0, 43.2, 42.1, 41.5, 25.6, 17.8, -4.9, -5.0 ppm.

^{31}PNMR (162 MHz, $CDCl_3$): δ 22.2 ppm.

HRMS (EI) *m/z*: calculated for $C_{11}H_{22}O_7PSi$ [M – *t*-Bu] 325.0872, observed 325.0921 (Δ = 4.9 mmu).

Characterization data for **3.63** proved consistent with previously reported literature data.[102]

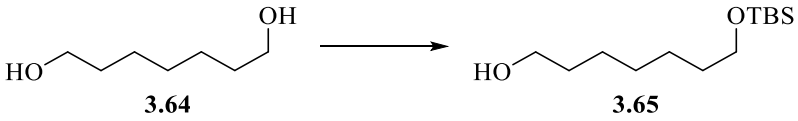

3.64 **3.65**

7-(*tert*-Butyldimethylsilyl)heptan-1-ol (3.65): In accordance with Wilke *et al*,[139] to an oven dried round-bottom flask containing a Teflon stir bar and 1,7-heptanediol **3.64** (10 g, 75.6 mmol, 1.0 equiv.) was added anhydrous acetonitrile (150 mL), hexanes passed through 10 g of activated alumina (450 mL), and triethylamine (12.7 mL, 90.4 mmol, 1.2 equiv.). The reaction mixture was stirred for 15 min at ambient temperature, upon which, *t*-butyldimethylsilyl chloride (11.4 g, 75.6 mmol, 1.0 equiv.) was added and the biphasic reaction was stirred vigorously for 48 h under inert atmosphere. Upon completion, the reaction was quenched with saturated aqueous NH_4Cl (300 mL), and diluted with EtOAc (200 mL). The layers were separated, and the aqueous layer was re-extracted (2 × 75 mL) with EtOAc. The combined organic layers were washed with brine (300 mL), dried ($MgSO_4$), filtered, and concentrated *in vacuo*. The crude residue

was purified by flash chromatography with a solvent gradient (100 mL 2%; 100 mL 5%; 100 mL 10%; 100 mL 15%; 100 mL 20%; 100 mL 25%; 200 mL 50% EtOAc in hexanes) to yield 14.2 g (57.6 mmol, 76%) of **3.65** as colorless oil.

R_f = 0.28 (silica gel, 20% EtOAc in hexanes).

^{1}HNMR (400 MHz, $CDCl_3$): δ 3.62 (t, J = 6.6 Hz, 2H, -CH_2-), 3.58 (t, J = 6.6 Hz, 2H, -CH_2-), 1.58 – 1.46 (m, 4H, 2 × -CH_2-), 1.37 – 1.22 (m, 7H, 3 × -CH_2-, -OH), 0.87 (s, 9H, O-TBS *t*-Bu), 0.03 (s, 6H, 2 × O-TBS -CH_3) ppm.

^{13}CNMR (100 MHz, $CDCl_3$): δ 63.3, 63.1, 32.8, 32.7, 29.2, 26.0, 25.8, 25.7, 18.4, -5.3 ppm.

HRMS (EI) *m/z*: Calculated for $C_{10}H_{20}O_7Si$ [M – *t*-Bu] 311.0716, Observed 259.1331 (Δ = 3.4 mmu).

Characterization data for **3.65** proved consistent with previously reported literature data.[140]

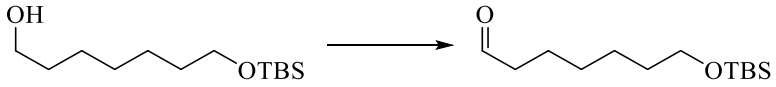

3.65 **3.66**

7-(*tert*-Butyldimethylsilyloxy)heptanal (3.66): To a round-bottom flask charged with PCC (1.46 g, 6.79 mmol, 1.2 eq.), silica gel (3 g), and CH_2Cl_2 (10 mL) was added alcohol **3.65** (1.40 g, 5.66 mmol, 1 equiv.) dissolved in DCM (10 mL). The reaction stirred at ambient temperature for 2 h, and monitored by TLC (silica gel, 10% EtOAc in hexanes). Upon completion, the reaction mixture was concentrated, and the dark brown suspension was added directly to a pre-equilibrated (silica gel, 10% EtOAc in hexanes) column, and purified to yield 0.97 g of a colorless oil (3.97 mmol, 70%).

R_f = 0.54 (silica gel, 10% EtOAc in hexanes).

^{1}HNMR (400 MHz, $CDCl_3$): δ 9.75 (t, J = 1.8 Hz, 1H, -CHO), 3.58 (t, J = 6.5 Hz, 2H, -CH_2-), 2.41 (dt, J = 1.9, 7.3 Hz, 2H, -CH_2-), 1.67 – 1.58 (m, 2H, -CH_2-), 1.52 – 1.46 (m, 2H, -CH_2-), 1.35 – 1.31 (m, 4H, 2 × -CH_2-), 0.87 (s, 9H, O-TBS *t*-Bu), 0.02 (s, 6H, 2 × O-TBS -CH_3) ppm.

^{13}CNMR (100 MHz, $CDCl_3$): δ 202.8, 63.1, 43.9, 32.6, 29.0, 26.0, 25.6, 22.1, 18.4, -5.3 ppm.

HRMS (EI) *m/z*: Calculated for $C_{10}H_{20}O_7Si$ [M – *t*-Bu] 311.0716, Observed 259.1331 (Δ = 3.4 mmu).

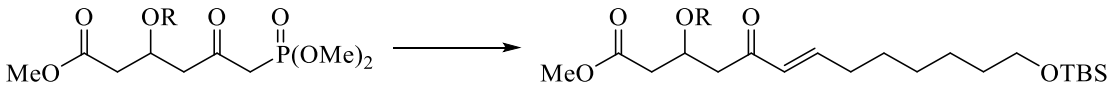

3.63, R = TBS **3.67**

(*E*)-Methyl-3,13-*bis*-(*tert*-butyldimethylsilyloxy)-5-oxotridec-6-enoate (3.67): Phosphonate **3.63** (302 mg, 0.79 mmol, 1.2 equiv.) was diluted in isopropanol (4 mL, dried over 4 Å ms) and cooled to 0 ºC. Cesium carbonate (257.4 mg, 0.79 mmol, 1.2 equiv.) was added to the solution, and the reaction stirred at 0 ºC for 2 h. A solution of TBS-aldehyde **3.66** (161 mg, 0.66 mmol, 1.0 equiv.) in dry isopropanol (4 mL)

was added dropwise to the reaction mixture, and allowed to warm to ambient temperature while stirring overnight. Upon completion, the reaction was diluted with EtOAc (10 mL) and quenched with 1.0 M HCl solution (4 mL). The layers were separated, and washed with EtOAc (3 × 5 mL). The combined organic layers were washed with brine, dried ($MgSO_4$), filtered, and concentrated *in vacuo*. The crude residue was purified by flash chromatography (10% EtOAc in hexanes) to yield **3.67** as 296.8 mg of clear, colorless oil (0.59 mmol, 75%).

R_f = 0.36 (silica gel, 10% EtOAc in hexanes; *p*-anisaldehyde stain).

^{1}HNMR (300 MHz, $CDCl_3$): δ 6.82 (dt, *J* = 15.9, 6.9 Hz, 1H, -C*H*=), 6.07 (dt, *J* = 15.9, 1.5 Hz, 1H, =C*H*-), 4.59 (p, *J* = 6.0 Hz, 1H, -C*H*-), 3.65 (s, 3H, -OCH_3), 3.57 (t, *J* = 6.4 Hz, 2H, -CH_2-), 2.82 (dd, *J* = 6.5, 15.7 Hz, 1H, -C*H*H-), 2.70 (dd, *J* = 5.9, 15.7 Hz, 1H, -C*H*H-), 2.54 (dd, *J* = 5.9, 14.8 Hz, 1H, -C*H*H-), 2.45 (dd, *J* = 6.4, 14.8 Hz, 1H, -C*H*H-), 2.23 – 2.16 (m, 2H, -CH_2-), 1.51 – 1.42 (m, 4H, 2 × -CH_2-), 1.35 – 1.28 (m, 4H, 2 × -CH_2-), 0.87 (s, 9H, O-TBS *t*-Bu), 0.81 (s, 9H, O-TBS *t*-Bu), 0.04 (s, 3H, O-TBS -CH_3), 0.03 (s, 6H, 2 × O-TBS -CH_3), 0.01 (s, 3H, O-TBS -CH_3) ppm.

^{13}CNMR (75 MHz, $CDCl_3$): δ 198.3, 171.5, 148.3, 131.0, 66.2, 63.1, 51.5, 47.2, 45.5, 32.7, 32.4, 29.0, 28.0, 25.9, 25.7, 25.6, 18.3, 17.9, -4.8, -5.0, -5.3 ppm.

HRMS (EI) *m/z*: Calculated for $C_{22}H_{43}O_5Si_2$ [M – *t*-Bu] 443.2649, Observed 443.2669 (Δ = 2.0 mmu).

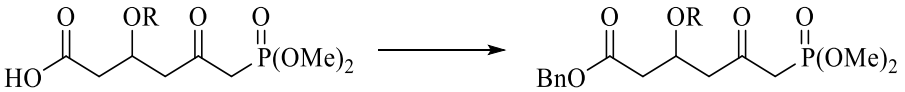

3.36, R = TBS **S-3**

Benzyl 3-(*tert*-butyldimethylsilyloxy)-6-(dimethoxyphosphoryl)-5-oxohexanoate (S-3). To a solution of **3.36** (610 mg, 1.66 mmol, 1.0 equiv.) in acetone (17 mL, 0.1 M) was added potassium carbonate (275 mg, 1.99 mmol, 1.2 equiv.), and stirred for 10 min. Benzyl bromide (983 μL, 8.23 mmol, 5.0 equiv.) was added to the solution and allowed to stir overnight (8-12 h). Upon completion, the reaction was quenched with water (15 mL), and diluted with EtOAc (30 mL). The layers were separated, and washed with EtOAc (3 × 10 mL). The combined organic layers were washed with brine, dried ($MgSO_4$), filtered and concentrated. The crude product was purified *via* flash chromatography (10% EtOAc in hexanes) to yield 680.0 mg (1.18 mmol, 71%) of **S-3** as clear, colorless oil.

R_f = 0.51 (silica gel, 40% acetone in hexanes; *p*-anisaldehyde stain).

^{1}HNMR (400 MHz, $CDCl_3$): δ 7.36 – 7.28 (m, 5H, 5 × -C*H*- Ph), 5.09 (dd, *J* = 7.5, 12.3 Hz, 2H, Bn -CH_2-), 4.56 (p, *J* = 6.0 Hz, 1H, -C*H*-), 3.77 (s, 3H, -OCH_3), 3.74 (s, 3H, -OCH_3), 3.07 (dd, *J* = 1.1, 22.6 Hz, 2H, -CH_2-), 2.87 (d, *J* = 6.2 Hz, 2H, -CH_2-), 2.58 (dd, *J* = 5.7, 15.1 Hz, 1H, -C*H*H-), 2.50 (dd, *J* = 6.2, 15.1 Hz, 1H, -C*H*H-), 0.81 (s, 9H, O-TBS *t*-Bu), 0.03 (d, *J* = 1.0 Hz, 6H, 2 × O-TBS -CH_3) ppm.

^{13}CNMR (100 MHz, $CDCl_3$): δ 200.1, 170.7, 135.8, 128.6, 128.3, 128.3, 66.4, 65.4, 51.0, 43.0, 42.2, 41.8, 25.7, 17.9, -4.8, -4.9 ppm.

^{31}PNMR (121 MHz, $CDCl_3$): δ 19.4 ppm.

HRMS (EI) *m/z*: calculated for $C_{17}H_{26}O_7PSi$ [M – *t*-Bu] 401.1185, observed 401.1176 (Δ = 0.9 mmu).

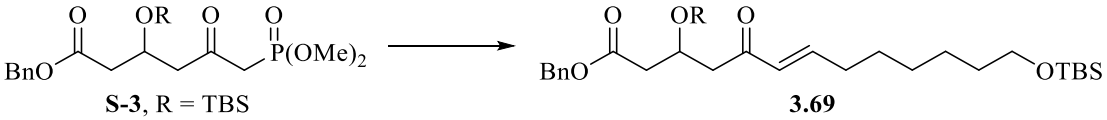

S-3, R = TBS **3.69**

(*E*)-Benzyl-3,13-*bis*-(*tert*-butyldimethylsilyloxy)-5-oxotridec-6-enoate (3.69): Phosphonate **S-3** (250 mg, 0.55 mmol, 1.2 equiv.) was diluted in isopropanol (4 mL, dried over 4 Å ms) and cooled to 0 ºC. Cesium carbonate (192.2 mg, 0.59 mmol, 1.3 equiv.) was added to the solution, and the reaction stirred at 0 ºC for 2 h. A solution of TBS-aldehyde **3.66** (111.2 mg, 0.45 mmol, 1.0 equiv.) in dry isopropanol (4 mL) was added to the reaction mixture dropwise, and allowed to warm to ambient temperature while stirring overnight. Upon completion, the reaction was diluted with EtOAc (10 mL) and quenched with 1.0 M HCl solution (4 mL). The layers were separated, and washed with EtOAc (3 × 5 mL). The combined organic layers were washed with brine, dried ($MgSO_4$), filtered, and concentrated *in vacuo*. The crude residue was purified by flash chromatography (5% EtOAc in hexanes) to yield **3.69** as 179.2 mg of clear, colorless oil (0.31 mmol, 69%), and stored in the freezer.

R_f = 0.37 (silica gel, 10% EtOAc in hexanes; *p*-anisaldehyde stain).

^{1}HNMR (400 MHz, $CDCl_3$): δ 7.39 – 7.34 (m, 5H, 5 × -C*H*- Ph), 6.82 (dt, *J* = 15.8, 6.9 Hz, 1H, -C*H*=), 6.08 (dt, *J* = 15.8, 1.4 Hz, 1H, =C*H*-), 5.16 (d, *J* = 12.4 Hz, 1H, -CH*H*-), 5.09 (d, *J* = 12.3 Hz, 1H, -CH*H*-), 4.65 (p, *J* = 6.1 Hz, 1H, -C*H*-), 3.61 (t, *J* = 6.5 Hz, 2H, -CH_2-), 2.86 (dd, *J* = 6.6, 15.6 Hz, 1H, -CH*H*-), 2.75 (dd, *J* = 5.8, 15.6 Hz, 1H, -CH*H*-), 2.63 (dd, *J* = 5.6, 14.9 Hz, 1H, -CH*H*-), 2.55 (dd, *J* = 6.2, 14.9 Hz, 1H, -CH*H*-), 2.25 – 2.18 (m, 2H, -CH_2-), 1.57 – 1.43 (m, 4H, 2 × -CH_2-), 1.38 – 1.32 (m, 2H, -CH_2-), 0.91 (s, 9H, O-TBS *t*-Bu), 0.84 (s, 9H, O-TBS *t*-Bu), 0.06 (s, 9H, 3 × O-TBS -CH_3), 0.03 (s, 3H, O-TBS -CH_3) ppm.

^{13}CNMR (100 MHz, $CDCl_3$): δ 198.4, 170.9, 148.4, 131.0, 128.5, 128.3, 128.2, 66.3, 66.2, 63.2, 47.1, 42.6, 32.7, 32.5, 29.0, 28.0, 26.0, 25.7, 25.6, 18.4, 17.9, -4.8, -4.9, -5.2 ppm.

HRMS (EI) *m/z*: Calculated for $C_{28}H_{47}O_5Si_2$ [M – *t*-Bu] 519.2962, Observed 519.2933 (Δ =2.9 mmu).

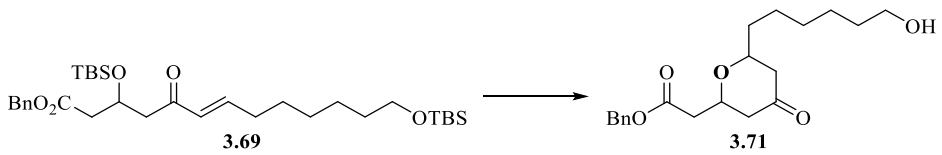

Benzyl 2-(6-(6-hydroxyhexyl)-4-oxotetrahydro-2*H*-pyran-2-yl)acetate (3.71): A 1.5 mL polypropylene Eppendorf® tube was charged with *bis*-silyl protected **3.69** (40 mg, 0.069 mmol, 1.0 equiv.), diluted in acetonitrile (700 μL, 0.1 M), and added pyridine (28 μL, 0.35 mmol, 5.0 equiv.). The reaction mixture was vortexed to homogeneity, upon which 48% HF (126 μL, 3.5 mmol, 50 equiv.) was added. The reaction was mixture was vortexed again, centrifuged, and left overnight. The reaction was quenched with water (2 × 1 mL), and diluted with EtOAc (2 × 2 mL). The aqueous layer was re-extracted with EtOAc, and the combined organic layers were washed with brine, dried ($MgSO_4$), filtered, and concentrated to dryness *in vacuo*. Column chromatography purified the product to afford **3.71** as clear, colorless oil.

^{1}HNMR (400 MHz, $CDCl_3$): δ 7.34 – 7.30 (m, 10H, 2 × C_6H_5), 5.13 (s, 4H, 2 x -CH_2-), 4.53 (tt, J = 4.9, 8.4 Hz, 1H, -C*H*-), 4.13 – 4.00 (m, 2H, 2 × -C*H*-), 3.60 (dt, J = 3.0, 6.6 Hz, 4H, 2 × -CH_2-), 3.57 – 3.52 (m, 1H, -C*H*-), 2.69 (dt, J = 16.0, 8.1 Hz, 2H, 2 × -CH*H*-), 2.58 – 2.47 (m, 4H, 4 × -CH*H*-), 2.44 – 2.34 (m, 2H, 2 × -CH*H*-), 2.34 – 2.14 (m, 4H, 4 × -CH*H*-), 1.54 – 1.44 (m, 8H, 4 × -CH_2-), 1.43 – 1.14 (m, 12H, 6 × -CH_2-) ppm.

^{13}CNMR (100 MHz, $CDCl_3$): δ 206.6, 206.4, 170.1, 170.0, 135.7, 135.6, 128.6, 128.4, 128.3, 128.24, 128.18, 77.0, 73.2, 72.9, 68.5, 66.6, 66.5, 62.89, 62.87, 47.6, 47.0, 46.7, 46.4, 41.3, 40.1, 36.1, 33.9, 32.64, 32.61, 29.1, 29.0, 25.6, 25.5, 25.13, 25.10 ppm.

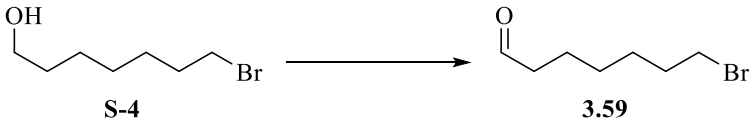

7-Bromoheptanal (3.59): To a round-bottom flask charged with 7-bromoheptanol **S-4** (1.40 g, 5.66 mmol, 1.0 equiv.) dissolved in CH_2Cl_2 (10 mL), was added a mixture of PCC (1.46 g, 6.79 mmol, 1.2 equiv.) and silica gel (3 g). The reaction was stirred under inert atmosphere at ambient temperature for 5 h, and monitored by TLC (silica gel, 10% EtOAc in hexanes). Upon completion, CH_2Cl_2 was carefully evaporated, to yield dark brown powder. Crude material was added directly to a pre-equilibrated column (silica gel, 10% EtOAc in hexanes), and yielded 0.97 g (3.97 mmol, 70%) of aldehyde **3.59** as clear, colorless oil.

R_f = 0.36 (silica gel, 10% EtOAc in hexanes).

^{1}HNMR (400 MHz, $CDCl_3$): δ 9.75 (t, J = 1.7 Hz, 1H, -C*H*O), 3.39 (t, J = 6.7 Hz, 2H, -CH_2-), 2.43 (dt, J = 1.7, 7.2 Hz, 2H, -CH_2-), 1.89 – 1.80 (m, 2H, -CH_2-), 1.63 (p, J = 7.5 Hz, 2H, -CH_2-), 1.50 – 1.28 (m, 4H, 2 × -CH_2-) ppm.

^{13}CNMR (100 MHz, $CDCl_3$): δ 202.5, 43.7, 33.7, 32.4, 28.2, 27.8, 21.8 ppm.

Characterization data for **3.59** proved consistent with previously reported literature data.[141]

S-5 **3.59**

7-bromoheptanal **(3.59):** To a round-bottom flask charged with 7-bromo-1-alkene **S-5** (400 mg, 2.09 mmol, 1.0 equiv.) in an equal mixture of *t*-butanol in deionized water (20 mL), was added potassium ferricyanide (2.07 g, 6.27 mmol, 3.0 equiv.) and potassium carbonate (867 mg, 6.27 mmol, 3.0 equiv.). A solution of potassium osmate dihydrate (15 mg, 0.04 mmol, 2 mol%) was prepared in 15% *w*/*w* NaOH (0.5 mL) and added to the vigorously stirred biphasic solution of **S-5**, sealed with a glass stopper and stirred overnight at ambient temperature. The reaction was quenched with saturated aqueous NH_4Cl (30 mL), and the organic layers were extracted with CH_2Cl_2 (3 × 20 mL). The combined organic layers were washed with brine, dried ($MgSO_4$), filtered, and concentrated *in vacuo* to yield the crude diol as clear and stable oil. The crude diol in DCM (8.5 mL), was added a portion of lead tetraacetate (1.1 g, 2.50 mmol, 1.2 equiv.), and left to stir for 90 min at ambient temperature, under inert atmosphere. The reaction mixture was concentrated to 20% volume *in vacuo* and added directly to a pre-equilibrated column (silica gel, 10% EtOAc in hexanes) for isolation of 288.3 mg of **3.59** (1.5 mmol, 72%) as clear, colorless oil.

Characterization data was identical to PCC oxidation method (*vide supra*), with comparable yields; two-step dihydroxylation/oxidative cleavage is method of choice due to cost of commercial starting bromide.[142]

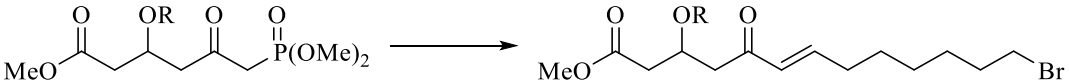

3.63, R = TBS **S-6**

(*E*)-Methyl 13-bromo-3-(*tert*-butyldimethylsilyloxy)-5-oxotridec-6-enoate (S-6): Phosphonate **3.63** (426.8 mg, 1.16 mmol, 1.2 equiv.) was diluted in isopropanol (5 mL, dried over 4 Å ms) and cooled to 0 ºC. Cesium carbonate (379 mg, 1.16 mmol, 1.2 equiv.) was added to the solution, and the reaction stirred at 0 ºC for 2 h. A solution of 7-bromoheptanal **3.59** (180 mg, 0.93 mmol, 1.0 equiv.) in dry isopropanol (5 mL) was added to the reaction mixture dropwise, and allowed to warm to ambient temperature while stirring overnight. Upon completion, the reaction was diluted with EtOAc (15 mL) and quenched with 1.0 M HCl solution (5 mL). The layers were separated, and washed with EtOAc (3 × 10 mL). The combined organic layers were washed with brine, dried ($MgSO_4$), filtered, and concentrated *in vacuo*. The crude residue was purified by flash chromatography (5% EtOAc in hexanes) to yield **S-6** as 326.0 mg of clear, colorless oil (0.73 mmol, 78%).

$\mathbf{R_f}$ = 0.34 (silica gel, 10% EtOAc in hexanes).

^{1}HNMR (400 MHz, $CDCl_3$): δ 6.81 (dt, *J* = 15.8, 6.9 Hz, 1H, -C*H*=), 6.08 (dt, *J* = 15.8, 1.5 Hz, 1H, =C*H*-), 4.59 (p, *J* = 6.0 Hz, 1H, -C*H*-), 3.65 (s, 3H, -OCH_3), 3.39 (t, *J* = 6.7 Hz, 2H, -CH_2Br), 2.82 (dd, *J* = 6.7, 15.7 Hz, 1H, -CH*H*-), 2.71 (dd, *J* = 6.0, 15.7 Hz, 1H, -CH*H*-), 2.54 (dd, *J* = 5.6, 14.8 Hz, 1H, -CH*H*-), 2.46 (dd, *J* = 6.4, 14.8 Hz, 1H, -CH*H*-), 2.24 – 2.18 (m, 2H, -CH_2-), 1.87 – 1.80 (m, 2H, -CH_2-), 1.51 – 1.40 (m, 4H, 2 × -CH_2-), 1.37 – 1.31 (m, 2H, -CH_2-), 0.81 (s, 9H, O-TBS *t*-Bu), 0.04 (s, 3H, O-TBS -CH_3), 0.01 (s, 3H, O-TBS -CH_3) ppm.

^{13}CNMR (100 MHz, $CDCl_3$): δ 198.3, 171.5, 147.9, 131.1, 66.2, 51.5, 47.3, 42.5, 33.7, 32.6, 33.3, 28.3, 27.9, 27.8, 25.7, 17.9, -4.7, -5.0 ppm.

HRMS (EI) *m/z*: Calculated for $C_{10}H_{20}O_7Si$ [M – *t*-Bu] 311.0716, Observed 259.1331 (Δ = 3.4 mmu).

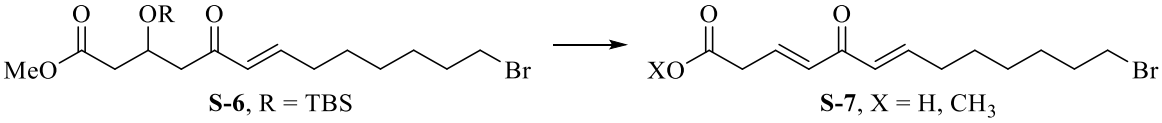

S-6, R = TBS **S-7**, X = H, CH_3

Elimination By-Product Mixture (S-7): In accordance with Barluenga's procedure,[108] a pre-formed solution of 3-hydroxypropionitrile (38 µL, 0.56 mmol, 10.0 equiv.) and 60% dispersion sodium hydride (9 mg, 0.22 mmol, 4.0 equiv.) in THF (0.4 mL) was added to a solution of **S-6** (25 mg, 5.6 µmol, 1.0 equiv.) in THF (0.4 mL) at 0 ºC. Upon addition, the clear and colorless solution turned deep red, which indicated elimination pathways from this system. The reaction was immediately quenched with 1 N HCl solution, and underwent aqueous work-up. Characterization was based on the crude residue obtained, and believed to contain a mixture of elimination by-products including those of ester starting material and free acid. Because neither purification or additional analysis of the obtained mixture was performed, spectral notation is only reported for new diagnostic signals (δ 7.0 – 3.0 ppm).

R_f = 0.23 (silica gel, 10% EtOAc in hexanes).

^{1}HNMR (400 MHz, $CDCl_3$): δ 7.06 (dt, *J* = 15.7, 7.2 Hz, 1H, -C*H*=), 6.90 (ddt, *J* = 15.9, 5.3, 1.6 Hz, 1H, =C*H*-), 6.86 (dt, *J* = 15.8, 6.9 Hz, 1H, =C*H*-), 6.36 (qt, *J* = 13.5, 1.4 Hz, 1H, -C*H*=), 6.11 (dt, *J* = 15.9, 1.6 Hz, 1H, -C*H*=), 5.90 (dt, *J* = 15.9, 1.5 Hz, 1H, =C*H*-), 3.89 (dt, *J* = 6.2, 0.5 Hz, "4.5H," 2 × -CH_2-), 3.72 (s, "3.7H," -OCH_3), 3.44 (dd, *J* = 7.2, 1.5 Hz, 2H, 2 × -CH*H*-), 3.89 (t, *J* = 6.8 Hz, "3.7H," 2 × -CH_2-), 3.27 (dd, *J* = 7.0, 1.6 Hz, 1H, -CH*H*-) ppm.

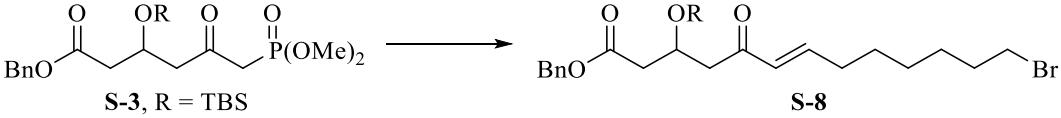

S-3, R = TBS **S-8**

(*E*)-Benzyl 13-bromo-3-(*tert*-butyldimethylsilyloxy)-5-oxotridec-6-enoate (S-8): Phosphonate **S-3** (73.2 mg, 0.16 mmol, 1.2 equiv.) was diluted in isopropanol (1 mL, dried over 4 Å ms) and cooled to 0 ºC.

Cesium carbonate (56.3 mg, 0.17 mmol, 1.3 equiv.) was added to the solution, and the reaction stirred at 0 ºC for 2 h. A solution of 7-bromoheptanal **3.59**[143] (25.7 mg, 0.133 mmol, 1.0 equiv.) in dry isopropanol (5 mL) was added to the reaction mixture dropwise, and allowed to warm to ambient temperature while stirring overnight. Upon completion, the reaction was diluted with EtOAc (15 mL) and quenched with 1.0 M HCl solution (5 mL). The layers were separated, and washed with EtOAc (3 × 10 mL). The combined organic layers were washed with brine, dried ($MgSO_4$), filtered, and concentrated *in vacuo*. The crude residue was purified by flash chromatography (5% EtOAc in hexanes) to yield **S-8** as 42.5 mg of clear, colorless oil (0.081 mmol, 61%).

R_f = 0.45 (silica gel, 10% EtOAc in hexanes).

^{1}HNMR (300 MHz, $CDCl_3$): δ 7.33 (s, 5H, 5 × –C*H*- Ph), 6.78 (dt, *J* = 15.9, 7.0 Hz, 1H, -C*H*=), 6.06 (dt, *J* = 15.9, 1.3 Hz, 1H, =C*H*-), 5.13 (d, *J* = 12.4 Hz, 1H, -CH*H*-), 5.06 (d, *J* = 12.4 Hz, 1H, -CH*H*-), 4.61 (p, *J* = 6.1 Hz, 1H, -C*H*-), 3.39 (t, *J* = 6.7 Hz, 2H, -CH_2-), 2.82 (dd, *J* = 15.7, 6.7 Hz, 1H, -CH*H*-), 2.72 (dd, *J* = 15.7, 5.7 Hz, 1H, -CH*H*-), 2.59 (dd, *J* = 14.8, 5.7 Hz, 1H, -CH*H*-), 2.52 (dd, *J* = 14.8, 6.2 Hz, 1H, -CH*H*-), 2.23 – 2.16 (m, 2H, -CH_2-), 1.84 (p, *J* = 7.4 Hz, 2H, -CH_2-), 1.48 – 1.29 (m, 6H, 3 × -CH_2-), 0.83 (s, 9H, O-TBS *t*-Bu), 0.03 (s, 3H, O-TBS -CH_3), 0.00 (s, 3H, O-TBS -CH_3) ppm.

^{13}CNMR (75 MHz, $CDCl_3$): δ 198.3, 170.9, 147.9, 135.8, 131.1, 128.5, 128.2, 128.1, 66.2, 66.1, 47.1, 42.6, 33.7, 32.6, 32.3, 28.3, 27.9, 27.8, 25.7, 17.9, -4.81, -4.95 ppm.

HRMS (EI) *m/z*: Calculated for $C_{10}H_{20}O_7Si$ (M – *t*-Bu) 311.0716, Observed 259.1331 (Δ = 3.4 mmu).

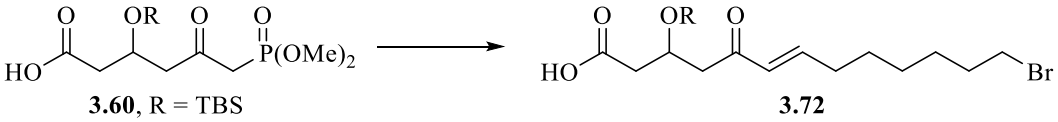

3.60, R = TBS **3.72**

(*E*)-13-Bromo-3-(*tert*-butyldimethylsilyloxy)-5-oxotridec-6-enoic acid (3.72): Phosphonate **3.60** (230 mg, 0.62 mmol, 1.2 equiv.) was dissolved in isopropanol (4 mL, dried over 4 Å MS) and cooled to 0 ºC. Cesium carbonate (390 mg, 1.2 mmol, 1.9 equiv.) was added in one portion, and the mixture was stirred at 0 ºC for 2 hours. To the reaction mixture, a solution of known bromoaldehyde **3.59**[143] (99 mg, 0.51 mmol, 1.0 equiv.) in isopropanol (1 mL, dried over 4 Å MS, 0.1 M overall reaction mixture) was added dropwise. The reaction mixture was warmed to 30 ºC and stirred overnight. The reaction was diluted with EtOAc (10 mL), and quenched by the addition of 1.0 M HCl solution (4 mL). The mixture was extracted with EtOAc (2 × 10 mL), and the combined organic layers were washed with brine, dried with $MgSO_4$, filtered, and concentrated *in vacuo*. Purification *via* column chromatography (20% EtOAc in hexanes) yielded 179.9 mg of **3.72** (0.413 mmol, 81%) as clear, colorless oil.

R_f = 0.29 (silica gel, 20% EtOAc in hexanes).

^{1}HNMR (400 MHz, $CDCl_3$): δ 9.70 (br s, 1H, -CO_2H), 6.81 (dt, J = 15.9, 6.9 Hz, 1H, -C*H*=), 6.08 (dt, J = 15.9, 1.5 Hz, 1H, =C*H*-), 4.59 (p, J = 5.9 Hz, 1H, -C*H*-), 3.38 (t, J = 6.7 Hz, 2H, -CH_2-), 2.84 (dd, J = 15.9, 6.4 Hz, 1H, -CH*H*-), 2.72 (dd, J = 15.9, 6.0 Hz, 1H, -CH*H*-), 2.60 (dd, J = 15.1, 5.5 Hz, 1H, -CH*H*-), 2.49 (dd, J = 15.1, 6.0 Hz, 1H, -CH*H*-), 2.24 – 2.17 (m, 2H, -CH_2-), 1.89 – 1.78 (m, 2H, -CH_2-), 1.51 – 1.29 (m, 8H, 4 × -CH_2-), 0.82 (s, 9H, O-TBS *t*-Bu), 0.06 (s, 3H, O-TBS -CH_3), 0.02 (s, 3H, O-TBS -CH_3) ppm.

^{13}CNMR (100 MHz, $CDCl_3$): δ 198.2, 176.5, 148.3, 131.0, 66.0, 46.9, 42.3, 33.7, 32.5, 32.3, 28.3, 27.8, 27.7, 25.7, 17.9, -4.8, -5.0 ppm.

HRMS (EI) *m/z*: Calculated for $C_{15}H_{26}BrO_4Si$ [M – *t*-Bu] 377.0784, Observed 377.0789 (Δ = 0.5 mmu).

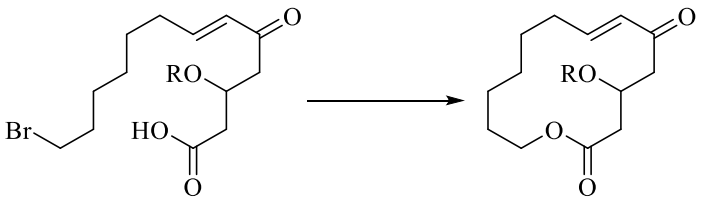

3.72, R = TBS **S-9**

(*E*)-4-(*tert*-Butyldimethylsilyloxy)oxacyclotetradec-7-ene-2,6-dione (S-9): To a flask charged with bromoacid **3.72** (120 mg, 0.28 mmol, 1.0 equiv.) in anhydrous DMF (28 mL, 0.01 M), was added cesium carbonate (162.1 mg, 0.50 mmol, 1.8 equiv.) under argon atmosphere at 0 ºC. The reaction was left to warm to room temperature as it stirred overnight, upon which the reaction mixture was diluted with EtOAc (40 mL) and washed with brine. The aqueous layer was re-extracted with EtOAc, and the combined organic layers were washed with water (3 × 40 mL) and brine, dried ($MgSO_4$), filtered, and concentrated to dryness *in vacuo*. The residue was purified by column chromatography (silica gel, 10% EtOAc in hexanes) to afford 66.3 mg of macrolactone **S-9** (0.19 mmol, 68%) as clear, pale-yellow oil.

R_f = 0.54 (silica gel, 10% EtOAc in hexanes).

^{1}HNMR (400 MHz, $CDCl_3$): δ 6.80 (ddd, J = 16.0, 8.1, 6.6 Hz, 1H, =C*H*-), 6.05 (dt, J = 16.0, 1.4 Hz, 1H, =C*H*-), 4.54 (ddt, J = 8.2, 4.3, 6.0 Hz, 1H, -C*H*-), 4.15 (ddd, J = 11.1, 7.3, 3.1 Hz, 1H, -CH*H*-), 4.08 – 4.01 (m, 1H, -CH*H*-), 3.00 (dd, J = 13.8, 8.2 Hz, 1H, -CH*H*-), 2.70 (dd, J = 13.8, 6.0 Hz, 1H, -CH*H*-), 2.52 (dd, J = 14.7, 4.3 Hz, 1H, -CH*H*-), 2.47 (dd, J = 14.7, 6.1 Hz, 1H, -CH*H*-), 2.39 – 2.21 (m, 2H, -CH_2-), 1.65 – 1.54 (m, 4H, 2 × -CH_2-), 1.48 – 1.39 (m, 4H, 2 × -CH_2-), 0.85 (s, 9H, O-TBS *t*-Bu), 0.06 (s, 3H, O-TBS -CH_3), 0.05 (s, 3H, O-TBS -CH_3) ppm.

^{13}CNMR (100 MHz, $CDCl_3$): δ 198.8, 170.4, 149.5, 131.8, 67.3, 64.7, 47.0, 42.5, 32.2, 27.4, 27.2, 25.8, 25.7, 25.5, 18.0, -4.8, -4.8 ppm.

HRMS (EI) *m/z*: Calculated for $C_{12}H_{25}O_4Si$ [M – *t*-Bu] 297.1522, Observed 297.1518 (Δ = 0.4 mmu).

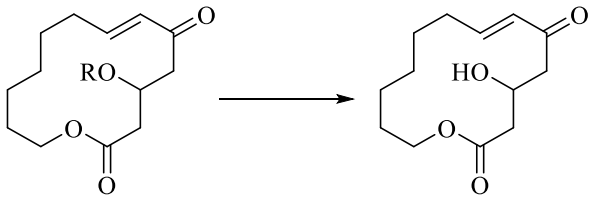

S-9 **3.36**

(*E*)-4-Hydroxyoxacyclotetradec-7-ene-2,6-dione (3.36): To a 1.5 mL polypropylene Eppendorf® tube charged with macrolactone **S-9** (16 mg, 0.045 mmol, 1.0 equiv.), was added acetonitrile (450 μL, 0.1 M) and pyridine (18 μL, 0.225 mmol, 5.0 equiv.). The reaction mixture was vortexed to homogeneity, upon which 48% HF (82 μL, 0.450 mmol, 50 equiv.) was added. The reaction was mixture was vortexed again, centrifuged, and left for 5 h. The reaction was quenched with water (2 × 1 mL), and diluted with EtOAc (2 × 2 mL). The aqueous layer was re-extracted with EtOAc, and the combined organic layers were washed with brine, dried ($MgSO_4$), filtered, and concentrated to dryness *in vacuo*. The product was purified by column chromatography (silica gel, 20% EtOAc in hexanes) to afford 10.8 mg of **3.36** (0.045 mmol, quant.) as clear, colorless oil.

R_f = 0.28 (silica gel, 40% EtOAc in hexanes).

^{1}HNMR (400 MHz, $CDCl_3$): δ 6.81 (dt, *J* = 16.0, 7.3 Hz, 1H, =C*H*-), 6.07 (dt, *J* = 16.0, 1.4 Hz, 1H, =C*H*-), 4.33 – 4.27 (m, 1H, -C*H*-), 4.17 (t, *J* = 5.4 Hz, 2H, -CH_2-), 3.73 (br s, 1H, -O*H*), 2.92 (d, *J* = 5.7 Hz, 2H, -CH_2-), 2.62 (dd, *J* = 16.1, 3.6 Hz, 1H, -CH*H*-), 2.52 (dd, *J* = 16.1, 8.4 Hz, 1H, -CH*H*-), 2.36 (dd, *J* = 7.1, 1.6 Hz, 1H, -CH*H*-), 2.32 (dd, *J* = 7.1, 1.4 Hz, 1H, -CH*H*-), 1.66 – 1.57 (m, 4H, 2 × -CH_2-), 1.44 – 1.31 (m, 4H, 2 × -CH_2-) ppm.

^{13}CNMR (100 MHz, $CDCl_3$): δ 201.5, 171.8, 151.9, 132.5, 66.7, 64.4, 41.6, 39.6, 32.6, 27.8, 27.7, 25.9, 25.6 ppm.

HRMS (EI) *m/z*: Calculated for $C_{13}H_{20}O_4$ [M] 240.1362, Observed 240.1348 (Δ = 1.4 mmu).

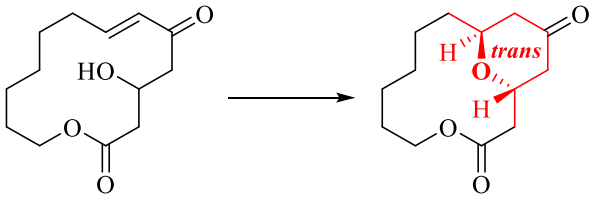

3.36 **3.73**

***trans*-Tetrahydropyran-5-one (3.73):** To a 5 mm NMR tube charged with **3.36** (3.5 mg, 14.57 μmol, 1.0 equiv.) in $CDCl_3$ (0.5 mL), was added *p*-toluenesulfonic acid monohydrate (1.6 mg), of which, most did not go into solution. Instantaneous conversion of material was realized *via* ^{1}HNMR and TLC (silica gel, 20% EtOAc in hexanes) monitoring, upon which, the mixture was filtered, concentrated, and purified by

column chromatography (silica gel, 20% EtOAc in hexanes) to afford 2.9 mg of ***trans*-3.73** (12.09 μmol, 83%) as clear, colorless oil.

R_f = 0.19 (silica gel, 20% EtOAc in hexanes).

^{1}HNMR (400 MHz, $CDCl_3$): δ 4.74 (ddt, *J* = 12.2, 6.3, 3.8 Hz, 1H, -C*H*-), 4.47 (ddd, *J* = 11.2, 6.4, 2.4 Hz, 1H, -CH*H*-), 4.17 (dddd, *J* = 10.8, 8.7, 3.9, 1.9 Hz, 1H, -C*H*-), 3.97 (ddd, *J* = 11.2, 9.4, 1.9 Hz, 1H, -CH*H*-), 2.71 (dd, *J* = 12.3, 1.4 Hz, 1H, -CH*H*-), 2.67 (ddd, *J* = 14.3, 6.2, 1.2 Hz, 1H, -CH*H*-), 2.42 (ddd, *J* = 14.1, 4.1, 1.7 Hz, 1H, -CH*H*-), 2.34 (dd, *J* = 13.7, 3.4 Hz, 1H, -CH*H*-), 2.32 – 2.26 (m, 1H, -CH*H*-), 2.24 (ddd, *J* = 14.4, 4.3, 1.7 Hz, 1H, -CH*H*-), 1.92 – 1.82 (m, 1H, -CH*H*-), 1.73 – 1.43 (m, 5H, 5 × -CH*H*-), 1.43 – 1.26 (m, 4H, 2 × -CH_2-) ppm.

^{13}CNMR (100 MHz, $CDCl_3$): δ 206.5, 170.4, 70.8, 69.9, 66.7, 48.2, 46.1, 39.6, 33.4, 26.8, 25.4, 25.1, 22.1 ppm.

HRMS (EI) *m/z*: Calculated for $C_{13}H_{18}O_3$ [M – H_2O] 222.1256, Observed 222.1270 (Δ = 1.4 mmu).

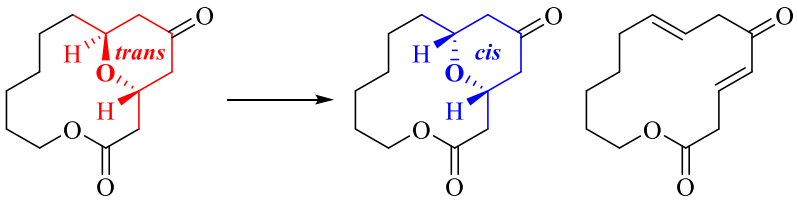

3.73 **3.74** **3.76**

To a 5 mm NMR tube charged with ***trans*-3.73** (2.5 mg, 10.4 μmol, 1.0 equiv.) in $CDCl_3$ (0.5 mL), was added *p*-toluenesulfonic acid monohydrate (1.1 mg), and carefully brought to 80 ºC. The length of the tube should be at least 5" and only be heated to the height of the solvent, to help prevent bumping. The reaction was heated at 80 ºC for 5 h, and monitored by ^{1}HNMR and TLC. Upon consumption of starting material, the reaction was filtered, concentrated, and purified by column chromatography (silica gel, 10% EtOAc in hexanes) to afford 1.1 mg of ***cis*-3.74** (4.58 μmol, 62%) as colorless oil. Trace amount of putative elimination by-product **3.76** was isolated, and submitted to ^{1}HNMR analysis; based on relative peak intensities from reaction mixture, it is assumed that elimination occurred by as much as 30% of total yield.

***cis*-Tetrahydropyran-5-one (3.74)**

R_f = 0.25 (silica gel, 20% EtOAc in hexanes).

^{1}HNMR (300 MHz, $CDCl_3$): δ 4.32 (ddd, *J* = 11.0, 10.1, 2.9 Hz, 1H, -CH*H*-), 4.18 (ddd, *J* = 11.0, 4.7, 4.0 Hz, 1H, -CH*H*-), 3.95 (dddd, *J* = 11.5, 7.7, 6.4, 2.7 Hz, 1H, -C*H*-), 3.58 (m, 1H, -C*H*-), 2.51 (d, *J* = 7.7 Hz, 1H, -CH*H*-), 2.50 (d, *J* = 6.4 Hz, 1H, -CH*H*-), 2.41 (ddd, *J* = 14.4, 2.7, 1.6 Hz, 1H, -CH*H*-), 2.32 (ddd, *J* = 14.4, 3.1, 1.6 Hz, 1H, -CH*H*-), 2.36 – 2.18 (m, 2H, -CH_2-), 1.93 – 1.78 (m, 1H, -CH*H*-), 1.77 – 1.27 (m, 9H, -CH*H*- and 4 × -CH_2-) ppm.

^{13}CNMR (100 MHz, $CDCl_3$): δ 206.1, 171.0, 77.2, 74.3, 64.4, 48.3, 47.1, 42.3, 33.6, 26.1, 25.2, 24.4, 24.2 ppm.

HRMS (ESI+ TOF) *m/z*: Calculated for $C_{13}H_{20}O_4Na$ [$(M + Na)^+$] 263.1259, Observed 263.1276 (Δ = 1.7 mmu).

Diene by-product (3.76)

R_f = 0.44 (silica gel, 20% EtOAc in hexanes).

^{1}HNMR (300 MHz, $CDCl_3$): δ 6.84 (dt, *J* = 16.0, 7.3 Hz, 1H, =C*H*-), 6.23 (dt, *J* = 16.0, 1.3 Hz, 1H, -C*H*=), 5.55 – 5.34 (m, 2H, 2 × -C*H*=), 4.16 (t, *J* = 5.4 Hz, 1H, -CH*H*-), 4.08 (t, *J* = 5.4 Hz, 1H, -CH*H*-), 3.22 – 3.15 (m, 2H, -CH_2-), 2.37 – 2.30 (m, 2H, -CH_2-), 2.09 – 2.02 (m), 1.74 – 1.49 (m), 1.44 – 1.24 (m) ppm. Accurate signal elucidation not possible due to low sample size and contamination of water (δ 1.56 ppm) and grease (δ 1.25, 0.87 – 0.84 ppm).[135] It was assumed that the multiplet at 2.09 – 2.02 is a single diastereotopic C8 proton (paired proton buried in multiplets) that was overlapping a residual solvent peak, such at the beta methyl singlet of EtOAc (δ 2.05).[135]

^{13}CNMR (75 MHz, $CDCl_3$): δ 194.0, 174.0, 139.0, 135.9, 132.2, 124.5, 64.0, 38.8, 29.8, 27.9, 26.6, 22.6, 18.1 ppm.

HRMS (ESI TOF+) *m/z*: Calculated for $C_{13}H_{18}O_3Na$ [$(M + Na)^+$] 245.1154, Observed 245.1126 (Δ = 2.8 mmu).

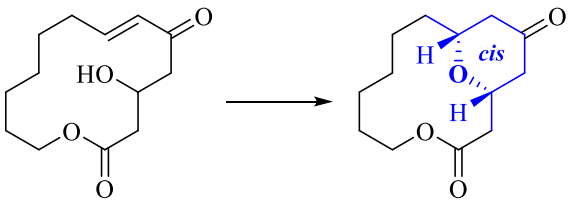

3.36 **3.74**

cis-Tetrahydropyran-5-one (**3.74**): To a 5 mm NMR tube charged with **3.36** (4.7 mg, 19.56 μmol, 1.0 equiv.) in $CDCl_3$ (0.5 mL), was added Amberlyst-15® hydrogen form (5 mg) and carefully heated to 80 ºC for 5 h. The reaction was monitored by ^{1}HNMR and TLC, and upon consumption of starting material, the mixture was filtered, concentrated, and purified by column chromatography (silica gel, 10% EtOAc in hexanes) to afford 3.6 mg of ***cis*-3.74** (14.87 μmol, 76%) as clear, colorless oil.

Characterization data identical to the *cis*-pyranone previously obtained *via* thermodynamic interconversion.

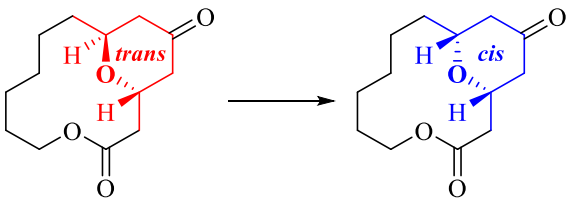

3.73 **3.74**

cis-Tetrahydropyran-5-one (**3.74**): To a 5 mm NMR tube charged with ***trans*-3.73** (2.7 mg, 11.24 μmol, 1.0 equiv.) in $CDCl_3$ (0.5 mL), was added Amberlyst-15® hydrogen form (5 mg) and heated to 80 ºC for 4 h. The reaction was monitored by ^{1}HNMR, following key proton shifts in the range of δ 4.74 – 3.58 (H3, H7, $H13_A$, $H13_B$). Upon completion, the reaction mixture was filtered, and purified by column chromatography (silica gel, 10% EtOAc in hexanes) to afford 2.2 mg of ***cis*-3.74** (9.33 μmol, 83%; 69% over two steps from oxa-conjugate precursor **3.36**) as clear, colorless oil.

Characterization data identical to the *cis*-pyranone previously obtained *via* Amberlyst-15®-mediated thermodynamic interconversion, with comparable yield.

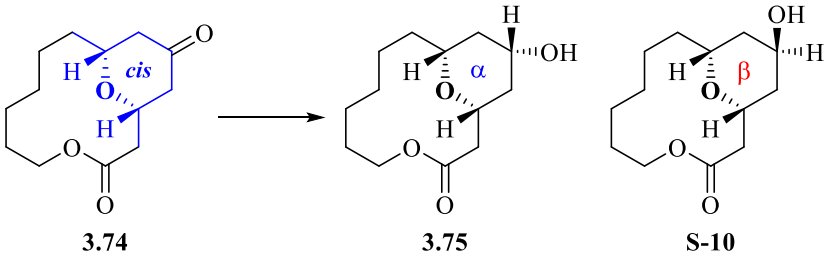

3.74 **3.75** **S-10**

***α*-*cis*-Tetrahydropyran-5-ol (3.75):** To a vial charged with *cis*-pyranone **3.74** (2.6 mg, 10.8 μmol, 1.0 equiv.) in methanol (0.25 mL) at 0 ºC, was added $NaBH_4$ (1.2 mg, 32.5 μmol, 3.0 equiv.) and stirred for 90 min. Upon completion, the reaction mixture was quenched with one drop of acetic acid, and diluted with EtOAc and water. The layers were separated, and the aqueous later was re-extracted with EtOAc. The combined organic layers were washed with brine, dried ($MgSO_4$), filtered, and concentrated *in vacuo*. The residue was purified by column chromatography (silica gel, 20% EtOAc in hexanes) to afford 2.2 mg of the *α*-*cis*-product **3.75** (9.16 μmol, 84%), and trace amount of the *β*-*cis*-product **S-10** (0.83 μmol, 7%) as clear, colorless oils.

syn:

R_f = 0.38 (silica gel, 50% EtOAc in hexanes).

^{1}HNMR (400 MHz, $CDCl_3$): δ 4.36 (dt, *J* = 3.2, 11.0 Hz, 1H, -CH*H*-), 4.06 (dt, *J* = 11.0, 4.6 Hz, 1H, -CH*H*-), 3.81 (dddd, *J* = 11.0, 11.0, 4.6, 4.6 1H, -C*H*-), 3.66 (m, 1H, -C*H*-), 3.27 (m, 1H, -C*H*-), 2.43 – 2.41 (m, 2H, -CH_2-), 1.96 (ddt, *J* = 12.0, 4.7, 1.9 Hz, 1H, -CH*H*-), 1.88 – 1.76 (m, 2H, 2 × -CH*H*-), 1.74 – 1.66 (m, 1H, -CH*H*-), 1.61 – 1.32 (m, 6H, 3 × -CH_2-), hydroxyl proton absent (H/D exchange) ppm.

^{13}CNMR (100 MHz, $CDCl_3$): δ 172.1, 76.3, 73.4, 68.1, 63.9, 42.2, 41.7, 40.6, 33.2, 29.7, 26.2, 25.5, 24.8, 23.7 ppm.

HRMS (ESI+ TOF) *m/z*: Calculated for $C_{13}H_{22}O_4Na$ [$(M + Na)^+$] 265.1410, Observed 265.1408 (Δ = 0.2 mmu).

Characterization data for **S-10** proved consistent with previously reported literature data.[61]

3.8 References

(1) Wright, A. E.; Botelho, J. C.; Guzmán, E.; Harmody, D.; Linley, P.; McCarthy, P. J.; Pitts, T. P.; Pomponi, S.; Reed, J. K. *J. Nat. Prod.* **2007**, *70* (3), 412–416.
(2) D'Ambrosio, M.; Guerriero, A.; Pietra, F.; Debitus, C. *Helv. Chim. Acta* **1996**, *79* (1), 51–60.
(3) Donia, M.; Hamann, M. T. *Lancet Infect. Dis.* **2003**, *3*, 338–348.
(4) Nasir, N. M.; Ermanis, K.; Clarke, P. A. *Org. Biomol. Chem.* **2014**, *12*, 3323–3335.
(5) Fuwa, H. *Heterocycles* **2012**, *85* (6), 1255–1298.
(6) Clarke, P. A.; Santos, S. *Eur. J. Org. Chem.* **2006**, No. 9, 2045–2053.
(7) Kang, E. J.; Lee, E. *Chem. Rev.* **2005**, *105*, 4348–4378.
(8) Yeung, K.; Paterson, I. *Chem. Rev.* **2005**, *105*, 4237–4313.
(9) Faul, M. M.; Huff, B. E. *Chem. Rev.* **2000**, *100*, 2407–2473.
(10) Julien, B.; Tian, Z.-Q.; Reid, R.; Reeves, C. D. *Chem. Biol.* **2006**, *13*, 1277–1286.
(11) Piel, J. *Proc. Natl. Acad. Sci.* **2002**, *99* (22), 14002–14007.
(12) Irschik, H.; Kopp, M.; Weissman, K. J.; Buntin, K.; Piel, J.; Müller, R. *ChemBioChem* **2010**, *11*, 1840–1849.
(13) Helfrich, E. J. N.; Piel, J. *Nat. Prod. Rep.* **2016**, *33*, 231–316.
(14) Berkhan, G.; Hahn, F. *Angew. Chem. Int. Ed.* **2014**, *53*, 14240–14244.
(15) Sudek, S.; Lopanik, N. B.; Waggoner, L. E.; Hildebrand, M.; Anderson, C.; Liu, H.; Patel, A.; Sherman, D. H.; Haygood, M. G. *J. Nat. Prod.* **2007**, *70*, 67–74.
(16) Oja, T.; Palmu, K.; Lehmussola, H.; Leppäranta, O.; Hännikäinen, K.; Niemi, J.; Mäntsälä, P.; Metsä-Ketelä, M. *Chem. Biol.* **2008**, *15*, 1046–1057.
(17) Luhavaya, H.; Dias, M. V. B.; Williams, S. R.; Hong, H.; Oliveira, L. G. De; Leadlay, P. F. *Angew. Chem. Int. Ed.* **2015**, *54*, 13622–13625.
(18) Pöplau, P.; Frank, S.; Morinaka, B. I.; Piel, J. *Angew. Chem. Int. Ed.* **2013**, *52*, 13215–13218.
(19) Cutignano, A.; Bruno, I.; Bifulco, G.; Casapullo, A.; Gomez-paloma, L.; Riccio, R. *Eur. J. Org. Chem.* **2001**, No. 4, 775–778.
(20) Kito, K.; Ookura, R.; Yoshida, S.; Namikoshi, M.; Ooi, T.; Kusumi, T. *Org. Lett.* **2008**, *10* (2), 225–228.
(21) Pettit, G. R.; Xu, J.; Chapuis, J.; Pettit, R. K.; Tackett, L. P.; Doubek, D. L.; Hooper, J. N. A.; Schmidt, J. M. *J. Med. Chem.* **2004**, *47*, 1149–1152.
(22) Cichewicz, R. H.; Valeriote, F. A.; Crews, P. *Org. Lett.* **2004**, *6* (12), 1951–1954.
(23) Pettit, G. R.; Herald, C. L.; Doubek, D. L.; Herald, D. L.; Arnold, E.; Clardy, J. *J. Am. Chem. Soc.* **1982**, *104* (24), 6846–6848.
(24) Sikorska, J.; Hau, A. M.; Anklin, C.; Parker-nance, S.; Davies-coleman, M. T.; Ishmael, J. E.; Mcphail, K. L. *J. Org. Chem.* **2012**, *77*, 6066–6075.
(25) Oku, N.; Takada, K.; Fuller, R. W.; Wilson, J. A.; Peach, M. L.; Pannell, L. K.; Mcmahon, J. B.; Gustafson, K. R. *J. Am. Chem. Soc.* **2010**, *132*, 10278–10285.
(26) Miller-wideman, M.; Makkar, N.; Tran, M.; Isaac, B.; Biest, N.; Stonard, R. *J. Antibiot.* **1992**, *45* (6), 914–921.
(27) Yin, J.; Kouda, K.; Tezuka, Y.; Tran, Q. Le; Miyahara, T.; Chen, Y.; Kadota, S. *Planta Med.* **2004**, *70*, 54–58.
(28) Searle, P. A.; Molinski, T. F. *J. Am. Chem. Soc.* **1995**, *117*, 8126–8131.
(29) Pavan, M.; Bo, G. *Curr. Physiol. Comp. Oecol.* **1953**, *3*, 307–312.
(30) Cardani, C.; Ghiringhelli, D.; Mondelli, R.; Quilioo, A. *Tetrahedron Lett.* **1965**, *29*, 2537–2545.
(31) Arundale, E.; Mikeska, L. *Chem. Rev.* **1952**, *51* (3), 505–555.
(32) Youngsaye, W.; Lowe, J. T.; Pohlki, F.; Ralifo, P.; Panek, J. S. *Angew. Chem. Int. Ed.* **2007**, *46* (48), 9211–9214.
(33) Custar, D. W.; Zabawa, T. P.; Scheidt, K. A. *J. Am. Chem. Soc.* **2008**, *130* (3), 804–805.
(34) Custar, D. W.; Zabawa, T. P.; Hines, J.; Crews, C. M.; Scheidt, K. A. *J. Am. Chem. Soc.* **2009**, *131* (34), 12406–12414.
(35) Woo, S. K.; Kwon, M. S.; Lee, E. *Angew. Chem. Int. Ed.* **2008**, *47* (17), 3242–3244.
(36) Vintonyak, V. V; Maier, M. E. *Org. Lett.* **2008**, *10* (6), 1239–1242.
(37) Vintonyak, V. V; Kunze, B.; Sasse, F.; Maier, M. E. *Chemistry*, **2008**, *14* (35), 11132–11140.
(38) Ulanovskaya, O.; Janjic, J.; Suzuki, M.; Sabharwal, S. S.; Schumacker, P. T.; Kron, S. J.; Kozmin, S. *Nat. Chem. Biol.* **2008**, *4* (7), 418–424.
(39) Tu, W.; Floreancig, P. E. *Angew. Chem. Int. Ed.* **2009**, *48* (25), 4567–4571.

(40) Cui, Y.; Tu, W.; Floreancig, P. E. *Tetrahedron* **2010**, *66* (26), 4867–4873.
(41) Cui, Y.; Balachandran, R.; Day, B. W.; Floreancig, P. E. *J. Org. Chem.* **2012**, *77*, 2225–2235.
(42) Yadav, J. S.; Krishana, G. G.; Kumar, S. N. *Tetrahedron* **2010**, *66* (2), 480–487.
(43) Martinez-Solorio, D.; Jennings, M. P. *J. Org. Chem.* **2010**, *75* (12), 4095–4104.
(44) Paterson, I.; Miller, N. *Chem. Commun.* **2008**, No. 39, 4708–4710.
(45) Raghavan, S.; Samanta, P. K. *Org. Lett.* **2012**, *14* (9), 2346–2349.
(46) Ghosh, A. K.; Shurrush, K. A.; Dawson, Z. L. *Org. Biomol. Chem.* **2013**, *11* (44), 7768–7777.
(47) Fuwa, H.; Naito, S.; Goto, T.; Sasaki, M. *Angew. Chem.* **2008**, *120* (25), 4815–4817.
(48) Taylor, R. E.; Kartika, R.; Gruffi, T. R. *Org. Lett.* **2008**, *10* (21), 5047–5050.
(49) Yang, Z.; Zhang, B.; Zhao, G.; Yang, J.; Xie, X.; She, X. *Org. Lett.* **2011**, *13* (21), 5916–5919.
(50) Dong, X.; Mattingly, C.; Tseng, M. T.; Cho, M. J.; Liu, Y.; Adams, V. R.; Mumper, R. J. *Cancer Res.* **2009**, *69* (9), 3918–3926.
(51) Bai, Y.; Davis, D. C.; Dai, M. *Angew. Chem. Int. Ed.* **2014**, *53*, 6519–6522.
(52) Yu, M.; Schrock, R. R.; Hoveyda, A. H. *Angew. Chem. Int. Ed.* **2015**, *54* (1), 215–220.
(53) Kim, H.; Park, Y.; Hong, J. *Angew. Chem. Int. Ed.* **2009**, *48* (41), 7577–7581.
(54) Guinchard, X.; Roulland, E. *Org. Lett.* **2009**, *11* (20), 4700–4703.
(55) Fuwa, H.; Saito, A.; Sasaki, M. *Angew. Chem.* **2010**, *122* (17), 3105–3108.
(56) Athe, S.; Chandrasekhar, B.; Roy, S.; Pradhan, T. K.; Ghosh, S. *J. Org. Chem.* **2012**, *77*, 9840–9845.
(57) Jung, H. H.; Floreancig, P. E. *Org. Lett.* **2006**, *8* (9), 1949–1951.
(58) Jung, H. H.; Floreancig, P. E. *J. Org. Chem.* **2007**, *72*, 7359–7366.
(59) Baldwin, J. *J. Chem. Soc., Chem. Commun.* **1976**, 734–736.
(60) Fischbach, M.; Walsh, C. T. *Chem. Rev.* **2006**, *106* (8), 3468–3496.
(61) Fuwa, H.; Kawakami, M.; Noto, K.; Muto, T.; Suga, Y. *Chem. Eur. J.* **2013**, *19*, 8100–8110.
(62) Menzella, H. G.; Reid, R.; Carney, J. R.; Chandran, S. S.; Reisinger, S. J.; Patel, K. G.; Hopwood, D.; Santi, D. V. *Nat. Biotechnol.* **2005**, *23* (9), 1171–1176.
(63) Menzella, H. G.; Carney, J. R.; Santi, D. V. *Chem. Biol.* **2007**, *14* (2), 143–151.
(64) Sherman, D. H. *Nat. Biotechnol.* **2005**, *23* (9), 1083–1084.
(65) Khosla, C.; Harbury, P. B. *Nature* **2001**, *409* (6817), 247–252.
(66) Gay, D. C.; Gay, G.; Axelrod, A. J.; Jenner, M.; Kohlhaas, C.; Kampa, A.; Oldham, N. J.; Piel, J.; Keatinge-Clay, A. T. *Structure* **2014**, *22*, 444–451.
(67) Nising, C. F.; Bräse, S. *Chem. Soc. Rev.* **2008**, *37*, 1218–1228.
(68) Nising, C. F.; Bräse, S. *Chem. Soc. Rev.* **2012**, *41*, 988–999.
(69) Hu, J.; Bian, M.; Ding, H. *Tetrahedron Lett.* **2016**, *57* (50), 5519–5539.
(70) Perry, M. A.; Rychnovsky, S. D.; Sizemore, N. In *Synthesis of Saturated Oxygenated Heterocycles I*; Cossy, J., Ed.; Springer-Verlag, 2014; pp 43–95.
(71) Beesley, R. M.; Ingold, C. K.; Thorpe, J. F. *J. Chem. Soc. Trans.* **1915**, *107*, 1080–1106.
(72) Cope, A. C.; Martin, M. M.; McKervey, M. A. *Q. Rev. Chem. Soc.* **1966**, *20*, 119–152.
(73) Yang, J.; Xue, H. In *Stereoselective Synthesis of Drugs and Natural Products*; John Wiley & Sons, Inc., 2013; pp 551–581.
(74) Sharma, G. V. M.; Reddy, S. V.; Ramakrishna, K. V. S. *Org. Biomol. Chem.* **2012**, *10* (18), 3689–3695.
(75) Kuhnert, S. M.; Maier, M. E. *Org. Lett.* **2002**, *4* (4), 643–646.
(76) Petri, A. F.; Bayer, A.; Maier, M. E. *Angew. Chem. Int. Ed.* **2004**, *43*, 5821–5823.
(77) Kanematsu, M.; Yoshida, M.; Shishido, K. *Angew. Chem. Int. Ed.* **2011**, *50*, 2618–2620.
(78) Kobayashi, H.; Kanematsu, M.; Yoshida, M.; Shishido, K. *Chem. Commun.* **2011**, *47*, 7440–7442.
(79) Kanematsu, M.; Shishido, K. *J. Synth. Org. Chem. Jpn.* **2012**, *70* (11), 1196–1205.
(80) Hilli, F.; White, J. M.; Rizzacasa, M. *Tetrahedron Lett.* **2002**, *43* (47), 8507–8510.
(81) Hilli, F.; White, J. M.; Rizzacasa, M. *Org. Lett.* **2004**, *6* (8), 1289–1292.
(82) Hilli, F.; White, J. M.; Rizzacasa, M. A. *Tetrahedron* **2011**, *67*, 5054–5068.
(83) Yamaguchi, M.; Inanaga, J.; Hirata, K.; Saeki, H.; Katsuki, T. *Bull. Chem. Soc. Jpn.* **1979**, *52* (7), 1989–1993.
(84) Horner, L.; Hoffman, H.; Wippel, H. G. *Chemistry*, **1958**, *91*, 61–63.
(85) Horner, L.; Hoffman, H.; Wippel, H. G.; Klahre, G. *Chemistry*, **1959**, *92*, 2499–2505.
(86) Wadsworth, W. S.; Emmons, W. D. *J. Am. Chem. Soc.* **1961**, *83* (7), 1733–1738.
(87) Bisceglia, J. Á.; Orelli, L. R. *Curr. Org. Chem.* **2012**, *16*, 2206–2230.
(88) Stevens, D. C.; Hari, T. P. A.; Boddy, C. N. *Nat. Prod. Rep.* **2013**, *30*, 1391–1411.
(89) Wilke, B. I. Examining Polyketide Synthase Mechanisms Through Biomimetic Synthesis, Syracuse

University, 2013.
(90) Matsuya, Y.; Kawaguchi, T.; Nemoto, H. *Org. Lett.* **2003**, *5* (16), 2939–2941.
(91) Magauer, T.; Martin, H. J.; Mulzer, J. *Chemistry*, **2010**, *16* (2), 507–519.
(92) Florence, G. J.; Cadou, R. F. *Tetrahedron Lett.* **2010**, *51* (44), 5761–5763.
(93) Chatterjee, A. K.; Choi, T.-L.; Sanders, D. P.; Grubbs, R. H. *J. Am. Chem. Soc.* **2003**, *125* (37), 11360–11370.
(94) Gradillas, A.; Pørez-castells, J. *Angew. Chem. Int. Ed.* **2006**, *45*, 6086–6101.
(95) Xuan, R.; Oh, H.-S.; Lee, Y.; Kang, H.-Y. *J. Org. Chem.* **2008**, *73* (4), 1456–1461.
(96) Parenty, A.; Moreau, X.; Niel, G.; Campagne, J.-M. *Chem. Rev.* **2013**, *113*, PR1-PR40.
(97) Corey, E. J.; Nicolaou, K. *J. Am. Chem. Soc.* **1974**, *96* (17), 5614–5616.
(98) Rychnovsky, S.; Rogers, B. *J. Org. Chem.* **1993**, *58*, 3511–3515.
(99) Hari, T. P. A.; Wilke, B. I.; Davey, J. A.; Boddy, C. N. *J. Org. Chem.* **2016**, *81*, 415–423.
(100) Ferrié, L.; Boulard, L.; Pradaux, F.; Bouzbouz, S.; Capdevielle, P.; Cossy, J. *J. Org. Chem.* **2008**, *73*, 1864–1880.
(101) Houghton, S. R.; Furst, L.; Boddy, C. N. *J. Org. Chem.* **2009**, *74* (4), 1454–1463.
(102) Heathcock, C. H.; Hadley, C. R.; Rosen, T.; Theisen, P. D.; Hecker, S. J. *J. Med. Chem.* **1987**, *30* (10), 1858–1873.
(103) Karanewsky, D. S.; Malley, M. F.; Gougoutas, J. Z. *J. Org. Chem.* **1991**, *56* (11), 3744–3747.
(104) Harada, K.; Matsushita, A.; Sasaki, H.; Kawachi, Y. Process For Preparation of Oxyglutaric Acid Ester Derivatives. US005717124A, 1998.
(105) Hari, T. P. A.; Labana, P.; Boileau, M.; Boddy, C. N. *ChemBioChem* **2014**, *15* (18), 2656–2661.
(106) Iakobson, G.; Beier, P. *Beilstein J. Org. Chem.* **2012**, *8*, 1185–1190.
(107) Dijkstra, G.; Kruizinga, W. H.; Kellogg, R. M. *J. Org. Chem.* **1987**, *52*, 4230–4234.
(108) Barluenga, S.; Moulin, E.; Lopez, P.; Winssinger, N. *Chem. Eur. J.* **2005**, *11*, 4935–4952.
(109) Laganis, E. D.; Chenard, B. L. *Tetrahedron Lett.* **1984**, *25* (51), 5831–5834.
(110) Ramesh, C.; Ravindranath, N.; Das, B. *J. Org. Chem.* **2003**, *68*, 7101–7103.
(111) Wei, Y.; Zuo, L.; Ye, D. Y.; Hu, W. *Chin. Chem. Lett.* **2009**, *20*, 1157–1160.
(112) Wang, B.; Sun, H.; Sun, Z. *J. Org. Chem.* **2009**, *74*, 1781–1784.
(113) Yan, H.; Oh, J.-S.; Song, C. E. *Org. Biomol. Chem.* **2011**, *9*, 8119–8121.
(114) Fernandes, R. A.; Gholap, S. P.; Mulay, S. V. *RSC Adv.* **2014**, *4*, 16438–16443.
(115) Mouloungui, Z.; Delmas, M.; Gaset, A. *J. Org. Chem.* **1989**, *54* (16), 3936–3941.
(116) Pascariu, A.; Ilia, G.; Bora, A.; Iliescu, S.; Popa, A.; Dehelean, G.; Pacureanu, L. *Cent. Eur. J. Chem.* **2003**, *4*, 491–542.
(117) Zhao, Q.; Sun, J. of M. C. A. : C. M. and kinetics of H. – W. – E. reaction in liquid – liquid phase-transfer catalytic system; Li, F.; He, J.; Liu, B. *J. Mol. Catal. A Chem.* **2015**, *400*, 111–120.
(118) Kruizinha, W. H.; Kellogg, R. M. *J. Am. Chem. Soc.* **1981**, *103*, 5183–5189.
(119) Keinan, E.; Eren, D. *J. Org. Chem.* **1986**, *51* (16), 3165–3169.
(120) Ostrowicki, A.; Koepp, E.; Vögtle, F. *Top. Curr. Chem.* **1991**, *161*, 37–67.
(121) Galli, C.; Mandohi, L. *J. Org. Chem.* **1991**, *56*, 3045–3047.
(122) Bhattacharjee, A.; Soltani, O.; De Brabander, J. K. *Org. Lett.* **2002**, *4* (4), 481–484.
(123) Nasveschuk, C. G.; Rovis, T. *J. Org. Chem.* **2008**, *73*, 612–617.
(124) Reddy, P. J.; Reddy, A. S.; Yadav, J. S.; Reddy, B. V. S. *Tetrahedron Lett.* **2012**, *53* (32), 4054–4055.
(125) Desilylation by treatment with HF at room temperature was capable of providing sufficient acidity to mediate the oxa-conjugate assembly of the pyran products with lower selectivity for the *trans*-pyranone (*d.r.* = 5:2).
(126) Stewart, J. J. P. *J. Mol. Model* **2007**, *13*, 1173–1213.
(127) Lee, C.; Yang, W.; Parr, R. G. *Phys. Rev. B* **1988**, *37* (2), 785–789.
(128) Miehlich, B.; Savin, A.; Stoll, H.; Preuss, H. *Chem. Phys. Lett.* **1989**, *157* (3), 200–206.
(129) Becke, A. D. *J. Chem. Phys.* **1993**, *98*, 5648–5652.
(130) Reiter, M.; Turner, H.; Gouverneur, V. *Chem. Eur. J.* **2006**, *12* (27), 7190–7203.
(131) Fuwa, H.; Mizunuma, K.; Matsukida, S.; Sasaki, M. *Tetrahedron* **2011**, *67*, 4995–5010.
(132) Mitsunobu, O.; Yamada, M.; Mukaiyama, T. *Bull. Chem. Soc. Jpn.* **1967**, *40* (4), 935–939.
(133) Pangborn, A. B.; Giardello, M.; Grubbs, R. H.; Rosen, R. K.; Timmers, F. J. *Organometallics* **1996**, *15* (5), 1518–1520.
(134) Armarego, W. L. F.; Chai, C. L. L. *Purification of Laboratory Chemicals*, 6th ed.; Elsevier Ltd, 2009.
(135) Fulmer, G. R.; Miller, A. J. M.; Sherden, N. H.; Gottlieb, H. E.; Nudelman, A.; Stoltz, B. M.; Bercaw, J. E.; Goldberg, K. I. *Organometallics* **2010**, *29*, 2176–2179.

(136) Hoye, T. R.; Danielson, M. E.; May, A. E.; Zhao, H. *Angew. Chem. Int. Ed.* **2008**, *47* (50), 9743–9746.
(137) McAllister, L.; Hixon, M. S.; Schwartz, R.; Kubitz, D. S.; Janda, K. D. *Bioconjugate Chem.* **2007**, *18* (2), 559–566.
(138) Wang, B.; Liu, J.; Tang, X.; Cheng, C.; Gu, J.; Dai, L.; Yu, H. *Tetrahedron Lett.* **2010**, *51* (2), 309–312.
(139) Wilke, B. I.; Dornan, M. H.; Yeung, J.; Boddy, C. N.; Pinto, A. *Tetrahedron Lett.* **2014**, *55* (16), 2600–2602.
(140) Nishida, A.; Kawahara, N.; Nishida, M.; Yonemitsu, O. *Tetrahedron* **1996**, *52* (29), 9713–9734.
(141) Kuwahara, S.; Morihiro, E.; Nemoto, A.; Hiramatsu, A. *Biosci. Biotech. Biochem.* **1992**, *56* (9), 1417–1419.
(142) Sigma-Aldrich. Price (as of 25/08/16): 7-bromo-1-heptanol ($335 CAD, 5 g), 7-bromo-1-heptene ($229 CAD, 5 g).
(143) Bestmann, H. J.; Kellermann, W.; Pecher, B. *Synthesis*, **1993**, *1*, 149–152.
(144) Leadlay, P. F.; Staunton, J.; Oliynyk, M.; Bisang, C.; Corte, J.; Frost, E.; Hughes, Z. A.; Jones, M. A. *J. Ind. Microbiol. Biotech.* **2001**, *27*, 360–367.
(145) Westley, J. W.; Blount, J. F.; Evans, R. H.; Stempel, A.; Berger, J. *J. Antibiot.* **1974**, *XXVII* (8), 597–604.
(146) Hotta, K.; Chen, X.; Paton, R. S.; Minami, A.; Li, H.; Swaminathan, K.; Mathews, I. I.; Watanabe, K.; Oikawa, H.; Houk, K. N.; Kim, C. *Nature* **2012**, *483*, 355–359.

· Chapter 4 ·

Formal Synthesis of Neopeltolide by Transannular Oxa-Conjugate Addition

4.1 Applications of Semi-Synthesis for Natural Product Drug Development

Natural products and their derivatives provide an excellent source for lead candidates in drug discovery by representing extensive chemical diversity and therapeutic applications. Of all new small-molecule drugs approved over the last four decades, it is estimated that 65% share natural product origins.[1] Despite significant potential as lead candidates, initial research into their biochemical and pharmacological effects is often hampered by extremely-limited amounts of active pharmaceutical ingredient (API) from source organisms. Synthetic chemistry offers a plausible solution to access sufficient material for preliminary biological evaluation, which was highlighted in **Chapter 2** by the elegant work on anticancer candidate neopeltolide **4.1** (Figure 4.1). However, except for Halaven® (Chapter 1, § 1.3.2), total synthesis is predominantly an academic exercise for natural products; in drug development, semi-synthesis often represents the only practical option for process-scale.

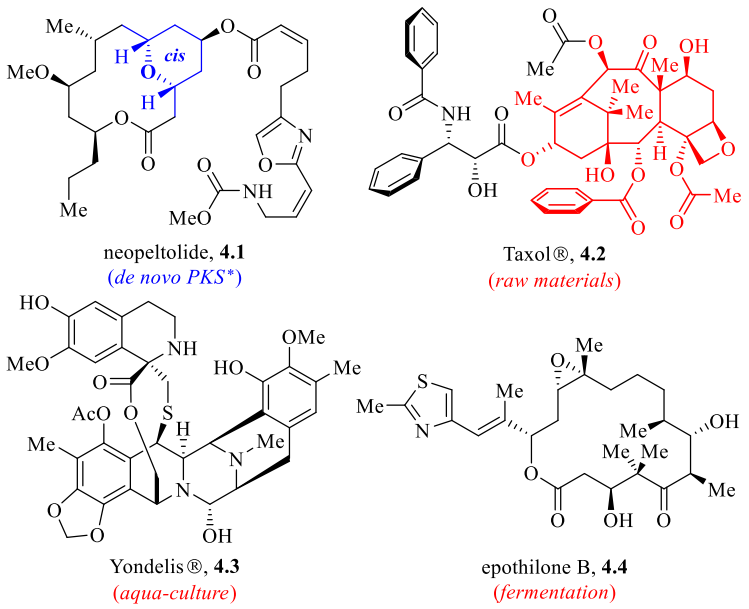

Figure 4.1 – Within drug development, semi-synthesis has proven instrumental for production of complex natural products using a variety of techniques. Our proposed* *de novo* PKS semi-synthesis could benefit potential commercial production of neopeltolide **4.1**, or other THP-bearing polyketide products.

To illustrate, the blockbuster anticancer agent Taxol® **4.2** required semi-synthesis for commercial-viability due to scarce isolation of its API from the bark of Pacific Yew trees. Unsustainable large-scale harvesting addressed initial supply needs[2] but was replaced by chemical conversion of advanced precursor 10-deacetyl-baccatin III (highlighted in **red**, Figure 4.1), which was extracted from needles of a related tree species, the European Yew.[3] Clinical production currently employs fermentation to access the API, providing a greener alternative.[4]

Marine-derived natural products like anticancer agents neopeltolide **4.1** and clinically-approved Yondelis® **4.3** present greater difficulties due to inherent obstacles in their discovery. Many marine candidates fail to reach preclinical stages of development because of extremely low natural abundance, and highly-complex chemical scaffolds that make syntheses intractable. In an ambitious effort, an aquaculture program was launched to secure sufficient material for Yondelis® to enter clinical trials.[5] This program averaged approximately one milligram of **4.3** per metric tonne of biomass collected, which required a more efficient semi-synthetic commercialization that would not be at risk to external factors like climate changes.[6,7] Clinical production currently employs fermentation of advanced precursor from a related organism,[8] and is chemically-converted to Yondelis®.[5]

The application of microbial fermentation for semi-synthesis of natural products candidates was introduced in **Chapter 1** by production of epothilone **4.4** and erythromycin analogues (Chapter 1, § 1.4.1). In fact, six of seven epothilone compounds to enter clinical trials were produced using this strategy.[9] However, most of these derivatives have been reported by researchers that discovered the producing myxobacterium strain,[9] suggesting fermentation strategies can be limited by the ability to secure access to appropriate cultures. Moreover, fermentation is not a feasible option for uncharacterized biosynthetic pathways or unidentified producing organisms of active compounds like neopeltolide. A potential solution to overcome these limitations has been to engineer well-characterized biosynthetic pathways to increase or modify production of a desired metabolite.

4.1.1 De Novo Biosynthetic Pathways for Natural Product Semi-Synthesis

Metabolic engineering is the practice of harnessing genetic and regulatory processes within a cell to optimize production of a certain substance. This technique has enabled industrial production of 1,3-propanediol from a recombinant producing strain and simple sugar materials *via* fermentation.[10] Combining genes from various natural producing-strains in a new host allowed the switch from glycerol to glucose as the non-native carbon source. Although structurally-simplistic, this accomplishment demonstrated the ability to design fermentation pathways to produce chemicals from renewable sources. Likewise, production of antimalarial drug precursor artemisinic acid **4.6** has been reported using engineered yeast in a heterologous host (Figure 4.2).[11] Clinical production combines this *de novo* biosynthetic production with short chemical routes[12,13] to semi-synthetically access an approximated one-third of global demand for **4.7** at reduced costs.[14]

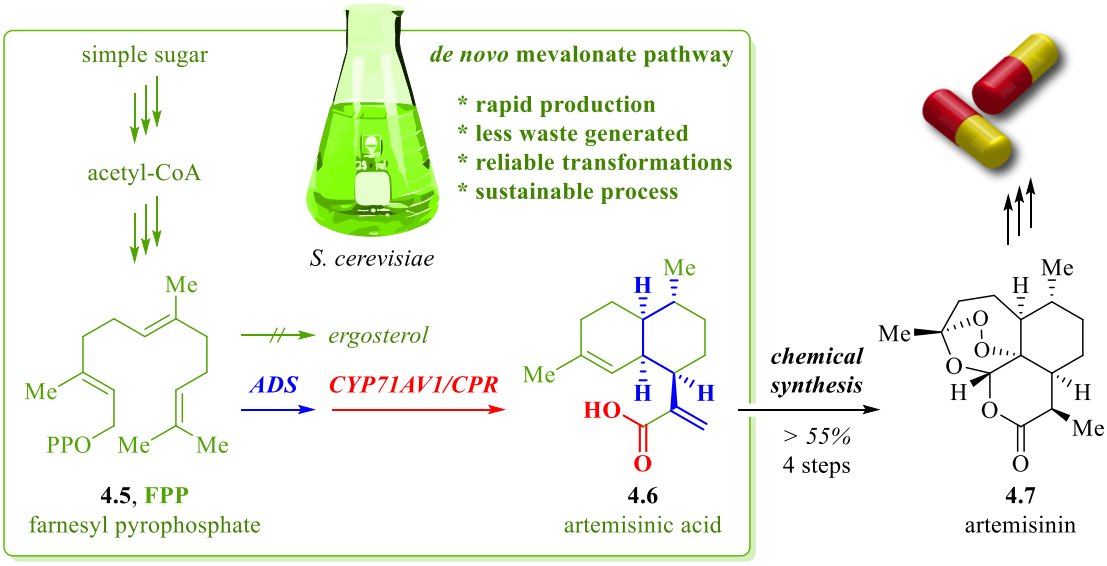

Figure 4.2 – The *de novo* biosynthetic production of artemisinic acid **4.6** in a heterologous host was engineered for upregulation of FPP **4.5** and downregulation of native sterols, like ergosterol. The engineered host expressed native and non-native proteins to furnish the advanced scaffold.[11] Artemisinin **4.7** can be rapidly accessed in good yield *via* chemical synthesis.[12,13]

The selected examples of semi-synthetic applications in natural product drug development highlighted how combining biosynthesis and synthetic chemistry can address supply limitations from producing hosts. This chapter discusses the application of our transannular oxa-conjugate addition strategy to assemble the 2,6-*cis*-tetrahydropyran (THP) ring system of the neopeltolide macrocyclic core using a biosynthetically-inspired macrocyclic precursor. Because of the strategic position of the functional groups required for this transformation, engineered biosynthetic pathways could be designed to produce advanced oxa-conjugate substrates. The long-term goal is *in vivo* or *in vitro* production of these compounds, which would establish reliable and sustainable access to complex THP-bearing polyketides.[15–18]

4.2 Designing a *De Novo* PKS Pathway for Semi-Synthesis of Neopeltolide

Due to its appealing architecture, promising biological activity, and extremely-limited natural supply, neopeltolide has become a topic of considerable interest in the decade since Wright's 2007 discovery.[19] The first report from the Panek research group proposed a partial stereochemical reassignment,[20] and was independently-confirmed by Scheidt and coworkers[21] to establish absolute configuration (refer to Chapter 2, § 2.2). Since then, combined efforts from more than 20 independent research groups have published reports of partial and completed syntheses of neopeltolide and first-generation analogues (Table 4.1).[20–40] While its structural elements are not trivial, neopeltolide has become a *de facto* target for synthetic chemists to highlight innovation and creativity in state-of-the-art strategies to assemble *cis*-pyranyl scaffolds.

Table 4.1 – Summary of neopeltolide total and formal syntheses (2007-2016).

Compound	Research Group	Publication Year	Linear Steps	Avg. Yield/Step	Linear Yield	Ref. #
(+)-neopeltolide	Panek	2007	20	80.5%	1.3%	20
(+)-neopeltolide	Scheidt	2008	16	72.6%	0.6%	21
(+)-macrocycle	Maier	2008	19[a]	92.6%	23.0%	22
(+)-neopeltolide	Lee	2008	15	83.5%	6.7%	23
(+)-neopeltolide	Fuwa	2008	23	88.2%	11.8%	24
(+)-neopeltolide	Kozmin	2008	15	82.3%	5.4%	25
(+)-neopeltolide	Paterson	2008	18	86.2%	6.9%	26
(+)-macrocycle	Taylor	2008	14	88.8%	18.9%	27
(+)-macrocycle	Floreancig	2009	13[b]	82.0%	7.6%	28
(+)-macrocycle	Hong	2009	14	84.4%	9.3%	29
(+)-neopeltolide	Roulland	2009	18	86.3%	7.1%	30
(+)-neopeltolide	Fuwa[c]	2009	25	94.0%	21.5%	31
(+)-macrocycle	Yadav	2010	15	85.3%	9.2%	32
(–)-macrocycle	Jennings	2010	24	86.1%	2.8%	33
(+)-macrocycle	She	2011	10	85.7%	21.4%	34
(+)-macrocycle	Sharma	2012	23	81.3%	1.0%	35
(+)-macrocycle	Raghavan	2012	21	84.4%	2.8%	36
(+)-macrocycle[d]	S. Ghosh	2012	20	83.3%	2.6%	37
(+)-neopeltolide	A. Ghosh	2013	21	82.7%	1.6%	38
(+)-neopeltolide	Fuwa[*]	2013	13	87.1%	16.8%	39
(+)-neopeltolide	Hoveyda	2015	9	85.5%	28.2%	40

[a] – Completion of natural product accomplished later that same year[41] in *via* Mitsunobu esterification (19.8% overall).
[b] – Completion of natural product was accomplished early 2010[42] in 88% yield over two steps (6.3% overall).
[c] – Modified route and yields reported in publication on analogue design, based on 2008 report.
[d] – Synthesis of *cis*-tetrahydropyran-4-one macrocyclic core; other "macrocycle" entries are *cis*-tetrahydropyran-4-ol.
[*] – Modified route based on 2010 report;[43] however, the earlier report is omitted due to unreported yields therein.

These publications have demonstrated the versatility of modern synthetic chemistry, and strategies for selectively accessing pyran systems. Their combined efforts have established the pharmacophoric elements of neopeltolide, and offered a temporary solution for preparing sufficient material for preliminary biological testing and elucidation of a putative target. Unfortunately, these syntheses did not provide a lasting solution to the supply issue faced by neopeltolide and pyran-bearing polyketide natural products. The combination of polyketide synthase (PKS) biosynthesis and organic chemistry presents an attractive opportunity for efficient and scalable production of neopeltolide, and to allow modification to produce other complex polyketides. We believe our transannular oxa-conjugate addition strategy can be applied to

advanced *de novo* PKS fermentation intermediates like **4.8** for rapid, scalable, and efficient semi-synthesis of natural products like neopeltolide using simple, renewable sources (Figure 4.3).

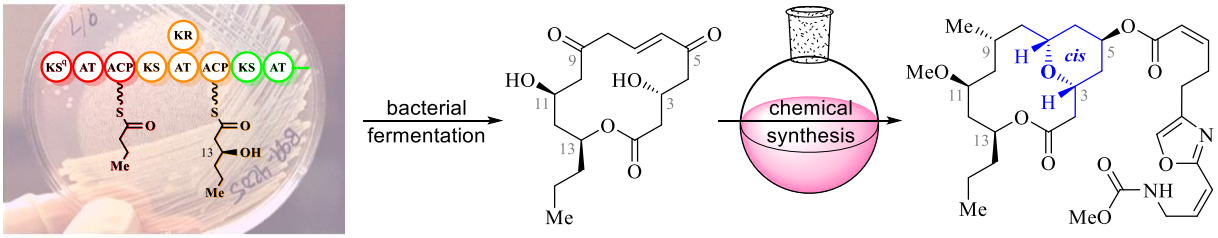

de novo PKS pathway **4.8** (+)-neopeltolide, **4.1**

Figure 4.3 – A combined *de novo* PKS biosynthetic-chemosynthetic strategy for production of complex polyketide natural products like neopeltolide, using advanced precursors with biosynthetically-accessible functional groups.

Research milestones for the neopeltolide study are divided into two distinct stages where using chemical synthesis to access *cis*-THP products from *de novo* PKS intermediates represents the final and long-term goal. The immediate goal of this project has thus been to establish and evaluate foundations of diastereoselective transannular oxa-conjugate assembly of 2,6-*cis*-tetrahydropyran ring systems, and apply this chemistry to the synthesis of neopeltolide. Our first milestone was achieved by acid-mediated addition of racemic *β'*-hydroxy into an *α,β*-unsaturated ketone model (**Chapter 3**), and confirmed the chemical viability of our key synthetic transformation. This chapter reports the efforts toward our second milestone.

4.3 Assembly of Complex Natural Products *via* Macrocyclic Stereocontrol

Conformational analysis is an indispensable tool when attempting to assess the reactivity of organic molecules. Barton's pioneering work with cyclic alkanes was the first to couple conformational analysis and reactivity,[44] where he demonstrated the effect of substituent positioning on reactivity. The explicit use of macrocycle conformation as stereochemical elements was later established by Still in his synthesis of the 10-membered macrolactone natural product periplanone B (**4.12**, Figure 4.4).[45] Using conformational analysis, Still clearly showed that macrocyclic frameworks possessing olefins (and by extension, macrocycles with sp^2 centers), can adopt at least two ground state conformations where opposite faces of the olefin are exposed to reactivity.[46] He proposed that there exists a propensity for reagents in intermolecular reactions to approach macrocyclic π-bonds of the lower-energy conformations peripherally, with kinetically-controlled attack of the olefin occurring from outside of the ring face and not the interior. Implicit with this *inter*molecular hypothesis was that all other factors, such as reaction type, nature of reagents, and the development of any stereoelectronic or electrostatic interactions in the ground state or transition state are ignored. The model assumes that the π-facial bias from a given substrate conformation is significantly large, such that all other interactions are considered negligible.

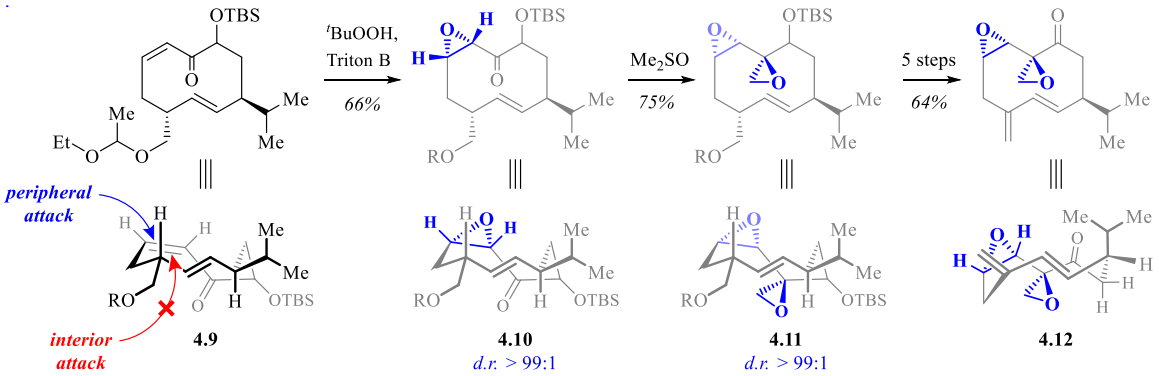

Figure 4.4 – The basis of macrocyclic stereocontrol was proposed by Still from his 1979 synthesis of periplanone B **4.12**. Both epoxides were installed as exclusive products *via* peripheral attack of the macrocyclic framework.

The peripheral attack hypothesis helped to rationalize many of the seemingly intractable issues that were associated with medium- and large-ring stereocontrol,[47] and has since been employed successfully in over 30 literature examples including epoxidation,[48–50] hydrogenation,[51,52] hydride reduction,[53–55] and conjugate addition transformations.[56] For in-depth discussion of macrocyclic stereocontrol, the peripheral model and its application to natural product synthesis, please refer to the 2009 review by Carreira and Kvaerno,[47] and the selected references embedded within this section.

4.3.1 Macrocyclic Stereocontrol in Neopeltolide Synthesis

Despite the limited reports of macrocyclic stereocontrol in literature, the neopeltolide core has been identified to possess amenable native architecture to act as a stereochemical element. Floreancig and coworkers used this strategy to rationalize the stereoselective (*d.r.* = 9:1) hydrogenation of an alkene in the functionalized core, to set the C9 methyl stereocenter (Figure 4.5).[28] A crystal structure of **4.13** showed that the molecule prefers a curved conformation, and suggested that alkene hydrogenation occurred preferentially from the sterically more-accessible convex face to afford the desired stereochemical orientation at C9. To prepare the C9-epimeric analogue **4.16**,[42] they relied on Crabtree's catalyst[57] to coordinate to the tetrahydropryanyl oxygen and facilitate interior attack of the concave face; the modest selectivity of the process highlighted the unfavorability of nucleophilic attack imposed by conformational biases of the macrocyclic backbone. Based on this success, substrate-controlled hydrogenation has since been employed by Fuwa,[39,43] She,[34] and Hoveyda[40] using macrocyclic neopeltolide precursors with defined C5 alcohols. In fact, both axial and equatorial C5 alcohol orientations proved to be substantially more selective, and higher-yielding transformations compared to Floreancig's pyranone precursor. Similarly, Floreancig and coworkers also used alkenyl precursor **4.13** to introduce polar groups *via* late-stage diversification to improve physical properties, such as water solubility.[42] Under macrocyclic stereocontrol, diol **4.17** and epoxide **4.18** analogues were prepared as single diastereoisomers.

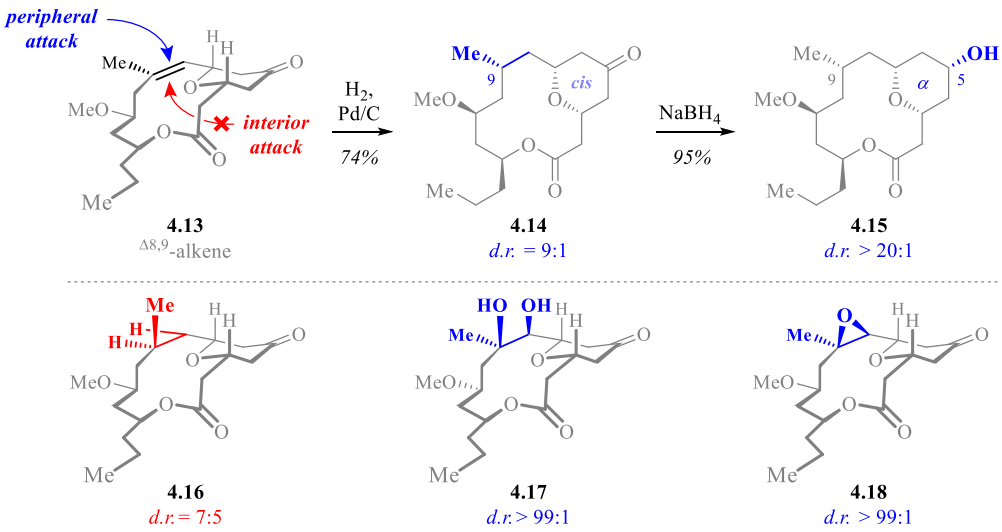

Figure 4.5 – Floreancig and coworkers demonstrated conformational biases imposed by the macrocyclic core of neopeltolide controlled the stereochemical hydrogenation of the $^{\Delta 8,9}$-alkene **4.13** with good selectivity.

The highly-selective reduction of *cis*-pyranone **4.14** to *α*-**4.15** was also substrate-controlled (Figure 4.5), and was first demonstrated by Scheidt and coworkers.[21] To date, this macrocyclic stereocontrol strategy has also been employed by the research groups of Paterson,[26] Hong,[29] Floreancig,[42] A. K. Ghosh,[38] and Dai,[58] with excellent selectivities. Moreover, pyranone reduction ($NaBH_4$) in our ketone model (Chapter 3, § 3.5.2) proved to be facile and highly selective (*d.r.* = 12:1) for the *α*-diastereoisomer.[59] It is worth questioning whether the lack of native substitution along the macrocyclic framework diminished the stereocontrol, and could account for the reduced selectivity observed in our model system.

4.3.2 Macrocyclic Stereocontrol for Transannular Systems

The peripheral attack model has been particularly successful for *inter*molecular reactions where the transition state for addition to the sp^2 centers does not significantly perturb the conformation of the macrocycle.[46] In these reactions, the ground state conformational preferences are predictive of the transition state conformational preferences. Intermolecular transformations like those in Figure 4.5, clearly follow these boundary conditions for peripheral attack. However, it is often difficult to predict the effect of conformational biases in the context of the requisite interior attack of *intra*molecular reactions. Recently, Evans and coworkers demonstrated that a transannular conjugate addition failed to generate the computationally-predicted product during their synthesis of tetracycline (Figure 4.6).[60] Using the ground state conformation model for macrocyclic stereocontrol, the 4a-4 *syn*-diastereomer **4.23** was predicted to be favored, but under the reaction conditions investigated, the *anti*-diastereomer **4.22** was generated with exclusive selectivity. In this instance, Curtin-Hammett kinetics predominated,[61] with the less-favored conformation **4.20** being significantly more reactive than the favored **4.21**.

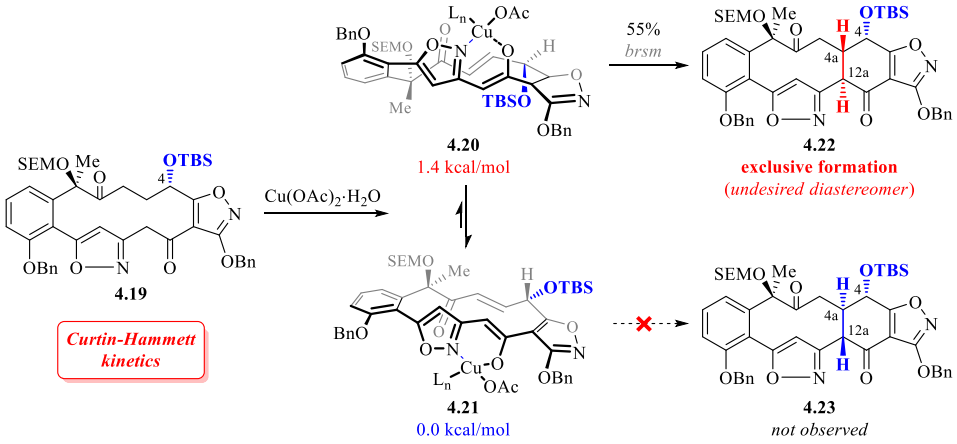

Figure 4.6 – Evans and coworkers demonstrated transannular conjugate addition for C4a-C12a bond construction operated under Curtin-Hammett kinetics *via* unfavored conformation **4.20**, to yield the undesired diastereomer.

To address the second milestone from our neopeltolide study, we wished to apply foundations of transannular oxa-conjugate addition from our *α,β*-unsaturated ketone model to access the fully-elaborated macrocyclic core of neopeltolide. Selectivity of this strategy toward assembly of the *cis*-THP ring system hinged upon hypothesized conformational biases imposed by the macrocyclic framework. We anticipated the native configuration of the macrocyclic backbone would act as an additional stereochemical element in our system, and improve the stereocontrol of the key transannular oxa-conjugate addition. Success of this milestone would provide further validation to this synthetic transformation, and would support preliminary investigation into designing *de novo* PKS modules for neopeltolide and other THP-bearing natural products.[15–18] Herein reports the efforts toward the design and synthesis of our transannular oxa-conjugate assembly of the 2,6-*cis*-tetrahydropyan ring in neopeltolide.

Results & Discussion

4.4 Toward a Transannular Oxa-Conjugate Precursor for Neopeltolide

Retrosynthetic analysis for the transannular oxa-conjugate addition strategy for *cis*-THP assembly of the macrocyclic core of neopeltolide was based on the successful olefination used in our ketone model system (Figure 4.7). Like Rizzacasa's synthesis of apicularen A,[62] we expected pre-organization of the macrocyclic backbone would provide favorable energetic barriers to enable highly-selective addition of our diastereomeric mixture of C3 nucleophiles under thermodynamic control. We envisioned macrocyclic precursor **4.24** could be accessed by Yamaguchi esterification, following olefination of the two fragments. The fully-elaborated C7-C16 fragment **4.25** would be derived from commercial material by a desymmetrizing esterase and sequential asymmetric allylation reactions. Acid phosphonate **4.26** would be constructed as the C3 racemate to evaluate our key thermodynamic interconverting process.

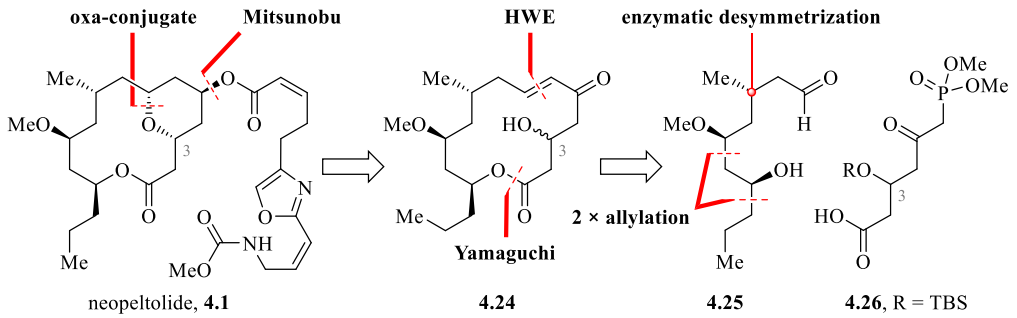

Figure 4.7 – Retrosynthetic analysis for transannular oxa-conjugate assembly of the *cis*-THP in the macrocyclic core of neopeltolide. Olefination of enantiopure **4.25** and C3-racemic fragment **4.26** would establish the full carbon-framework.

In designing our retrosynthesis, we originally wanted to focus on a linear approach to access the full carbon framework of the macrocyclic core, as it would resemble the general machinery of PKS biosynthesis (Chapter 1, § 1.2.1). Such a biomimetic approach would enable *in vitro* biosynthetic studies where synthetic intermediates could be derivatized as thioester substrates, and assessed in feeding experiments with individually-expressed domains or *de novo* modules for enzymatic function. Ultimately, the biomimetic strategy was abandoned for this stage of the study (*vide infra*), but represents ongoing research for entry to the longer-term *de novo* synthesis. Herein the efforts toward the convergent construction of our oxa-conjugate precursor are reported.

4.4.1 Rapid Development of Racemic C1-C6 Framework

Substantial experimental work was investigated to develop a viable route to the C1-C6 diprotic phosphonate coupling fragment **4.26** (see Chapter 3, § 3.5.1 for selected details). Rapid preparation was achieved in a 4-step sequence from commercially-available dimethyl-1,3-acetonedicarboxylate (**4.27**, Figure 4.8), to provide the C1-C6 framework in 68% overall yield.

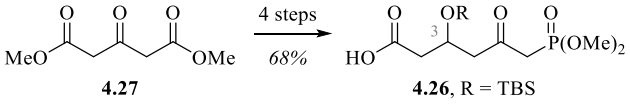

Figure 4.8 – Rapid and high-yielding generation of C1-C6 coupling fragment **4.26** for the transannular oxa-conjugate assembly of the *cis*-THP of neopeltolide. This route is highly-amenable to modifications of hydroxyl- and carboxyl-protecting groups.

The advantage of this sequence was that it readily prepared the *seco*-acid required for macrocyclization by Yamaguchi esterification,[63] and circumvented ester cleavage and potential *β*-elimination of the HWE product. Additionally, the process is highly-amenable to various hydroxyl- and carboxyl- protecting groups. In the potential event the C7-C16 region within the fully-functionalized linear framework of our HWE product was sensitive to classic desilylation conditions, preparation of alternative phosphonate fragments would prove more economical with respect to time, difficulty, and cost of reagents.

4.4.2 Bio-Inspired Development of C7-C16 Fragment is Abandoned

The sequential-asymmetric-allylation strategy for development of the C7-C16 coupling fragment required aldehyde **4.30** as a key intermediate (Figure 4.9). A highlight of this route to accessing the C7-C13 framework of neopeltolide included use of pig liver esterase (PLE) for desymmetrization of the C9-methyl group *via* enzymatic hydrolysis,[64] affording the half-acid in high enantiomeric purity (*ee* > 95%) and yield (94%). Success of this process was validated by Hoye's NMR strategy[65] for determining absolute configuration of remote stereogenic centers. Additionally, Mosher's analysis[19] provided support for the success of enzymatic desymmetrization, corroborating the highly enantioselective process. Completion of aldehyde **4.30** was achieved in 58% yield, over 7 steps from commercially-available materials.

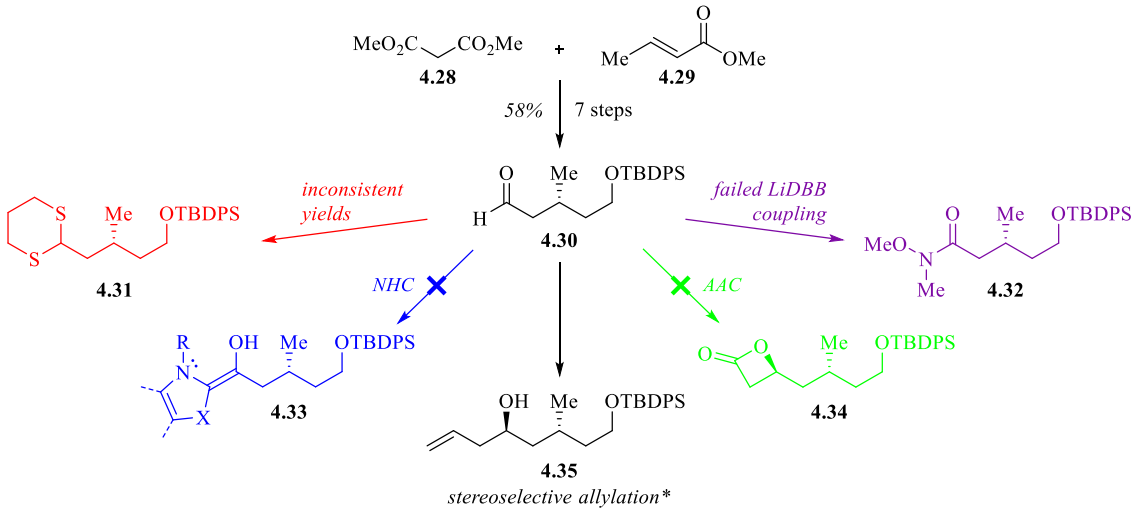

Figure 4.9 – Selection of failed biomimetic Umpolung strategies toward accessing the desired C7-C13 framework of neopeltolide. Ultimately, Brown's stereoselective conditions[74] for allylation were identified as the most efficient alternative.

Initial attempts of step-wise, linear chain extension (biomimetic) of key **4.30** *via* Umpolung[68] protocol were beset with failure (Figure 4.9). Generation of dithiane **4.31** for its addition into enantioenriched (2*S*)-propyloxirane† proved too inconsistent for this early stage of synthesis (yields ranged from 27 – 72%). Rychnovsky's method[69] of coupling Weinreb amide[70] **4.32** with an LiDBB-derived *β*-alkoxy alkyllithium reagent failed, in part due to the challenge of consistently maintaining reaction temperatures below -78 ºC for 48 h. Furthermore, unsuccessful attempts of biomimetic linear-elongation *via N*-heterocyclic carbene (NHC)-catalyzed **4.33** epoxide-opening,[71] and Nelson's cinchona-catalyzed acid chloride-aldehyde cyclocondensation (AAC)[72] accentuated use of the convergent chemistry employed in our ketone model system. A comprehensive discussion of these and other synthetic routes can be found in

† Preparation of enantioenriched (2*S*)-propyloxirane *via* Jacobsen's method for kinetic resolution[155] would prove valuable for the outlined Umpolung strategies. Epoxide-opening by thiophenol readily affords the required *β*-hydroxylsulfide (for reductive lithiation by LiDBB),[27] in addition to use of epoxide as the coupling partner for the NHC-catalyzed strategy.

my 2012 M.Sc. thesis ("Efforts Toward an Oxa-Conjugate Addition Based Approach to (+)-Neopeltolide Synthesis").[73]

To overcome challenges faced by a biomimetic Umpolung strategy, asymmetric allylation of **4.30** readily accessed the desired C7-C13 framework of neopeltolide. Screening conditions for diastereoselective generation of homoallylic alcohol **4.35** determined Brown's selective allylation conditions provided superior yield and selectivity (86%, *d.r.* = 13:2) compared with Leighton's asymmetric allylsilane.[75]

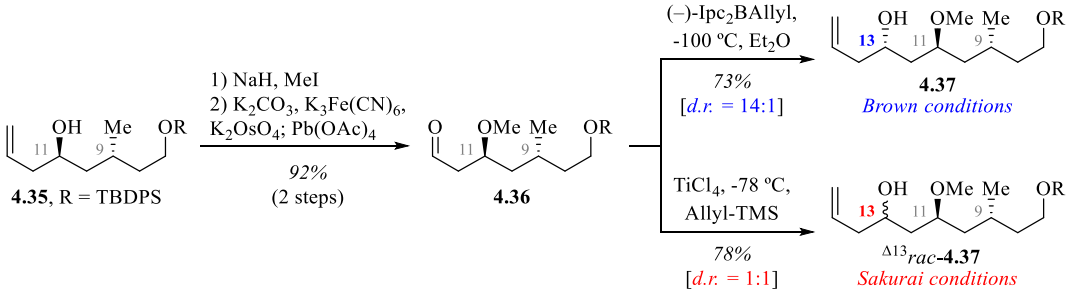

Scheme 4.1 – Completion of the C7-C16 framework of neopeltolide using Brown's conditions[74] provided superior selectivity for the sequential-asymmetric-allylation strategy.

With homoallylic alcohol **4.35** in hand, a second stereoselective allylation would rapidly complete the C7-C16 fragment (Scheme 4.1). Alkylation of **4.35** as the requisite C11-methyl ether, followed by Sharpless dihydroxylation[76] and subsequent oxidative cleavage, readily-provided aldehyde **4.36** in excellent yield. Treatment of **4.36** under Sakurai allylation conditions[77] proved non-selective, yielding an equal mixture of C13 diastereoisomers ($^{\Delta 13}$*rac*-**4.37**). It is uncertain what limited selectivity of this transformation; however, it was proposed that the C11-methoxy does not provide the required-level of *β*-alkoxy chelation-control to achieve 1,3-asymmetric induction. Ultimately, a second allylation under Brown's stereoselective conditions[74] provided homoallylic alcohol **4.37** in good yield with high diastereoselectivity (*d.r.* = 14:1), completing the carbon framework of C7-C16 fragment.

4.4.3 Tandem Hydrogenation/Hydrogenolysis Yields Complete C7-C16 Fragment

From commercially-available materials, homoallylic alcohol **4.37** was generated in 8 linear steps (40% overall; 89% average step yield), installing three stereogenic centers with high selectivity. However, choice of protecting group for the free alcohol of **4.37** still required careful consideration. Choice of protection was critical for success of the convergent synthesis of neopeltolide, and heavily-influenced by its surrounding functional groups present during unmasking. Prior to HWE coupling, the chosen protecting group must be stable to TBDPS desilylating conditions to avoid selective oxidation, or additional protecting group manipulation. Conversely, if coupling preceded deprotection, conditions must be mild to suppress C3-desylilation due to the facile pyran formation observed in the model system (Chapter 3, § 3.5.1).

Moreover, the allyl group must be reduced prior to coupling to prevent saturating the requisite conjugated-ketone system. Lastly, our ester model demonstrated difficulties associated with use of PMB protecting groups;[78] this protecting group caused difficulty during oxidation chemistry and for its cleavage. Based on these considerations, protection as the benzyl ether represented a superior choice. It was envisaged to be stable under basic- or acidic-desilylation conditions, as well as undergo single-step allyl hydrogenation/hydrogenolysis to unmask the C13-alcohol prior to HWE coupling.

A synthetic model evaluated the tandem hydrogenation/benzyl cleavage strategy using our previously-generated aldehyde **4.38** (Scheme 4.2).[79] Grignard conditions[80] successfully provided the racemic homoallylic alcohol, and was subsequently protected as the desired benzyl ether **4.39** in moderate yield. Two-step desilylation and oxidation generated model **4.40** to screen conditions for the tandem sequence. Initial attempts by classic hydrogenation conditions using Pd/C successfully yielded unmasked alcohol **4.41**; however, presence of ester side-product **4.42** was realized in as high as 30% of isolated crude product. We believed use of freshly-distilled methanol and addition of molecular sieves could effectively suppress formation of this side-reaction.

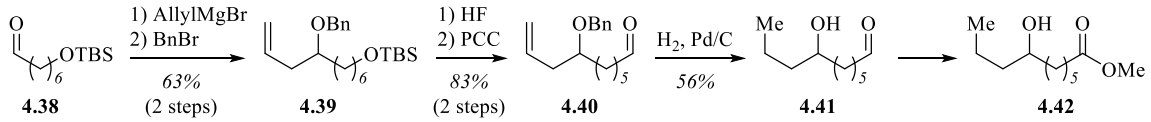

Scheme 4.2 – Synthetic model validated tandem hydrogenation/benzyl cleavage.

Limited quantities of **4.41** permitted a single attempt to couple with phosphonate **4.26** under the HWE conditions used in our ketone model (Scheme 4.3).[59] Despite the presence of side-product **4.42**, trace generation of diagnostic signals in the alkene region suggested conversion to **4.43** was viable, albeit, not optimized. Based on this preliminary result, benzylation of homoallylic alcohol **4.37** for completion of the C7-C16 framework of neopeltolide was initiated.

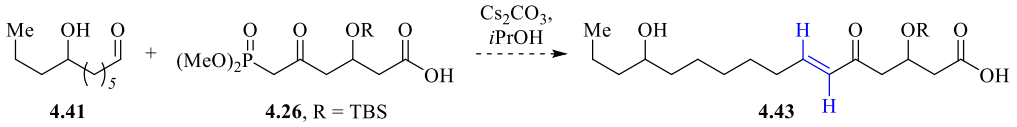

Scheme 4.3 – Preliminary coupling under previously-employed conditions revealed generation of olefin peaks, however the scale of the reaction was too small for isolation or characterization of products.

Completion of the C7-C16 framework for neopeltolide was efficient, and began with TBAI-catalyzed benzylation of **4.37** (Scheme 4.4).[81] Alcohol **4.44** was afforded in high yield under acidic (HF) or basic (TBAF) desilylation conditions. Oxidation by Swern[82] or PCC[83] conditions generated aldehyde **4.45** with excellent spectroscopic purity; however, Swern conditions afforded greater conversion and yield with quantities of **4.44** in excess of 50 mg. Initial efforts to prepare fragment **4.25** by

hydrogenation/hydrogenolysis were plagued by co-isolation of desired aldehyde product and its hydrate. Use of freshly-distilled methanol and 4 Å molecular sieves did not significantly curb formation of hydrate side-product. Attempts to optimize the reaction using decreased catalyst-loading (< 10% *w/w*) highlighted the chemoselectivity of the process, where the greater accessibility of the allyl group generated **4.46** prior to cleavage of the benzyl ether. Extended reaction times failed to generate desired aldehyde and required 20% *w/w* catalyst loading.

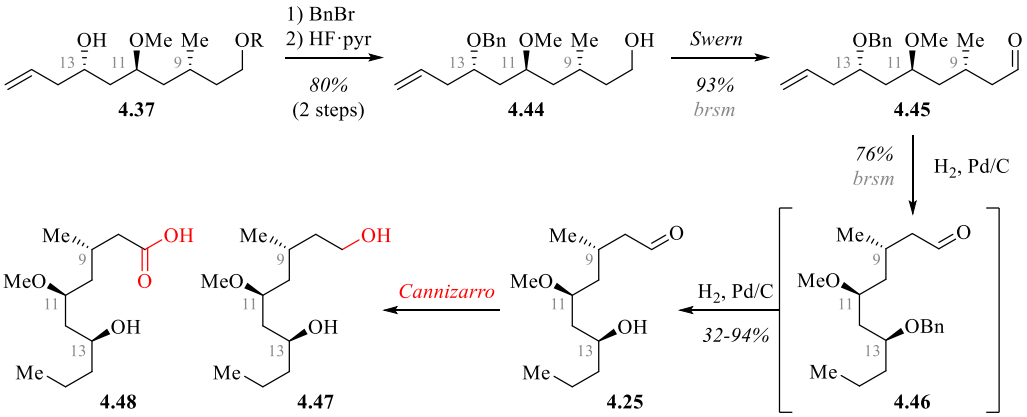

Scheme 4.4 – Synthesis of unmasked C7-C16 fragment of neopeltolide *via* tandem hydrogenation/benzyl cleavage yielded inconsistent ratios of aldehyde **4.25** and its corresponding hydrate.

Improved yields and suppressed generation of hydrate were realized when purification using silica gel was omitted. This observation suggested mildly-acidic conditions sufficiently activated the carbonyl and facilitated weak nucleophilic attack. Moreover, **4.25** has limited storage-life and must be used immediately, as it readily undergoes disproportionation *via* Cannizarro-type reaction[84,85] to afford its corresponding alcohol **4.47** and carboxylic acid **4.48** as reduction and oxidation by-products, respectively. Attempts to recycle these by-products were not made due to limited quantity of material, and the number of subsequent transformations required. Restricted by stability of **4.25**, and supported by satisfactory spectral-purity of the crude product obtained by celite filtration, material was telescoped into olefination attempts with its phosphonate coupling partner.

4.4.4 Model Olefination Conditions Fail with Neopeltolide Framework

HWE coupling conditions that relied on cesium carbonate in isopropanol[59] failed to generate the desired *α,β*-unsaturated ketone **4.49** (Figure 4.10). Numerous modifications that probed reaction times, temperatures, stoichiometry, and concentrations also failed to generate desired product from pure **4.25**. Use of varying mixtures of desired aldehyde and hydrate did not furnish **4.49**, but resulted in recovery of pure **4.25**. This observation supported Villieras' report[86] that the ratio of aldehyde-to-hydrate should not influence the coupling reaction due to equilibrium favoring the aldehyde under basic conditions.

Consequently, it was hypothesized that carbanion-formation of the diprotic system failed due to ineffective deprotonation of the weakly-acidic *α*-methylene of acid phosphonate **4.26** (Figure 4.10). This hypothesis was supported by observation that there are very few examples of similar phosphonate compounds for HWE coupling in literature, of which our model system represented one of them.[59,87]

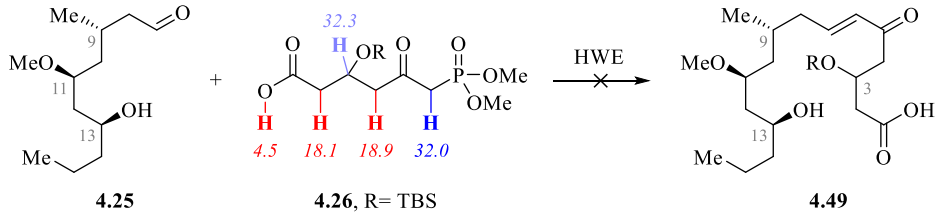

4.25 **4.26**, R= TBS **4.49**

Figure 4.10 – The weak acidity of key methylene (**blue**) in diprotic phosphonate **4.26** was believed to hinder formation of active carbanion species needed for HWE coupling by competing sites. The pKa values were estimated using JChem software.

Interestingly, coupling between aldehyde **4.25** and methyl ester phosphonate **4.50** proceeded quickly and cleanly (Scheme 4.5). This result supported the hypothesis of ineffective carbanion-formation of diprotic **4.26**. Unfortunately, like the ketone model system (Chapter 3, § 3.5.1), fully-derivatized ester system **4.51** failed to hydrolyze cleanly under a variety of conditions and readily underwent *β*-elimination. In addition to conventional base-mediated hydrolysis, other failed conditions included use of barium hydroxide octahydrate,[88] enzyme-controlled base hydrolysis (PLE),[64] non-hydrolytic cleavages,[89,90] heterogeneous sonochemistry,[91] and LiCl-assisted microwave irradiation.[92] Mild hydrolysis of methyl esters by barium hydroxide proved successful in accessing many unique chemical scaffolds from literature[93,94] including a complex intermediate of swinholide A,[95] and substrates sensitive to conventional strategies.[96] Because of these combined observations, we were prompted to investigate phosphonate alternatives with highly-labile ester groups under non-basic conditions.[64,88,89,92,97]

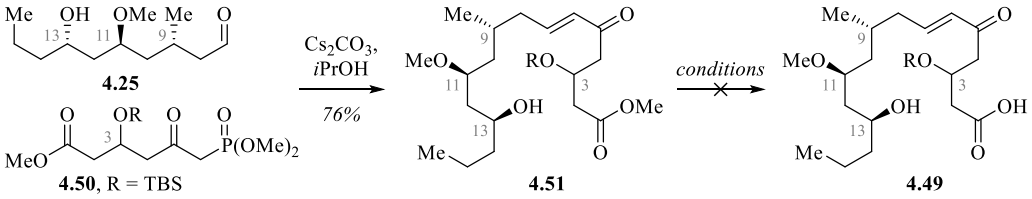

Scheme 4.5 – HWE coupling with ester phosphonate **4.50** proceeded quickly and efficiently; however, only trace *seco*-acid was observed under a variety of conditions, predominantly leading to *β*-elimination or no-reaction.

Initial efforts focussed on methylene acetal esters that can be removed under very mild acidic conditions, and have been used when traditional hydrolytic methods were precluded by issues of acid- or base-stability.[98–100] Synthesis of 2-(trimethylsilyl)ethoxymethyl (SEM) ester phosphonate **4.52** proceeded smoothly,[100,101] and was coupled with aldehyde **4.25** by treatment with cesium carbonate in isopropanol (Scheme 4.6). Modest conversion was attributed to poor stability of the SEM-acetal, as observed by base-mediated decomposition of **4.52** during carbanion formation. Additionally, treatment by SiO_2 proved

effective at ester hydrolysis with concomitant β-elimination to yield diene **4.54** as a by-product. It is believed that free acid was formed and adsorbed to the column during initial purification. Alternative acetal phosphonates displayed similar conversion and stability issues. Based on these results and an inability to generate alternative ester-phosphonates using various substituents and procedures,[102–104] this methodology was abandoned without significant screening.

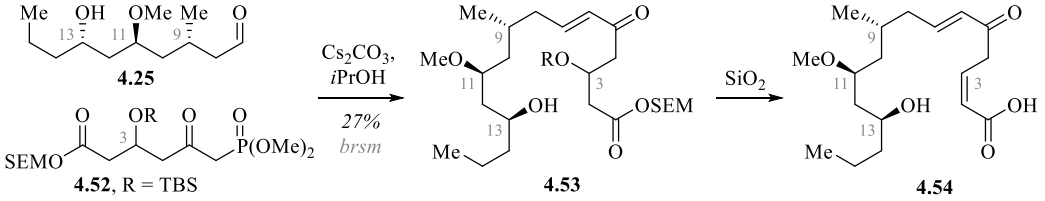

Scheme 4.6 – Stability of SEM-ester phosphonate **4.52** resulted in poor conversion and facile formation of by-products *via* elimination. Employing alternative esters and reaction conditions furnished similar decomposition pathways.

To circumvent challenges of ester-phosphonate formation and subsequent hydrolysis of the resulting HWE product, we explored direct esterification of diprotic phosphonate **4.26** with our C7-C16 fragment of neopeltolide (Scheme 4.7). This would prove more step-economical, and potentially enhance reactivity of HWE olefination since it would be *intra*- versus *inter*molecular transformation. Keck esterification conditions[103] using EDC as the activating-carbodiimide was chosen for the sterically-demanding reaction. Crude material revealed promising new diagnostic signals. The H13 peak shifted downfield, and more-complex splitting-patterns were observed because of the diastereomeric mixture. Unfortunately, the limited material was highly-unstable and could not be isolated from indistinguishable by-products. Attempts to optimize conversion, or telescope material to ring-closure failed to generate any desired macrocyclic product **4.56**.

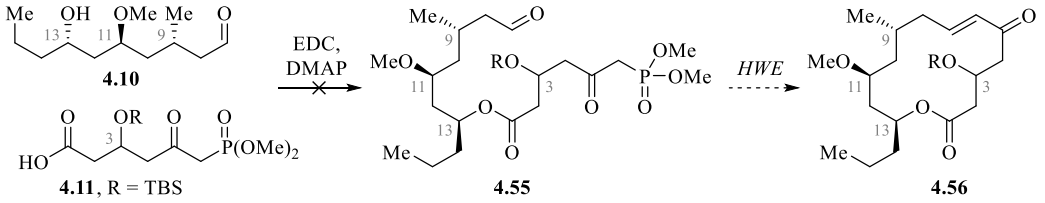

Scheme 4.7 –Direct esterification of C7-C16 fragment **4.25** and diprotic phosphonate **4.26** by Keck protocol generated highly-unstable intermediate **4.55** with low conversion, limiting the exploration of this sequence.

Exploration of alternative routes to generate the full-carbon framework to the macrocyclic core of neopeltolide did not reveal a strategy that was superior to direct-coupling with diprotic phosphonate **4.26**. Consequently, a more detailed screen of reaction conditions was performed to optimize the HWE coupling of aldehyde **4.25** and phosphonate **4.26**.

4.4.5 Screening Conditions for HWE Coupling

The success of HWE coupling can be variable under phase-transfer (PT) conditions,[105] and is heavily influenced by many factors such as solvent, base-catalyst, temperature, additives, carbanion (phosphonate) and carbonyl (aldehyde) compounds.[106] Use of diprotic reagents in PT systems is unfavorable, and can exacerbate reaction variability. To identify optimal reaction conditions for the neopeltolide system and prevent additional loss of advanced aldehydic material, a thorough screen of these factors was performed using a model aldehyde (Figure 4.11). Key observations from this process are discussed below, however a detailed summary of all screened conditions can be found in Appendix II.

Commercial octanal **4.57** was initially tested with diprotic phosphonate **4.26** under the previous HWE coupling conditions that relied on cesium carbonate in isopropanol.[59] As expected, these conditions yielded minimal conversion to desired **4.58**, and formation of *β*-elimination and other undesired peaks were observed. A negative control that lacked phosphonate indicated similar by-products were still produced. These were identified as aldolization compound **4.60** and its dehydration product **4.61** (Figure 4.11), which have been observed with aliphatic aldehydes in phase-transfer HWE reactions at elevated temperatures.[86]

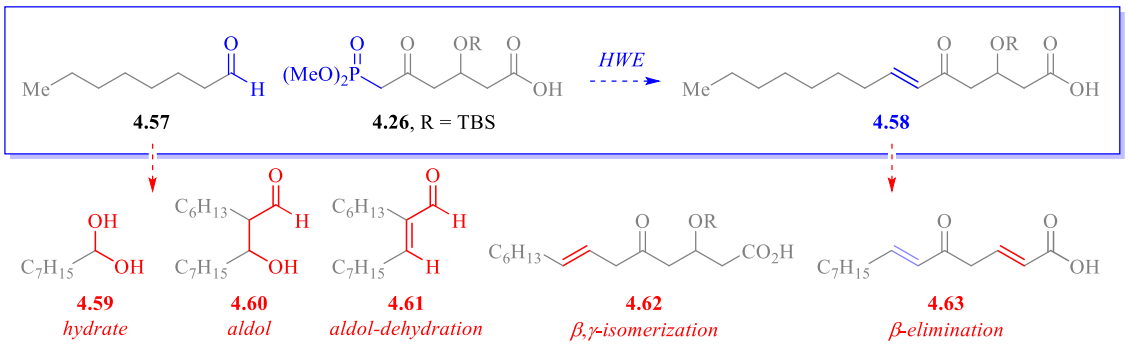

Figure 4.11 – Summary of the desired HWE coupling product (**blue**), and easily-identifiable products of common side-reactions in alkaline conditions (**red**).

Barium hydroxide is an effective base for PT-HWE,[105,107–109] and its mild reaction conditions were used to couple *β*-ketophosphonates with base-sensitive aldehydes in the production of complex natural products such as scytophycin C[110] and (–)-brevenal.[111] Unfortunately, both **4.60** and **4.61** were observed with barium hydroxide under negative control, and prompted an investigation of solvents for suppression of side-reactions (Table 4.2). The small screen indicated isopropanol and DMF facilitated formation of aldol side-products with both bases, while little-to-no detection was observed with acetonitrile and THF solvent systems. Apart from MeCN, this screen showed that polar systems facilitate side-reactions because of improved base solubility. We believed the limited dissolving power of MeCN mimicked non-polar conditions of THF, where a less-stable conjugate base hinders deprotonation at the alpha carbon. In fact,

non-polar systems are known to promote PT-HWE coupling reactions, and THF is the most-commonly employed solvent.[106]

Two-phase systems commonly employ quaternary "-onium" salts or cyclic ethers as catalytic additives to transfer active species.[112] The anionic intermediates of Wittig and HWE olefination reactions have proven successful in the absence of these additives, but required hydrated solvent systems.[105–109,112] The low solubility of barium hydroxide and cesium carbonate in organic systems is improved by hydration. Small amounts of water create thin interfacial layers on the solid base that have similar effects to PT catalytic additives, and improves mass transfer of the carbanion.[113] In our system, hydrated solvents promoted uncharacterized elimination side-reactions from as little as 2.5% *v/v* water (entry 13 & 17, Table 4.3). Water increases overall basicity of the system by disrupting reticular energies of bases to provide greater access to basic sites of the solid. This strategy was used in our first-generation model to achieve thermal disruption of the base lattice, however increased temperatures promoted aldol dehydration and elimination side-reactions (entry 17).[86] Powdered $Ba(OH)_2{\cdot}8H_2O$ yielded similar observations in a system that was previously non-reactive (entry 9), but proved beneficial with activated forms of the base.

Table 4.2 – Negative controls were run for $Ba(OH)_2$ and Cs_2CO_3 in a small screen of solvents to evaluate stability of **4.57**.

Entry[a]	Solvent	Base		Yield[b]	Notes
1	*i*PrOH	$Ba(OH)_2{\cdot}8H_2O$	1.9 equiv.	–	**4.60** and **4.61** formation
2	DMF	$Ba(OH)_2{\cdot}8H_2O$	1.9 equiv.	–	**4.60** and **4.61** formation
3	THF	$Ba(OH)_2{\cdot}8H_2O$	1.9 equiv.	+	No reaction
4	MeCN	$Ba(OH)_2{\cdot}8H_2O$	1.9 equiv.	+	Trace **4.60** side-product
5	*i*PrOH	Cs_2CO_3	1.9 equiv.	–	**4.60** and **4.61** formation
6	DMF	Cs_2CO_3	1.9 equiv.	–	**4.60** and **4.61** formation
7	THF	Cs_2CO_3	1.9 equiv.	+	Trace **4.60** and **4.61** side-products
8	MeCN	Cs_2CO_3	1.9 equiv.	+	Trace **4.60** and **4.61** side-products

[a] – Conditions: octanal **4.57** (1.0 equiv.) in solvent (0.1 M) under argon, for 12 h at ambient temperature.
[b] – Yield is presented as qualitative observation based on TLC and ^{1}HNMR analysis of crude material, indicating relative stability (+) or erosion (–) of aldehyde material.

The microcrystalline structure of barium hydroxide is crucial to its activity in HWE reactions and activated forms of the solid base-catalyst have suppressed undesired side-reactions of starting materials and products.[108,110] In fact, using C-100 (the activated form of barium hydroxide heated at 100 ºC), generated our desired **4.58** as major product (entry 23). We found powdered form of C-200 base-catalyst was superior, and reliably favored desired olefination when performed at ambient temperature using 3.5 equivalents relative to phosphonate **4.26**. The reaction proved surprisingly facile under these conditions and favored **4.58** in as little as 60 minutes (entry 51). Overnight conditions provided optimal conversion, as side-reactions increased with extended reaction times (≥ 24 h).

Table 4.3 – Summary of observations from select screening HWE conditions used to optimize our system. Conditions are presented to highlight single-modifications and improve comparability. Full details can be found in the supporting information.

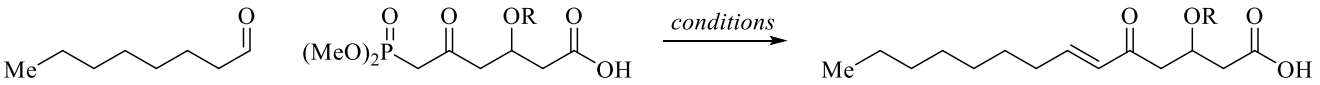

4.57 **4.26**, R = TBS **4.58**

Entry	Solvent		Base[a]		Temp.	Time	Notes	Yield[b]
9	THF	0.1 M	$Ba(OH)_2{\cdot}8H_2O$	1.9 equiv.	22 ºC	12 h	whole crystals	trace formation of any products (< 5% conversion)
11			Cs_2CO_3				30 min. depro	trace formation of any products (< 5% conversion)
13	$THF_{aq.}$	0.1 M	$Ba(OH)_2{\cdot}8H_2O$	1.9 equiv.	22 ºC	12 h	5% *v*/*v* hydration	elimination by-products > **4.57** > hydrate **4.59**
17					45 ºC		3% *v*/*v* hydration	dehydration **4.61** > elimination by-products >> **4.57**
23	THF	0.1 M	C-100 (pow.)	1.9 equiv.	22 ºC	12 h	activated base	**4.58** ≥ **4.57** > dehydration **4.61** > aldol **4.60**
25	THF	0.1 M	C-200 (pow.)	1.9 equiv.	-60 º C	12 h	-	negligible formation of any products
27				1.9 equiv.	4 ºC	24 h		**4.58** ≥ **4.57** >> hydrate **4.59** > *β*,*γ*-**4.62**
35	THF	0.1 M	C-200 (pow.)	1.5 equiv.	22 ºC	12 h	-	**4.26** >> complex mixture of erosion products
39				5.0 equiv.				**4.58** > *β*,*γ*-**4.62** >> **4.57** > *β*-elimination **4.63**
51	THF	0.1 M	C-200 (pow.)	3.5 equiv.	22 ºC	1 h	-	**4.58** ≥ **4.57** >> *β*,*γ*-**4.62** > hydrate **4.59**
54						18 h		**4.58** >>> *β*,*γ*-**4.62** >> hydrate **4.59**
56	THF	0.1 M	DBU	4.0 equiv.	22 ºC	12 h	$Zn(OTf)_2$, TMEDA	dehydration **4.61** > *β*-elimination **4.63** >>> **4.58**
58	THF	0.1 M	C-200 (pow.)	3.5 equiv.	22 ºC	15 h	5.0 M HCl quench	**4.58** >> *β*,*γ*-**4.62** > *β*-elimination **4.63**
59							sat. NH_4Cl quench	**4.58** >>> *β*,*γ*-**4.62**
61							no quench	**4.58** > *β*-elimination **4.63** > *β*,*γ*-**4.62**
62	THF	0.05 M	C-200 (pow.)	3.5 equiv.	22 ºC	15 h	-	**4.58** >> *β*,*γ*-**4.62** >> **4.57** >> aldol **4.60**
65		0.5 M						**4.58** > *β*,*γ*-**4.62** > *β*-elimination **4.63**
66	THF	0.1 M	C-200 (pow.)	3.5 equiv.	22 ºC	15 h	simultaneous addition of **4.26** and **4.57**	1:20:20 (**4.57**-*to*-**4.58**-*to*-all side products)
67	MeCN							4:10:3 (**4.57**-*to*-**4.58**-*to*-all side products)
68	THF	0.1 M	C-200 (pow.)	3.5 equiv.	22 ºC	15 h	-	3:23:23 (**4.57**-*to*-**4.58**-*to*-all side products)
69	MeCN							4:11:6 (**4.57**-*to*-**4.58**-*to*-all side products)

[a] – Carbanion-formation achieved by 40-minute incubation prior to aldehyde addition, unless otherwise specified.
[b] – Major products are presented; a more detailed evaluation can be found in the supplemental information.

With reliable conditions, we wished to compare them to Helquist's zinc-promoted HWE conditions (entry 56).[87] Their mild conditions were reported for diprotic phosphonate systems using a zinc triflate promoter in the presence of DBU and TMEDA additive. These conditions failed with our system and promoted aldol dehydration and elimination side-products. It should be noted that the carboxylate was in the *β*-position of their diprotic system and could provide significantly different electronic effects compared to the *ζ*-position of our system. Similarly, mild Masamune-Roush conditions (DBU, LiCl),[114] and alternative reaction additives provided mixtures of side-products.

Isolation of coupled product **4.58** required a proton source, but needed to be mild-enough conditions to prevent concomitant desilylation of the C3 alcohol. Considerable suppression of *β,γ*-isomerization product was observed during acidic quench with a saturated solution of ammonium chloride (entry 59). Moreover, under optimized conditions, use of anhydrous acetonitrile provided a greater ratio of desired product to side-products, compared to THF (entry 66-69). Although conversion was slower, we believed this could allow aldehyde **4.25** to be recovered and recycled into subsequent coupling reactions.

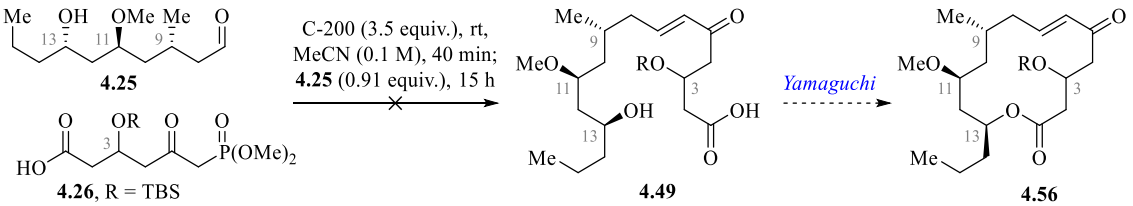

Scheme 4.8 – HWE coupling under the newly-optimized conditions failed to provide *seco*-acid **4.49**, and prompted a hypothesis where the free alcohol inhibited the reaction.

With great disappointment, the newly-optimized conditions failed to yield the full carbon framework of neopeltolide **4.49** (Scheme 4.8). Other successful combinations from the screen were tested, but little-to-no coupling product was observed. Because of continued difficulties, we questioned whether the C13 free alcohol of aldehyde fragment **4.25** inhibited desired olefination. Within phase-transfer systems, presence of weakly-acidic amino- and hydroxy-protons have poisoned base-catalysts and inhibited the reaction.[105–107] To rapidly investigate this hypothesis, we designed a second-generation *α,β*-unsaturated ketone model system of neopeltolide that lacked substituents at C9 and C11 positions.

4.5 A Second-Generation *α,β*-Unsaturated Ketone Model System

The presented difficulties of fragment coupling under HWE conditions[115] aligned with low-reactivity reported in liquid-solid phase-transfer (LS-PT).[106,113] We believed the free C13 alcohol could coordinate to solid base-catalyst to neutralize carbanion formation by occupying the limited basic sites of its solid surface. Accordingly, we designed a second-generation *α,β*-unsaturated ketone model to feature a protecting group that was stable to HWE conditions and readily-labile under mild conditions (Figure 4.12).

Methoxymethyl ether (MOM) protection was chosen for the C13-alcohol,[116] which previously demonstrated extremely facile deprotection by treatment with SiO_2 during investigation of labile ester phosphonates (§ 4.4.4).

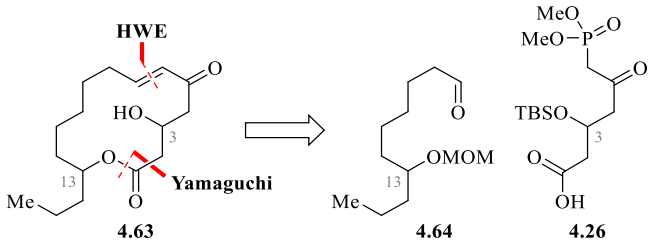

Figure 4.12 – Retrosynthetic analysis for oxa-conjugate precursor **4.63** of the second-generation *α,β*-unsaturated ketone model featuring the requisite C13 *n*-propyl from neopeltolide.

The second-generation model was designed to complement our first-generation system,[59] and featured reversible acid-mediated *β'*-hydroxy attack into an *α,β*-unsaturated ketone for assembly of the *cis*-THP. In addition to validating our HWE inhibition hypothesis, native propyl substitution would provide preliminary insight into remote stereocontrol by the lactone stereocenter during THP assembly. Rizzacasa reported that the lactone configuration in apicularen A was sufficient to control both THP stereogenic centers (Chapter 3, § 3.3.2).[117] Herein, synthesis of our second-generation *α,β*-unsaturated ketone model system for transannular oxa-conjugate assembly of the 2,6-*cis*-THP of neopeltolide is reported.

4.5.1 Development of Ketone Model to Evaluate Native C13 Substitution

Synthesis of aldehyde **4.64** proceeded smoothly in a five-step sequence from previously-prepared **4.38** (Scheme 4.9). HWE coupling conditions using microcrystalline C-200 base-catalyst in MeCN successfully generated the full carbon framework **4.66**, albeit in low yield. When performed at extended times (18 h), mildly-elevated temperatures (35 ºC), and with addition of THF (50% *v*/*v*), conversion was modestly improved. However, with sufficient material prepared, acid **4.66** was subjected to deprotection conditions without further optimization.

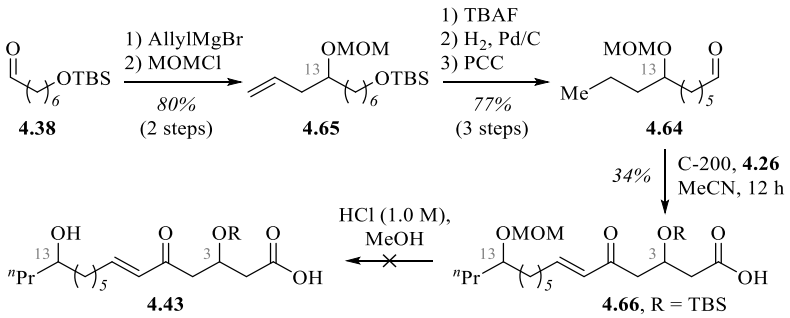

Scheme 4.9 – HWE olefination of C13-Protected aldehyde **4.64** and diprotic phosphonate **4.26** modestly-yielded the desired coupling product **4.66**. Deprotection of under mildly-acidic conditions facilitated decomposition and did not furnish *seco*-acid **4.43**.

The MOM-protected alcohol proved more robust than our MOM-protected ester phosphonate, and was stable to SiO_2 conditions during purification.[99] Treatment with methanolic HCl (1.0 N) also failed to provide desired *seco*-acid **4.43**; however, formation of cleanly deprotected *β*-TBS alcohol **4.67** was observed (Figure 4.13). Contrary to observations from our first-generation model (Chapter 3, § 3.5.1), spontaneous formation of pyranone products from this linear system was not detected. This may suggest oxa-conjugate addition requires more forcing conditions to activate the *α*,*β*-unsaturated carbonyl and/or lower entropic barriers. Further investigation is required to better understand the requirements that facilitate THP assembly in these linear systems. Efforts to suppress undesired desilylation were not attempted, and **4.67** was subjected to similar conditions and monitored for cleavage of the MOM-acetal. The obtained *seco*-acid could still cyclize by Yamaguchi esterification,[63] and was believed would preferentially yield macrocyclic product to *β*-lactone product with superior chemoselectivity. Unfortunately, prolonged exposure resulted in erosion of **4.67** *via* conjugate addition (**4.68**) and retro-aldol-type mechanisms (**4.42**, Figure 4.13).

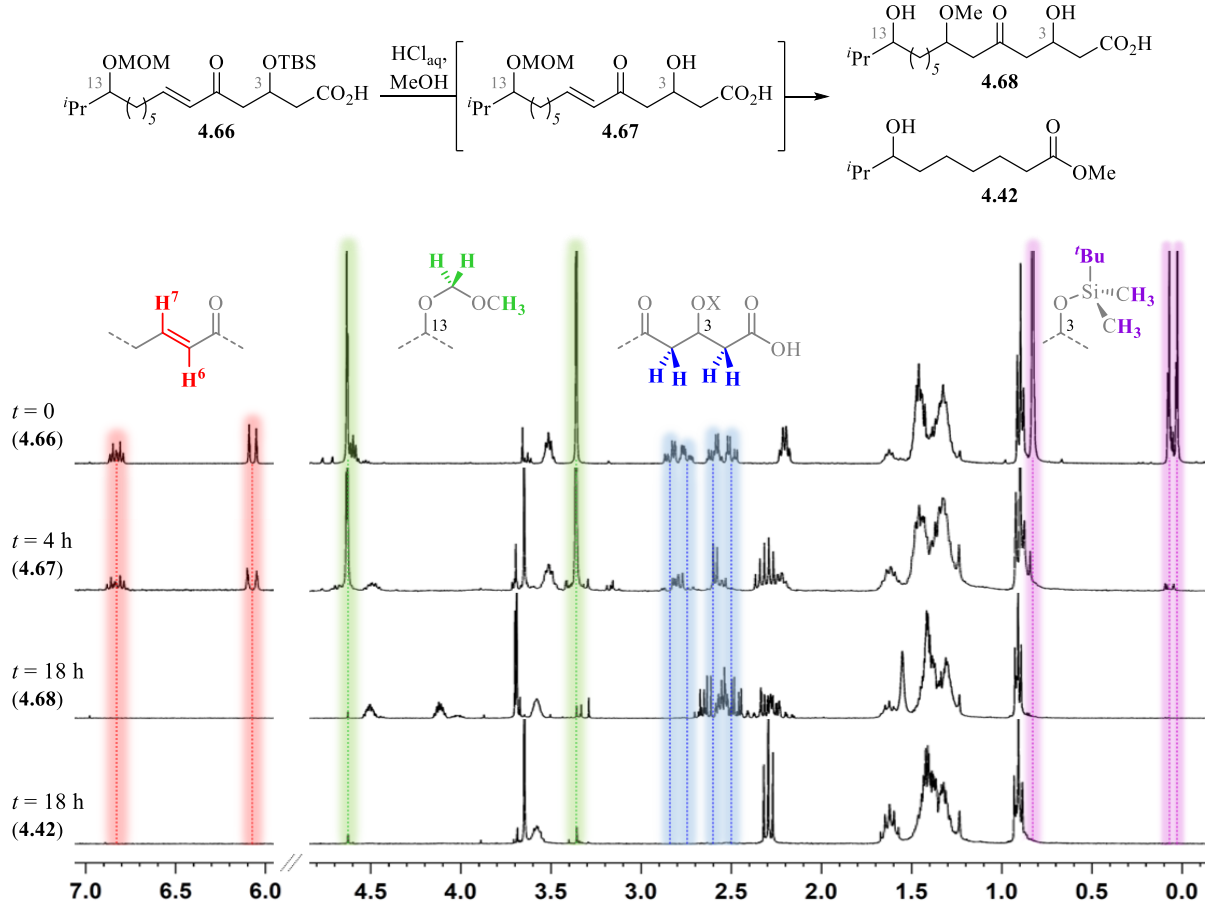

Figure 4.13 – Aqueous HCl (1.0 N) desilylates **4.66**, but failed to cleave the desired MOM acetal. Extended exposure resulted in formation of separable by-products *via* conjugate addition **4.68** and retro-aldol **4.42** mechanisms.

This work indicated deprotection of C13-protected MOM-acetal required more forcing conditions. Use of Lewis-acid-mediated deprotection conditions[90,118,119] caused concerns of stability for both the C3-TBS-alcohol and requisite C11-methyl ether of the coupled natural product framework. Likewise, C13-protected **4.64** did not improve coupling to appreciable levels, suggesting free-alcohol was not an inhibiting factor. Based on these considerations, **4.64** was screened for optimal MOM-acetal-deprotection conditions prior to olefination. A panel of acids (HCl, HBr, HF, TFA) and solvents (MeOH, THF, MeCN, *i*PrOH, 1,4-dioxane, CH_2Cl_2) were evaluated, and it was determined that HCl (12 N) in anhydrous THF reliably accessed desired aldehyde **4.41** in good yield.

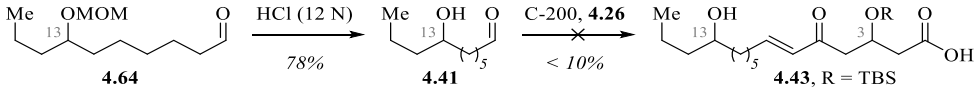

Scheme 4.10 – A small screen of conditions revealed concentrated HCl (12 N) in THF reliably furnished **4.41** in good yield. Distressingly, the optimized olefination conditions did not generate desired **4.43** product.

Having demonstrated that protection of the C13 alcohol does not significantly improve HWE coupling reaction with diprotic phosphonate **4.26**, and complicated unmasking of the *seco*-acid required for macrocyclization, we refocused efforts toward further-optimizing our olefination conditions. Thus, an exhaustive screen systematically evaluated combinations of reaction conditions with our HWE model system.

4.5.2 Thermodynamic Equilibration Achieves Exclusive Formation of cis-Pyranone

The secondary screening process identified that carbanion formation continued to limit the success of olefination. Using time-course experiments in various deuterated solvents, facile coupling was observed by instantaneous formation of alkene product signals in trace amounts (< 5% relative-to-C*H*O); however, product formation did not increase with extended reaction times. Stability of aldehyde was not affected during periods greater than 2 weeks at ambient temperature, which supported concerns of inadequate basicity. Anhydrous conditions can degrade crystalline structures of the base-catalyst by extracting surface water and causing contraction of the lattice.[113] Decreased alkalinity caused by limited access to basic sites exacerbates difficulties of carbanion formation *via* abstraction of the weakly acidic alpha proton. Ultimately, conditions were identified that relied on aqueous THF (3% *v*/*v*, 0.076 M) as a solvent, and cesium carbonate (1.3 equiv.) as our phase-transfer base-catalyst. Details of this fortuitous discovery are outlined in the supporting information.

Our newly-optimized conditions successfully-coupled aldehyde **4.41** with phosphonate **4.26** to afford desired *α*,*β*-unsaturated **4.43** in modest yield (Scheme 4.11). Macrocyclization was accomplished by Yamaguchi esterification, to provide an inseparable mixture of diastereomers that was desilylated by

treatment with HF to yield **4.63** (*d.r.* = 1:1). Because quantities were limited (1.3 mg), the key oxa-conjugate addition was performed using our previously-reported conditions[59,117,120,121] in a single attempt.

Addition of Amberlyst-15® slowly converted *β'*-hydroxy enone **4.63** to relative *trans*-pyranone product with modest selectivity (*d.r.* = 5:4). Unlike our first-generation model, formation of this kinetic product was not instantaneous, and in fact did not fully-convert (approximately 80% conversion) after 15 hours at ambient temperature (Figure 4.11). It should be noted that *p*-TsOH was employed as our proton source in the first-generation system to achieve the high reaction rate. Disappointingly, formation of elimination product appeared in this mixture that resembled by-product from the earlier model; based on this observation, it was believed to be diene **4.72** (*vide infra*). The complex mixture of stereoisomers was heated at 80 ºC for 6 hours to fully consume residual precursor, and interconverted kinetic *trans*-**4.70** product with exclusive formation of *cis*-pyranone diastereomers. The relative ratio of *cis*-THP isomers was 2:1, however absolute identification was not possible.

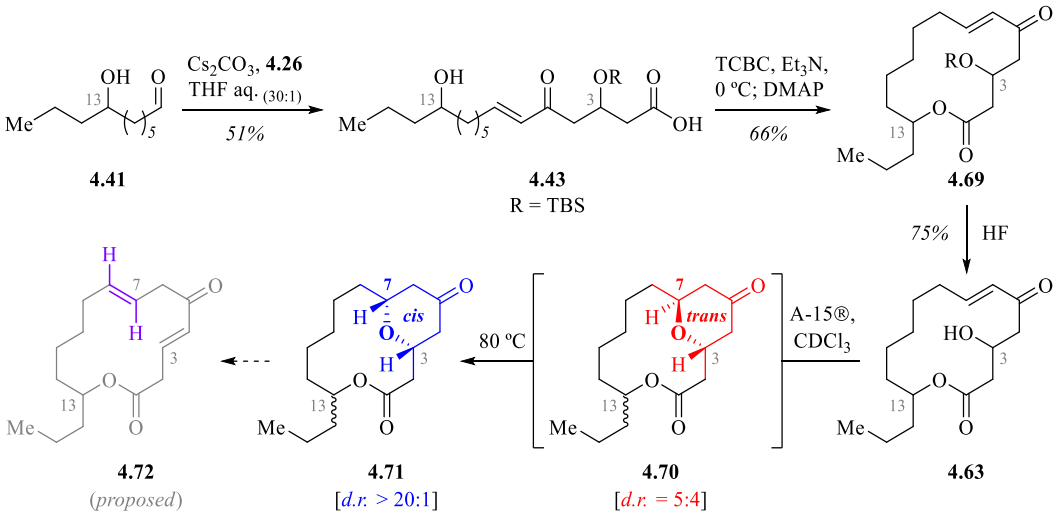

Scheme 4.11 – Second-generation *α,β*-unsaturated ketone model validates selective transannular oxa-conjugate assembly of *cis*-THP under thermodynamic control. The sequence was performed once and was not optimized.

The C13-propyl substituent resulted in a dramatic increase in relative selectivity during thermodynamic equilibration (*d.r.* > 20:1). Comparatively, our first-generation ketone model afforded *cis*-pyranone product with good diastereoselectivity under thermodynamic Amberlyst-15® conditions (*d.r.* > 9:1). It is unclear whether 1,7-stereocontrol of the lactone stereocenter sufficiently accounted for the improved selectivity.[122] However, we expected native conformational biases imparted by the macrocyclic backbone of neopeltolide would further enhance selectivity during pyran formation.[123]

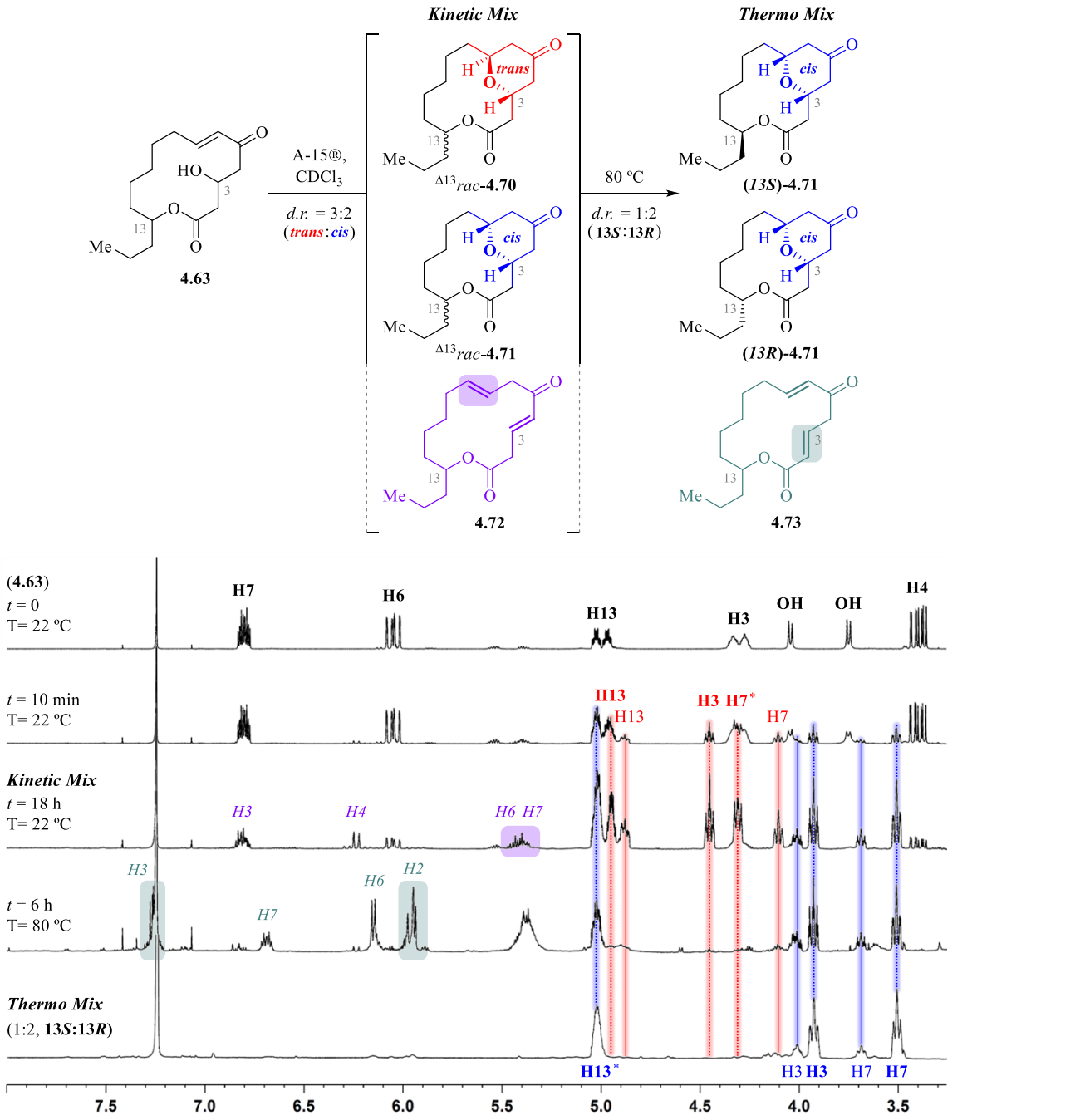

Figure 4.14 – Acid-mediated transannular oxa-conjugate addition successfully furnished pyran products. Kinetic *trans*-pyranone product is exclusively converted to *cis*-pyranone by thermodynamic equilibration, and favors our (13*R*)-epimer. Major products are **bolded**; putative products are *italicized*. Missing signals buried beneath peaks labeled with an asterisk.

Like the first-generation model, formation of elimination by-product was realized under acid-mediated conditions (Figure 4.14). Under kinetic control, we proposed formation of diene **4.72** could occur by an unproductive pathway that isomerizes to the non-conjugated β,γ-unsaturated ketone system, and subsequent dehydration of the C3-alcohol. Gouverneur noted Brønsted acid-mediated pyran formation of hydroxy enones commonly competed with dehydration of their hydroxy nucleophile while establishing

cationic Pd-catalyzed cyclization conditions.[124] Rizzacasa observed similar elimination in their acid-mediated transannular oxa-conjugate addition of apicularen A, under thermodynamic conditions.[120] In our system, we proposed **4.73** was generated by an alternative unproductive pathway under thermodynamic equilibration. Retro-cyclization could establish conjugation into the ester carbonyl, which would not re-cyclize to desired pyranone product and could eliminate the *β'*-hydroxy C7-stereocenter *via* E1cB mechanism. This hypothesis is supported by the inability to generate pyran products with our *α,β*-unsaturated ester model system (Chapter 3, § 3.4.2). Deuterium labeling could be used to determine mechanistic details of elimination by-product formation. At this point, we questioned whether the fully-elaborated macrocyclic backbone of neopeltolide would suppress elimination. Nevertheless, the study verified our strategy and demonstrated that distal stereochemical elements can affect selectivity of THP formation.

Selective reduction of *cis*-pyranone mixture **4.71** into the desired C5-alcohol was accomplished by treatment with $NaBH_4$, favoring *α*-product (*α*:*β* > 15:1) as an inseparable mixture of *cis*-pyranyl C13-diastereomers (*d.r.* = 5:1). Comparison to Fuwa's report[39] suggested our minor *cis*-product possessed the configuration of **4.74** (Scheme 4.12). This configuration boasts native C3-, C7-, and C13-configuration of the neopeltolide macrocyclic core, and the epimeric C5-configuration used to append the side-chain under Mitsunobu esterification conditions. Consequently, we proposed our major product possessed the configuration of **4.76**. Due to extremely-limited quantity of material and inability to separate all diastereoisomers cleanly, optical rotations were not possible to accurately identity the major product. Use of single-dimensional NOESY experiments with a 600 MHz cryo-probe were also inconclusive at this scale.

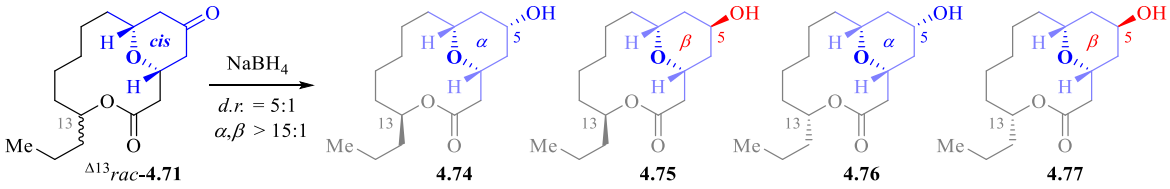

Scheme 4.12 – Possible *cis*-stereoisomers from the reduction of $^{\Delta 13}$*rac*-**4.71** (enantiomers were excluded). Results suggested remote stereocontrol by the lactone center improves selectivity from our first-generation model.

Repeating the sequence with enantiopure alcohol **4.41** would help eliminate ambiguity, however the second-generation *α,β*-unsaturated ketone model provided support to our transannular oxa-conjugate addition strategy to assemble the 2,6-*cis*-THP of neopeltolide. This work demonstrated olefination of free C13-hydroxy is possible under optimized conditions, and suggested previous failures were partly due to capricious reaction conditions leading to limited carbanion formation. Facile macrocyclization by Yamaguchi esterification afforded our key oxa-conjugate precursor, and yielded kinetically-favored *trans*-pyranone by acidic treatment with Amberlyst-15®. Under thermodynamic conditions, equilibration to *cis*-

pyranone was achieved with exclusive selectivity. This result suggested distal stereochemical elements can affect control for diastereoselective pyran formation, which was believed to be reinforced by rigidifying elements of the native neopeltolide backbone.[125] Lastly, the sequence of HWE-to-selective ketone reduction was performed as a single-attempt due to limited material; this caveat provided encouragement and confidence for completion of the macrocyclic core of neopeltolide.

4.6 Transannular Oxa-Conjugate Addition Generates Neopeltolide Core

Based on the success of the second-generation model, re-design of our C7-C16 neopeltolide framework featured MOM-acetal protection of the C13-alcohol. Confidence in deprotection, as well as our newly-optimized and reproducible olefination reaction, prompted development of aldehyde **4.25** despite minimal quantities of precursor materials.

4.6.1 Optimized Conditions Furnish C3-Diastereomeric Oxa-Conjugate Precursors

Development of fragment **4.25** began with hydrogenation of homoallylic alcohol **4.37**, and subsequent protection as MOM-acetal **4.78** in excellent yield (Scheme 4.13). Desilylation and oxidation provided precursor **4.79**, which was recently published by Mineeva in a failed synthetic effort toward neopeltolide.[126] Their independent strategy employed sequential Keck asymmetric allylations[127] and substrate-controlled hydrogenation to access **4.79** in 9.8% overall yield over 15 steps from a commercial ester. Comparatively, this work accessed the common intermediate in 13 linear steps from racemic methyl glutarate (**S-12**) in 31.5% overall yield.

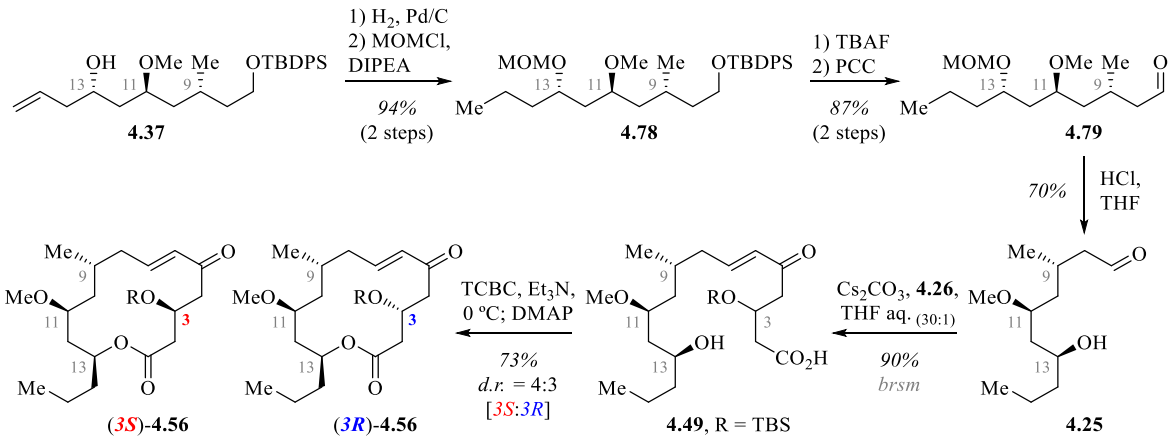

Scheme 4.13 – Optimized MOM-deprotection and HWE olefination conditions were employed to generate the full carbon framework of **4.49**, and macrocyclized by Yamaguchi esterification as a separable mixture of C3-diastereomers.

The C13-MOM-acetal was cleaved in moderate yield (70%) using our optimized deprotection conditions, and represented the poorest yield of our synthesis. The full carbon framework of neopeltolide **4.49** was *finally* isolated in excellent yield based on recovered starting material, under the most-recent

coupling conditions. Although conversion remained modest, with nearly 10 mg of **4.49** in hand, macrocyclization by highly-diluted Yamaguchi esterification conditions afforded a separable mixture of diastereomers (*3S*)-**4.56** and (*3R*)-**4.56** (*d.r.* = 4:3). These diastereomers were retroactively-assigned based on extensive 1D- and 2D-NMR analysis of the pyran products they generated.

Desilylation of diastereomers (*3S*)- and (*3R*)-**4.56** by treatment with HF at ambient temperature readily provided all four pyranyl diastereoisomers by spontaneous oxa-conjugate addition (Scheme 4.14). Oxa-conjugate precursors (*3R*)- and (*3S*)-**4.24** were not isolated, but trace signals of these free-hydroxyl compounds could be identified from crude materials (< 5%). From native (*3R*)-**4.56**, facile oxa-conjugate addition yielded a mixture of pyranyl products that favored *trans*-**4.80** as kinetic product (*d.r.* ~ 40:1). This supported our previous results from first- and second-generation models, which suggested *trans*-products are kinetically-favored under acid-mediated transannular oxa-conjugate addition in 14-membered macrocyclic systems. Similarly, spontaneous cyclization from epimeric (*3S*)-**4.56** furnished a mixture of pyranyl products that favored kinetic *trans*-**4.82** (*d.r.* ~ 9:5).

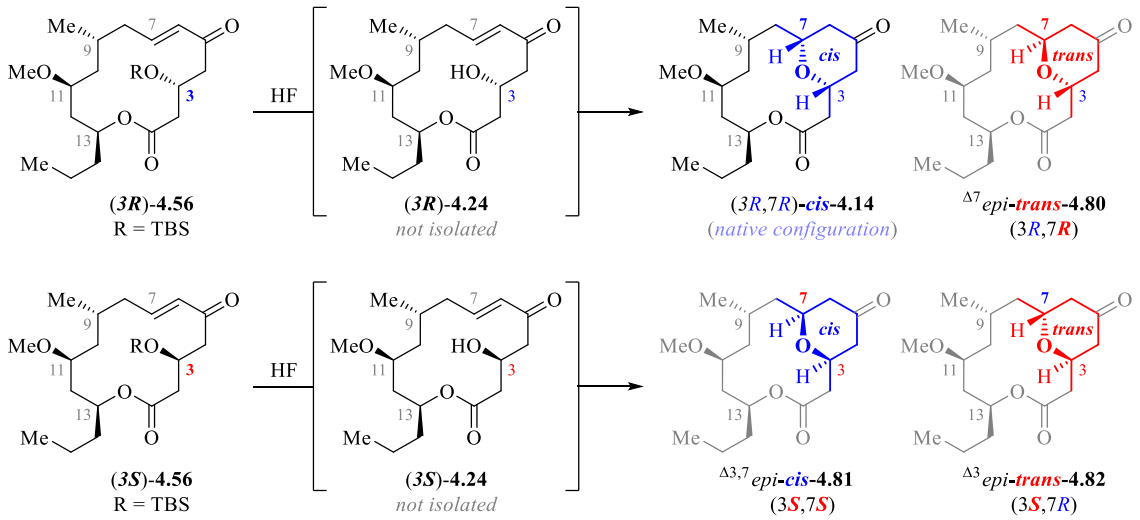

Scheme 4.14 – Acid-mediated desilylation facilitated spontaneous oxa-conjugate addition without isolation of *β'*-hydroxy enone intermediates. Kinetic conditions favored the formation of *trans*-pyranone diastereoisomers.

Ultimately, both kinetic mixtures are expected to coalesce into the thermodynamically-preferred product under our equilibration conditions. However, due to limited material we were restricted to single attempts at thermodynamic equilibration for the obtained kinetic mixtures. We believed equilibration of these products could provide a rapid route to accessing the desired configuration for the macrocyclic framework of neopeltolide.

4.6.2 Native cis-THP Configuration of Neopeltolide is Not Energetic Minimum

A computational approach was used to evaluate relative energies of all diastereomeric oxa-conjugate precursors, as well as the *cis*- and *trans*-products to determine if thermodynamic control would access desired *cis*-**4.14** (Figure 4.16). Structures were subjected to PM6[128] optimization prior to B3LYP/6-31++G** energy minimization.[129–131] Potential energies of energy-minimized structures were computed. Vibrational analysis was performed, and no imaginary frequencies were identified, suggesting the geometries of each compound occupied a local minimum. Potential energies calculated by DFT are proficient for comparing stability between conformations of the same molecule and between configurational isomers. However, it should be noted that DFT is poor at recapitulating the difference in free energy (or heats of formation) between molecules with different types and number of bonds (*vide infra*).[132]

From precursor (*3R*)-**4.24**, our computational analysis determined *trans*-**4.80** to be in a twist-boat conformation and approximately 1.1 kcal/mol higher in energy than the native *cis*-**4.14** chair conformation. Likewise, *trans*-**4.82** diastereoisomer from (*3S*)-**4.24** was predicted to adopt a twist-boat conformation and calculated to be approximately 6.45 kcal/mol higher in energy than the *cis*-**4.81** chair conformer. These conformer profiles, coupled with the high diastereoselectivity obtained experimentally for *trans*-product, suggested that the transannular oxa-conjugate additions operated under Curtin-Hammett kinetics (Figure 4.15). Directing this outcome may be an interplay of two conformations from each oxa-conjugate precursor, where the macrocyclic backbone of conformers I and III are in extended parallel relationships that generate staggered ring systems akin to Scheidt's transition state for pyran formation (Chapter 2, § 2.2.2).[21] Conversely, conformers II and IV lead to energetically-favored *cis*-pyran products, but proceed with the macrocyclic backbone in perpendicular relationships that could significantly-hinder nucleophilic addition. We hypothesized that these conformational biases facilitated the observed product distributions in our kinetic mixtures, and triggered Curtin-Hammett kinetics to predominate. Additional conformational analysis, including thorough computations on plausible transition states is required to gain better insight into the experimental results.

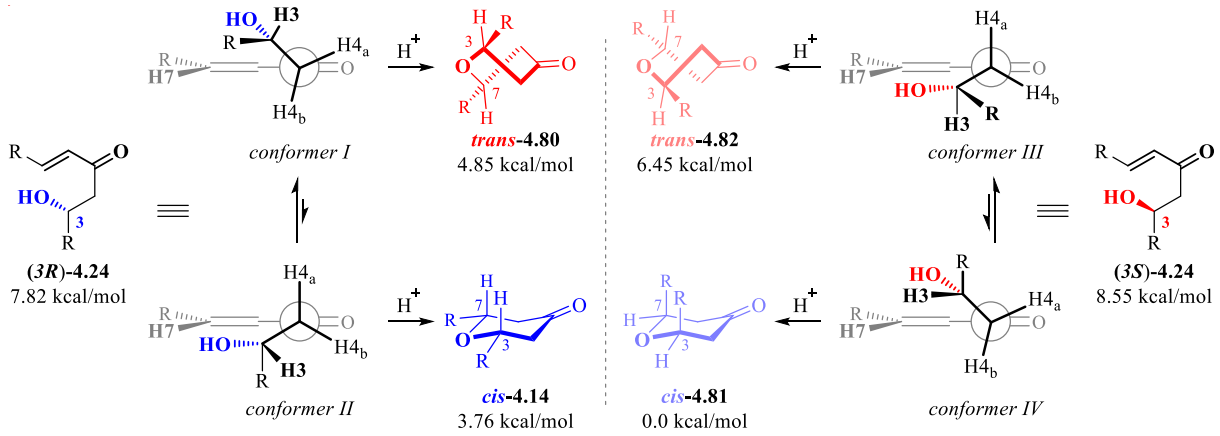

Figure 4.15 – An interplay of two conformations may be responsible for the observed stereochemical outcomes from macrocyclic oxa-conjugate addition precursors (***3R***)- and (***3S***)-**4.24** under kinetic conditions, to favor *trans*-products.

Surprisingly, our computational data indicated that epimeric *cis*-**4.81** was the energetic minimum, and not the native *cis*-**4.14** configuration for the bicyclic core of neopeltolide. In fact, the 3.76 kcal/mol barrier favoring undesired *cis*-**4.81** is larger than relative energy differences calculated for assembly of native configurations of 2,6-disubstituted pyrans from transannular oxa-conjugate addition systems for apicularen A,[117] aspergillide A-B,[133] laulimalide,[121] and our first-generation ketone model.[59] A comparison of relative energy differences for *cis*- and *trans*-pyran formation within these systems can be found in the supporting information. This observation suggested spontaneous pyran formation is unlikely during biosynthesis and that a highly-specific enzyme such as the putative pyran synthase may be required to assemble the native configuration of neopeltolide.[134]

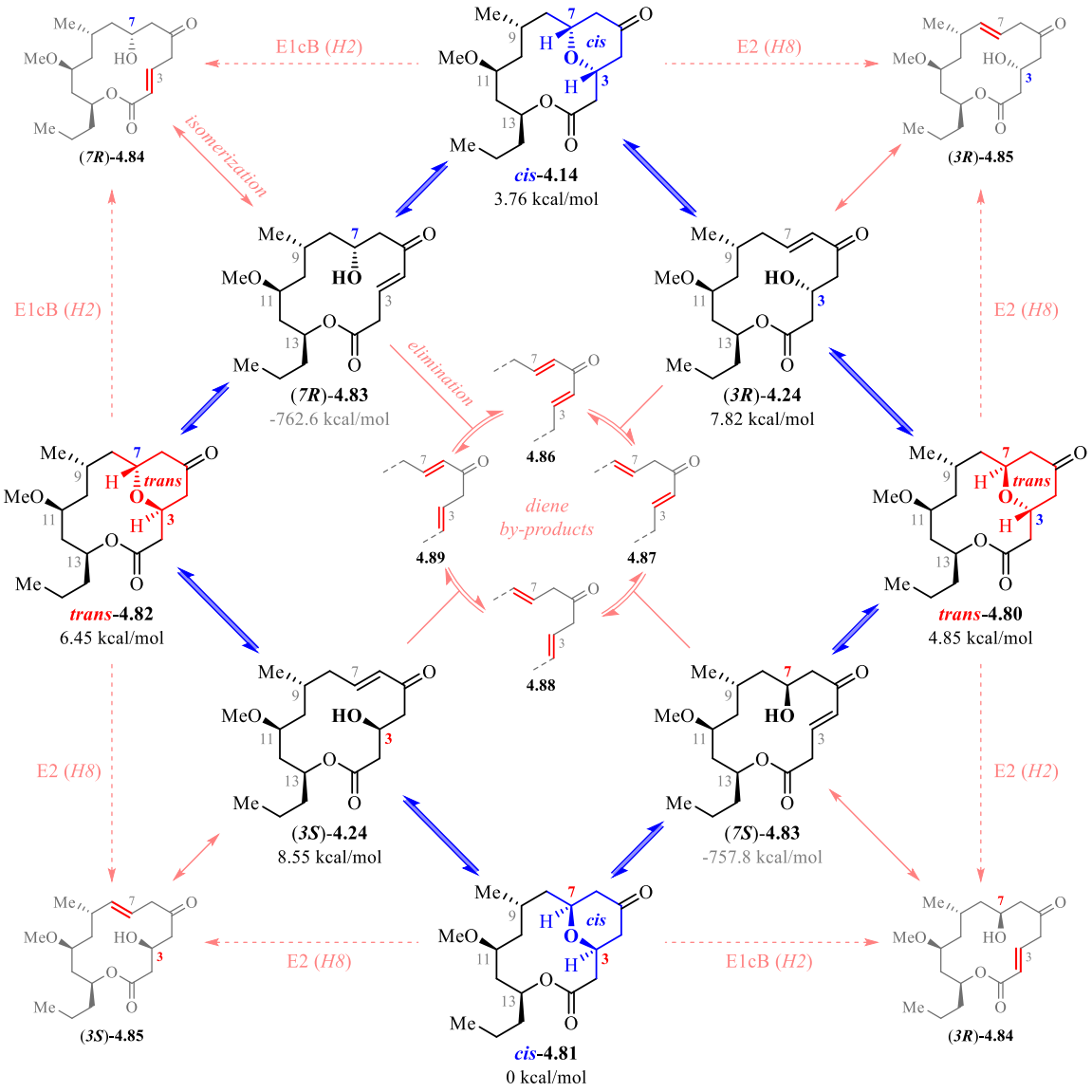

Figure 4.16 – Map of potential pathways during acid-mediated (Amberlyst-15®) transannular oxa-conjugate addition assembly of the *cis*-THP from the macrocyclic core of neopeltolide **4.14**. Under thermodynamic conditions, **blue** arrows indicate equilibration pathways; **red** arrows denote non-productive pathways that lead to undesired isomerization and elimination by-products; dashed arrows represent plausible pathways, but are not believed to play a role.

Evaluation of our thermodynamic equilibration was restricted to a single opportunity with each kinetic mixture. Under thermodynamic equilibration conditions from the first- and second-generation *α,β*-unsaturated ketone model systems (Amberlyst-15® in $CDCl_3$ at 80 ºC), each reaction was performed in a 2.5 mm NMR tube and monitored using a 600 MHz instrument (Figure 4.17-18). Using the kinetic mixture obtained from precursor (*3R*)-**4.24**, exclusive formation of *cis*-pyranone products was achieved after 15 hours under thermodynamic control. Within five hours at 80 ºC, more than 90% of *trans*-**4.80** was consumed, according to relative integrations of peaks. The reaction mixture indicated an increase to the relative abundance of both *cis*-isomers in identical selectivity that favored desired *cis*-**4.14** (*d.r.* = 5:4),

which were now major products (Figure 4.17). After 15 hours under thermodynamic control, complete conversion of *trans*-product was realized, with minimal increase in non-productive pathway by-products (*vide infra*).

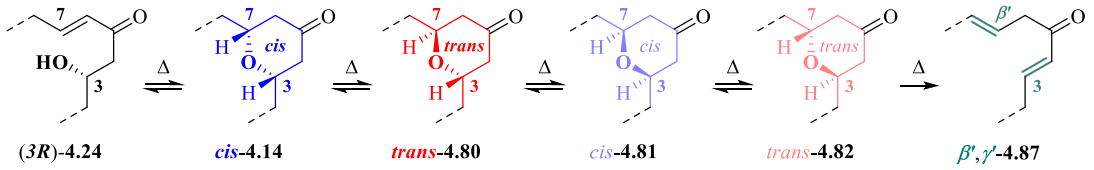

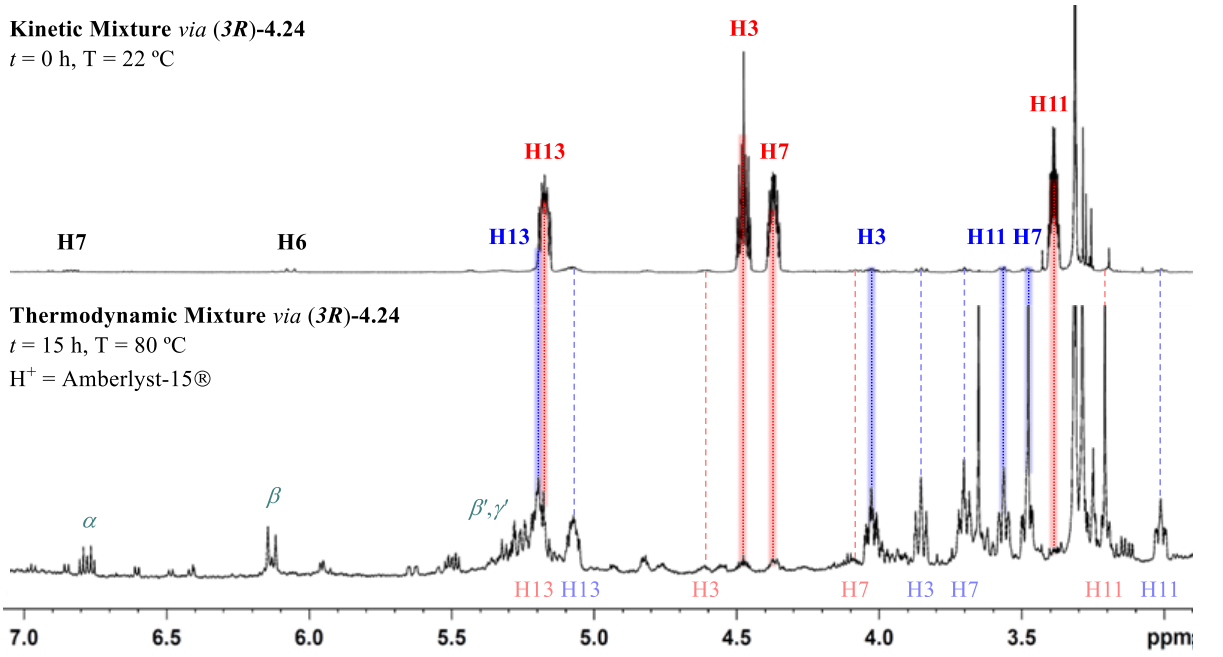

	cis-4.14	*trans*-4.80	*cis*-4.81	*trans*-4.82	*Notes*
Kinetic (*3R*)	1.0	40	0.8	0.5	- majority of *trans*-THPs equilibrate within 5 h - formation of signals δ 5.1 – 5.3 ppm resemble pattern for *β',γ'*-elimination **4.87** (~ 15%) - unidentified signals δ 5.5 – 7.0 and 4.5 – 4.8 ppm potentially C7 regio-isomeric intermediates or by-products of non-productive pathways
Thermodynamic					
t = 5 h	1.0	0.14	0.76	0.04	
t = 10 h	1.0	0.11	0.71	0.05	
t = 15 h	1.0	*trace*	0.54	*trace*	

Figure 4.17 – Acid-mediated thermodynamic conditions facilitated equilibration of the predominantly *trans*-**4.80** kinetic mixture obtained *via* oxa-conjugate precursor (***3R***)-**4.24**. Generation of native *cis*-configuration **4.14** was favored over the lower-energy *cis*-diastereomer **4.81** (*d.r.* = 9:5). Bolded lines and labels indicate products with 3*R*-configuration.

Upon completion, selectivity for native *cis*-**4.14** had improved, and was favored in comparison to energetically-preferred *cis*-**4.81** (*d.r.* = 9:5). This observation could suggest formation of C7 *β'*-hydroxy enone (*7S*)-**4.83** imposed an energetic barrier to hinder formation of the energetic minimum. Unfortunately, our computational data suffered the limitation of recapitulating energetic differences for regio-isomers by DFT analysis and could not provide accurate comparisons for our C7-nucleophilic products (*R/S*)-**4.83**. Synthesis of these isomers could greatly-benefit the re-evaluation of this study by providing experimental

details of product formation and distribution from these precursors, including potential formation of by-products *via* non-productive pathways. Lastly, based on relative energy difference between *cis*-**4.14** and *trans*-**4.80**, our experimental data exceeded the computationally-predicted equilibration ratio at 80 ºC of 82:18 for *cis*-to-*trans* product distribution for (*3R*)-isomers. However, this prediction does not include the complex mixture of equilibration products, and it is difficult to predict interconversion to the energetic minimum *cis*-**4.81** isomer.

Under thermodynamic Amberlyst-15® conditions, unidentified olefin signals that closely-resembled the *α,β*-unsaturated-*β',γ'* diene system of **4.87** were observed. Similar signals were previously-reported in apicularen A[120] and both of our model systems (Chapter 4, § 4.5.2).[59] Re-evaluation of this transformation is required to determine if these are intermediates from our equilibration pathway, or by-products of non-productive pathways. Likewise, evaluation of modified or alternative reaction conditions should be screened to suppress formation of by-products under thermodynamic control, like the 20% decrease observed in our first-generation model.

To improve direct-comparison to results from our (*3R*)-kinetic mixture, identical acid-mediated thermodynamic conditions were employed with the diastereomeric (*3S*)-mixture (Figure 4.18). The kinetic mixture of *cis*-**4.81** and *trans*-**4.82** (*d.r.* = 5:9) provided a distribution of products that favored our computationally-predicted energetic minimum under thermodynamic control. Within 5 hours, approximately 75% of material had equilibrated to *cis*-**4.81** with surprising formation of desired *cis*-**4.14** (*d.r.* ~ 5:1, **4.81**:**4.14**). Extended reaction times did not result in complete consumption of *trans*-**4.82**, and suggested that the mixture was not completely at its thermodynamic minimum. Surprisingly, the observed selectivity did not align with our computationally-predicted equilibrium ratio at 80 ºC of greater than 99% formation of energetically-favored *cis*-**4.81** for (*3S*)-isomers. Based on this observation, we believe structural biases inherent to the fully-elaborated macrocyclic backbone of neopeltolide could lower energetic barriers to promote formation of its native configuration *cis*-**4.14**. Reproducing our computational data and re-evaluation of the oxa-conjugate sequence is critical to advance this study, and would provide additional insight to thermodynamic control in our system.

Unlike our previous substrates, thermodynamic equilibration of the (*3S*)-kinetic mixture did not generate signals consistent with non-productive diene by-product **4.87** (Figure 4.18). However, new signals that resembled *α,β*-unsaturation suggested formation of ester **4.84** from the non-productive pathway was observed. This hypothesis was supported by a new signal (*δ* 5.43 ppm) believed could represent H7. Generation of C7 *β'*-hydroxy enone intermediates (7*R*)- and (7*S*)-**4.83** could be used as authentic standards to better identify new alkene signals during our thermodynamic equilibration sequence. Additionally,

separate evaluation of C7 regio-isomers could potentially reveal an equilibration intermediate that favors non-productive pathways, or other beneficial insights.

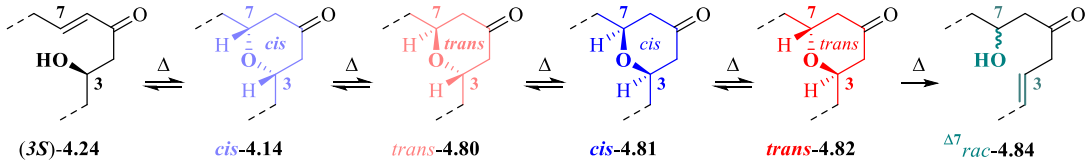

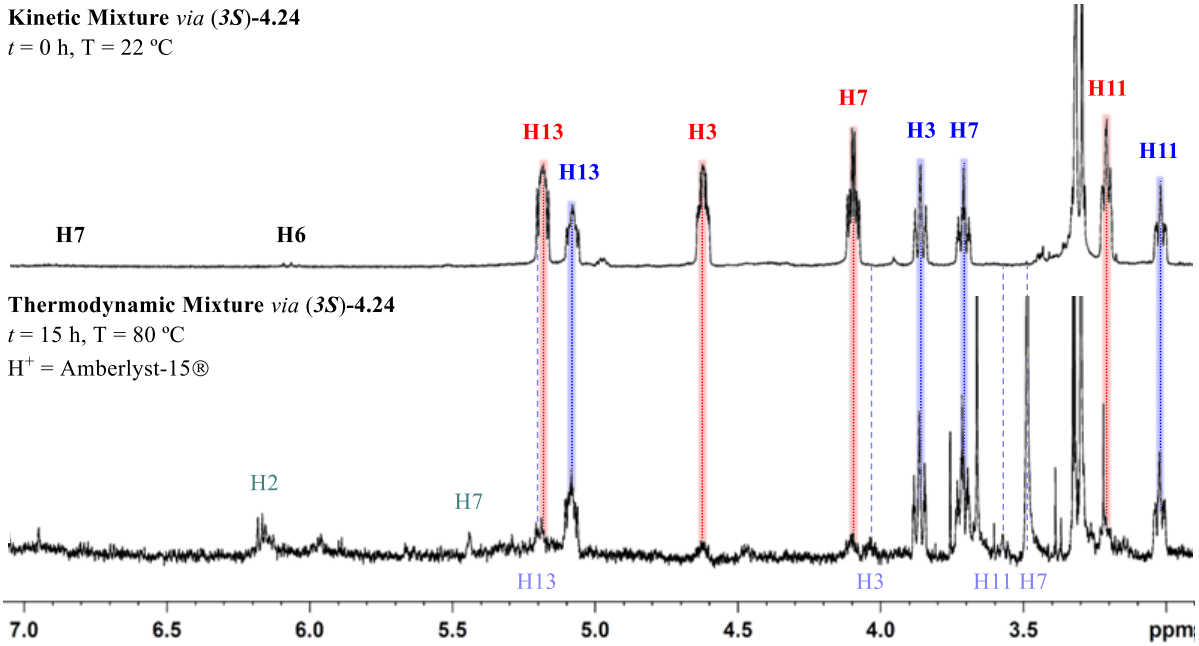

	cis-4.14	*trans*-4.80	***cis*** -4.81	***trans*** -4.82	*Notes*
Kinetic (*3S*)	-	-	1.0	1.8	- thermodynamic equilibration plateaued near 5 h
Thermodynamic					- no elimination signals δ 5.1 – 5.3 ppm
t = 5 h	0.22	-	1.0	0.26	- buried signal δ 7.2 – 7.3 ppm, and those shown above, consistent with non-productive pathway by-products α,β-unsaturated ester **4.84** (~10%)
t = 15 h	0.18	-	1.0	0.15	

Figure 4.18 – Acid-mediated thermodynamic conditions facilitated equilibration of the kinetic mixture obtained *via* oxa-conjugate precursor (***3S*)-4.24**. Generation of energetic minimum ***cis*-4.81** was favored over native *cis*-configuration **4.14** (*d.r.* ~ 5:1), and ***trans*-4.82** (*d.r.* > 5:1). Bolded lines and labels indicate products with 3*S*-configuration.

This work demonstrated that transannular oxa-conjugate addition is an effective strategy for pyran assembly, and is a novel approach toward assembly of the 2,6-*cis*-THP in neopeltolide. Acidic desilylation conditions did not result in any observable cyclization products in homologous systems of aspergillide A–C,[133] apicularen A,[62] or laulimalide.[121] However, spontaneous formation of all pyranyl diastereoisomers under acid-mediated desilylation conditions represented great promise for this strategy within neopeltolide and other 14-membered macrocyclic frameworks. Curtin-Hammett kinetics operated under our desilylation conditions, where *trans*-pyranone products were favored from each C3 diastereomer. Based on modest differences between relative energy profiles (E_{rel}), it was assumed that the activation energies of the oxa-conjugate addition from each ground state conformer were similar ($\Delta G_1^{\ddagger} \sim \Delta G_2^{\ddagger}$ or $\Delta G^0 \sim \Delta\Delta G^{\ddagger}$). If the

additions proceeded with modest transition state barriers, it is possible that the key transannular oxa-conjugate addition may have been in competition with barriers of interconversion. Competitive barriers could slow the interconversion of nucleophilic conformers *via* memory effect (refer to Figure 4.15), and would effectively lock our oxa-conjugate precursors as conformationally-immobile systems. This potential conformational memory effect caveat would directly impact our thermodynamic equilibration process.

Our computational study showed (3*S*,7*S*)-*cis*-**4.81** was favored over native *cis*-configuration by 3.76 kcal/mol, which predicted exclusive formation under thermodynamic equilibration (80 ºC). Our experimental observations indicated that the reversible E1cB elimination/oxa-conjugate addition sequence modestly favored native *cis*-diastereoisomer from the (3*R*)-*β'*-hydroxy nucleophile (*d.r.* = 9:5), and as a minor product with the (3*S*)-epimer. The observed thermodynamic product distributions suggested that they did not reach the thermodynamic minimum under the evaluated conditions. The limited equilibration to the thermodynamic product could be due to macrocyclic stereocontrol imposed by conformational biases, coupled to conformational memory. If barriers existed that limited the necessary conformational interconversion of our oxa-conjugate precursors compared to the nucleophilic addition sequence, the coalescing of products to our desired *cis*-configured pyran may not occur. However, we believe distal stereochemical elements and intrinsic conformational biases of the macrocyclic backbone lower reaction barriers to suppress relative energy differences between *cis*-isomers, similar to Hong's use of Thorpe-Ingold effect.[135] These results suggested stereocontrol of the nucleophilic oxygen is important to diastereoselectivity. Additional work is required to investigate whether optimized reaction conditions can improve diastereoselectivity for *cis*-**4.14**, while minimizing non-productive reaction pathways. Comprehensive assessment of C7 *β'*-hydroxy ketone **4.83** could provide insight into its role in non-productive pathways and subsequent product distribution.

4.7 Conclusions & Future Direction: Advancing from Early Milestones

This chapter highlighted a wealth of information produced to achieve the second milestone of our neopeltolide study. Transannular oxa-conjugate addition has been employed to generate the *cis*-THP from the macrocyclic core of neopeltolide using *β'*-hydroxy nucleophilic attack into an *α,β*-unsaturated ketone system (Figure 4.19). Attack was extremely facile within the 14-membered macrocyclic backbone. Acid-mediated desilylation facilitated spontaneous ring-closure of all four THP diastereoisomers. Experimental and computational data indicated that addition is reversible and can successfully be performed under kinetic control to access *trans*-pyranone products, or thermodynamic control to access the *cis*-pyranones. Unfortunately, we determined that the energetic minimum is not the native configuration from neopeltolide. Interconversion *via* our thermodynamic equilibration pathway was limited to modest-selectivity for desired

cis-**4.14**; however, it was generated as major and minor products from our (*3R*)- and (*3S*)-precursors, respectively. Optimization is required to address selectivity of this transformation. We expect the results will establish economical routes for stereoselective synthesis of 2,6-*cis*-disubstituted tetrahydropyrans in natural products like neopeltolide and other THP-bearing polyketides.

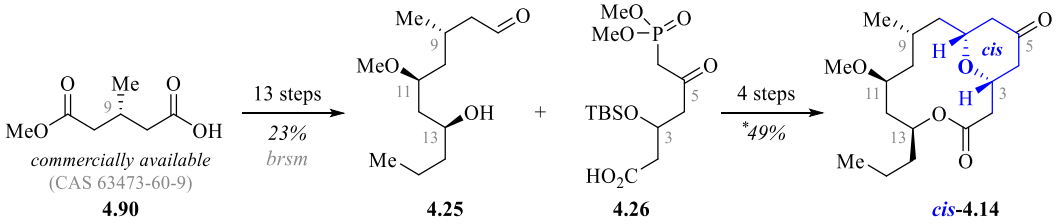

Figure 4.19 – Synthetic summary of my diastereoselective transannular oxa-conjugate addition strategy to accessing the THP of the macrocyclic core of neopeltolide. HWE coupling of enantiopure **4.25** with the racemic **4.26** highlights this route, which required 21 total steps (17 longest linear) in 11.3% overall yield. *Because of an unrecorded yield for the thermodynamic equilibration, the oxa-conjugate sequence was modestly estimated as 75% based on the results from the first-generation model (76-83%).

In **Chapter 2**, synthetic contributions toward accessing the *cis*-THP of neopeltolide were detailed. Unoptimized data from our transannular oxa-conjugate addition strategy compares admirably with these previous accomplishments (Figure 4.20). Including thermodynamic equilibration as a separate step, this work required 17 linear steps to access the macrocyclic core of neopeltolide from commercially-available (*3R*)-methylglutarate **4.90**, which was employed by Panek (18 steps)[20] and Taylor (14 steps).[27] The linear steps of this sequence equals the average from all published syntheses to date, but is dramatically lower when comparing total steps. Although a yield for our thermodynamic equilibration was not determined, the overall efficiency of our synthesis ranks well against published works, and boasts room for optimization. The long-term milestone of a *de novo* PKS pathway in the second-stage of this study could further improve the efficiency of our process.

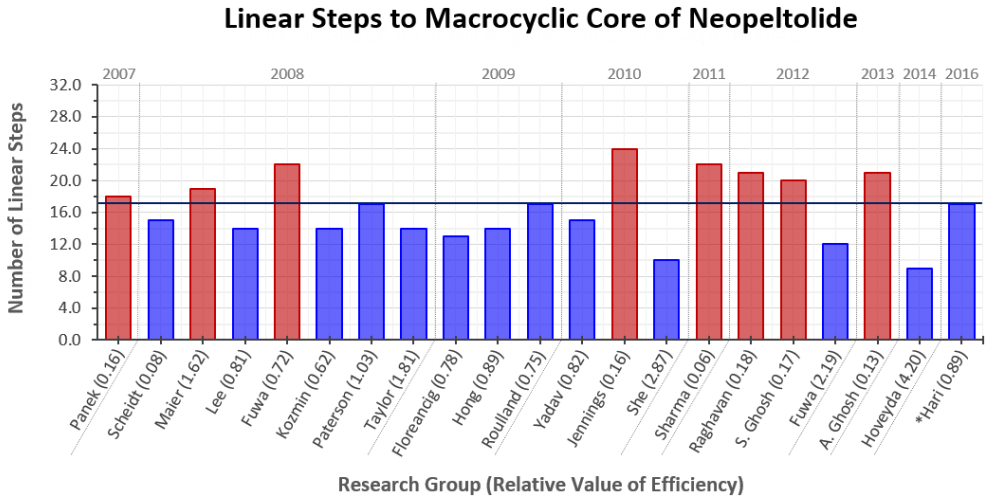

Figure 4.20 – Summary of neopeltolide syntheses to date, where the trendline (**—**) represents the mean number of linear steps (17). Colors indicate routes with longer (**red**) or equal/shorter (**blue**) step-count. Bracketed values are comparative efficiencies based on overall yield as a measure of steps, and normalized to the mean; higher values suggest routes with greater relative efficiency.

Moving forward, re-evaluation of the key transannular oxa-conjugate addition sequence is imperative. Difficulties experienced during HWE olefination depleted significant quantities of aldehyde coupling partner **4.25**, and restricted evaluation to single attempts with each C3-diastereoisomer. Fortunately, the synthetic route has been established and should allow rapid generation of required materials. Preparation of C7-C16 fragment **4.25** should be straightforward and follow the outlined procedures within this chapter. Conversely, because our computational data revealed the native pyranyl configuration of neopeltolide is not the energetic minimum, preparation of enantiopure (*3R*)-**4.26** should benefit our strategy (Figure 4.21). Experimentally, our desired *cis*-**4.14** pyranone was not generated from oxa-conjugate precursor (*3S*)-**4.24** under kinetic conditions, and only modestly by thermodynamic equilibration (*d.r.* = 1:5, **4.14**:**4.81**). However, thermodynamic conditions successfully converted approximately half of our (*3R*)-kinetic mixture into desired *cis*-product (*d.r.* = 9:5, **4.14**:**4.81**). Generation of defined C3 alcohol phosphonate should eliminate potential competition with barriers of interconversion caused by conformational-immobility (conformational memory effect) that may have influenced the experimental results from our first-generation synthesis of neopeltolide. We anticipate that the use of a pre-configured nucleophile, coupled with conformational biases imposed by the neopeltolide core, will facilitate macrocyclic stereocontrol akin to Sharma's activated mercurinium ion system[35] for transannular assembly of the desired *cis*-**4.14** product.

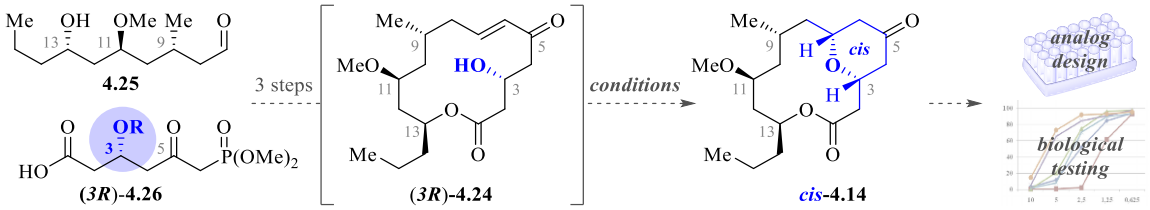

Figure 4.21 – Use of enantiopure phosphonate would allow deeper-investigation of our transannular oxa-conjugate addition strategy, and to optimize reaction conditions. Trisubstituted pyranyl analogues of neopeltolide could be prepared from the diastereoisomeric family of oxa-conjugate pyranone products, and evaluated for biological activity.

Regeneration of precursor material **4.24** would allow a proper evaluation and optimization of our transannular oxa-conjugate addition strategy under kinetic and thermodynamic conditions. Screening alternative reaction conditions should generate sufficient quantities of all four pyranone products to allow clean isolation and characterization. From the distribution of generated pyranone isomers, three are novel compounds. These products could facilitate derivatization into a pyranyl library of neopeltolide analogues, which is a study that has not been addressed previously and could uncover novel substrates with promising activity. Please refer to **Chapter 7** for additional details about these, and other potential future directions for the neopeltolide study.

Neopeltolide has established its place in the synthetic community as an exciting compound with attractive activity and chemical scaffold. This work joined us with 22 international groups that represent an inspiring collection of research and accomplishments. With our neopeltolide study, we hope to contribute to the field of natural product synthesis by opening doors to *in vivo* or *in vitro* chemoenzymatic production of advanced precursors that can be chemically-converted into THP-bearing compounds by oxa-conjugate addition. We believe this strategy can be developed to facilitate rapid, reliable, and sustainable production of bioactive compounds for drug discovery.

4.8 Experimental

4.8.1 General Procedures

All reactions were carried out using oven-dried glassware under an inert atmosphere (nitrogen, or argon gas) with dry solvents under anhydrous conditions, unless otherwise noted. Anhydrous solutions of THF, Et_2O, and CH_2Cl_2 were obtained from an anhydrous solvent delivery system;[136] other solvents were freshly distilled.[137] Yields refer to chromatographically and spectroscopically (^{1}HNMR) homogenous materials, unless otherwise stated. Reagents were commercially purchased at the highest quality and used without further purification, unless otherwise stated. Reactions were monitored by TLC carried out on 0.25 Mm Silicycle silica gel plates (60F-254) using either UV light as a visualizing agent, or an aqueous solution of CAM, *p*-anisaldehyde or iodine$_{(s)}$, and heat as a developing agent. Preparative thin-layer chromatography (PTLC) separations were carried out on 0.25 Mm Silicycle silica gel plates (60F-254). NMR spectra were recorded on Bruker Avance 300 or 400 MHz, Avance II 300 MHz, or Avance III 600 MHz instruments, and calibrated using residual undeuterated solvent ($CDCl_3$: δ H = 7.26 ppm, δ C = 77.0 ppm)[138] as internal references. Data is reported as follows: chemical shift (multiplicity abbreviations: s = singlet, d = doublet, t = triplet, q = quartet, p = pentet, m = multiplet, br = broad), J = coupling constant (Hz), integration, peak assignment. Infrared (IR) spectra were recorded on an ABB Bomen MB Series Arid-Zone™ Infrared Spectrometer. HRMS were recorded by positive ion electrospray on Kratos Analytical Concept 11A mass spectrometer with an electron beam of 70 eV (Ottawa-Carleton Mass Spectrometry Centre).

4.8.2 Experimental Procedures and Physical Data of Compounds

All the experimental procedures are representative, and arranged to reflect the synthetic procedures shown in the schemes.

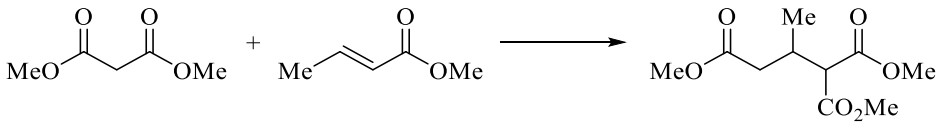

4.28 **4.29** **S-11**

Trimethyl-2-methylpropane-1,1,3-tricarboxylate (S-11). In a modified version of procedure by Lane *et al*,[139] sodium methoxide (5.6 g, 0.10 mol, 0.25 equiv.) was dissolved in THF (580 mL, 0.7 M). Over 10 min, dimethyl malonate **4.28** (50 mL, 0.44 mol, 1.05 equiv.) was added at ambient temperature. To the stirring solution, methyl crotonate **4.29** (44 mL, 0.42 mol, 1.0 equiv.) was added over 10 min, and the reaction mixture was heated at 50 ºC overnight. The reaction was cooled to 0 ºC, and quenched by slow addition of 10% *v*/*v* acetic acid (250 mL). The mixture stirred for 30 min, and was concentrated *in vacuo*. The resulting oil was washed with 0.5 M sodium bicarbonate, and the organics were extracted with ethyl acetate (2 × 75 mL). The combined organic layers were further washed with brine, dried ($MgSO_4$), filtered, and concentrated *in vacuo* to yield a clear, colorless oil (94.4 g, 0.41 mmol, 98%), which was spectroscopically pure enough for use in the next step.

R_f = 0.38 (silica gel, 40% EtOAc in hexanes).

^{1}HNMR (400 MHz, $CDCl_3$): δ 3.70 (s, 3H, -OCH_3), 3.69 (s, 3H, -OCH_3), 3.64 (s, 3H, -OCH_3), 3.41 (d, J = 7.2 Hz, 1H, -C*H*-), 2.76 – 2.65 (m, 1H, -C*H*-), 2.50 (dd, J = 15.9, 5.1 Hz, 1H, -CH*H*-), 2.28 (dd, J = 16.0, 8.4 Hz, 1H, -CH*H*-), 1.02 (d, J = 6.9 Hz, 3H, -CH_3) ppm.

^{13}CNMR (100 MHz, $CDCl_3$): δ 172.5, 168.8, 166.9, 55.9, 52.5, 51.6, 41.1, 38.4, 30.2, 17.5 ppm.

Characterization data for **S-11** proved consistent with previously reported literature data.[139,140]

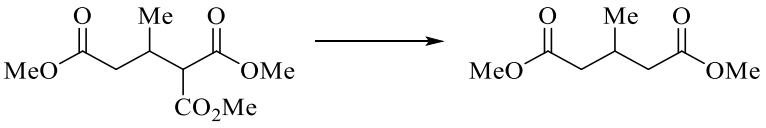

S-11 **S-12**

Dimethyl-3-methylglutarate (S-12). To tricarboxylate **S-11** (7.70 g, 33.0 mmol, 1.0 equiv.), DMSO (36.0 mL), water (1.2 mL), and finely ground NaCl (3.82 g, 66.0 mmol, 2.0 equiv.) was added and stirred in an open system. The reaction refluxed at 210 ºC in a sand bath until completion by TLC (silica gel, 10% EtOAc in hexanes), upon which the mixture was cooled to ambient temperature and poured over a liter of ice water. Extraction with ether and brine (3 × 75 mL), followed by evaporation of the dried ($MgSO_4$) organic extracts yielded 5.23 g (30.0 mmol, 91%) of **S-12** as clear, pale yellow oil.

R_f = 0.25 (silica gel, 10% EtOAc in hexanes).

^{1}HNMR (400 MHz, $CDCl_3$): δ 3.65 (s, 6H, 2 × -OCH_3), 2.55 – 2.33 (m, 3H, -C*H*-, 2 × -CH*H*-), 2.22 (dd, J = 15.1, 7.5 Hz, 2H, 2 × -CH*H*-), 0.99 (d, J = 6.6 Hz, 3H, -CH_3) ppm.

^{13}CNMR (100 MHz, $CDCl_3$): δ 172.8, 51.5, 40.6, 27.4, 19.9 ppm.

Characterization data for **S-12** proved consistent with previously reported literature data.[140–142]

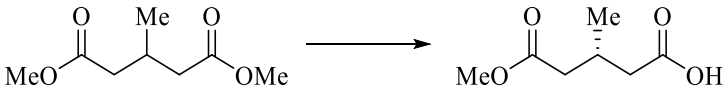

S-12 **4.90**

(*R*)-5-Methoxy-3-methyl-5-oxopentanoic acid (4.90). Meso **S-12** (0.96 mL, 5.83 mmol, 1 equiv.) was dissolved in 0.1 M KPhos buffer (30 mL) plus methanol (10 % *v*/*v*), and cooled to 0 ºC. Esterase from hog liver (PLE, 400 units) was added, and a pH of 7 was maintained for the solution. Hydrolysis proceeded until 1 equivalent (11.6 mL) of base had been consumed, at which point the solution was brought to a pH > 10. The resulting solution was washed with ether (2 × 30 mL) to remove unreacted diester, and the aqueous layer was acidified to pH < 1 with concentrated HCl. Thick emulsions formed during the washing stage, and was run through a long column of sand and cotton. Extraction of the filtrate was performed with ether (3 × 70 mL), and washed with brine (4 × 30 mL) until neutral. The combined organic layers were dried ($MgSO_4$), filtered, and concentrated *in vacuo* to yield 860 mg (5.37 mmol, 94% yield) of **4.90** as clear colorless oil.[140]

R_f = 0.18 (silica gel, 20% EtOac in hexanes).

^{1}HNMR (400 MHz, $CDCl_3$): δ 10.68 (br s, 1H, -CO_2H), 3.66 (s, 3H, -OCH_3), 2.51 – 2.21 (m, 5H, -C*H*-, 2 × -CH_2-), 1.04 (d, J = 6.6 Hz, 3H, -CH_3) ppm.

^{13}CNMR (100 MHz, $CDCl_3$): δ 178.3, 172.8, 51.6, 40.5, 40.4, 27.2, 19.9 ppm.

Characterization data for **4.89** proved consistent with previously reported literature data.[142,143]

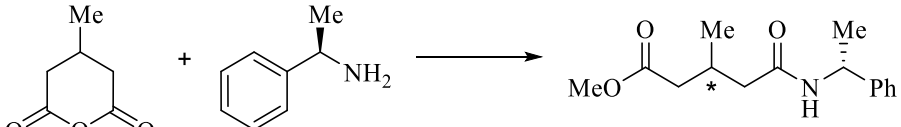

S-13 **S-14** ***syn*** **S-15** ***anti*** **S-16**

(*R*/*S*)-Methyl 3-methyl-5-oxo-5-((*R*)-1-phenylethylamino)pentanoate (S-15/S-16). In accordance with Hoye and Koltun,[65] anhydride **S-13** (101.2 mg, 0.79 mmol, 1.0 equiv.), **S-14** (101 µL, 0.79 mmol, 1.0 equiv.), and DMAP (100 mg, 0.82 mmol, 1.03 equiv.) were dissolved in 2 mL of anhydrous CH_2Cl_2. The mixture stirred for 1 h under inert atmosphere. At this point, DCC (163 mg, 0.79 mmol, 1.0 equiv.) was added as one portion, followed by the addition of 1 mL of dry MeOH. The reaction mixture stirred overnight, and was filtered through a plug of silica. The solution was washed with 5% HCl (2 × 2 mL) and saturated $NaHCO_3$ (2 mL), dried over $MgSO_4$ and concentrated to yield compounds *syn* **S-15** and *anti* **S-16** as a mixture with a 2:1 ratio. The crude material was used for spectroscopic analysis, and was not purified.

^{1}HNMR (300 MHz, $CDCl_3$): δ 7.32 – 7.17 (m, 5H, 5 × -C*H*- Ph), 6.18 (br s, 1H, -N*H*), 5.08 (p, *J* = 7.2 Hz, 1H, -C*H*-), 3.62 (s, 3H, -OCH_3; *anti*), 3.60 (s, 3H, -OCH_3; *syn*), 2.48 – 1.99 (m, 5H, 2 × -CH_2-; -C*H*-), 1.43 (d, *J* = 7.0 Hz, 3H, -CH_3), 0.97 (d, *J* = 6.6 Hz, 3H, -CH_3; *syn*), 0.95 (d, *J* = 6.6 Hz, 3H, -CH_3; *anti*) ppm.

^{13}CNMR (75 MHz, $CDCl_3$): δ 173.1, 170.7, 143.3 (*syn*), 143.2, 128.6, 127.2, 126.1, 126.0 (*syn*), 51.40, 51.39 (*syn*), 48.6 (*syn*), 48.5, 43.0, 42.9 (*syn*), 40.3, 40.2 (*syn*), 28.6, 28.1 (*syn*), 21.8, 21.7 (*syn*), 19.8, 19.7 (*syn*) ppm.

Characterization data for **S-15** and **S-16** proved consistent with previously reported literature data.[65]

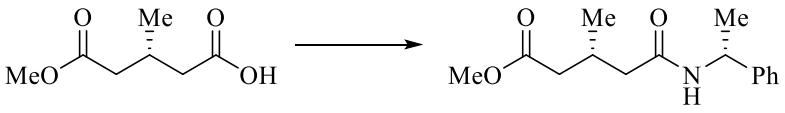

4.90 ***syn* S-15**

***syn*-(*R*)-Methyl 3-methyl-5-oxo-5-((*R*)-1-phenylethylamino)pentanoate (S-15).** Acid **4.90** (20.5 mg, 0.13 mmol, 1.0 equiv.), DCC (26.4 mg, 0.13 mmol, 1.0 equiv.), and DMAP (1.6 mg, 0.01 mmol, 0.1 equiv.) were dissolved in 0.4 mL of anhydrous CH_2Cl_2. The mixture formed a thick white precipitate. After the mixture stirred for 5 min, (*R*)-*α*-methylbenzylamine **S-14** (15.9 µL, 0.13 mmol, 1.0 equiv.) was added neat. The reaction mixture stirred for 2 h, and was filtered through a plug of silica. The solution was dried ($MgSO_4$), filtered, and concentrated to yield **S-15** as crude material. Spectral comparisons of crude **S-15** against the diastereomeric mixture of **S-15**/**S-16** supported high enantioselectivity (*ee* > 95%) from the enzymatic desymmetrization process.

^{1}HNMR (400 MHz, $CDCl_3$): δ 7.36 – 7.26 (m, 5H, 5 × -C*H*- Ph), 5.87 (br s, 1H, -N*H*), 5.12 (p, *J* = 7.3 Hz, 1H, -C*H*-), 3.64 (s, 3H, -OCH_3; *syn*), 3.61 (s, "0.09H," –OCH_3; *anti*), 2.47 – 2.18 (m, 4H, 2 × -CH_2-), 2.08 (dd, *J* = 7.0, 13.9 Hz, 1H, -C*H*-), 1.47 (d, *J* = 7.0 Hz, 3H, -CH_3), 1.00 (d, *J* = 6.9 Hz, 3H, -CH_3; *syn*) ppm.

^{13}CNMR (100 MHz, $CDCl_3$): δ 173.1, 170.6, 143.3, 128.7, 128.5, 127.3, 126.8, 126.1, 125.7, 51.5, 48.7, 43.1, 40.2, 28.3, 21.8, 19.9 ppm.

Characterization data for **S-15** proved consistent with previously reported literature data.[65,142]

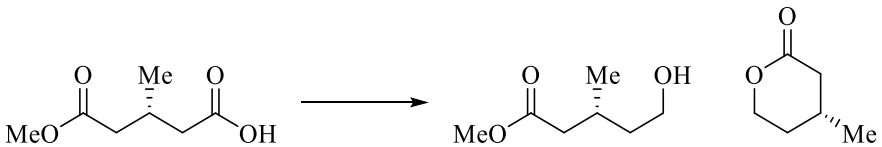

4.89 **S-17** **S-18**

To a stirring flask charged with dried acid **4.90** (1.0 g, 6.24 mmol, 1 equiv.), was added dry THF (25 mL) and stirred under inert atmosphere at -78 °C. Once cooled, $BH_3{\cdot}Me_2S$ (0.5 mL, 12.48 mmol, 2 equiv.) was added dropwise *via* syringe, and the mixture was then allowed to warm to room temperature. The reaction mixture was monitored for progression by ^{1}HNMR (methyl doublet; δ 1.04 – 0.93), and upon complete conversion of **4.90**, was quenched by carefully adding 0.5 mL of alcohol (H_2O or methanol), and evaporated

to dryness. The crude material was dried ($MgSO_4$), filtered, and concentrated *in vacuo* to yield 721.0 mg (5.00 mmol, 84%) as a mixture (**S-17**:**S-18** > 20:1) of clear, colorless oil. The crude material was telescoped directly into subsequent silyl protection.

(3*R*)-5-Hydroxy-3-methylpentanoic acid methyl ester (S-17)

R_f = 0.36 (silica gel, 20% EtOAc in hexanes).

^{1}HNMR (400 MHz, $CDCl_3$): δ 3.84 – 3.74 (m, 2H, -C*H*$_2$-), 3.63 (s, 3H, -OC*H*$_3$), 2.39 – 2.04 (m, 3H, -C*H*- & -C*H*$_2$-), 1.61 – 1.35 (m, 2H, -C*H*$_2$-), 0.93 (d, *J* = 6.5 Hz, 3H, -C*H*$_3$) ppm.

^{13}CNMR (100 MHz, $CDCl_3$): δ 173.5, 61.1, 51.3, 41.5, 38.0, 27.3, 19.7 ppm.

(3*R*)-3-Methyltetrahydro-2*H*-pyranone (S-18)

^{1}HNMR (400 MHz, $CDCl_3$): δ 4.40 (ddd, *J* = 11.3, 5.0, 4.0 Hz, 1H, -CH*H*-), 4.25 (ddd, *J* = 11.5, 10.7, 4.0 Hz, 1H, -CH*H*-), 2.66 (dd, *J* = 11.6, 1.7 Hz, 1H, -CH*H*-), 2.10 – 2.04 (m, 2H, -C*H*$_2$-), 1.90 (ddq, *J* = 14.0, 4.0, 1.5 Hz, 1H, -CH*H*-), 1.55 – 1.45 (m, 1H, -C*H*-), 1.05 (d, *J* = 6.3 Hz, 3H, -C*H*$_3$) ppm.

Characterization data for **S-17** and **S-18** proved consistent with previously reported literature data.[27,140,144,145]

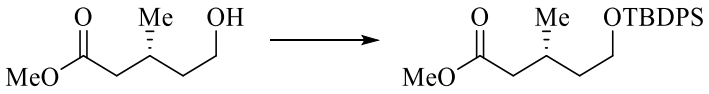

S-17 **S-19**

(3*R*)-Methyl-5-(*tert*-butyldiphenylsilyloxy)-3-methylpentanoate (S-19). Freshly-obtained alcohol **S-17** (2.96 g, 20.5 mmol, 1 equiv.) was diluted in anhydrous DMF (27 mL, 0.8 M), and TBDPSCl (6.33 mL, 26.7 mmol, 1.3 equiv.) was added under inert atmosphere. To this solution, imidazole (4.19 g, 61.5 mmol, 3.0 equiv.) was added and left to stir overnight at ambient temperature. The reaction mixture was diluted in EtOAc (50 mL) and washed with saturated ammonium chloride. The organic layers were then washed with brine, dried ($MgSO_4$), filtered, and concentrated *in vacuo*. Purification *via* flash chromatography (2% EtOAc in hexanes) separated unreacted ester, lactone **S-18** and silanol by-products from the desired product, and yielded 7.81 g (20.3 mmol, quant.; 84% yield over 2 steps) of **S-19** as clear, colorless oil.

R_f = 0.37 (silica gel, 10% EtOAc in hexanes).

^{1}HNMR (400 MHz, $CDCl_3$): δ 7.64 (dd, *J* = 1.6, 7.8 Hz, 4H, 4 × -C*H*- Ph), 7.42 – 7.32 (m, 6H, 6 × -C*H*- Ph), 3.67 (t, *J* = 6.4 Hz, 2H, -C*H*$_2$-), 3.63 (s, 3H, -OC*H*$_3$), 2.31 (dd, *J* = 13.9, 5.0 Hz, 1H, -CH*H*-), 2.20 – 2.05 (m, 2H, -C*H*- & -CH*H*-), 1.63 – 1.39 (m, 2H, -C*H*$_2$-), 1.02 (s, 9H, O-TBDPS *t*-Bu), 0.89 (d, *J* = 6.4 Hz, 3H, -C*H*$_3$) ppm.

^{13}CNMR (100 MHz, $CDCl_3$): δ 173.7, 135.7, 134.1, 129.8, 127.7, 62.1, 51.4, 41.6, 39.3, 27.6, 26.7, 19.8, 19.1 ppm.

HRMS (EI) *m/z*: calculated for $C_{19}H_{23}O_3Si$ [M – *t*-Bu] 327.1417, observed 327.1424 (Δ = 0.7 mmu).

IR (thin film) ν_{max}: 3074, 2930, 1736, 1474, 1216, 1109 cm^{-1}.

$[\alpha]_D^{20}$ = + 3.4° (*c* = 0.021, $CHCl_3$; *l* = 10 mm; α = + 0.0071°).

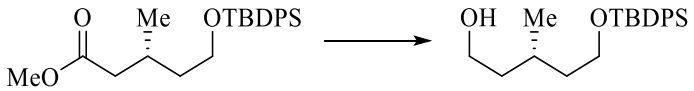

S-19 **S-20**

(3*S*)-5-(*tert*-Butyldiphenylsilyloxy)-3-methylpentan-1-ol (S-20). Under inert atmosphere, **S-19** (3.90 g, 10.1 mmol, 1.0 equiv.) was diluted in anhydrous diethyl ether to yield an overall concentration of 0.1 M, and placed into an ice bath with vigorous stirring. $LiAlH_4$ (268.3 mg, 7.1 mmol, 0.7 equiv.) was added in portions, and stirred for 5 h while monitored by TLC (silica gel, 20% EtOAc in hexanes). Upon completion, the reaction was quenched using modified Fieser conditions[146,147] with 40 µL distilled water per mmol $LiAlH_4$, and stirred for 10 min. To precipitate the aluminum salt, 40 µL of 15% *w*/*w* NaOH per mmol $LiAlH_4$ was added, followed by a second aliquot of distilled water. The resulting mixture was extracted with Et_2O, and washed with saturated ammonium chloride (1 × 30 mL) and brine (2 × 30 mL). Organic layers were dried ($MgSO_4$), filtered, and concentrated *in vacuo*. The crude residue was purified by flash chromatography (10% EtOAc in hexanes), and yielded 3.48 (9.77 mmol, 97% yield) of **S-20** as clear, colorless oil.

R_f = 0.22 (silica gel, 20% EtOAc in hexanes).

^{1}HNMR (400 MHz, $CDCl_3$): *δ* 7.70 – 7.64 (m, 4H, 4 × -C*H*- Ph), 7.45 – 7.33 (m, 6H, 6 × -C*H*- Ph), 3.78 – 3.57 (m, 4H, 2 × -CH_2-), 1.82 – 1.68 (m, 1H, -C*H*-), 1.61 – 1.55 (m, 2H, -CH_2-), 1.47 – 1.29 (m, 2H, -CH_2-), 1.05 (s, 9H, O-TBDPS *t*-Bu), 0.86 (d, *J* = 6.7 Hz, 3H, -CH_3) ppm.

^{13}CNMR (100 MHz, $CDCl_3$): *δ* 135.6, 134.0, 129.6, 127.6, 62.1, 61.1, 39.9, 39.6, 26.9, 26.4, 19.8, 19.2 ppm.

$[\alpha]_D^{20}$ = + 3.1° (*c* = 0.094, $CHCl_3$; *l* = 10 mm; α = + 0.0288°).

Characterization data for **S-20** proved consistent with previously reported literature data.[148,149]

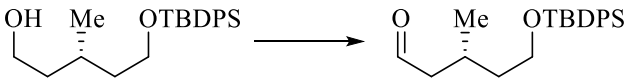

S-20 **4.30**

(3*R*)-5-(*tert*-Butyldiphenylsilyloxy)-3-methylpentanal (4.30). To a round-bottom flask charged with **S-21** (2.45 g, 6.9 mmol, 1.0 equiv.) dissolved in CH_2Cl_2 (70.0 mL), was added a mixture of PCC (1.94 g, 9.0 mmol, 1.3 equiv.) and silica gel (3.88 g). The reaction was stirred under inert atmosphere for 5 h at ambient temperature, and monitored by TLC (silica gel, 10% EtOAc in hexanes). Upon completion, CH_2Cl_2 was carefully evaporated, to yield a dark brown powder. To a pre-equilibrated column (silica gel, 10% EtOAc in hexanes), purification yielded 2.12 g (6.0 mmol, 87%) of **4.30** as clear, colorless oil.

R_f = 0.29 (silica gel, 10% EtOAc in hexanes).

^{1}HNMR (400 MHz, $CDCl_3$): δ 9.70 (t, *J* = 2.2 Hz, 1H, -C*H*O), 7.67 – 7.61 (m, 4H, 4 × -C*H*- Ph), 7.44 - 7.33 (m, 6H, 6 × -C*H*- Ph), 3.68 (t, *J* = 6.3 Hz, 2H, -CH_2-), 2.41 – 2.14 (m, 3H, -C*H*-, -CH_2-), 1.62 – 1.42 (m, 2H, -CH_2-), 1.03 (s, 9H, O-TBDPS *t*-Bu), 0.91 (d, *J* = 6.5 Hz, 3H, -CH_3) ppm.

^{13}CNMR (75 MHz, $CDCl_3$): δ 202.9, 135.5, 133.8, 129.6, 127.6, 61.5, 50.8, 39.2, 20.0, 19.2 ppm.

HRMS (EI) *m/z*: calculated for $C_{18}H_{21}O_2Si$ [M – *t*-Bu] 297.1311, observed 297.1329 (Δ = 1.8 mmu).

IR (thin film) ν_{max}: 3070, 2960, 2858, 2705, 1724, 1111 cm^{-1}.

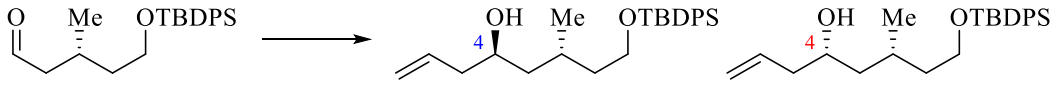

4.30 **4.35** **$^{\Delta 4}$*epi*-4.35**

Two flame-dried reaction flasks were prepared in accordance with Brown's procedure for asymmetric allylation.[74] In the first, **4.30** (1.41 g, 3.98 mmol, 1.0 equiv.) was dissolved in anhydrous ether (6 mL) and cooled to -100 ºC under inert atmosphere. In the second flask, (+)-Ipc_2BAllyl (5 mL, 1.0 M in pentanes) was transferred *via* a dry glass syringe from its ampule to the flask, and cooled to -100 ºC while stirring. The first flask was cannulated into the second, with anhydrous ether (4 mL) rinse. The reaction mixture warmed to -78 ºC, and monitored by TLC (silica gel, 10% EtOAc in hexanes). Upon completion, the reaction was quenched with MeOH and stirred for 20 min. Addition of 15% NaOH (2 mL) induced a pale-yellow color from the clear mixture, and was stirred for an additional 10 min. Addition of 30% aqueous H_2O_2 (4 mL) induced an opaque white solution and exothermed. The reaction mixture was refluxed for 1 h, upon which the mixture was diluted in ether (40 mL) and washed with brine (3 × 50 mL). The organic layer was dried ($MgSO_4$), filtered, and concentrated *in vacuo*. Purification *via* flash chromatography (0-10% gradient of EtOAc in hexanes) yielded 1.37 g (3.45 mmol, 86%, *d.r.* = 13:2) of **4.35**, and **$^{\Delta 4}$*epi*-4.35** as clear, colorless oils.

(4*R*,6*R*)-8-(*tert*-Butyldiphenylsilyloxy)-6-methyloct-1-en-4-ol (4.35)

R_f = 0.23 (silica gel, 10% EtOAc in hexanes).

^{1}HNMR (400 MHz, $CDCl_3$): δ 7.66 – 7.64 (m, 4H, 4 × -C*H*- Ph), 7.43 – 7.34 (m, 6H, 6 × -C*H*- Ph), 5.85 – 5.75 (m, 1H, -C*H*=), 5.12 – 5.07 (m, 2H, =CH_2), 3.73 – 3.64 (m, 3H, -C*H*, -CH_2-), 2.27 – 2.20 (m, 1H, -CH*H*-), 2.14 – 2.07 (m, 1H, -CH*H*-), 1.81 (m, 1H, -C*H* -), 1.64 – 1.54 (m, 2H, -CH*H*-), 1.47 – 1.32 (m, 2H, 2 × -CH*H*-), 1.18 (ddd, *J* = 13.8, 9.2, 3.8 Hz, 1H, -CH*H*-), 1.02 (s, 9H, O-TBDPS *t*-Bu), 0.85 (d, *J* = 6.8 Hz, 3H, -CH_3) ppm.

^{13}CNMR (100 MHz, $CDCl_3$): δ 135.6, 134.9, 134.1, 129.5, 127.6, 118.0, 68.4, 62.1, 44.3, 42.6, 40.2, 26.9, 26.2, 19.5, 19.2 ppm.

HRMS (EI) *m/z*: calculated for $C_{21}H_{27}O_2Si$ [M – *t*-Bu] 339.1780, observed 339.1797 (Δ = 1.7 mmu).

IR (thin film) ν_{max}: 3409, 3071, 2922, 2857, 1641, 1472, 1106, 1087, 1028 cm^{-1}.

$[\alpha]_D^{20}$ = + 1.8° (*c* = 0.037, $CHCl_3$; *l* = 10 mm; α = + 0.0067°).

(4*S*,6*R*)-8-(*tert*-Butyldiphenylsilyloxy)-6-methyloct-1-en-4-ol ($^{\Delta 4}$*epi*-4.35)

R_f = 0.20 (silica gel, 10% EtOAc in hexanes).

^{1}HNMR (400 MHz, $CDCl_3$): δ 7.65 (dd, *J* = 7.7, 1.7 Hz, 4H, 4 × -C*H*- Ph), 7.44 – 7.33 (m, 6H, 6 × -C*H*- Ph), 5.87 – 5.74 (m, 1H, -C*H*=), 5.14 – 5.07 (m, 2H, =CH_2), 3.75 – 3.62 (m, 3H, -CH_2- & -C*H*-), 2.25- 2.17 (m, 1H, -CH*H*-), 2.13 – 2.03 (m, 1H, -CH*H*-), 1.88 – 1.74 (m, 2H, 2 × -CH*H*-), 1.70 – 1.59 (m, 1H, -CH*H*-), 1.38 – 1.29 (m, 1H, -CH*H*-), 1.03 (s, 9H, O-TBDPS *t*-Bu), 0.86 (d, *J* = 6.6 Hz, 3H, -CH_3) ppm.

$[\alpha]_D^{20}$ = + 8.7° (*c* = 0.034, $CHCl_3$; *l* = 10 mm; α = + 0.0299°).

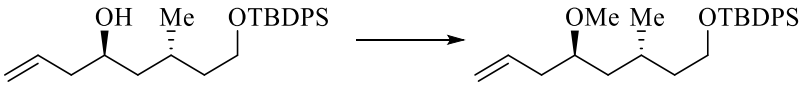

4.35 **S-21**

***tert*-Butyl-((3*R*,5*R*)-5-methoxy-3-methyloct-7-enyloxy)diphenylsilane (S-21).** NaH (220 mg, 5.5 mmol, 2.2 equiv.) was dissolved in anhydrous THF (5.0 mL), and cooled to 0 °C. Dropwise, a solution of **4.35** (1.0 g, 2.52 mmol, 1.0 equiv.) in THF was added. Iodomethane (215 µL, 3.5 mmol, 1.4 equiv.) was added to the solution, and the reaction mixture stirred overnight and left to warm to ambient temperature. Upon completion (silica gel, 10% EtOAc in hexanes), the reaction was cooled to 0 °C, and diluted with 5 mL of H_2O. The aqueous layer was extracted with EtOAc (2 × 10 mL). The combined organic layers were washed with brine (3 × 10 mL), dried ($MgSO_4$), filtered, and concentrated *in vacuo*. Purification through a plug of silica (60% EtOAc in hexanes) yielded 1.01 g (2.45 mmol, 98%) of **S-21** as clear, colorless oil.

R_f = 0.51 (silica gel, 10% EtOAc in hexanes).

^{1}HNMR (400 MHz, $CDCl_3$): δ 7.65 (dd, *J* = 7.8, 1.5 Hz, 4H, -C*H*- Ph), 7.42 – 7.33 (m, 6H, -C*H*- Ph), 5.77 (ddt, *J* = 7.0, 7.0, 10.2 Hz, 1H, -C*H*-), 5.07 – 5.01 (m, 2H, -CH_2-), 3.72 – 3.62 (m, 2H, -CH_2-), 3.30 (s, 3H, -OCH_3), 3.29 – 3.22 (m, 1H, -C*H*-), 2.29 – 2.16 (m, 2H, -CH_2-), 1.82 – 1.71 (m, 1H, -C*H*-), 1.63 – 1.55 (m, 1H, -C*H*-), 1.46 (ddd, *J* = 14.0, 8.6, 5.2 Hz, 1H, -C*H*-), 1.40 – 1.30 (m, 2H, -CH_2-), 1.15 (ddd, *J* = 14.1, 8.8, 4.4 Hz, 2H, -CH_2-), 1.02 (s, 9H, O-TBDPS *t*-Bu), 0.82 (d, *J* = 6.7 Hz, 3H, -CH_3) ppm.

^{13}CNMR (100 MHz, $CDCl_3$): δ 135.6, 134.9, 134.1, 129.5, 127.6, 116.9, 78.3, 62.1, 56.4, 41.6, 40.2, 38.1, 26.9, 26.2, 19.7, 19.2 ppm.

HRMS (EI) *m/z*: calculated for $C_{22}H_{29}O_2Si$ [M – *t*-Bu] 353.1937, observed 353.1927 (Δ = 1.0 mmu).

IR (thin film) ν_{max}: 2953, 2856, 1640, 1456, 1371, 1110, 1087 cm^{-1}.

$[\alpha]_D^{20}$ = – 4.0° (*c* = 0.037, $CHCl_3$; *l* = 10 mm; α = – 0.0148°).

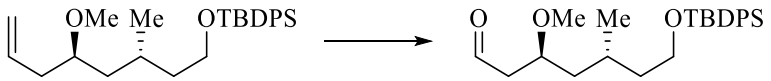

S-21 **4.36**

(3*S*,5*R*)-7-(*tert*-butyldiphenylsilyloxy)-3-methoxy-5-methylheptanal (4.36). Purified **S-21** (0.200 g, 0.487 mmol, 1.0 equiv.) was dissolved in an equal mixture of *t*-BuOH and water (7 mL). To this was added potassium carbonate (0.202 g, 1.461 mmol, 3.0 equiv.) potassium ferricyanide (0.481 g, 1.461 mmol, 3.0 equiv.), and a solution of potassium osmate (VI) dihydrate (18 mg, 0.049 mmol, 0.1 equiv.) in 15% NaOH (0.2 mL). The reaction mixture stirred overnight under inert atmosphere and temperature, and was monitored by TLC (10% EtOAc in hexanes). Upon completion, the mixture was diluted in water, and extracted with EtOAc (3 × 10 mL). Combined organics were washed with brine (3 × 30 mL), and dried ($MgSO_4$), filtered, and concentrated *in vacuo*. The crude product was diluted in anhydrous CH_2Cl_2 (2 mL), and lead tetraacetate (0.260 g, 0.584 mmol, 1.2 equiv.) was added at ambient temperature. The reaction stirred for 1 h, and was concentrated to remove 75% of the CH_2Cl_2. The resulting brown paste was loaded directly on a pre-equilibrated column (2% EtOAc in hexanes), and yielded **4.36** in 189.2 mg (0.459 mmol, 94%, 2 steps) as a clear, colorless oil.

$\mathbf{R_f}$ = 0.31 (silica gel, 10% EtOAc in hexanes).

^{1}HNMR (400 MHz, $CDCl_3$): δ 9.78 (dd, *J* = 2.0, 2.5 Hz, 1H, -C*H*O), 7.64 (dd, *J* = 1.6, 7.9 Hz, 4H, 4 × -C*H*- Ph), 7.43 – 7.33 (m, 6H, 6 × -C*H*- Ph), 3.78 – 3.62 (m, 3H, -C*H*- & -CH_2-), 3.30 (s, 3H, -OCH_3), 2.57 (ddd, *J* = 2.6, 6.6, 16.2 Hz, 1H, -CH*H*-), 2.49 (ddd, *J* = 2.0, 5.2, 16.2 Hz, 1H, -CH*H*-), 1.84 – 1.73 (m, 1H, -C*H*-), 1.64 – 1.55 (m, 2H, -CH_2-), 1.40 – 1.31 (m, 1H, -CH*H*-), 1.18 (ddd, *J* = 5.0, 8.4, 13.8 Hz, 1H, -CH*H*-), 1.02 (s, 9H, O-TBDPS *t*-Bu), 0.86 (d, *J* = 6.6 Hz, 3H, -CH_3) ppm.

^{13}CNMR (100 MHz, $CDCl_3$): δ 201.6, 135.6, 134.0, 129.6, 127.6, 74.4, 61.9, 56.8, 48.3, 42.1, 39.9, 26.9, 26.1, 19.7, 19.2 ppm.

HRMS (EI) *m/z*: calculated for $C_{20}H_{23}O_2Si$ [M – (*t*-Bu + MeOH)] 323.1467, observed 323.1491 (Δ = 2.4 mmu).

IR (thin film) ν_{max}: 3071, 2961, 1725, 1110, 1087 cm^{-1}.

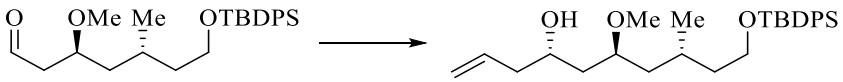

4.36 **4.37**

(4*S*,6*S*,8*R*)-10-(*tert*-butyldiphenylsilyloxy)-6-methoxy-8-methyldec-1-en-4-ol (4.37). Two flame-dried reaction flasks were prepared in accordance with Brown's procedure for asymmetric allylation.[74] In the first, **4.36** (1.8 g, 4.36 mmol, 1.0 equiv.) was dissolved in anhydrous ether (6 mL) and cooled to -100 ºC under inert atmosphere. In the second flask, (–)-Ipc_2BAllyl (5 mL, 1.0 M in pentanes) was transferred *via*

a dry glass syringe from its ampule to the flask, and cooled to -100 ºC while stirring. The first flask was cannulated into the second, with anhydrous ether (4 mL) rinse. The reaction mixture warmed to -78 ºC, and monitored by TLC (silica gel, 10% EtOAc in hexanes). Upon completion, the reaction was quenched with MeOH and stirred for 20 min. Addition of 15% NaOH (2 mL) induced a pale-yellow color from the clear mixture, and was stirred for an additional 10 min. Addition of 30% aqueous H_2O_2 (4 mL) induced an opaque white solution and exothermed. The reaction mixture was refluxed for 1 h, upon which the mixture was diluted in ether (40 mL) and washed with brine (3 × 50 mL). The organic layer was dried ($MgSO_4$), filtered, and concentrated *in vacuo*. Purification *via* flash chromatography (gradient 5 - 20% EtOAc in hexanes) yielded 1.45 g (3.2 mmol, 73%, d.r. = 14:1) of **4.37** as clear, colorless oil.

R_f = 0.51 (silica gel, 20% EtOAc in hexanes).

^{1}HNMR (400 MHz, $CDCl_3$): δ 7.65 (dd, *J* = 7.8, 1.6 Hz, 4H, 4 × -C*H*- Ph), 7.45 – 7.32 (m, 6H, 6 × -C*H*- Ph), 5.81 (ddt, *J* = 17.3, 10.3, 7.1 Hz, 1H, =C*H*-), 5.11 – 5.06 (m, 2H, =CH_2), 12.8 6.3 2.8 3.92 (ddd, *J* = 12.8, 6.3, 2.8 Hz, 1H, -C*H*-), 3.75 – 3.60 (m, 2H, -CH_2-), 3.56 – 3.50 (m, 1H, -C*H*-), 3.33 (s, 3H, -OCH_3), 2.97 (d, *J* = 2.7 Hz, 1H, -O*H*), 2.27 – 2.12 (m, 2H, -CH_2-), 1.82 – 1.54 (m, 4H, 4 × -CH*H*-), 1.50 (ddd, *J* = 14.7, 6.3, 2.5 Hz, 1H, -CH*H*-), 1.34 (ddd, *J* = 13.8, 8.1, 6.2 Hz, 1H, -CH*H*-), 1.16 (ddd, *J* = 12.3, 9.0, 5.0 Hz, 1H, -CH*H*-), 1.03 (s, 9H, O-TBDPS *t*-Bu), 0.85 (d, *J* = 6.6 Hz, 3H, -CH_3) ppm.

^{13}CNMR (100 MHz, $CDCl_3$): δ 135.6, 135.0, 134.05, 134.03, 129.5, 127.6, 117.5, 77.5, 68.0, 61.9, 56.8, 42.3, 41.2, 39.8, 39.0, 26.9, 26.3, 20.0, 19.2 ppm.

HRMS (ESI+ TOF) *m/z*: calculated for $C_{28}H_{42}O_3SiNa$ [(M + Na)$^+$] 477.2801, observed 477.2823 (Δ = 2.2 mmu).

IR (thin film) ν_{max}: 3446, 3071, 2926, 1640, 1427, 1187, 1105, 1085 cm^{-1}.

$[\alpha]_D^{20}$ = + 10.3º (*c* = 9.9 mg/2.5 mL $CHCl_3$; *l* = 100 mm; α = + 0.0407º).

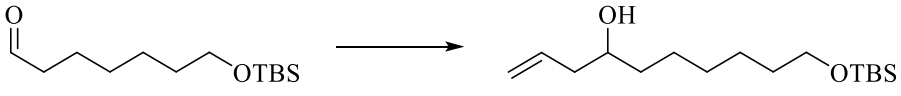

4.38 **S-22**

10-(*tert*-Butyldimethylsilyloxy)dec-1-en-4-ol (S-22). Aldehyde **4.38**[150] (0.5 g, 2.05 mmol, 1.0 equiv.) was dissolved in anhydrous Et_2O (7 mL), and cooled to -78 ºC. Allylmagnesium bromide (840 µL, 4.90 mmol, 2.4 equiv.) was added dropwise under inert atmosphere, and the reaction was left to stir at ambient temperature. Upon completion (silica gel, 10% EtOAc in hexanes), the mixture was quenched with NH_4Cl, diluted in Et_2O (15 mL), and washed with brine (3 × 20 mL). The combined organic layers were dried ($MgSO_4$), filtered, and concentrated *in vacuo*. The crude product was purified *via* flash chromatrography (5 – 10% EtOAc in hexanes), and yielded 504 mg (1.76 mmol, 86%) of **S-22** as clear, pale yellow oil.

R_f = 0.32 (silica gel, 10% EtOAc in hexanes; CAM stain).

^{1}HNMR (300 MHz, $CDCl_3$): δ 5.81 (dddd, J = 17.6, 9.6, 7.9, 6.5 Hz), 5.15 – 5.09 (m, 2H, =CH_2), 3.66 – 3.58 (m, 1H, -C*H*-), 3.58 (t, J = 6.5 Hz, 2H, -CH_2-), 2.28 (dddt, J = 13.4, 6.5, 4.2, 1.3 Hz, 1H, -CH*H*-), 2.11 (dtt, J = 14.0, 7.9, 1.1 Hz, 1H, -CH*H*-), 1.55 – 1.41 (m, 6H, 3 × -CH_2-), 1.36 – 1.27 (m, 6H, 3 × -CH_2-), 0.87 (s, 9H, O-TBS *t*-Bu), 0.03 (s, 6H, 2 × O-TBS -CH_3) ppm.

^{13}CNMR (75 MHz, $CDCl_3$): δ 134.9, 118.1, 70.6, 63.2, 41.9, 36.7, 32.8, 29.4, 25.9, 25.7, 25.6, 18.3, -5.3 ppm.

Characterization data for **S-22** proved consistent with previously reported literature data.[151]

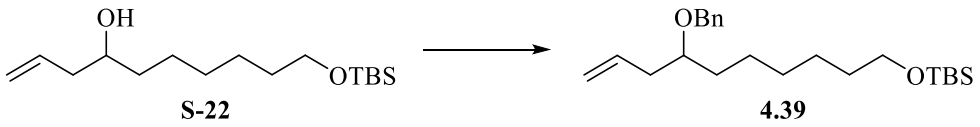

S-22 **4.39**

((7-Benzyloxy)dec-9-en-1-yl)oxy)-*tert*-butyldimethylsilane (4.39). Homoallylic alcohol **S-22** (150 mg, 0.53 mmol, 1.0 equiv.) was dissolved in a 2:1 mixture of DMF and THF (3 mL, 0.3 M) under inert atmosphere. TBAI (20 mg, 0.5 mmol, 10 mol %), 60% dispersion NaH (64 mg, 1.6 mmol, 3.0 equiv.), and freshly distilled BnBr (97 μL, 0.79 mmol, 1.5 equiv.) were added, and the reaction mixture stirred overnight at ambient temperature. Upon completion (silica gel, 10% EtOAc in hexanes), the reaction mixture was diluted with EtOAc (15 mL) and carefully quenched with distilled water (5 mL), and $NaHCO_3$ (5 mL). The aqueous layer was extracted with EtOAc (2 × 10 mL), and the combined organic layers were washed with brine, dried ($MgSO_4$), filtered, and concentrated *in vacuo*. The crude material was purified *via* flash chromatography (2 – 5% EtOAc in hexanes), and yielded 139.5 mg (0.39 mmol, 73%) of **4.39** as clear, colorless oil.

R_f = 0.37 (silica gel, 10% EtOAc in hexanes).

^{1}HNMR (400 MHz, $CDCl_3$): δ 7.35 – 7.31 (m, 5H, 5 × -C*H*- Ph), 5.83 (ddt, J = 17.1, 10.1, 7.1 Hz, 1H, =C*H*-), 5.10 – 5.02 (m, 2H, =CH_2), 4.55 (d, J = 11.6 Hz, 1H, -CH*H*-), 4.47 (d, J = 11.6 Hz, 1H, -CH*H*-), 3.57 (t, J = 6.6 Hz, 2H, -CH_2-), 3.41 (p, J = 5.8 Hz, 1H, -C*H*-), 2.35 – 2.26 (m, 2H, -CH_2-), 1.53 – 1.42 (m, 4H, 2 × -CH_2-), 1.36 – 1.21 (m, 6H, 3 × -CH_2-), 0.88 (s, 9H, O-TBS *t*-Bu), 0.03 (s, 6H, 2 × O-TBS -CH_3) ppm; residual BnBr contamination δ 7.29 – 7.25 (m, "1.37" H, -C*H*- Ph), 4.55 (s, "0.56" H, -CH_2-) ppm.

^{13}CNMR (100 MHz, $CDCl_3$): δ 139.0, 135.1, 128.4, 127.8, 127.4, 116.8, 78.6, 70.9, 63.3, 38.3, 33.8, 32.9, 29.5, 26.0, 25.8, 25.4, 18.4, -5.2 ppm.

HRMS (EI) *m/z*: calculated for $C_{16}H_{34}O_2Si$ [M – C_7H_7] 286.2328, observed 286.2355 (Δ = 2.7 mmu).

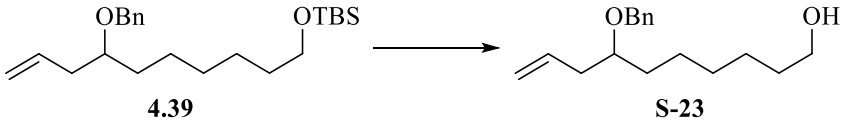

4.39 **S-23**

(7-Benzyloxy)dec-9-en-1-ol (S-23). Di-protected **4.39** (40 mg, 0.11 mmol, 1.0 equiv.) was added to a 1.5-mL polypropylene Eppendorf® tube and dissolved in acetonitrile (1.1 mL, 0.1 M). Pyridine (44 μL, 0.55 mmol, 5.0 equiv.) was added, and the solution was vortexed to homogeneity. Carefully, 48% HF (200 μL, 5.5 mmol, 50 equiv.) was added, and the reaction mixture was again vortexed, centrifuged, and left for 5 h. The reaction was quenched with water (2 × 1 mL), and diluted with EtOAc (2 × 2 mL). The aqueous layer was re-extracted with EtOAc, and the combined organic layers were washed with brine, dried ($MgSO_4$), filtered, and concentrated *in vacuo*. The crude product was purified by column chromatography (silica gel, 20% EtOAc in hexanes), and yielded 28.8 mg of **S-23** (0.11 mmol, quant.) as clear, colorless oil.

R_f = 0.13 (silica gel, 10% EtOAc in hexanes).

^{1}HNMR (400 MHz, $CDCl_3$): δ 7.36 – 7.29 (m, 4H, 4 × -C*H*- Ph), 7.27 – 7.25 (m, 1H, -C*H*- Ph), 5.83 (ddt, *J* = 17.2, 10.2, 7.1 Hz, 1H, -C*H*=), 5.09 – 5.03 (m, 2H, =CH_2), 4.55 (d, *J* = 11.6 Hz, 1H, -CH*H*-), 4.47 (d, *J* = 11.6 Hz, 1H, -CH*H*-), 3.61 (t, *J* = 6.6 Hz, 2H, -CH_2-), 3.42 (p, *J* = 5.9 Hz, 1H, -C*H*-), 2.38 – 2.24 (m, 2H, -CH_2-), 1.58 – 1.47 (m, 4H, 2 × -CH_2-), 1.39 – 1.22 (m, 6H, 3 ×-CH_2-) ppm.

^{13}CNMR (100 MHz, $CDCl_3$): δ 138.9, 135.1, 128.3, 127.7, 127.5, 116.9, 78.5, 70.9, 63.0, 38.3, 33.7, 32.8, 29.5, 25.7, 25.3 ppm.

HRMS (EI) *m/z*: calculated for $C_{10}H_{19}O_2$ [M – C_7H_7] 171.1385, observed 171.1378 (Δ = 0.7 mmu).

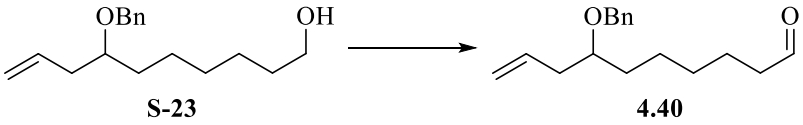

S-23 **4.40**

7-Benzyloxy-dec-9-enal (4.40). Alcohol **S-23** (22 mg, 0.08 mmol, 1.0 equiv.) was dissolved in CH_2Cl_2 (10 mL), and a mixture of PCC (24 mg, 0.11 mmol, 1.3 equiv.) and silica gel (50 mg) were added under inert atmosphere. The reaction stirred at ambient temperature, and was monitored by TLC (silica gel, 10% EtOAc in hexanes). Upon completion, CH_2Cl_2 was evaporated, and the obtained dark brown powder was added directly to a pre-equilibrated column (silica gel, 10% EtOAc in hexanes). Purification yielded 16.5 mg of aldehyde **4.40** (0.06 mmol, 79%; 83% BRSM), along with 2.1 mg of recovered starting material, as clear, colorless oils.

R_f = 0.43 (silica gel, 10% EtOAc in hexanes).

^{1}HNMR (400 MHz, $CDCl_3$): δ 9.73 (t, *J* = 1.8 Hz, 1H, -C*H*O), 7.32 (d, *J* = 4.5 Hz, 4 × -C*H*- Ph), 7.29 – 7.25 (m, 1H, -C*H*- Ph), 5.82 (ddt, *J* = 17.2, 10.2, 7.1 Hz, 1H, -C*H*=), 5.11 – 5.01 (m, 2H, =CH_2), 4.56 (d, *J* 11.6 Hz, 1H, -CH*H*-), 4.45 (d, *J* = 11.6 Hz, 1H, -CH*H*-), 3.41 (p, *J* = 5.8 Hz, 1H, -C*H*-), 2.39 (td, *J* = 7.3,

1.8 Hz, 2H, -C*H*$_2$-), 2.36 – 2.25 (m, 2H, -C*H*$_2$-), 1.60 (dt, *J* = 14.8, 7.4 Hz, 2H, -C*H*$_2$-), 1.55 – 1.40 (m, 4H, 2 × -C*H*$_2$-), 1.36 – 1.24 (m, 4H, 2 × -C*H*$_2$-) ppm.

^{13}CNMR (100 MHz, $CDCl_3$): δ 202.7, 138.9, 134.9, 128.3, 127.7, 127.5, 116.9, 78.3, 70.9, 43.8, 38.2, 33.6, 29.2, 25.1, 22.0 ppm.

HRMS (ESI+ TOF) *m/z*: calculated for $C_{17}H_{24}O_2Na$ [(M + Na)$^+$] 283.1674, observed 283.1707 (Δ = 3.3 mmu).

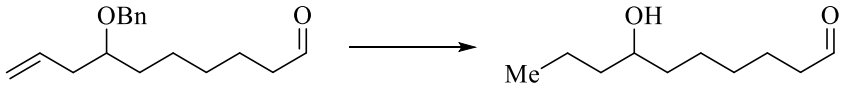

4.40 **4.41**

7-hydroxydecenal (4.41). To a 25-mL round-bottom flask charged with a teflon stirring bar, a solution of alcohol **4.40** (15 mg, 0.058 mmol) was prepared using 0.6 mL of HPLC-grade MeOH. Carefully, Pd/C (10 mg) was added and the system was sealed with a three-way valve. One valve was connected to a PIAB vacuum system, and the other to a double-balloon filled with H_2 gas. The flask was carefully evacuated of atmosphere while the solution stirred, and back-filled with hydrogen. This process was repeated (5×) to ensure complete voiding of ambient atmosphere. The stirred under a blanket of H_2 gas, and was periodically evacuated and back-filled with H_2 gas. Upon completion of the reaction (silica gel, 10% EtOAc in hexanes), the solution was filtered through a celite plug, and concentrated to yield 5.6 mg (0.033 mmol, 56%) of **4.41** as clear, colorless oil. The obtained crude product was spectroscopically pure enough to continue to subsequent steps.

R_f = 0.40 (silica gel, 30% acetone in hexanes; CAM stain).

^{1}HNMR (300 MHz, $CDCl_3$): δ 9.75 (t, *J* = 1.7 Hz, 1H, -C*H*O), 3.62 – 3.55 (m, 1H, -C*H*-), 2.42 (dt, *J* = 1.8, 7.3 Hz, 2H, -C*H*$_2$-), 1.63 (p, *J* = 7.3 Hz, 2H, -C*H*$_2$-), 1.48 – 1.28 (m, 10H, 5 × -C*H*$_2$-), 0.91 (t, *J* = 6.6 Hz, 3H, -C*H*$_3$) ppm.

^{13}CNMR (100 MHz, $CDCl_3$): δ 202.7, 71.6, 43.8, 39.7, 37.2, 29.2, 25.4, 22.0, 18.8, 14.1 ppm.

HRMS (ESI+ TOF) *m/z*: calculated for $C_{10}H_{20}O_2Na$ [(M + Na)$^+$] 195.1361, observed 195.1387 (Δ = 2.6 mmu).

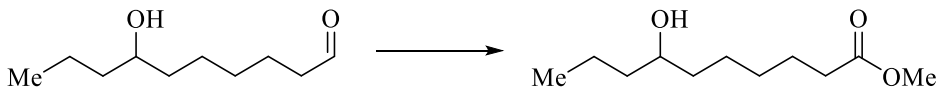

4.41 **4.42**

Methyl 7-hydroxydecanoate (4.42). Formation of **4.42** was the result of undesired side-reactions during work with the C7-C16 fragment of the C13-propyl model (second-generation ketone model). This ester was observed as a minor side-product from the tandem hydrogenation/hydrogenolysis reaction, as well as a

major product formed while screening acid-mediated acetal deprotection conditions of the olefinated framework (*vide infra*).

R_f = 0.34 (silica gel, 30% acetone in hexanes; *p*-anisaldehyde stain).

^{1}HNMR (400 MHz, $CDCl_3$): δ 3.65 (s, 3H, -OC*H*$_3$), 3.60 – 3.55 (m, 1H, -C*H*-), 2.30 (t, *J* = 7.4 Hz, 2H, -C*H*$_2$-), 1.62 (p, *J* = 7.4 Hz, 2H, -C*H*$_2$-), 1.47 – 1.38 (m, 6H, 3 × -C*H*$_2$-), 1.37 – 1.29 (m, 4H, 2 × -C*H*$_2$-), 0.91 (t, *J* = 6.9 Hz, 3H, -C*H*$_3$) ppm.

^{13}CNMR (100 MHz, $CDCl_3$): δ 174.2, 71.6, 51.5, 39.7, 37.2, 34.0, 29.2, 25.3, 24.9, 18.8, 14.1 ppm.

HRMS (ESI+ TOF) *m/z*: calculated for $C_{11}H_{22}O_3Na$ [$(M + Na)^+$] 225.1467, observed 225.1468 (Δ = 0.1 mmu).

Characterization data for **4.42** proved consistent with previously reported literature data.[152]

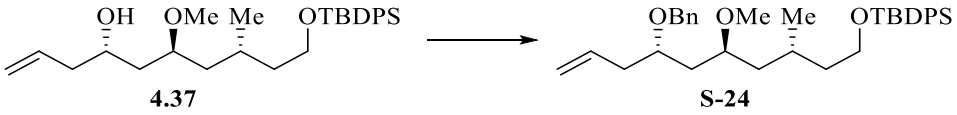

4.37 **S-24**

((3*R*,5*S*,7*S*)-7-Benzyloxy-5-methoxy-3-methyldec-9-enyloxy)-*tert*-butyldiphenylsilane (S-24). Purified homoallylic alcohol **4.37** (750 mg, 1.64 mmol, 1.0 equiv.) was dissolved in a 2:1 mixture of DMF and THF (5.5 mL, 0.3 M). To the solution was added TBAI (59 mg, 0.16 mmol, 10 mol %), 60% dispersion NaH (198 mg, 4.9 mmol, 3.0 equiv.), and freshly distilled BnBr (300 μL, 2.5 mmol, 1.5 equiv.) under inert atmosphere. The reaction mixture stirred overnight at ambient temperature. Upon completion (silica gel, 10% EtOAc in hexanes), the reaction mixture was diluted with EtOAc (25 mL) and carefully quenched with distilled water (15 mL), and $NaHCO_3$ (15 mL). The aqueous layer was extracted with EtOAc (2 × 20 mL), and the combined organic layers were washed with brine, dried ($MgSO_4$), filtered, and concentrated *in vacuo* to yield crude oil. Purification *via* flash chromatography (2–5% EtOAc in hexanes), yielded 768 mg (1.41 mmol, 86%) of **S-24** as clear, colorless oil.

R_f = 0.52 (silica gel, 10% EtOAc in hexanes).

^{1}HNMR (300 MHz, $CDCl_3$): δ 7.67 – 7.63 (m, 4H, 4 × -C*H*- Ph), 7.42 – 7.30 (m, 6H, 6 × -C*H*- Ph), 5.83 (ddt, *J* = 17.2, 10.1, 7.0 Hz, 1H, -C*H*=), 5.13 – 5.02 (m, 2H, =C*H*$_2$), 4.62 (d, *J* = 11.5 Hz, 1H, -CH*H*-), 4.44 (d, *J* = 11.5 Hz, 1H -CH*H*-), 3.72 – 3.61 (m, 3H, -C*H*- & -C*H*$_2$-), 3.45 (ddd, *J* = 12.7, 7.2, 5.7 Hz, 1H, -C*H*-), 3.20 (s, 3H, -OC*H*$_3$), 2.33 (t, *J* = 6.1 Hz, 2H, -C*H*$_2$-), 1.83 – 1.68 (m, 1H, -CH*H*-), 1.67 – 1.46 (m, 4H, 4 × -CH*H*-), 1.40 – 1.27 (m, 1H, -CH*H*-), 1.17 – 1.06 (m, 1H, -CH*H*-), 1.02 (s, 9H, O-TBDPS *t*-Bu), 0.84 (d, *J* = 6.6 Hz, 3H, -C*H*$_3$) ppm; residual BnBr contamination δ 7.31 – 7.26 (m, "0.82" H, 5 × -C*H*- Ph), 4.55 (s, "0.33" H, -C*H*$_2$-) ppm.

^{13}CNMR (100 MHz, $CDCl_3$): δ 135.6, 134.6, 134.1, 129.5, 128.3, 127.83, 127.76, 127.57, 127.45, 117.2, 75.6, 75.4, 71.1, 62.0, 56.3, 42.1, 40.2, 40.1, 38.7, 26.8, 26.2, 19.9, 19.2 ppm.

HRMS (EI) *m/z*: calculated for $C_{31}H_{39}O_3Si$ [M – *t*-Bu] 487.2668, observed 487.2661 (Δ = 0.7 mmu).

IR (thin film) ν_{max}: 3071, 2928, 1641, 1427, 1216, 1087, 1027 cm^{-1}.

$[\alpha]_D^{20}$ = + 17.2° (*c* = 10.1 mg/2.5 mL, $CHCl_3$; *l* = 100 mm; α = + 0.0694°).

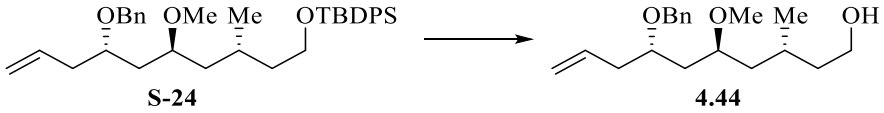

S-24 **4.44**

(3*R*,5*S*,7*S*)-7-Benzyloxy-5-methoxy-3-methyldec-9-en-1-ol (4.44). [*Method A*] To a 15-mL polypropylene Falcon tube charged with **S-24** (600 mg, 1.10 mmol, 1.0 equiv.), was added acetonitrile (11 mL, 0.1 M) and pyridine (443 μL, 5.5 mmol, 5.0 equiv.). The reaction mixture was vortexed to homogeneity, upon which 48% HF (1.9 mL, 55 mmol, 50 equiv.) was added. The reaction was mixture was again vortexed, then centrifuged and left for 5 h. The reaction was monitored by TLC (silica gel, 30% acetone in hexanes), and upon completion was quenched with water (2 × 10 mL), and diluted with EtOAc (15 mL). The aqueous layer was re-extracted with EtOAc (2 × 10 mL), and the combined organic layers were washed with brine, dried ($MgSO_4$), filtered, and concentrated *in vacuo*. The product was purified (silica gel, 10 – 30% EtOAc in hexanes), and yielded 314.6 mg of **4.44** (1.02 mmol, 93%) as clear, colorless oil. [*Method B*] To a stirring solution of **S-24** (58 mg, 0.106 mmol, 1.0 equiv.) in anhydrous THF (1.0 mL), was added TBAF (68 μL, 0.234 mmol, 2.2 equiv.) under inert atmosphere. The reaction stirred at ambient temperature overnight, upon which it was diluted with EtOAc (5mL) and quenched by NH_4Cl (3 mL). The aqueous layer was re-extracted, and the combined organic layers were washed with brine, dried, filtered and concentrated *in vacuo*. The crude product was purified under the same conditions above, to afford 25.3 mg (0.083 mmol, 78%) of **4.44** as clear, colorless oil.

R_f = 0.27 (silica gel, 30% acetone in hexanes).

^{1}HNMR (400 MHz, $CDCl_3$): *δ* 7.35 – 7.31 (m, 4H, 4 × -C*H*- Ph), 7.30 – 7.25 (m, 1H, -C*H*- Ph), 5.84 (ddt, *J* = 17.3, 10.2, 7.1 Hz, 1H, =C*H*-), 5.13 – 5.04 (m, 1H, =CH_2), 4.63 (d, *J* = 11.4 Hz, 1H, -CH*H*-), 4.44 (d, *J* = 11.4 Hz, 1H, -CH*H*-), 3.74 – 3.53 (m, 3H, -C*H*- & -CH_2-), 3.44 (ddd, *J* = 12.1, 7.1, 5.2 Hz, 1H, -C*H*-), 3.24 (s, 3H, -OCH_3), 2.37 – 2.31 (m, 2H, -CH_2-), 1.78 – 1.64 (m, 1H, -CH*H*-), 1.61 – 1.49 (m, 4H, 2 × -CH_2-), 1.44 – 1.32 (m, 1H, -CH*H*-), 1.16 (ddd, *J* = 13.9, 8.0, 5.2 Hz, 1H, -CH*H*-), 0.92 (d, *J* = 6.6 Hz, 3H, -CH_3) ppm.

^{13}CNMR (100 MHz, $CDCl_3$): *δ* 138.7, 134.5, 128.4, 127.9, 127.6, 117.4, 76.0, 75.5, 71.2, 60.9, 56.6, 42.0, 40.2, 40.1, 38.6, 26.3, 20.3 ppm.

HRMS (EI) *m/z*: calculated for $C_{12}H_{23}O_3$ [M – C_7H_7] 215.1647, observed 215.1635 (Δ = 1.2 mmu).

IR (thin film) ν_{max}: 3416, 3071, 2928, 1460, 1427, 1216, 1187, 1104, 1089 cm^{-1}.

$[\alpha]_D^{20}$ = – 6.4° (*c* = 14.1 mg/2.5 mL, $CHCl_3$; *l* = 100 mm; α = – 0.0358°).

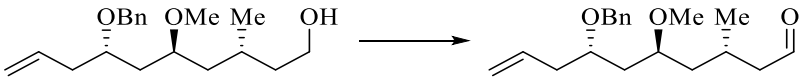

4.44 **4.45**

(3*S*,5*S*,7*S*)-7-Benzyloxy-5-methoxy-3-methyldec-9-enal (4.45). [*Method A*] A round-bottom flash, equipped with a magnetic stirrer, containing oxalyl chloride (196 μL, 0.391 mmol, 1.2 equiv.) and CH_2Cl_2 (3.0 mL/mmol alcohol) was cooled to -78 ºC under inert atmosphere. Anhydrous DMSO (58.5 μL, 0.816 mmol, 2.5 equiv.) was added dropwise, and the solution stirred for 15 min while holding temperature. A solution of freshly-dried **4.44** (74.5 mg, 0.243 mmol, 1.0 equiv.) in CH_2Cl_2 (0.5 mL/mmol alcohol) was added dropwise, and stirred for an additional 15 min while holding temperature. Triethylamine (227.3 μL, 1.63 mmol, 5.0 equiv.) was added to the solution dropwise, and turned the reaction mixture thick and grey/yellow in color. The reaction mixture stirred for 80 min at -78 ºC, and monitored by TLC (silica gel, 10% EtOAc in hexanes) while warmed to ambient temperature. Upon completion, the mixture was diluted with CH_2Cl_2 and quenched with water. The aqueous layer was acidified with aqueous 1M HCl solution, and re-extracted. The combined organic layers were washed with brine, dried, filtered, and evaporated *in vacuo*. The crude paste was purified immediately (silica gel, 10% EtOAc in hexanes), and yielded 59.3 mg of **4.45** (0.195 mmol, 80%; 93% BRSM) and 10.3 mg of recovered alcohol **4.44** (0.034 mmol, 14%). [*Method B*] Alcohol **4.44** (20.4 mg, 0.066 mmol, 1 eq.) was dissolved in CH_2Cl_2 (0.3 mL), and added PCC (17.2 mg, 0.08 mmol, 1.2 eq.) and silica gel (40 mg), and CH_2Cl_2 (0.6 mL) under inert atmospher. The reaction stirred at ambient temperature for 2 hours, and was monitored by TLC (silica gel, 10% EtOAc in hexanes). Upon completion, the reaction mixture was concentrated, and the dark brown suspension was added directly to a pre-equilibrated (silica gel, 10% EtOAc in hexanes) column. Purification yielded 12.9 mg of **4.32** as colorless oil (0.042 mmol, 65%; 80% BRSM) and 4.1 mg of recovered alcohol. Both methods provided product of identical spectroscopic purity; as with most Swern oxidations,[82] maintenance of temperature is critical to reliability of yield.

R_f = 0.21 (silica gel, 10% EtOAc in hexanes).

^{1}HNMR (400 MHz, $CDCl_3$): δ 9.70 (t, *J* = 2.1 Hz, 1H, -C*H*O), 7.32 (d, *J* = 4.6 Hz, 4H, 4 × -C*H*- Ph), 7.30 – 7.24 (m, 1H, -C*H*- Ph), 5.83 (ddt, *J* = 17.2, 10.2, 7.1 Hz, 1H, -C*H*=), 5.16 – 5.00 (m, 2H, =CH_2), 4.63 (d, *J* = 11.4 Hz, 1H, -CH*H*-), 4.43 (d, *J* = 11.4 Hz, 1H, -CH*H*-), 3.64 (dtd, *J* = 9.0, 5.6, 3.5 Hz, 1H, -C*H*-), 3.44 (ddd, *J* = 12.4, 8.2, 4.6 Hz, 1H, -C*H*-), 3.23 (s, 3H, -OCH_3), 2.41 – 2.32 (m, 3H, -C*H*- & -CH_2-), 2.25- 2.18 (m, 2H, -CH_2-), 1.66 – 1.50 (m, 3H, -CH*H*- & -CH_2-), 1.26 (ddd, *J* = 14.1, 7.8, 4.8 Hz, 1H, -CH*H*-), 0.97 (d, *J* = 6.4 Hz, 3H, -CH_3) ppm.

^{13}CNMR (100 MHz, $CDCl_3$): δ 202.6, 138.7, 134.4, 128.4, 127.9, 127.6, 117.5, 75.6, 75.4, 71.2, 56.4, 51.3, 41.7, 40.0, 38.5, 25.0, 20.3 ppm.

HRMS (ESI+ TOF) *m/z*: calculated for $C_{19}H_{30}O_3Na$ [$(M+Na)^+$] 329.2093, observed 329.2071 (Δ = 2.2 mmu).

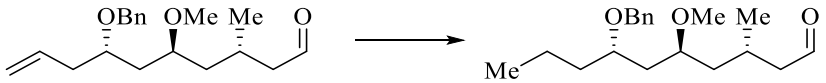

4.45 **4.46**

(3*S*,5*S*,7*S*)-7-(benzyloxy)-5-methoxy-3-methyldecanal (4.46). *The following product was obtained during attempts to optimize a tandem hydrogenation/benzyl cleavage step, and demonstrates the rate of selectivity in the process.* To a 25-mL round-bottom flask charged with a teflon stirring bar, a solution of alcohol **4.45** (22 mg, 0.072 mmol) was prepared using 2.4 mL of HPLC-grade MeOH (0.03 M), to which Pd/C (2 mg) was carefully added and the system was sealed with a three-way valve. One valve was connected to a PIAB vacuum system, and the other to a double-balloon filled with H_2 gas. The flask was carefully evacuated of atmosphere with stirring of the solution, and back-filled with hydrogen. This process was repeated (5×) to ensure complete voiding of air. The stirred under a blanket of H_2 gas, and was periodically evacuated of atmosphere and back-filled with H_2 gas. Upon completion of the reaction (silica gel, 10% EtOAc in hexanes), the solution was filtered through a celite plug, and concentrated for analysis by ^{1}HNMR. The crude material was purified (silica gel, 10% EtOAc in hexanes) to yield 8.8 mg of **4.46** (0.029 mmol, 40%; 76% BRSM) and 10.4 mg (0.034 mmol, 48%) of unreacted as clear, colorless oil.

R_f = 0.41 (silica gel, 20% EtOAc in hexanes).

^{1}HNMR (300 MHz, $CDCl_3$): δ 9.71 (t, *J* = 2.2 Hz, 1H, -C*H*O), 7.32 (d, *J* = 4.7 Hz, 4H, 4 × -C*H*- Ph), 7.29 – 7.24 (m, 1H, -C*H*- Ph), 4.57 (d, *J* = 11.4 Hz, 1H, -CH*H*-), 4.42 (d, *J* = 11.4 Hz, 1H, -CH*H*-), 3.56 (td, *J* = 9.4, 5.5 Hz, 1H, -C*H*-), 3.47 – 3.39 (m, 1H, -C*H*-), 3.25 (s, 3H, -OCH_3), 2.38 (ddd, *J* = 18.7, 8.6, 1.7 Hz, 1H, -CH*H*-), 2.27 – 2.17 (m, 2H, -C*H*- & -CH*H*-), 1.67 – 1.46 (m, 5H, 2 × -CH_2- & 1 × -CH*H*-), 1.45 – 1.33 (m, 2H, -CH_2-), 1.30 – 1.24 (m, 1H, -CH*H*-), 0.97 (d, *J* = 6.2 Hz, 3H, -CH_3), 0.91 (t, *J* = 7.3 Hz, 3H, -CH_3) ppm.

^{13}CNMR (75 MHz, $CDCl_3$): δ 202.6, 138.9, 128.4, 127.9, 127.5, 75.9, 75.8, 71.0, 56.4, 51.4, 41.8, 40.1, 36.5, 25.1, 20.3, 18.3, 14.4 ppm.

LRMS (ESI+ TOF) *m/z*: calculated for $C_{19}H_{30}O_3Na$ [$(M + Na)^+$] 329.2, observed 329.2.

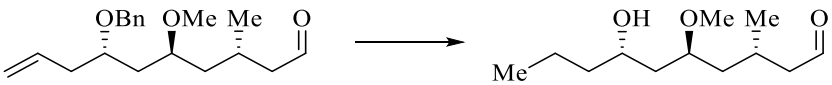

4.45 **4.25**

(3*S*,5*S*,7*S*)-7-hydroxy-5-methoxy-3-methyldecanal (4.25). To a 25-mL round-bottom flask charged with a teflon stirring bar, a solution of aldehyde **4.45** (80 mg, 0.26 mmol) was prepared using 3.5 mL of HPLC-grade MeOH (0.075 M), to which Pd/C (60 mg) was carefully added and the system was sealed with a

three-way valve. One valve was connected to a PIAB vacuum system, and the other to a double-balloon filled with H_2 gas. The flask was carefully evacuated of atmosphere with stirring of the solution, and back-filled with hydrogen. This process was repeated (5×) to ensure complete voiding of air. The flask was left to stir with a blanket of H_2 gas, periodically evacuating and back-filling the flask. Upon completion of the reaction (silica gel, 10% EtOAc in hexanes), the solution was filtered through a celite plug, and concentrated for analysis by ^{1}HNMR to reveal spectroscopically-pure product (74.5 mg, 0.24 mmol, 94%). Purification of the crude material was not performed, as it promotes formation of the polar hydrate. It should be noted that use of aldehyde **4.46** under these conditions will afford **4.25** in similar yields. Product must be used immediately, or frozen under vacuum, as it readily undergoes disproportionation *via* Cannizarro[85,153]-type reaction to afford the corresponding alcohol and carboxylic acid as reduction and oxidation side-products, respectively.

R_f = 0.21 (silica gel, 10% EtOAc in hexanes).

^{1}HNMR (600 MHz, $CDCl_3$): δ 9.75 – 9.74 (m, 1H, -C*H*O), 3.88 (m, 1H, -C*H*-), 3.55 (ddt, *J* = 8.5, 5.4, 4.2 Hz, 1H, -C*H*-), 3.36 (s, 3H, -OCH_3), 2.76 (br s, 1H, -O*H*), 2.46 -2.41 (m, 1H, -CH*H*-), 2.31 – 2.20 (m, 2H, -CH*H*- & -C*H*-), 1.76 – 1.64 (m, 2H, 2 × -CH*H*-), 1.49 (ddd, *J* = 14.8, 5.9, 2.4 Hz, 1H, -CH*H*-), 1.47 – 1.41 (m, 2H, 2 × -CH*H*-), 1.39 – 1.32 (m, 2H, 2 × -CH*H*-), 1.29 (ddd, *J* = 14.1, 7.9, 4.5 Hz, 1H, -CH*H*-), 1.00 (d, *J* = 6.4 Hz, 3H, -CH_3), 0.92 (t, *J* = 7.0 Hz, 3H, -CH_3) ppm.

^{13}CNMR (150 MHz, $CDCl_3$): δ 202.4, 77.5, 68.4, 56.8, 51.3, 40.9, 40.1, 39.4, 25.1, 20.3, 18.8, 14.1 ppm.

HRMS (ESI+ TOF) *m/z*: calculated for $C_{12}H_{24}O_3Na$ [$(M + Na)^+$] 239.1623, observed 239.1624 (Δ = 0.1 mmu).

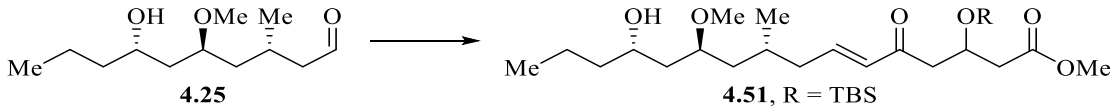

4.25 **4.51**, R = TBS

(*E*)-Methyl-3-(*O*-TBS)-(13*S*)-hydroxy-(11*S*)-methoxy-(9*R*)-methyl-5-oxohexadec-6-enoate (4.51). To a solution of methyl phosphonate **4.50** (6.3 mg, 16.8 μmol, 1.2 equiv.) in isopropanol (150 μL, dried over 4 Å ms), was added cesium carbonate (8.7 mg, 26.8 μmol, 2.0 equiv.) under inert atmosphere. The mixture was stirred for 2 h at ambient temperature. A solution of **4.25** (2.9 mg, 13.4 μmol, 1.0 equiv.) in dry isopropanol (150 μL) was added to the reaction mixture dropwise, and monitored by TLC (silica gel, 20% EtOAc in hexanes; *p*-anisaldehyde stain). The reaction converted all starting material to product within 2 h, with no apparent side- or by-products. Upon completion, the reaction was diluted with EtOAc (5 mL), and quenched by the addition of 1.0 M HCl solution (1 mL). The mixture was extracted with EtOAc (2 × 3 mL), and the combined organic layers were washed with brine (2 × 5 mL), dried ($MgSO_4$), filtered, and concentrated *in vacuo*. Purification *via* column chromatography (20% acetone in hexanes) yielded 4.8 mg

4.51 (10.2 μmol, 76%) as clear, colorless oil. This reaction was performed once, and remains open to optimization.

R_f = 0.30 (silica gel, 20% EtOAc in hexanes).

^{1}HNMR (400 MHz, $CDCl_3$): δ 6.80 (dt, *J* = 15.7, 7.5 Hz, 1H, -C*H*=), 6.09 (dt, *J* = 15.8, 1.2 Hz, 1H, =C*H*-), 4.60 (p, *J* = 5.9 Hz, 1H, -C*H*-), 3.91 – 3.83 (m, 1H, -C*H*-), 3.65 (s, 3H, -CO_2CH_3), 3.59 – 3.52 (m, 1H, -C*H*-), 3.35 (s, 3H, -OCH_3), 2.82 (dd, *J* = 15.7, 6.5 Hz, 1H, -CH*H*-), 2.72 (d, *J* = 15.7, 5.9 Hz, 1H, -CH*H*-), 2.54 (dd, *J* = 14.8, 5.6 Hz, 1H, -CH*H*-), 2.46 (dd, *J* = 14.8, 6.4 Hz, 1H, -CH*H*-), 2.29 – 2.20 (m, 1H, -CH*H*-), 2.10 – 2.03 (m, 1H, -CH*H*-), 1.87 – 1.76 (m, 1H, -C*H*-), 1.74 – 1.65 (m, 2H, 2 × -CH*H*-), 1.51 – 1.44 (m, 2H, 2 × -CH*H*-), 1.41 – 1.29 (m, 4H, -CH_2-, -O*H*, & -CH*H*-), 1.22 – 1.17 (m, 1H, -CH*H*-), 0.93 (d, *J* = 6.7 Hz, 3H, -CH_3), 0.91 (t, *J* = 7.0 Hz, 3H, -CH_3), 0.81 (s, 9H, O-TBS *t*-Bu), 0.04 (s, 3H, O-TBS -CH_3), 0.01 (s, 3H, O-TBS -CH_3) ppm.

^{13}CNMR (100 MHz, $CDCl_3$): δ 198.1, 171.5, 146.4, 132.4, 77.5, 68.5, 66.1, 56.9, 51.5, 47.4, 42.5, 40.9, 40.3, 40.1, 39.6, 29.4, 25.7, 19.8, 18.8, 17.9, 14.1, -4.7, -5.0 ppm.

HRMS (ESI+ TOF) *m/z*: calculated for $C_{25}H_{48}O_6SiNa$ [$(M + Na)^+$] 495.3118, observed 495.3132 (Δ = 1.4 mmu).

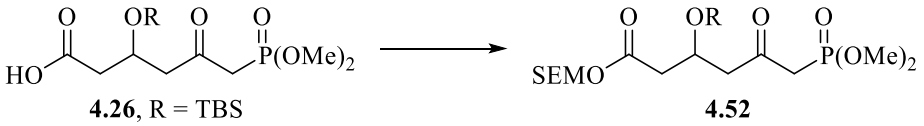

4.26, R = TBS **4.52**

3-(*O*-TBS)-5-oxo-5-((2-(trimethylsilyl)ethoxy)methoxy)pentanoic acid (4.52). To a cooled (0 ºC) solution of **4.26** (100 mg, 0.27 mmol, 1.0 equiv.) in THF (1.4 mL, 0.2 M) was added either triethylamine (76 μL, 0.54 mmol, 2.0 equiv.) *OR* potassium carbonate (176 mg, 0.54 mmol, 2.0 equiv.), and stirred for 10 min under inert atmosphere. Carefully, 2-(Trimethylsilyl)ethoxymethyl chloride (62 μL, 0.35 mmol, 1.3 equiv.) was added to the solution and stirred overnight at ambient temperature. Upon completion, the reaction was quenched with water (1.5 mL), and diluted with EtOAc (3 mL). The layers were separated, and washed with EtOAc (3 × 2 mL). The combined organic layers were washed with brine, dried ($MgSO_4$), filtered, and concentrated. The crude product was purified *via* flash chromatography (10-50% EtOAc in hexanes), and yielded 106.3 mg (0.21 mmol, 79%) of **4.52** as clear, colorless oil.

R_f = 0.29 (silica gel, 5% MeOH in CH_2Cl_2; *p*-anisaldehyde stain).

^{1}HNMR (400 MHz, $CDCl_3$): δ 5.27 (d, *J* = 6.2 Hz, 1H, -CH*H*-), 5.23 (d, *J* = 6.2 Hz, 1H, -CH*H*-), 4.55 (p, *J* = 6.0 Hz, 1H, -C*H*-), 3.78 (d, *J* = 1.3 Hz, 3H, -CH_3), 3.75 (d, *J* = 1.3 Hz, 3H, -CH_3), 3.68 (dd, *J* = 9.0, 7.7 Hz, 2H, -CH_2-), 3.09 (dd, *J* = 22.7, 1.6 Hz, 2H, -CH_2-), 2.88 (d, *J* = 6.0 Hz, 2H, -CH_2-), 2.56 (dd, *J* = 15.3, 5.8 Hz, 1H, -CH*H*-), 2.49 (dd, *J* = 15.3, 6.2 Hz, 1H, -CH*H*-), 0.97 – 0.91 (m, 2H, -CH_2-), 0.82 (s, 9H, O-TBS *t*-Bu), 0.06 (s, 3H, -CH_3), 0.05 (s, 3H, -CH_3), 0.00 (s, 9H, TMS *t*-Bu) ppm.

^{13}CNMR (100 MHz, $CDCl_3$): δ 199.9 (d, J = 6.5 Hz), 170.5, 89.1, 68.0, 65.3, 53.1 (d, J = 4.2 Hz), 53.0 (d, J = 4.2 Hz), 51.0, 43.1, 42.2, 41.8, 25.7, 18.1, 17.9, -1.4, -4.8, -4.9 ppm.

^{31}PNMR (162 MHz, $CDCl_3$): δ 22.3 ppm.

HRMS (ESI+ TOF) *m/z*: calculated for $C_{20}H_{43}O_8PSi_2Na$ [$(M + Na)^+$] 521.2132, observed 521.2119 (Δ = 1.3 mmu).

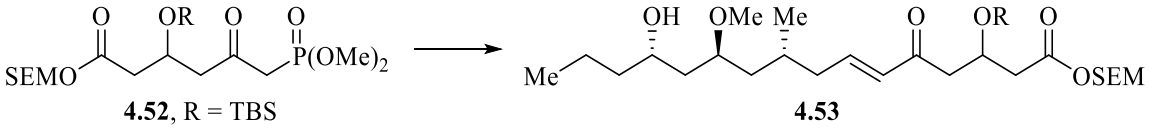

4.52, R = TBS **4.53**

(2-(Trimethylsilyl)ethoxy)-Methyl-(*E*)-3-(*O*-TBS)-(13*S*)-hydroxy-(11*S*)-methoxy-(9*R*)-methyl-5-oxohexadec-6-enoate (4.53): Phosphonate **4.52** (32 mg, 64 μmol, 1.25 equiv.) was dissolved in isopropanol (0.4 mL, dried over 4 Å MS), and cooled to 0 ºC. Cesium carbonate (33.2 mg, 102 μmol, 2.0 equiv.) was added in one portion, and the mixture stirred at 0 ºC for 2 hours. To the reaction mixture, a solution of aldehyde **4.25** (11 mg, 51 μmol, 1.0 equiv.) in isopropanol (0.2 mL, dried over 4 Å MS, 0.1 M overall reaction mixture) was added dropwise. The reaction mixture was warmed to 30 ºC and stirred overnight. The reaction was diluted with EtOAc (10 mL), and quenched by the addition of 1.0 M HCl solution (4 mL). The mixture was extracted with EtOAc (2 × 10 mL), and the combined organic layers were washed with brine, dried ($MgSO_4$), filtered, and concentrated *in vacuo* to provide 14.6 mg of crude material. Purification *via* column chromatography (20% EtOAc in hexanes) furnished 5.3 mg of spectroscopically-sufficient **4.53** (9.0 μmol, 27% BRSM) and 3.8 mg of recovered **4.25** as clear, colorless oils. Attempts to further-purify the limited material resulted in clean hydrolysis of the SEM-acetal ester, and revealed formation of β-elimination by-products.

R_f = 0.38 (silica gel, 20% EtOAc in hexanes).

^{1}HNMR (400 MHz, $CDCl_3$): δ 6.81 (dt, J = 15.8, 7.5 Hz, 1H, -C*H*=). 6.09 (d, J = 15.8 Hz, 1H, =C*H*-), 5.28 (d, J = 6.4 Hz, 1H, -CH*H*-), 5.23 (d, J = 6.4 Hz, 1H, -CH*H*-), 4.60 (dq, J = 11.2, 5.8 Hz, 1H, -C*H*-), 3.90 – 3.84 (m, 1H, -C*H*-), 3.68 (t, J = 8.4 Hz, 2H, -CH_2-), 3.58 – 3.53 (m, 1H, -C*H*-), 3.35 (s, 3H, -OCH_3), 2.83 (dd, J = 15.7, 6.6 Hz, 1H, -CH*H*-), 2.75 (dd, J = 15.7, 5.7 Hz, 1H, -CH*H*-), 2.58 (dd, J = 15.2, 6.1 Hz, 1h, -CH*H*-), 2.51 (dd, J = 15.2, 6.3 Hz, 1H, -CH*H*-), 2.27 – 2.21 (m, 1H, -CH*H*-), 2.09 – 2.02 (m, 1H, -CH*H*-), 1.85 – 1.77 (m, 1H, -C*H*-), 1.73 – 1.66 (m, 2H, 2 × -CH*H*-), 1.57 – 1.43 (m, 2H, 2 × -CH*H*-), 1.40 – 1.30 (m, 4H, -CH_2-, -O*H*, & -CH*H*-), 1.22 (t, J = 6.3 Hz, 2H, -CH_2-), 1.20 – 1.17 (m, 1H, -CH*H*-), 0.93 (d, J = 7.0 Hz, 3H, -CH_3), 0.91 (t, J = 7.1 Hz, 3H, -CH_3), 0.82 (s, 9H, O-TBS *t*-Bu), 0.05 (s, 3H, O-TBS -CH_3), 0.02 (s, 3H, O-TBS -CH_3), 0.00 (s, 9H, TMS *t*-Bu) ppm.

^{13}CNMR (100 MHz, $CDCl_3$): δ 198.3, 170.8, 146.6, 132.4, 89.1, 77.5, 68.5, 68.0, 66.0, 56.9, 47.3, 42.7, 40.9, 40.3, 40.1, 39.6, 29.4, 25.7, 21.9, 19.8, 18.8, 17.9, 14.1, -1.4, -4.8, -4.9 ppm.

HRMS (ESI+ TOF) *m/z*: calculated for $C_{30}H_{60}O_7Si_2Na$ [$(M + Na)^+$] 611.3775, observed 611.3822 (Δ = 4.7 mmu).

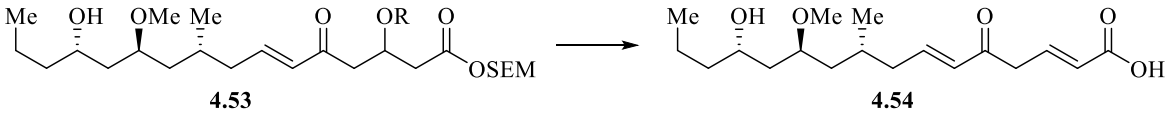

4.53 **4.54**

Elimination By-Product (4.54): The obtained ester **4.53** was treated with SiO_2 and dry-loaded onto a pre-equilibrated column (10% EtOAc in hexanes). The silica gel proved sufficiently-acidic for ester hydrolysis, in addition to undesired *β*-elimination of the C3-TBS alcohol as a major by-product.

R_f = 0.19 (silica gel, 20% EtOAc in hexanes).

^{1}HNMR (400 MHz, $CDCl_3$): δ 7.30 (dd, *J* = 9.4, 6.7 Hz, 2H, 2 × -C*H*=), 6.69 (p, *J* = 7.4 Hz, 2H, 2 × =C*H*-), 6.19 (dd, *J* = 9.3, 0.7 Hz, 1H, 2 × -C*H*=), 6.01 (dt, *J* = 15.4, 1.3 Hz, 2H, 2 × =C*H*-), 5.99 (d, *J* = 6.7 Hz, 1H, 2 × =C*H*-), 3.95 – 3.88 (m, 2H, 2 × -C*H*-), 3.63 – 3.56 (m, 2H, 2 × -C*H*-), 3.39 (s, 6H, 2 × -OCH_3), 3.35 – 3.28 (m, 2H, 2 × -CH*H*-), 2.33 – 2.23 (m, 2H, 2 × -CH*H*-), 2.15 – 2.05 (m, 2H, 2 × -CH*H*-), 1.89 – 1.78 (m, 2H, 2 × -CH*H*-), 1.78 – 1.69 (m, 4H, 4 × -CH*H*-), 1.54 (dd, *J* = 6.0, 2.4 Hz, 2H, 2 × -CH*H*-), 1.51 – 1.33 (m, 10H, 10 × -CH*H*-), 1.29 – 1.19 (m, 4H, 4 × -CH*H*-), 0.97 (d, *J* = 6.6 Hz, 6H, 2 × -CH_3), 0.94 (t, *J* = 7.4 Hz, 6H, 2 × -CH_3) ppm.

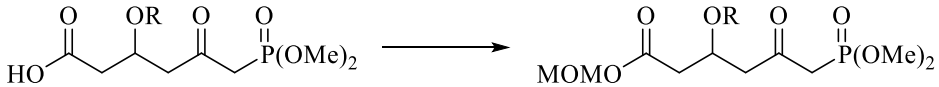

4.26, R = TBS **S-25**

3-(*tert*-Butyldimethylsilyloxy)-5-(methoxymethoxy)-5-oxopentanoic acid (S-25). To a cooled (0 ºC) and stirring solution of **4.26** (140 mg, 0.37 mmol, 1.0 equiv.) in anhydrous CH_2Cl_2 (1.5 mL, 0.25 M) was added DIPEA (662 µL, 3.79 mmol, 10.0 equiv.), TBAI (13.5 mg, 0.04 mmol, 10 mol%) and MOMCl (153 µL, 1.85 mmol, 5.0 equiv.). The reaction mixture was covered with tinfoil and stirred under inert atmosphere for 5 h at ambient temperature. Upon completion, the mixture was quenched with $NaHCO_3$ and diluted with EtOAc (25 mL). The aqueous layer was extracted with EtOAc (2 × 20 mL), and the combined organic layers were washed with brine, dried ($MgSO_4$), filtered, and concentrated *in vacuo* to yield a crude amber oil. Purification of the residue was accomplished *via* flash chromatography (5% MeOH in CH_2Cl_2), and yielded **S-25** as clear, colorless oil. The MOM-ester is reported to be cleavable by mildly-acidic SiO_2;[99] it was believed purification facilitated erosion of the compound and further-diminished the limited conversion. Alternative conditions did not improve the conversion of the reaction.

R_f = 0.48 (silica gel, 5% MeOH in CH_2Cl_2; *p*-anisaldehyde stain).

^{1}HNMR (400 MHz, $CDCl_3$): δ 5.20 (d, J = 7.4 Hz, 2H, -CH_2-), 4.55 (p, J = 6.1 Hz, 1H, -CH-), 3.79 (d, J = 1.0 Hz, 3H, -OCH_3), 3.75 (d, J = 1.0 Hz, 3H, -OCH_3), 3.44 (s, 3H, -CH_3), 3.09 (d, J = 22.6 Hz, 2H, -CH_2-), 2.89 (d, J = 5.9 Hz, 2H, -CH_2-), 2.59 (dd, J = 15.2, 5.9 Hz, 1H, -CHH-). 2.50 (dd, J = 15.2, 6.1 Hz, 1H, -CHH-), 0.83 (s, 9H, O-TBS *t*-Bu), 0.06 (s, 3H, O-TBS -CH_3). 0.05 (s, 3H, O-TBS -CH_3) ppm.

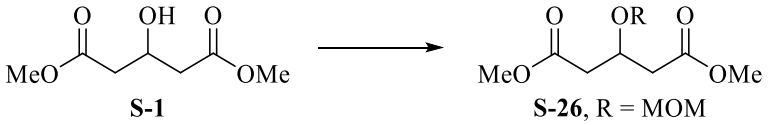

S-1 **S-26**, R = MOM

Dimethyl 3-(methoxymethoxy)pentanedioate (S-26). To a stirring solution of **S-1** (2.5 g, 14.1 mmol, 1.0 equiv.) in anhydrous CH_2Cl_2 (56 mL, 0.25 M) was added DIPEA (24.7 mL, 141 mmol, 10.0 equiv.), TBAI (0.5 g, 1.4 mmol, 10 mol%) and MOMCl (5.6 mL, 70.5 mmol, 5.0 equiv.). The reaction mixture was covered with tinfoil and stirred under argon atmosphere for 6 h at ambient temperature. Upon completion, the mixture was quenched with $NaHCO_3$ and diluted with EtOAc (25 mL). The aqueous layer was extracted with EtOAc (2 × 20 mL), and the combined organic layers were washed with brine, dried ($MgSO_4$), filtered, and concentrated *in vacuo*. Purification of the amber residue was accomplished *via* flash chromatography (10% acetone in hexanes), and yielded 2.87 g (1.11 mmol, 92%) of **S-26** as clear, colorless oil.

R_f = 0.44 (silica gel, 30% acetone in hexanes; CAM stain).

^{1}HNMR (400 MHz, $CDCl_3$): δ 4.67 (s, 2H, -CH_2-), 4.42 -4.36 (m, 1H, -CH-), 3.67 (s, 6H, 2 × -CO_2CH_3), 3.33 (s, 3H, -OCH_3), 2.67 (dd, J = 15.6, 6.9 Hz, 2H, 2 × -CHH-), 2.60 (dd, J = 15.6, 5.7 Hz, 2H, 2 × -CHH-) ppm.

^{13}CNMR (100 MHz, $CDCl_3$): δ 171.2, 96.6, 71.6, 55.7, 51.7, 39.9 ppm.

HRMS (ESI+ TOF) *m/z*: calculated for $C_9H_{16}O_6Na$ [$(M + Na)^+$] 243.0845, observed 243.0849 (Δ = 0.4 mmu).

Characterization data for **S-26** proved consistent with previously reported literature data.[154]

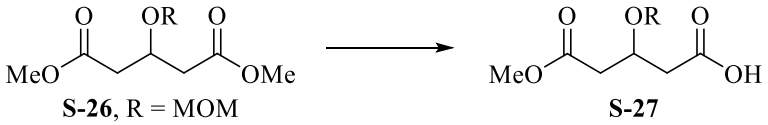

S-26, R = MOM **S-27**

5-Methoxy-3-(methoxymethoxy)-5-oxopentanoic acid (S-27). Purified **S-26** (1.5 g, 6.76 mmol, 1.0 equiv.) was dissolved to homogeneity in a mixture of THF, MeOH, and water (24 mL:12 mL:6 mL, 0.2 M). A solution of 1.0 M NaOH (6.7 mL, 1.0 equiv.) was added, and the mixture stirred at 30 ºC for 8 h, while monitored by TLC (silica gel, 30% acetone in hexanes; CAM stain). Upon completion, the mixture was quenched with saturated NH_4Cl, diluted in EtOAc (50 mL) and extracted (3 × 10 mL). The aqueous layer was acidified, and re-extracted with EtOAc (30 mL). The combined organic layers were dried

($MgSO_4$), filtered, and concentrated to afford 1.03 g (5.00 mmol, 74%) of **S-27** as clear, colorless oil. If necessary, residual diester can be removed using a short column of silica gel (25% acetone in hexanes).

R_f = 0.18 (silica gel, 30% acetone in hexanes; CAM stain).

^{1}HNMR (400 MHz, $CDCl_3$): δ 4.69 (s, 2H, -C*H*$_2$-), 4.38 (p, *J* = 6.3 Hz, 1H, -C*H*-), 3.68 (s, 3H, -CO_2C*H*$_3$), 3.34 (s, 3H, -C*H*$_3$), 2.70 (dd, *J* = 15.7, 6.8 Hz, 1H, -CH*H*-), 2.70 (d, *J* = 2.6 Hz, 1H, -CH*H*-), 2.68 (d, *J* = 2.0 Hz, 1H, -CH*H*-), 2.62 (dd, *J* = 15.7, 5.7 Hz, 1H, -CH*H*-) ppm.

^{13}CNMR (100 MHz, $CDCl_3$): δ 175.8, 171.2, 96.7, 71.4, 55.8, 51.8, 39.70, 39.65 ppm.

HRMS (ESI+ TOF) *m/z*: calculated for $C_8H_{14}O_6Na$ [$(M + Na)^+$] 229.0688, observed 229.0670 (Δ = 1.8 mmu).

IR (thin film) ν_{max}: 3020, 2954, 2359, 1733, 1507, 1437, 1214, 919, 668 cm^{-1}.

Characterization data for **S-27** proved consistent with previously reported literature data.[154]

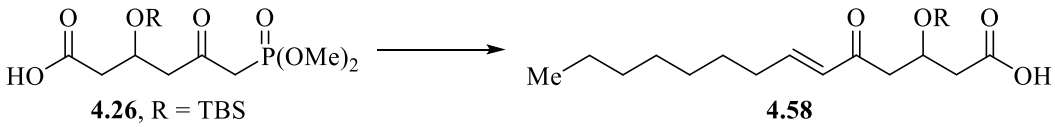

4.26, R = TBS **4.58**

(*E*)-3-(*tert*-Butyldimethylsilyloxy)-4-oxotetradec-6-enoic acid (4.58). *This compound was used as a model for screening olefination conditions; the following represents the second- and third-generations of optimized conditions.* [*Method A*] Phosphonate **4.26** (1.0 equiv.) was dissolved in anhydrous MeCN (0.1 M) under inert atmosphere. C-200 (3.5 equiv.) was added, and the mixture stirred for 40 min at ambient temperature. A solution of octyl aldehyde **4.57** (0.91 equiv.) in dry MeCN, was added to the stirring solution dropwise, and the reaction was monitored by TLC (silica gel, 20% EtOAc in hexanes using CAM stain to monitor product formation; 5% MeOH in CH_2Cl_2 using *p*-anisaldehyde to monitor consumption of phosphonate). Upon completion, the mixture was diluted in EtOAc and quenched by a saturated solution of NH_4Cl (3 × initial volume), washed with brine, dried ($MgSO_4$), filtered, and concentrated *in vacuo*. Crude **4.58** was yielded in 75 – 90%, with (< 10%) remaining starting material. [*Method B*] To a stirring solution of phosphonate **4.26** (1.0 equiv.) in aqueous THF (30:1 *v*/*v*, ≤ 0.076 M), was added Cs_2CO_3 (1.2 equiv.) and left to stir for 2 h under ambient atmosphere and temperature. Octyl aldehyde **4.57** (0.91 equiv.) in aqueous THF, was added to the stirring solution dropwise, and the reaction was monitored by TLC (silica gel, 20% EtOAc in hexanes using CAM stain to monitor product formation; 5% MeOH in CH_2Cl_2 using *p*-anisaldehyde to monitor consumption of phosphonate). The potential formation of a biphasic system suggests the reaction stalled, and requires additional solvent or to be worked up. Upon completion, the mixture was diluted in EtOAc and quenched by 1.0 M HCl (3 × initial volume), washed with brine, dried ($MgSO_4$), filtered, and concentrated *in vacuo*. Crude **4.58** was yielded in 80 – 90%, with varying amounts

of unreacted starting materials. Flash chromatography (silica gel, 10% EtOAc in hexanes) separated the three components efficiently.

R_f = 0.24 (silica gel, 20% EtOAc in hexanes; CAM stain).

^{1}HNMR (300 MHz, $CDCl_3$): δ 6.87 (dt, *J* = 15.9, 6.9 Hz, 1H, -C*H*=), 6.11 (dt, *J* = 15.9, 1.5 Hz, 1H, =C*H*-), 4.64 (p, *J* = 5.8 Hz, 1H, -C*H*-), 2.89 (dd, *J* =15.9, 6.3 Hz, 1H, -CH*H*-), 2.77 (dd, *J* = 15.9, 6.1 Hz, 1H, -CH*H*-), 2.66 (dd, *J* = 15.2, 5.5 Hz, 1H, -CH*H*-), 2.54 (dd, *J* = 15.2, 5.5 Hz, 1H, -CH*H*-), 2.23 (dq, *J* = 1.3, 7.0 Hz, 2H, -CH_2-), 1.48 (p, *J* = 7.3 Hz, 2H, -CH_2-), 1.33 – 1.26 (m, 8H, 4 × -CH_2-), 0.90 (t, *J* = 6.5 Hz, 3H, -CH_3), 0.87 (s, 9H, O-TBS *t*-Bu), 0.12 (s, 3H, O-TBS -CH_3), 0.07 (s, 3H, O-TBS -CH_3) ppm; acid proton absent (H/D exchange).

^{13}CNMR (75 MHz, $CDCl_3$): δ 198.2, 174.6, 149.1, 130.8, 66.0, 46.6, 42.0, 32.6, 31.7, 29.2, 29.0, 28.0, 25.7, 22.6, 17.9, 14.1, -4.8, -5.0 ppm.

HRMS (ESI+ TOF) *m/z*: calculated for $C_{20}H_{38}O_4SiNa$ [$(M + Na)^+$] 393.2437, observed 393.2416 (Δ = 2.1 mmu).

IR (thin film) ν_{max}: 3002, 2944, 2254, 1716, 1636, 1437, 1375, 1039 cm^{-1}.

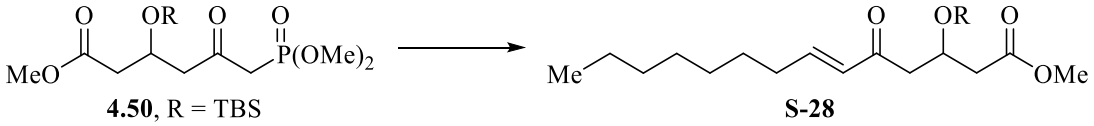

4.50, R = TBS **S-28**

(*E*)-Methyl-3-(*tert*-Butyldimethylsilyloxy)-4-oxotetradec-6-enoate (S-28). Phosphonate **4.50** (11.3 mg, 29.5 µmol, 1.0 equiv.) was dissolved in dry *i*PrOH (0.05 M), and Cs_2CO_3 (17.3 mg, 53.1 µmol, 1.8 equiv.) was added at ambient temperature. The mixture stirred for 1 h. A solution of octyl aldehyde **4.57** (4.7 µL, 26.8 µmol, 0.91 equiv.) in dry *i*PrOH, was added to the mixture dropwise, and the reaction was monitored by TLC (silica gel, 20% EtOAc in hexanes using CAM stain to monitor product formation; 5% MeOH in CH_2Cl_2 using *p*-anisaldehyde to monitor consumption of phosphonate). Upon completion, the mixture was diluted in EtOAc and quenched by 1.0 M HCl (3 × initial volume), washed with brine, dried ($MgSO_4$), filtered, and concentrated *in vacuo* to yield 12.1 mg of crude product with no remaining aldehyde (< 4%). Characterization was assigned from crude material, which contained residual phosphonate (3:1, product:phosphonate).

R_f = 0.72 (silica gel, 20% EtOAc in hexanes; CAM stain).

^{1}HNMR (300 MHz, $CDCl_3$): δ 6.82 (dt, *J* = 15.8, 6.9 Hz, 1H, =C*H*-), 6.07 (dt, *J* = 15.8, 1.7 Hz, 1H, -C*H*=), 4.59 (p, *J* = 6.1 Hz, 1H, -C*H*-), 3.64 (s, 3H, -CO_2CH_3), 2.82 (dd, *J* = 15.6, 6.5 Hz, 1H, -CH*H*-), 2.70 (dd, *J* = 15.6, 6.0 Hz, 1H, -CH*H*-), 2.54 (dd, *J* = 14.9, 5.9 Hz, 1H, -CH*H*-), 2.45 (dd, *J* = 14.9, 6.4 Hz, 1H, -CH*H*-), 2.19 (dq, *J* = 1.4, 7.3 Hz, 2H, -CH_2-), 1.65 – 1.20 (m, "10 H," 5 × -CH_2-), 0.86 (t, *J* = 6.6 Hz, 3H, -CH_3), 0.81 (s, 9H, O-TBS *t*-Bu), 0.04 (s, 3H, O-TBS -CH_3), 0.01 (s, 3H, O-TBS -CH_3) ppm.

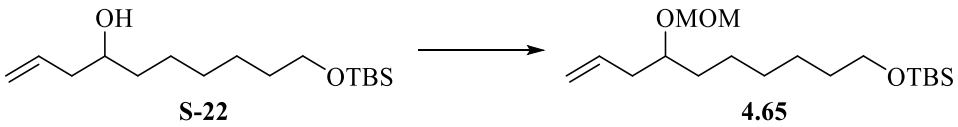

S-22 **4.65**

5-Allyl-13,13,14,14-tetramethyl-2,4,12-trioxa-13-silapentadecane (4.65). Homoallylic alcohol **S-22** (350 mg, 1.22 mmol, 1.0 equiv.) was diluted in CH_2Cl_2 (5 mL) under inert atmosphere. To this solution was added DIPEA (2.2 mL, 12.4 mmol, 10 equiv.), TBAI (45 mg, 0.12 mmol, 10 mol %), and MOMCl (510 μL, 6.25 mmol, 5.0 equiv.). The reaction was protected from light, and stirred for 6 h at ambient temperature. The reaction was monitored (silica gel, 10% EtOAc in hexanes), and upon completion was quenched with $NaHCO_3$ and diluted with EtOAc (20 mL). The aqueous layer was extracted with EtOAc (2 × 10 mL), and the combined organic layers were washed with brine, dried ($MgSO_4$), filtered, and concentrated *in vacuo*. Purification of the crude amber residue was accomplished *via* flash chromatography (5 – 10% EtOAc in hexanes), and yielded 366 mg (1.11 mmol, 93%) of **4.65** as clear, colorless oil.

$\mathbf{R_f}$ = 0.45 (silica gel, 10% EtOAc in hexanes; CAM stain).

^{1}HNMR (400 MHz, $CDCl_3$): δ 5.80 (ddt, *J* = 17.2, 10.2, 7.1 Hz, 1H, -C*H*-), 5.09 – 5.02 (m, 2H, =CH_2), 4.66 (d, *J* = 6.9 Hz, -CH*H*-), 4.62 (d, *J* = 6.9 Hz, -CH*H*-), 3.58 (p, *J* = 5.9 Hz, 1H, -C*H*-), 3.57 (t, *J* = 6.6 Hz, 2H, -CH_2-), 3.56 (s, 3H, -OCH_3), 2.27 (dd, *J* = 7.0, 5.9 Hz, 2H, -CH_2-), 1.48 (q, *J* = 6.6 Hz, 4H, 2 × -CH_2-), 1.37 – 1.23 (m, 6H, 3 × -CH_2-), 0.87 (s, 9H, O-TBS *t*-Bu), 0.02 (s, 6H, 2 × O-TBS -CH_3) ppm.

^{13}CNMR (100 MHz, $CDCl_3$): δ 134.9, 117.0, 95.4, 76.8, 63.3, 55.5, 38.9, 34.1, 32.8, 29.5, 26.0, 25.8, 25.3, 18.4, -5.2 ppm.

HRMS (EI) *m/z*: calculated for $C_{17}H_{35}O_2Si$ [M – MeOH] 299.2406, observed 299.2390 (Δ = 1.6 mmu).

IR (thin film): 2929, 2857, 2359, 1472, 1361, 1255, 1149, 1099, 1042, 916, 668 cm^{-1}.

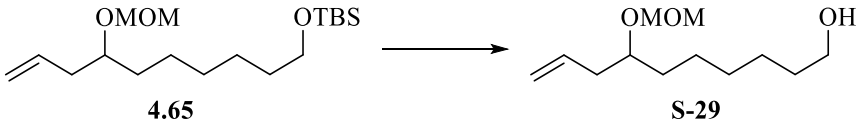

4.65 **S-29**

7-(Methoxymethoxy)dec-9-en-1-ol (S-29). A stirring solution of di-protected **4.65** (360 mg, 1.1 mmol, 1.0 equiv.) in THF (5.5 mL, 0.2 M) was prepared under inert atmosphere, to which 5.5 mL of TBAF (5.5 mmol of commercial 1.0 M solution, 5.0 equiv.) was slowly added at ambient temperature. After 3 hours, total consumption of starting material was realized (silica gel, 10% EtOAc in hexanes), with a large baseline spot visible under CAM stain. The reaction was quenched with NH_4Cl, diluted with EtOAc (15 mL), and washed with brine (3 × 20 mL). The combined organic layers were dried ($MgSO_4$), filtered, and concentrated *in vacuo*. Purification of the crude yellow oil was accomplished *via* flash chromatography (silica gel, 20 – 50% EtOAc in hexanes) to yield 239 mg (1.1 mmol, quant.) of **S-29** as clear, colorless oil.

$\mathbf{R_f}$ = 0.37 (silica gel, 30% acetone in hexanes; CAM stain).

^{1}HNMR (400 MHz, $CDCl_3$): δ 5.80 (ddt, J = 17.3, 10.2, 7.1 Hz, 1H, -C*H*-), 5.09 – 5.02 (m, 2H, =CH_2), 4.66 (d, J = 6.9 Hz, -CH*H*-), 4.62 (d, J = 6.9 Hz, 1H, -CH*H*-), 3.62 (t, J = 6.6 Hz, 2H, -CH_2-), 3.58 (p, J = 5.8 Hz, 1H, -C*H*-), 3.36 (s, 3H, -OCH_3), 2.27 (ddt, J = 7.1, 5.9, 1.2 Hz, 2H, -CH_2-), 1.55 (p, J = 7.0 Hz, 2H, -CH_2-), 1.50 – 1.45 (m, 2H, -CH_2-), 1.38 – 1.28 (m, 6H, 3 × -CH_2-) ppm.

^{13}CNMR (100 MHz, $CDCl_3$): δ 134.8, 117.0, 95.4, 76.8, 63.0, 55.5, 38.9, 34.1, 32.7, 29.5, 25.7, 25.3 ppm.

HRMS (ESI+ TOF) *m/z*: calculated for $C_{12}H_{24}O_3Na$ [$(M + Na)^+$] 239.1623, observed 239.1601 (Δ = 2.2 mmu).

IR (thin film): 3648, 3002, 2943, 2359, 2293, 2253, 1635, 1437, 1375, 1038, 918 cm^{-1}.

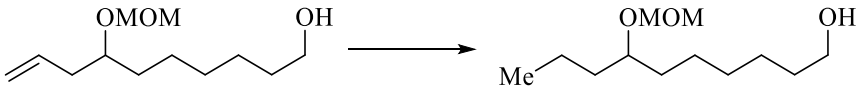

S-29 **S-30**

7-(Methoxymethoxy)decan-1-ol (S-30). To a 50-mL round-bottom flask charged with a teflon stirring bar, a solution of alcohol **S-29** (230 mg) was prepared using 10 mL of HPLC-grade MeOH. Carefully, Pd/C (150 mg) was added and the system was sealed with a three-way valve. One valve was connected to a PIAB vacuum system, and the other to a double-balloon filled with H_2 gas. The flask was carefully evacuated of atmosphere, and back-filled with hydrogen. This process was repeated (5×) to ensure the vessel was completely voided of ambient atmosphere. The flask stirred under a blanket of H_2 gas, and periodically evacuated and back-filled with H_2 gas. Upon completion of the reaction (silica gel, 30% acetone in hexanes), the solution was filtered through a celite plug, and concentrated to yield 182 mg (0.83 mmol, 84%) of **S-30** as clear, colorless oil. The obtained crude product was spectroscopically pure enough to continue to subsequent steps.

R_f = 0.43 (silica gel, 30% acetone in hexanes; CAM stain).

^{1}HNMR (400 MHz, $CDCl_3$): δ 4.63 (s, 2H, -CH_2-), 3.62 (t, J = 6.6 Hz, 2H, -CH_2-), 3.51 (p, J = 5.7 Hz, 1H, -C*H*-), 3.47 (s, 1H, -O*H*), 3.36 (s, 3H, -OCH_3), 1.55 (p, J = 6.8 Hz, 2H, -CH_2-), 1.49 – 1.41 (m, 4H, 2 × -CH_2-), 1.38 – 1.28 (m, 8H, 4 × -CH_2-), 0.90 (t, J = 7.2 Hz, 3H, -CH_3) ppm.

^{13}CNMR (100 MHz, $CDCl_3$): δ 95.4, 77.3, 63.0, 55.5, 36.6, 34.2, 32.8, 29.6, 25.7, 25.2, 18.6, 14.3 ppm.

HRMS (ESI+ TOF) *m/z*: calculated for $C_{12}H_{26}O_3Na$ [$(M + Na)^+$] 241.1780, observed 241.1781 (Δ = 0.1 mmu).

IR (thin film): 3587, 3000, 2944, 1635, 1437, 1375, 1039, 918 cm^{-1}.

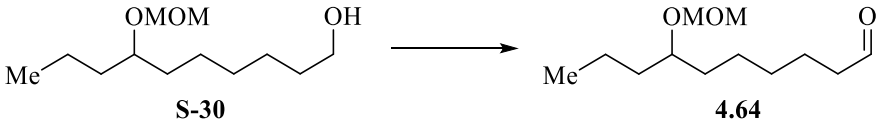

S-30 **4.64**

7-(Methoxymethoxy)decanal (4.64). Purified **S-30** (181.3 mg, 0.83 mmol, 1.0 equiv.) was dissolved in anhydrous CH_2Cl_2 (8.5 mL), and a mixture of PCC (224 mg, 1.04 mmol, 1.2 equiv.) and silica gel (500 mg) was added under inert atmosphere. The reaction stirred for 4 h at ambient temperature, and was monitored by TLC (silica gel, 10% EtOAc in hexanes). Upon completion, CH_2Cl_2 was evaporated, and the obtained dark brown powder was added to a pre-equilibrated column (silica gel, 2% EtOAc in hexanes). Purification yielded 165.1 mg (0.72 mmol, 86%) of **4.64** as clear, colorless oil.

$\mathbf{R_f}$ = 0.59 (silica gel, 30% acetone in hexanes; CAM stain).

^{1}HNMR (300 MHz, $CDCl_3$): δ 9.75 (t, J = 1.8 Hz, 1H, -C*H*O), 4.63 (s, 2H, -CH_2-), 3.51 (p, J = 5.6, 1H, -C*H*-), 3.36 (s, 3H, -CH_3), 2.41 (dt, J = 7.3, 1.8 Hz, 2H, -CH_2-), 1.62 (p, J = 7.3 Hz, 2H, -CH_2-), 1.50 – 1.41 (m, 4H, 2 × -CH_2-), 1.38 – 1.26 (m, 6H, 3 × -CH_2-), 0.90 (t, J = 7.2 Hz, 3H, -CH_3) ppm.

^{13}CNMR (100 MHz, $CDCl_3$): δ 202.8, 95.4, 77.2, 55.5, 43.9, 36.6, 34.0, 29.3, 25.0, 22.1, 18.6, 14.2 ppm.

HRMS (ESI+ TOF) *m/z*: calculated for $C_{12}H_{24}O_3Na$ [$(M + Na)^+$] 239.1637, observed 239.1647 (Δ = 1.0 mmu).

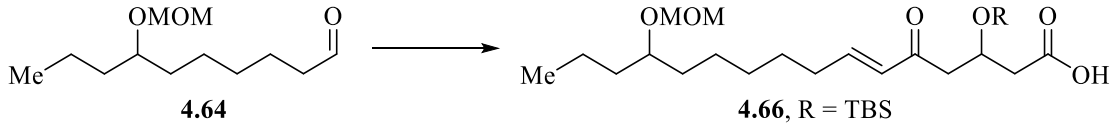

4.64 **4.66**, R = TBS

(*E*)-3-(*tert*-Butyldimethylsilyloxy)-13-(methoxymethoxy)-5-oxohexadec-6-enoic acid (4.66). To a stirring solution of phosphonate **4.26** (71 mg, 0.192 mmol, 1.3 equiv.) in anhydrous MeCN (1.5 mL), was added activated barium hydroxide‡ (230 mg, 0.74 mmol, 5.0 equiv.). The resulting mixture stirred at ambient temperature for 2 hours. A solution of aldehyde **4.64** (32 mg, 0.148 mmol, 1.0 equiv.) in MeCN (1.5 mL, 0.05 M overall) was added dropwise, and stirred overnight. The reaction was monitored (silica gel, 30% acetone in hexanes), and revealed product formation was extremely slowly. The reaction mixture was heated to 36 ºC, and stirred for an additional 18 h. The reaction mixture was diluted in EtOAc (10 mL), and quenched with aqueous HCl (3 × 3 mL, 1.0 M). The combined organic layers were washed with brine, dried ($MgSO_4$), filtered, and concentrated *in vacuo*. The crude oil was purified *via* flash chromatography (silica gel, 10 – 30% acetone in hexanes), and yielded 23 mg (0.05 mmol, 34%) of **4.66** as an inseparable mixture (*d.r.* = 3:1) of diastereomers.

‡ The octahydrate salt, $Ba(OH)_2{\cdot}8H_2O$, was heated at temperatures of 200 ºC for a minimum of 2 h, and finely-ground prior to use in the reaction; this is commonly referred to as C-200, and has been suggested that the micro-crystalline structure of the salt is crucial to catalytic activity in HWE olefinations.[108,110]

R_f = 0.36 (silica gel, 30% acetone in hexanes; *p*-anisaldehyde stain).

^{1}HNMR (400 MHz, $CDCl_3$): δ 6.83 (dt, *J* = 15.8, 6.9 Hz, 1H, -C*H*=), 6.07 (d, *J* = 15.9 Hz, 1H, =C*H*-), 4.631 (s, 2H, -CH_2-, *major*), 4.626 (s, "0.7H," -CH_2-, *minor*), 4.60 (p, *J* = 5.9 Hz, 1H, -C*H*-), 3.51 (p, *J* = 5.7 Hz, 1H, -C*H*-), 3.36 (s, 3H, -OCH_3, *major*), 3.35 (s, "1.8H," -OCH_3, *minor*), 2.84 (dd, 16.1, 6.8 Hz, 1H, -CH*H*-). 2.75 (dd, *J* = 16.1, 5.9 Hz, 1H, -CH*H*-), 2.60 (dd, *J* = 15.1, 5.6 Hz, 1H, -CH*H*-), 2.23 – 2.17 (m, 2H, -CH_2-), 1.50 – 1.41 (m, 8H, 4 × -CH_2-), 1.37 – 1.26 (m, 4H, 2 × -CH_2-), 0.89 (t, *J* = 7.1 Hz, 3H, -CH_3), 0.83 (s, 3H, O-TBS *t*-Bu, minor) 0.82 (s, 9H, O-TBS *t*-Bu, *major*), 0.08 (s, "1H," O-TBS -CH_3, *minor*), 0.07 (s, 3H, O-TBS -CH_3, major), 0.03 (s, "1H," O-TBS -CH_3, *minor*), 0.02(s, 3H, O-TBS -CH_3, *major*) ppm; unassigned peaks/contamination δ 2.33 (t, *J* = 7.5 Hz, 1H), 1.66 – 1.57 (m, 1H, -CH*H*-), 1.37 – 1.26 (m, "1H," -CH*H*-) ppm.

^{13}CNMR (100 MHz, $CDCl_3$): δ 198.2, 175.3, 148.6, 131.0, 95.3, 77.2, 66.1, 55.5, 46.8, 46.7 (*minor*), 42.2, 42.0 (*minor*), 36.6, 34.2, 34.1 (*minor*), 32.5, 39.3, 29.2 (*minor*), 28.0, 25.7, 25.0, 24.9 (*minor*), 18.5, 17.9, 14.2, -4.8, -5.0 ppm; unassigned peaks/contamination δ 33.9, 25.6, 24.7 ppm.

HRMS (ESI+ TOF) *m/z*: calculated for $C_{24}H_{46}O_6SiNa$ [$(M + Na)^+$] 481.2961, observed 481.2943 (Δ = 1.8 mmu).

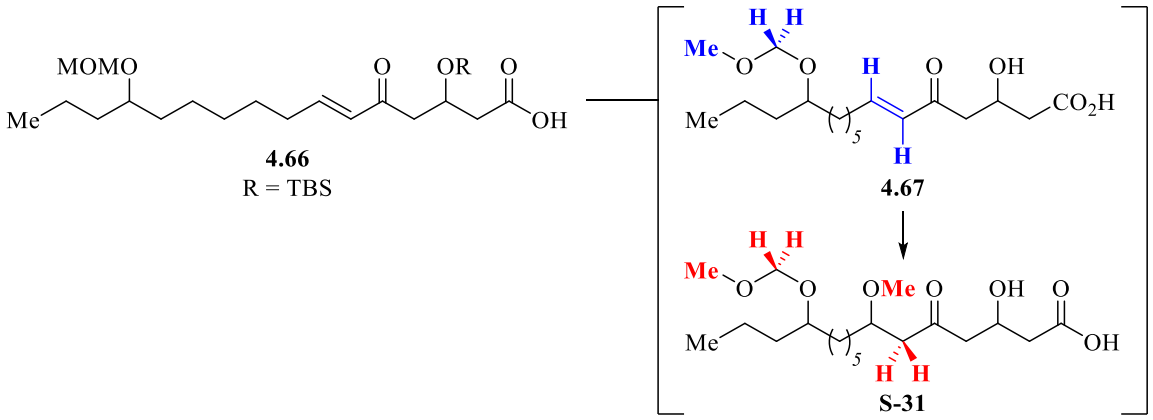

To a stirring solution of **4.66** (21.2 mg, 0.045 mmol, 1.0 equiv.) in a mixture of MeOH and water (10:1, 0.5 mL), aqueous HCl solution (70 µL, 1.0 N) was added and stirred at ambient temperature. After 5 h, the reaction was diluted with EtOAc (10 mL) and washed with brine (3 mL). Spectral data of the crude material revealed clean desilylation of the C3-TBS, but not the desired deacetalization of the C13-MOM. Additionally, conjugate attack by methanol yielded a 1:2 mixture of **4.67**-to-(**S-31**), which was not purified. Please note that for this mixture of products, only the diagnostic signals of **4.67** (highlighted in **blue**) and **S-31** (highlighted in **red**) are reported.

(*E*)-3-hydroxy-13-(methoxymethoxy)-5-oxohexadec-6-enoic acid (4.67)

^{1}HNMR (300 MHz, $CDCl_3$): δ 6.88 (dt, J = 16.0, 7.0 Hz, 1H, =C*H*-), 6.08 (dt, J = 16.0, 1.4 Hz, 1H, -C*H*=), 4.64 (s, 2H, -CH_2-), 3.37 (s, 3H, -OCH_3) ppm.

3-hydroxy-7-methoxy-13-(methoxymethoxy)-5-oxohexadec-6-enoic acid (S-31)

^{1}HNMR (300 MHz, $CDCl_3$): δ 3.65 (s, "6H," C13 -OCH_3), 3.36 (s, "6H," -OCH_3), 2.59 (d, J = 6.3 Hz, "4H," -CH_2-) ppm.

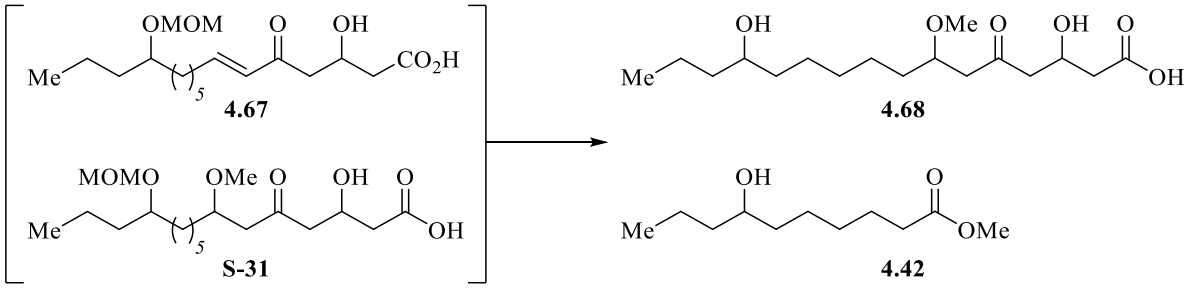

The crude mixture of **4.67**/**S-31** was re-submitted to the same reaction conditions, and monitored by TLC (silica gel, 30% acetone in hexanes). The reaction produced two distinct products after 18 h, upon which it was diluted with EtOAc and washed with brine. Purification of the residue *via* flash chromatography (silica gel, 10 – 30% acetone in hexanes) yielded conjugate addition (**4.68**) and retro-aldol (**4.42**) erosion products.

3,13-dihydroxy-7-methoxy-5-oxohexadecanoic acid (4.68)

R_f = 0.25 (silica gel, 30% acetone in hexanes; *p*-anisaldehyde stain).

^{1}HNMR (400 MHz, $CDCl_3$): δ 4.50 (dddt, J = 2.0, 7.3, 12.0, 4.9 Hz, 1H, -C*H*-), 4.11 (dt, J = 5.0, 9,8 Hz, 1H, -C*H*-), 3.69 (s, 3H, -OCH_3), 3.61 – 3.55 (m, 1H, -C*H*-), 2.64(dd, J = 8.5, 15.5 Hz, 1H, -CH*H*-), 2.59 – 2.52 (m, 2H, -CH_2-), 2.47 (dd, J = 5.3, 15.2 Hz, 1H, -CH*H*-), 2.30 (ddd, J = 1.4, 7.8, 14.4 Hz, 1H, -CH*H*-), 2.26 (ddd, J = 1.5, 5.8, 14.4 Hz, 1H, -CH*H*-), 1.67 – 1.60 (m, 1H, -CH*H*-), 1.48 – 1.37 (m, 10H, 8 × -CH*H*- & 2 × -O*H*), 1.35 – 1.28 (m, 5H, 5 × -CH*H*-), 0.91 (t, J = 7.0 Hz, 3H, -CH_3) ppm.

^{13}CNMR (100 MHz, $CDCl_3$): δ 206.5, 170.7, 72.93, 72.87, 71.62, 71.59, 68.46, 68.40, 51.89, 46.71, 46.69, 46.45, 46.43, 39.94, 39.93, 39.72, 39.71, 37.3, 33.89, 33.86, 29.30, 29.28, 25.50, 25.47, 18.8, 14.1 ppm.

Methyl 7-hydroxydecanoate (4.42)

Characterization data identical to ester by-product generated as a minor product during evaluation of tandem hydrogenation/hydrogenolysis conditions (*vide infra*). Characterization data for **4.42** proved consistent with previously reported literature data.[152]

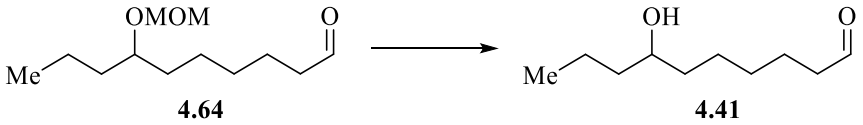

4.64 **4.41**

7-hydroxydecanal (4.28). A stirring solution of MOM-protected aldehyde **4.64** (17.5 mg, 0.081 mmol, 1.0 equiv.) in anhydrous THF (0.85 mL) was carefully evacuated of atmosphere, and back-filled with inert gas. This process was repeated three times, upon which concentrated HCl (60 μL, 12 M) was added and stirred at ambient temperature. The reaction was monitored (silica gel, 30% acetone in hexanes) for consumption of the starting material. Upon completion, the reaction was cooled to 0 ºC, diluted with EtOAc (5 mL) and quenched with $NaHCO_3$ (3 mL). The aqueous layer was re-extracted with EtOAc (3 mL). The combined organic layers were washed with water (3 mL), and brine (2 × 4 mL), dried ($MgSO_4$), filtered, and evaporated *in vacuo*, to yield 11 mg of **4.41** (0.063 mmol, 78%). This crude alcohol was spectroscopically pure-enough to be used directly in the subsequent step.

Characterization data was identical to **4.41** previously obtained *via* tandem hydrogenation/hydrogenolysis of benzyl ether conditions (*vide supra*).

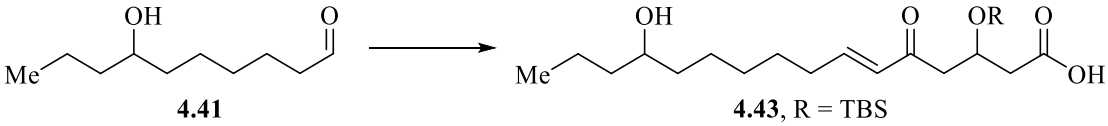

4.41 **4.43**, R = TBS

(*E*)-3-(*tert*-Butyldimethylsilyloxy)-13-hydroxy-5-oxohexadec-6-enoic acid (4.43). Phosphonate **4.26** (28.3 mg, 0.077 mmol, 1.2 equiv.) was dissolved in aqueous THF (0.4 mL, 30:1 THF:H_2O), and cesium carbonate (32.5 mg, 0.100 mmol, 1.5 equiv.) was added in one portion. The mixture stirred for 2 hours at ambient temperature. A solution of aldehyde **4.41** (11 mg, 0.064 mmol, 1.0 equiv.) in aqueous THF (0.43 mL, 30:1 THF:H_2O, 0.076 M overall reaction mixture) was added dropwise, and the reaction mixture was stirred overnight, and monitored by TLC for appearance of a deep red-purple spot (silica gel, 30% acetone in hexanes; *p*-anisaldehyde stain). The reaction stalled if the mixture becomes biphasic, and requires additional solvent to be added dropwise. Upon completion, the reaction was diluted with EtOAc (10 mL), and quenched by the addition of 1.0 M HCl solution (1 mL). The mixture was extracted with EtOAc (2 × 3 mL), and the combined organic layers were washed with brine (2 × 2 mL), dried ($MgSO_4$), filtered, and concentrated *in vacuo*. Purification *via* column chromatography (20% acetone in hexanes) yielded 4.8 mg of recovered aldehyde **4.41**, and 7.6 mg of acid **4.43** (0.018 mmol, 51% BRSM) as clear, colorless oil. This procedure represents a single attempt; the given yield was not optimized, nor is it considered indicative for the efficiency of this process.

R_f = 0.33 (silica gel, 30% acetone in hexanes; *p*-anisaldehyde stain).

^{1}HNMR (300 MHz, $CDCl_3$): δ 6.84 (dt, *J* = 15.9, 7.0 Hz, 1H, =C*H*-), 6.07 (dt, *J* = 15.9, 1.4 Hz, 1H, -C*H*=), 4.60 (p. *J*= 5.8 Hz, 1H, -C*H*-), 3.63 – 3.55 (m, 1H, -C*H*-), 2.85 (dd, *J* = 6.4, 15.9 Hz, 1H, -CH*H*-), 2.77 (dd, *J* = 6.2, 15.9 Hz, 1H, -CH*H*-), 2.62 (dd, *J* = 5.7, 15.6 Hz, 1H, -CH*H*-), 2.51 (dd, *J* = 5.2, 15.6 Hz, 1H, -CH*H*-), 2.24 (dd, *J* = 1.4, 7.1 Hz, 1H, -CH*H*-), 2.19 (dd, *J* = 1.4, 7.4 Hz, 1H, -CH*H*-), 1.52 – 1.26 (m, 12H, 6 × -CH_2-), 0.91 (t, *J* = 6.9 Hz, 3H, -CH_3), 0.84 (s, 9H, O-TBS *t*-Bu), 0.09 (s, 3H, O-TBS -CH_3), 0.04 (s, 3H, O-TBS -CH_3) ppm.

^{13}CNMR (75 MHz, $CDCl_3$): δ 198.1, 173.8, 148.8, 130.9, 71.6, 66.0, 46.5, 41.8, 39.7, 37.2, 32.4, 29.1, 27.9, 25.7, 25.3, 18.8, 17.9, 14.1, -4.8, -5.0 ppm.

HRMS (ESI+ TOF) *m/z*: calculated for $C_{22}H_{42}O_5SiNa$ [$(M + Na)^+$] 437.2699, observed 437.2700 (Δ = 0.1 mmu).

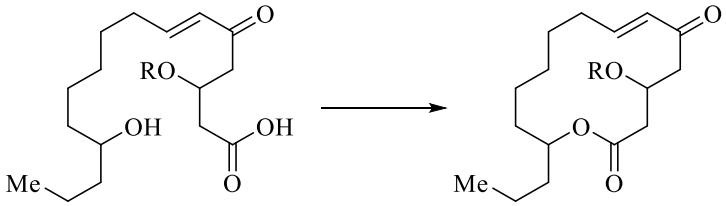

4.43, R = TBS **4.69**

(*E*)-4-(*tert*-Butyldimethylsilyloxy)-14-propyloxacyclotetradec-7-ene-2,6-dione (4.69). To a cooled (0 ºC) solution of acid **4.43** (7.5 mg, 0.018 mmol, 1.0 equiv.) in THF (350 µL, 0.05 M), was and added triethylamine (15.2 µL, 0.11 mmol, 6.0 equiv.) under inert atmosphere. This solution stirred for 15 min, upon which 2,4,6-trichlorobenzoyl chloride (14.2 µL, 0.09 mmol, 5.0 equiv.) was added to afford a colorless, murky solution. The mixture stirred for 2 h, and warmed to ambient temperature. Upon consumption of starting material (silica gel, 30% acetone in hexanes; *p*-anisaldehyde stain), this solution was added dropwise over a 12 h period to a second flask containing powdered DMAP (55 mg, 0.45 mmol, 25.0 equiv.) in toluene (18 mL, 0.001 M). The clear, pale yellow reaction stirred at ambient temperature, and was monitored by TLC (silica gel, 10% EtOAc in hexanes; *p*-anisaldehyde stain). Upon completion, the reaction was evaporated *in vacuo*, diluted with hexanes, and the white residues passed through a silica plug. Careful purification *via* column chromatography (1 – 5% gradient of EtOAc in hexanes) yielded 4.7 mg of macrocycle **4.69** (0.012 mmol, 66%) as clear, colorless oil. This non-selective preparation of **4.69** yielded an inseparable mixture of diastereomers (*d.r.* = 1:1).

R_f = 0.27 (silica gel, 10% EtOAc in hexanes; *p*-anisaldehyde stain).

^{1}HNMR (300 MHz, $CDCl_3$): δ 6.84 (m, 2H, 2 × =C*H*-), 6.04 (ddt, *J* = 20.1, 15.9, 1.5 Hz, 2H, 2 × -C*H*=), 5.00 – 4.88 (m, 2H, 2 × -C*H*-), 4.50 – 4.37 (m, 2H, 2 × -C*H*-), 3.23 (dd, *J* = 7.1, 13.3 Hz, 1H, -CH*H*-), 2.95 (dd, *J* = 8.5, 12.7 Hz, 1H, --CH*H*-), 2.75 (dd, *J* = 4.6, 12.7 Hz, 1H, -CH*H*-), 2.65 (dd, *J* = 6.9, 13.3 Hz, 1H, -CH*H*-), 2.60 (dd, *J* = 7.9, 16.7 Hz, 1H, -CH*H*-), 2.53 (d, *J* = 3.4 Hz, 1H, -CH*H*-), 2.48 – 2.45 (m, 2H, 2 × -CH*H*-), 2.36 – 2.18 (m, 4H, 2 × -CH_2-), 1.54 – 1.48 (m, 4H, -CH_2-, 2× -CH*H*-), 1.48 – 1.42 (m, 4H, 4 × -

CH*H*-), 1.42 – 1.33 (m, 6H, 6 × -CH*H*-), 1.33 – 1.20 (m, 10H, 4 × -C*H*$_2$-, 2 × -CH*H*-), 0.87 (dt, *J* = 1.9, 7.3 Hz, 6H, 2 × -C*H*$_3$), 0.86 (s, 9H, O-TBS *t*-Bu), 0.85 (s, 9H, O-TBS *t*-Bu), 0.083 (s, 3H, O-TBS -C*H*$_3$), 0.077 (s, 3H, O-TBS -C*H*$_3$), 0.06 (s, 3H, O-TBS -C*H*$_3$), 0.04 (s, 3H, O-TBS -C*H*$_3$) ppm.

^{13}CNMR (75 MHz, $CDCl_3$): *δ* 199.6, 198.1, 170.5, 170.0, 150.1, 149.1, 132.2, 131.8, 73.9, 73.8, 67.4, 66.8, 47.3, 45.8, 42.4, 42.1, 37.2, 36.8, 33.2, 32.8, 32.4, 31.5, 27.9, 27.1, 26.4, 25.8, 25.7, 24.9, 23.8, 18.6, 18.5, 17.9, 13.94, 13.90, -4.9, -5.0 ppm.

HRMS (ESI+ TOF) *m/z*: calculated for $C_{22}H_{40}O_4SiNa$ [(M + Na)$^+$] 419.2594, observed 419.2586 (Δ = 0.8 mmu).

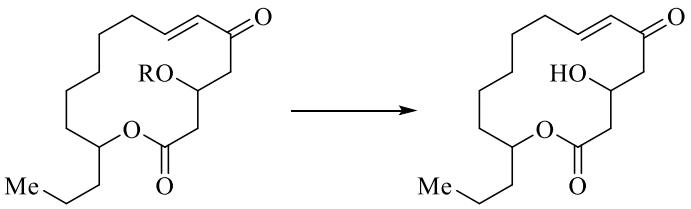

4.69, R = TBS **4.63**

(*E*)-4-Hydroxy-14-propyloxacyclotetradec-7-ene-2,6-dione (4.63). Macrolactone **4.69** (3.5 mg, 8.8 μmol, 1.0 equiv.) was added to a 1.5 mL polypropylene Eppendorf tube, and dissolved in acetonitrile (120 μL, 0.07 M). Pyridine (4.8 μL, 61.9 μmol, 7.0 equiv.) was added, and the reaction mixture was vortexed to homogeneity. To this solution, 48% HF (12 μL, 0.6 mmol, 70 equiv.) was added, and the reaction mixture was again vortexed, centrifuged, and left for 5 h at ambient temperature. The reaction was quenched with water (2 × 1 mL) and diluted with EtOAc (2 × 2 mL). The aqueous layer was re-extracted with EtOAc, and the combined organic layers were washed with brine, dried ($MgSO_4$), filtered, and concentrated *in vacuo*. The product was carefully purified using pipette chromatography (silica gel, 10 - 20% acetone in hexanes) to afford a 1.8 mg diastereomeric mixture of **4.63** (6.4 μmol, 73%) as clear, colorless oil. This procedure represents a single attempt; the obtained yield was not optimized, nor considered indicative for the efficiency of this process.

R$_f$ = 0.36 (silica gel, 30% acetone in hexanes; *p*-anisaldehyde stain).

^{1}HNMR (600 MHz, $CDCl_3$): *δ* 6.80 (dddd, *J* = 4.5, 5.6, 9.9, 16.1 Hz, 2H, 2 × -C*H*=). 6.07 (ddd, *J* = 0.6, 2.2, 16.1 Hz, 1H, =C*H*-), 6.03 (ddd, *J* = 0.7, 2.2, 16.1 Hz, 1H, =C*H*-), 5.02 (ddd, *J* = 10.1, 7.8, 5.1, 2.5 Hz, 1H, -C*H*-), 4.97 (dddd, *J* = 10.2, 7.7, 5.1, 2.6 Hz, 1H, -C*H*-), 4.34 (qd, *J* = 8.7, 4.2 Hz, 1H, -C*H*-), 4.28 (tdd, *J* = 11.8, 5.6, 2.3 Hz, 1H, -C*H*-), 4.05 (d, *J* = 10.0 Hz, 1H, -O*H*), 3.75 (d, *J* = 10.1 Hz, 1H, -O*H*), 3.42 (dd, *J* = 15.1, 3.2 Hz, 1H, -CH*H*-), 3.38 (dd, *J* = 13.9, 9.7 Hz, 1H, -CH*H*-), 2.74 (ddd, *J* = 16.8, 4.1, 1.5 Hz, 1H, -CH*H*-), 2.66 (ddd, *J* = 17.0, 5.6, 1.2 Hz, 1H, -CH*H*-), 2.58 (ddd, *J* = 13.9, 5.5, 1.2 Hz, 1H, -CH*H*-), 2.51 (ddd, *J* = 15.4, 4.7, 1.5 Hz, 1H, -CH*H*-), 2.48 – 2.44 (m, 2H, 2 × -CH*H*-), 2.42 (dd, *J* = 15.1, 1.9 Hz, 1H, -CH*H*-), 2.38 (dd, *J* = 14.9, 9.5 Hz, 1H, -CH*H*-), 2.27 – 2.18 (m, 2H, 2 × -CH*H*-), 1.73 – 1.66 (m, 2H, 2 × -

CH*H*-), 1.64 – 1.52 (m, 4H, 4 × -CH*H*-), 1.52 – 1.44 (m, 4H, 4 × -CH*H*-), 1.44 – 1.36 (m, 4H, 4 × -CH*H*-), 1.35 – 1.18 (m, 10H, 4 × -CH_2- & 2 × -CH*H*-), 0.87 (td, *J* = 7.4, 3.1 Hz, 6H, 2 × -CH_3) ppm.

^{13}CNMR (150 MHz, $CDCl_3$): δ 203.6, 199.7, 172.7, 171.1, 153.4, 151.9, 132.9, 132.4, 74.3, 73.8, 66.7, 66.5, 42.7, 40.0, 38.9, 37.9, 37.0, 36.9, 34.0, 33.9, 32.8, 32.7, 28.11, 28.08, 26.72, 26.69, 25.5, 25.4, 18.68, 18.66, 13.85, 13.82 ppm.

HRMS (ESI+ TOF) *m/z*: calculated for $C_{16}H_{26}O_4Na$ [(M + Na)$^+$] 305.1729, observed 305.1750 (Δ = 2.1 mmu).

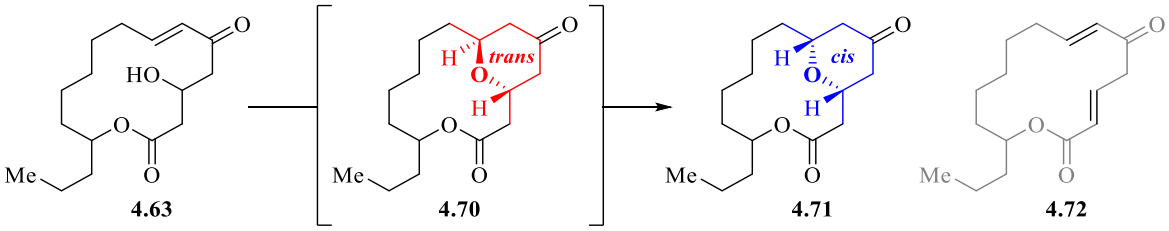

To a 2.5 mm NMR tube charged with oxa-conjugate precursor **4.63** (1.3 mg, 4.6 μmol, 1.0 equiv.) in $CDCl_3$ (0.3 mL), was added Amberlyst-15® hydrogen form (~ 30 beads) at ambient temperature. The mixture was monitored by ^{1}HNMR and TLC (silica gel, 30% acetone in hexanes) hourly. Within 4 h, ^{1}HNMR and TLC showed a complex mixture of compounds with higher R_f values. The reaction was left overnight, to little effect. The relative diastereoselectivity slightly favored the *trans*-pyranone products (*d.r.* ~ 5:4, based on ^{1}HNMR analysis of crude reaction mixture). The reaction was heated to 80 ºC, and was monitored by ^{1}HNMR. Key proton shifts in the range of δ 5.07 – 3.35 (H3, H7, H13, OH) monitored thermodynamic conversion. Upon completion, the reaction mixture was carefully filtered, and even-more carefully purified by column chromatography in a glass pipette (silica gel, 10% freshly-distilled acetone in freshly-distilled hexanes) to afford relative ***cis*-4.71** as colorless oil (*d.r.* > 50:1). Product was concentrated under a stream of nitrogen. This procedure represents the single attempt at oxa-conjugate addition, and subsequent equilibration. Characterization of kinetic ***trans*-4.70** was retroactively-based on spectral analysis of crude reaction mixture. This was accomplished using differences between it and signals from both the starting material **4.63** and thermodynamic product ***cis*-4.71**. Not all signals were accounted for, and may be buried. Characterization is reported for key proton shifts (H3, H7, H13); the complex mixture presented far too much ambiguity to accurately assign remaining signals.

***trans*-5-Propyl-4,15-dioxabicyclo[9.3.1]pentadecane-3,13-dione (4.70).**

^{1}HNMR (600 MHz, $CDCl_3$): δ 5.05 – 4.98 (m, 3H, -C*H*- ***trans*** minor; -C*H*- ***cis*** major; -C*H*- ***cis*** minor), 4.95 (ddd, *J* = 13.3, 7.1, 3.7 Hz, 1H, -C*H*- ***trans*** major), 4.90 – 4.85 (m, 1H, -C*H*- ***trans*** minor), 4.45 (tt, *J* = 10.8, 2.9 Hz, 1H, -C*H*- ***trans*** major), 4.33 – 4.29 (m, 1H, -C*H*- ***trans*** major), 4.11 (tt, *J* = 10.8, 2.3 Hz, -C*H*- ***trans*** minor), 4.01 (tt, *J* = 10.3, 3.5 Hz, 1H, -C*H*- ***cis*** minor), 3.93 (tt, *J* = 11.2, 2.7 Hz, 1H, -C*H*- ***cis***

major), 3.71 – 3.67 (m, 1H, -C*H*- ***cis*** minor), 3.53 – 3.48 (m, 1H, -C*H*- ***cis*** major) ppm; based on crude reaction mixture, and reported as whole numbers to represent the following kinetic ratios (*trans* major: 1H = 1.00H, *trans* minor: 1H = 0.70H | *cis* major: 1H = 1.00H, *cis* minor: 1H = 0.31H).

^{13}CNMR (150 MHz, $CDCl_3$): δ 206.7, 206.4, 169.7, 75.9, 75.8, 73.7, 72.1, 68.2, 68.0, 48.8, 47.7, 47.0, 46.8, 45.5, 42.9, 38.6, 37.9, 35.9, 34.9, 34.4, 30.3, 28.7, 25.2, 24.8, 24.5, 21.7, 21.4, 19.0, 18.74, 13.96, 13.91 ppm; missing second *C*1 carbonyl signal.

***cis*-5-Propyl-4,15-dioxabicyclo[9.3.1]pentadecane-3,13-dione (4.71).**

R_f = 0.13 (silica gel, 10% acetone in hexanes; *p*-anisaldehyde stain).

^{1}HNMR (600 MHz, $CDCl_3$): δ 5.05 – 4.98 (m, 2H, -C*H*- ***cis*** major; -C*H*- ***cis*** minor), 4.01 (tt, *J* = 10.3, 3.5 Hz, 1H, -C*H*- ***cis*** minor), 3.93 (tt, *J* = 11.2, 2.7 Hz, 1H, -C*H*- ***cis*** major), 3.71 – 3.67 (m, 1H, -C*H*- ***cis*** minor), 3.53 – 3.48 (m, 1H, -C*H*- ***cis*** major), 2.67 (dt, *J* = 14.2, 3.8 Hz, 1H, -CH*H*- ***cis*** minor), 2.48 (dt, *J* = 11.7, 3.8 Hz, 1H, -CH*H*- ***cis*** major), 2.44 – 2.40 (m, 2H), 2.38 – 2.29 (m, 2H), 2.25 (dd, *J* = 11.6, 3.9 Hz, 1H, -CH*H*- ***cis*** major), 2.23 (dd, *J* = 11.6, 3.3 Hz, 1H, -CH*H*- ***cis*** major), 1.98 – 1.91 (m, 1H, -CH*H*-, ***cis*** major), 1.90 – 1.86 (m, 1H, -CH*H*- ***cis*** minor), 1.76 – 1.70 (m, 1H), 1.65 – 1.62 (m, 1H), 1.49 – 1.37 (m), 1.36 – 1.30 (m), 1.21 – 1.85 (m), 1.17 – 1.05 (m), 0.91 (dt, *J* = 7.3 Hz, 3H, -CH_3), 0.87 – 0.82 (m) ppm; when possible, reported as whole numbers to represent the following thermodynamic product ratio (*cis* major: 1H = 1.0H, *cis* minor: 1H = 0.2H).

^{13}CNMR (150 MHz, $CDCl_3$): δ 206.0, 171.9, 78.5, 75.0, 73.0, 48.4, 47.2, 42.7, 37.4, 32.5, 32.4, 27.0, 25.4, 22.0, 18.7, 14.0 ppm.

HRMS (ESI+ TOF) *m/z*: calculated for $C_{16}H_{26}O_4Na$ [$(M + Na)^+$] 305.1729, observed 305.1747 (Δ = 1.8 mmu).

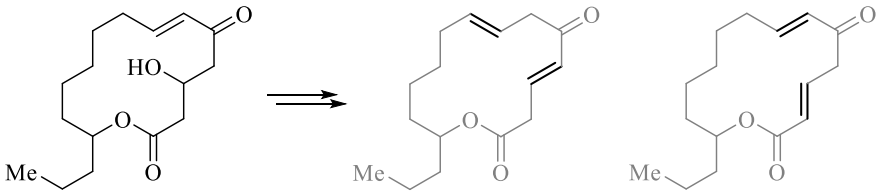

4.63 **4.72** **4.73**

Formation of putative elimination side-products was proposed based on crude reaction mixtures. Key peaks that suggested formation of isomerization compound **4.72** were observed as a minor by-product of acid-mediated transannular oxa-conjugate addition under kinetic conditions, while conjugated ester **4.73** was observed as a minor by-product under thermodynamic conditions. Characterization was proposed based on key signals.

***β',γ'*-Unsaturated Ketone Diene (4.72)**

^{1}HNMR (600 MHz, $CDCl_3$): δ 6.84 – 6.79 (m, 1H, -C*H*=), 6.23 (dt, *J* = 15.9, 1.4 Hz, 1H, =C*H*-), 5.47 – 5.37 (m, 2H, 2 × -C*H*=) ppm.

***α,β*-Unsaturated Ester Diene (4.73)**

^{1}HNMR (600 MHz, $CDCl_3$): δ 7.26 (dd, *J* = 9.4, 6.2 Hz, 1H, -C*H*=), 6.69 (dtd, *J* = 15.6, 7.3, 1.9 Hz, 1H, -C*H*=), 6.15 (dd, *J* = 9.3, 0.9 Hz, 1H, -C*H*=), 5.94 (d, *J* = 7.0 Hz, 1H, -C*H*=) ppm.

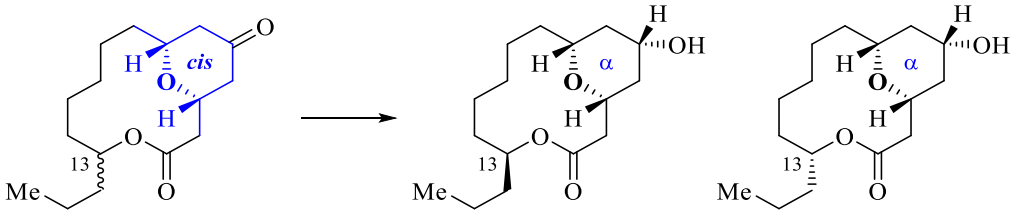

***α*-*cis*-13-Hydroxy-5-propyl-4,15-dioxabicyclo[9.3.1]pentadecan-3-one.** In a 150 µL low-volume HPLC vial insert, the obtained *cis*-pyranone **4.71** (≤ 200 µg) in HPLC-grade MeOH (100 µL) was added $NaBH_4$ (3 equiv.), agitated, centrifuged, and left at ambient temperature. After 5 h, the reaction mixture was carefully extracted with $CDCl_3$ and dried under a low stream of nitrogen. LC-SPE-NMR was conducted using an Agilent 1260 interfaced with a Prospekt 2 (Spark Holland) solid-phase extraction module, using HySphere Resin GP cartridges. Separation relied on a reverse phase Agilent Zorbax C18 column (100 mm × 2.1 mm I.D., 3.5 µm particle size). Mobile phases throughout the analysis were water (H_2O, Phase A) and acetonitrile (MeCN, Phase B). The chromatography method had a flow-rate of 0.25 mL/min. The mobile phase was held at 30% Phase B over 3 minutes, followed by a linear gradient to 100% Phase B over 14 minutes. A 4-minute hold at 100% Phase B flushed the column and was re-equilibrated at 30% Phase B for an additional 4-minutes, for a total run-time of 25 minutes. Peak-trapping was conducted over the entire run into new cartridges, at 5-minute intervals (total of 5 cartridges). Ten trapping experiments were performed with trapping on the same set of solid-phase cartridges. Compounds were eluted from the cartridges using deuterated acetonitrile (CD_3CN, 60 µL), and NMR spectra was recorded on a Bruker Avance III instrument, with cryoprobe operating at 600 MHz. We proposed the major product is **4.74**, and the minor product is its C13 epimer, **4.76**.

^{1}HNMR (600 MHz, CD_3CN): δ 4.96 (dq, *J* = 5.6, 7.3 Hz, 1H, -C*H*-), 4.92 – 4.89 (m, 0.2H, -C*H*-), 3.74 – 3.68 (m, 1.2H, 2 × -C*H*-), 3.59 (tt, *J* = 2.4, 11.3 Hz, 1H, -C*H*-), 3.40 – 3.37 (m, 0.2H, -C*H*-), 3.24- 3.20 (m, 1H, -C*H*-), 2.89 – 2.87 (m, 1H, -CH*H*-), 2.64 (dd, *J* = 3.7, 14.2 Hz, 0.2H, -CH*H*-), 2.36 (dd, *J* = 2.9, 11.7 Hz, 1H, -CH*H*-), 2.28 (t, *J* = 11.2 Hz, 1H, -CH*H*-), 1.78 (ddt, *J* = 12.3, 4.6, 1.8 Hz, 1.2H, 2 × -CH*H*-), 1.62 – 1.59 (m), 1.57 – 1.52 (m), 1.50 – 1.46 (m), 1.44 – 1.39 (m), 1.37 – 1.30 (m), 1.18 – 1.13 (m, 1.3H, 2 × -CH*H*-), 1.10 – 1.04 (m), 0.92 (t, *J* = 7.3 Hz, 3H, -CH_3) ppm; missing peaks for major isomer are assumed

to be buried under LC-SPE acetonitrile peaks. Possible signals representing *β*-isomers: *δ* 4.12 (p, *J* = 2.7 Hz, 0.08H, -C*H*-), 4.02 (ddd, *J* = 9.0, 2.7 Hz, 0.08H, -C*H*-), 3.52 – 3.48 (m, 0.08H, -C*H*-), 2.76 (t, *J* = 3.0 Hz, -C*H*-) ppm.

HRMS (ESI+ TOF) *m/z*: calculated for $C_{16}H_{28}O_4Na$ [(M + Na)$^+$] 307.1885, observed 307.1905 (Δ = 2.0 mmu).

LC-SPE (t_R): 10-15 min.

Observed peaks proved consistent with literature data.[39]

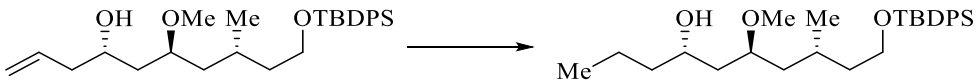

4.37 **S-32**

(4*S*,6*S*,8*R*)-10-(*tert*-Butyldiphenylsilyloxy)-6-methoxy-8-methyldecan-4-ol (S-32). To a 50-mL round-bottom flask charged with a teflon stirring bar, a solution of alcohol **4.37** (400 mg, 0.88 mmol) was prepared using 12 mL of HPLC-grade MeOH at ambient temperature. Carefully, Pd/C (175 mg) was added and the system was sealed with a three-way valve. One valve was connected to a PIAB vacuum system, and the other to a double-balloon filled with H_2 gas. The flask was carefully evacuated of atmosphere, and back-filled with hydrogen. This process was repeated (5×) to ensure complete voiding of air. The reaction stirred vigorously under a blanket of H_2 gas, and was periodically evacuated and back-filled with H_2 gas. Upon completion of the reaction (silica gel, 20% EtOAc in hexanes), the solution was filtered through a celite plug, and concentrated to yield 399 mg (quant.) of **S-32** as clear, colorless oil.

R_f = 0.40 (silica gel, 20% EtOAc in hexanes; CAM stain).

^{1}HNMR (400 MHz, $CDCl_3$): *δ* 7.66 – 7.63 (m, 4H, 4 × -C*H*- Ph), 7.42 – 7.34 (m, 6H, 6 × -C*H*- Ph), 3.90 – 3.84 (m, 1H, -C*H*-), 3.73 – 3.62 (m, 2H, -CH_2-), 3.32 (s, 3H, -CH_3), 2.93 (br s, 1H, -O*H*), 1.79 – 1.57 (m, 4H, -C*H*-, 3 × -CH*H*-), 1.51 – 1.40 (m, 3H, 3 × -CH*H*-), 1.38 – 1.29 (m, 3H, -CH*H*-, -CH_2-), 1.18 (ddd, *J* = 13.8, 7.4, 5.6 Hz, 1H, -CH*H*-), 1.03 (s, 9H, O-TBDPS *t*-Bu), 0.91 (t, *J* = 7.0 Hz, 3H, -CH_3), 0.85 (d, *J* = 6.7 Hz, 3H, -CH_3) ppm.

^{13}CNMR (150 MHz, $CDCl_3$): *δ* 135.6, 134.0, 129.5, 127.6, 77.8, 68.5, 61.8, 56.7, 41.0, 40.0, 39.7, 39.1, 26.8, 26.3, 20.0, 19.2, 18.8, 14.1 ppm.

HRMS (ESI+ TOF) *m/z*: calculated for $C_{28}H_{44}O_3SiNa$ [(M + Na)$^+$] 479.2957, observed 479.2946 (Δ = 1.1 mmu).

IR (thin film) ν_{max}: 3447, 2928, 1589, 1463, 1427, 1379, 1187, 1105, 1085 cm^{-1}.

$[\alpha]_D^{20}$ = + 11.3º (*c* = 11.9 mg/2.5 mL, $CHCl_3$; *l* = 100 mm; α = + 0.0537º).

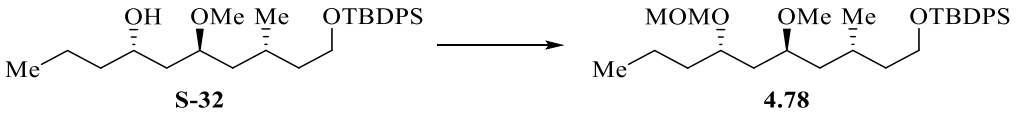

S-32 **4.78**

(5*S*,7*S*,9*R*)-7-Methoxy-9,14,14-trimethyl-13,13-diphenyl-5-propyl-2,4,12-trioxa-13-silapentadecane (4.78). Homoallylic alcohol **S-32** (395 mg, 0.87 mmol, 1.0 equiv.) was dissolved in CH_2Cl_2 (3.5 mL), under inert atmosphere. To this solution was added DIPEA (1.5 mL, 8.7 mmol, 10 equiv.), TBAI (32.5 mg, 0.09 mmol, 10 mol %), and MOMCl (350 μL, 4.4 mmol, 5.0 equiv.). The reaction mixture was protected from light, and stirred for 6 h at ambient temperature while monitored by TLC (silica gel, 10% EtOAc in hexanes). Upon completion, the reaction was quenched with $NaHCO_3$ and diluted with EtOAc (20 mL). The aqueous layer was extracted with EtOAc (2 × 10 mL), and the combined organic layers were washed with brine, dried ($MgSO_4$), filtered, and concentrated *in vacuo*. Purification of the amber residue *via* flash chromatography (5 – 10% EtOAc in hexanes) yielded 408 mg (0.81 mmol, 94%) of **4.78** as clear, colorless oil.

R_f = 0.36 (silica gel, 10% EtOAc in hexanes; CAM stain).

^{1}HNMR (600 MHz, $CDCl_3$): δ 7.65 (d, *J* = 7.2 Hz, 4H, 4 × -C*H*- Ph), 7.40 (t, *J* = 7.2 Hz, 2H, 2 × -C*H*- Ph), 7.36 (t, *J* = 7.2 Hz, 4H, 4 × -C*H*- Ph), 4.66 (d, *J* = 6.7 Hz, 1H, -CH*H*-), 4.63 (d, *J* = 6.7 Hz, 1H, -CH*H*-), 3.72 – 3.65 (m, 3H, -C*H*- & -CH_2-), 3.44 – 3.40 (m, 1H, -C*H*-), 3.37 (s, 3H, -CH_2OCH_3), 3.29 (s, 3H, -CHOCH_3), 1.77 (dt, *J* = 6.4, 12.8 Hz, 1H, -C*H*-), 1.65 – 1.59 (m, 1H, -CH*H*-), 1.58 – 1.48 (m, 4H, 2 × -CH*H*- & -CH_2-), 1.47 – 1.41 (m, 1H, -CH*H*-), 1.38 – 1.33 (m, 3H, -CH*H*- & -CH_2-), 1.13 (ddd, *J* = 13.7, 8.2, 5.7 Hz, 1H, -CH*H*-), 1.03 (s, 9H, O-TBDPS *t*-Bu), 0.90 (t, *J* = 7.2 Hz, 3H, -CH_3), 0.86 (d, *J* = 6.6 Hz, 3H, -CH_3) ppm.

^{13}CNMR (150 MHz, $CDCl_3$): δ 135.6, 134.1, 129.5, 127.6, 95.9, 75.5, 75.0, 62.0, 55.9, 55.6, 42.0, 40.4, 40.1, 37.5, 26.8, 26.2, 19.9, 19.2, 18.2, 14.3 ppm.

HRMS (ESI+ TOF) *m/z*: calculated for $C_{30}H_{48}O_4SiNa$ [$(M + Na)^+$] 523.3220, observed 523.3216 (Δ = 0.4 mmu).

IR (thin film) ν_{max}: 2927, 1589, 1463, 1427, 1379, 1187, 1091, 1039 cm^{-1}.

$[\alpha]_D^{20}$ = + 14.1° (*c* = 7.7 mg/2.5 mL, $CHCl_3$; *l* = 100 mm; α = + 0.0434°).

4.78 **S-33**

(3*R*,5*S*,7*S*)-5-Methoxy-7-(methoxymethoxy)-3-methyldecan-1-ol (S-33). Di-protected **4.78** (400 mg, 0.8 mmol, 1.0 equiv.) was dissolved in THF (4.0 mL, 0.2 M) under inert atmosphere. To the solution, TBAF (3.2 mL, 3.2 mmol of commercial 1.0 M solution, 5.0 equiv.) was added dropwise, at ambient temperature. After 3 hours, total consumption of starting material was realized (silica gel, 30% acetone in hexanes), with

a large baseline spot visible under CAM stain. The reaction was quenched with NH_4Cl, diluted with EtOAc (15 mL), and washed with brine (3 × 20 mL). The combined organic layers were dried ($MgSO_4$), filtered, and concentrated *in vacuo* to yield a crude yellow oil. Purification of the residue (silica gel, 20% acetone in hexanes) yielded 185 mg (0.71 mmol, 88%) of **S-33** as clear, colorless oil.

R_f = 0.41 (silica gel, 30% acetone in hexanes; CAM stain).

^{1}HNMR (600 MHz, $CDCl_3$): δ 4.67 (d, *J* = 7.0 Hz, 1H, -CH*H*-), 4.64 (d, *J* = 7.0 Hz, 1H, -CH*H*-), 3.72 – 3.67 (m, 2H, -CH_2-), 3.67 – 3.63 (m, 1H, -C*H*-), 3.42 (dtd, *J* = 12.4, 4.7, 3.0 Hz, 1H, -C*H*-), 3.38 (s, 3H, -OCH_3), 3.32 (s, 3H, -OCH_3), 1.77 – 1.71 (m, 1H, -C*H*-), 1.64 – 1.40 (m, 8H, 3 × -CH_2-; -CH*H*-; -O*H*), 1.39 – 1.31 (m, 2H, -CH_2-), 1.19 (ddd, *J* = 14.0, 8.1, 5.1 Hz, 1H, -CH*H*-), 0.94 (d, *J* = 6.7 Hz, 3H, -CH_3), 0.91 (t, *J* = 7.4 Hz, 3H, -CH_3) ppm.

^{13}CNMR (150 MHz, $CDCl_3$): δ 95.8, 75.9, 75.0, 60.9, 56.1, 55.6, 41.8, 40.2, 40.1, 37.4, 26.2, 20.3, 18.2, 14.2 ppm.

HRMS (ESI+ TOF) *m/z*: calculated for $C_{14}H_{30}O_4Na$ [$(M + Na)^+$] 285.2042, observed 285.2022 (Δ = 2.0 mmu).

IR (thin film) ν_{max}: 3428, 2930, 1458, 1379, 1215, 1144, 1090, 1036 cm^{-1}.

$[\alpha]_D^{20}$ = + 11.7° (*c* = 9.2 mg/2.5 mL, $CHCl_3$; *l* = 100 mm; α = + 0.0431°).

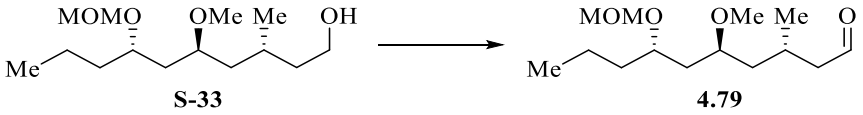

S-33 **4.79**

(3*S*,5*S*,7*S*)-5-methoxy-7-(methoxymethoxy)-3-methyldecanal (4.79). Alcohol **S-33** (30 mg, 0.11 mmol, 1.0 equiv.) was dissolved in CH_2Cl_2 (1.2 mL), and a mixture of PCC (30 mg, 0.14 mmol, 1.2 equiv.) and silica gel (60 mg) was added under inert atmosphere. The reaction stirred for 5 h at ambient temperature, and was monitored by TLC (silica gel, 30% acetone in hexanes). Upon completion, CH_2Cl_2 was evaporated, and the obtained dark brown powder was added directly to a pre-equilibrated column (silica gel, 20% EtOAc in hexanes). Purification yielded 26.4 mg (0.10 mmol, 92%) of **4.79**, and 2.1 mg of recovered **S-33** as clear, colorless oils.

R_f = 0.58 (silica gel, 30% acetone in hexanes; CAM stain).

^{1}HNMR (400 MHz, $CDCl_3$): δ 9.73 (t, *J* = 2.2 Hz, 1H, -C*H*O), 4.66 (d, *J* = 6.8 Hz, 1H, -CH*H*-), 4.63 (d, *J* = 6.8 Hz, 1H, -CH*H*-), 3.67 (dtd, *J* = 9.7, 5.7, 4..0 Hz, 1H, -C*H*-), 3.42 (ddd, *J* = 12.5, 8.0, 4.5 Hz, 1H, -C*H*-), 3.37 (s, 3H, -OCH_3), 3.31 (s, 3H, -OCH_3), 2.41 (ddd, *J* = 18.8, 8.4, 1.8 Hz, 1H, -CH*H*-), 2.28 – 2.21 (m, 2H, -CH*H*- & -C*H*-), 1.63 (ddd, *J* = 14.5, 8.1, 3.9 Hz, 1H, -CH*H*-), 1.58 (dd, *J* = 8.0, 5.5 Hz, 1H, -CH*H*-), 1.54 – 1.44 (m, 3H, -CH_2- & -CH*H*-), 1.38- 1.24 (m, 3H, -CH_2- & -CH*H*-), 0.99 (d, *J* = 6.2 Hz, 3H, -CH_3), 0.90 (t, *J* = 7.3 Hz, 3H, -CH_3) ppm.

^{13}CNMR (100 MHz, $CDCl_3$): δ 202.6, 95.9, 75.5, 75.0, 56.0, 55.7, 51.4, 41.6, 40.1, 37.4, 25.1, 20.3, 18.3, 14.3 ppm.

HRMS (ESI+ TOF) *m/z*: calculated for $C_{14}H_{28}O_4Na$ [$(M + Na)^+$] 283.1885, observed 283.1869 (Δ = 1.6 mmu).

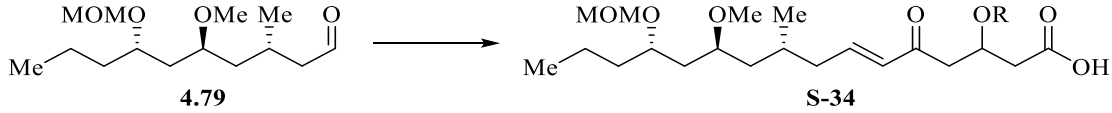

(9*R*,11*S*,13*S*)-(*E*)-3-(TBS)-11-methoxy-13-(MOM)-9-methyl-5-oxohexadec-6-enoic acid (S-34). Phosphonate **4.26** (3.7 mg, 0.010 mmol, 1.0 equiv.) was dissolved in a solution of THF (0.08 M), and Cs_2CO_3 (4 mg, 0.012 mmol, 1.2 equiv.) was added in one portion under inert atmosphere. The mixture stirred for 2h at ambient temperature. A solution of aldehyde **4.79** (2.2 mg, 84.5 µmol, 0.85 equiv.) in THF was added dropwise. The reaction mixture stirred overnight, and monitored by TLC for disappearance of a deep red-purple spot (silica gel, 30% acetone in hexanes; *p*-anisaldehyde stain). Upon completion, the reaction was diluted with EtOAc (10 mL), and quenched by addition of 1.0 M HCl solution (3 mL). The mixture was extracted with EtOAc (2 × 10 mL), and the combined organic layers were washed with brine (2 × 10 mL), dried ($MgSO_4$), filtered, and concentrated *in vacuo*. Purification (silica gel, 20% acetone in hexanes) yielded 2.6 mg of **S-34** as an inseparable mixture (*d.r.* ~ 3:1) of diastereomers (51.7 µmol, 61%). **R_f** = 0.44 (silica gel, 30% acetone in hexanes; *p*-anisaldehyde stain).

^{1}HNMR (400 MHz, $CDCl_3$): δ 6.87 – 6.79 (m, 1H, -C*H*=), 6.07 (dd, *J* = 15.8, 4.6 Hz, 1H, =C*H*-), 4.68 – 4.62 (m, 0.3H, -C*H*-), 4.66 (s, 2H, -CH_2-), 4.64 (s, 0.7H, -CH_2-), 4.61 – 4.56 (m, 1H, -C*H*-), 3.71 – 3.65 (m, 1.3H, 2 × -C*H*-), 3.44 – 3.35 (m, 1.3H, 2 × -C*H*-), 3.39 (s, 3H, -OCH_3), 3.38 (s, 1H, -OCH_3), 3.32 (s, 3H, -OCH_3), 3.31 (s, 1H, -OCH_3), 2.91 – 2.75 (m, 2.7H, 2 × -CH_2-), 2.63 – 2.57 (m, 1.6H, 3 × -CH*H*-), 2.51 (dd, *J* = 15.3, 4.6 Hz, 1.3H, 2 × -CH*H*-), 2.25 – 2.15 (m, 1.3H, 2 × -CH*H*-), 2.15 – 2.08 (m, 1.3H, 2 × -CH*H*-), 1.88 – 1.80 (m, 1.3H, 2 × -C*H*-), 1.67 – 1.17 (m, 8 ×-CH*H*-), 1.01 (d, *J* = 6.2 Hz, 1H, -CH_3), 0.94 – 0.88 (m, 3 × -CH_3), 0.85 (s, 12H, 2 × O-TBS *t*-Bu), 0.09 (s, 4H, 2 × O-TBS -CH_3), 0.05 (s, 4H, 2 × O-TBS -CH_3) ppm; presented characterization was normalized to the unidentified major C3 diastereomer.

HRMS (ESI+ TOF) *m/z*: calculated for $C_{26}H_{50}O_7SiNa$ [$(M + Na)^+$] 525.3224, observed 525.3217 (Δ = 0.7 mmu).

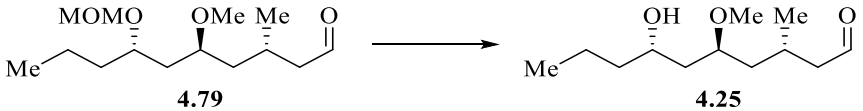

(3*S*,5*S*,7*S*)-7-Hydroxy-5-methoxy-3-methyldecanal (4.10). A stirring solution of MOM-protected aldehyde **4.79** (18.8 mg, 72.25 µmol, 1.0 equiv.) in anhydrous THF (700 µL) was carefully evacuated of atmosphere,

and back-filled with inert gas. This process was repeated three times, upon which concentrated HCl (49 μL, 12 M) was added. The reaction mixture was stirred at room temperature, and monitored by TLC (silica gel, 30% acetone in hexanes) for consumption of the starting material. Upon completion, the reaction was cooled to 0 ºC, diluted with EtOAc (5 mL) and quenched with $NaHCO_3$ (3 mL). The aqueous layer was re-extracted with EtOAc (3 mL). The combined organic layers were washed with water (3 mL), and brine (2 × 4 mL), dried ($MgSO_4$), filtered, and evaporated *in vacuo*. Purification yielded 10.9 mg of **4.25** (50.42 mmol, 70%) as clear, colorless oil. The obtained product must be kept under inert atmosphere and used quickly, as the product readily undergoes Cannizarro-like disproportionation mechanism to afford alcohol and carboxylic acid side-products.

Characterization data was identical to the fully-functionalized aldehyde previously obtained *via* tandem hydrogenation/hydrogenolysis of benzyl ether (*vide supra*); however, the presented conditions provided consistent formation of the desired product in comparable yield.

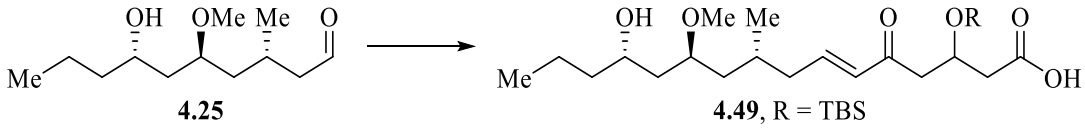

4.25 **4.49**, R = TBS

(9*R*,11*S*,13*S*,*E*)-3-(TBS)-13-hydroxy-11-methoxy-9-methyl-5-oxohexadec-6-enoic acid (4.49). The purified phosphonate **4.26** (11.9 mg, 33.3 μmol, 1.1 equiv.) was dissolved in aqueous THF (200 μL, 30:1 THF:H_2O). Cesium carbonate (13.6 mg, 41.7 μmol, 1.3 equiv.) was added in one portion, and the mixture stirred for 2 h at ambient temperature. A solution of aldehyde **4.25** (6.7 mg, 31.0 μmol, 1.0 equiv.) in aqueous THF (150 μL, 30:1 THF:H_2O, 0.076 M overall reaction mixture) was added to the solution dropwise, and rinsed with additional aqueous THF (2 × 50 μL). The reaction mixture stirred overnight, and was monitored by TLC for appearance of a deep red-purple spot (silica gel, 30% acetone in hexanes; *p*-anisaldehyde stain). A potential biphasic solution indicates the reaction has stalled, and requires additional solvent to be added dropwise. Upon completion, the reaction was diluted with EtOAc (10 mL), and quenched by the addition of 1.0 M HCl solution (1 mL). The mixture was extracted with EtOAc (2 × 3 mL), and the combined organic layers were washed with brine (2 × 2 mL), dried ($MgSO_4$), filtered, and concentrated *in vacuo*. Purification (silica gel, 20% acetone in hexanes) yielded 2.5 mg of recovered aldehyde **4.25**, and 7.7 mg of acid **4.49** (0.017 mmol, 90% brsm) as clear, colorless oil.

R_f = 0.40 (silica gel, 30% acetone in hexanes; *p*-anisaldehyde stain).

^{1}HNMR (600 MHz, $CDCl_3$): δ 6.82 (td, *J* = 15.7, 7.5 Hz, 2H, 2 × -C*H*=), 6.08 (ddt, *J* = 15.7, 12.3, 1.3 Hz, 2H, 2 × =C*H*-), 4.62 – 4.55 (m, 2H, 2 × -C*H*-), 3.93 (dtdd, *J* = 14.5, 7.3, 4.7, 2.3 Hz, 2H, 2 × -C*H*-), 3.56 (td, *J* = 8.9, 4.2 Hz, 2H, 2 × -C*H*-), 3.37 (s, 3H, -OCH_3), 3.36 (s, 3H, -OCH_3), 2.90 (dd, *J* = 15.4, 6.2 Hz, 1H, -CH*H*-), 2.83 (dd, *J* = 6.3, 1.1 Hz, 2H, -CH_2-), 2.78 (dd, *J* = 15.4, 6.3 Hz, -CH*H*-), 2.58 (dt, *J* = 15.0,

6.5 Hz, 2H, 2 × -CH*H*-), 2.51 (ddd, *J* = 15.0, 4.9 Hz, 2 × -CH*H*-), 2.23 – 2.15 (m, 3H, 3 × -CH*H*-), 2.12 (ddd, *J* = 14.5, 7.8, 1.0 Hz, 1H, -CH*H*-), 1.88 – 1.80 (m, 2H, 2 × -C*H*-), 1.80 – 1.70 (m, 4H, 4 × -CH*H*-), 1.50 – 1.40 (m, 6H, 2 × -CH_2-; 2 × -O*H*-), 1.39 – 1.29 (m, 6H, 2 × CH_2-; 2 × -CH*H*-), 1.16 (ddq, *J* = 19.9, 14.2, 4.3 Hz, 2H, 2 × -CH*H*-), 0.95 (d, *J* = 6.6 Hz, 3H, -CH_3), 0.94 (d, *J* = 6.7 Hz, 3H, -CH_3), 0.913 (t, *J* = 7.1 Hz, 3H, -CH_3), 0.907 (t, *J* = 7.2 Hz, 3H, -CH_3), 0.844 (s, 9H, O-TBDPS *t*-Bu), 0.842 (s, 9H, O-TBS *t*-Bu), 0.09 (s, 6H, 2 × O-TBS -CH_3), 0.04 (s, 6H, 2 × O-TBS -CH_3) ppm; acid proton absent (H/D Exchange).

^{13}CNMR (150 MHz, $CDCl_3$): δ 198.3, 198.1, 173.8, 173.6, 147.2, 147.0, 132.5, 132.3, 77.8, 77.7, 68.5, 66.3, 66.2, 57.1, 57.0, 46.7, 46.4, 42.0, 41.9, 40.5, 40.4, 40.3, 40.09, 40.07, 39.1, 38.8, 29.3, 29.2, 25.7, 19.99, 19.95, 18.71, 18.66, 17.89, 17.88, 14.1, -4.8, -5.0 ppm.

HRMS (ESI+ TOF) *m/z*: calculated for $C_{24}H_{46}O_6SiNa$ [$(M + Na)^+$] 481.2961, observed 481.2950 (Δ = 1.1 mmu).

IR (thin film) ν_{max}: 3462, 2930, 1716, 1374, 1254, 1216, 1084 cm^{-1}.

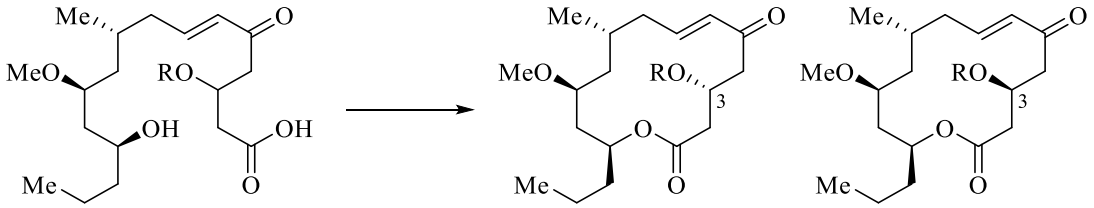

Purified acid **4.49** (11.4 mg, 24.9 μmol, 1.0 equiv.) was dissolved in anhydrous THF (700 μL, 0.04 M), and cooled to 0 ºC. Under inert atmosphere, triethylamine (29.4 μL, 0.21 mmol, 8.0 equiv.) was added, and the resulting solution stirred for 15 min. To the mixture, 2,4,6-trichlorobenzoyl chloride (27.3 μL, 0.17 mmol, 7.0 equiv.) was added to afford a colorless, murky solution, and stirred for 2 h while warming to ambient temperature. Upon consumption of starting material (silica gel, 30% Et_2O in hexanes; *p*-anisaldehyde stain), this solution was added dropwise over a 12 h period to a second flask containing powdered DMAP (106 mg, 0.87 mmol, 35.0 equiv.) in toluene (35 mL, < 0.001 M). The clear, pale yellow reaction was left to stir at ambient temperature, while monitored by TLC (silica gel, 30% Et_2O in hexanes; *p*-anisaldehyde stain). Upon completion, the reaction was evaporated carefully under a stream of nitrogen, diluted with hexanes, and the white residues passed through a silica plug. Careful purification *via* column chromatography (5 – 30% gradient of Et_2O in hexanes) yielded a separable mixture of macrocycle (***3R***)-**4.56** (3.4 mg, 7.7 μmol, 31%) and macrocycle (***3S***)-**4.56** (4.6 mg, 10.5 μmol, 42%) as clear, colorless oils. This preparation of (***3R***)- and (***3S***)-diastereomers afforded an overall yield of 73% (*d.r.* = 2:3). Products were evaporated under a stream of nitrogen.

(*3R*)-*β'*-(TBS)-Silyloxy-enone (4.56)

R_f = 0.22 (silica gel, 30% Et_2O in hexanes; *p*-anisaldehyde stain).

^{1}HNMR (600 MHz, $CDCl_3$): δ 6.84 (ddd, *J* = 16.2, 9.3, 4.4 Hz, 1H, -C*H*=), 6.03 (6.03 (ddd, *J* = 16.2, 2.2, 0.8 Hz, 1H, =C*H*-), 5.06 (dtd, *J* = 7.6, 5.7, 1.9 Hz, 1H, -C*H*-), 4.45 (dddd, *J* = 9.3, 7.2, 5.5, 1.8 Hz, 1H, -C*H*-), 3.69 (dd, *J* = 14.0, 9.7 Hz, 1H, -CH*H*-), 3.34 (dtd, *J* = 12.5, 3.9, 2.2 Hz, 1H, -C*H*-), 3.21 (s, 3H, -OCH_3), 2.55 (dd, *J* = 15.7, 7.1 Hz, 1H, -CH*H*-), 2.47 – 2.43 (m, 1H, -CH*H*-), 2.41 (dd, *J* = 15.7, 1.7 Hz, 1H, -CH*H*-), 2.39 (dd, *J* = 13.3, 6.1 Hz, 1H, -CH*H*-), 2.10 (dt, *J* = 16.4, 10.1 Hz, 1H, -CH*H*-), 1.93 (ddd, *J* = 14.7, 11.3, 2.2 Hz, 1H, -CH*H*-), 1.90 – 1.83 (m, 1H, -C*H*-), 1.69 – 1.64 (m, 1H, -CH*H*-), 1.61 – 1.57 (m, 2H, -CH_2-), 1.43 (ddd, *J* = 14.8, 10.1, 2.0 Hz, 1H, -CH*H*-), 1.39 – 1.33 (m, 3H, -CH_2- & -CH*H*-), 1.03 (d, *J* = 6.7 Hz, 3H, -CH_3), 0.88 (t, *J* = 7.3 Hz, 3H, -CH_3), 0.86 (s, 9H, O-TBS *t*-Bu), 0.074 (s, 3H, O-TBS -CH_3), 0.065 (s, 3H, O-TBS -CH_3) ppm.

^{13}CNMR (150 MHz, $CDCl_3$): δ 199.9, 170.1, 150.0, 132.8, 75.1, 71.7, 66.8, 56.8, 43.9, 42.6, 41.37, 41.32, 38.2, 37.0, 30.0, 25.6, 24.1, 17.9, 17.8, 14.1, -4.998, -5.003 ppm.

HRMS (ESI+ TOF) *m/z*: calculated for $C_{24}H_{46}O_6SiNa$ [$(M + Na)^+$] 463.2856, observed 463.2851 (Δ = 0.5 mmu).

(*3S*)-*β'*-(TBS)-Silyloxy-enone (4.56)

R_f = 0.28 (silica gel, 30% Et_2O in hexanes; *p*-anisaldehyde stain).

^{1}HNMR (600 MHz, $CDCl_3$): δ 6.84 (ddd, *J* = 16.1, 8.9, 6.3 Hz, 1H, -C*H*=), 5.99 (dt, *J* = 16.1, 1.2 Hz, 1H, =C*H*-), 5.16 (dtd, *J* = 10.2, 6.3, 1.3 Hz, 1H, -C*H*-), 4.46 (qd, *J* = 7.1, 3.0 Hz, 1H, -C*H*-), 3.35 – 3.30 (m, 1H, -C*H*-), 3.32 (s, 3H, -OCH_3), 2.95 (dd, *J* = 13.7, 7.8 Hz, 1H, -CH*H*-), 2.92 (dd, *J* = 13.7, 7.2 Hz, 1H, -CH*H*-), 2.54 (dd, *J* = 14.6, 6.4 Hz, 1H, -CH*H*-), 2.49 (dd, *J* = 14.6, 3.0 Hz, 1H, -CH*H*-), 2.34 – 2.29 (m, 1H, -CH*H*-), 2.10 – 2.04 (m, 1H, -CH*H*-), 1.81 (ddd, *J* = 15.0, 10.2, 3.0 Hz, 1H, -CH*H*-), 1.77 – 1.68 (m, 2H, 2 × -CH*H*-), 1.58 – 1.52 (m, 1H, -CH*H*-), 1.49 – 1.42 (m, 2H, 2 × -CH*H*-), 1.33 – 1.27 (m, 3H, -CH_2- & -CH*H*-), 1.03 (d, *J* = 6.5 Hz, -CH_3), 0.88 (t, *J* = 7.3 Hz, 3H, -CH_3), 0.85 (s, 9H, O-TBS *t*-Bu), 0.06 (s, 3H, O-TBS -CH_3), 0.02 (s, 3H, -CH_3) ppm.

^{13}CNMR (150 MHz, $CDCl_3$): δ 199.6, 169.9, 148.6, 132.8, 76.4, 71.9, 66.9, 56.7, 46.0, 42.7, 42.3, 40.8, 38.6, 37.7, 30.8, 25.7, 23.5, 18.4, 18.0, 13.9, -4.8, -4.9 ppm.

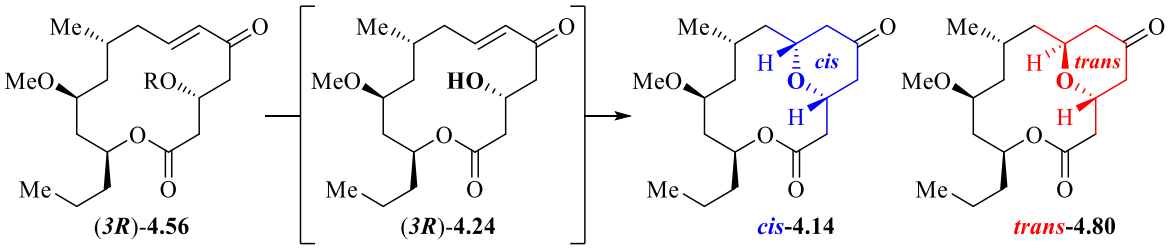

Macrolactone (*3R*)-**4.56** (3.3 mg, 7.5 μmol, 1.0 equiv.) was added to a 1.5 mL polypropylene Eppendorf tube, and dissolved in acetonitrile (75 μL, 0.1 M) and pyridine (3 μL, 37.5 μmol, 5.0 equiv.). The mixture was vortexed to homogeneity, upon which 48% HF (15 μL, 0.75 mmol, 100 equiv.) was added. The reaction mixture was again vortexed, centrifuged, and left for 5 h. The reaction was quenched with water (2 × 1 mL) and diluted with EtOAc (2 × 2 mL). The aqueous layer was re-extracted with EtOAc, and the combined organic layers were washed with brine, dried ($MgSO_4$), filtered, and concentrated under a stream of nitrogen. The product was carefully-purified *via* column chromatography in a glass pipette (silica gel, 10 - 20% acetone in hexanes) to afford 2.1 mg of our kinetic product mixture favoring ***trans*-4.80** (6.4 μmol, 87%; *d.r.* > 20:1 according to relative ^{1}HNMR integration) as clear, colorless oil. Due to the high selectivity of the reaction, the R_f and HRMS data has confidently been assigned to ***trans*-4.80** stereoisomer.

(3*R*,7*R*)-*cis*-neopeltolide macrocyclic core (*cis*-4.14)

^{1}HNMR (600 MHz, $CDCl_3$): δ 5.22 – 5.18 (buried m, 1H, -C*H*-, H13), 4.03 (dddd, 11.3, 10.7, 4.1, 2.9 Hz, 1H, -C*H*-, H3), 3.56 (dddd, *J* = 10.8, 9.4, 2.8, 1.8 Hz, 1H, -C*H*-, H11), 3.48 (dt, *J* = 9.5, 3.9 Hz, 1H, -C*H*-, H7) ppm.

Because of the reaction scale, cleanly-isolating material for spectroscopic analysis of remaining signals was not possible. However, the key identifying signals that were presented are fully-consistent with the characterization data reported by the following groups: Scheidt (2008),[21] Paterson (2009),[26] Floreancig (2009),[28] Roulland (2009),[30] Fuwa (2009),[31] S. Ghosh (2012).[37]

(3*R*,7*S*)-*trans*-$^{\Delta 7}$*epi*-neopeltolide macrocyclic core (*trans*-4.80)

^{1}HNMR (600 MHz, $CDCl_3$): δ 5.19 (dddd, *J* = 10.7, 7.8, 5.3, 1.4 Hz, 1H, -C*H*-, H13), 4.49 (tt, *J* = 9.8, 4.3 Hz, 1H, -C*H*-, H3), 4.38 (ddt, *J* = 9.1, 7.0, 4.3 Hz, 1H, -C*H*-, H7), 3.40 (ddt, *J* = 9.6, 6.6, 3.4 Hz, 1H, -C*H*-, H11), 3.33 (s, 3H, -OCH_3), 2.71 (dd, *J* = 14.2, 4.2 Hz, 1H, -CH*H*-), 2.56 (dd, *J* = 15.1, 4.8 Hz, 1H, -CH*H*-), 2.49 (dd, *J* = 12.1, 4.3 Hz, 1H, -CH*H*-), 2.47 – 2.42 (m, 2H, 2 × -CH*H*-), 2.38 (dd, *J* = 15.2, 6.9 Hz, 1H, -CH*H*-), 1.78 (ddd, *J* = 15.3, 10.9, 3.4 Hz, 1H, -CH*H*-), 1.77 – 1.73 (m, 1H, -C*H*-), 1.68 – 1.63 (m, 2H, 2 × -CH*H*-), 1.61 – 1.55 (m, 2H, 2 × -CH*H*-), 1.53 – 1.47 (m, 1H, -CH*H*-), 1.42 (ddd, *J* = 14.9, 8.8, 4.2 Hz, 1H, -CH*H*-), 1.36 – 1.30 (m, 2H, -CH_2-), 1.99, (ddd, *J* = 13.4, 9.4, 3.6 Hz, 1H, -CH*H*-), 0.95 (d, *J* = 7.1 Hz, 3H, -CH_3), 0.90 (t, *J* = 7.4 Hz, 3H, -CH_3) ppm.

^{13}CNMR (150 MHz, $CDCl_3$): δ 206.8, 169.9, 77.6, 73.7, 70.1, 67.8, 56.6, 46.0, 45.5, 42.2, 42.0, 39.9, 38.8, 37.4, 24.0, 23.8, 18.6, 13.9 ppm.

R_f = 0.46 (silica gel, 30% Et_2O in hexanes; *p*-anisaldehyde stain).

HRMS (ESI+ TOF) *m/z*: calculated for $C_{18}H_{30}O_5Na$ [(M + Na)$^+$] 349.1991, observed 349.1975 (Δ = 1.6 mmu).

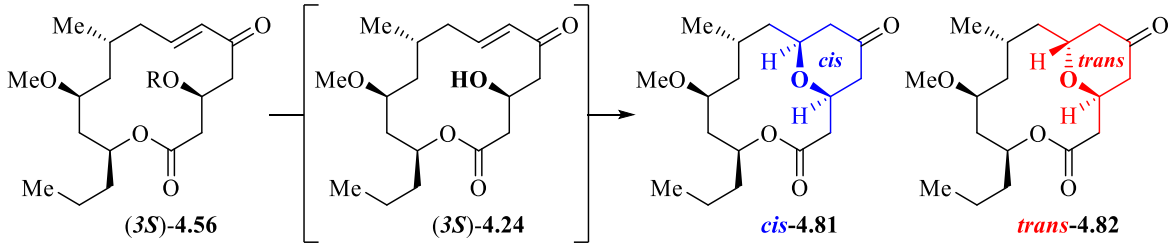

Macrolactone (*3R*)-**4.56** (4.3 mg, 9.8 µmol, 1.0 equiv.) was added to a 1.5 mL polypropylene Eppendorf tube, and dissolved in acetonitrile (100 µL, 0.1 M) and pyridine (4 µL, 39.6 µmol, 5.0 equiv.). The mixture was vortexed to homogeneity, upon which 48% HF (20 µL, 1.0 mmol, 100 equiv.) was added. The reaction mixture was again vortexed, centrifuged, and left for 5 h. The reaction was quenched with water (2 × 1 mL) and diluted with EtOAc (2 × 2 mL). The aqueous layer was re-extracted with EtOAc, and the combined organic layers were washed with brine, dried ($MgSO_4$), filtered, and concentrated to dryness under a stream of nitrogen. The product was carefully-purified *via* column chromatography in a glass pipette (silica gel, 10 - 20% acetone in hexanes) to afford 2.7 mg of an inseparable kinetic mixture of ***cis*-4.81** and ***trans*-4.82** (8.3 µmol, 84%; *d.r.* = 5:9) as clear, colorless oil.

R_f = 0.56 (silica gel, 40% EtOAc in hexanes; CAM stain).

HRMS (ESI+ TOF) *m/z*: calculated for $C_{18}H_{30}O_5Na$ [(M + Na)$^+$] 349.1991, observed 349.2009 (Δ = 1.8 mmu).

(3*S*,7*S*)-*cis*-$^{\Delta 3,7}$*epi*-neopeltolide macrocyclic core (*cis*-4.81)

^{1}HNMR (600 MHz, $CDCl_3$): δ 5.07 (dddd, *J* = 11.2, 8.6, 5.0, 1.6 Hz, 1H, -C*H*-, H13), 3.85 (ddt, *J* = 11.7, 10.8, 2.2 Hz, 1H, -C*H*-, H3), 3.70 (tt, 10.9, 3.0 Hz, 1H, -C*H*-, H7), 3.29 (s, 3H, -OCH_3), 3.01 (dddd, *J* = 11.1, 8.4, 3.5, 1.4 Hz, 1H, -C*H*-, H11), 2.55 – 2.53 (m, 1H, -CH*H*-), 2.47 – 2.34 (m, 4H, 4 × -CH*H*-), 2.19 (dd, *J* = 14.8, 10.6 Hz, 1H, -CH*H*-), 1.91 (dd, *J* = 15.3, 11.9 Hz, 1H, -CH*H*-), 1.89 – 1.84 (m, 1H, -C*H*-), 1.76 – 1.71 (m, 1H, -CH*H*-), 1.71 – 1.65 (m, 3H, 3 × -CH*H*-), 1.51 – 1.38 (m, 3H, 3 × -CH*H*-), 1.37 – 1.29 (m, 2H, -CH_2-), 0.95 (d, *J* = 7.0 Hz, 3H, -CH_3), 0.91 (t, *J* = 7.6 Hz, 3H, -CH_3) ppm.

^{13}CNMR (150 MHz, $CDCl_3$): δ 205.4, 171.7, 75.6, 74.5, 74.0, 56.9, 48.3, 47.5, 45.5, 42.4, 39.6, 39.2, 36.8, 24.5, 24.0, 18.9, 13.9 ppm; one missing *C*-O signal presumed buried beneath solvent signal.

(3*S*,7*R*)-*trans*-$^{\Delta 3}$*epi*-neopeltolide macrocyclic core (*trans*-4.82)

^{1}HNMR (600 MHz, $CDCl_3$): δ 5.18 (dq, *J* = 8.0, 5.3 Hz, 1H, -C*H*-, H13), 4.61 (11.3, 8.0, 4.5, 2.3 Hz, 1H, -C*H*-, H3), 4.08 (dt, *J* = 5.2, 9.7 Hz, 1H, -C*H*-, H7), 3.31 (s, 3H, -OCH_3), 3.20 (ddt, *J* = 9.0, 7.5, 2.4 Hz, 1H, -C*H*-, C11), 2.60 – 2.55 (m, 2H, 2 × -CH*H*-), 2.45 – 2.38 (m, 2H, 2 × -CH*H*-), 2.34 (dd, *J* = 12.6, 2.2 Hz, 1H, -CH*H*-), 2.29 (dd, *J* = 8.2, 8.2 Hz, -CH*H*-), 1.81 (ddd, *J* = 14.7, 10.3, 2.8 Hz, 1H, -CH*H*-), 1.71 – 1.65 (m, 1H, -CH*H*-), 1.63 – 1.57 (m, 3H, 2 × -CH*H*- & -C*H*-), 1.51 – 1.38 (m 1H, -CH*H*-), 1.37 – 1.29 (m, 2H, -CH_2-), 1.22 – 1.99 (m, 2H, 2 × -CH*H*-), 0.97 (d, *J* = 6.7 Hz, 3H, -CH_3), 0.90 (t, *J* = 7.4 Hz, 3H, -CH_3) ppm.

^{13}CNMR (150 MHz, $CDCl_3$): δ 206.5, 171.5, 76.9, 73.7, 72.0, 69.9, 56.3, 46.6, 46.4, 43.5, 40.7, 40.1, 39.4, 37.2, 27.8, 23.0, 18.6, 13.8 ppm.

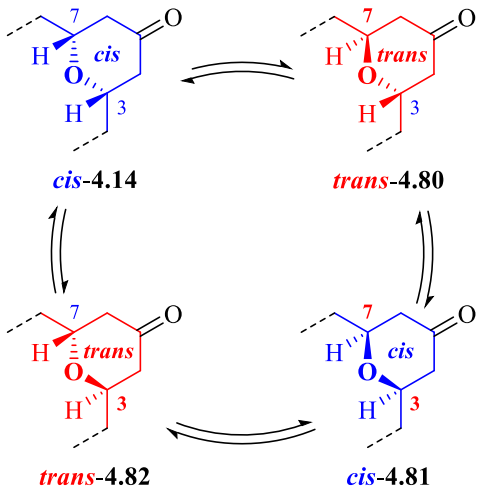

Thermodynamic Equilibration of (3*R*)-Kinetic Mixture. The kinetic 3*R* mixture of ***cis*-4.14** and ***trans*-4.80** (2.1 mg, 6.4 µmol, 1.0 equiv.) was added to a 2.5 mm NMR tube, and dissolved in $CDCl_3$ (0.2 mL). Amberlyst-15® hydrogen form (approx. 15 beads) was added, and the mixture was heated to 80 ºC in an oil bath for 5 h. The reaction was monitored by ^{1}HNMR, and followed key proton shifts in the range of δ 5.3 – 2.8 ppm (H3, H7, H11, H13). The mixture reacted under these conditions with continued monitoring by ^{1}HNMR; equilibration appeared to plateau beyond the 5 h, and formation of by-products from non-productive pathways increased beyond the 15 h mark. Despite the limited quantity, and based on my misfortune, it is highly recommended to avoid 2.5-mm NMR tubes to prevent lost material during reflux. Upon completion, the reaction mixture was dried under a stream of nitrogen. LC-SPE-NMR was conducted using an Agilent 1260 interfaced with a Prospekt 2 (Spark Holland) solid-phase extraction module, using HySphere Resin GP cartridges. Separation relied on a reverse phase Agilent Zorbax C18 column (100 mm × 2.1 mm I.D., 3.5 µm particle size). Mobile phases throughout the analysis were water (H_2O, Phase A) and acetonitrile (MeCN, Phase B). The chromatography method had a flow-rate of 0.25 mL/min. The

mobile phase was held at 30% Phase B over 3 minutes, followed by a linear gradient to 100% Phase B over 14 minutes. A 4-minute hold at 100% Phase B flushed the column and was re-equilibrated at 30% Phase B for an additional 4-minutes, for a total run-time of 25 minutes. Peak-trapping was conducted over the entire run into new cartridges, at 5-minute intervals (total of 5 cartridges). Ten trapping experiments were performed with trapping on the same set of solid-phase cartridges. Compounds were eluted from the cartridges using deuterated acetonitrile (CD_3CN, 60 µL), and NMR spectra was recorded on a Bruker Avance III instrument, with cryoprobe operating at 600 MHz.

Characterization data for *cis*-**4.14** proved consistent with previously reported data;[21,26,28,30,31,37] because of scale, clean isolation of *cis*-**4.81** was not achieved, but diagnostic signals were identical to the ones observed in our 3*S* kinetic mixture.

	***cis*-4.14**	***trans*-4.80**	***cis*-4.81**	***trans*-4.82**
Kinetic* (3*R*) *Mixture	1.0	40	0.8	0.5
***Thermodynamic Mixture* (5 h)**	1.0	0.14	0.76	0.04
***Thermodynamic Mixture* (10 h)**	1.0	0.11	0.71	0.05
***Thermodynamic Mixture* (15 h)**	1.0	-	0.54	-

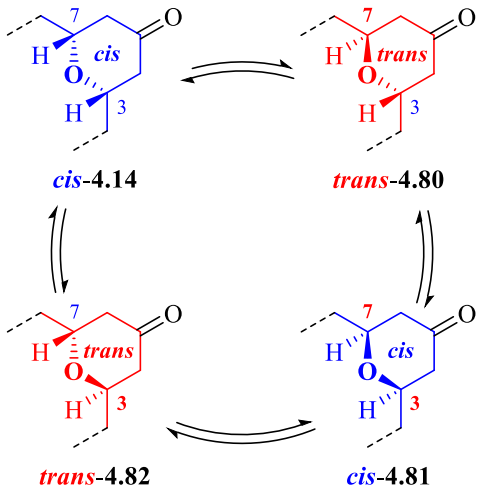

Thermodynamic Equilibration of (3*S*)-Kinetic Mixture. The kinetic 3*S* mixture of ***cis*-4.81** and ***trans*-4.82** (2.7 mg, 8.3 µmol, 1.0 equiv.) was added to a 2.5 mm NMR tube, and dissolved in $CDCl_3$ (0.2 mL). Amberlyst-15® hydrogen form (approx.. 15 beads) was added, and the mixture was heated to 80 ºC in an oil bath for 5 h. The reaction was monitored by ^{1}HNMR, and followed key proton shifts in the range of δ 5.3 – 2.8 ppm (H3, H7, H11, H13). The mixture was reacted under these conditions with continued monitoring by ^{1}HNMR; equilibration appeared to plateau beyond the 5 h, and formation of by-products from non-productive pathways increased beyond the 15 h mark. Upon completion, the reaction mixture was dried under a stream of nitrogen. LC-SPE-NMR were conducted using the same procedure described for the thermodynamic equilibration of (3*R*)-kinetic mixture (*vide supra*). Peak-trapping was conducted over

the entire run into new cartridges, at 5-minute intervals (total of 5 cartridges). Ten trapping experiments were performed with trapping on the same set of solid-phase cartridges. Compounds were eluted from the cartridges using deuterated acetonitrile (CD_3CN, 60 µL), and NMR spectra was recorded on a Bruker Avance III instrument, with cryoprobe operating at 600 MHz.

Characterization data for *cis*-**4.14** proved consistent with previously reported data;[21,26,28,30,31,37] similar issues with scale prevented clean isolation of *cis*-**4.81**, but diagnostic signals were identical to the starting mixture.

	***cis*-4.14**	***trans*-4.80**	***cis*-4.81**	***trans*-4.82**
Kinetic* (3*S*) *Mixture	-	-	1.0	1.8
***Thermodynamic Mixture* (5 h)**	0.22	-	1.0	0.26
***Thermodynamic Mixture* (15 h)**	0.18	-	1.0	0.15

4.9 References

(1) Newman, D. J.; Cragg, G. M. *J. Nat. Prod.* **2016**, *79* (3), 629–661.
(2) Ganem, B.; Franke, R. R. *J. Org. Chem.* **2007**, *72* (11), 3981–3987.
(3) Oberlies, N. H.; Kroll, D. J. *J. Nat. Prod.* **2004**, *67*, 129–135.
(4) Che, C.-T.; Haynes, R. K.; Höfle, G.; Wright, A. E.; Sennett, S. H.; McCarthy, P. J.; Kingston, D. G. I. In *The American Society of Pharmacognosy 50 Years of Progress in Natural Products Research 1959-2009*; Cragg, G. M., Beutler, J. A., Jones, W. P., Eds.; 2009; pp 212–248.
(5) Cuevas, C.; Francesch, A. *Nat. Prod. Rep.* **2009**, No. 26, 322–33.
(6) Kingston, D. G. I. *J. Org. Chem.* **2008**, *73* (11), 3975–3984.
(7) Mittermeier, R.; Mittermeier, C. G.; Brooks, T. M.; Pilgrim, J. D.; Konstant, W. R.; da Fonseca, G. B.; Kormos, C. *Proc. Natl. Acad. Sci.* **2003**, *100* (18), 10309–10313.
(8) Ikeda, Y.; Idemoto, H.; Hirayama, F.; Yamamoto, K.; Iwao, K.; Asao, T.; Munakata, T. *J. Antibiot.* **1983**, *36* (10), 1279–1283.
(9) Altmann, K.-H.; Gaugaz, F. Z.; Schiess, R. *Mol. Divers.* **2011**, *15*, 383–399.
(10) Nakamura, C. E.; Whited, G. M. *Curr. Opin. Biotechnol.* **2003**, *14* (5), 454–459.
(11) Ro, D.; Paradise, E. M.; Ouellet, M.; Fisher, K. J.; Newman, K. L.; Ndungu, J. M.; Ho, K. A.; Eachus, R. A.; Ham, T. S.; Kirby, J.; Chang, M. C. Y.; Withers, S. T.; Shiba, Y.; Sarpong, R.; Keasling, J. D. *Nature* **2006**, *440*, 940–943.
(12) Paddon, C. J.; Westfall, P. J.; Pitera, D. J.; Benjamin, K.; Fisher, K.; McPhee, D.; Leavell, M. D.; Tai, a; Main, a; Eng, D.; Polichuk, D. R.; Teoh, K. H.; Reed, D. W.; Treynor, T.; Lenihan, J.; Fleck, M.; Bajad, S.; Dang, G.; Dengrove, D.; Diola, D.; Dorin, G.; Ellens, K. W.; Fickes, S.; Galazzo, J.; Gaucher, S. P.; Geistlinger, T.; Henry, R.; Hepp, M.; Horning, T.; Iqbal, T.; Jiang, H.; Kizer, L.; Lieu, B.; Melis, D.; Moss, N.; Regentin, R.; Secrest, S.; Tsuruta, H.; Vazquez, R.; Westblade, L. F.; Xu, L.; Yu, M.; Zhang, Y.; Zhao, L.; Lievense, J.; Covello, P. S.; Keasling, J. D.; Reiling, K. K.; Renninger, N. S.; Newman, J. D. *Nature* **2013**, *496* (7446), 528–532.
(13) Kopetzki, D.; Lévesque, F.; Seeberger, P. H. *Chem. Eur. J.* **2013**, *19* (17), 5450–5456.
(14) Peplow, M. Sanofi launches malaria drug production https://www.chemistryworld.com/news/sanofi-launches-malaria-drug-production/6068.article.
(15) Khosla, C.; Harbury, P. B. *Nature* **2001**, *409* (6817), 247–252.
(16) Menzella, H. G.; Reid, R.; Carney, J. R.; Chandran, S. S.; Reisinger, S. J.; Patel, K. G.; Hopwood, D.; Santi, D. V. *Nat. Biotechnol.* **2005**, *23* (9), 1171–1176.
(17) Sherman, D. H. *Nat. Biotechnol.* **2005**, *23* (9), 1083–1084.
(18) Menzella, H. G.; Carney, J. R.; Santi, D. V. *Chem. Biol.* **2007**, *14* (2), 143–151.
(19) Wright, A. E.; Botelho, J. C.; Guzmán, E.; Harmody, D.; Linley, P.; McCarthy, P. J.; Pitts, T. P.; Pomponi, S.; Reed, J. K. *J. Nat. Prod.* **2007**, *70* (3), 412–416.
(20) Youngsaye, W.; Lowe, J. T.; Pohlki, F.; Ralifo, P.; Panek, J. S. *Angew. Chem. Int. Ed.* **2007**, *46* (48), 9211–9214.
(21) Custar, D. W.; Zabawa, T. P.; Scheidt, K. A. *J. Am. Chem. Soc.* **2008**, *130* (3), 804–805.
(22) Vintonyak, V. V; Maier, M. E. *Org. Lett.* **2008**, *10* (6), 1239–1242.
(23) Woo, S. K.; Kwon, M. S.; Lee, E. *Angew. Chem. Int. Ed.* **2008**, *47* (17), 3242–3244.
(24) Fuwa, H.; Naito, S.; Goto, T.; Sasaki, M. *Angew. Chem.* **2008**, *120* (25), 4815–4817.
(25) Ulanovskaya, O.; Janjic, J.; Suzuki, M.; Sabharwal, S. S.; Schumacker, P. T.; Kron, S. J.; Kozmin, S. *Nat. Chem. Biol.* **2008**, *4* (7), 418–424.
(26) Paterson, I.; Miller, N. *Chem. Commun.* **2008**, No. 39, 4708–4710.
(27) Taylor, R. E.; Kartika, R.; Gruffi, T. R. *Org. Lett.* **2008**, *10* (21), 5047–5050.
(28) Tu, W.; Floreancig, P. E. *Angew. Chem. Int. Ed.* **2009**, *48* (25), 4567–4571.
(29) Kim, H.; Park, Y.; Hong, J. *Angew. Chem. Int. Ed.* **2009**, *48* (41), 7577–7581.
(30) Guinchard, X.; Roulland, E. *Org. Lett.* **2009**, *11* (20), 4700–4703.
(31) Fuwa, H.; Saito, A.; Naito, S.; Konoki, K.; Yotsu-Yamashita, M.; Sasaki, M. *Chem. Eur. J.* **2009**, *15*, 12807–12818.
(32) Yadav, J. S.; Krishana, G. G.; Kumar, S. N. *Tetrahedron* **2010**, *66* (2), 480–487.
(33) Martinez-Solorio, D.; Jennings, M. P. *J. Org. Chem.* **2010**, *75* (12), 4095–4104.
(34) Yang, Z.; Zhang, B.; Zhao, G.; Yang, J.; Xie, X.; She, X. *Org. Lett.* **2011**, *13* (21), 5916–5919.
(35) Sharma, G. V. M.; Reddy, S. V.; Ramakrishna, K. V. S. *Org. Biomol. Chem.* **2012**, *10* (18), 3689–3695.

(36) Raghavan, S.; Samanta, P. K. *Org. Lett.* **2012**, *14* (9), 2346–2349.
(37) Athe, S.; Chandrasekhar, B.; Roy, S.; Pradhan, T. K.; Ghosh, S. *J. Org. Chem.* **2012**, *77*, 9840–9845.
(38) Ghosh, A. K.; Shurrush, K. A.; Dawson, Z. L. *Org. Biomol. Chem.* **2013**, *11* (44), 7768–7777.
(39) Fuwa, H.; Kawakami, M.; Noto, K.; Muto, T.; Suga, Y. *Chem. Eur. J.* **2013**, *19*, 8100–8110.
(40) Yu, M.; Schrock, R. R.; Hoveyda, A. H. *Angew. Chem. Int. Ed.* **2015**, *54* (1), 215–220.
(41) Vintonyak, V. V; Kunze, B.; Sasse, F.; Maier, M. E. *Chemistry*, **2008**, *14* (35), 11132–11140.
(42) Cui, Y.; Tu, W.; Floreancig, P. E. *Tetrahedron* **2010**, *66* (26), 4867–4873.
(43) Fuwa, H.; Saito, A.; Sasaki, M. *Angew. Chem.* **2010**, *122* (17), 3105–3108.
(44) Barton, D. H. R. *Experientia* **1950**, *1* (8), 316–320.
(45) Still, W. C. *J. Am. Chem. Soc.* **1979**, *101* (9), 2493–2495.
(46) Still, W. C.; Galynker, I. *Tetrahedron* **1981**, *37* (23), 3981–3996.
(47) Wzorek, J. S. Macrocyclic Stereocontrol in Organic Synthesis: I. Efforts toward the Synthesis of (-)-Tetracycline II. Analysis of the Peripheral Attack Model, Harvard University, 2012.
(48) Still, W. C.; Novack, V. J. *J. Am. Chem. Soc.* **1984**, *106*, 1148–1149.
(49) Stachel, S. J.; Danishefsky, S. J. *Tetrahedron Lett.* **2001**, *42*, 6785–6787.
(50) Paterson, I.; Norcross, R. D.; Ward, R. A.; Romea, P.; Lister, M. A. *J. Am. Chem. Soc.* **1994**, *116*, 11287–11314.
(51) Bäurle, S.; Blume, T.; Mengel, A.; Parchmann, C.; Skuballa, W.; Bäsler, S.; Schäfer, M.; Sülzle, D. *Angew. Chem. Int. Ed.* **2003**, *42*, 3961–3964.
(52) Llàcer, E.; Urpí, F.; Vilarrasa, J. *Org. Lett.* **2009**, *11* (15), 3198–3201.
(53) Nicolaou, K. C.; Adsool, V. A.; Hale, C. R. H. *Angew. Chem. Int. Ed.* **2011**, *50*, 5149–5152.
(54) Nicolaou, K. C.; Jiang, X.; Lindsay-Scott, P. J.; Corbu, A.; Yamashiro, S.; Bacconi, A.; Fowler, V. M. *Angew. Chem. Int. Ed.* **2011**, *50*, 1139–1144.
(55) Kende, A. S.; Liu, K.; Kaldor, I.; Dorey, G.; Koch, K. *J. Am. Chem. Soc.* **1995**, *117*, 8258–8270.
(56) Still, W. C.; MacPherson, L. J.; Harada, T.; Callahan, J. F. *Tetrahedron* **1984**, *40* (12), 2275–2281.
(57) Crabtree, R.; Davis, M. W. *J. Org. Chem.* **1986**, *51* (14), 2655–2661.
(58) Bai, Y.; Davis, D. C.; Dai, M. *Angew. Chem. Int. Ed.* **2014**, *53*, 6519–6522.
(59) Hari, T. P. A.; Wilke, B. I.; Davey, J. A.; Boddy, C. N. *J. Org. Chem.* **2016**, *81*, 415–423.
(60) Wzorek, J. S.; Knöpfel, T. F.; Sapountzis, I.; Evans, D. A. *Org. Lett.* **2012**, *14* (23), 5840–5843.
(61) Seeman, J. I. *Chem. Rev.* **1983**, *83* (2), 83–134.
(62) Hilli, F.; White, J. M.; Rizzacasa, M. A. *Tetrahedron* **2011**, *67*, 5054–5068.
(63) Yamaguchi, M.; Inanaga, J.; Hirata, K.; Saeki, H.; Katsuki, T. *Bull. Chem. Soc. Jpn.* **1979**, *52* (7), 1989–1993.
(64) Lam, L. K. P.; Hui, R. H. F.; Jones, J. B. *J. Org. Chem.* **1986**, *51* (11), 2047–2050.
(65) Hoye, T. *J. Am. Chem. Soc.* **1998**, *120*, 4638–4643.
(66) Dale, J. A.; Dull, D. L.; Mosher, H. S. *J. Org. Chem.* **1969**, *34* (9), 2543–2549.
(67) Mosher, H. S.; Dale, J. A.; Sullivan, G. R. *J. Org. Chem.* **1973**, *38* (12), 2143–2147.
(68) Gröbel, B. T.; Seebach, D. *Synthesis*, **1977**, *6*, 357–402.
(69) La Cruz, T. E.; Rychnovsky, S. D. *J. Org. Chem.* **2007**, *72* (7), 2602–2611.
(70) Nahm, S.; Weinreb, S. M. *Tetrahedron Lett.* **1981**, *22* (39), 3815–3818.
(71) Yadav, L. D. S.; Singh, S.; Rai, V. K. *Synlett* **2010**, *2*, 240–246.
(72) Zhu, C.; Shen, X.; Nelson, S. G. *J. Am. Chem. Soc.* **2004**, *126* (17), 5352–5353.
(73) Hari, T. P. A. Efforts Toward an Oxa-Conjugate Addition Based Approach to (+)-Neopeltolide Synthesis, University of Ottawa, 2012.
(74) Brown, H.; Jadhav, P. K. *J. Am. Chem. Soc.* **1983**, *105* (4), 2092–2093.
(75) Kubota, K.; Leighton, J. L. *Angew. Chem. Int. Ed.* **2003**, *42* (8), 946–948.
(76) Kolb, H. C.; VanNieuwenhze, M. S.; Sharpless, K. B. *Chem. Rev.* **1994**, *94*, 2483–2547.
(77) Hosomi, A.; Sakurai, H. *Tetrahedron Lett.* **1976**, *17* (16), 1295–1298.
(78) Wilke, B. I. Examining Polyketide Synthase Mechanisms Through Biomimetic Synthesis, Syracuse University, 2013.
(79) Kim, Y. J.; Wang, P.; Navarro-Villalobos, M.; Rohde, B. D.; Derryberry, J. M.; Gin, D. Y. *J. Am. Chem. Soc.* **2006**, *128* (36), 11906–11915.
(80) Ashby, E. C. *Q. Rev. Chem. Soc.* **1967**, *21* (2), 259.
(81) Czernecki, S.; Georgoulis, C.; Provelenghiou, C. *Tetrahedron Lett.* **1976**, *17* (39), 3535–3536.
(82) Omura, K.; Swern, D. *Tetrahedron* **1978**, *34* (11), 1651–1660.
(83) Corey, E.; Suggs, J. *Tetrahedron Lett.* **1975**, No. 31, 2647–2650.
(84) Cannizzaro, S. *Liebigs Ann. der Chemie und Pharm.* **1853**, *88*, 129–130.

(85) Geissman, T. A. *Org. React.* **2011**, *2* (3), 94–113.
(86) Villieras, J.; Rambaud, M. *Synthesis*, **1983**, *April*, 300–303.
(87) Schauer, D. J.; Helquist, P. *Synthesis*, **2006**, No. 21, 3654–3660.
(88) Inoue, K.; Sakai, K. *Tetrahedron Lett.* **1977**, No. 46, 4063–4066.
(89) Akiyama, T.; Hirofuji, H.; Hirose, A.; Ozaki, S. *Synth. Commun.* **1994**, *24* (15), 2179–2185.
(90) Goff, Dane, A.; Harris, R. N. I.; Bottaro, J. C.; Bedford, C. D. *J. Org. Chem.* **1986**, *51* (24), 4711–4714.
(91) Tuulmets, A.; Salmar, S.; Hagu, H. *J. Phys. Chem. B* **2003**, *107*, 12891–12896.
(92) Wu, X.-A.; Ying, P.; Liu, J.-Y.; Shen, H.-S.; Chen, Y.; He, L. *Synth. Commun.* **2009**, *39* (19), 3459–3470.
(93) Papot, S.; Rivault, F.; Tranoy, I.; Gesson, J.-P. *Synlett* **2002**, *1* (28), 164–166.
(94) Anderson, M. O.; Moser, J.; Sherrill, J.; Guy, R. K. *Synlett* **2004**, No. 13, 2391–2393.
(95) Paterson, I.; Yeung, K.-S.; Ward, R. A.; Smith, J. D.; Cumming, J. G.; Lamboley, S. *Tetrahedron* **1995**, *51* (34), 9467–9486.
(96) Nambu, M.; White, J. D. *Chem. Commun.* **1996**, No. 14, 1619–1620.
(97) Manchand, P. S. *Chem. Commun.* **1971**, *1* (13), 667.
(98) Kocienski, P. J. *Protecting Groups*, 3rd ed.; Thieme Verlag, 2005.
(99) Wuts, P. G. M. *Greene's Protective Groups in Organic Synthesis*, 5th ed.; Wiley, 2014.
(100) Logush, E. W. *Tetrahedron Lett.* **1984**, *25* (38), 4195–4198.
(101) Earley, J.; Adams, C. M. *Encyclopedia of Reagents for Organic Synthesis: 2-(Trimethylsilyl)ethoxymethyl Chloride*; 2008; pp 1–5.
(102) Guindon, Y.; Yoakim, C.; Bernstein, M. A.; Morton, H. E. *Tetrahedron Lett.* **1985**, *26* (9), 1185–1188.
(103) Boden, E.; Keck, G. E. *J. Org. Chem.* **1985**, *50*, 2394–2395.
(104) Steglich, W.; Höfle, G. *Angew. Chem. Int. Ed.* **1969**, *8* (12), 981–981.
(105) Sinisterra, J. V.; Barrios, J.; Mouloungui, Z. *Bull. Soc. Chim. Belg.* **1991**, *100* (3), 267–275.
(106) Pascariu, A.; Ilia, G.; Bora, A.; Iliescu, S.; Popa, A.; Dehelean, G.; Pacureanu, L. *Cent. Eur. J. Chem.* **2003**, *4*, 491–542.
(107) Barrios, J.; Marinas, J. M.; Sinisterra, J. V. *Bull. Chem. Soc. Belg.* **1986**, *95* (2), 107–117.
(108) Alvarez-lbarra, C.; Arias, S.; Baiion, G.; Fernandez, M. J.; Rodriguez, M.; Sinisterra, V. *J. Chem. Soc., Chem. Commun.* **1987**, 1509–1511.
(109) Ibarra, C. A.; Arias, S.; Fernandez, M. J.; Sinisterra, J. V. *J. Chem. Soc., Perkin Trans. II* **1989**, 503–508.
(110) Paterson, I.; Yeung, K.-S.; Smaill, J. B. *Synlett* **1993**, *October*, 774–776.
(111) Crimmins, M. T.; Shamszad, M.; Mattson, A. E. *Org. Lett.* **2010**, *12* (11), 2614–2617.
(112) Weber, W. P.; Gokel, G. W. *Phase Transfer Catalysis in Organic Synthesis*; Springer-Verlag, 1977; Vol. 4.
(113) Mouloungui, Z.; Delmas, M.; Gaset, A. *J. Org. Chem.* **1989**, *54* (16), 3936–3941.
(114) Blanchette, M. A.; Choy, W.; Davis, J. T.; Essenfeld, A. P.; Masamune, S.; Roush, W. R. *Tetrahedron Lett.* **1984**, *25* (21), 2183–2186.
(115) Bisceglia, J. Á.; Orelli, L. R. *Curr. Org. Chem.* **2012**, *16*, 2206–2230.
(116) The decision to protect C13-alcohol as the MOM-ether was also guided by the fact that moms are there for you when you need them most, and will do anything to help you.
(117) Hilli, F.; White, J. M.; Rizzacasa, M. *Org. Lett.* **2004**, *6* (8), 1289–1292.
(118) Michel, B. Y. *Synlett* **2008**, No. 18, 2893–2894.
(119) Boeckman, R. K.; Potenza, J. C. *Tetrahedron Lett.* **1985**, *26*, 1411–1414.
(120) Hilli, F.; White, J. M.; Rizzacasa, M. *Tetrahedron Lett.* **2002**, *43* (47), 8507–8510.
(121) Houghton, S. R.; Furst, L.; Boddy, C. N. *J. Org. Chem.* **2009**, *74* (4), 1454–1463.
(122) Clayden, J. *Chem. Soc. Rev.* **2009**, *38*, 817–829.
(123) Still, W. C.; Novack, V. J. *J. Am. Chem. Soc.* **1984**, *106*, 1149–1150.
(124) Reiter, M.; Turner, H.; Gouverneur, V. *Chem. Eur. J.* **2006**, *12* (27), 7190–7203.
(125) Yang, J.; Xue, H. In *Stereoselective Synthesis of Drugs and Natural Products*; John Wiley & Sons, Inc., 2013; pp 551–581.
(126) Mineeva, I. V. *Russ. J. Org. Chem.* **2015**, *51* (8), 1083–1092.
(127) Keck, G. E.; Castellino, S.; Wiley, M. R. *J. Org. Chem.* **1986**, *51*, 5478–5480.
(128) Stewart, J. J. P. *J. Mol. Model* **2007**, *13*, 1173–1213.
(129) Lee, C.; Yang, W.; Parr, R. G. *Phys. Rev. B* **1988**, *37* (2), 785–789.
(130) Miehlich, B.; Savin, A.; Stoll, H.; Preuss, H. *Chem. Phys. Lett.* **1989**, *157* (3), 200–206.
(131) Becke, A. D. *J. Chem. Phys.* **1993**, *98*, 5648–5652.
(132) Based on personal correspondance with collaborator, Dr. James Davey, who performed the computational analysis.

(133) Kanematsu, M.; Shishido, K. *J. Synth. Org. Chem. Jpn.* **2012**, *70* (11), 1196–1205.
(134) Pöplau, P.; Frank, S.; Morinaka, B. I.; Piel, J. *Angew. Chem. Int. Ed.* **2013**, *52*, 13215–13218.
(135) Beesley, R. M.; Ingold, C. K.; Thorpe, J. F. *J. Chem. Soc. Trans.* **1915**, *107*, 1080–1106.
(136) Pangborn, A. B.; Giardello, M.; Grubbs, R. H.; Rosen, R. K.; Timmers, F. J. *Organometallics* **1996**, *15* (5), 1518–1520.
(137) Armarego, W. L. F.; Chai, C. L. L. *Purification of Laboratory Chemicals*, 6th ed.; Elsevier Ltd, 2009.
(138) Fulmer, G. R.; Miller, A. J. M.; Sherden, N. H.; Gottlieb, H. E.; Nudelman, A.; Stoltz, B. M.; Bercaw, J. E.; Goldberg, K. I. *Organometallics* **2010**, *29*, 2176–2179.
(139) Lane, J. W.; Spencer, K. L.; Shakya, S. R.; Kallan, N. C.; Stengel, P. J.; Remarchuk, T. *Org. Process Res. Dev.* **2014**, *18* (12), 1641–1651.
(140) Alvarez, E.; Cuvigny, T.; du Penhoat, C. H.; Julia, M. *Tetrahedron* **1988**, *44* (1), 119–126.
(141) James, D.; Stille, J. *J. Org. Chem.* **1976**, *41* (9), 1504–1511.
(142) Patel, P.; Reddy, C. N.; Gore, V.; Chourey, S.; Ye, Q.; Ouedraogo, Y. P.; Gravel, S.; Powell, W. S.; Rokach, J. *ACS Med. Chem. Lett.* **2014**, *5*, 815–819.
(143) Peschiulli, A.; Gun, Y.; Connon, S. J.; Enzymes, G. M. I. *J. Org. Chem.* **2008**, *73*, 2454–2457.
(144) Mohr, P.; Herold, P.; Tamm, C. *Helv. Chim. Acta* **1983**, *66* (3), 744–745.
(145) Zhang, C.; Schneiderman, D. K.; Cai, T.; Tai, Y.-S.; Fox, K.; Zhang, K. *ACS Sustain. Chem. Eng.* **2016**, *4*, 4396–4402.
(146) Paquette, L. A.; Ollevier, T.; Desyroy, V. Lithium Aluminum Hydride http://dx.doi.org/10.1002/047084289X.rl036.pub2.
(147) Ho, T.-L.; Fieser, M.; Fieser, L.; Danheiser, R.; Roush, W. In *Lithium aluminum hydride. Fieser and Fieser's Reagents for Organic Synthesis*; John Wiley & Sons, Inc., 2006.
(148) Ito, H.; Inoue, T.; Iguchi, K. *Org. Lett.* **2008**, *10* (17), 3873–3876.
(149) Zhang, Y.; Deng, L.; Zhao, G. *Org. Biomol. Chem.* **2011**, *9*, 4518–4526.
(150) Boger, D. L.; Mathvink, R. J. *J. Am. Chem. Soc.* **1990**, *112*, 4008–4011.
(151) Ribes, C.; Falomir, E.; Murga, J.; Marco, J. A. *Org. Biomol. Chem.* **2009**, *7*, 1355–1360.
(152) Ono, M.; Kishida, M.; Ikegami, Y.; Takaki, Y.; Okawa, M.; Kinjo, J.; Yoshimitsu, H.; Nohara, T.; Miyahara, K. *J. Nat. Med.* **2011**, *65*, 95–102.
(153) Cannizarro, S. *Liebigs Ann.* **1853**, *88* (1), 129–130.
(154) Novak, L.; Rohaly, J.; Poppe, L.; Hornyanszky, G.; Kolonits, P.; Zelei, I.; Feher, I.; Fekete, J.; Szabo, E.; Zahorszky, U.; Javor, A.; Szantay, C. *Liebigs. Ann. Chem.* **1992**, *1992* (2), 145–157.
(155) Schaus, S. E.; Brandes, B. D.; Larrow, J. F.; Tokunaga, M.; Hansen, K. B.; Gould, A. E.; Furrow, M. E.; Jacobsen, E. N. *J. Am. Chem. Soc.* **2002**, *124* (7), 1307–1315.

EFFORTS TOWARD DEVELOPMENT OF A GENERALIZED CHEMOENZYMATIC MACROCYCLIZATION TOOL

· Study II ·

Abstract

The macrolactonization of polyketide natural products is a particularly demanding step for chemical synthesis. In many case, ring-closure only occurs under a very limited set of highly-optimized reaction conditions, or in some cases not at all. Consequently, a wealth of cyclization strategies have been developed to access this privileged scaffold, where carboxyl-activation of *seco*-acids remains the prototypical method (**Chapter 5**). Biosynthetically, these scaffolds are regio- and stereoselectively cyclized by thioesterase (TE) catalytic domains with exceptional efficiency. In this study, we have used phylogenic analysis and *in vitro* biochemical characterization to develop and support an evolutionary model in which the plasticity of TEs increases long-term fitness through retained ability to generate and access chemical diversity (**Chapter 6**). We biochemically showed with recombinant TE from the erythromycin pathway how small, evolutionarily-accessible changes to the substrate can lead to multiple different chemistries, including hydrolysis, macrocyclization, transesterification, and unprecedented dimerization and macrodiolide formation.

· Chapter 5 ·

Macrocyclization Strategies in Natural Product Synthesis

5.1 Macrolactones: A Privileged Scaffold in Natural Products

Preceding chapters demonstrated a rich diversity of structural scaffolds and biological activities in polyketide natural products. Macrocyclic lactones represent a particularly important class within this family, where 10- to 18-membered frameworks are the most common naturally-occurring ring sizes (Figure 5.1). These frameworks rarely adhere to drug-like "rule of five" properties,[1] yet a 2014 review[2] reported 68 registered macrocyclic drugs and 35 in clinical trials.* Most of these agents are used for treatment of infections like the macrolide antibiotic erythromycin A (**5.5**),[3] or anticancer therapeutics like epothilone B (**5.7**).[4] As a direct result of their clinical-relevance,[2] improved generation of macrolactones and other macrocyclic products has garnered significant attention from synthetic chemists and biologists alike.

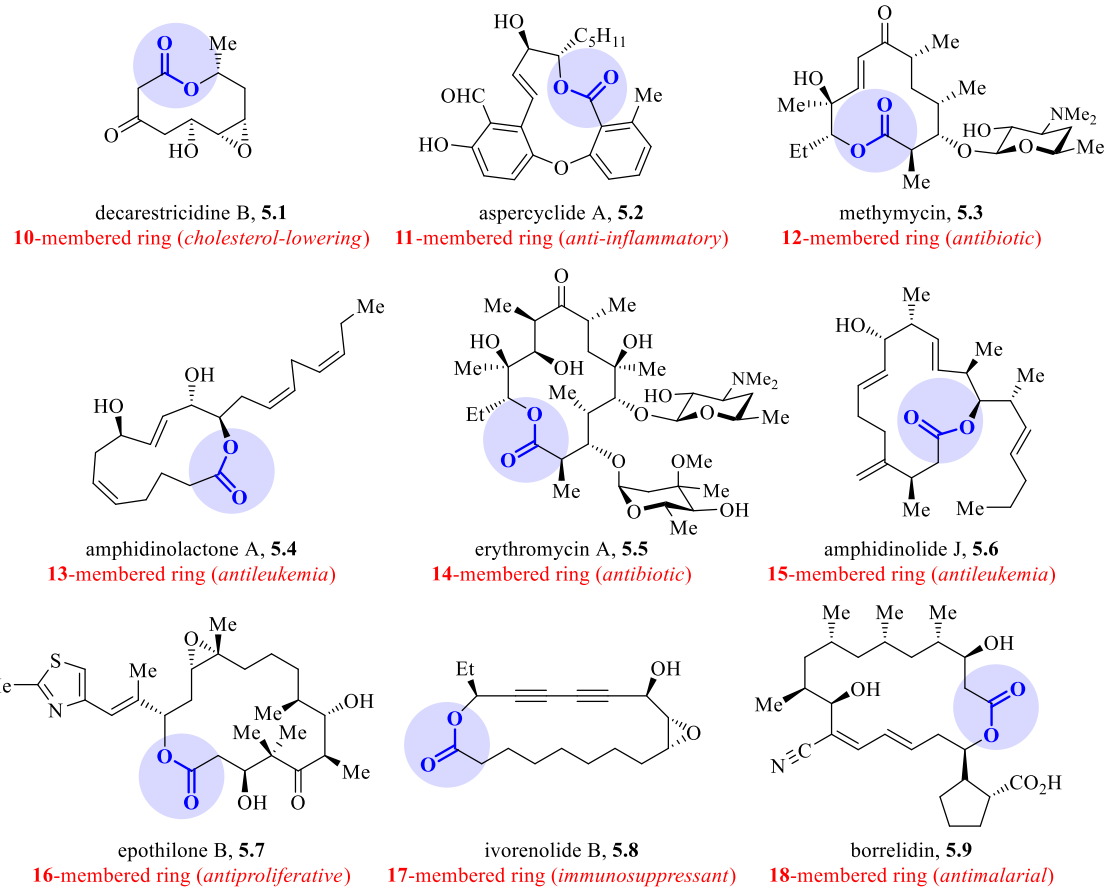

Figure 5.1 – Macrocyclic lactones represent a complex class of natural products with varying ring sizes that display great structural diversity, and assorted therapeutic applications.[3–11] Lactone bonds are highlighted in **blue**.

Although macrocyclic scaffolds have proven to be a pharmacologically-privileged molecular class, their development into clinical agents remains comparatively-limited (< 5% of the drug market, n = 1453).[12]

* "*Macrocycle*" was defined as being a cyclic compound of at least 12 atoms in size; the data set was admittedly incomplete due to disclosure, but considered leads from phase II studies onward.

Fundamental difficulties in accessing these scaffolds is intensified for highly-oxygenated and stereochemically-rich macrolactone polyketide natural products. Generation of these complex metabolites challenge synthetic chemists despite a growing catalogue of macrocyclization strategies (Figure 5.2).[13–18] Due to frequently being late-stage transformations, limitations on available materials make screening conditions and optimization techniques increasingly demanding. Synthetic difficulties stem from entropic- and enthalpic-barriers that prevent cyclization. Although multiple solutions have been reported to this problem, unsuccessful ring-closure still encumbers many total syntheses.

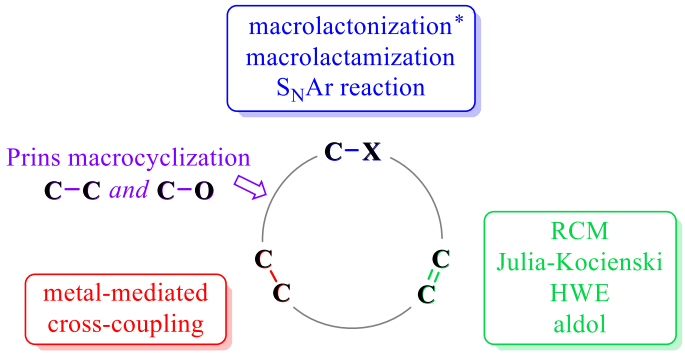

Figure 5.2 – Common bond formations in macrocyclization reactions. For the purposes of this dissertation, only select macrolactonization techniques that rely on activation of *seco*-acids will be highlighted.

This chapter highlights ring-closure as the most decisive step for synthesis of macrocyclic polyketides. While it is beyond the scope of this dissertation to address the many ways of accessing macrocyclic ring systems or to evaluate respective efficiencies, basic details of select strategies will be presented with emphasis on macrolactones. Specifically, prototypical ring-closures that involve lactonization *via* carboxyl-activation of the *seco*-acid will be discussed. This strategy most-closely resembles mechanistic details of macrocyclization in polyketide synthase (PKS) biosynthesis, though it has not produced a synthetic variation that rivals the efficiency of PKS systems.

5.2 General Difficulties Associated with Chemical Synthesis of Macrolactones

Macrolactones are key structural features of many diverse polyketides and other families of biologically-active natural products. The covalent lactone bond adds significant conformational biases by coupling distal parts of the molecule, which can entropically-favor the bioactive orientation by dramatically reducing other conformations. Macrolactonization may also enhance binding affinity, improve selectivity, offer protection against degradation, and lead to exceptional physico-chemical stability of the corresponding macrocycle.[16,18] Polyketide biosynthesis has evolved to exploit these features and biosynthetically-produce macrolactone metabolites with exceptional efficiency.[19]

Kinetic factors that govern chemical macrolactonization were studied by Illuminati and Mandolini using simple ω-bromo alkanoic acids.[20] They evaluated macrolactonization of 3- to 23-membered ring systems, and confirmed that size does matter (Figure 5.3). Results were summarized to illustrate ease of lactonization (log k_{intra}, panel **A**), probability of *intra*- versus *inter*molecular attack ($\Delta S^{\ddagger}$, panel **B**), and relative transition-state strain energies ($\Delta H^{\ddagger}$, panel **C**).[20] The study illustrated that as ring sizes grew larger, observed ring-strain became negligible; however, larger ring sizes decreased chemoselectivity and increased probability of intermolecular reactions that could yield diolide and oligomeric products. The principal method for favoring intramolecular macrolactonization is to employ a high-dilution technique, where the substrate is slowly added to a large volume of solvent, akin to ring-closing metathesis (RCM) procedures.[21,22]

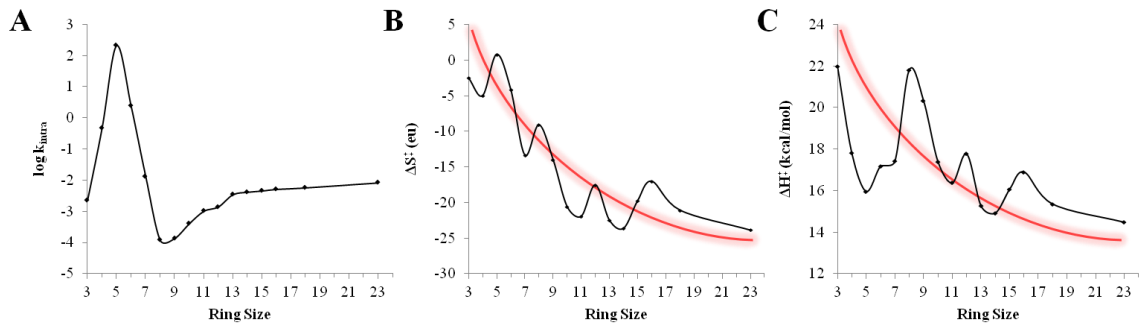

Figure 5.3 – Kinetics profile of cyclising ω-bromoacids highlighting reactivity (A), entropy (B), and enthalpy activation for lactone formation. As ring sizes increase, they exhibit strain-free characteristics comparable to linear counterparts; however, are less likely to react intramolecularly ($\Delta S > \Delta H$).[20]

Activated *seco*-acids and high-dilution techniques have addressed the general trends of macrolactonization kinetics, but not the influence of electronics, steric and conformational biases, regio- and stereoselectivity of complex systems. These influences are typically controlled by specific reagents, strategically-installed reactive groups, and calculated use of protecting groups. Inherently, these requirements contribute to decreased efficiency, atom- and redox-economy, and overall yields of synthetic routes.

Synthesis of macrolactones from their corresponding *seco*-acid is the most-frequently employed chemical strategy (Figure 5.4). Extensive methodologies exist, and esterification has generally been classified by the mode of activation used to facilitate ring-closure.[13,17] Both strategies involve chemoselective reactions that polarize the targeted moiety to increase electrophilicity. Common methods of carboxylic acid-activation increase electrophilicity of the carbonyl group *via* formation of thioesters (*vide infra*, § 5.3.2), *O*-acyl *iso*-ureas (§ 5.3.3), and mixed-anhydrides (§ 5.3.4).

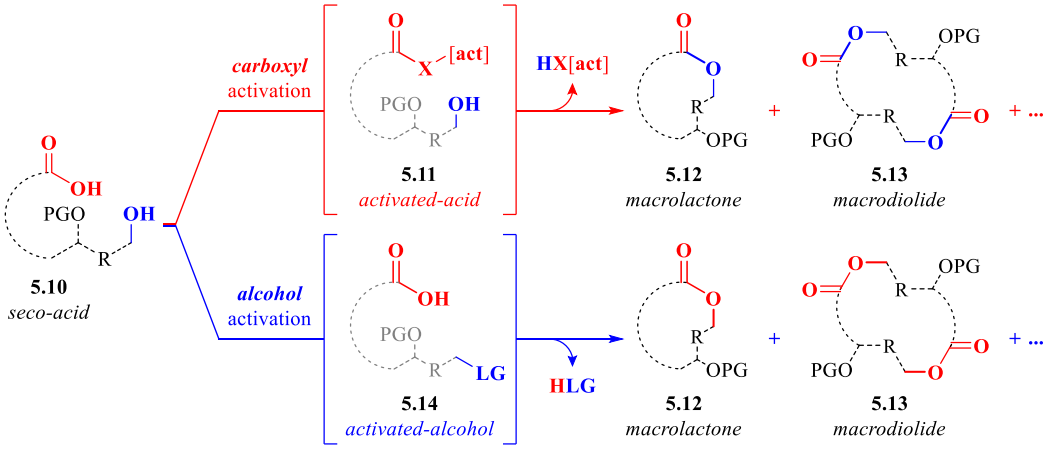

Figure 5.4 – Two synthetic methods of macrolactone assembly *via* activation of linear *seco*-acids. These techniques often require high-dilutions to suppress intermolecular attack, and use of protecting groups to achieve regioselectivity.

Although less prevalent, alcohol-activation methodologies exist for macrolactonization and typically involve its conversion into a better leaving group (Figure 5.4). For example, the ubiquitous role of Mitsunobu conditions[23] in generation of oxophosphonium ion intermediates for synthesis of macrocyclic natural products.[13] Similarly, alcohol-activation *via* conversion to labile groups such as alkyl halides,[24] mesylates,[25] and sulfonium ions[26] facilitate macrolactonization by S_N2 displacement.[13] Application of these chemistries have proven most effective with relatively simple scaffolds. The Boddy Lab reported this methodology for synthesis of laulimalide[27] and neopeltolide[28] model systems (**Chapter 3**); however, this strategy has not been employed for preparation of the fully-functionalized frameworks of these polyketide compounds.[29,30] Because alcohol-activation is not a mimic to the biosynthesis of macrolactones and thus, beyond the scope of this dissertation, the following sections will not detail its common strategies. The reader is encouraged to read excellent reviews covering these and complementary techniques for alcohol-activation.[13–18]

5.3 Accessing Macrolactones *via* Carboxyl-Activation Strategies

In this section, prototypical carboxyl-activation macrolactonization strategies will be highlighted. Synthetic examples are limited to thioester, carbodiimide, and mixed-anhydride techniques, and include references to literature examples. Once again, the reader is encouraged to review cited material for in-depth analysis of these and complementary activation techniques beyond the scope of this document.[13–18]

5.3.1 PKS Biosynthesis: A Muse for Synthetic Chemistry

The general machinery of PKS biosynthesis was outlined in Chapter 1 (§ 1.2.1), and illustrated that assembly of macrolactone metabolites is governed by thioesterase (**TE**) domains.[19] Once the enzymatically-programmed chain length is constructed, a TE acts as the final enzymatic process of modular

PKS assembly (Figure 5.5).[19] This domain operates *via* two-step mechanism between the incoming acyl-carrier protein (**ACP**) and a catalytic triad of amino acid residues in the TE domain active site. The serine (Ser) side-chain alcohol is activated by a conserved histidine-aspartic acid (His-Asp) dyad, and loads thioester intermediate **5.15** by nucleophilic attack. Cyclo-release of intermediate **5.17** as the macrolactone product occurs by intramolecular hydroxyl attack, though intermolecular attack of exogenous water can release a linear hydrolysis product. Post-PKS tailoring enzymes can catalyze additional modifying chemistries, such as monooxygenase-catalyzed epoxidation and hydratase-catalyzed C5-alcohol installation within decarestricidine B (Figure 5.5).[5]

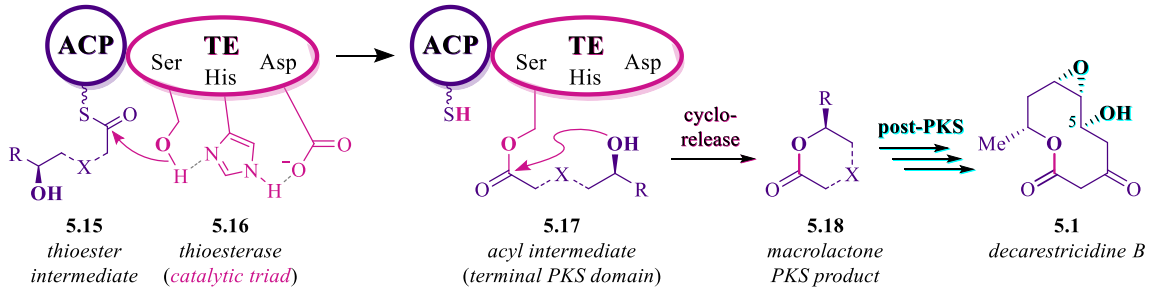

Figure 5.5 – Summary of two-step macrolactone production in PKS biosynthesis. During the loading stage, active site serine replaces the thioester bond to the ACP. In the offloading stage, intramolecular nucleophilic attack releases a macrolactone PKS product. Post-PKS tailoring enzymes can further modify offloaded products.

Enzyme-mediated pre-organization of the linear substrate is critical for success of biosynthetic macrolactonization.[19] Unlike highly-specific PKS enzymes, synthetic strategies toward macrolactonization have not evolved to a similar extent. In the absence of biosynthetic machinery and organizational programming, chemical synthesis of macrolactones must rely upon the generation of activated species. Not surprisingly, the most common approach involves activation of the acid.

5.3.2 Macrolactonization via Activating Thioester Reagents

Motivated by PKS biosynthesis, chemical synthesis employed thioesters as activating agents for bioinspired macrocyclizations of lactone products (Figure 5.6). Corey and Nicolaou first reported this strategy using a double-activation technique in their 1974 synthesis of zearalenone.[31] The general mechanism of this strategy involves mild formation of a 2-pyridine thioester **5.21** from its ω-hydroxy acid **5.19** *via* Mukaiyama condensation.[32] This intermediate species is doubly-activated by intramolecular proton transfer, making cyclization of zwitterion **5.22** electrostatically-driven to furnish the desired lactone.

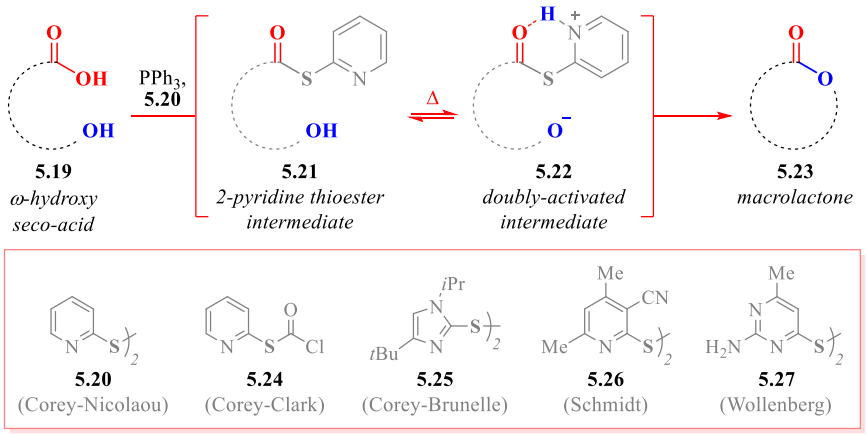

Figure 5.6 – Synthetic macrolactonization of thioester intermediates is a mimic of PKS biosynthesis.[19] Corey-Nicolaou conditions were first-reported, but have seen various modifications to the thioester reagent.[31,33–36]

The Corey-Nicolaou strategy for activation of acids was the first general methodology for preparation of macrolactones, and has been used to generate 6- to 48-membered lactone rings in numerous total syntheses.[13] Popularity emerged from room-temperature-activation and relatively mild conditions, particularly with respect to acid- and base-sensitive molecules. Difficulty removing co-products resulted in variations of thioester reagents like thionylchloroformate **5.24**, which does not require use of triphenylphosphine (Figure 5.6).[34] Other variants improved cyclization rates and selectivity.[33,35,36] Gerlach and Thalmann reported silver ion induced reactions furnished significantly-increased rates by creating a trivalent sulfur species *via* chelation with the alkoxide of **5.22**.[37] This popular modification was used to modestly (40%) cyclize 16-membered macrosphelide A when classical conditions failed and other common activation strategies afforded the condensed 12-membered regio-isomer or partial epimerization.[38]

In the decades since Corey and Nicolaou's seminal report, a large diversity of macrocyclization methodologies relying on varying acid-activation techniques have been developed.[13–18] While many of these alternatives proved highly-robust, the pioneering approach is still prized for its mild reaction conditions, as was seen in the macrolactonization of the highly-sensitive polyene aplyolide A.[39]

5.3.3 Macrolactonization via Activating Carbodiimide Reagents

Carbodiimide reagents are commonly used as an acid-activating strategy in lactonization (Figure 5.7).[40] The first report of carbodiimide-mediated cyclization of a *seco*-acid was Woodward's 1958 synthesis of the six-membered Ring-E within the polycyclic framework of reserpine.[41] General mechanistic details of this strategy involves formation of an activated *O*-acylurea **5.29** ester intermediate from hydroxy acid **5.19** and carbodiimide reagent **5.28**. Because alcohols are much poorer nucleophiles than amines, intermediate **5.29** can undergo intramolecular rearrangement to form undesired *N*-acylurea **5.31** by-product, with no formation of desired lactone. Two decades later,[42] Steglich published a bimolecular esterification

strategy that employed DMAP as an acylating catalyst[43] to suppress formation of *N*-acylurea by-products. Boden and Keck further-modified conditions for *in situ* formation of **5.29** using a proton source (for example, the HCl salt of DMAP) to mediate its requisite proton-transfer step. This modification facilitated intramolecular ring-closure *via* attack of *ω*-hydroxy nucleophile **5.30**, and has found broad application in total synthesis due to elimination of undesired **5.31** by-products.

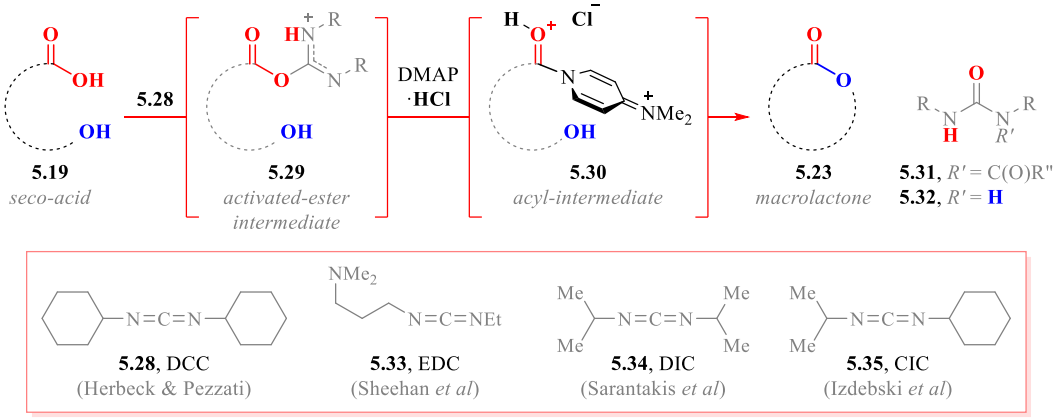

Scheme 5.7 – Carbodiimides are dehydration agents and often used to activate carboxylic acids for amide and ester synthesis.[40] Steglich's carbodiimide/DMAP-mediated esterification conditions[42] were modified to include proton sources for *in situ* formation of activated species, and elimination of insoluble *N*-acylurea by-product **5.31**.[44]

Main disadvantages of this technique include the need for excess carbodiimide reagent, and formation of urea by-products that can make purification intractable.[45] Modified carbodiimide reagents were developed to prevent formation of **5.31**, or to facilitate simplified purification from **5.32** by-products (Figure 5.7). EDC **5.33** and its urea by-product are water soluble,[46] enabling efficient removal during aqueous workup. Conversely, the urea by-products from DIC **5.34**[47] and CIC **5.35**[48] are relatively soluble in CH_2Cl_2, and have been monumental in evolving this strategy for solid phase synthesis.[40] As a result, carbodiimide reagents have become a staple within peptide synthesis and for macrolactamization reactions.

5.3.4 Macrolactonization via Formation of Mixed-Anhydrides

Activation of carboxylic acids *via* formation of anhydrides is a historically-useful strategy for synthesis of macrolactones (Figure 5.8).[49,50] In 1979, Yamaguchi and coworkers determined stoichiometric amounts of DMAP facilitated rapid esterification when employed with sterically-hindered 2,4,6-trichlorobenzoyl chloride (TCBC, **5.36**).[51] Mixed anhydride **5.37** is pre-formed by treatment of hydroxy acid **5.19** with **5.36**, in the presence of base. Regioselective acyl transfer with DMAP promotes alkoxide attack of **5.38**, whereby the resulting tetrahedral intermediate collapses to yield desired lactone. This

methodology has successfully been applied to generating hundreds of cyclic compounds,† and is the most widely-used method of lactonization in organic synthesis.[13,52]

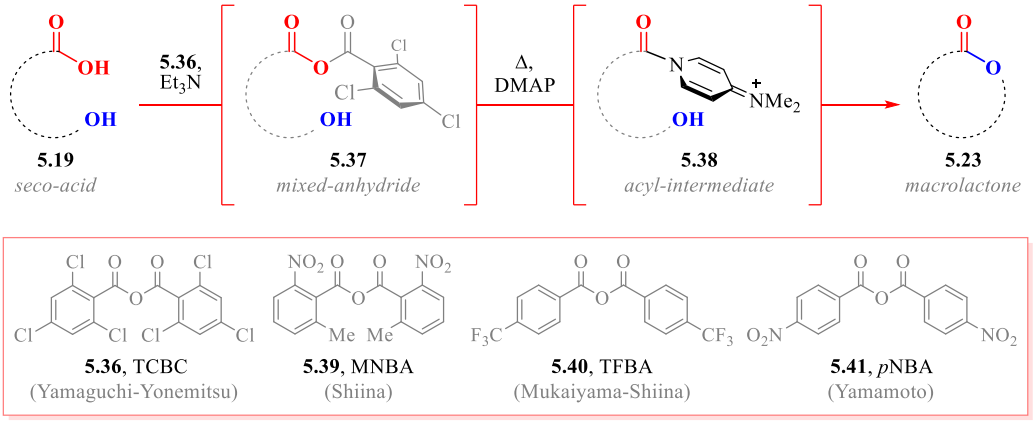

Figure 5.8 – Formation of mixed anhydrides is the paradigm macrolactonization strategy. Activation is traditionally under basic conditions, but Lewis-acid-mediated methodologies have been reported with reagents like **5.40** and **5.41**.[53,54]

The main drawback to Yamaguchi's macrolactonization procedure is the common use of highly-alkaline conditions and refluxing temperatures, which can facilitate erosion of compounds. Use of 2-methyl-6-nitro-benzoic acid **5.39** was reported to afford desired macrolactonization with reduced basicity, and at ambient temperatures.[55,56] Moreover, **5.39** furnished higher-yields and product ratios of monomer-to-dimer in cyclization reactions, compared to **5.36** under similar conditions. Alternatively, anhydride formation can be achieved under acidic conditions, and demonstrated most-effective for preparation of medium-sized macrolactones.[53,54] These conditions promote cyclization *via* Lewis-acid coordination between the mixed anhydride and *ω*-hydroxy, and represent a growing list of variations and modifications that improve reactivity,[57–60] selectivity,[56] and overall popularity of the strategy.[13]

5.4 Macrolactone Synthesis *via* Alternative Strategies

In **Chapter 2**, synthetic efforts toward the macrolactone core of neopeltolide were examined and detailed a variety of common ring-closing strategies beyond carboxyl-activation of *seco*-acids. The wealth of macrolactonization strategies developed over the last 50 years is reflective of associated challenges with the chemical transformation. Despite the growing number of synthetic strategies, it is often that ring-closure only occurs under a very limited set of highly-optimized reaction conditions, or in some cases not at all (Figure 5.9). This section highlights select failures of cyclization strategies toward accessing macrolactone metabolites.

† To illustrate organic chemists' propensity towards macrocyclization under Yamaguchi conditions, greater-than 60% of neopeltolide syntheses relied on this strategy to access its macrocyclic core (Chapter 2, § 2.9.4).

Woodward and coworkers used Corey-Nicolaou macrolactonization conditions in the only successful total synthesis of erythromycin to date (Figure 5.9).[61] Generation of **5.42** failed using numerous activating thioester reagents,[33,37,62,63] and lactonization techniques that relied on formation of mixed-anhydrides or activated amides.[50,64] Structural and reactivity relationships were exhaustively evaluated using a 17-membered isomeric library that differed in protecting groups and C9-configuration. Successful macrolactonization was realized with a single 9*S*-isomer using modified Corey-Nicolaou conditions.‡ They suggested cyclic protecting groups and *S*-configuration were essential to set conformational requirements needed for successful ring-closure.[61]

Similarly, Molinski and coworkers were plagued by complex mixtures of products when common strategies for macrolactonization *via* anhydride formation were employed toward their synthesis of enigmazole (Figure 5.9).[51,55,57,65,66] While trace formation of precursor **5.43** was observed under Mukaiyama[32] and Keck[44] conditions, the undesired 16-membered regio-isomer was both kinetically- and thermodynamically-preferred. Poor regioselectivity was caused by conformational bias imposed by free-rotation of the C12-C13 bond. Desired selective macrolactonization was achieved by an altered order of transformations that left the framework rigidified with a C12-C13 olefin during ring-closure.[65]

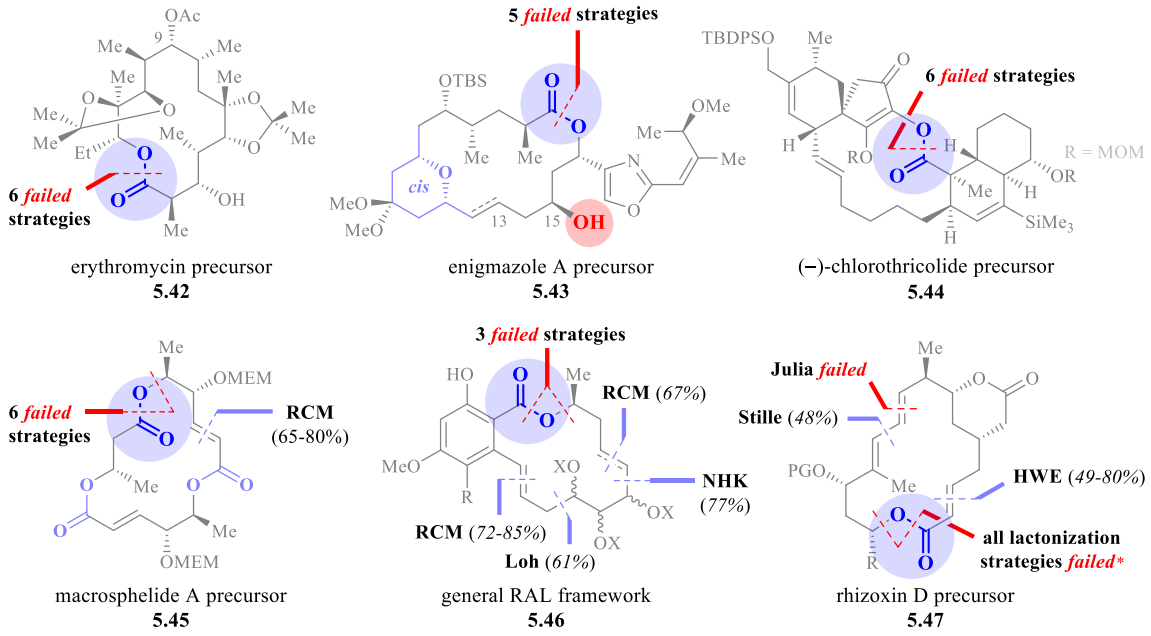

Figure 5.9 – Small sample of ring-closure difficulties experienced in the chemical synthesis of various macrolactone polyketides.

Prototypical carboxyl-activating macrolactonization strategies do not guarantee successful ring-closure. Roush published multiple reports toward assembly of (–)-chlorothricolide,[67] and required

‡ Three isomers generated observable lactone; two were poor-yielding (10% and 15%). All three were 9*S*-configured.[61]

treatment by Palomo's reagent BOP-Cl[68] to modestly-generate precursor **5.44** in 50% yield. Phosphorous-based activating reagents are rarely-employed for macrolactonization, but common carboxyl-activating conditions and modifications were hampered by poor yields and formation of by-products. In some cases, macrolactonization strategies fail so utterly that alternative bond-forming reactions are needed. The lactonization of **5.45** was laden with issues caused by base-lability.[38] Subsequently, neutral RCM strategies have since been employed to efficiently generate macrosphelide A and analogues for structural-activity relationship studies.[69] Metal-mediated cyclization techniques have become increasingly popular in macrolactone synthesis, as illustrated by work on cochliomycins A-C,[70–74] and pæcilomycin E and F[73–79] of the resorcylic acid lactone (RAL) scaffold **5.46**. Generation of these metabolites relied on RCM (Ru), Loh-type α-allylation (In),[80] and Nozaki-Hiyama-Kishi γ-allylation (Cr/Ni)[81] reactions to effect ring-closure.

Unfortunately, macrolactonization is commonly a late-stage transformation and limited material exacerbates difficulties of screening and optimizing conditions. Leahy and coworkers underscored this challenge with their synthesis of rhozoxin D.[82] Multiple lactonization strategies and Julia olefination protocol failed to yield desired precursor **5.47**, which was finally afforded in fair yield (49%) using phase-transfer HWE conditions of barium hydroxide in aqueous THF. Analogous macrocyclic precursors of rhizoxin D have been reported by other groups (6) using HWE conditions (55-84%),[83] and most-recently by Pattenden and coworkers[84] using Stille cross-coupling.

The selection of chemical macrolactonization difficulties was not exhaustive, but highlighted a delicate balance between controlling *essential* attributes like reactivity, stereo-, regio-, and chemoselectivity with *desired* ones, including step/redox economy, minimal protecting group use/manipulation, yield, or reaction reproducibility. There exists a need for a selective mechanism to generate macrolactone products that can overcome unfavorable enthalpic and entropic concerns, while limiting polymerization.

5.5 Thioesterase-Mediated Macrolactonization: A Potential Chemoenzymatic Tool

Thioesterase (TE) domains catalyze macrolactonization in many PKS and non-ribosomal peptide synthetase (NRPS) biosynthetic pathways.[19] Because of the incredible selectivity and relative efficiency at which TEs convert linear substrates into macrolactone scaffolds, they have the potential to address some of the significant difficulties experienced in chemical cyclization reactions. With an increased understanding of PKS/NRPS biosynthesis and advances in protein engineering, TEs make attractive candidates to be developed as general macrolactonization biocatalysts.

Isolated TE domains demonstrated retention of autonomous catalytic activity for *in vivo* and *in vitro* experiments (Figure 5.10). Most TEs exhibit flexibility in the loading stage, but display stringent

substrate-selectivity and fail to effectively process non-native substrates. In fact, when separated from their upstream modules, PKS TE domains predominantly-catalyze hydrolysis of thioester substrates. However, isolated epothilone TE facilitated regioselective *in vitro* production of epothilone C **5.49** by ring-closure of *N*-acetylcysteamine (NAC) thioester **5.48**.[85] Similar work was conducted with methymycin/pikromycin (PIK TE), where exclusive production of **5.51** was realized *in vitro* with native linear framework of SNAC-derivative **5.50** (Figure 5.10). Conversely, C7-*hydroxy*-**5.50** was hydrolyzed exclusively, indicating small modifications to linear frameworks can dramatically-alter selectivity. This result clearly highlighted that substrate-selectivity must be carefully characterized to ensure TEs are used with appropriately-functionalized substrates.

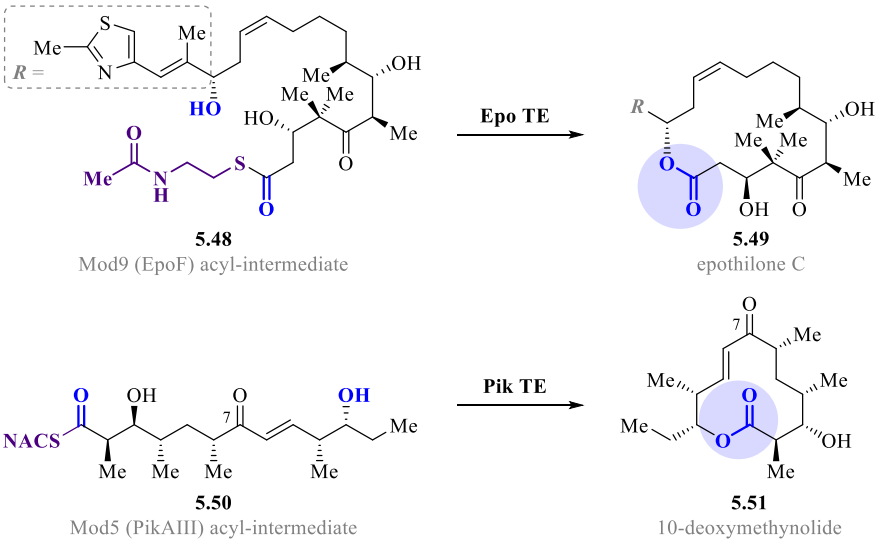

Figure 5.10 – Synthetic phosphopantetheinyl mimics (**SNAC**) promoted *in vitro* acylation of linear substrates **5.48** and **5.50**, and generated native macrolactone products from epothilone and pikromycin biosynthetic pathways, respectively.

Present knowledge of factors that control TE-mediated hydrolysis and macrocyclization during substrate off-loading is limited and remains unclear. Understanding the molecular basis for substrate-specificity of TEs is critical to manipulating these enzymes for macrolactonization of non-native linear polyketide substrates. Additionally, known libraries of macrocyclizing TEs must be probed for selectivity to provide necessary insights into their relative promiscuity, and to identify an enzyme possessing broad substrate-tolerance. Libraries of synthetic substrates improve *in vitro* characterization of TE activity by accessing greater diversity to be assayed biochemically as an empirical method of elucidating recognition elements. These studies will enable rational protein engineering[86–88] and directed evolution[89–91] to modulate substrate-specificity for macrocyclization and to relax substrate-selectivity of non-native linear scaffolds, thus providing a chemoenzymatic tool to facilitate production of novel drug-like macrocyclic molecules.

5.6 Conclusions

This chapter highlighted that despite an ever-expanding synthetic toolbox, the intramolecular assembly of ester bonds remains one of the most-challenging chemical transformations in macrolactone production. Biosynthetically, thioesterase catalytic domains generate complex macrolactone scaffolds from highly-oxygenated, stereo-enriched linear substrates with incredible selectivity under physiological conditions. Ergo, modular PKS enzymes have the potential to address challenges associated with the chemical synthesis of macrolactones, and offers an exciting strategy to access structurally-diverse libraries of novel macrocyclic compounds for drug discovery. However, this potential remains unrealized at present, and first requires the identification of an thioesterase domain with broad substrate-tolerance.

5.7 References

(1) Lipinski, C. A.; Lombardo, F.; Dominy, B. W.; Feeney, P. J. *Adv. Drug Deliv. Rev.* **2001**, *46*, 3–26.
(2) Giordanetto, F.; Kihlberg, J. *J. Med. Chem.* **2014**, *57*, 278–295.
(3) McGuire, J. M.; Bunch, R. L.; Anderson, R. C.; Boaz, H. E.; Flynn, E. H.; Powell, H. M.; Smith, J. W. *Antibiot. Chemother.* **1952**, *2*, 281.
(4) Altmann, K.-H.; Gaugaz, F. Z.; Schiess, R. *Mol. Divers.* **2011**, *15*, 383–399.
(5) Gohrt, A.; Zeeck, A.; Hutter, K.; Kirsch, R.; Kluge, H.; Thiericke, R. *J. Antibiot.* **1992**, *45* (1), 66–73.
(6) Singh, S. B.; Jayasuriya, H.; Zink, D. L.; Polishook, J. D.; Dombrowski, A. W.; Zweerink, H. *Tet. Lett.* **2004**, *45*, 7605–7608.
(7) Donin, M. N.; Pagano, J.; Dutcher, J. D.; McKee, C. M. *Antibiot. Annu.* **1953**, 179–189.
(8) Takahashi, Y.; Kubota, T.; Kobayashi, J. *Heterocycles* **2007**, *72* (1), 567–572.
(9) Kobayashi, J.; Sato, M.; Ishibashi, M. *J. Org. Chem.* **1993**, *58*, 2645–2646.
(10) Wang, Y.; Liu, Q.; Xue, J.; Zhou, Y.; Yu, H.; Yang, S.; Zhang, B.; Zuo, J.; Li, Y.; Yue, J. *Org. Lett.* **2014**, *16*, 2062–2065.
(11) Azcárate, I. G.; Marin-García, P.; Camacho, N.; Pérez-Benavente, S.; Puyet, A.; Diez, A.; Ribas de Pouplana, L.; Bautista, J. M. *Br. J. Pharmacol.* **2013**, *169*, 645–658.
(12) Kinch, M. S.; Haynesworth, A.; Kinch, S. L.; Hoyer, D. *Drug Discov. Today* **2014**, *19* (8), 1033–1039.
(13) Parenty, A.; Moreau, X.; Niel, G.; Campagne, J.-M. *Chem. Rev.* **2013**, *113*, PR1-PR40.
(14) Crane, E.; Scheidt, K. *Angew. Chem. Int. Ed.* **2010**, *49* (45), 8316–8326.
(15) Wessjohann, L.; Ruijter, E. In *Topics in Current Chemistry*; 2005; Vol. 243, pp 137–184.
(16) Kopp, F.; Marahiel, M. A. *Nat. Prod. Rep.* **2007**, *24*, 735–749.
(17) Tsakos, M.; Schaffert, E. S.; Clement, L. L.; Villadsen, N. L.; Poulsen, T. B. *Nat. Prod. Rep.* **2015**, 605–632.
(18) Marti-Centelles, V.; Pandey, M. D.; Burguete, M. I.; Luis, S. V. *Chem. Rev.* **2015**, *115* (16), 8736–8834.
(19) Horsman, M. E.; Hari, T. P. A.; Boddy, C. N. *Nat. Prod. Rep.* **2016**, *33*, 183–202.
(20) Illuminati, G.; Mandolini, L. *Acc. Chem. Res.* **1981**, *14* (4), 95–102.
(21) Ziegler, K.; Eberle, H.; Ohlinger, H. *Justus Liebigs Ann. Chem.* **1933**, *504* (1), 94–130.
(22) Wilke, G. *Angew. Chem. Int. Ed.* **2003**, *42* (41), 5000–5008.
(23) Mitsunobu, O.; Yamada, M.; Mukaiyama, T. *Bull. Chem. Soc. Jpn.* **1967**, *40* (4), 935–939.
(24) Hunsdiecker, H.; Erlbach, H. *Chem. Ber.* **1947**, *80*, 129–137.
(25) Vedejs, E.; Larsen, S. D. *J. Am. Chem. Soc.* **1984**, *106* (4), 3030–3032.
(26) Matsuyama, H.; Nakamura, T.; Kamigata, N. *J. Org. Chem.* **1989**, *54* (22), 5218–5223.
(27) Houghton, S. R.; Furst, L.; Boddy, C. N. *J. Org. Chem.* **2009**, *74* (4), 1454–1463.
(28) Hari, T. P. A.; Wilke, B. I.; Davey, J. A.; Boddy, C. N. *J. Org. Chem.* **2016**, *81*, 415–423.
(29) Crimmins, M. T. *Curr. Opin. Drug Discov. Devel.* **2002**, *5* (6), 944–959.
(30) Fuwa, H. *Mar. Drugs* **2016**, *14* (65).
(31) Corey, E. J.; Nicolaou, K. *J. Am. Chem. Soc.* **1974**, *96* (17), 5614–5616.
(32) Mukaiyama, T.; Matsueda, R.; Suzuki, M. *Tet. Lett.* **1970**, No. 22, 1901–1904.
(33) Corey, E. J.; Brunelle, D. J. *Tet. Lett.* **1976**, *38*, 3409–3412.
(34) Corey, E. J.; Clark, D. A. *Tet. Lett.* **1979**, *31*, 2875–2878.
(35) Schmidt, U.; Heermann, D. *Angew. Chem. Int. Ed.* **1979**, *18*, 308–309.
(36) Nimitz, S.; Wollenberg, R. H. *Tet. Lett.* **1978**, *38*, 3523–3526.
(37) Gerlach, H.; Thalmann, A. *Helv. Chim. Acta* **1974**, *57* (8), 2661–2663.
(38) Kusaka, S. I.; Dohi, S.; Doi, T.; Takahashi, T. *Tet. Lett.* **2003**, *44* (49), 8857–8859.
(39) Hansen, T. V.; Stenstrøm, Y. *Tetrahedron* **2001**, *12*, 1407–1409.
(40) Han, S.-Y.; Kim, Y.-A. *Tetrahedron* **2004**, *60* (11), 2447–2467.
(41) Woodward, R. B.; Bader, F. E.; Bickel, H.; Frey, A. J.; Kierstead, R. W. *Tetrahedron* **1958**, *2*, 1–57.
(42) Neises, B.; Steglich, W. *Angew. Chem. Int. Ed.* **1978**, *17* (7), 522–524.
(43) Steglich, W.; Höfle, G. *Angew. Chem. Int. Ed.* **1969**, *8* (12), 981–981.
(44) Boden, E.; Keck, G. E. *J. Org. Chem.* **1985**, *50*, 2394–2395.
(45) El-Faham, A.; Albericio, F. *Chem. Rev.* **2011**, *111* (11), 6557–6602.
(46) Sheehan, J. C.; Cruickshank, P. A.; Boshart, G. L. *J. Org. Chem.* **1961**, *26* (7), 2525–2528.
(47) Sarantakis, D.; Teichman, J.; Lien, E. L.; Fenichel, R. L. *Biochem. Biophys. Res. Commun.* **1976**, *73* (2), 336–342.

(48) Izdebski, J.; Pachulska, M.; Orłowska, A. *Int. J. Pept. Protein Res.* **1994**, *44* (5), 414–419.
(49) Baker, W.; Ollis, W. D.; Zealley, T. S. *J. Chem. Soc.* **1952**, 1447–1451.
(50) Taub, D.; Girotra, N. N.; Hoffsommer, R. D.; Kuo, C. H.; Slates, H. L.; Weber, S.; Wendler, N. L. *Chem. Commun.* **1967**, *13*, 225–226.
(51) Yamaguchi, M.; Inanaga, J.; Hirata, K.; Saeki, H.; Katsuki, T. *Bull. Chem. Soc. Jpn.* **1979**, *52* (7), 1989–1993.
(52) Wang, Z. In *Comprehensive Organic Name Reactions and Reagents*; 2010; pp 3109–3114.
(53) Shiina, I.; Mukaiyama, T. *Chem. Lett.* **1994**, *23* (4), 677–680.
(54) Ishihara, K.; Karumi, Y.; Kubota, M.; Yamamoto, H. *J. Am. Chem. Soc.* **1995**, *117*, 4413–4414.
(55) Shiina, I.; Kubota, M.; Ibuka, R. *Tet. Lett.* **2002**, *43*, 7535–7539.
(56) Shiina, I.; Kubota, M.; Oshiumi, H.; Hashizume, M. *J. Org. Chem.* **2004**, *69* (6), 1822–1830.
(57) Hikota, M.; Tone, H.; Horita, K.; Yonemitsu, O. *J. Org. Chem.* **1990**, *55*, 7–9.
(58) Okuno, Y.; Isomura, S.; Nishibayashi, A.; Hosoi, A.; Fukuyama, K.; Ohba, M.; Takeda, K. *Synth. Commun.* **2014**, *44* (19), 2854–2860.
(59) Okuno, Y.; Isomura, S.; Sugamata, A.; Tamahori, K.; Fukuhara, A.; Kashiwagi, M.; Kitagawa, Y.; Kasai, E.; Takeda, K. *ChemSusChem* **2015**, *8*, 3587–3589.
(60) Okuno, Y.; Isomura, S.; Kamakura, T.; Sano, F.; Tamahori, K.; Goto, T.; Hayashida, T.; Kitagawa, Y.; Fukuhara, A.; Takeda, K. *ChemSusChem* **2015**, *8*, 1711–1715.
(61) Woodward, R. B.; Au-Yeung, B. W.; Balaram, P.; Browne, L. J.; Ward, D. E.; Card, P. J.; Chen, C. H. *J. Am. Chem. Soc.* **1981**, *103* (11), 3213–3215.
(62) Corey, E.; Nicolaou, K.; Melvin Jr, L. S. *J. Am. Chem. Soc.* **1975**, *97* (3), 653–654.
(63) Masamune, S.; Kamata, S.; Schilling, W. *J. Am. Chem. Soc.* **1975**, *97* (12), 3515–3516.
(64) Staab, H. A.; Wendel, K. *Angew. Chem.* **1961**, *73* (1), 26.
(65) Skepper, C. K.; Quach, T.; Molinski, T. F. *J. Am. Chem. Soc.* **2010**, *132*, 10286–10292.
(66) Hikota, M.; Sakurai, Y.; Horita, K.; Yonemitsu, O. *Tet. Lett.* 1990, pp 6367–6370.
(67) Roush, W. R.; Sciotti, R. J. *J. Am. Chem. Soc.* **1998**, *120*, 7411–7419.
(68) Diago-Meseguer, J.; Palomo-Coll, A. L. *Synthesis*, **1980**, *July*, 547–551.
(69) Matsuya, Y.; Kawaguchi, T.; Nemoto, H. *Org. Lett.* **2003**, *5* (16), 2939–2941.
(70) Pal, P.; Jana, N.; Nanda, S. *Org. Biomol. Chem.* **2014**, *12* (41), 8257–8274.
(71) Wang, L.; Gao, Y.; Liu, J.; Cai, C.; Du, Y. *Tetrahedron* **2014**, *70*, 2616–2620.
(72) Bolte, B.; Basutto, J. A.; Bryan, C. S.; Garson, M. J.; Banwell, M. G.; Ward, J. S. *J. Org. Chem.* **2015**, *80*, 460–470.
(73) Ma, X.; Bolte, B.; Banwell, M. G.; Willis, A. C. *Org. Lett.* **2016**, *18*, 4226–4229.
(74) Mahankali, B.; Srihari, P. *Eur. J. Org. Chem.* **2015**, 3983–3993.
(75) Mohapatra, D. K.; Reddy, D. S.; Mallampudi, N. A.; Yadav, J. S. *Eur. J. Org. Chem.* **2014**, 5023–5032.
(76) Pal, P.; Jana, N.; Nanda, S. *Org. Biomol. Chem.* **2014**, *12*, 8257–8274.
(77) Bhunia, N.; Das, B. *Synthesis*, **2015**, *47*, 1499–1509.
(78) Srihari, P.; Mahankali, B.; Rajendraprasad, K. *Tetrahedron Lett.* **2012**, *53*, 56–58.
(79) Jana, N.; Nanda, S. *Tetrahedron: Asymmetry* **2012**, *23*, 802–808.
(80) Tan, K.-T.; Chng, S.-S.; Cheng, H.-S.; Loh, T.-P. *J. Am. Chem. Soc.* **2003**, *125*, 2958–2963.
(81) Okude, Y.; Hirano, S.; Hiyama, T.; Nozaki, H. *J. Am. Chem. Soc.* **1977**, *99* (9), 3179–3181.
(82) Lafontaine, J. A.; Provencal, D. P.; Gardelli, C.; Leahy, J. W. *J. Org. Chem.* **2003**, *68*, 4215–4234.
(83) Hong, J.; White, J. D. *Tetrahedron* **2004**, *60* (681), 5653–5681.
(84) Mitchell, I. S.; Pattenden, G.; Stonehouse, J. *Org. Biomol. Chem.* **2005**, *3*, 4412–4431.
(85) Boddy, C. N.; Schneider, T. L.; Hotta, K.; Walsh, C. T.; Khosla, C. *J. Am. Chem. Soc.* **2003**, *125* (12), 3428–3429.
(86) Wong, F. T.; Khosla, C. *Curr. Opin. Chem. Biol.* **2012**, *16*, 117–123.
(87) Williams, G. J. *Curr. Opin. Struct. Biol.* **2013**, *23* (4), 603–612.
(88) Lutz, S. *Curr. Opin. Biotechnol.* **2010**, *21*, 734–743.
(89) Turner, N. J. *Nat. Chem. Biol.* **2009**, *5* (8), 567–573.
(90) Toscano, M. D.; Woycechowsky, K. J.; Hilvert, D. *Angew. Chem. Int. Ed.* **2007**, *46*, 3212–3236.
(91) Shivange, A. V; Marienhagen, J.; Mundhada, H.; Schenk, A.; Schwaneberg, U. *Curr. Opin. Chem. Biol.* **2009**, *13*, 19–25.

· Chapter 6 ·

Probing the Specificity of the 6-Deoxyerythronolide B Thioesterase

6.1 Harnessing PKS for Chemoenzymatic Synthesis of Macrocyclic Products

Engineered modular polyketide synthases (PKSs) have a potential to be extraordinarily effective platforms for the chemoenzymatic production of complex natural products. Native PKS biosynthetic machineries assemble simple, readily-available cellular building blocks, and tailor growing frameworks into large, complex, chiral metabolites (Figure 6.1).[1–9] As highlighted in **Chapter 5**, the total chemical synthesis of macrocyclic scaffolds is particularly demanding and fails to rival the overall efficiency of PKS systems. Thus, there exists a potential benefit of developing PKS systems into chemoenzymatic tools.

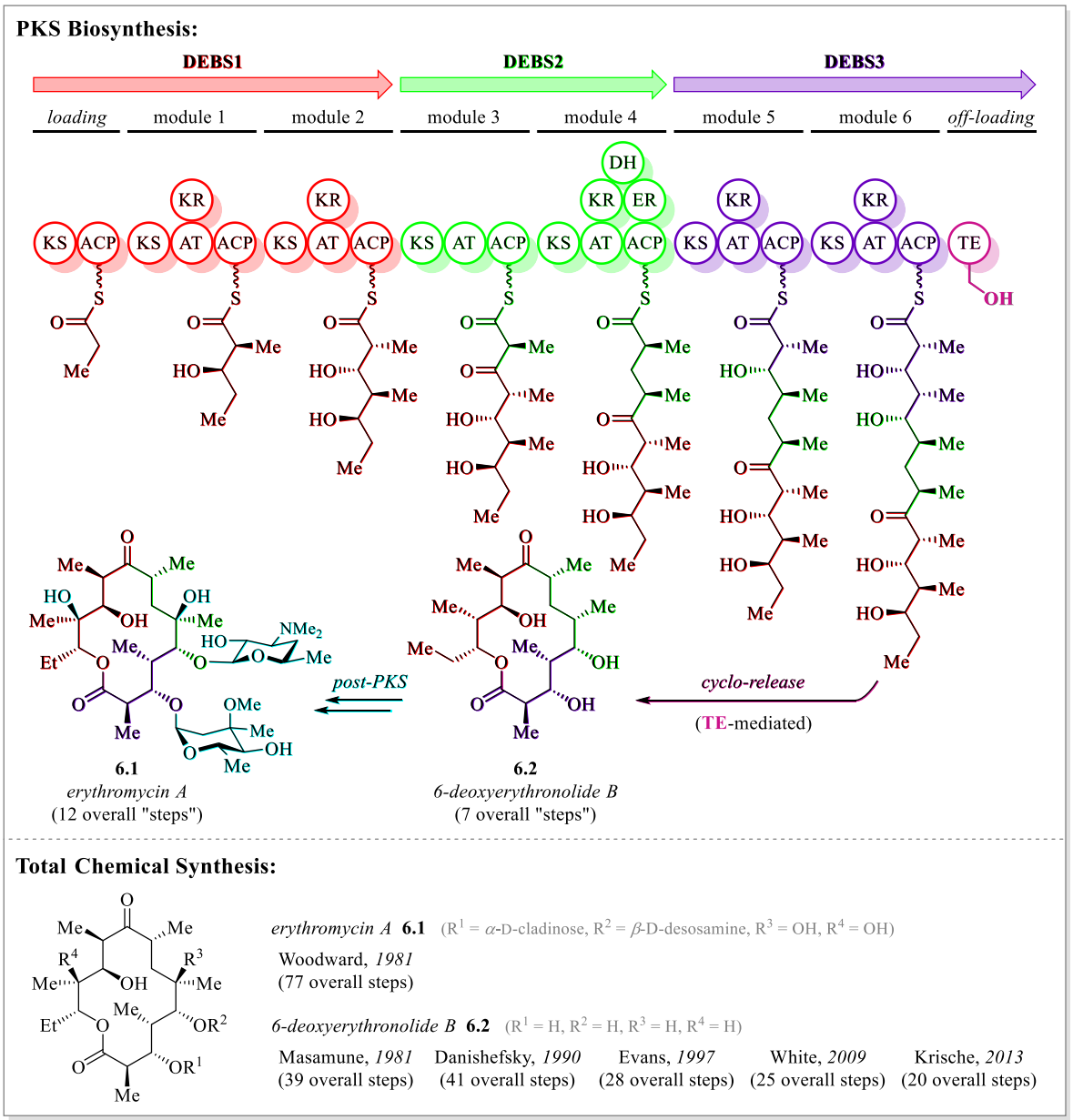

Figure 6.1 – The paradigm model of modular PKS systems is 6-deoxyerythronolide B synthase (DEBS), which produces the macrocyclic core of erythromycin A. Total chemical synthesis has suffered by their structural complexity, indicating a potential benefit of harnessing PKS systems in chemoenzymatic synthesis or as free-standing biocatalysts.

Macrocyclizing thioesterase (TE) catalytic domains from PKS biosynthetic pathways represent a particularly attractive candidate for development of a macrocyclization biocatalyst. These enzymes have been reported to effectively mediate ring-closure of their polyfunctional native substrates with extremely-high selectivity under physiological conditions.[10] Harnessing these specific enzymes to macrocyclize non-native substrates would generate a much-needed addition to the current biocatalysis toolbox. Moreover, it could enable combinatorial biosynthesis and PKS protein engineering studies that seek to assemble *de novo* pathways, such as the *de novo* neopeltolide pathway described in the earlier chapters of this dissertation, by providing a catalytic domain capable of off-loading non-native substrates from the terminal PKS protein. Key first steps in this development process involve the identification of an appropriate enzyme from the library of known macrocyclizing TEs, and characterization of its substrate-selectivity.

Phylogenetic analysis of many type-I PKS catalytic domains indicated that substrate-specificity, or reactivity of domains, often have a primary sequence determinant. For example, acyltransferase (AT) domains cluster into malonyl-CoA- and methylmalonyl-CoA-specific clades.[11–14] Similarly, *β*-ketosynthase (KS) domains from *trans*-AT pathways cluster based on substitution patterns at the *α*- and *β*-carbons of upstream polyketide intermediates.[15,16] Lastly, ketoreductase (KR) domains cluster into type-A or type-B, based on facial selectivity for delivery of hydride from NADPH.[17–19]

Conversely, our phylogenetic analysis highlighted that TEs are unique among PKS domains because they do not cluster based on reactivity (please refer to Appendix II, § S2.4.1).[20] PKS TEs catalyze the PKS turnover step by releasing a completed polyketide chain from the mega-protein to which it was covalently-linked (Figure 6.2).[21] Polyketide release can occur *via* hydrolysis of acyl-PKS intermediates to generate free acids like ambruticin[22] and gephyronic acid (**6.5**),[23] nucleophilic attack by intramolecular alcohols to generate macrolactones like epothilone[24,25] and erythromycin (**6.1**),[26] or dimerization with a second equivalent of acyl-PKS to generate macrodiolides like the predicted biosyntheses of disorazol[27] and elaiophylin (**6.8**).[28] Phylogenetic analysis distinctly showed that TEs do not cluster based on the type of reaction they catalyze. Thus, while factors that control the chemistry for off-loading remain unclear, it is abundantly-clear that a primary sequence determinant does not exist that can predict macrocyclization activity for these domains.

More-detailed analysis of sequence diversity for PKS TEs indicated that the main determinant for clustering of TE domains is the type of biosynthetic module that the TE is directly-fused to (PKS, *trans*-AT PKS, NRPS). In some cases, the phylogeny of the producing organism also appeared to be important.[10] Consequently, unlike other PKS catalytic domains, predicting and characterizing specificity or reactivity of TEs relies on experimental characterization and observation.[10,29–31]

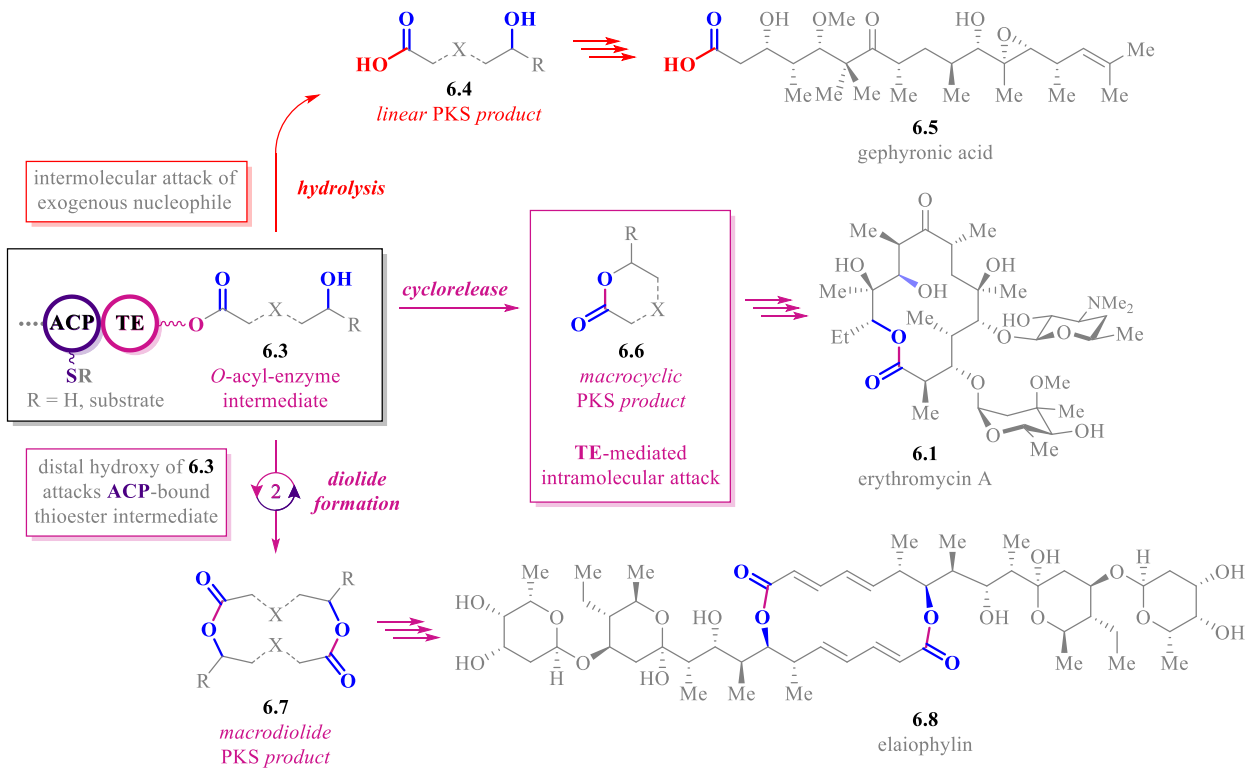

Figure 6.2 – Highlighting various known chemistries of PKS TE proteins. Post-PKS tailoring can produce a diverse range of metabolites after completed polyketide chains are off-loaded from protein.

6.1.1 Research Milestones of Biocatalytic Thioesterase Study

Research milestones of the thioesterase biocatalyst study are divided into two stages, where development of a TE domain as a commercially-available general macrolactonizing biocatalytic tool represents the final and long-term goal for this research (Figure 6.3). The immediate goal of this study has thus been to identify an appropriate TE domain through evaluation and characterization of its boundaries of promiscuity, and necessary elements for successful ring-closure of non-native linear substrates. This information will guide protein engineering experiments to expand the limits of viable frameworks, electrophiles, or nucleophiles to optimize cyclization.

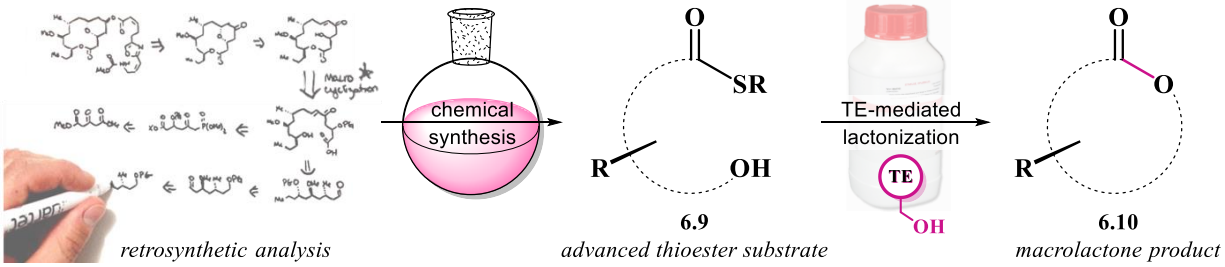

Figure 6.3 – A combined synthetic-biosynthetic approach for production of macrolactone natural products using a thioesterase catalytic domain as a biocatalyst for ring-closure of advanced thioester frameworks.

To address the immediate goal, we focused on the best-studied PKS macrocyclizing TE domain, which is from the erythromycin biosynthetic pathway (DEBS TE). This is the only PKS TE that has been reported to macrocyclize non-native substrates as an excised, stand-alone, recombinant purified protein. This chapter discusses our on-going characterization of DEBS TE activity with additional evolutionarily-related non-native substrates, and shows that this enzyme is both highly substrate-selective and capable of catalyzing a high-diversity of chemistries that include hydrolysis, esterification, macrocyclization, and an unprecedented formation of macrodiolide product. Moreover, we propose an evolutionary model using the screening hypothesis to account for these observations. Based on our data, it is likely that wild-type DEBS TE is too substrate-selective to be used as a general biocatalyst for macrocycle formation, or for use in *de novo* engineered PKS pathways. Consequently, we believe TEs with broader substrate-tolerance must be identified to develop a stand-alone macrocyclizing biocatalyst, and for the combinatorial biosynthetic field to successfully generate functionalized *de novo* PKS pathways.

6.2 6-Deoxyerythronolide B Synthase as a Model of Study

In vitro biochemical characterization of DEBS TE indicated that macrocyclization activity is substrate-selective, with hydrolytic activity predominating in virtually all substrates investigated. For example, small changes to oxidation state within substrates known to undergo macrocyclization (Figure 6.4a), as well as the configuration of *O*-nucleophiles, have completely abolished formation of macrocyclic metabolites (Figure 6.4b).[29,32,33] The related TE from pikromycin biosynthesis (PIK TE) demonstrated similar high substrate-specificity for macrocyclization, suggesting that this is a general phenomenon of type-I PKS TEs.[31,33]

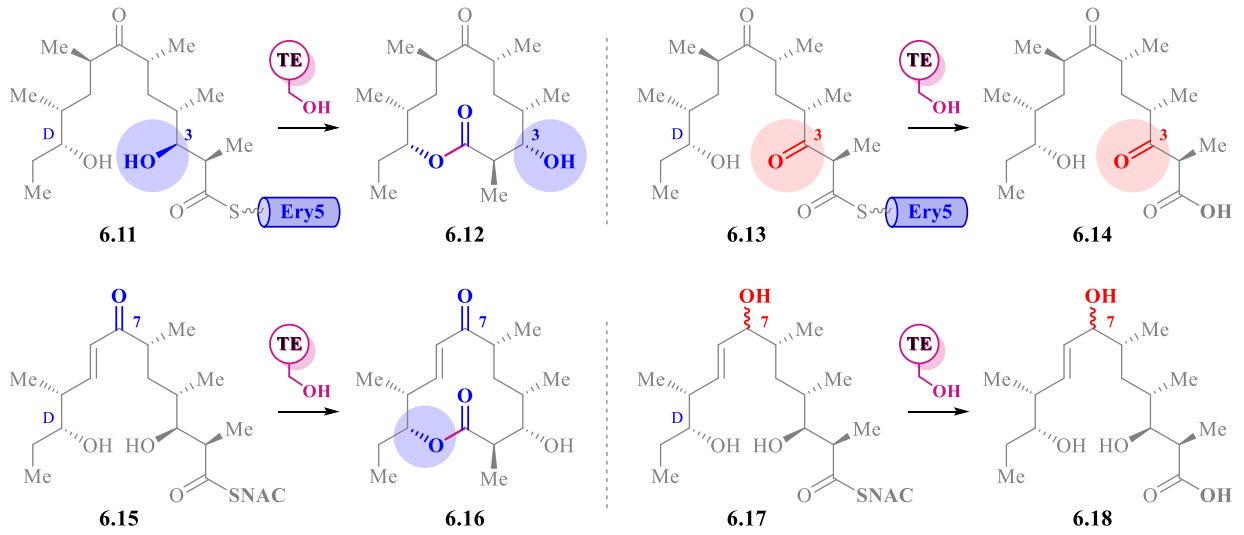

Figure 6.4a – Highly-selective DEBS TE-mediated macrocyclization demonstrated the effects of C3 oxidation state *in vivo*, and C7 oxidation state for *in vitro* experiments.

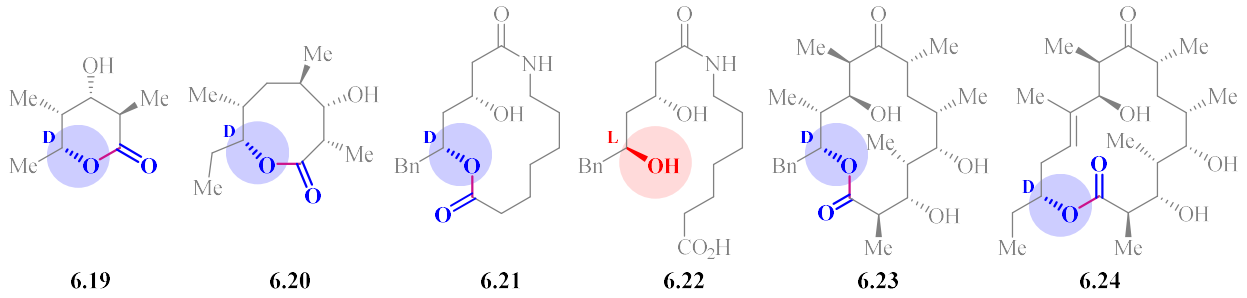

Figure 6.4b – Select panel of metabolites produced by DEBS TE from a range of linear chain lengths. Only substrates with D-configured† *O*-nucleophiles were successfully macrocyclized; substrates with L-configured *O*-nucleophiles yielded hydrolysis products exclusively.

Very little is known about underlying factors that influence selectivity of TE-biochemistry.[10] Early studies of recombinant DEBS TE provided crystallographic analysis and generated multiple high-resolution structures of the enzyme.[34] The fully-functionalized linear framework of native 6-deoxyerythronolide was computationally-docked into crystallographically-derived DEBS TE binding cavity. Analysis of the docked structure revealed key hydrogen-bonding interactions between the alcohol-rich substrate and hydrophilic residues in the binding cavity (Figure 6.5). From this result, model-**I** was proposed, and suggested hydrogen-bonding was the key mechanism that controlled substrate-selectivity in TE-catalyzed offloading (hydrolysis or macrocyclization).

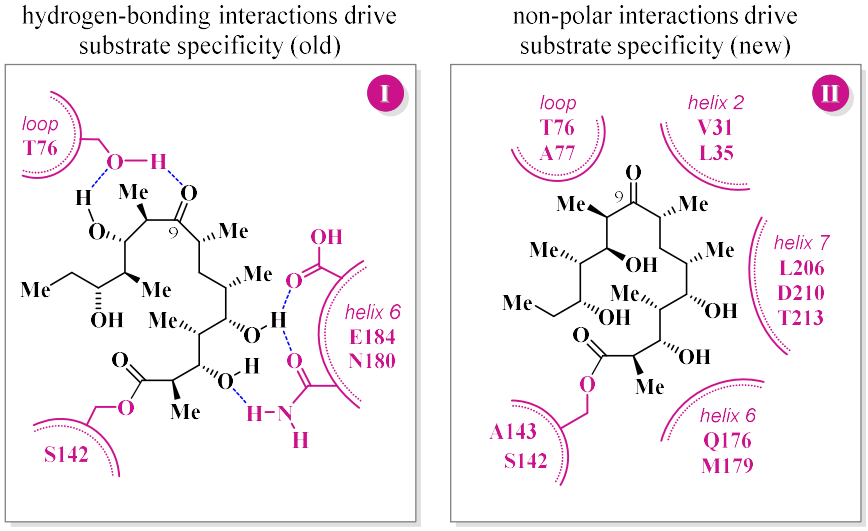

Figure 6.5 – Comparison of substrate-binding and selectivity models for DEBS TE catalytic active site. Early model proposed hydrogen-bonding interactions between enzyme and full-linear framework of 6-deoxyerythronolide B.[34] Updated model indicated no specific or direct contacts between substrate and binding-cavity are observed, and hydrophobic packing drives recognition.[35]

To experimentally probe the role of hydrogen-bonding interactions in mediating substrate recognition and acyl-enzyme intermediate formation in DEBS TE, former Boddy Lab graduate Dr. Meng

† During biosynthesis, Cahn-Ingold-Prelog[89] *R*- and *S*-priorities of reduced intermediates can interchange. Consequently, the D- and L-system is preferred when discussing PKS intermediates.

Wang conducted a site-directed mutagenesis study.[35,36] Proteins were prepared where hydrogen-bond donors and acceptors within DEBS TE binding cavity were mutated to either alanine or phenylalanine residues, and activities for these mutants were characterized with substrates possessing or lacking hydrogen bond donors or acceptors. This study indicated no significant change in substrate-specificity was observed when hydrogen bond donors and acceptors were mutated, and suggested hydrogen-bonding does not play a significant role in substrate recognition. Based on this result, an updated model-**II** was proposed where hydrophobic interactions controlled substrate-selectivity for the formation of acyl-enzyme intermediates.

While an updated model on substrate loading was established, not enough data was available to provide a clear model on substrate-selectivity for TE-mediated macrocyclization. Previous *in vivo* work indicated that DEBS TE has moderate substrate-tolerance for ring sizes, however the structural complexity of macrocyclization precursors has prevented systematic examination of the roles that ring size and stereochemistry play on reactivity. To enable such a study, a synthetically-tractable model substrate for TE-mediated macrocyclization was necessary. This subsection summarizes contributions made toward *in vitro* evaluation of our first-generation simplified analogues for 6-deoxyerythronolide B (**6.2**).

Initial work indicated that DEBS TE displayed improved catalytic efficiency with short peptidyl thioester-containing substrates, in comparison to their polyketide analogues.[37] Motivated by this discovery, simplified linear *N*-acetylcysteamine (NAC) thioester analogues of **6.2** were prepared for *in vitro* analysis with purified DEBS TE by Dr. Atahualpa Pinto – also a graduate of the Boddy Lab (Figure 6.6).[32,38] Our initial hypothesis proposed that absolute stereochemistry of the nucleophilic alcohol required D-configuration for macrocyclization, and was supported by the ability of DEBS TE to generate an *in vivo* macrolactone library of various ring sizes (6-, 8-, 12-, 14-, and 16-membered) using D-configured nucleophiles. When treated with purified DEBS TE, our panel of diastereomeric substrates showed that macrocycle **6.21** was obtained from D-configured substrate **6.28**, and that hydrolysis predominated from L-configured substrates **6.27** and **6.29** to afford the respective *seco*-acids. Unexpectedly, D-configured substrate **6.25** did not generate any macrocyclic product, which indicated that absolute stereochemistry is not sufficient to predict ring-closure.

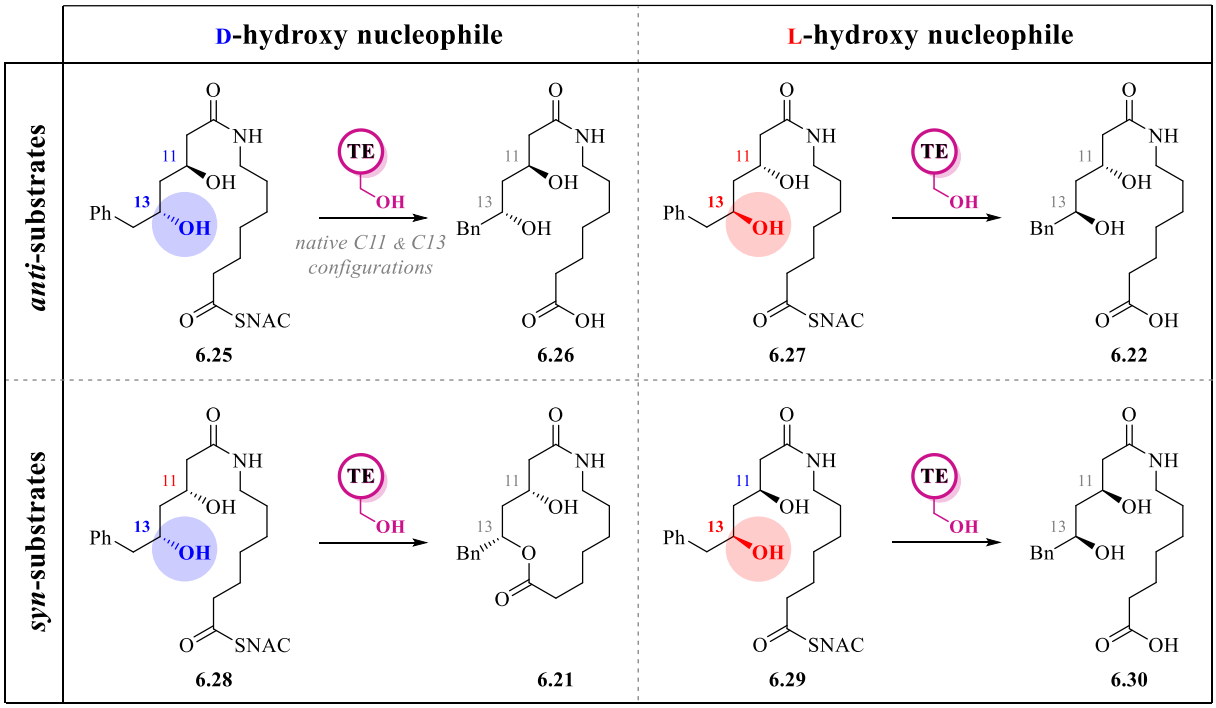

Figure 6.6 – Summary of key observations from *in vitro* testing of first-generation simplified analogues with DEBS TE.

While this small library provided the first non-native substrate to be macrocyclized by DEBS TE, and an entry to probing the specificity of this PKS enzyme, it also highlighted that small changes proved significant in affecting product distribution. Thus, unlike many PKS catalytic domains that display moderate substrate-selectivity due to the substrate being covalently-bound to enzyme, substrate-selectivity with TEs appears to be a capricious activity.

Results & Discussion

6.3 Development of Second-Generation Acyl-Intermediate Models

To continue our investigation of substrate-specificity for DEBS TE-mediated macrocyclization, we designed substrates that were biosynthetically-related to our first-generation analogues (Figure 6.7). Our second-generation model could be envisaged as arising from a biosynthetic gain of dehydratase (DH) function, resulting in conversion of the substrate's C11 *β*-hydroxy functionality into an *α*,*β*-unsaturated carbonyl. The relationship between our first- and second-generation models is comparable to what is seen for the complete framework of acyl-intermediates **6.27** and **6.28**, which are cyclo-released by DEBS TE and PIK TE, respectively.

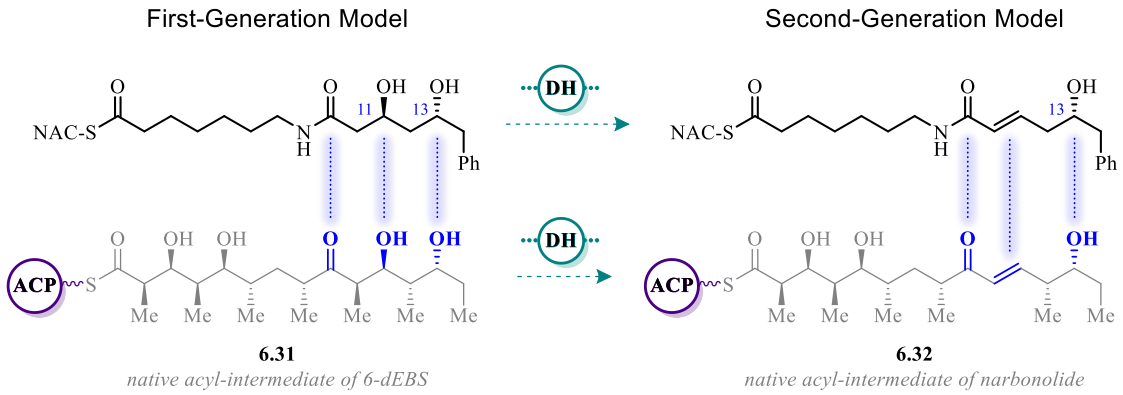

Figure 6.7 – Second-generation simplified model based on the known relationship between native acyl-intermediates **6.31** and **6.32**, and their off-loaded macrocyclic products. Designed for rapid investigation into the off-loading function of DEBS TE *via* evolutionarily-accessible substrate modifications, such as gain of dehydratase.

It was hypothesized that generation of both C13-enantiomers for our second-generation model would provide a negative control for this investigation, as no L-configured alcohol has been reported to successfully cyclize *in vivo* or *in vitro* by DEBS TE. Herein, development of our second-generation of analogues to probe the specificity of DEBS TE-mediated macrocyclization is reported.

6.3.1 Design & Convergent Synthesis of Second-Generation Analogue Panel

Design of second-generation analogues was heavily-based on salient features included in our first-generation panel (Figure 6.8).[32,36,38] Accordingly, a phenyl chromophore was incorporated at the distal end of our linear framework, in addition to amidation of the requisite C9 carbonyl. DEBS TE proved amenable to these structural elements,[37,39] and the chromophoric element improved detection for UV traces obtained by LC-MS. Inclusion of the peptidyl bond significantly increased overall efficiency of substrate synthesis, and suppressed the possibility of forming a six-membered hemiketal, as was previously observed.[33] Lastly, *N*-acetyl cysteamine (NAC) thioester is a synthetic mimic of the phosphopantetheinyl arm within acyl carrier proteins (ACPs), which facilitates acylation of the TE using non-native substrates.

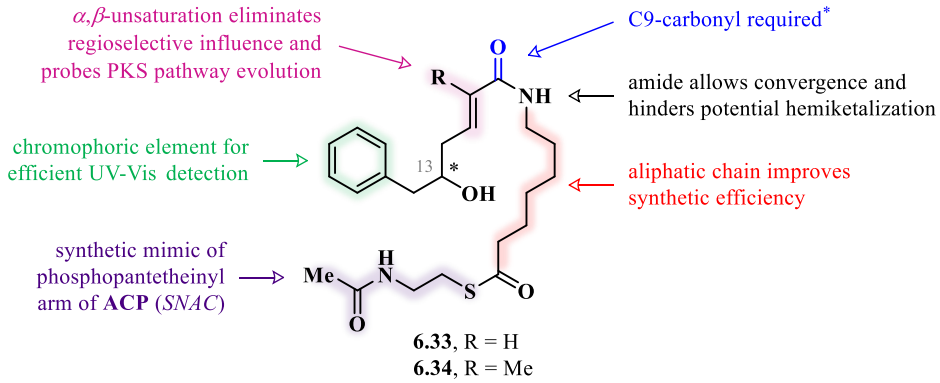

Figure 6.8 – Analysis of design elements for second-generation model to investigate DEBS TE-mediated *in vitro* macrocyclization.

Substrate **6.34** was envisioned as a derivative to **6.33** through modulation of specificity within the acyltransferase domain from malonyl-CoA-specific to methylmalonyl-CoA-specific loading. This panel of substrates could be expected to arise *via* evolution of PKS pathways, thus enabling us to provide preliminary insights into the relationship between substrate selectivity and PKS pathway evolution.

Initial investigation with the racemic mixture of **6.33** strongly-suggested production of our desired macrocyclic metabolite by treatment with DEBS TE, and prompted generation of enantiopure substrates. Synthesis of D-**6.33** was accomplished in a single-attempt over seven linear steps (Scheme 6.1). Because our primary goal was to probe substrate-specificity of DEBS TE-mediated ring-closure, we did not address the potential optimization of yields. Asymmetric allylation of phenylacetaldehyde (**6.35**) under Brown's conditions[40,41] set desired D-configuration of stereogenic C13 carbon with good selectivity. The resulting homoallylic alcohol was protected as silyl ether **6.36** and its allylic double bond was oxidized to yield aldehyde **6.37**. Under Horner-Wadsworth-Emmons olefination conditions,[42] this was coupled with triethylphosphonoacetate (**6.38**) to furnish *α,β*-(*E*)-unsaturated ester in moderate yield. Saponification of the ethyl ester afforded carboxylic acid **6.39**, which was treated with EDC·HCl and cross-coupled with known[36] amine **6.40** to yield the complete linear framework. Thioester **6.41** was deprotected by treatment with HF and pyridine to complete the synthesis of our D-configured **6.33** substrate.[32] Enantiomeric L-**6.33** substrate was prepared in identical fashion using (+)-Ipc$_2$BAllyl reagent, and yielded comparable yields and selectivity (refer to experimental section). Substrates were stored in DMSO as 50 mM stock solutions.

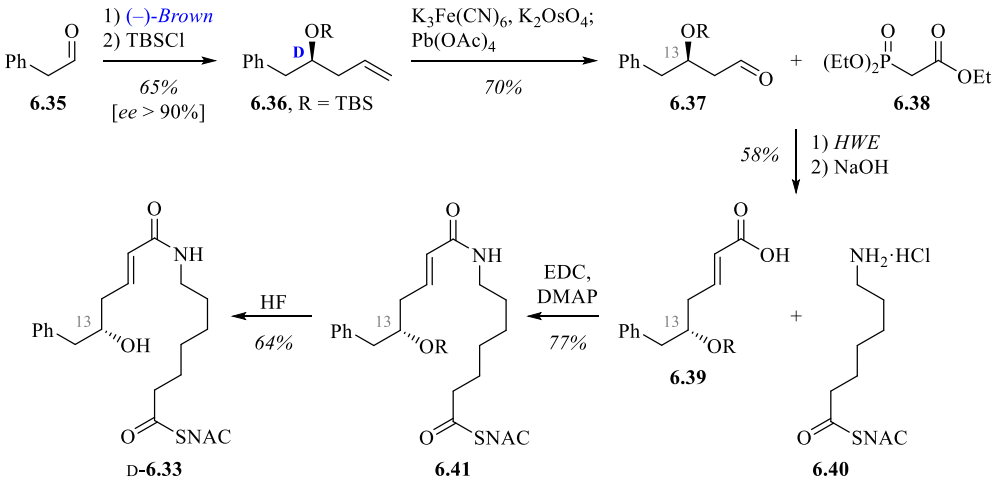

Scheme 6.1 – Synthesis of D-enantioenriched substrate **6.33** was performed without optimization. The L-enantioenriched substrate *ent*-**6.29** was prepared in identical fashion using (+)-Ipc$_2$BAllyl for the asymmetric Brown allylation.[40]

Substrate **6.34** was generated using an analogous route, starting with racemic aldehyde **6.37** (Scheme 6.2). Wittig coupling[43] with methyl 2-(triphenylphophoranylide)-propionate **6.42** afforded C13-racemic methyl-substituted *α,β*-unsaturated ester in modest yield. Once again, substrate synthesis was

performed as a single attempt without optimization of yields. Carboxylic acid **6.43** was generated under standard saponification conditions, and coupled with free amine **6.40** to provide the complete carbon framework **6.44**. Acid-mediated desilylation yielded methyl-substituted NAC-thioester **6.34** in 10% overall yield from phenylacetaldehyde (seven linear steps). Enantioenriched material was not prepared because preliminary *in vitro* characterization revealed exclusive formation of hydrolysis product (*vide infra*).

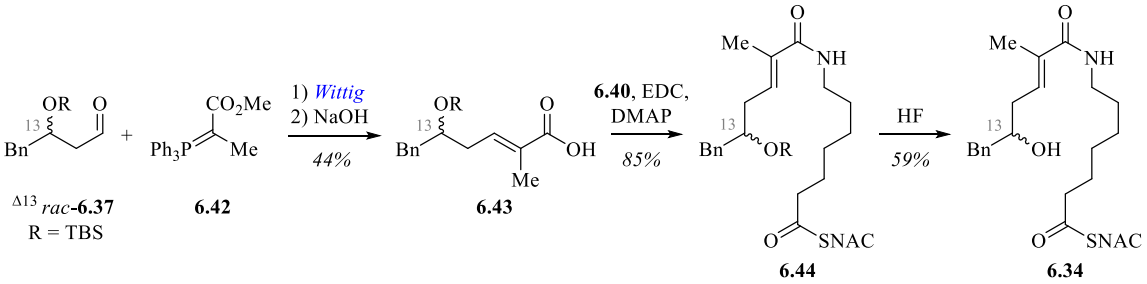

Scheme 6.2 – Synthesis of racemic methyl-substituted substrate **6.34** was rapidly-achieved using analogous chemistries.

With our small panel of second-generation analogues in hand, we proceeded to probe the influence of PKS pathway evolution enzyme-mediated macrocyclization by wild-type DEBS TE.

6.3.2 Unprecedented Macrodiolide Observed by In Vitro Incubation with DEBS TE

To evaluate the ability of wild-type DEBS TE-mediated *in vitro* macrolactonization, enzymatic assays of D-**6.33**, enantiomeric L-**6.33**, and *rac*-**6.34** were prepared in triplicate. Purified recombinant DEBS TE protein[35] (15 μM) was treated with each NAC-thioester substrate (2.5 mM) in 50 mM phosphate buffer (pH 7.4), using DMSO (10% *v*/*v*) as a solubility additive.‡ Assays were incubated for 18 h at ambient temperature, quenched and analyzed for product formation by LC-MS. The results obtained for D-**6.33** and L-**6.33** supported our initial stereochemical hypothesis that suggested D-configured alcohols are necessary for macrocyclization (Figure 6.9). The D-configured alcohol **6.33** was successfully converted into 14-member ring macrolactone **6.47**, whereas enantiomeric L-**6.33** generated free-acid as the predominant assay product (*vide infra*).

Analysis of product distribution obtained with D-**6.33** revealed a suite of TE-mediated PKS linear and cyclic metabolites (Figure 6.9). Major product peaks included parent substrate **6.33** (t_R = 14.64 min; $[M + H]^+$ 435 *m/z*), hydrolysis product **6.46** (t_R = 13.40 min; $[M + H]^+$ 334 *m/z*) and desired ring-closed macrolactone **6.47** (t_R = 16.96 min; $[M + H]^+$ 316 *m/z*). Formation of **6.47** represented the second literature example of a non-native linear substrate to be cyclized by DEBS TE. Commonly, an absence of required structural features on non-native backbones limits hydrophobic interactions that induce favorable conformations (§ 6.3.1), allowing small, exogenous nucleophiles to enter the active site. This facilitates

‡ Negative controls were prepared in identical fashion using bovine serum albumin (BSA) or heat-shocked DEBS TE protein.

cleavage of acyl-enzyme intermediates by water to afford hydrolysis products, or transesterification with an intermolecular alcohol to generate esters, as was recently observed *in vitro*.[44] Accordingly, formation of glycerolysis adduct **6.45** (t_R = 12.72 min; $[M + H]^+$ 408 *m/z*) was an expected side-product resulting from its function in the expression and purification of excised DEBS TE.[36]

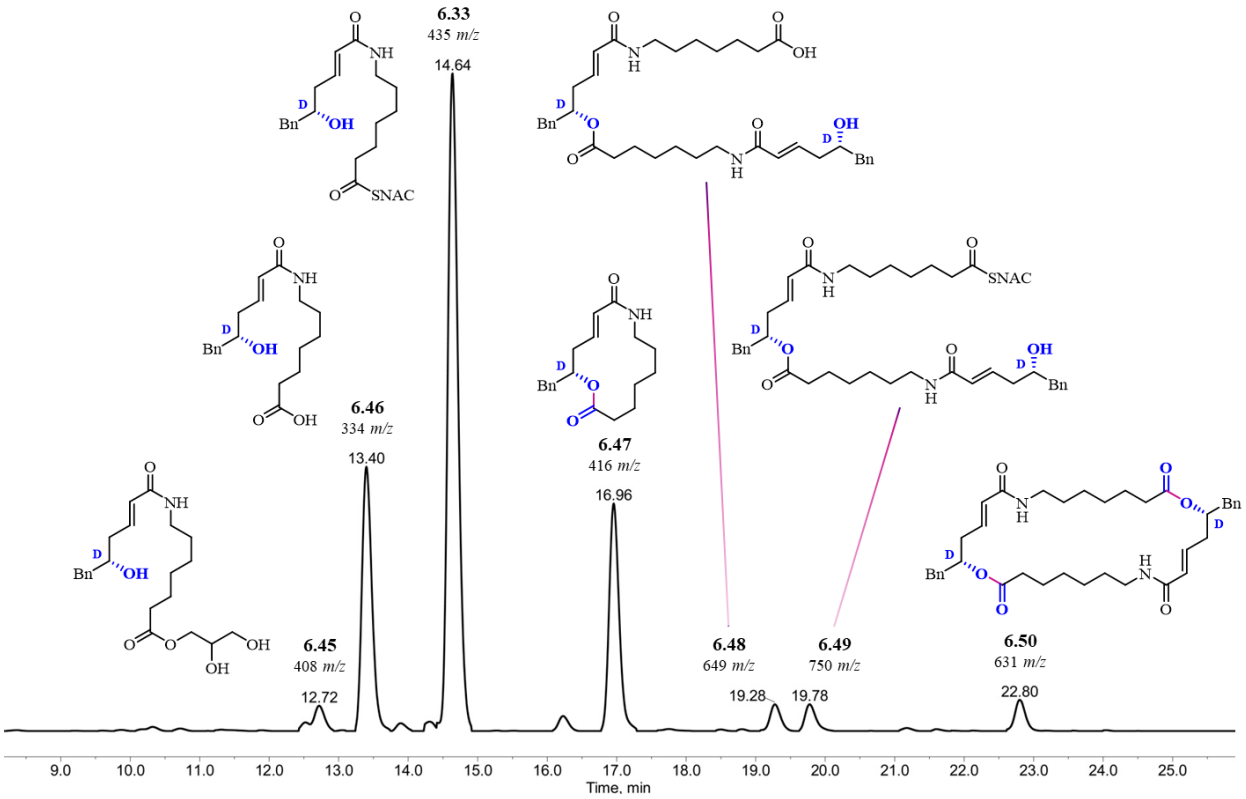

Figure 6.9 – LC-MS analysis from *in vitro* enzymatic assays of D-configured NAC-thioester **6.33** with wild-type DEBS TE. The UV (254 nm) trace between 8-and-26 minutes is shown, with retention times and $[M + H]^+$ data included above product peaks. Trace contamination present in sample highlighted (*) accordingly; intensities of these peaks are consistent with negative controls.

Unexpectedly, C_2-symmetrical, head-to-tail dimerized macrodiolide product **6.50** (t_R = 22.80 min; $[M + H]^+$ 631 *m/z*) was identified as a minor product (Figure 6.9). Corresponding linear-dimer metabolites were also observed as minor products, including dimeric *seco*-acid **6.48** (t_R = 19.28 min; $[M + H]^+$ 649 *m/z*) and NAC-thioester **6.49** (t_R = 19.78 min; $[M + H]^+$ 750 *m/z*). Structures of the dimeric compounds were consistent with ^{1}HNMR and MS/MS data collected on these compounds (refer to § 6.4.3). Formation of macrodiolide and linear-dimer structures was unprecedented for DEBS TE, though PKS[27,28,45,46] and non-ribosomal peptide synthetase (NRPS)[47–49] TEs have been proposed to catalyze this chemistry. We believed TE-bound monomer was attacked by the nucleophilic alcohol of our NAC-thioester monomer substrate D-**6.33** to generate dimeric species **6.49** *via* retro-transfer. This linear-dimer metabolite was subsequently loaded to a vacant TE active site to be processed (refer to § 6.4.4).

Analysis of product distribution obtained with enantiomeric L-**6.33** was consistent with our stereochemical hypothesis (Figure 6.10). Expected peaks included parent substrate **6.33** (t_R = 14.61 min; $[M + H]^+$ 416 *m/z*), and hydrolysis product *ent*-**6.46** (t_R = 13.40 min; $[M + H]^+$ 334 *m/z*) as major products, in addition to minor product peak of glycerolysis adduct *ent*-**6.45** (t_R = 12.70 min; $[M + H]^+$ 408 *m/z*). Interestingly, trace presence of species with identical retention times and masses predicted for that of macrocyclic product *ent*-**6.47** (t_R = 16.95 min; $[M + H]^+$ 316 *m/z*) and dimerized free-acid *ent*-**6.48** (t_R = 19.25 min; $[M + H]^+$ 649 *m/z*) were also observed. Because LC-MS data does not provide information about configuration of products, the sample was re-evaluated under prolonged incubation periods with DEBS TE and indicated comparable distribution and intensity of product peaks.

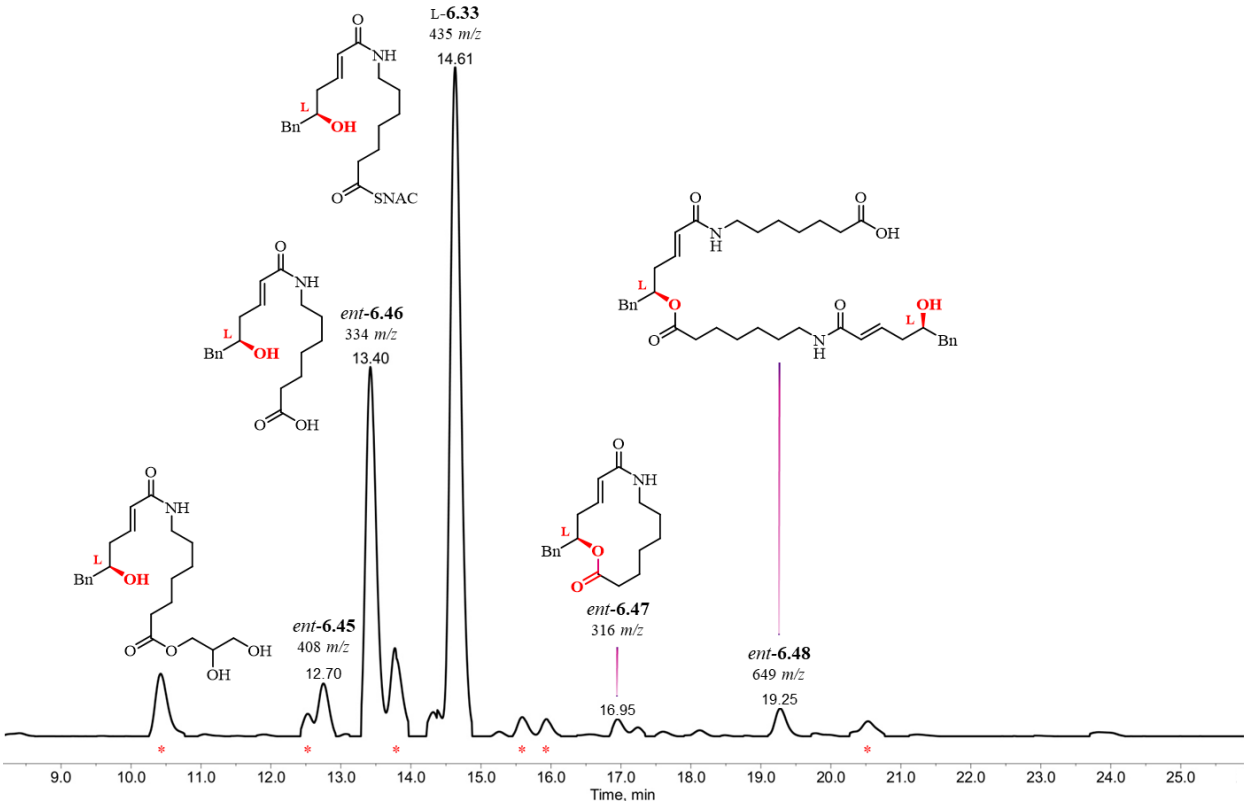

Figure 6.10 – LC-MS analysis from *in vitro* enzymatic assays of L-configured NAC-thioester **6.33** with wild-type DEBS TE. The UV (254 nm) trace between 8-and-26 minutes is shown, with retention times and $[M + H]^+$ data included above product peaks. Trace contamination present in sample highlighted (*) accordingly; intensities of these peaks are consistent with negative controls.

Putative *ent*-**6.47** was believed could result from conversion of trace residual D-configured **6.33** (L-**6.33** *ee* 90%, see experimental details); however, the complete suite of dimerized PKS products including *ent*-**6.49–6.50** was not observed under any evaluated incubation periods. While spontaneous formation of *ent*-**6.47** and *ent*-**6.48** would be consistent with reported probability of intra- and intermolecular attack ($\Delta S^{\ddagger}$) for assembly of macrolactones[50] (Chapter 5, § 5.2), this explanation was rejected based on several inconsistencies observed in our negative control assays. Thus, we proposed formation of putative *ent*-**6.48**

could be enzyme-mediated, whereby *seco*-acid **6.46** attacked TE-bound monomer *via* retro-transfer. It is unclear why linear acid *ent*-**6.48** was the only dimeric metabolite observed, but it is possible that it displays a lower Michaelis constant (K_m) value. To date, no study has been reported on changes in K_m as TE-mediated conversion of monomers to corresponding dimeric-metabolites. This remains an active area of investigation within our research group.

To investigate the observed trace production, both D- and L-configured NAC-thioester substrates **6.33** were incubated with site-directed mutagenesis protein DEBS D169A TE (refer to Appendix II). Dr. Meng Wang previously-produced this protein for his examination of hydrogen-bonding interactions in DEBS TE binding cavity (§ 6.3.1),[35] which mutated aspartic acid of the catalytic triad to an alanine residue. The alanine residue inactivates the protein but maintains proper folding, thus acting as a negative control. Analysis of each *in vitro* assay with DEBS D169A TE was consistent with our previous negative controls that used bovine serum albumin (BSA) or heat-shocked DEBS TE protein.[§] Trace production of metabolites were observed, and suggested very low-level protein activity. We propose that the D169A TE mutant displayed residual oxyanion hole-based activity,[10] despite its inactive catalytic binding site. Because the mutant cannot generate an acyl-enzyme intermediate, the presence of a binding site and oxyanion hole could facilitate activity by inducing required pre-organization akin to the large bowl-shaped hydrophobic site within the surfactin TE,[51] or the application of Lewis acids in template synthesis of macrocyclic compounds.[52]

Biochemical analysis of our methyl-substituted NAC-thioester derivative **6.34** relied on its racemic mixture, and predominantly led to formation of hydrolysis product *rac*-**6.52** (Figure 6.11). Peaks corresponding to species with masses predicted for transesterified glycerolysis adduct *rac*-**6.51** and macrocyclic product *rac*-**6.53** did not exceed our arbitrary intensity-threshold for spontaneous background production based on negative controls. Trace formation of a species with the predicted mass for dimeric acid *rac*-**6.54** supported our hypothesis of displaying a lower K_m value. We proposed addition of the α-methyl group substantially increased allylic 1,3-strain[53] across the amide bond, and effectively obstructed access to the *s-trans* configuration required for successful enzyme-mediated macrocyclization. Limited production of macrocyclization with *rac*-**6.34** suggested DEBS TE was unable to overcome intrinsic unfavorability of the reactive conformation for the substrate.

[§] Trace observation of hydrolyzed and cyclic monomer products are observed on comparable levels from negative control assays using bovine serum albumin (BSA) or heat-shocked DEBS TE protein with NAC-thioester analogs D-**6.33**, L-**6.33**, and *rac*-**6.34**.

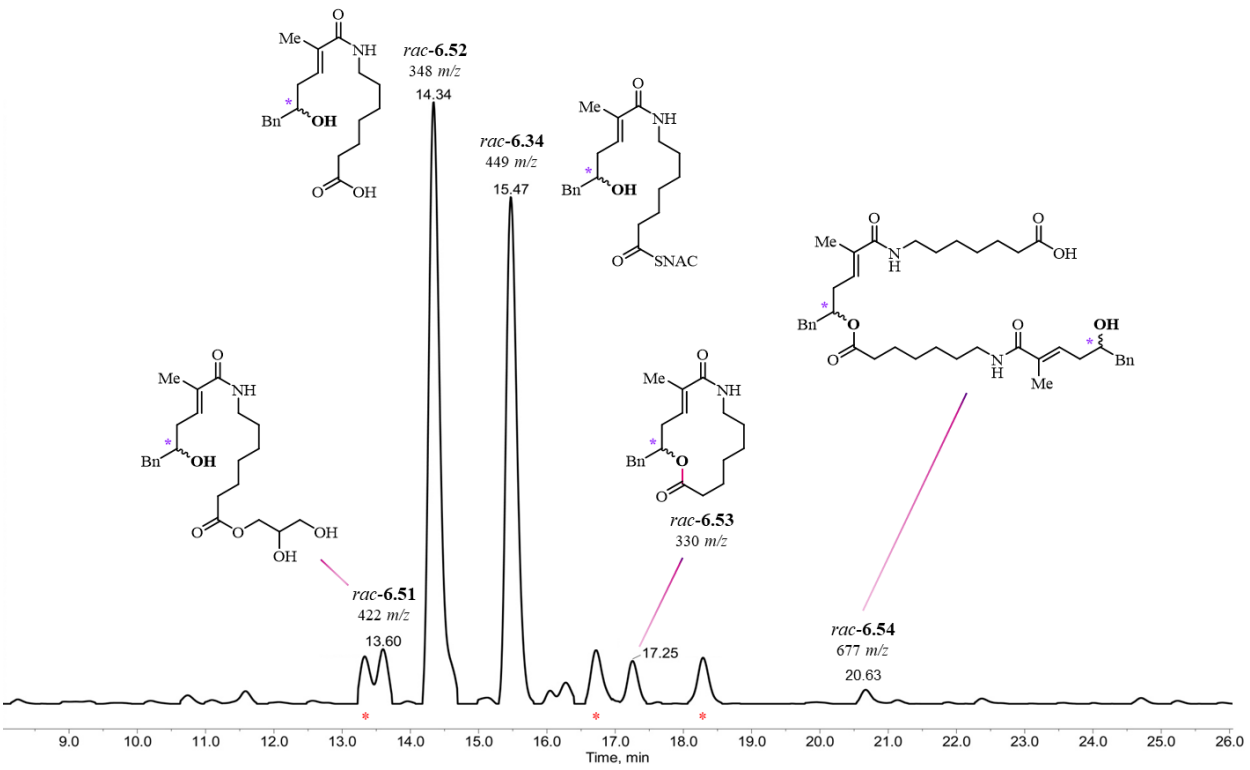

Figure 6.11 – LC-MS analysis from *in vitro* enzymatic assays of racemic NAC-thioester **6.34** with wild-type DEBS TE. The UV (254 nm) trace between 8-and-26 minutes is shown, with retention times and $[M + H]^+$ data included above product peaks. Trace contamination present in sample highlighted (*) accordingly; intensities of these peaks are consistent with negative controls.

6.3.3 Steady-State Kinetics Consistent with Catalytic Efficiencies of PKS TEs

Steady-state kinetic characterization for catalyzed consumption of NAC-thioester analogues D-**6.33**, L-**6.33**, and *rac*-**6.34** provided the turnover rate (k_{cat}), Michaelis constant (K_m), and specificity constant (k_{cat}/K_m) when the enzyme could not be saturated (Figure 6.12). DEBS TE-mediated consumption was monitored by Ellman's reagent, collecting data points every 30-seconds for 30-minutes across substrate concentrations between 0.25 mM and 5.00 mM. Enzymatic activity with D-**6.33** and L-**6.33** displayed Michaelis-Menten kinetics with turnover rates of 0.228 ± 0.015 min^{-1} and 0.114 ± 0.008 min^{-1} respectively, and a K_M of 2.8 ± 0.4 mM and 1.3 ± 0.2 mM respectively. Specificity constants were 1.4 ± 0.4 $M^{-1}s^{-1}$ for D-**6.33**, and 1.5 ± 0.3 $M^{-1}s^{-1}$ for its enantiomer.

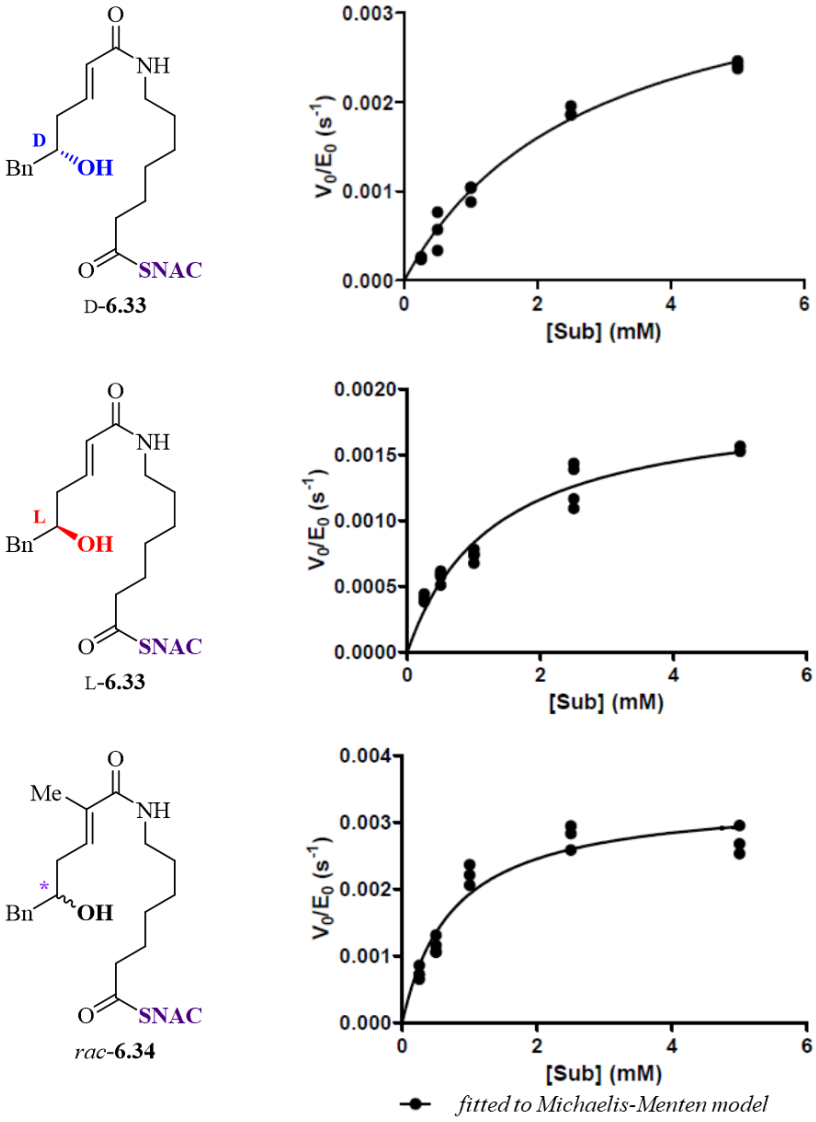

Best-Fit Values	
V_{max}	0.003825
K_M	2.775
Std. Error	
V_{max}	0.0002489
K_M	0.3707

Best-Fit Values	
V_{max}	0.001919
K_M	1.307
Std. Error	
V_{max}	0.0001313
K_M	0.2149

Best-Fit Values	
V_{max}	0.003377
K_M	0.7529
Std. Error	
V_{max}	0.0002022
K_M	0.1352

Figure 6.12a – Kinetic characterization using Ellman's reagent to monitor TE-consumption. Initial reaction rates ($mM \cdot s^{-1}$) plotted against concentrations of D-and L-configured NAC-thioester analogue **6.33**, and racemic NAC-analogue **6.34**. Data was based on triplicate assay data points for five different substrate concentrations.

Racemic methyl-substituted NAC-thioester derivative **6.34** also fit the Michaelis-Menten model, providing a k_{cat} of 0.20 ± 0.01 min^{-1} and K_M of 0.75 ± 0.13 mM. This data was consistent with observed catalytic efficiencies for characterized modular PKS TE domains.[29–33,35,37,54–57] For example, our data was in excellent agreement with the specificity constants for DEBS TE processing of *N*-Boc-7-aminoheptanoate NAC-thioester (1.5 ± 0.1 $M^{-1}s^{-1}$), and our first-generation analogue **6.28** (1.2 ± 0.5 $M^{-1}s^{-1}$).

6.3.4 Collision-Induced Dissociation Confirms Formation of Macrodiolide

Motivated by our unprecedented experimental observations, we attempted to isolate macrodiolide **6.50**, as well as dimeric *seco*-acid **6.48** and NAC-thioester **6.49** products using LC-SPE-NMR. However,

analysis indicated that wild-type DEBS TE only sparsely-produced these dimerized metabolites *in vitro*, and there was not sufficient material for complete structural characterization by NMR alone. Therefore, we decided to pursue additional support for our putative dimeric products using tandem mass spectrometry data that could be obtained from sub-microgram levels of assay sample. Low-resolution mass-spectrometry (LRMS) data with MS/MS fragmentation was acquired by optimizing the collision energy of the *q*TOF to 20 V against observed parent masses of 316 Da and 631 Da to unambiguously differentiate between two non-covalently-bound monomers and putative macrodiolide. We hoped covalently-bound dimer would generate a distinct fragmentation pattern of credible high-mass fragments that could not be generated from our corresponding monomer.

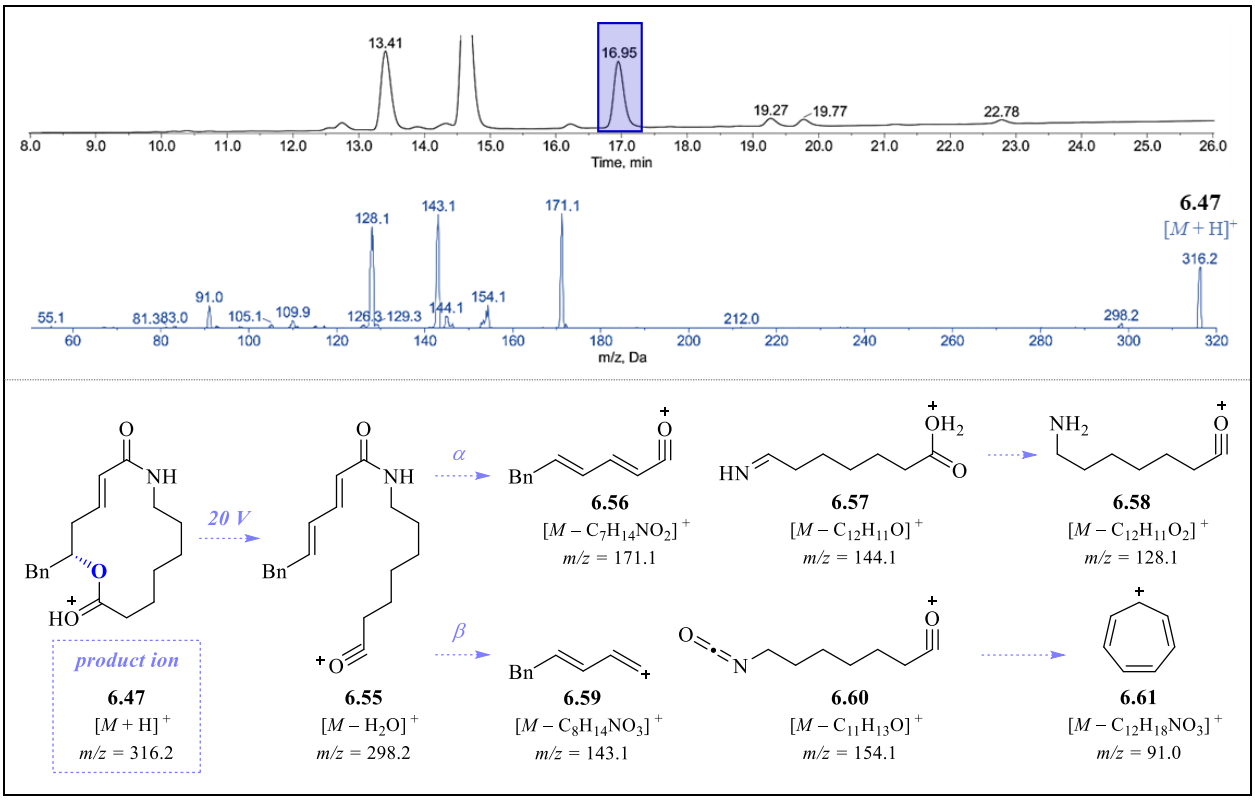

Figure 6.13 – LC-MS/MS analysis from *in vitro* enzymatic assays of D-**6.33** with wild-type DEBS TE. MS2 data collected for parent ion scan (316 Da), and shown between 16.787 and 17.328 min over a mass range of 50-to-320 Da. Select fragmentation ions are proposed for major peaks.

Analysis of crude enzymatic assay material using product ion scan mass of 316 Da provided a fragmentation pattern fully-consistent with our cyclic lactone monomer **6.47** (Figure 6.13). The molecular ion for **6.47** was identified ([*M* + H]$^+$ 316.2 *m/z*), and major fragments with *m/z* of 171.1, 143.1, and 128.0 were also observed. Fragmentation from *α*-cleavage of amide and ester bonds could produce acylium cations of conjugated system **6.56** (171.1 *m/z*), and free-amine **6.58** (128.0 *m/z*) as sister ions. Amine **6.58** could also be generated by hydrolysis of fragment **6.57** (144.1 *m/z*). Vinylic-cleavage is intrinsically-

unfavorable relative to loss of an amine fragment, and was supported by minor diene fragment **6.59** (143.1 *m/z*) and sister isocyanate ion **6.60** (154.1 *m/z*). Finally, formation of tropylium cation **6.61** (91.0 *m/z*) is a common fragment from benzylic compounds. These low-mass fragments served as a benchmark for comparison with observed fragmentations from our putative macrodiolide product.

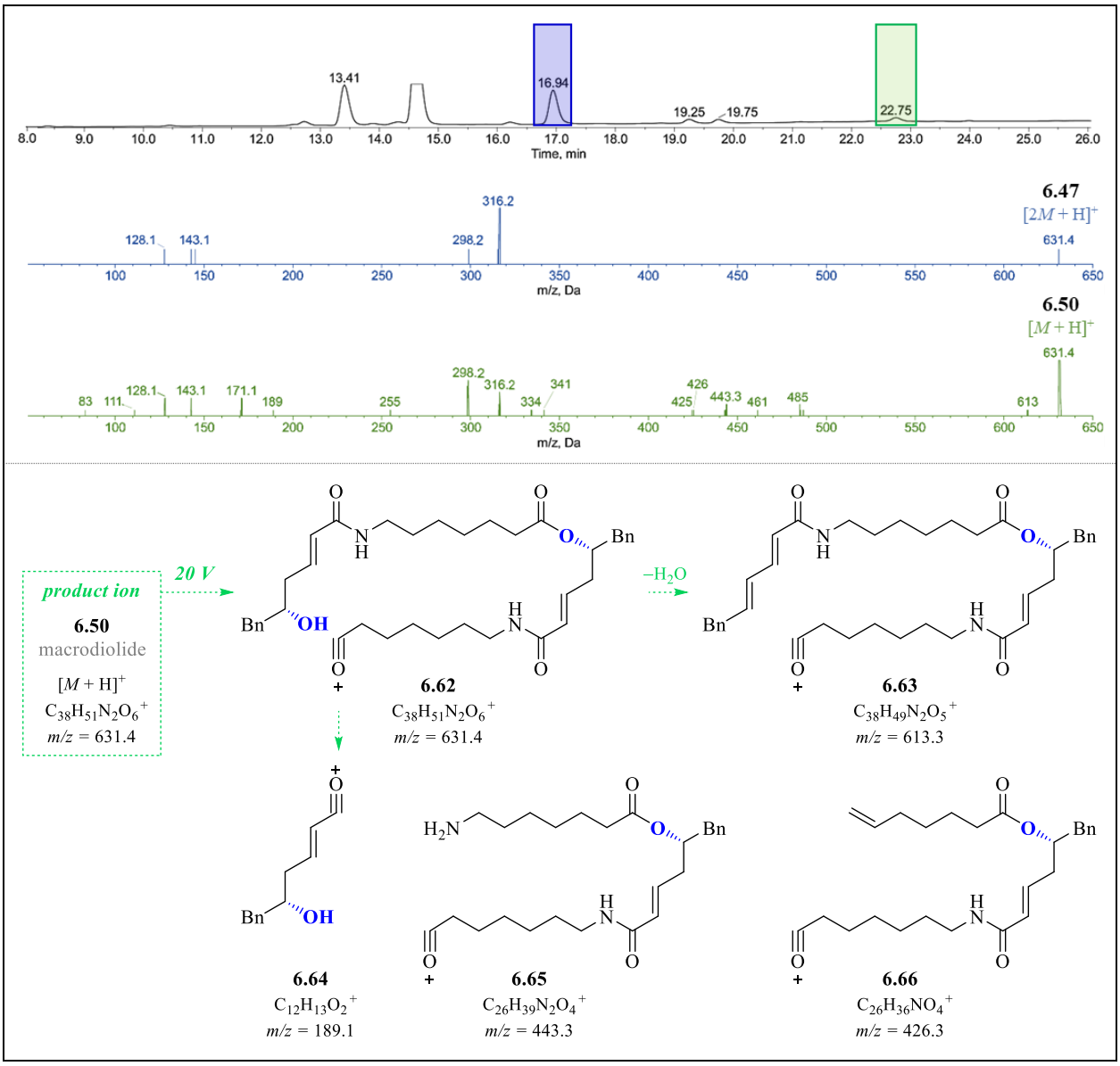

Figure 6.14 – LC-MS/MS analysis from *in vitro* enzymatic assays of D-**6.33** with wild-type DEBS TE. MS2 data collected for parent ion scan (631 Da), and ionization shown for 16.735–17.429 min (trace **1**) and 22.490–23.240 min (trace **2**) over a mass range of 50-*to*-631 Da. Large-mass fragments unambiguously indicated formation of C_2-symmetrical 28-membered macrodiolide **6.50**.

Analysis of MS/MS data using product ion scan mass of 631 Da unambiguously confirmed TE-mediated formation of covalently-bound macrodiolide **6.50** from our *in vitro* assays (Figure 6.14). Ionization patterns of our cyclic monomer **6.47** (trace **1**) failed to generate larger-mass fragments between its molecular ion ([*M* + H]$^+$ 316.2 *m/z*) and non-covalently bound dimer ([2*M* + H]$^+$ 631.4 *m/z*). This

observation was further-substantiated by the ionization pattern of our macrodiolide product **6.50** (trace **2**). α-Cleavage of either amide or ester bond for molecular ion **6.50** would produce fragments of the same mass (631.4 *m/z*). In addition to observation of previously-proposed fragments with *m/z* of 171.1, 143.1, and 128.0 (Figure 6.13), successive α-cleavage of **6.62** would generate conjugated system **6.63** ($[M - H_2O]^+$ 613.3 *m/z*) as hydrolysis product or sister acylium ions **6.64** (189.1 *m/z*) and **6.65** (443.3 *m/z*). Minor high-mass fragment **6.66** (426.3 *m/z*) could be generated from each proposed high-mass fragment, though corresponding sister ions from β-cleavage of **6.62** (205.1 *m/z*) and **6.63** (187.1 *m/z*) were not observed.

Tandem mass spectrometry was used to differentiate between covalently-bound dimer $[(M + H)^+]$ and two non-covalently-bound monomers $[(2M + H)^+]$. Credible ionization patterns with high-mass fragments provided additional support to the unique retention times from our UV (254 nm) traces and limited LC-SPE-NMR data. Based on these observations, we unambiguously confirmed unprecedented formation of 28-membered macrodiolide **6.50** by treatment with recombinant wild-type DEBS TE.

6.3.5 DEBS TE Tolerable of Exogenous Nucleophilic Attack

Two plausible mechanisms exist for TE-mediated dimerization (Figure 6.15), and preliminary support has been reported from *in vitro* investigation of recombinant protein from enterobactin[47,48] and elaiophylin biosyntheses.[27,45,46] The biochemically-characterized enterobactin NRPS thioesterase (Ent TE) trimerizes a 2,3-dihydroxybenzoyl-L-serinyl monomer, and mediates ring-closure to generate a macrotriolide. Using top-down mass spectrometry, a mutant of Ent TE was shown to accumulate monomeric and dimeric acyl-enzyme intermediates without hydrolytic release. Based on this observation, it was postulated that dimer formed by *inter*molecular *O*-nucleophilic attack (catalytic binding-site serine) of the monomeric TE-intermediate onto a second equivalent of activated thioester.[47] Two iterations of interdomain transfers between covalent thioester intermediates from upstream carrier proteins generate the required backbone, and undergoes *intra*molecular cyclotrimerization to release 12-membered enterobactin (refer to Pathway **A**, Figure 6.15).

Alternatively, the proposed mechanism for dimerization of PKS product elaiophylin (**6.8**, Figure 6.2) was influenced by its strong homology to PKS TEs that mediate ring-closure *via* intramolecular attack of a distal *O*-nucleophile. Conformational biases of rigidifying hemiketal and unsaturated structural elements impede intramolecular attack for 10-membered ring formation.[27] Under these conditions, TE-bound monomer is attacked by the distal hydroxy nucleophile of activated thioester, to afford linear dimer attached to the upstream site *via* retro-transfer. Iterative enzyme-loading of dimeric acyl-enzyme intermediate to the vacant TE active site eliminates conformational biases and mediates facile cyclodimerization to release 20-membered elaiophylin (refer to Pathway **B**, Figure 6.15).

Formation of linear dimeric NAC-thioester **6.49** in our present study strongly suggested that a second equivalent of monomer attacked electrophilic monomer-TE acyl-enzyme intermediate D-**6.67** to generate **6.49** (Figure 6.15). This type of mechanism for cyclodimerization was also proposed for mixed NRPS-PKS TE of conglobatin,[58] as well as the NRPS TEs of gramicidin,[49] and related depsipeptide framework of thiocoraline.[59] Accordingly, we proposed that iterative nucleophilic attack of the seryl side-chain alcohol of monomer DEBS TE loaded NAC-thioester **6.49** to generate a dimeric acyl-enzyme intermediate D-**6.68***. Formation of dimeric free-acid **6.48** and macrodiolide **6.50** can occur *via* subsequent hydrolysis and ring-closure, respectively.

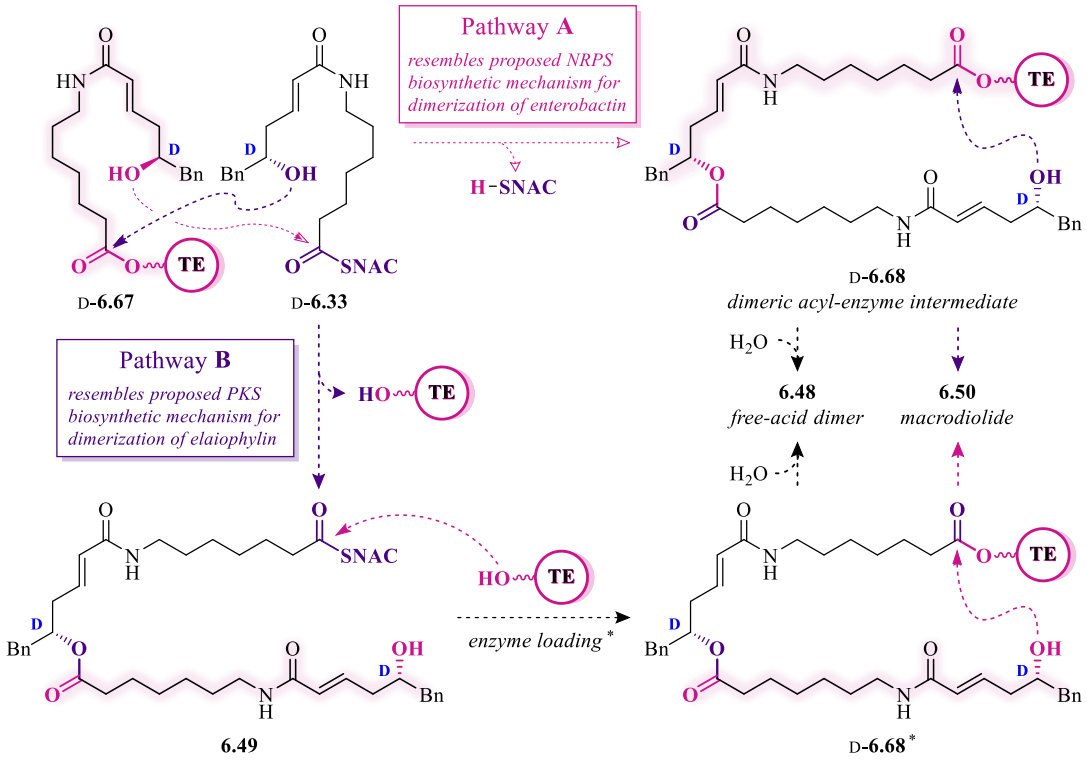

Figure 6.15 – Plausible mechanisms for generation of dimeric metabolites. Observation of dimeric NAC-thioester **6.49** supports Pathway **B** mechanism for dimerization. Iterative enzyme loading generates dimeric acyl-enzyme intermediate **6.68***, which can be cleaved by exogenous water or TE-mediated ring-closure to afford dimerized free-acid **4.48** and macrodiolide **6.50**, respectively.

Following publication of this work,[20] Leadlay and coworkers reported similar results from *in vitro* investigation of Ela TE-mediated diolide formation using NAC-thioesters of putative monomeric PKS precursors.[45] HPLC-MS analysis revealed the presence of a species with the predicted mass for a linear NAC-thioester dimer that, when purified from reaction mixture, produced macrodiolide in the presence of fresh enzyme. Unfortunately, insufficient quantities of **6.49** were produced by our enzymatic assay and prevented analogous evaluation of diolide formation with fresh DEBS TE. While dimeric NAC-thioester **6.49** could not be isolated, Leadlay's result was consistent with our own experimental observations, and supported the mechanism of Pathway B (Figure 6.15) for *in vitro* macrodiolide formation since Pathway A

would not generate dimeric NAC-species. Consequently, we proposed that the same iterative mechanism would operate in the event of DEBS TE-mediated *in vivo* dimerization, because published structures for dimeric PKS TE domains reveal that functional communications between TE active sites is highly-improbable.[10,45,55,60]

Proposed Pathway B mechanism requires an exogenous nucleophile (specifically, a second equivalent of monomeric substrate D-**6.33**) to attack TE acyl-enzyme intermediate D-**6.67** and release a linear thioester. This type of transesterification activity is common with glycerol and type-I PKS TEs,[44] as well as with type-II fungal PKS pathway responsible for zearalenone biosynthesis (Zea TE).[61] In the case of Zea TE, a wide range of simple exogenous nucleophiles accessed the acyl-enzyme intermediate *in vitro*. Based on this result, we hypothesized that if dimer formation occurred *via* exogenous nucleophilic attack by a second equivalent of our monomeric substrate D-**6.33** onto D-**6.67**, then our acyl-enzyme intermediate should be tolerable to attack by other exogenous nucleophiles. We therefore investigated the ability of D-**6.33** to undergo DEBS TE-catalyzed transesterification with exogenous alcohols.

A panel of alcohols were incubated with D-**6.33** to generate the corresponding ester adducts (Table 6.1). Formation of esters **6.69**–**6.78** was consistent with our proposed mechanism for dimer formation, and provided additional support to Pathway B-type mechanism. Comparison of relative initial rates of transesterification indicated that primary alcohols are preferred substrates. As was seen with the transesterification catalyzed by fungal Zea TE, 1-butanol was the most kinetically-competent alcohol substrate for DEBS TE.[61] This similar substrate-specificity in two diverse TEs suggested transesterification may be a broadly-conserved activity for PKS TEs.

Interestingly, both *n*-pentanol and *n*-hexanol effectively suppressed all TE-mediated reactivity. We hypothesized that the long, linear, hydrophobic structures displayed sufficient homology with D-**6.33** (and native DEBS active site binding cavity), and prevented our NAC-thioester from binding. Effectively, these would behave kinetically as competitive inhibitors to raise the K_m, without affecting turnover rate (k_{cat}). Additional *in vitro* exploration of recombinant PKS TEs is imperative to testing these hypotheses.

Motivated by the results with exogenous *O*-nucleophiles, we initiated preliminary exploration of transamidation by a small panel of exogenous amines. Our early results indicated cross-coupling was not mediated by DEBS TE, though optimization of assay conditions remains part of on-going research.

Table 6.1 – Normalized-abundance of substrate (D-configured NAC-thioester **6.33**) and products from *in vitro* enzymatic assays provide relative-velocities (V_{rel}) for DEBS TE-mediated *in vitro* cross-coupling with exogenous *O*-nucleophiles.

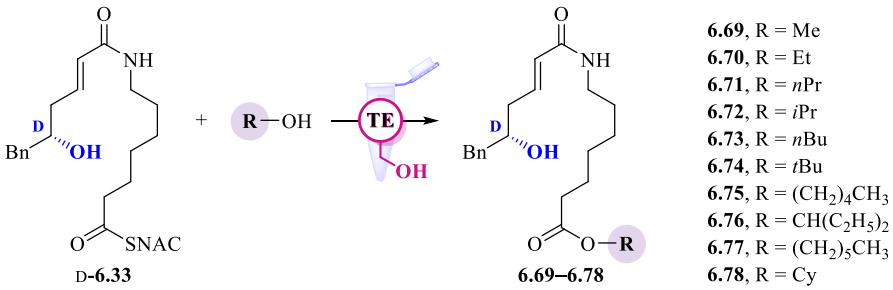

D-**6.33** → **6.69–6.78**

6.69, R = Me
6.70, R = Et
6.71, R = *n*Pr
6.72, R = *i*Pr
6.73, R = *n*Bu
6.74, R = *t*Bu
6.75, R = $(CH_2)_4CH_3$
6.76, R = $CH(C_2H_5)_2$
6.77, R = $(CH_2)_5CH_3$
6.78, R = Cy

nucleophile	*hydrolysis* (**6.46**)	*SNAC* (D-**6.33**)	*macrocycle* (**6.47**)	*adduct* (**6.69–6.78**)	V_{rel}
butan-1-ol	10.79 ± 0.57	64.33 ± 1.99	6.09 ± 0.63	18.79 ± 0.79	1.00 ± 0.08
propan-1-ol	13.96 ± 1.76	59.54 ± 4.80	10.56 ± 0.67	15.94 ± 2.37	0.85 ± 0.16
methanol	19.73 ± 1.43	57.67 ± 1.49	15.41 ± 0.10	7.19 ± 0.17	0.38 ± 0.03
ethanol	20.21 ± 0.51	56.98 ± 0.40	16.06 ± 0.36	6.75 ± 0.48	0.36 ± 0.04
cyclohexanol	23.50 ± 0.61	62.12 ± 1.80	7.92 ± 1.16	6.46 ± 0.03	0.34 ± 0.02
pentan-3-ol	16.05 ± 0.16	67.43 ± 2.19	10.92 ± 0.73	4.76 ± 0.10	0.26 ± 0.02
pentan-1-ol	5.55 ± 0.48	92.41 ± 2.04	0.36 ± 0.10	4.33 ± 1.32	0.22 ± 0.08
hexan-1-ol	5.95 ± 0.11	94.80 ± 6.22	0.75 ± 0.12	3.44 ± 0.74	0.17 ± 0.05
t-butanol	23.76 ± 0.17	54.46 ± 0.06	19.18 ± 0.10	2.60 ± 0.02	0.14 ± 0.01
propan-2-ol	23.29 ± 0.21	56.01 ± 0.97	18.46 ± 0.76	2.24 ± 0.00	0.12 ± 0.01

6.3.6 A Fitness-Based Model for Evolution of Thioesterase Substrate Tolerance

The screening hypothesis suggests that long-term evolutionary selection favors pathways that can be readily 'screened' in the face of new environments to support chemical diversity.[62,63] In part, the diversity in a multistep pathway is dependent on substrate tolerance of late-stage enzymes. This tolerance permits plasticity in upstream components of the pathway, and fitness-based screening of newly-released metabolites. In addition, off-loading enzymes should be able to process diverse substrates and introduce substantial new chemical diversity to amplify potential new compounds accessible from upstream modifications.

Our results suggested a model for an evolution of type-I polyketide chemical diversity in the context of TE-mediated off-loading. We proposed that TEs are intrinsically non-selective toward the possible chemistries they catalyze,[64] and readily-perform hydrolysis, esterification, amidation, and ring-closure of macrocyclic and macrodiolide products. This range of reactivity expands chemical diversity accessible from a PKS pathway. As one metabolite, such as a macrodiolide, becomes essential to improving fitness in a particular producing environment,[65,66] the TE evolves under pressure to enrich for the corresponding

reactivity. This is supported by our phylogenetic analysis (Appendix II, § S2.4.1), which is consistent with convergent evolution of macrodiolide-forming activity. A corollary to this hypothesis is that small changes to the substrate should lead to loss of selectivity for the type of TE-mediated chemistry. This has been observed by *in vitro* characterization of the DEBS TE domain, where subtle structural changes have led to dramatic changes in reactivity, from hydrolysis, to macrocycle formation, and unprecedented macrodiolide formation.

This screening hypothesis and fitness-based model is sufficient to account for the observed experimental TE activity results in literature. It can also be used predicatively. For example, polyketide natural products have been isolated with functional groups derived from TE-mediated hydrolysis, macrolactonization, macrolactamization, and dimerization. However, no transesterification-derived polyketide products have been isolated to date. Having observed kinetic preference for *n*-butanol in two diverse TEs, we predict that an *n*-butanol ester is likely natively-produced by a yet-unidentified PKS pathway. Furthermore, since the presence of *n*-butanol is required for this activity, we predict that it will be observed in a native producer of butanol, such as the genus *Clostridium*.[67] At least three of the forty sequenced genomes (*Clostridium khuyveri* DSM 555, *Clostridium botulinum* A2 BoNT, and *Clostridium botulinum* H04402 065) encode a TE,[68] and possess a butanol dehydrogenase A (bdhA) orthologue.[69,70] This represents an active field of study toward industrial applications such as renewable production of high-value biofuels.[71–75]

6.4 Conclusions & Future Directions

This chapter presented ongoing work to probe substrate-selectivity of wild-type DEBS TE toward enzyme-catalyzed macrolactonization. Our two generations of simplified NAC-thioester analogues yielded the first two examples of recombinant DEBS TE-mediated *in vitro* ring-closure using non-native linear substrates. These analogues also highlighted dramatic effects on substrate-enzyme interactions and product distributions based on small, evolutionarily-accessible structural modifications. We proposed that the observed range of enzyme-mediated chemistries was due to plasticity within DEBS TE, and that substrate-selectivity of macrocyclizing TEs evolved from broadly-functioning proteins as a response to increase the likelihood of producing a bioactive compound. This fitness-based model has implications for bacterial TE engineering, and suggests that most TEs will not macrocyclize substrates effectively. However, we believe that TEs can be activated for previously-suppressed chemistries and to exhibit relaxed substrate-selectivity. Stimulating directed-evolution for vestigial chemistries will likely require extensive protein engineering to achieve preparative *in vitro* production from TEs with selective macrocyclization activity.[76–78] Based on

this assumption, a better understanding of substrate-enzyme interactions is needed to provide insights into the controlling factors of TE-mediated catalysis.

Early conclusions from our two generations of simplified analogues suggested that wild-type DEBS TE is likely too substrate-selective to be developed as an effective macrocyclizing chemoenzymatic tool. Our initial stereochemical hypothesis that stated D-configured nucleophiles are required for successful intramolecular attack proved accurate, though not wholly-sufficient at predicting ring-closure or to explain observed selectivity of DEBS TE-mediated macrocyclization. Hydrolysis predominated with D-configured **6.25** and our racemic mixture of methyl derivative **6.34**. Remarkably, analogue **6.25** possessed the relative and absolute stereochemistry at C11 and C13 analogous to the native precursor. To probe the observed selectivity, we have been engaged in obtaining high-resolution structural data of acyl-enzyme intermediates.[79] Specifically, we hope non-hydrolyzable phosphonate-based covalent inhibitors of Pinto's **6.25** and **6.28** will provide contrasting details of acyl-enzyme interactions in D-configured C13-substrates that were hydrolyzed and macrocyclized by DEBS TE, respectively.[60,79] This remains an active source of collaborative research with the Martin Schmeing Lab[80] at McGill University.

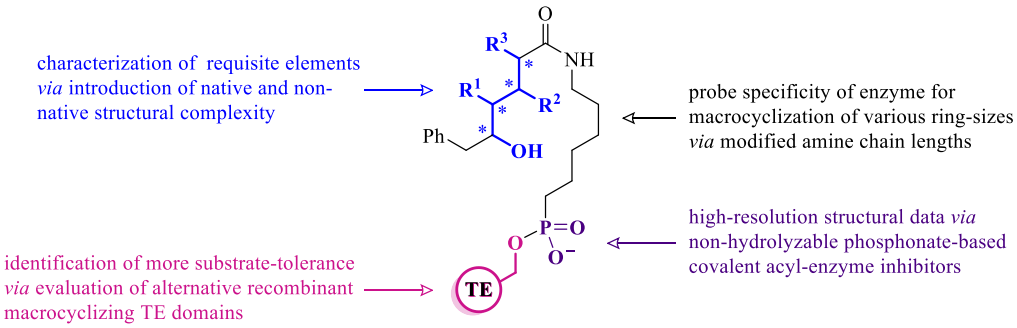

Figure 6.16 – Building analogue libraries introduces structural elements that can identify functional groups that are necessary and sufficient to predict TE-mediated ring-closure from a panel of recombinant proteins. Crystal structures can be obtained *via* covalent acyl-enzyme inhibitors, and used in-turn to guide next-generation analogue development.

To advance the study, it is necessary to expand our analogue library through introduction of native and non-native structural complexity. Initial efforts should involve modifications to our existing library, such as selectively-oxidizing first-generation analogues or allow free rotation *via* hydrogenation of second-generation analogues to evaluate effects on product distributions. Emphasis should then be placed on developing synthetically-tractable, asymmetric production of the C9-C13 PKS framework that allows easy derivatization. The hydrophobic model for substrate-enzyme recognition suggests that native alkylation may play an important role in dictating the conformation of the substrate within the catalytic site, and thus

its reactivity. On-going work in our lab is focused on the effect of introducing these structural elements,[**] and to evaluate if they are sufficient in making our substrates macrocyclization competent.

Similarly, to rapidly populate our analogue library and to probe substrate-specificity with respect to ring size, each C9-C13 fragment should be coupled to amines of varying length. Using commercial materials, unsubstituted aliphatic chains like **6.40** could easily be prepared for production of precursors to common macrolactone ring-sizes (12-, 14-, 16-, and 18-membered). This strategy effectively quadruples our library, and should provide key insights into the regioselectivity of TE-mediated transformations. Early exploration of precursors to 12-membered ring systems of our second-generation analogues has begun (refer to experimental). Previous reports indicated that DEBS TE possessed sufficient substrate tolerance to exclusively-generate 12-membered macrocyclic metabolites *in vitro* using fully-elaborated native pikromycin backbone.[33,81] Because these metabolites are structurally-homologous, we expect these truncated amino NAC-thioesters will readily undergo ring-closure in similar fashion with our analogues.

Lastly, because our data suggested DEBS TE is too selective, it is imperative to the success of the study that alternative TEs are used for biochemical characterization with all analogues generated. To identify a macrocyclizing enzyme with broad substrate tolerance, a diverse panel of known TEs from PKS and NRPS biosynthetic pathways should be expressed and purified.[10] The chosen panel could be used to guide design of next-generation analogues to install native structural elements. Once identified, a long-term goal of the study would be to evolve the most-promising TE candidates *via* protein engineering and directed evolution using detailed information of substrate-enzyme interactions procured through the combination of biochemical characterization and high-resolution structural data.[80] Please refer to **Chapter 7** for additional details about these studies, and other potential future directions for the development of a thioesterase as a macrocyclizing biocatalytic tool.

The field of biocatalysis is incredibly active and the potential to harness TE catalytic domains to perform macrocyclization of non-native substrates offers incredible possibilities for *de novo* pathways and as a standalone chemoenzymatic tool. With this study, we hope to contribute to a better understanding of the molecular interactions that control specificity and promiscuity for these enzymes, and identify a suitable TE with broad substrate-tolerance. It is with great anticipation that the cumulative knowledge gained will serve as foundations for future efforts aimed at attenuating hydrolytic activity, and leveraging the catalytic efficiency of macrocyclizing TEs for production of novel frameworks and possible drug candidates.

[**] Preliminary exploration of C12-methylated derivatives to our first-generation model suggested selective formation of enzyme-mediated products including putative macrocycle and macrodiolide metabolites.

6.5 Experimental

6.5.1 General Procedures

All reactions were carried out using oven-dried glassware under an inert atmosphere (nitrogen, or argon gas) with dry solvents under anhydrous conditions, unless otherwise noted. Anhydrous solutions of THF, Et_2O, and CH_2Cl_2 were obtained from an anhydrous solvent delivery system;[82] other solvents were freshly distilled.[83] Yields refer to chromatographically and spectroscopically (^{1}HNMR) homogenous materials, unless otherwise stated. Reagents were commercially purchased at the highest quality and used without further purification, unless otherwise stated. Reactions were monitored by TLC carried out on 0.25 Mm Silicycle silica gel plates (60F-254) using either UV light as a visualizing agent, or an aqueous solution of CAM, *p*-anisaldehyde or iodine$_{(s)}$, and heat as a developing agent. Preparative thin-layer chromatography (PTLC) separations were carried out on 0.25 Mm Silicycle silica gel plates (60F-254). NMR spectra were recorded on Bruker Avance 300 or 400 MHz, Avance II 300 MHz, or Avance III 600 MHz instruments, and calibrated using residual undeuterated solvent ($CDCl_3$: δ H = 7.26 ppm, δ C = 77.0 ppm)[84] as internal references. Data is reported as follows: chemical shift (multiplicity abbreviations: s = singlet, d = doublet, t = triplet, q = quartet, p = pentet, m = multiplet, br = broad), *J* = coupling constant (Hz), integration, peak assignment. Infrared (IR) spectra were recorded on an ABB Bomen MB Series Arid-Zone™ Infrared Spectrometer. HRMS were recorded by positive ion electrospray on Kratos Analytical Concept 11A mass spectrometer with an electron beam of 70 eV (Ottawa-Carleton Mass Spectrometry Centre). ESI-LC-MS/MS analysis was performed on an API2000 System equipped with a turbo-ion spray ESI probe interfaced with a Prominence UFLC. A reverse phase BDS Hypersil C18 column (100 mm × 2.1 mm I.D., 3 µm particle size) was employed. Mobile phases throughout experimental were *A*: 5% MeCN:95% H_2O with 0.05% formic acid, and *B*: 95% MeCN:5% H_2O with 0.05% formic acid. Chemical separation was performed using a gradient from 0% *B* to 100% *B* over 30 min, with a flow rate of 0.2 mL/min. An ionization voltage of 5500 V and probe temperature of 250 °C were used in the ESI TurboSpray probe, and masses were scanned over 300 – 800 *m*/*z*.

6.5.2 Experimental Procedures and Physical Data of Compounds

All the experimental procedures are representative of single-run and unoptimized procedures, and arranged to reflect the synthetic procedures shown in the schemes. Spectral traces can be found in the supplemental information (Appendix I).

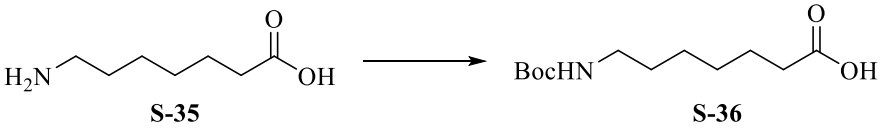

S-35 **S-36**

7-*tert*-Butyloxycarbonylamino heptanoic acid (**S-36**). To a stirring solution of 7-aminoheptanoic acid **S-35** (300 mg, 2.06 mmol, 1.0 equiv.) and Boc-anhydride (0.57 mL, 2.47 mmol, 1.2 equiv.) in an equal mixture of 1,4-dioxane and water (0.3 M overall), was added potassium carbonate (1.15 g, 8.24 mmol, 4.0 equiv.) under inert atmosphere. The solution was stirred overnight at ambient temperature. The reaction mixture was concentrated *in vacuo*, and the crude residue was dissolved in water (20 mL) and washed with EtOAc (2 × 20 mL). The aqueous phase was acidified (pH < 2) and extracted with EtOAc (3 × 20 mL). Combined organic extracts were dried ($MgSO_4$), filtered, and concentrated *in vacuo* to afford acid **S-36** (474.5 mg, 1.94 mmol, 94%) as colorless oil, which slowly crystallized as colorless solid.

^{1}HNMR (400 MHz, $CDCl_3$): δ 4.49 (br s, 1H, -N*H*-), 3.09 (q, J = 6.7 Hz, 2H, -CH_2-), 2.33 (t, J = 7.5 Hz, 2H, -CH_2-), 1.62 (p, J = 7.4 Hz, 2H, -CH_2-), 1.47 – 1.43 (m, 2H, -CH_2-), 1.42 (s, 9H, Boc *t*-Bu), 1.36 – 1.29 (m, 4H, 2 × -CH_2-) ppm.

Characterization data for **S-36** proved consistent with previously reported literature data.[85]

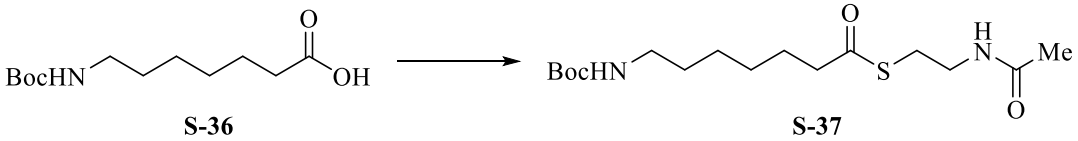

S-36 **S-37**

1-(2-Acetamidoethylthio)-7-(*tert*-butoxycarbonylamino)-heptanethioate (**S-37**). To a stirring solution of *N*-Boc-7-aminoheptanoic acid **S-36** (474.5 mg, 1.94 mmol, 1.0 equiv.) in THF (13 mL) was added EDC·HCl (631.0 mg, 4.06 mmol, 2.1 equiv.), DMAP (150.0 mg, 1.22 mmol, 0.63 equiv.) and *N*-acetylcysteamine (340.0 µL, 2.32 mmol, 1.2 equiv.). The reaction was stirred for 18 h at ambient temperature, then quenched with water. The mixture was extracted with ethyl acetate (50 mL), washed with water (30 mL), saturated $NaHCO_3$ (30 mL), and brine (30 mL). The organic layer was dried ($MgSO_4$), filtered, and concentrated *in vacuo*. The crude residue was purified *via* flash chromatography (40% acetone in hexanes) to afford **S-37** (612.1 mg, 1.77 mmol, 91%) as white powder.

R_f = 0.22 (silica gel, 40% acetone in hexanes).

^{1}HNMR (300 MHz, $CDCl_3$): δ 5.87 (br s, 1H, -N*H*-), 4.49 (br s, 1H, -N*H*-), 3.41 (q, J = 6.3 Hz, 2H, -CH_2-NH-), 3.08 (q, J = 6.5 Hz, 2H, -CH_2-NH-), 3.01 (t, J = 6.3, 2H, -CH_2-S-), 2.55 (t, J = 7.5 Hz, 2H, -CH_2-CO-), 1.95 (s, 3H, -CH_3), 1.69 – 1.60 (m, 4H, 2 × -CH_2-), 1.42 (s, 9H, *t*-Bu), 1.32 – 1.30 (m, 4H, -CH_2-) ppm.

^{13}CNMR (75 MHz, $CDCl_3$): δ 200.0, 170.3, 156.0, 79.1, 43.9, 40.4, 39.7, 29.8, 28.5, 28.4, 28.4, 26.3, 25.5, 23.2 ppm.

HRMS (EI) *m/z*: calculated for $C_{12}H_{21}N_2O_3S$ [M – C_4H_9O] 273.1273, observed 273.1285 (Δ 1.2 mmu).

Characterization data for **S-37** proved consistent with previously reported literature data.[37]

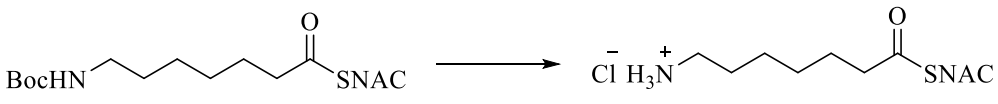

S-37 **6.40**

7-(2-Acetamidoethylthio)-7-oxoheptan-1-ammonium chloride (**6.36**). Boc-protected aminothioester **S-37** (340 mg, 0.98 mmol, 1.0 equiv.) was dissolved in HCl/dioxane (2.5 mL, 9.8 mmol, 10.0 equiv.), and stirred at ambient temperature under inert atmosphere. After 45 minutes, solvent was evaporated *in vacuo* and amine **6.40** was isolated (240.9 mg, 0.98 mmol, quant.) as a white powder.

^{1}HNMR (400 MHz, D_2O): δ 3.24 (t, J = 6.3 Hz, 2H, -CH_2-NH-), 2.91 (t, J = 6.3 Hz, 2H, -CH_2-S-), 2.84 (br t, J = 7.6 Hz, 2H, -CH_2-NH_2), 2.52 (t, J = 7.3 Hz, 2H, -CH_2-CO-), 1.81 (s, 3H, -CH_3), 1.55 – 1.48 (m, 4H, -CH_2-), 1.26 – 1.20 (m, 4H, 2 × -CH_2-) ppm.

^{13}CNMR (100 MHz, D_2O): δ 204.9, 174.4, 43.2, 39.4, 38.6, 28.0, 27.4, 26.4, 25.2, 25.0, 21.8 ppm.

Characterization data for **6.40** proved consistent with previously reported literature data.[32]

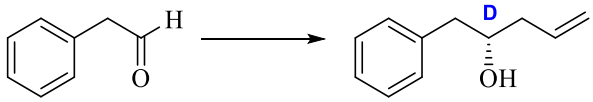

6.35 **S-38**

(D)-1-Phenylpent-4-en-2-ol (**S-38**). Two flame-dried reaction flasks were prepared in accordance with Brown's procedure for asymmetric allylation.[40] In the first, phenylacetaldehyde **6.35** (600 mg, 5.0 mmol, 1.0 equiv.) was dissolved in anhydrous ether (6 mL) and cooled to -100 ºC under inert atmosphere. In the second flask, (–)-Ipc_2BAllyl (5 mL, 1.0 M in pentanes) was transferred *via* a dry glass syringe from its ampule to the flask, and cooled to -100 ºC while stirring. The first flask was cannulated into the second, with anhydrous ether (4 mL) rinse. The reaction mixture warmed to -78 ºC, and monitored by TLC (silica gel, 10% EtOAc in hexanes). Upon completion, the reaction was quenched with MeOH and stirred for 20 min. Addition of 15% NaOH (2 mL) induced a pale-yellow color from the clear mixture, and was stirred for an additional 10 min. Addition of 30% aqueous H_2O_2 (4 mL) induced an opaque white solution and exothermed. The reaction mixture was refluxed for 1 h, upon which the mixture was diluted in ether (40 mL) and washed with brine (3 × 50 mL). The organic layer was dried ($MgSO_4$), filtered, and concentrated *in vacuo*. Crude material was purified *via* flash chromatography (50% CH_2Cl_2 in hexanes), and yielded 525 mg (3.24 mmol, 65%) of **S-38** as clear, colorless oil (*ee* > 90% by chiral GC).

R_f = 0.23 (silica gel, 10% EtOAc in hexanes).

^{1}HNMR (300 MHz, $CDCl_3$): δ 7.30 – 7.20 (m, 5H, 5 × -C*H*- Ph), 5.85 (dddd, *J* = 16.6, 10.7, 7.3, 7.3 Hz, 1H, -C*H*-), 5.11 – 5.17 (m, 2H, -CH_2-), 3.88 (dq, *J* = 4.7, 8.0 Hz, 1H, -C*H*-), 2.81 (dd, *J* = 13.6, 4.9 Hz, 1H, -CH*H*-), 2.72 (dd, *J* = 13.6, 8.0 Hz, 1H, -CH*H*-), 2.38 – 2.15 (m, 2H, -CH_2-), 1.66 (d, *J* = 3.5 Hz, -O*H*) ppm.

^{13}CNMR (100 MHz, $CDCl_3$): δ 138.6, 134.6, 129.4, 128.6, 126.5, 71.6, 43.3, 41.2 ppm.

Characterization data for **S-38** proved consistent with previously reported literature data.[32]

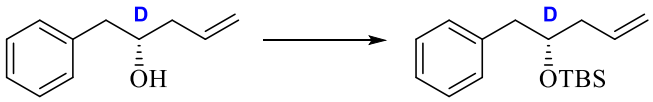

S-38 **6.36**

(D)-*tert*-Butyldimethyl(1-phenylpent-4-en-2-yloxy)silane (**6.36**). Homoallylic alcohol **S-38** (329.1 mg, 2.0 mmol, 1.0 equiv.) was dissolved in anhydrous DMF (2.0 mL, 1.0 M) under inert atmosphere, and TBSCl (367.0 mg, 2.4 mmol, 1.2 equiv.) was added to the solution. Imidazole (341.0 mg, 5.0 mmol, 2.5 equiv.) was added, and stirred overnight. The reaction mixture was quenched with saturated ammonium chloride, and diluted in EtOAc (20 mL). Organic layers were washed with water (4 × 10 mL), and an increasing-gradient concentration of brine. The combined organic layers were dried ($MgSO_4$), filtered, and concentrated *in vacuo*. Crude material was purified *via* gradient flash chromatography (0 – 5% EtOAc in hexanes), and quantitatively yielded 561 mg of **6.36** as clear, colorless oil.

R_f = 0.71 (silica gel, 10% EtOAc in hexanes).

^{1}HNMR (300 MHz, $CDCl_3$): δ 7.29 – 7.12 (m, 5H, 5 × -C*H*- Ph), 5.85 (ddt, *J* = 17.9, 10.6, 7.2 Hz, 1H, -C*H*-), 5.19 – 4.98 (m, 2H, -CH_2-), 3.91 – 3.80 (m, 1H, -C*H*-), 2.75 (dd, *J* = 13.3, 5.7 Hz, 1H, -CH*H*-), 2.65 (dd, *J* = 13.3, 7.0 Hz, 1H, -CH*H*-), 2.25 – 2.16 (m, 2H, -CH_2-), 0.82 (s, 9H, O-TBS *t*-Bu), -0.08 (s, 3H, O-TBS -CH_3), -0.25 (s, 3H, O-TBS -CH_3) ppm.

^{13}CNMR (100 MHz, $CDCl_3$): δ 139.3, 135.1, 129.8, 128.1, 126.0, 117.1, 73.5, 43.5, 41.7, 25.9, 18.1, 14.2, -4.7, -5.0 ppm.

Characterization data for **6.36** proved consistent with previously reported literature data.[86]

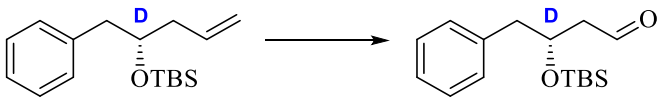

6.36 **6.37**

(D)-3-(*tert*-Butyldimethylsilyloxy)-4-phenylbutanal (**6.37**). Purified **6.36** (601.4 mg, 2.0 mmol, 1.0 equiv.) was diluted in an equal mixture of *t*-BuOH and water (20 mL) at ambient temperature. To this solution was added potassium carbonate (830.0 mg, 6.0 mmol, 3.0 equiv.), potassium ferricyanide (1.54 g,

4.68 mmol, 3.0 equiv.), and a solution of potassium osmate (VI) dihydrate (8 mg, 0.02 mmol, 0.01 equiv.) in NaOH (15% *w*/*v*, 0.3 mL). The reaction mixture was stirred overnight at ambient temperature. Upon completion by TLC (silica gel, 10% EtOAc in hexanes), the mixture was diluted in water and EtOAc, and washed with brine (3 × 30 mL). Combined organic layers were dried ($MgSO_4$), filtered, and concentrated *in vacuo*. The crude product was diluted in anhydrous CH_2Cl_2 (8.0 mL). Lead tetraacetate (1.06 g, 2.4 mmol, 1.2 equiv.) was added under inert atmosphere, and stirred vigorously for 1 h while being monitored by TLC. Upon completion, the mixture was concentrated to remove 75% of the CH_2Cl_2, and loaded directly on a pre-equilibrated column (10% EtOAc in hexanes). The two-step sequence yielded 389.4 mg of **6.37** (1.40 mmol, 70%, 2 steps) as a clear, colorless oil.

R_f = 0.31 (silica gel, 10% EtOAc in hexanes).

^{1}HNMR (300 MHz, $CDCl_3$): δ 9.76 (t, *J* = 2.3 Hz, 1H, -C*H*O), 7.30 – 7.14 (m, 5H, 5 × -C*H*- Ph), 4.40 – 4.32 (m, 1H, -C*H*-), 2.85 (dd, *J* = 13.3, 6.5 Hz, 1H, -CH*H*-), 2.76 (dd, *J* = 13.3, 6.6 Hz, 1H, -CH*H*-), 2.49 (dd, *J* = 5.7, 2.4 Hz, 2H, -CH_2-), 0.84 (s, 9H, O-TBS *t*-Bu), -0.01 (s, 3H, O-TBS -CH_3), -0.12 (s, 3H, O-TBS -CH_3) ppm.

^{13}CNMR (75 MHz, $CDCl_3$): δ 201.8, 137.8, 129.7, 128.5, 126.7, 69.6, 50.5, 44.6, 25.8, 18.1, -4.8, -5.0 ppm.

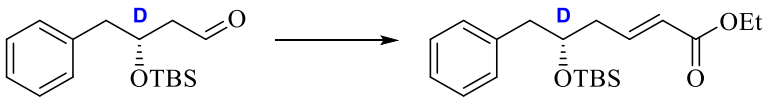

6.37 **S-39**

(D)-(*E*)-Ethyl 5-(*tert*-butyldimethylsilyloxy)-6-phenylhex-2-enoate (**S-39**). To a stirring solution of **6.37** (575 mg, 2.06 mmol, 1.0 equiv.) and triethyl phosphonoacetate **6.38** (0.47 mL, 2.30 mmol, 1.1 equiv.) in THF (14 mL), freshly powdered KOH (231 mg, 4.12 mmol, 2.0 equiv.) was added and stirred for 1 h at ambient temperature. Upon completion by TLC (silica gel, 10% EtOAc in hexanes), the mixture was diluted in Et_2O (3 × 10 mL), and washed with brine (3 × 30 mL). Combined organic layers were dried ($MgSO_4$), filtered, and concentrated *in vacuo*. The crude product was purified by flash chromatography (10% EtOAc in hexanes), and yielded 435.7 mg of **S-39** (1.25 mmol, 63%) as a clear, colorless oil.

R_f = 0.41 (silica gel, 10% EtOAc in hexanes).

^{1}HNMR (300 MHz, $CDCl_3$): δ 7.29 – 7.11 (m, 5H, 5 × -C*H*- Ph), 6.98 (dt, *J* = 7.6, 7.6 Hz, 1H, -C*H*-), 5.81 (dt, *J* = 15.6, 1.4 Hz, 1H, -C*H*-), 4.18 (q, *J* = 7.1 Hz, 2H, -CH_2-), 4.00 – 3.89 (m, 1H, -C*H*-), 2.72 (d, *J* = 6.4 Hz, 2H, -CH_2-), 2.36 – 2.27 (m, 2H, -CH_2-), 1.27 (t, *J* = 7.1 Hz, 3H, -CH_3), 0.83 (s, 9H, O-TBS *t*-Bu), -0.06 (s, 3H, O-TBS -CH_3), -0.22 (s, 3H, O-TBS -CH_3) ppm.

^{13}CNMR (75 MHz, $CDCl_3$): δ 166.4, 145.7, 138.5, 129.7, 128.2, 126.3, 123.6, 72.7, 60.2, 44.0, 39.8, 25.8, 18.0, 14.3, -4.9, -5.0 ppm.

HRMS (EI) *m/z*: calculated for $C_{16}H_{23}O_3Si$ [M – *t*-Bu] 291.1416, observed 291.1410 (Δ 0.6 mmu).

IR (thin film) ν_{max}: 2936, 1724, 1656, 1091 cm^{-1}.

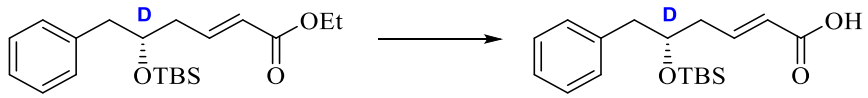

S-39 **6.39**

(D)-(*E*)-5-(*tert*-Butyldimethylsilyloxy)-6-phenylhex-2-enoic acid (**6.39**). To a solution of **S-39** (250 mg, 0.72 mmol, 1.0 equiv.) in a mixture of MeOH, THF, and water (3:2:1, 0.1 M), LiOH (1.3 mL, 1.0 M) was added and stirred for 6 h at ambient temperature. Upon completion by TLC (silica gel, 20% EtOAc in hexanes; CAM stain), the mixture was quenched with saturated NH_4Cl, diluted in EtOAc (20 mL) and washed with brine (3 × 20 mL). The aqueous layer was acidified (pH < 2), and re-extracted with EtOAc (15 mL). The combined organic layers were dried ($MgSO_4$), filtered, and concentrated *in vacuo*. The crude product was purified by flash chromatography (15% EtOAc in hexanes) to afford 211.5 mg (0.66 mmol, 92%) of **6.39** as clear, colorless oil.

R_f = 0.24 (silica gel, 20% EtOAc in hexanes).

^{1}HNMR (300 MHz, $CDCl_3$): δ 7.30 – 7.12 (m, 5H, 5 × -C*H*- Ph), 7.04 – 7.13 (m, 1H, -C*H*-), 5.82, (d, *J* = 15.6 Hz, 1H, -C*H*-), 3.97 (p, *J* = 6.0 Hz, 1H, -C*H*-), 2.72 (dd, *J* = 6.3, 4.8 Hz, 2H, -CH_2-), 2.43 – 2.26 (m, 2H, -CH_2-), 0.84 (s, 9H, O-TBS *t*-Bu), -0.05 (s, 3H, O-TBS -CH_3), -0.20 (s, 3H, O-TBS -CH_3) ppm.

^{13}CNMR (75 MHz, $CDCl_3$): δ 170.8, 148.7, 138.4, 129.7, 128.3, 126.3, 122.7, 72.5, 44.0, 39.9, 25.8, 18.0, -4.9, -5.1 ppm.

HRMS (EI): calculated for $C_{14}H_{19}O_3Si$ [M – *t*-Bu] 263.1103, observed 263.1099 (Δ 0.4 mmu).

IR (thin film) ν_{max}: 3022, 1700, 1649, 1490 cm^{-1}.

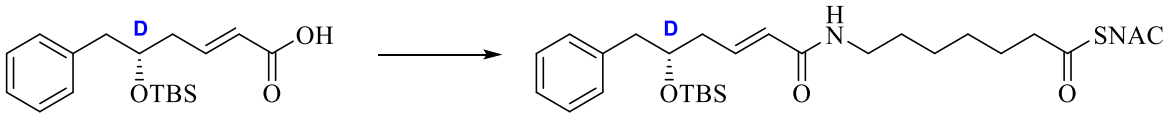

6.39 **6.41**

(D)-(*E*)-*S*-2-Acetamidoethyl-7-(5-(TBS)-6-phenylhex-2-enamido)heptanethioate (**6.41**). The purified acid **6.39** (53.7 mg, 0.168 mmol, 1.0 equiv.) was dissolved in CH_2Cl_2 (1.7 mL), to which EDC·HCl (48.2 mg, 0.251 mmol, 1.5 equiv.), DMAP (2.1 mg, 0.017 mmol, 0.1 equiv.), and amine **6.40** (51.2 mg, 0.235 mmol, 1.4 equiv.) were added. The reaction mixture stirred for 10 min at ambient temperature, and triethylamine (34.9 µL, 0.251 mmol, 1.5 equiv.) was added. The reaction stirred overnight under inert atmosphere, and monitored by TLC (silica gel, 5% MeOH in CH_2Cl_2). Upon completion, the reaction was quenched with NH_4Cl (1.0 mL), and extracted with EtOAc (5 × 2 mL). Combined organic extracts were washed with brine (3 × 4 mL), dried ($MgSO_4$), filtered, and concentrated *in vacuo*. The crude residue was

purified by flash chromatography (3% MeOH in CH_2Cl_2), to furnish 71.2 mg of amide **6.41** (0.130 mmol, 77%) as a clear, yellow oil.

R_f = 0.45 (silica gel, 5% MeOH in CH_2Cl_2).

^{1}HNMR (400 MHz, $CDCl_3$): δ 7.28 – 7.09 (m, 5H, 5 × -C*H*- Ph), 6.81 (dt, *J* = 15.1, 7.5 Hz, 1H, -C*H*-), 5.99 (br s, 1H, -N*H*-), 5.74 (d, *J* = 15.3 Hz, 1H, -C*H*-), 5.47 (t, *J* = 5.3 Hz, 1H, -N*H*-), 3.93 (p, *J* = 5.8 Hz, 1H, -C*H*-), 3.41 (q, *J* = 6.0 Hz, 2H, -CH_2-NH-), 3.29 (dd, *J* = 12.8, 5.6 Hz, 2H, -CH_2-NH-), 3.00 (t, *J* = 6.3 Hz, -CH_2-S-), 2.70 (dd, *J* = 6.3, 3.6 Hz, 2H, -CH_2-), 2.55 (t, *J* = 7.3 Hz, 2H, -CH_2-CO-), 2.38 – 2.23 (m, 2H, -CH_2-), 1.95 (s, 3H, -CH_3), 1.68 – 1.61 (m, 2H, -CH_2-), 1.56 – 1.45 (m, 2H, -CH_2-), 1.38 – 1.27 (m, 4H, 2 × -CH_2-), 0.81 (s, 9H, O-TBS *t*-Bu), -0.08 (s, 3H, O-TBS -CH_3), -0.25 (s, 3H, O-TBS -CH_3) ppm.

^{13}CNMR (100 MHz, $CDCl_3$): δ 200.0, 170.4, 169.4, 138.8, 132.5, 131.8, 129.8, 128.2, 126.2, 73.0, 44.1, 43.9, 39.7, 39.4, 36.1, 29.4, 28.6, 28.4, 26.4, 25.9, 25.5, 23.2, 18.0, -4.8, -5.0 ppm.

HRMS (EI) *m/z*: calculated for $C_{25}H_{39}N_2O_4SSi$ [M – *t*-Bu] 491.2400, observed 491.2392 (Δ 0.8 mmu).

IR (thin film) ν_{max}: 3321, 2933, 1653, 1558, 1087 cm^{-1}.

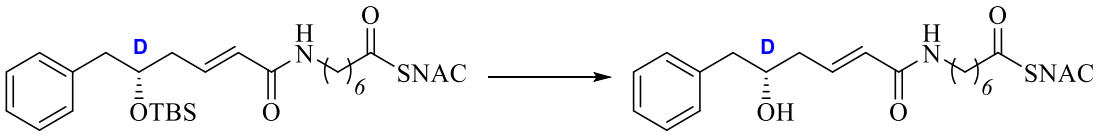

6.41 D-**6.33**

(D)-(*E*)-*S*-2-Acetamidoethyl-7-(5-hydroxy-6-phenylhex-2-enamido)heptanethioate (D-**6.33**). Purified NAC-substrate **6.41** (40.0 mg, 0.073 mmol, 1.0 equiv.) was added to a 1.5 mL Eppendorf tube and dissolved in MeCN (910 µL). To this solution was added pyridine (29.4 µL, 0.365 mmol, 5.0 equiv.), and 48% aqueous HF (131 µL, 3.645 mmol, 50 equiv.). The mixture was vortexed to homogeneity, and proceeded without stirring for 5 h at ambient temperature. Upon completion by TLC (silica gel, 5% MeOH in CH_2Cl_2), the mixture was diluted with 2 volumes of water. The resulting solution was carefully extracted with EtOAc (5 × 3 mL), and washed with brine (2 × 4 mL). The organic extracts were combined, dried ($MgSO_4$), filtered, and concentrated *in vacuo*. Crude product was purified by flash chromatography (5% MeOH in CH_2Cl_2), and yielded free diol D-**6.33** (20.1 mg, 0.047 mmol, 64%) as clear, colorless oil.

R_f = 0.32 (silica gel, 5% MeOH in CH_2Cl_2).

^{1}HNMR (400 MHz, $CDCl_3$): δ 7.33 – 7.16 (m, 5H, 5 × -C*H*- Ph), 6.84 (dt, *J* = 15.0, 7.4 Hz, 1H, -C*H*-), 6.02 (br s, 1H, -N*H*-), 5.86 (d, *J* = 15.3 Hz, 1H, -C*H*-), 5.62 (t, *J* = 5.1 Hz, 1H, -N*H*-), 3.96 (tt, *J* = 7.8, 4.7 Hz, 1H, -C*H*-), 3.40 (dd, *J* = 12.4, 6.0 Hz, 2H, -CH_2-NH-), 3.29 (dd, *J* = 13.1, 6.8 Hz, 2H, -CH_2-NH-), 3.00 (t, *J* = 6.4 Hz, 2H, -CH_2-S-), 2.82 (dd, *J* = 13.7, 4.8 Hz, 1H, -CH*H*-), 2.71 (dd, *J* = 13.6, 8.1 Hz, 1H, -CH*H*-), 2.54 (t, *J* = 7.3 Hz, 2H, -CH_2-CO-), 2.45 – 2.28 (m, 2H, -CH_2-), 1.94 (s, 3H, -CH_3), 1.72 – 1.57 (m, 2H, -CH_2-), 1.56 – 1.45 (m, 2H, -CH_2-), 1.36 – 1.28 (m, 4H, 2 × -CH_2-) ppm.

^{13}CNMR (100 MHz, $CDCl_3$): δ 200.1, 170.5, 165.7, 140.4, 137.9, 129.4, 128.7, 126.7, 126.4, 71.4, 43.9, 43.6, 39.7, 39.3, 39.2, 29.3, 28.6, 28.3, 26.3, 25.4, 23.2 ppm.

HRMS (EI) *m/z*: calculated for $C_{23}H_{32}N_2O_3S$ [M – H_2O] 416.2134, observed 416.2125 (Δ 0.9 mmu).

LCMS (t_R): 14.66 min.

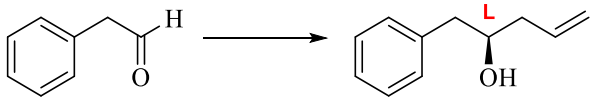

6.35 **S-40**

(L)-1-Phenylpent-4-en-2-ol (**S-40**). Using (+)-Ipc_2BAllyl (5 mL, 1.0 M in pentanes), homoallylic alcohol **S-40** was prepared in identical fashion to **S-38** (*vide supra*). Crude material was purified *via* flash chromatography (50% CH_2Cl_2 in hexanes), and yielded 518 mg (3.19 mmol, 64%) of **S-40** as clear, colorless oil (*ee* 90% by chiral GC).

R_f = 0.23 (silica gel, 10% EtOAc in hexanes).

^{1}HNMR (300 MHz, $CDCl_3$): δ 7.30 – 7.20 (m, 5H, 5 × -C*H*- Ph), 5.85 (dddd, *J* = 16.6, 10.7, 7.2, 7.2 Hz, 1H, -C*H*-), 5.12 – 5.18 (m, 2H, -CH_2-), 3.87 (dq, *J* = 4.7, 8.0 Hz, 1H, -C*H*-), 2.81 (dd, *J* = 13.6, 4.9 Hz, 1H, -CH*H*-), 2.71 (dd, *J* = 13.6, 8.0 Hz, 1H, -CH*H*-), 2.38 – 2.15 (m, 2H, -CH_2-), 1.66 (d, *J* = 3.5 Hz, -O*H*) ppm.

^{13}CNMR (100 MHz, $CDCl_3$): δ 138.6, 134.7, 129.4, 128.6, 126.5, 71.7, 43.3, 41.2 ppm.

Characterization data for **S-40** proved consistent with previously reported literature data.[32]

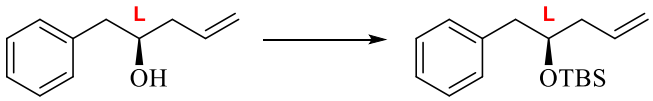

S-40 ***ent*-6.36**

(L)-*tert*-Butyldimethyl(1-phenylpent-4-en-2-yloxy)silane (*ent*-**6.36**). Homoallylic alcohol **S-40** (515.0 mg, 3.18 mmol, 1.0 equiv.) was dissolved in anhydrous DMF (3.2 mL, 1.0 M) under inert atmosphere, and TBSCl (574.3 mg, 3.81 mmol, 1.2 equiv.) was added to the solution. Imidazole (540.4 mg, 7.94 mmol, 2.5 equiv.) was added, and stirred overnight. The reaction mixture was quenched with saturated ammonium chloride, and diluted in EtOAc (20 mL). Organic layers were washed with water (4 × 10 mL), and an increasing-gradient concentration of brine. The combined organic layers were dried ($MgSO_4$), filtered, and concentrated *in vacuo*. Crude material was purified *via* gradient flash chromatography (0 – 5% EtOAc in hexanes), and yielded *ent*-**6.36** (860.1 mg, 3.11 mmol, 98%) as clear, colorless oil.

R_f = 0.72 (silica gel, 10% EtOAc in hexanes).

^{1}HNMR (300 MHz, $CDCl_3$): δ 7.27 – 7.13 (m, 5H, 5 × -C*H*- Ph), 5.85 (dddd, *J* = 16.7, 10.7, 7.1, 7.1 Hz, 1H, -C*H*-) 5.08 – 5.00 (m, 2H, -CH_2), 3.86 (dq, *J* = 7.1, 5.6 Hz, 1H, -C*H*-), 2.75 (dd, *J* = 13.3, 5.4 Hz, 1H, -CH*H*-), 2.65 (dd, *J* = 13.5, 7.1 Hz, 1H, -CH*H*-), 2.24 – 2.17 (m, 2H, -CH_2-), 0.82 (s, 9H, O-TBS *t*-Bu), -0.08 (s, 3H, O-TBS-CH_3), -0.25 (s, 3H, O-TBS-CH_3) ppm.

^{13}CNMR (100 MHz, $CDCl_3$): δ 139.3, 135.1, 129.8, 128.1, 126.0, 117.1, 73.5, 43.5, 41.7, 25.9, 18.1, 14.1, -4.7, -5.0 ppm.

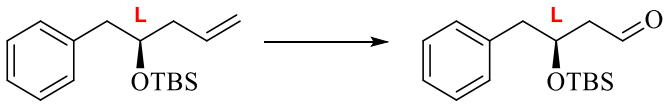

ent-**6.36** *ent*-**6.37**

(L)-3-(*tert*-Butyldimethylsilyloxy)-4-phenylbutanal (*ent*-**6.37**). Homoallylic alcohol *ent*-**6.36** (1.64 g, 5.90 mmol, 1.0 equiv.) was diluted in an equal mixture of *t*-BuOH and water (20 mL) at ambient temperature. To this solution was added potassium carbonate (2.52 g, 17.7 mmol, 3.0 equiv.), potassium ferricyanide (5.83 g, 17.7 mmol, 3.0 equiv.), and a solution of potassium osmate (VI) dihydrate (20 mg, 0.054 mmol, 0.01 equiv.) in NaOH (15% *w*/*v*, 0.3 mL). The reaction mixture was stirred overnight at ambient temperature. Upon completion by TLC (silica gel, 10% EtOAc in hexanes), the mixture was diluted in water and EtOAc, and washed with brine (3 × 30 mL). Combined organic layers were dried ($MgSO_4$), filtered, and concentrated *in vacuo*. The crude product was diluted in anhydrous CH_2Cl_2 (8.0 mL). Lead tetraacetate (3.2 g, 7.1 mmol, 1.2 equiv.) was added under inert atmosphere, and stirred vigorously for 1 h while being monitored by TLC. Upon completion, the mixture was concentrated to remove 75% of the CH_2Cl_2, and loaded directly on a pre-equilibrated column (10% EtOAc in hexanes). The two-step sequence yielded 1.23 g of *ent*-**6.37**(4.43 mmol, 72%, 2 steps) as a clear, colorless oil.

R_f = 0.31 (silica gel, 10% EtOAc in hexanes).

^{1}HNMR (400 MHz, $CDCl_3$): δ 9.76 (t, *J* = 2.4 Hz, 1H, -C*H*O), 7.34 – 7.08 (m, 5H, 5 × -C*H*- Ph), 4.36 (p, *J* = 6.1 Hz, 1H, -C*H*-), 2.85 (dd, *J* = 13.4, 6.3 Hz, 1H, -CH*H*-), 2.76 (dd, *J* = 13.4, 6.7 Hz, 1H, -CH*H*-), 2.49 (dd, *J* = 5.7, 2.3 Hz, 2H, -CH_2-), 0.83 (s, 9H, O-TBS *t*-Bu), -0.01 (s, 3H, O-TBS -CH_3), -0.12 (s, 3H, O-TBS -CH_3) ppm.

^{13}CNMR (100 MHz, $CDCl_3$): δ 202.0, 137.8, 129.7, 128.4, 126.6, 69.6, 50.4, 44.5, 25.8, 18.0, -4.8, -4.9 ppm.

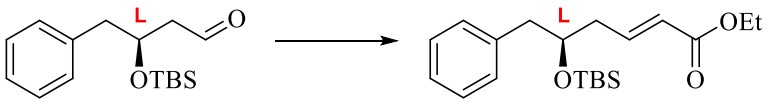

ent-**6.37** **S-41**

(L)-(*E*)-Methyl 5-(*tert*-butyldimethylsilyloxy)-6-phenylhex-2-enoate (**S-41**). To a stirring solution of *ent*-**6.37** (105.0 mg, 0.377 mmol, 1.0 equiv.) and triethyl phosphonoacetate **6.38** (83.1 µL, 0.415 mmol, 1.1 equiv.) in THF (2.5 mL), freshly powdered KOH (44 mg, 0.75 mmol, 2.0 equiv.) was added and stirred for 1 h at ambient temperature. Upon completion by TLC (silica gel, 10% EtOAc in hexanes), the mixture was diluted in Et_2O (3 × 10 mL), and washed with brine (3 × 30 mL). Combined organic layers were dried ($MgSO_4$), filtered, and concentrated *in vacuo*. The crude product was purified by flash chromatography (10% EtOAc in hexanes), and yielded 80.1 mg of **S-41** (0.229 mmol, 61%) as a clear, colorless oil.

R_f = 0.43 (silica gel, 10% EtOAc in hexanes).

^{1}HNMR (400 MHz, $CDCl_3$): δ 7.28 – 7.12 (m, 5H, 5 × -C*H*- Ph), 6.97 (dt, *J* = 15.3, 7.5 Hz, 1H, -C*H*-), 5.81 (dt, *J* = 15.7, 1.3 Hz, 1H, -C*H*-), 4.17 (q, *J* = 7.2 Hz, 2H, -CH_2-), 3.94 (p, *J* = 6.0 Hz, 1H, -C*H*-), 2.71 (d, *J* = 6.4 Hz, 2H, -CH_2-), 2.38 – 2.25 (m, 2H, -CH_2-), 1.27 (t, *J* = 7.1 Hz, 3H, -CH_3), 0.83 (s, 9H, O-TBS *t*-Bu), -0.06 (s, 3H, O-TBS -CH_3), -0.22 (s, 3H, O-TBS -CH_3) ppm.

^{13}CNMR (100 MHz, $CDCl_3$): δ 166.4, 145.7, 138.6, 129.7, 128.3, 126.3, 123.6, 72.7, 60.2, 44.0, 39.8, 25.8, 25.5, 18.0, 14.3, -4.8, -5.0 ppm.

HRMS (EI) *m/z*: calculated for $C_{16}H_{23}O_3Si$ [M – *t*-Bu] 291.1416, observed 291.1391 (Δ 2.5 mmu).

IR (thin film) ν_{max}: 2936, 1724, 1656, 1091 cm^{-1}.

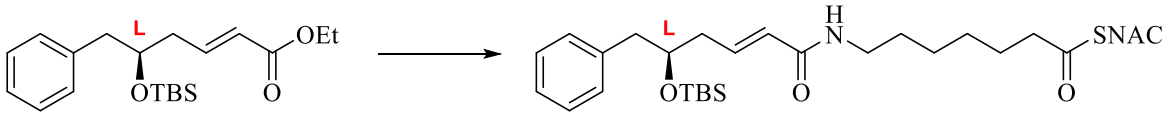

S-41 *ent*-**6.41**

(L)-(*E*)-*S*-2-Acetamidoethyl-7-(5-(TBS)-6-phenylhex-2-enamido)heptanethioate (*ent*-**6.41**). Purified **S-41** (40.0 mg, 0.115 mmol, 1.0 equiv.) was dissolved to homogeneity in a mixture MeOH, THF, and water (3:2:1, 0.1 M). A solution of NaOH (0.2 mL, 1.0 M) was added, and stirred at ambient temperature while being monitored by TLC (5% MeOH in CH_2Cl_2; CAM stain). Upon completion, the mixture was quenched with saturated NH_4Cl, diluted in EtOAc (2 mL), and washed with brine (3 × 3 mL). The combined organic layers were dried ($MgSO_4$), filtered, and concentrated *in vacuo*.

The crude acid **S-42** (30.5 mg) was dissolved in anhydrous CH_2Cl_2 (1 mL), to which EDC·HCl (27.4 mg, 0.143 mmol, 1.5 equiv.), DMAP (1.2 mg, 0.009 mmol, 0.1 equiv.), and amine **6.40** (32.7 mg, 0.133 mmol, 1.4 equiv.) were added. The resulting solution was stirred for 10 min at ambient temperature. Triethylamine (19.8 µL, 0.143 mmol, 1.5 equiv.) was added, and the reaction mixture stirred overnight while monitored

by TLC (silica gel, 5% MeOH in CH_2Cl_2). Upon completion, the reaction was quenched with NH_4Cl (1.0 mL), and extracted with EtOAc (5 × 2 mL). The combined organic extracts were washed with brine (3 × 4 mL), dried ($MgSO_4$), filtered, and concentrated *in vacuo*. The crude residue was purified by flash chromatography (3% MeOH in CH_2Cl_2), and furnished 39.1 mg of amide *ent*-**6.41** (0.071 mmol, 62% over 2 steps) as clear, yellow oil.

R_f = 0.43 (silica gel, 5% MeOH in CH_2Cl_2).

^{1}HNMR (300 MHz, $CDCl_3$): δ 7.26 – 7.11 (m, 5H, 5 × -C*H*- Ph), 6.81 (dt, *J* = 15.1, 7.5 Hz, 1H, -C*H*-), 6.07 (br s, 1H, -N*H*-), 5.75 (d, *J* = 15.3 Hz, 1H, -C*H*-), 5.59 – 5.56 (m, 1H, -N*H*-), 3.92 (p, *J* = 6.2 Hz, 1H, -C*H*-), 3.39 (q, *J* = 6.2 Hz, 2H, -CH_2-NH-), 3.31 – 3.25 (m, 2H, -CH_2-NH-), 3.00 (t, *J* = 6.4 Hz, 2H, -CH_2-S-), 2.69 (dd, *J* = 6.2, 2.4 Hz, 2H, -CH_2-), 2.54 (t, *J* = 7.4 Hz, 2H, -CH_2-CO-), 2.29 (dd, *J* = 11.9, 5.9 Hz, 2H, -CH_2-), 1.94 (s, 3H, -CH_3), 1.68 – 1.59 (m, 2H, -CH_2-), 1.52 – 1.44 (m, 2H, -CH_2-), 1.36 – 1.28 (m, 4H, 2 × -CH_2-), 0.81 (s, 9H, *t*-Bu), -0.09 (s, 3H, O-TBS -CH_3), -0.26 (s, 3H, O-TBS -CH_3) ppm.

^{13}CNMR (75 MHz, $CDCl_3$): δ 199.9, 170.3, 165.5, 140.7, 138.7, 129.7, 128.2, 126.2, 126.0, 72.7, 43.9, 43.8, 39.9, 39.7, 39.2, 29.3, 28.5, 28.3, 26.3, 25.8, 25.4, 23.2, 18.0, -4.8, -5.1 ppm.

HRMS (EI) *m/z*: calculated for $C_{25}H_{39}N_2O_4SSi$ [M – *t*-Bu] 491.2400, observed 491.2421 (Δ -2.1 mmu).

IR (thin film) ν_{max}: 3321, 2933, 1653, 1558, 1087 cm^{-1}.

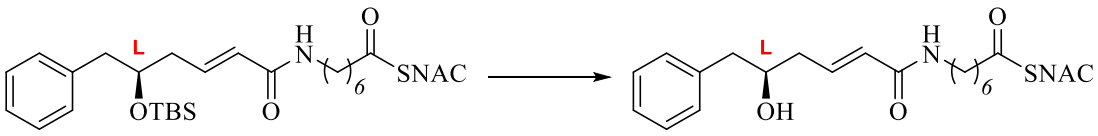

ent-**6.41** L-**6.33**

(L)-(*E*)-*S*-2-Acetamidoethyl-7-(5-hydroxy-6-phenylhex-2-enamido)heptanethioate (L-**6.33**). Purified NAC-substrate *ent*-**6.41** (13.6 mg, 0.025 mmol, 1.0 equiv.) was added to a 1.5 mL Eppendorf tube and dissolved in MeCN (250 µL). To this solution was added pyridine (10.1 µL, 0.125 mmol, 5.0 equiv.), and 48% aqueous HF (45 µL, 1.25 mmol, 50 equiv.). The mixture was vortexed to homogeneity, and proceeded without stirring for 5 h at ambient temperature. Upon completion by TLC (silica gel, 5% MeOH in CH_2Cl_2), the mixture was diluted with water (2 volumes). The resulting solution was carefully extracted with EtOAc (5 × 3 mL), washed with brine (2 × 4 mL), and the organic extracts were combined, dried ($MgSO_4$), filtered, and concentrated *in vacuo*. Crude product was purified by flash chromatography (5% MeOH in CH_2Cl_2), and yielded diol L-**6.33** (6.5 mg, 0.015 mmol, 60%) as clear, colorless oil.

R_f = 0.31 (silica gel, 5% MeOH: CH_2Cl_2).

^{1}HNMR (300 MHz, $CDCl_3$): δ 7.34 – 7.15 (m, 5H, 5 × -C*H*- Ph), 6.84 (dt, *J* = 15.0, 7.4 Hz, 1H, -C*H*-), 5.98 (br s, 1H, -N*H*-), 5.85 (d, *J* = 15.3 Hz, 1H, -C*H*-), 5.57 (m, 1H, -N*H*-), 3.96 (dt, *J* = 12.5, 4.8 Hz, 1H, -C*H*-), 3.44 – 3.34 (m, 2H, -CH_2-NH-), 3.29 (dt, *J* = 12.5, 4.8 Hz, 2H, -CH_2-NH-). 3.00 (t, *J* = 6.3 Hz, 2H,

-C*H*$_2$-S-), 2.86 – 2.66 (m, 2H, -C*H*$_2$-), 2.54 (t, *J* = 7.3 Hz, 2H, -C*H*$_2$-CO-), 2.43 – 2.29 (m, 2H, -C*H*$_2$-), 1.94 (s, 3H, -C*H*$_3$), 1.70 – 1.58 (m, 2H, -C*H*$_2$-), 1.56 – 1.44 (m, 2H, -C*H*$_2$-), 1.35 – 1.31 (m, 4H, 2 × -C*H*$_2$-) ppm.
^{13}CNMR (100 MHz, $CDCl_3$): δ 200.1, 170.3, 165.6, 140.2, 137.9, 129.4, 128.7, 126.7, 126.5, 71.4, 43.8, 43.5, 39.7, 39.3, 39.2, 29.3, 28.6, 28.3, 26.3, 25.5, 23.3 ppm.
HRMS (ESI+ TOF) *m/z*: calculated for $C_{23}H_{34}N_2O_4SNa$ [$(M + Na)^+$] 457.2137, observed 457.2129 (Δ 1.8 mmu).
LCMS (t_R): 14.62 min.

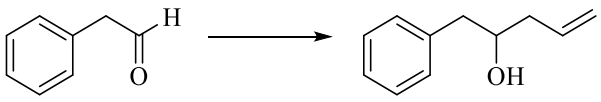

6.35 **S-43**

1-Phenylpent-4-en-2-ol (**S-43**). Phenylacetaldehyde **6.35** (4.0 g, 33.3 mmol, 1.0 equiv.) was dissolved in anhydrous ethyl ether (110 mL) under inert atmosphere, and cooled to 0 °C. Allyl magnesium bromide (1.0 M solution in Et_2O, 12.8 mL, 73.3 mmol, 2.2 equiv.) was added dropwise over 5 minutes, and stirred overnight while warming to ambient temperature. The reaction was monitored by TLC (silica gel, 20% EtOAc in hexanes), and upon completion was diluted in Et_2O (40 mL) and quenched with saturated NH_4Cl (20 mL). The organic layers were washed with brine (3 × 50 mL), dried ($MgSO_4$), filtered, and concentrated *in vacuo*. The crude product was purified *via* flash chromatography (5% EtOAc in hexanes), and yielded 4.73 g (29.1 mmol, 88%) of **S-43** as clear, pale yellow oil.
R_f = 0.38 (silica gel, 20% EtOAc in hexanes).
^{1}HNMR (300 MHz, $CDCl_3$): δ 7.34 – 7.19 (m, 5H, 5 × -C*H*- Ph), 5.92 – 5.79 (m, 1H, -C*H*-), 5.18 – 5.11 (m, 2H, -C*H*$_2$), 3.92 – 3.83 (m, 1H, -C*H*-), 2.81 (dd, *J* = 5.0, 13.6 Hz, 1H, -CH*H*-), 2.71 (dd, *J* = 7.9, 13.6 Hz, 1H, -CH*H*-), 2.38 – 2.15 (m, 2H, -C*H*$_2$-), 1.65 (d, *J* = 3.6 Hz, 1H, -O*H*) ppm.
^{13}CNMR (100 MHz, $CDCl_3$): δ 138.4, 134.7, 129.4, 128.6, 126.5, 118.2, 71.7, 43.3, 41.2 ppm.
Characterization data for **S-43** proved consistent with previously reported literature data.[32]

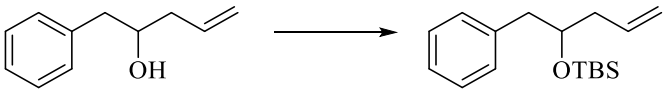

S-43 *rac*-**6.36**

***tert*-Butyldimethyl(1-phenylpent-4-en-2-yloxy)silane** (*rac*-**6.36**). Homoallylic alcohol **S-43** (1.0 g, 6.16 mmol, 1.0 equiv.) was dissolved in anhydrous DMF (7.5 mL, 1.0 M) under inert atmosphere, and TBSCl (1.2 g, 7.7 mmol, 1.2 equiv.) was added at ambient temperature. Imidazole (1.1 g, 15.5 mmol, 2.5 equiv.) was added, and the reaction mixture stirred overnight while being monitored by TLC (silica gel, 10% EtOAc in hexanes). Upon completion, the reaction mixture was quenched with saturated ammonium chloride, and

diluted in EtOAc (40 mL). The organic layers were then washed with water (4 × 20 mL), and an increasing-gradient concentration of brine. Combined organic layers were dried ($MgSO_4$), filtered, and concentrated *in vacuo*. The crude product was purified *via* flash chromatography (0 – 5% EtOAc in hexanes), and yielded *rac*-**6.36** (1.64 g, 5.9 mmol, 96%) as clear, colorless oil.

R_f = 0.72 (silica gel, 10% EtOAc in hexanes).

^{1}HNMR (400 MHz, $CDCl_3$): δ 7.26 – 7.14 (m, 5H, 5 × -C*H*- Ph), 5.85 (dddd, *J* = 7.1, 7.1, 10.4, 17.0 Hz, 1H, -C*H*-), 5.06 – 5.00 (m, 2H, -CH_2), 3.89 – 3.83 (m, 1H, -C*H*-), 2.74 (dd, *J* = 5.5, 13.4 Hz, 1H, -CH*H*-), 2.65 (dd, *J* = 7.2, 13.4 Hz, 1H, -CH*H*-), 2.27 – 2.15 (m, 2H, -CH_2-), 0.82 (s, 9H, O-TBS *t*-Bu), -0.08 (s, 3H, O-TBS -CH_3), -0.26 (s, 3H, O-TBS -CH_3) ppm.

^{13}CNMR (100 MHz, $CDCl_3$): δ 139.3, 135.1, 129.8, 128.1, 126.0, 117.1, 73.5, 43.5, 41.7, 31.6, 25.9, 18.1, 14.1, -4.7, -5.1 ppm.

HRMS (EI) *m/z*: calculated for $C_{13}H_{19}OSi$ [M – *t*-Bu] 219.1205, observed 219.1182 (Δ = 2.3 mmu).

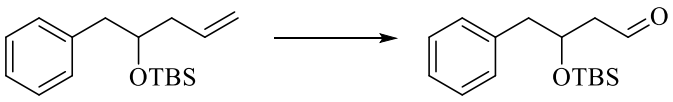

rac-**6.36** *rac*-**6.37**

3-(*tert*-Butyldimethylsilyloxy)-4-phenylbutanal (*rac*-**6.37**). Purified homoallylic alcohol *rac*-**6.36** (1.0 g, 3.61 mmol, 1.0 equiv.) was diluted in an equal mixture of *t*-BuOH and water (20 mL) at ambient temperature. To this solution was added potassium carbonate (1.5 g, 10.8 mmol, 3.0 equiv.), potassium ferricyanide (4.0 g, 10.8 mmol, 3.0 equiv.), and a solution of potassium osmate (VI) dihydrate (13 mg, 1 mol%) in NaOH (15% *w*/*v*, 0.3 mL). The reaction mixture stirred overnight and was monitored by TLC (silica gel, 10% EtOAc in hexanes). Upon completion, the mixture was diluted in water, extracted with EtOAc (3 × 10 mL), and washed with brine (3 × 30 mL). Combined organic layers were dried ($MgSO_4$), filtered, and concentrated *in vacuo*. The crude product was diluted in anhydrous CH_2Cl_2 (8.0 mL), followed by addition of lead tetraacetate (1.9 g, 4.3 mmol, 1.2 equiv.). The reaction stirred for 1 h while monitored by TLC. Upon completion consumption of diol, the mixture was concentrated to remove 75% of the CH_2Cl_2, and loaded directly on a pre-equilibrated column (10% EtOAc in hexanes). The two-step sequence yielded *rac*-**6.37** (754.2 mg, 2.71 mmol, 75%, 2 steps) as a clear, colorless oil.

R_f = 0.31 (silica gel, 10% EtOAc in hexanes).

^{1}HNMR (400 MHz, $CDCl_3$): δ 9.76 (t, *J* = 2.3 Hz, 1H, -C*H*O), 7.29 – 7.14 (m, 5H, 5 × -C*H*- Ph), 4.36 (p, *J* = 6.2 Hz, 1H, -C*H*-), 2.85 (dd, *J* = 6.3, 13.4 Hz, 1H, -CH*H*-), 2.76 (dd, *J* = 6.7, 13.4 Hz, 1H, -CH*H*-), 2.49 (dd, *J* = 2.4, 5.7 Hz, 2H, -CH_2-), 0.84 (s, 9H, O-TBS *t*-Bu), -0.01 (s, 3H, O-TBS -CH_3), -0.12 (s, 3H, O-TBS -CH_3) ppm.

^{13}CNMR (100 MHz, $CDCl_3$): δ 201.9, 137.8, 129.7, 128.4, 126.6, 69.6, 50.4, 44.5, 25.8, 18.0, -4.8, -4.9 ppm.

HRMS (EI) *m/z*: calculated for $C_{12}H_{17}O_2Si$ [M – *t*-Bu] 221.0998, observed 221.0993 (Δ = 0.5 mmu).

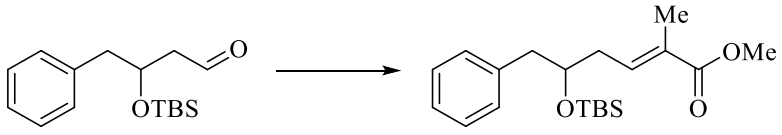

rac-**6.37** **S-44**

Methyl-(*E*)-5-((*tert*-butyldimethylsilyl)oxy)-2-methyl-6-phenylhex-2-enoate (**S-44**). Aldehyde *rac*-**6.37** (754.2 mg, 2.71 mmol, 1.0 equiv.) and known ylide[87,88] methyl 2-(triphenylphosphanylidene)-propanoate **6.42** (1.89 g, 5.42 mmol, 2.0 equiv.) were dissolved in benzene (27 mL), and stirred at reflux for 18 h under inert atmosphere. Upon completion by TLC (silica gel, 10% EtOAc in hexanes), the reaction mixture was cooled to room temperature and concentrated *in vacuo*. The crude residue was purified by flash chromatography (10% EtOAc in hexanes), and afforded ester **S-44** (652.6 mg, 1.87 mmol, 69%) as clear, pale yellow oil.

R_f = 0.38 (silica gel, 10% EtOAc in hexanes).

^{1}HNMR (300 MHz, $CDCl_3$): δ 7.29 – 7.10 (m, 5H, 5 × -C*H*- Ph), 6.87 – 6.80 (m, 1H, -C*H*-), 3.96 (p, *J* = 6.1 Hz, 1H, -C*H*-), 3.73 (s, 3H, -OCH_3), 2.72 (d, *J* = 6.3 Hz, 2H, -CH_2-), 2.33 – 2.27 (m, 2H, -CH_2-), 1.77 (d, *J* = 1.3 Hz, 3H, -CH_3), 0.83 (s, 9H, O-TBS *t*-Bu), -0.06 (s, 3H, O-TBS-CH_3), -0.22 (s, 3H, O-TBS-CH_3) ppm.

^{13}CNMR (75 MHz, $CDCl_3$): δ 168.6, 138.8, 138.7, 129.9, 128.9, 128.2, 126.2, 72.9, 51.7, 44.1, 36.3, 25.8, 18.0, 12.6, -4.9, -5.1 ppm.

HRMS (EI) *m/z*: calculated for $C_{16}H_{23}O_3Si$ [M – *t*-Bu] 291.1416, observed 291.1417 (Δ -0.1 mmu).

IR (thin film): ν_{max} = 2951, 1717, 1652, 1089 cm^{-1}.

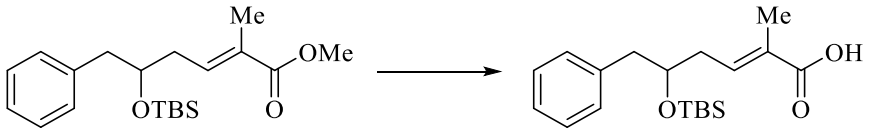

S-44 **6.43**

(*E*)-5-(*tert*-Butyldimethylsilyloxy)-2-methyl-6-phenylhex-2-enoic acid (**6.43**). Purified **S-44** (652 mg, 1.87 mmol, 1.0 equiv.) was dissolved to homogeneity in a mixture MeOH, THF, and water (3:2:1, 20 mL). A solution of NaOH (2.4 mL, 1.0 M) was added, and the mixture stirred for 12 h at ambient temperature, while monitored by TLC (silica gel, 20% EtOAc in hexanes; CAM stain). Upon completion, the mixture was quenched with saturated NH_4Cl, diluted in EtOAc (25 mL) and washed with brine (3 × 20 mL). The

aqueous layer was acidified (pH < 2), and re-extracted with EtOAc (20 mL). The combined organic layers were dried ($MgSO_4$), filtered, and concentrated *in vacuo*. The crude product was purified by flash chromatography (15% EtOAc in hexanes), and yielded 400.4 mg of acid **6.43** (1.20 mmol, 64%) as clear, colorless oil.

R_f = 0.37 (silica gel, 20% EtOAc in hexanes).

^{1}HNMR (300 MHz, $CDCl_3$): δ 7.33 – 7.15 (m, 5H, 5 × -C*H*- Ph), 7.04 (td, *J* = 7.4, 1.3 Hz, 1H, -C*H*-), 4.02 (p, *J* = 6.0 Hz, 1H, -C*H*-), 2.76 (dd, *J* = 6.3, 3.3 Hz, 2H, -CH_2-), 2.36 (t, *J* = 6.6 Hz, 2H, -CH_2-), 1.81 (d, *J* = 1.1 Hz, 3H, -CH_3), 0.87 (s, 9H, O-TBS *t*-Bu), -0.01 (s, 3H, O-TBS -CH_3), -0.17 (s, 3H, O-TBS -CH_3) ppm.

^{13}CNMR (75 MHz, $CDCl_3$): δ 172.9, 141.6, 138.6, 129.7, 128.4, 128.3, 126.3, 72.8, 44.2, 36.5, 25.8, 18.0, 12.3, -4.8, -5.1 ppm.

HRMS (EI) *m/z*: calculated for $C_{15}H_{21}O_3Si$ [M – *t*-Bu] 277.1260, observed 277.1286 (Δ -2.6 mmu).

IR (thin film) ν_{max}: 3027, 2862, 1686, 1653, 1098 cm^{-1}.

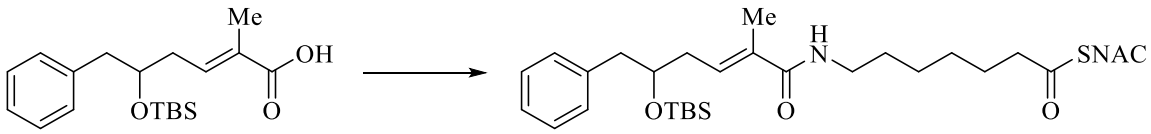

6.43 **6.44**

(*E*)-S-2-Acetamidoethyl-7-(5-(TBS)-2-methyl-6-phenylhex-2-enamido)heptanethioate (**6.44**). Acid **6.43** (40.0 mg, 0.12 mmol, 1.0 equiv.) was dissolved in anhydrous CH_2Cl_2 (1.2 mL). EDC·HCl (34.4 mg, 0.179 mmol, 1.5 equiv.), DMAP (1.5 mg, 0.012 mmol, 0.1 equiv.), and amine **6.40** (41.3 mg, 0.167 mmol, 1.4 equiv.) were added under inert atmosphere, and left to stir at ambient temperature. After 10 min, triethylamine (19.8 µL, 0.143 mmol, 1.5 equiv.) was added, and the solution stirred overnight. Upon completion (silica gel, 5% MeOH in CH_2Cl_2), the reaction was quenched with NH_4Cl (1.0 mL), and extracted with EtOAc (5 × 5 mL). The combined organic extracts were washed with brine (3 × 10 mL), dried ($MgSO_4$), filtered, and concentrated *in vacuo*. The crude oil was purified by flash chromatography (3% MeOH in CH_2Cl_2), to furnish NAC-thioester **6.44** (57.2 mg, 0.101 mmol, 85%) as clear, yellow oil.

R_f = 0.50 (silica gel, 5% MeOH in CH_2Cl_2).

^{1}HNMR (400 MHz, $CDCl_3$): δ 7.29 -7.08 (m, 5H, 5 × -C*H*- Ph), 6.30 (dt, *J* = 1.4, 7.3 Hz, 1H, -C*H*-), 6.08 (br s, 1H, -N*H*-), 5.65 (t, *J* = 5.5 Hz, 1H, -N*H*-), 3.94 (p, *J* = 6.0 Hz, 1H, -C*H*-), 3.39 (dd, *J* = 12.4, 6.1 Hz, 2H, -CH_2-NH-), 3.26 (dd, *J* = 13.6, 6.3 Hz, 2H, -CH_2-NH-), 2.99 (t, *J* = 6.4 Hz, 2H, -CH_2-S-), 2.71 (d, *J* = 6.3 Hz, 2H, -CH_2-), 2.54 (t, *J* = 7.4 Hz, 2H, -CH_2-CO-), 2.27 (t, *J* = 6.5 Hz, 2H, -CH_2-), 1.93 (s, 3H, -CH_3), 1.76 (s, 3H, -CH_3), 1.69 – 1.62 (m, 2H, -CH_2-), 1.55 – 1.45 (m, 2H, -CH_2-), 1.36 – 1.30 (m, 4H, 2 × -CH_2-), 0.82 (s, 9H, O-TBS *t*-Bu), -0.07 (s, 3H, O-TBS -CH_3), -0.22 (s, 3H, O-TBS -CH_3) ppm.

^{13}CNMR (100 MHz, $CDCl_3$): δ 200.0, 170.4, 169.4, 138.8, 132.5, 131.8, 129.8, 128.2, 126.2, 73.0, 44.1, 43.9, 39.7, 39.4, 36.1, 29.4, 28.6, 28.4, 26.4, 25.8, 25.5, 23.2, 18.0, 13.1, -4.7, -5.0 ppm.

HRMS (EI) *m/z*: calculated for $C_{26}H_{41}N_2O_4SSi$ [M – *t*-Bu] 505.2556, observed 505.2581 (Δ -2.5 mmu).

IR (thin film) ν_{max}: 2933, 1700, 1653, 1087 cm^{-1}.

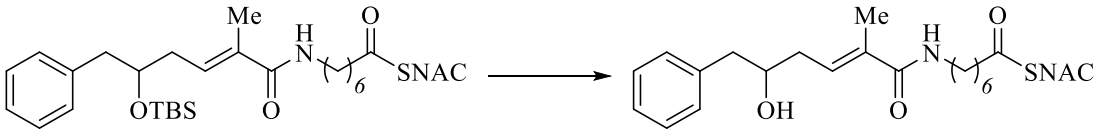

6.44 **6.34**

(*E*)-S-2-Acetamidoethyl 7-(5-hydroxy-2-methyl-6-phenylhex-2-enamido)heptanethioate (**6.34**). The purified NAC-substrate **6.44** (42.0 mg, 0.075 mmol, 1.0 equiv.) was added to a 1.5 mL Eppendorf tube and dissolved in MeCN (940 µL). To this solution was added pyridine (30.3 µL, 0.376 mmol, 5.0 equiv.), and 48% aqueous HF (135 µL, 3.76 mmol, 50 equiv.). The mixture was vortexed to homogeneity, and proceeded without stirring for 5 h at ambient temperature. Upon completion by TLC (silica gel, 5% MeOH in CH_2Cl_2), the mixture was diluted with water (2 volumes). The resulting solution was carefully extracted with EtOAc (5 × 3 mL), washed with brine (2 × 4 mL), and the organic extracts were combined, dried ($MgSO_4$), filtered, and concentrated *in vacuo*. Crude product was purified by flash chromatography (5% MeOH in CH_2Cl_2), and yielded diol **6.34** (19.8 mg, 0.044 mmol, 59%) as clear, colorless oil.

R_f = 0.27 (silica gel, 5% MeOH in CH_2Cl_2).

^{1}HNMR (400 MHz, $CDCl_3$): δ 7.32 – 7.17 (m, 5H, 5 × -C*H*- Ph), 6.37 (dt, *J*= 1.3, 7.3 Hz, 1H, -C*H*-), 6.03 (br s, 1H, -N*H*-), 5.83 (t, *J* = 5.2 Hz, -N*H*-), 3.95 (ddt, *J* = 7.9, 7.0, 5.2 Hz, 1H, -C*H*-), 3.39 (dd, *J* = 12.4, 6.0 Hz, 2H, -CH_2-NH-), 3.27 (dd, *J* = 13.3, 6.8 Hz, 2H, -CH_2-NH-), 2.99 (t, *J* = 6.4 Hz, 2H, -CH_2-S-), 2.82 (dd, *J* = 13.5, 5.0 Hz, 1H, -CH*H*-), 2.73 (dd, *J* = 13.6, 8.0 Hz, 1H, -CH*H*-), 2.54 (t, *J* = 7.3 Hz, 2H, -CH_2-CO-), 2.39 – 2.30 (m, 2H, -CH_2-), 1.94 (s, 3H, -CH_3), 1.83 (d, *J* = 1.1 Hz, 3H, -CH_3), 1.68 – 1.60 (m, 2H, -CH_2-), 1.54 – 1.48 (m, 2H, -CH_2-), 1.36 – 1.29 (m, 4H, 2 × -CH_2-) ppm.

^{13}CNMR (100 MHz, $CDCl_3$): δ 200.1, 170.5, 169.4, 138.1, 133.3, 131.4, 129.4, 128.7, 126.7, 72.0, 43.9, 43.7, 39.7, 39.5, 35.6, 29.3, 28.5, 28.3, 26.3, 25.4, 23.2, 13.1 ppm.

HRMS (EI) *m/z*: calculated for $C_{24}H_{34}N_2O_3S$ [M – H_2O] 430.2290, observed 430.2317 (Δ -2.7 mmu).

LCMS (t_R): 15.46 min.

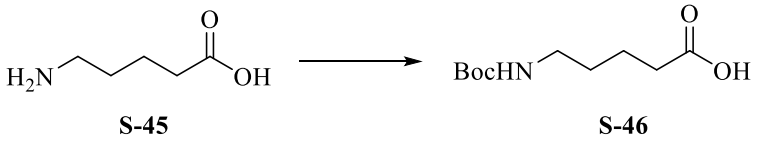

S-45 **S-46**

5-*tert*-Butyloxycarbonylamino pentanoic acid (**S-46**). Commercial 5-aminopentanoic acid **S-45** (1.0 g, 8.5 mmol, 1.0 equiv.) and Boc-anhydride (2.36 mL, 10.2 mmol, 1.2 equiv.) were dissolved in an equal mixture of 1,4-dioxane and water (0.3 M). To this solution was added potassium carbonate (4.72 g, 34.2 mmol, 4.0 equiv.), and was stirred overnight at room temperature. The reaction mixture was concentrated *in vacuo*, and the crude residue was dissolved in water (30 mL) and washed with EtOAc (2 × 30 mL). The aqueous phase was acidified (pH < 2), and extracted with EtOAc (3 × 30 mL). Combined organic extracts were dried ($MgSO_4$), filtered, and concentrated *in vacuo* to afford acid **S-46** (1.45 g, 6.7 mmol, 78%) colorless oil, which slowly crystallized as colorless solid.

^{1}HNMR (400 MHz, $CDCl_3$): δ 4.54 (br s, 1H, -N*H*-), 3.12 (q, J = 6.4 Hz, 2H, -CH_2-), 2.36 (t, J = 7.4 Hz, 2H, -CH_2-), 1.68 – 1.61 (m, 2H, -CH_2-), 1.52 (p, J = 7.8 Hz, 2H, -CH_2-), 1.42 (s, 9H, Boc *t*-Bu) ppm.

^{13}CNMR (100 MHz, $CDCl_3$): δ 177.8, 158.2, 79.3, 40.1, 33.3, 29.4, 28.4, 21.8 ppm.

Characterization data for **S-46** proved consistent with previously reported literature data.[85]

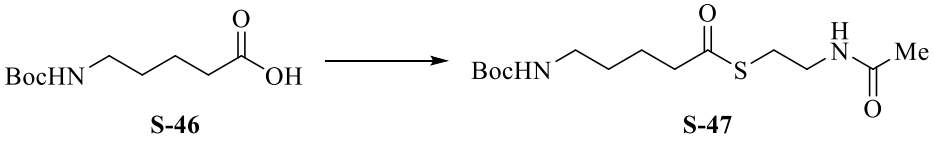

S-46 **S-47**

1-(2-Acetamidoethylthio)-5-(*tert*-butoxycarbonylamino)-pentanethioate (**S-47**). To a stirring solution of *N*-Boc-5-aminopentanoic acid **S-46** (500 mg, 2.3 mmol, 1.0 equiv.) in THF (16 mL) was added EDC·HCl (0.75 g, 4.83 mmol, 2.1 equiv.), DMAP (177 mg, 1.45 mmol, 0.63 equiv.) and *N*-acetylcysteamine (400 µL, 2.76 mmol, 1.2 equiv.). The reaction was stirred for 18 h at ambient temperature, then quenched with water. The mixture was extracted with ethyl acetate (50 mL), washed with water (30 mL), saturated $NaHCO_3$ (30 mL) and brine (30 mL). The combined organic layers were dried ($MgSO_4$), filtered, and concentrated *in vacuo* to afford **S-47** (662 mg, 2.08 mmol, 90%) as white paste.

^{1}HNMR (300 MHz, $CDCl_3$): δ 5.98 (br s, 1H, -N*H*-), 4.55 (br s, 1H, -N*H*-), 3.41 (dd, J = 12.3, 6.0 Hz, 2H, -CH_2-NH-), 3.10 (q, J = 6.6 Hz, 2H, -CH_2-NH-), 3.01 (dd, J = 6.6, 5.6 Hz, 2H, -CH_2-S-), 2.58 (t, J = 7.2 Hz, 2H, -CH_2-CO-), 1.95 (s, 3H, -CH_3), 1.73 – 1.60 (m, 6H, 3 × -CH_2-), 1.42 (s, 9H, *t*-Bu) ppm.

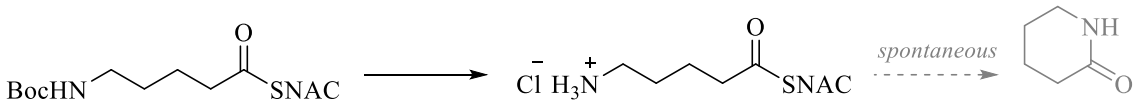

S-47 **S-48** **S-49**

7-(2-Acetamidoethylthio)-7-oxoheptan-1-ammonium chloride (**S-48**). Boc-protected amino thioester **S-47** (515 mg, 1.62 mmol, 1.0 equiv.) was dissolved in HCl/Dioxane (4.1 mL, 16.2 mmol, 10.0 equiv.), and stirred at ambient temperature under inert atmosphere. After 45 minutes, solvent was evaporated *in vacuo* and free amine **S-48** was isolated (156.2 mg, 0.67 mmol, 41%) as a white powder. Spontaneous formation of 6-membered lactam **S-49** could be observed as a side-product.

^{1}HNMR (400 MHz, D_2O): δ 3.23 (t, J = 6.2 Hz, 2H, -CH_2-NH-), 2.91 (t, J = 6.2 Hz, 2H, -CH_2-S-), 2.86 (br t, J = 5.7 Hz, 2H, -CH_2-NH_2), 2.57 (t, J = 6.7 Hz, 2H, -CH_2-CO-), 1.81 (s, 3H, -CH_3), 1.59 – 1.53 (m, 4H, 2 × -CH_2-) ppm.

^{13}CNMR (100 MHz, D_2O): δ 206.1, 176.8, 45.1, 41.5, 41.1, 30.6, 28.4, 24.4, 24.3 ppm; sample was dissolved in D_2O, but spectrum was mistakenly tuned to $CDCl_3$.

Characterization data for **S-48** proved consistent with previously reported literature data.[32]

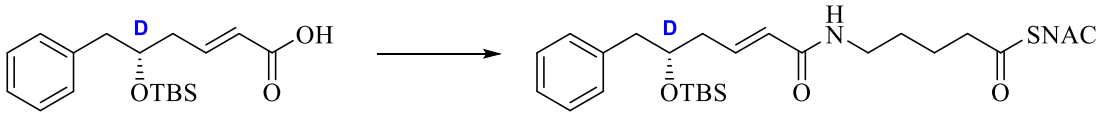

D-**6.39** **S-50**

(D)-(*E*)-*S*-2-Acetamidoethyl-5-(3-(TBS)-6-phenylhex-2-enamido)pentanethioate (**S-50**). In a single attempt, purified acid D-**6.39** (53.7 mg, 0.168 mmol, 1.0 equiv.) was dissolved in CH_2Cl_2 (1.7 mL), to which EDC·HCl (48.2 mg, 0.251 mmol, 1.5 equiv.), DMAP (2.1 mg, 0.017 mmol, 0.1 equiv.), and truncated amine **S-48** (51.2 mg, 0.235 mmol, 1.4 equiv.) were added. After 5 min of stirring at ambient temperature, triethylamine (34.9 µL, 0.251 mmol, 1.5 equiv.) was added, and the solution stirred overnight under inert atmosphere. Upon completion (silica gel, 5% MeOH in CH_2Cl_2), the reaction was quenched with NH_4Cl (1.0 mL) and extracted with EtOAc (5 × 2 mL). Combined organic extracts were washed with brine (3 × 4 mL), dried ($MgSO_4$), filtered, and concentrated *in vacuo*. The crude residue was not purified, but indicated formation of new compound with comparable signals to previously-generated heptanthioate D-**6.41** (*vide supra*).

^{1}HNMR (400 MHz, $CDCl_3$): δ 7.26 – 7.11 (m, 5H, 5 × -CH- Ph), 6.82 (dt, J = 15.3, 7.4 Hz, 1H, -CH=), 6.30 (br s, 1H, -NH-), 5.75 (d, J = 15.3 Hz, 1H, =CH-), 5.68 (t, J = 6.2 Hz, 1H, -NH-), 3.92 (p, J = 6.0 Hz, 1H, -CH-), 3.42 (d, J = 6.0 Hz, 1H, -CHH-NH-), 3.37 (d, J = 6.0 Hz, 1H, -CHH-NH-), 3.29 (dd, J = 6.4 Hz, 2H, -CH_2-NH-), 3.00 (t, J = 6.4 Hz, 2H, -CH_2-S-), 2.76 (dd, J = 9.4, 6.8 Hz, 2H, -CH_2-), 2.58 (t, J = 7.3 Hz, 2H, -CH_2-CO-), 2.36 – 2.26 (m, 2H, -CH_2-), 1.95 (s, 3H, -CH_3), 1.73 – 1.52 (m, 3H, 3 × -CHH-), 1.47 –

1.40 (m, 1H, -CH*H*-), 0.81 (s, 9H, O-TBS *t*-Bu), -0.08 (s, 3H, O-TBS -CH_3), -0.25 (s, 3H, O-TBS -CH_3) ppm; characterization was based on crude material.

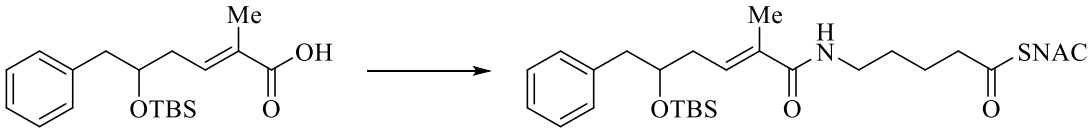

rac-**6.43** **S-50**

(*E*)-S-2-Acetamidoethyl-5-(3-(TBS)-2-methyl-6-phenylhex-2-enamido)pentanethioate (**S-51**). In a single attempt, acid *rac*-**6.43** (33.9 mg, 0.10 mmol, 1.0 equiv.) was dissolved in CH_2Cl_2 (1 mL). To the resulting solution, EDC·HCl (29.2 mg, 0.15 mmol, 1.5 equiv.), DMAP (1.3 mg, 0.01 mmol, 0.1 equiv.), and truncated amine **S-48** (31 mg, 0.14 mmol, 1.4 equiv.) were added. The reaction mixture stirred for 10 min, and triethylamine (21.1 µL, 0.152 mmol, 1.5 equiv.) was added. The mixture stirred overnight at ambient temperature, and monitored by TLC (silica gel, 5% MeOH in CH_2Cl_2). Upon completion, the reaction was quenched with NH_4Cl (1.0 mL), and extracted with EtOAc (5 × 5 mL). The combined organic extracts were washed with brine (3 × 10 mL), dried ($MgSO_4$), filtered, and concentrated to dryness *in vacuo*. The obtained crude residue was not purified or characterized, but indicated formation of new compound with comparable signals to previously-generated heptantioate methyl derivative **6.44** (*vide supra*).

6.6 References

(1) Staunton, J.; Weissman, K. J. *Nat. Prod. Rep.* **2001**, *18* (4), 380–416.
(2) Khosla, C.; Harbury, P. B. *Nature* **2001**, *409* (6817), 247–252.
(3) Weissman, K. J.; Leadlay, P. F. *Nat. Rev. Microbiol.* **2005**, *3* (12), 925–936.
(4) Hertweck, C. *Angew. Chem. Int. Ed.* **2009**, *48* (26), 4688–4716.
(5) Caffrey, P. *Comput. Struct. Biotechnol. J.* **2012**, *3* (4), 1–8.
(6) Keatinge-Clay, A. T. *Nat. Prod. Rep.* **2012**, *29* (10), 1050–1073.
(7) Khosla, C.; Herschlag, D.; Cane, D. E.; Walsh, C. T. *Biochemistry* **2014**, *53* (18), 2875–2883.
(8) Lowry, B.; Li, X.; Robbins, T.; Cane, D. E.; Khosla, C. *ACS Cent. Sci.* **2016**, *2* (1), 14–20.
(9) Weissman, K. J. *Beilstein J. Org. Chem.* **2017**, *13*, 348–371.
(10) Horsman, M. E.; Hari, T. P. A.; Boddy, C. N. *Nat. Prod. Rep.* **2016**, *33*, 183–202.
(11) Jenke-Kodama, H.; Sandmann, A.; Müller, R.; Dittmann, E. *Mol. Biol. Evol.* **2005**, *22* (10), 2027–2039.
(12) Ridley, C. P.; Lee, H. Y.; Khosla, C. *Proc. Natl. Acad. Sci.* **2008**, *105* (12), 4595–4600.
(13) Yadav, G.; Gokhale, R. S.; Mohanty, D. *J. Mol. Biol.* **2003**, *328* (2), 335–363.
(14) Hill, P.; Piel, J.; Aris-Brosou, S.; Krištůfek, V.; Boddy, C. N.; Dijkhuizen, L. *J. Ind. Microbiol. Biotech.* **2014**, *41* (1), 75–85.
(15) Nguyen, T. A.; Ishida, K.; Jenke-Kodama, H.; Dittmann, E.; Gurgui, C.; Hochmuth, T.; Taudien, S.; Platzer, M.; Hertweck, C.; Piel, J. *Nat. Biotechnol.* **2008**, *26* (2), 225–233.
(16) Teta, R.; Gurgui, M.; Helfrich, E. J. N.; Kunne, S.; Schneider, A.; Van Echten-Deckert, G.; Mangoni, A.; Piel, J. *ChemBioChem* **2010**, *11* (18), 2506–2512.
(17) Caffrey, P. *ChemBioChem* **2003**, *4* (7), 654–657.
(18) Reid, R.; Piagentini, M.; Rodriguez, E.; Ashley, G.; Viswanathan, N.; Carney, J.; Santi, D. V.; Hutchinson, C. R.; McDaniel, R. *Biochemistry* **2003**, *42*, 72–79.
(19) Keatinge-Clay, A. T. *Nat. Prod. Rep.* **2016**, *33* (2), 141–149.
(20) Hari, T. P. A.; Labana, P.; Boileau, M.; Boddy, C. N. *ChemBioChem* **2014**, *15* (18), 2656–2661.
(21) Kohli, R. M.; Walsh, C. T. *Chem. Commun.* **2003**, 297–307.
(22) Julien, B.; Tian, Z.-Q.; Reid, R.; Reeves, C. D. *Chem. Biol.* **2006**, *13* (12), 1277–1286.
(23) Young, J.; Stevens, D. C.; Carmichael, R.; Tan, J.; Rachid, S.; Boddy, C. N.; Müller, R.; Taylor, R. E. *J. Nat. Prod.* **2013**, *76* (12), 2269–2276.
(24) Tang, L.; Shah, S.; Chung, L.; Carney, J.; Katz, L.; Khosla, C.; Julien, B. *Science* **2000**, *287* (5453), 640–642.
(25) Molnár, I.; Schupp, T.; Ono, M.; Zirkle, R.; Milnamow, M.; Nowak-Thompson, B.; Engel, N.; Toupet, C.; Stratmann, A.; Cyr, D. D.; Gorlach, J.; Mayo, J. M.; Hu, A.; Goff, S.; Schmid, J.; Ligon, J. M. *J. Chem. Biol.* **2000**, *7* (2), 97–109.
(26) Donadio, S.; Staver, M. J.; McAlpine, J. B.; Swanson, S. J.; Katz, L. *Science* **1991**, *252* (5006), 675–679.
(27) Haydock, S. F.; Mironenko, T.; Ghoorahoo, H. I.; Leadlay, P. F. *J. Biotechnol.* **2004**, *113* (1–3), 55–68.
(28) Kopp, M.; Irschik, H.; Pradella, S.; Müller, R. *Chembiochem* **2005**, *6* (7), 1277–1286.
(29) Gokhale, R. S.; Hunziker, D.; Cane, D. E.; Khosla, C. *Chem. Biol.* **1999**, *6* (2), 117–125.
(30) Boddy, C. N.; Schneider, T. L.; Hotta, K.; Walsh, C. T.; Khosla, C. *J. Am. Chem. Soc.* **2003**, *125* (12), 3428–3429.
(31) Aldrich, C. C.; Venkatraman, L.; Sherman, D. H.; Fecik, R. A. *J. Am. Chem. Soc.* **2005**, *127* (25), 8910–8911.
(32) Pinto, A.; Wang, M.; Horsman, M.; Boddy, C. N. *Org. Lett.* **2012**, *14* (9), 2278–2281.
(33) He, W.; Wu, J.; Khosla, C.; Cane, D. E. *Bioorg. Med. Chem. Lett.* **2006**, *16*, 391–394.
(34) Tsai, S.-C.; Miercke, L. J. W.; Krucinski, J.; Gokhale, R.; Chen, J. C.-H.; Foster, P. G.; Cane, D. E.; Khosla, C.; Stroud, R. M. *Proc. Natl. Acad. Sci.* **2001**, *98* (26), 14808–14813.
(35) Wang, M.; Boddy, C. N. *Biochemistry* **2008**, *47* (45), 11793–11803.
(36) Wang, M. Characterizing Structure and Function of Thioesterase from Polyketide Synthase, Syracuse University, 2009.
(37) Wang, M.; Opare, P.; Boddy, C. N. *Bioorg. Med. Chem. Lett.* **2009**, *19* (5), 1413–1415.
(38) Pinto, A. Synthesis and Biosynthesis of Polyketide Natural Products, Syracuse University, 2011.
(39) Jacobsen, J. R.; Hutchinson, C. R.; Cane, D. E.; Khosla, C. *Science*, **1997**, *277*, 367–369.
(40) Brown, H.; Jadhav, P. K. *J. Am. Chem. Soc.* **1983**, *105* (4), 2092–2093.
(41) Jadhav, P. K.; Bhat, K. S.; Perumal, P. T.; Brown, H. C. *J. Org. Chem.* **1986**, *51* (4), 432–439.
(42) Wadsworth, W. S.; Emmons, W. D. *J. Am. Chem. Soc.* **1961**, *83* (7), 1733–1738.
(43) Wittig, G.; Schöllkopf, U. *Chem. Ber.* **1954**, *87* (9), 1318–1330.

(44) Hughes, A. J.; Tibby, M. R.; Wagner, D. T.; Brantley, J. N.; Keatinge-Clay, A. T. *Chem. Commun. (Camb).* **2013**.
(45) Zhou, Y.; Prediger, P.; Dias, L. C.; Murphy, A. C.; Leadlay, P. F. *Angew. Chem.* **2015**, *127*, 5321–5324.
(46) Sheng, Y.; Lam, P. W.; Shahab, S.; Santosa, D. A.; Proteau, P. J.; Zabriskie, T. M.; Mahmud, T. *J. Nat. Prod.* **2015**, *78*, 2768–2775.
(47) Shaw-Reid, C. A.; Kelleher, N. L.; Losey, H. C.; Gehring, A. M.; Berg, C.; Walsh, C. T. *Chem. Biol.* **1999**, *6* (6), 385–400.
(48) Trauger, J. W.; Kohli, R. M.; Mootz, H. D.; Marahiel, M. A.; Walsh, C. T. *Nature* **2000**, *407* (6801), 215–218.
(49) Hoyer, K. M.; Mahlert, C.; Marahiel, M. A. *Chem. Biol.* **2007**, *14* (1), 13–22.
(50) Illuminati, G.; Mandolini, L. *Acc. Chem. Res.* **1981**, *14* (4), 95–102.
(51) Bruner, S. D.; Weber, T.; Kohli, R. M.; Schwarzer, D.; Marahiel, M. A.; Walsh, C. T.; Stubbs, M. T. *Structure* **2002**, *10* (3), 301–310.
(52) Arion, V. B.; Gerbeleu, N. V; Burgess, J. *Template Synthesis of Macrocyclic Compounds*; Wiley-VCH, 1999.
(53) Hoffmann, R. W. *Chem. Rev.* **1989**, *89* (8), 1841–1860.
(54) Sharma, K. K.; Boddy, C. N. *Bioorg. Med. Chem. Lett.* **2007**, *17* (11), 3034–3037.
(55) Lu, H.; Tsai, S.-C.; Khosla, C.; Cane, D. E. *Biochemistry* **2002**, *41* (42), 12590–12597.
(56) Scaglione, J. B.; Akey, D. L.; Sullivan, R.; Kittendorf, J. D.; Rath, C. M.; Kim, E.-S.; Smith, J. L.; Sherman, D. H. *Angew. Chem. Int. Ed. Engl.* **2010**, *49* (33), 5726–5730.
(57) Beck, Z. Q.; Aldrich, C. C.; Magarvey, N. A.; Georg, G. I.; Sherman, D. H. *Biochemistry* **2005**, *44* (41), 13457–13466.
(58) Zhou, Y.; Murphy, A. C.; Samborskyy, M.; Prediger, P.; Dias, L. C.; Leadlay, P. F. *Chem. Biol.* **2015**, *22* (6), 745–754.
(59) Robbel, L.; Hoyer, K. M.; Marahiel, M. A. *FEBS J.* **2009**, *276* (6), 1641–1653.
(60) Akey, D. L.; Kittendorf, J. D.; Giraldes, J. W.; Fecik, R. A.; Sherman, D. H.; Smith, J. L. *Nat. Chem. Biol.* **2006**, *2* (10), 537–542.
(61) Wang, M.; Zhou, H.; Wirz, M.; Tang, Y.; Boddy, C. N. *Biochemistry* **2009**, *48* (27), 6288–6290.
(62) Firn, R. D.; Jones, C. G. *Nat. Prod. Rep.* **2003**, *20* (4), 382–391.
(63) Firn, R. D.; Jones, C. G. *J. Exp. Bot.* **2009**, *60* (3), 719–726.
(64) Gupta, R. D. *Sustain. Chem. Process.* **2016**, *4* (2), 1–7.
(65) Copley, S. D. *Biochem. Soc. Trans.* **2014**, *42*, 1684–1691.
(66) Martínez-Núñez, M. A.; Pérez-Rueda, E. *Sustain. Chem. Process.* **2016**, *4:3*, 1–5.
(67) Gheshlaghi, R.; Scharer, J. M.; Moo-Young, M.; Chou, C. P. *Biotechnol. Adv.* **2009**, *27* (6), 764–781.
(68) Letzel, A.-C.; Pidot, S. J.; Hertweck, C. *Nat. Prod. Rep.* **2013**, *30* (3), 392–428.
(69) Walter, K. A.; Bennett, G. N.; Papoutsakis, E. T. *J. Bacteriol.* **1992**, *174* (22), 7149–7158.
(70) Petersen, D. J.; Welch, R. W.; Rudolph, F. B.; Bennett, G. N. *J. Bacteriol.* **1991**, *173* (5), 1831–1834.
(71) Alper, H.; Stephanopoulos, G. *Nat. Rev. Microbiol.* **2009**, *7* (10), 715–723.
(72) Sauer, M. *FEMS Microbiol. Lett.* **2016**, *363* (13), 1–4.
(73) Herman, N. A.; Kim, S.; Li, J. S.; Cai, W.; Koshino, H. *bioRxiv (preprint)* **2017**, 1–36.
(74) Sreekumar, S.; Baer, Z. C.; Pazhamalai, A.; Gunbas, G.; Grippo, A.; Blanch, H. W.; Clark, D. S.; Toste, F. D. *Nat. Protoc.* **2015**, *10* (3), 528–537.
(75) Peralta-Yahya, P. P.; Zhang, F.; del Cardayre, S. B.; Keasling, J. D. *Nature* **2012**, *488* (7411), 320–328.
(76) Khersonsky, O.; Tawfik, D. S. *Annu. Rev. Biochem.* **2010**, *79*, 471–505.
(77) Tokuriki, N.; Tawkfik, D. S. *Science*, **2009**, *324*, 203–208.
(78) Kaltenbach, M.; Tokuriki, N. *J. Exp. Zool. (Mol. Dev. Evol.)* **2014**, *322B*, 468–487.
(79) Argyropoulos, P.; Bergeret, F.; Pardin, C.; Reimer, J. M.; Pinto, A.; Boddy, C. N.; Schmeing, T. M. *Biochim. Biophys. Acta* **2016**, *1860* (3), 486–497.
(80) The Schmeing Lab, http://www.med.mcgill.ca/biochem/schmeinglab/Schmeing_Lab_website/Home.html.
(81) Mortison, J. D.; Kittendorf, J. D.; Sherman, D. H. *J. Am. Chem. Soc.* **2009**, *131*, 15784–15793.
(82) Pangborn, A. B.; Giardello, M.; Grubbs, R. H.; Rosen, R. K.; Timmers, F. J. *Organometallics* **1996**, *15* (5), 1518–1520.
(83) Armarego, W. L. F.; Chai, C. L. L. *Purification of Laboratory Chemicals*, 6th ed.; Elsevier Ltd, 2009.
(84) Fulmer, G. R.; Miller, A. J. M.; Sherden, N. H.; Gottlieb, H. E.; Nudelman, A.; Stoltz, B. M.; Bercaw, J. E.; Goldberg, K. I. *Organometallics* **2010**, *29*, 2176–2179.
(85) Gavande, N.; Kim, H.-L.; Doddareddy, M. R.; Johnston, G. A. R.; Chebib, M.; Hanrahan, J. R. *ACS Med. Chem. Lett.* **2013**, *4*, 402–407.

(86) Kumar, D.; Reddy, C.; Das, B. *Synthesis*, **2011**, *2011* (19), 3190–3194.
(87) Denmark, S. E.; Kobayashi, T.; Regens, C. S. *Tetrahedron* **2010**, *66* (26), 4745–4759.
(88) McClymont, K. Gephyronic Acid: A Chemical-Biological Approach to Biosynthetic Pathway Discovery, University of Ottawa, 2013.
(89) Cahn, R. S.; Ingold, C.; Prelog, V. *Angew. Chem. Int. Ed.* **1966**, *5* (4), 385–415.

· Chapter 7 ·

Future Directions: Combining Lessons from Both Doctoral Studies

7.1 Chemoenzymatic Synthesis of Polyketide Natural Products

The polyketide family of natural products are structurally-diverse compounds that represent a wide range of activities. Their highly-oxygenated and stereochemically-rich frameworks are valued within drug discovery, where clinical derivatives exceed $20B USD annually.[1] These substrates often feature rigidifying biases imposed by macrocyclic lactone frameworks and substituted five- and six-membered oxacycles,[2–9] which can control their bioactive conformation. Within the Boddy Lab, we use synthetic chemistry, biochemistry, and molecular biology to determine how microorganisms build complex polyketide natural products. With this knowledge, we then try to harness or mimic native biosynthesis to produce biologically-active polyketides and analogues.[10–15]

The theme of my graduate work combined synthetic chemistry and biosynthesis for production of macrocyclic polyketide natural products. My research focused on validating a transannular oxa-conjugate addition strategy to access 2,6-*cis*-tetrahydropyran (THP) ring systems, as demonstrated by synthesis of the macrocyclic core to neopeltolide (**7.1**, Figure 7.1). This work identified acid-mediated transannular attack of a *β'*-hydroxy nucleophile into an *α,β*-unsaturated ketone selectively generated *trans*-pyranone products using kinetic conditions, and desired *cis*-product under thermodynamic control.

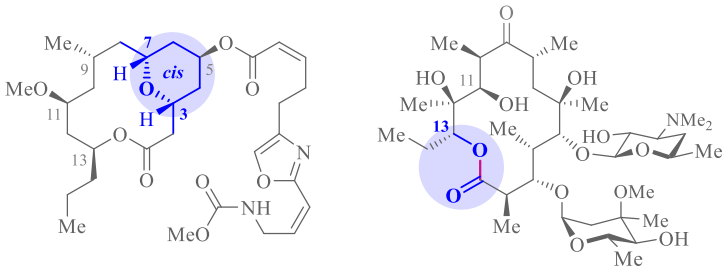

Figure 7.1 – Research from this dissertation focussed on chemoenzymatic strategies to synthesize macrocyclic polyketide natural products using two distinct studies.

In the second study, specificity of the macrolactonizing thioesterase (TE) domain from the 6-deoxyerythronolide B synthase (DEBS) biosynthetic pathway was probed. This is the paradigm pathway for type-I polyketide systems, and is responsible for producing the macrocyclic core of clinically-relevant erythromycin (**7.2**, Figure 7.1). This work discovered an unexpected suite of metabolites were produced by *in vitro* incubation with DEBS TE, suggesting an evolutionary fitness model within the protein and plasticity of its available chemistries.

The aim of this chapter is to summarize the current state of the two presented studies, and introduce potential areas of research for future direction.

7.2 Development of a *De Novo* PKS Pathway for Neopeltolide

Since its 2007 discovery,[16] neopeltolide **7.1** has received considerable attention from the research community.[17] Unfortunately, that attention has not provided a lasting solution to supply issues faced by **7.1** and many polyketide products. Our neopeltolide study is divided into two stages (Figure 7.3), where *de novo* polyketide synthase (PKS) pathway design represents the long-term milestone. The chemistry that fulfills the requirement of synthesizing tetrahydropyran (THP) ring systems using functional groups easily-accessible by engineered PKS proteins is oxa-conjugate addition. Presented work from this dissertation encompassed the first stage of research for the study. The collective results provided a foundation to direct the focus of on-going experiments and entry into the second stage of research toward development of a chemoenzymatic synthesis for pyran-bearing polyketides using *de novo* PKS pathways.

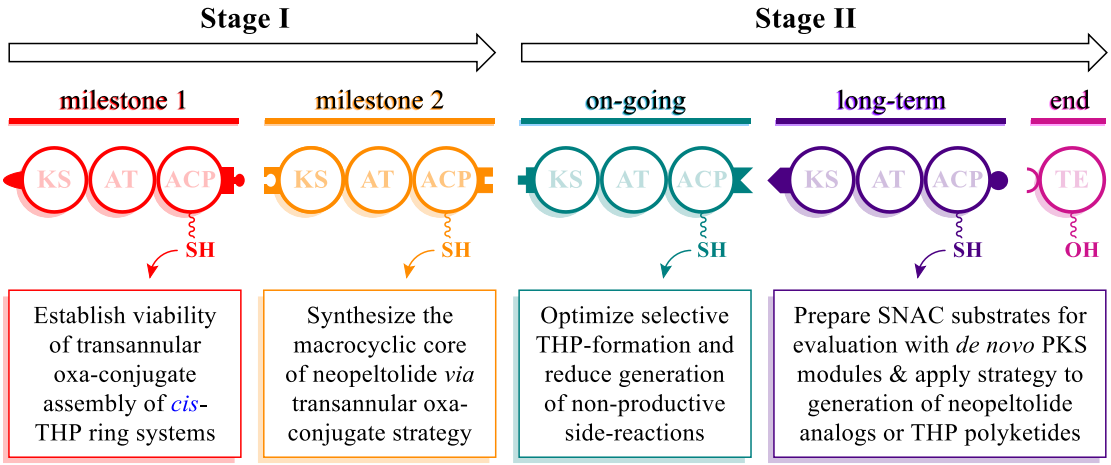

Figure 7.2 – Summary of the two stages of the neopeltolide study, whereby the results in this thesis represent the first stage and entry into the second.

In this section, select on-going research and future projects are proposed based on the current state of the neopeltolide study, and lessons learned from this doctoral work. Herein, projects are presented in a natural progression from unresolved matters toward our long-term milestone.

7.2.1 Current State of the Neopeltolide Study and Knowledge Acquired in Stage I

The chemical viability of transannular oxa-conjugate addition for selective assembly of our desired *cis*-THP ring system was established using a simplified model system (Scheme 7.1).[14] This work demonstrated that acid-mediated addition of a *β'*-hydroxy nucleophile into an *α,β*-unsaturated ketone embedded within a 14-membered macrolactone was superior to acid- or base-mediated additions into an *α,β*-unsaturated ester system (Chapter 3, § 3.4). Selectivity was controlled by reaction conditions and supported by computational data (§ 3.5.2). With good yield and diastereoselectivity, kinetic conditions generated *trans*-THP product **7.4** and thermodynamic conditions generated desired *cis*-THP **7.5**. We

hypothesized that conformational biases inherent to the 14-membered macrocyclic backbone lowered the reaction energy barrier, and exacerbated energetic differences between *cis*- and *trans*-diastereomers to enhance selectivity.[18] Similarly, the reversibility of the reaction demonstrated a potential application of racemic nucleophiles for diastereoselective assembly of pyrans. This work represented the first reported example of acid-mediated transannular oxa-conjugate assembly of 2,6-*cis*-THPs under thermodynamic control.

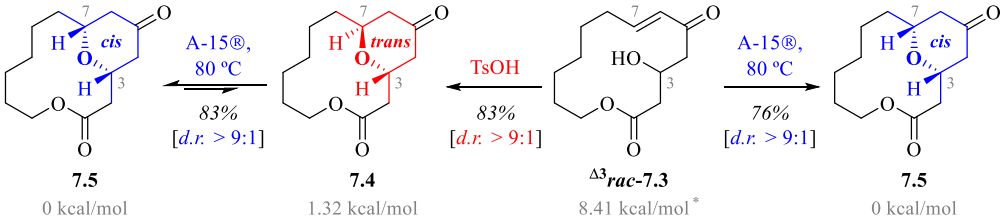

Scheme 7.1 – Summary of *α,β*-unsaturated ketone model for transannular oxa-conjugate addition assembly of *cis*-THP; acid-mediated thermodynamic control selectively furnishes the *cis*-pyranone product (Chapter 3). *C3 average.

Inspired by the success of our ketone model system (milestone 1), we evaluated the transannular oxa-conjugate addition strategy within the native core of neopeltolide (Figure 7.2). The fully-elaborated macrocyclic precursor was prepared from known material (12 steps from **S-20**, 19% overall),[19] as a separable mixture of C3 epimers (*d.r.* = 4:3, *3S*:*3R*). Acid-mediated desilylation spontaneously-furnished all four THP diastereoisomers, and favored kinetic *trans*-pyranone products (Chapter 4, § 4.6.2). Exclusive formation of *cis*-THP products was achieved by thermodynamic interconversion of the kinetic mixtures. Unfortunately, computational data determined the native macrocyclic configuration was not energetically-favored, and thermodynamic control did not achieve similar levels of selectivity seen in our model system for desired product. Our experimental observations indicated that the reversible E1cB elimination/oxa-conjugate addition sequence modestly favored native *cis*-diastereoisomer from the (3*R*) *β'*-hydroxy nucleophile (*d.r.* = 9:5, **7.7**:**7.9**), and as a minor product with the (3*S*) epimer. Moreover, we believe distal stereochemical elements and intrinsic conformational biases of the macrocyclic backbone lower the reaction barrier to suppress relative energy differences between the *cis*-isomers, similar to Hong's use of Thorpe-Ingold effect.[20] This work compared favorably to the efficiency of published syntheses of neopeltolide, and boasts room for improvement *via* optimization of our strategy.

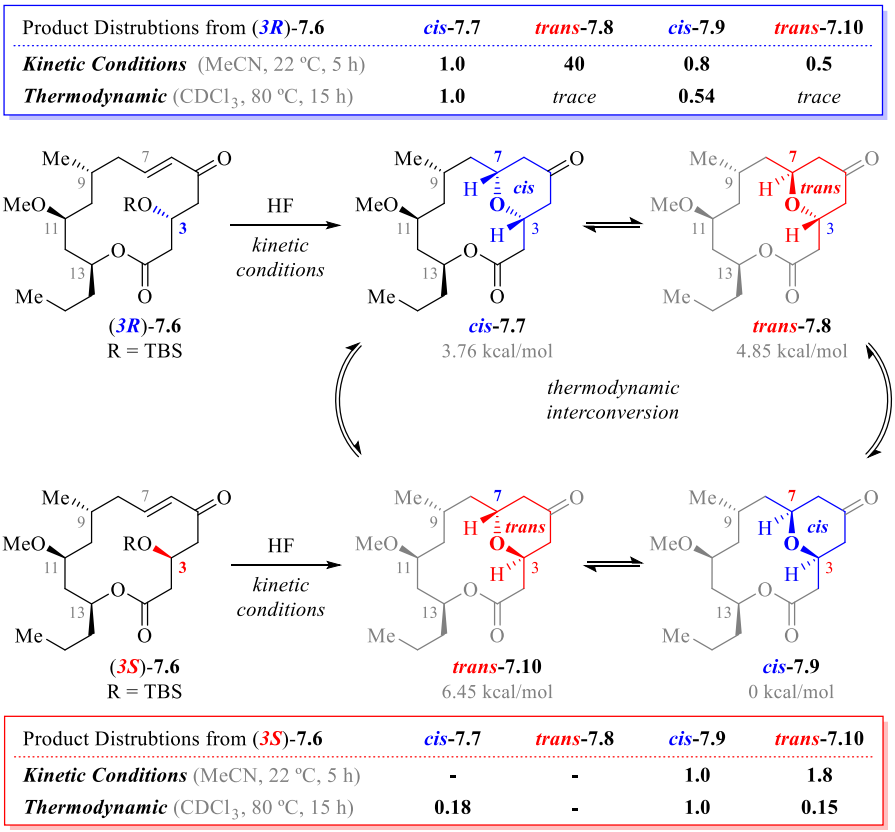

Figure 7.3 – Summary of product distributions obtained under kinetic and thermodynamic conditions using our transannular oxa-conjugate addition strategy for pyran formation (Chapter 4). Native configuration *cis*-**7.7** is not the energetic minimum, though is favored from (*3R*)-**7.6** and generated from (*3S*)-**7.6** precursors by thermodynamic control.

My doctoral work achieved the first two milestones of the neopeltolide study and constitutes the first stage of research. This data provides the necessary foundation to explore entry into the second stage of the study, where proposed research for this transition is outlined below.

7.2.2 Optimization of Oxa-Conjugate Addition for Selective Pyran Assembly (On-Going)

Experimental results from our key transannular oxa-conjugate addition within the macrocyclic core of neopeltolide indicated the reaction was less facile than our model systems. This observation was supported by computational data that revealed the native pyran configuration was not the energetic minimum. Limited material restricted our experimental results to single trials and requires re-evaluation to confirm reproducibility, as well as to improve desired selectivity. Because material was exhausted and must be regenerated, it allows additional investigation of our system. Thermodynamic interconversion of native-configured precursor (*3R*)-**7.6** proved superior in accessing the desired *cis*-THP ring system; thus, generation of enantiopure diprotic C3-phosphonate could suppress formation of undesired pyranyl isomers and non-productive side-products (Aim 1). Likewise, development of the C7 *β'*-hydroxy conjugated ketone system would provide insight to product distribution from regio-isomeric oxa-conjugate precursors (Aim

2). Using the precursors from Aims 1 and 2, our transannular oxa-conjugate addition strategy should be screened under a host of reaction conditions (Aim 3), and could facilitate the generation of a library of novel pyran analogues for neopeltolide (Aim 4).

Aim 1: Synthesis of Enantiopure C3-Hydroxy Phosphonate

To control C3 stereochemistry of our C1-C6 fragment, selective preparation of (*3R*)-**7.11** could be accomplished using chemical or chemoenzymatic syntheses (Figure 7.4). Though multiple strategies exist, desymmetrization of *meso*-glutaric anhydrides using *cinchona*-based sulfonamide catalysts[21–23] and Ni_2-Schiff base catalysts[24] have proven highly-selective to access enantiomeric hemiesters. Likewise, chiral auxiliaries or directing groups represent attractive chemical strategies to selectively assemble our desired phosphonate. In fact, the latter was employed by Heathcock to prepare (*3R*)-**7.11** over 9 steps from the ethyl ester of our prochiral 3-hydroxy diester.[25]

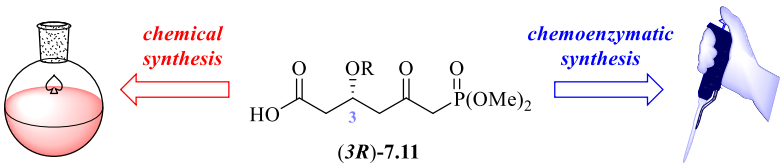

Figure 7.4 – Preparation of enantiopure C3-hydroxy phosphonate (***3R*)-7.33** could be accomplished *via* chemical or chemoenzymatic synthesis.

Esterases are cofactor- and metal-free biocatalysts for broad chemical applications, including desymmetrization reactions of prochiral materials.[26] For example, pig liver esterase (PLE) has extensively been used for highly-selective desymmetrization of *meso*-glutararic substrates *via* enzymatic hydrolysis. Like the selective installation of the C9-methyl in our C7-C16 fragment, PLE (or similar esterases) could provide optically-pure C3 hydroxy material. Alternatively, an industrial process was recently published for *de novo* production of the stabilized triphenylphosphonium ylide of **7.11** for Wittig coupling.[27] The one-pot chemoenzymatic strategy employed two biocatalysts over seven steps (59% overall, *ee* = 98%), in high substrate concentrations and multi-gram scale. This homologous species could be evaluated for our requisite olefination, or readily-converted to phosphonate (*3R*)-**7.11** *via* an advanced anhydride intermediate of the sequence.[28]

Aim 2: Development of C7 *β'*-Hydroxy *α,β*-Unsaturated Ketone System

Computational analysis for the equilibrium pathway to our transannular oxa-conjugate addition strategy for pyran assembly generally-supported our experimental observations for product formation; kinetic conditions favored *trans*-THP products and thermodynamic conditions favored *cis*-products. However, favored formation of native *cis*-pyran relative to its energetically-preferred *cis*-isomer, in addition

to unidentified side-products believed to be from non-productive pathways, were observed under thermodynamic control. These results fostered a hypothesis that a bottleneck in the interconversion process was caused by an energetic barrier imposed by our C7 *β'*-hydroxy nucleophilic regio-isomers. Unfortunately, our computational data did not permit accurate comparisons for our C7 products (*R/S*)-**7.12**. Generation of C7 *β'*-hydroxy enone substrates would allow experimental evaluation of product distribution from these equilibration pathway intermediates (Figure 7.5).

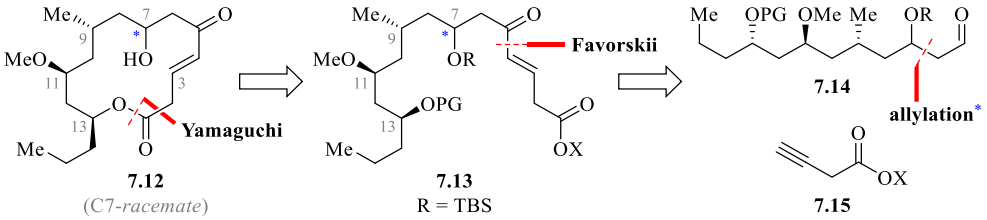

Figure 7.5 – Potential retrosynthetic strategy to generate C7 *β'*-hydroxy enone regio-isomer **7.12** for transannular oxa-conjugate addition pyran assembly in neopeltolide. *Non-selective or asymmetric allylation conditions can be employed.

Synthesis of **7.12** could be accomplished by linear elongation of our C7-C16 aldehyde fragment, allowing simultaneous generation of all four oxa-conjugate precursors. It is believed that non-selective Grignard allylation would provide a separable mixture of diastereomeric precursors, though asymmetric allylation conditions exist.[29–32] Additionally, the less-acidic environment of the C7 hydroxy nucleophile should effectively suppress the possibility of undesired elimination during formation of the requisite *seco*-acid for Yamaguchi esterification. It is worth noting this strategy resembles our originally-planned biomimetic synthesis and the biosynthetic building of PKS products.

Aim 3: Investigation of Oxa-Conjugate Addition Reaction Conditions

The initial results from our thermodynamic interconversion in our neopeltolide system provided experimental support to our computational data; however, demonstrating reaction reproducibility remains imperative (Figure 7.6). Product distribution should be evaluated using both C3- and C7-hydroxy nucleophilic oxa-conjugate precursors, which could provide insight to our hypothesized equilibration pathway energetic barrier (Aim 2). Use of NMR time-course experiments would prove instrumental for detailing product formation under kinetic and thermodynamic conditions. These experiments are believed could identify equilibration pathway intermediates that facilitate formation of non-productive side-products, and possibly dictate conditions for suppression.

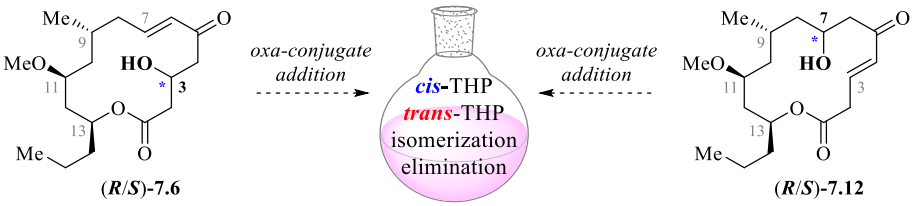

Figure 7.6 – Product distribution can be evaluated with C3- and C7-hydroxy oxa-conjugate precursors under a screen of acid- and base-mediated reaction conditions.

Because pyran formation was incredibly facile under acid-mediated desilylating kinetic conditions, screening alternative proton sources should be evaluated first. Examination of both Lewis and Brønsted acids could improve selectivity of our desired THP isomer,[33] akin to the results from our first-generation ketone model.[14] Screening of temperatures should also be investigated, and whether the reaction can be telescoped in one pot under thermodynamic desilylation conditions. Similarly, base-mediated oxa-conjugate addition (TBAF desilylation) should be analyzed within this system, despite limited success in our first-generation model. Base-mediated intramolecular oxa-conjugate addition has effectively generated pyrans under kinetic and thermodynamic control, including Fuwa's simplified linear neopeltolide fragment.[32,34]

Aim 4: Preparation of Pyranyl Analogues for Neopeltolide

All four pyranyl diastereoisomers were generated for the macrocyclic core of neopeltolide with our acid-mediated transannular oxa-conjugate addition strategy. The small scale of this work did not allow clean isolation, but screening reaction conditions in Aim 3 should generate sufficient material for thorough characterization of each isomer. Each pyranone product can generate two natural analogues of neopeltolide by reduction of the C5 ketone and subsequent coupling to the oxazole-bearing sidechain (Figure 7.7). Though the pharmacophoric elements of neopeltolide reported the pyran is essential for activity,[32] a focused study of pyranyl analogues has not been addressed. In fact, six of the potential products of the 8-member library of trisubstituted pyranyl stereoisomers represent novel substrates with unknown biological activity (**7.17-7.22**). Analogue **7.16** was generated by Maier and coworkers,[35] and reported with comparable nanomolar cytotoxicity to **7.1** in multiple cell lines.

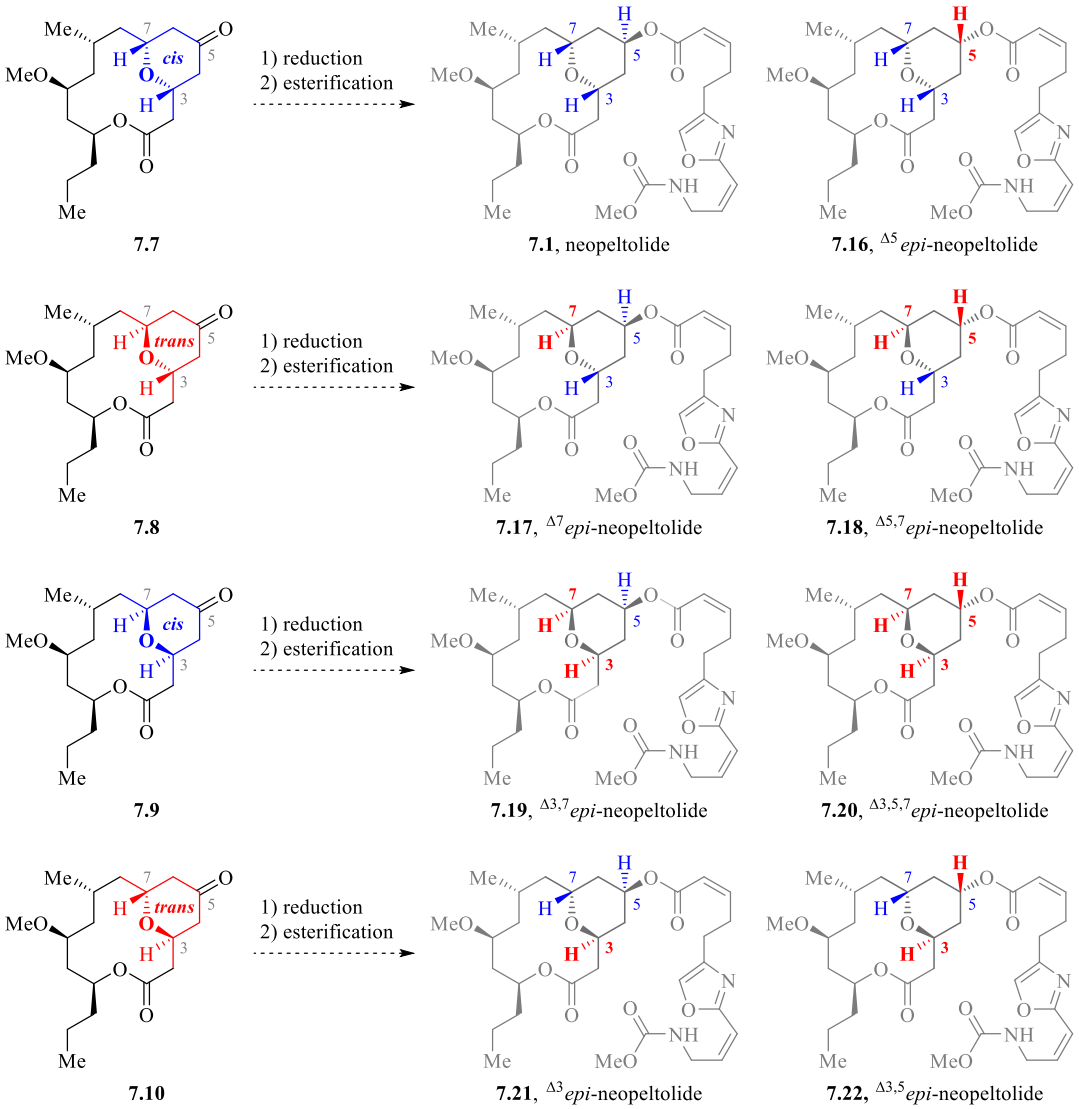

Figure 7.7 – Reduction of the four pyran stereoisomers would allow rapid generation of a small library of novel neopeltolide analogues. The configuration of the C5 stereocenter could be controlled by reaction conditions.

These four aims surrounding optimization of oxa-conjugate addition for selective pyran assembly would deliver a significant amount of impactful data for our neopeltolide study. More importantly, it is believed that my doctoral research provided an excellent foundation for these proposals, and would not require significant amounts of new effort.

7.2.3 Toward a De Novo Synthesis of Neopeltolide (Long-Term)

Extensive research in the field of modular PKS biosynthetic pathways has seen researchers engineer mutant proteins for *in vivo* and *in vitro* production of unnatural polyketides. These achievements have largely been limited to predictable point mutations or simplified *de novo* systems. As established in **Chapter 6**, use of recombinant catalytic domains with unnatural substrates can be unpredictable. For entry

to the second stage of our neopeltolide study and long-term goal of designing a *de novo* PKS pathway for producing transannular oxa-conjugate precursors, research should be conducted in top-down fashion to increase the likelihood of success.

Aim 5: Evaluation of Enzyme-Mediated Cyclization within Neopeltolide

Thioesterase-mediated cyclization of the neopeltolide framework could be addressed with rapid preparation of a synthetic linear acyl chain substrate from parent macrocycle **7.7** (Figure 7.8).[36] Because the genome for the producing organism of neopeltolide was not sequenced and re-isolation has not been realized, a panel of known catalytic TE domains excised from PKS systems should be investigated (*vide infra*).[37] Using methodology akin to the research of Chapter 6, *N*-acetylcysteamine (NAC) thioester **7.23** would be treated with purified TE proteins and analyzed by HPLC-MS for production of free-acid **7.25** or macrocycle **7.7** *via* hydrolytic cleavage or cyclo-release pathways, respectively.

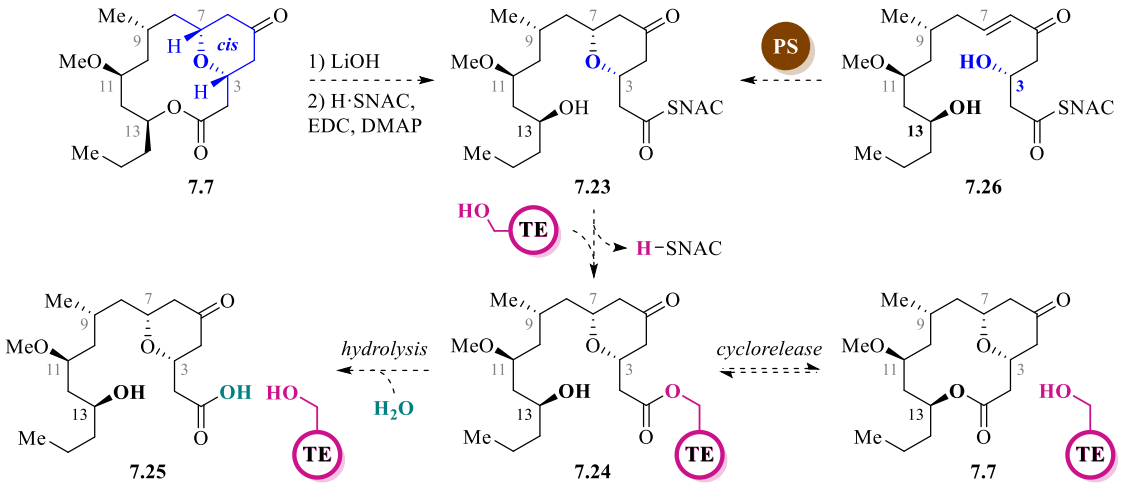

Figure 7.8 – Macrocycle **7.7** allows preliminary evaluation of enzyme-mediated cyclizations by thioesterase and pyran synthase domains, and would provide insight for rational design of our *de novo* pathway.

Likewise, NAC-thioester **7.26** could be generated from previously-prepared *seco*-acid of our HWE olefination (Chapter 4, § 4.6.1), and screened against the same TE panel for effect of the proximal *β*-hydroxy (C3) nucleophile. In event of cyclization, chemoselectivity should furnish energetically-preferred 14-membered macrocyclic oxa-conjugate precursor over linear beta-lactone.[†] Moreover, substrate **7.26** should also be evaluated for *in vitro* pyran formation with putative pyran synthase (PS) catalytic domains isolated from biosynthetic pathways for compounds that include pederin,[38] misakinolide,[39] salinomycin,[40] ambruticin,[41] or sorangicin A.[42]

[†] The *seco*-acid derived from C7 *β'*-hydroxy intermediate **7.13** (Figure 7.5, Aim 2) could also be used to prepare its linear NAC-thioester substrate for *in vitro* evaluation with TE and PS domains.

Aim 6: Rational Design of *De Novo* System for Production of Neopeltolide

The long-term milestone of this study will be rife with challenges resulting from domain substrate specificities and modular interactions intrinsic to PKS proteins. A major challenge with domain or module swapping is disruption of protein-protein interactions within chimeric synthases needed for efficient processing of acyl intermediates.[43] These combinatorial techniques have been met with only limited success to date,[51–53] suggesting much remains to be learned to achieve the flexibility of LEGO® analogies.[49] Accordingly, use of whole or unmodified proteins is an attractive strategy to minimize challenges associated with turnover of nascent polyketide chains between modules, and to facilitate the necessary cloning and purification steps.

Thailandamide A was elucidated in 2012 as a cryptic polyene product from a *trans*-AT PKS biosynthetic pathway of *Burkholderia thailandensis*.[50] Because native ThaN protein houses three modules that perform necessary chemistries and provide the proper stereochemistry required in our system, issues with poor homodimerization could be suppressed (Figure 7.9).[43] These modules should first be evaluated individually for function with appropriate NAC-thioesters,‡ and then in conjugation with its downstream partner. Ultimately, the TE domain identified from Aim 5 can be fused to ThaN for enzyme-mediated cyclo-release of our macrocyclic oxa-conjugate precursor (*3R*)-**7.6**.

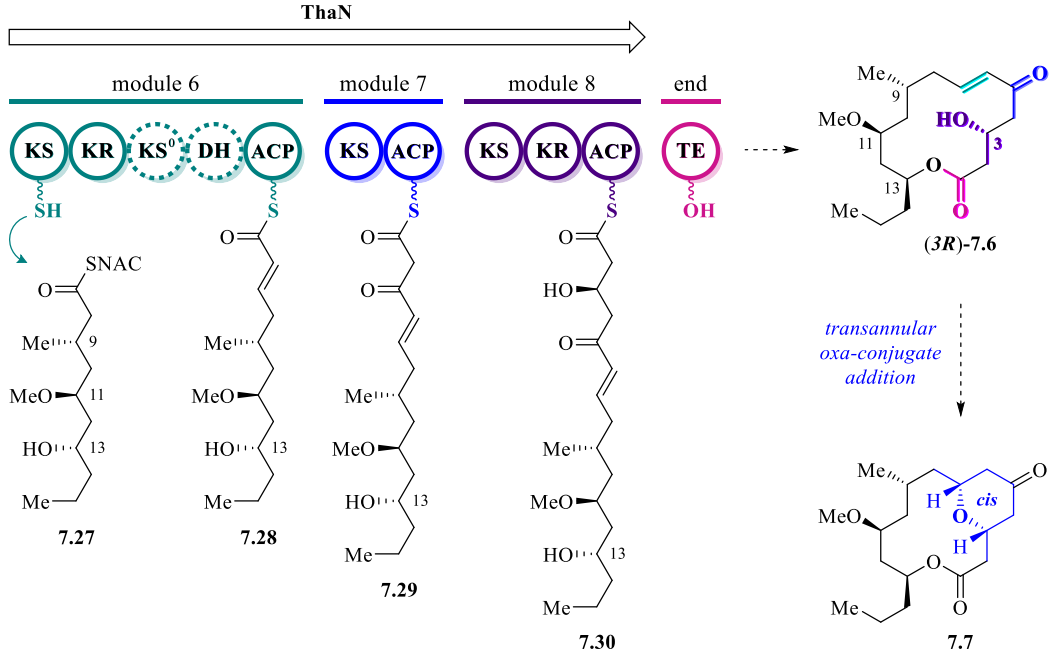

Figure 7.9 – The ThaN protein from the biosynthetic pathway of thailandamide A contains three modules that natively-perform the requisite chemistry that could selectively-assemble the full-carbon framework of the macrocyclic core to neopeltolide from a derivatized version of our C7-C16 fragment.

‡ NAC-thioester substrates **7.27**-**7.30** can be prepared from the C7-C16 fragment used in the chemical synthesis of **7.7** (§ 4.4.3).

This retro-biosynthetic approach has many challenges unique to the current capabilities of modern protein engineering. However, continued research in the expanding field presents opportunity to harness biosynthetic enzymes and exploit their astounding natural diversity. The potential of this methodology is particularly appealing for production of compounds like neopeltolide, whose native pathways have not been elucidated. Unfortunately, limited examples of *de novo* pathways exist at present. In fact, this strategy presents greater challenges and required effort than our chemical synthesis, and likely pushes the limits of feasibility despite employing a whole protein and its native modules. Nevertheless, by systematically-expanding our *de novo* system in top-down fashion, we would contribute to, and incorporate modifications based on evolving knowledge and capabilities.

7.3 Development of a Macrocyclizing Biocatalytic Thioesterase

Thioesterase proteins are typically found at the terminus of final elongation modules in PKS biosynthetic systems, and mediate regio- and stereoselective ring-closure during cyclo-released off-loading. Because these enzymes circumvent challenges associated with the chemical synthesis of macrolactone scaffolds from linear intermediates, TEs represent attractive candidates for development of macrocyclizing chemoenzymatic tools. Our thioesterase study is divided into two stages, where the long-term goal is to optimize and engineer a substrate-tolerant TE to expand its limits of promiscuity toward macrocyclization-competent frameworks (Figure 7.10). Presented work from this dissertation contributed to the on-going first stage of research toward identifying and characterizing a suitable TE. Our results suggested that wild-type DEBS TE is likely too substrate-selective to be developed as a generalized macrocyclizing biocatalyst, but highlighted a plasticity of activities to access and generate unprecedented chemical diversity.

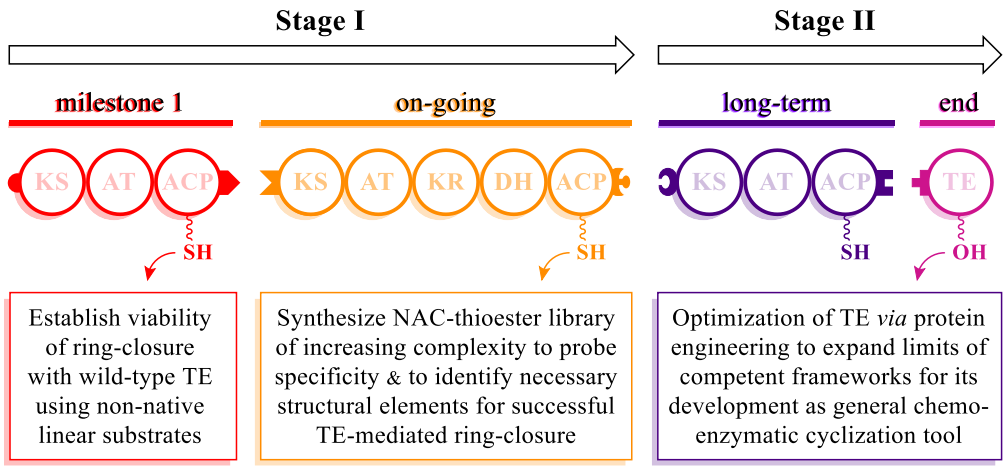

Figure 7.10 – Summary of the two stages of the macrocyclizing biocatalytic thioesterase study, whereby results in this dissertation represent contributions toward the first stage using wild-type DEBS TE from the erythromycin biosynthetic pathway. Multiple iterations of Stage I will likely be required to identify a suitable catalytic domain that displays broad substrate-tolerance.

In this section, a selection of on-going research and future projects are proposed based on the current state of the thioesterase study, and lessons learned from using DEBS TE for this doctoral work. Herein, projects are presented to facilitate thorough *in vitro* characterization of TE domains like DEBS, toward the identification of a suitable macrocyclizing TE with broad substrate-tolerance.

7.3.1 Current State of the Biocatalytic TE Study & Knowledge Acquired using DEBS TE

The viability of wild-type DEBS TE-mediated ring-closure was established using two generations of simplified, linear NAC-thioester analogues of the native framework (Figure 7.11).[11,15] This work yielded the first two examples of non-native substrates to be cyclized *in vitro* by treatment with recombinant DEBS TE as a stand-alone enzyme. The first-generation system adhered to our hypothesis that stated ring-closure required D-configured nucleophiles (Chapter 6, § 6.2), but revealed that absolute stereochemistry was not sufficient at predicting cyclization-competency (Figure 7.11a). Substrate-selectivity of DEBS TE was probed using our second-generation system that converted the C11 *β*-hydroxy functionality into an *α,β*-unsaturated carbonyl (Figure 7.11b). The modification showed that small, evolutionarily-accessible changes to substrate frameworks can dramatically increase chemical diversity. *In vitro* incubation of DEBS TE with D-configured **7.36** revealed a suite of enzyme-mediated metabolites were produced (§ 6.3.2), including unprecedented dimerization that afforded linear-dimeric and macrodiolide products.

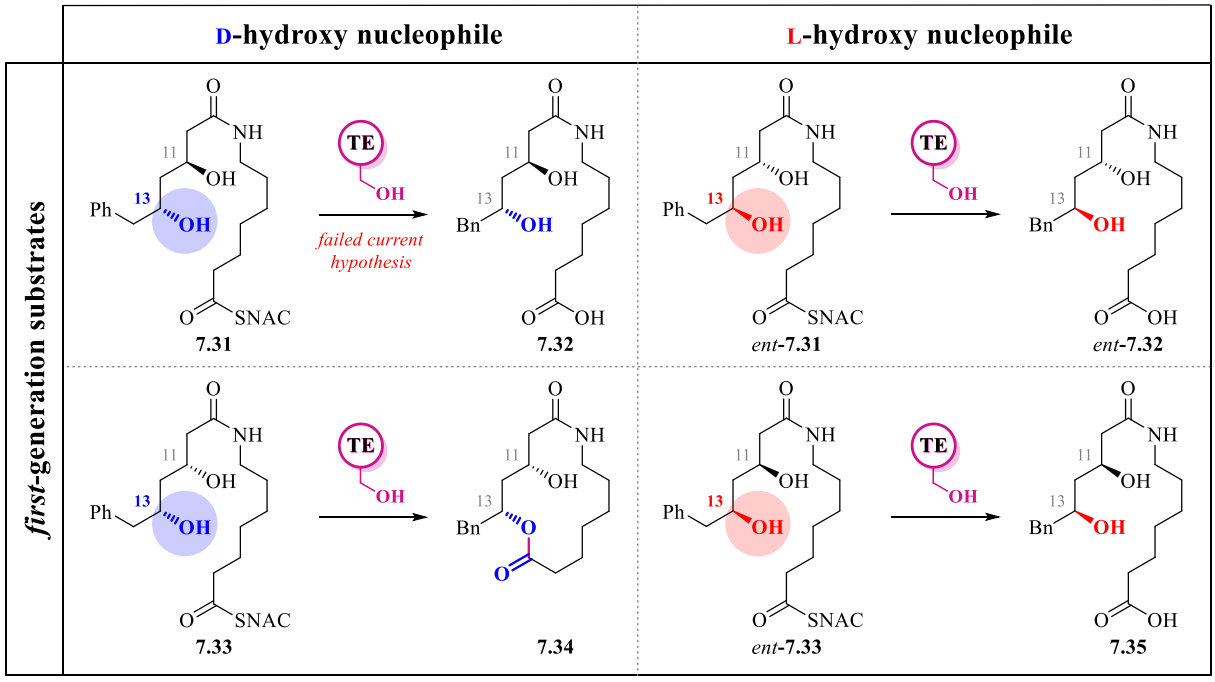

Figure 7.11a – Summary for first-generation of non-native substrates developed by the Boddy Lab for *in vitro* evaluation of DEBS TE-mediated macrocyclization during off-loading from the enzyme. Transformations that failed our working hypothesis that states D-nucleophiles are required for ring-closure are indicated, accordingly.

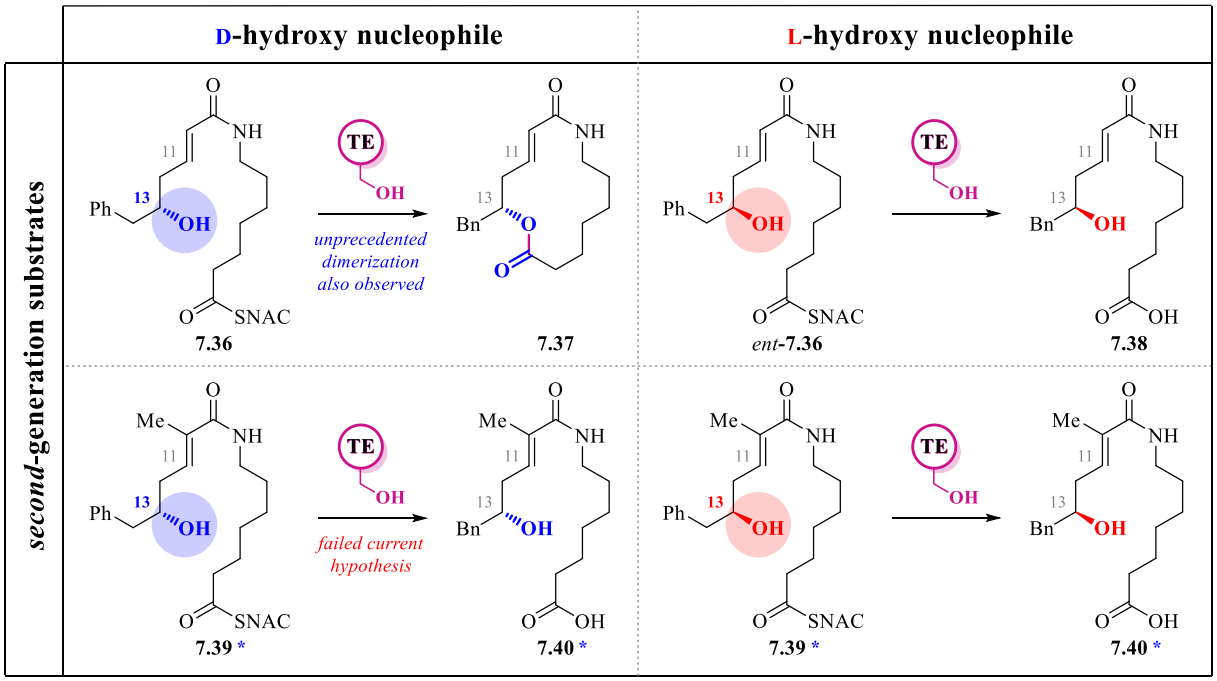

Figure 7.11b – Summary for second-generation of non-native substrates that probed selectivity of DEBS TE-mediated *in vitro* macrocyclization during off-loading. *Prepared as racemic mixture.

Unprecedented dimerization was confirmed using data that included unique UV-Vis retention times, tandem mass-spectrometry, and LC-SPE-NMR analyses (§ 6.4.3). To account for the suite of enzyme-mediated dimeric metabolites, we proposed that TE-bound monomer D-**7.41** was attacked by the distal hydroxy nucleophile of a second equivalent of NAC-thioester D-**7.36** (Figure 7.12), to generate linear NAC-thioester dimer **7.42** *via* retro-transfer. Observation of **7.42** was critical to our proposed mechanism because it would not be produced by the alternative TE-mediated dimerization pathway (§ 6.4.4). This linear metabolite would subsequently be loaded to a vacant TE active site, whereby D-**7.43** could be processed to yield dimeric free-acid or C_2-symmetrical macrodiolide **7.44** during off-loading.

Based on our experimental observations, we proposed a fitness-based evolutionary model that suggested TEs are intrinsically non-selective toward the possible chemistries they catalyze during enzyme-mediated off-loading. This screening hypothesis accounted for chemical diversity observed during our *in vitro* biochemical characterization of DEBS TE, which included hydrolysis, transesterification, macrocyclization, dimerization and macrodiolide formation. Our hypothesized convergent evolution of macrodiolide-forming activity was supported by phylogenetic analysis of 138 modular TE domains (Appendix II, § S2.4.1) that revealed TE domains are unique among PKS enzymes, and do not cluster based on substrate-specificity or function. Thus, while factors that control TE-mediated chemistries for off-loading remain unclear, it is abundantly-clear that a primary sequence determinant does not exist that can predict macrocyclization activity and requires biochemical characterization and observation.

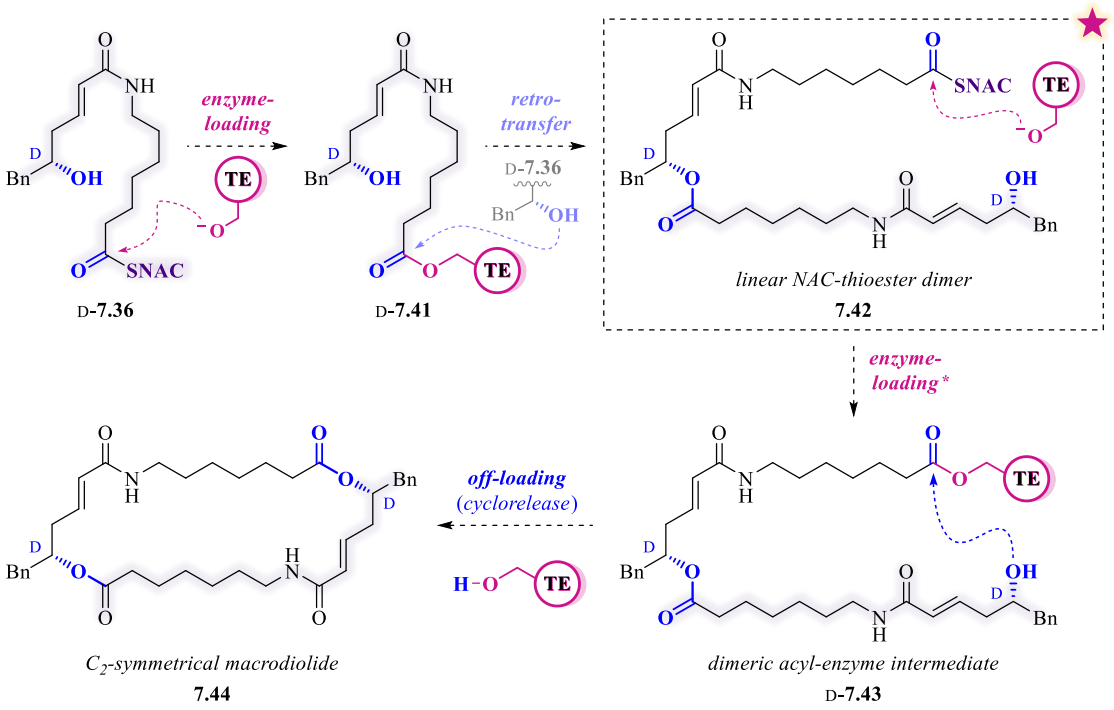

Figure 7.12 – Proposed mechanism for DEBS TE-mediated macrodiolide formation. Observation of linear NAC-thioester dimer **7.42** supported iterative enzyme-loading* of monomer D-**7.36**. Dimeric acyl-enzyme intermediate D-**7.43** is off-loaded to generate dimeric free-acid by hydrolysis (not shown), or intramolecular ring-closure to yield C_2-symmetrical macrodiolide **7.44**.

My doctoral work contributed to an on-going first-stage in our study toward the characterization of DEBS TE for its potential development as a general macrocyclizing biocatalyst. Our data indicated that wild-type DEBS TE is incredibly substrate-selective, and requires additional investigation to better understand the molecular interactions needed to effect ring-closure.

7.3.2 Development of Precursor Library for Identification & Characterization of Suitable TE

Experimental results from our small library of simplified NAC-thioester analogues indicated that small, evolutionarily-accessible structural changes can dramatically alter DEBS TE-mediated product distribution. Additional investigation of substrate-selectivity is necessary to complement our preliminary data, and to improve our understanding of molecular interactions needed to predict enzyme-mediated macrocyclization using non-native substrates. Consequently, we must identify tractable strategies to rapidly-populate libraries of fragments and substrates to probe macrocyclization competency *via* roles of regio- and stereoselectivity (Aim 7). Similarly, development of amine fragments with varying chain lengths would evaluate effects of ring size on product distribution observed with DEBS TE (Aim 8). To identify a macrocyclizing enzyme with broad substrate tolerance, the library of analogues developed through Aims 7 and 8 should be evaluated against a panel of known TE domains from PKS (bacterial and fungal) and NRPS

biosynthetic pathways (Aim 9). Characterization data generated from these aims would ultimately be used to direct protein engineering and explore Stage II of our study.

Aim 7: Design Synthetically-Tractable Complexity to Probe Substrate-Selectivity

Library development by systematic incorporation of structural complexity is an insurmountable endeavour for most native PKS frameworks with current synthetic and enzymatic platforms, as highlighted by the 1024 (2^{10}) possible diastereomeric frameworks for DEBS. Selective preparation of triketide δ-lactones or similarly small, chiral polyketide synthons of the C9-C13 framework for DEBS is an attractive approach to rapidly populate a library of novel NAC-thioester analogues (Figure 7.13). This strategy would facilitate use of our previously-employed cross-coupling methodology, and provide insights to substrate-enzyme interactions surrounding the nucleophilic alcohol. These types of compounds have previously been synthesized using multi-step sequences,[51–53] and produced *in vivo* using bi- and trimodular PKS pathways on non-preparative scales.[54–62] Though numerous strategies are available, Córdova's amino-acid-catalyzed asymmetric synthesis should be employed to efficiently generate enantiopure triketide δ-lactones.[63,64] Alternating D- and L-proline catalysts would generate four diastereomers *via* incorporation of propionyl aldehyde **7.46**, and can be readily coupled with a desired amine (*vide infra*) to afford analogues **7.52-7.55** in four total steps. Addition of acetaldehyde would generate desmethylated products akin to biosynthetic loading of malonyl-CoA extender units, and a broad range of C10- and C12-alkylated products would also be possible using aldehydes successfully-employed in the seminal report.[§]

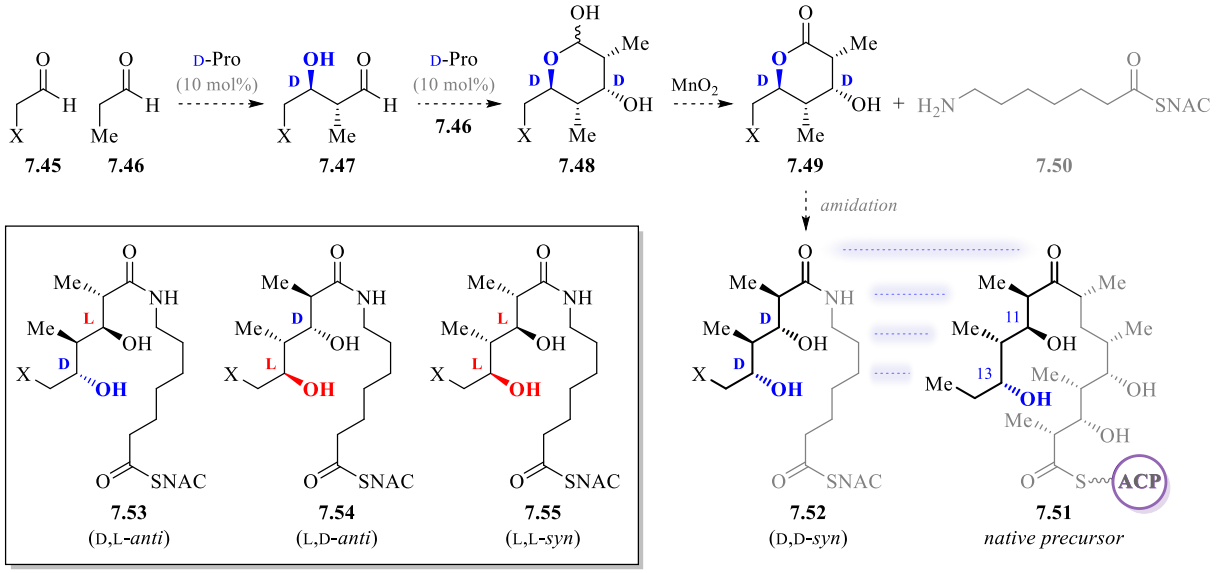

Figure 7.13 – Amino-acid-catalyzed asymmetric synthesis provides a synthetically tractable strategy that could rapidly populate analogue libraries to probe substrate-selectivity of TEs using commercial reagents.

[§] Their reported range of aldehydes (RCHO, R = Me, Et, *i*Pr, *i*Bu, *c*-hex, Bn) gave moderate yields with selectivities ≥ 99%.

Completion of each 16-membered diastereomeric panel could be realized, in part by MacMillan's proline-catalyzed/Mukaiyama aldol sequence,[65] or by conventional use of Evans-type chiral auxiliaries or directing groups to afford *syn*-aldol adducts (refer to Appendix II). However, the four potential isomers obtained include all *syn/anti* combinations between C11- and C13-nucleophiles, and should provide sufficient data to highlight regio- and stereoselectivity of TE-mediated processes. To illustrate the tractability of this strategy, a theoretical library of 4096 (4^6) triketides could selectively be prepared by swapping between aldehydes employed in the seminal report,[63] and could be used to introduce native homology from other PKS frameworks in our TE panel (*vide infra*). Moreover, modulation of precursor **7.45** should be explored to incorporate chemical handles (e.g., terminal olefin, alkyne, azide, halide) that would broaden the synthetic utility of the corresponding triketide building blocks.[66,67] These scaffolds could be expanded to improve the pharmacological properties of current polyketide-based therapeutics, or to interrogate cellular processes *via* bio-orthogonal chemistries.[68–73]

Aim 8: Rapid Library Development for Continued Mapping of Substrate-Specificity

The convergent methodology used to populate our small library of macrocyclization precursors significantly increased synthetic efficiency, and the peptidyl bond eliminated undesired hemiketalization side-reactions. To evaluate substrate-specificity toward common macrolactone ring sizes (Figure 7.14), amines with varying lengths of unsubstituted aliphatic backbones could be prepared in three steps from commercial acids. We believe that 14-, 16-, and 18-membered precursors like **7.57-7.59** would provide key insights into substrate-specificity and regioselectivity of TE-mediated chemistries. Longer-term milestones would include derivatization of hydrocarbon backbones with structural complexity that adheres to prototypical PKS architecture, or mimics specific native metabolites from the panel of recombinant TEs (*vide infra*). These modulations have potential to grow our library of macrocyclization precursors at exponential rates, using minimal effort.

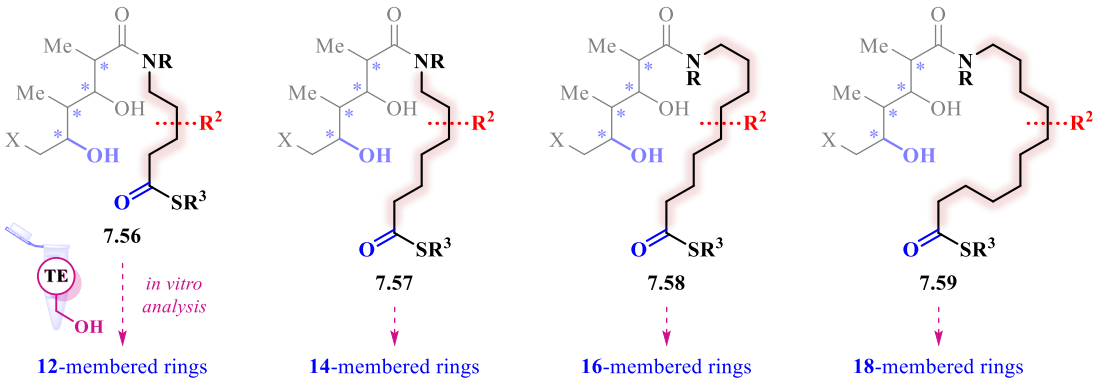

Figure 7.14 – Cross-coupling C9-C13 fragments with amines of varying chain lengths would evaluate TE-mediated cyclization of common macrocyclic ring sizes, and alternative thioesters would probe substrate loading. Structural complexity could be introduced into the aliphatic backbone as a long-term milestone.

In vitro investigation of isolated PKS modules and domains rely on electrophilic thioesters for diffusive enzyme loading *in lieu* of upstream transfer.[74] Historically, NAC-thioesters have been the most widely-used due to mimicking the phosphopantetheinyl arm that tethers a growing polyketide chain, and its relative ease of production.[75] Recently, use of alternative thioesters have been reported that improved TE-catalysis in comparison to NAC,[76] suggesting a potential area for reaction optimization. To probe substrate-loading parameters of TE catalysis, amine fragments should be derivatized as a variety of thio- and oxoesters, and coupled to fragments from Aim 7. Similar work with PIK TE showed product formation could be selected by ester choice,[77,78] and highlighted thiophenol as highly-effective for catalyst-loading. Next-generation analogue design could be guided by biochemical characterization, where non-hydrolyzable phosphonate-based covalent inhibitors would be developed to obtain high-resolution structural data for interactions between enzymatic active-site and substrates of interest.

Aim 9: Identification of Macrocyclization Thioesterase with Broad Substrate-Tolerance[**]

Assembly of macrocyclic scaffolds using chemoenzymatic tools and engineered *de novo* pathways will only be useful if the TE efficiently produces desired product by cyclo-release. Thus, characterizing TE specificity is critical to design of robust engineered domains and synthases (Table 7.1). Our initial data suggested DEBS TE is too selective for general macrocyclization. Consequently, future analogue libraries prepared from Aims 7 and 8 must be evaluated against a diverse panel of known cyclizing TEs from characterized pathways. Diversity should examine contrasting structural elements when possible, such as Pld TE-mediated ring-closure of the native C7-hydroxy-containing pladienolide backbone **7.60**, which abolished all cyclization activity with PIK TE and DEBS TE using homologous 10-deoxymethynolide **7.61** systems.[79] Type-I PKS bacterial TEs have received considerable attention, but some type-II PKS fungal variants have recently demonstrated comparatively-relaxed stereotolerance toward macrocyclization.[80–82] Similarly, the NRPS TE responsible for cyclizing tyrocidine **7.73** displayed a broadly-tolerant specificity profile,[83] and was used to catalyze macrolactamization of more-than 100 linear peptides immobilized on solid-phase support.[84] Crytophycin **7.70** analogues were also prepared using on-resin methodology for lactonization by treatment with native Crp TE from its mixed PKS/NRPS pathway.[85] Because the success of this study relies on recognizing a TE that retained autonomous catalytic activity and displays superior kinetics with broad tolerance, this work will undoubtedly require multiple iterations of *in vitro* characterization (Stage I). This data will facilitate entry to the second stage, where the most-promising TE candidates are selected for rationally-designed protein engineering and directed-evolution studies.

[**] The diverse panel would also be used to identify a TE that mediates ring-closure for functionalized neopeltolide frameworks (Aim 5), and ultimately be used in our *de novo* PKS pathway (Aim 6).

Table 7.1 – Select examples of known macrocyclizing TE domains from characterized PKS, NRPS and mixed biosynthetic pathways. Prepared libraries of linear precursors should be evaluated with a diverse panel of TEs to increase likelihood of identifying a protein that displays broad substrate-tolerance for macrocyclization.

Thioesterase {PDB ID}	**Class**		**Nucleophilic Configuration**	**Ring-Size Formed**	**Native Off-Loaded Structures**
	type	***origin***			
Pladienolide (**Pld**)[86]	Type-I PKS[a]	*Streptomyces platensis*[87]	**D**-*hydroxy*	**12**	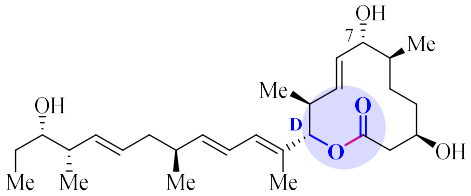 **7.60**
Pikromycin (**PIK**)[88] {**1MN6**}[89]	Type-I PKS[a]	*Streptomyces venezuelæ*[90]	**D**-*hydroxy*	**12** & **14**	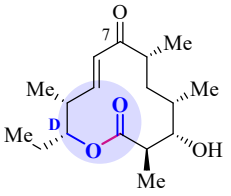 **7.61** (Chapter 5, § 5.7) 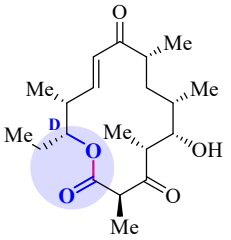 **7.62**
Deoxyerythronolide (**DEBS**⁂)[91] {**1KEZ**}[92]	Type-I PKS[a]	*Saccharopolyspora erythræa*[93]	**D**-*hydroxy*	**14**	**6.2** (Chapter 6, § 6.1)
Epothilone (**Epo**⁂)[94]	Type-I PKS[a]	*Sorangium cellulosum*[95]	**D**-*hydroxy*	**16**	**5.49** (Chapter 5, § 5.7)
Tylosin (**Tyl**)[96]	Type-I PKS[a]	*Streptomyces fradiæ*[97]	**D**-*hydroxy*	**16**	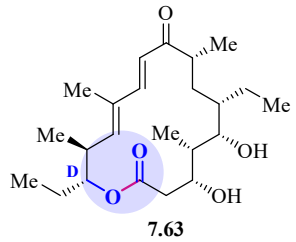 **7.63**

Soraphen A (**Sor**)[98]	Type-I PKS[a]	*S. cellulosum*[99]	**D**-*hydroxy*	**18**	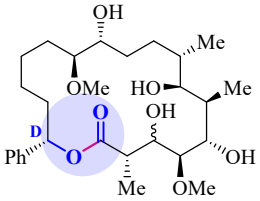 **7.64**
Pimaricin (**Pim**⁂)[100]	Type-I PKS[a]	*Streptomyces natalensis*[101]	**D**-*hydroxy*	**26**	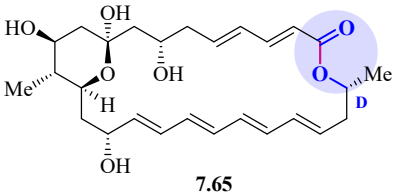 **7.65**
Dehydrocurvularin (**Dhc**⁂)[102]	Type-II PKS[b]	*Aspergillus terreus*[103,104]	**L**-*hydroxy*	**12**	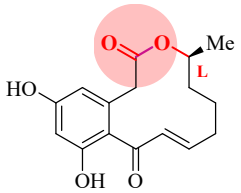 **7.66**
Radicicol (**Rdc**⁂)[105]	Type-II PKS[b]	*Pochonia chlamydosporia*[106]	**D**-*hydroxy*	**14**	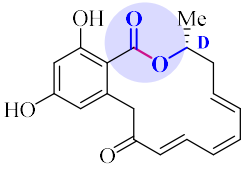 **7.67**
Zearalenone (**Zea**⁂)[107]	Type-II PKS[b]	*Fusarium sp.*[108]	**L**-*hydroxy*	**14**	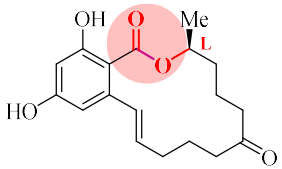 **7.68**

Borrelidin (**Bor**)[109]	Type-II PKS[a]	*Streptomyces parvulus*[110]	**D**-*hydroxy*	**18**	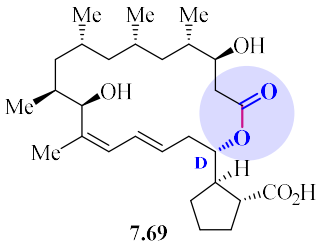 **7.69**
Cryptophycin (**Crp**)[111]	Hybrid PKS/NRPS	*Nostoc sp.*[112,113]	**D**-*hydroxy*	**16**	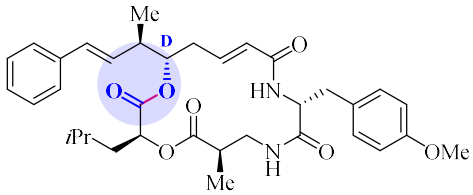 **7.70**
Bacitracin (**Bac**)[114]	NRPS	*Bacillus subtillis*[115]	**L**-Lys	**25** (dodecapeptido-lactam)	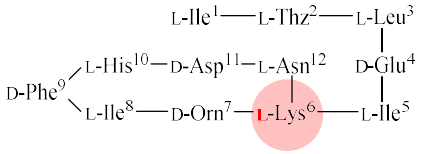 **7.71**
Surfactin (**Srf**)[116] {**2RON**}[117]	NRPS	*B. subtillis*[118]	**D**-*hydroxy*	**25** (lipopeptide)	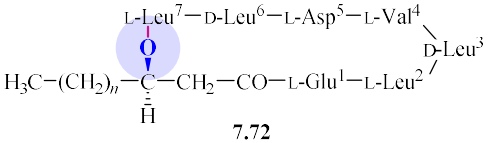 **7.72**
Tyrocidine (**Tyr**)[119]	NRPS	*Brevibacillus brevis*[120]	**D**-Phe	**30** (decapeptido-lactam)	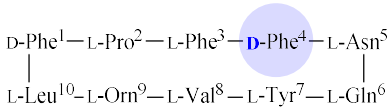 **7.73**

[a] – Bacterial producing organism.
[b] – Fungal producing organism.
♣ – TE expression vector currently present in Boddy Lab stock. Our library also has expression vectors to dimerizing type-I PKS of elaiphylin (Ela TE),[121] and NRPS TEs known to trimerize tetrapeptides, including valinomycin (Vlm TE)[122] and related cereulide (ces TE);[123] it may prove interesting to also evaluate using these domains.

Research has demonstrated the exciting potential of harnessing TEs to catalyze ring-closure of non-native frameworks, though it remains to be seen whether a suitable domain can be identified that can overcome physiological selectivities to be developed as a generalized biocatalyst. Unfortunately, this bottom-up approach for biochemical characterization of TE activity is a laborious undertaking, and will predominantly fail to produce desired cyclic metabolites. However, inherent value gained from these experiments is the mapping of specificity and selectivity profiles for the enzymes. In the event a suitable TE is not identified by these studies, the characterization data will support future, and yet identified avenues of research. For example, our unprecedented DEBS TE-mediated formations of C_2-symmetrical diolide **7.44** and linear dimeric metabolites like **7.42** represented an intriguing and relatively-rare variation in the mode of polyketide release from type-I PKS assembly lines.[124,125] Uncovering details to the molecular basis for such catalysis could enable a novel, mild, chemoenzymatic route to novel frameworks and possible drug candidates.

7.4 Concluding Remarks

Nature's evolution of strategies to assemble polyketide architectures has been a focal interest of interdisciplinary research programs dedicated to designing methods of innovative drug development, and sustainable alternatives to generate bioactive natural products. The theme of this dissertation was toward harnessing the potential of PKS biosynthetic systems for chemoenzymatic synthesis of polyketide natural products. Chemoenzymatic research provides an accelerated route to achieving biosynthetic fidelity with non-native systems based on strong, mechanistic, chemical, and biochemical understandings of the enzymatic systems. However, as noted by Keasling and coworkers in a recent review,[126] there exists a notable gap between the promise and reality of exploiting PKS machinery as a useful platform for accessing complex molecules. Encouragingly, the actual use of biosynthetic systems as chemoenzymatic tools has begun to bridge-the-gap with hypothetical applications due to increased knowledge of their enzymology,[127] and into structural features that mediate these protein-protein interactions.[128] This dissertation continued to narrow the divide between promise and reality for chemoenzymatic platforms. My cumulative results have begun to elucidate key details to fulfil the potential of PKS engineering of individual catalytic domains like DEBS TE, or engineered *de novo* pathways for products lacking genomic information, like neopeltolide.

7.5 References

(1) Yuzawa, S.; Keasling, J. D.; Katz, L. *J. Antibiot.* **2016**, *69* (7), 494–499.
(2) Butler, M. S.; Robertson, A. A. B.; Cooper, M. A. *Nat. Prod. Rep.* **2014**, *31* (11), 1612–1661.
(3) Schwecke, T.; Aparicio, J. F.; Molnár, I.; König, A.; Khaw, L. E.; Haydock, S. F.; Oliynyk, M.; Caffrey, P.; Cortés, J.; Lester, J. B.; Böhm, G.; Staunton, J.; Leadlay, P. F. *Proc. Natl. Acad. Sci.* **1995**, *92* (17), 7839–7843.
(4) Bauer, A. In *Topics in Heterocyclic Chemistry*; Cossy, J., Ed.; Springer, 2016; pp 209–270.
(5) Altmann, K.-H.; Gaugaz, F. Z.; Schiess, R. *Mol. Divers.* **2011**, *15*, 383–399.
(6) Newman, D. J.; Cragg, G. M. *J. Nat. Prod.* **2016**, *79* (3), 629–661.
(7) Denvir, J.; Neitch, S.; Fan, J.; Niles, R. M.; Boskovic, G.; Schreurs, B. G.; Primerano, D. A.; Alkon, D. L. *J. Alzheimers Dis.* **2015**, *46* (2), 483–490.
(8) Rothmeier, A. S.; Schneiders, U. M.; Wiedmann, R. M.; Ischenko, I.; Bruns, C. J.; Rudy, A.; Zahler, S.; Vollmar, A. M. *Int. J. Cancer* **2010**, *127* (5), 1096–1105.
(9) Bon, R. S.; Waldmann, H. *Acc. Chem. Res.* **2010**, *43* (8), 1103–1114.
(10) Wang, M.; Boddy, C. N. *Biochemistry* **2008**, *47* (45), 11793–11803.
(11) Pinto, A.; Wang, M.; Horsman, M.; Boddy, C. N. *Org. Lett.* **2012**, *14* (9), 2278–2281.
(12) Pinto, A.; Boddy, C. N. *Bioorg. Med. Chem. Lett.* **2012**, *22* (16), 5253–5256.
(13) Cole Stevens, D.; Henry, M. R.; Murphy, K. A.; Boddy, C. N. *Appl. Environ. Microbiol.* **2010**, *76* (8), 2681–2683.
(14) Hari, T. P. A.; Wilke, B. I.; Davey, J. A.; Boddy, C. N. *J. Org. Chem.* **2016**, *81*, 415–423.
(15) Hari, T. P. A.; Labana, P.; Boileau, M.; Boddy, C. N. *ChemBioChem* **2014**, *15* (18), 2656–2661.
(16) Wright, A. E.; Botelho, J. C.; Guzmán, E.; Harmody, D.; Linley, P.; McCarthy, P. J.; Pitts, T. P.; Pomponi, S.; Reed, J. K. *J. Nat. Prod.* **2007**, *70* (3), 412–416.
(17) Fuwa, H. *Mar. Drugs* **2016**, *14* (65).
(18) Yang, J.; Xue, H. In *Stereoselective Synthesis of Drugs and Natural Products*; John Wiley & Sons, Inc., 2013; pp 551–581.
(19) Ito, H.; Inoue, T.; Iguchi, K. *Org. Lett.* **2008**, *10* (17), 3873–3876.
(20) Beesley, R. M.; Ingold, C. K.; Thorpe, J. F. *J. Chem. Soc. Trans.* **1915**, *107*, 1080–1106.
(21) Oh, S. H.; Rho, H. S.; Lee, J. W.; Lee, J. E.; Youk, S. H.; Chin, J.; Song, C. E. *Angew. Chem. Int. Ed.* **2008**, *47* (41), 7872–7875.
(22) Peschiulli, A.; Gun, Y.; Connon, S. J.; Enzymes, G. M. I. *J. Org. Chem.* **2008**, *73*, 2454–2457.
(23) Park, S. E.; Nam, E. H.; Jang, H. Bin; Oh, J. S.; Some, S.; Lee, Y. S.; Song, C. E. *Adv. Synth. Catal.* **2010**, *352* (13), 2211–2217.
(24) Gopinath, P.; Watanabe, T.; Shibasaki, M. *Org. Lett.* **2012**, *14* (5), 1358–1361.
(25) Heathcock, C. H.; Hadley, C. R.; Rosen, T.; Theisen, P. D.; Hecker, S. J. *J. Med. Chem.* **1987**, *30* (10), 1858–1873.
(26) Lam, L. K. P.; Hui, R. H. F.; Jones, J. B. *J. Org. Chem.* **1986**, *51* (11), 2047–2050.
(27) Metzner, R.; Hummel, W.; Wetterich, F.; König, B.; Gröger, H. *Org. Process Res. Dev.* **2015**, *19* (6), 635–638.
(28) Radosevich, A. T.; Chan, V. S.; Shih, H. W.; Toste, F. D. *Angew. Chem. Int. Ed.* **2008**, *47* (20), 3755–3758.
(29) Taylor, R. E.; Kartika, R.; Gruffi, T. R. *Org. Lett.* **2008**, *10* (21), 5047–5050.
(30) Martinez-Solorio, D.; Jennings, M. P. *J. Org. Chem.* **2010**, *75* (12), 4095–4104.
(31) Yang, Z.; Zhang, B.; Zhao, G.; Yang, J.; Xie, X.; She, X. *Org. Lett.* **2011**, *13* (21), 5916–5919.
(32) Fuwa, H.; Kawakami, M.; Noto, K.; Muto, T.; Suga, Y. *Chem. Eur. J.* **2013**, *19*, 8100–8110.
(33) Ermanis, K.; Hsiao, Y.-T.; Kaya, U.; Jeuken, A.; Clarke, P. A. *Chem. Sci.* **2017**, *8*, 482–490.
(34) Fuwa, H.; Ichinokawa, N.; Noto, K.; Sasaki, M. *J. Org. Chem.* **2012**, *77*, 2588–2607.
(35) Petri, A. F.; Bayer, A.; Maier, M. E. *Angew. Chem. Int. Ed.* **2004**, *43*, 5821–5823.
(36) Boddy, C. N.; Schneider, T. L.; Hotta, K.; Walsh, C. T.; Khosla, C. *J. Am. Chem. Soc.* **2003**, *125* (12), 3428–3429.
(37) Wang, M.; Opare, P.; Boddy, C. N. *Bioorg. Med. Chem. Lett.* **2009**, *19* (5), 1413–1415.
(38) Pöplau, P.; Frank, S.; Morinaka, B. I.; Piel, J. *Angew. Chem. Int. Ed.* **2013**, *52*, 13215–13218.
(39) Ueoka, R.; Uria, A. R.; Reiter, S.; Mori, T.; Karbaum, P.; Peters, E. E.; Helfrich, E. J. N.; Morinaka, B. I.; Gugger, M.; Takeyama, H.; Matsunaga, S.; Piel, J. *Nat. Chem. Biol.* **2015**, *11* (9), 705–712.
(40) Luhavaya, H.; Dias, M. V. B.; Williams, S. R.; Hong, H.; Oliveira, L. G. De; Leadlay, P. F. *Angew. Chem.*

Int. Ed. **2015**, *54*, 13622–13625.
(41) Berkhan, G.; Hahn, F. *Angew. Chem. Int. Ed.* **2014**, *53*, 14240–14244.
(42) Unpublished details from a collaborating colleague.
(43) Weissman, K. J.; Müller, R. *ChemBioChem* **2008**, *9* (6), 826–848.
(44) Menzella, H. G.; Reid, R.; Carney, J. R.; Chandran, S. S.; Reisinger, S. J.; Patel, K. G.; Hopwood, D.; Santi, D. V. *Nat. Biotechnol.* **2005**, *23* (9), 1171–1176.
(45) Chandran, S. S.; Menzella, H. G.; Carney, J. R.; Santi, D. V. *Chem. Biol.* **2006**, *13* (5), 469–474.
(46) Menzella, H. G.; Carney, J. R.; Santi, D. V. *Chem. Biol.* **2007**, *14* (2), 143–151.
(47) Aldrich, C. C.; Venkatraman, L.; Sherman, D. H.; Fecik, R. A. *J. Am. Chem. Soc.* **2005**, *127* (25), 8910–8911.
(48) Cane, D. E. *J. Biol. Chem.* **2010**, *285* (36), 27517–27523.
(49) Sherman, D. H. *Nat. Biotechnol.* **2005**, *23* (9), 1083–1084.
(50) Ishida, K.; Lincke, T.; Hertweck, C. *Angew. Chem. Int. Ed.* **2012**, *51* (22), 5470–5474.
(51) Wilkinson, A. L.; Hanefeld, U.; Wilkinson, B.; Leadlay, P. F.; Staunton, J. *Tetrahedron Lett.* **1998**, *39*, 9827–9830.
(52) Akagawa, K.; Kudo, K. *Chem. Commun.* **2017**, DOI: 10.1039/C7CC04033D.
(53) Yu, Z.; Liu, X.; Dong, Z.; Xie, M.; Feng, X. *Angew. Chem. Int. Ed.* **2008**, *47*, 1308–1311.
(54) Aggarwal, R.; Caffrey, P.; Leadlay, P. F.; Smith, C. J.; Staunton, J. *J. Chem. Soc., Chem. Commun.* **1995**, 1519–1520.
(55) McDaniel, R.; Kao, C. M.; Fu, H.; Hevezi, P.; Gustafsson, C.; Betlach, M.; Ashley, G.; Cane, D. E.; Khosla, C. *J. Am. Chem. Soc.* **1997**, *119*, 4309–4310.
(56) Lowry, B.; Robbins, T.; Weng, C.-H.; O'Brien, R. V; Cane, D. E. *J. Am. Chem. Soc.* **2013**, *135*, 16809–16812.
(57) Weissman, K. J.; Bycroft, M.; Cutter, A. L.; Hanefeld, U.; Frost, E. J.; Timoneyl, M. C.; Harris, R.; Handa, S.; Roddis, M.; Staunton, J.; Leadlay, P. F. *Chem. Biol.* **1998**, *5* (12), 743–754.
(58) Cortes, J.; Wiesmann, K. E. H.; Roberts, G. A.; Brown, M. J. B.; Staunton, J.; Leadlay, P. F. *Science,* **1995**, *268*, 1487–1489.
(59) Kao, C. M.; Luo, G.; Katz, L.; Cane, D. E.; Khosla, C. *J. Am. Chem. Soc.* **1995**, *117*, 9105–9106.
(60) Staunton, J.; Wilkinson, B. *Chem. Rev.* **1997**, *97*, 2611–2629.
(61) Kao, C. M.; Luo, G.; Katz, L.; Cane, D. E.; Khosla, C. *J. Am. Chem. Soc.* **1996**, *118*, 9184–9185.
(62) Regentin, R.; Kennedy, J.; Wu, N.; Carney, J. R.; Licari, P.; Galazzo, J.; Desai, R. *Biotechnol. Prog.* **2004**, *20*, 122–127.
(63) Córdova, A.; Engqvist, M.; Ibrahem, I.; Casas, J.; Sunden, H. *Chem. Commun.* **2005**, No. 15, 2047–2049.
(64) Casas, J.; Engqvist, M.; Ibrahem, I.; Kaynak, B.; Córdova, A. *Angew. Chem. Int. Ed.* **2005**, *44* (9), 1343–1345.
(65) Northrup, A. B.; MacMillan, D. W. C. *Science,* **2004**, *305*, 1752–1754.
(66) Hughes, A. J.; Tibby, M. R.; Wagner, D. T.; Brantley, J. N.; Keatinge-Clay, A. T. *Chem. Commun. (Camb).* **2013**.
(67) Koryakina, I.; Kasey, C.; McArthur, J. B.; Lowell, A. N.; Chemler, J. A.; Li, S.; Hansen, D. A.; Sherman, D. H.; Williams, G. J. *ACS Chem. Biol.* **2017**, *12* (1), 114–123.
(68) Patterson, D. M.; Nazarova, L. A.; Prescher, J. A. *ACS Chem. Biol.* **2014**, *9*, 592–605.
(69) Mckay, C. S.; Finn, M. G. *Chem. Biol.* **2014**, *21*, 1075–1101.
(70) Sletten, E. M.; Bertozzi, C. R. *Angew. Chem. Int. Ed.* **2009**, *48*, 6974–6998.
(71) Riva, E.; Wilkening, I.; Gazzola, S.; Li, W. M. A.; Smith, L.; Leadlay, P. F.; Tosin, M. *Angew. Chem. Int. Ed.* **2014**, *53*, 11944–11949.
(72) Dupuis, S. N.; Robertson, A. W.; Veinot, T.; Monro, S. M. A.; Douglas, S. E.; Syvitski, R. T.; Goralski, K. B.; McFarland, A.; Jakeman, D. L. *Chem. Sci.* **2012**, *3*, 1640–1644.
(73) Kennedy, J. *Nat. Prod. Rep.* **2008**, *25*, 25–34.
(74) Franke, J.; Hertweck, C. *Cell Chem. Biol.* **2016**, *23*, 1179–1192.
(75) Sharma, K. K.; Boddy, C. N. *Bioorg. Med. Chem. Lett.* **2007**, *17* (11), 3034–3037.
(76) Aldrich, C. C.; Beck, B. J.; Fecik, R. A.; Sherman, D. H. *J. Am. Chem. Soc.* **2005**, *127*, 8441–8452.
(77) Hansen, D. A.; Rath, C. M.; Eisman, E. B.; Narayan, A. R. H.; Kittendorf, J. D.; Mortison, J. D.; Yoon, Y. J.; Sherman, D. H. *J. Am. Chem. Soc.* **2013**, *135* (30), 11232–11238.
(78) Hansen, D. A.; Koch, A. A.; Sherman, D. H. *J. Am. Chem. Soc.* **2015**, *137* (11), 3735–3738.
(79) He, W.; Wu, J.; Khosla, C.; Cane, D. E. *Bioorg. Med. Chem. Lett.* **2006**, *16*, 391–394.
(80) Horsman, M. E.; Hari, T. P. A.; Boddy, C. N. *Nat. Prod. Rep.* **2016**, *33*, 183–202.

(81) Zhou, H.; Qiao, K.; Gao, Z.; Vederas, J. C.; Tang, Y. *J. Biol. Chem.* **2010**, *285* (53), 41412–41421.
(82) Heberlig, G. W.; Wirz, M.; Wang, M.; Boddy, C. N. *Org. Lett.* **2014**, *16*, 5858–5861.
(83) Trauger, J. W.; Kohli, R. M.; Mootz, H. D.; Marahiel, M. A.; Walsh, C. T. *Nature* **2000**, *407* (6801), 215–218.
(84) Kohli, R. M.; Walsh, C. T.; Burkart, M. D. *Nature* **2002**, *418*, 658–661.
(85) Seufert, W.; Beck, Z. Q.; Sherman, D. H. *Angew. Chem. Int. Ed.* **2007**, *46*, 9298–9300.
(86) Machida, K.; Arisawa, A.; Takeda, S.; Tsuchida, T.; Aritoku, Y.; Yoshida, M.; Ikeda, H. *Biosci. Biotech. Biochem.* **2008**, *72* (11), 2946–2952.
(87) Sakai, T.; Sameshima, T.; Matsfuji, M.; Kawamura, N.; Dobashi, K.; Mizui, Y. *J. Antibiot.* **2004**, *57* (3), 173–179.
(88) He, J.; Sundararajan, A.; Devitt, N. P.; Schilkey, F. D.; Ramaraj, T.; Melançon III, C. E. *Genome Announc.* **2016**, *4* (3), 1–2.
(89) Akey, D. L.; Kittendorf, J. D.; Giraldes, J. W.; Fecik, R. A.; Sherman, D. H.; Smith, J. L. *Nat. Chem. Biol.* **2006**, *2* (10), 537–542.
(90) Henkel, W.; Brockmann, H. *Antibiot. aus Actinomyceten* **1951**, *84*, 284–288.
(91) Oliynyk, M.; Samborskyy, M.; Lester, J. B.; Mironenko, T.; Scott, N.; Dickens, S.; Haydock, S. F.; Leadlay, P. F. *Nat. Biotechnol.* **2007**, *25*, 447–453.
(92) Tsai, S.-C.; Miercke, L. J. W.; Krucinski, J.; Gokhale, R.; Chen, J. C.-H.; Foster, P. G.; Cane, D. E.; Khosla, C.; Stroud, R. M. *Proc. Natl. Acad. Sci.* **2001**, *98* (26), 14808–14813.
(93) McGuire, J. M.; Bunch, R. L.; Anderson, R. C.; Boaz, H. E.; Flynn, E. H.; Powell, H. M.; Smith, J. W. *Antibiot. Chemother.* **1952**, *2*, 281.
(94) Molnár, I.; Schupp, T.; Ono, M.; Zirkle, R.; Milnamow, M.; Nowak-Thompson, B.; Engel, N.; Toupet, C.; Stratmann, A.; Cyr, D. D.; Gorlach, J.; Mayo, J. M.; Hu, A.; Goff, S.; Schmid, J.; Ligon, J. M. *J. Chem. Biol.* **2000**, *7* (2), 97–109.
(95) Höfle, G.; Bedorf, N.; Steinmetz, H.; Schomburg, D.; Gerth, K.; Reichenbach, H. *Angew. Chem. Int. Ed.* **1996**, *35* (13), 1567–1569.
(96) Fouces, R.; Mellado, E.; Diez, B.; Barredo, J. L. *Microbiology* **1999**, *145*, 855–869.
(97) Hamill, R. L.; Haney Jr., M. E.; Stamper, M.; Wiley, P. F. *Antibiot. Chemother.* **1961**, *May*, 328–334.
(98) Schupp, T.; Toupet, C.; Cluzel, B.; Neff, S.; Hill, S.; Beck, J. J.; Ligon, J. M. *J. Bacteriol.* **1995**, *177* (13), 3673–3679.
(99) Bedorf, N.; Schomburg, D.; Gerth, K.; Reichenbach, H.; Höfle, G. *Liebigs. Ann. Chem.* **1993**, 1017–1021.
(100) Aparicio, J. F.; Colina, A. J.; Ceballos, E.; Martı, J. F. *J. Biol. Chem.* **1999**, *274* (15), 10133–10139.
(101) Edelstein, P. H.; Edelstein, M. A. C. *J. Clin. Microbiol.* **1996**, *34* (1), 185–187.
(102) Xu, Y.; Espinosa-artiles, P.; Schubert, V.; Xu, Y.; Zhang, W.; Lin, M.; Gunatilaka, A. A. L. *Appl. Environ. Microbiol.* **2013**, *79* (6), 2038–2047.
(103) Musgrave, O. C. *J. Chem. Soc.* **1956**, 4301–4305.
(104) Munro, H. D.; Musgrave, O. C.; Templeton, R. *J. Chem. Soc.* **1967**, 947–948.
(105) Reeves, C. D.; Hu, Z.; Reid, R.; Kealey, J. T. *Appl. Environ. Microbiol.* **2008**, *74* (16), 5121–5129.
(106) Nozawa, K.; Nakajima, S. *J. Nat. Prod.* **1979**, *42* (9), 374–377.
(107) Kim, Y.-T.; Lee, Y.-R.; Jin, J.; Han, K.-H.; Kim, H.; Kim, J.-C.; Lee, T.; Yun, S.-H.; Lee, Y.-W. *Mol. Microbiol.* **2005**, *58* (4), 1102–1113.
(108) Chelkowski, J.; Visconti, A.; Manka, M. *Nahrung* **1984**, *28* (5), 493–496.
(109) Olano, C.; Wilkinson, B.; Moss, S. J.; Braña, A. F.; Méndez, C.; Leadlay, P. F. *Chem. Commun.* **2003**, 2780–2782.
(110) Keller-Schierlein, W. *Helv. Chim. Acta* **1967**, *50*, 731–753.
(111) Magarvey, N. A.; Beck, Z. Q.; Golakoti, T.; Ding, Y.; Huber, U.; Hemscheidt, T. K.; Abelson, D.; Moore, R. E.; Sherman, D. H. *ACS Chem. Biol.* **2006**, *1* (12), 766–779.
(112) Schwartz, E.; Hirsch, C. F.; Sesin, D. F.; Flor, J. E.; Chartrain, M.; Fromtling, E.; Harris, G. H.; Salvatore, M. J.; Liesch, J. M.; Yudin, K. *J. Ind. Microbiol. Biotech.. Microbiol.* **1990**, *5*, 113–123.
(113) Trimurtulu, G.; Ohtani, K.; Patterson, G. M. L.; Moore, R. E.; Corbett, T. H.; Valeriote, F. A.; Demchiko, L. *J. Am. Chem. Soc.* **1994**, *116*, 4729–4737.
(114) Eppelmann, K.; Doekel, S.; Marahiel, M. A. *J. Biol. Chem.* **2001**, *276* (37), 34824–34831.
(115) Johnson, B. A.; Anker, H.; Meleney, F. L. *Science,* **1945**, *102* (2650), 376–377.
(116) Cosmina, P.; Rodriguez, F.; de Ferra, F.; Grandi, G.; Perego, M.; Venema, G.; van Sinderen, D. *Mol. Microbiol.* **1993**, *8* (5), 821–831.
(117) Koglin, A.; Löhr, F.; Bernhard, F.; Rogov, V. V.; Frueh, D. P.; Strieter, E. R.; Mofid, M. R.; Güntert, P.;

Wagner, G.; Walsh, C. T.; Marahiel, M. A.; Dötsch, V. *Nature* **2008**, *454*, 907–912.
(118) Arima, K.; Kakinuma, A.; Tamura, G. *Biochem. Biophys. Res. Commun.* **1968**, *31* (3), 488–494.
(119) Mittenhuber, G.; Weckermann, R.; Marahiel, M. A. *J. Bacteriol.* **1989**, *171* (9), 4881–4887.
(120) Battersby, A. R.; Craig, L. C. *J. Am. Chem. Soc.* **1952**, *74* (16), 4019–4023.
(121) Haydock, S. F.; Mironenko, T.; Ghoorahoo, H. I.; Leadlay, P. F. *J. Biotechnol.* **2004**, *113* (1–3), 55–68.
(122) Matter, A. M.; Hoot, S. B.; Anderson, P. D.; Neves, S. S.; Cheng, Y.-Q. *PLoS One* **2009**, *4* (9), e7194.
(123) Ehling-Schulz, M.; Fricker, M.; Grallert, H.; Rieck, P.; Wagner, M.; Scherer, S. *BMC Microbiol.* **2006**, *6* (20), 1–11.
(124) Sharma, G. V. M.; Doddi, V. R. In *Natural Lactones and Lactams: Synthesis, Occurence and Biological Activity*; Janecki, T., Ed.; Wiley-VCH, 2014; pp 229–272.
(125) Zhou, Y.; Prediger, P.; Dias, L. C.; Murphy, A. C.; Leadlay, P. F. *Angew. Chem.* **2015**, *127*, 5321–5324.
(126) Poust, S.; Hagen, A.; Katz, L.; Keasling, J. D. *Curr. Opin. Biotechnol.* **2014**, *30*, 32–39.
(127) Khosla, C.; Herschlag, D.; Cane, D. E.; Walsh, C. T. *Biochemistry* **2014**, *53* (18), 2875–2883.
(128) Keatinge-Clay, A. T. *Nat. Prod. Rep.* **2012**, *29* (10), 1050–1073.

· Appendix I ·

Spectroscopic Data

S1.1 General Procedures

1-D and 2-D NMR spectra were recorded on Bruker Avance 300 or 400 MHz, Bruker Avance II 300 MHz, or Bruker Avance III 600 MHz instruments. Spectra were calibrated using residual undeuterated solvent ($CDCl_3$: δ H = 7.26 ppm, δ C = 77.0 ppm; D_2O: δ H = 4.79 ppm; CD_3CN: δ H = 1.94 ppm, δ C = 1.3, 118.3 ppm; CD_3OD: δ H = 3.31 ppm, δ C = 49.0 ppm; THF-d_8: δ H = 2.08, 6.97, 7.01, 7.09 ppm, δ C = 67.2, 25.3 ppm; $(CD_3)_2SO$ δ H = 2.50 ppm, δ C = 39.5 ppm;) as internal reference.

LC-SPE-NMR spectra were conducted using an Agilent 1260 interfaced with a Prospekt 2 (Spark Holland) solid-phase extraction module, using HySphere Resin GP cartridges. Separation relied on a reverse phase Agilent Zorbax C18 column (100 mm × 2.1 mm I.D., 3.5 µm particle size). Mobile phases throughout analysis were water (H_2O, Phase A) and acetonitrile (MeCN, Phase B). The chromatography method had a flow-rate of 0.25 mL/min. The mobile phase was held at 30% Phase B over 3 minutes, followed by a linear gradient to 100% Phase B over 14 minutes. A 4-minute hold at 100% Phase B flushed the column and was re-equilibrated at 30% Phase B for an additional 4-minutes, for a total run-time of 25 minutes. Peak-trapping was conducted over the entire run into new cartridges, at 5-minute intervals (total of 5 cartridges). Ten trapping experiments were performed with trapping on the same set of solid-phase cartridges. Compounds were eluted from the cartridges using deuterated acetonitrile (CD_3CN, 60 µL), and NMR spectra was recorded on a Bruker Avance III instrument, with cryoprobe operating at 600 MHz.

ESI-LC-MS/MS analysis was performed on an API2000 LC-MS/MS System (Applied Biosystems), equipped with a turbo-ion spray ESI probe interfaced with a Prominence UFLC (Shimadzu). A reverse phase BDS Hypersil C18 column (100 mm × 2.1 mm I.D., 3 µm particle size; Thermo Scientific) was employed. Mobile phases throughout experimental were 5% MeCN:95% H_2O with 0.05% formic acid (Phase A), and 95% MeCN:5% H_2O with 0.05% formic acid (Phase B). Chemical separation was performed using a gradient from 0% Phase B to 100% Phase B over 30 min, with a flow rate of 0.2 mL/min. HPLC UV absorption was monitored using 210 nm and 254 nm channels. Tandem mass spectrometry was performed using an ionization voltage of 5500 V, and probe temperature of 250 °C were used in the ESI TurboSpray probe, and masses were scanned over 300 – 800 *m*/*z*.

S1.2 A Transannular Oxa-Conjugate Addition Model of Neopeltolide (Chapter 3)

S1.2.1 First-Generation α,β-Unsaturated Ketone Model v1.1 (§ 3.5.1)

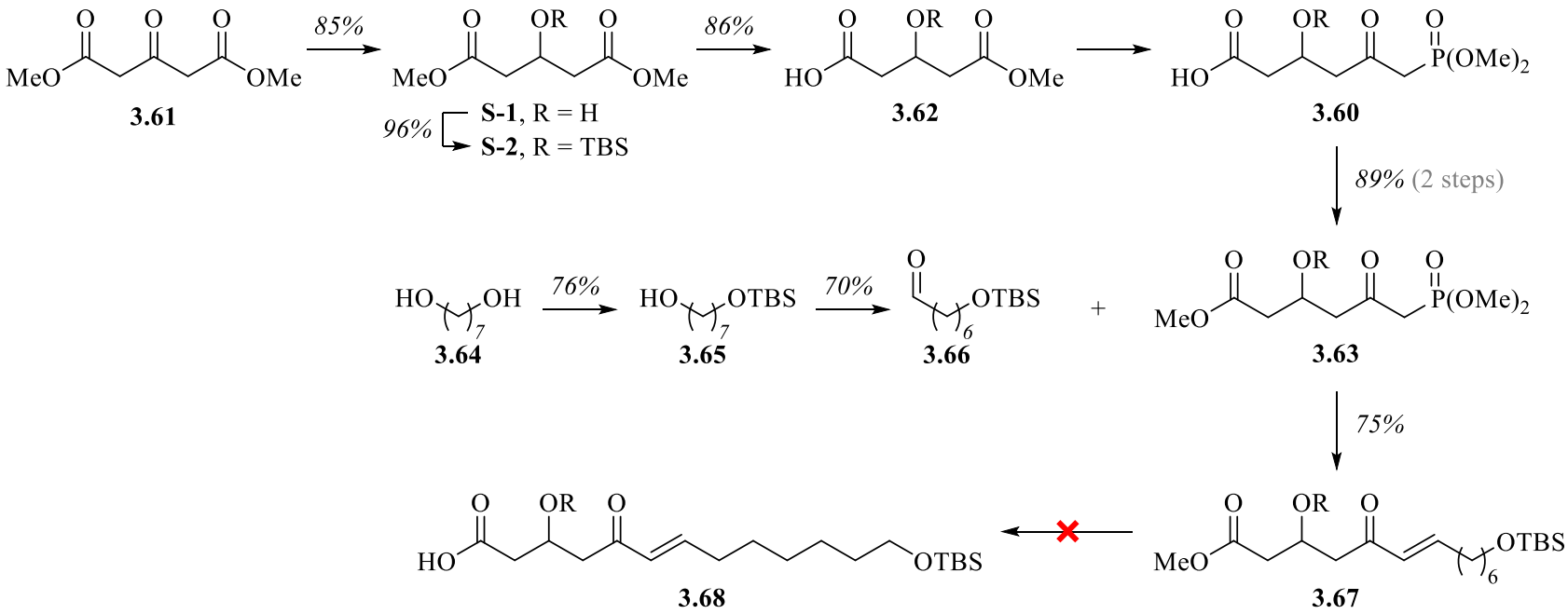

Figure S1 – Summary of the synthesis of first-generation *α,β*-unsaturated ketone model version 1.1.

Dimethyl-3-hydroxypentanedioate (**S-1**)

^{1}H NMR (400 MHz, $CDCl_3$)

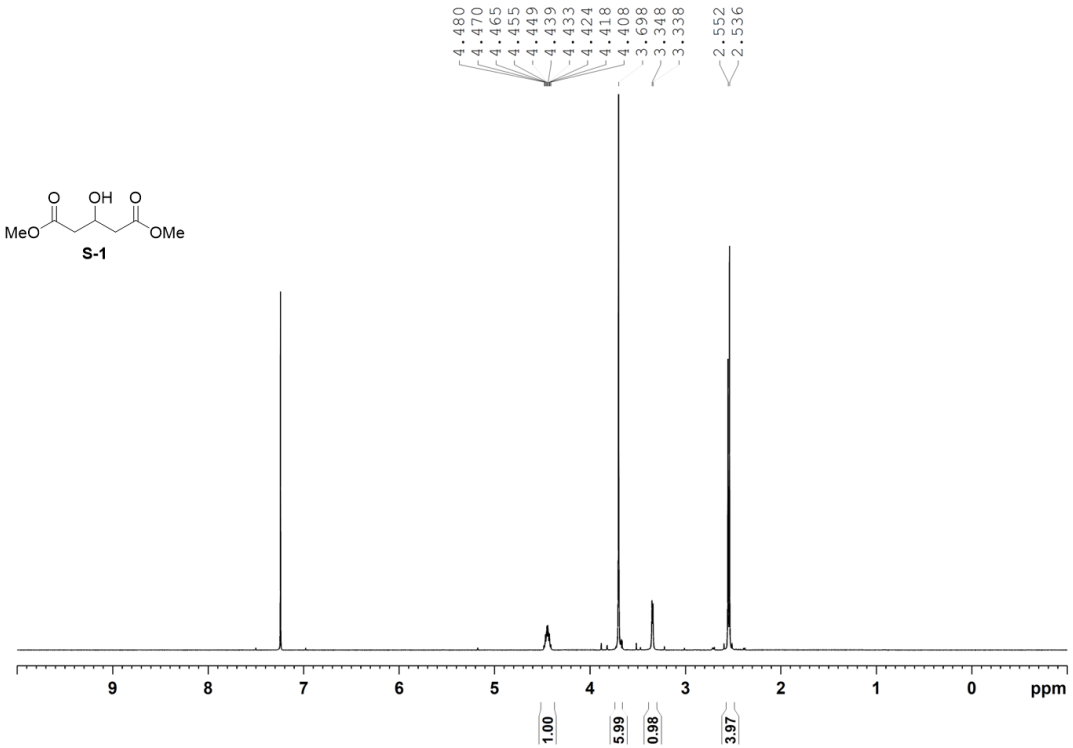

Dimethyl-3-hydroxypentanedioate (**S-1**)

^{13}C NMR (100 MHz, $CDCl_3$)

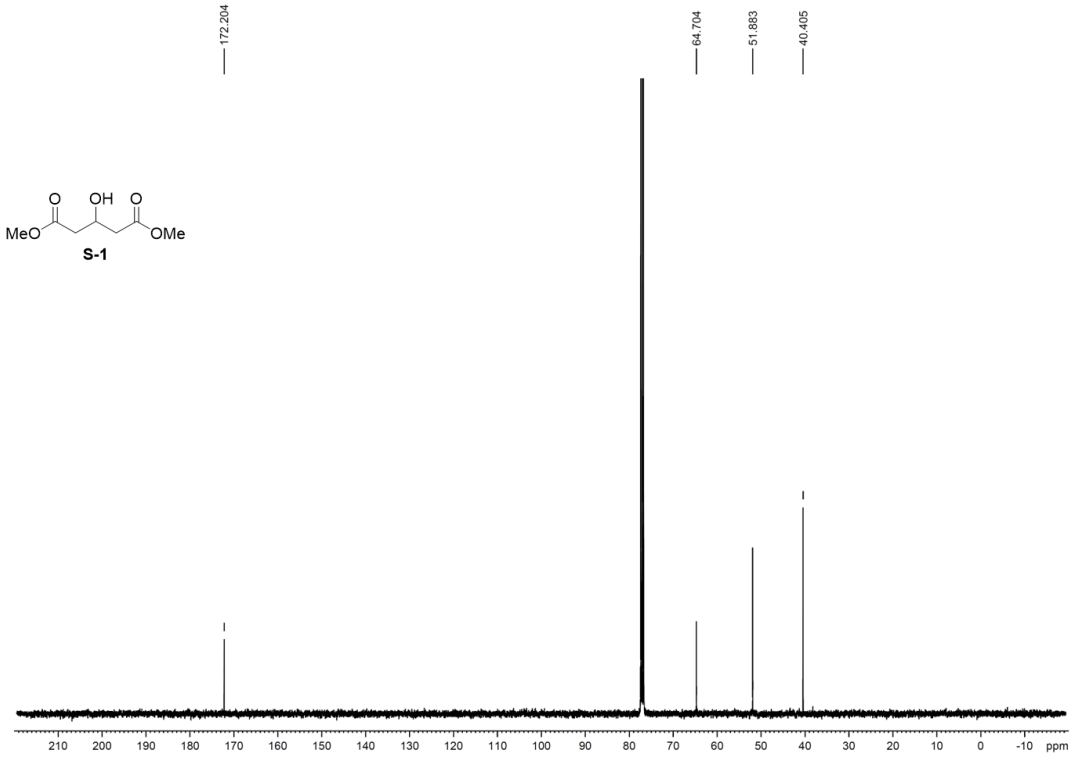

Dimethyl-3-(*tert*-butyldimethylsilyloxy)pentanedioate (**S-2**)

^{1}H NMR (300 MHz, $CDCl_3$)

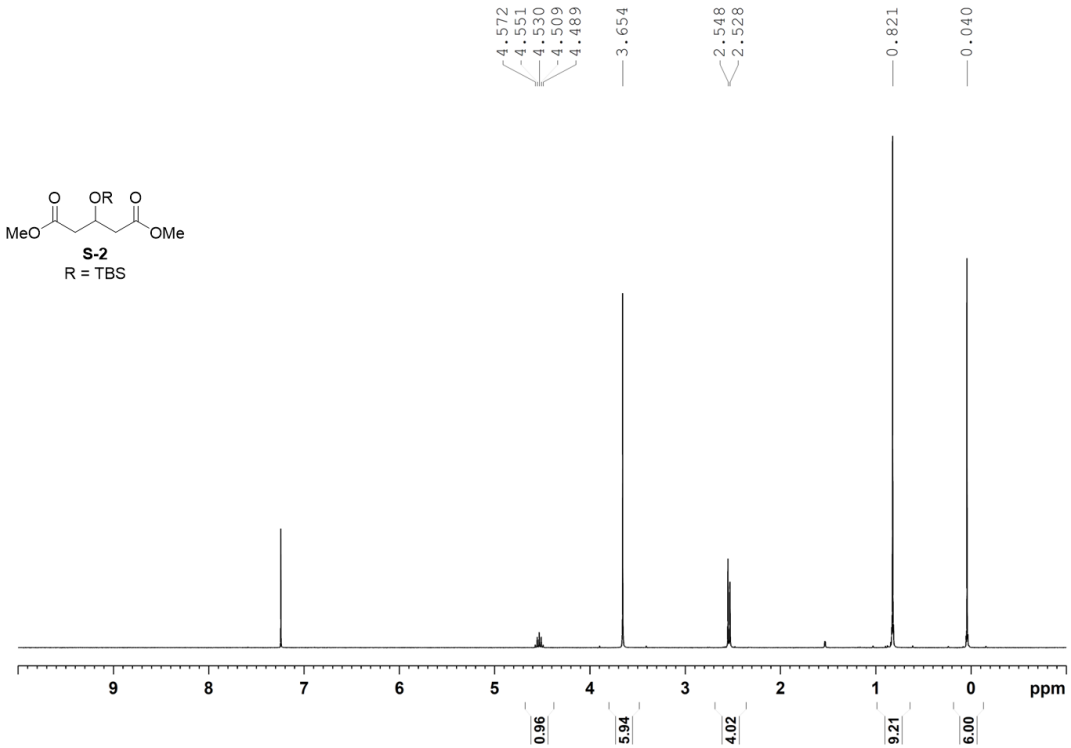

Dimethyl-3-(*tert*-butyldimethylsilyloxy)pentanedioate (**S-2**)

^{13}C NMR (100 MHz, $CDCl_3$)

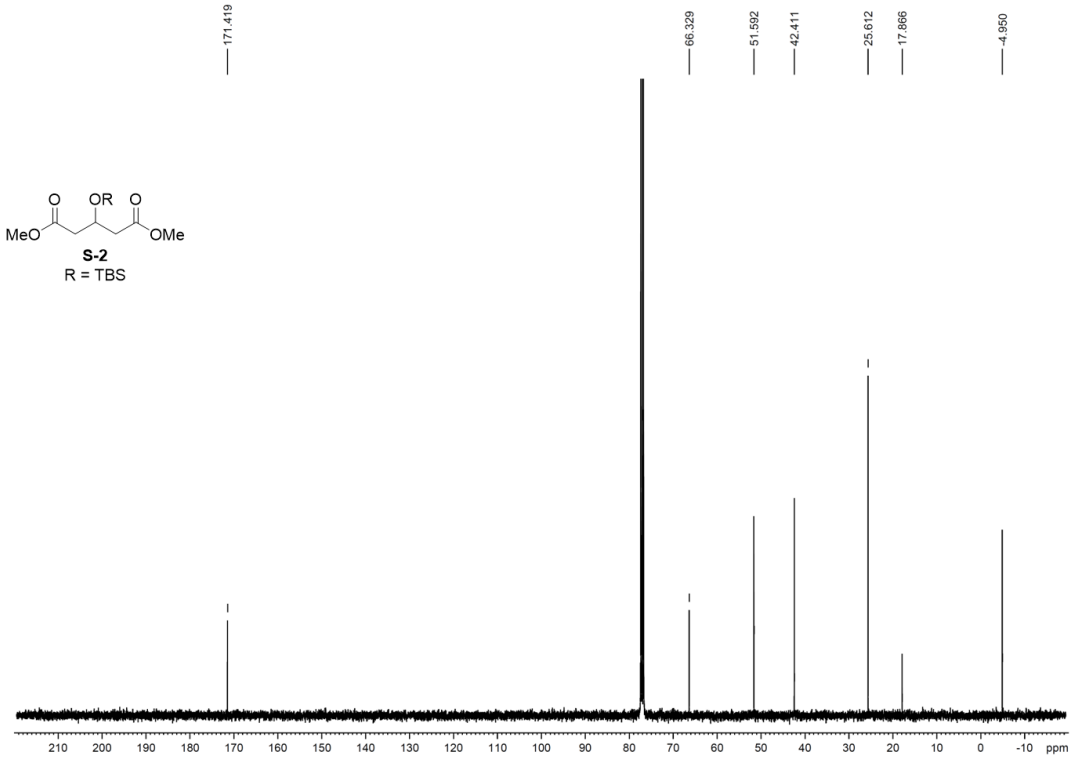

3-(*tert*-Butyldimethylsilyloxy)-5-methoxy-5-oxopentanoic acid (**3.62**)

^{1}H NMR (300 MHz, $CDCl_3$)

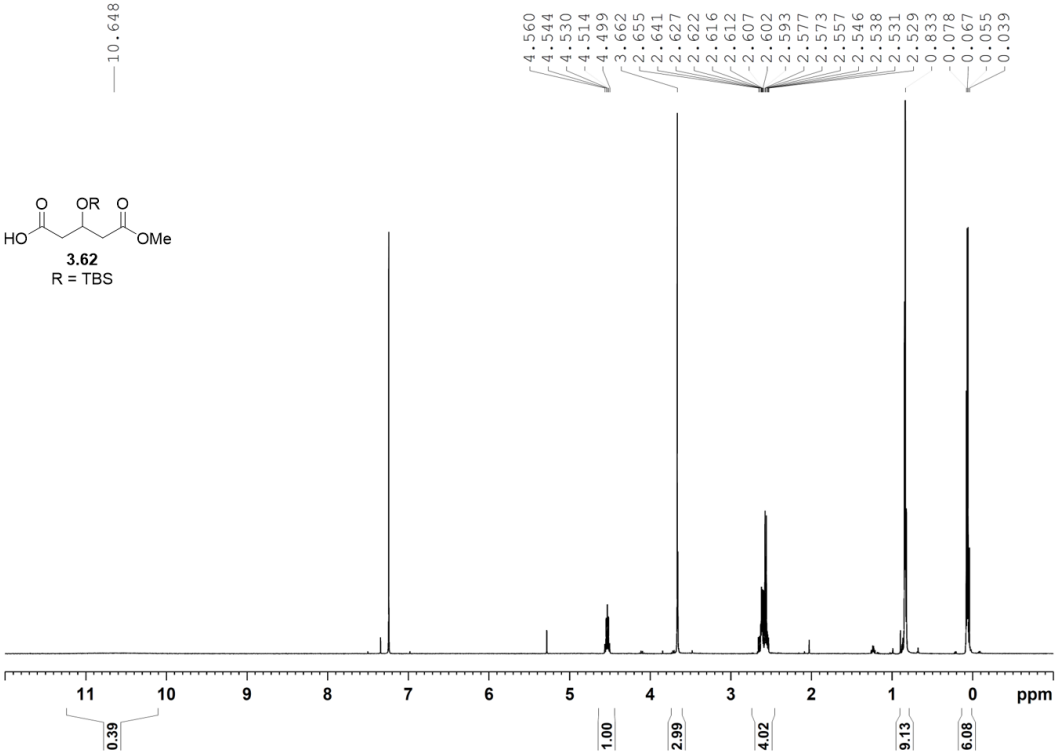

3-(*tert*-Butyldimethylsilyloxy)-5-methoxy-5-oxopentanoic acid (**3.62**)

^{13}C NMR (100 MHz, $CDCl_3$)

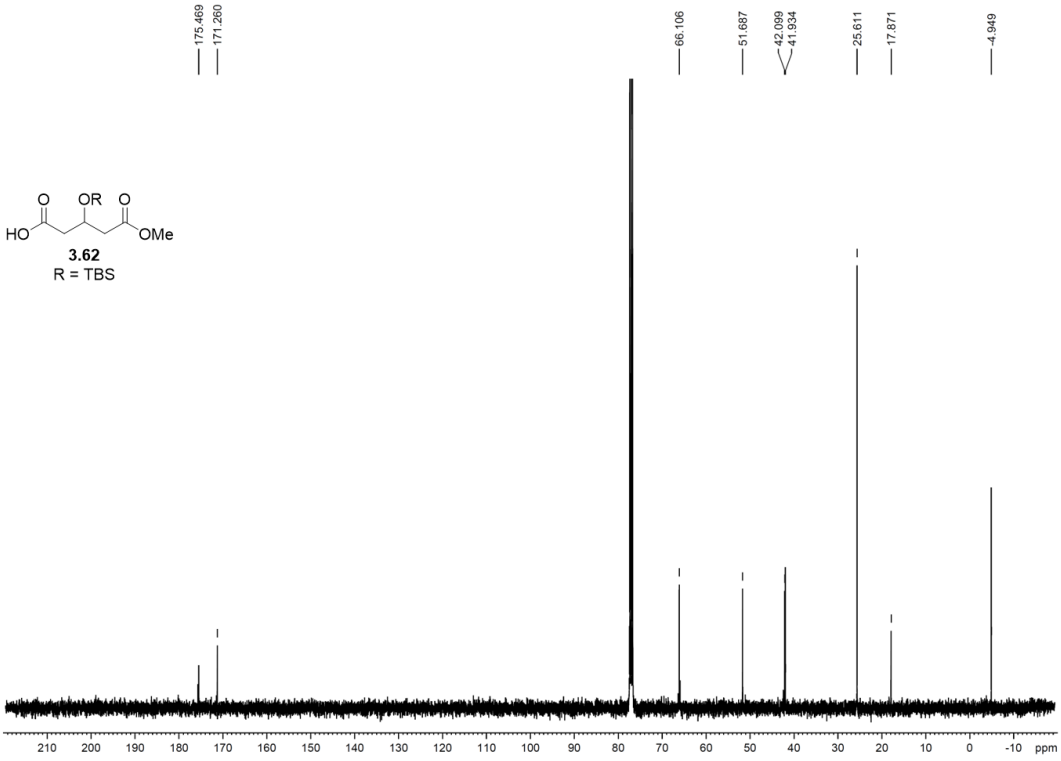

3-(*tert*-Butyldimethylsilyloxy)-6-(dimethoxyphosphoryl)-5-oxohexanoic acid (**3.60**)

^{1}H NMR (300 MHz, $CDCl_3$)

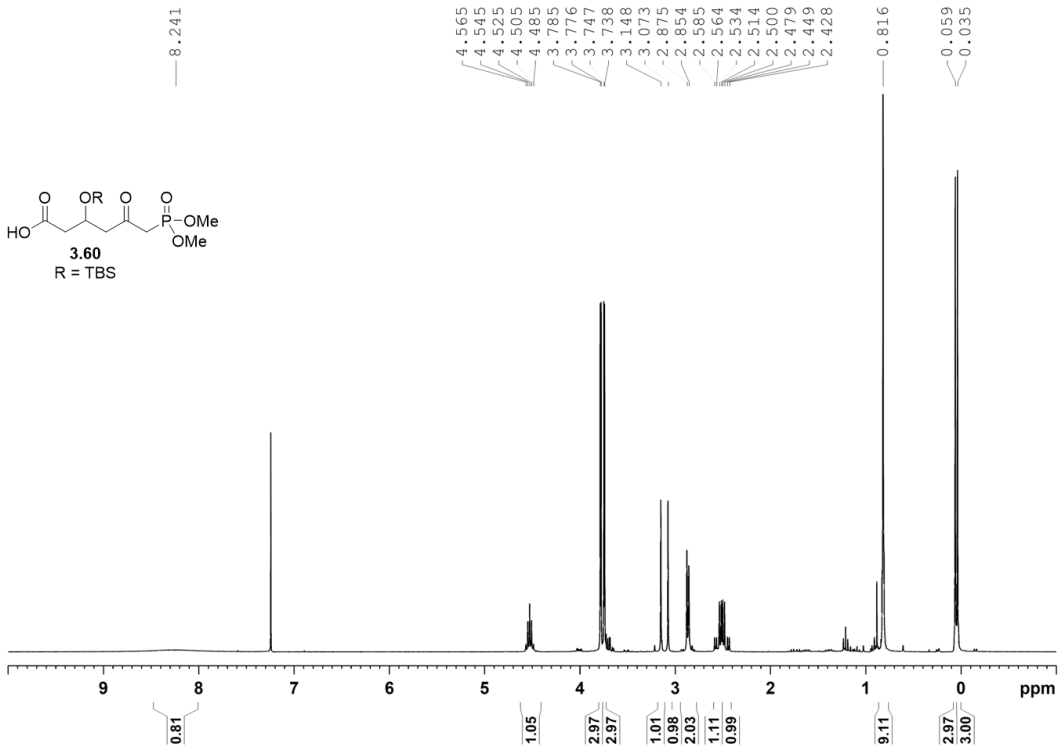

3-(*tert*-Butyldimethylsilyloxy)-6-(dimethoxyphosphoryl)-5-oxohexanoic acid (**3.60**)

^{13}C NMR (75 MHz, $CDCl_3$)

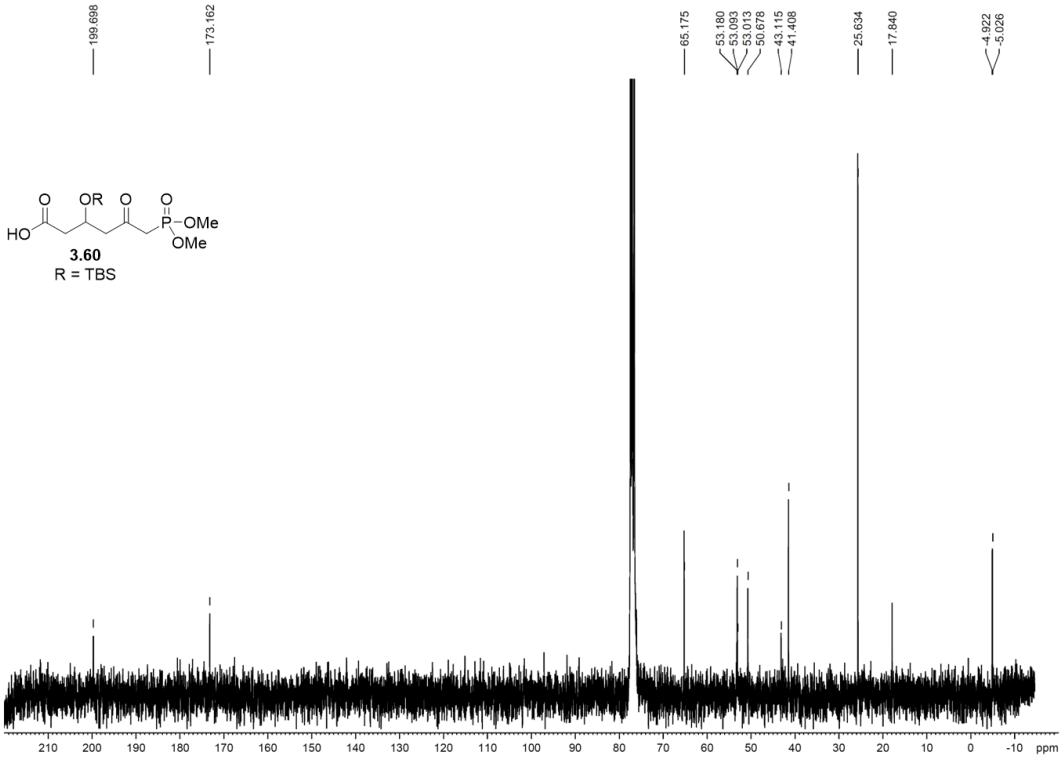

3-(*tert*-Butyldimethylsilyloxy)-6-(dimethoxyphosphoryl)-5-oxohexanoic acid (**3.60**)

^{31}P NMR (121 MHz, $CDCl_3$)

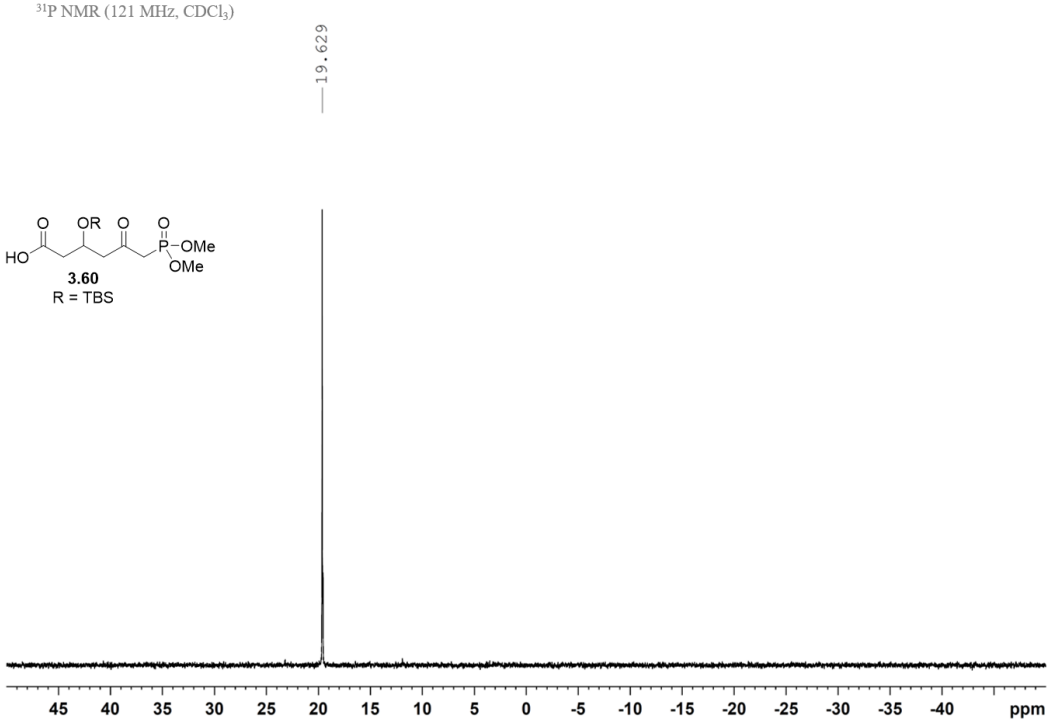

Methyl 3-(*tert*-Butyldimethylsilyloxy)-6-(dimethoxyphosphoryl)-5-oxohexanoate (**3.63**)

^{1}H NMR (400 MHz, $CDCl_3$)

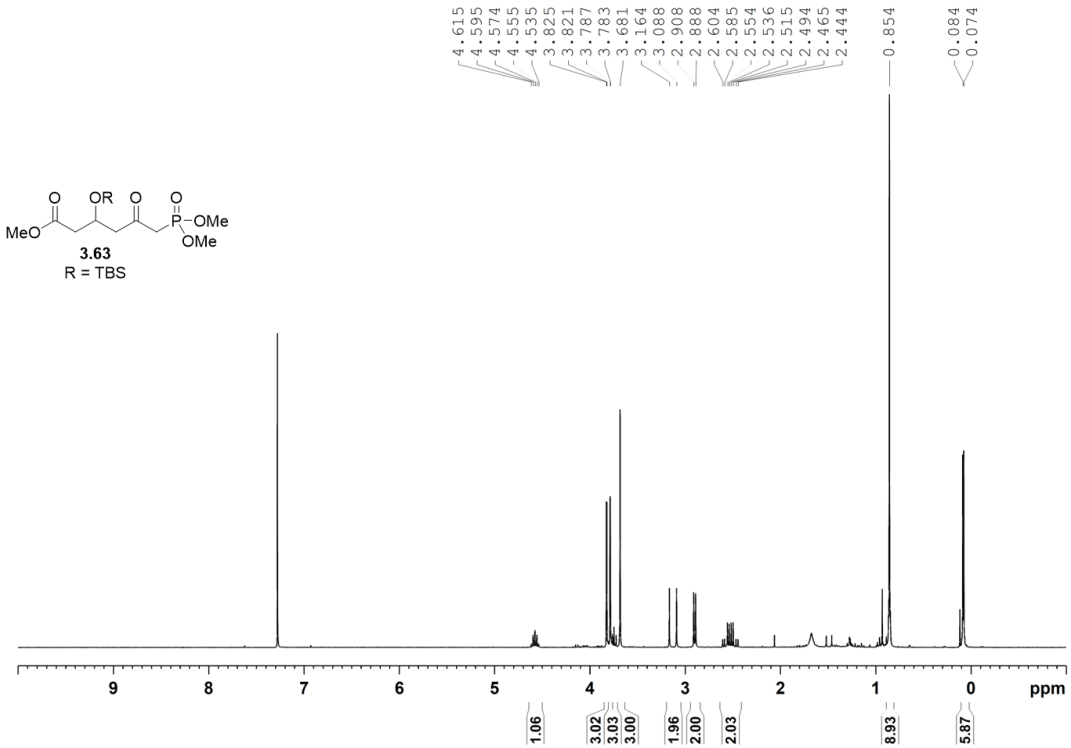

Methyl 3-(*tert*-Butyldimethylsilyloxy)-6-(dimethoxyphosphoryl)-5-oxohexanoate (**3.63**)

^{13}C NMR (100 MHz, $CDCl_3$)

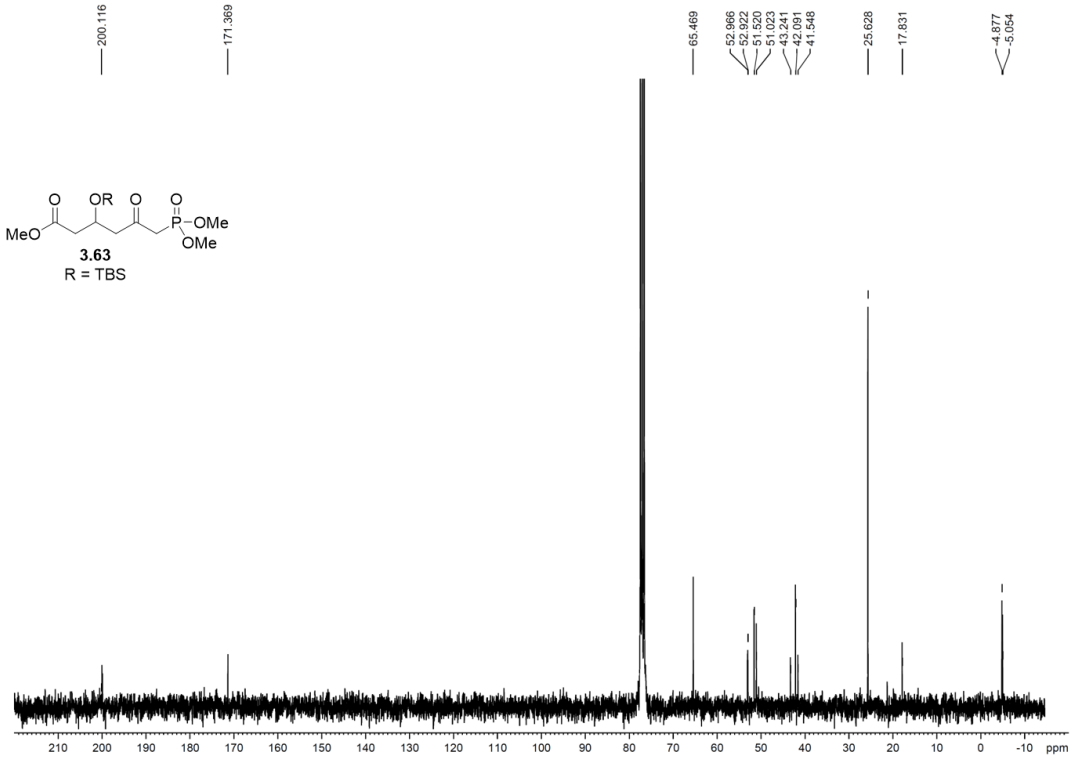

Methyl 3-(*tert*-Butyldimethylsilyloxy)-6-(dimethoxyphosphoryl)-5-oxohexanoate (**3.63**)

^{31}P NMR (162 MHz, $CDCl_3$)

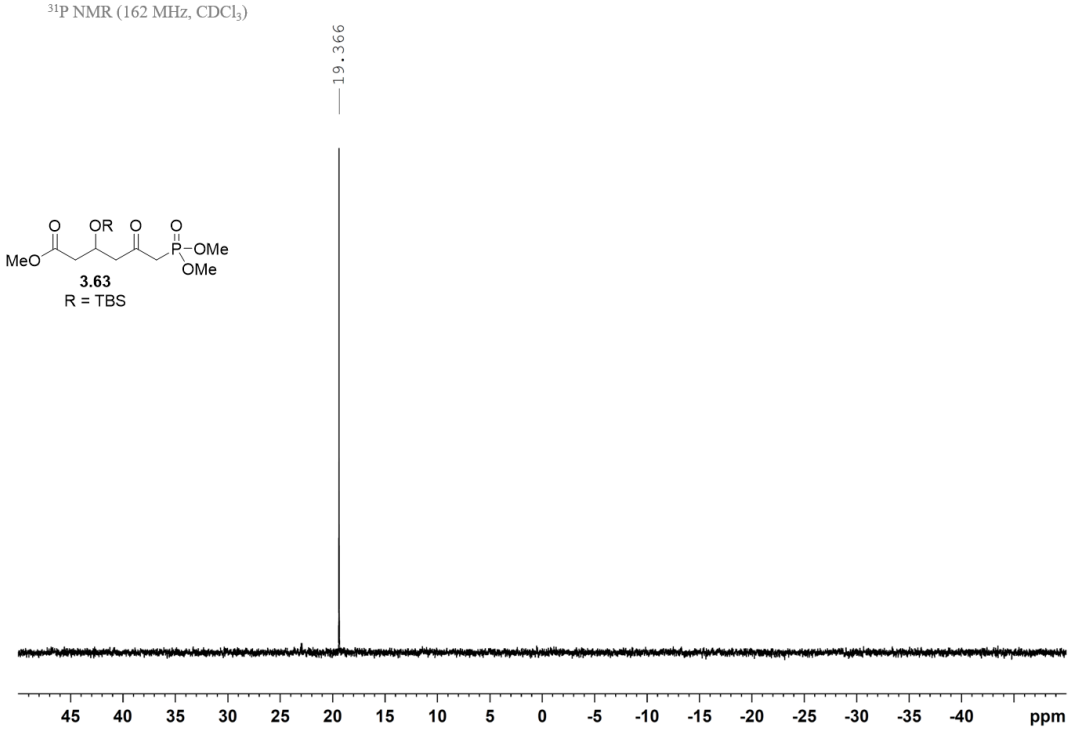

7-(*tert*-Butyldimethylsilyloxy)heptan-1-ol (**3.65**)

^{1}H NMR (400 MHz, $CDCl_3$)

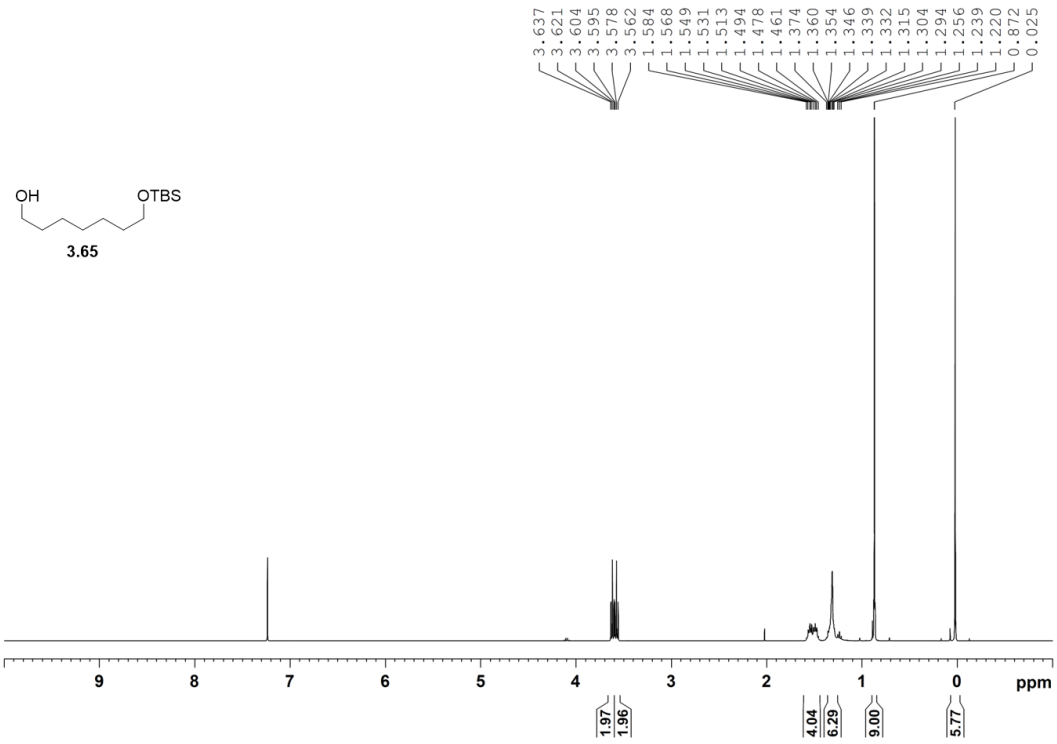

7-(*tert*-Butyldimethylsilyloxy)heptan-1-ol (**3.65**)

^{13}C NMR (100 MHz, $CDCl_3$)

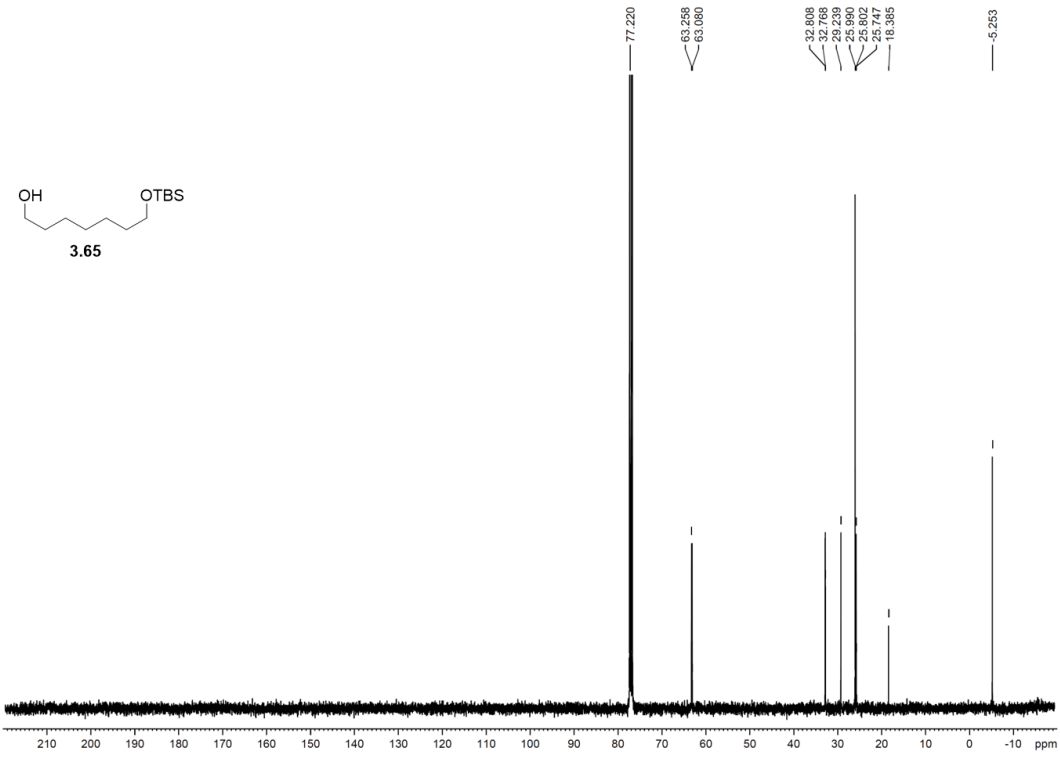

7-(*tert*-Butyldimethylsilyloxy)heptanal (**3.66**)

^{1}H NMR (400 MHz, $CDCl_3$)

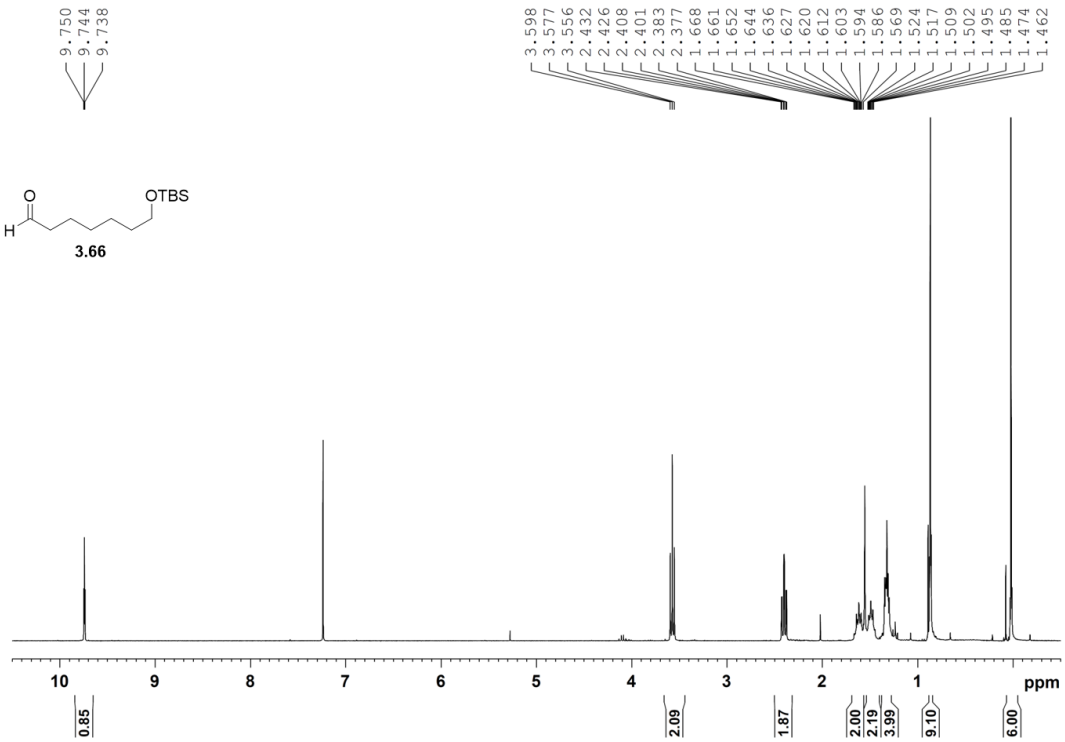

7-(*tert*-Butyldimethylsilyloxy)heptanal (**3.66**)

^{13}C NMR (100 MHz, $CDCl_3$)

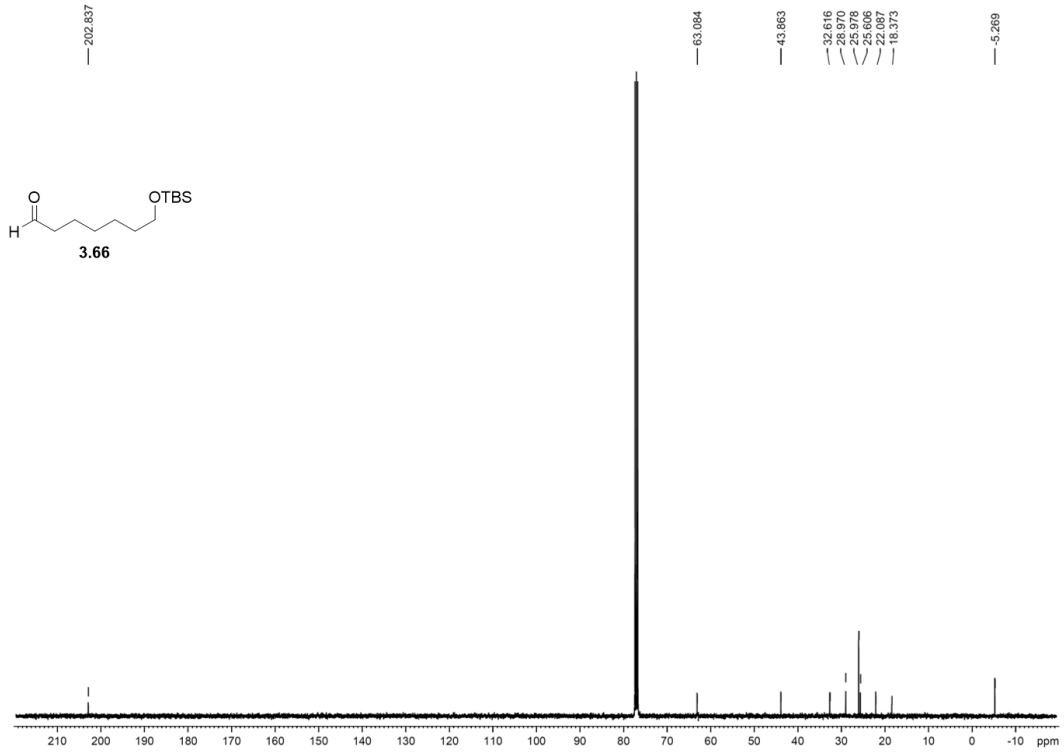

(*E*)-Methyl-3,13-*bis*-(*tert*-butyldimethylsilyloxy)-5-oxotridec-6-enoate (**3.67**)

^{1}H NMR (300 MHz, $CDCl_3$)

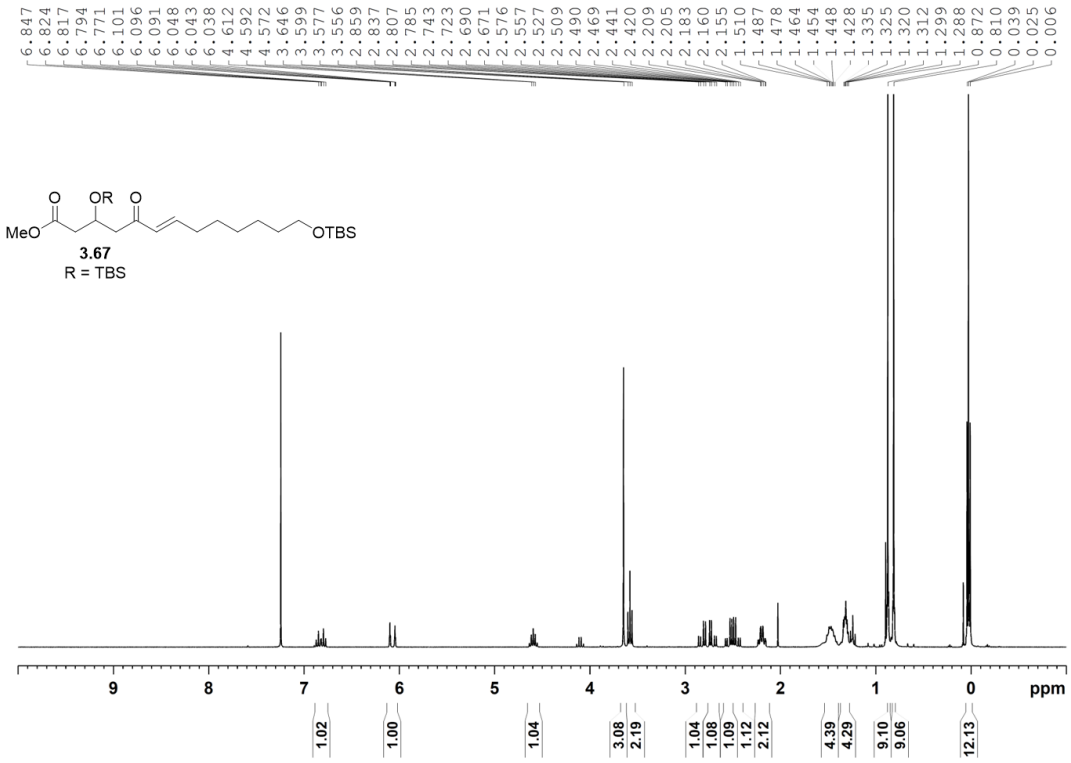

(*E*)-Methyl-3,13-*bis*-(*tert*-butyldimethylsilyloxy)-5-oxotridec-6-enoate (**3.67**)

^{13}C NMR (75 MHz, $CDCl_3$)

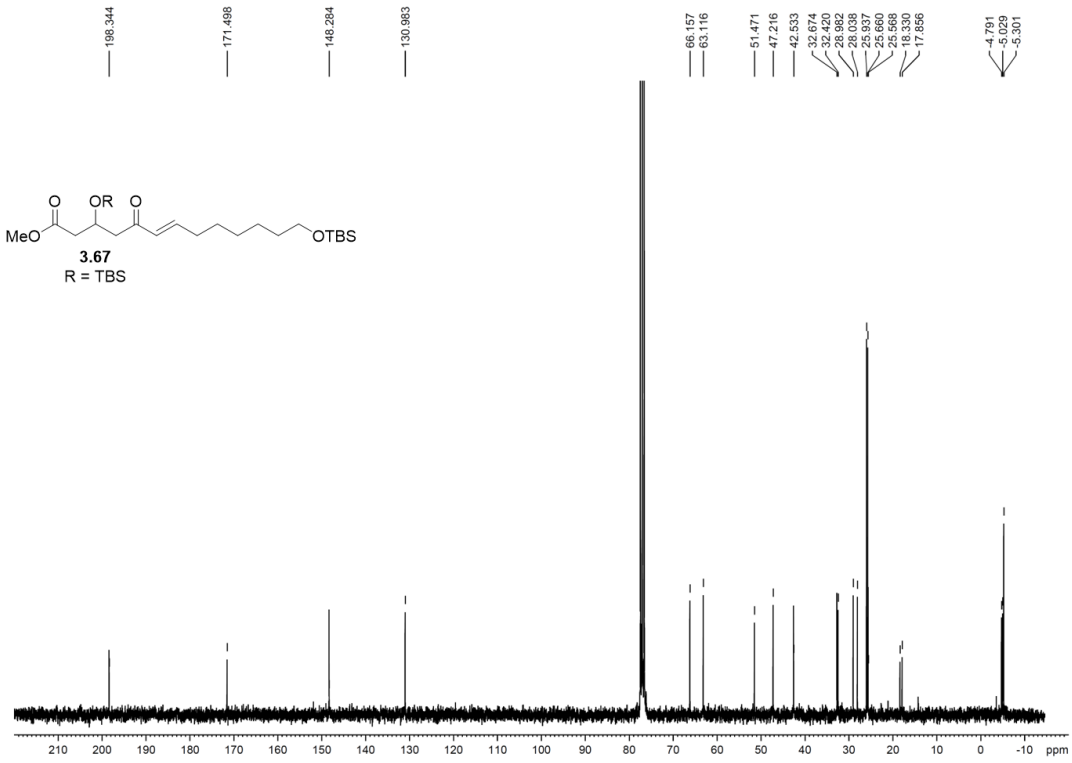

(*E*)-Methyl-3,13-*bis*-(*tert*-butyldimethylsilyloxy)-5-oxotridec-6-enoate (**3.67**)

HSQC (400 MHz, $CDCl_3$)

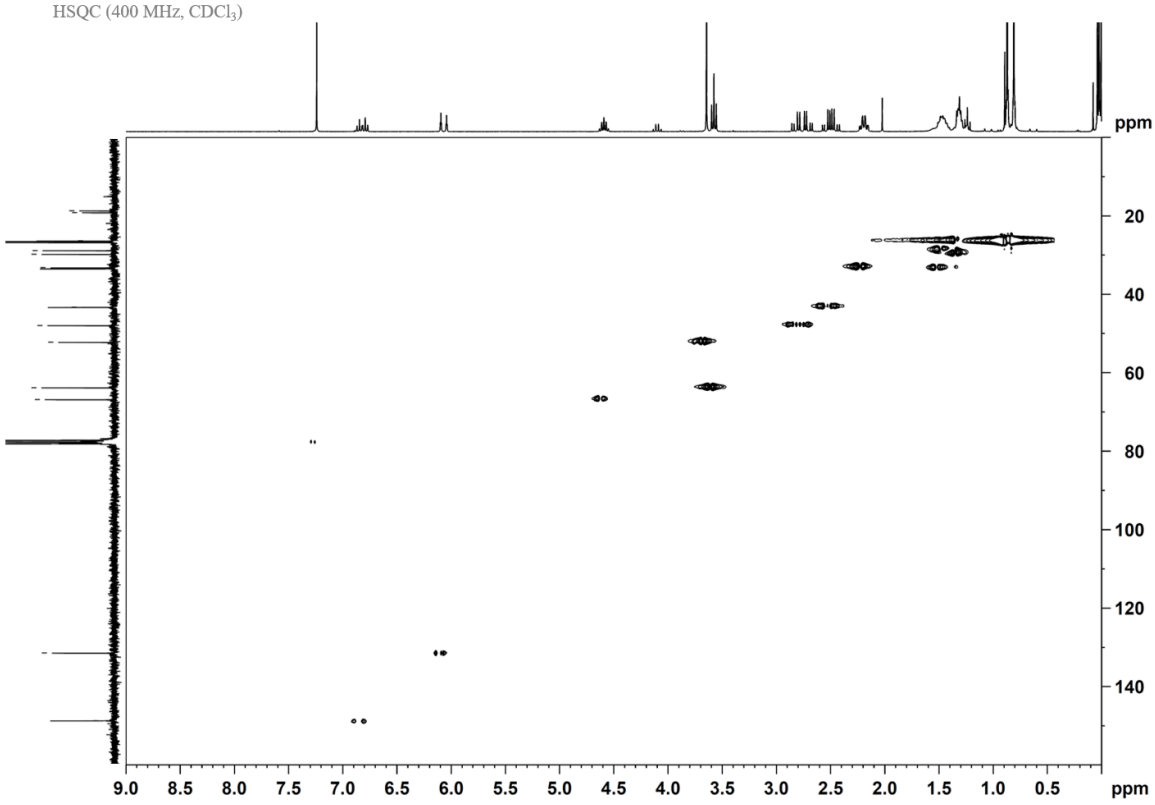

S1.2.2 First-Generation α,β-Unsaturated Ketone Model v1.2 (§ 3.5.1)

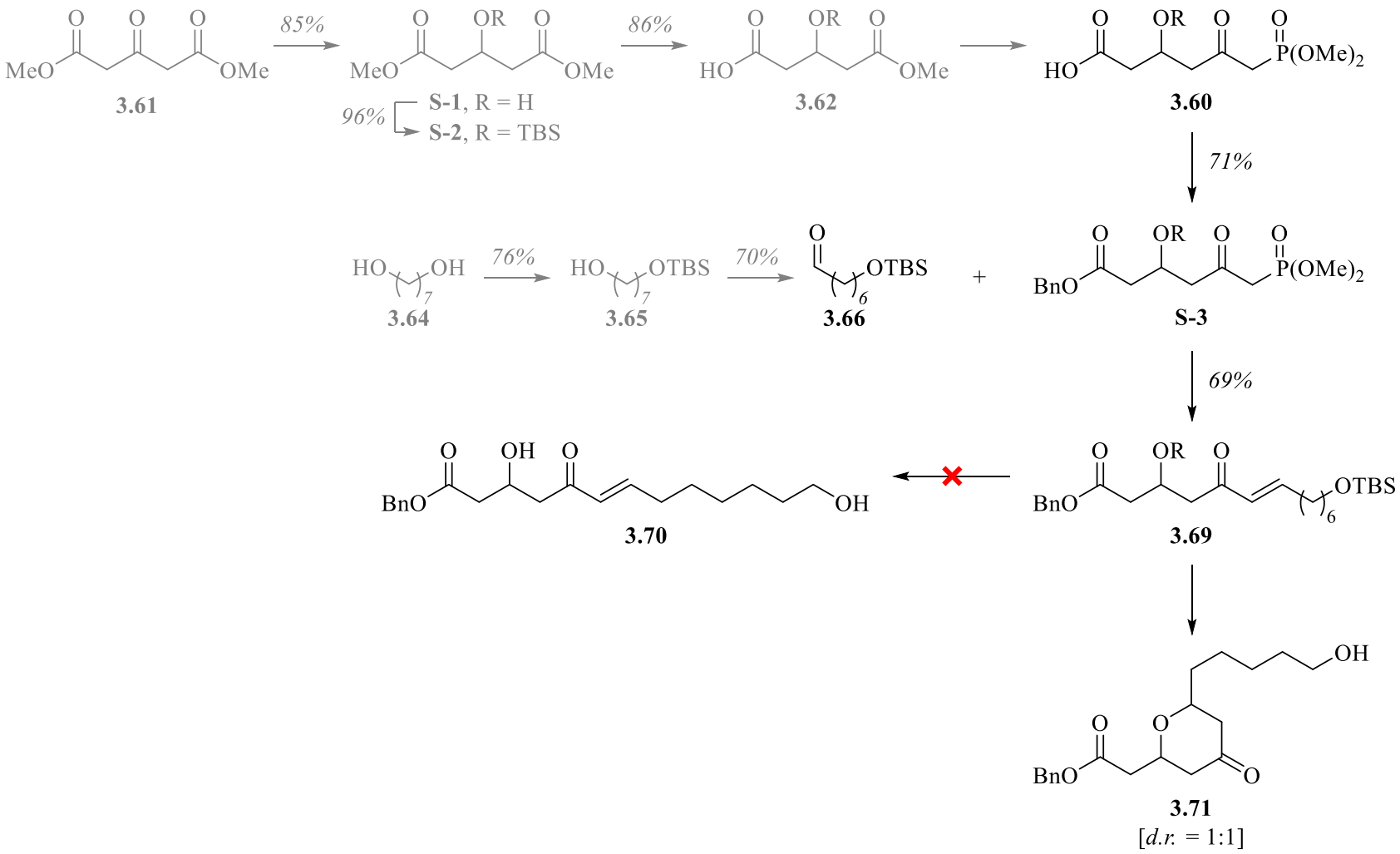

Figure S2 – Summary of the synthesis of first-generation *α,β*-unsaturated ketone model version 1.2.

Benzyl 3-(*tert*-butyldimethylsilyloxy)-6-(dimethoxyphosphoryl)-5-oxohexanoate (**S-3**)

^{1}H NMR (400 MHz, $CDCl_3$)

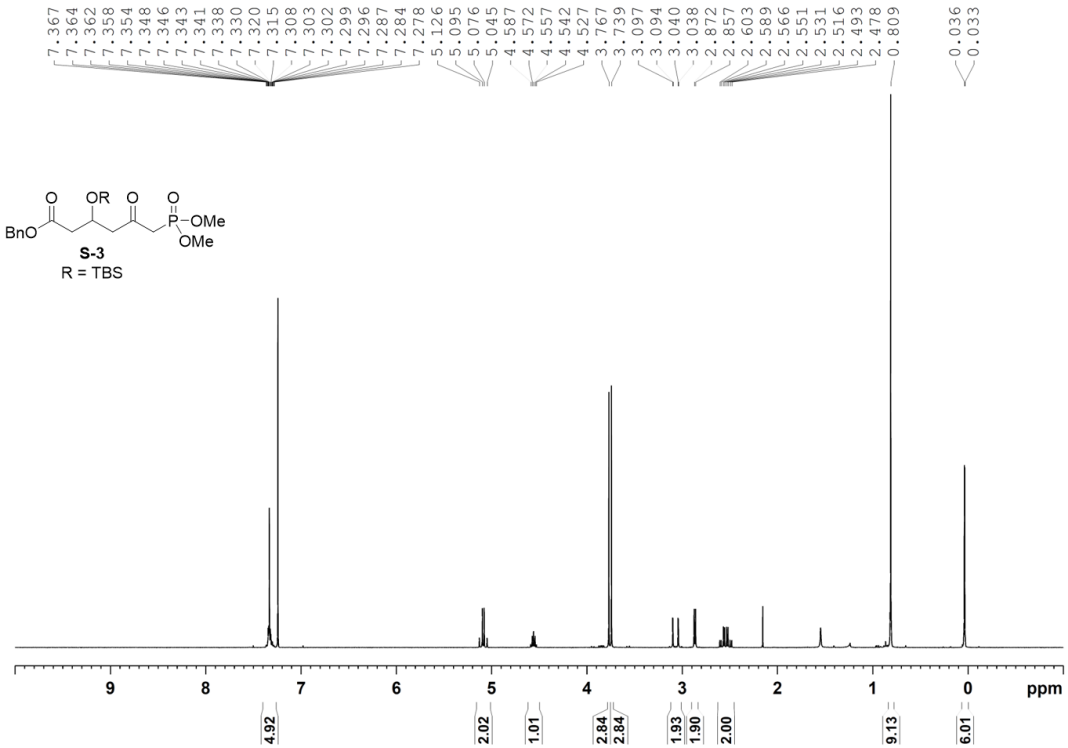

Benzyl 3-(tert-butyldimethylsilyloxy)-6-(dimethoxyphosphoryl)-5-oxohexanoate

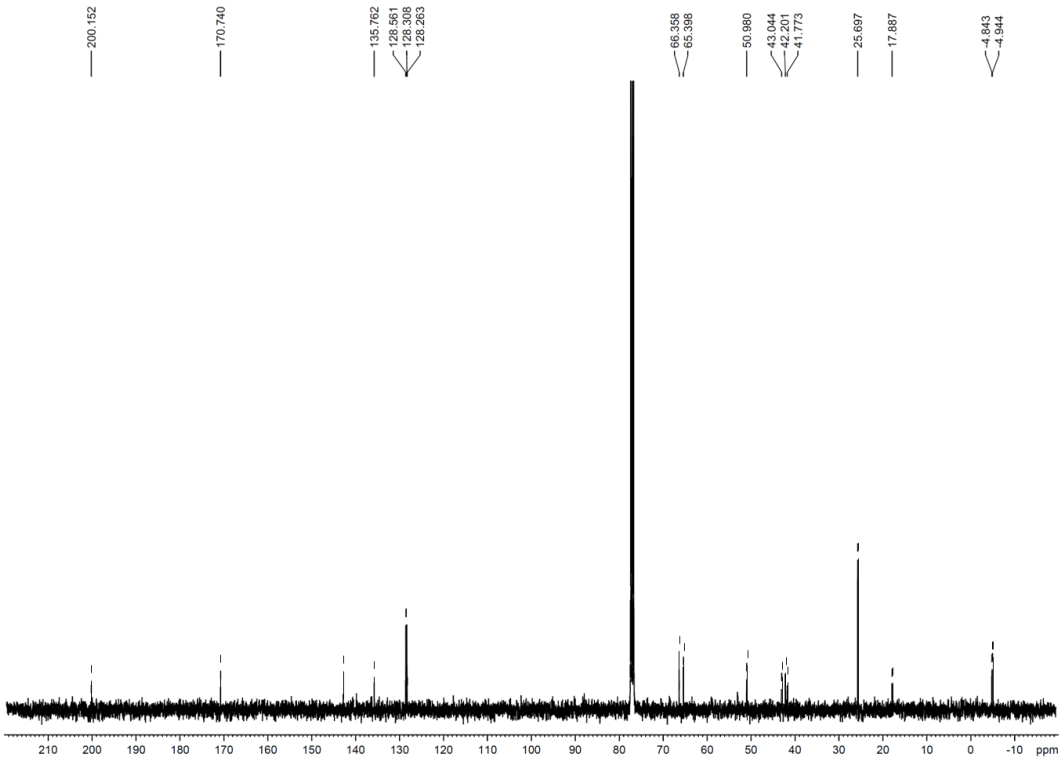

Benzyl 3-(*tert*-butyldimethylsilyloxy)-6-(dimethoxyphosphoryl)-5-oxohexanoate (**S-3**)

^{31}P NMR (121 MHz, $CDCl_3$)

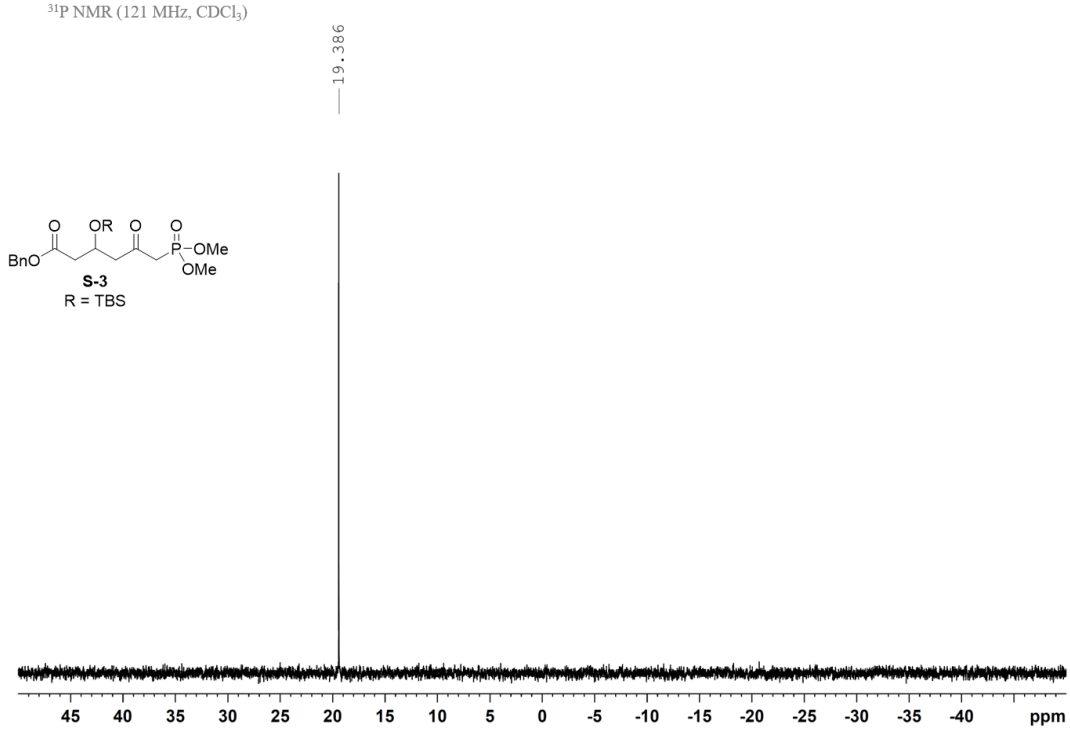

Benzyl 3-(*tert*-butyldimethylsilyloxy)-6-(dimethoxyphosphoryl)-5-oxohexanoate (**S-3**)

HSQC (400 MHz, $CDCl_3$)

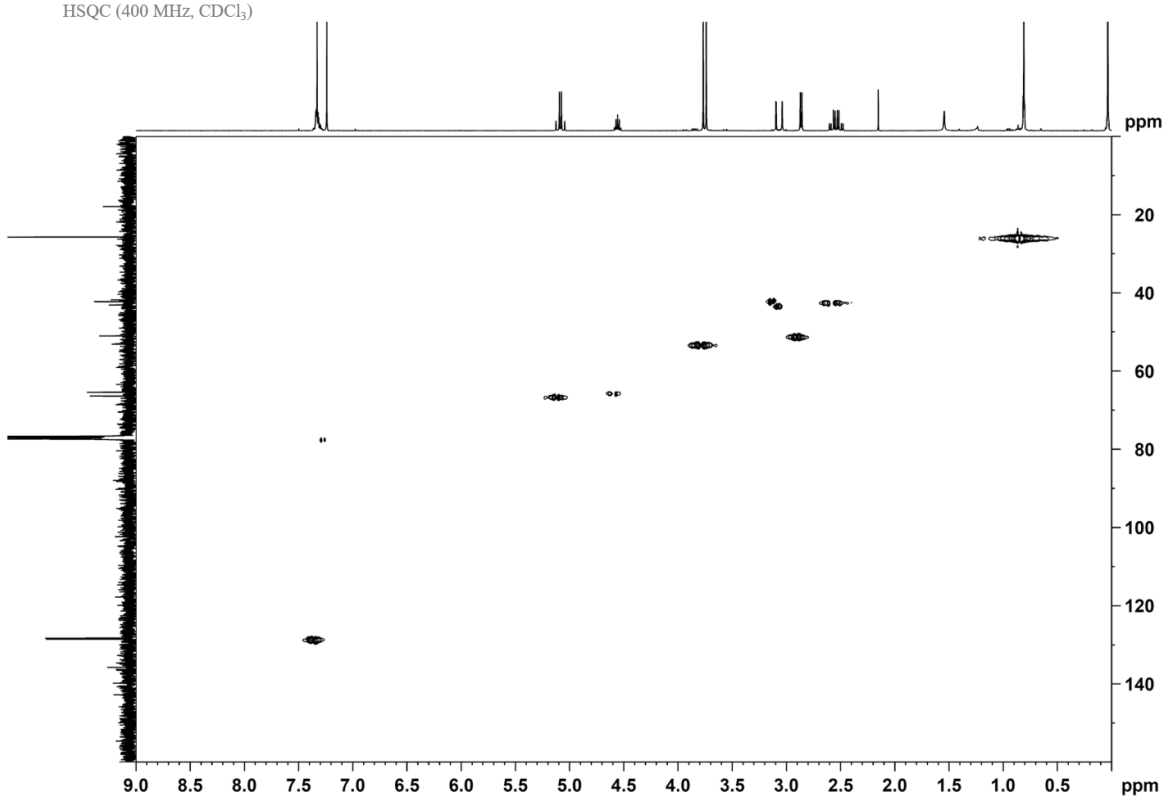

(*E*)-Benzyl-3,13-*bis*-(*tert*-butyldimethylsilyloxy)-5-oxotridec-6-enoate (**3.69**)

^{1}H NMR (400 MHz, $CDCl_3$)

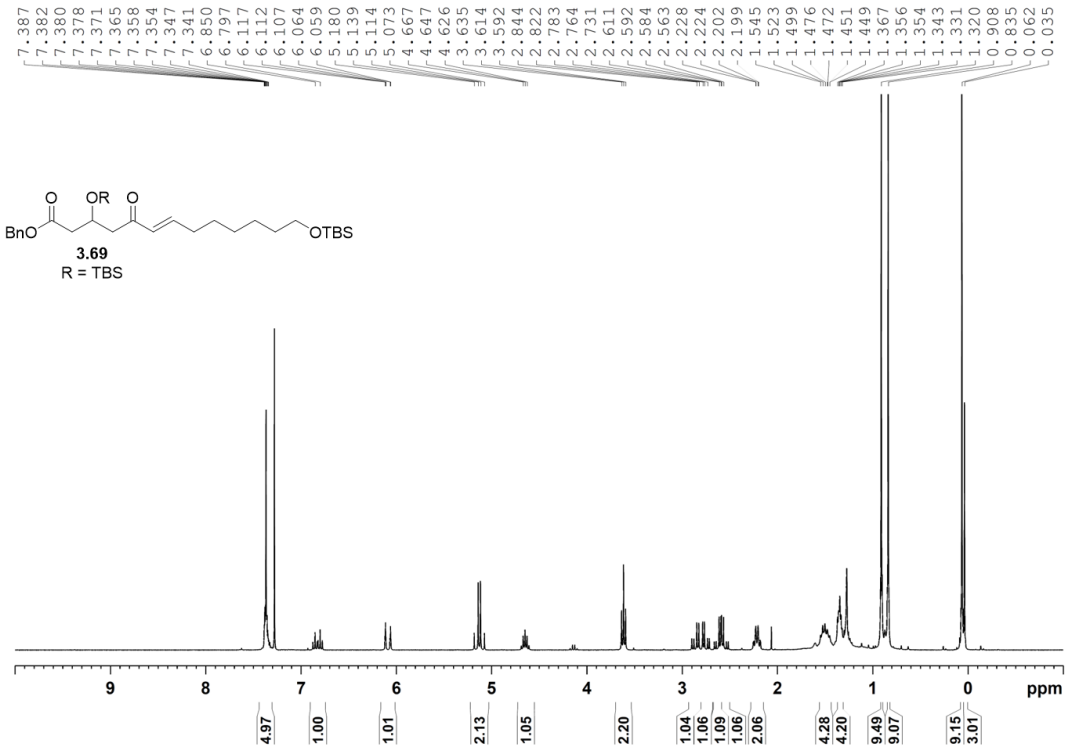

(*E*)-Benzyl-3,13-*bis*-(*tert*-butyldimethylsilyloxy)-5-oxotridec-6-enoate (**3.69**)

^{13}C NMR (100 MHz, $CDCl_3$)

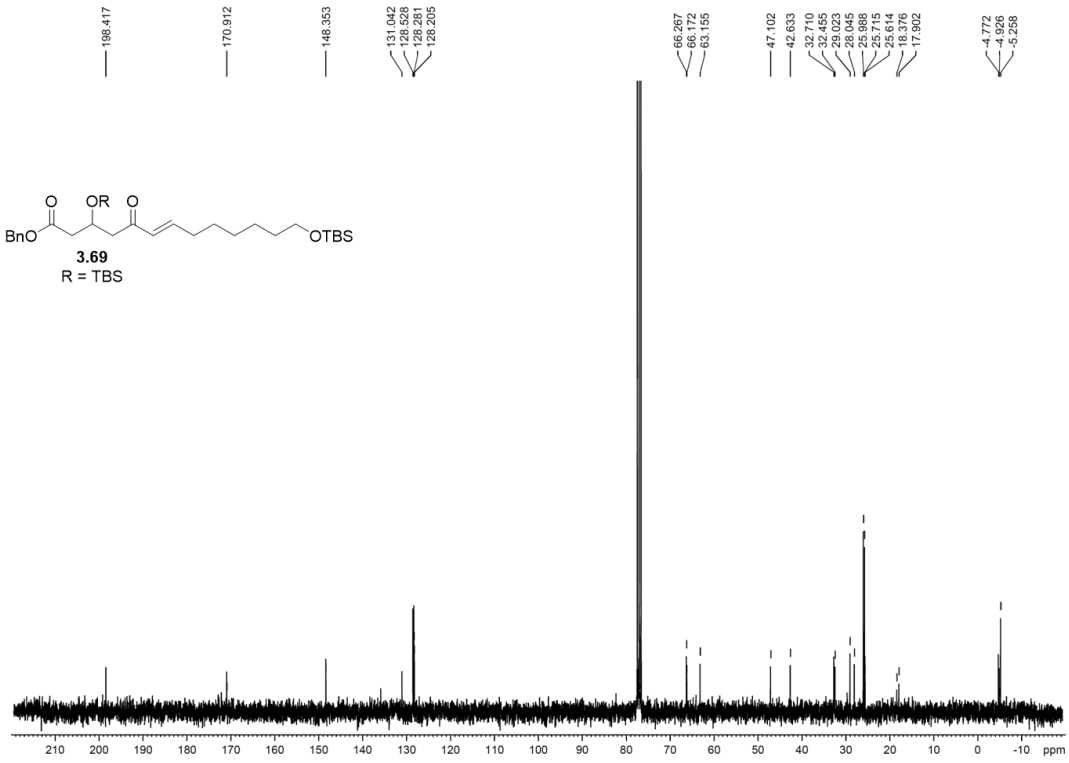

(*E*)-Benzyl-3,13-*bis*-(*tert*-butyldimethylsilyloxy)-5-oxotridec-6-enoate (**3.69**)

HSQC (400 MHz, $CDCl_3$)

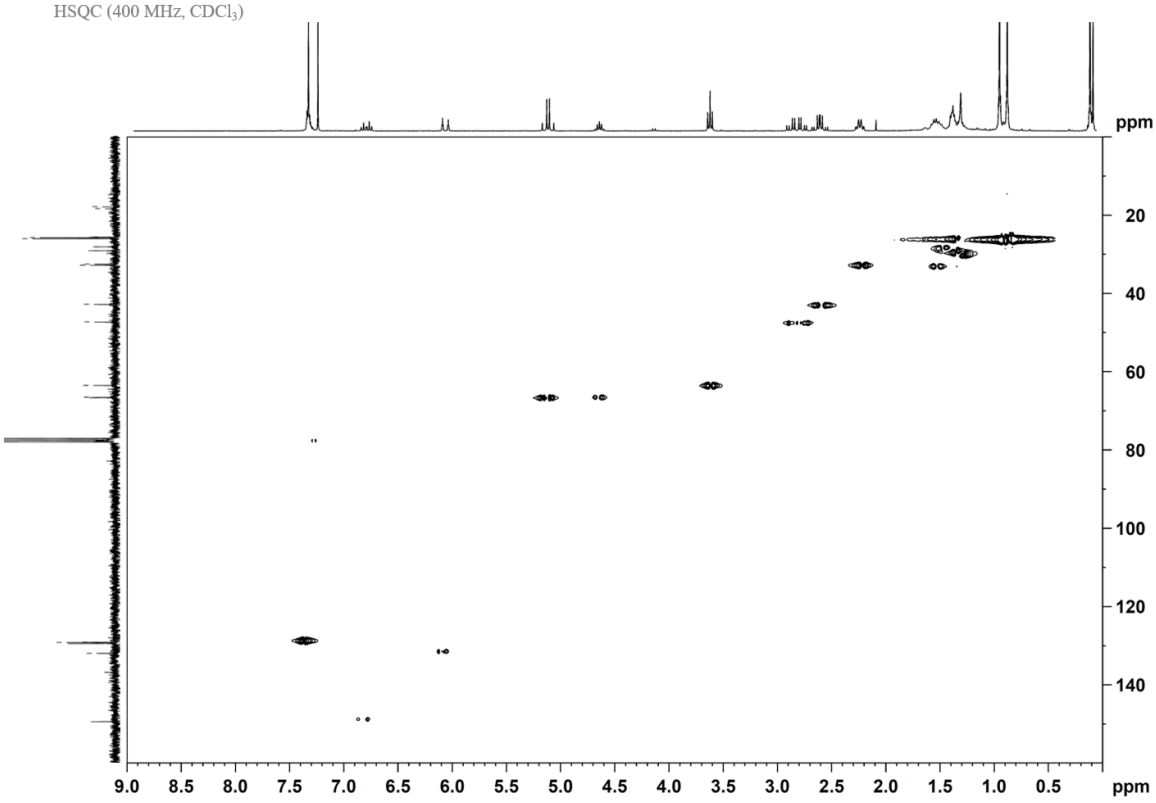

Benzyl 2-(6-(6-hydroxyhexyl)-4-oxotetrahydro-2*H*-pyran-2-yl)acetate (**3.71**)

^{1}H NMR (400 MHz, $CDCl_3$)

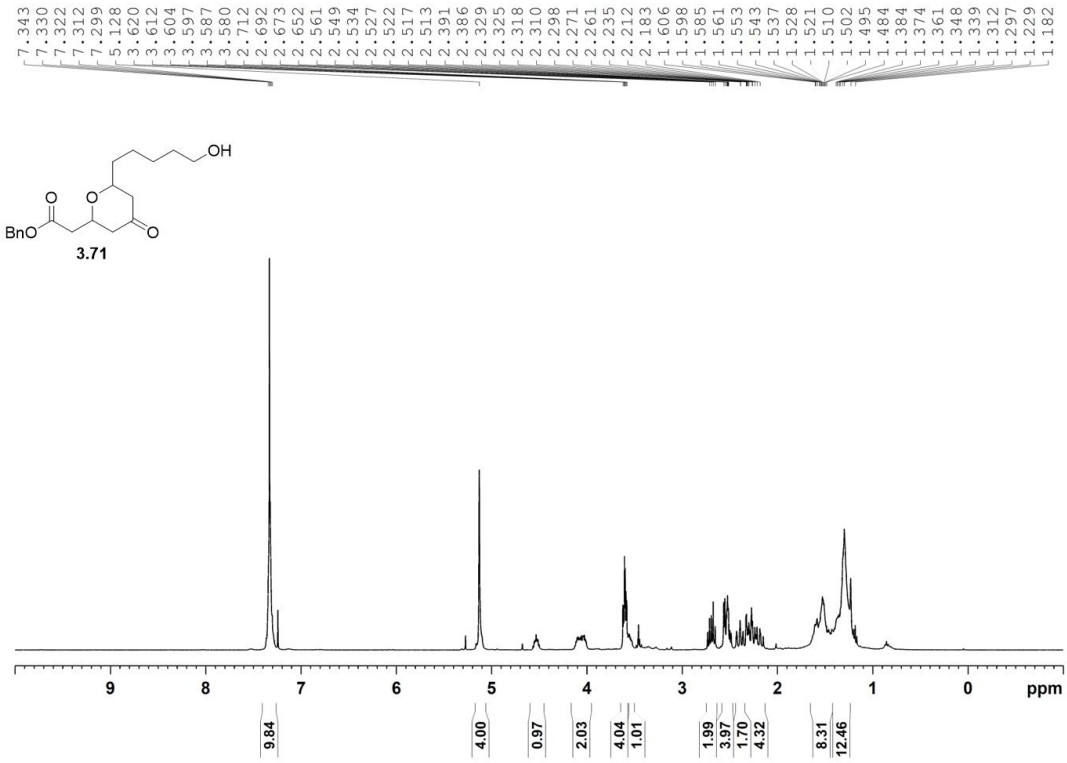

Benzyl 2-(6-(6-hydroxyhexyl)-4-oxotetrahydro-2*H*-pyran-2-yl)acetate (**3.71**)

^{13}C NMR (100 MHz, $CDCl_3$)

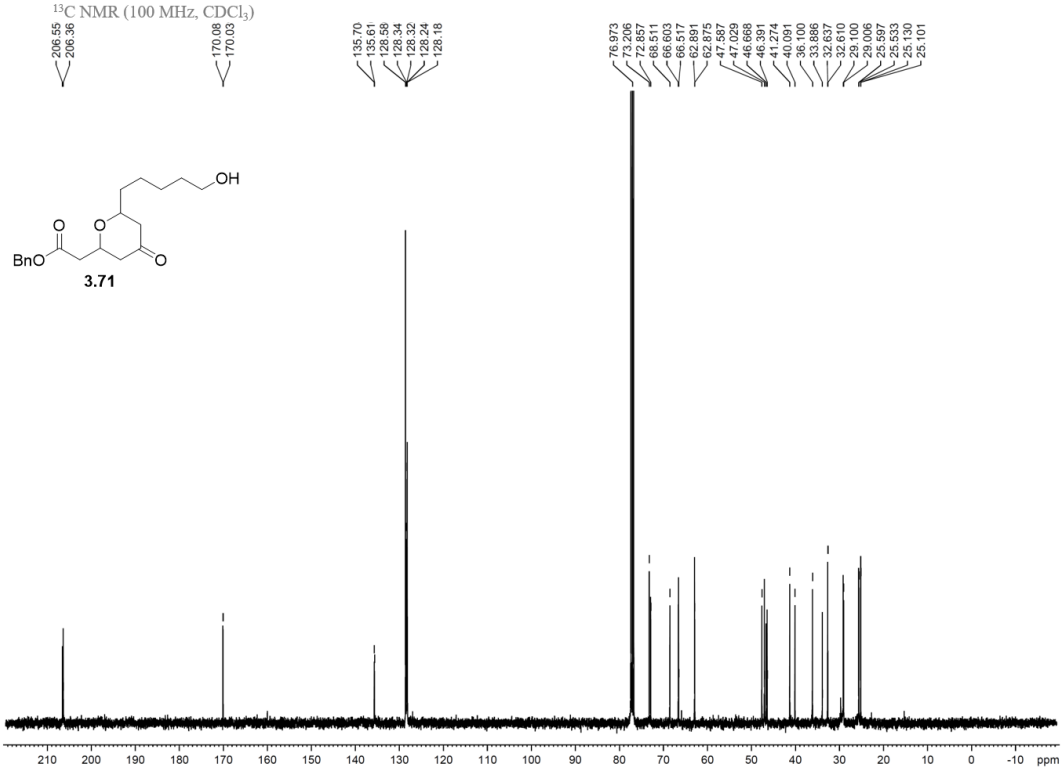

Benzyl 2-(6-(6-hydroxyhexyl)-4-oxotetrahydro-2*H*-pyran-2-yl)acetate (**3.71**)

COSY (400 MHz, $CDCl_3$)

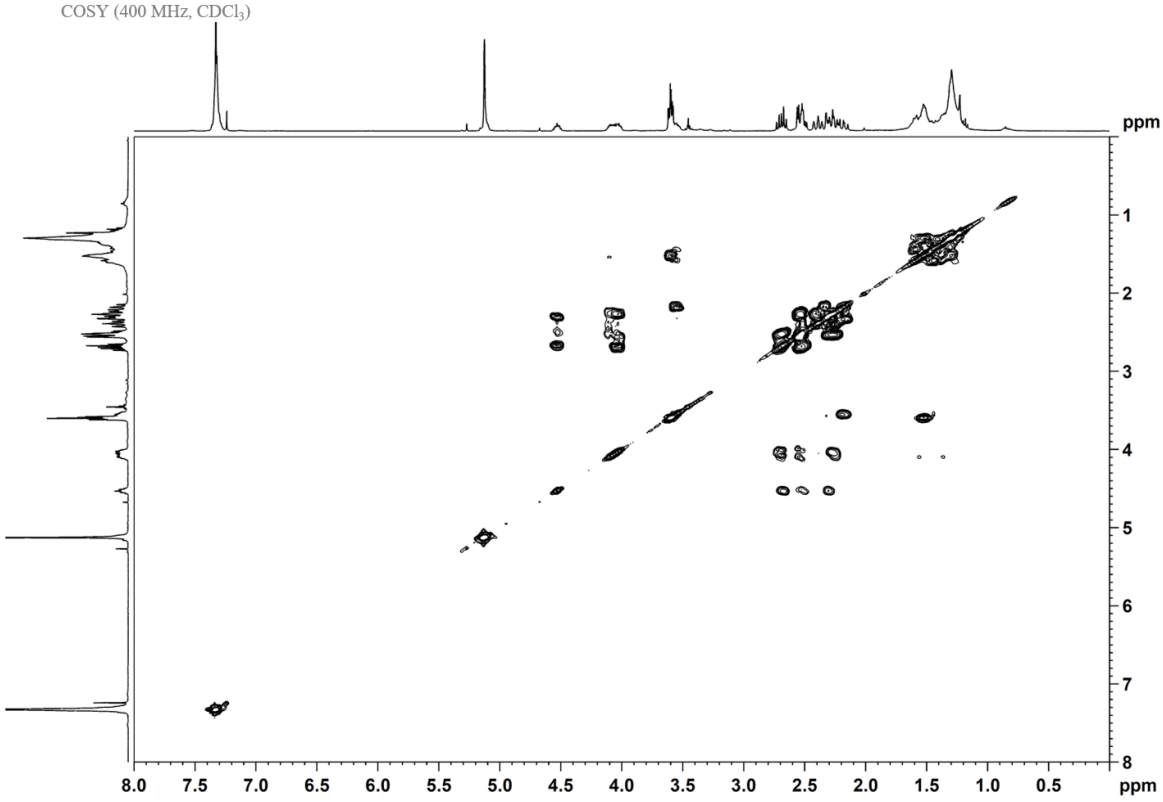

Benzyl 2-(6-(6-hydroxyhexyl)-4-oxotetrahydro-2*H*-pyran-2-yl)acetate (**3.71**)

HSQC (400 MHz, $CDCl_3$)

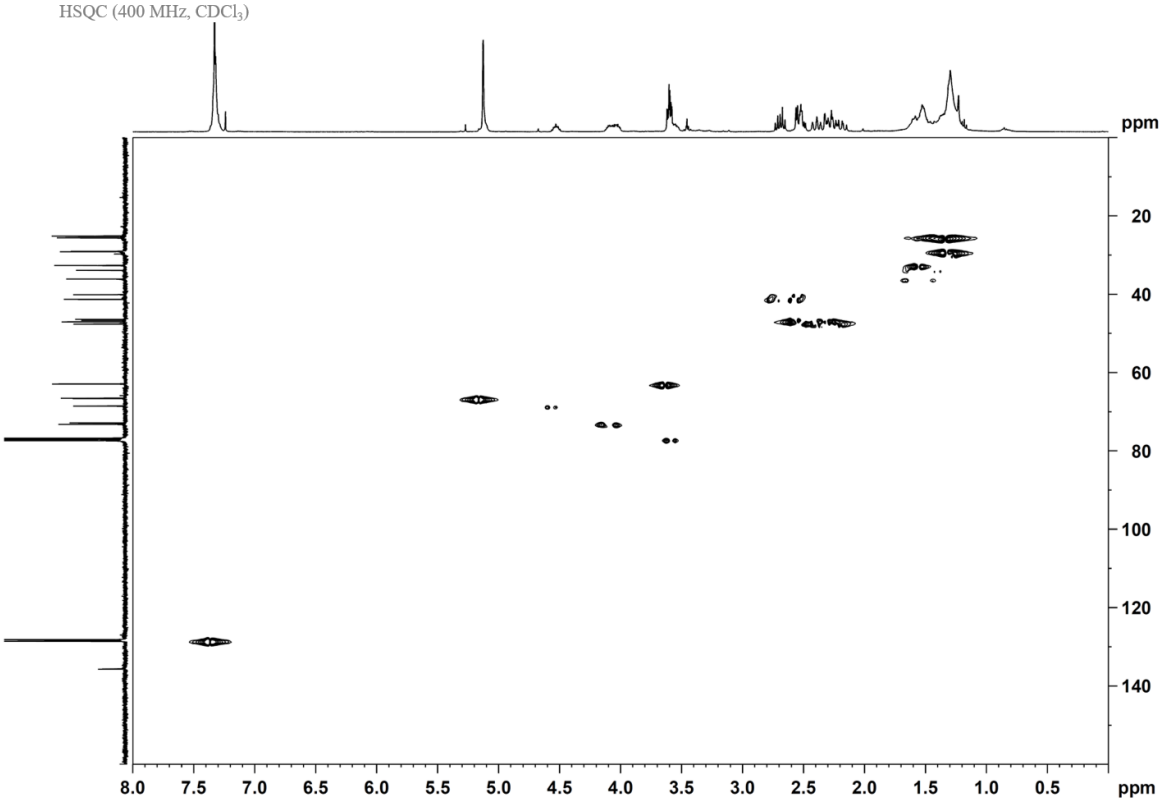

Benzyl 2-(6-(6-hydroxyhexyl)-4-oxotetrahydro-2*H*-pyran-2-yl)acetate (**3.71**)

HMBC (400 MHz, $CDCl_3$)

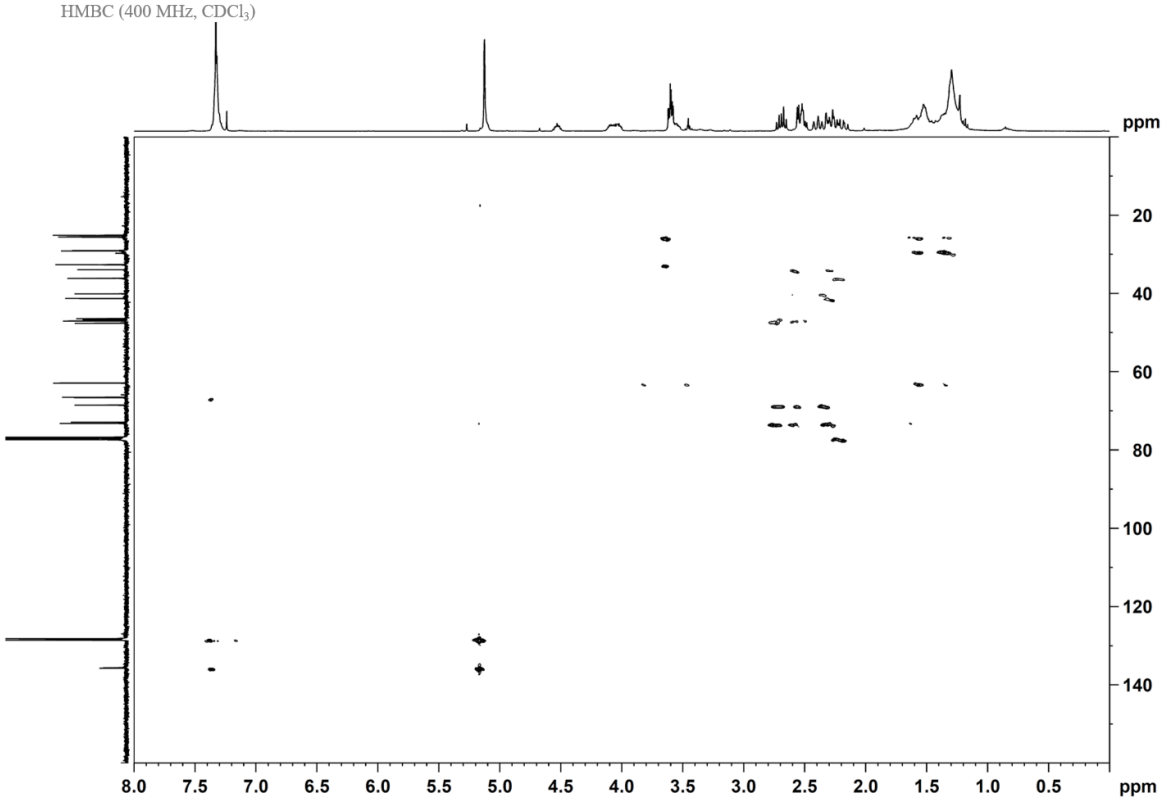

(*E*)-3,13-*bis*-(*O*-*tert*-butyldimethylsilyloxy)-5-oxotridec-6-enoic acid (**3.68**)

^{1}H NMR (400 MHz, $CDCl_3$)

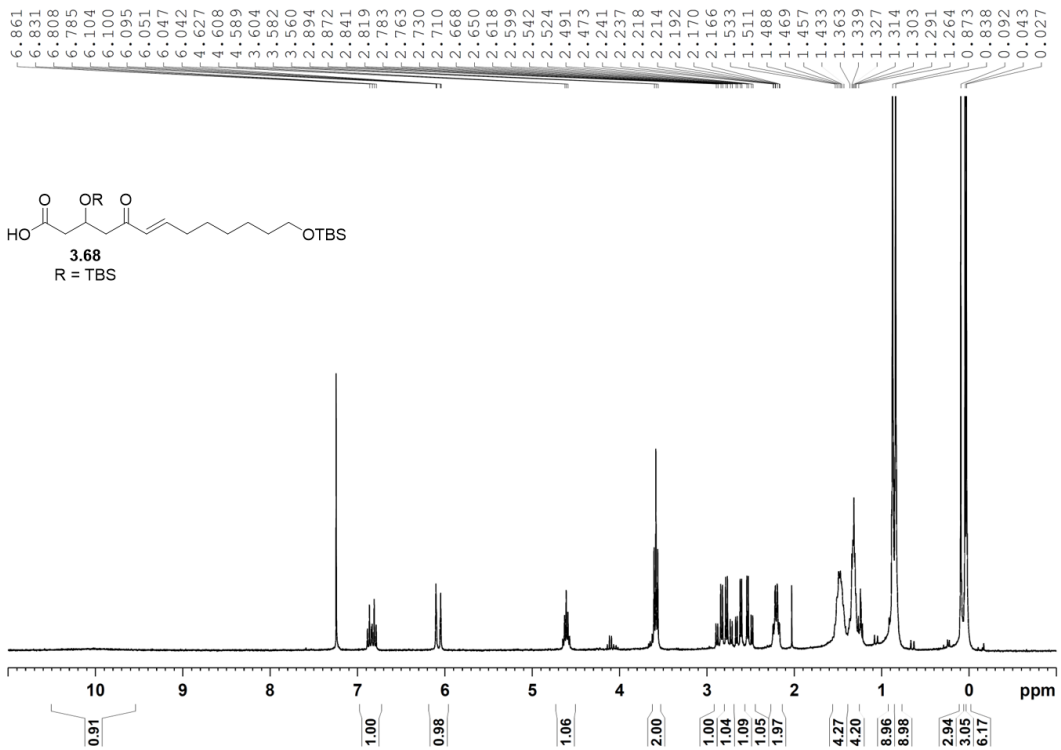

(*E*)-3,13-*bis*-(*O*-*tert*-butyldimethylsilyloxy)-5-oxotridec-6-enoic acid (**3.68**)

^{13}C NMR (100 MHz, $CDCl_3$)

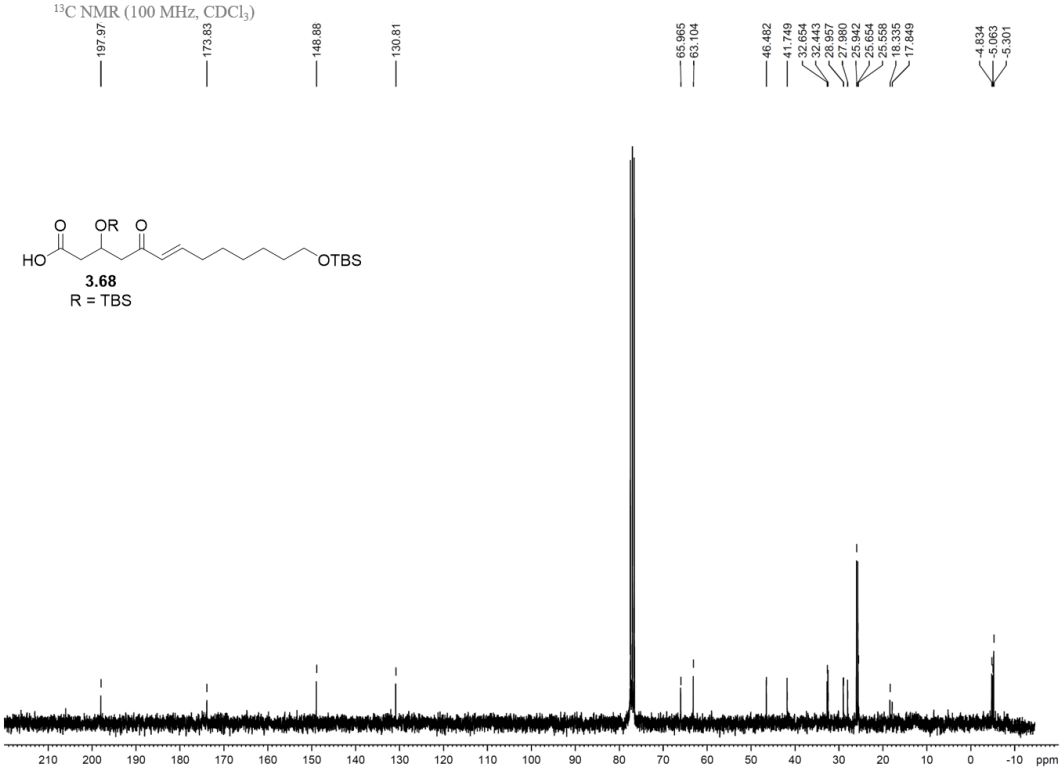

S1.2.3 First-Generation α,β-Unsaturated Ketone Model v2.1 (§ 3.5.1)

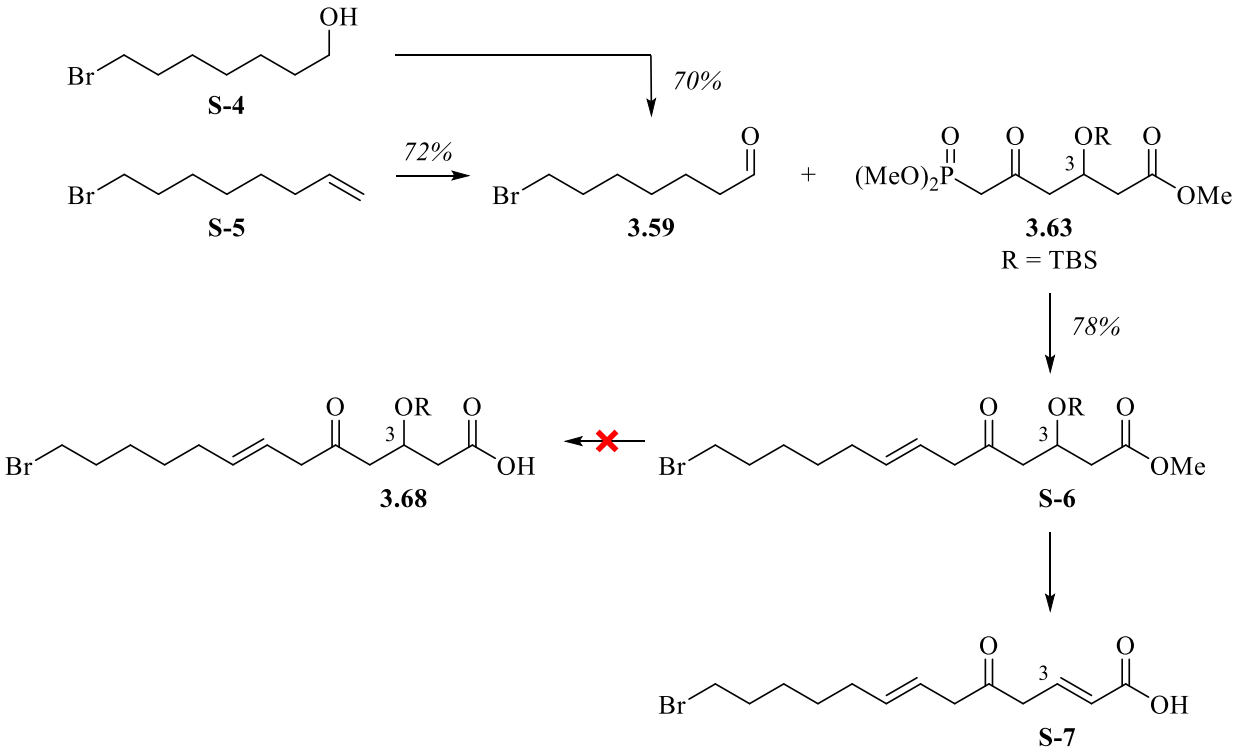

Figure S3 – Summary of the synthesis of first-generation *α,β*-unsaturated ketone model version 2.1.

7-Bromoheptanal (**3.59**)

^{1}H NMR (400 MHz, $CDCl_3$)

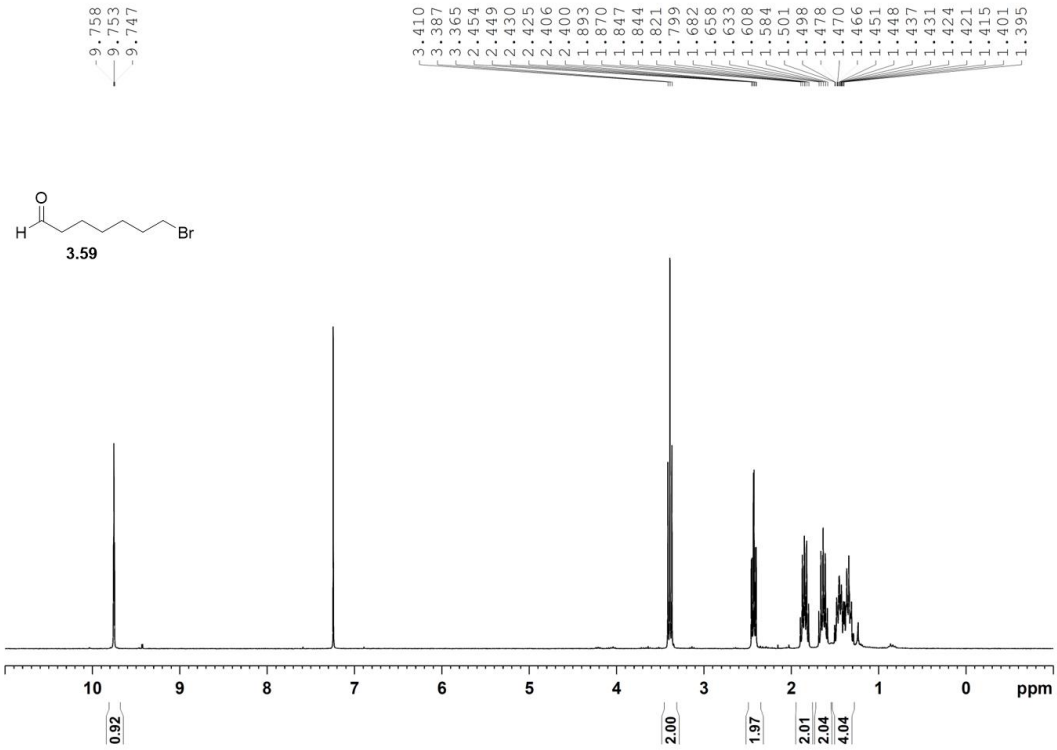

7-Bromoheptanal (**3.59**)

^{13}C NMR (100 MHz, $CDCl_3$)

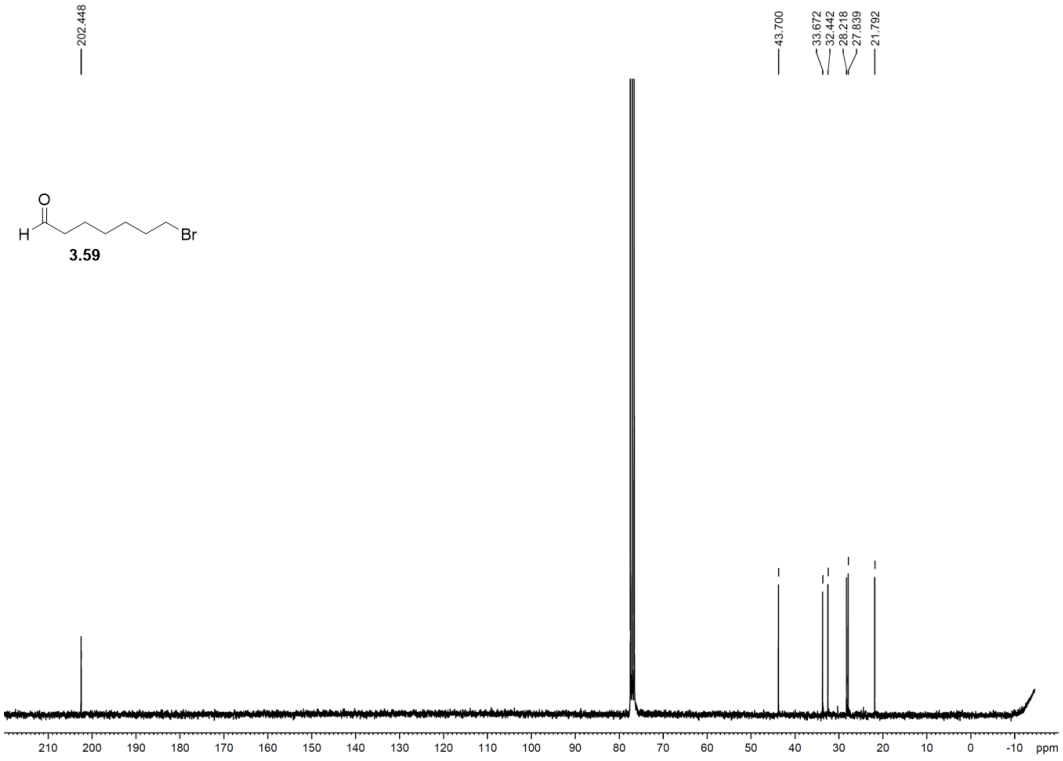

(*E*)-Methyl 13-bromo-3-(*tert*-butyldimethylsilyloxy)-5-oxotridec-6-enoate (**S-6**)

^{1}H NMR (400 MHz, $CDCl_3$)

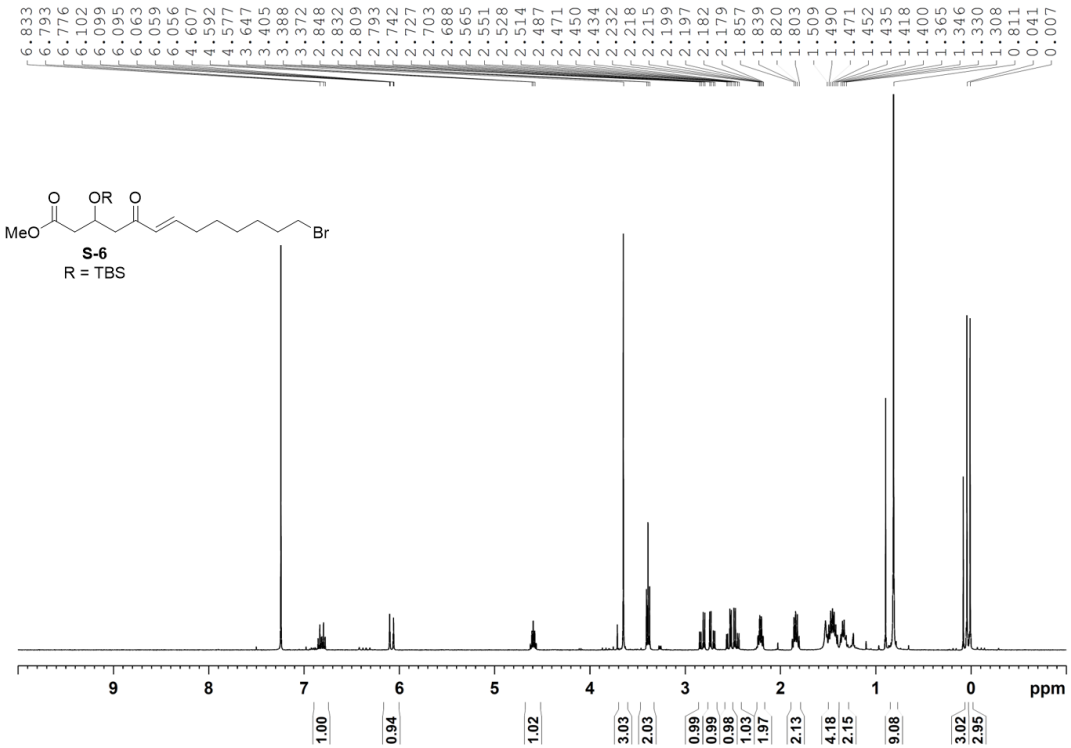

(*E*)-Methyl 13-bromo-3-(*tert*-butyldimethylsilyloxy)-5-oxotridec-6-enoate (**S-6**)

^{13}C NMR (100 MHz, $CDCl_3$)

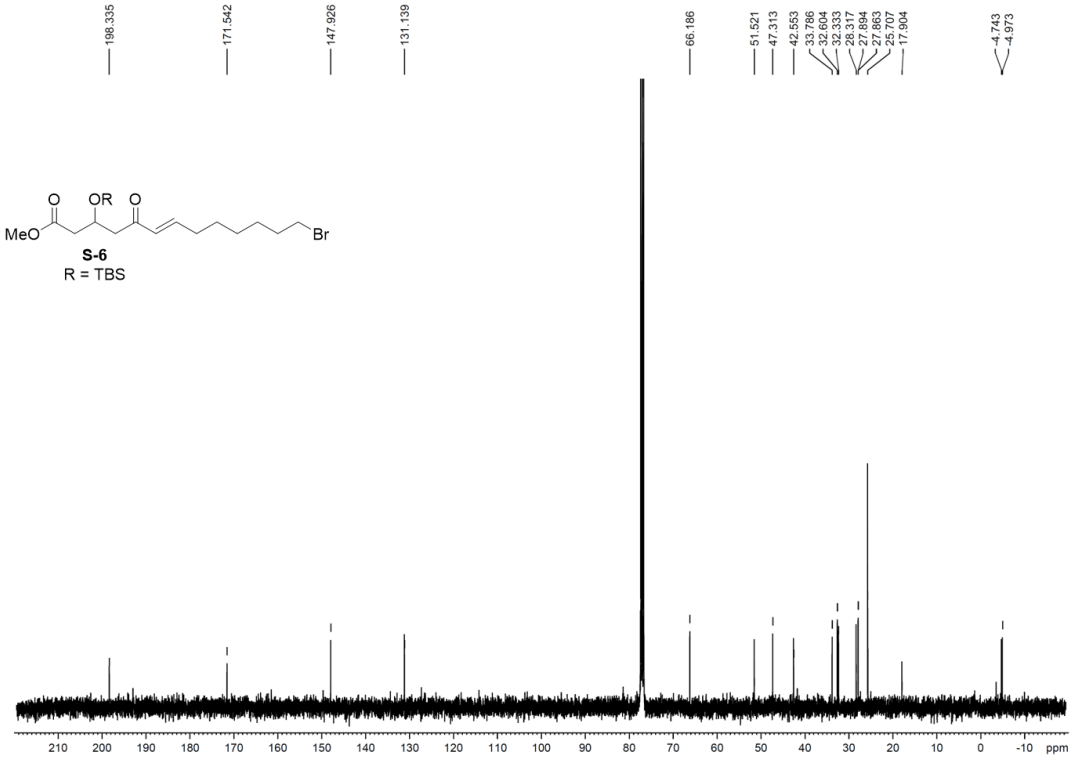

(*E*)-Methyl 13-bromo-3-(*tert*-butyldimethylsilyloxy)-5-oxotridec-6-enoate (**S-6**)

HSQC (400 MHz, $CDCl_3$)

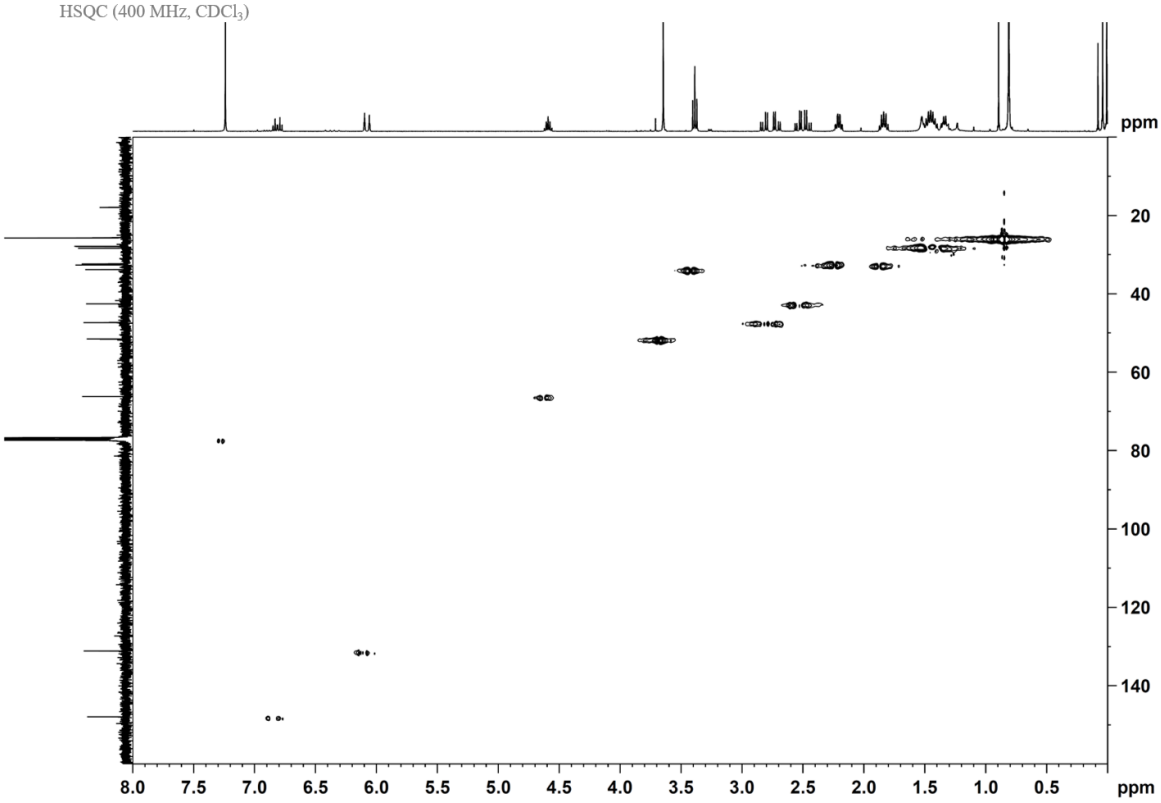

(2*E*,6*E*)-13-Bromo-5-oxotrideca-2,6-dienoic acid (*β*-elimination by-product, **S-7**)

^{1}H NMR (400 MHz, $CDCl_3$)

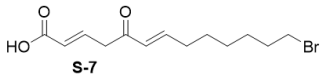

S-7

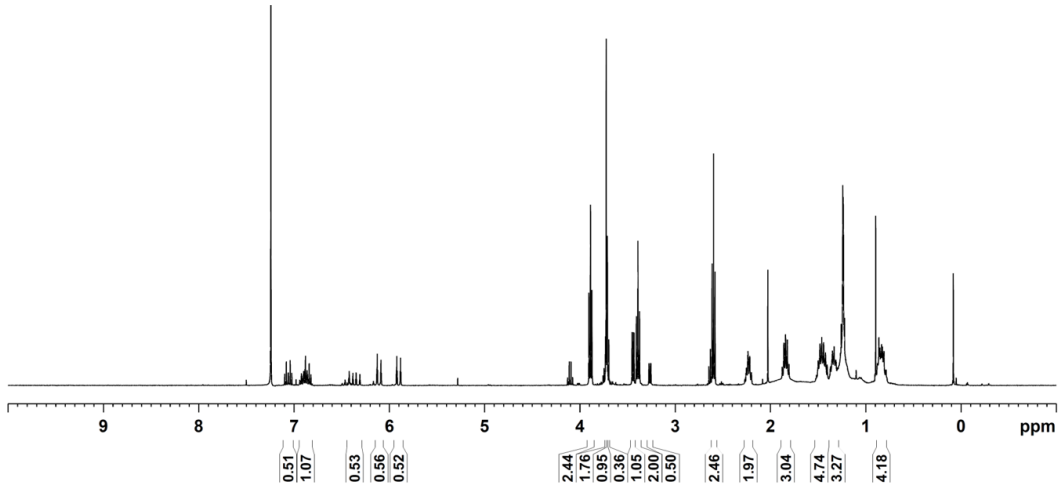

(*E*)-Methyl 13-bromo-3-(*tert*-butyldimethylsilyloxy)-5-oxotridec-6-enoate (**S-6**)

^{1}H NMR (400 MHz, $CDCl_3$)

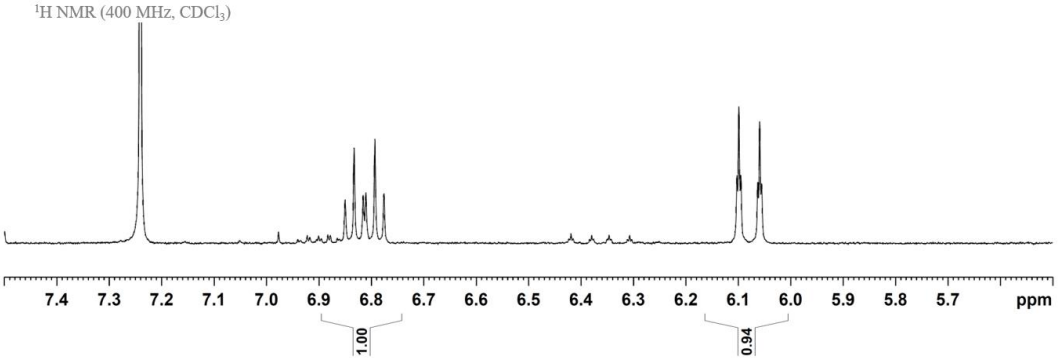

(2*E*,6*E*)-13-Bromo-5-oxotrideca-2,6-dienoic acid (*β*-elimination by-product, **S-7**)

^{1}H NMR (400 MHz, $CDCl_3$)

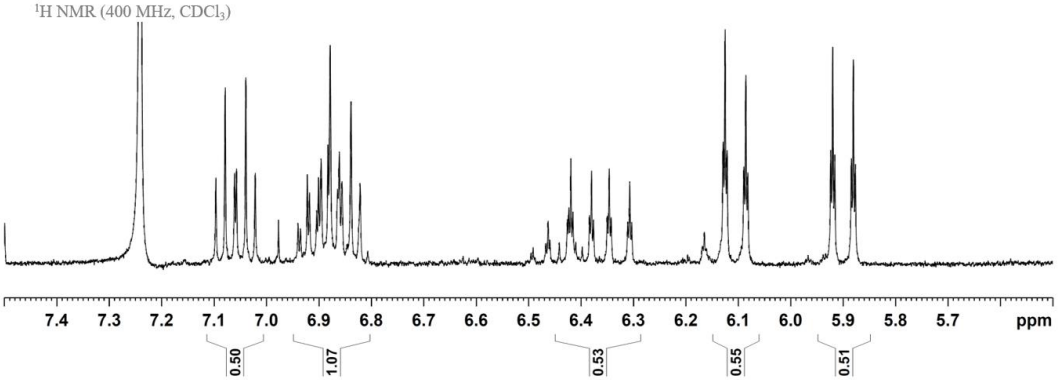

(*E*)-Methyl 13-bromo-3-(*tert*-butyldimethylsilyloxy)-5-oxotridec-6-enoate (**S-6**)

^{1}H NMR (400 MHz, $CDCl_3$)

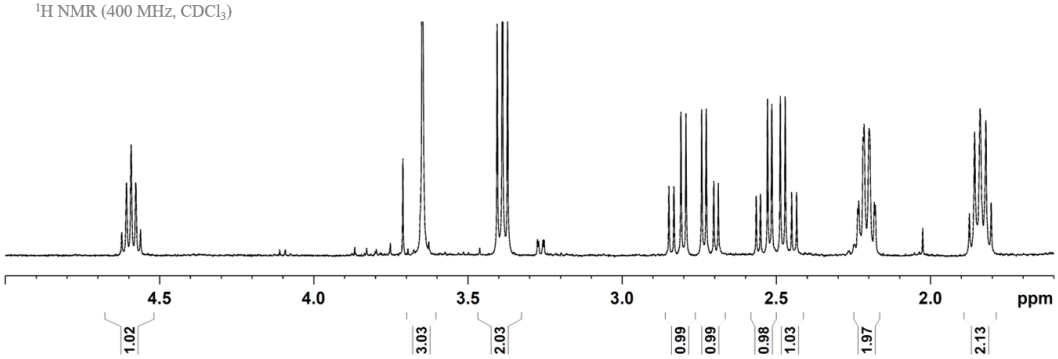

(2*E*,6*E*)-13-Bromo-5-oxotrideca-2,6-dienoic acid (*β*-elimination by-product, **S-7**)

^{1}H NMR (400 MHz, $CDCl_3$)

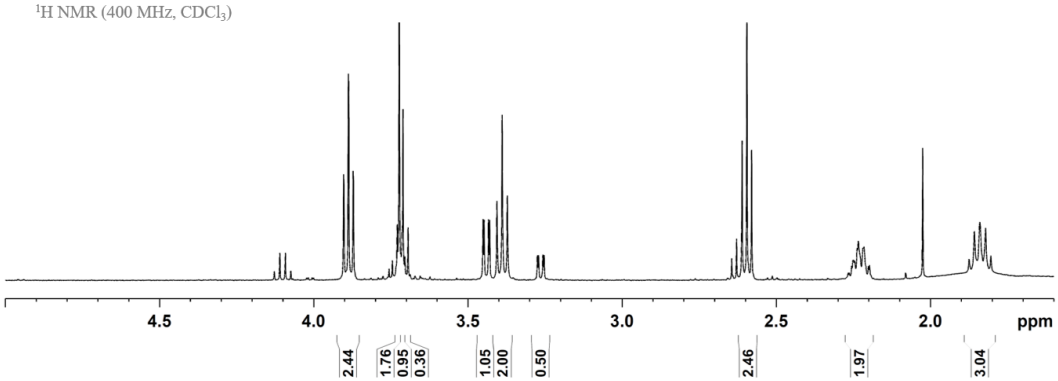

S1.2.4 First-Generation α,β-Unsaturated Ketone Model v2.2 (§ 3.5.1)

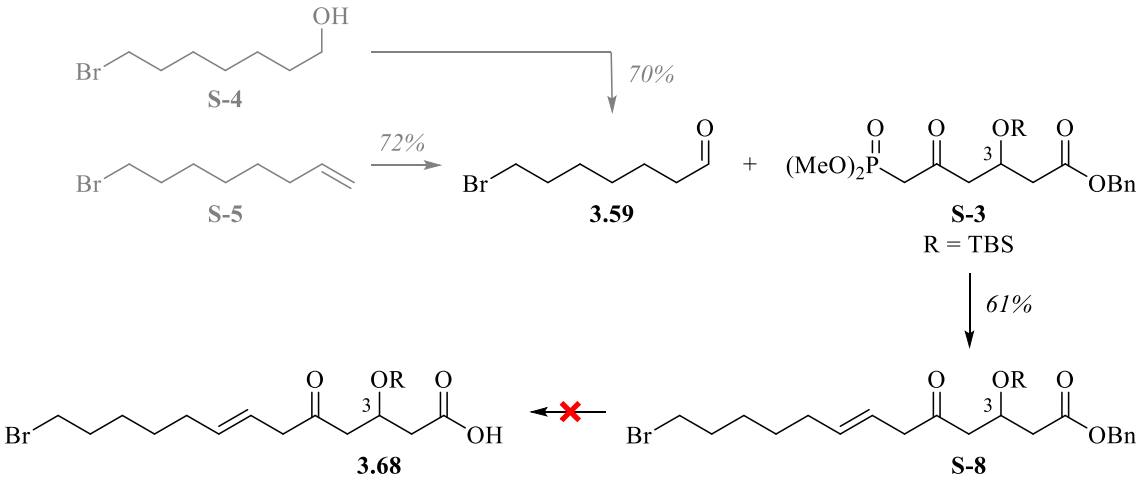

Figure S4 – Summary of the synthesis of first-generation *α,β*-unsaturated ketone model version 2.2.

(*E*)-Benzyl 13-bromo-3-(*tert*-butyldimethylsilyloxy)-5-oxotridec-6-enoate (**S-8**)

^{1}H NMR (300 MHz, $CDCl_3$)

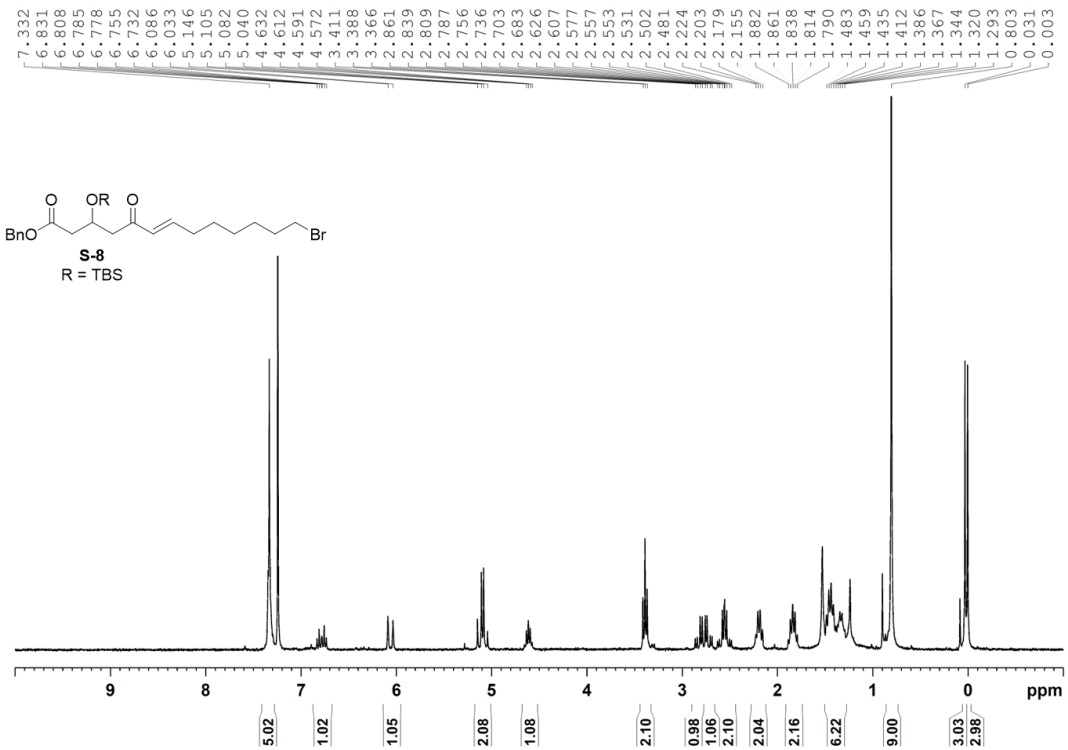

(*E*)-Benzyl 13-bromo-3-(*tert*-butyldimethylsilyloxy)-5-oxotridec-6-enoate (**S-8**)

^{13}C NMR (75 MHz, $CDCl_3$)

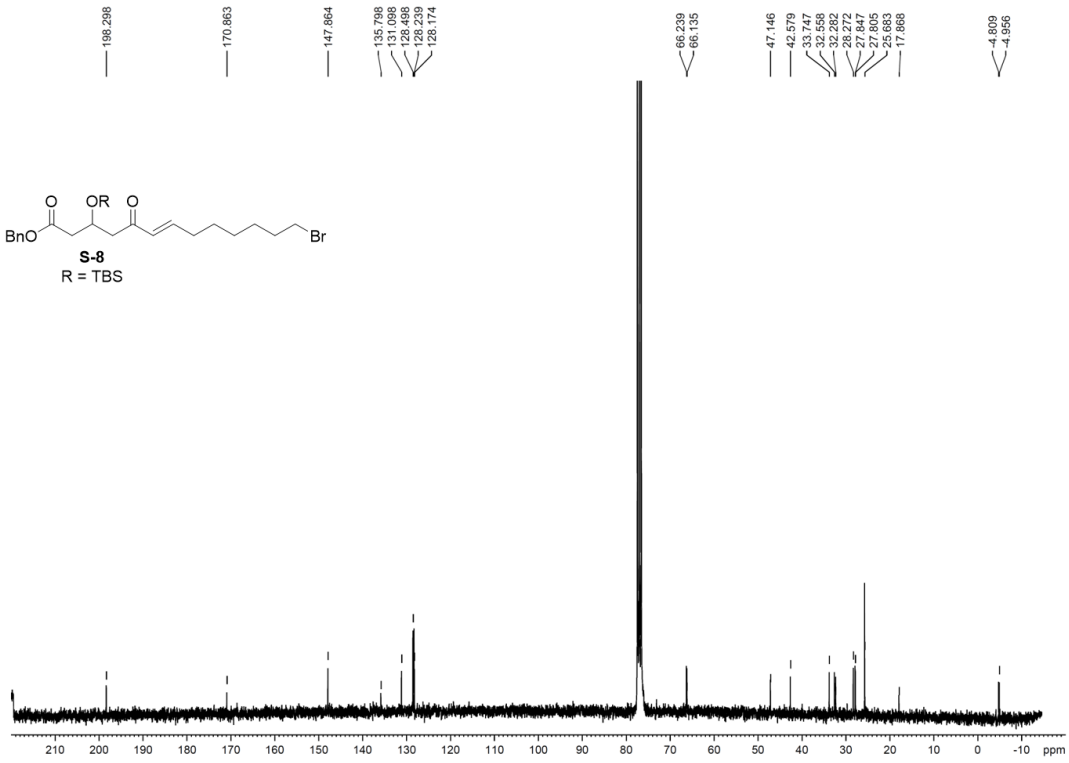

S1.2.5 First-Generation α,β-Unsaturated Ketone Model v2.3 (§ 3.5.1)

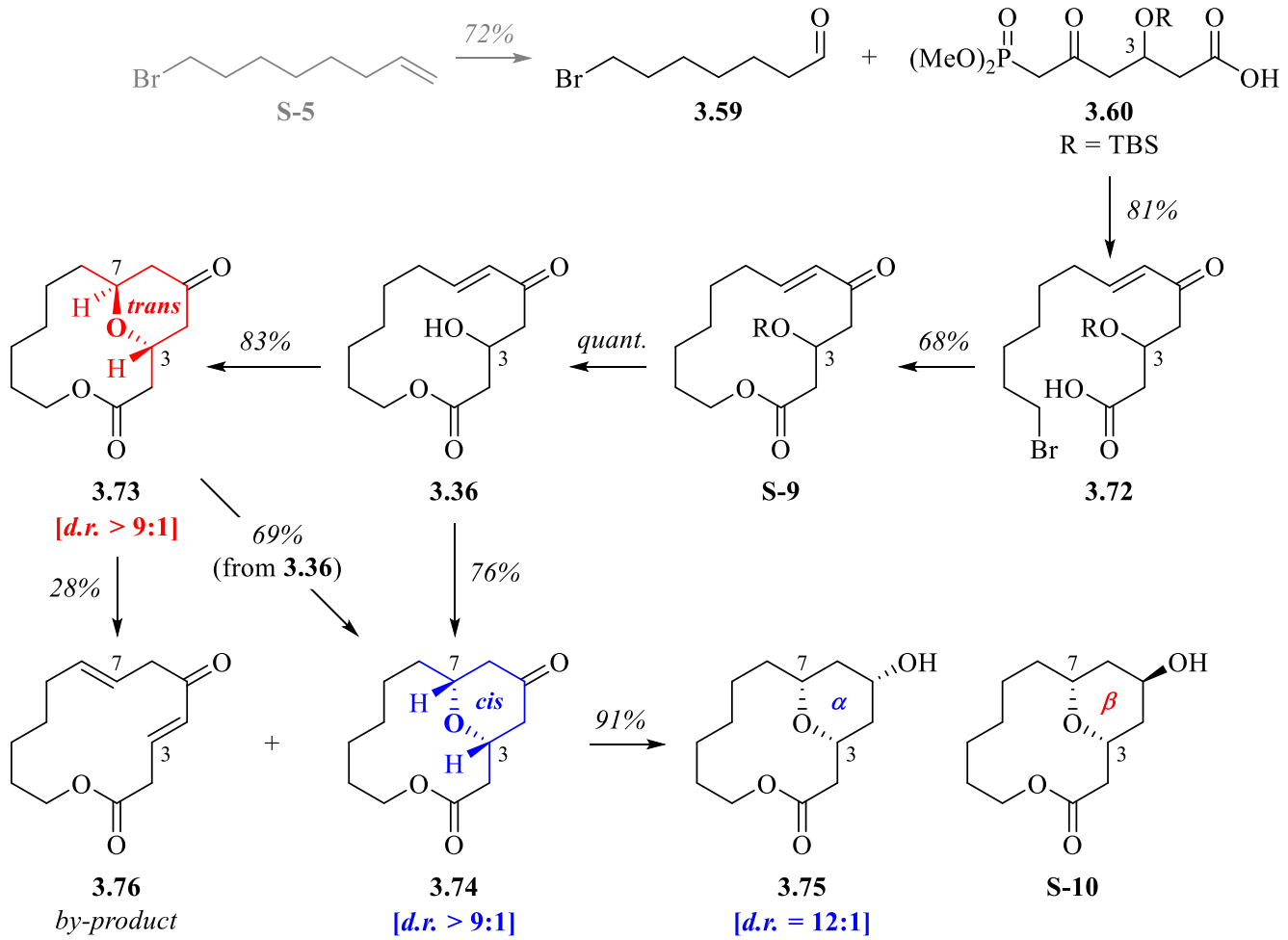

Figure S5 – Summary of the synthesis of first-generation *α,β*-unsaturated ketone model version 2.3.

(*E*)-13-Bromo-3-(*tert*-butyldimethylsilyloxy)-5-oxotridec-6-enoic acid (**3.72**)

^{1}H NMR (400 MHz, $CDCl_3$)

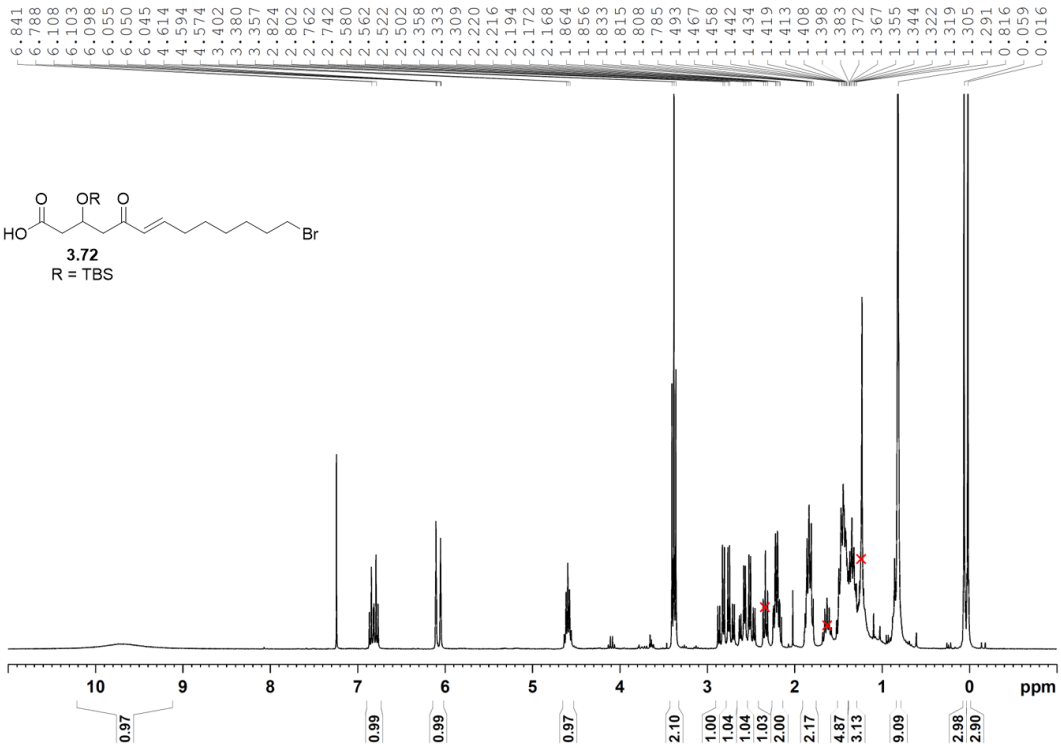

(*E*)-13-Bromo-3-(*tert*-butyldimethylsilyloxy)-5-oxotridec-6-enoic acid (**3.72**)

^{13}C NMR (100 MHz, $CDCl_3$)

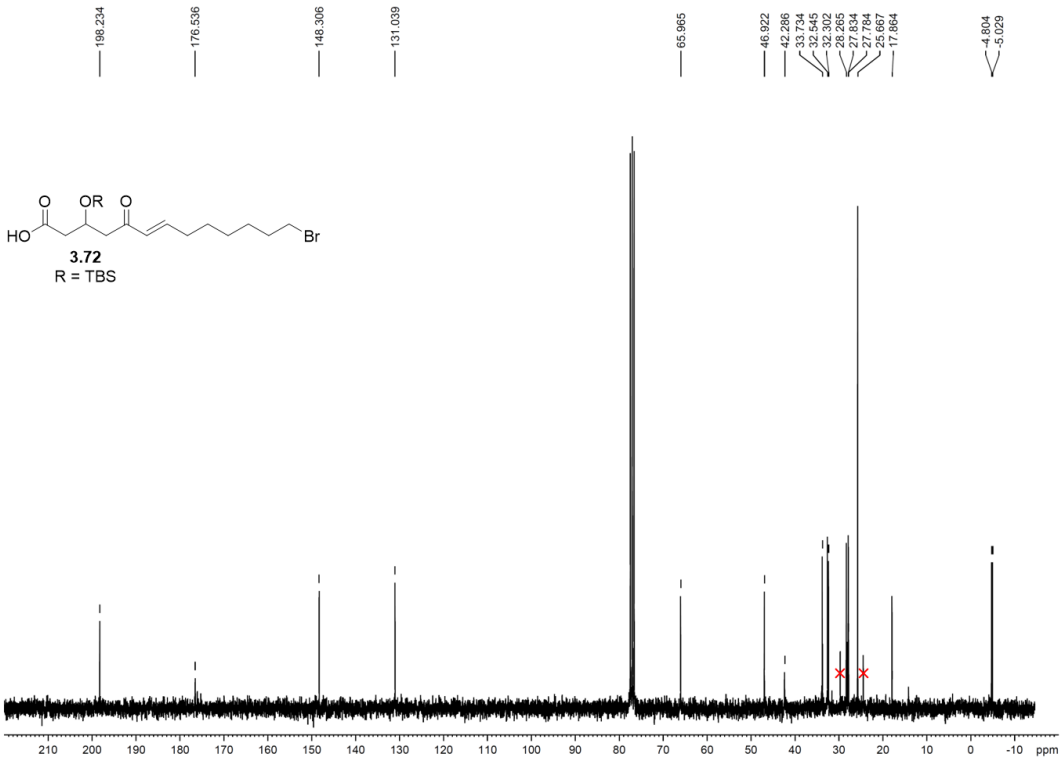

(*E*)-4-(*tert*-butyldimethylsilyloxy)oxacyclotetradec-7-ene-2,6-dione (**S-9**)

^{1}H NMR (400 MHz, $CDCl_3$)

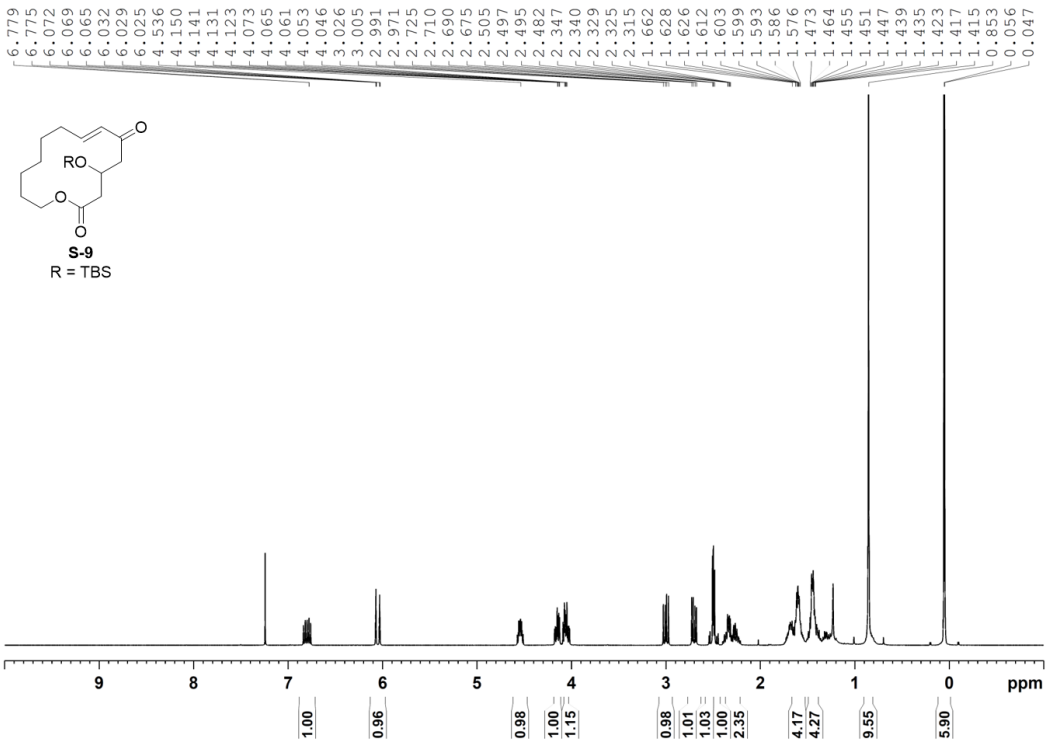

(*E*)-4-(*tert*-butyldimethylsilyloxy)oxacyclotetradec-7-ene-2,6-dione (**S-9**)

^{13}C NMR (100 MHz, $CDCl_3$)

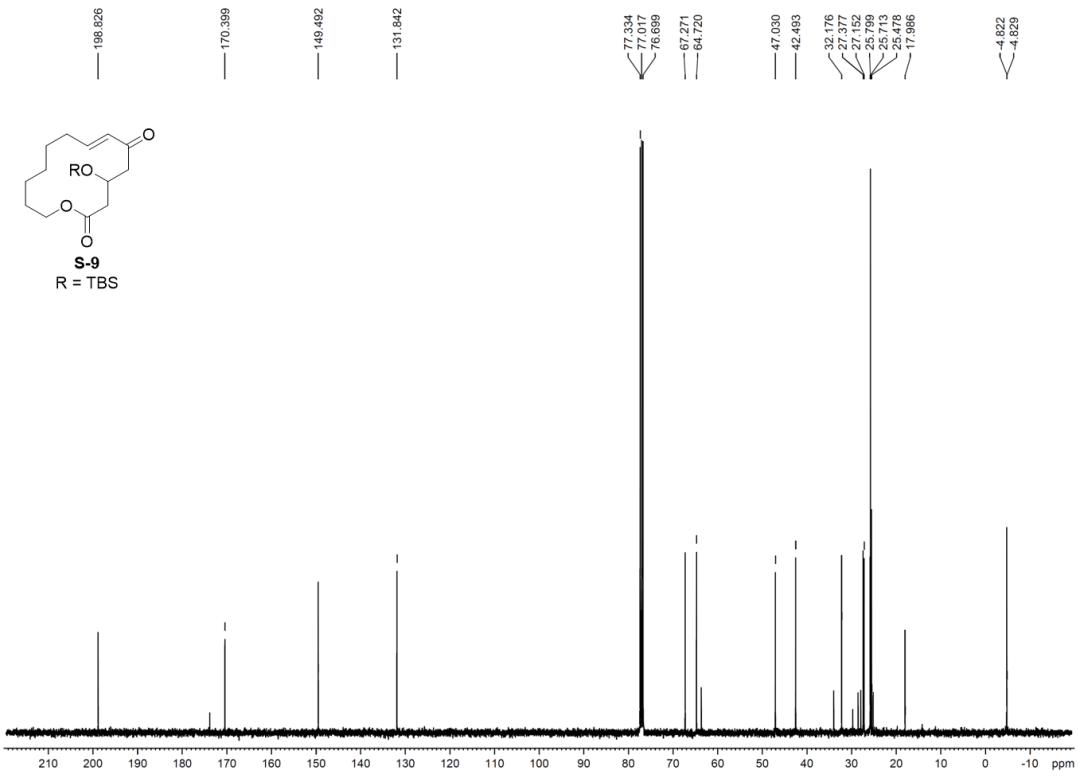

(*E*)-4-(*tert*-butyldimethylsilyloxy)oxacyclotetradec-7-ene-2,6-dione (**S-9**)

COSY (400 MHz, $CDCl_3$)

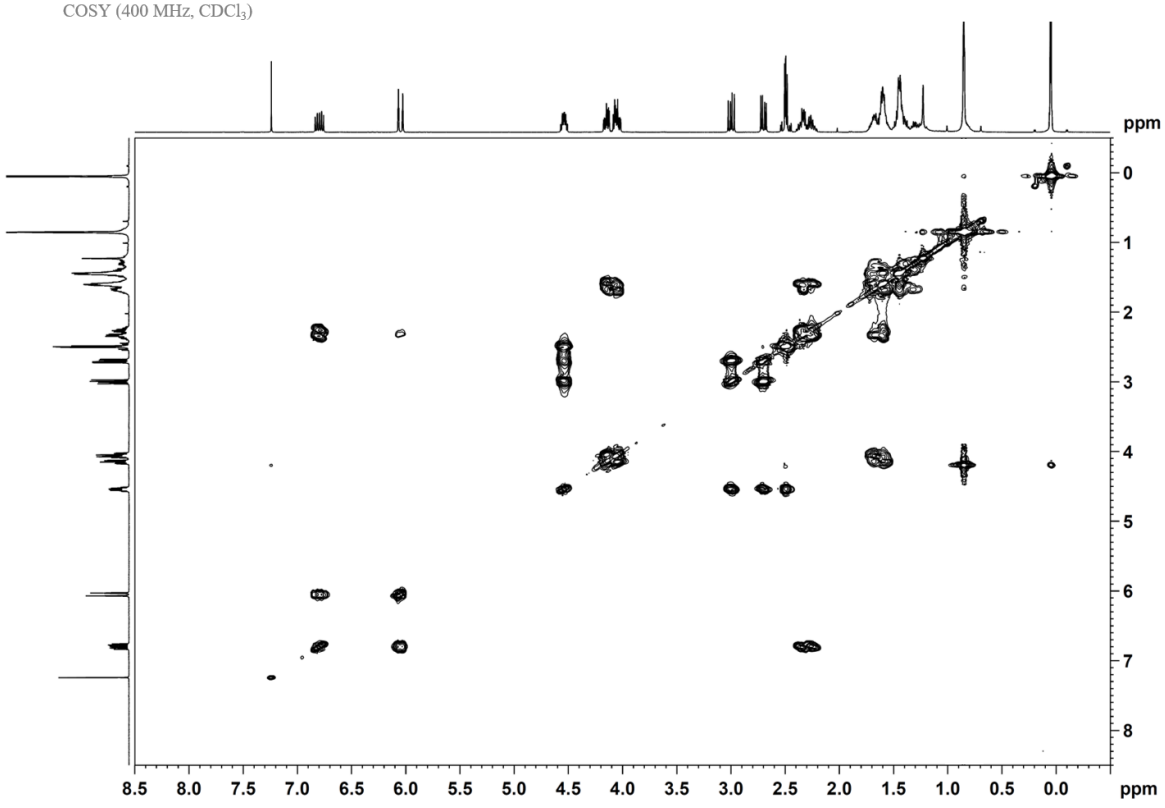

(*E*)-4-(*tert*-butyldimethylsilyloxy)oxacyclotetradec-7-ene-2,6-dione (**S-9**)

HSQC (400 MHz, $CDCl_3$)

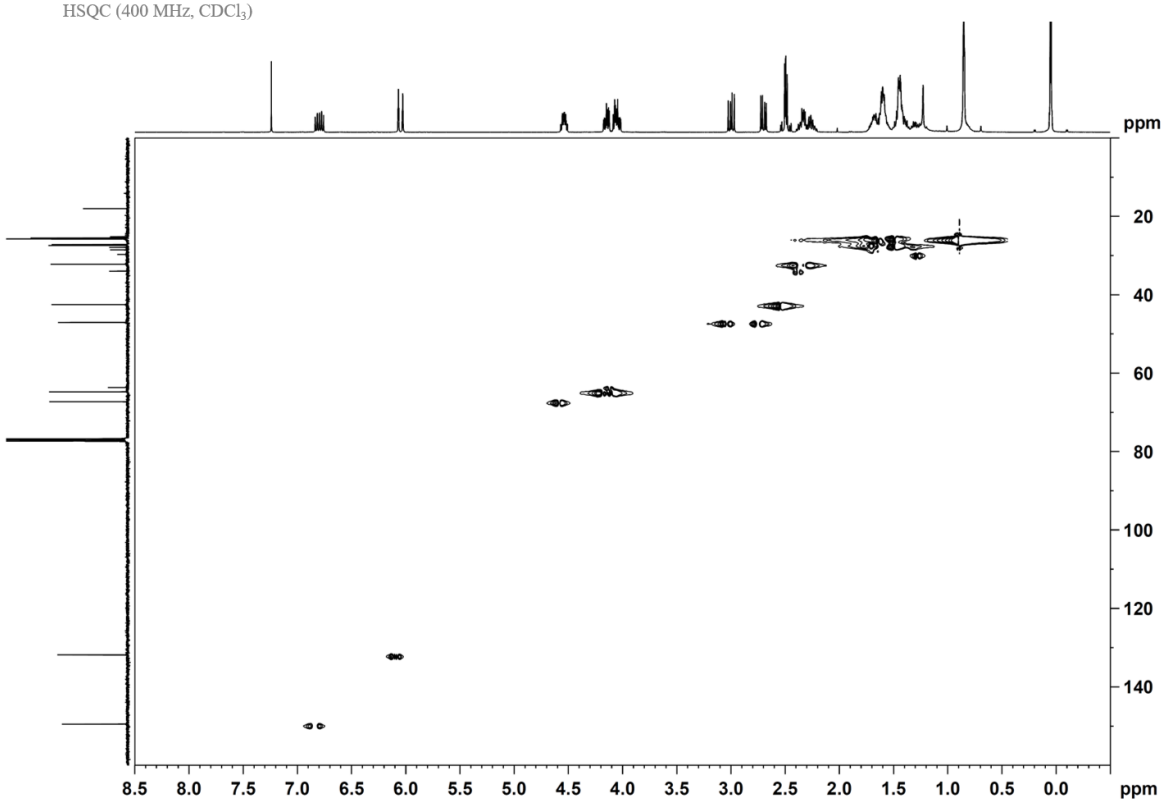

(*E*)-4-(*tert*-butyldimethylsilyloxy)oxacyclotetradec-7-ene-2,6-dione (**S-9**)

HMBC (400 MHz, $CDCl_3$)

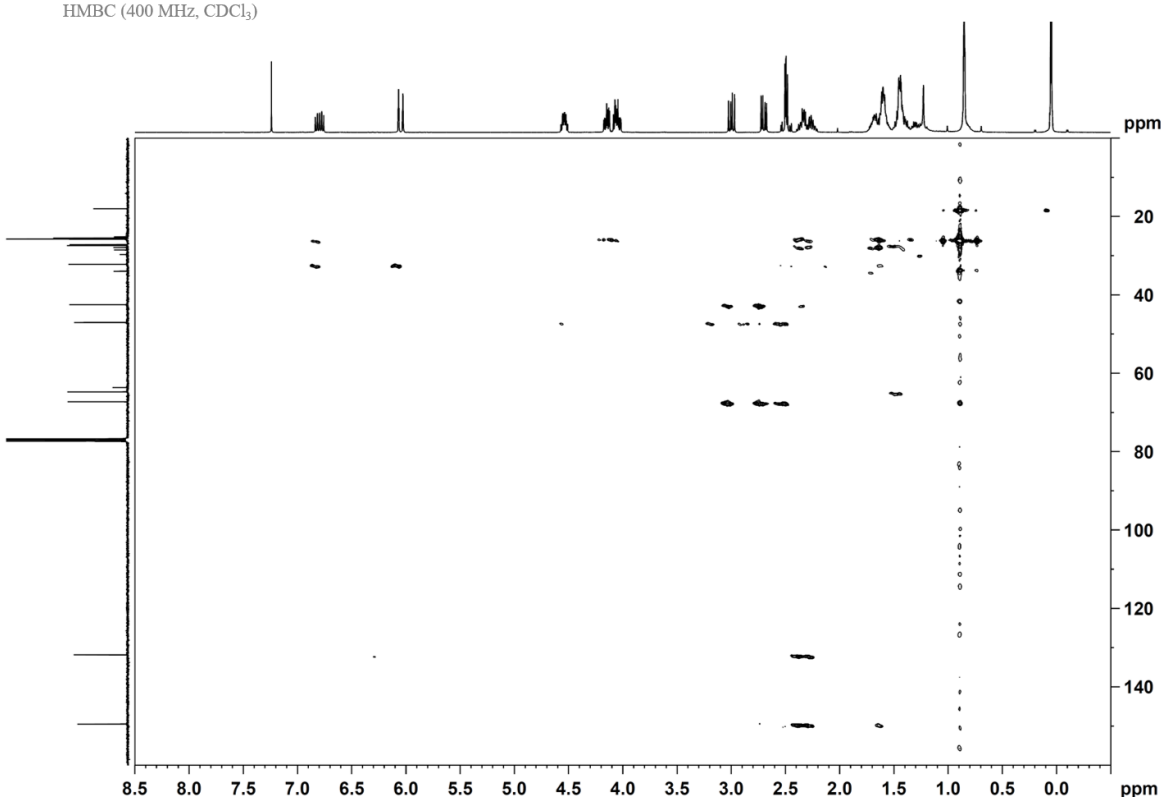

(*E*)-4-Hydroxyoxacyclotetradec-7-ene-2,6-dione (**3.36**)

^{1}H NMR (400 MHz, $CDCl_3$)

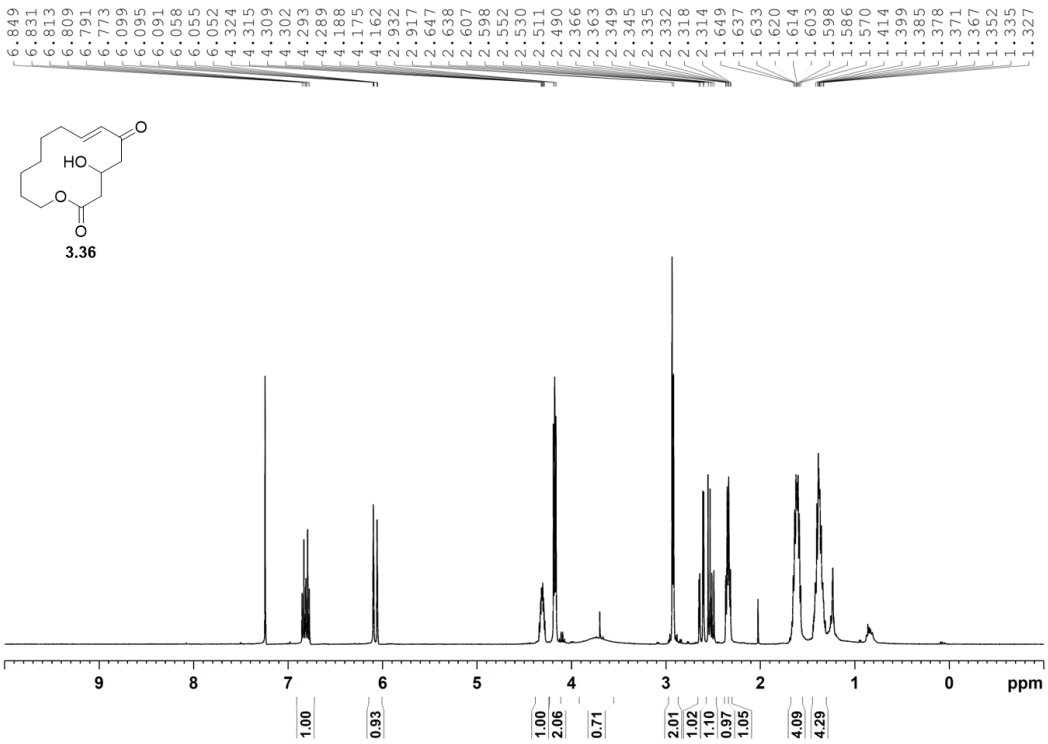

(*E*)-4-Hydroxyoxacyclotetradec-7-ene-2,6-dione (**3.36**)

^{13}C NMR (100 MHz, $CDCl_3$)

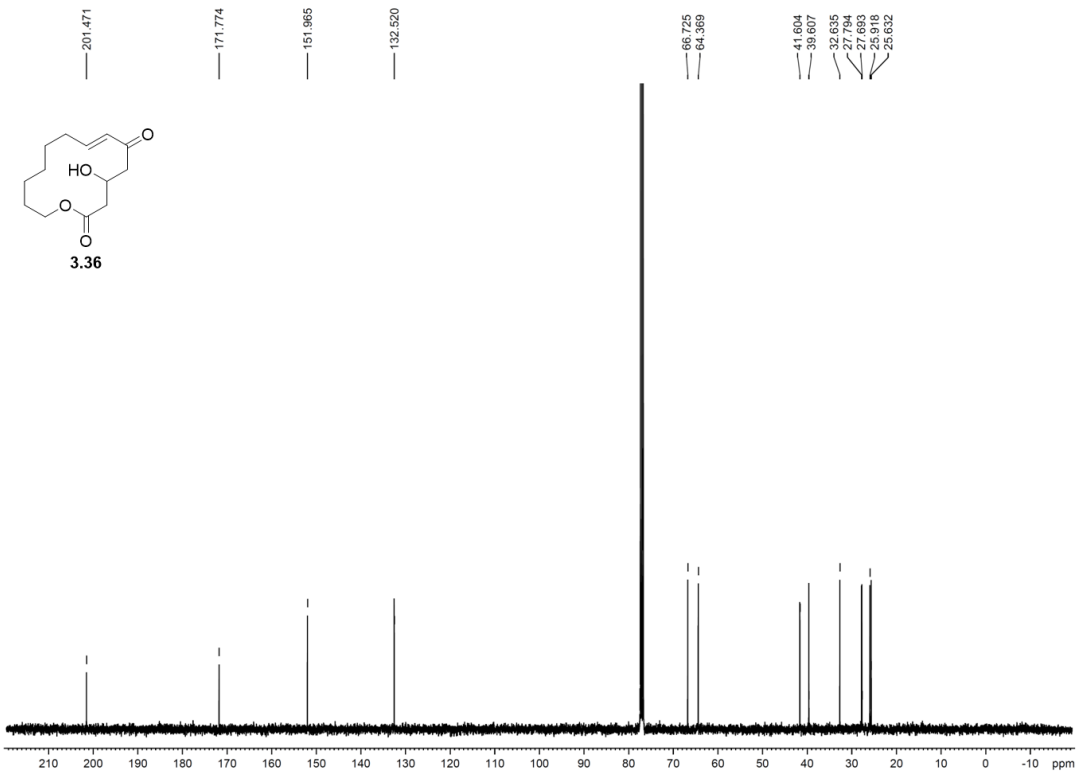

(*E*)-4-Hydroxyoxacyclotetradec-7-ene-2,6-dione (**3.36**)

COSY (400 MHz, $CDCl_3$)

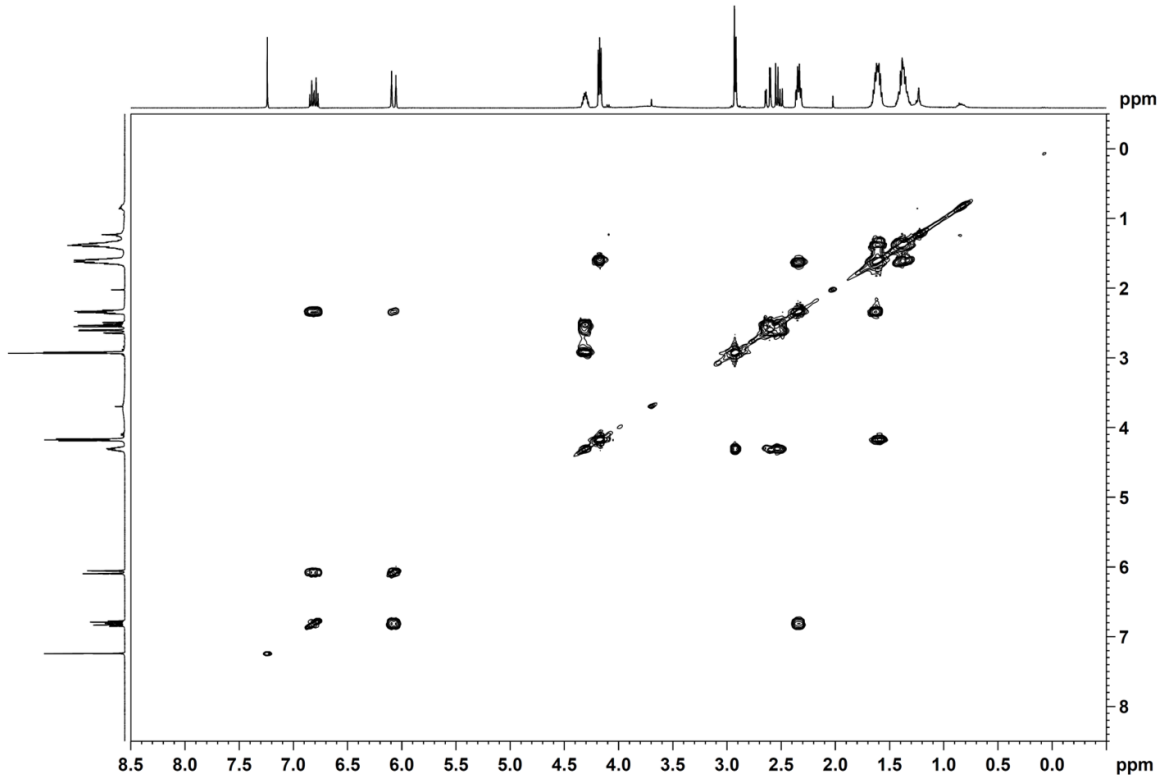

(*E*)-4-Hydroxyoxacyclotetradec-7-ene-2,6-dione (**3.36**)

HSQC (400 MHz, $CDCl_3$)

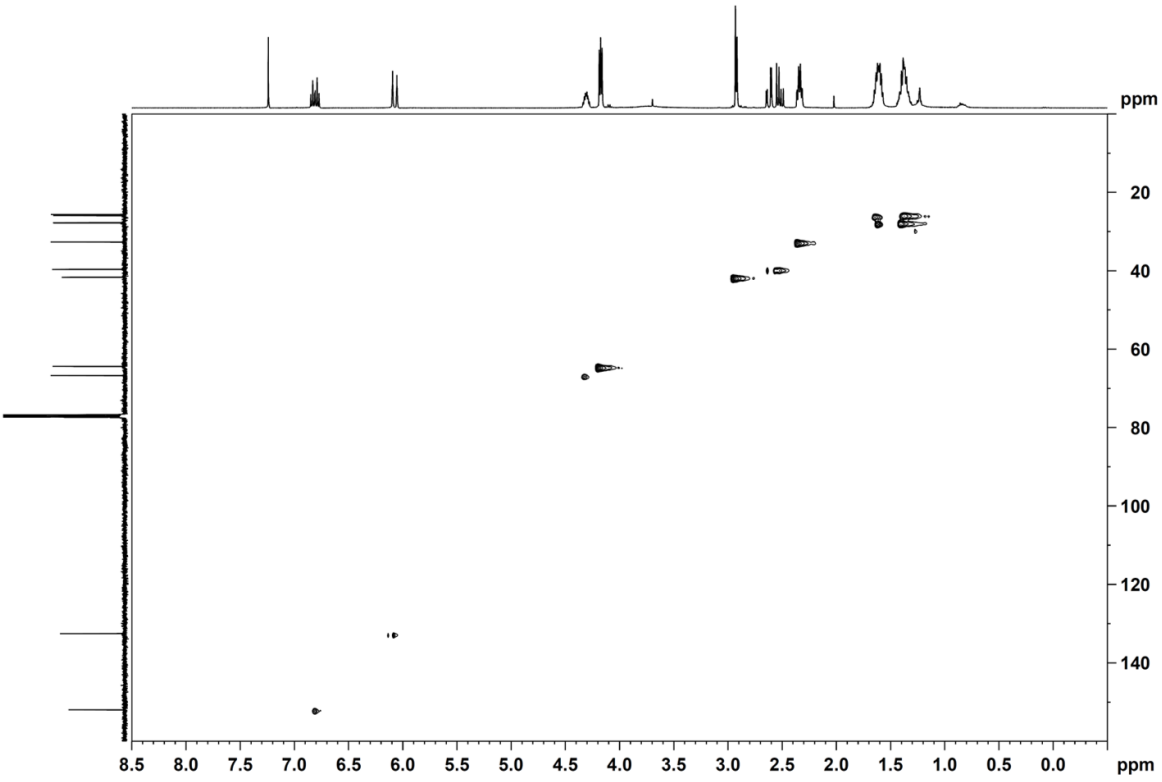

***trans*-4,15-Dioxabicyclo[9.3.1]pentadecane-3,13-dione (3.73)**

^{1}H NMR (400 MHz, $CDCl_3$)

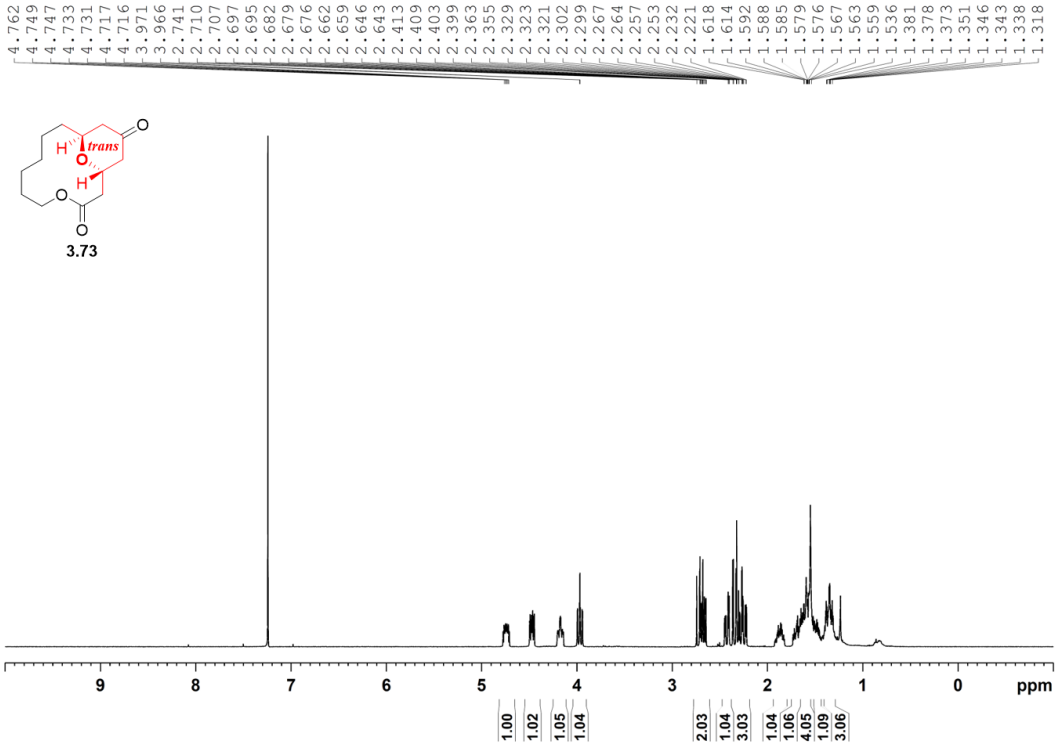

***trans*-4,15-Dioxabicyclo[9.3.1]pentadecane-3,13-dione (3.73)**

^{13}C NMR (100 MHz, $CDCl_3$)

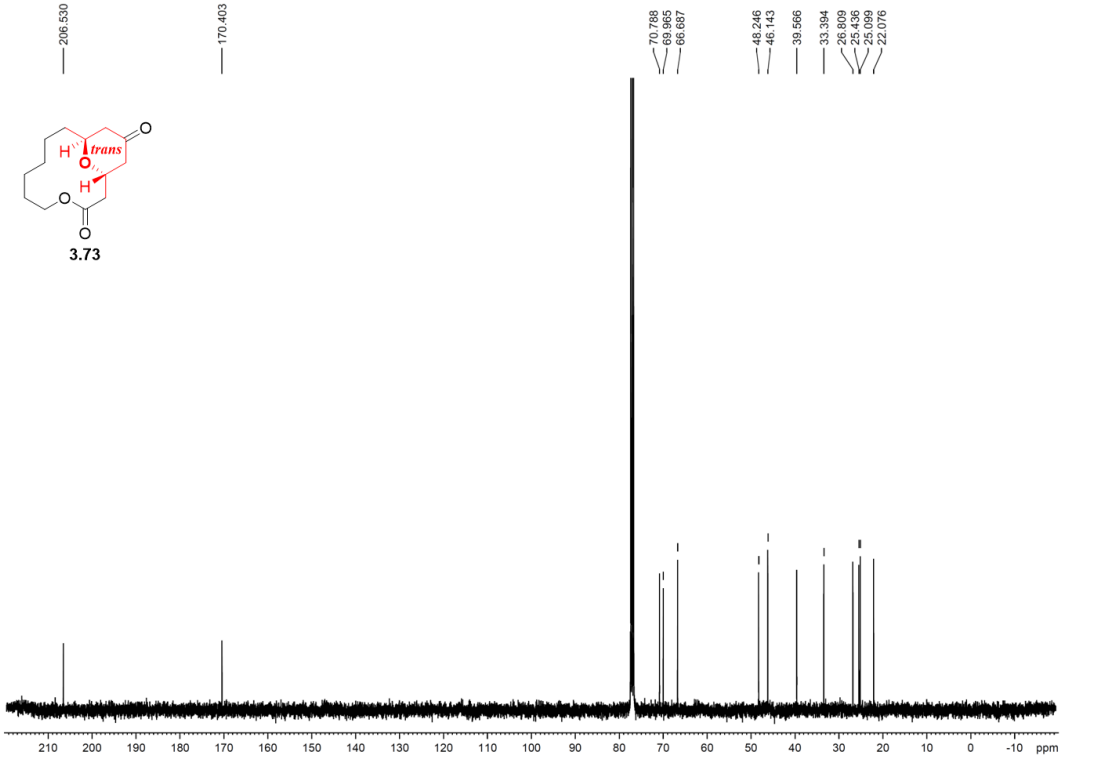

***trans*-4,15-Dioxabicyclo[9.3.1]pentadecane-3,13-dione (3.73)**

COSY (400 MHz, $CDCl_3$)

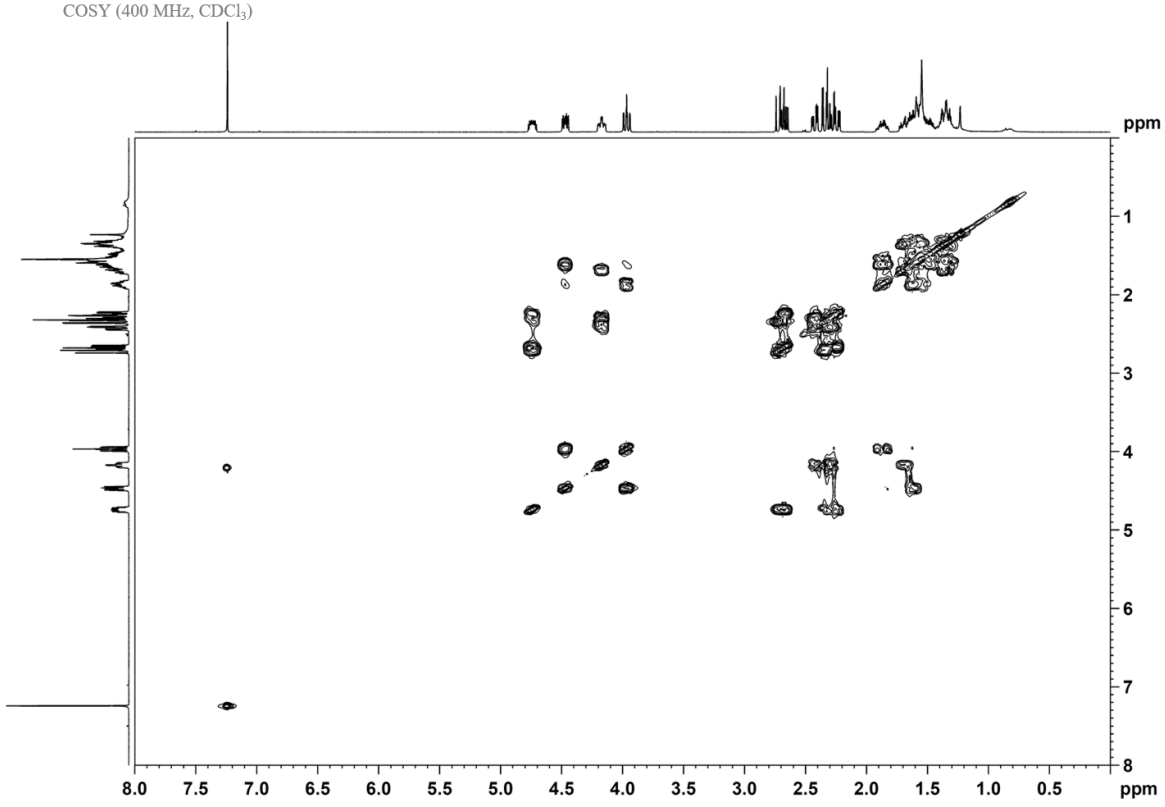

trans-4,15-Dioxabicyclo[9.3.1]pentadecane-3,13-dione (**3.73**)

HSQC (400 MHz, $CDCl_3$)

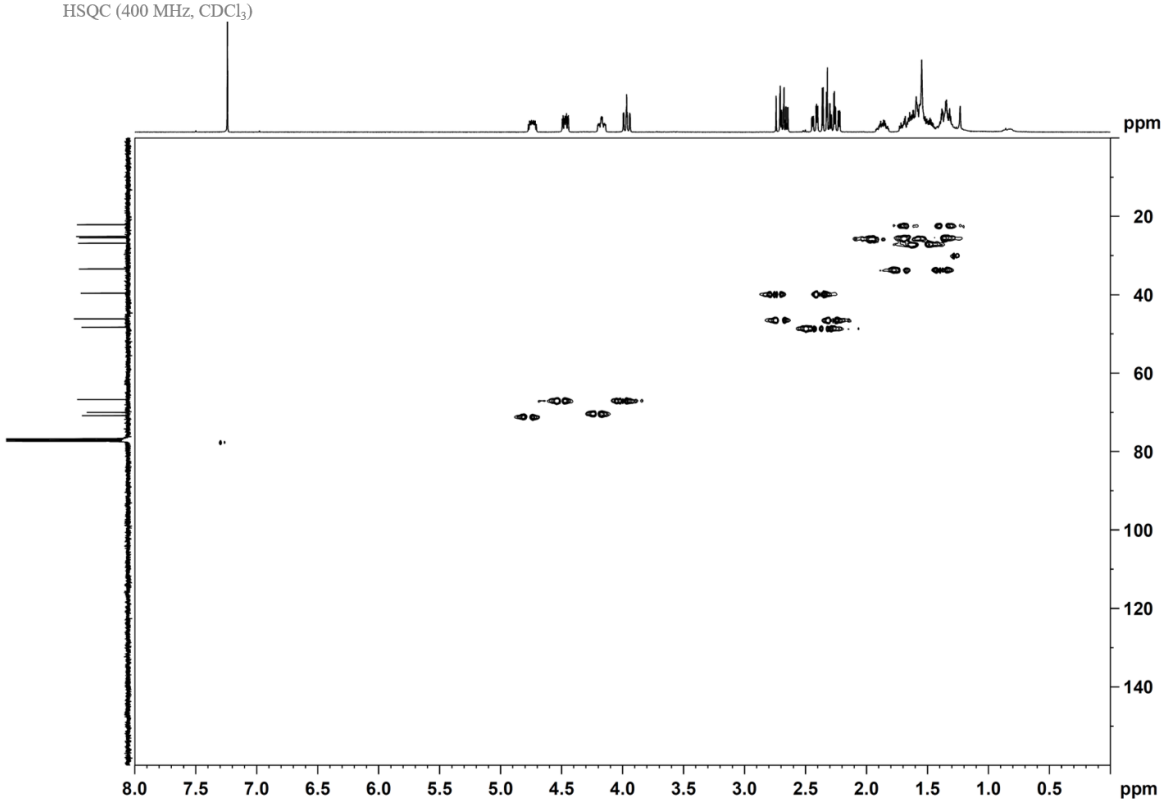

trans-4,15-Dioxabicyclo[9.3.1]pentadecane-3,13-dione (**3.73**)

NOESY (400 MHz, $CDCl_3$)

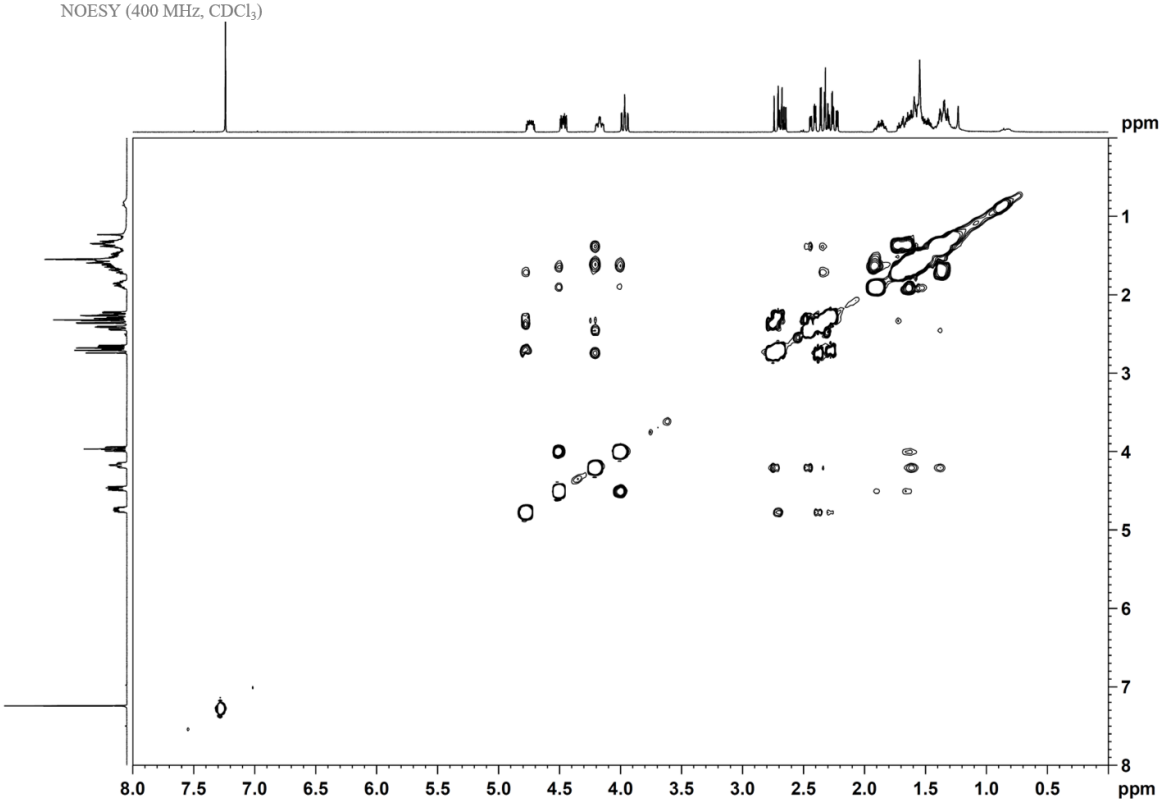

trans-4,15-Dioxabicyclo[9.3.1]pentadecane-3,13-dione (**3.73**)

TOCSY (400 MHz, $CDCl_3$)

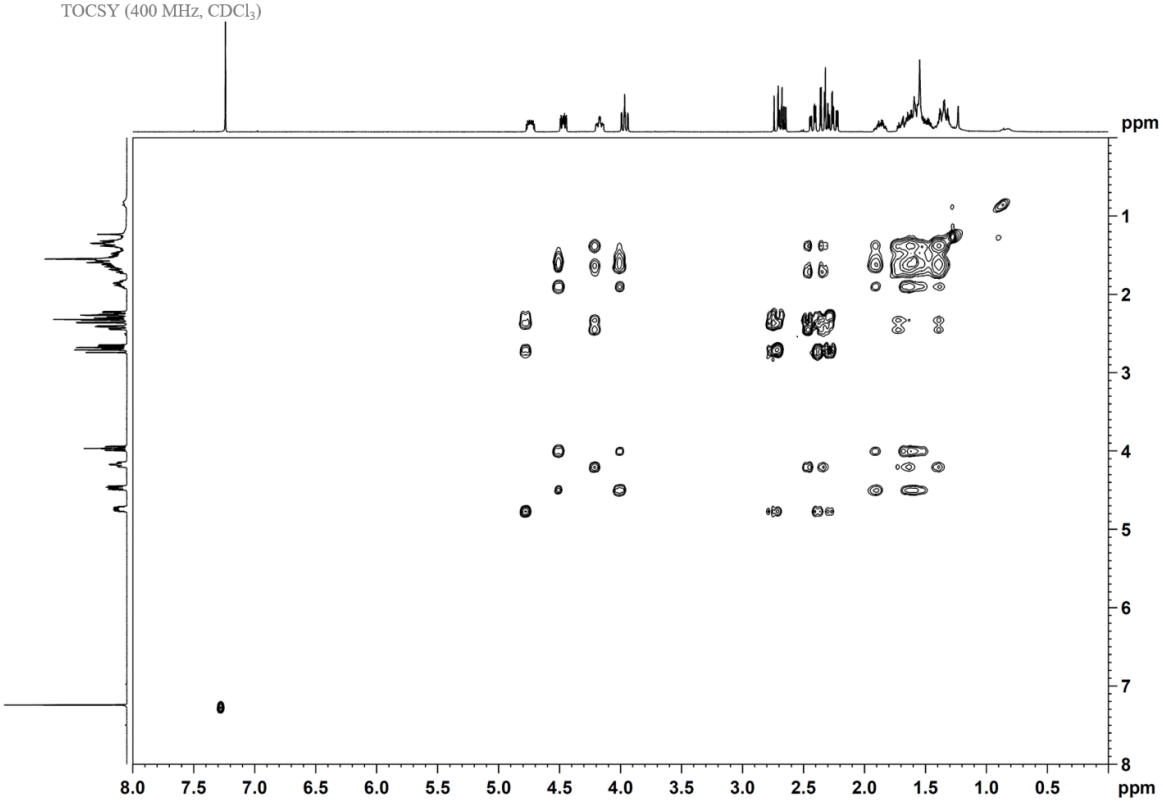

***cis*-4,15-Dioxabicyclo[9.3.1]pentadecane-3,13-dione (3.74)**

^{1}H NMR (400 MHz, $CDCl_3$)

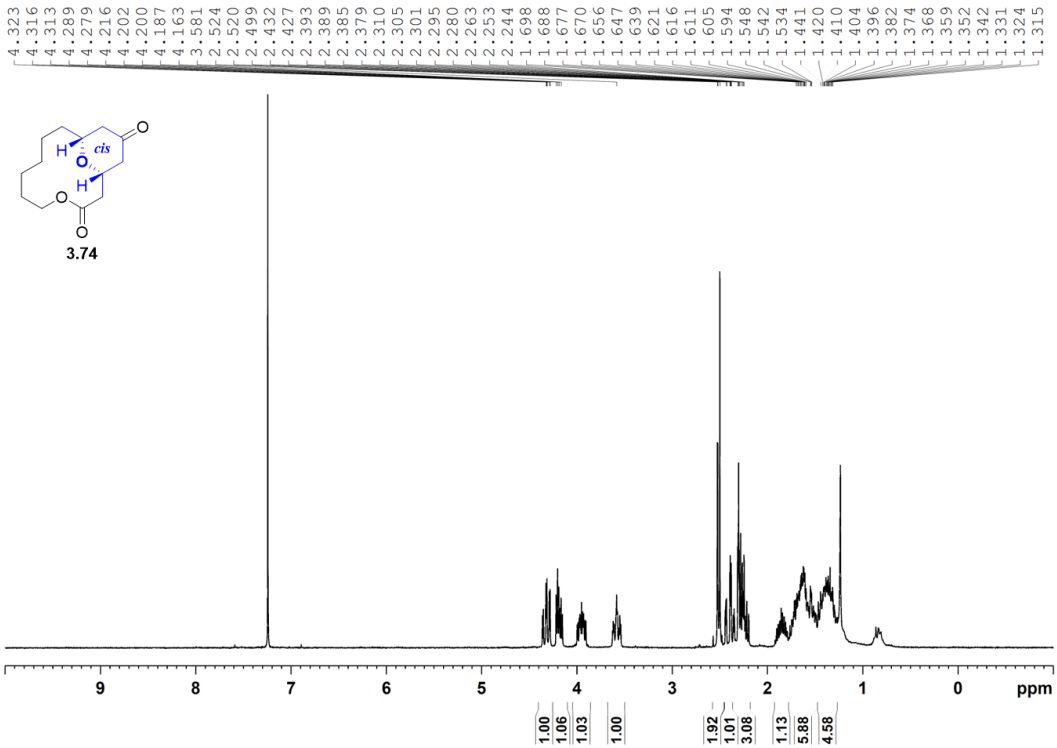

***cis*-4,15-Dioxabicyclo[9.3.1]pentadecane-3,13-dione (3.74)**

^{13}C NMR (100 MHz, $CDCl_3$)

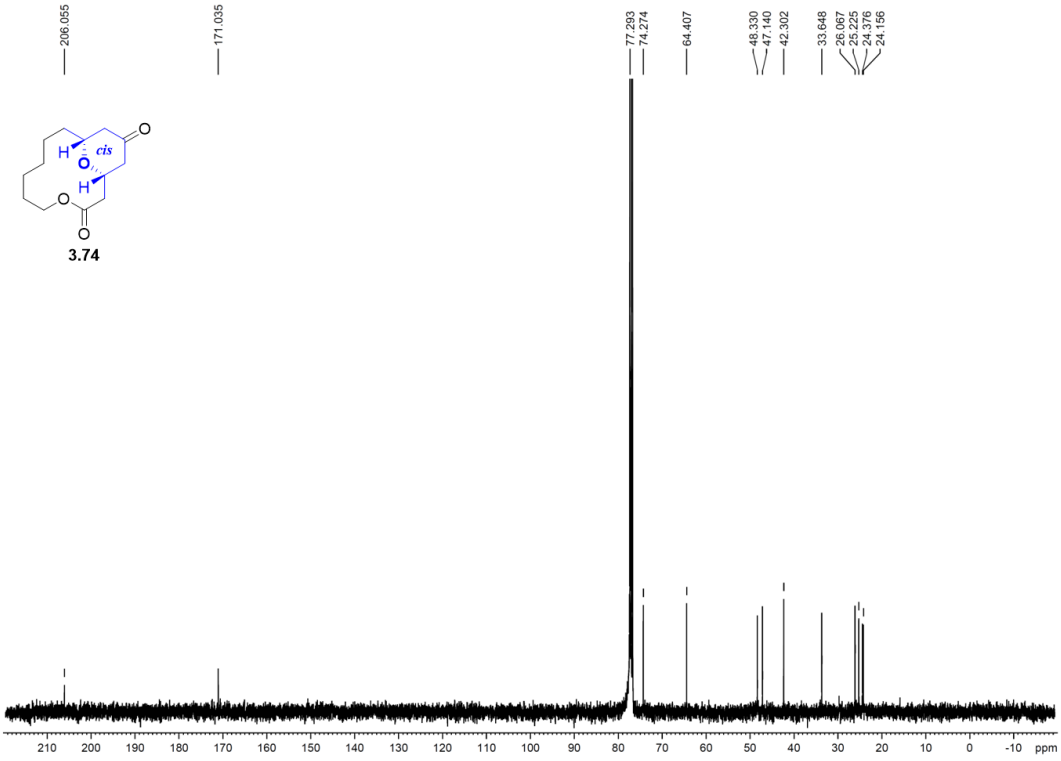

cis-4,15-Dioxabicyclo[9.3.1]pentadecane-3,13-dione (**3.74**)

COSY (400 MHz, $CDCl_3$)

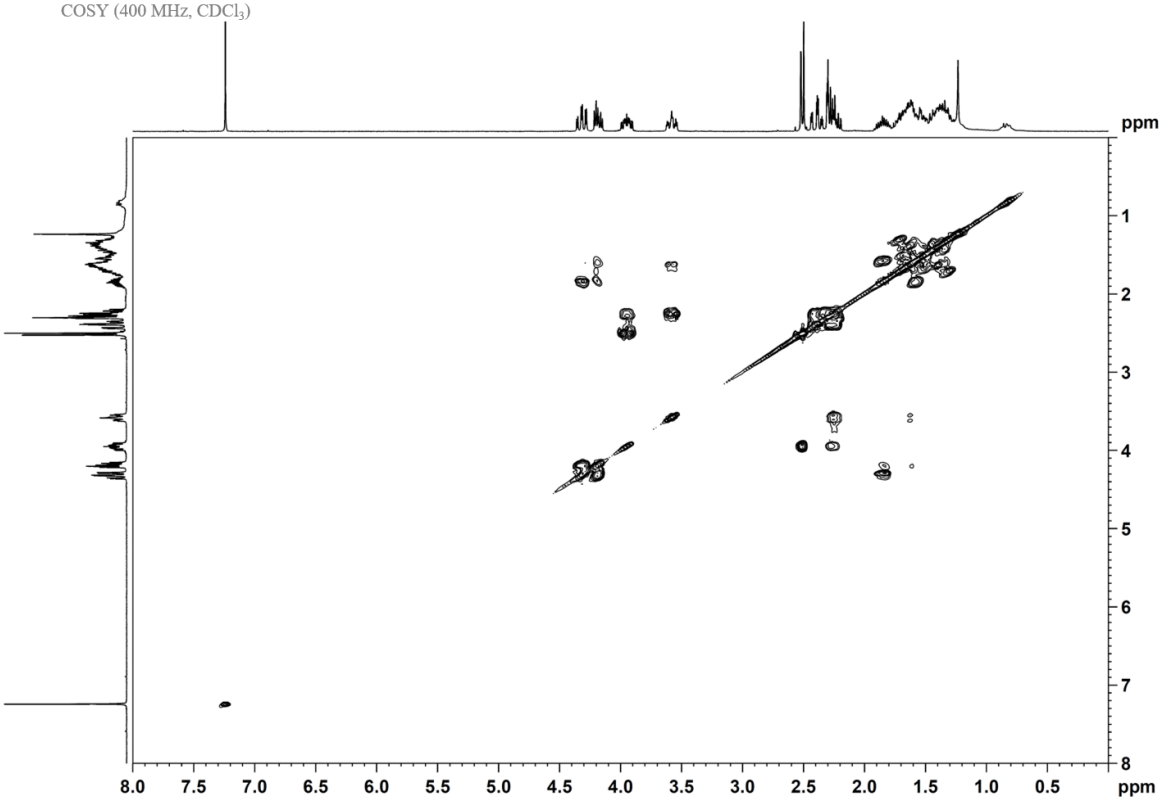

cis-4,15-Dioxabicyclo[9.3.1]pentadecane-3,13-dione (**3.74**)

HSQC (400 MHz, $CDCl_3$)

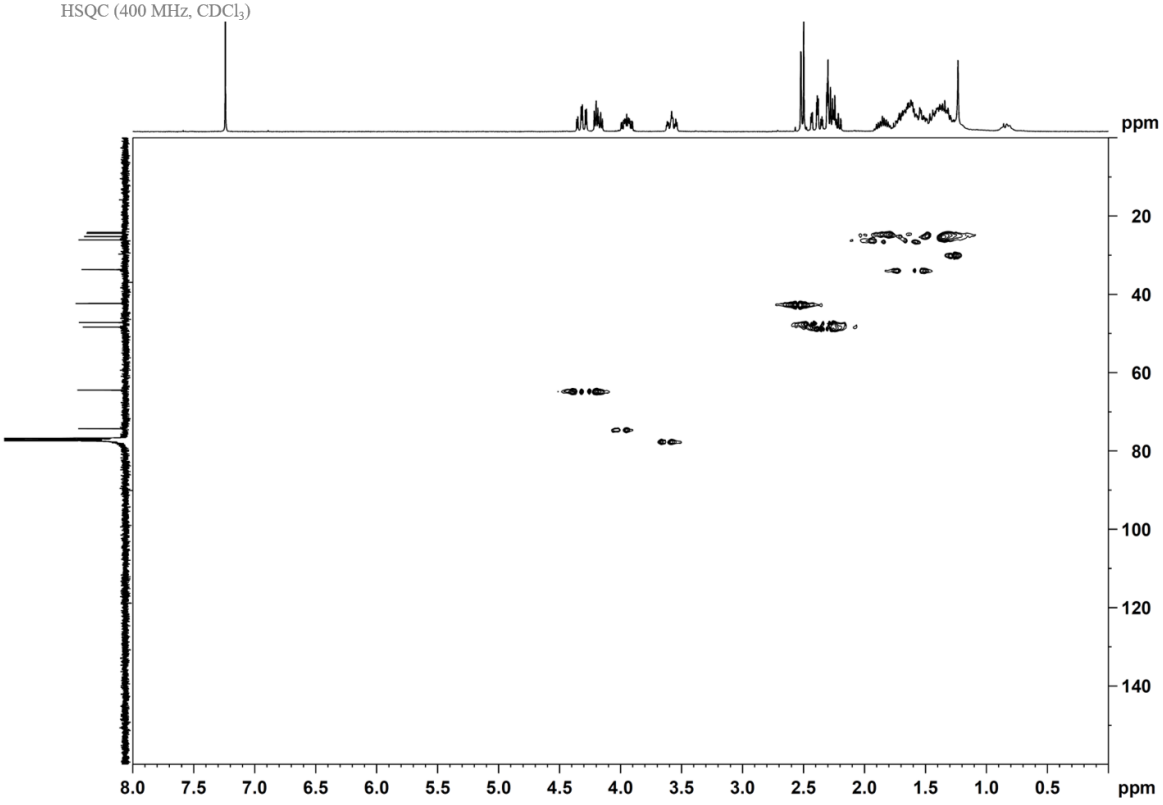

cis-4,15-Dioxabicyclo[9.3.1]pentadecane-3,13-dione (**3.74**)

NOESY (400 MHz, $CDCl_3$)

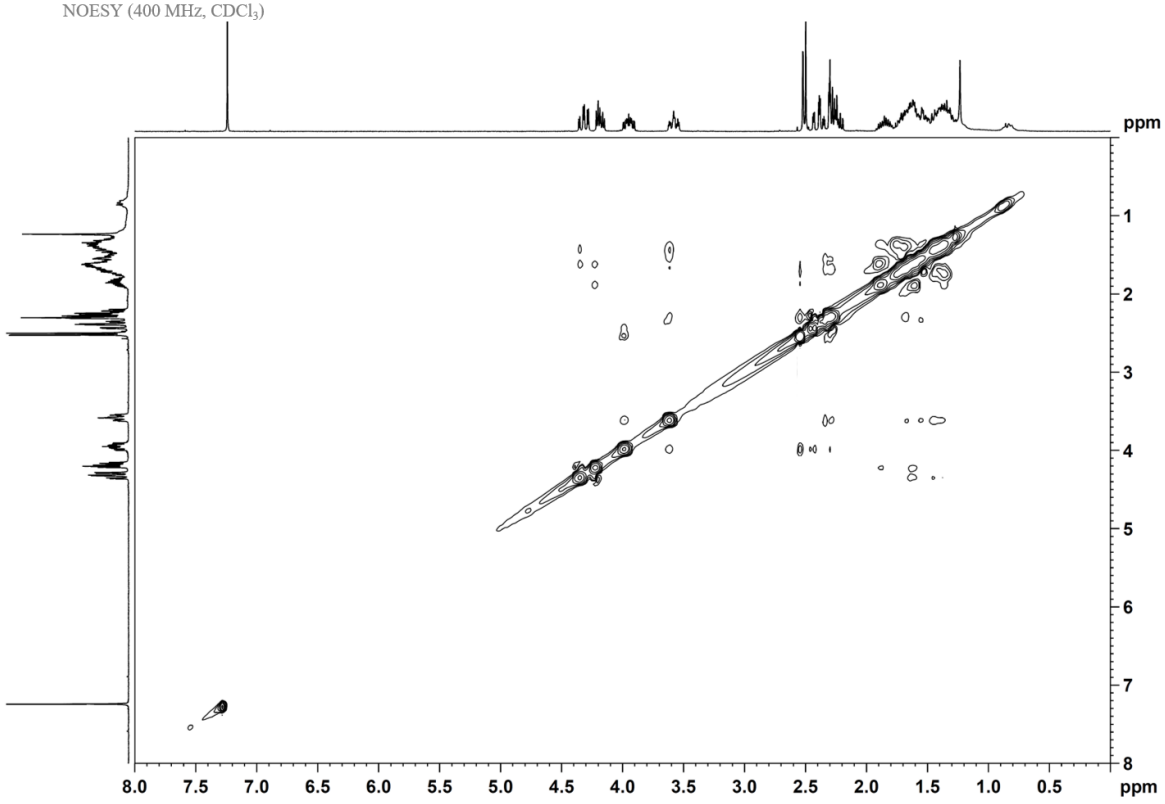

cis-4,15-Dioxabicyclo[9.3.1]pentadecane-3,13-dione (**3.74**)

TOCSY (400 MHz, $CDCl_3$)

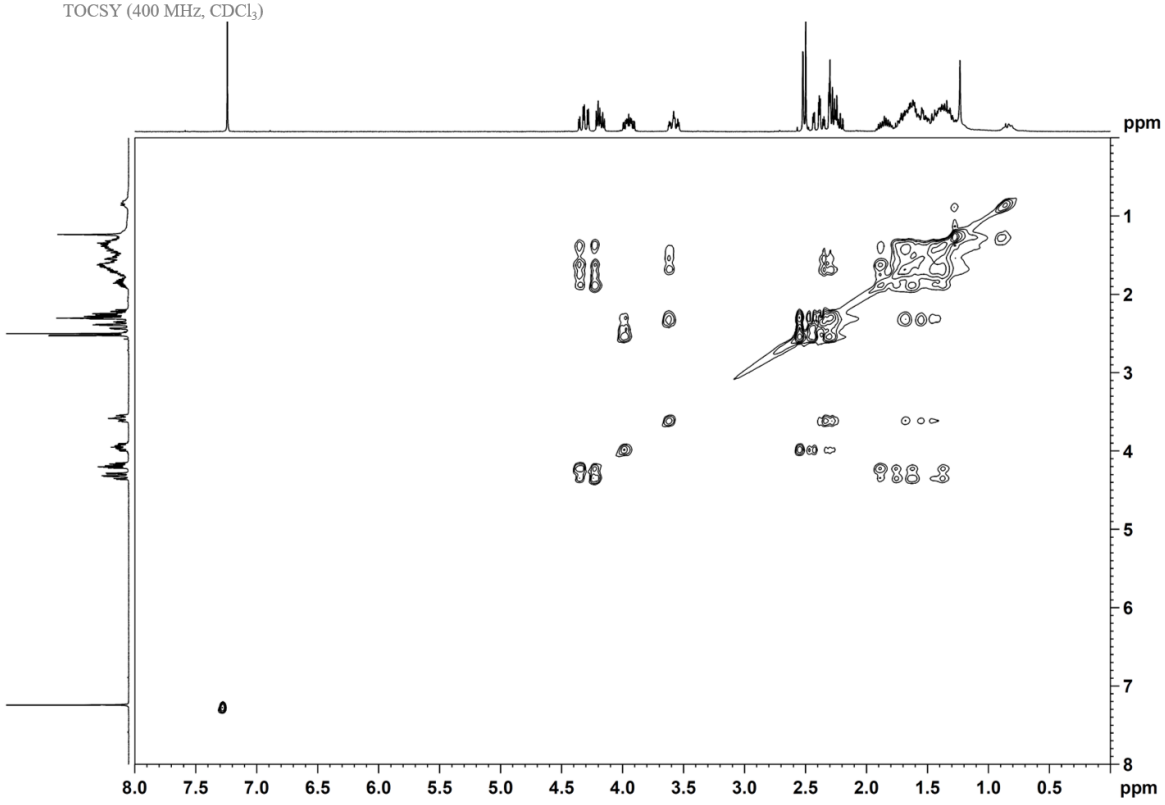

(4*E*,8*E*)-Oxacyclotetradeca-4,8-diene-2,6-dione (elimination by-product, **3.76**)

^{1}H NMR (400 MHz, $CDCl_3$)

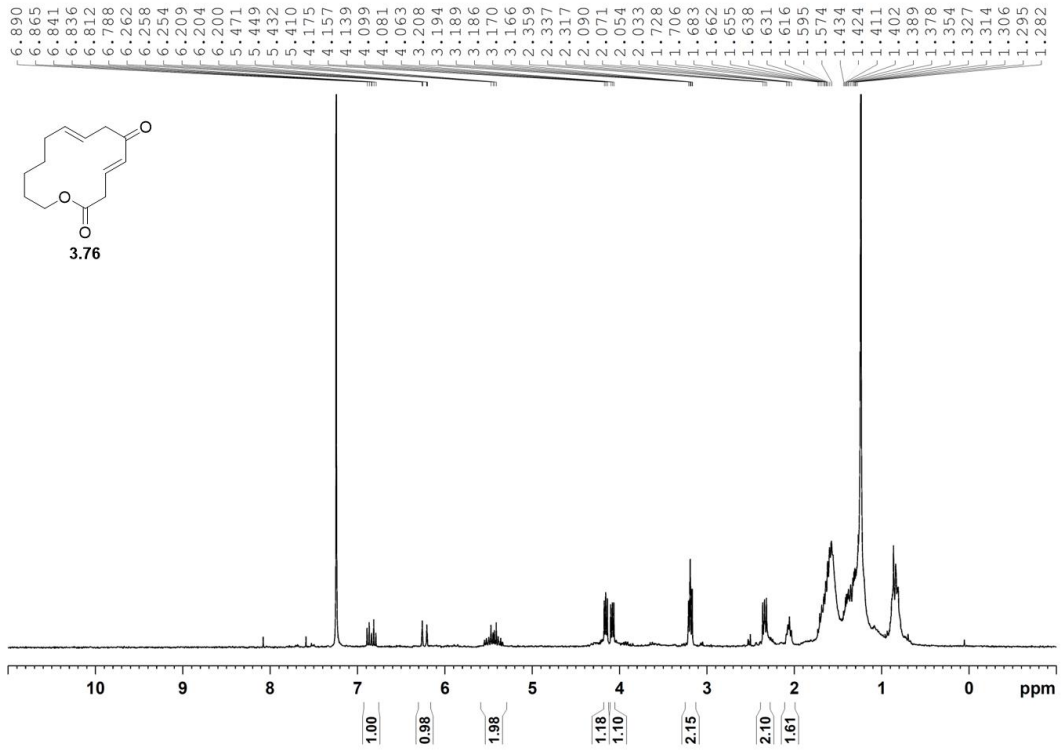

(4*E*,8*E*)-Oxacyclotetradeca-4,8-diene-2,6-dione (elimination by-product, **3.76**)

^{13}C NMR (100 MHz, $CDCl_3$)

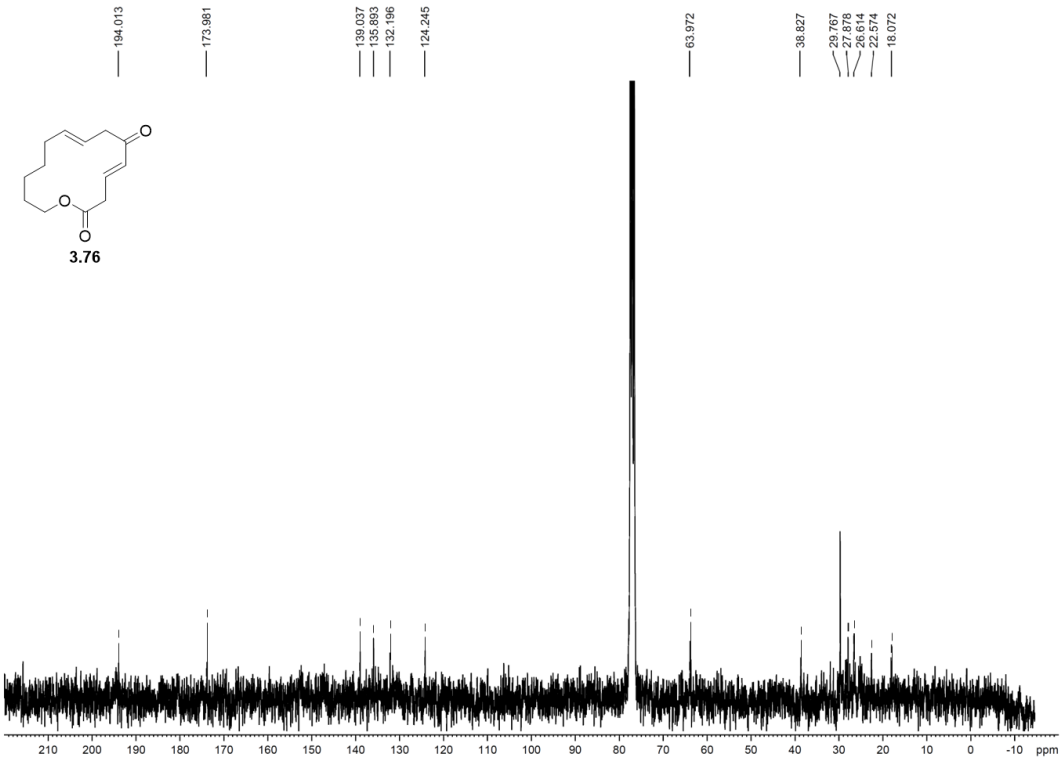

(4*E*,8*E*)-Oxacyclotetradeca-4,8-diene-2,6-dione (elimination by-product, **3.76**)

COSY (400 MHz, $CDCl_3$)

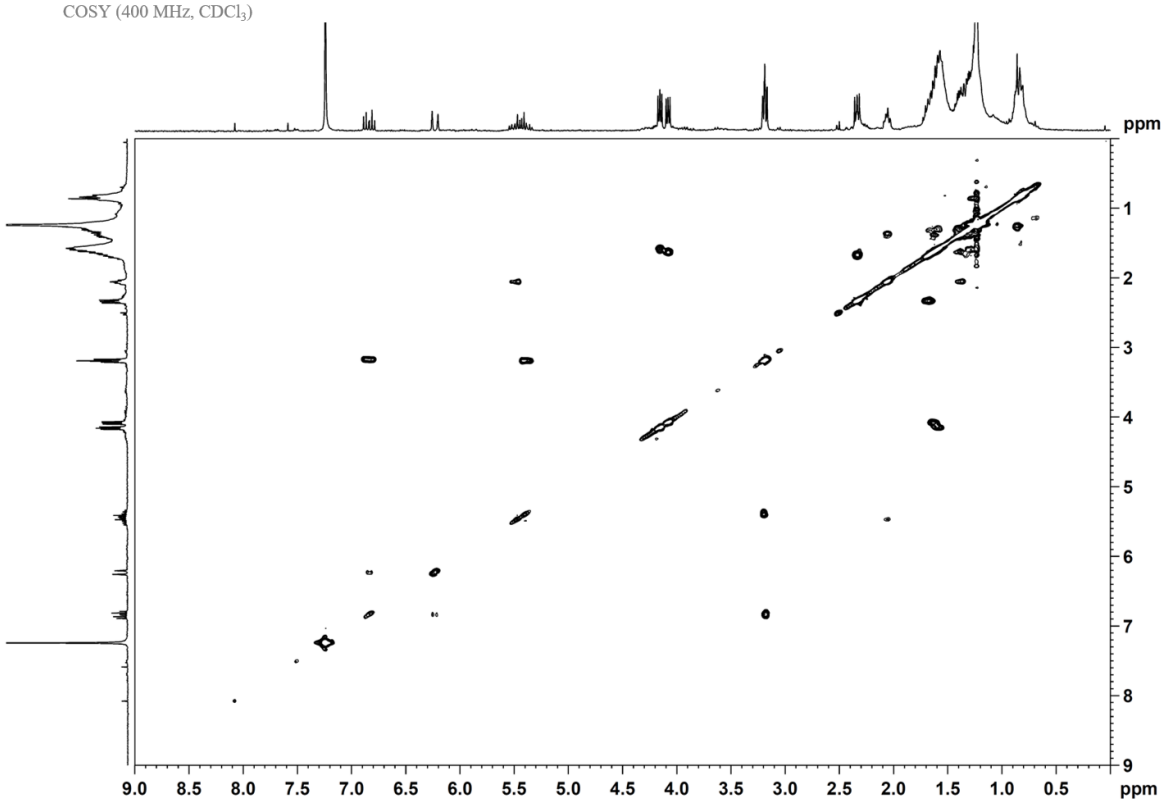

α-cis-13-Hydroxy-4,15-dioxabicyclo[9.3.1]pentadecane-3-one (**3.75**)

^{1}H NMR (400 MHz, $CDCl_3$)

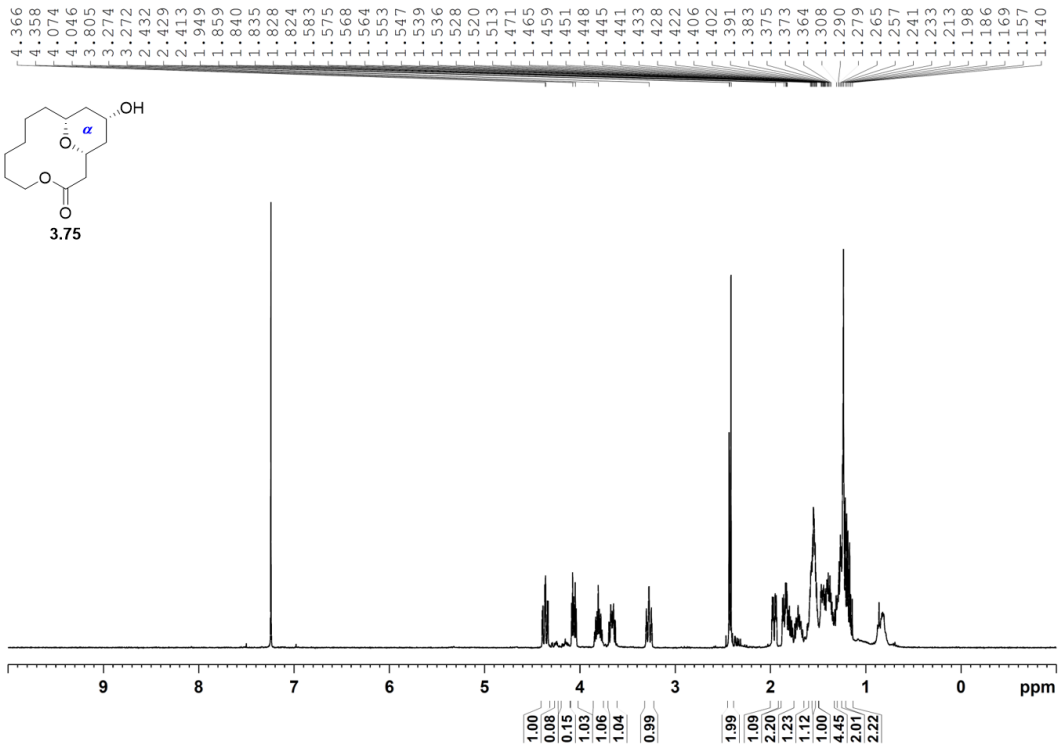

α-cis-13-Hydroxy-4,15-dioxabicyclo[9.3.1]pentadecane-3-one (**3.75**)

^{13}C NMR (100 MHz, $CDCl_3$)

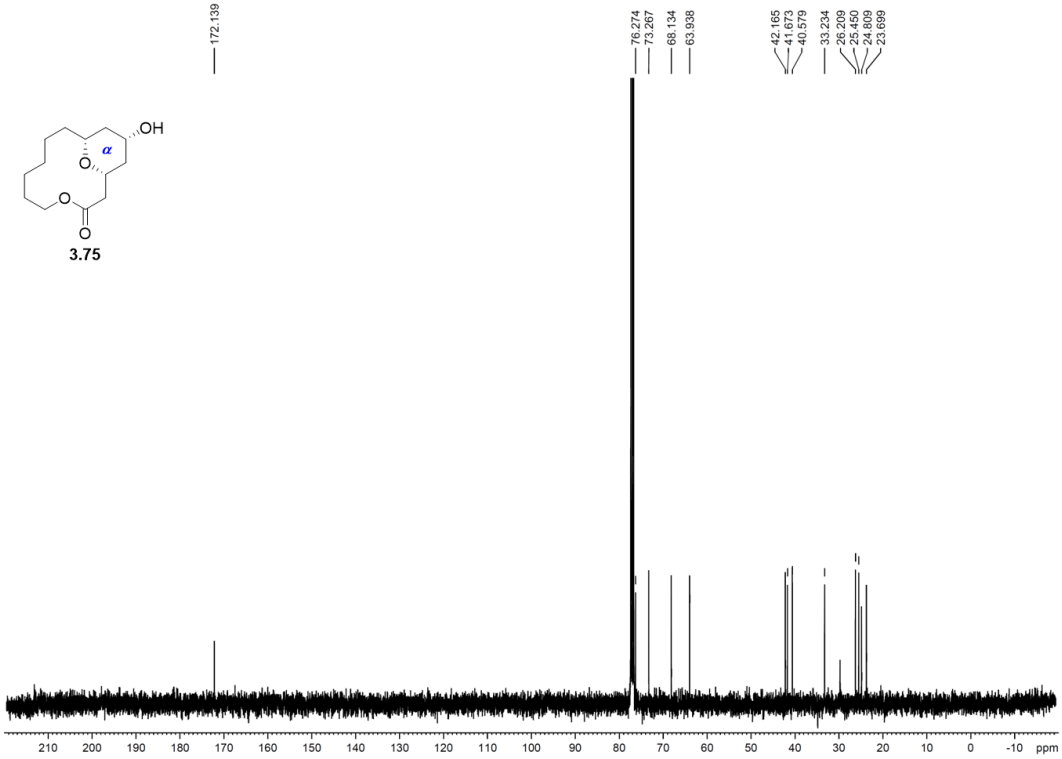

α-cis-13-Hydroxy-4,15-dioxabicyclo[9.3.1]pentadecane-3-one (**3.75**)

COSY (400 MHz, $CDCl_3$)

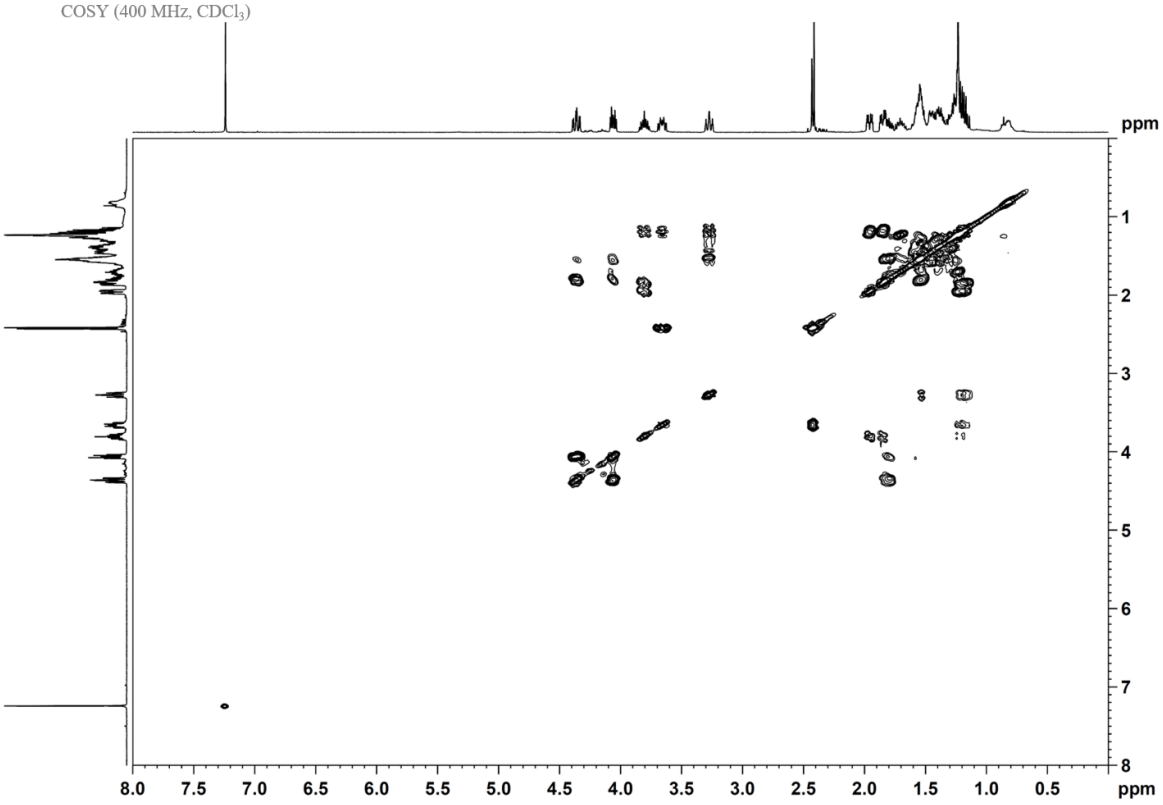

α-cis-13-Hydroxy-4,15-dioxabicyclo[9.3.1]pentadecane-3-one (**3.75**)

HSQC (400 MHz, $CDCl_3$)

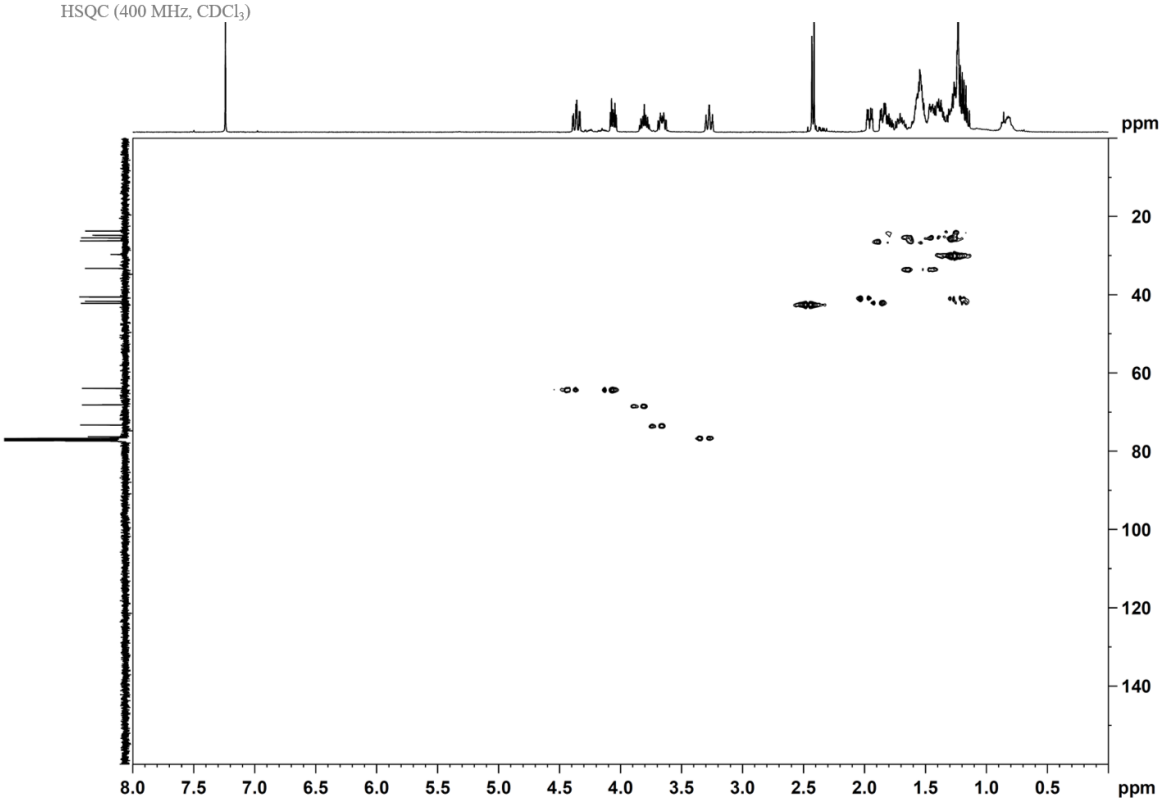

α-cis-13-Hydroxy-4,15-dioxabicyclo[9.3.1]pentadecane-3-one (**3.75**)

NOESY (400 MHz, $CDCl_3$)

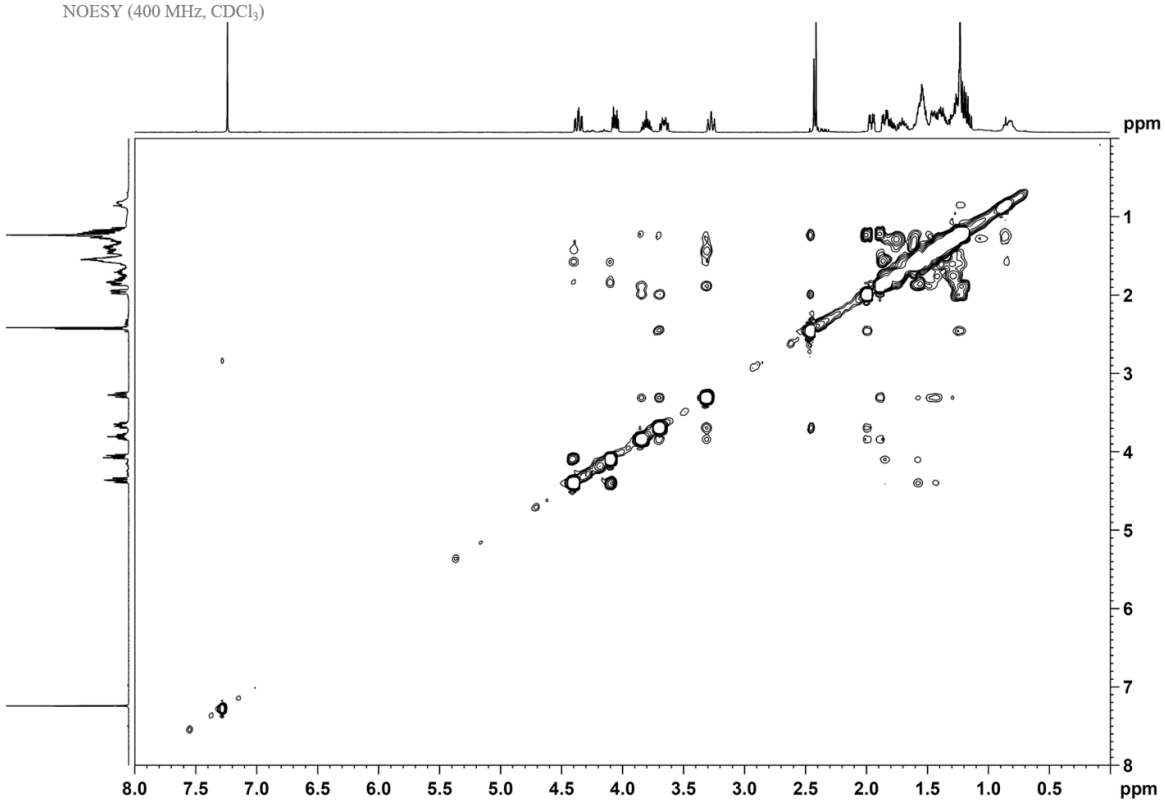

S1.3 Formal Synthesis of Neopeltolide by Transannular Oxa-Conjugate Addition (Chapter 4)

S1.3.1 Development of C7-C16 Framework (§ 4.4.2)

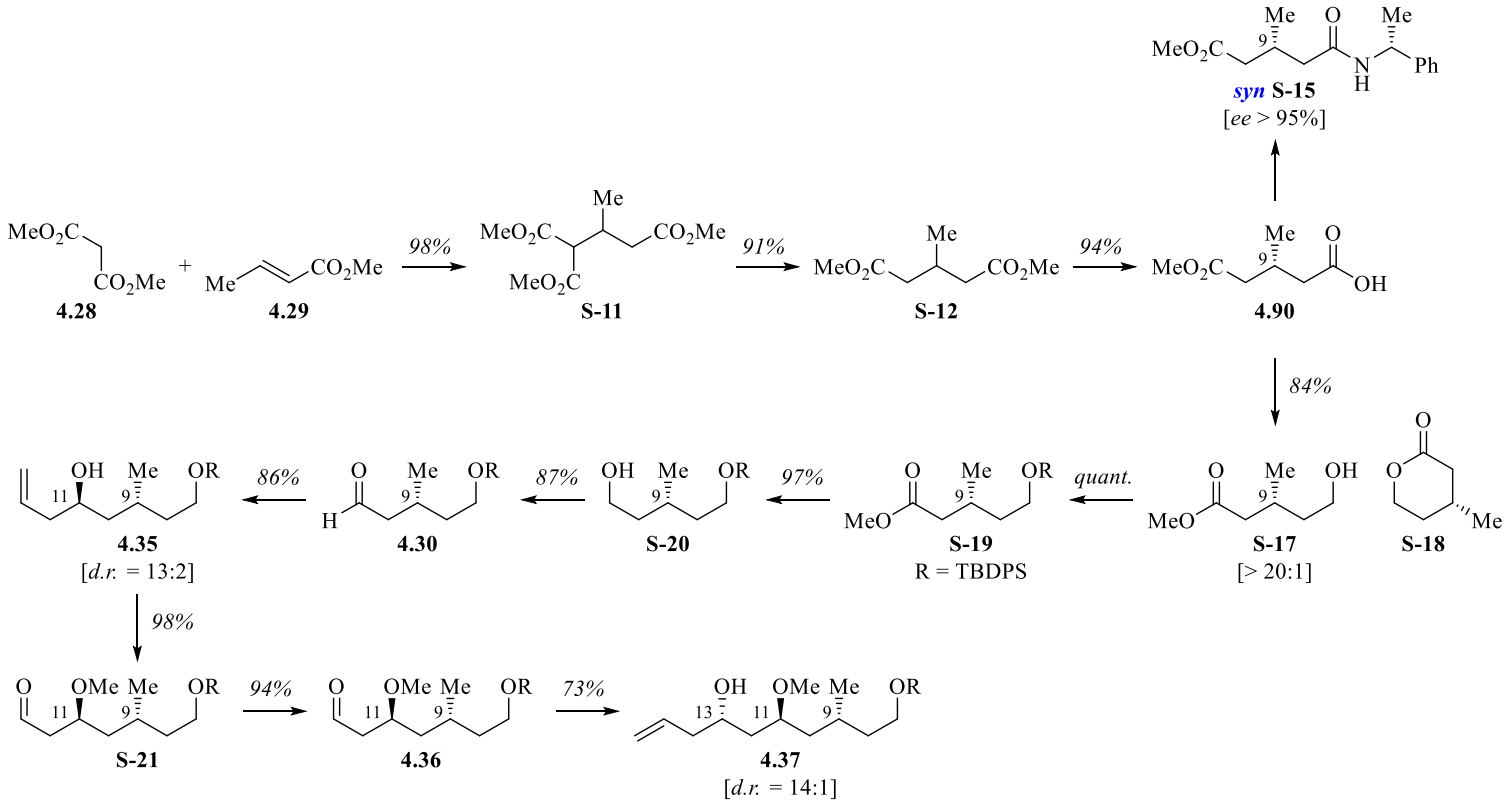

Figure S6 – Summary of the synthesis of the C7-C16 framework of neopeltolide macrocyclic core.

Trimethyl-2-methylpropane-1,1,3-tricarboxylate (**S-11**)

^{1}H NMR (400 MHz, $CDCl_3$)

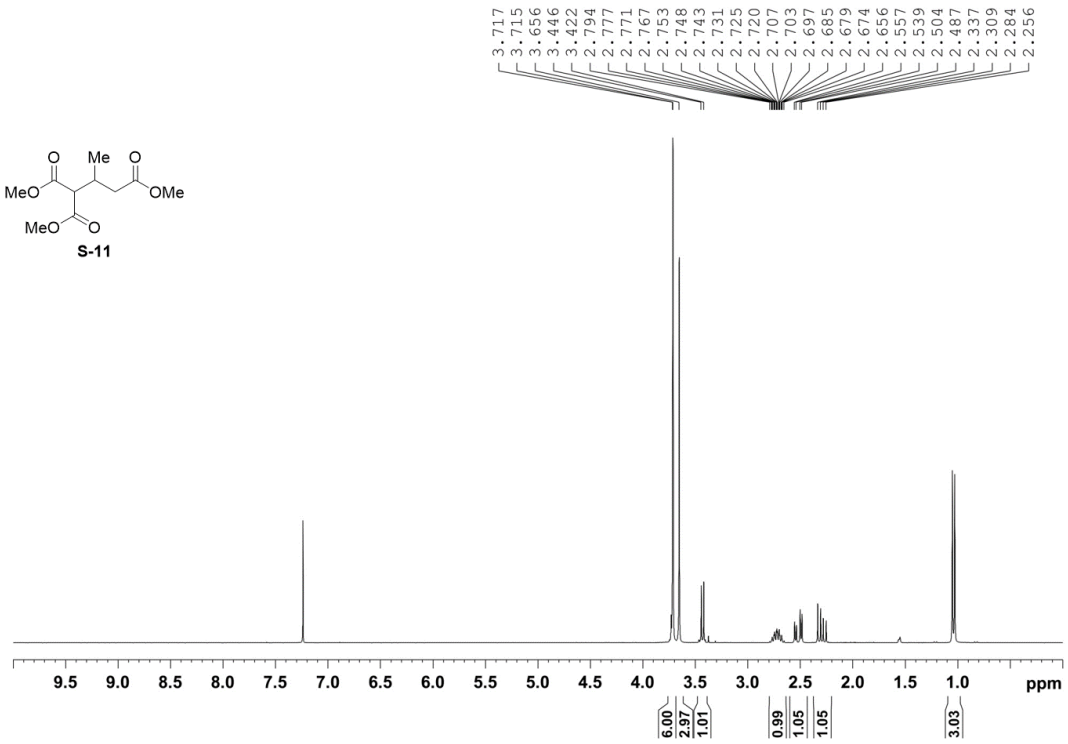

Trimethyl-2-methylpropane-1,1,3-tricarboxylate (**S-11**)

^{13}C NMR (100 MHz, $CDCl_3$)

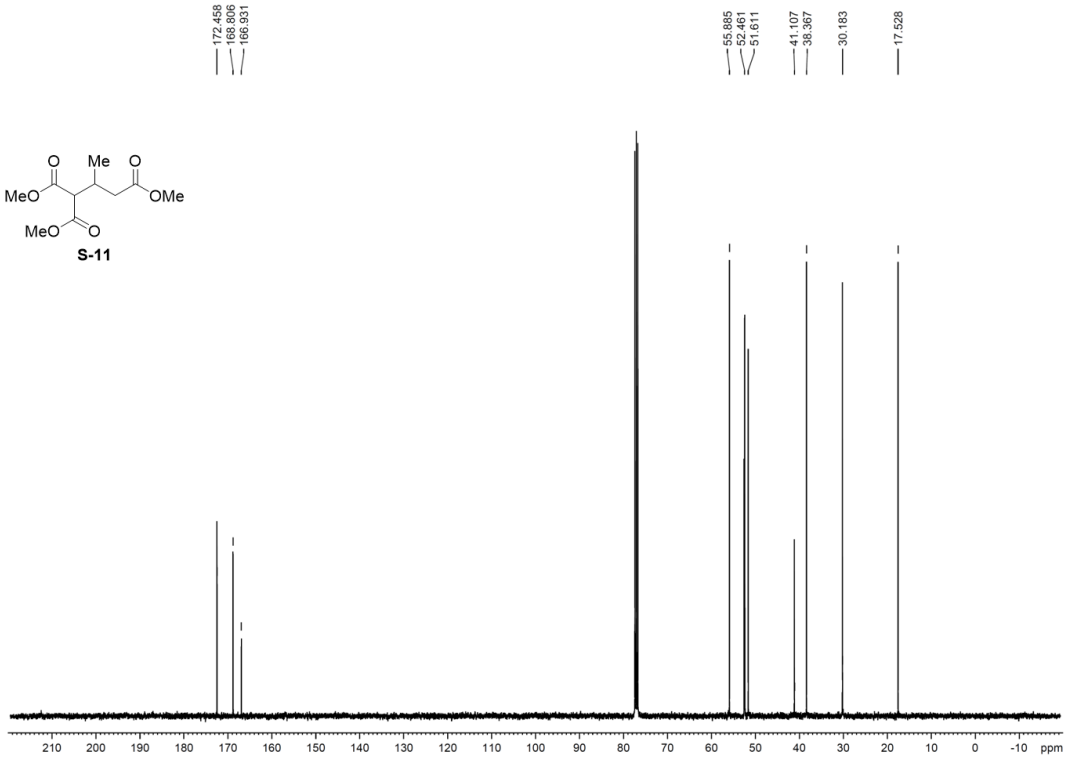

Dimethyl-3-methylglutarate (**S-12**)

^{1}H NMR (400 MHz, $CDCl_3$)

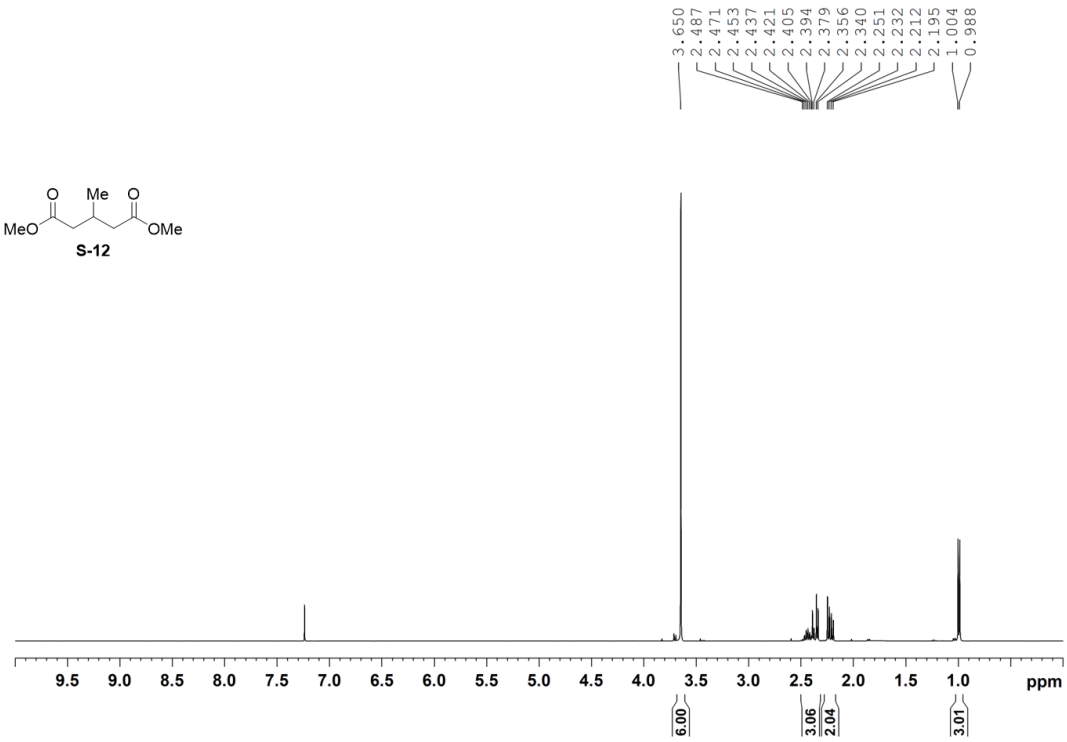

Dimethyl-3-methylglutarate (**S-12**)

^{13}C NMR (100 MHz, $CDCl_3$)

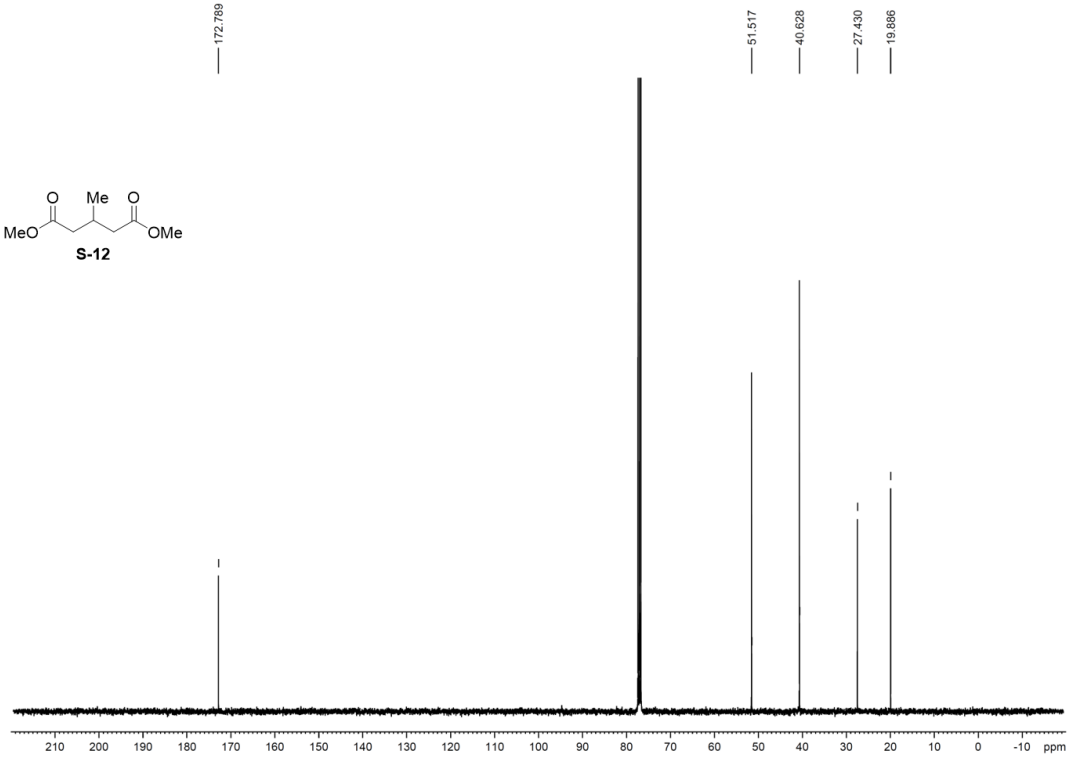

(*R*)-5-Methoxy-3-methyl-5-oxopentanoic acid **(4.90)**

^{1}H NMR (400 MHz, $CDCl_3$)

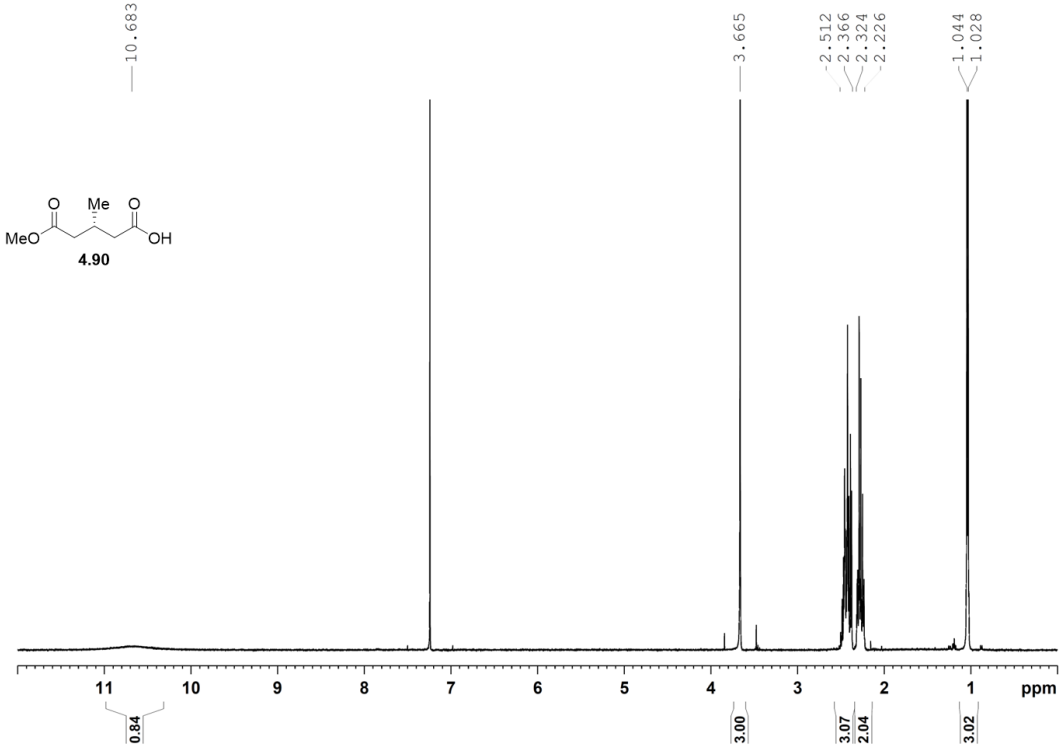

(*R*)-5-Methoxy-3-methyl-5-oxopentanoic acid **(4.90)**

^{13}C NMR (100 MHz, $CDCl_3$)

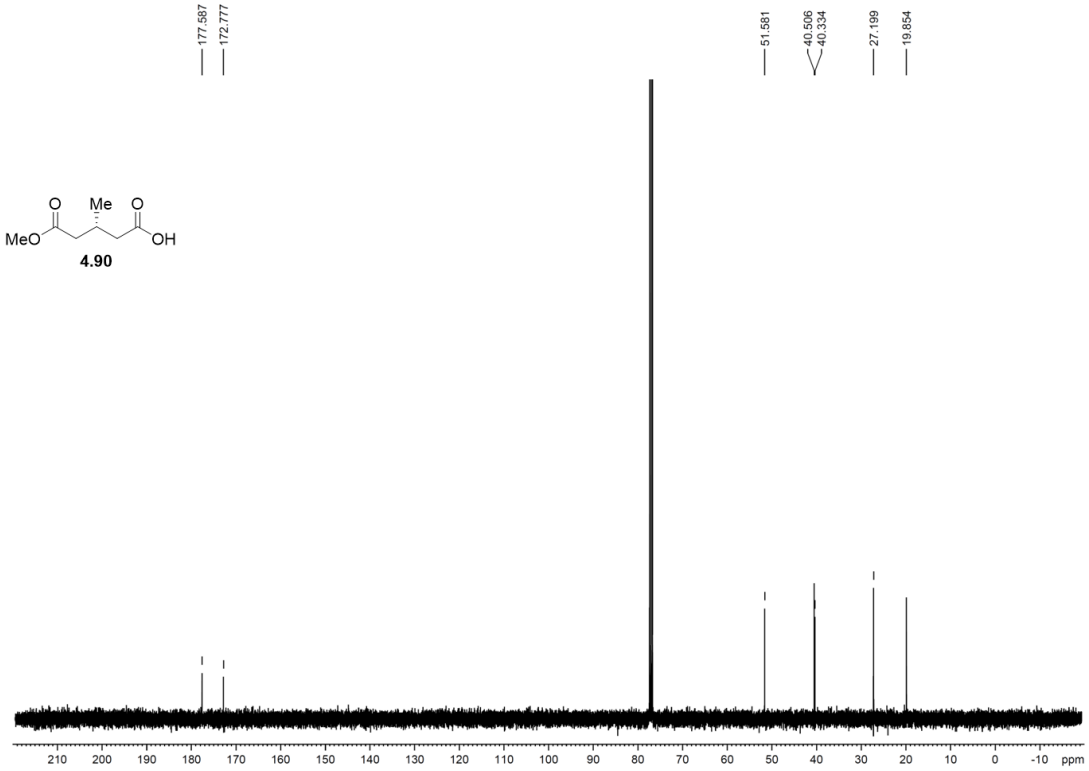

***syn*/*anti*-(*R*/*S*)-Methyl 3-methyl-5-oxo-5-((*R*)-1-phenylethylamino)pentanoate (S-15/S-16)**

^{1}H NMR (300 MHz, $CDCl_3$)

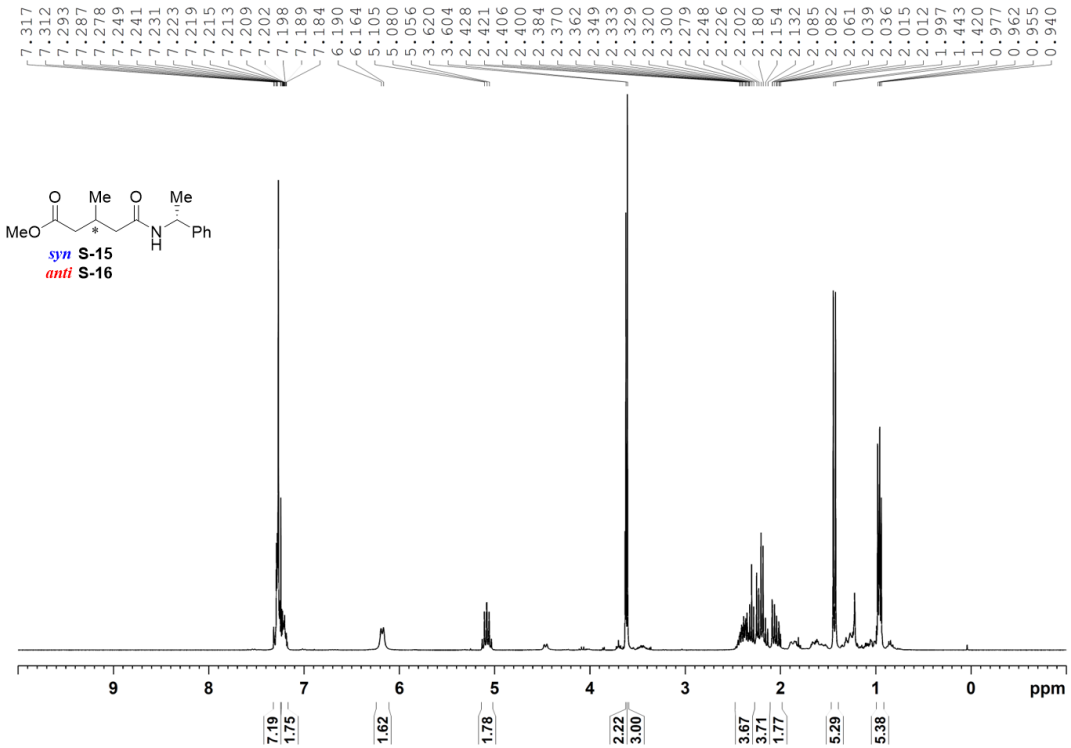

***syn*/*anti*-(*R*/*S*)-Methyl 3-methyl-5-oxo-5-((*R*)-1-phenylethylamino)pentanoate (S-15/S-16)**

^{13}C NMR (75 MHz, $CDCl_3$)

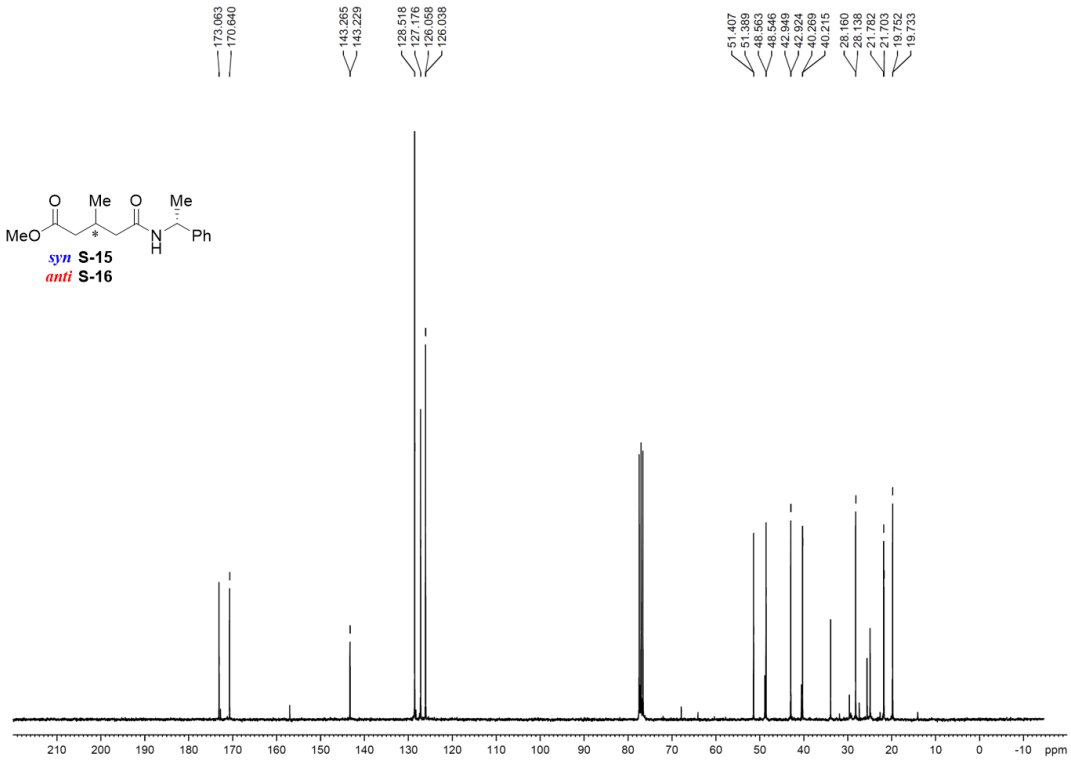

***syn*-(*R*)-Methyl 3-methyl-5-oxo-5-((*R*)-1-phenylethylamino)pentanoate (S-15)**

^{1}H NMR (400 MHz, $CDCl_3$)

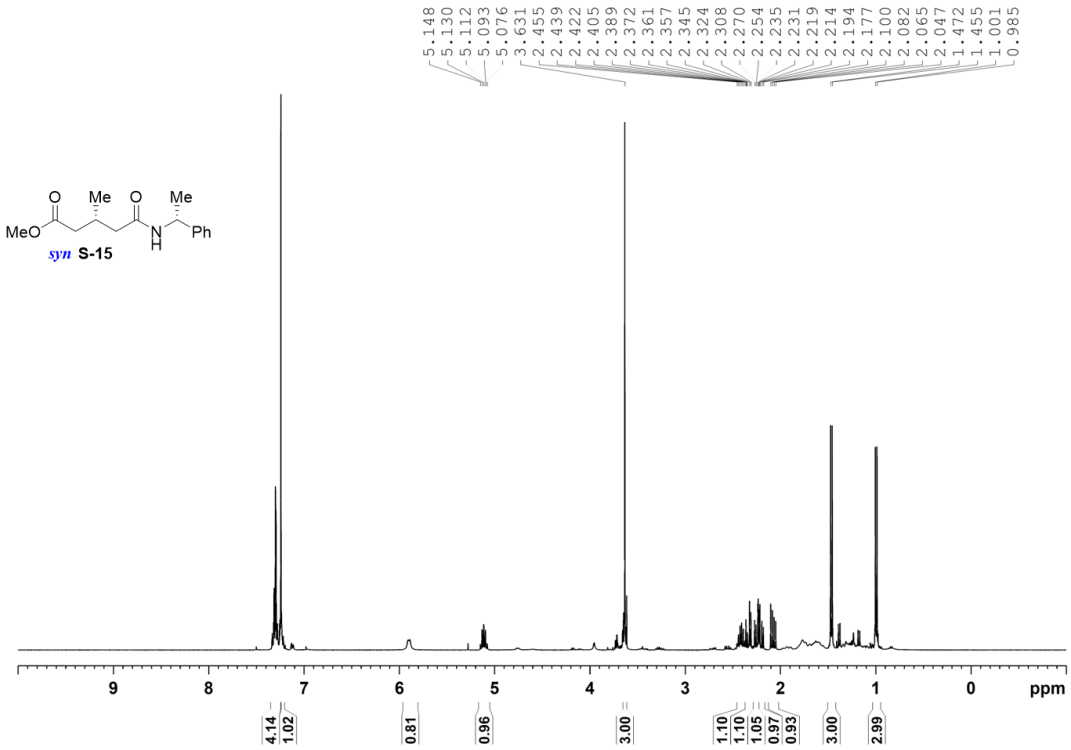

***syn*-(*R*)-Methyl 3-methyl-5-oxo-5-((*R*)-1-phenylethylamino)pentanoate (S-15)**

^{13}C NMR (100 MHz, $CDCl_3$)

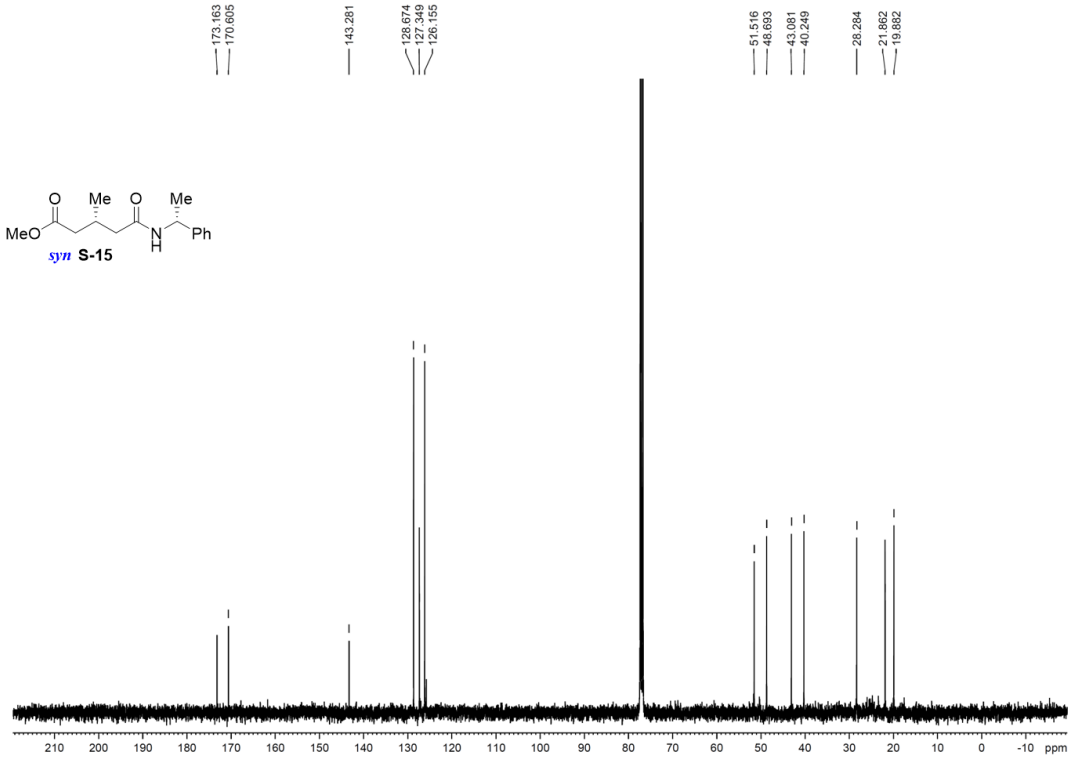

***syn*/*anti*-(*R*/*S*)-Methyl 3-methyl-5-oxo-5-((*R*)-1-phenylethylamino)pentanoate (S-15/S-16)**

^{13}C NMR (75 MHz, $CDCl_3$)

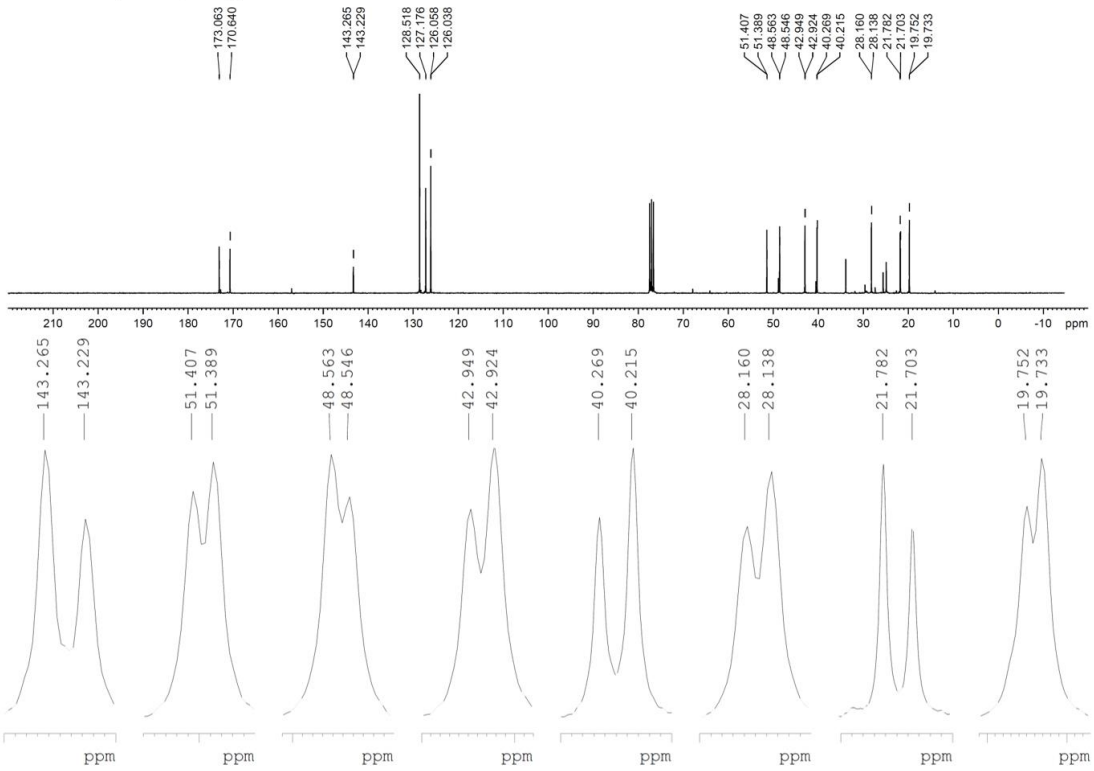

***syn*-(*R*)-Methyl 3-methyl-5-oxo-5-((*R*)-1-phenylethylamino)pentanoate (S-15)**

^{13}C NMR (100 MHz, $CDCl_3$)

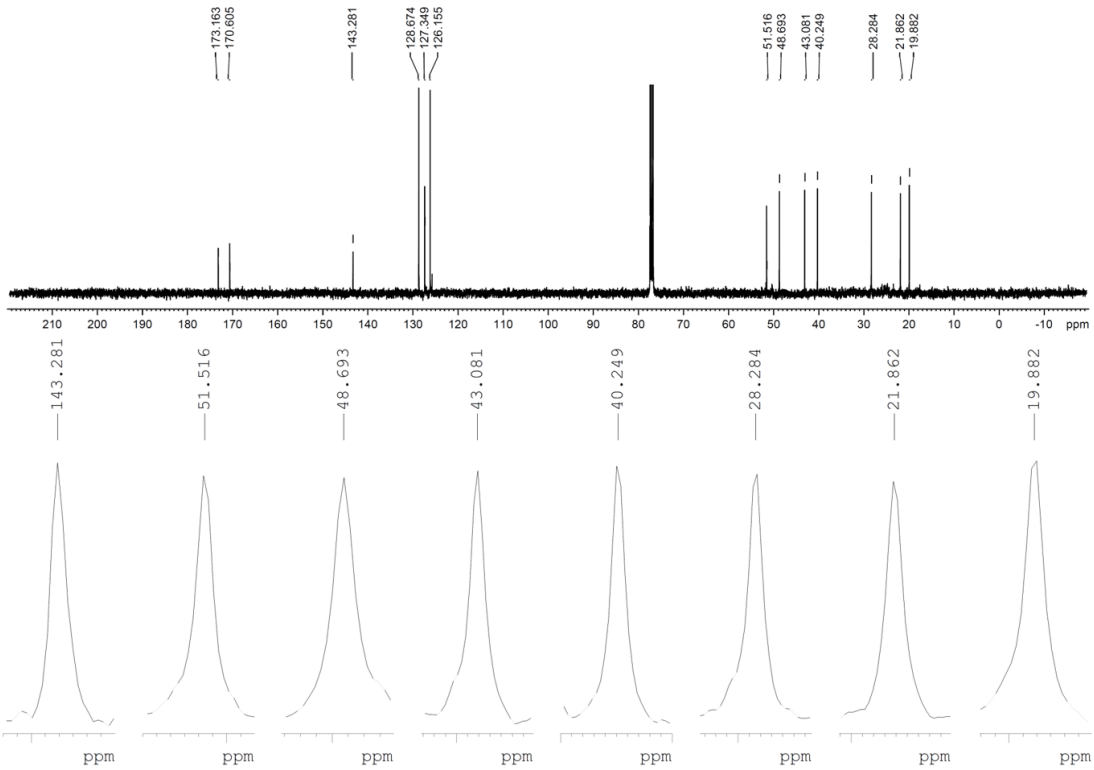

(3*R*)-5-Hydroxy-3-methylpentanoic acid methyl ester : (*R*)-4-Methyltetrahydro-2*H*-pyran-2-one (**S-17**:**S-18**)

^{1}H NMR (400 MHz, $CDCl_3$)

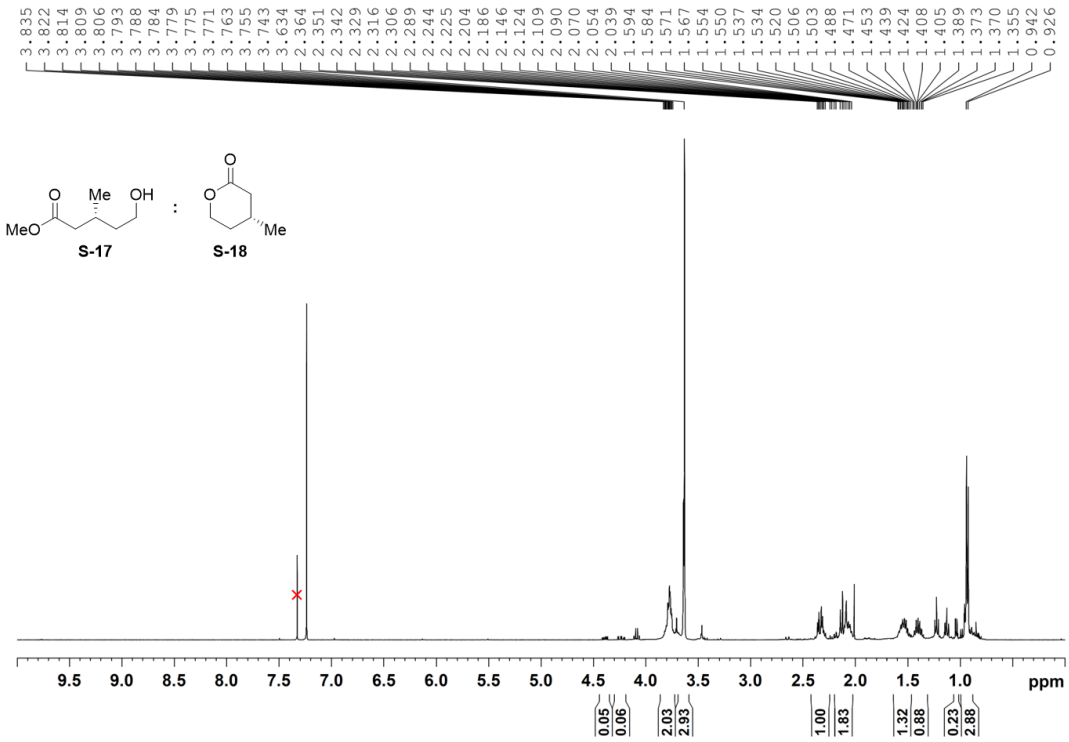

(3*R*)-5-Hydroxy-3-methylpentanoic acid methyl ester : (*R*)-4-Methyltetrahydro-2*H*-pyran-2-one (**S-17**:**S-18**)

^{13}C NMR (100 MHz, $CDCl_3$)

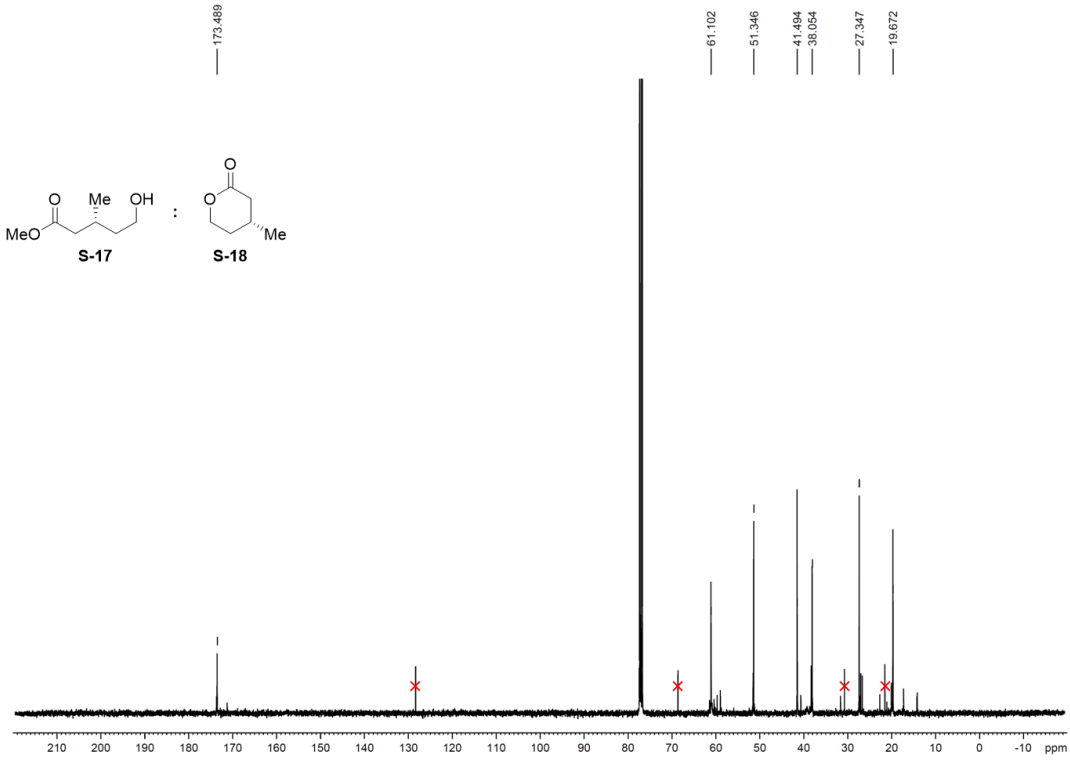

(*R*)-4-Methyltetrahydro-2*H*-pyran-2-one (**S-18**)

^{1}H NMR (400 MHz, $CDCl_3$)

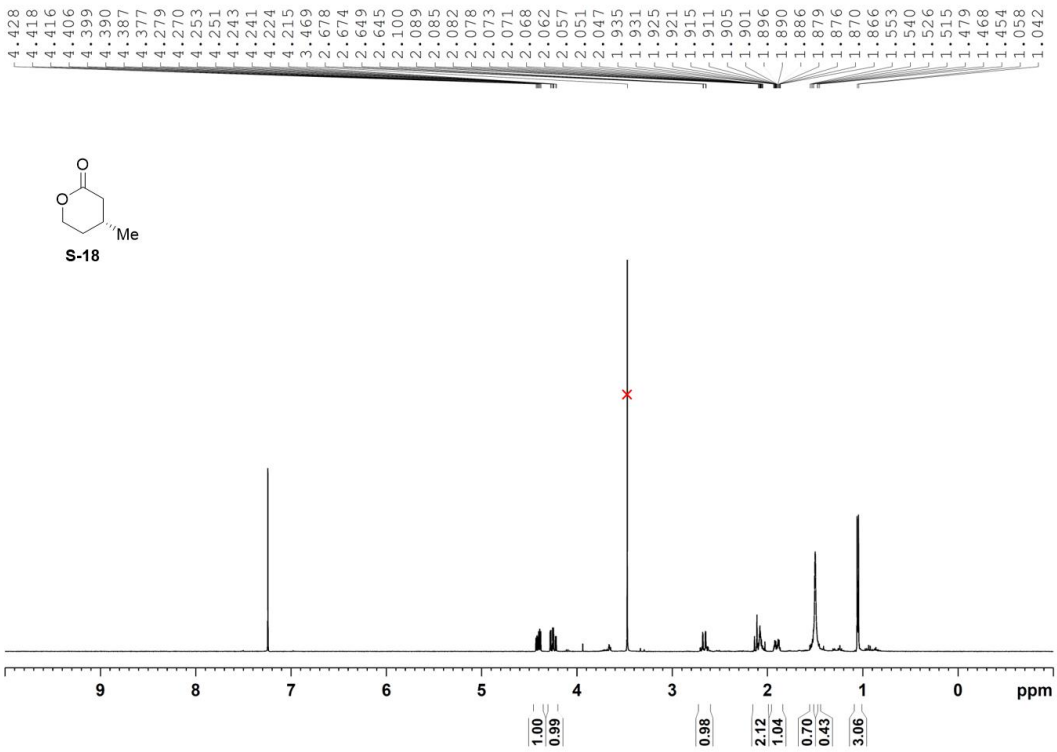

(3*R*)-Methyl 5-(*tert*-butyldiphenylsilyloxy)-3-methylpentanoate (**S-19**)

^{1}H NMR (400 MHz, $CDCl_3$)

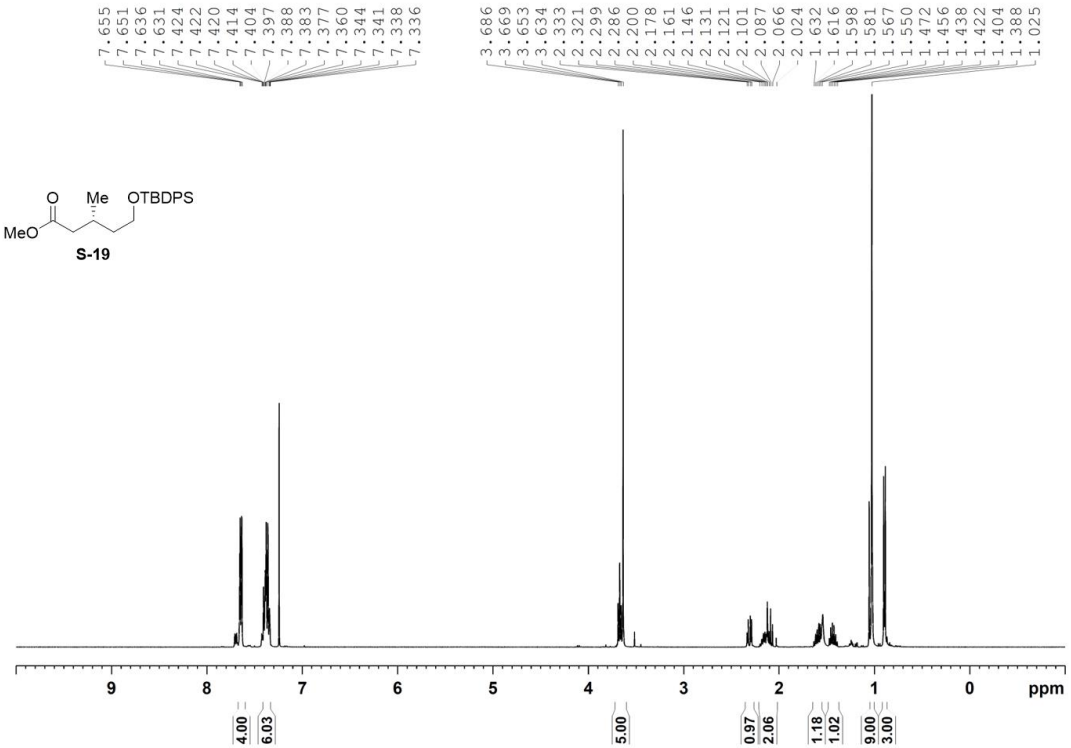

(3*R*)-Methyl 5-(*tert*-butyldiphenylsilyloxy)-3-methylpentanoate (**S-19**)

^{13}C NMR (100 MHz, $CDCl_3$)

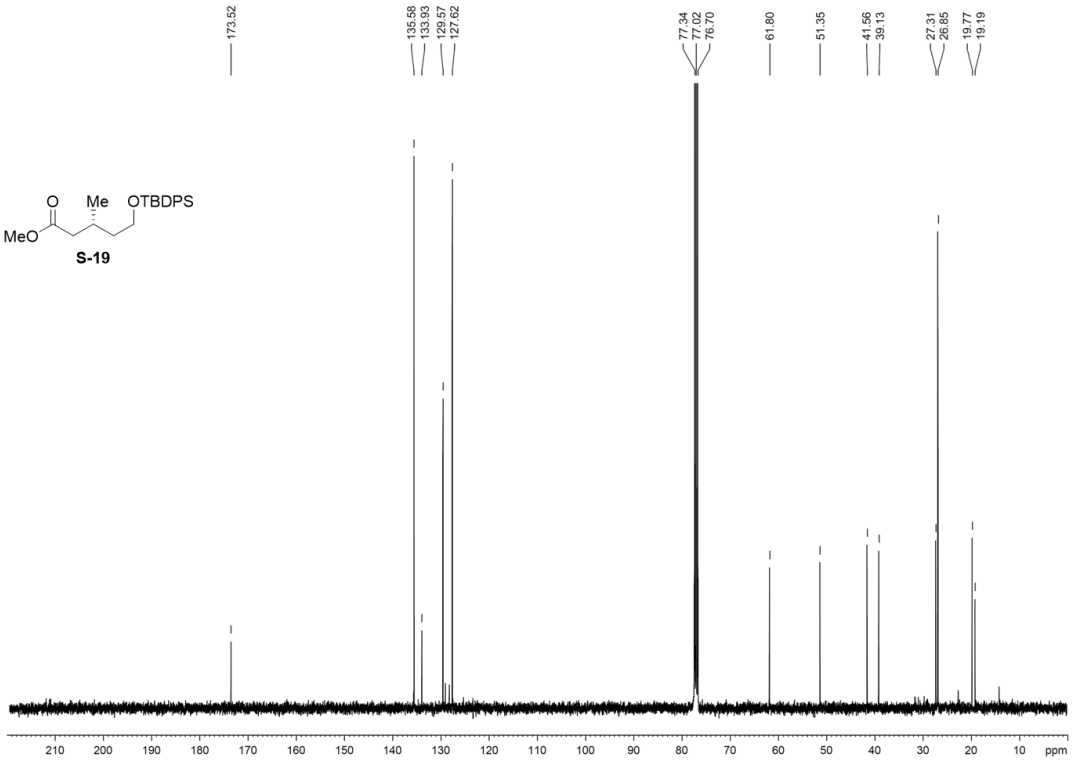

(3*R*)-Methyl 5-(*tert*-butyldiphenylsilyloxy)-3-methylpentanoate (**S-19**)

HSQC (400 MHz, $CDCl_3$)

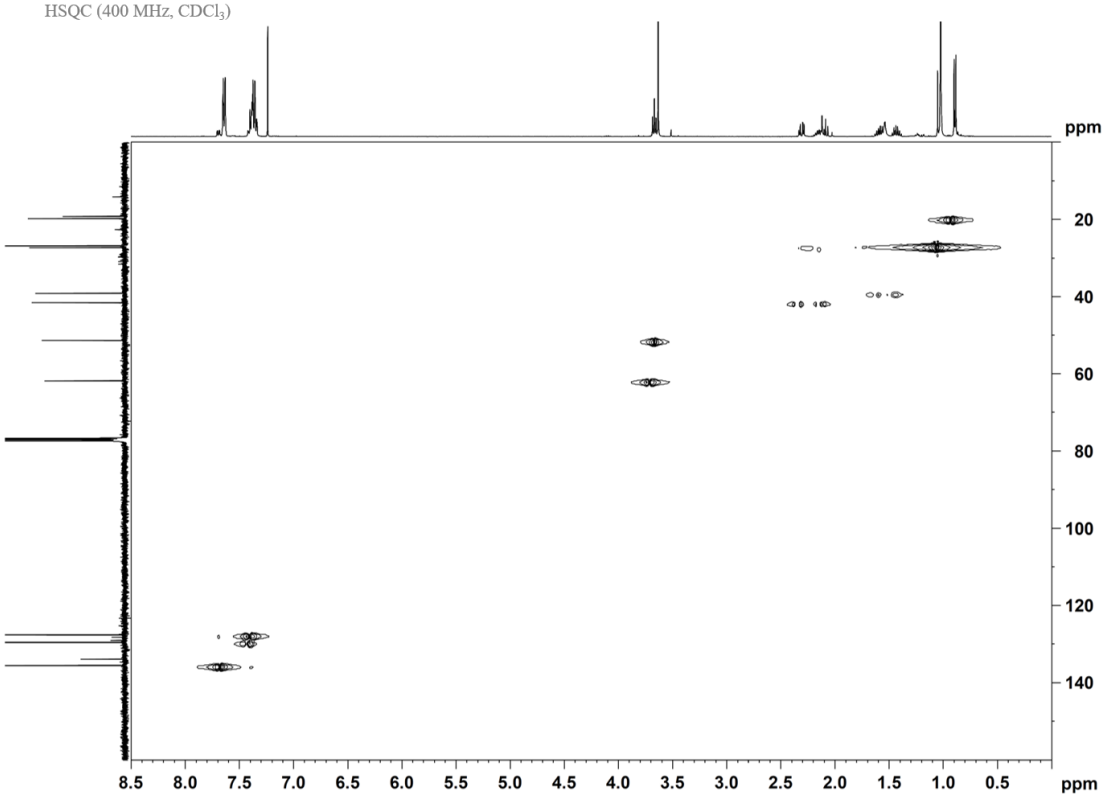

(3*S*)-5-(*tert*-Butyldiphenylsilyloxy)-3-methylpentan-1-ol (**S-20**)

^{1}H NMR (400 MHz, $CDCl_3$)

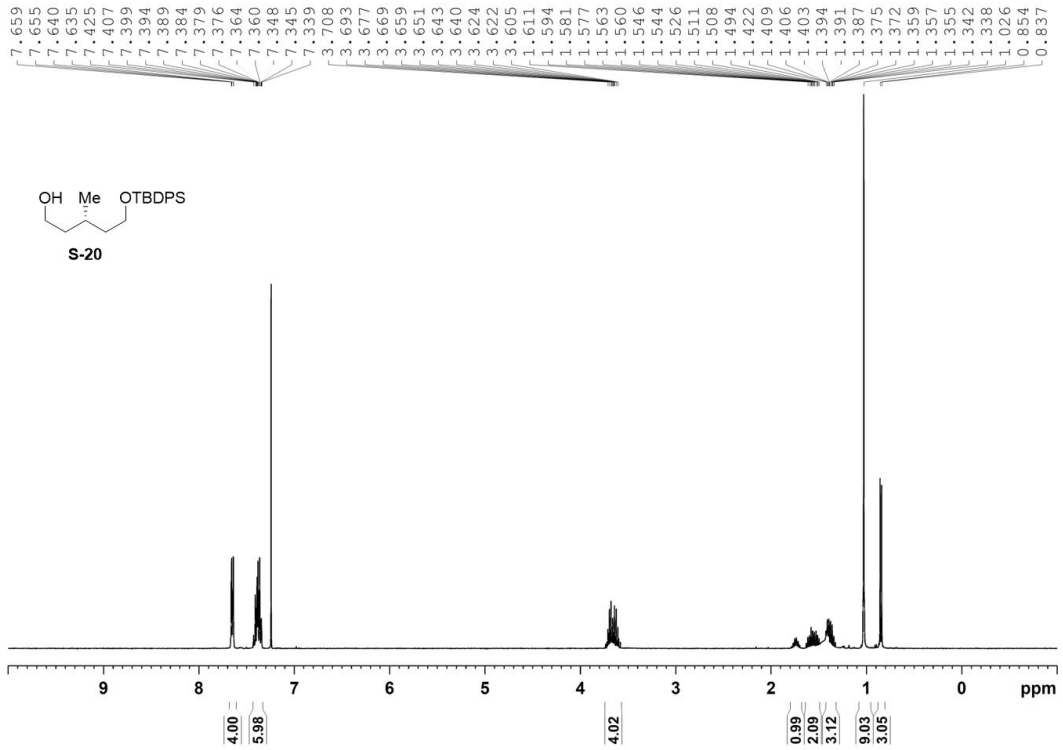

(3*S*)-5-(*tert*-Butyldiphenylsilyloxy)-3-methylpentan-1-ol (**S-20**)

^{13}C NMR (100 MHz, $CDCl_3$)

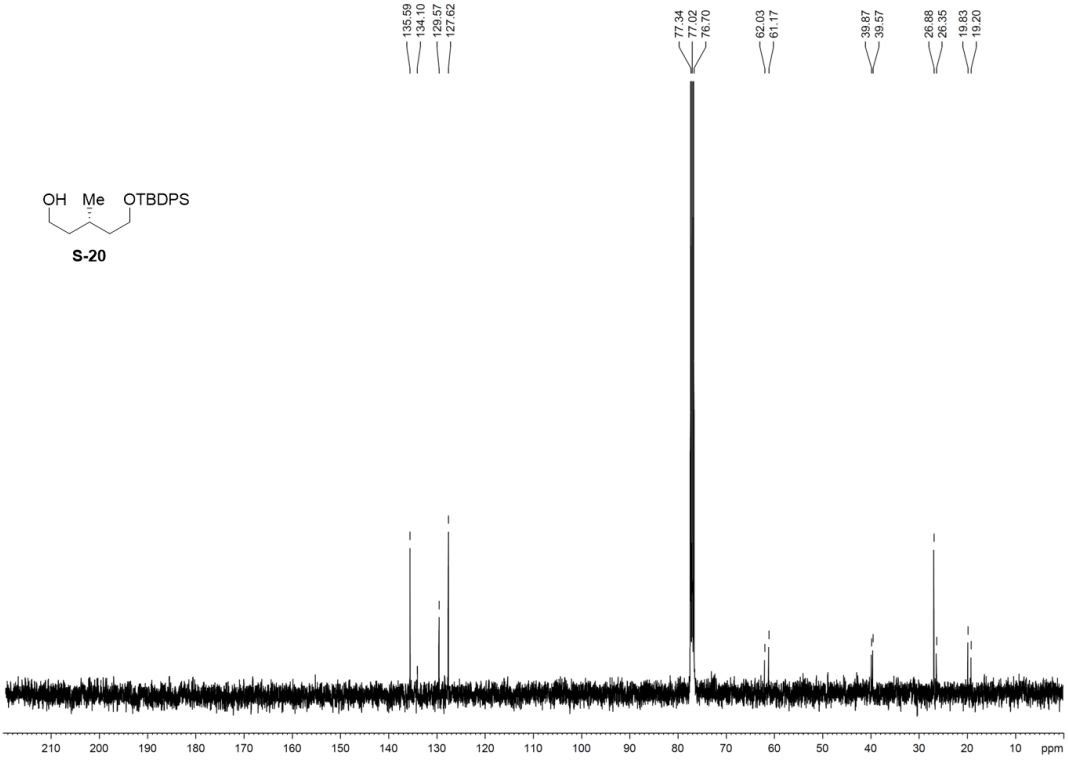

(3*R*)-5-(*tert*-Butyldiphenylsilyloxy)-3-methylpentanal (**4.30**)

^{1}H NMR (400 MHz, $CDCl_3$)

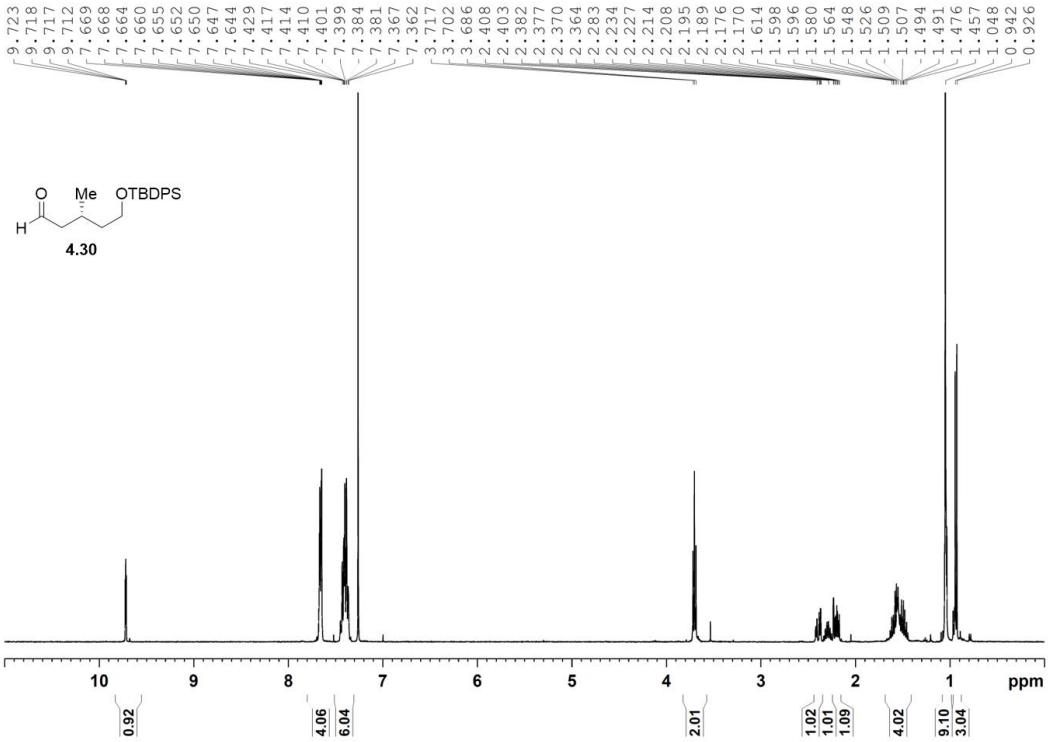

(3*R*)-5-(*tert*-Butyldiphenylsilyloxy)-3-methylpentanal (**4.30**)

^{13}C NMR (100 MHz, $CDCl_3$)

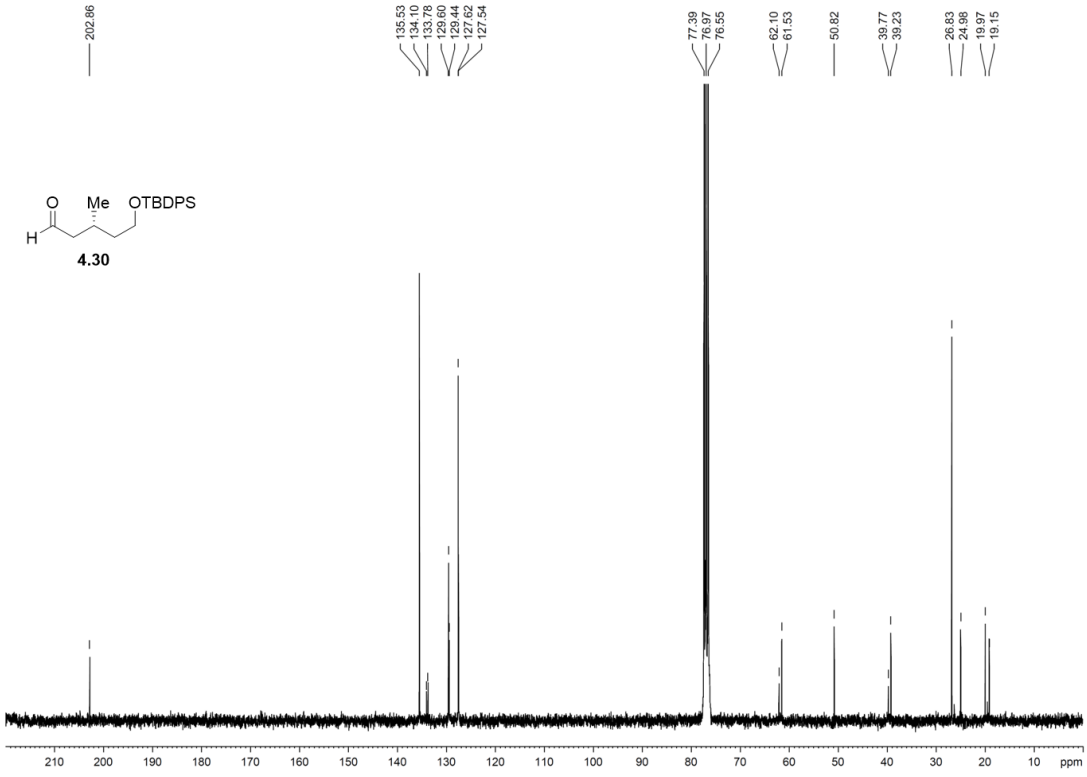

(4*R*,6*R*)-8-(*tert*-Butyldiphenylsilyloxy)-6-methyloct-1-en-4-ol (**4.35**)

^{1}H NMR (400 MHz, $CDCl_3$)

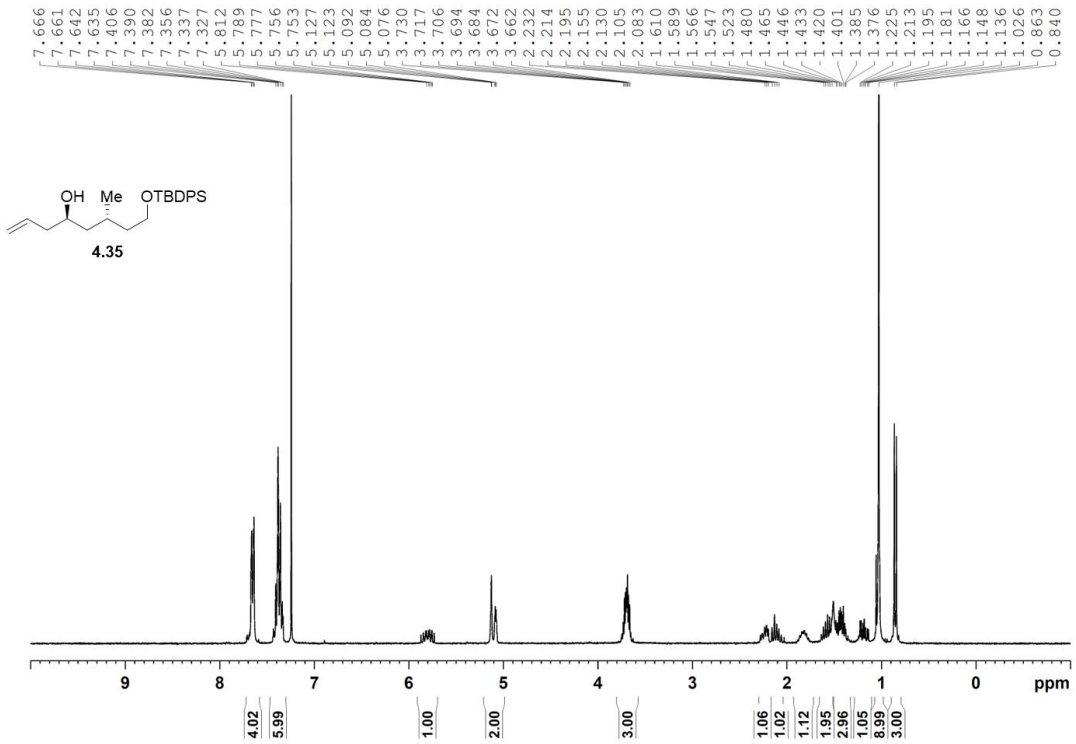

(4*R*,6*R*)-8-(*tert*-Butyldiphenylsilyloxy)-6-methyloct-1-en-4-ol (**4.35**)

^{13}C NMR (100 MHz, $CDCl_3$)

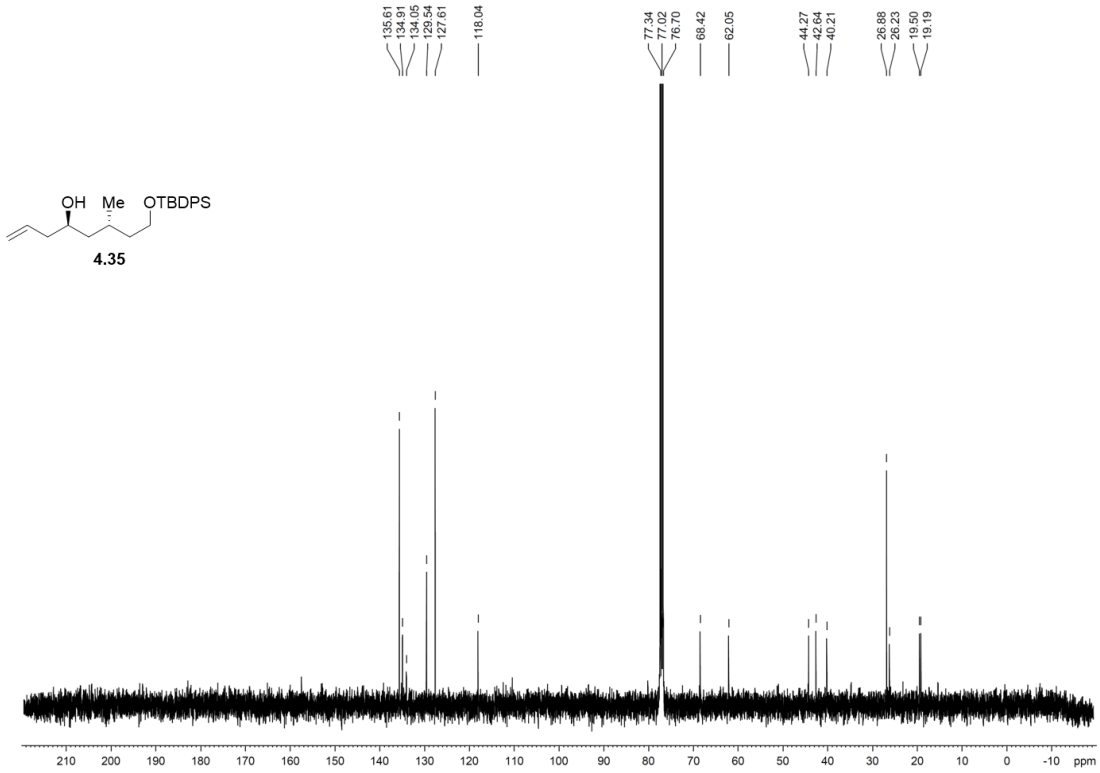

(4*R*,6*R*)-8-(*tert*-Butyldiphenylsilyloxy)-6-methyloct-1-en-4-ol (**4.35**)

^{1}H NMR (400 MHz, $CDCl_3$)

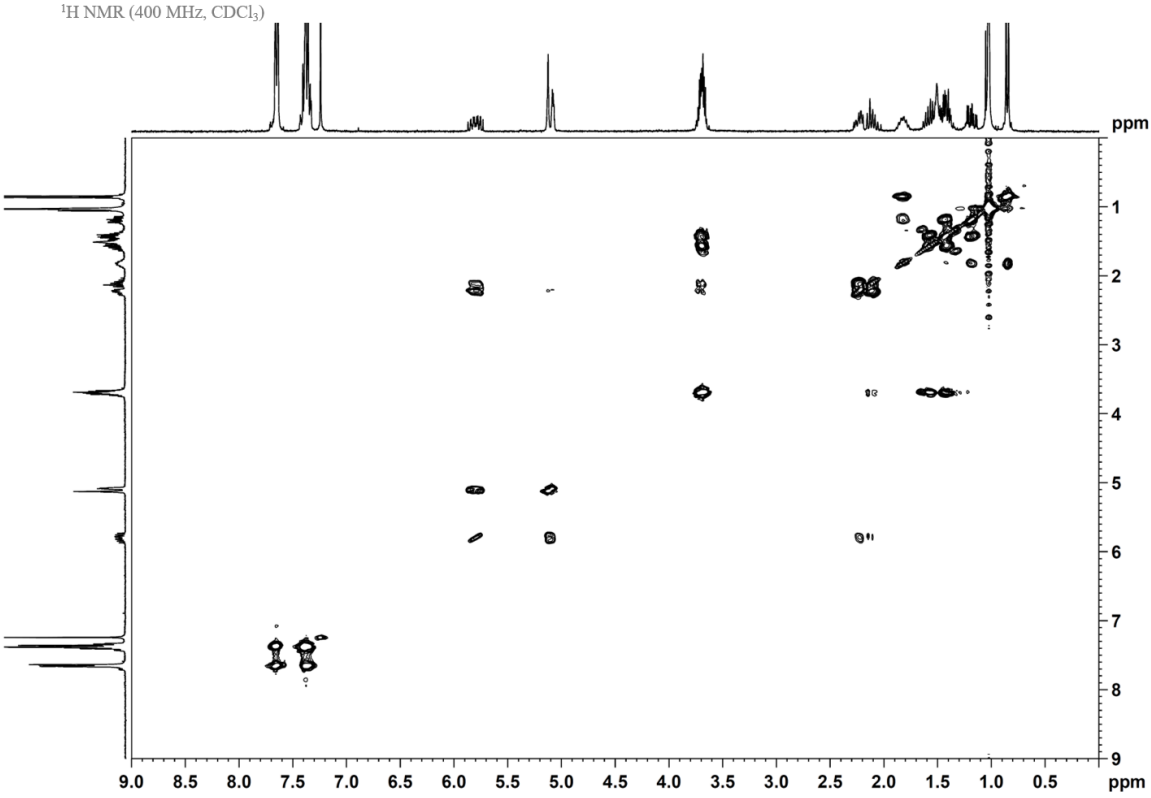

(4*R*,6*R*)-8-(*tert*-Butyldiphenylsilyloxy)-6-methyloct-1-en-4-ol (**4.35**)

HSQC (400 MHz, $CDCl_3$)

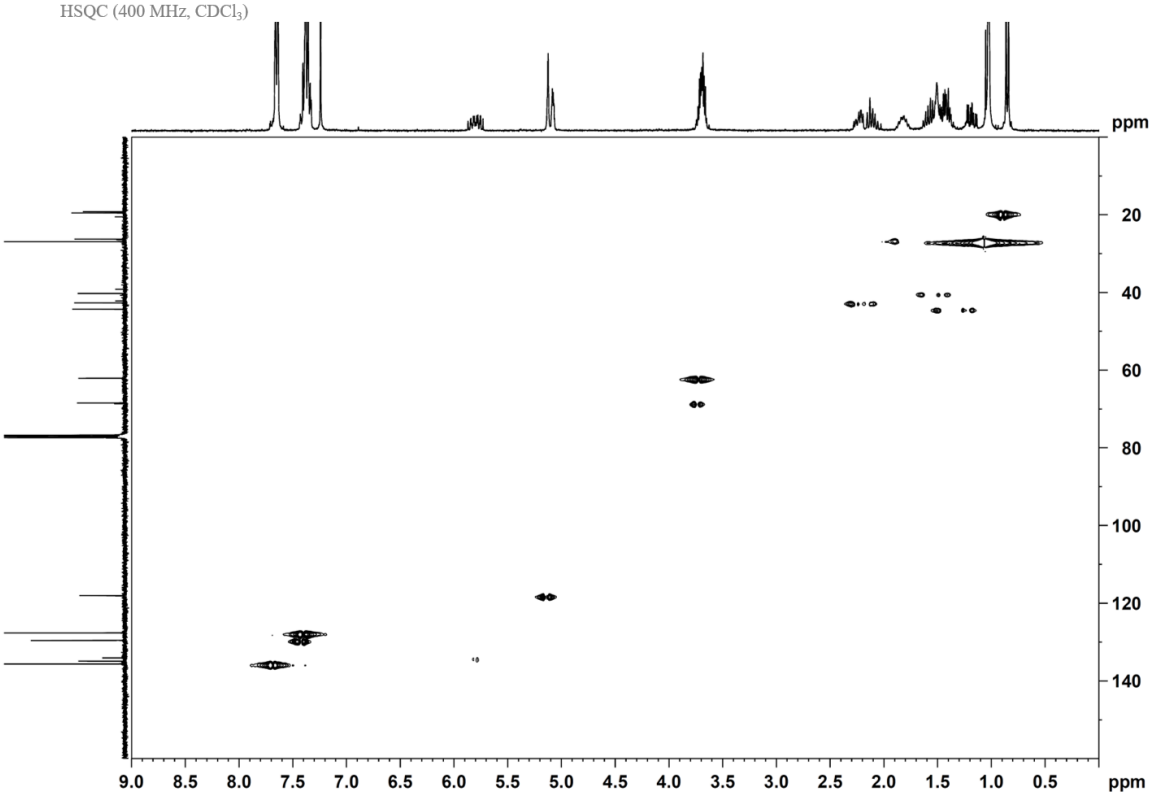

(4*S*,6*R*)-8-(*tert*-Butyldiphenylsilyloxy)-6-methyloct-1-en-4-ol ($^{\Delta 4}$*epi*-**4.35**)

^{1}H NMR (400 MHz, $CDCl_3$)

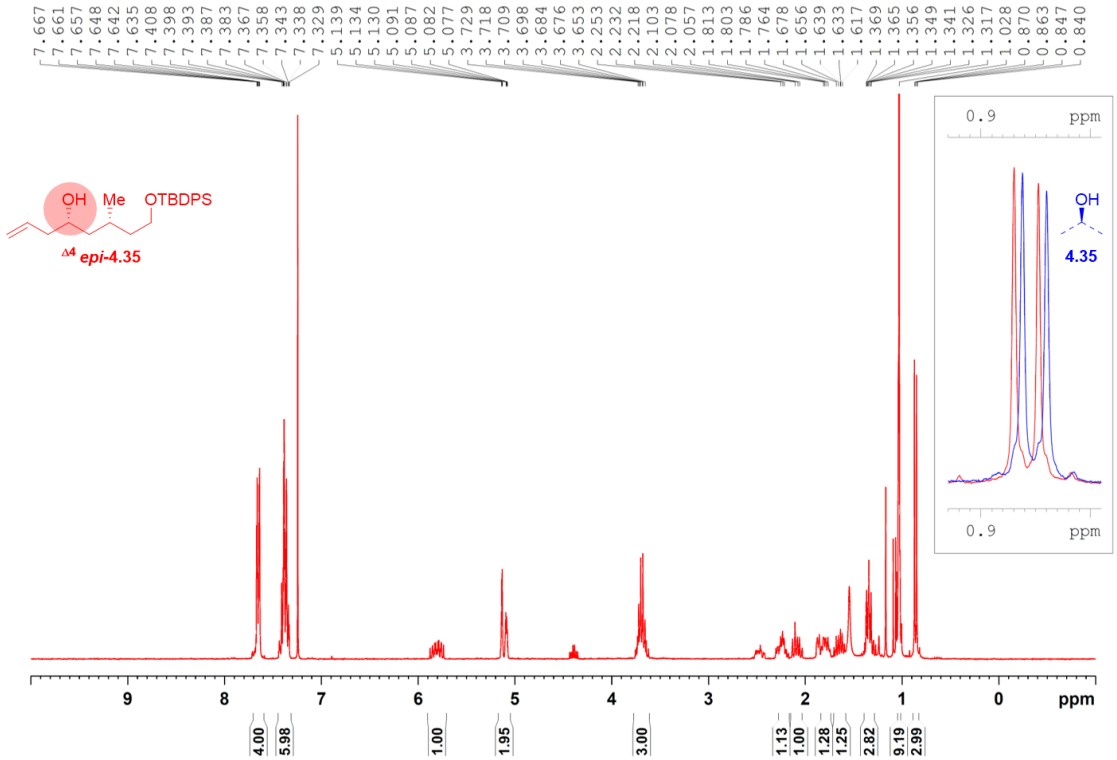

tert-Butyl-((3*R*,5*R*)-5-methoxy-3-methyloct-7-enyloxy)diphenylsilane (**S-21**)

^{1}H NMR (400 MHz, $CDCl_3$)

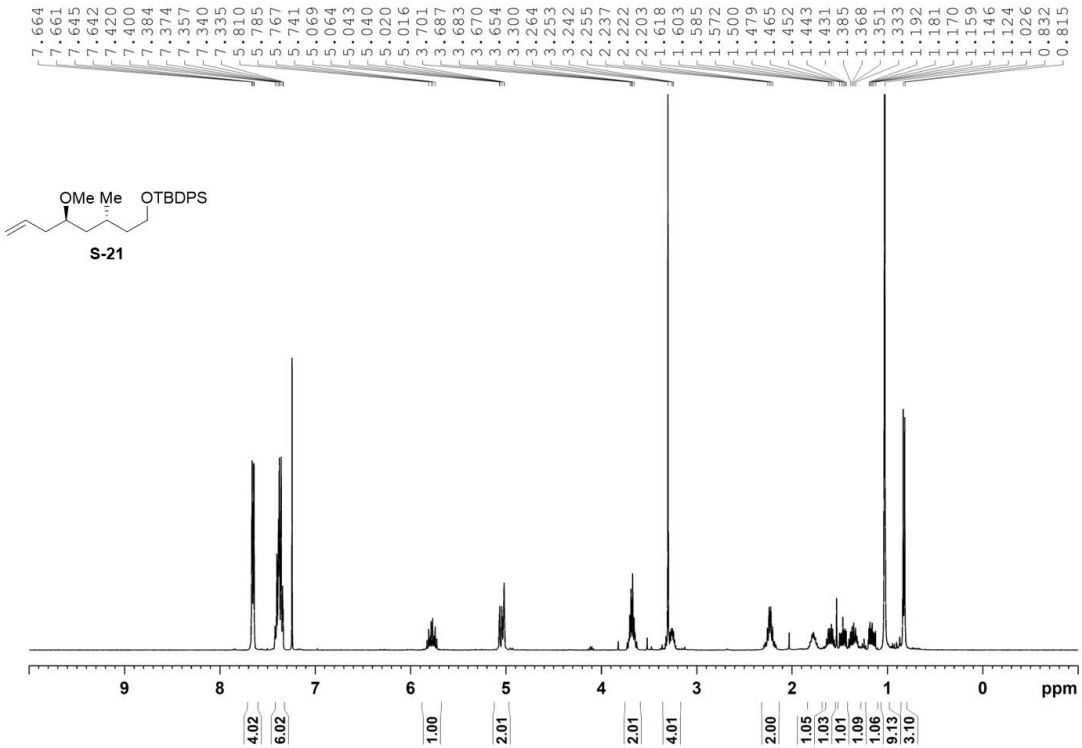

tert-Butyl-((3*R*,5*R*)-5-methoxy-3-methyloct-7-enyloxy)diphenylsilane (**S-21**)

^{13}C NMR (100 MHz, $CDCl_3$)

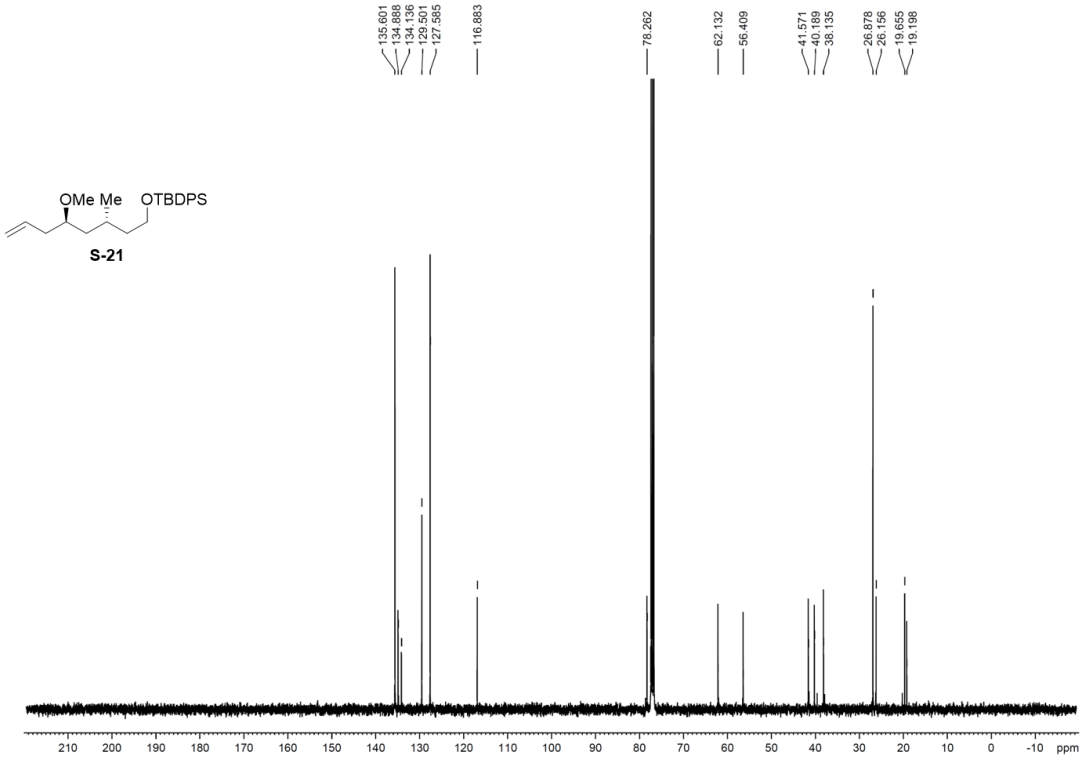

tert-Butyl-((3*R*,5*R*)-5-methoxy-3-methyloct-7-enyloxy)diphenylsilane (**S-21**)

COSY (400 MHz, $CDCl_3$)

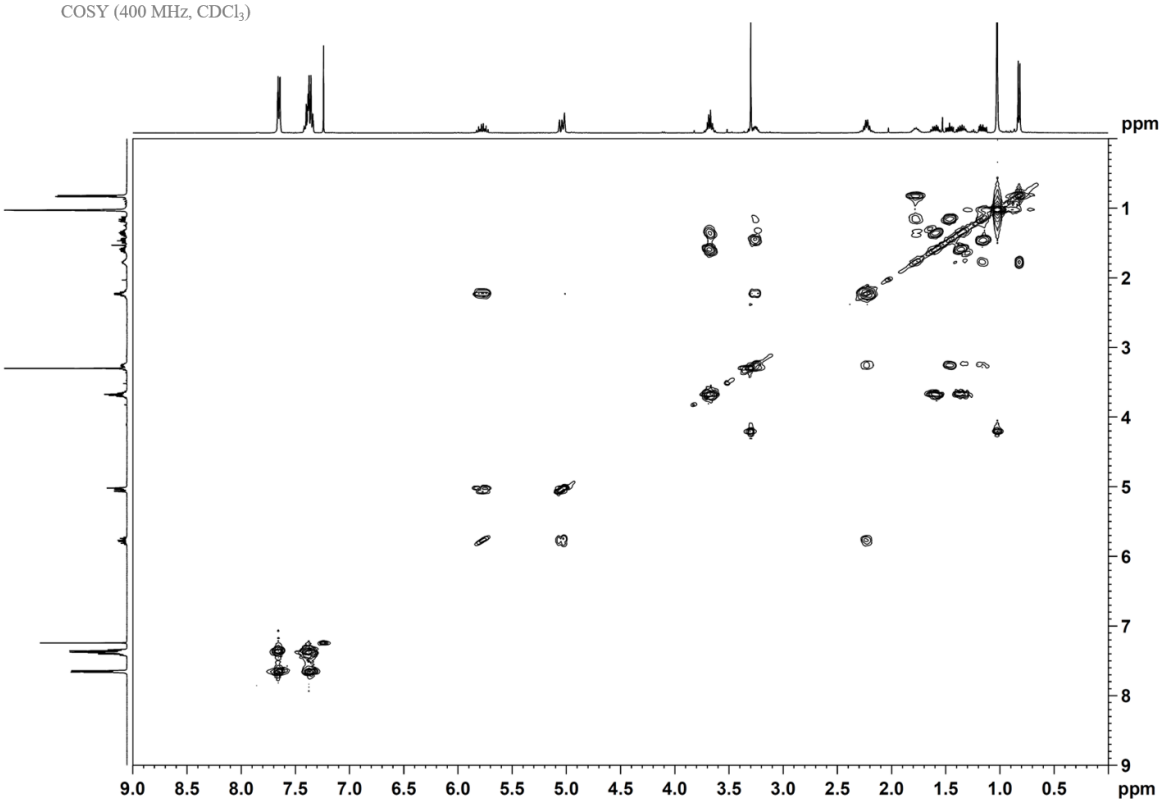

tert-Butyl-((3*R*,5*R*)-5-methoxy-3-methyloct-7-enyloxy)diphenylsilane (**S-21**)

HSQC (400 MHz, $CDCl_3$)

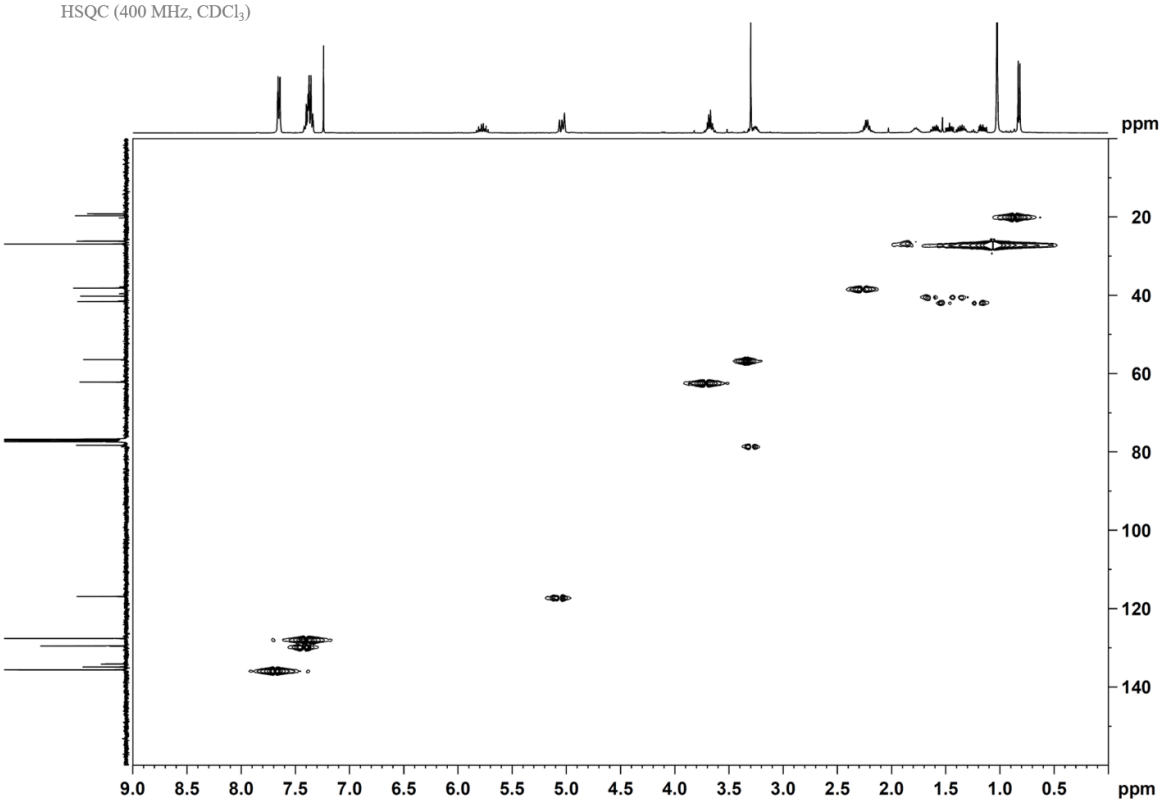

(3*S*,5*R*)-7-(*tert*-Butyldiphenylsilyloxy)-3-methoxy-5-methylheptanal (**4.36**)

^{1}H NMR (400 MHz, $CDCl_3$)

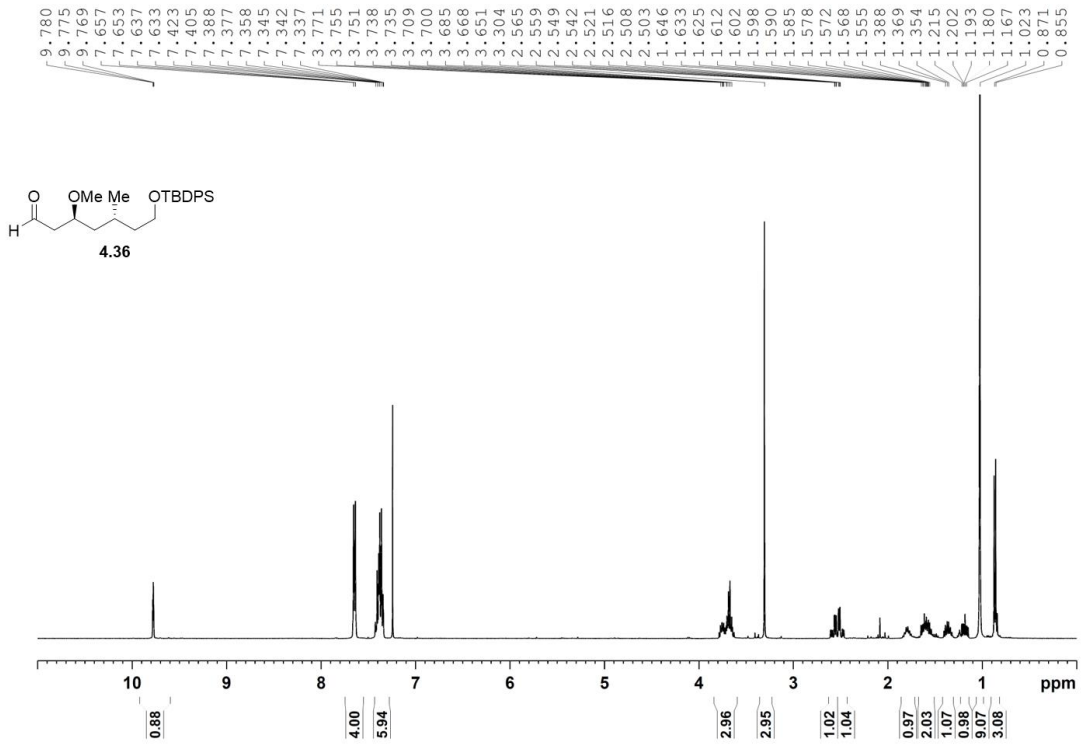

(3*S*,5*R*)-7-(*tert*-Butyldiphenylsilyloxy)-3-methoxy-5-methylheptanal (**4.36**)

^{13}C NMR (100 MHz, $CDCl_3$)

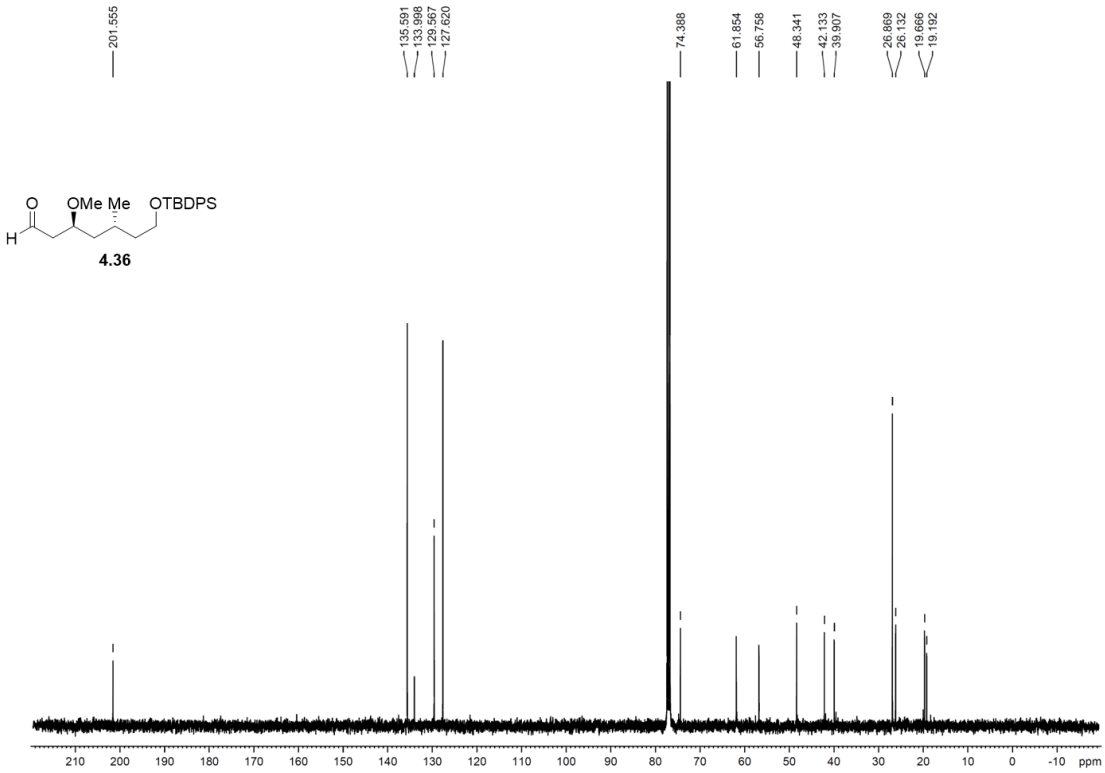

(3*S*,5*R*)-7-(*tert*-Butyldiphenylsilyloxy)-3-methoxy-5-methylheptanal (**4.36**)
COSY (400 MHz, $CDCl_3$)

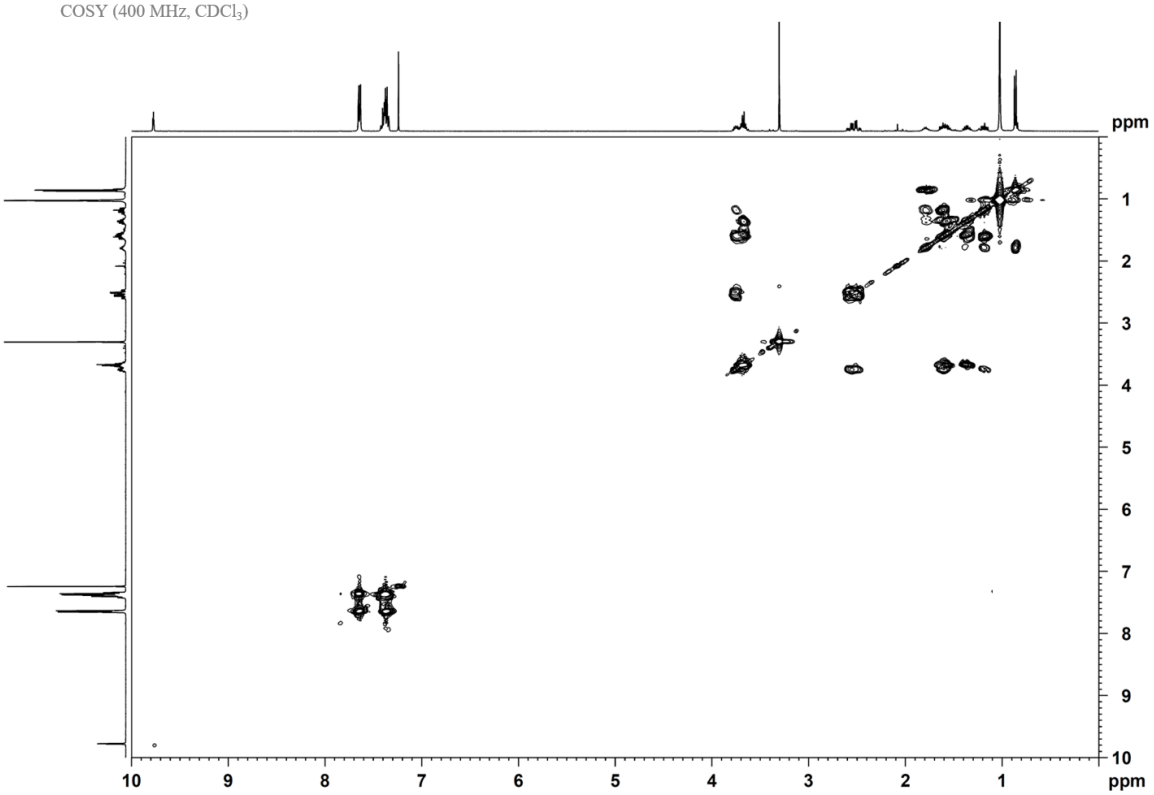

(3*S*,5*R*)-7-(*tert*-Butyldiphenylsilyloxy)-3-methoxy-5-methylheptanal (**4.36**)
HSQC (400 MHz, $CDCl_3$)

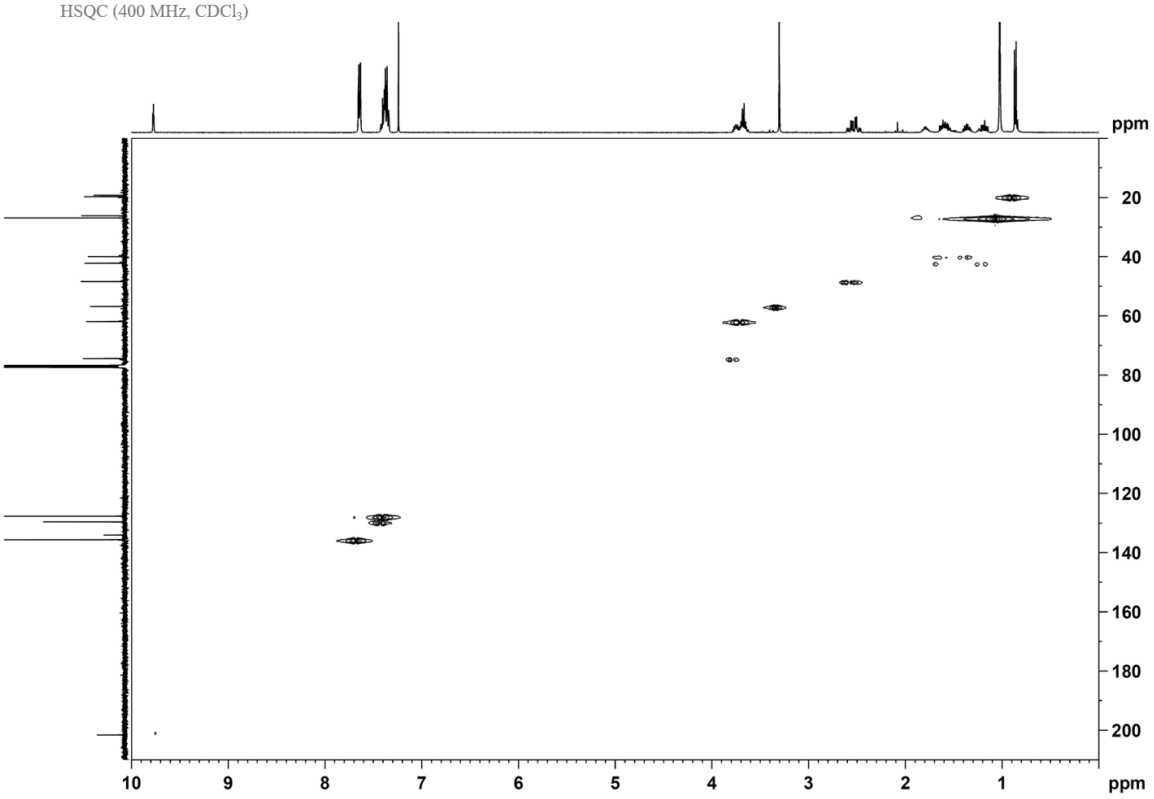

(4*S*,6*S*,8*R*)-10-(*tert*-Butyldiphenylsilyloxy)-6-methoxy-8-methyldecan-4-ol (**4.37**)

^{1}H NMR (400 MHz, $CDCl_3$)

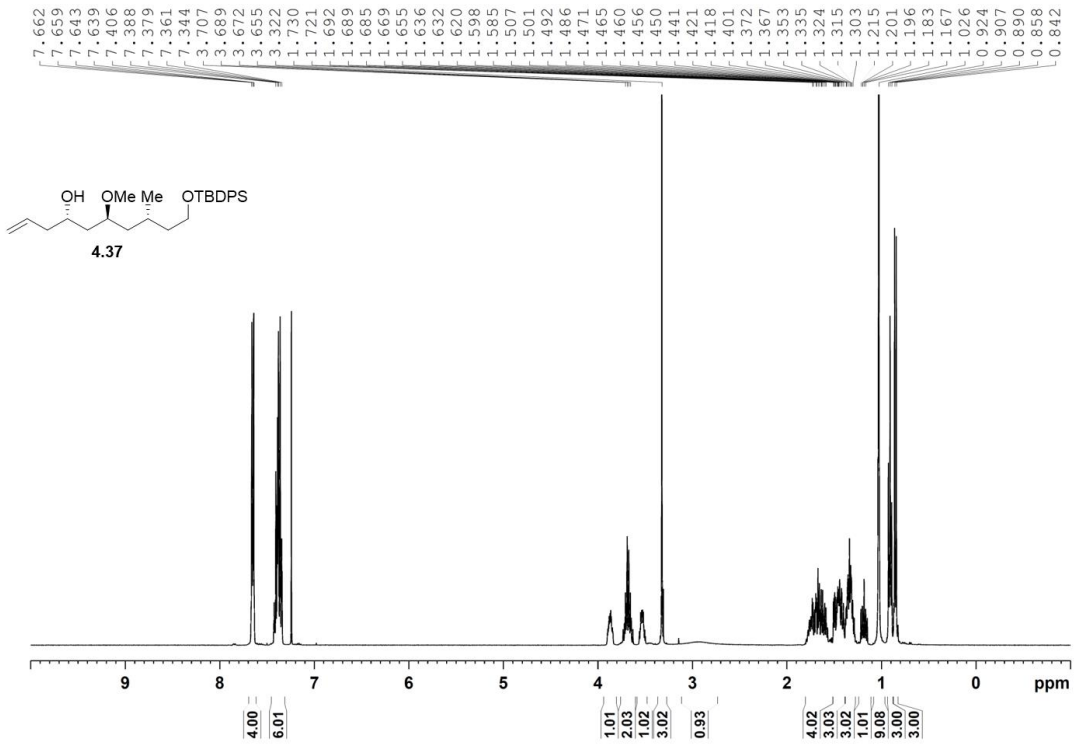

(4*S*,6*S*,8*R*)-10-(*tert*-Butyldiphenylsilyloxy)-6-methoxy-8-methyldecan-4-ol (**4.37**)

^{13}C NMR (100 MHz, $CDCl_3$)

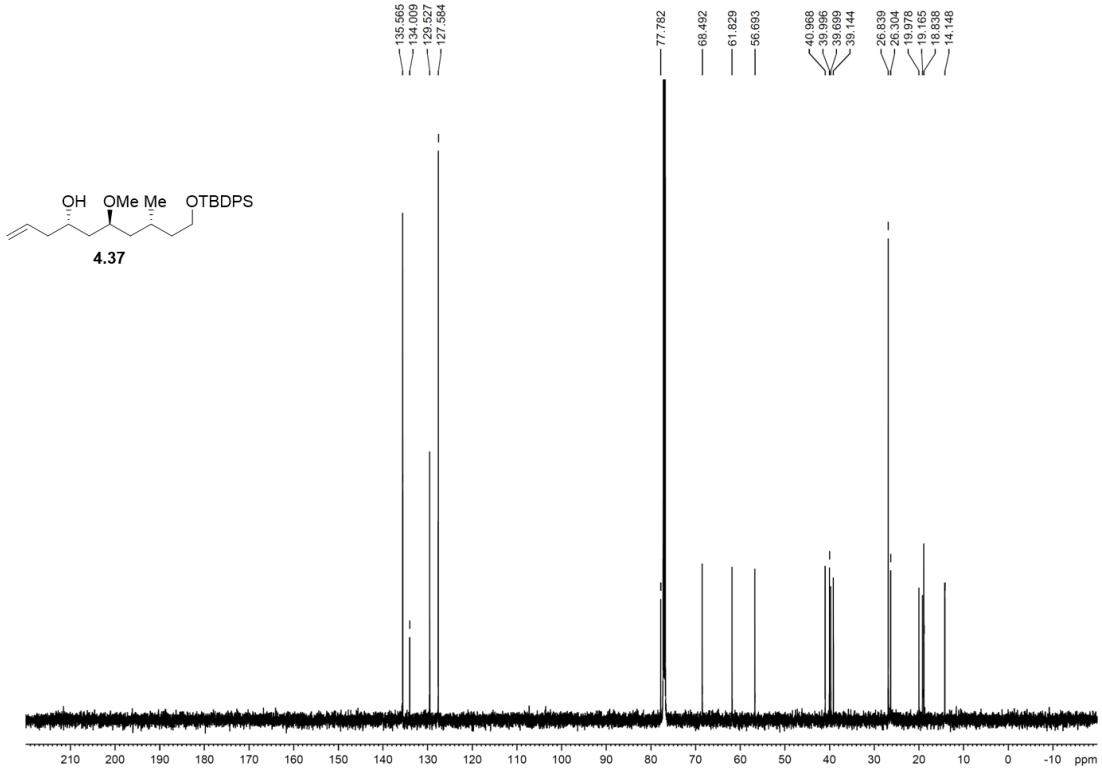

(4*S*,6*S*,8*R*)-10-(*tert*-Butyldiphenylsilyloxy)-6-methoxy-8-methyldecan-4-ol (**4.37**)

COSY (400 MHz, $CDCl_3$)

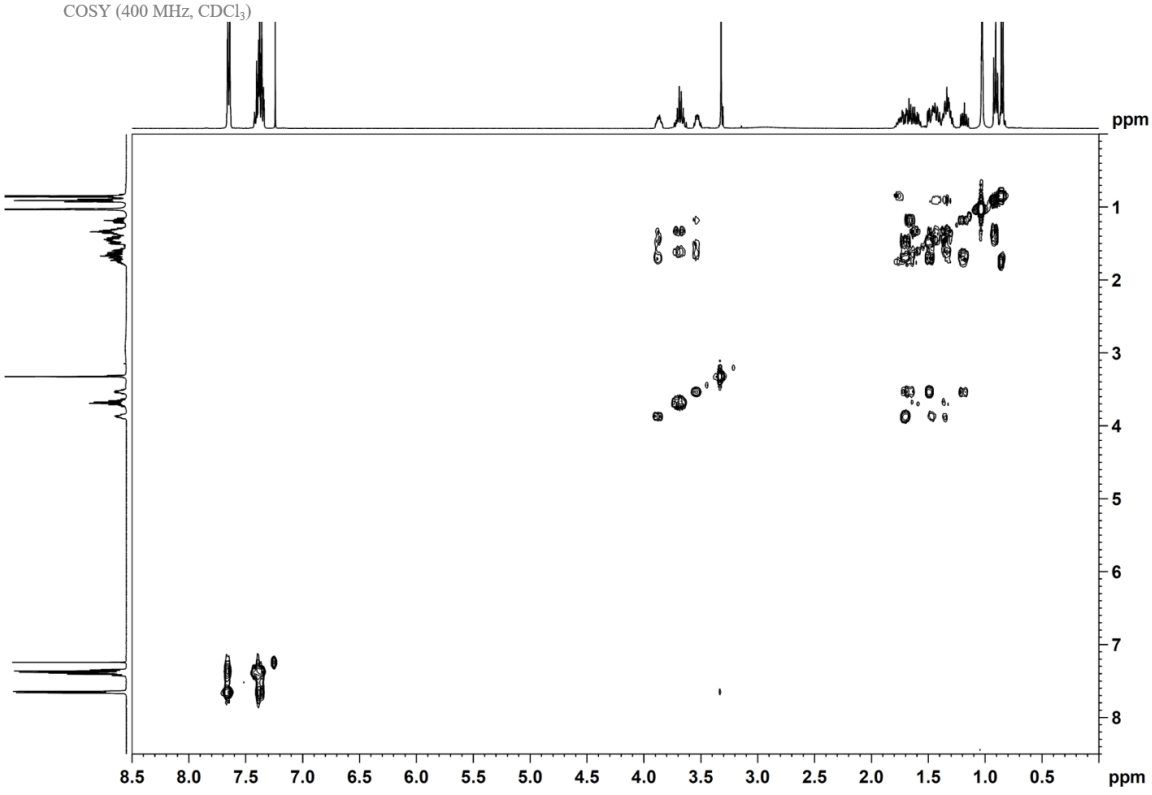

(4*S*,6*S*,8*R*)-10-(*tert*-Butyldiphenylsilyloxy)-6-methoxy-8-methyldecan-4-ol (**4.37**)

HSQC (400 MHz, $CDCl_3$)

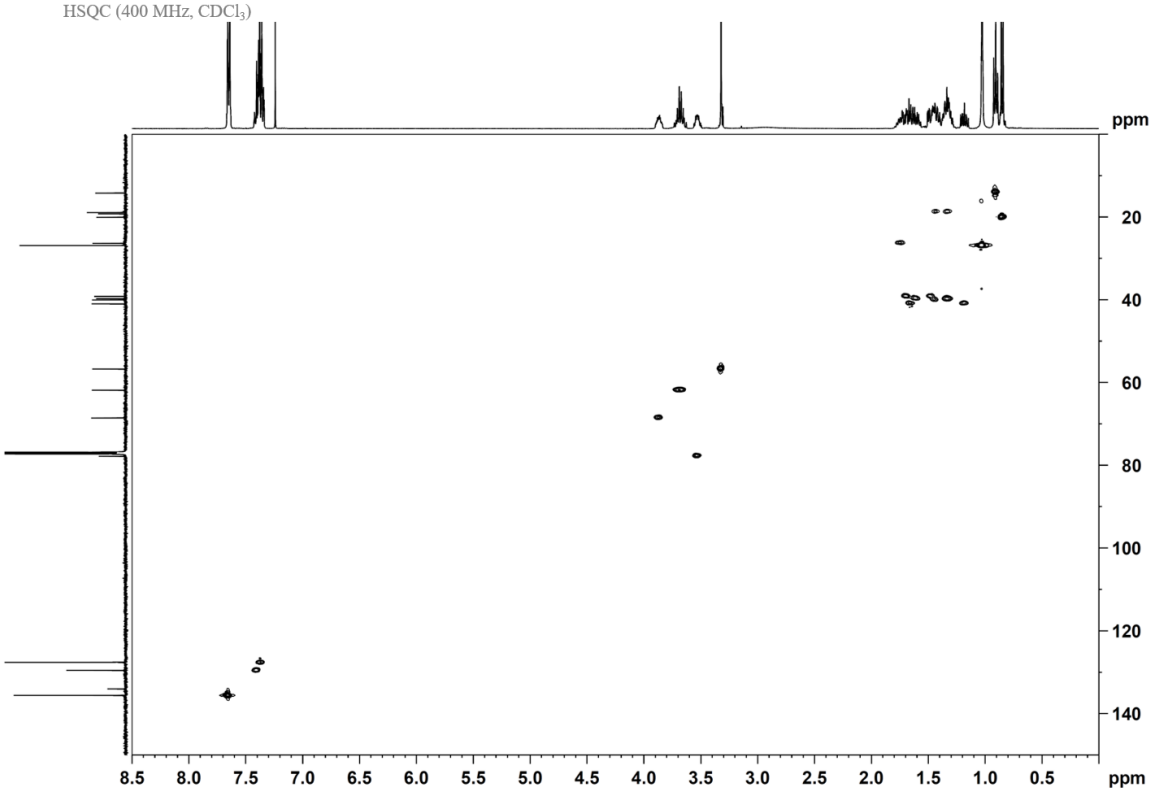

S1.3.2 Tandem Hydrogenation/Hydrogenolysis C13-Benzyl Ether Model (§ 4.4.3)

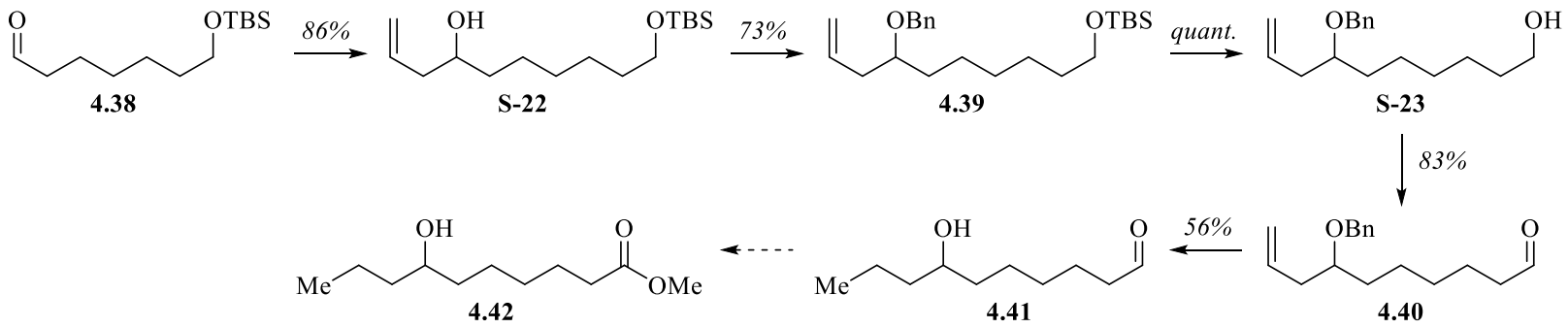

Figure S7 – Summary of the synthesis of C13 benzyl ether model for tandem hydrogenation/hydrogenolysis.

10-(*tert*-Butyldimethylsilyloxy)dec-1-en-4-ol (**S-22**)

^{1}H NMR (300 MHz, $CDCl_3$)

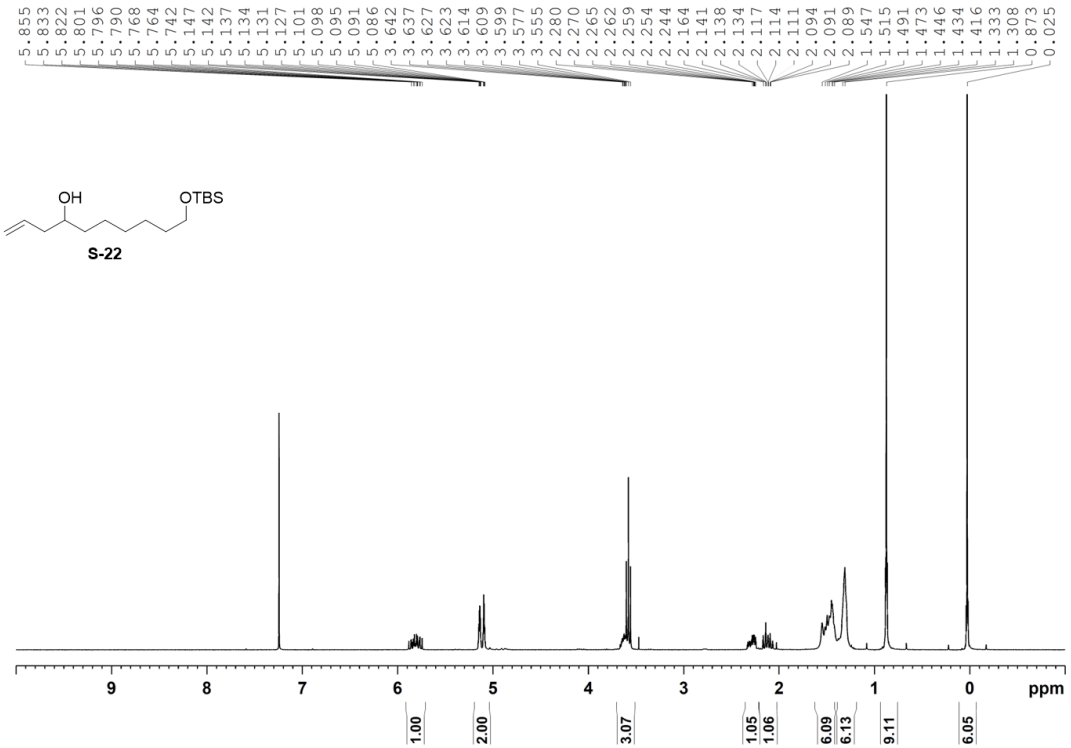

10-(*tert*-Butyldimethylsilyloxy)dec-1-en-4-ol (**S-22**)

^{13}C NMR (75 MHz, $CDCl_3$)

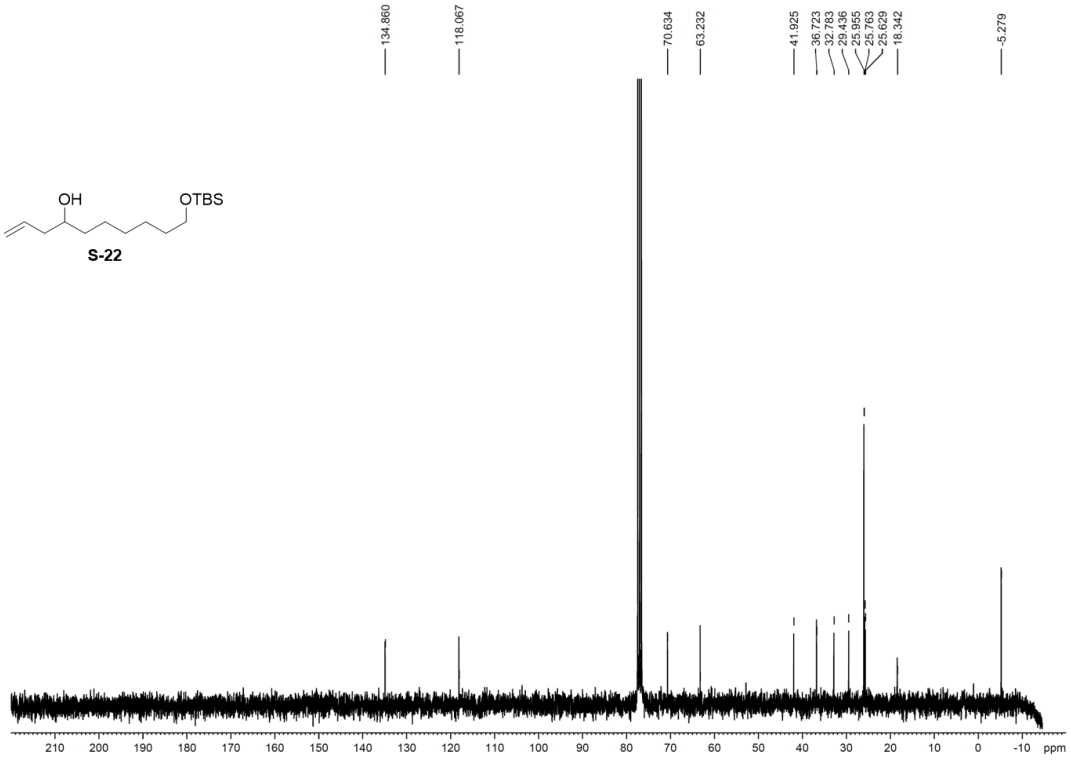

((7-(Benzyloxy)dec-9-en-1-yl)oxy)-*tert*-butyldimethylsilane (**4.39**)

^{1}H NMR (400 MHz, $CDCl_3$)

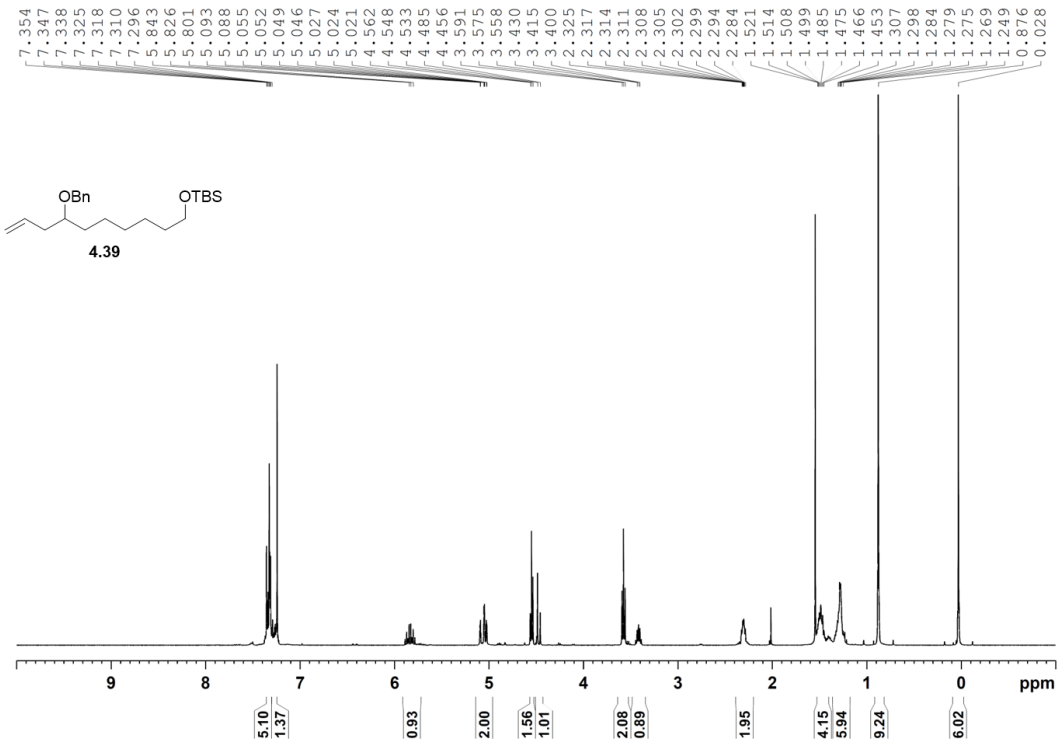

((7-(Benzyloxy)dec-9-en-1-yl)oxy)-*tert*-butyldimethylsilane (**4.39**)

^{13}C NMR (100 MHz, $CDCl_3$)

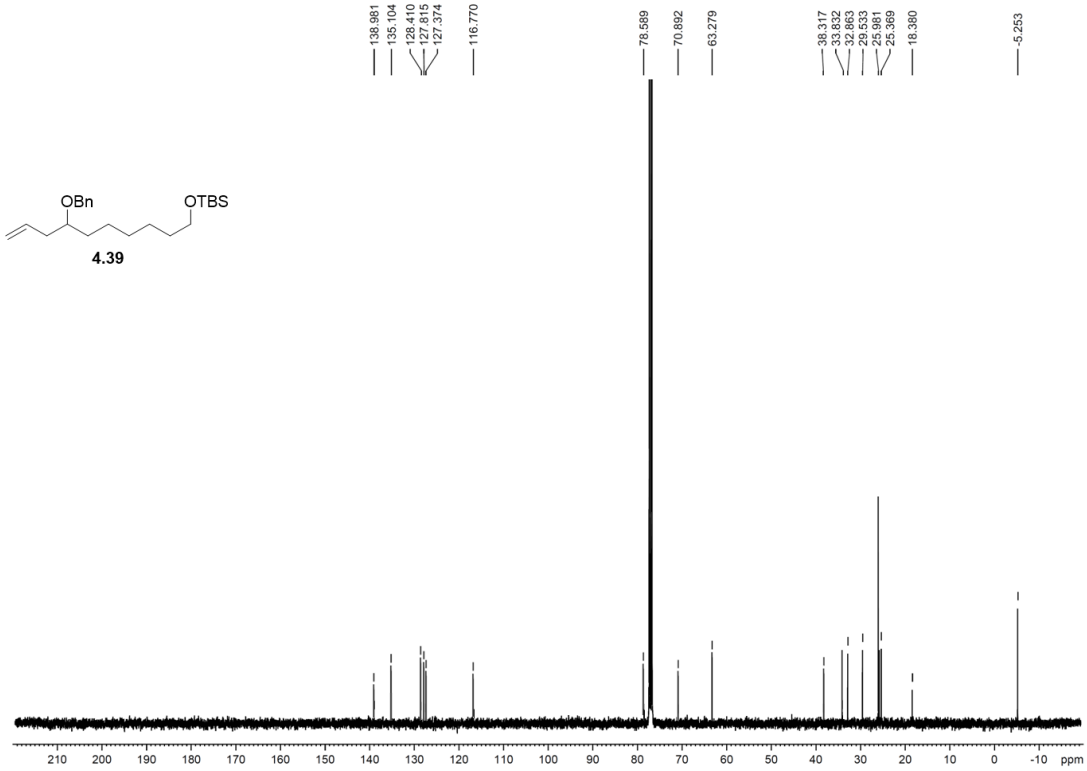

((7-(Benzyloxy)dec-9-en-1-yl)oxy)-*tert*-butyldimethylsilane (**4.39**)

COSY (400 MHz, $CDCl_3$)

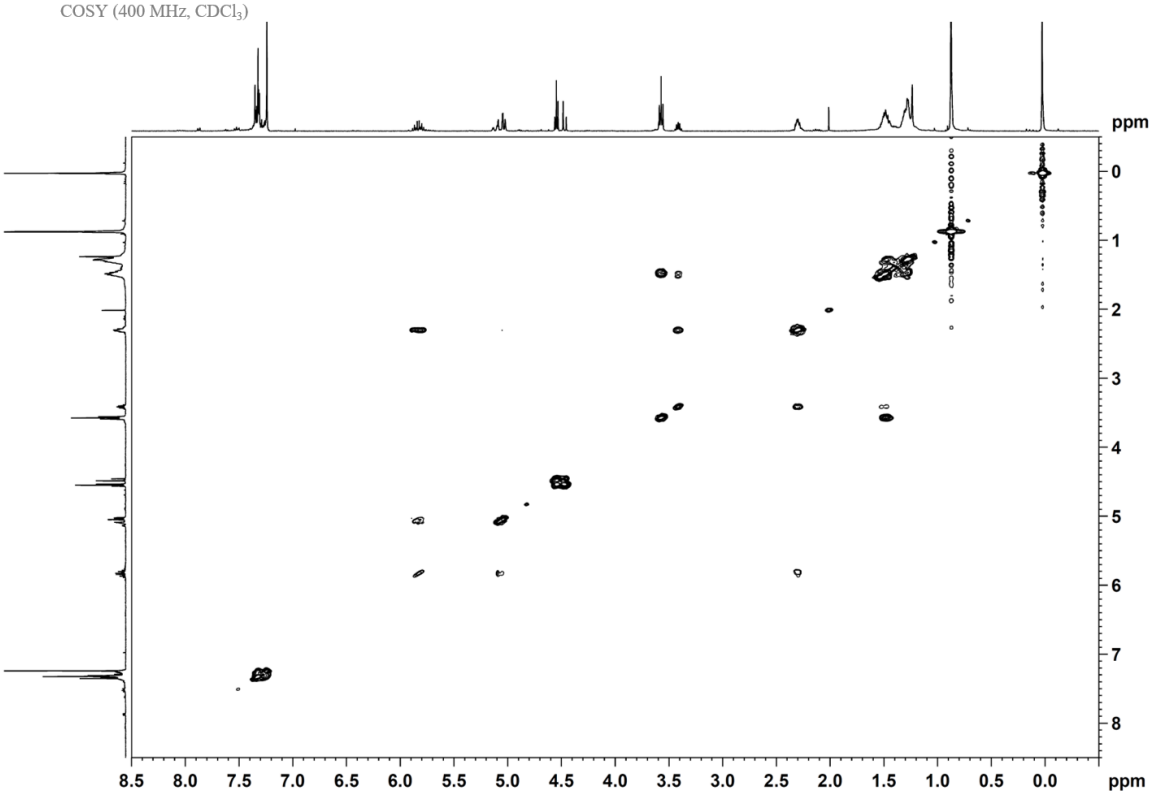

((7-(Benzyloxy)dec-9-en-1-yl)oxy)-*tert*-butyldimethylsilane (**4.39**)

HSQC (400 MHz, $CDCl_3$)

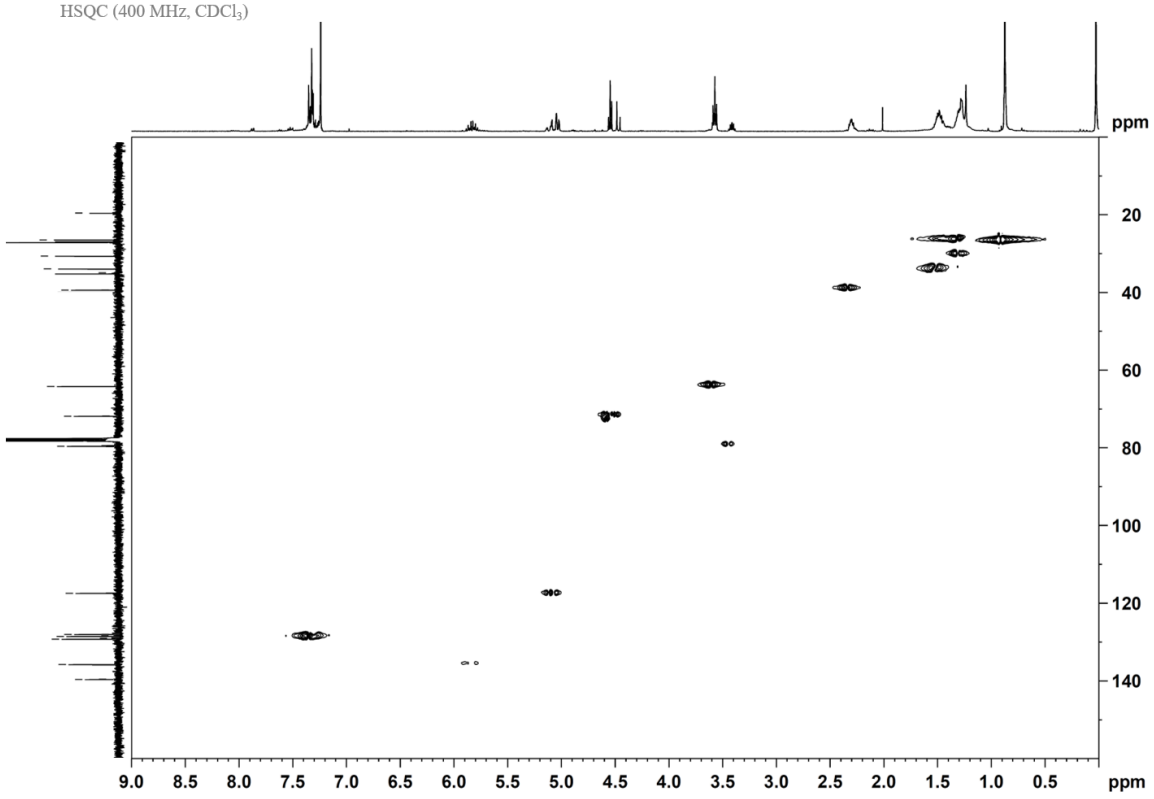

7-(Benzyloxy)dec-9-en-1-ol (**S-23**)

^{1}H NMR (400 MHz, $CDCl_3$)

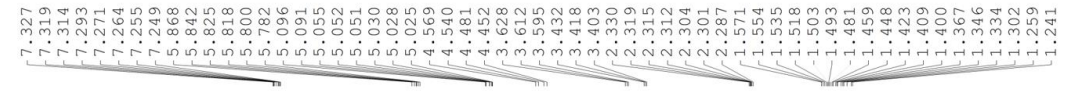

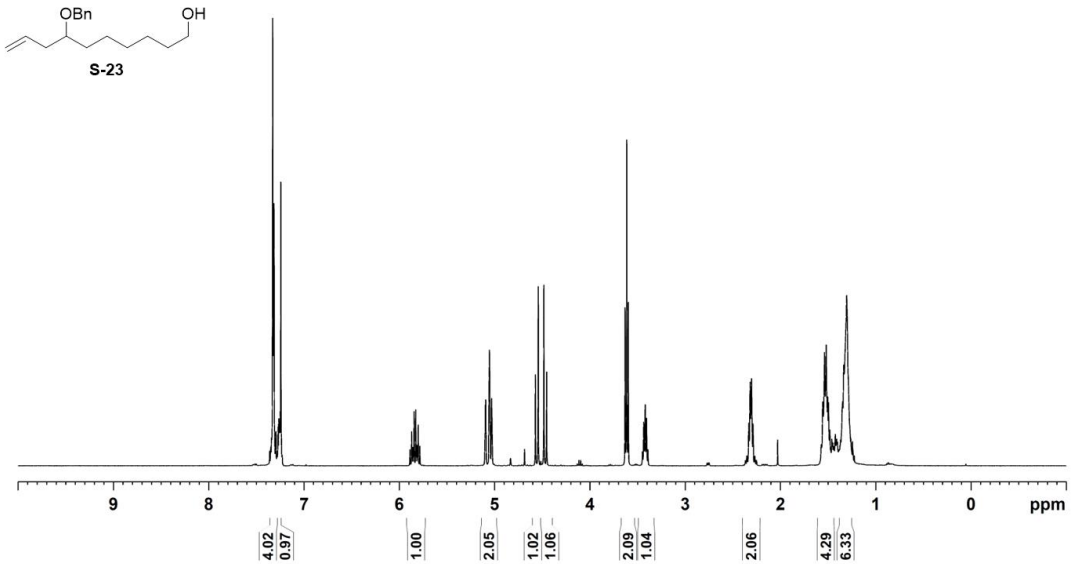

7-(Benzyloxy)dec-9-en-1-ol (**S-23**)

^{13}C NMR (100 MHz, $CDCl_3$)

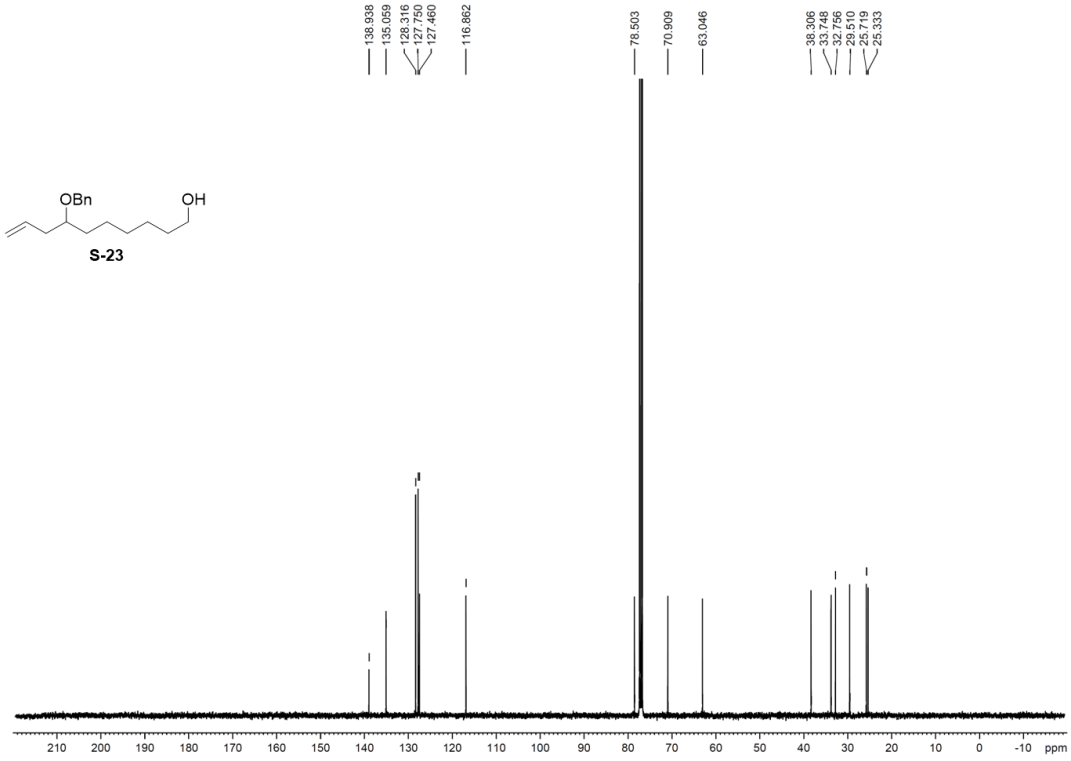

7-(Benzyloxy)dec-9-en-1-ol (**S-23**)

COSY (400 MHz, $CDCl_3$)

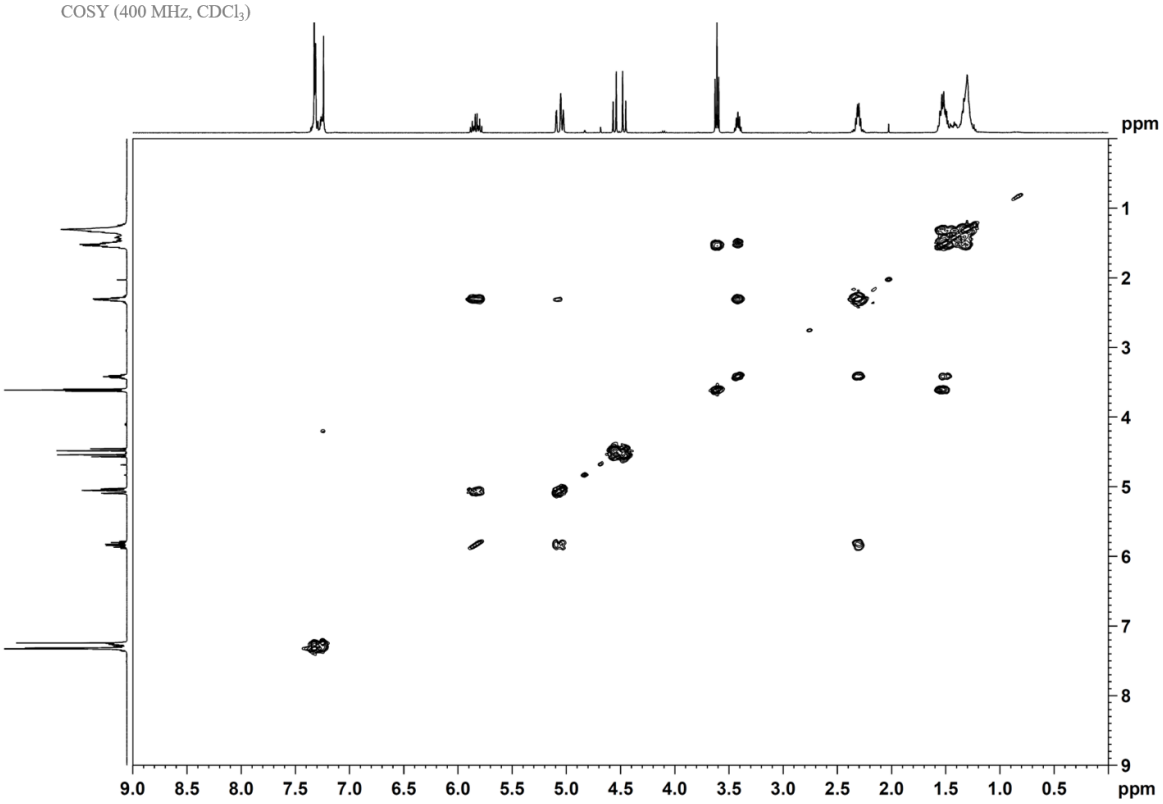

7-(Benzyloxy)dec-9-en-1-ol (**S-23**)

HSQC (400 MHz, $CDCl_3$)

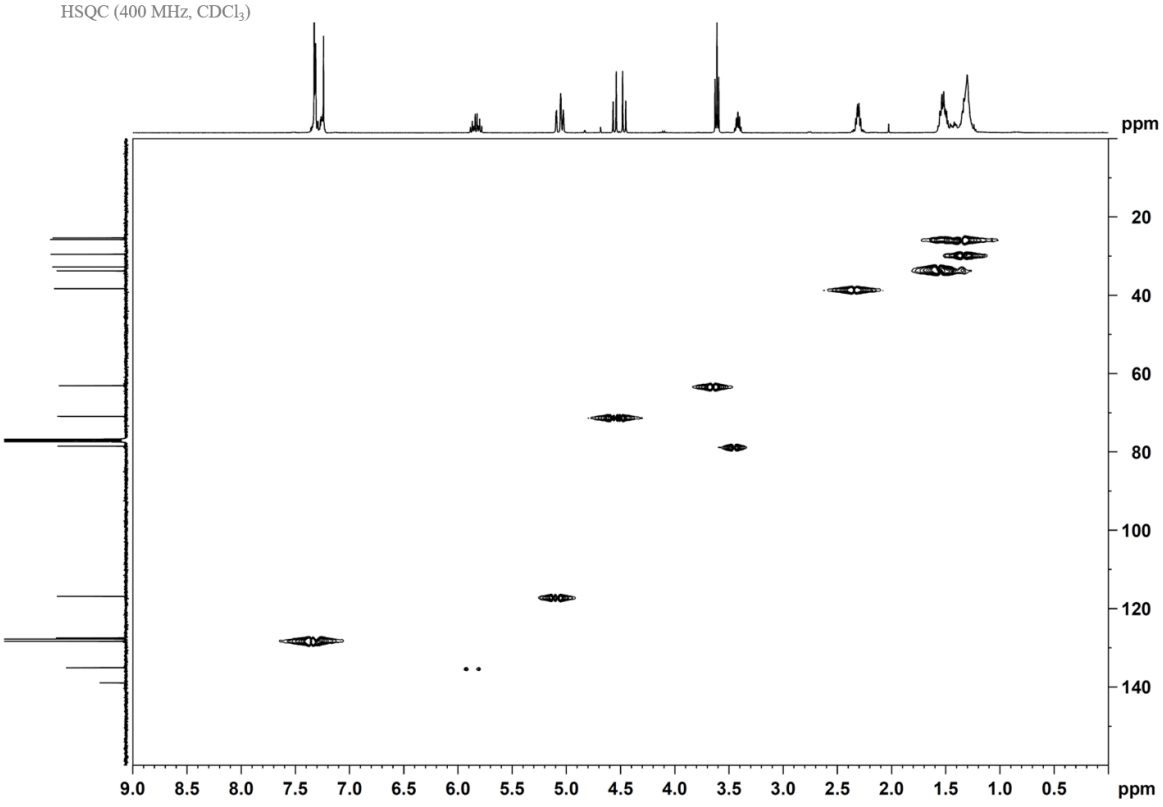

7-(Benzyloxy)dec-9-enal (**4.40**)

^{1}H NMR (400 MHz, $CDCl_3$)

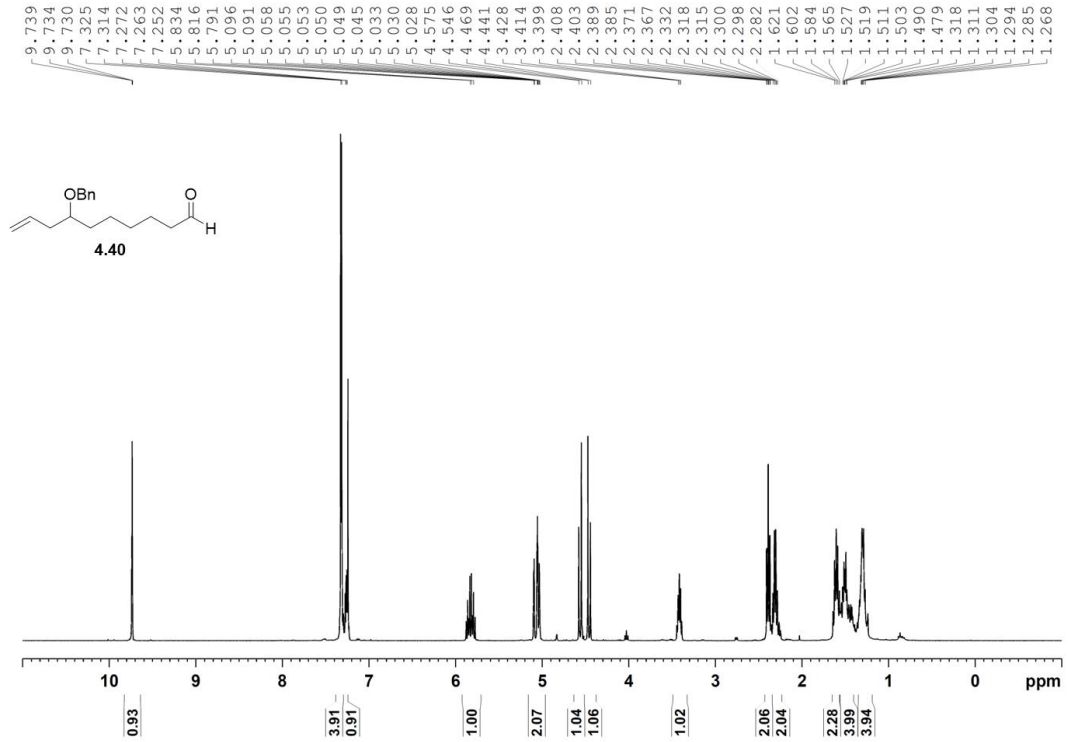

7-(Benzyloxy)dec-9-enal (**4.40**)

^{13}C NMR (100 MHz, $CDCl_3$)

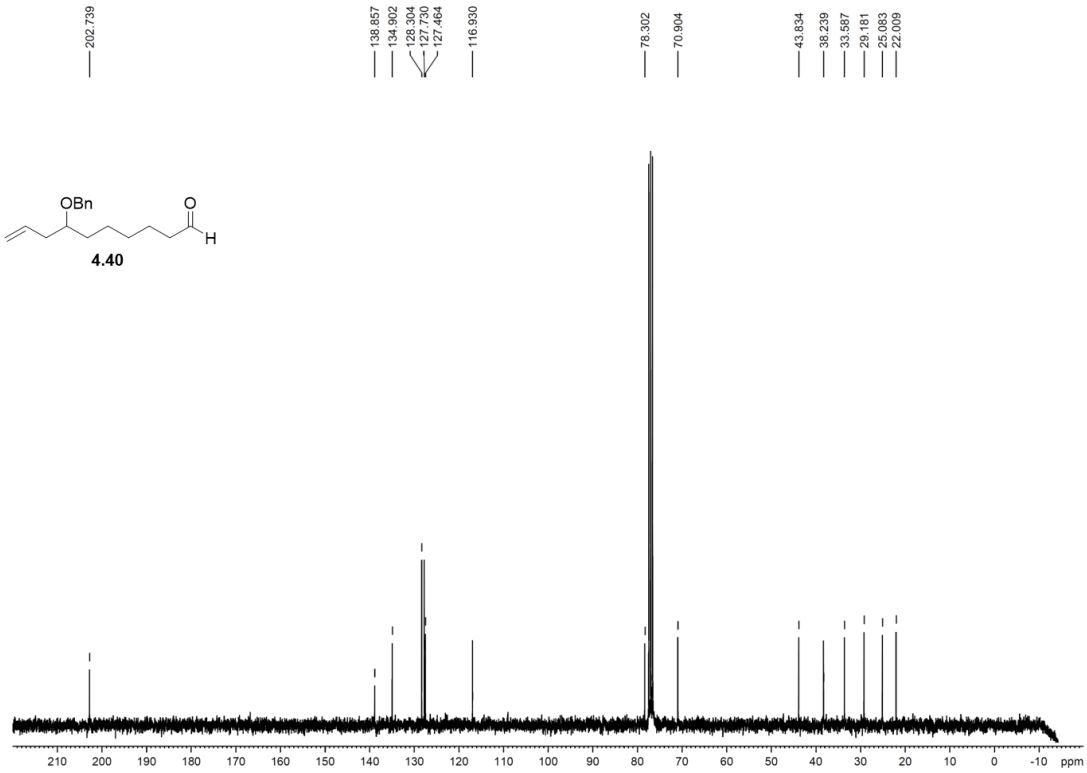

7-(Benzyloxy)dec-9-enal (**4.40**)

COSY (400 MHz, $CDCl_3$)

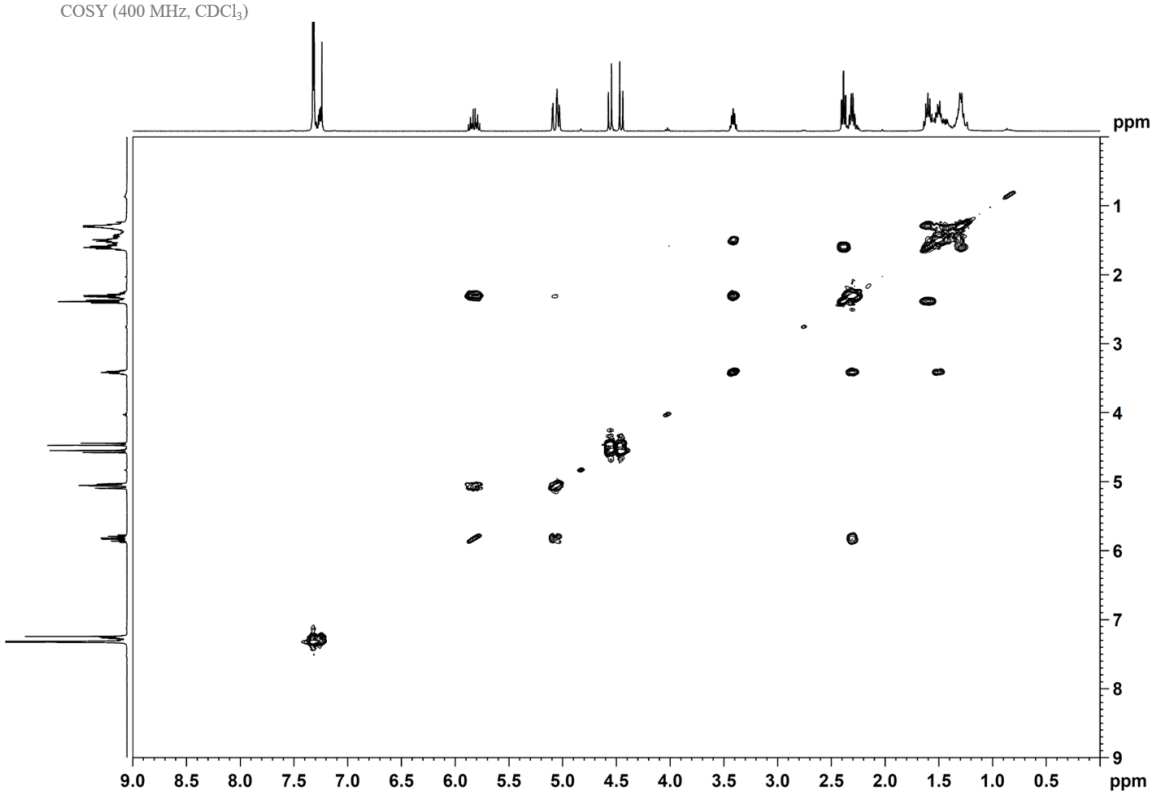

7-(Benzyloxy)dec-9-enal (**4.40**)

HSQC (400 MHz, $CDCl_3$)

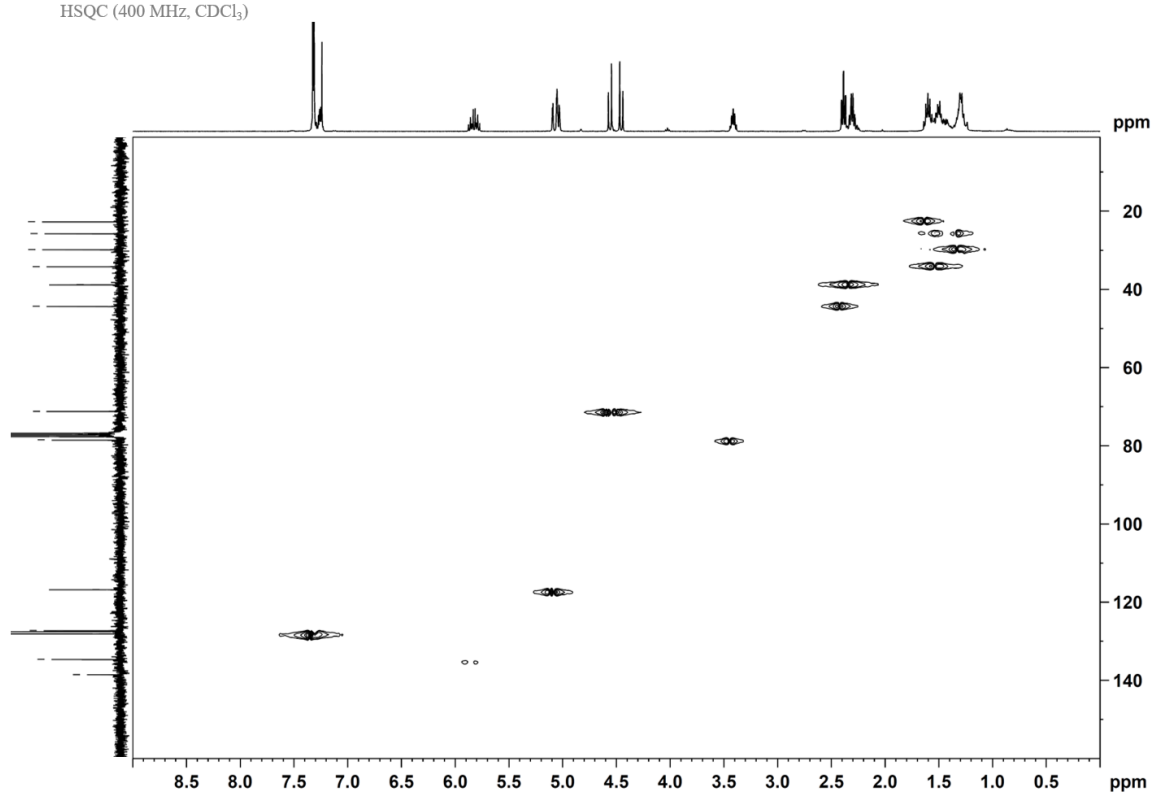

7-Hydroxydecanal (**4.41**)

^{1}H NMR (300 MHz, $CDCl_3$)

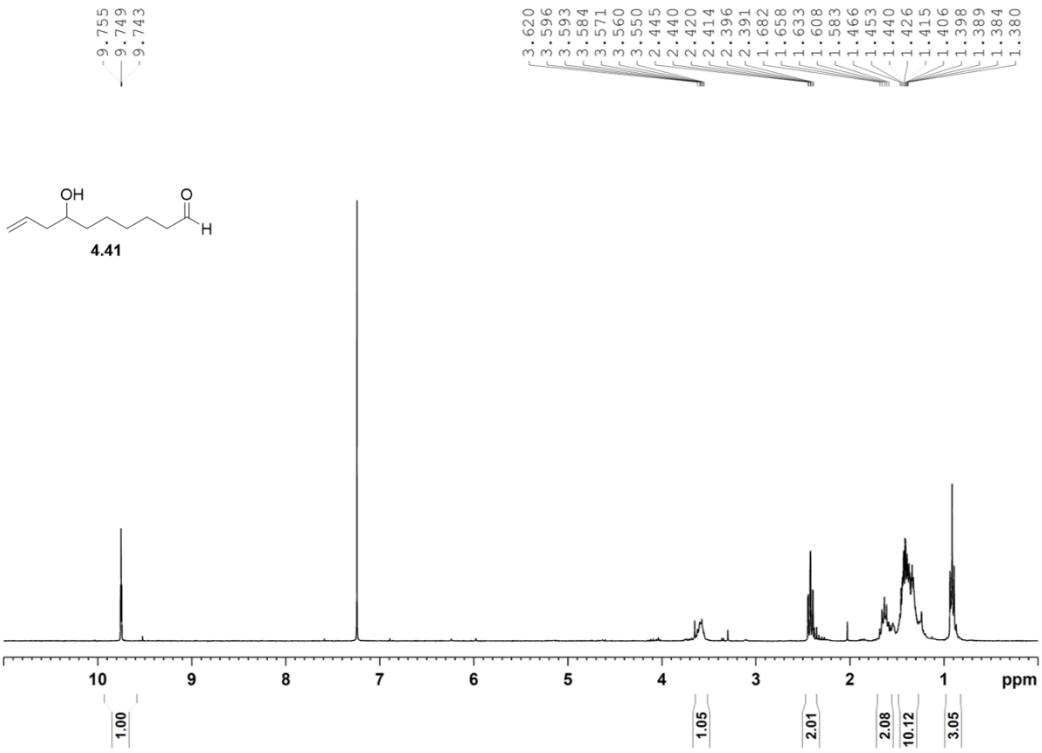

7-Hydroxydecanal (**4.41**)

^{13}C NMR (100 MHz, $CDCl_3$)

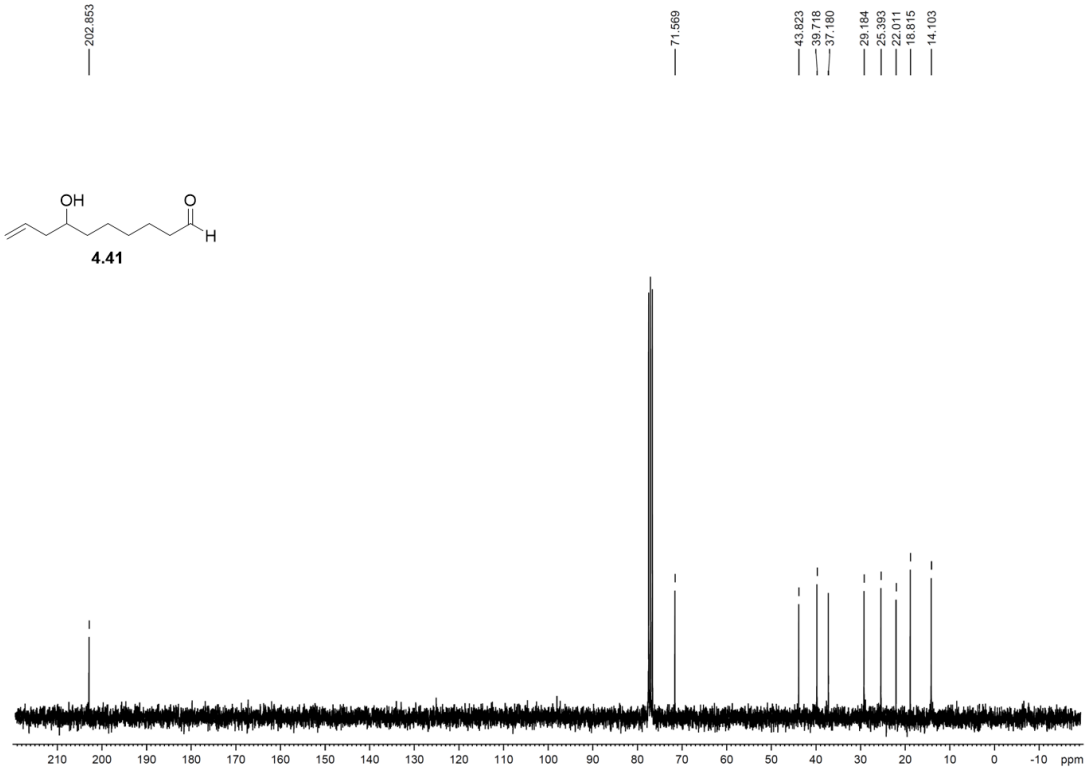

7-Hydroxydecanal (**4.41**)
COSY (300 MHz, $CDCl_3$)

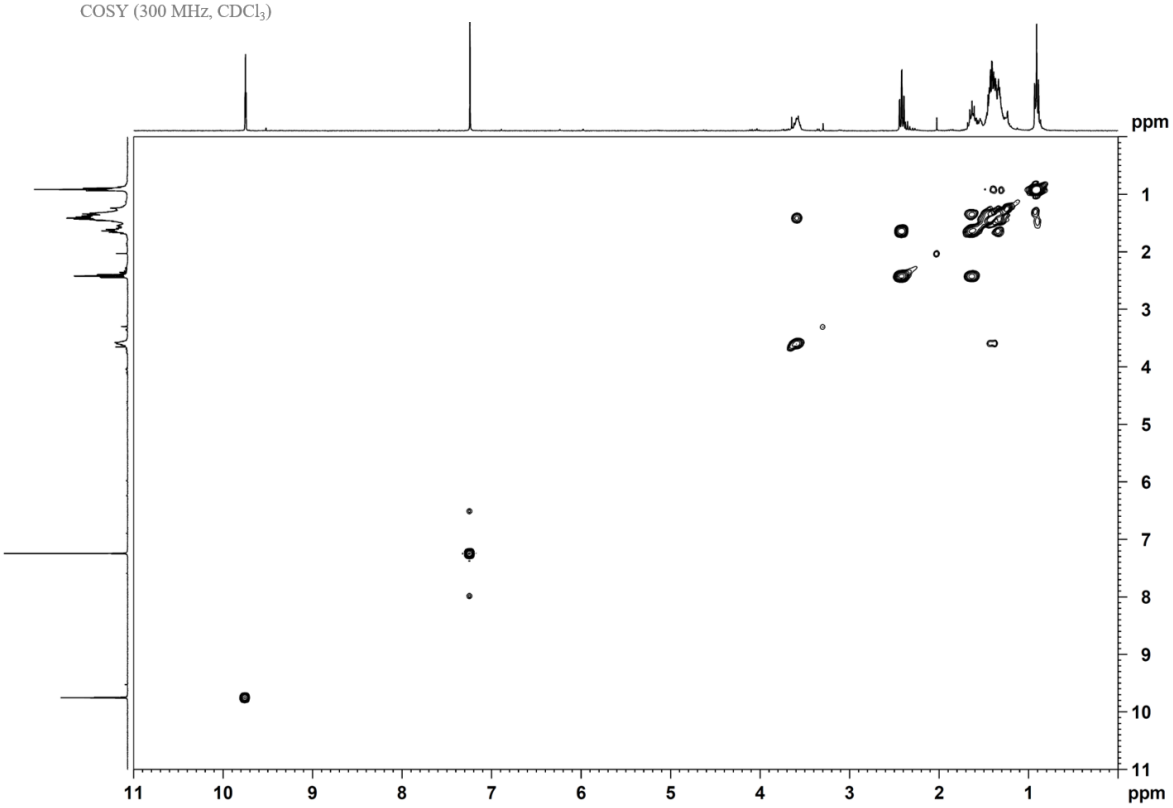

7-Hydroxydecanal (**4.41**)
HSQC (300 MHz, $CDCl_3$)

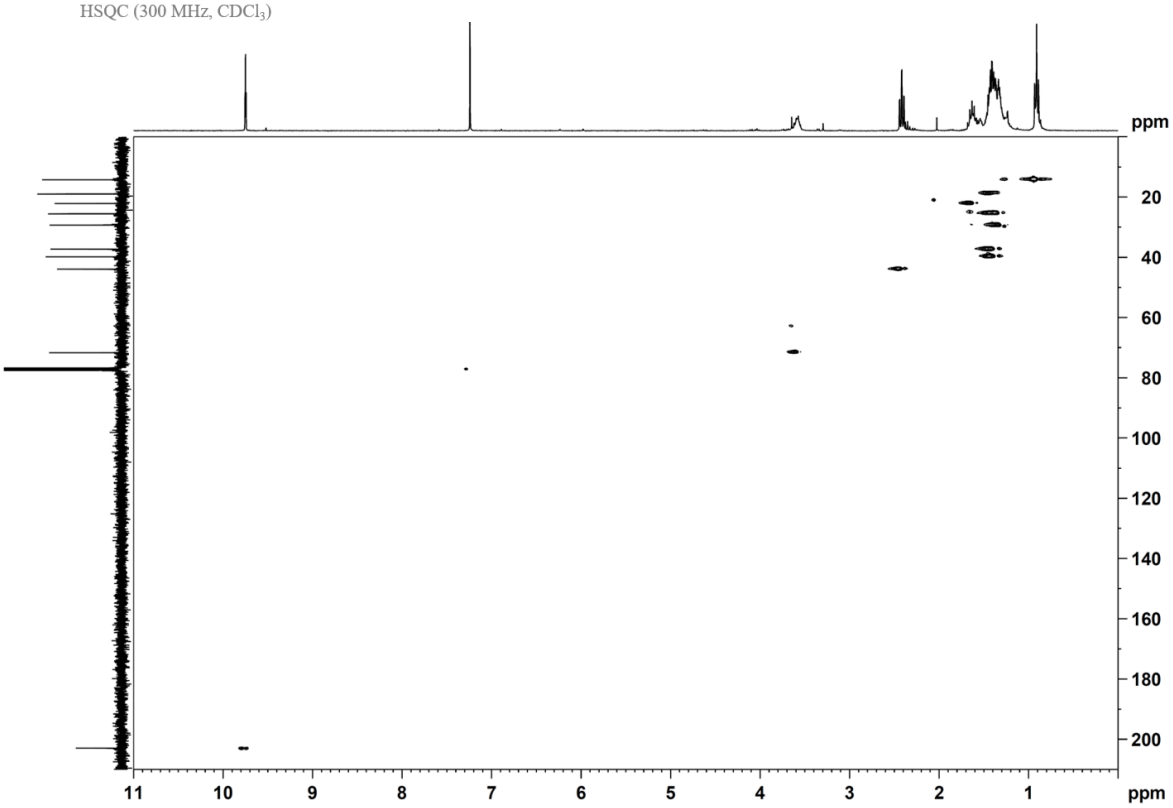

Methyl 7-hydroxydecanoate (**4.42**)

^{1}H NMR (400 MHz, $CDCl_3$)

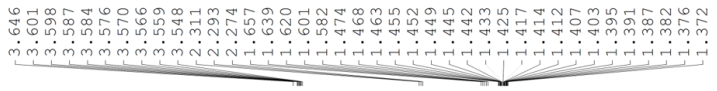

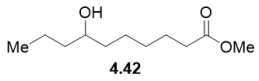

4.42

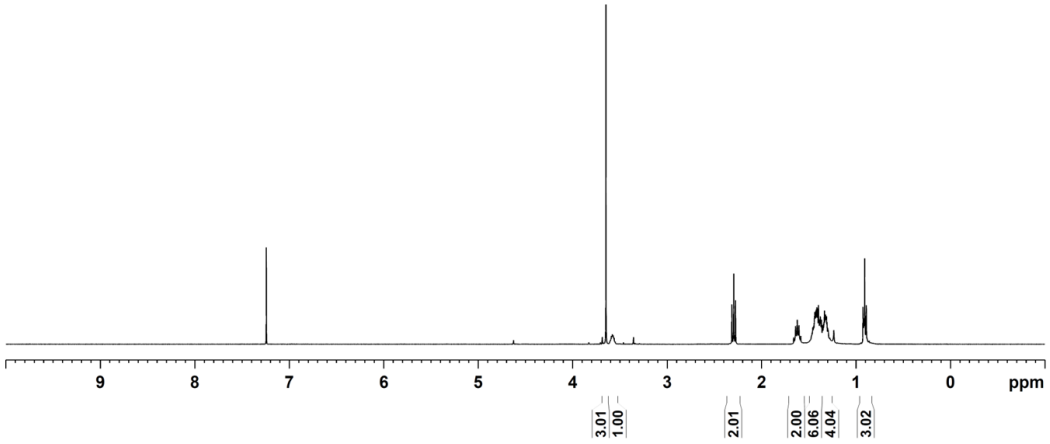

Methyl 7-hydroxydecanoate (**4.42**)

^{13}C NMR (100 MHz, $CDCl_3$)

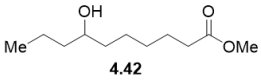

4.42

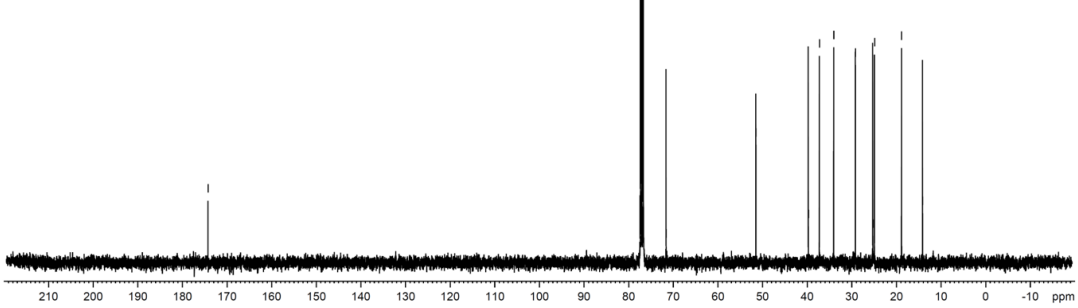

Methyl 7-hydroxydecanoate (**4.42**)

COSY (400 MHz, $CDCl_3$)

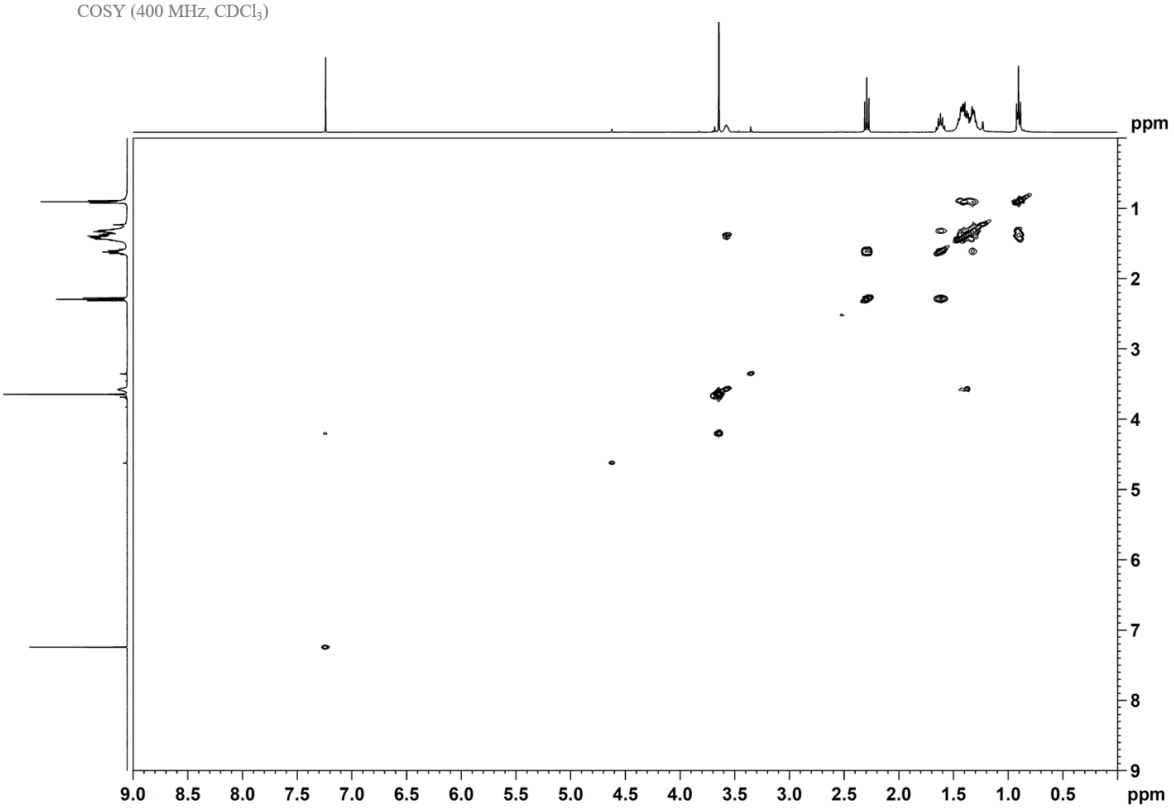

Methyl 7-hydroxydecanoate (**4.42**)

HSQC (400 MHz, $CDCl_3$)

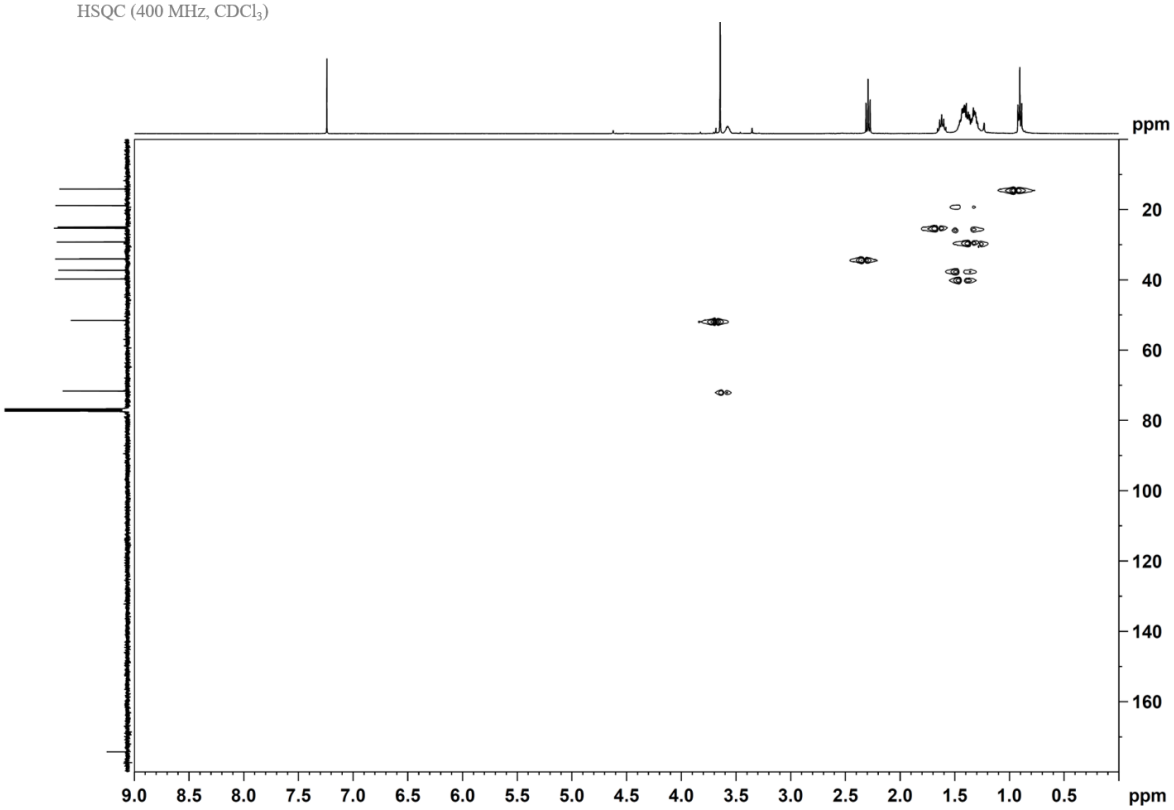

S1.3.3 Completed Carbon Framework for Macrocyclic Core v1 (§ 4.4.4)

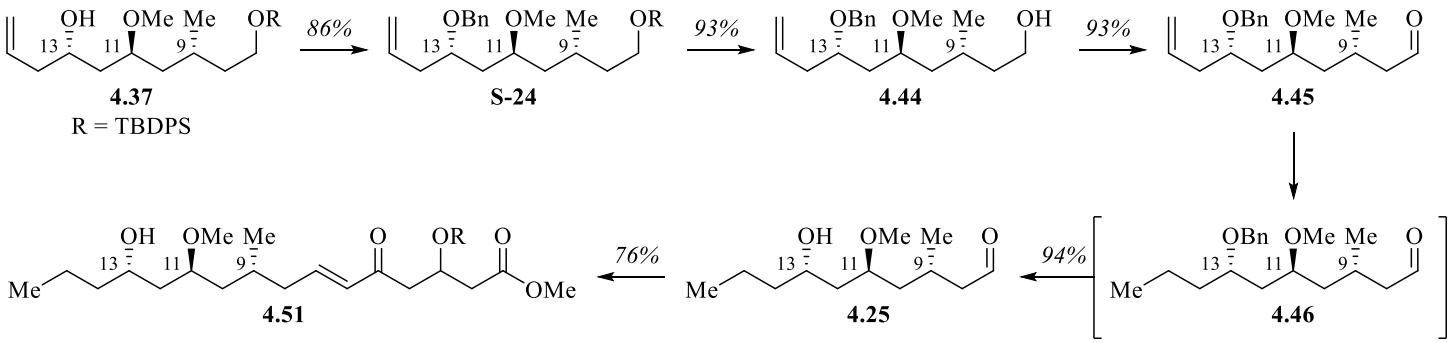

Figure S8 – Completed carbon framework to the macrocyclic core of neopeltolide achieved *via* HWE with methyl ester phosphonate.

((3*S*,5*S*,7*R*)-7-Benzyloxy-5-methoxy-3-methyldec-9-en-1-yl)-*tert*-butyldiphenylsilane (**S-24**)

^{1}H NMR (300 MHz, $CDCl_3$)

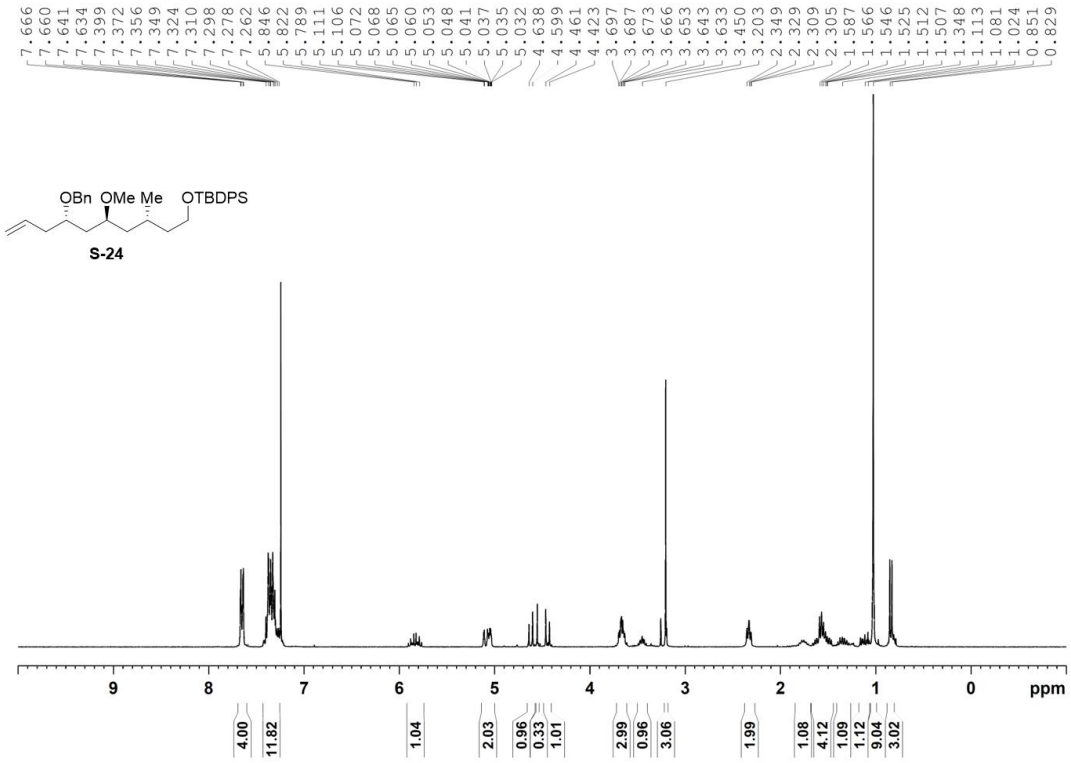

((3*S*,5*S*,7*R*)-7-Benzyloxy-5-methoxy-3-methyldec-9-en-1-yl)-*tert*-butyldiphenylsilane (**S-24**)

^{13}C NMR (100 MHz, $CDCl_3$)

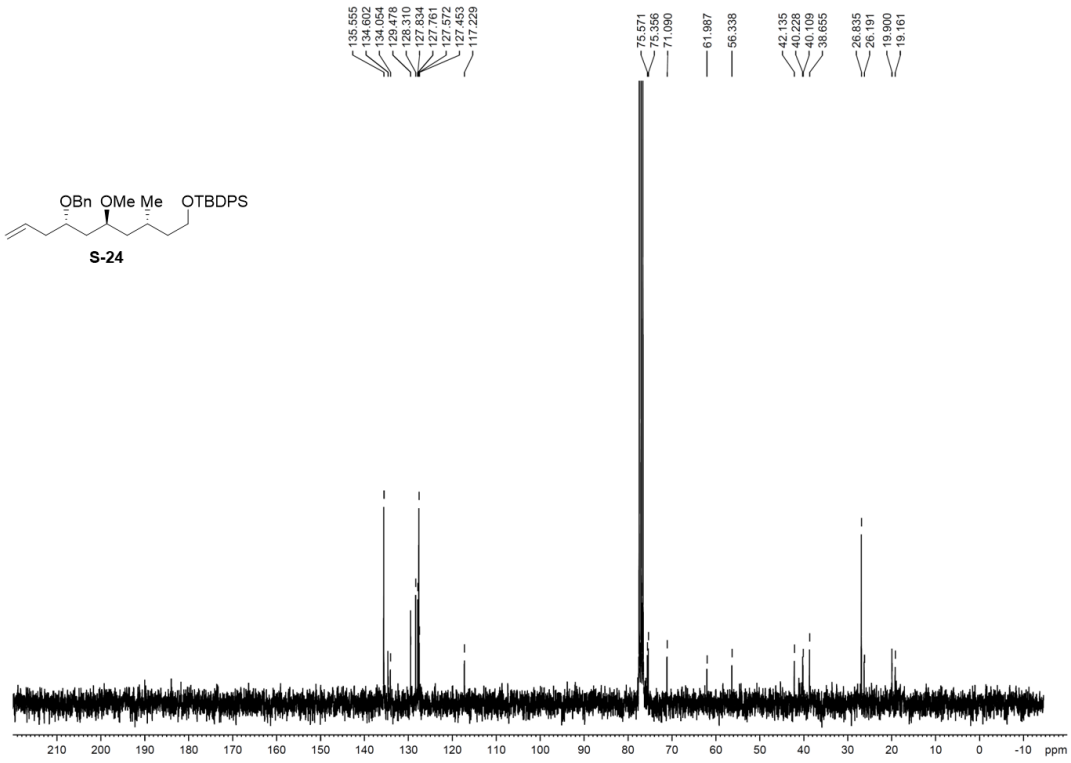

((3*S*,5*S*,7*R*)-7-Benzyloxy-5-methoxy-3-methyldec-9-en-1-yl)-*tert*-butyldiphenylsilane (**S-24**)

COSY (300 MHz, $CDCl_3$)

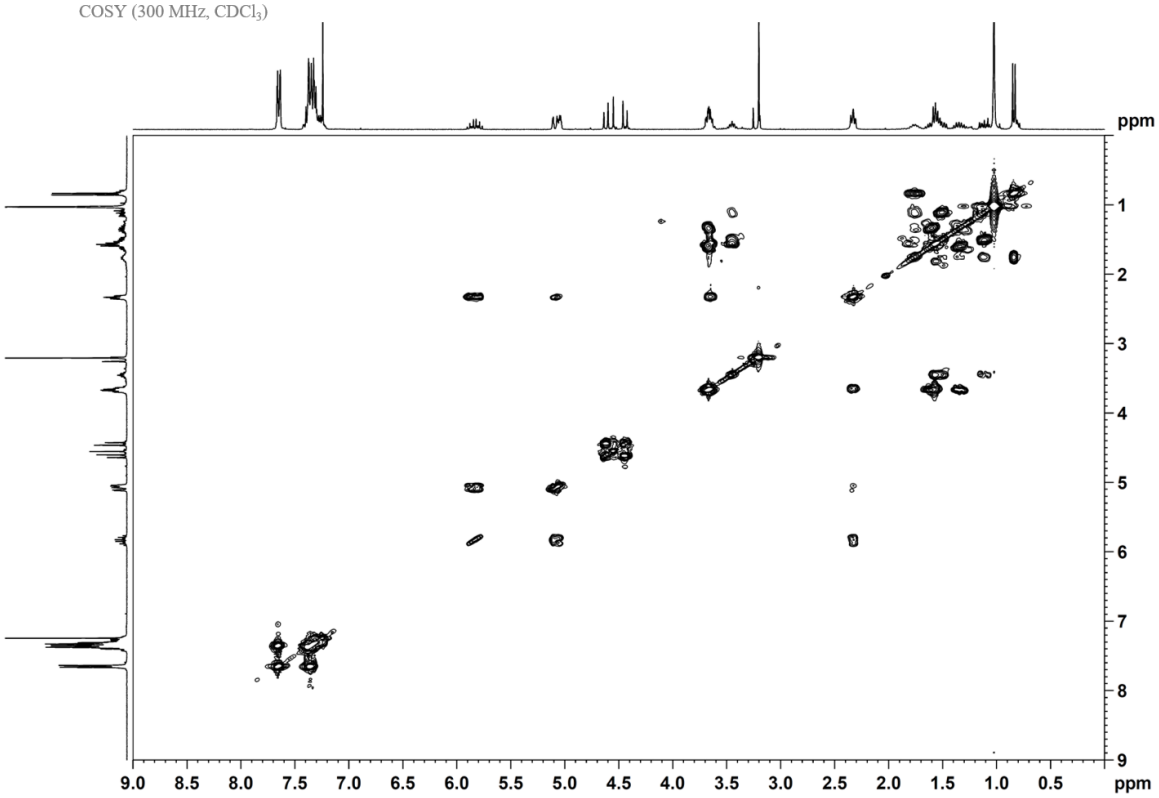

((3*S*,5*S*,7*R*)-7-Benzyloxy-5-methoxy-3-methyldec-9-en-1-yl)-*tert*-butyldiphenylsilane (**S-24**)

HSQC (300 MHz, $CDCl_3$)

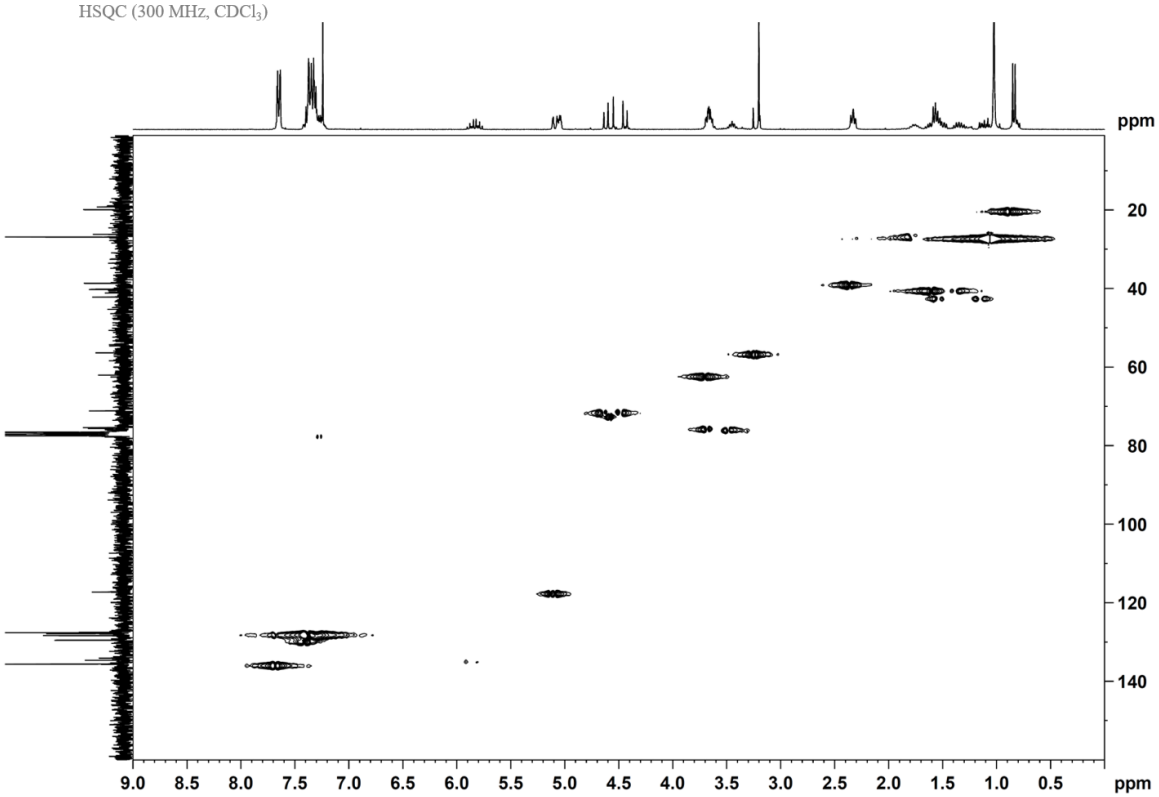

(3*R*,5*S*,7*S*)-7-Benzyloxy-5-methoxy-3-methyldec-9-en-1-ol (**4.44**)

^{1}H NMR (400 MHz, $CDCl_3$)

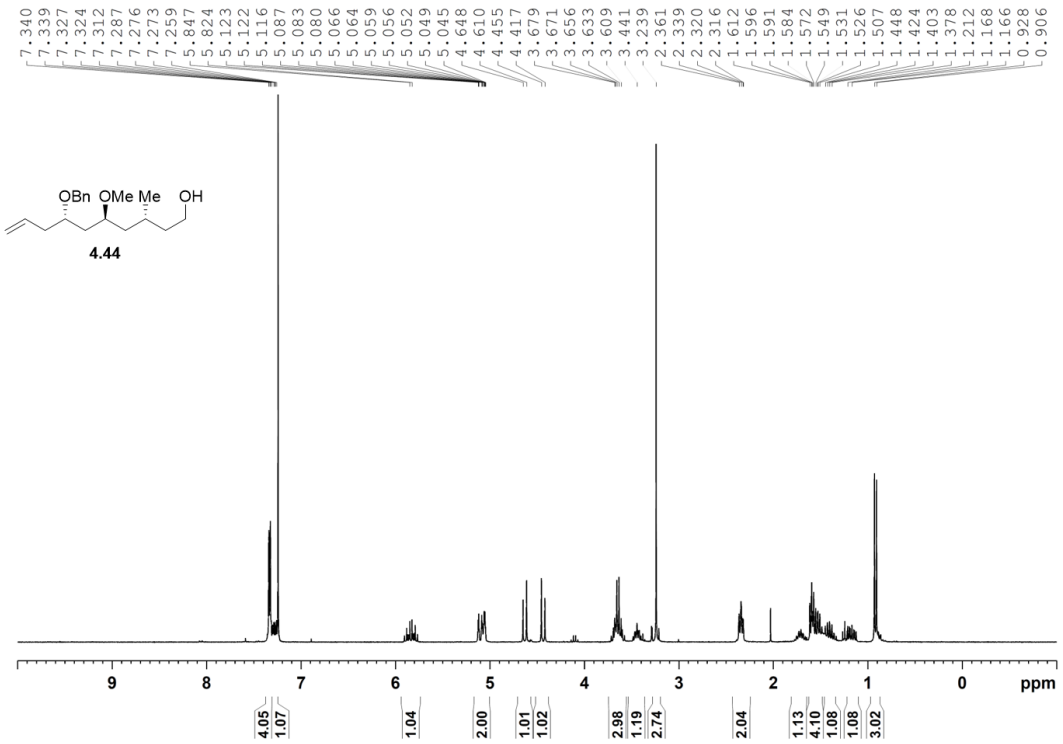

(3*R*,5*S*,7*S*)-7-Benzyloxy-5-methoxy-3-methyldec-9-en-1-ol (**4.44**)

^{13}C NMR (100 MHz, $CDCl_3$)

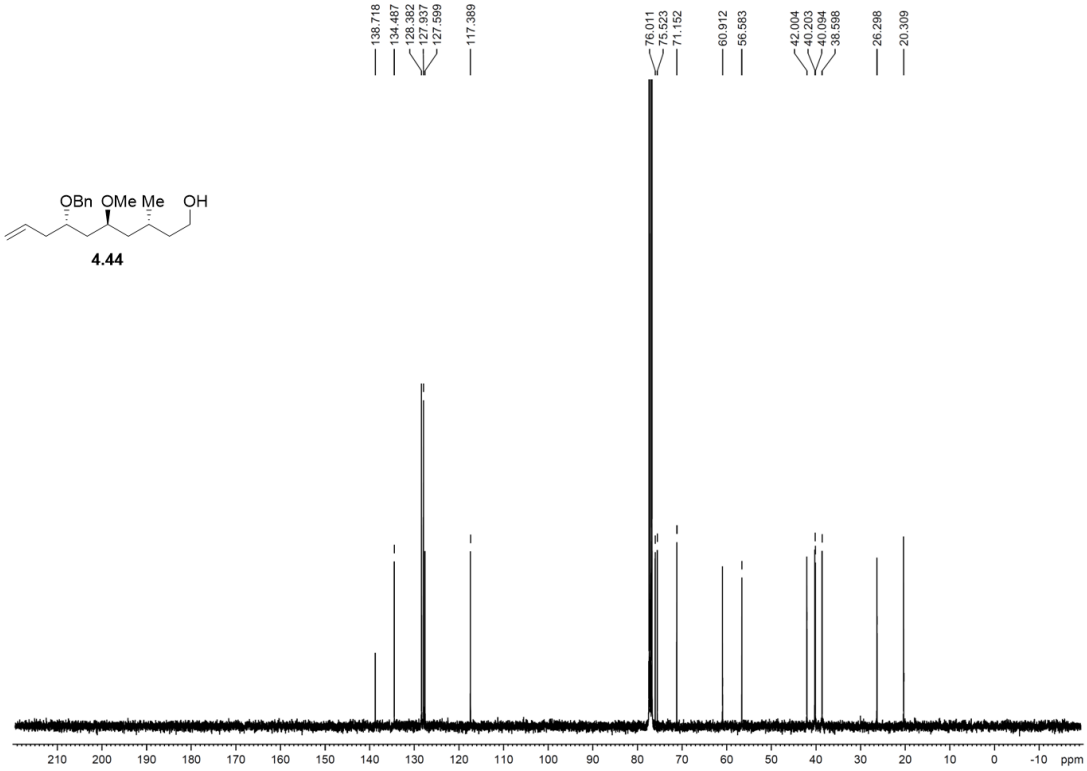

(3*R*,5*S*,7*S*)-7-Benzyloxy-5-methoxy-3-methyldec-9-en-1-ol (**4.44**)

COSY (400 MHz, $CDCl_3$)

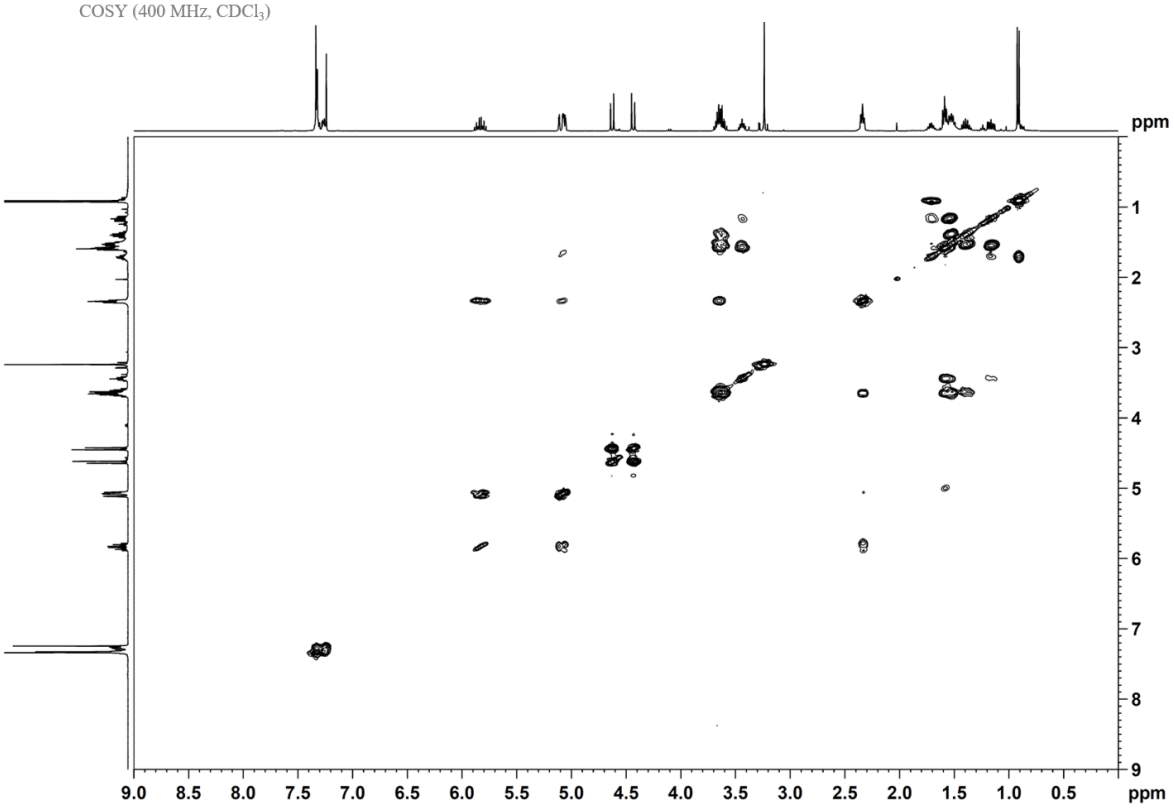

(3*R*,5*S*,7*S*)-7-Benzyloxy-5-methoxy-3-methyldec-9-en-1-ol (**4.44**)

HSQC (400 MHz, $CDCl_3$)

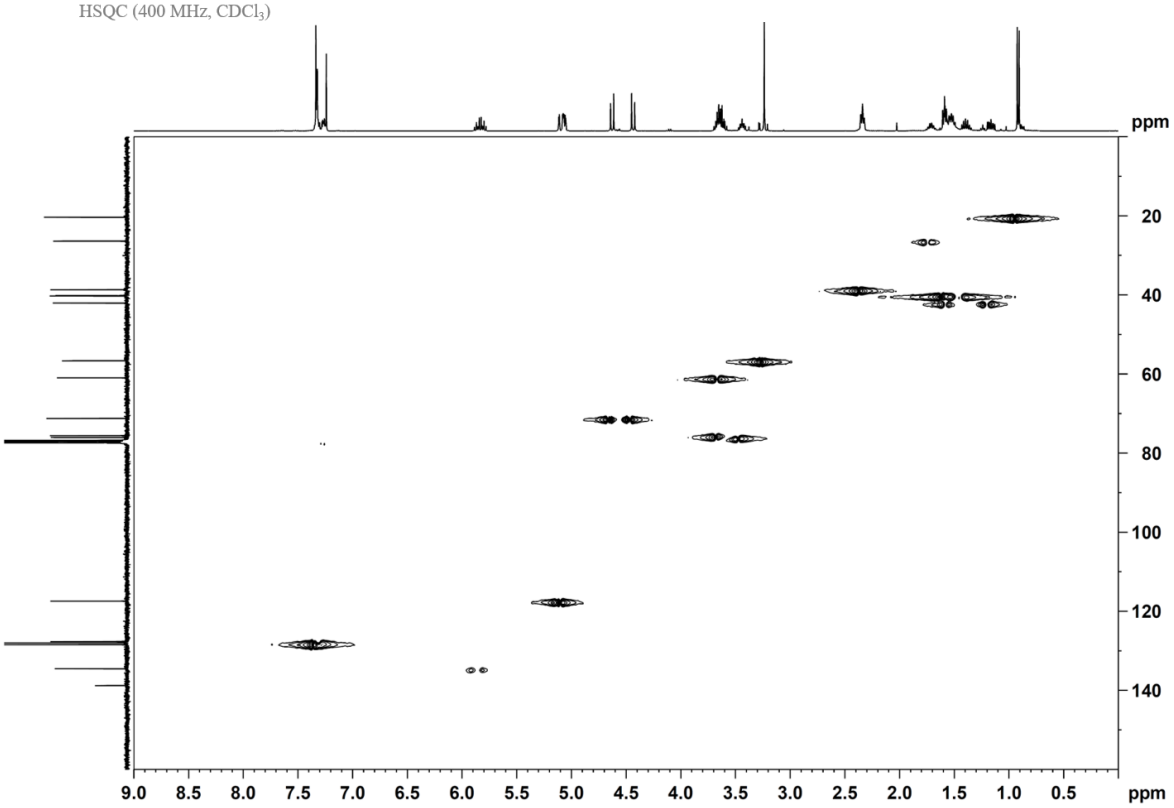

(3*S*,5*S*,7*S*)-7-Benzyloxy-5-methoxy-3-methyldec-9-enal (**4.45**)

^{1}H NMR (400 MHz, $CDCl_3$)

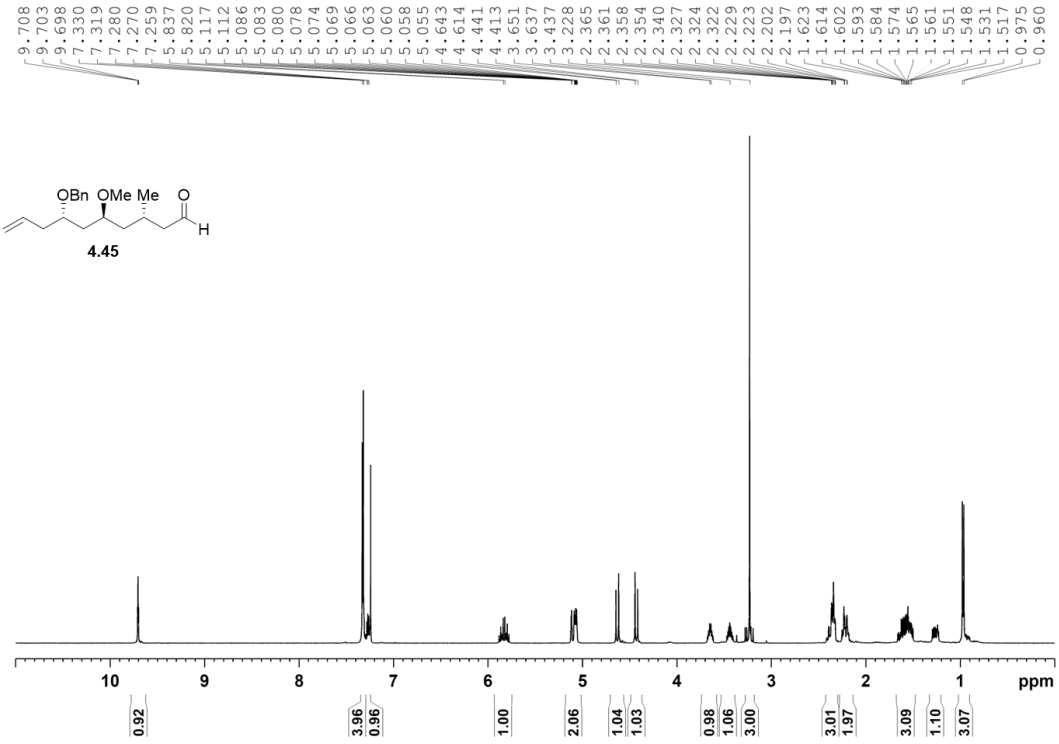

(3*S*,5*S*,7*S*)-7-Benzyloxy-5-methoxy-3-methyldec-9-enal (**4.45**)

^{13}C NMR (100 MHz, $CDCl_3$)

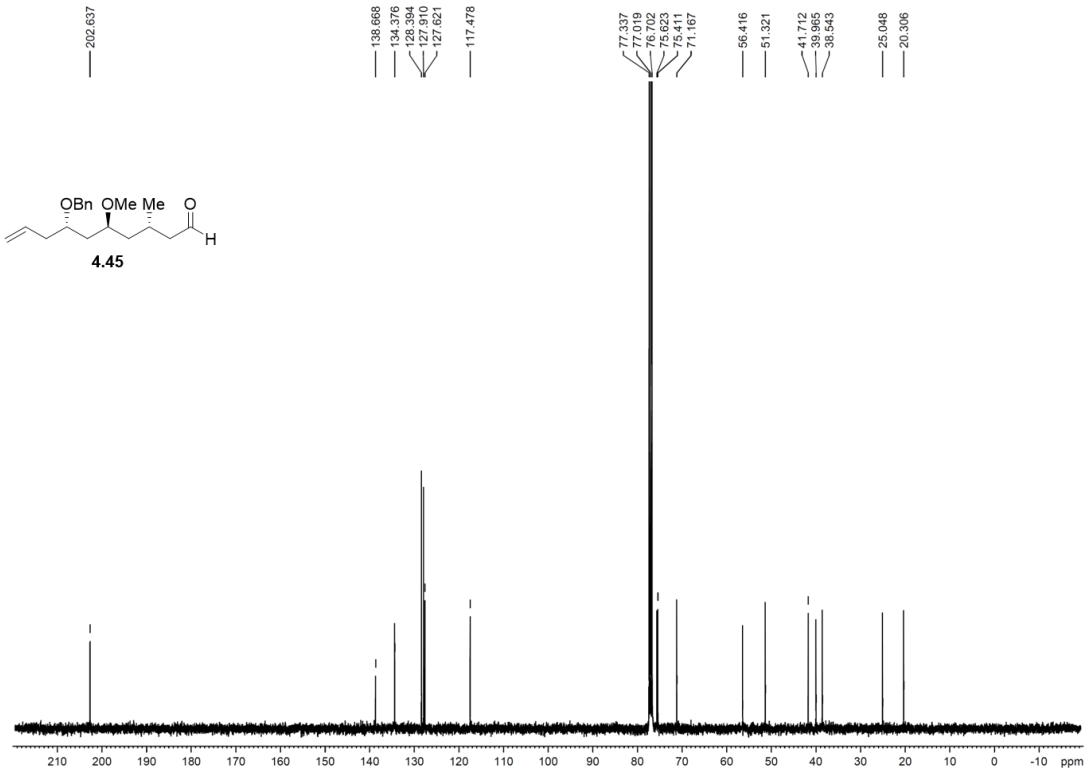

(3*S*,5*S*,7*S*)-7-Benzyloxy-5-methoxy-3-methyldec-9-enal (**4.45**)
COSY (400 MHz, $CDCl_3$)

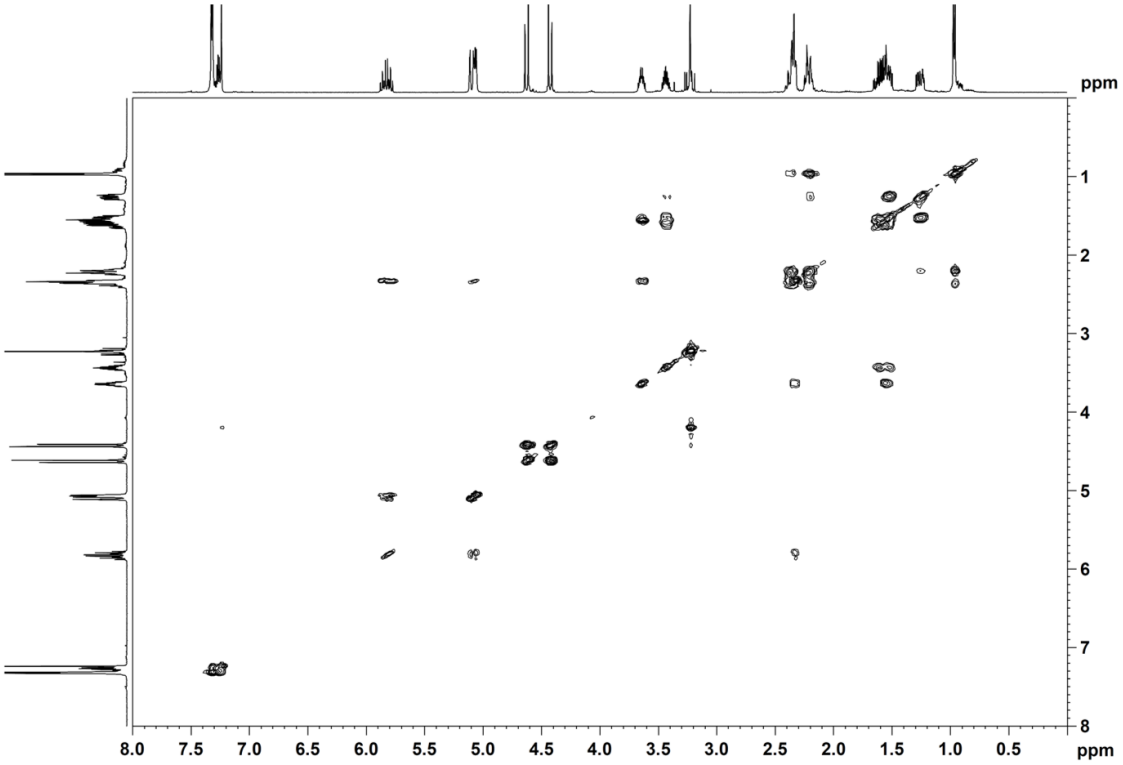

(3*S*,5*S*,7*S*)-7-Benzyloxy-5-methoxy-3-methyldec-9-enal (**4.45**)
HSQC (400 MHz, $CDCl_3$)

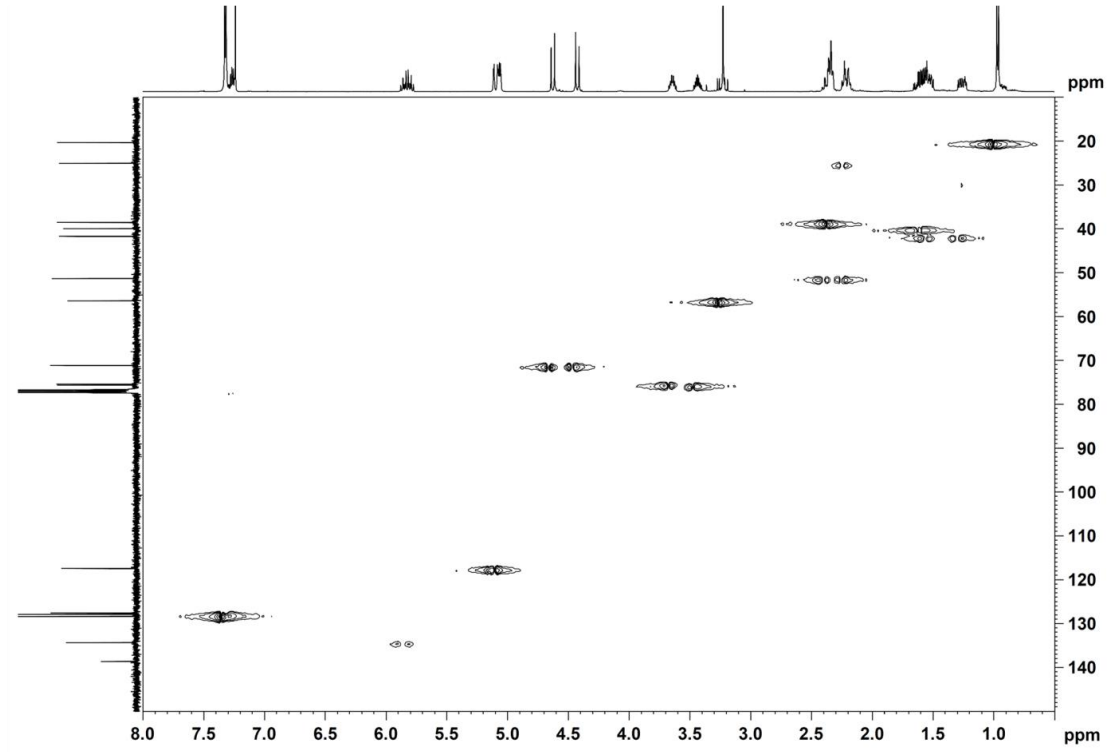

(3*S*,5*S*,7*S*)-7-Benzyloxy-5-methoxy-3-methyldecanal (**4.46**)

^{1}H NMR (300 MHz, $CDCl_3$)

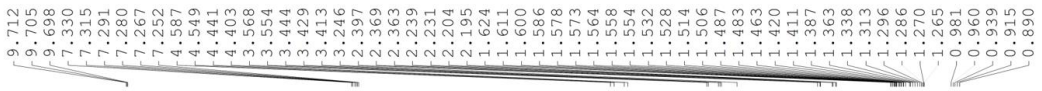

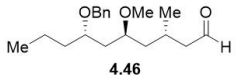

4.46

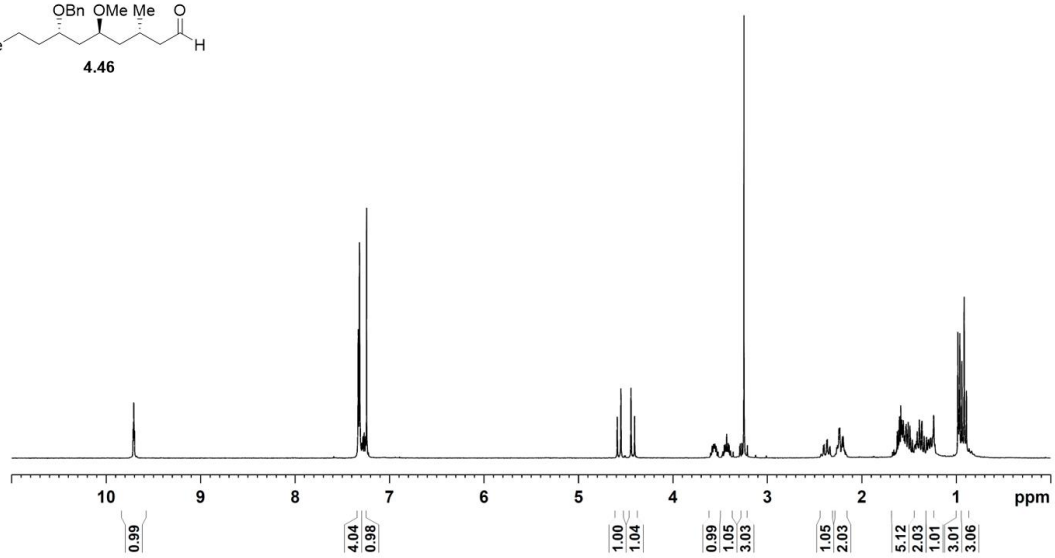

(3*S*,5*S*,7*S*)-7-Benzyloxy-5-methoxy-3-methyldecanal (**4.46**)

^{13}C NMR (75 MHz, $CDCl_3$)

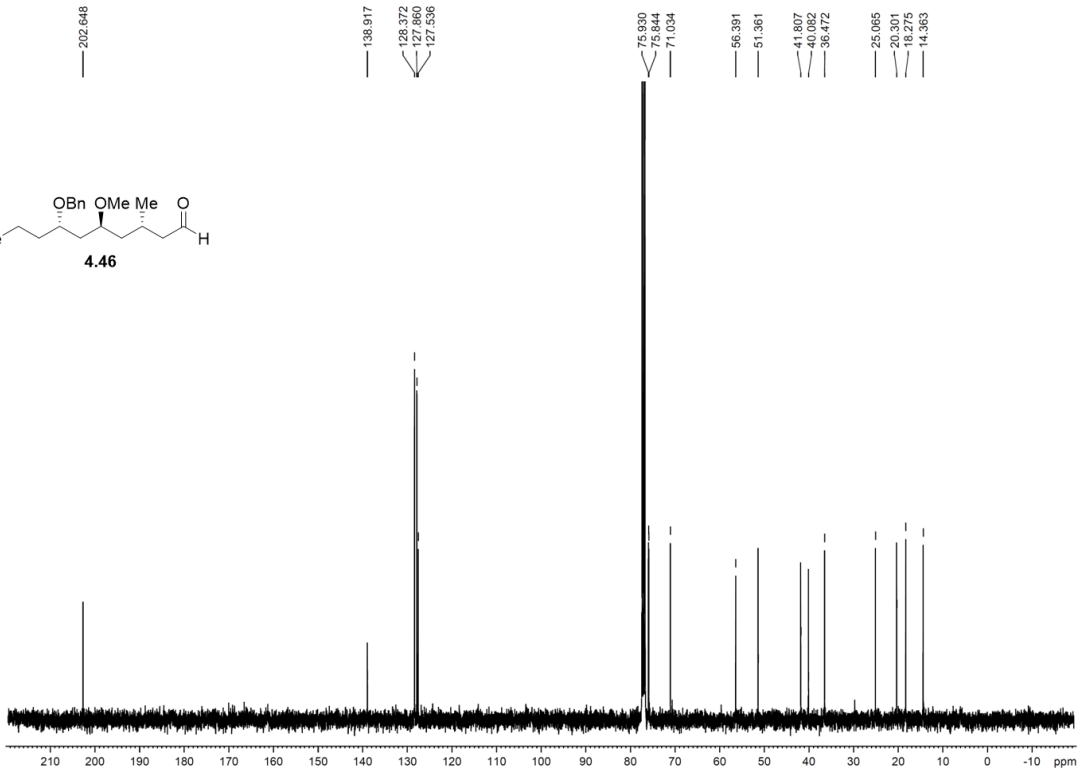

4.46

(3*S*,5*S*,7*S*)-7-Benzyloxy-5-methoxy-3-methyldecanal (**4.46**)

COSY (300 MHz, $CDCl_3$)

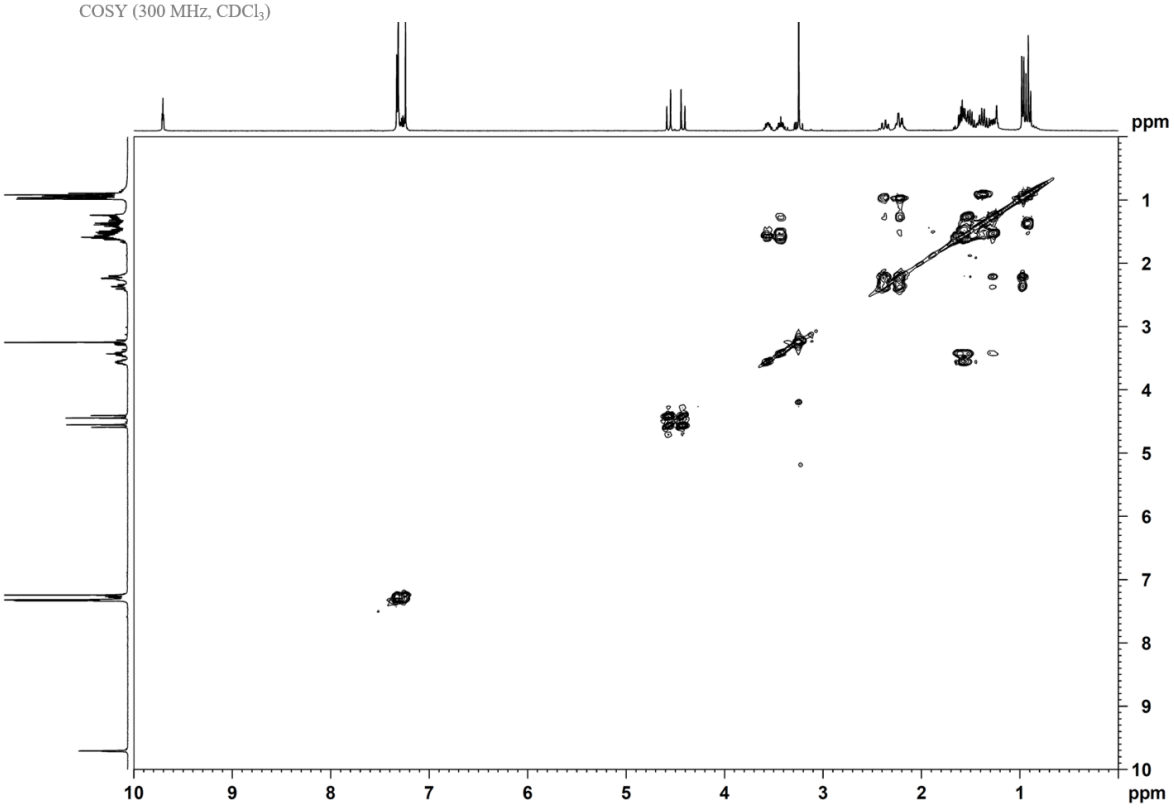

(3*S*,5*S*,7*S*)-7-Benzyloxy-5-methoxy-3-methyldecanal (**4.46**)

HSQC (300 MHz, $CDCl_3$)

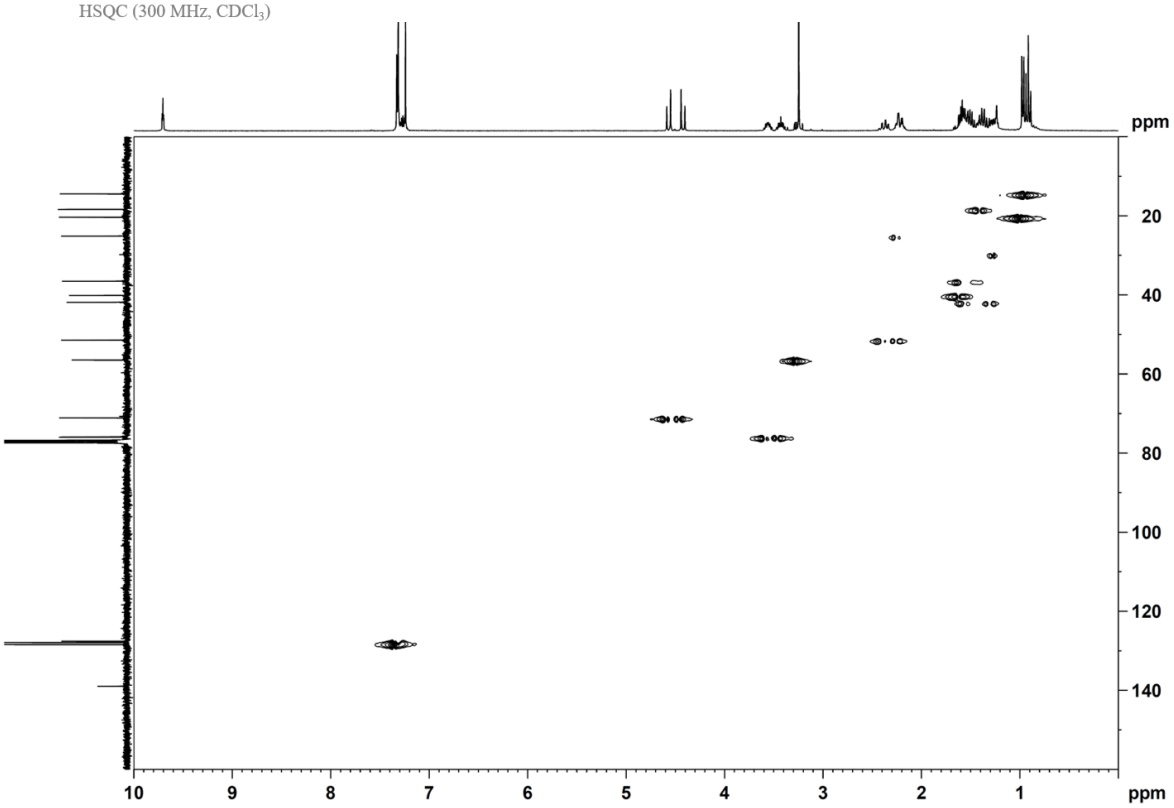

(3*S*,5*S*,7*S*)-7-Hydroxy-5-methoxy-3-methyldecanal (**4.25**)

^{1}H NMR (600 MHz, $CDCl_3$)

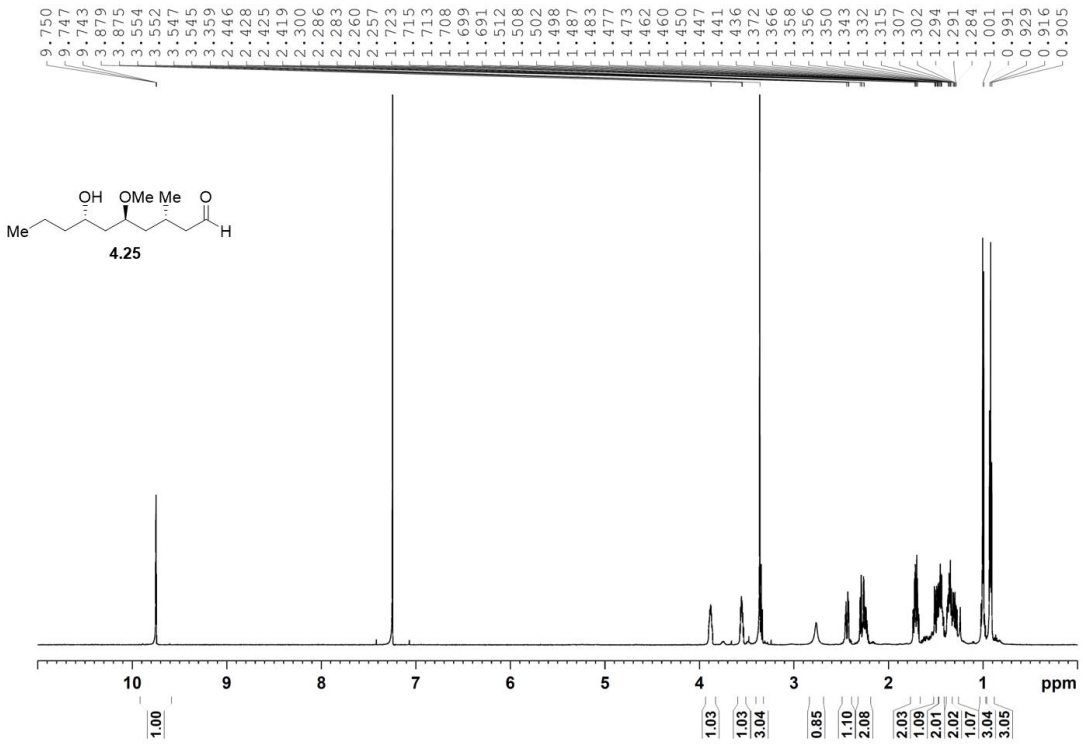

(3*S*,5*S*,7*S*)-7-Hydroxy-5-methoxy-3-methyldecanal (**4.25**)

^{13}C NMR (150 MHz, $CDCl_3$)

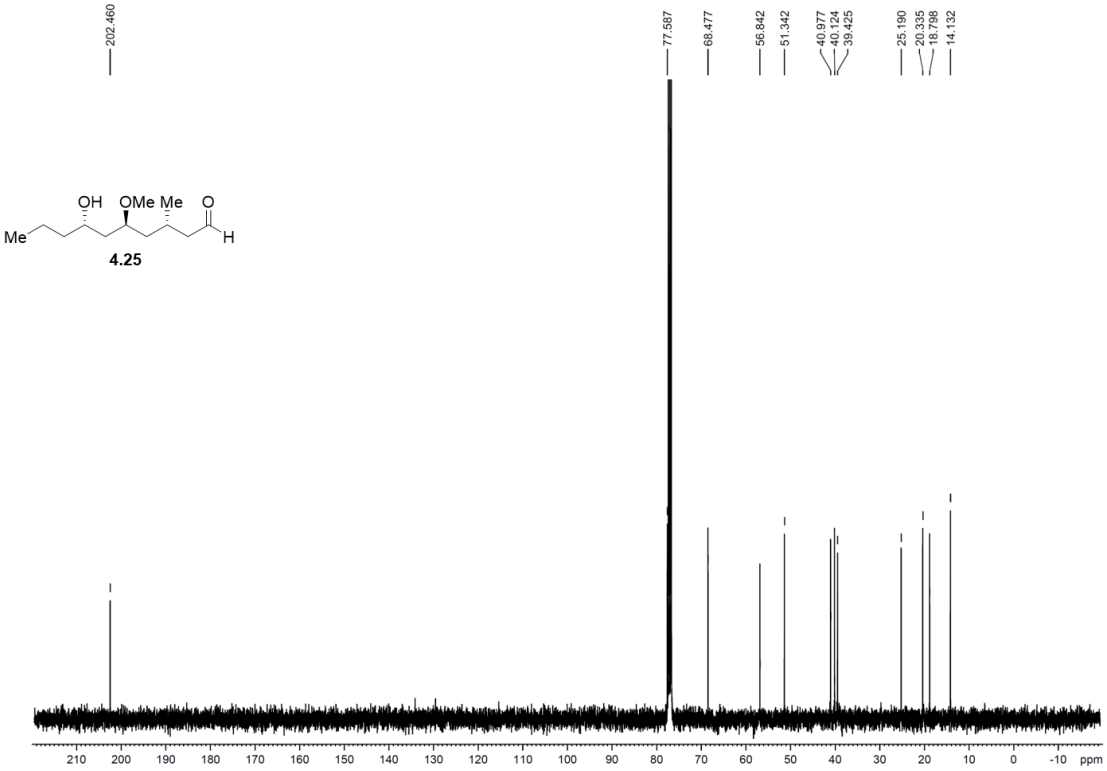

(3*S*,5*S*,7*S*)-7-Hydroxy-5-methoxy-3-methyldecanal (**4.25**)

COSY (600 MHz, $CDCl_3$)

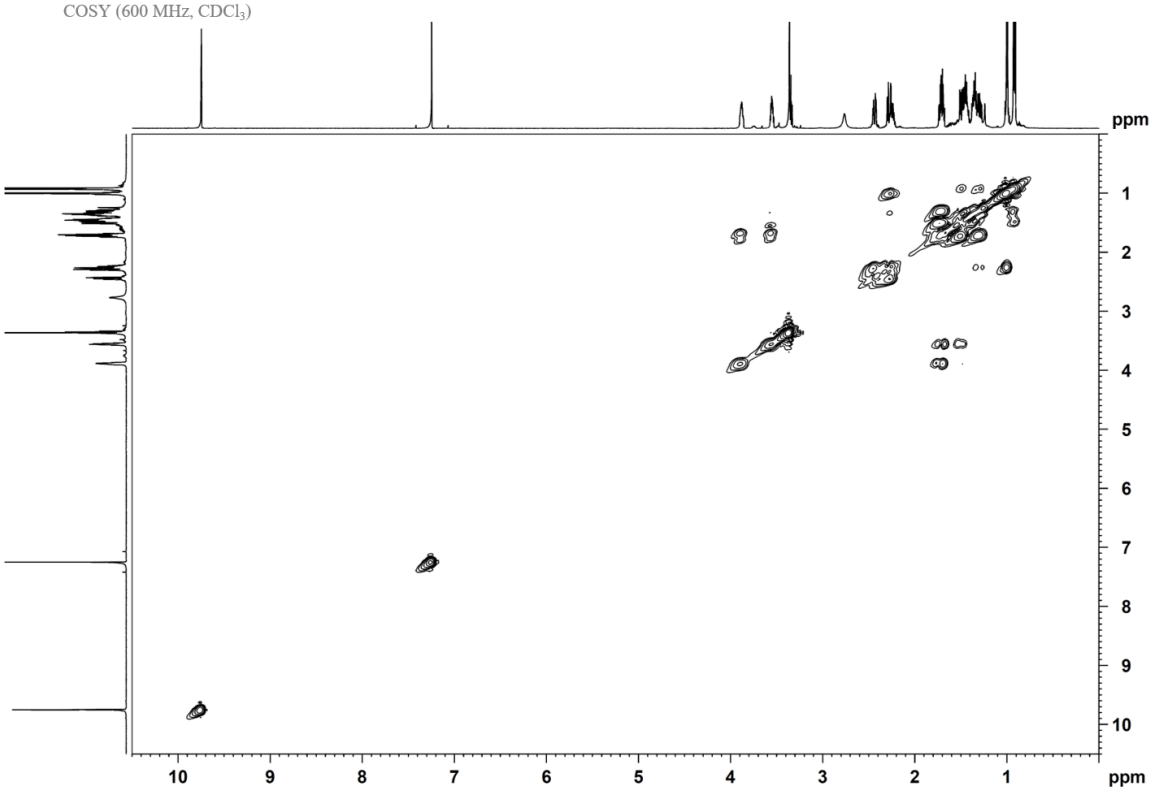

(3*S*,5*S*,7*S*)-7-Hydroxy-5-methoxy-3-methyldecanal (**4.25**)

HSQC (600 MHz, $CDCl_3$)

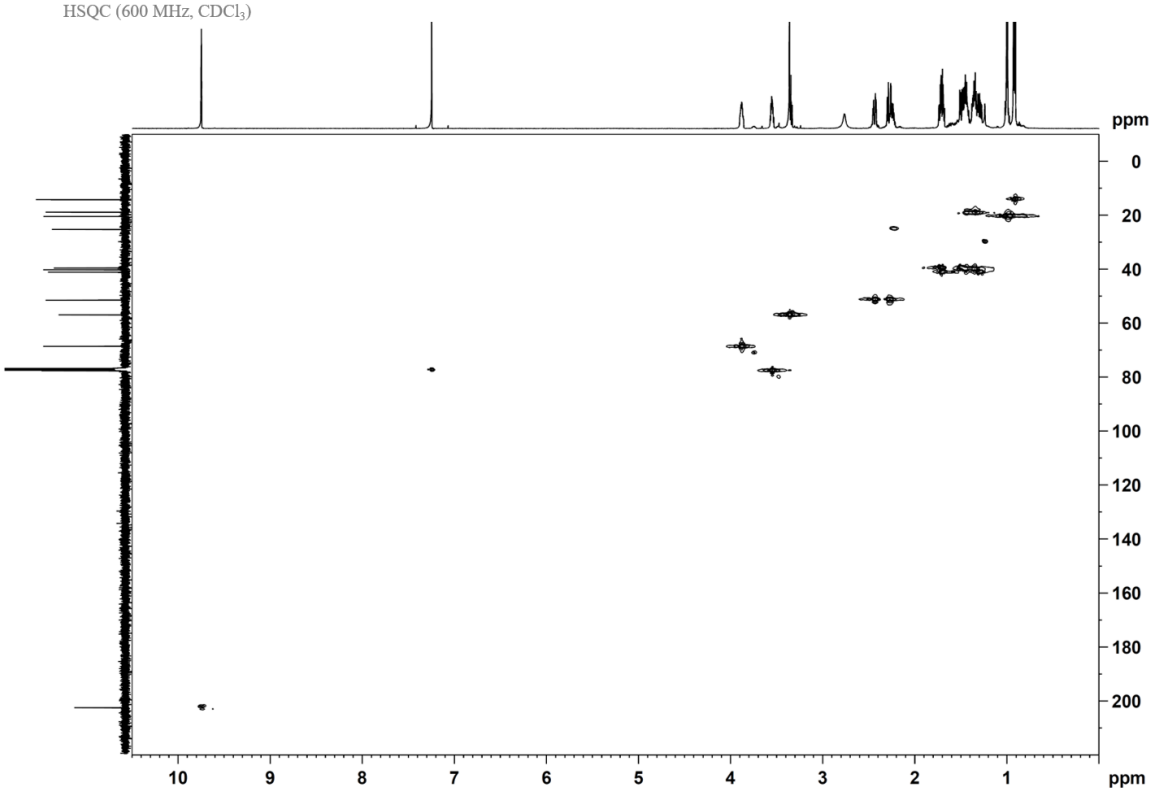

(*9R,11S,13S*)-(*E*)-Methyl-3-(*tert*-butyldimethylsilyloxy)-13-hydroxy-11-methoxy-9-methyl-5-oxohexadec-6-enoate (**4.51**)

^{1}H NMR (400 MHz, $CDCl_3$)

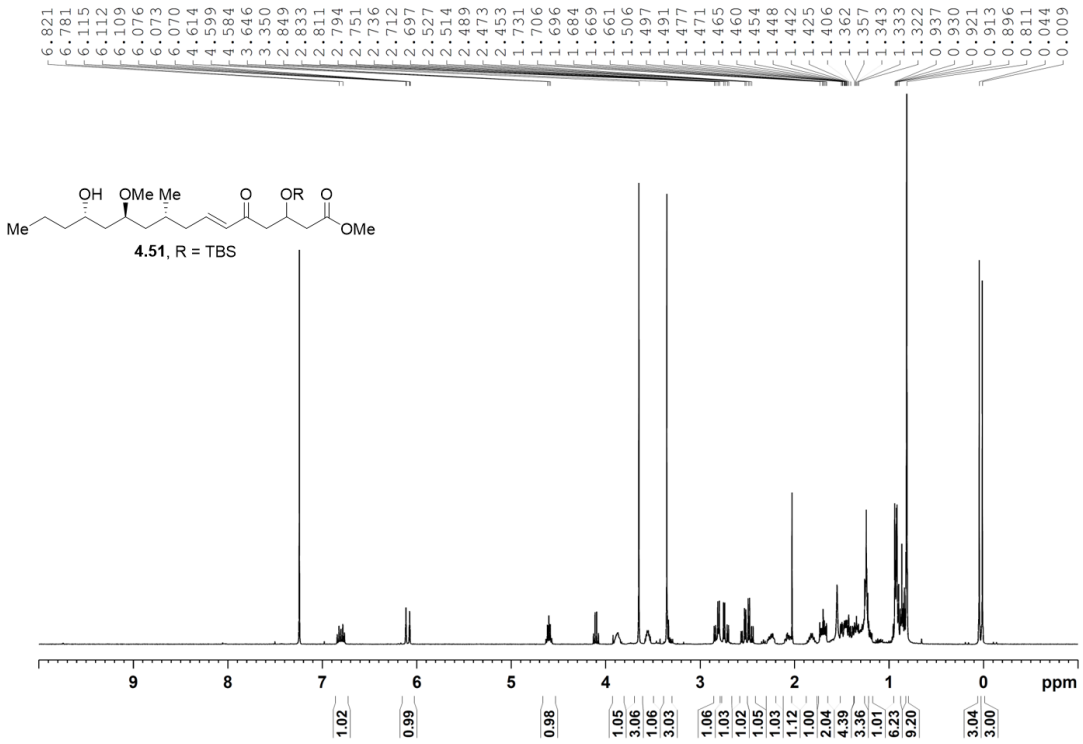

(*9R,11S,13S*)-(*E*)-Methyl-3-(*tert*-butyldimethylsilyloxy)-13-hydroxy-11-methoxy-9-methyl-5-oxohexadec-6-enoate (**4.51**)

^{13}C NMR (100 MHz, $CDCl_3$)

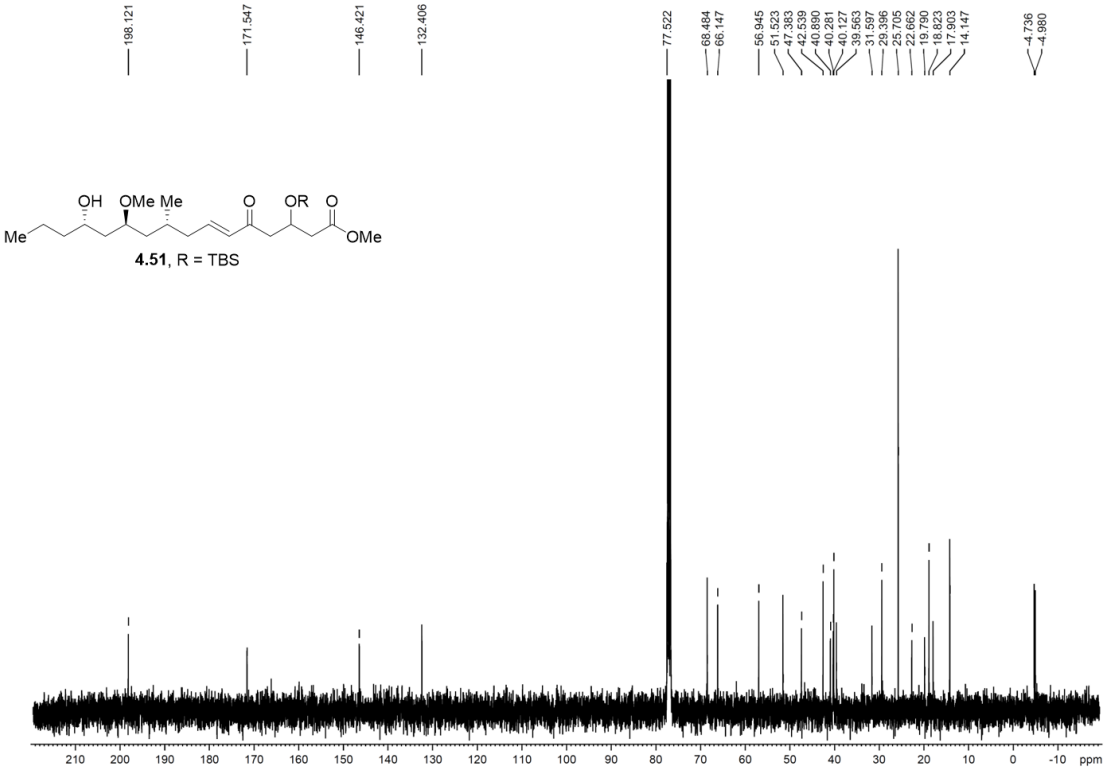

(*9R,11S,13S*)-(*E*)-Methyl-3-(*tert*-butyldimethylsilyloxy)-13-hydroxy-11-methoxy-9-methyl-5-oxohexadec-6-enoate (**4.51**)

COSY (400 MHz, $CDCl_3$)

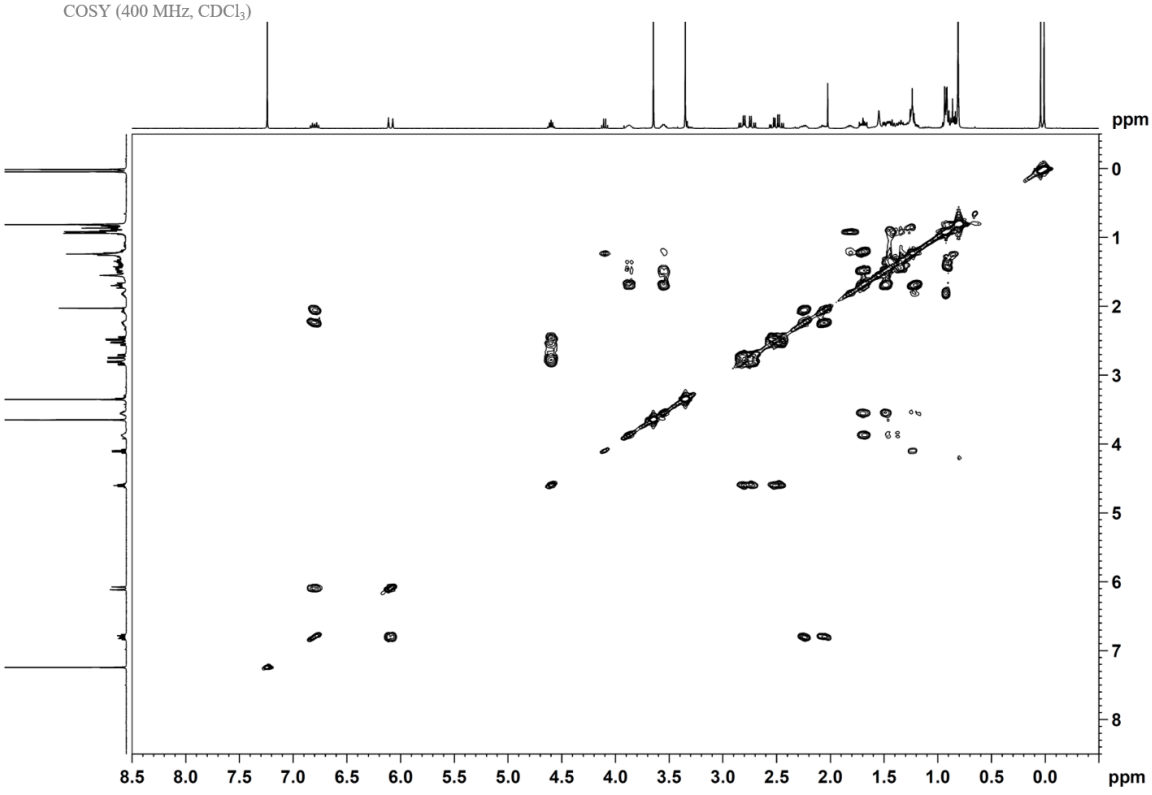

(*9R,11S,13S*)-(*E*)-Methyl-3-(*tert*-butyldimethylsilyloxy)-13-hydroxy-11-methoxy-9-methyl-5-oxohexadec-6-enoate (**4.51**)

HSQC (400 MHz, $CDCl_3$)

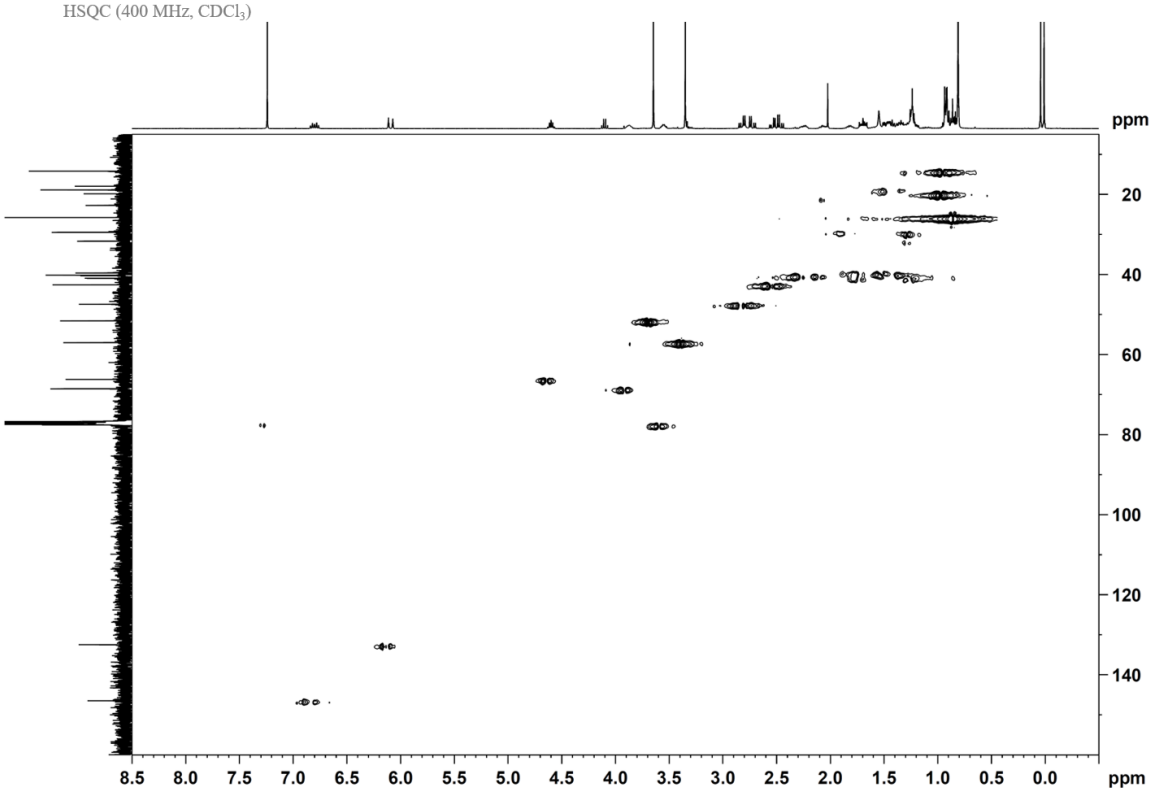

S1.3.4 Alternative C1-C6 Phosphonate Fragments & HWE Olefination Screening (§ 4.4.4/4.4.5)

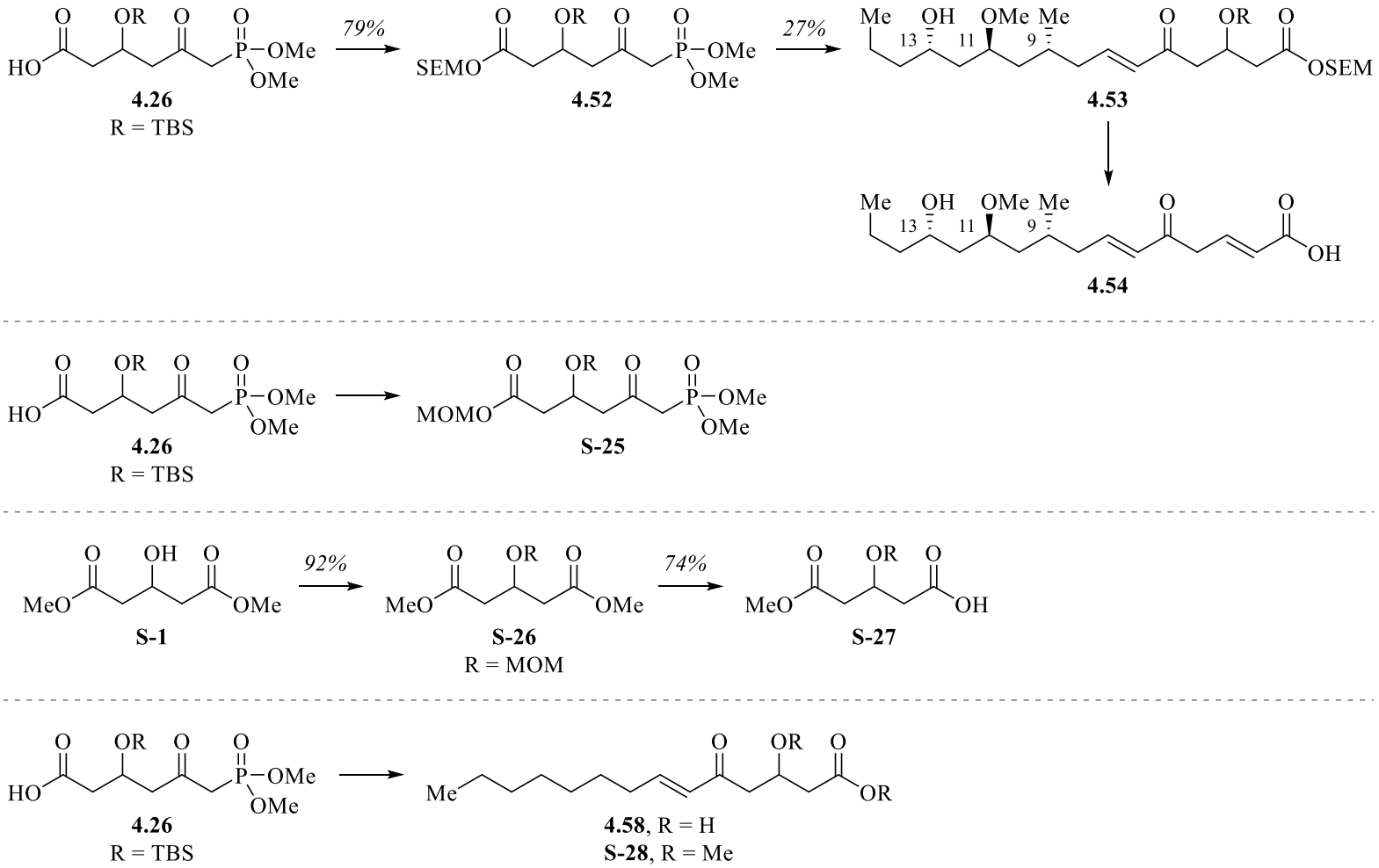

Figure S9 – Selection of alternative C1-C6 phosphonate fragment and HWE screening reactions.

3-(*tert*-Butyldimethylsilyloxy)-5-oxo-5-((2-(trimethylsilyl)ethoxy)methoxy)pentanoic acid (**4.52**)

^{1}H NMR (400 MHz, $CDCl_3$)

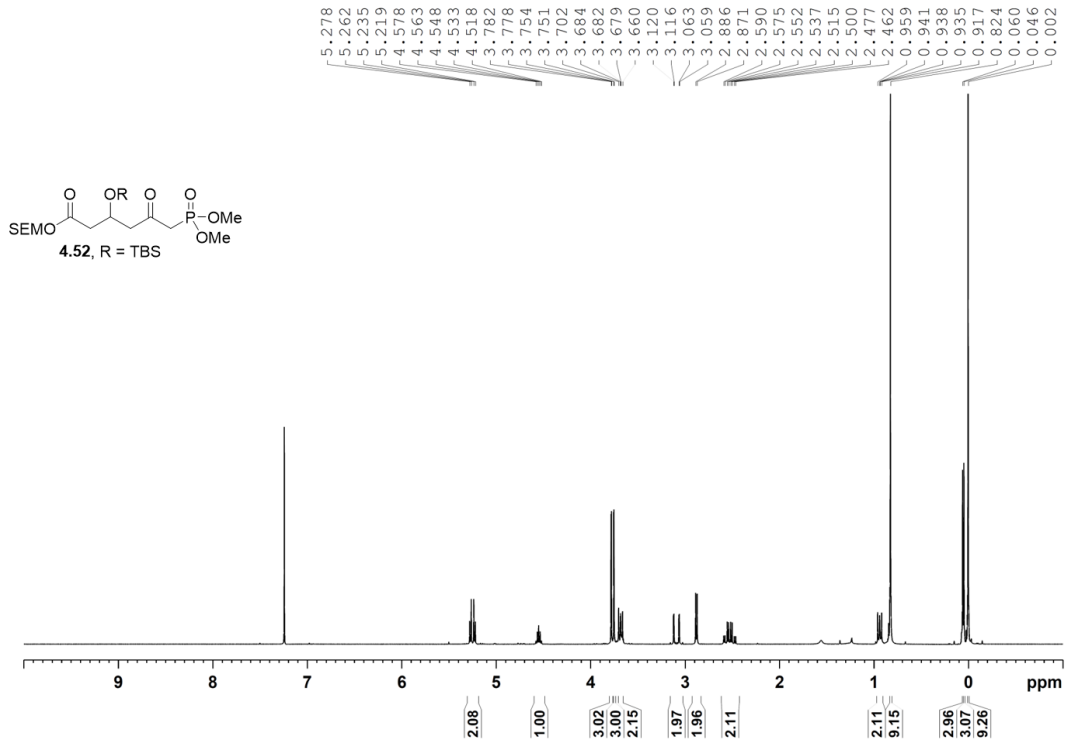

3-(*tert*-Butyldimethylsilyloxy)-5-oxo-5-((2-(trimethylsilyl)ethoxy)methoxy)pentanoic acid (**4.52**)

^{13}C NMR (100 MHz, $CDCl_3$)

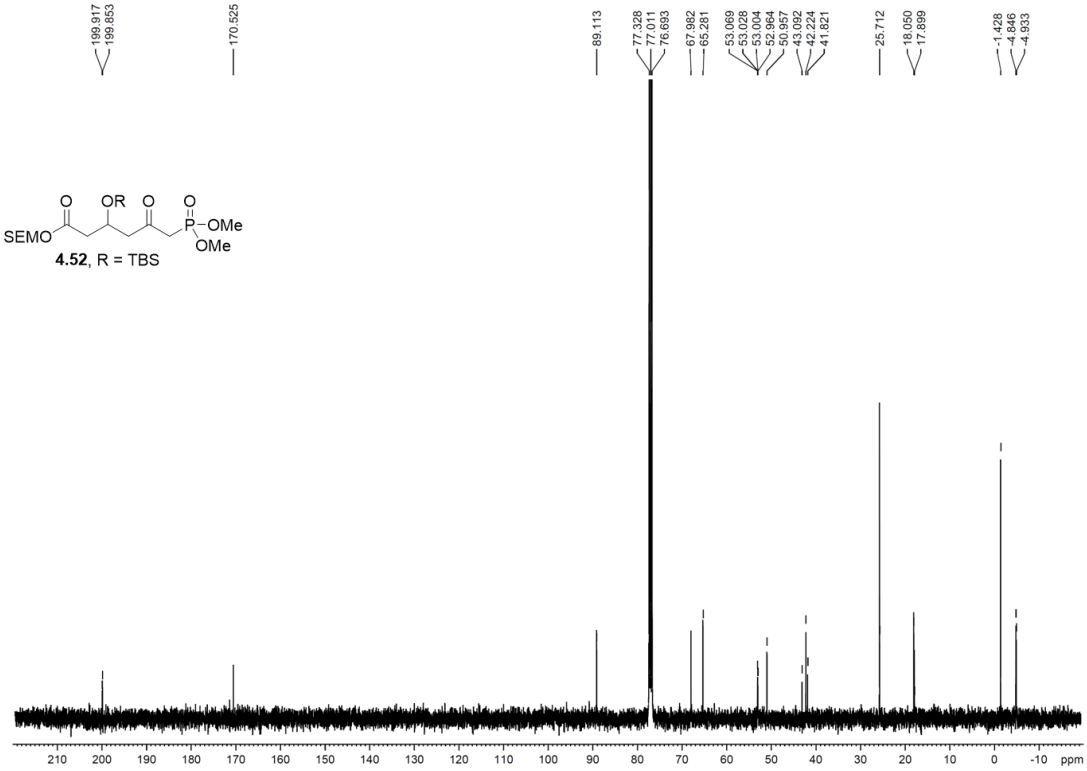

3-(*tert*-Butyldimethylsilyloxy)-5-oxo-5-((2-(trimethylsilyl)ethoxy)methoxy)pentanoic acid (**4.52**)
COSY (400 MHz, $CDCl_3$)

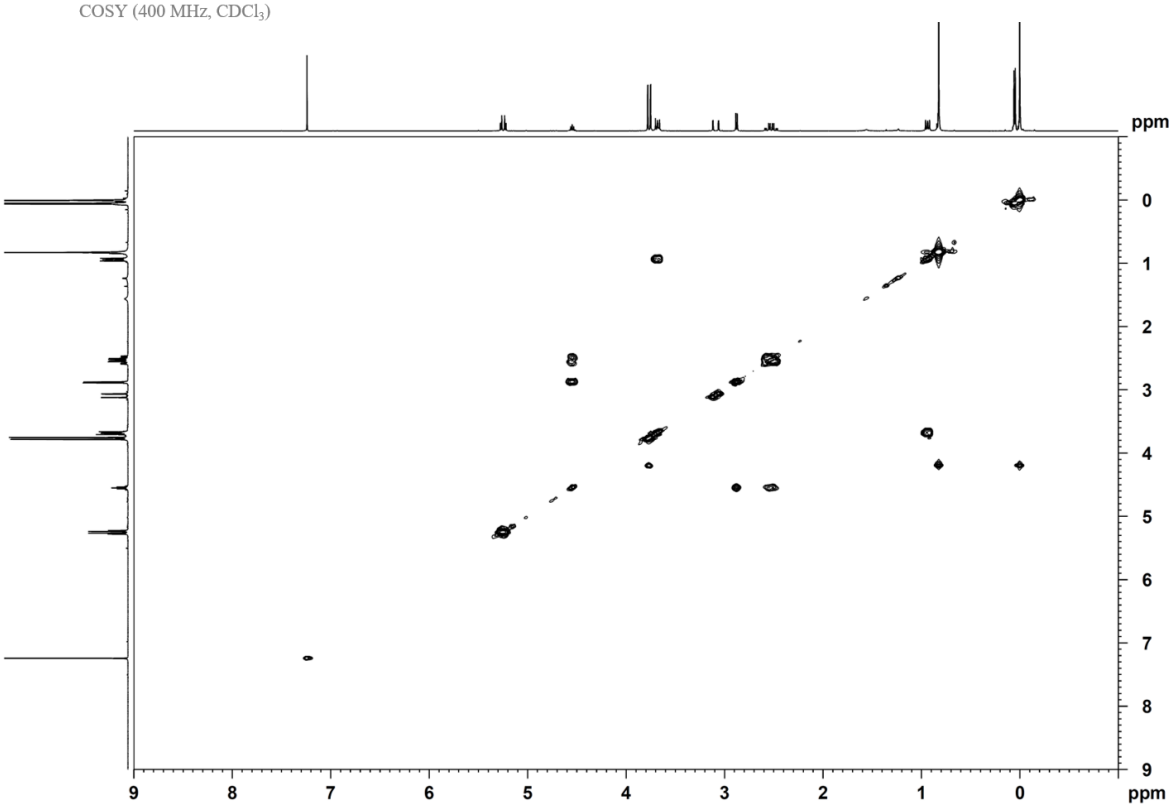

3-(*tert*-Butyldimethylsilyloxy)-5-oxo-5-((2-(trimethylsilyl)ethoxy)methoxy)pentanoic acid (**4.52**)
HSQC (400 MHz, $CDCl_3$)

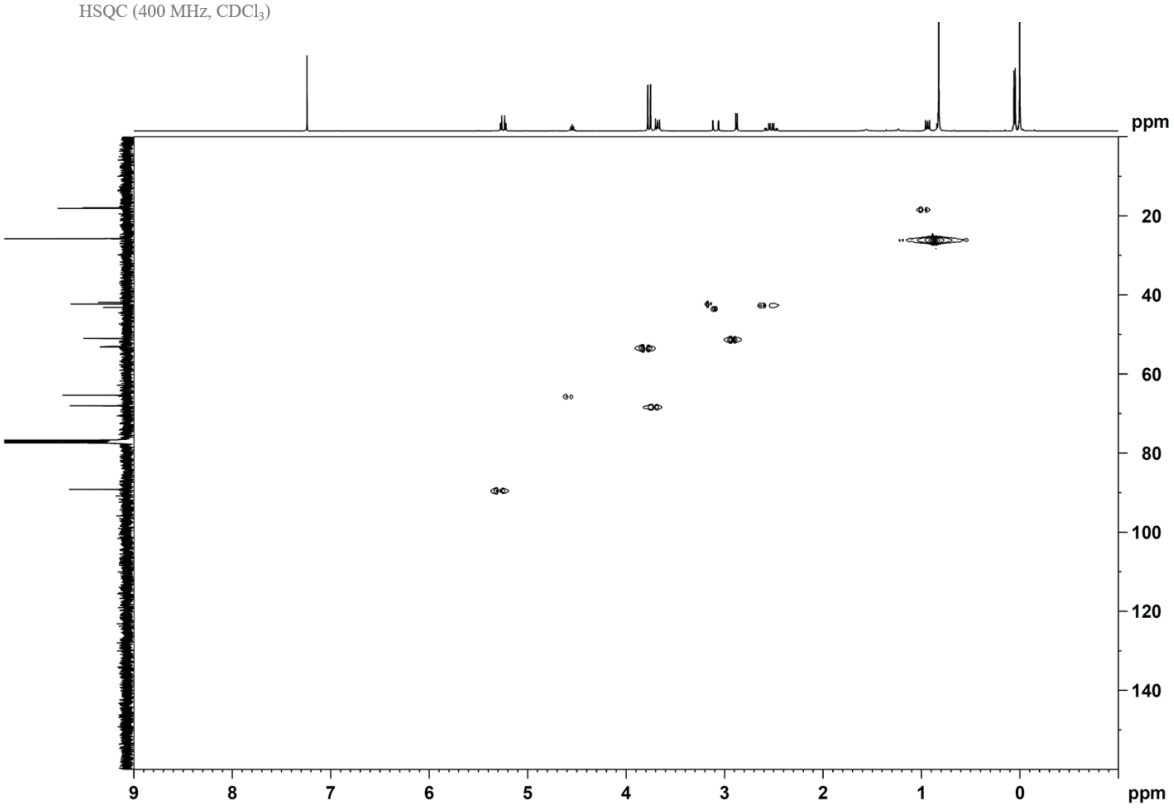

3-(*tert*-Butyldimethylsilyloxy)-5-oxo-5-((2-(trimethylsilyl)ethoxy)methoxy)pentanoic acid (**4.52**)

^{31}P NMR (162 MHz, $CDCl_3$)

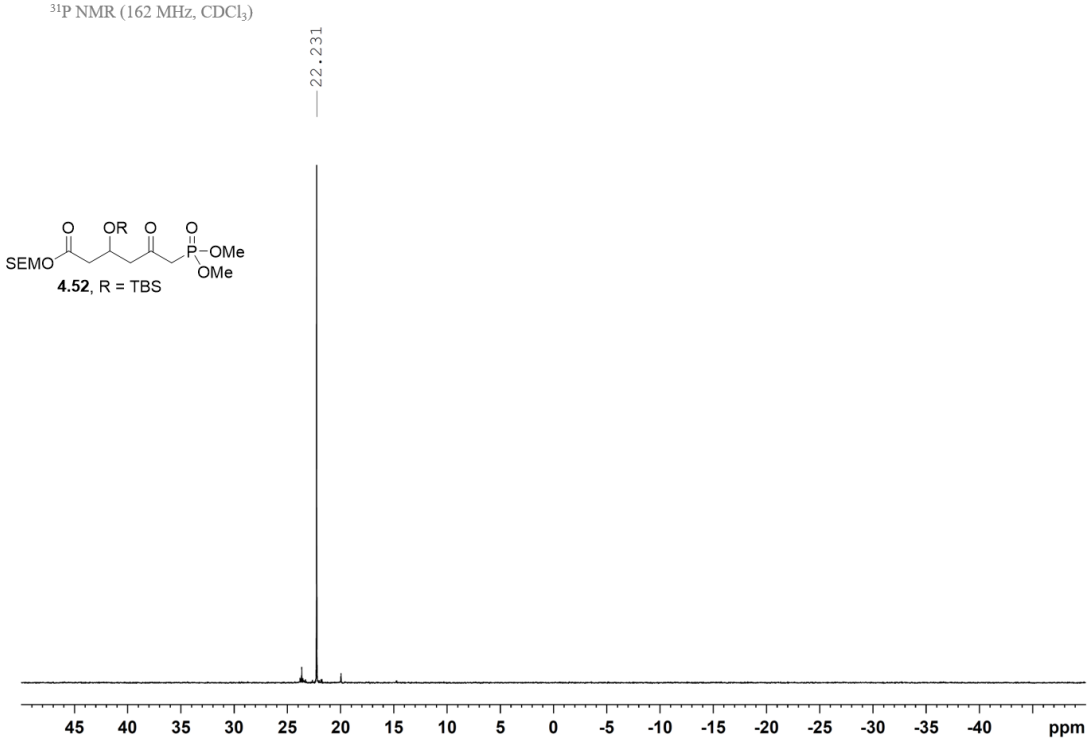

(2-(trimethylsilyl)ethoxy)methyl-(9*R*,11*S*,13*S*)-(*E*)-3-TBS-13-hydroxy-11-methoxy-9-methyl-5-oxohexadec-6-enoate (**4.53**)

^{1}H NMR (400 MHz, $CDCl_3$)

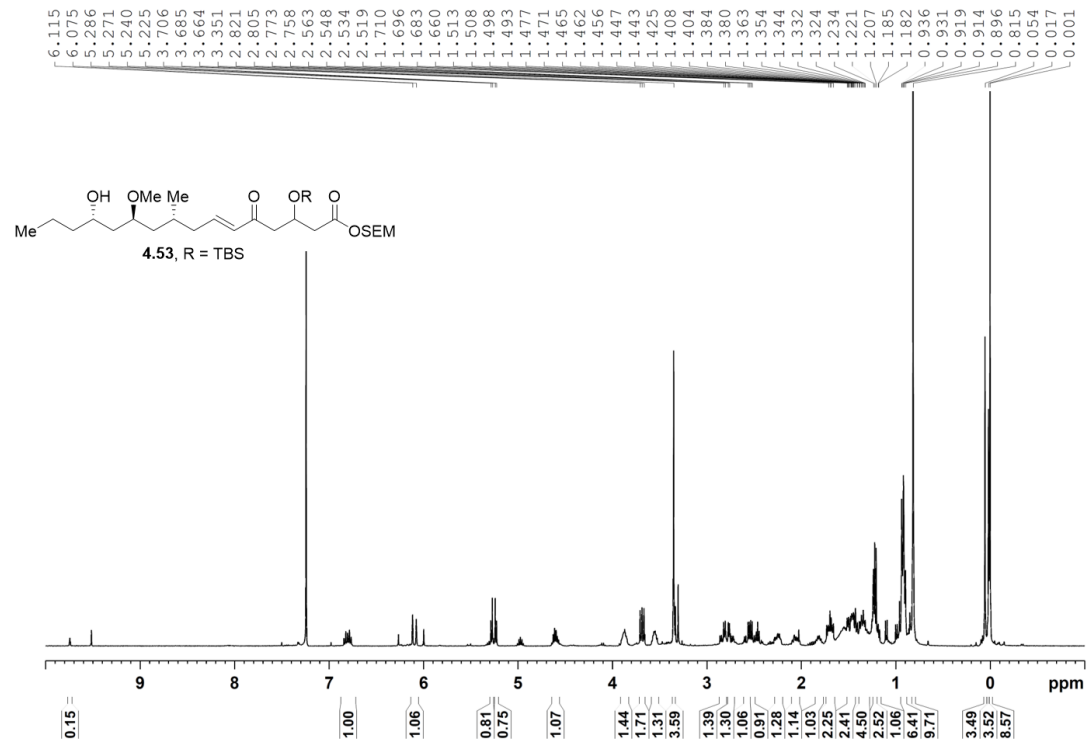

(2-(trimethylsilyl)ethoxy)methyl-(9*R*,11*S*,13*S*)-(*E*)-3-TBS-13-hydroxy-11-methoxy-9-methyl-5-oxohexadec-6-enoate (**4.53**)

^{13}C NMR (100 MHz, $CDCl_3$)

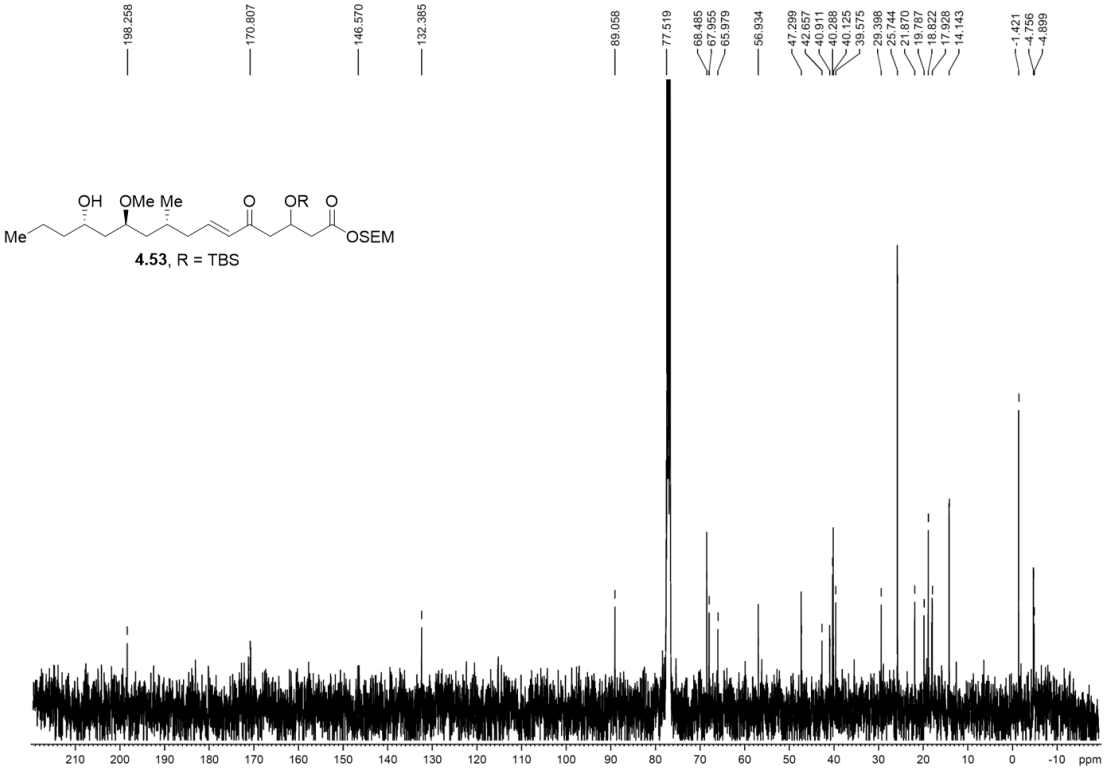

(2-(trimethylsilyl)ethoxy)methyl-(9*R*,11*S*,13*S*)-(*E*)-3-TBS-13-hydroxy-11-methoxy-9-methyl-5-oxohexadec-6-enoate (**4.53**)

COSY (400 MHz, $CDCl_3$)

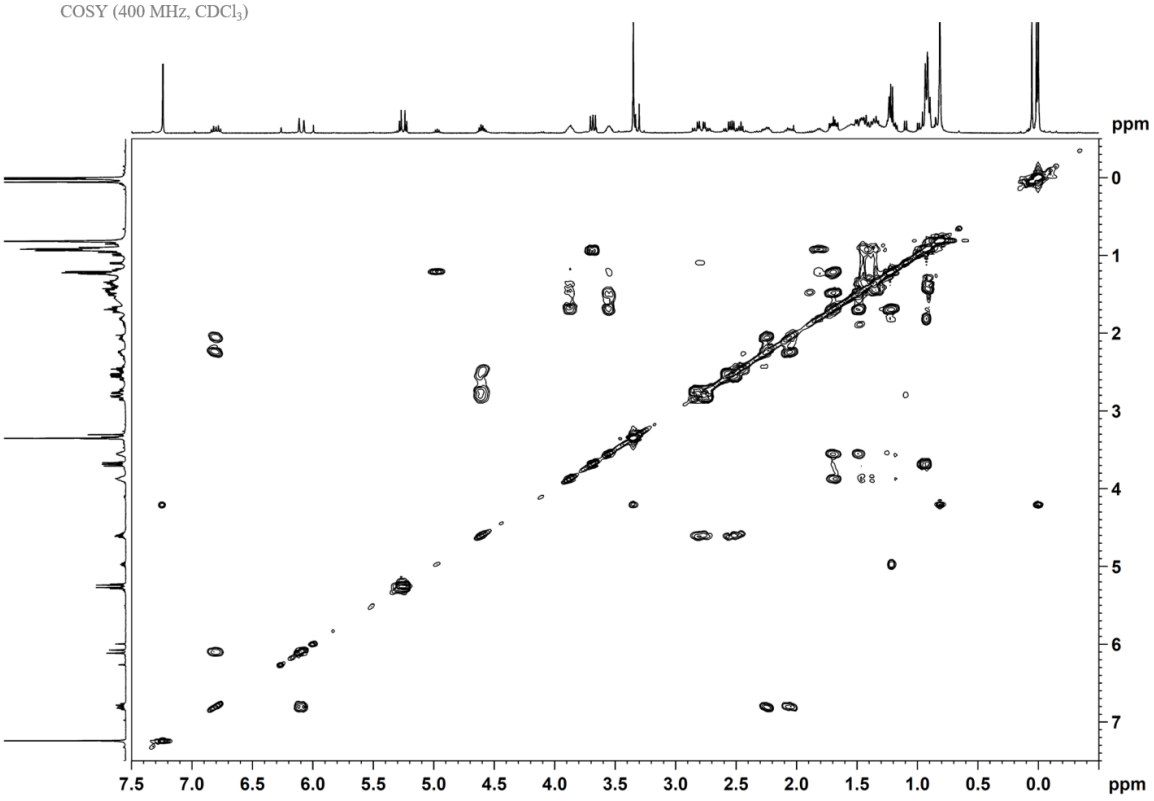

(2*E*,6*E*,9*R*,11*S*,13*S*)-13-Hydroxy-11-methoxy-9-methyl-5-oxohexadec-2,6-enoic acid (**4.54**)

^{1}H NMR (400 MHz, $CDCl_3$)

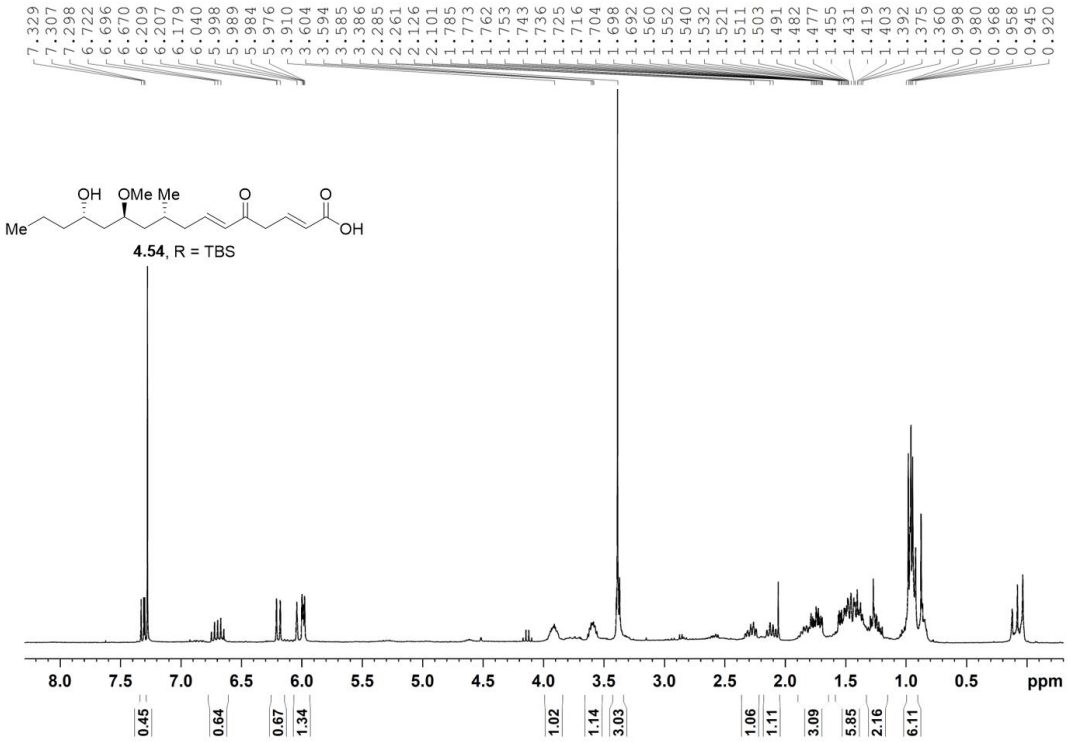

(2*E*,6*E*,9*R*,11*S*,13*S*)-13-Hydroxy-11-methoxy-9-methyl-5-oxohexadec-2,6-enoic acid (**4.54**)

COSY (400 MHz, $CDCl_3$)

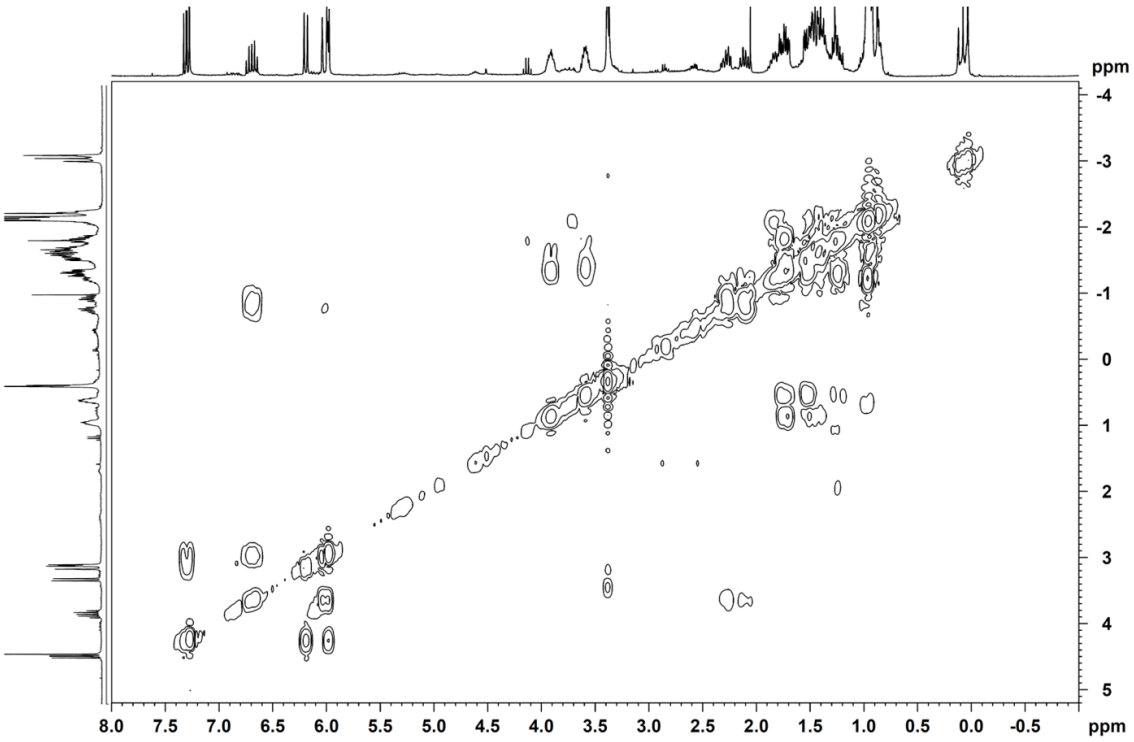

3-(*tert*-Butyldimethylsilyloxy)-5-(methoxymethoxy)-5-oxopentanoic acid (**S-25**)

^{1}H NMR (400 MHz, $CDCl_3$)

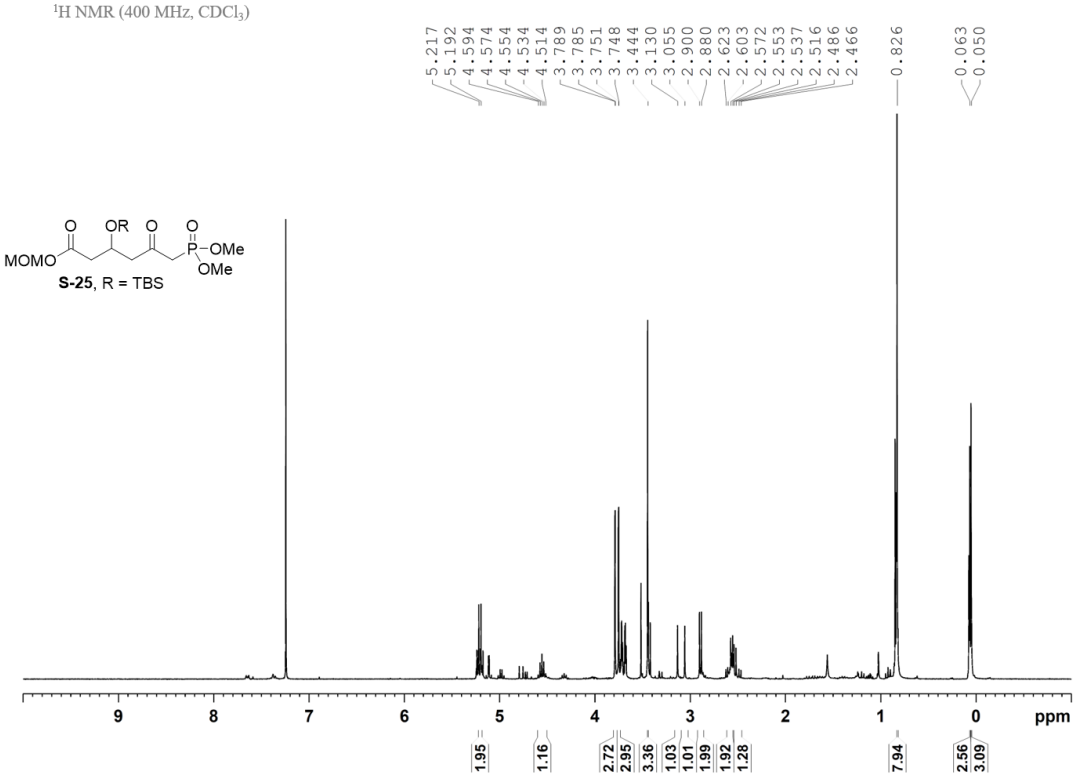

Dimethyl 3-(methoxymethoxy)pentanedioate (**S-26**)

^{1}H NMR (400 MHz, $CDCl_3$)

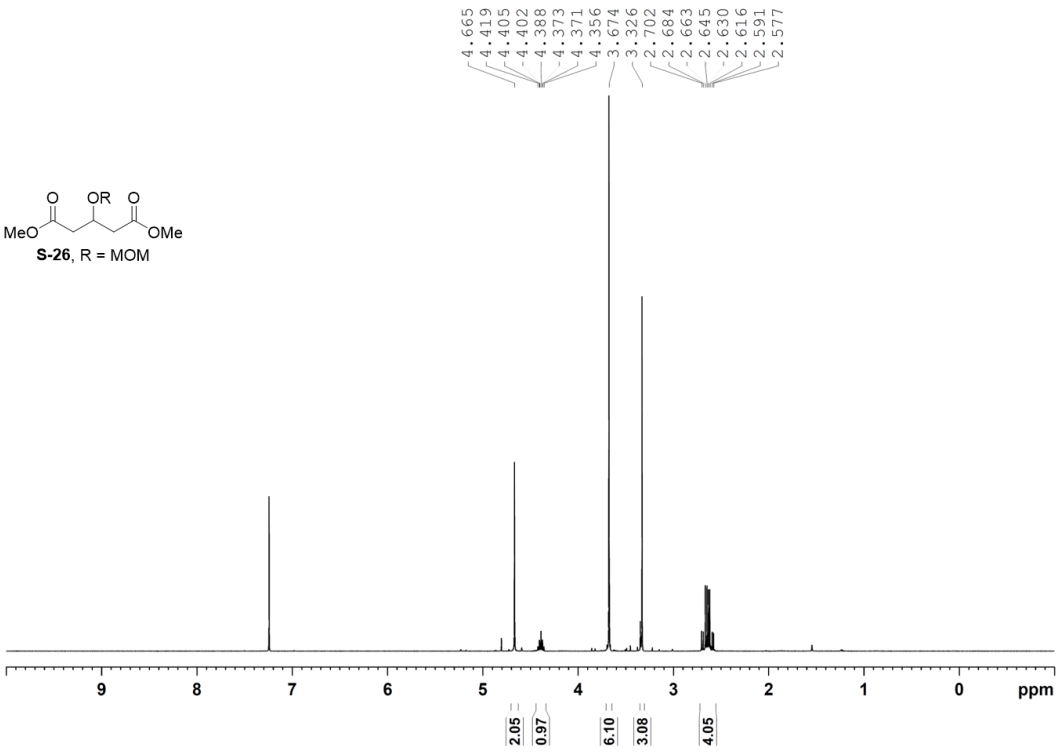

Dimethyl 3-(methoxymethoxy)pentanedioate (**S-26**)

^{13}C NMR (100 MHz, $CDCl_3$)

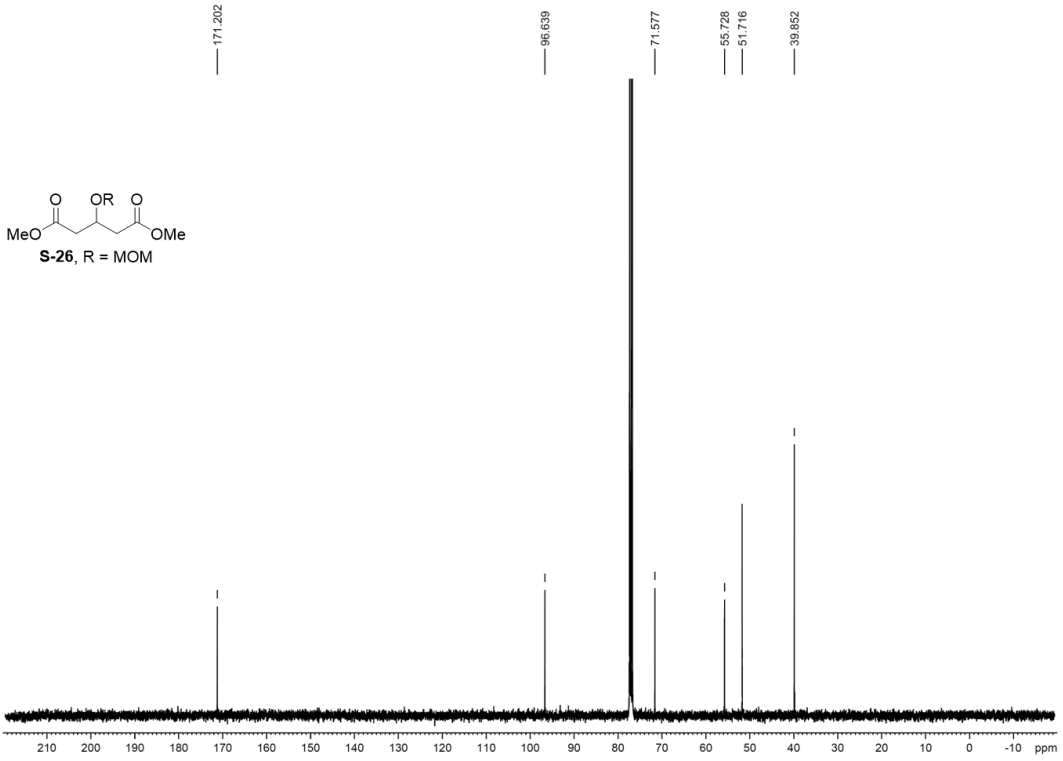

Dimethyl 3-(methoxymethoxy)pentanedioate (**S-26**)

COSY (400 MHz, $CDCl_3$)

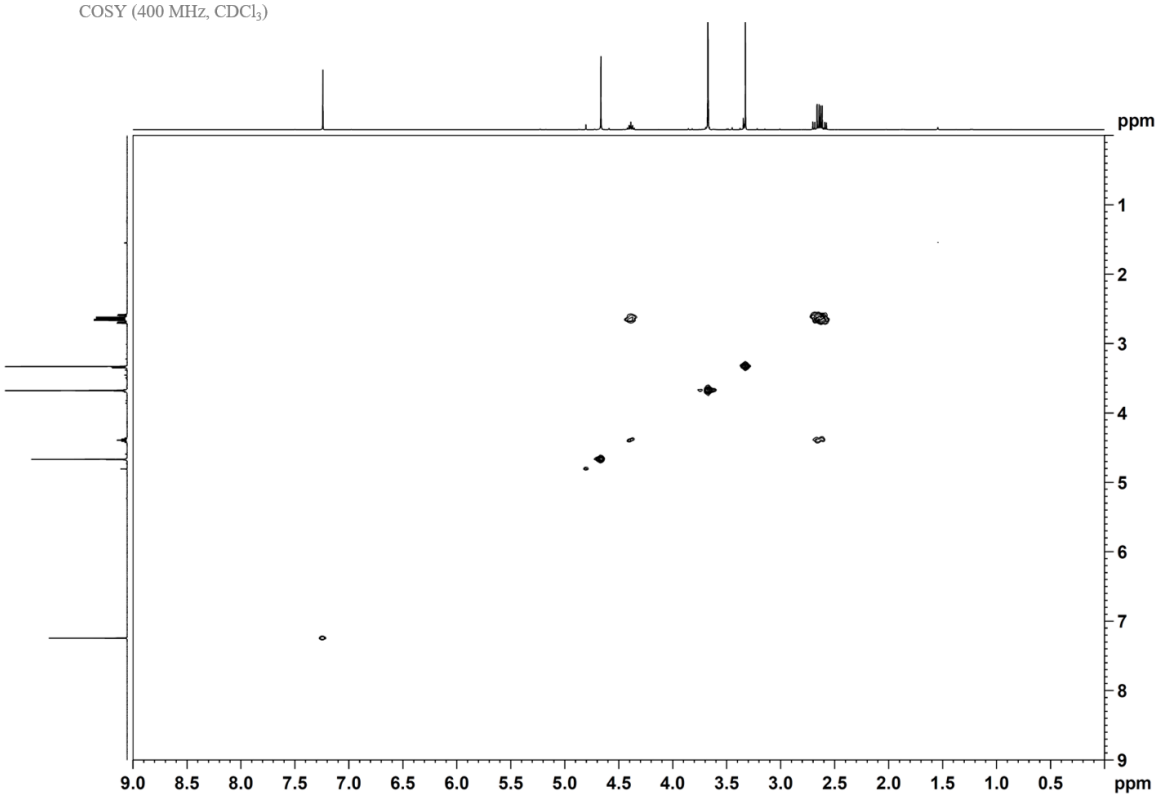

Dimethyl 3-(methoxymethoxy)pentanedioate (**S-26**)

HSQC (400 MHz, $CDCl_3$)

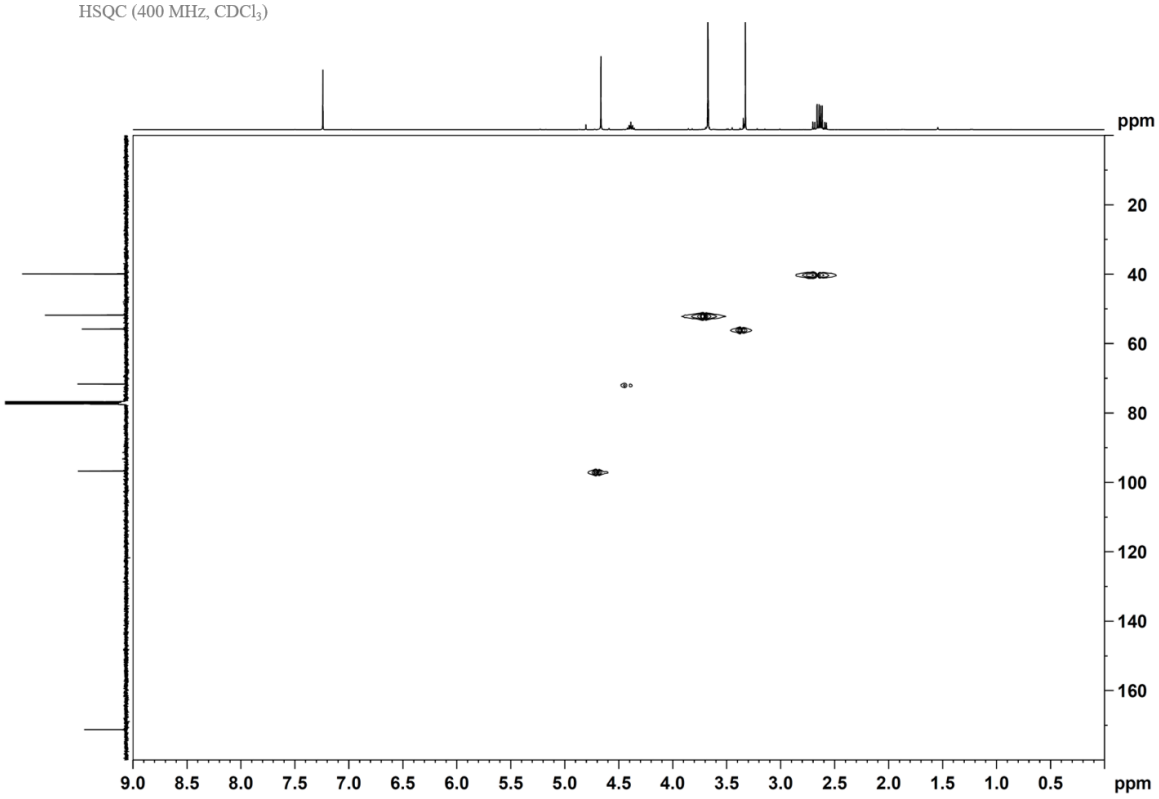

5-Methoxy-3-(methoxymethoxy)-5-oxopentanoic acid (**S-27**)

^{1}H NMR (400 MHz, $CDCl_3$)

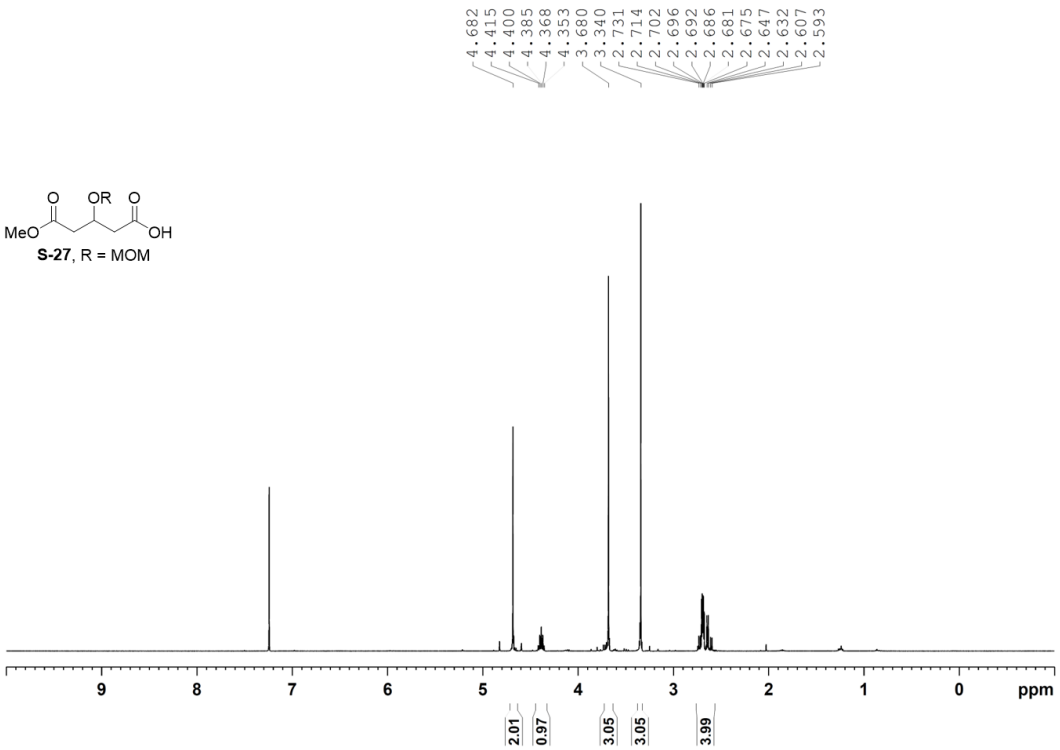

5-Methoxy-3-(methoxymethoxy)-5-oxopentanoic acid (**S-27**)

^{13}C NMR (100 MHz, $CDCl_3$)

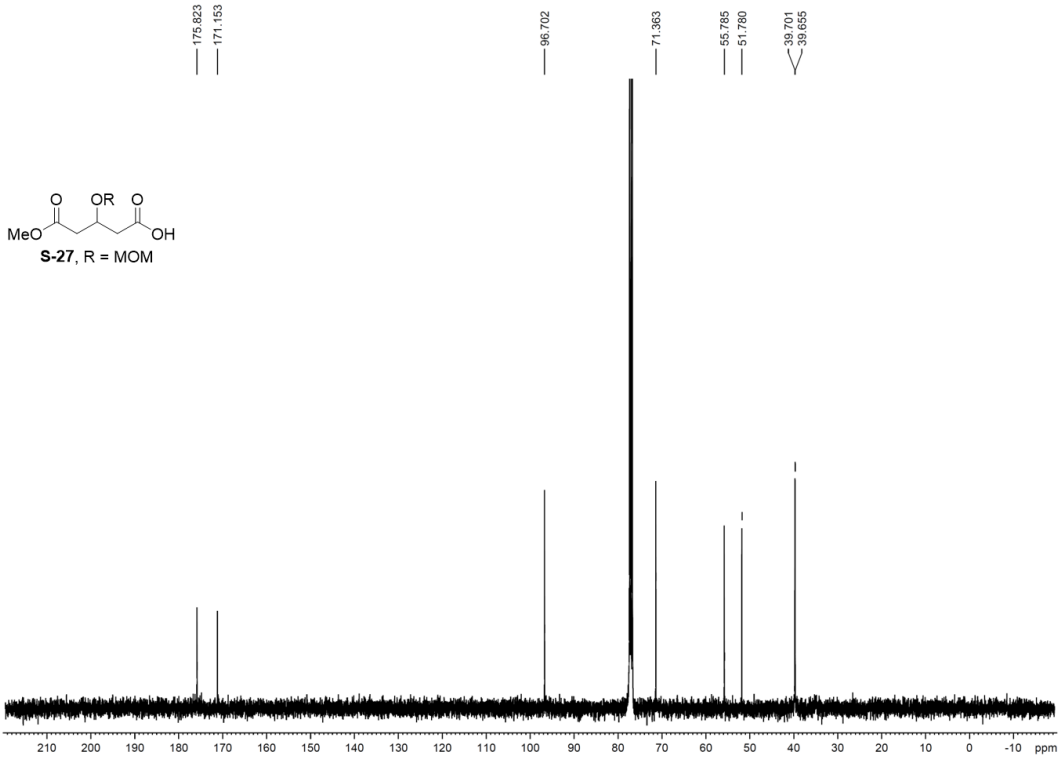

5-Methoxy-3-(methoxymethoxy)-5-oxopentanoic acid (**S-27**)

COSY (400 MHz, $CDCl_3$)

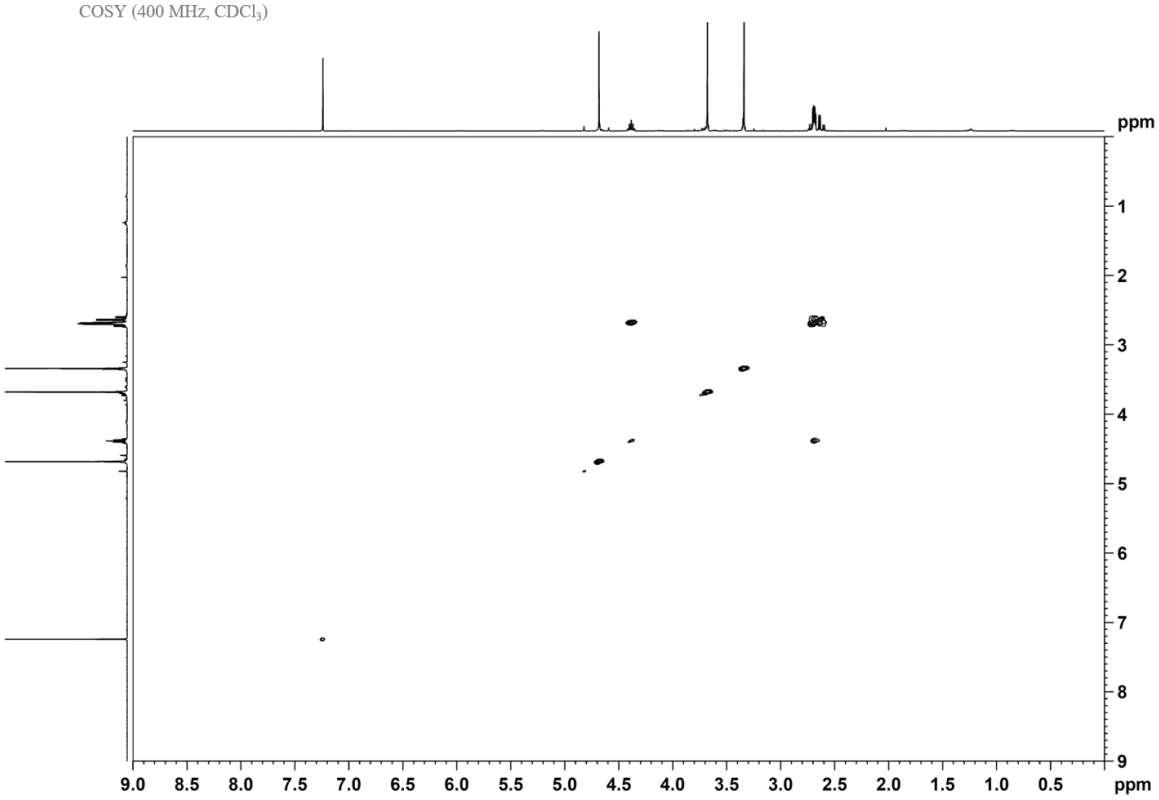

5-Methoxy-3-(methoxymethoxy)-5-oxopentanoic acid (**S-27**)

HSQC (400 MHz, $CDCl_3$)

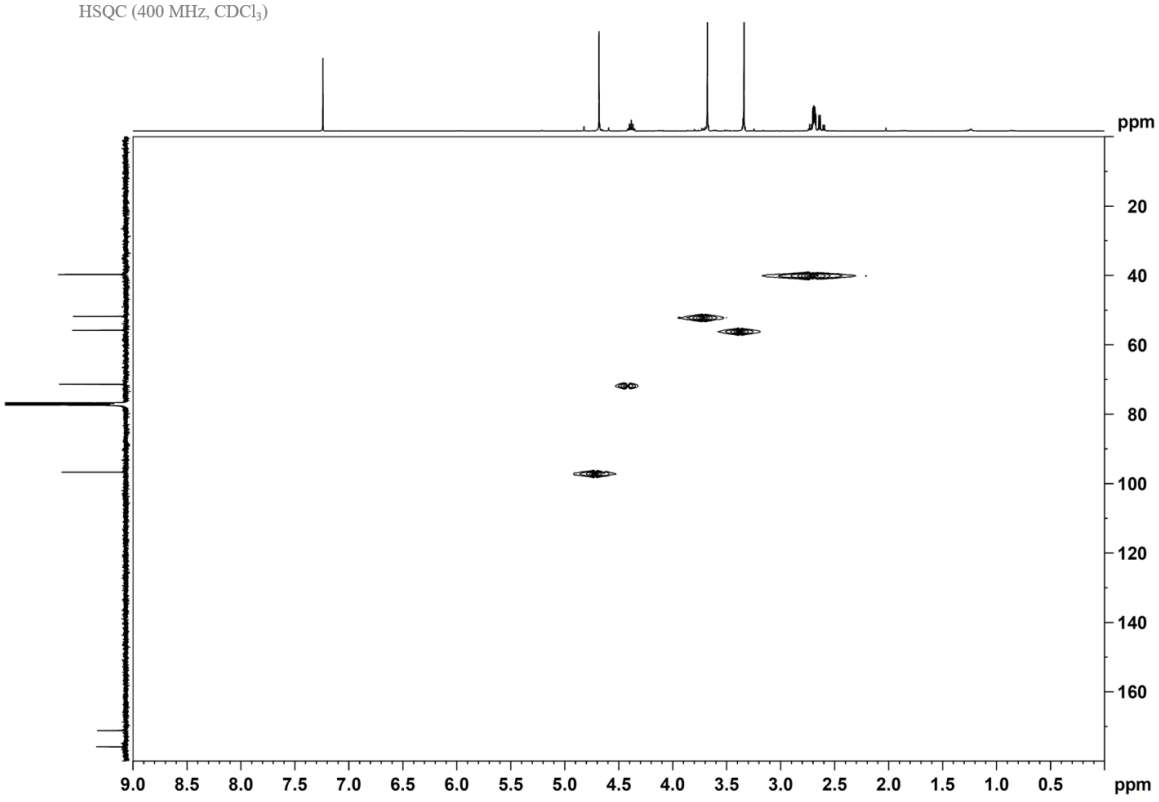

(*E*)-3-(*tert*-Butyldimethylsilyloxy)-5-oxotetradec-6-enoic acid (**4.58**)

^{1}H NMR (300 MHz, $CDCl_3$)

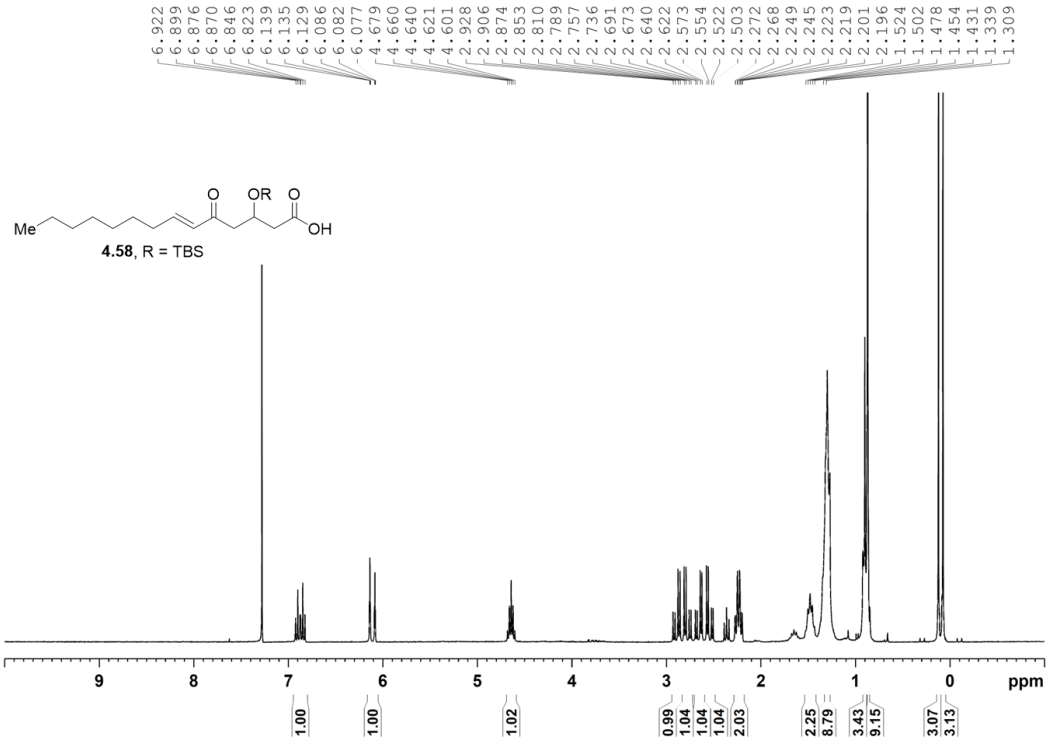

(*E*)-3-(*tert*-Butyldimethylsilyloxy)-5-oxotetradec-6-enoic acid (**4.58**)

^{13}C NMR (75 MHz, $CDCl_3$)

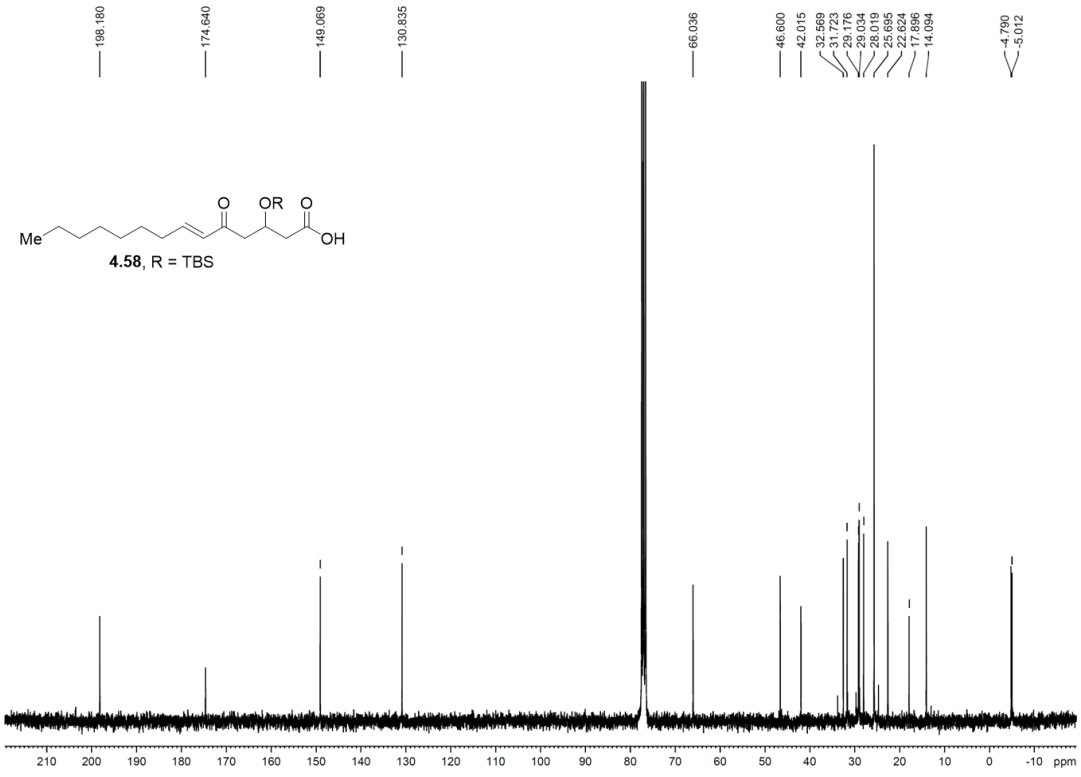

(*E*)-3-(*tert*-Butyldimethylsilyloxy)-5-oxotetradec-6-enoic acid (**4.58**)

COSY (300 MHz, $CDCl_3$)

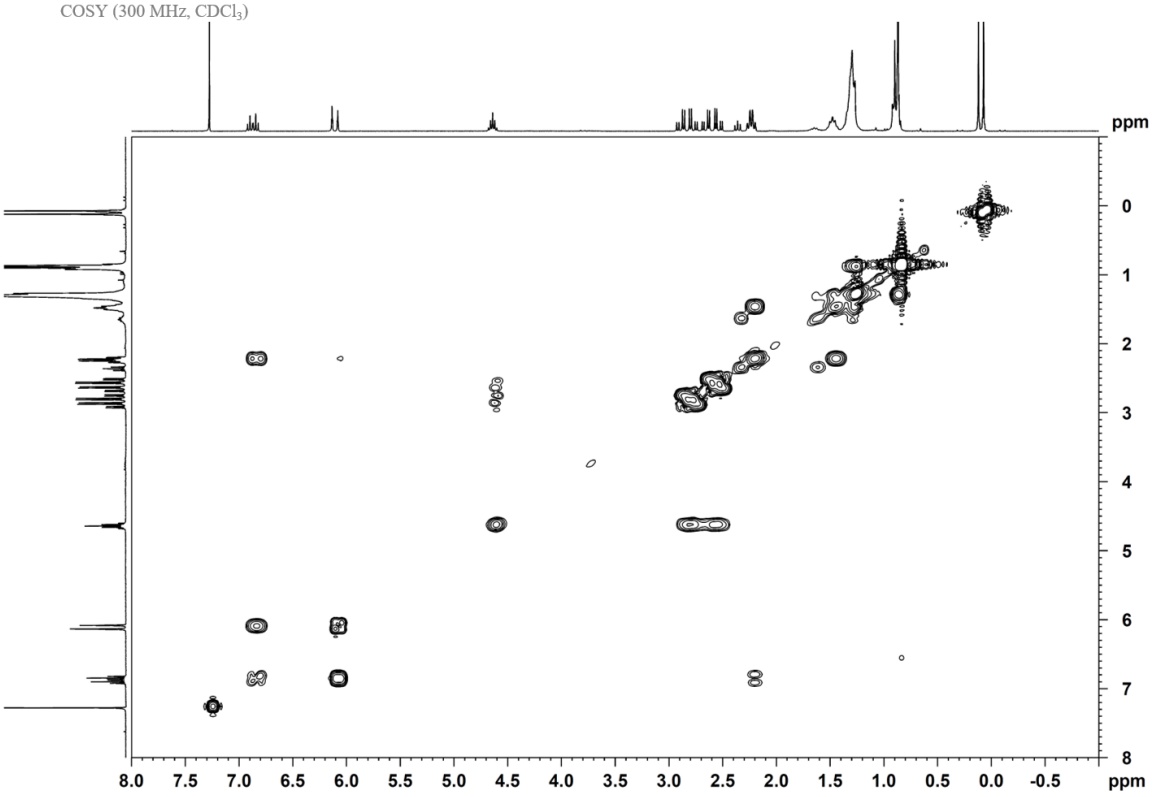

(*E*)-3-(*tert*-Butyldimethylsilyloxy)-5-oxotetradec-6-enoic acid (**4.58**)

HSQC (300 MHz, $CDCl_3$)

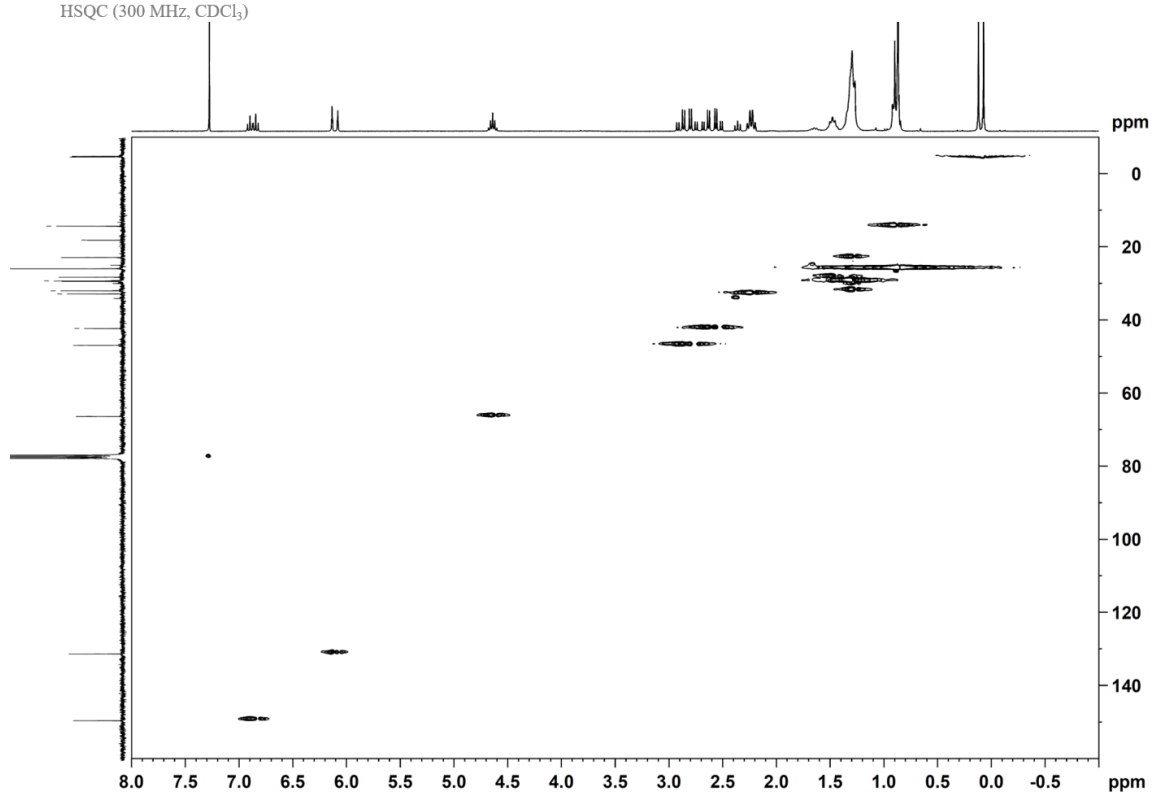

Methyl (*E*)-3-(*tert*-butyldimethylsilyloxy)-5-oxohexadec-6-enoate (**S-28**)

^{1}H NMR (300 MHz, $CDCl_3$)

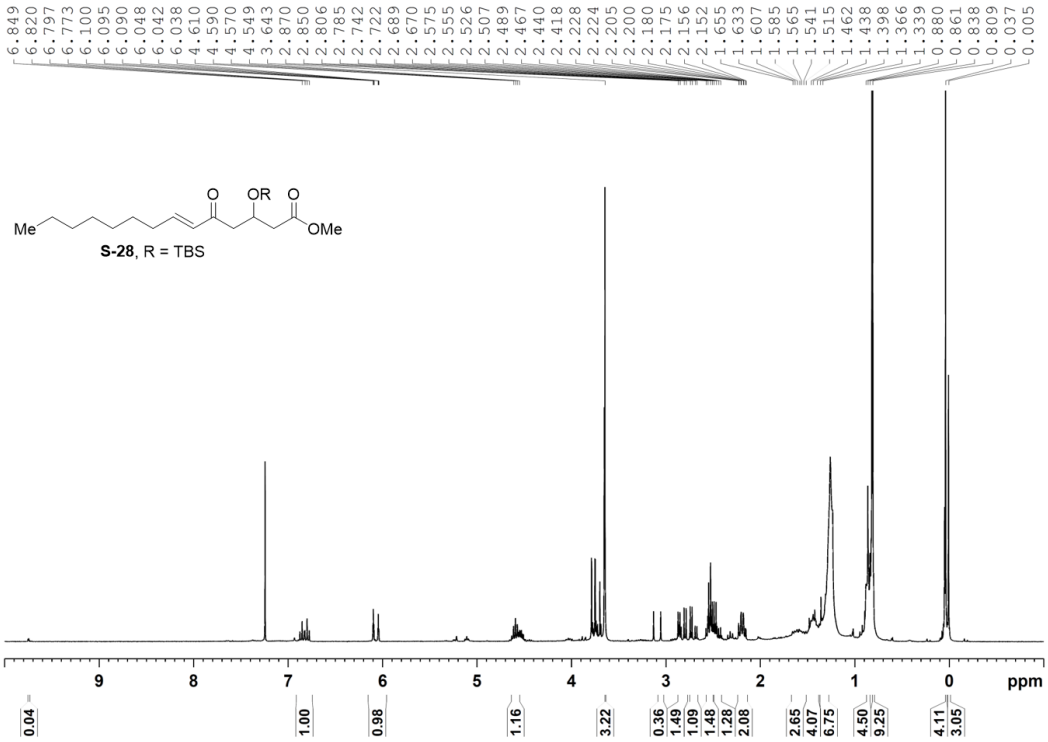

S1.3.5 Second-Generation α,β-Unsaturated Ketone Model Fragment Development (§ 4.5.1)

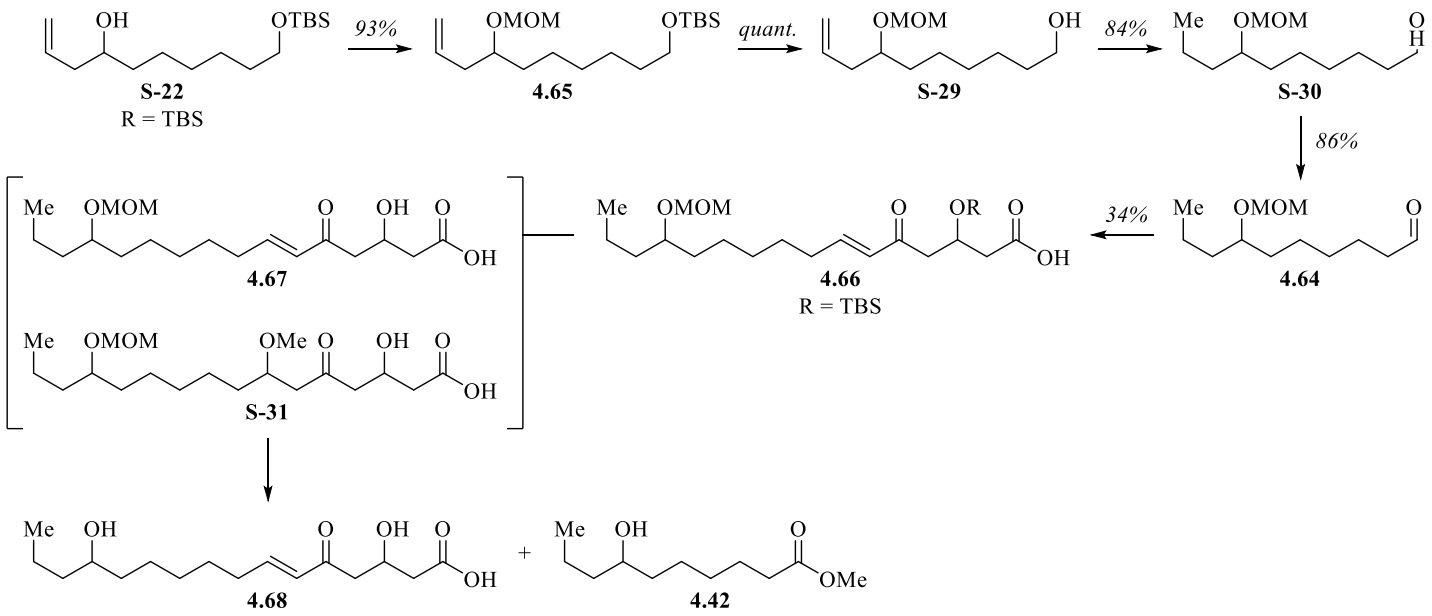

Figure S10 – Rapid development of C7-C16 fragment for second-generation *α,β*-unsaturated ketone model.

5-Allyl-13,13,14,14-tetramethyl-2,4,12-trioxa-13-silapentadecane (**4.65**)

^{1}H NMR (400 MHz, $CDCl_3$)

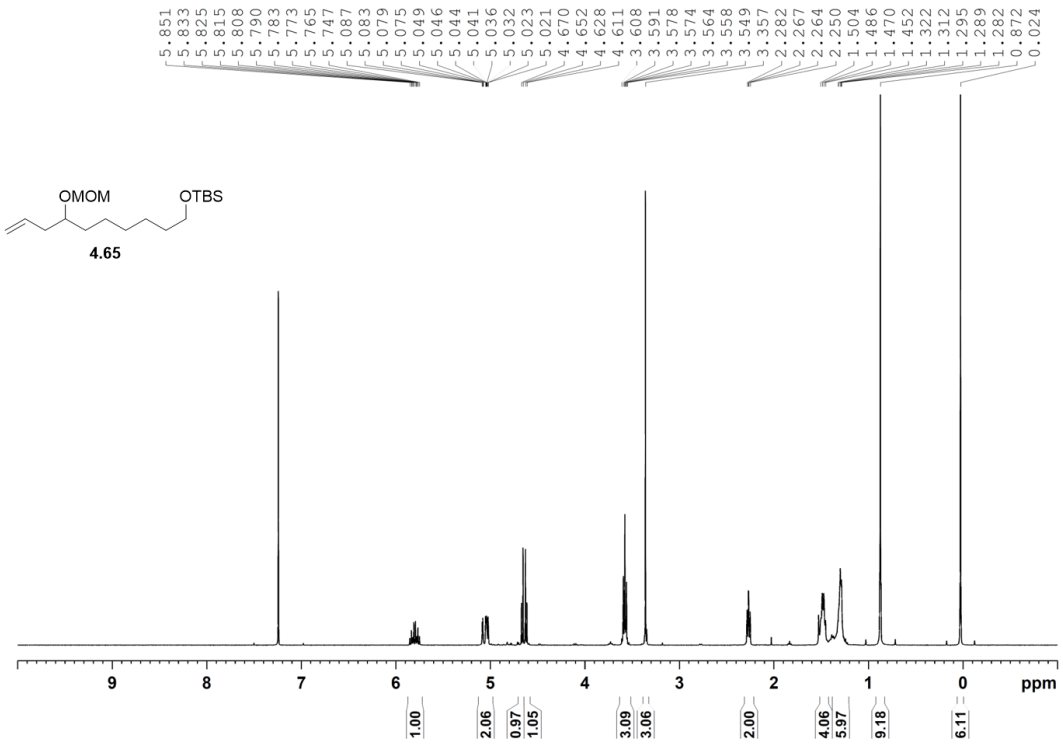

5-Allyl-13,13,14,14-tetramethyl-2,4,12-trioxa-13-silapentadecane (**4.65**)

^{13}C NMR (100 MHz, $CDCl_3$)

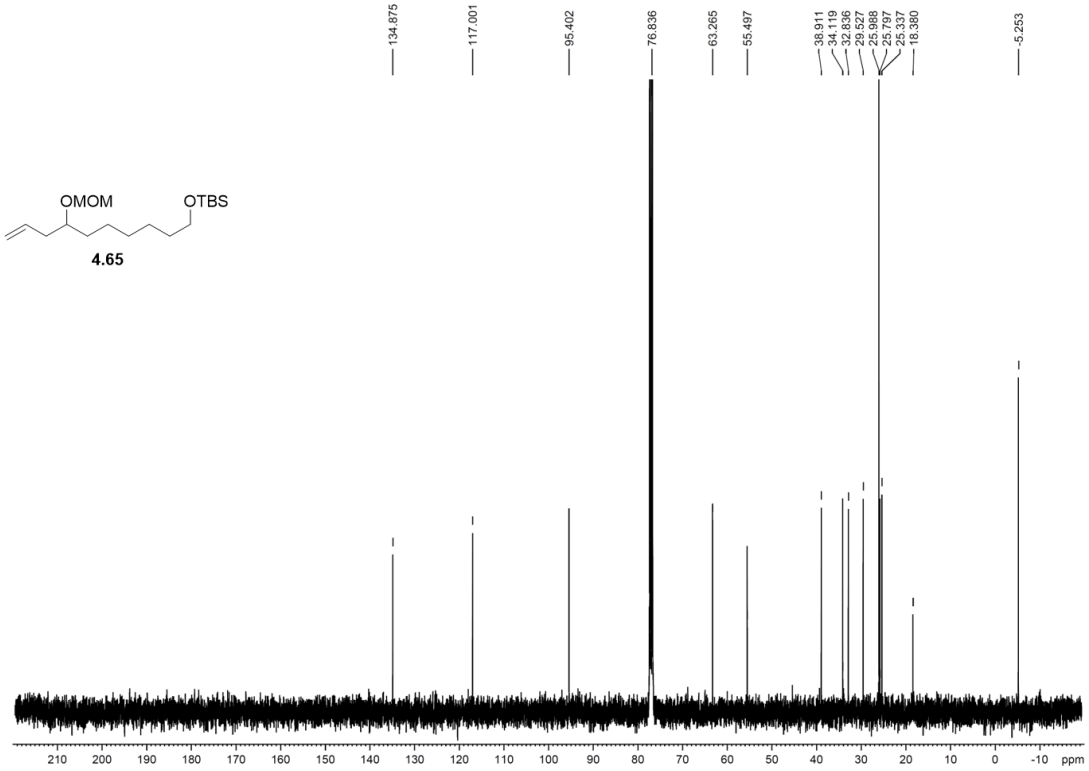

5-Allyl-13,13,14,14-tetramethyl-2,4,12-trioxa-13-silapentadecane (**4.65**)

COSY (400 MHz, $CDCl_3$)

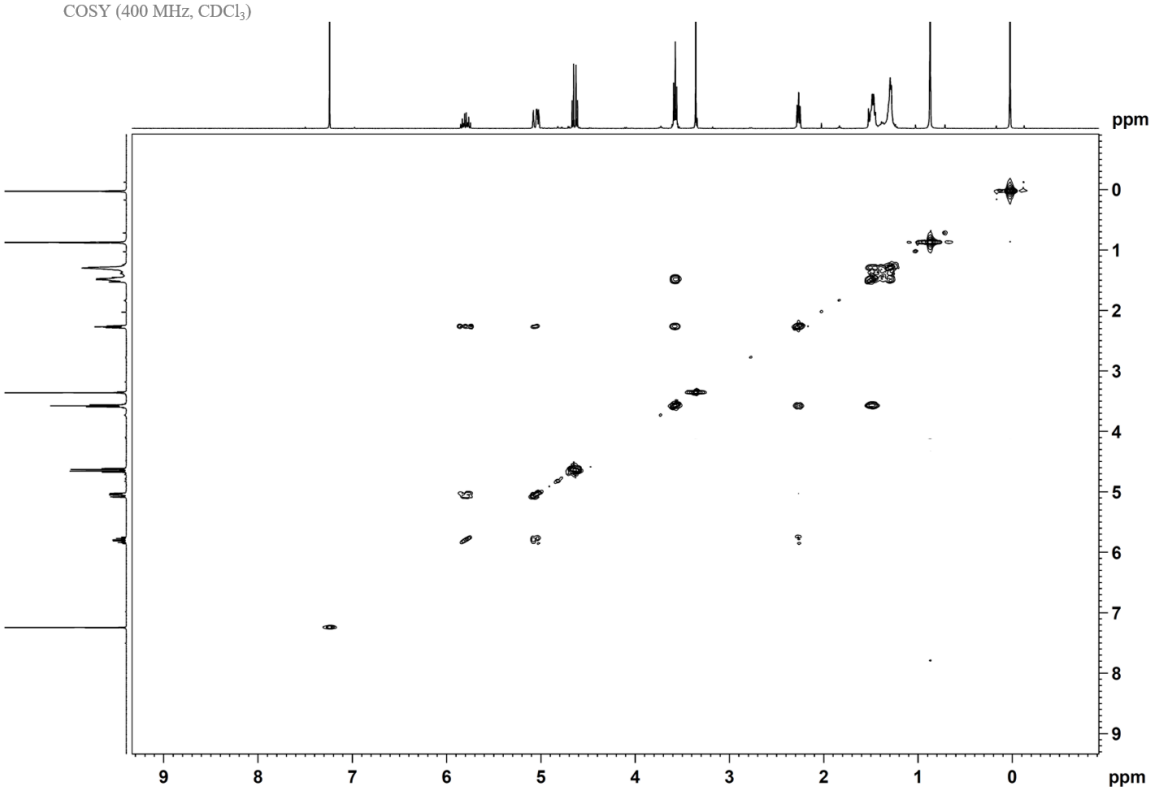

5-Allyl-13,13,14,14-tetramethyl-2,4,12-trioxa-13-silapentadecane (**4.65**)

HSQC (400 MHz, $CDCl_3$)

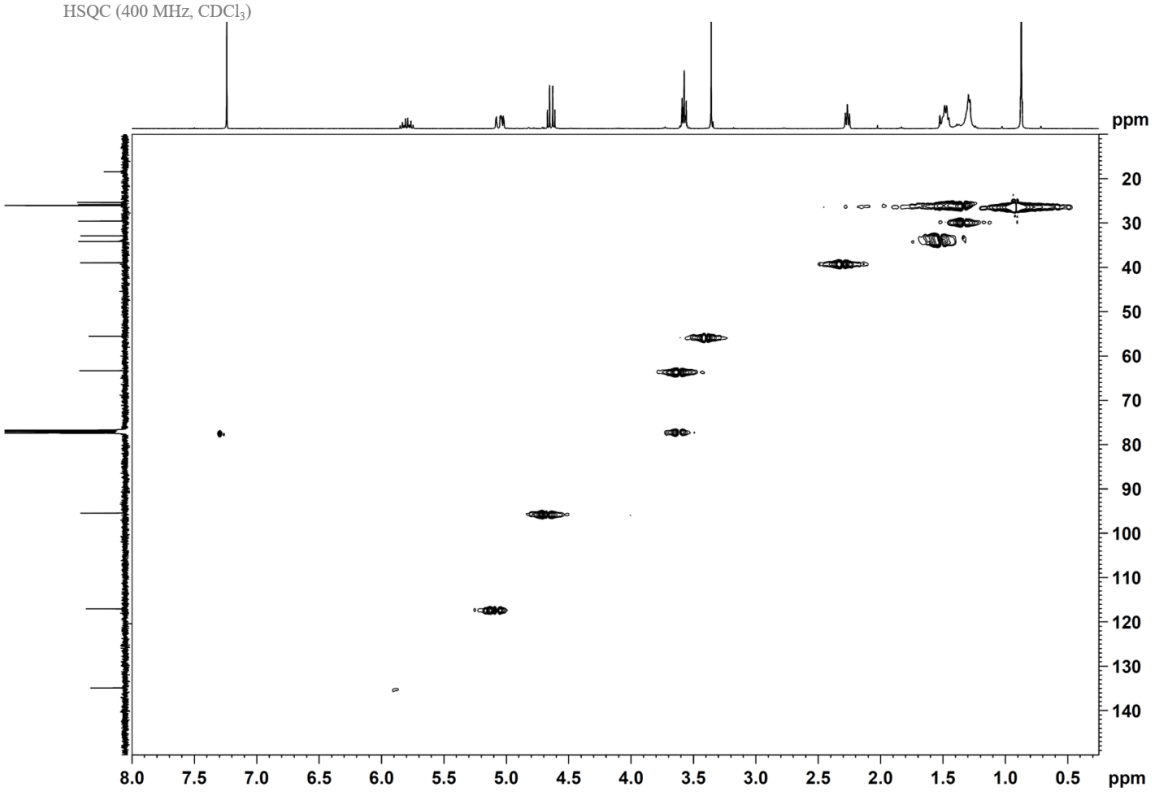

7-(Methoxymethoxy)dec-9-en-1-ol (**S-29**)

^{1}H NMR (400 MHz, $CDCl_3$)

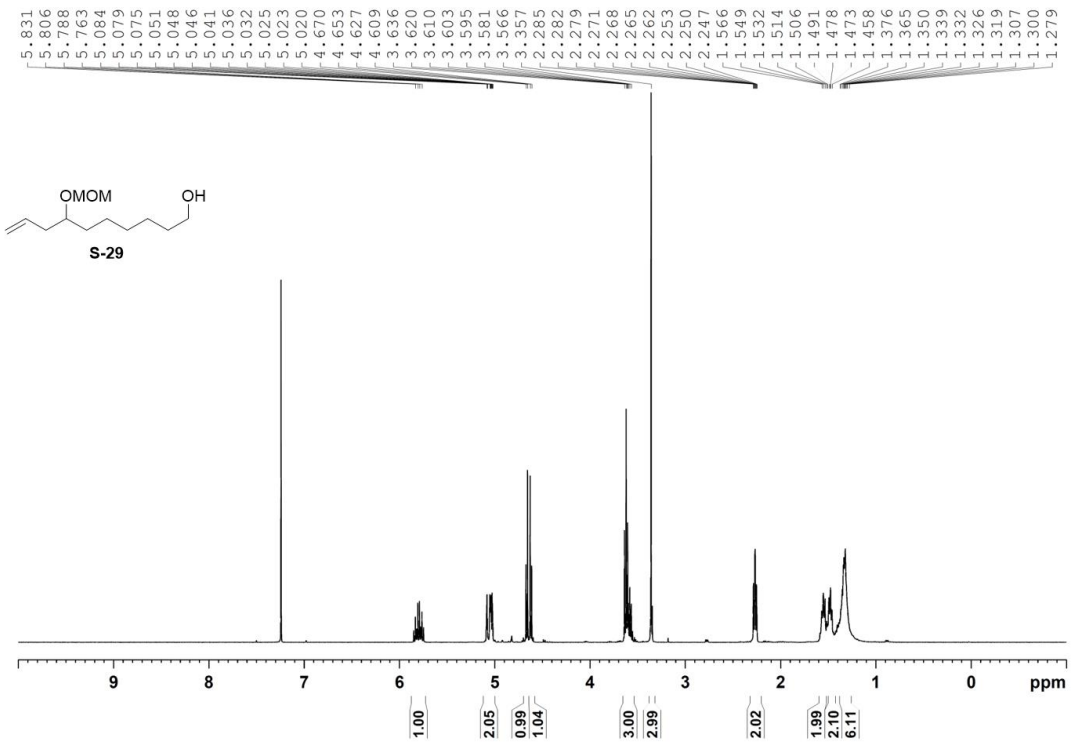

7-(Methoxymethoxy)dec-9-en-1-ol (**S-29**)

^{13}C NMR (100 MHz, $CDCl_3$)

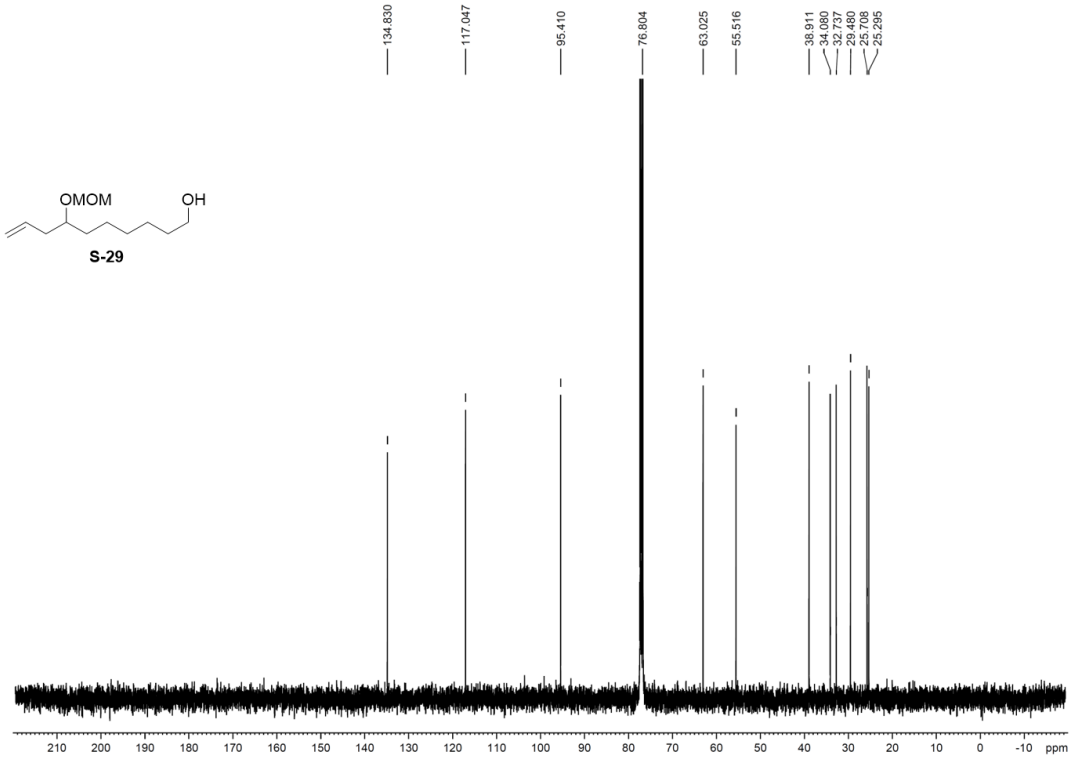

7-(Methoxymethoxy)dec-9-en-1-ol (**S-29**)

COSY (400 MHz, $CDCl_3$)

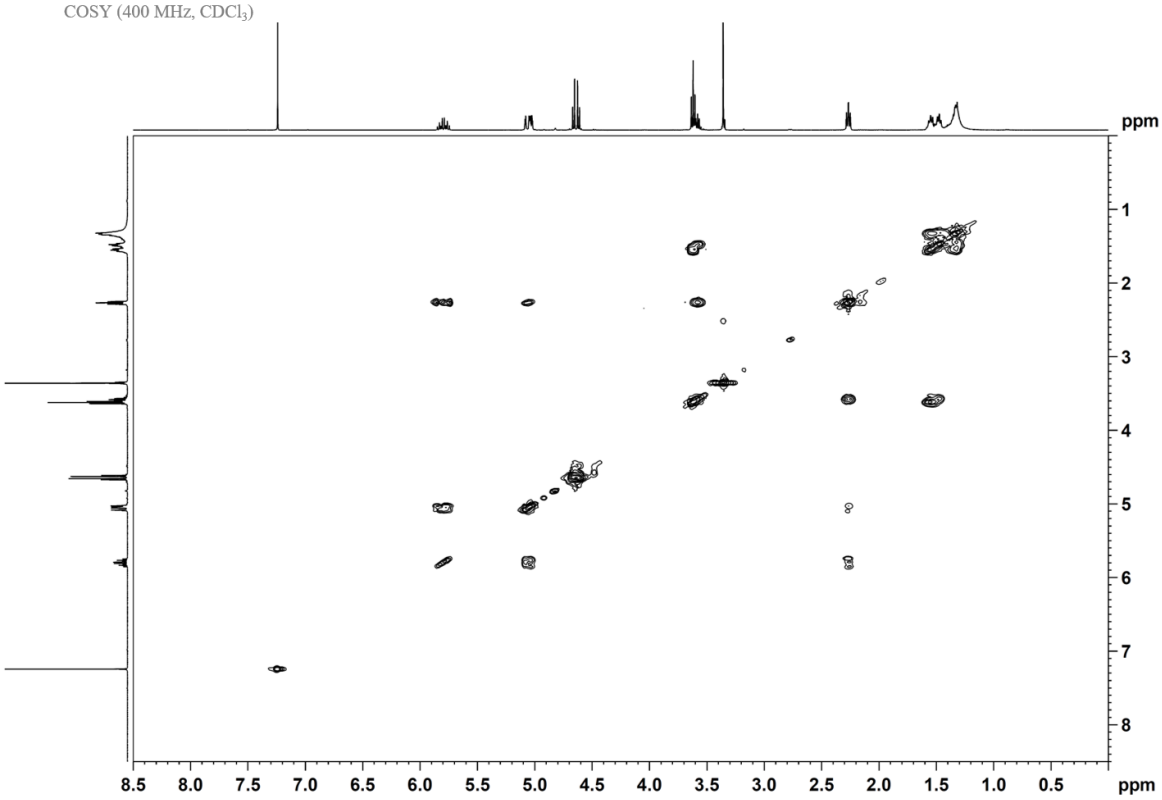

7-(Methoxymethoxy)dec-9-en-1-ol (**S-29**)

HSQC (400 MHz, $CDCl_3$)

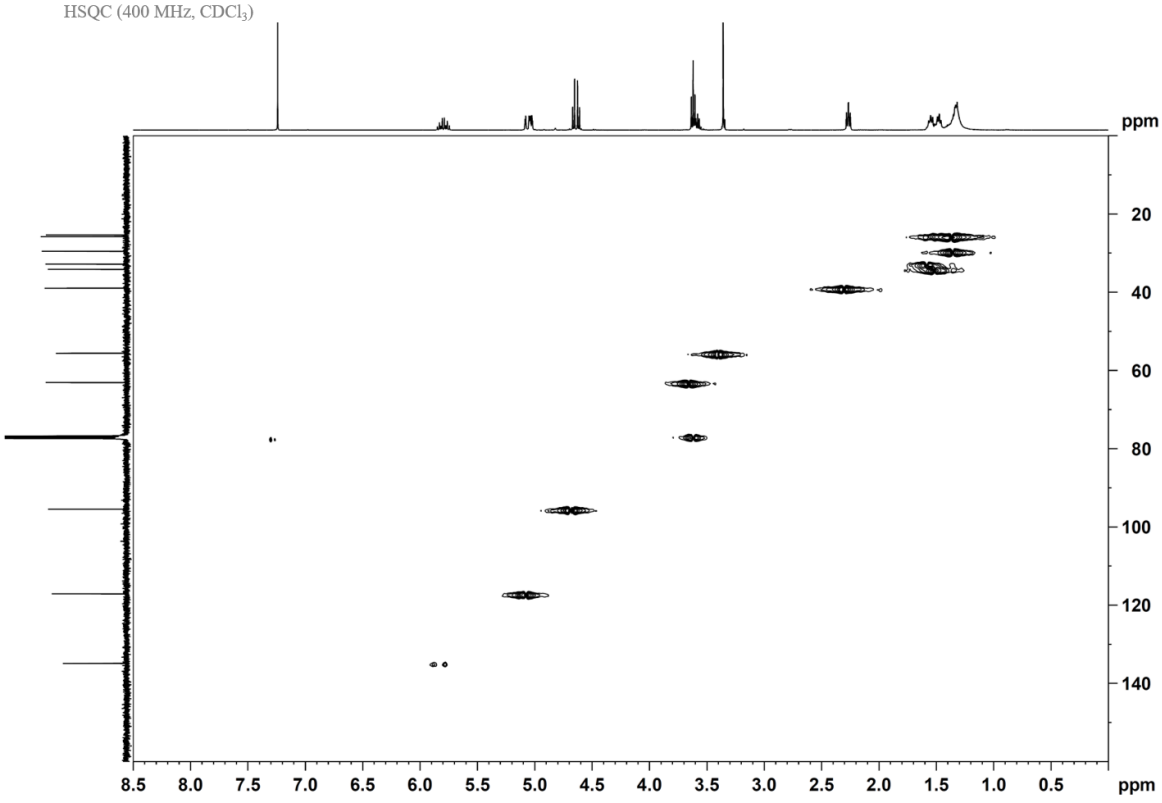

7-(Methoxymethoxy)decan-1-ol (**S-30**)

^{1}H NMR (400 MHz, $CDCl_3$)

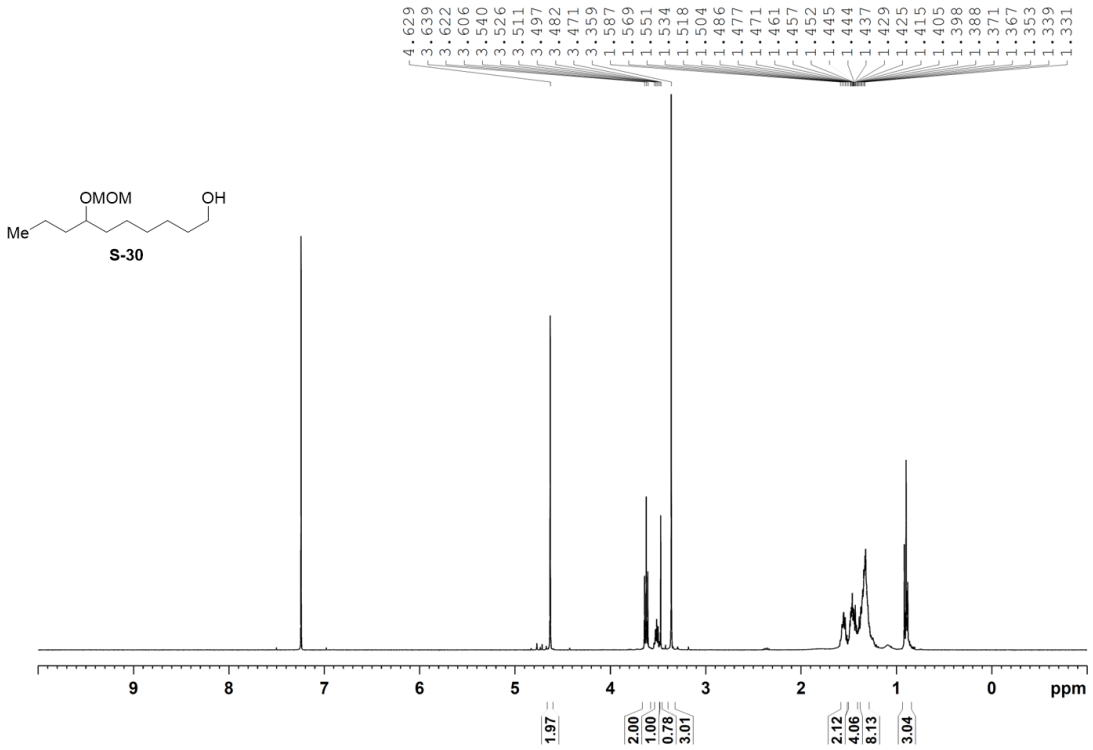

7-(Methoxymethoxy)decan-1-ol (**S-30**)

^{13}C NMR (100 MHz, $CDCl_3$)

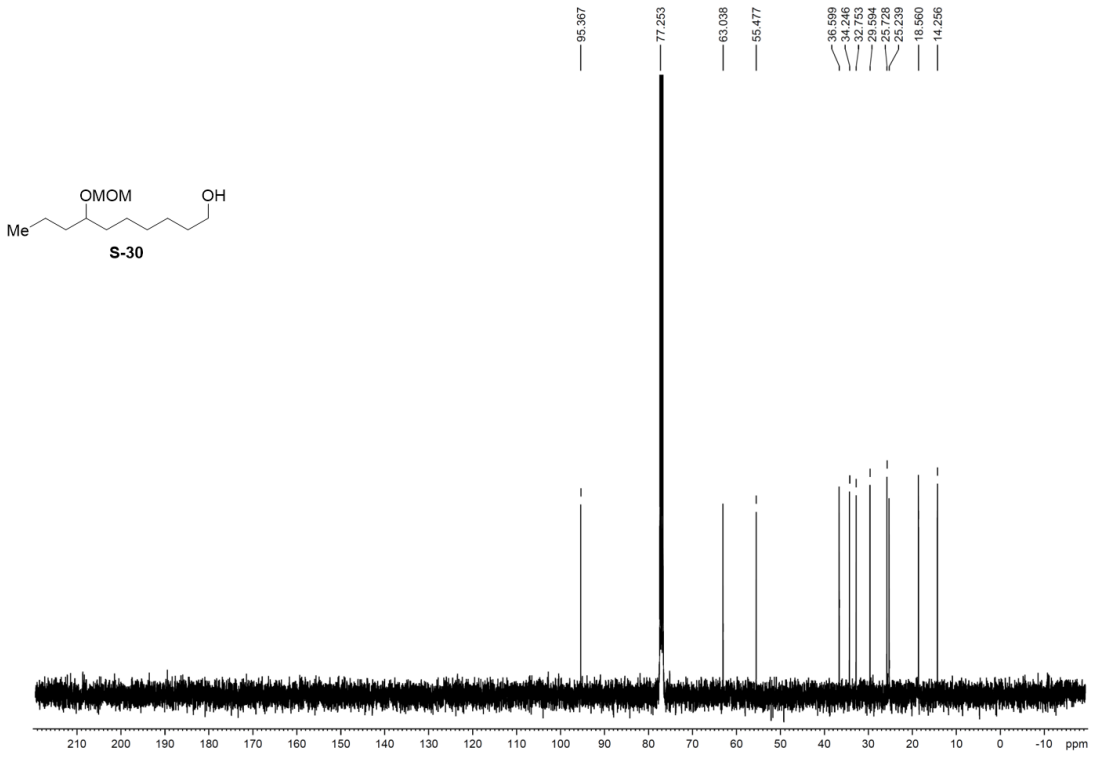

7-(Methoxymethoxy)decan-1-ol (**S-30**)

COSY (400 MHz, $CDCl_3$)

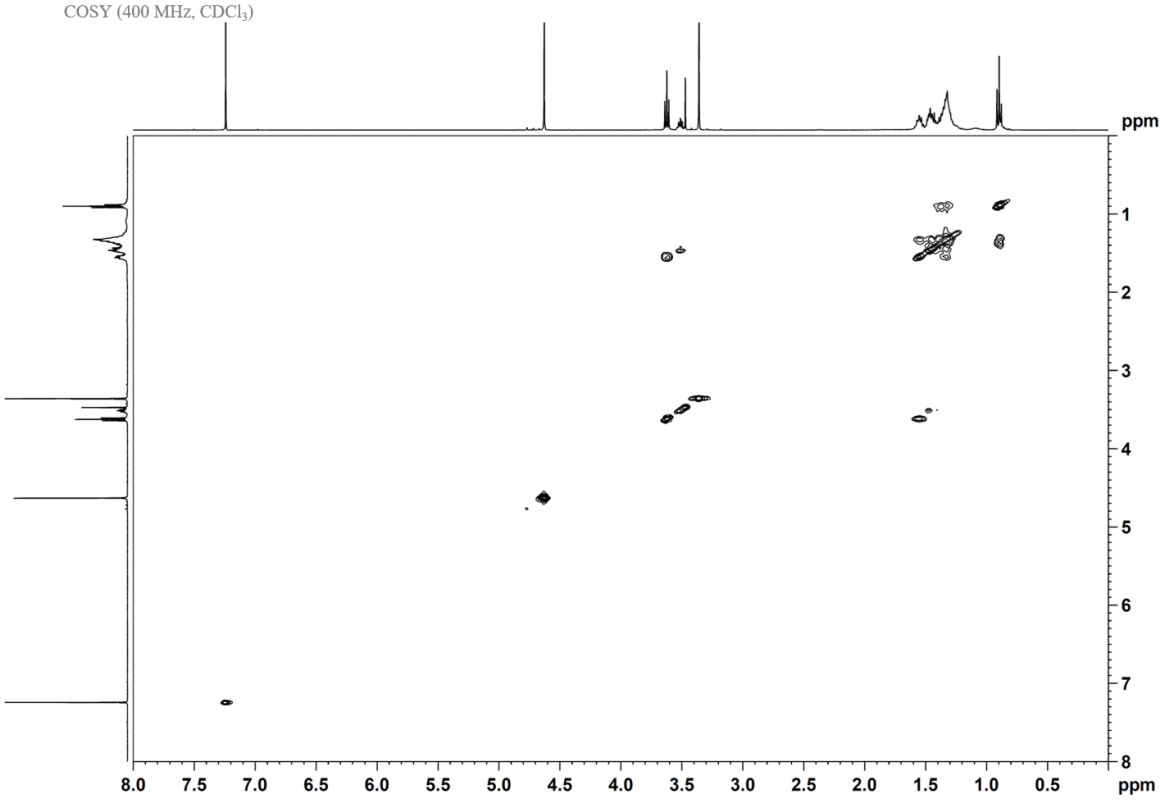

7-(Methoxymethoxy)decan-1-ol (**S-30**)

HSQC (400 MHz, $CDCl_3$)

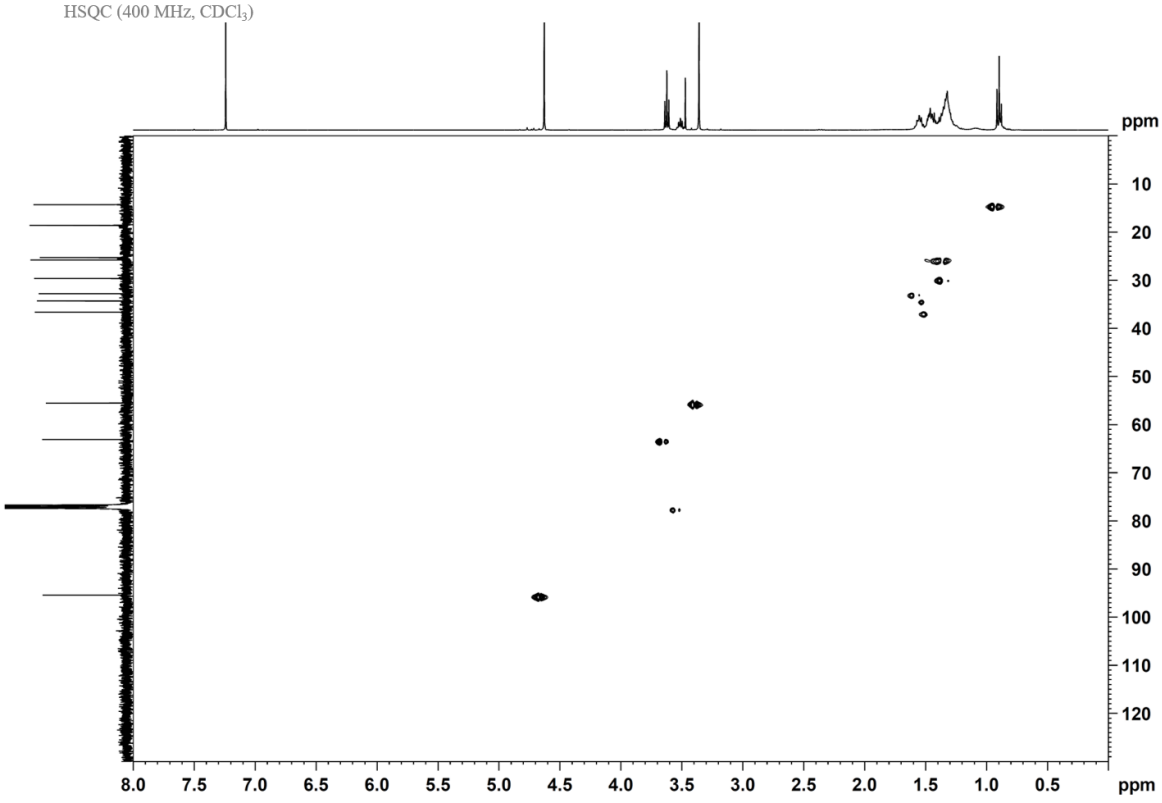

7-(Methoxymethoxy)decanal (**4.64**)

^{1}H NMR (400 MHz, $CDCl_3$)

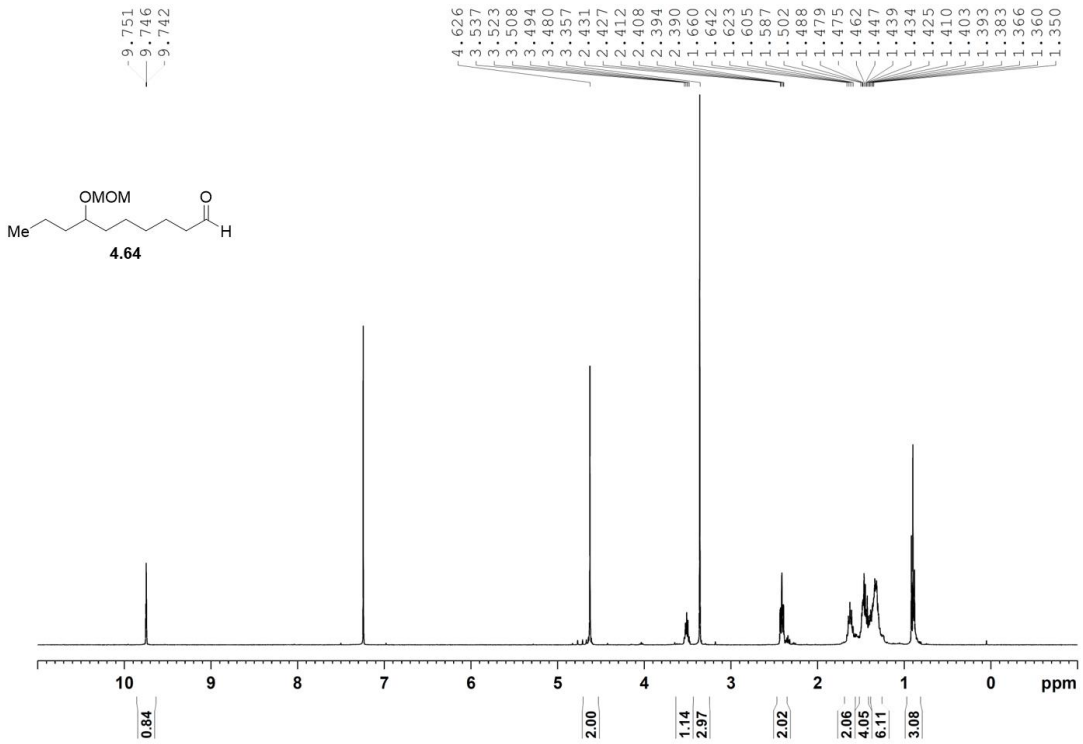

7-(Methoxymethoxy)decanal (**4.64**)

^{13}C NMR (100 MHz, $CDCl_3$)

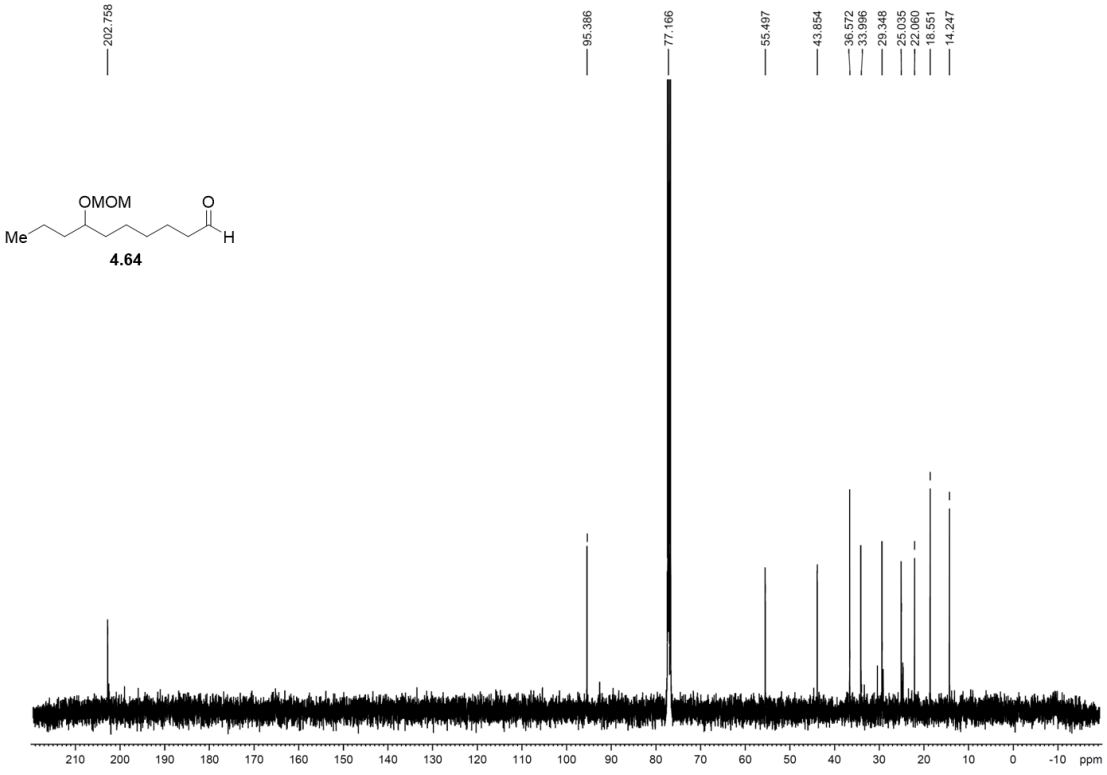

7-(Methoxymethoxy)decanal (**4.64**)
COSY (400 MHz, $CDCl_3$)

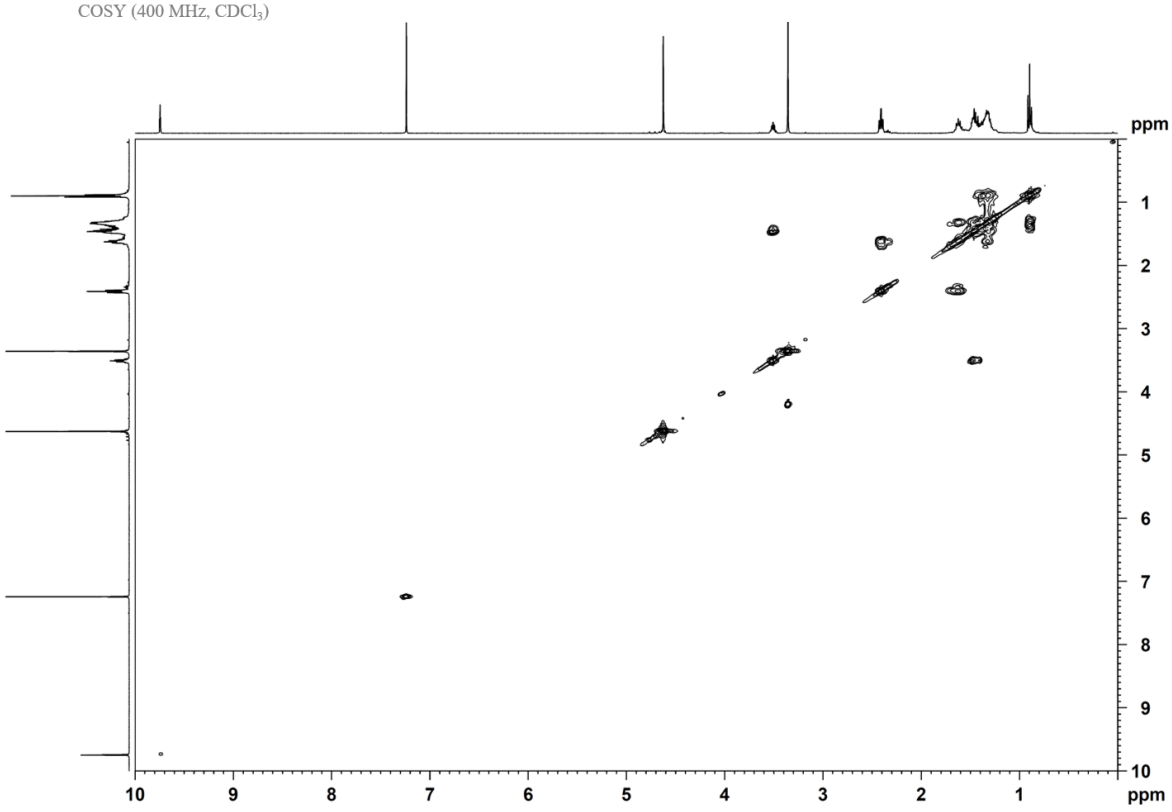

7-(Methoxymethoxy)decanal (**4.64**)
HSQC (400 MHz, $CDCl_3$)

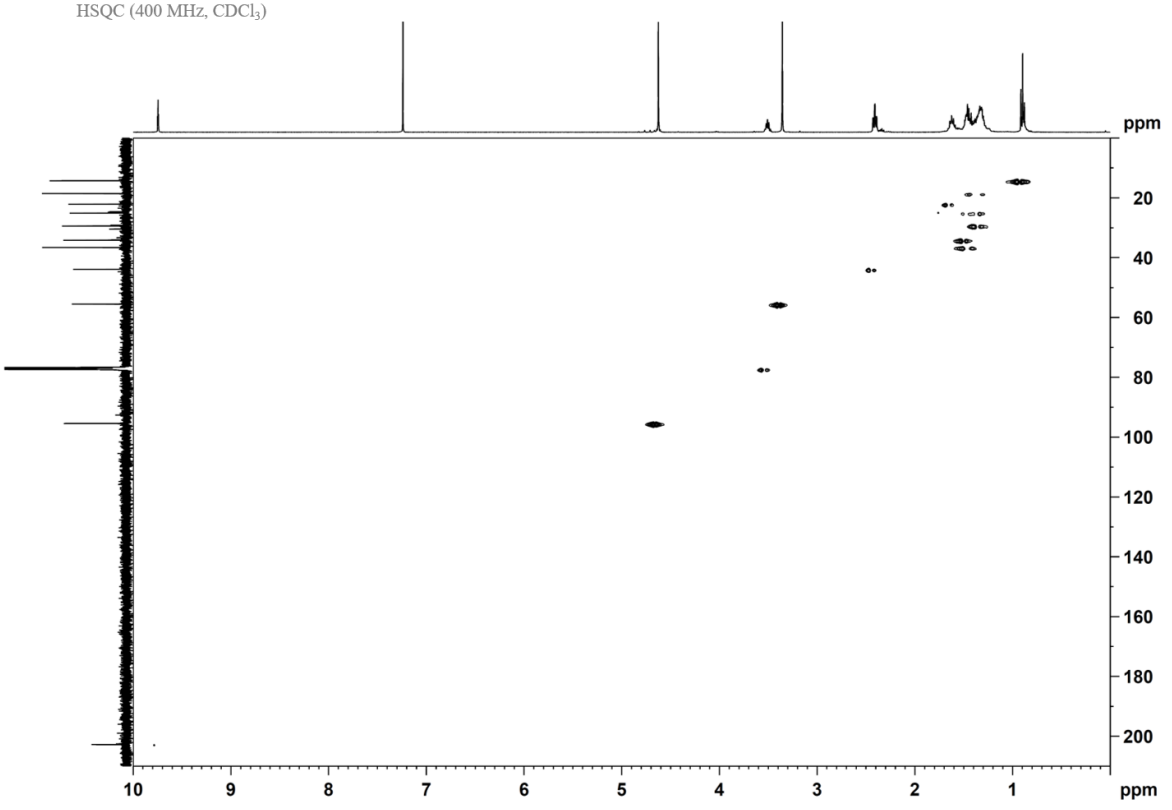

(*E*)-3-(TBS)-13-MOM-5-oxohexadec-6-enoic acid (**4.66**)

^{1}H NMR (400 MHz, $CDCl_3$)

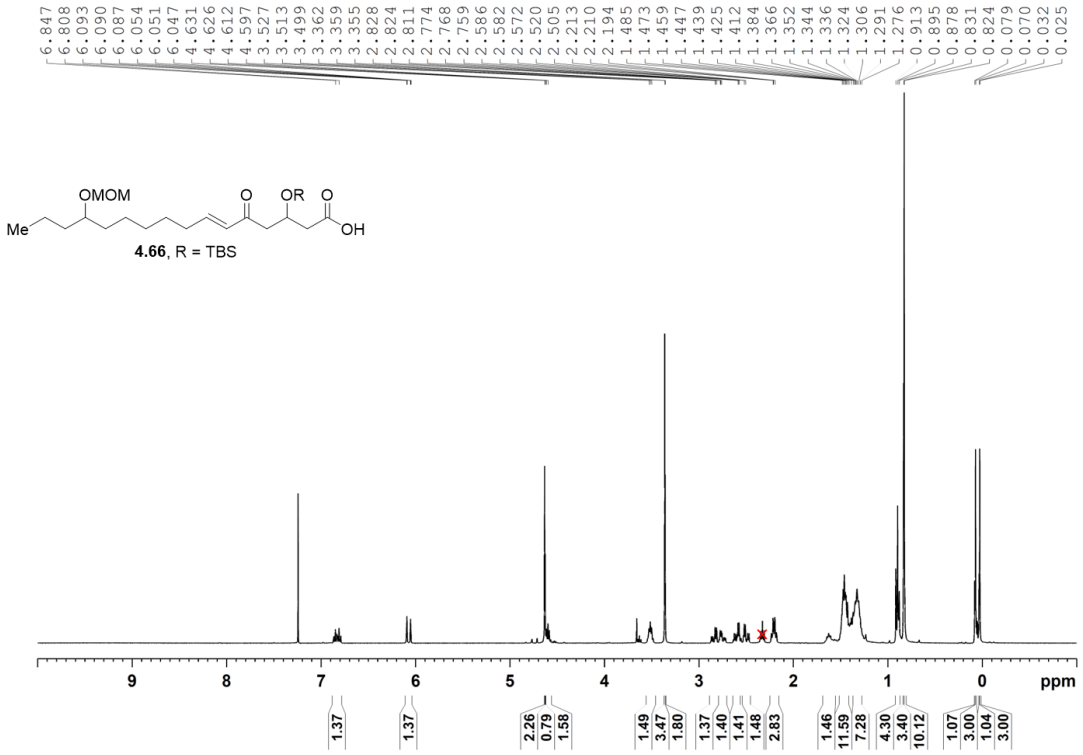

3-Hydroxy-13-(methoxymethoxy)-5-oxohexadecanoic acid (**4.67**) : 3-Hydroxy-7-methoxy-13-(methoxymethoxy)-5-oxohexadecanoic acid (**S-31**) [*d.r.* = 1:2, **4.67**:**S-31**], *crude reaction mixture*

^{1}H NMR (400 MHz, $CDCl_3$)

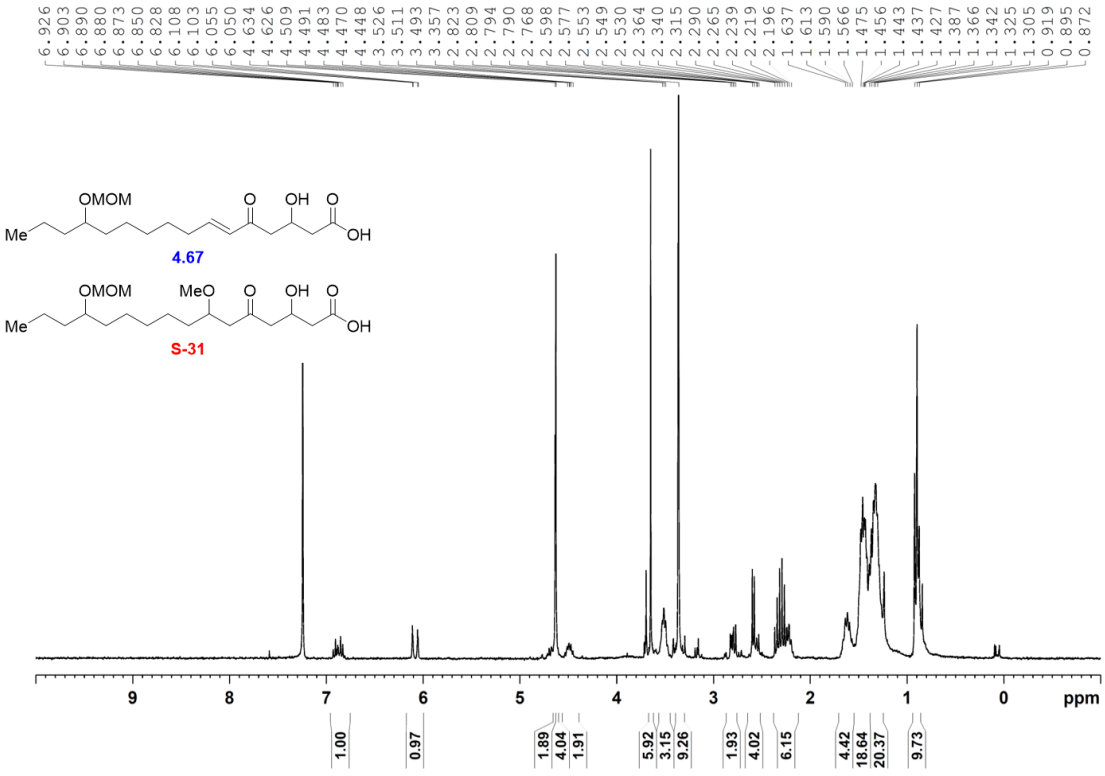

3,13-Dihydroxy-7-methoxy-5-oxohexadecanoic acid (**4.68**)

^{1}H NMR (400 MHz, $CDCl_3$)

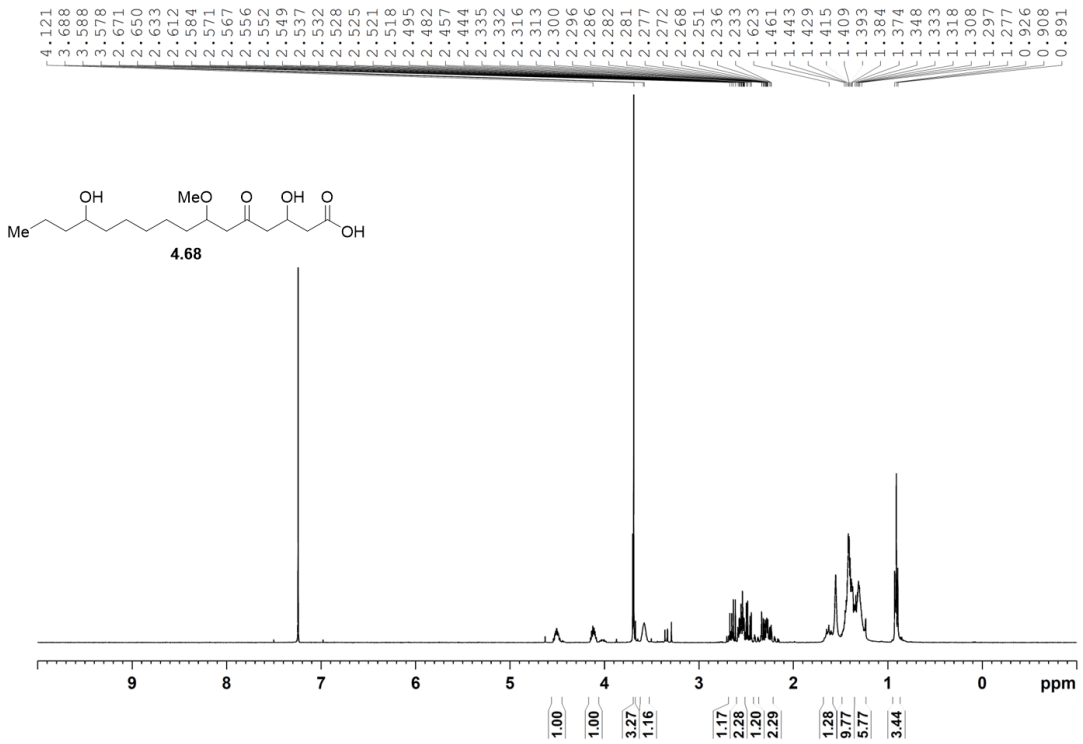

3,13-Dihydroxy-7-methoxy-5-oxohexadecanoic acid (**4.68**)

^{1}C NMR (100 MHz, $CDCl_3$)

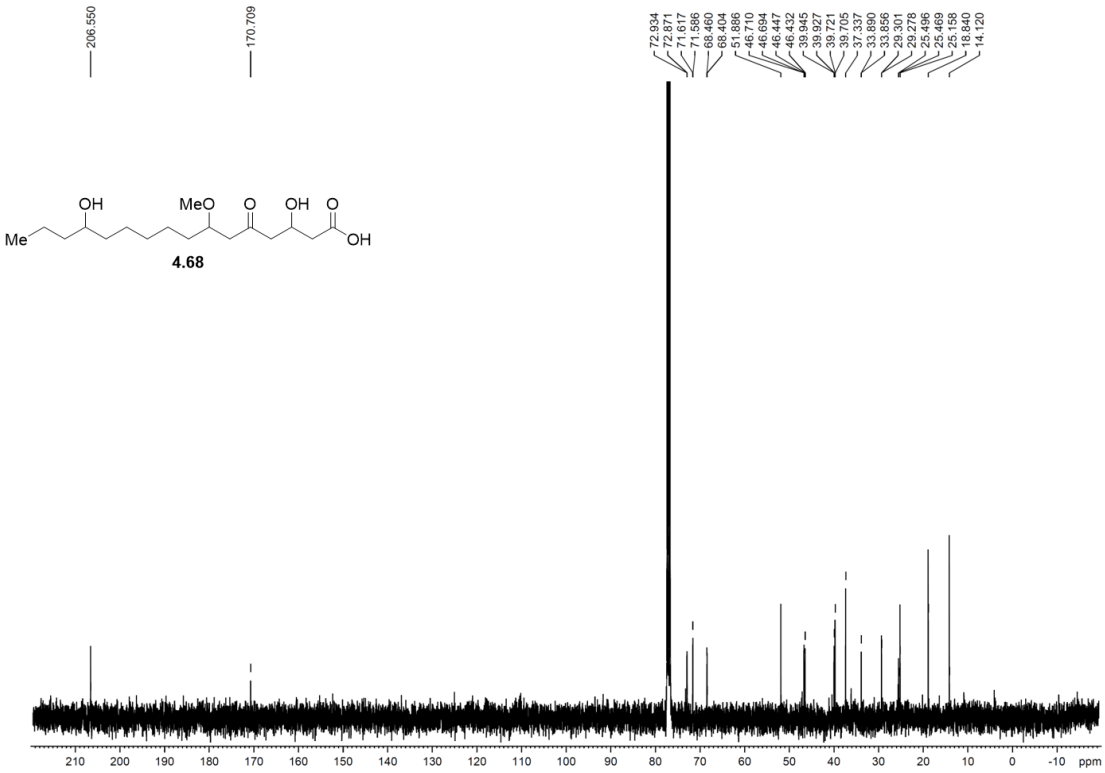

3,13-Dihydroxy-7-methoxy-5-oxohexadecanoic acid (**4.68**)

COSY (400 MHz, $CDCl_3$)

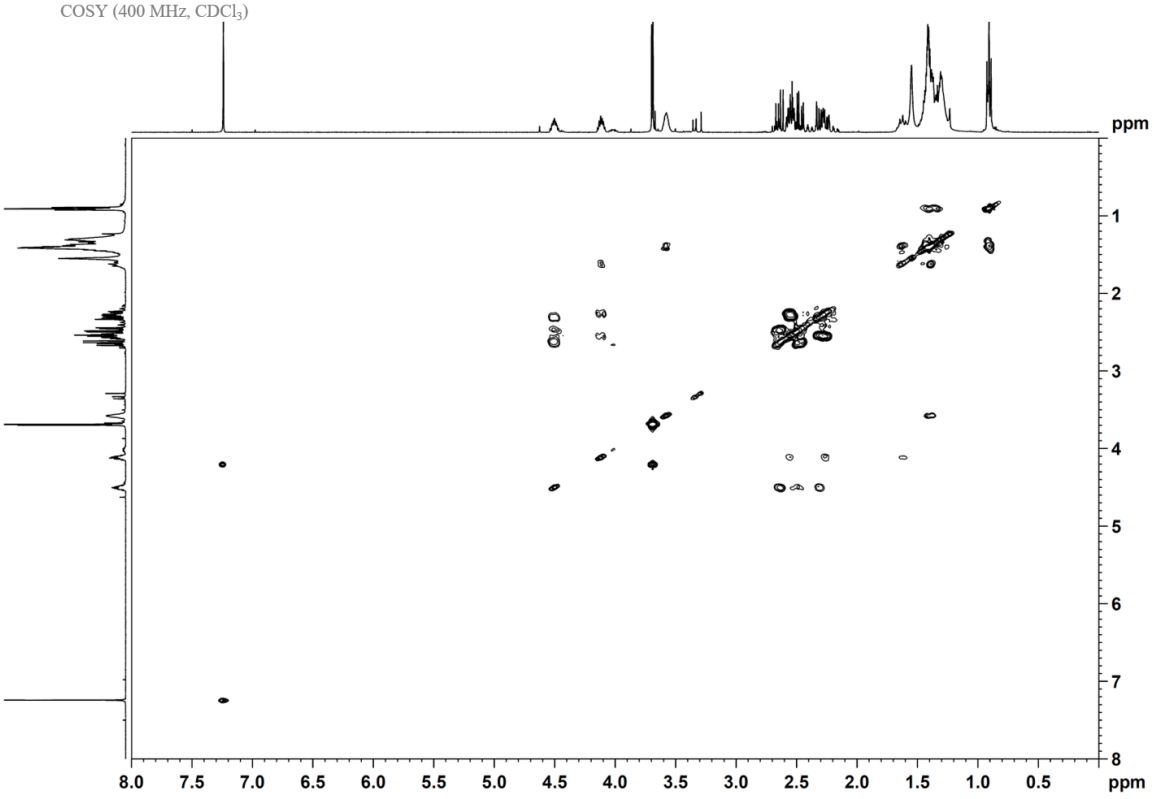

3,13-Dihydroxy-7-methoxy-5-oxohexadecanoic acid (**4.68**)

HSQC (400 MHz, $CDCl_3$)

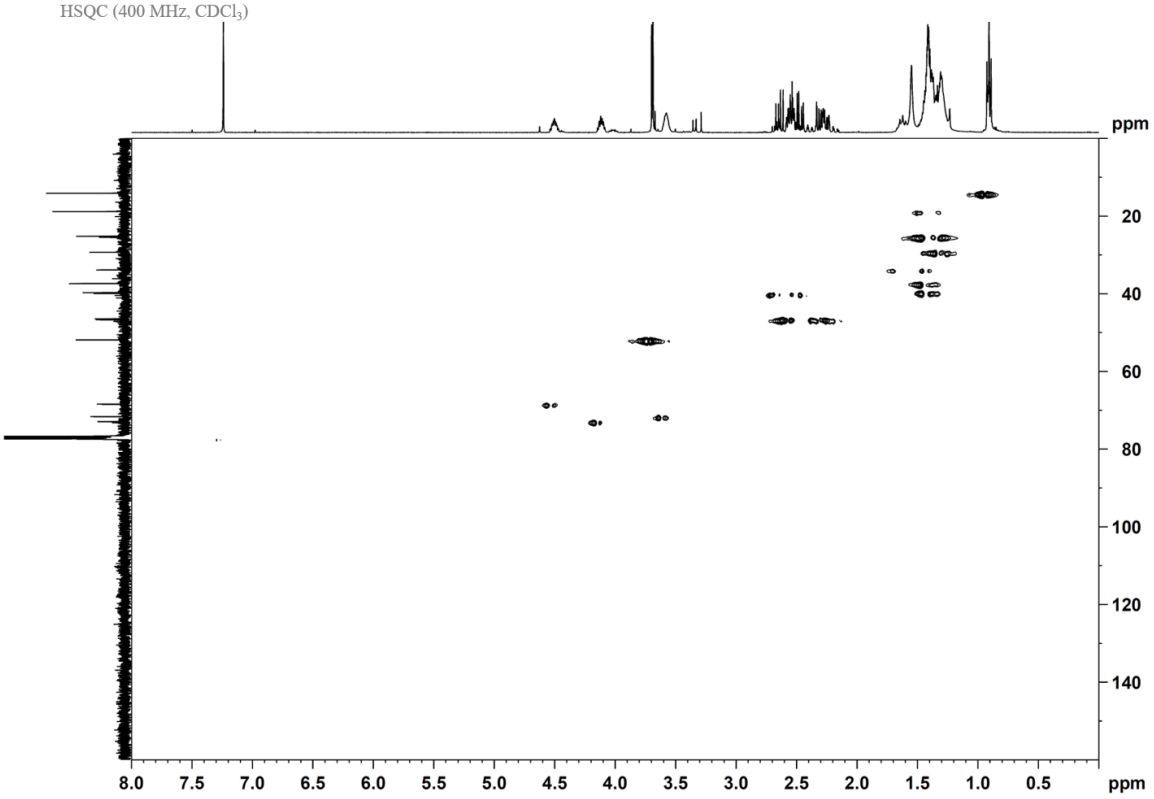

S1.3.6 Completion of Second-Generation α,β-Unsaturated Ketone Model (§ 4.5.2)

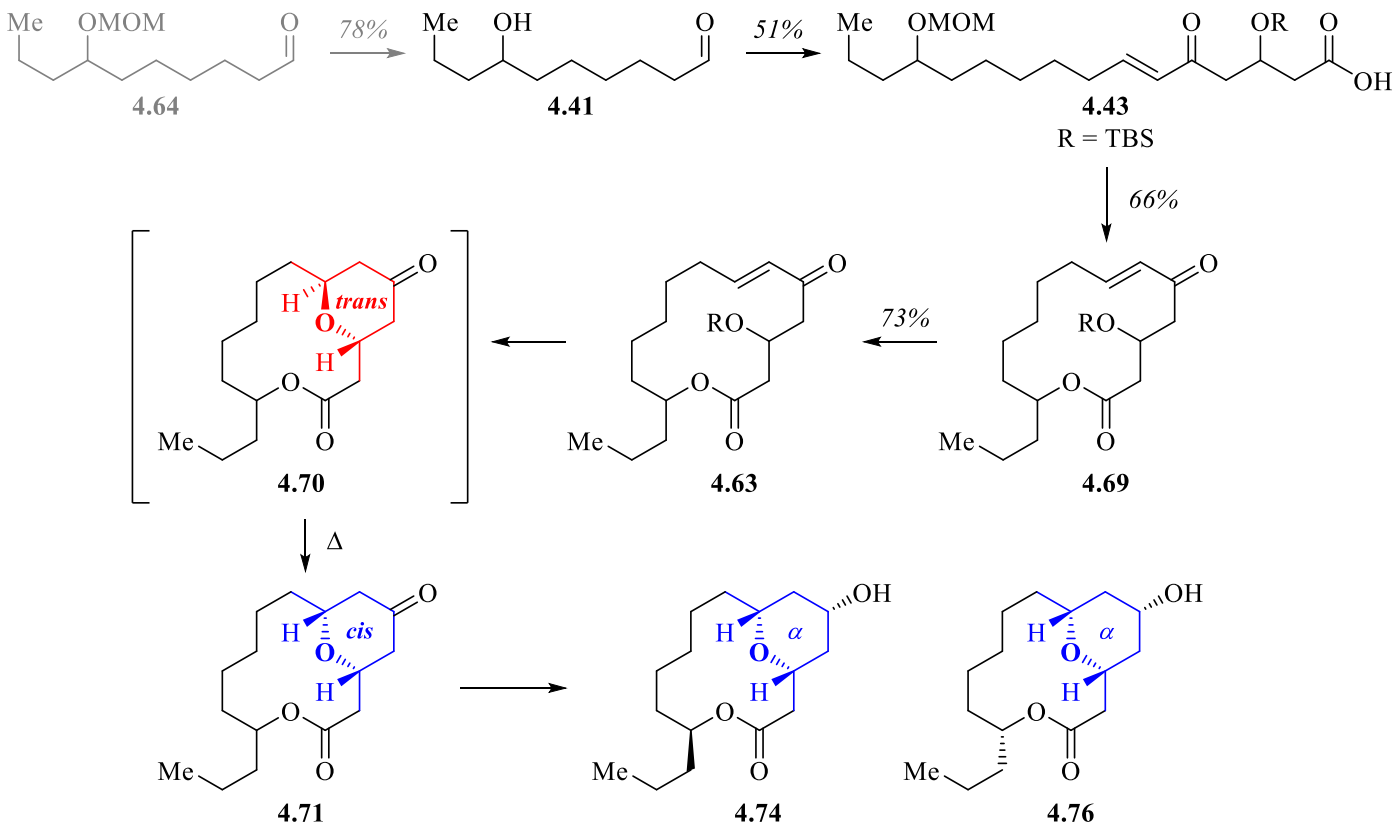

Figure S11 – Completion of second-generation *α,β*-unsaturated ketone model demonstrates transannular oxa-conjugate addition generates pyranyl products. Kinetic *trans*-pyranone mixture is exclusively-converted to *cis*-pyranone by thermodynamic equilibration.

(*E*)-3-(*tert*-Butyldimethylsilyloxy)-13-hydroxy-5-oxohexadec-6-enoic acid (**4.43**)

^{1}H NMR (300 MHz, $CDCl_3$)

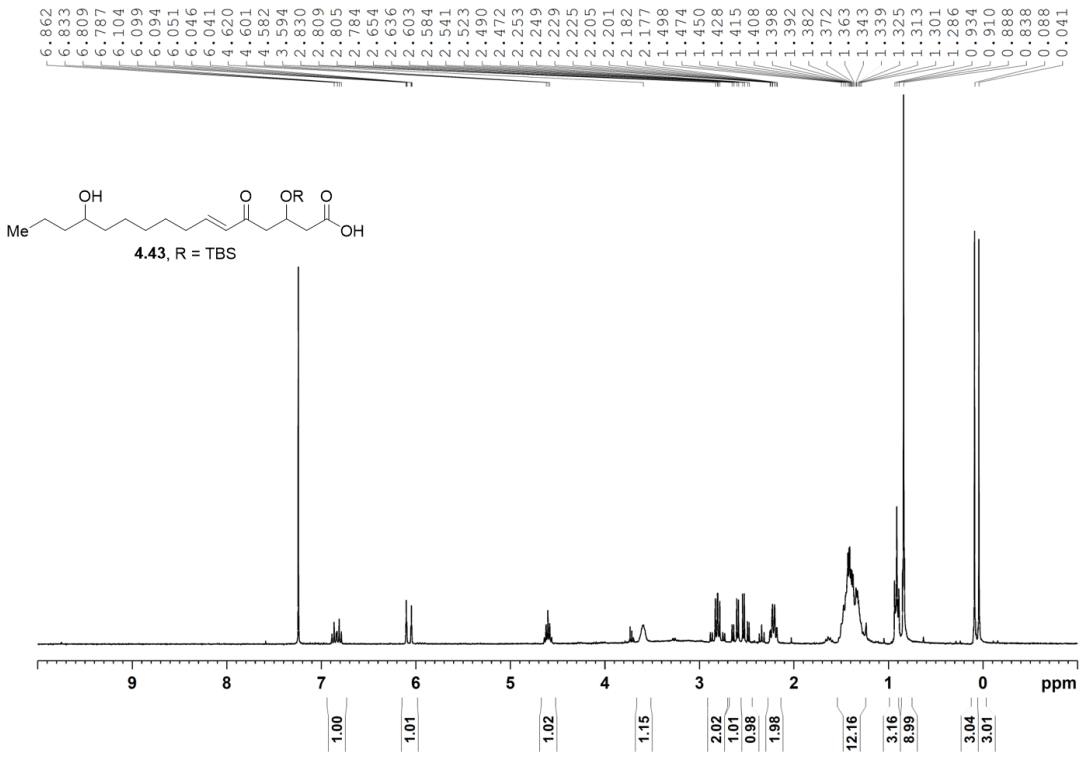

(*E*)-3-(*tert*-Butyldimethylsilyloxy)-13-hydroxy-5-oxohexadec-6-enoic acid (**4.43**)

^{13}C NMR (75 MHz, $CDCl_3$)

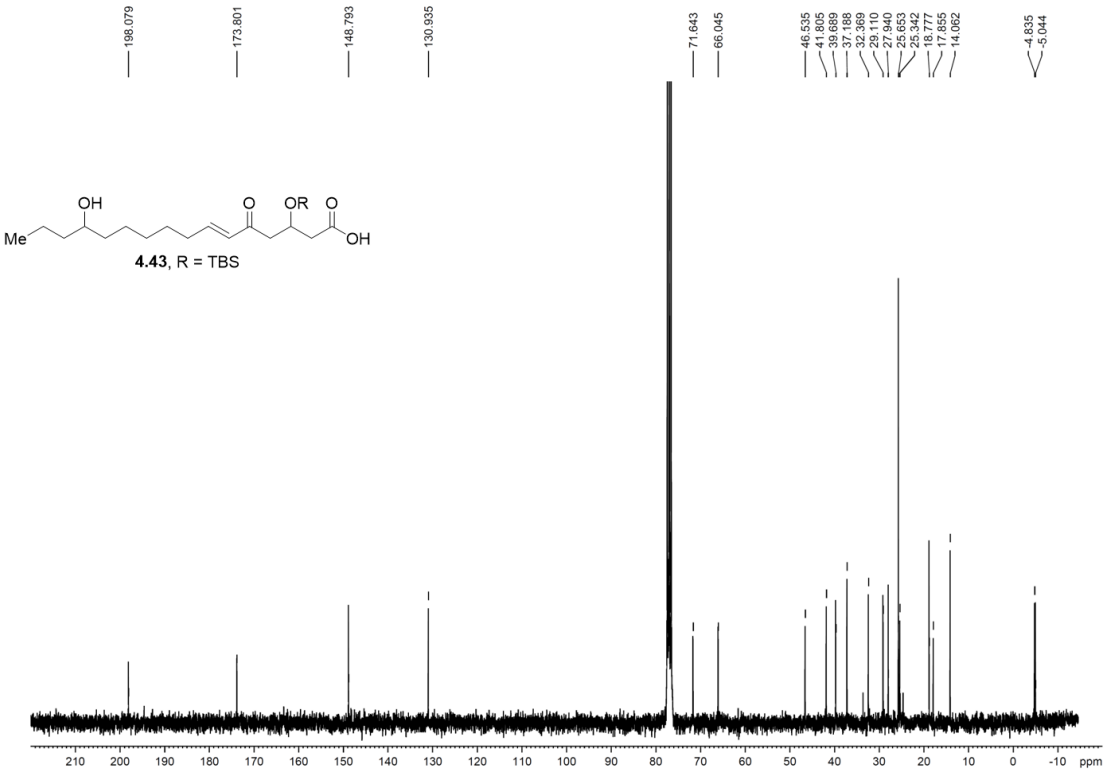

(*E*)-3-(*tert*-Butyldimethylsilyloxy)-13-hydroxy-5-oxohexadec-6-enoic acid (**4.43**)

COSY (300 MHz, $CDCl_3$)

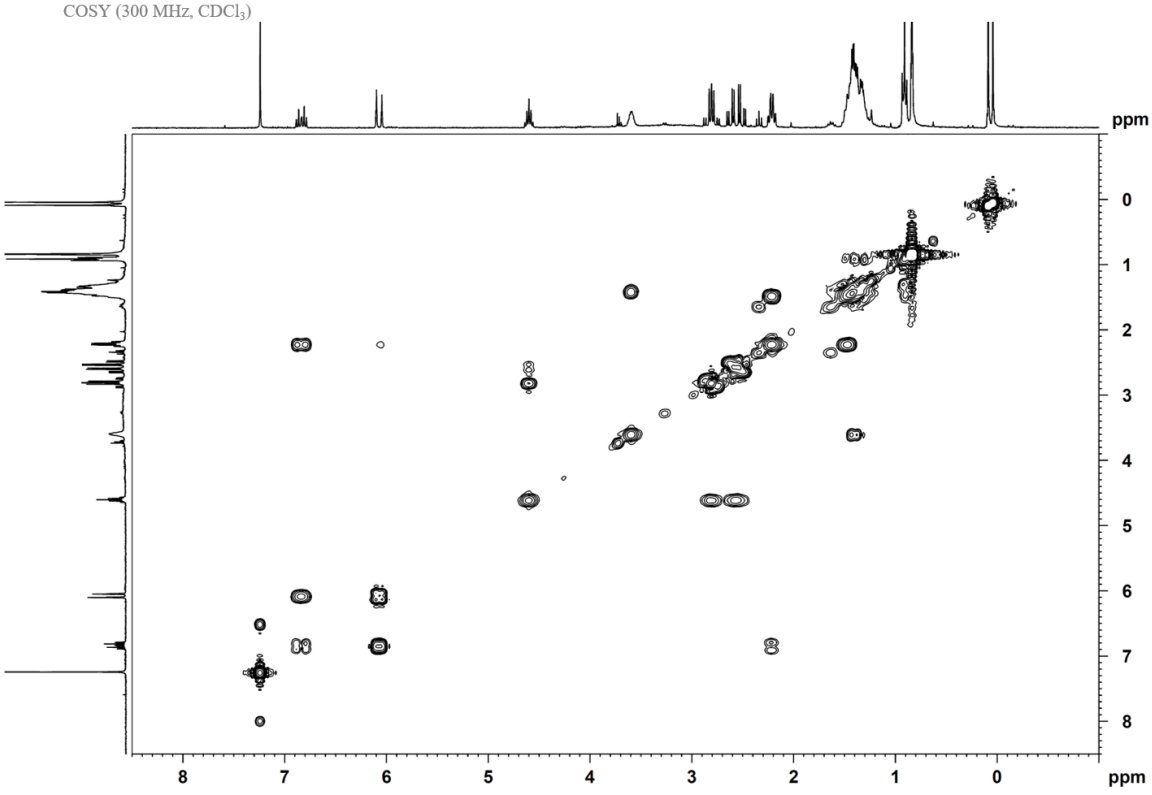

(*E*)-3-(*tert*-Butyldimethylsilyloxy)-13-hydroxy-5-oxohexadec-6-enoic acid (**4.43**)

HSQC (300 MHz, $CDCl_3$)

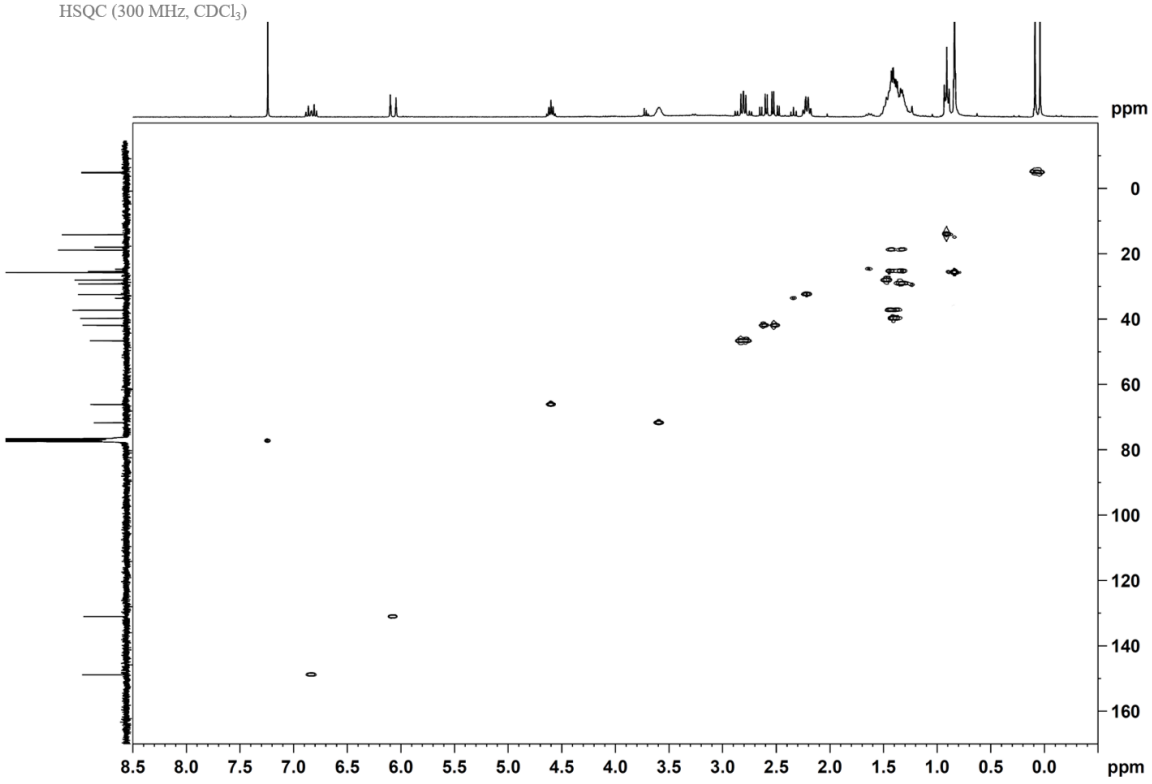

(*E*)-4-(*tert*-Butyldimethylsilyloxy)-14-propyloxacyclotetradec-7-ene-2,6-dione (**4.69**)

^{1}H NMR (300 MHz, $CDCl_3$)

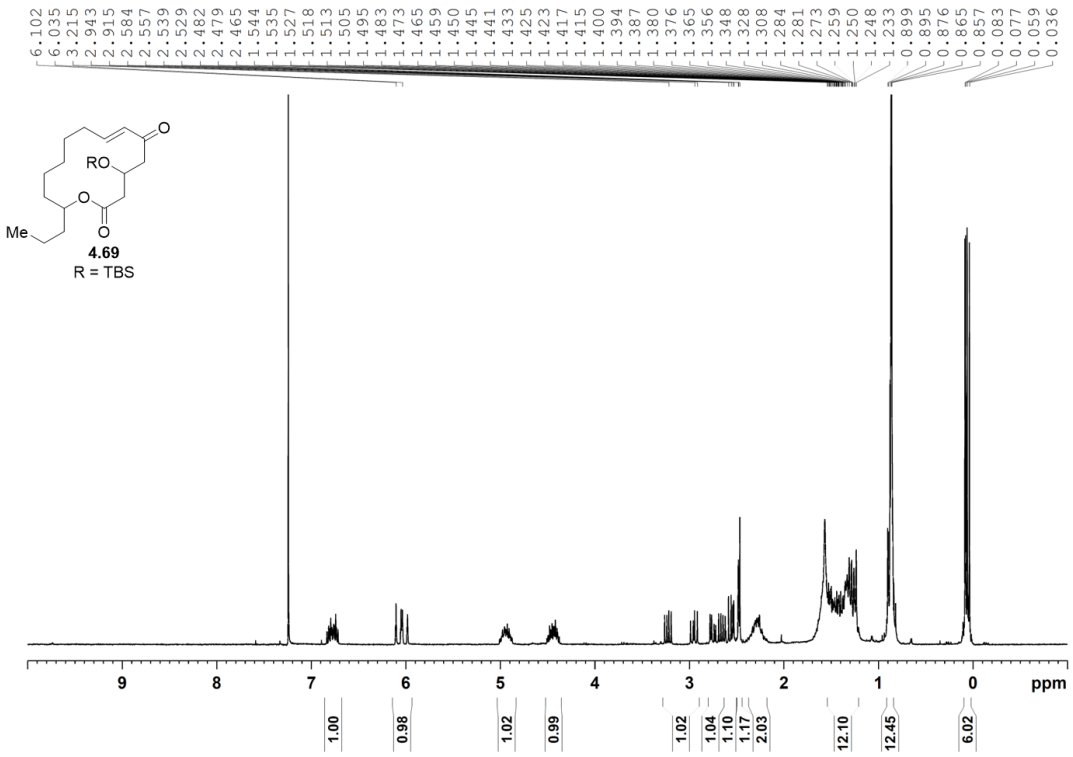

(*E*)-4-(*tert*-Butyldimethylsilyloxy)-14-propyloxacyclotetradec-7-ene-2,6-dione (**4.69**)

^{13}C NMR (75 MHz, $CDCl_3$)

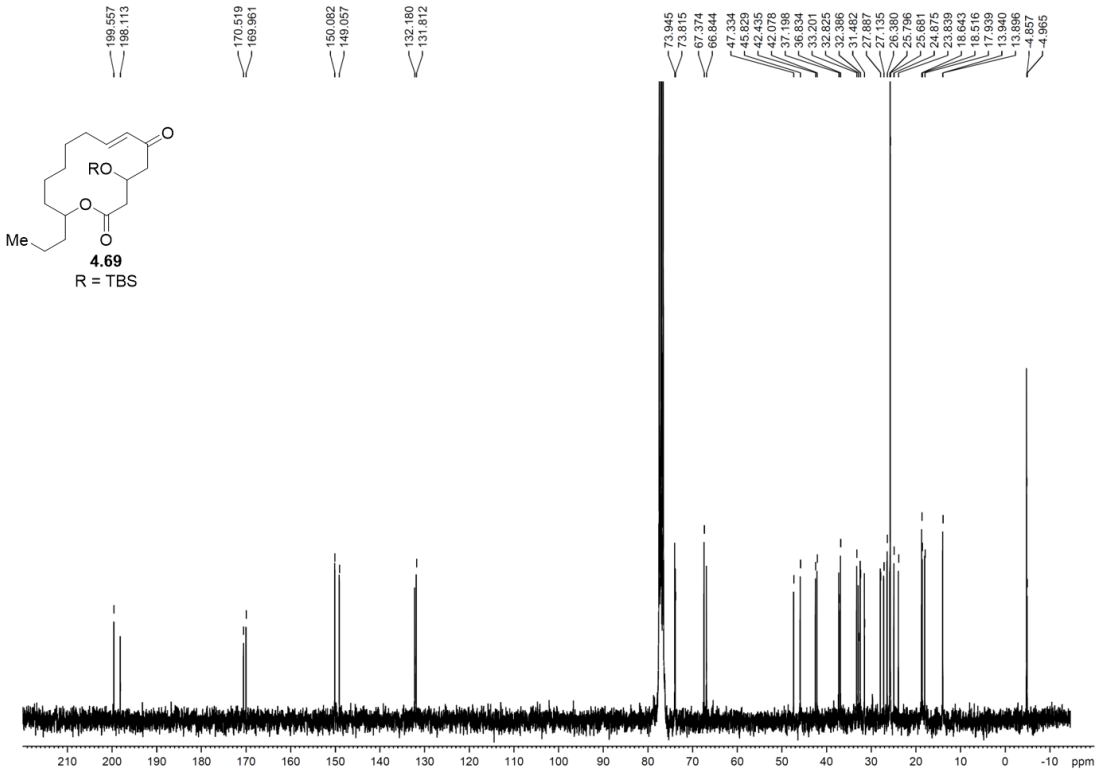

(*E*)-4-(*tert*-Butyldimethylsilyloxy)-14-propyloxacyclotetradec-7-ene-2,6-dione (**4.69**)

COSY (300 MHz, $CDCl_3$)

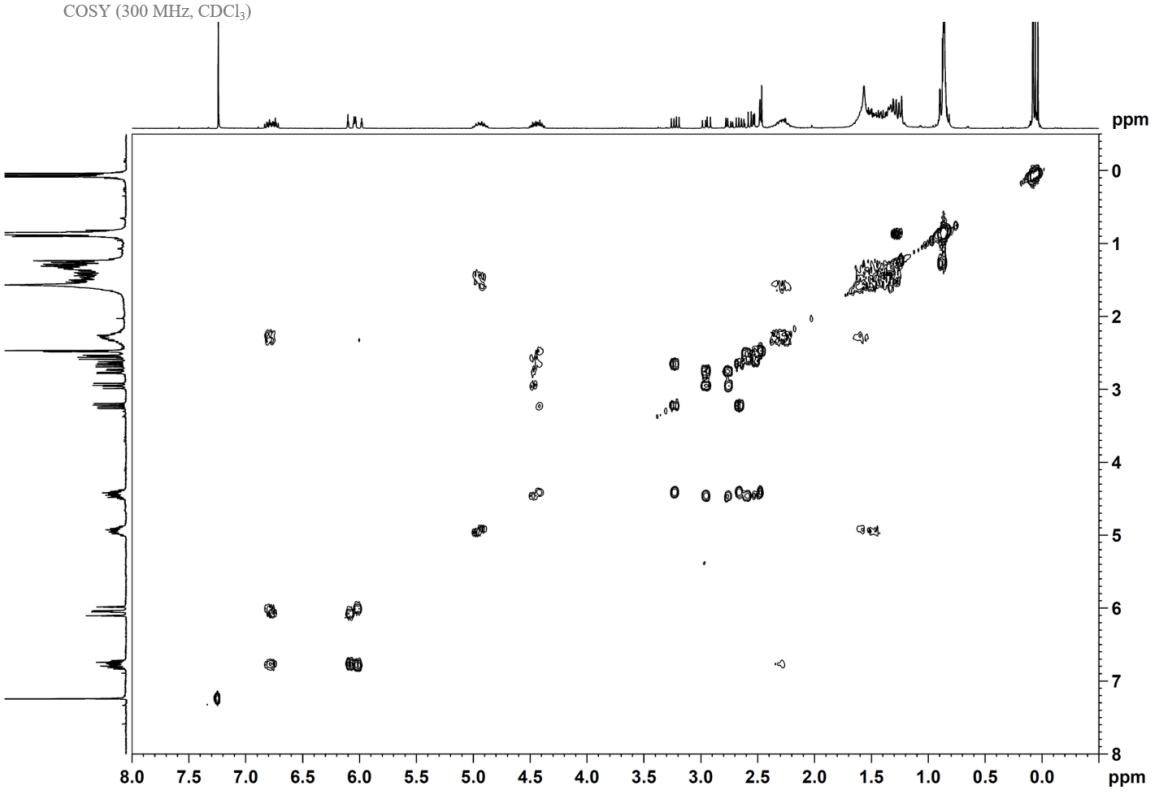

(*E*)-4-(*tert*-Butyldimethylsilyloxy)-14-propyloxacyclotetradec-7-ene-2,6-dione (**4.69**)

HSQC (300 MHz, $CDCl_3$)

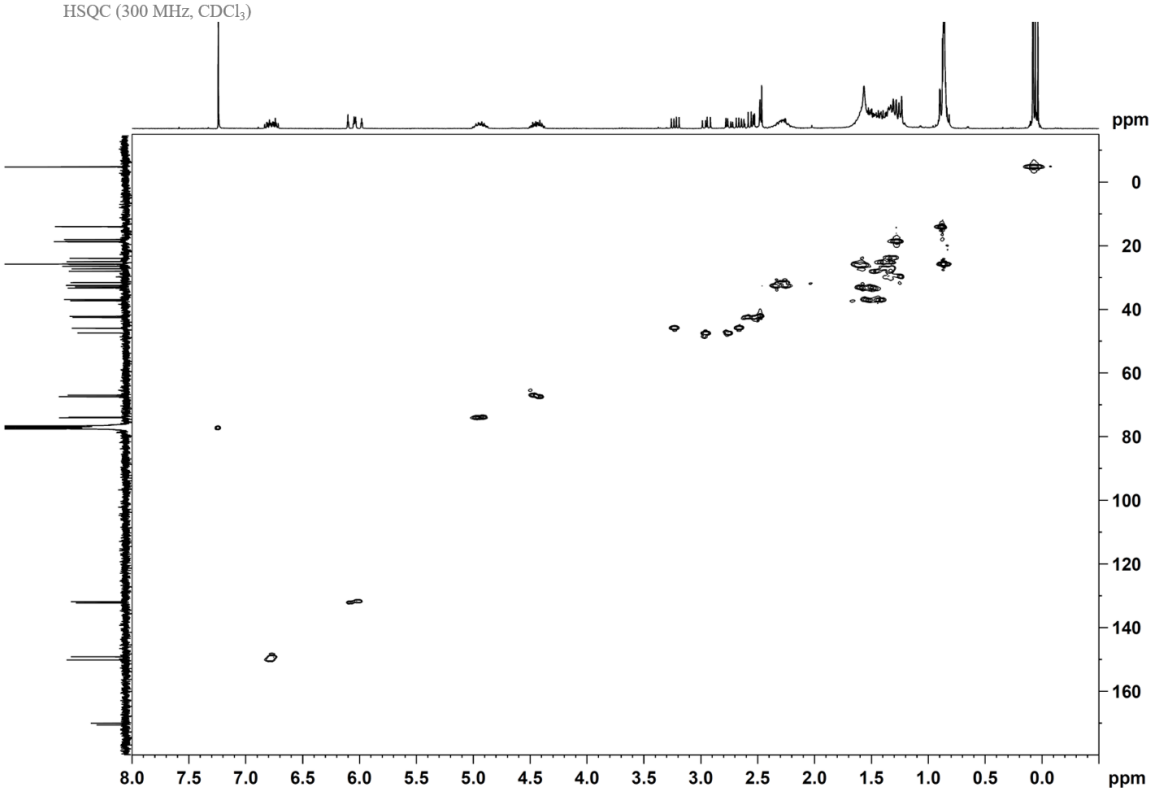

(*E*)-4-Hydroxy-14-propyloxacyclotetradec-7-ene-2,6-dione (**4.63**)

^{1}H NMR (600 MHz, $CDCl_3$)

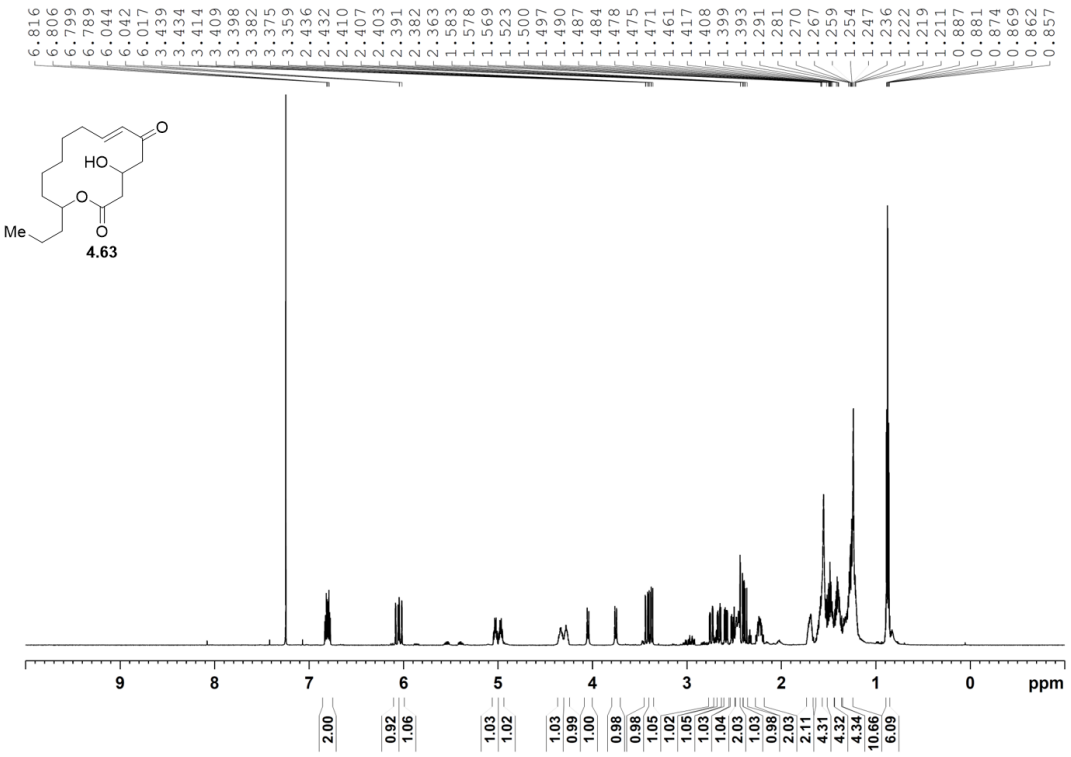

(*E*)-4-Hydroxy-14-propyloxacyclotetradec-7-ene-2,6-dione (**4.63**)

^{13}C NMR (150 MHz, $CDCl_3$)

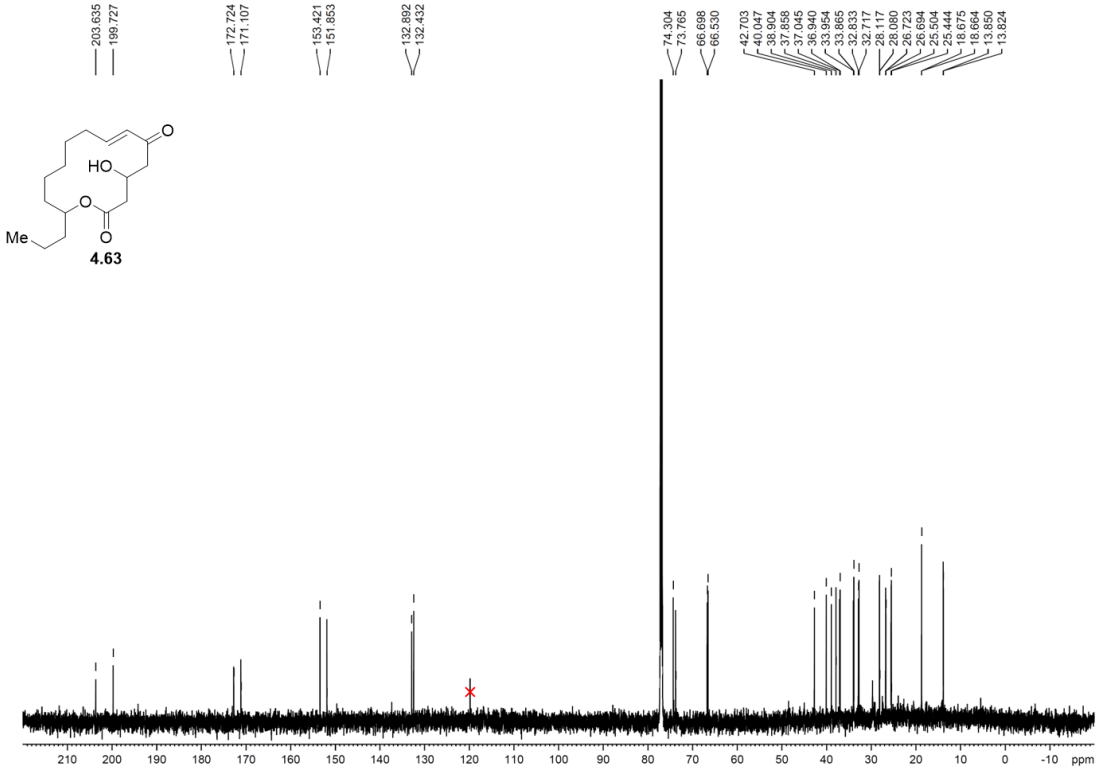

(*E*)-4-Hydroxy-14-propyloxacyclotetradec-7-ene-2,6-dione (**4.63**)

COSY (600 MHz, $CDCl_3$)

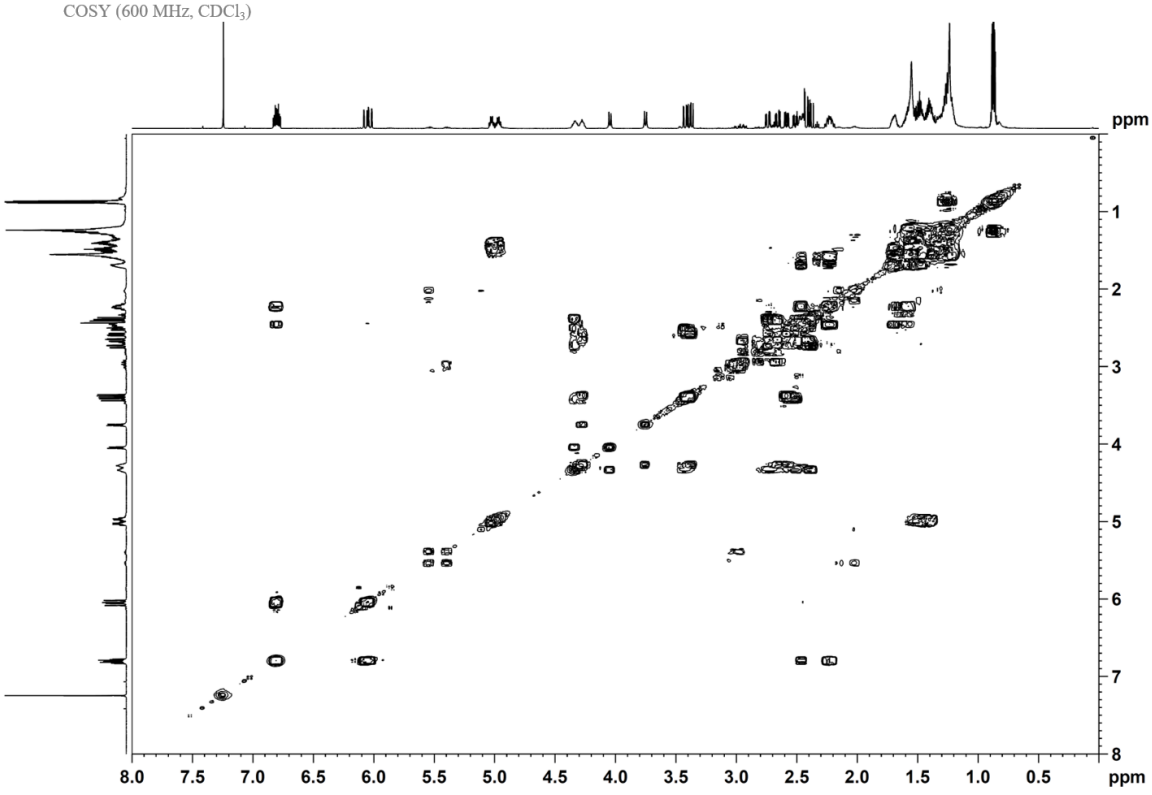

(*E*)-4-Hydroxy-14-propyloxacyclotetradec-7-ene-2,6-dione (**4.63**)

HSQC (600 MHz, $CDCl_3$)

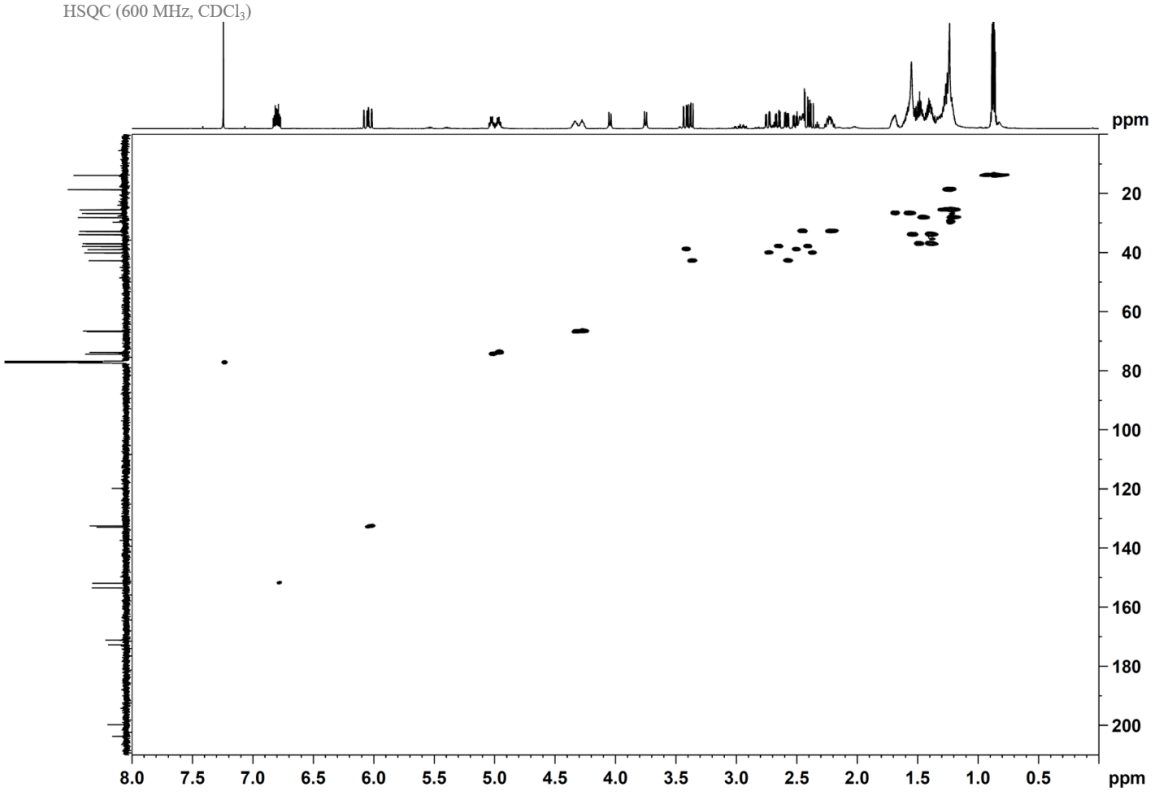

***trans*-5-Propyl-4,15-dioxabicyclo[9.3.1]pentadecane-3,13-dione (4.70)**

^{1}H NMR (600 MHz, $CDCl_3$)

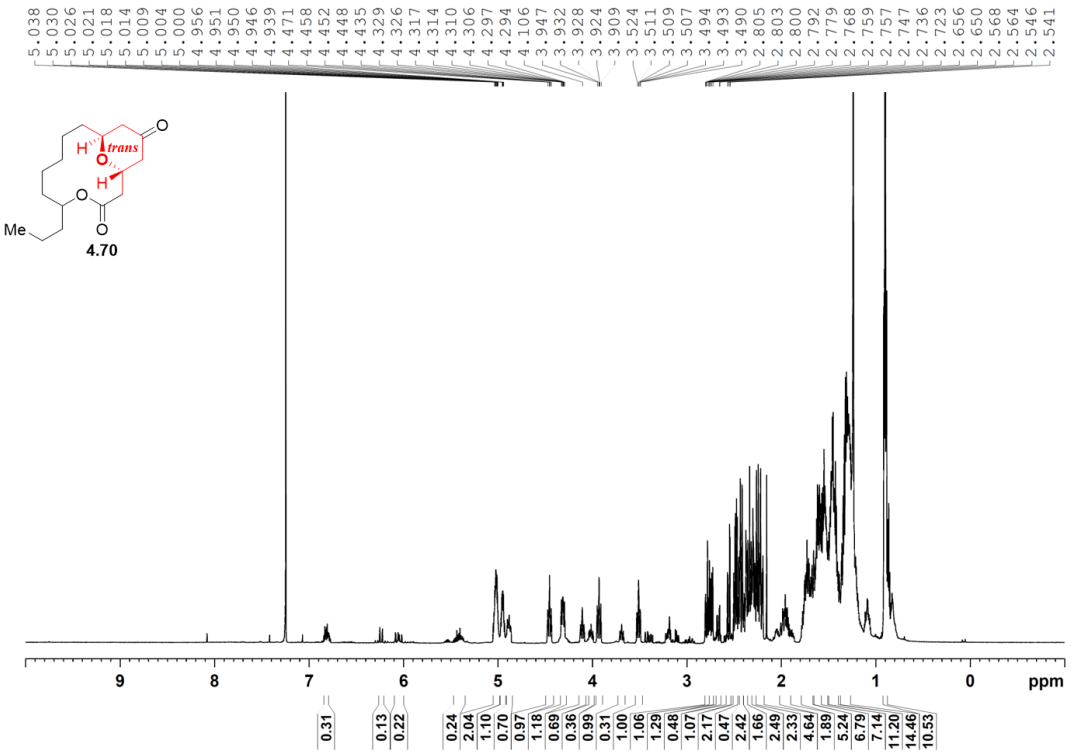

***trans*-5-Propyl-4,15-dioxabicyclo[9.3.1]pentadecane-3,13-dione (4.70)**

^{1}H NMR (600 MHz, $CDCl_3$)

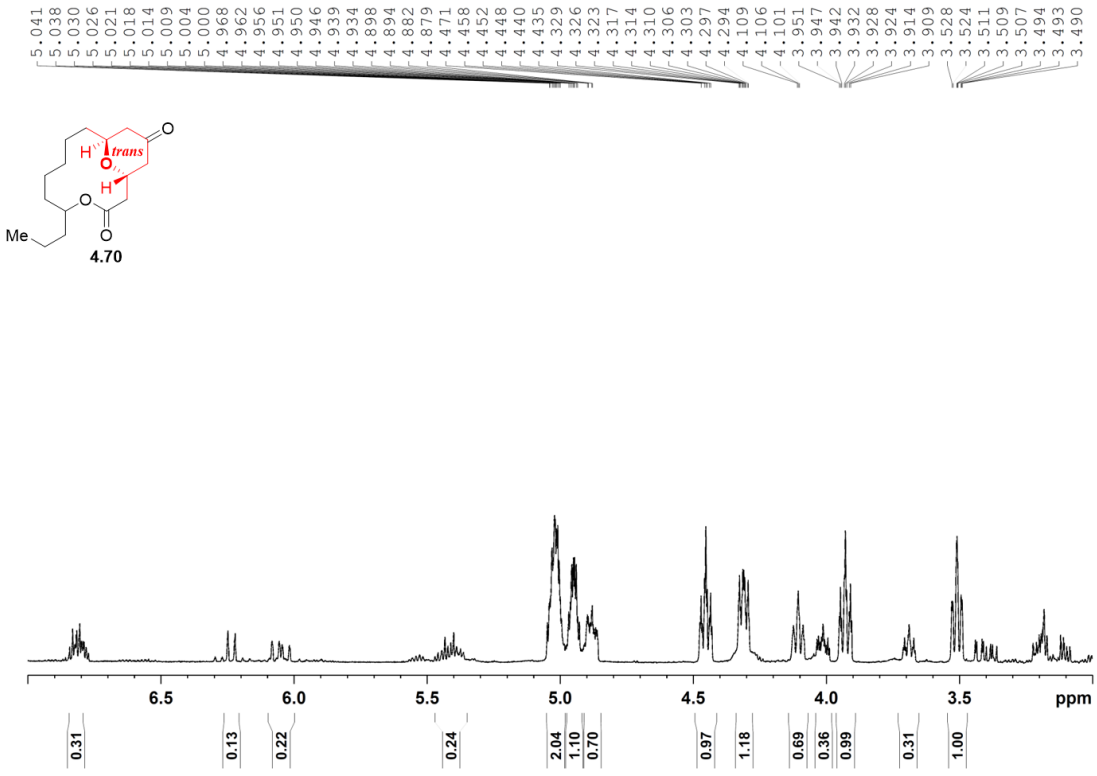

***trans*-5-Propyl-4,15-dioxabicyclo[9.3.1]pentadecane-3,13-dione (4.70)**

^{13}C NMR (150 MHz, $CDCl_3$)

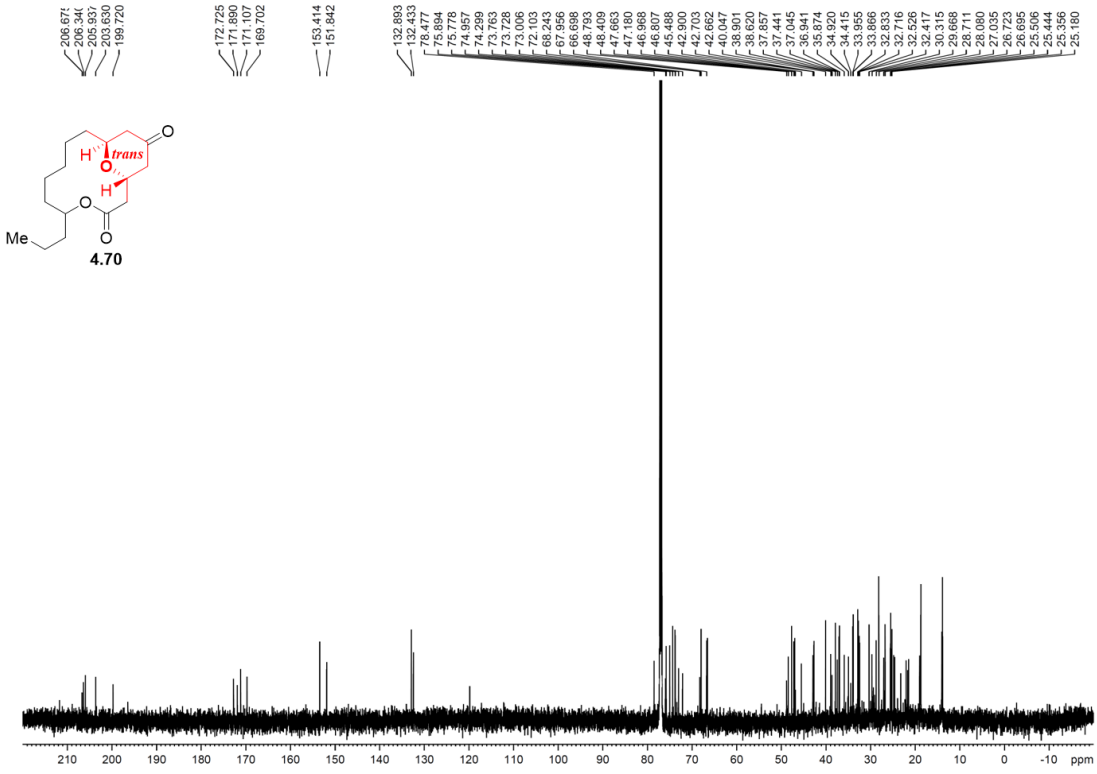

***trans*-5-Propyl-4,15-dioxabicyclo[9.3.1]pentadecane-3,13-dione (4.70)**

COSY (600 MHz, $CDCl_3$)

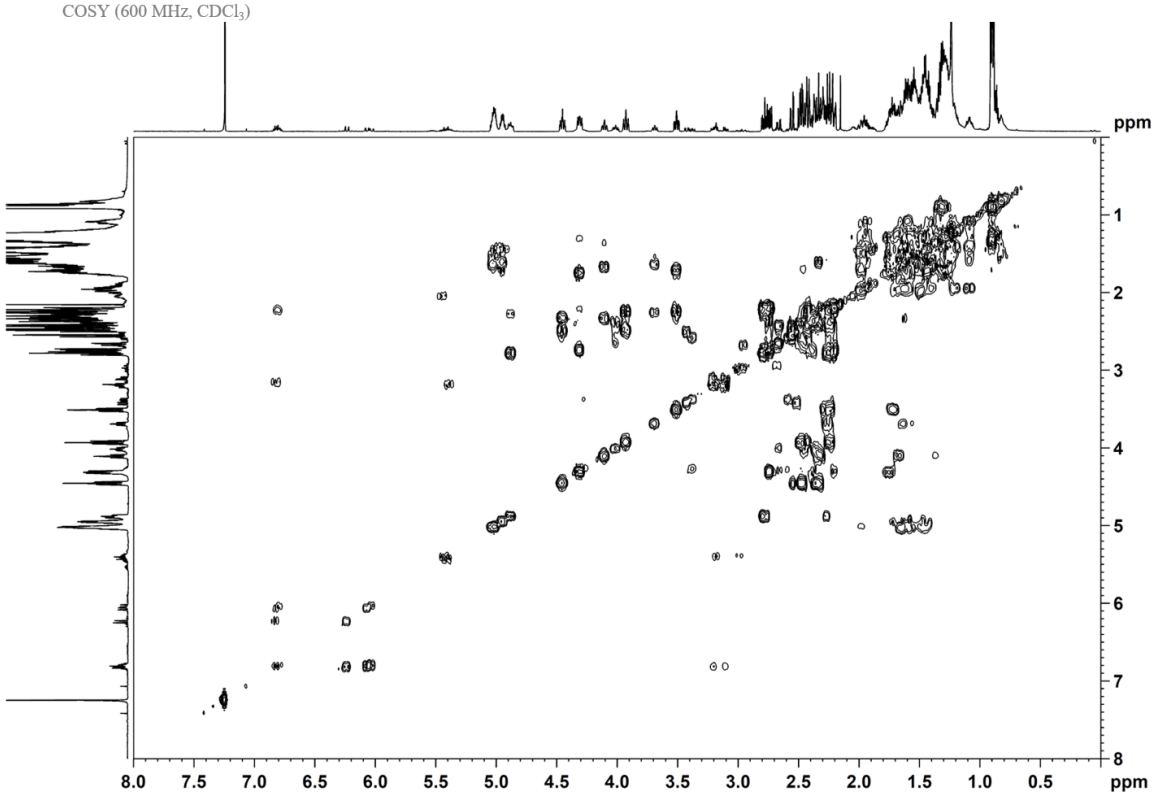

***cis*-5-Propyl-4,15-dioxabicyclo[9.3.1]pentadecane-3,13-dione (4.71)**

^{1}H NMR (600 MHz, $CDCl_3$)

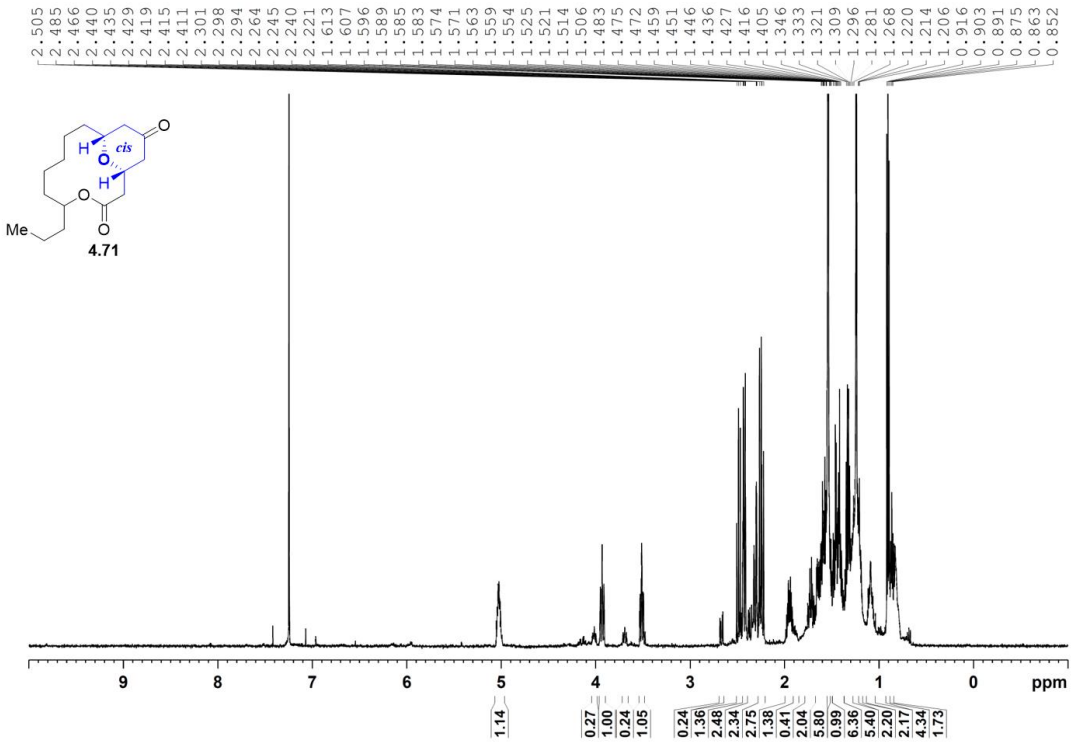

***cis*-5-Propyl-4,15-dioxabicyclo[9.3.1]pentadecane-3,13-dione (4.71)**

^{13}C NMR (150 MHz, $CDCl_3$)

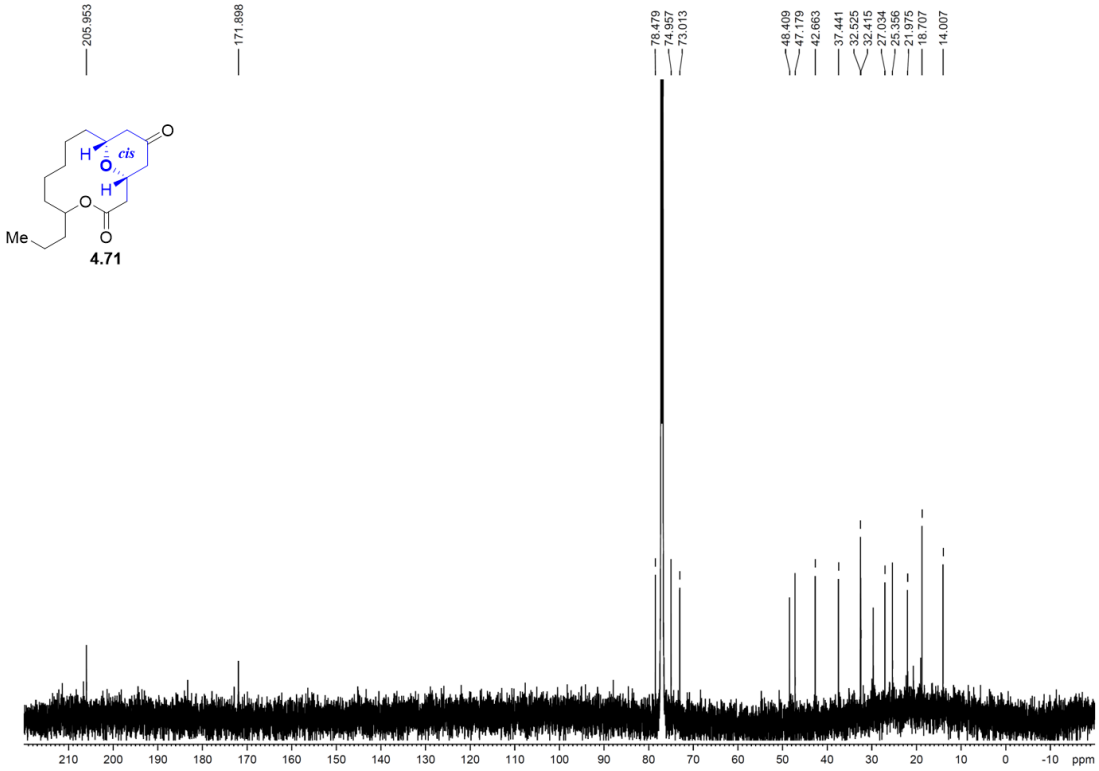

***cis*-5-Propyl-4,15-dioxabicyclo[9.3.1]pentadecane-3,13-dione (4.71)**

COSY (600 MHz, $CDCl_3$)

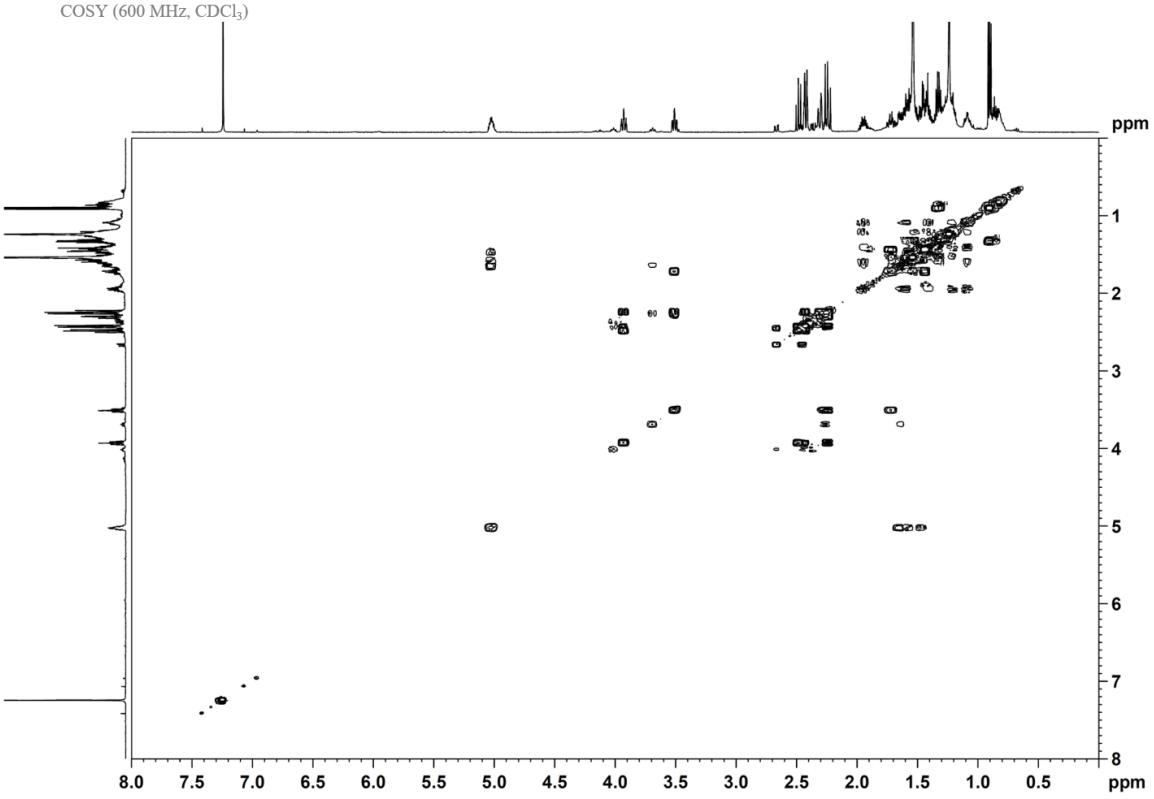

***cis*-5-Propyl-4,15-dioxabicyclo[9.3.1]pentadecane-3,13-dione (4.71)**

HSQC (600 MHz, $CDCl_3$)

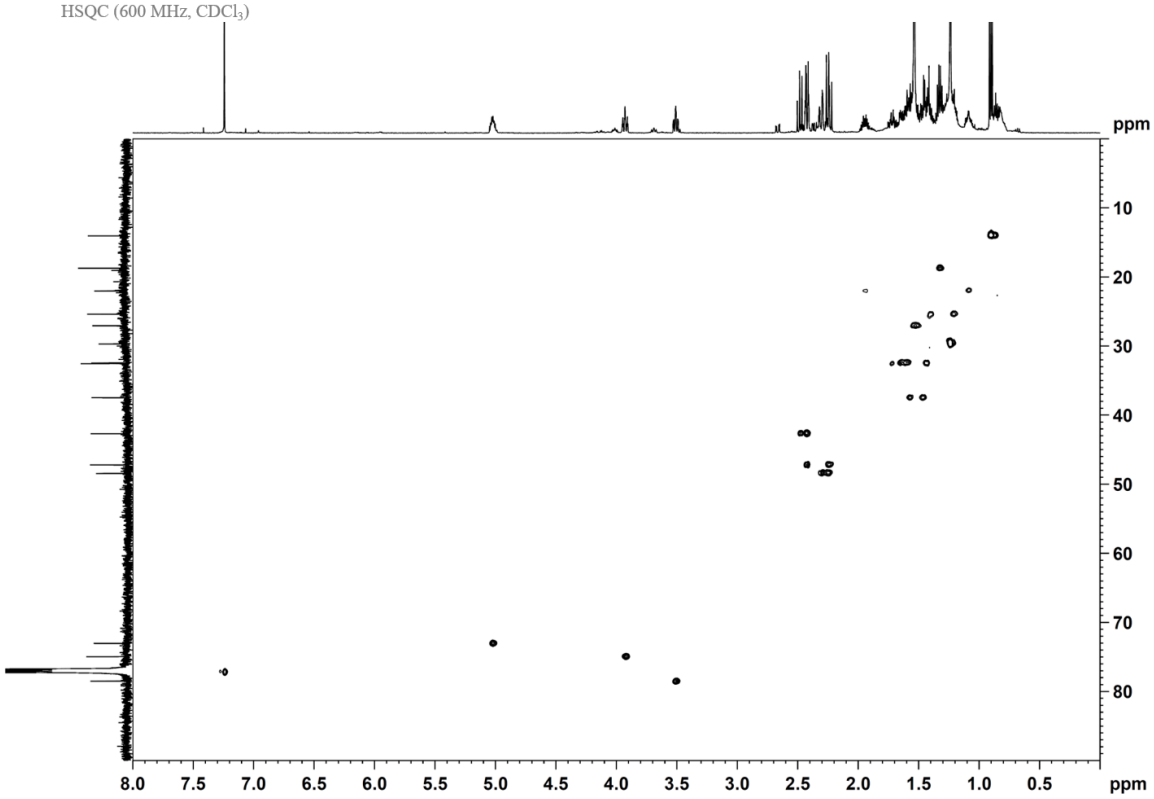

cis-5-Propyl-4,15-dioxabicyclo[9.3.1]pentadecane-3,13-dione (**4.71**)

2D NOESY (600 MHz, $CDCl_3$)

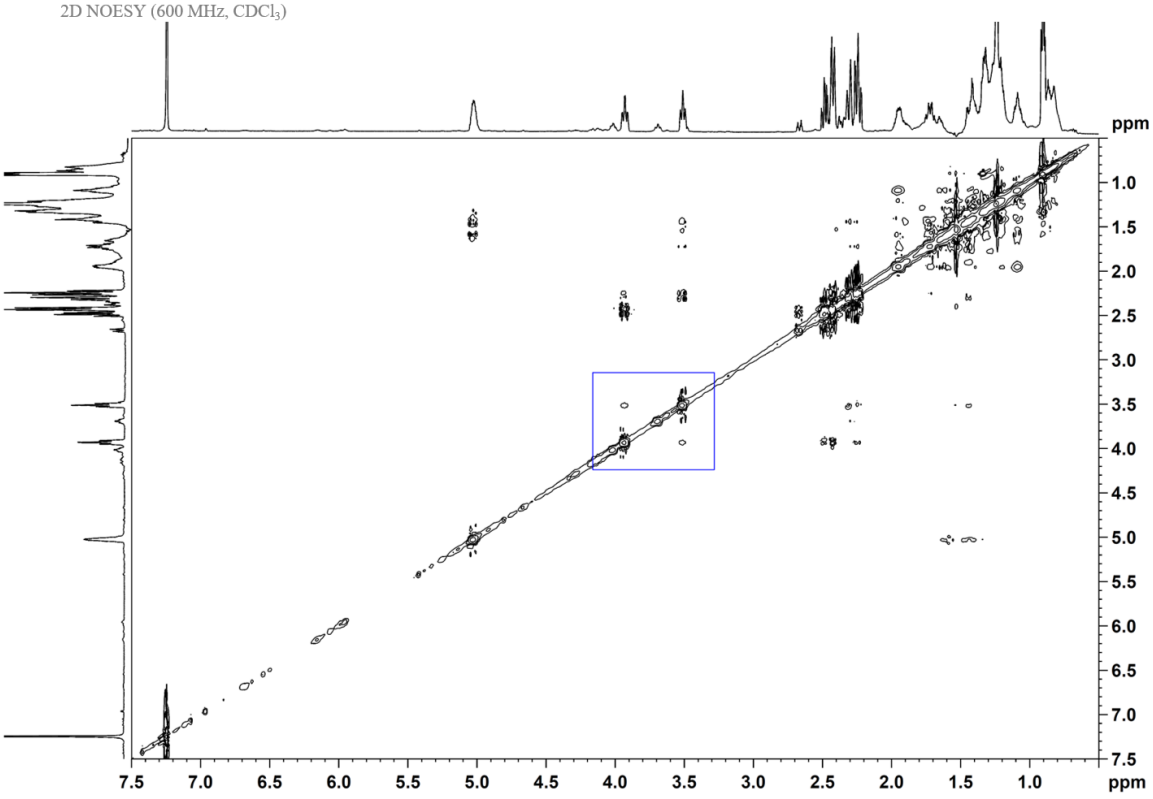

cis-5-Propyl-4,15-dioxabicyclo[9.3.1]pentadecane-3,13-dione (**4.71**)

1D Selective Gradient NOESY (600 MHz, $CDCl_3$)

δ 5.03 ppm (***H13***)

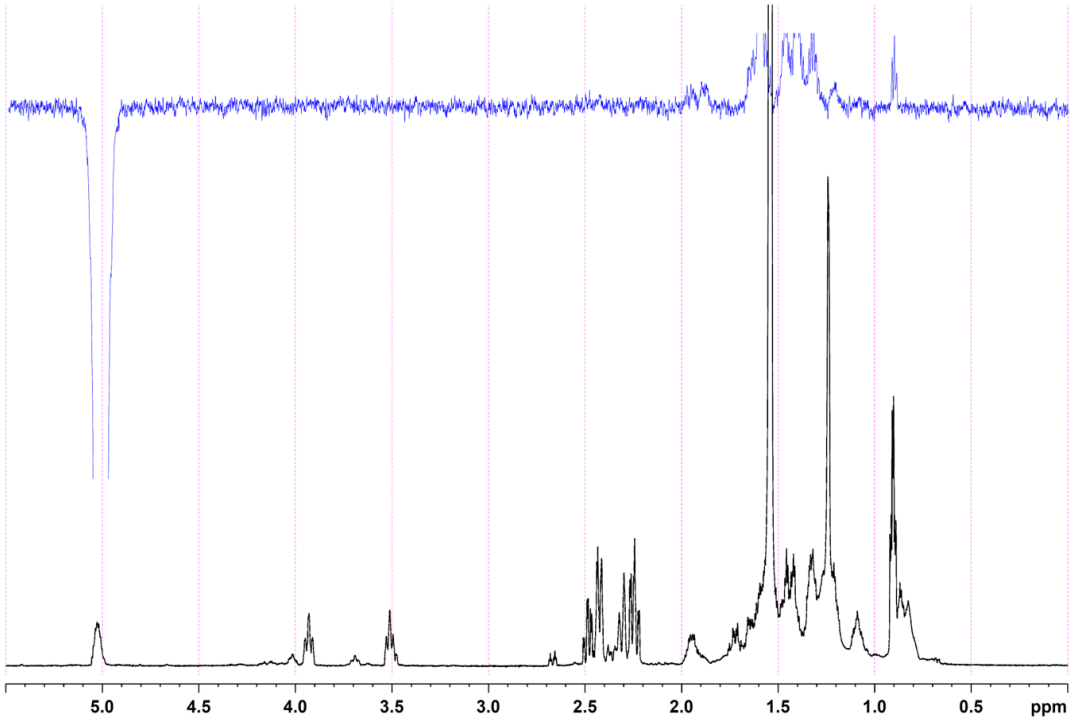

cis-5-Propyl-4,15-dioxabicyclo[9.3.1]pentadecane-3,13-dione (**4.71**)
1D Selective Gradient NOESY (600 MHz, $CDCl_3$)
δ 3.93 ppm (***H3***)

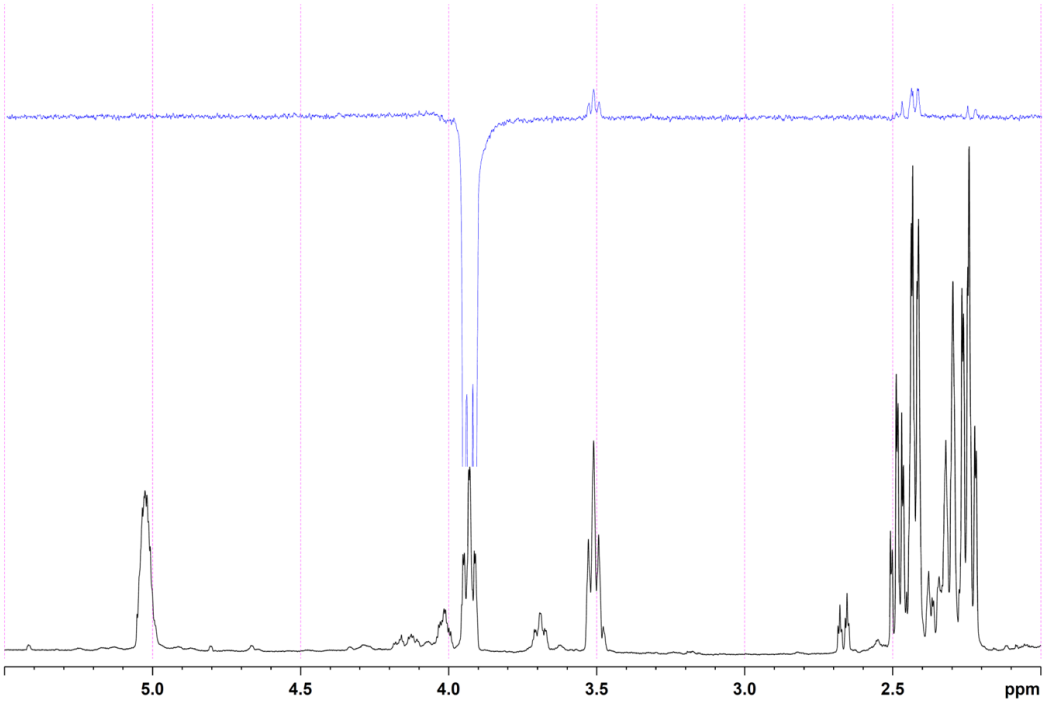

cis-5-Propyl-4,15-dioxabicyclo[9.3.1]pentadecane-3,13-dione (**4.71**)
1D Selective Gradient NOESY (600 MHz, $CDCl_3$)
δ 3.51 ppm (***H7***)

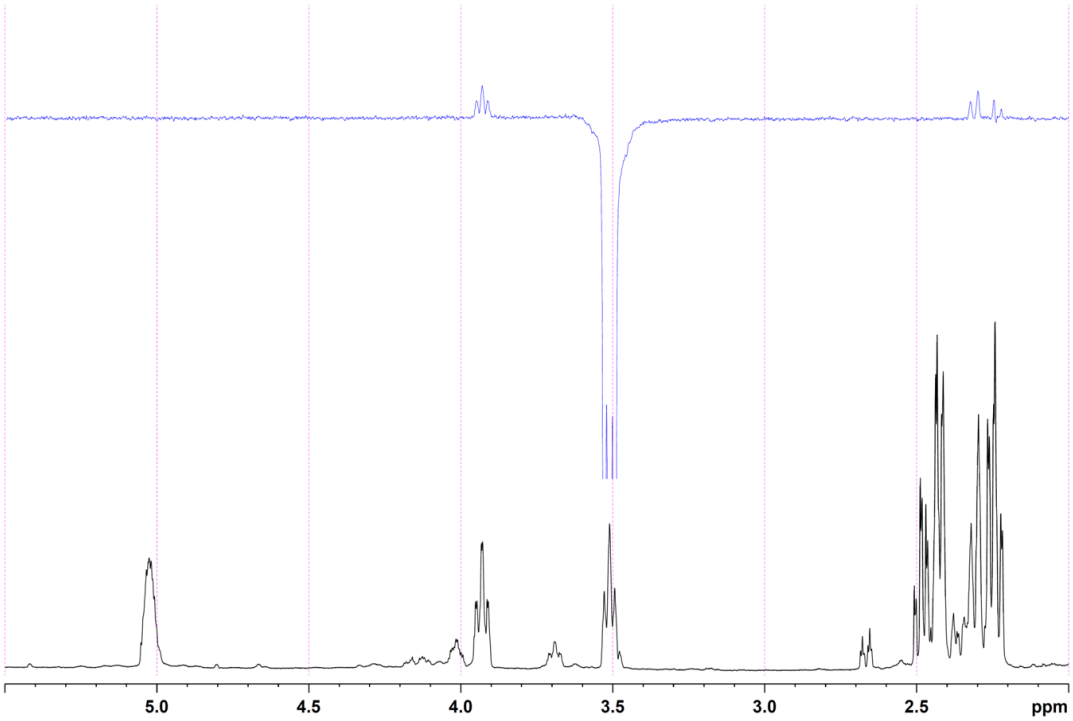

α-cis-13-Hydroxy-5-propyl-4,15-dioxabicyclo[9.3.1]pentadecan-3-one (mixture of C13-epimers, **4.74/4.76**)

^{1}H NMR (600 MHz, $CDCl_3$)

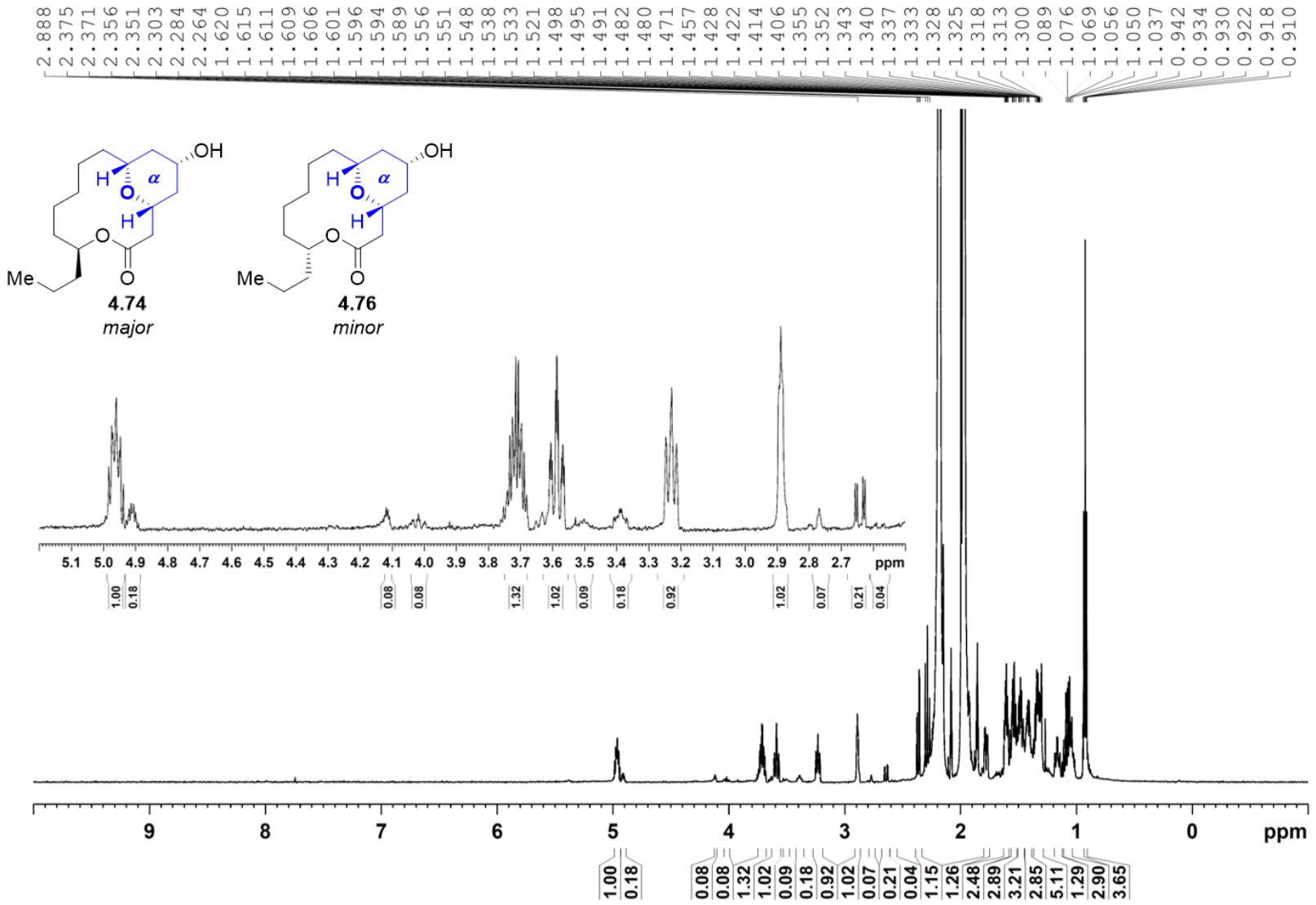

α-cis-13-Hydroxy-5-propyl-4,15-dioxabicyclo[9.3.1]pentadecan-3-one (mixture of C13-epimers, **4.74**/**4.76**)

COSY (600 MHz, $CDCl_3$)

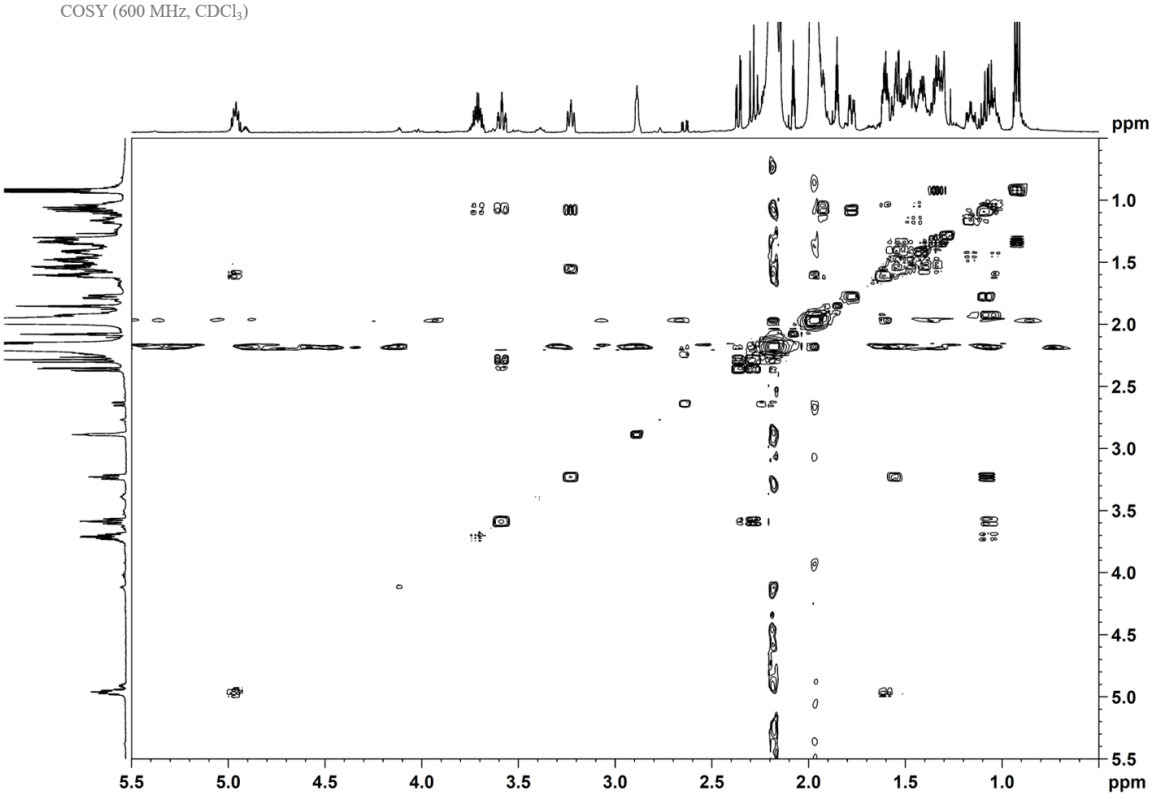

α-cis-13-Hydroxy-5-propyl-4,15-dioxabicyclo[9.3.1]pentadecan-3-one (**4.74**)

1D Selective Gradient NOESY (600 MHz, $CDCl_3$)

δ 4.981 ppm (***H13***)

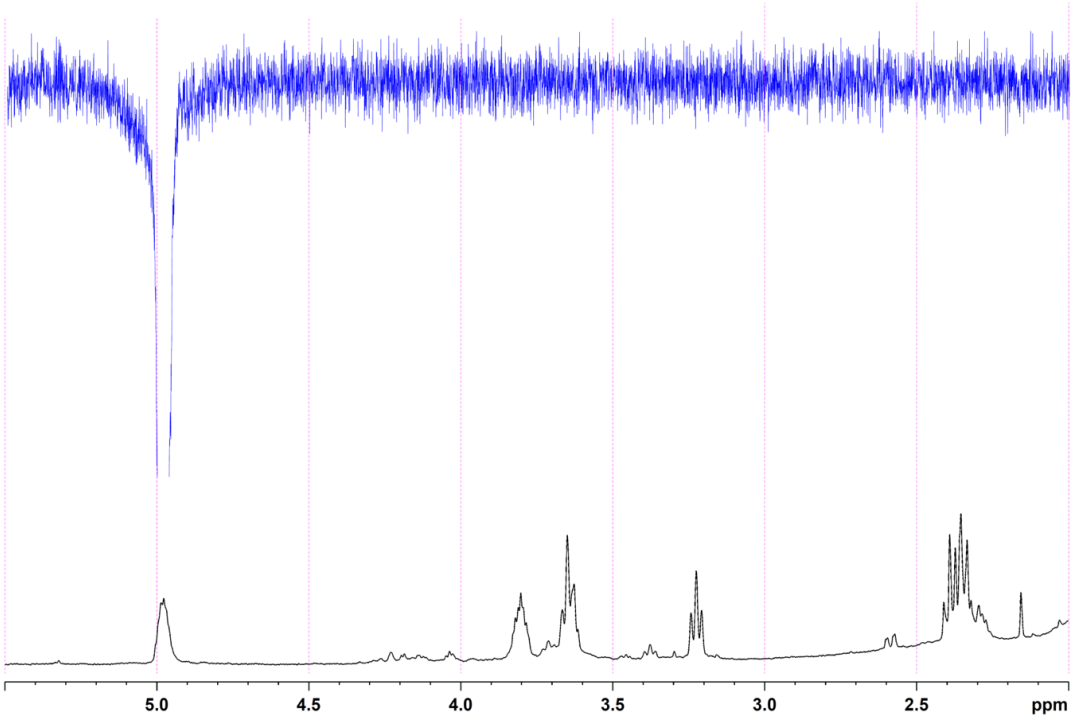

α-cis-13-Hydroxy-5-propyl-4,15-dioxabicyclo[9.3.1]pentadecan-3-one (**4.74**)
1D Selective Gradient NOESY (600 MHz, $CDCl_3$)
δ 3.811 ppm (***H3***)

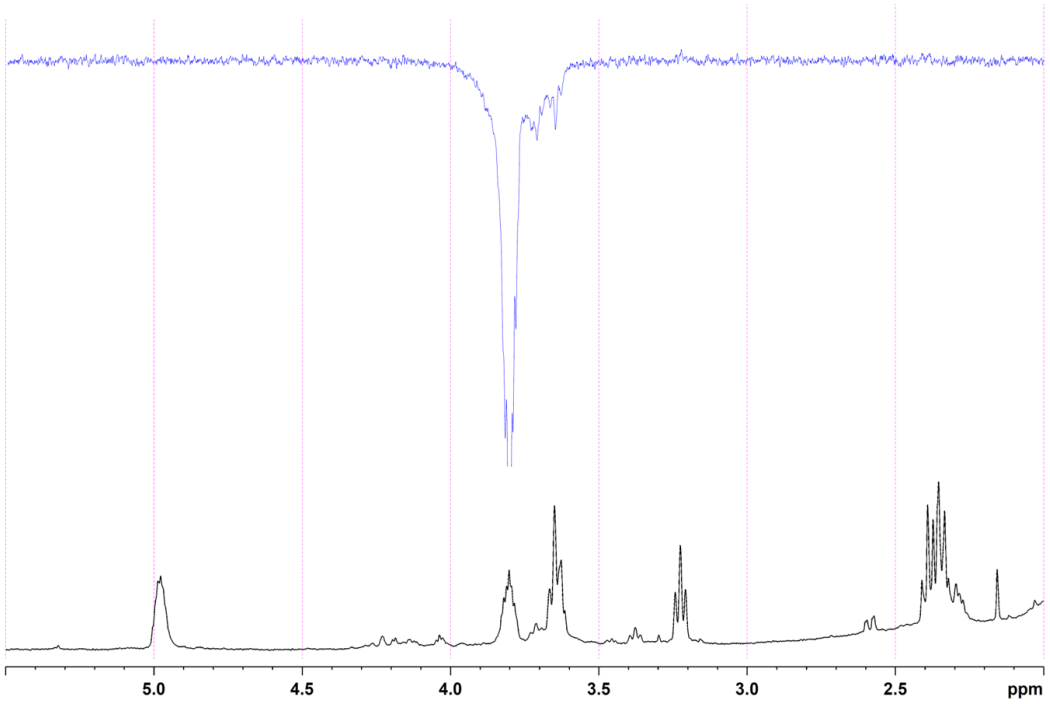

α-cis-13-Hydroxy-5-propyl-4,15-dioxabicyclo[9.3.1]pentadecan-3-one (**4.74**)
1D Selective Gradient NOESY (600 MHz, $CDCl_3$)
δ 3.649 ppm (***H5***)

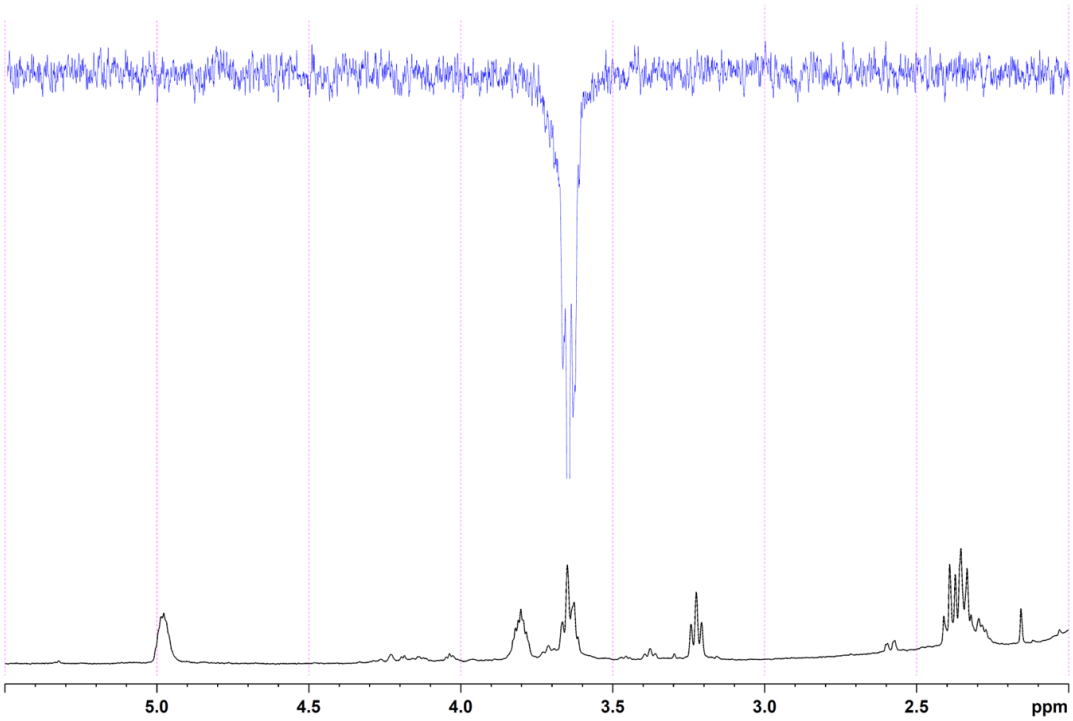

α-*cis*-13-Hydroxy-5-propyl-4,15-dioxabicyclo[9.3.1]pentadecan-3-one (**4.74**)

1D Selective Gradient NOESY (600 MHz, $CDCl_3$)

δ 3.225 ppm (***H7***)

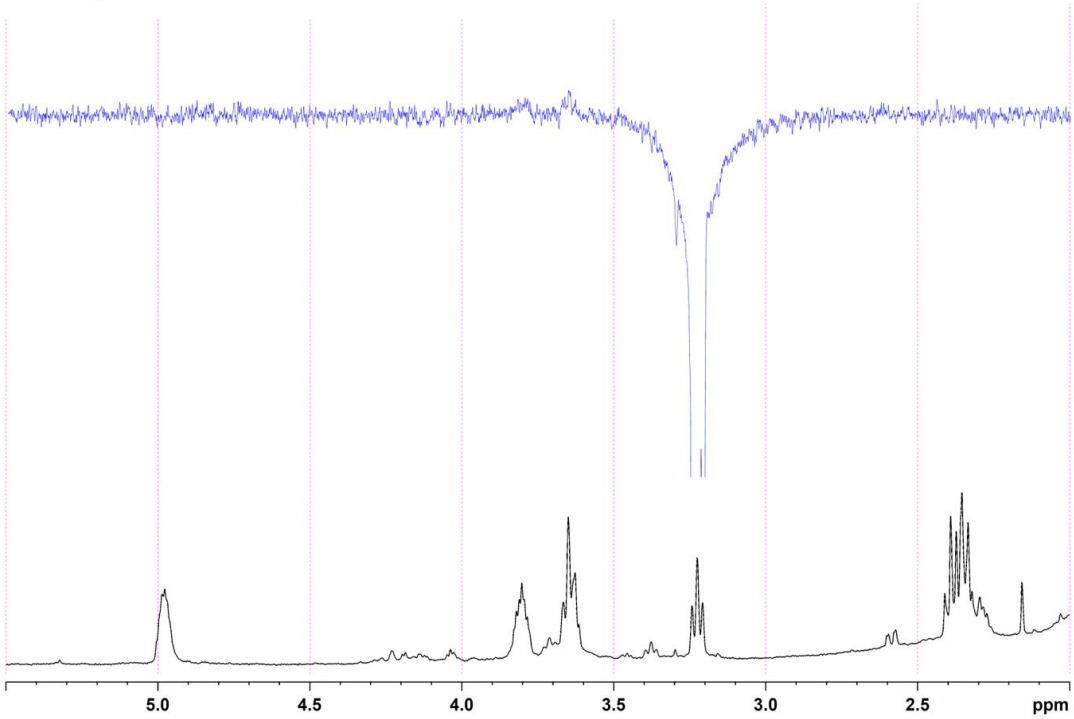

S1.3.7 Accessing Key Oxa-Conjugate Addition Precursors for the Neopeltolide Macrocyclic Core (§ 4.6.1)

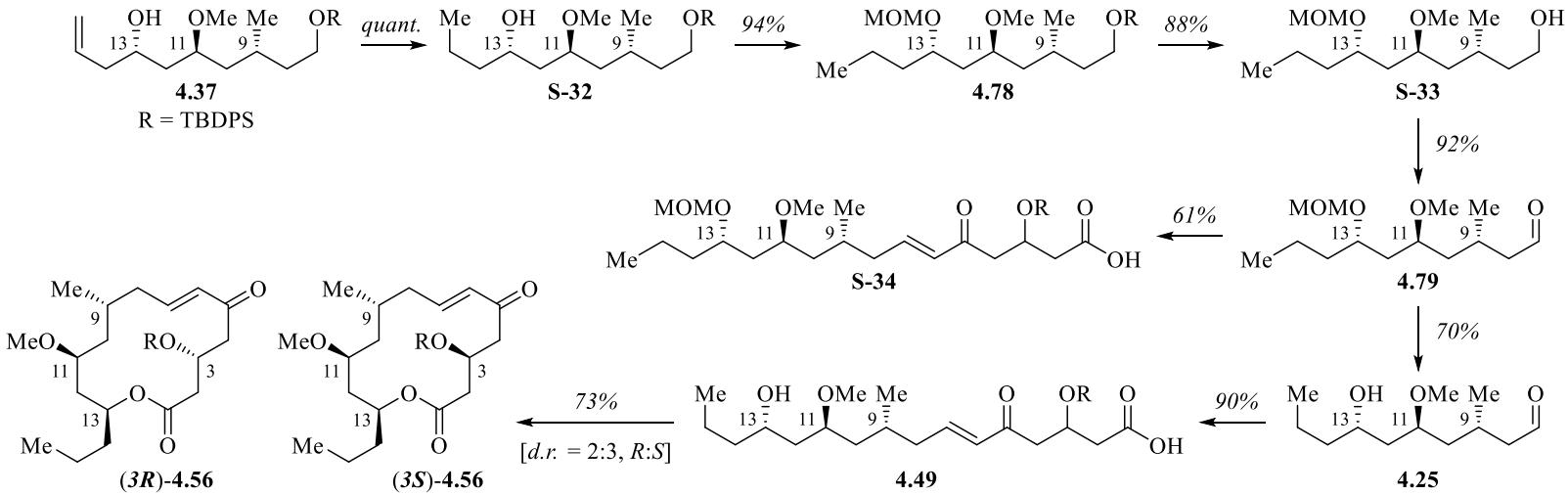

Figure S12 – Synthetic summary of C3-epimeric oxa-conjugate addition precursors to the macrocyclic core of neopeltolide.

(4*S*,6*S*,8*R*)-10-(*tert*-Butyldiphenylsilyloxy)-6-methoxy-8-methyldecan-4-ol (**S-32**)

^{1}H NMR (400 MHz, $CDCl_3$)

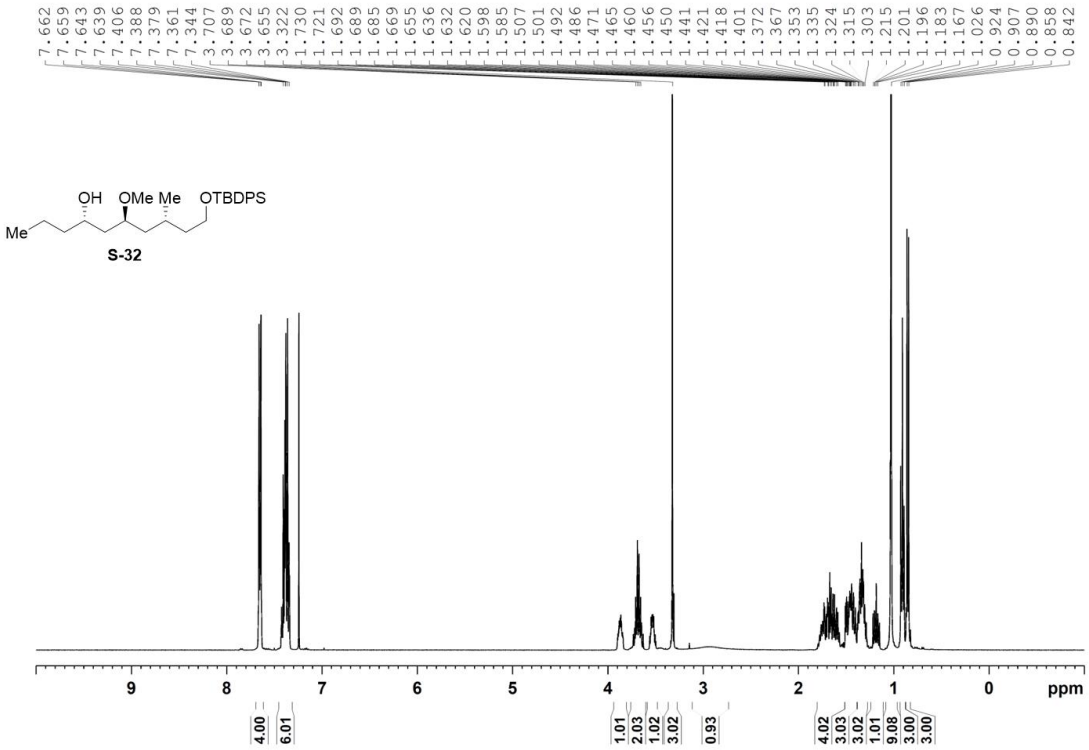

(4*S*,6*S*,8*R*)-10-(*tert*-Butyldiphenylsilyloxy)-6-methoxy-8-methyldecan-4-ol (**S-32**)

^{13}C NMR (150 MHz, $CDCl_3$)

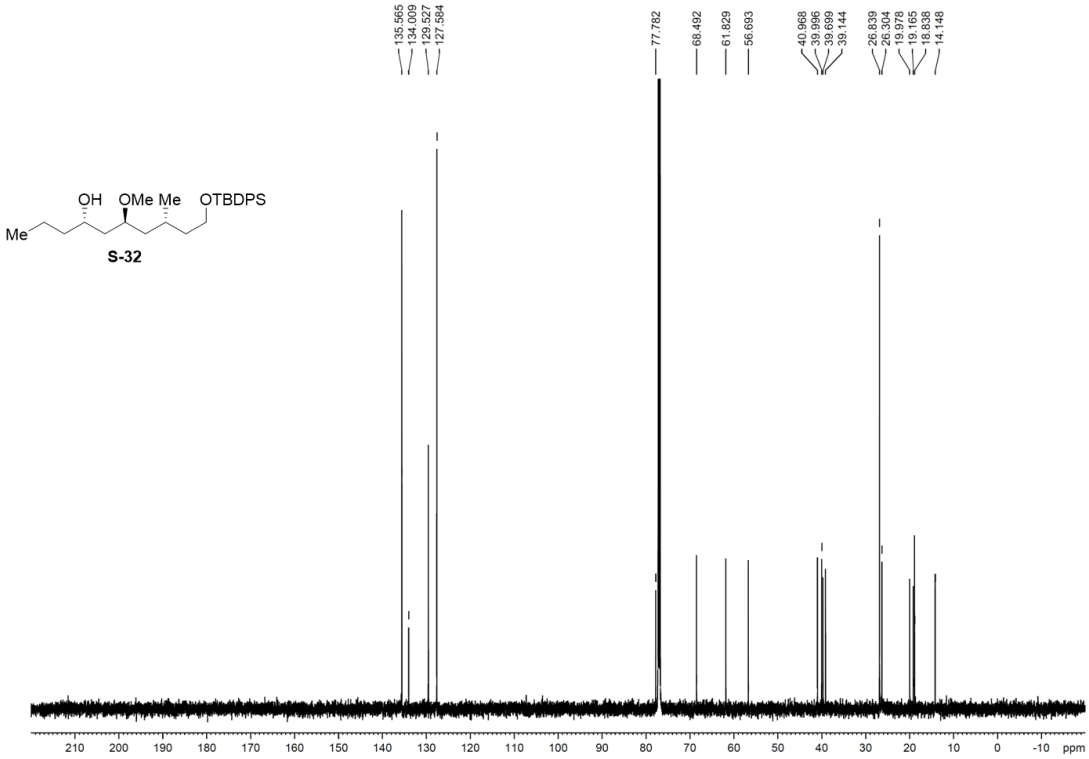

(4*S*,6*S*,8*R*)-10-(*tert*-Butyldiphenylsilyloxy)-6-methoxy-8-methyldecan-4-ol (**S-32**)

COSY (600 MHz, $CDCl_3$)

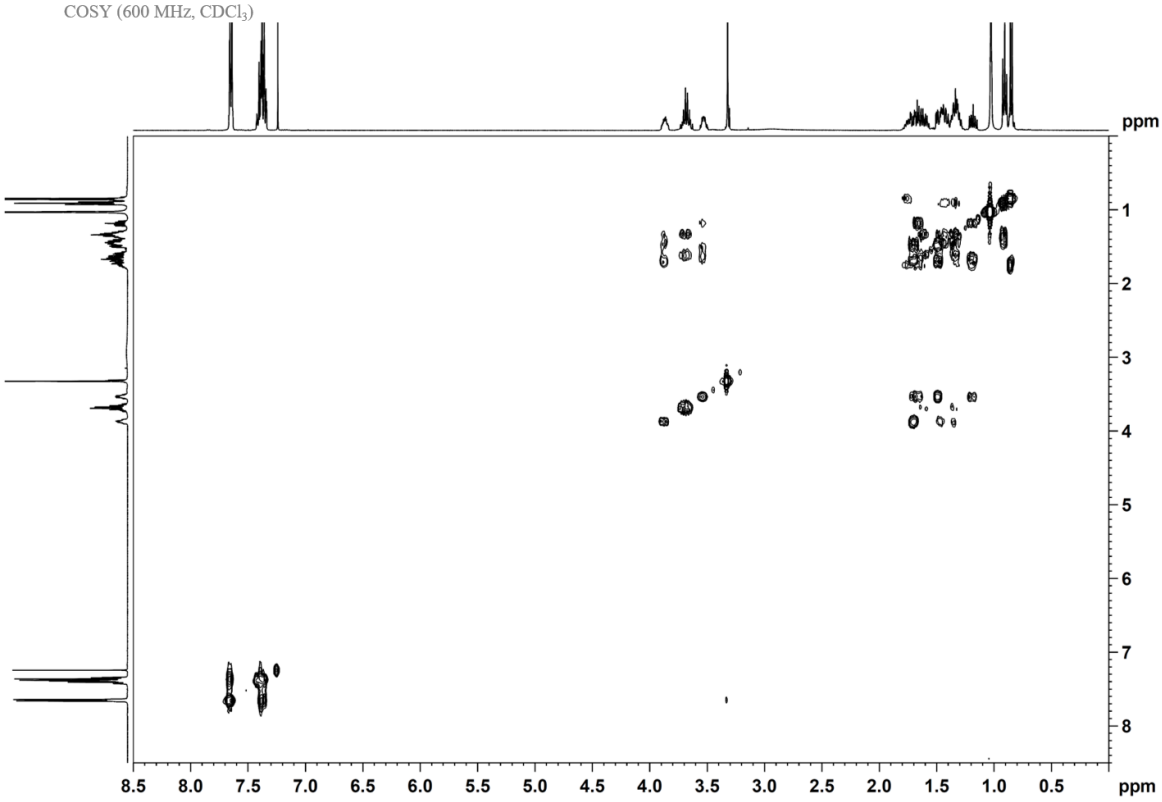

(4*S*,6*S*,8*R*)-10-(*tert*-Butyldiphenylsilyloxy)-6-methoxy-8-methyldecan-4-ol (**S-32**)

HSQC (600 MHz, $CDCl_3$)

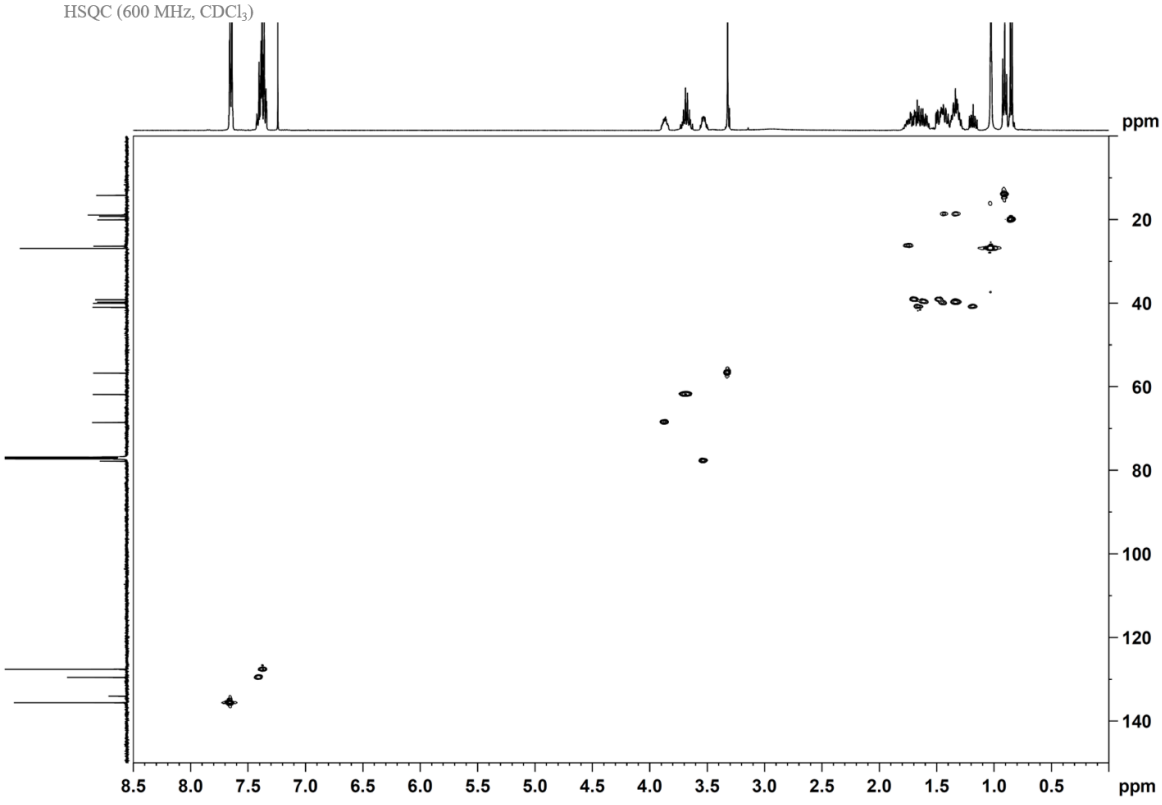

(5*S*,7*S*,9*R*)-7-Methoxy-9,14,14-trimethyl-13,13-diphenyl-5-propyl-2,4,12-trioxa-13-silapentadecane (**4.78**)

^{1}H NMR (600 MHz, $CDCl_3$)

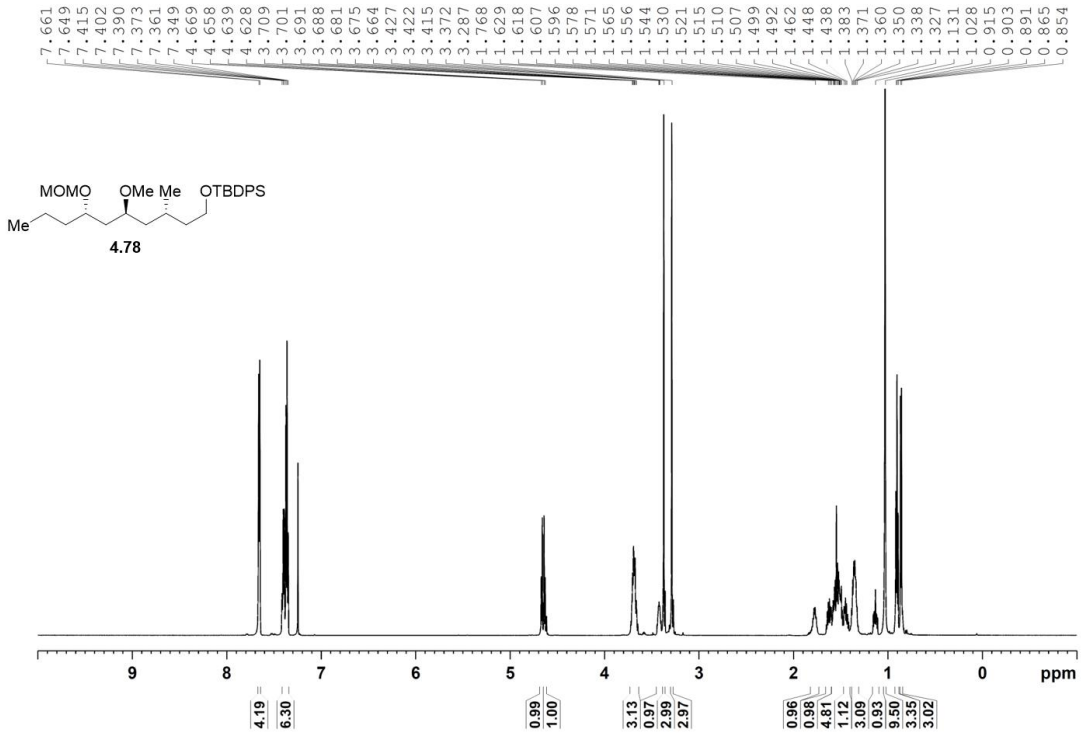

(5*S*,7*S*,9*R*)-7-Methoxy-9,14,14-trimethyl-13,13-diphenyl-5-propyl-2,4,12-trioxa-13-silapentadecane (**4.78**)

^{13}C NMR (150 MHz, $CDCl_3$)

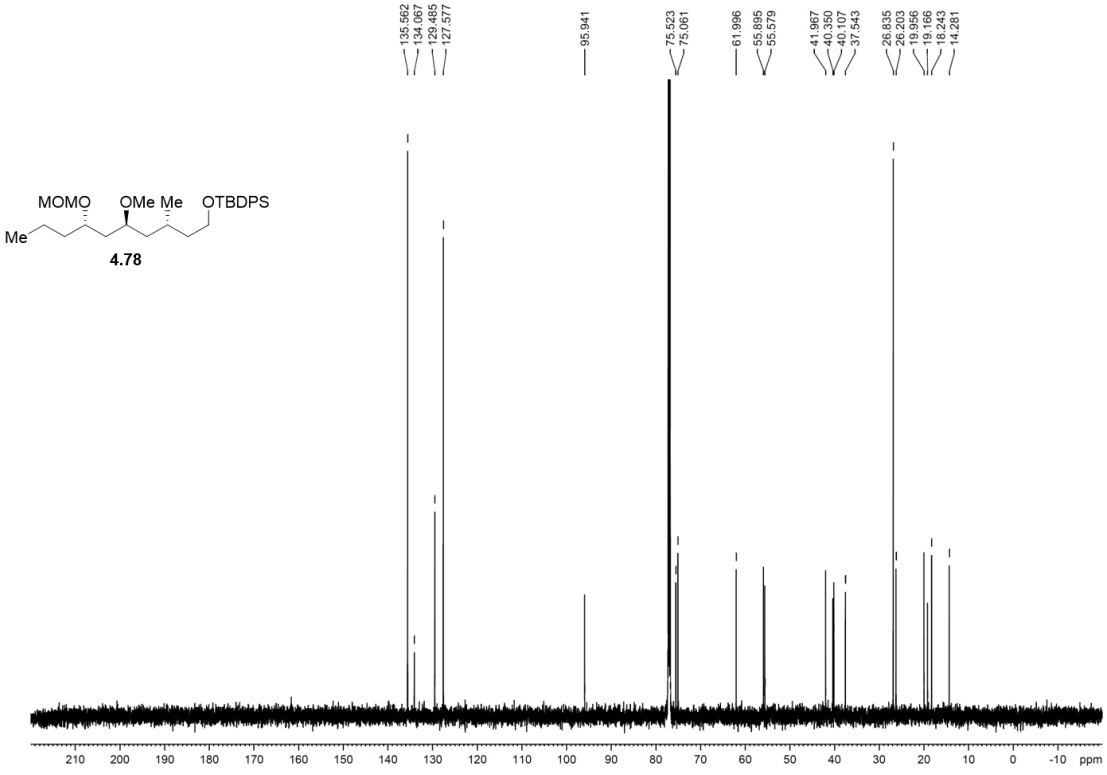

(5*S*,7*S*,9*R*)-7-Methoxy-9,14,14-trimethyl-13,13-diphenyl-5-propyl-2,4,12-trioxa-13-silapentadecane (**4.78**)

COSY (600 MHz, $CDCl_3$)

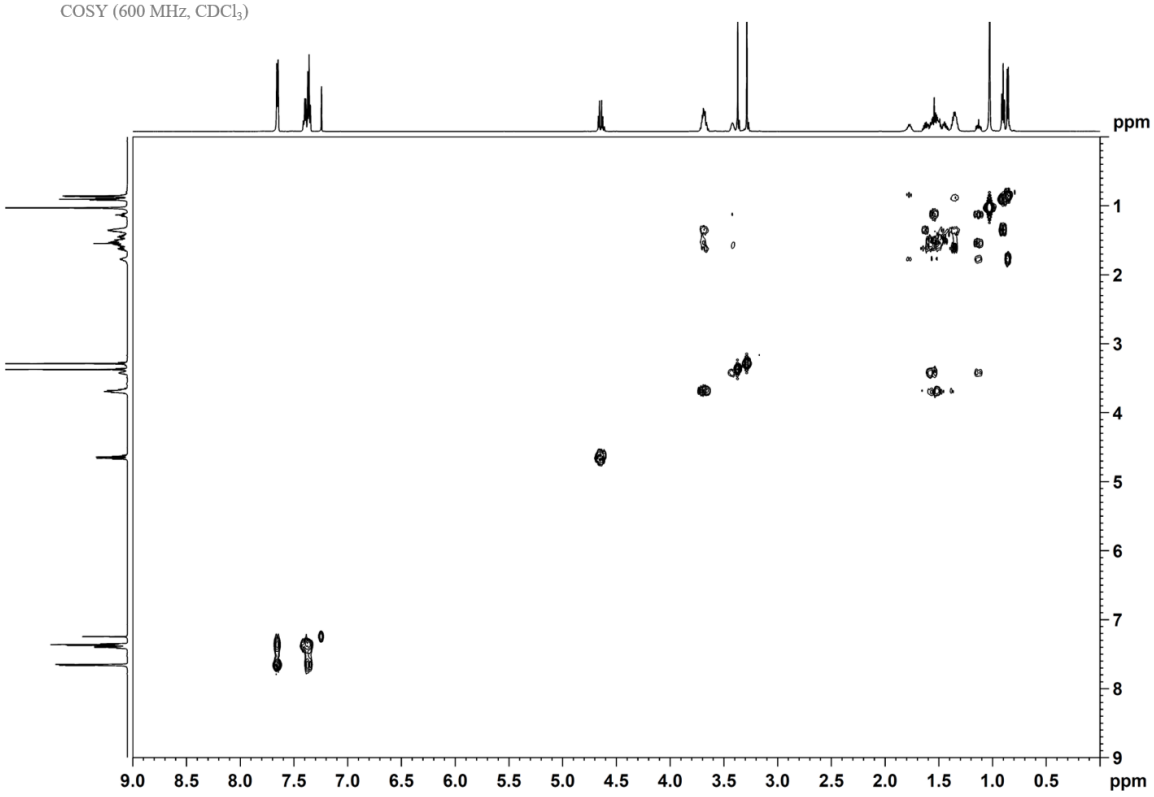

(5*S*,7*S*,9*R*)-7-Methoxy-9,14,14-trimethyl-13,13-diphenyl-5-propyl-2,4,12-trioxa-13-silapentadecane (**4.78**)

HSQC (600 MHz, $CDCl_3$)

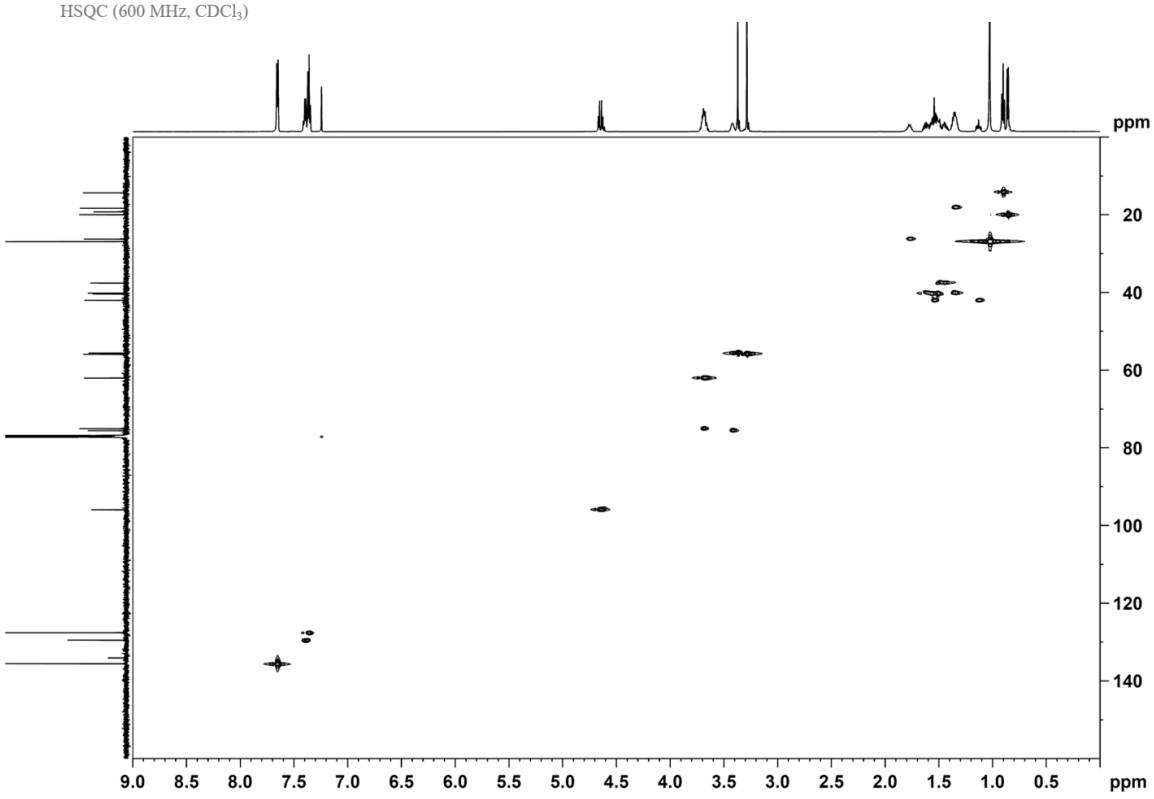

(3*R*,5*S*,7*S*)-5-Methoxy-7-(methoxymethoxy)-3-methyldecan-1-ol (**S-33**)

^{1}H NMR (600 MHz, $CDCl_3$)

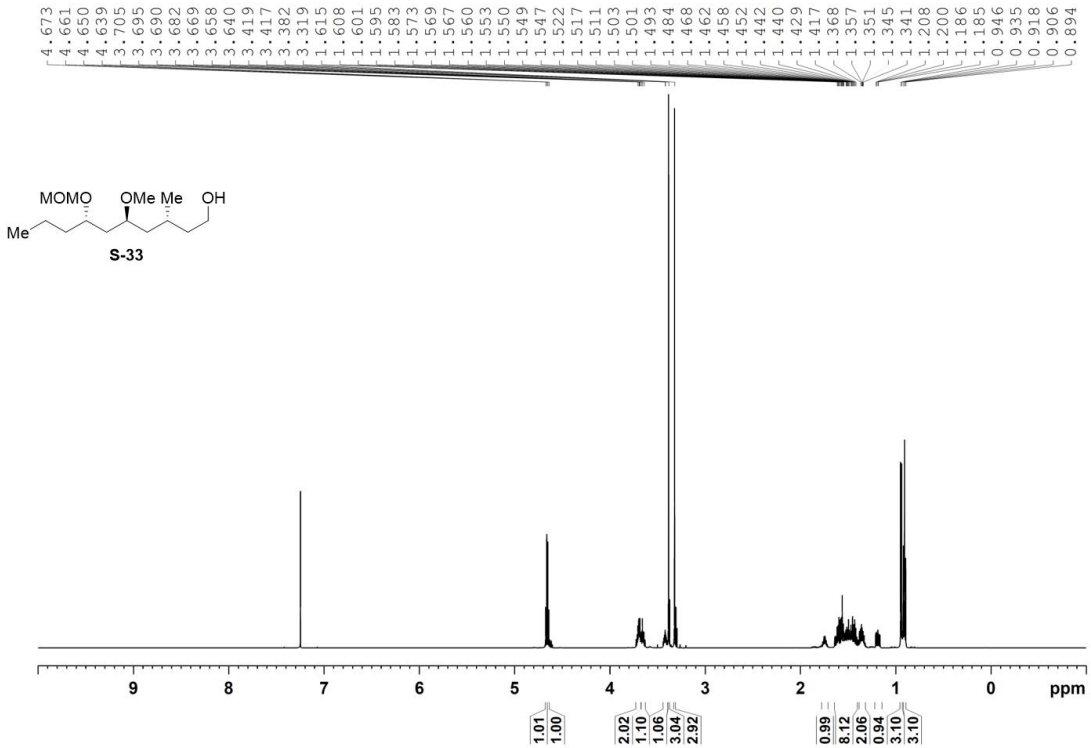

(3*R*,5*S*,7*S*)-5-Methoxy-7-(methoxymethoxy)-3-methyldecan-1-ol (**S-33**)

^{13}C NMR (150 MHz, $CDCl_3$)

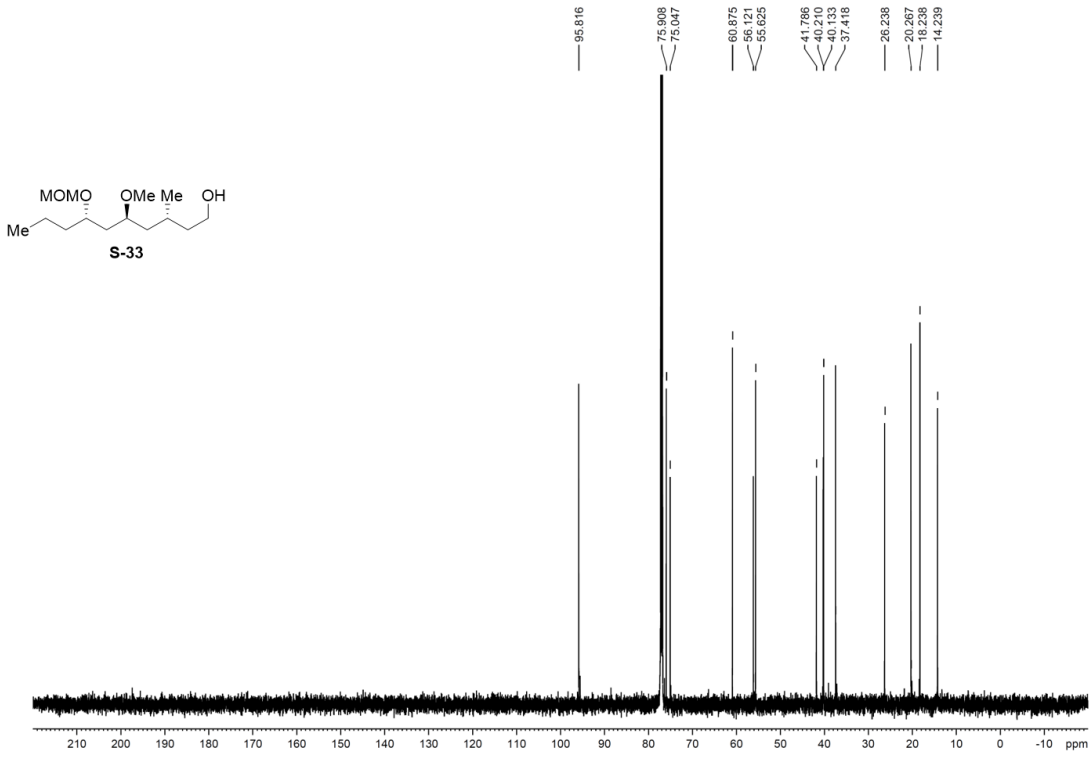

(3*R*,5*S*,7*S*)-5-Methoxy-7-(methoxymethoxy)-3-methyldecan-1-ol (**S-33**)

COSY (600 MHz, $CDCl_3$)

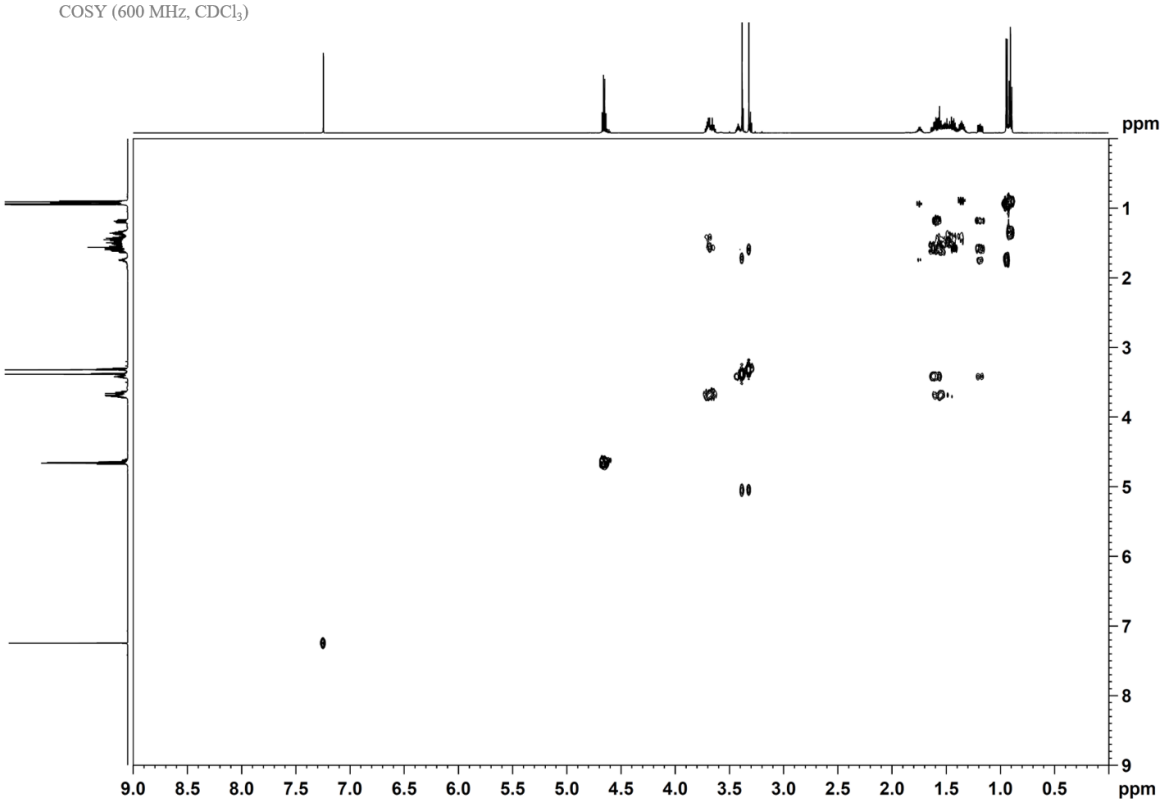

(3*R*,5*S*,7*S*)-5-Methoxy-7-(methoxymethoxy)-3-methyldecan-1-ol (**S-33**)

HSQC (600 MHz, $CDCl_3$)

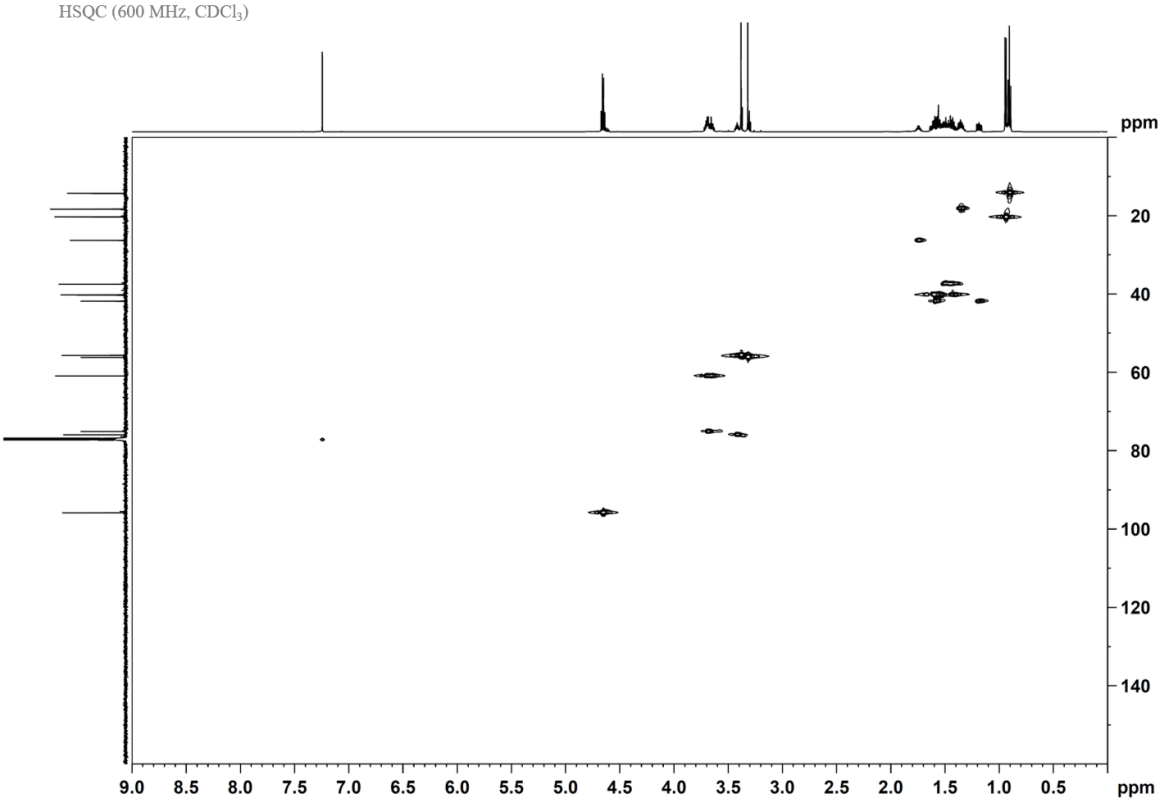

(3*S*,5*S*,7*S*)-5-Methoxy-7-(methoxymethoxy)-3-methyldecanal (**4.79**)

^{1}H NMR (600 MHz, $CDCl_3$)

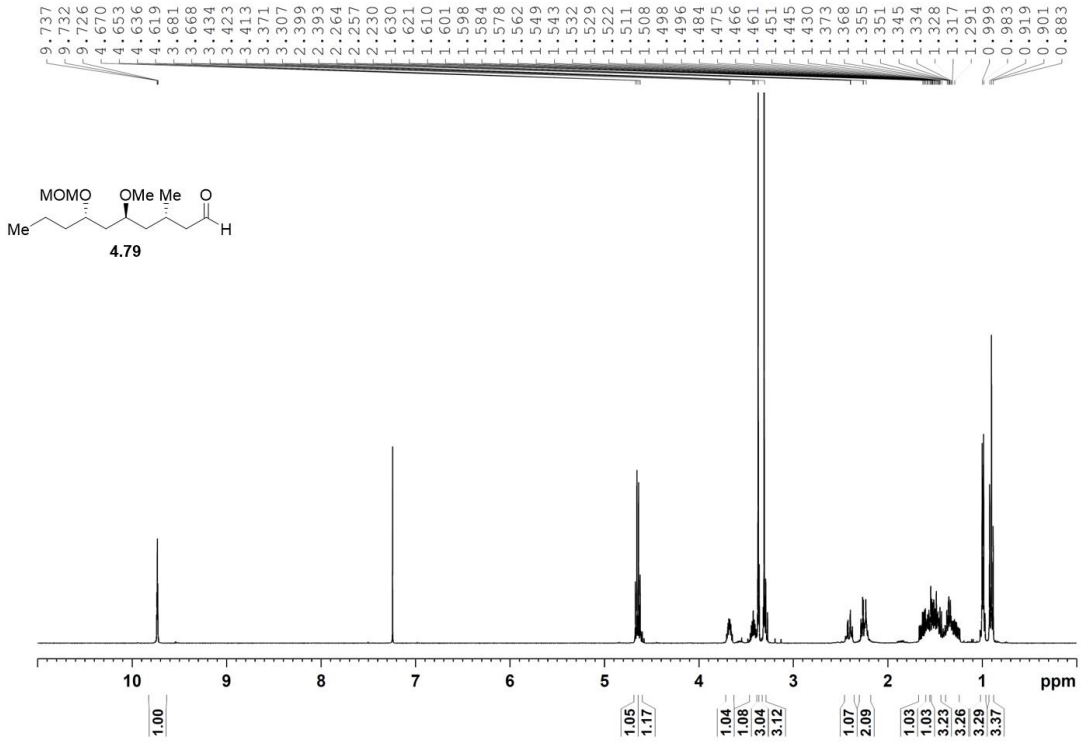

(3*S*,5*S*,7*S*)-5-Methoxy-7-(methoxymethoxy)-3-methyldecanal (**4.79**)

^{13}C NMR (150 MHz, $CDCl_3$)

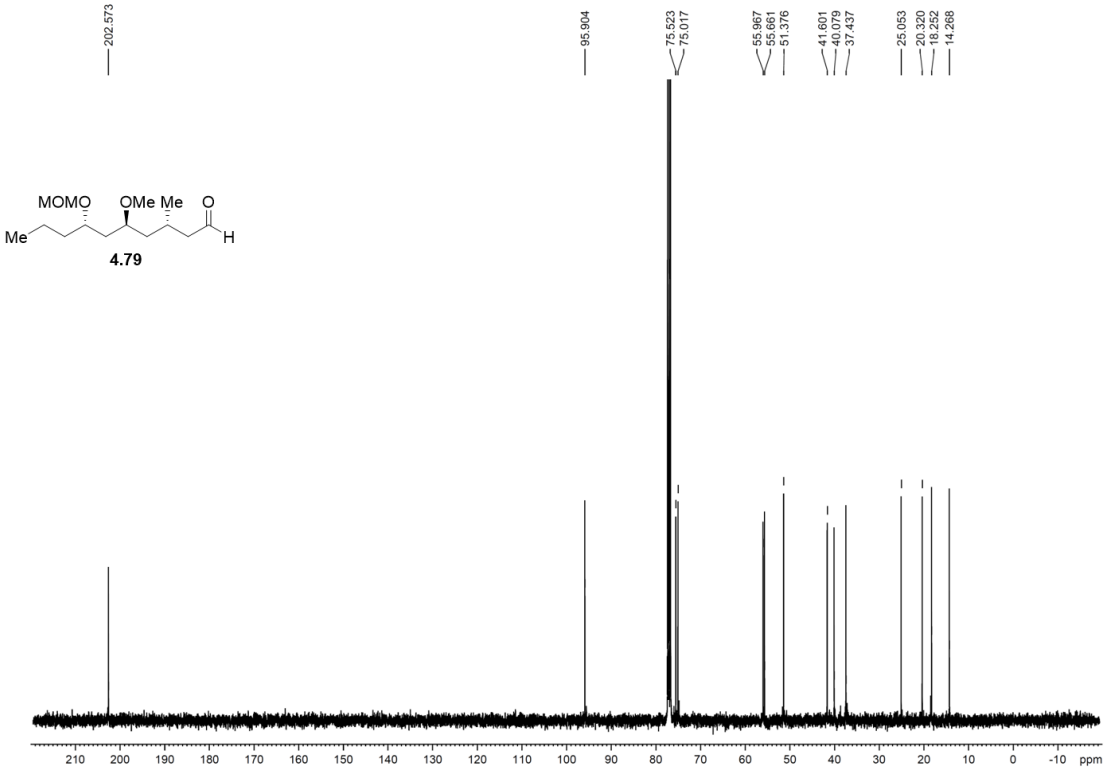

(3*S*,5*S*,7*S*)-5-Methoxy-7-(methoxymethoxy)-3-methyldecanal (**4.79**)
COSY (600 MHz, $CDCl_3$)

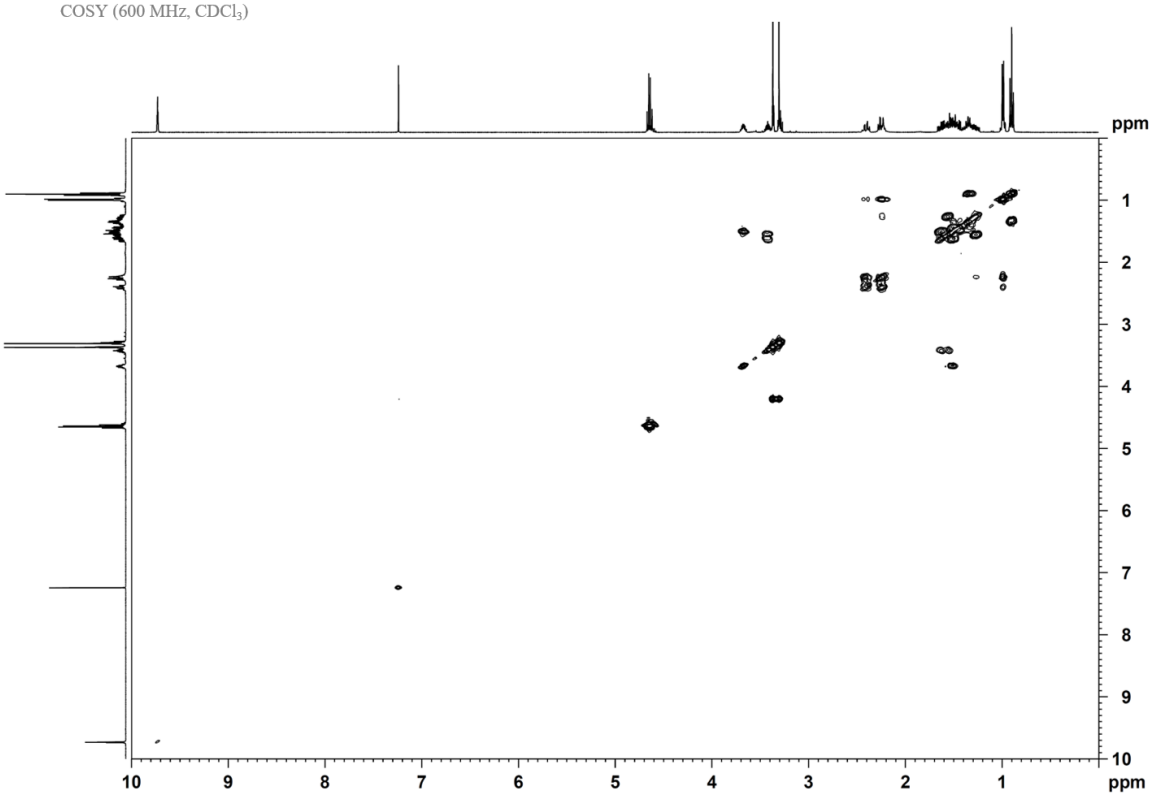

(3*S*,5*S*,7*S*)-5-Methoxy-7-(methoxymethoxy)-3-methyldecanal (**4.79**)
HSQC (600 MHz, $CDCl_3$)

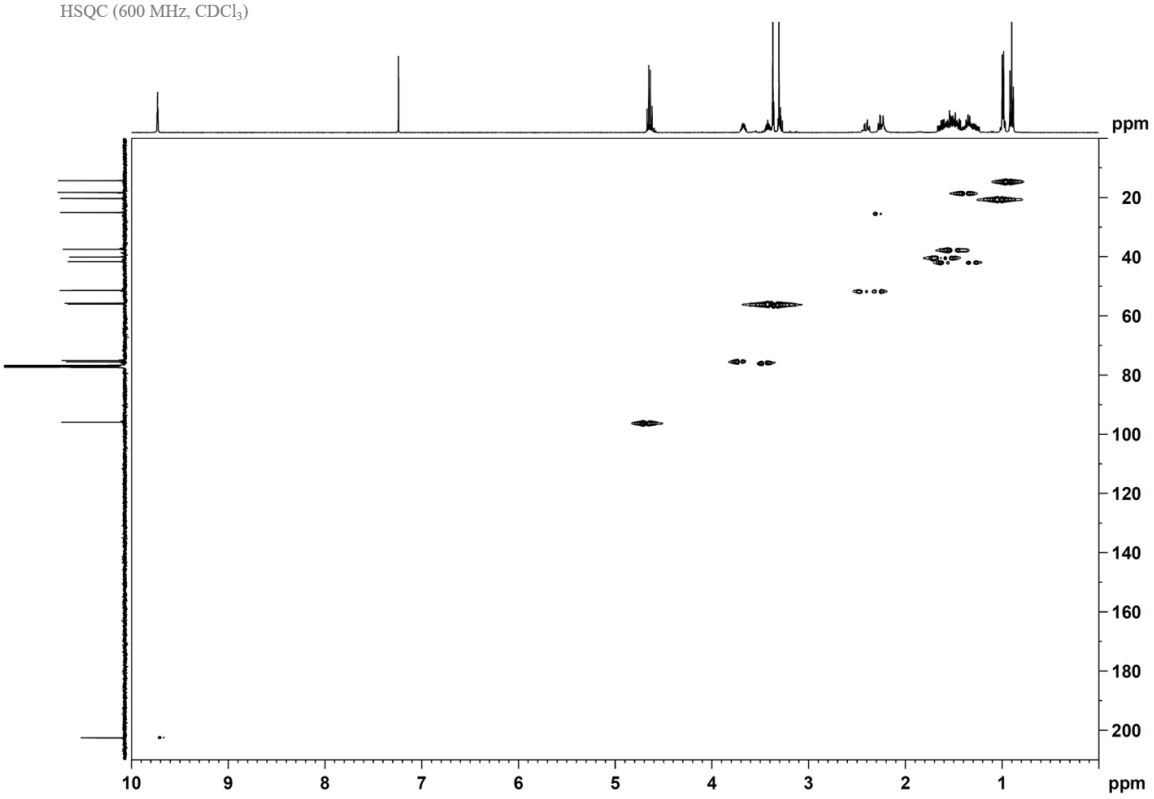

(9*R*,11*S*,13*S*)-(*E*)-3-(*tert*-Butyldimethylsilyloxy)-13-(methoxymethoxy)-11-methoxy-9-methyl-5-oxohexadec-6-enoic acid (**S-34**)

^{1}H NMR (100 MHz, $CDCl_3$)

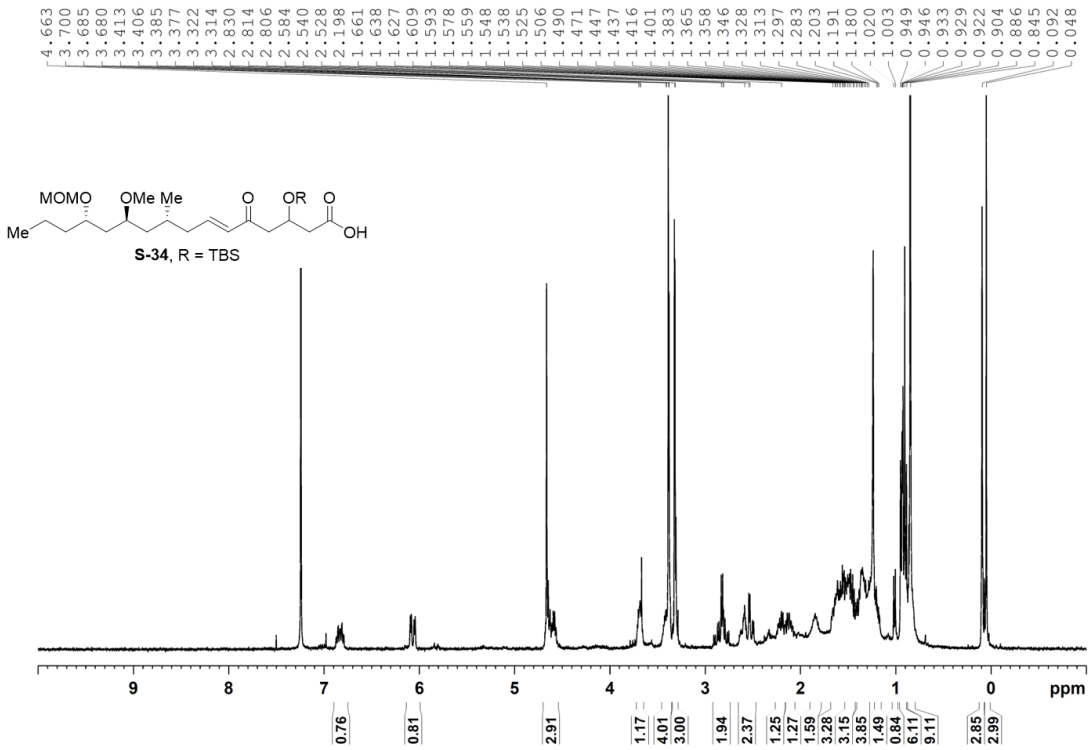

(9*R*,11*S*,13*S*)-(*E*)-3-(*tert*-Butyldimethylsilyloxy)-13-(methoxymethoxy)-11-methoxy-9-methyl-5-oxohexadec-6-enoic acid (**S-34**)

COSY (400 MHz, $CDCl_3$)

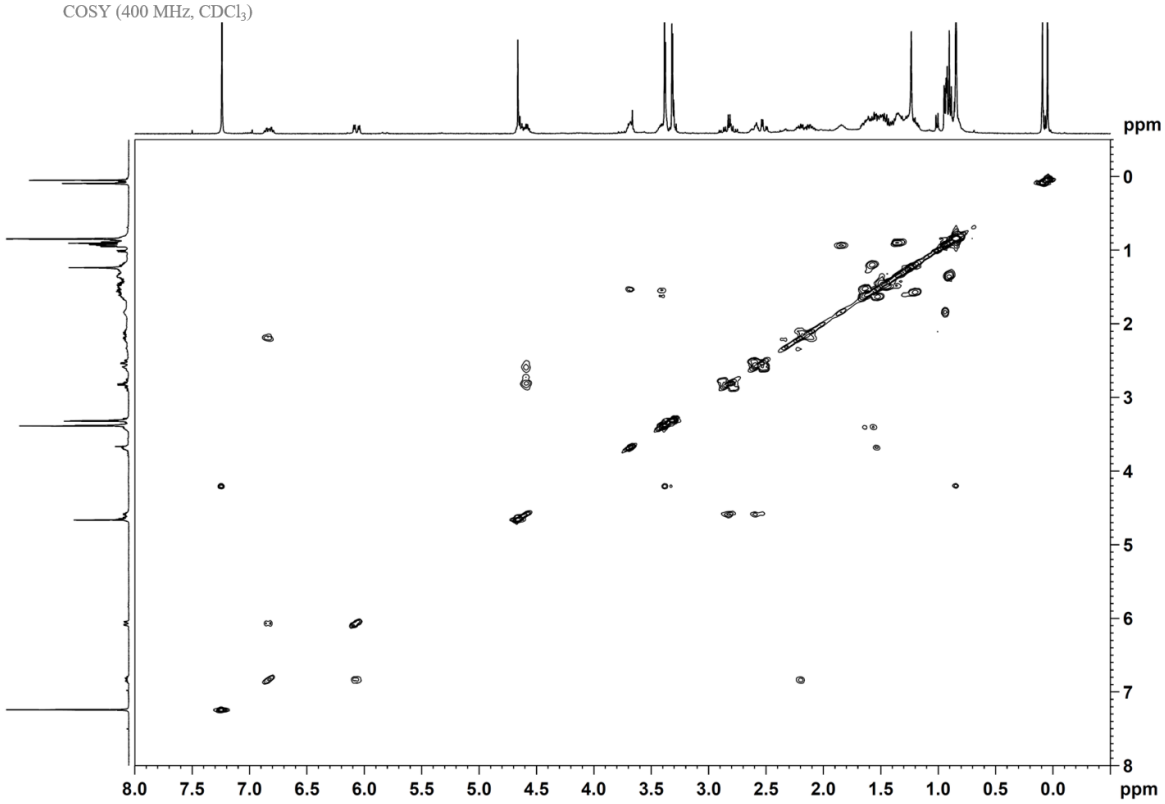

(9*R*,11*S*,13*S*)-(*E*)-3-(*tert*-Butyldimethylsilyloxy)-13-(methoxymethoxy)-11-methoxy-9-methyl-5-oxohexadec-6-enoic acid (**S-34**)

HSQC (400 MHz, $CDCl_3$)

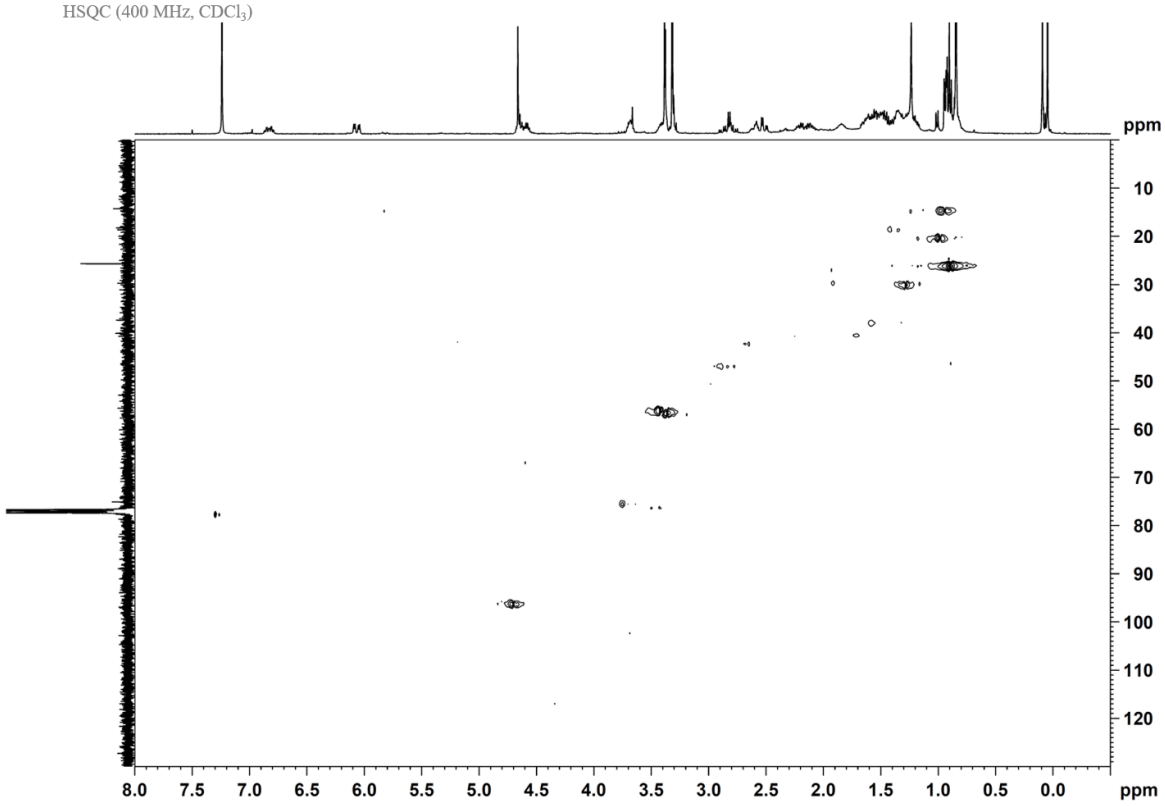

(9*R*,11*S*,13*S*)-(*E*)-3-(*tert*-Butyldimethylsilyloxy)-13-hydroxy-11-methoxy-9-methyl-5-oxohexadec-6-enoic acid (**4.49**)

^{1}H NMR (600 MHz, $CDCl_3$)

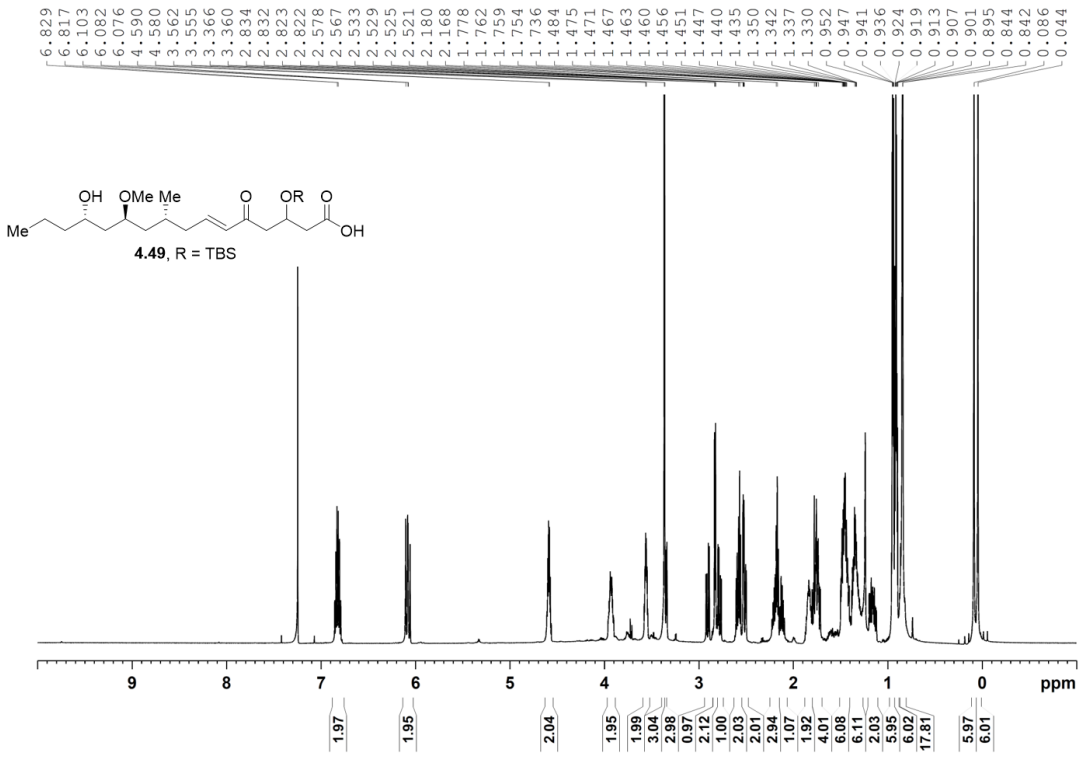

(9*R*,11*S*,13*S*)-(*E*)-3-(*tert*-Butyldimethylsilyloxy)-13-hydroxy-11-methoxy-9-methyl-5-oxohexadec-6-enoic acid (**4.49**)

^{13}C NMR (150 MHz, $CDCl_3$)

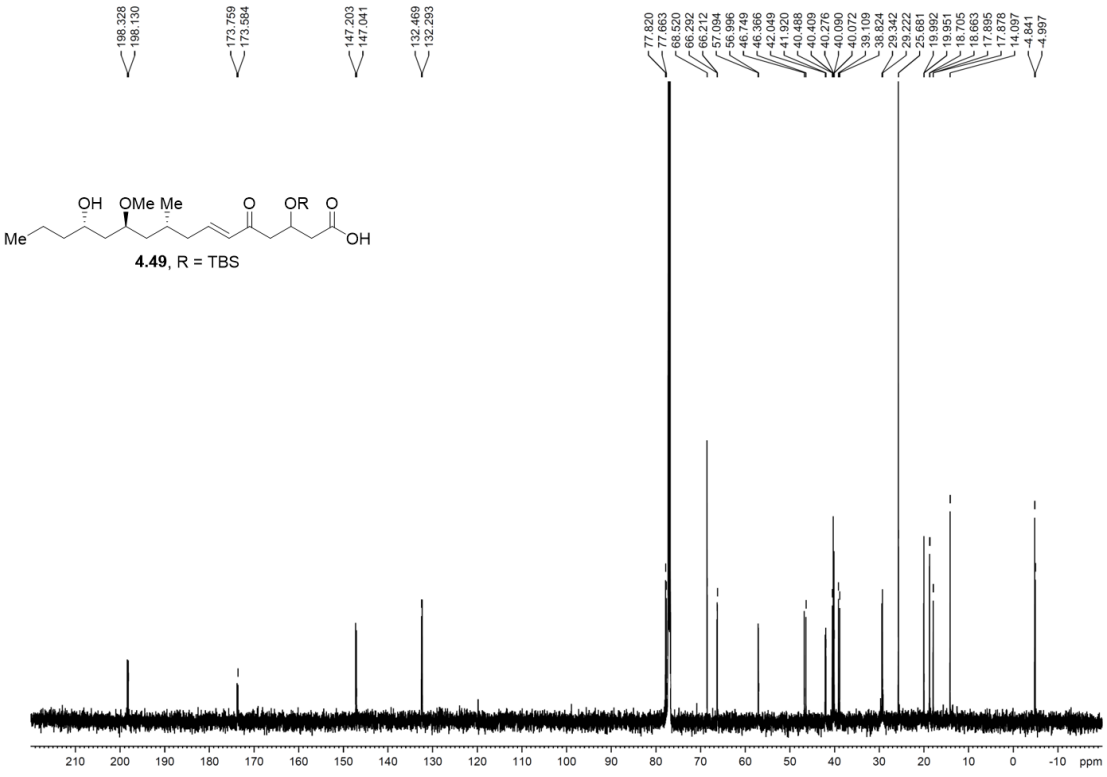

(9*R*,11*S*,13*S*)-(*E*)-3-(*tert*-Butyldimethylsilyloxy)-13-hydroxy-11-methoxy-9-methyl-5-oxohexadec-6-enoic acid (**4.49**)

COSY (600 MHz, $CDCl_3$)

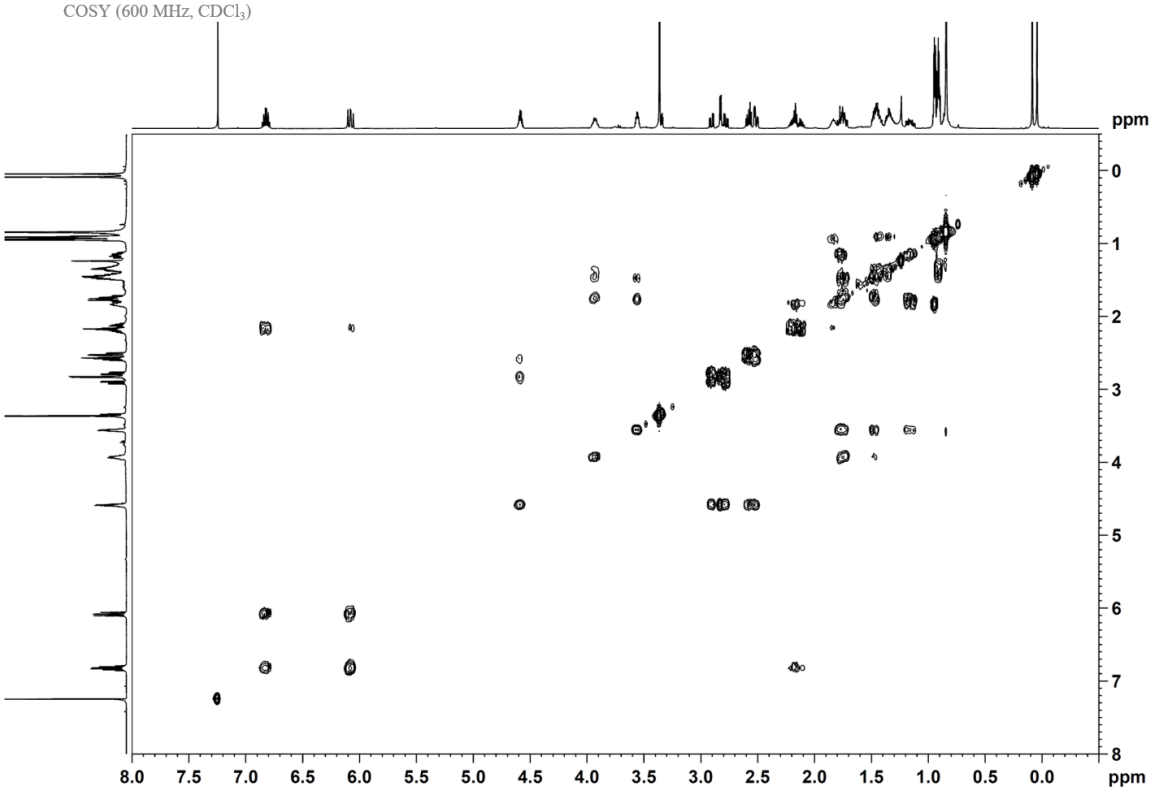

(9*R*,11*S*,13*S*)-(*E*)-3-(*tert*-Butyldimethylsilyloxy)-13-hydroxy-11-methoxy-9-methyl-5-oxohexadec-6-enoic acid (**4.49**)

HSQC (600 MHz, $CDCl_3$)

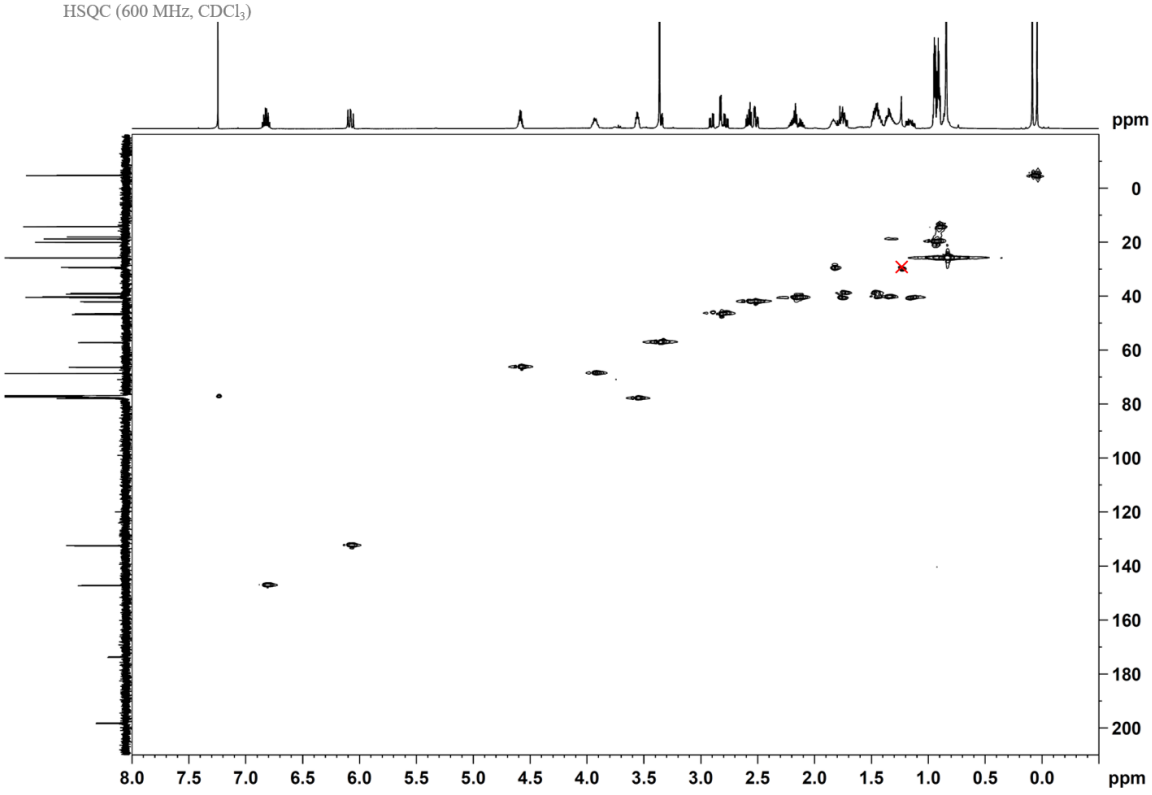

(3*R*,9*R*,11*S*,13*S*)-(*E*)-3-TBS-11-methoxy-9-methyl-13-propyloxacyclotetradec-6-ene-1,5-dione (3*R*-**4.56**)

^{1}H NMR (600 MHz, $CDCl_3$)

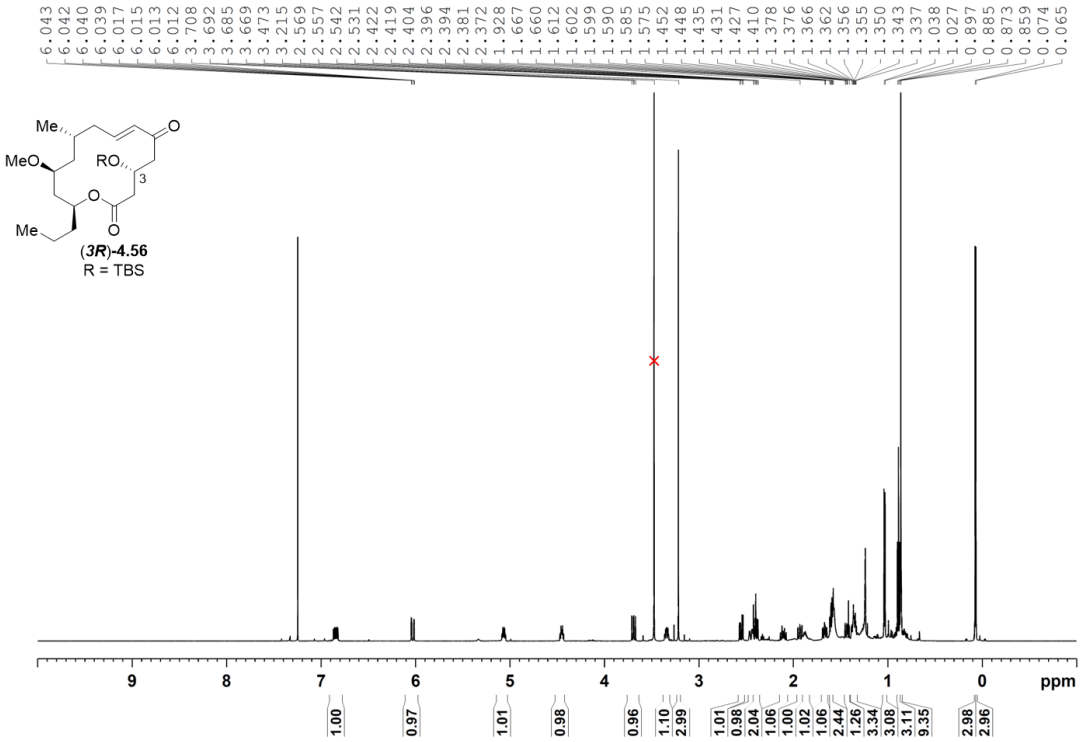

(3*R*,9*R*,11*S*,13*S*)-(*E*)-3-TBS-11-methoxy-9-methyl-13-propyloxacyclotetradec-6-ene-1,5-dione (3*R*-**4.56**)

^{13}C NMR (150 MHz, $CDCl_3$)

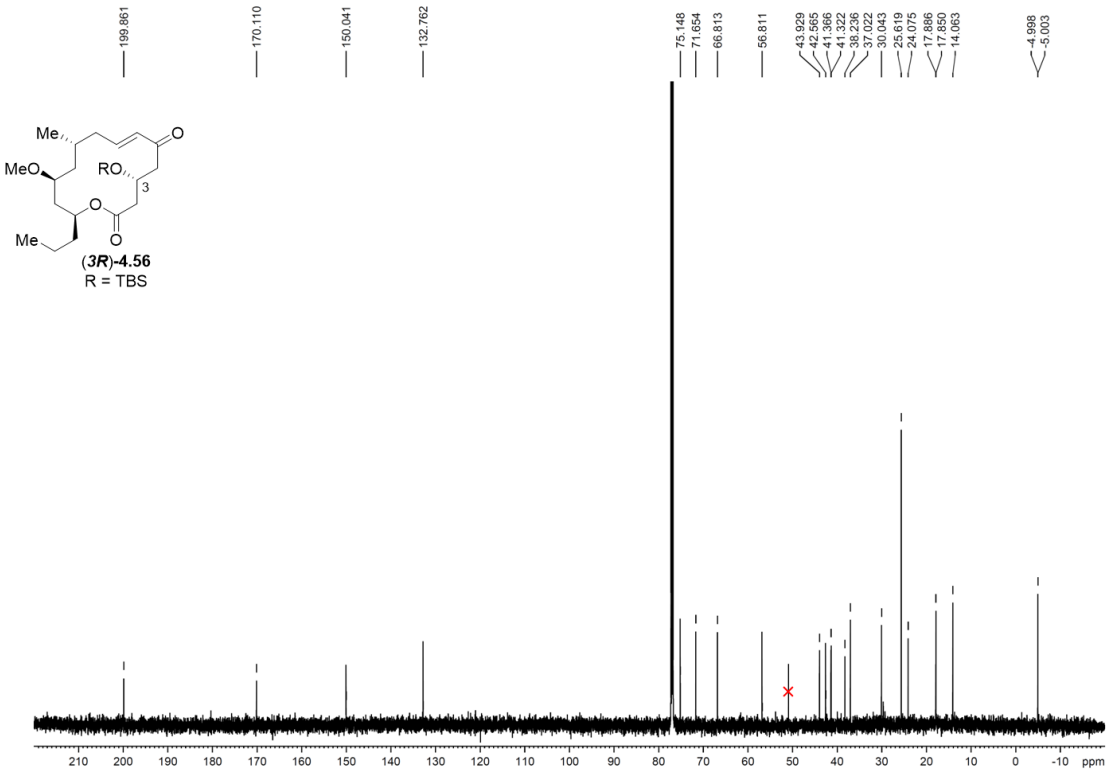

(3*R*,9*R*,11*S*,13*S*)-(*E*)-3-TBS-11-methoxy-9-methyl-13-propyloxacyclotetradec-6-ene-1,5-dione (3*R*-**4.56**)

COSY (600 MHz, $CDCl_3$)

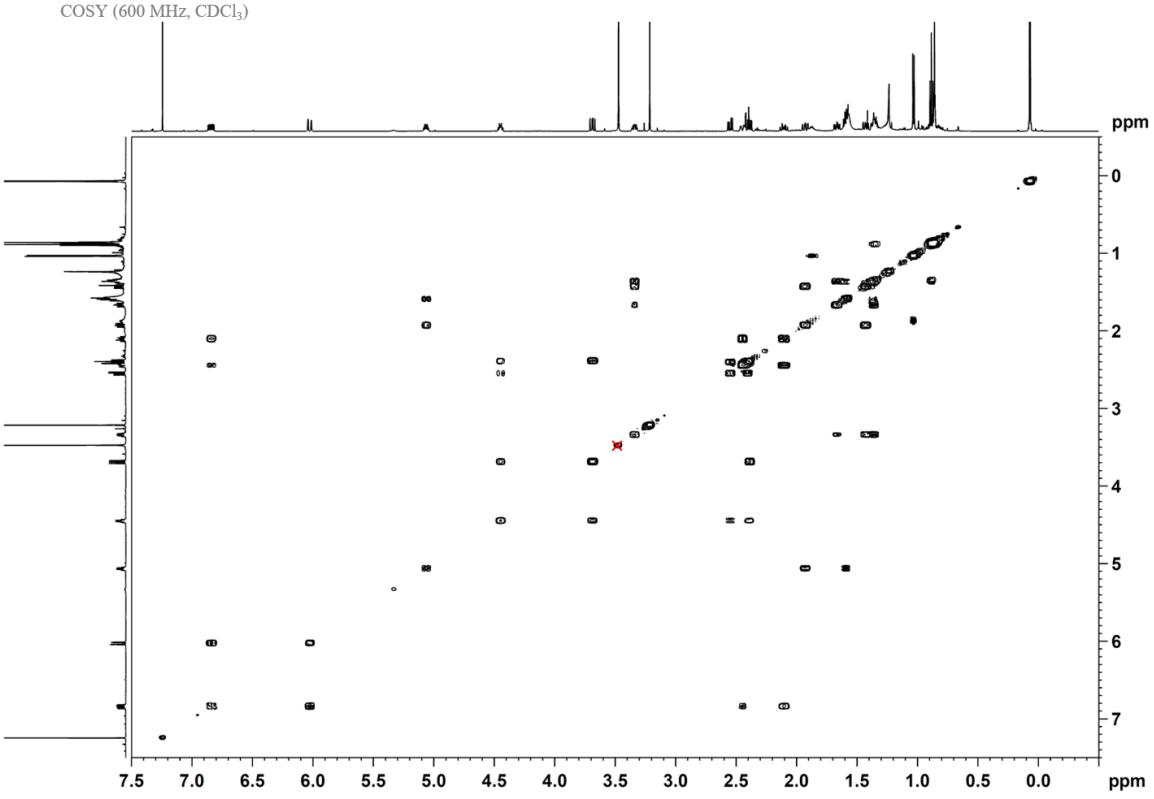

(3*R*,9*R*,11*S*,13*S*)-(*E*)-3-TBS-11-methoxy-9-methyl-13-propyloxacyclotetradec-6-ene-1,5-dione (3*R*-**4.56**)

HSQC (600 MHz, $CDCl_3$)

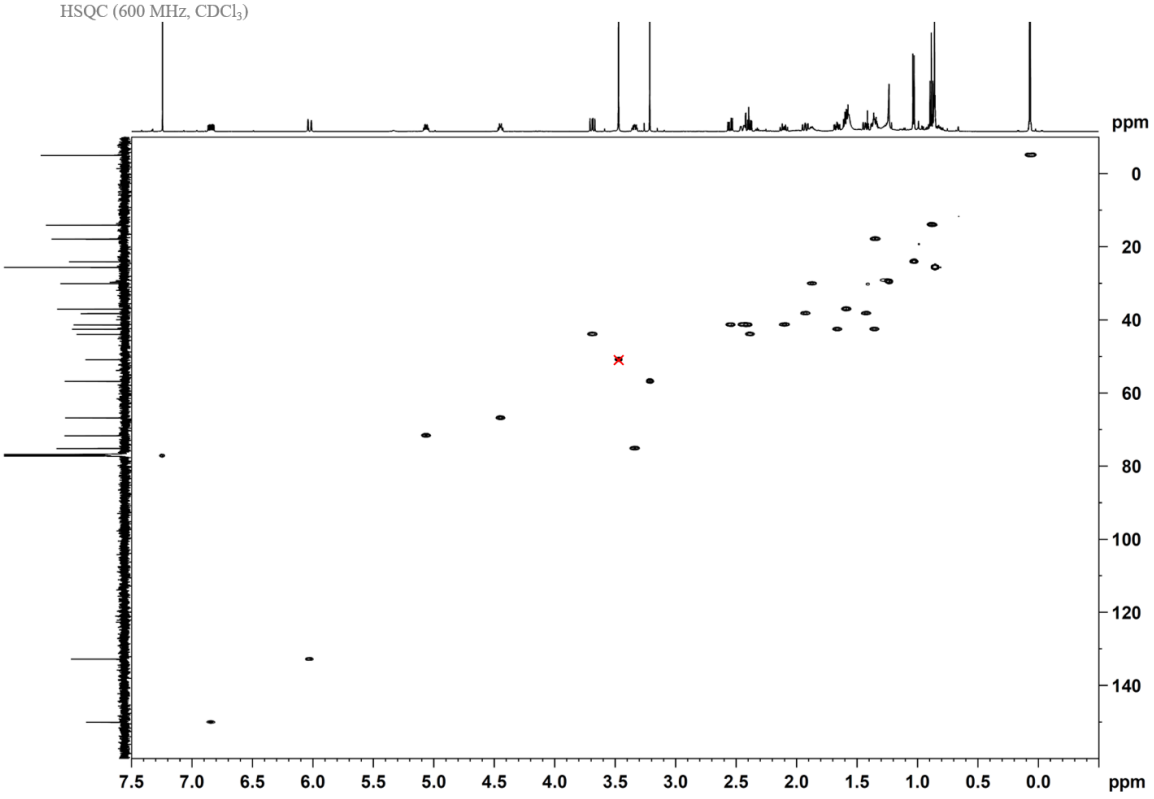

(3*R*,9*R*,11*S*,13*S*)-(*E*)-3-TBS-11-methoxy-9-methyl-13-propyloxacyclotetradec-6-ene-1,5-dione (3*R*-**4.56**)

2D NOESY (600 MHz, $CDCl_3$)

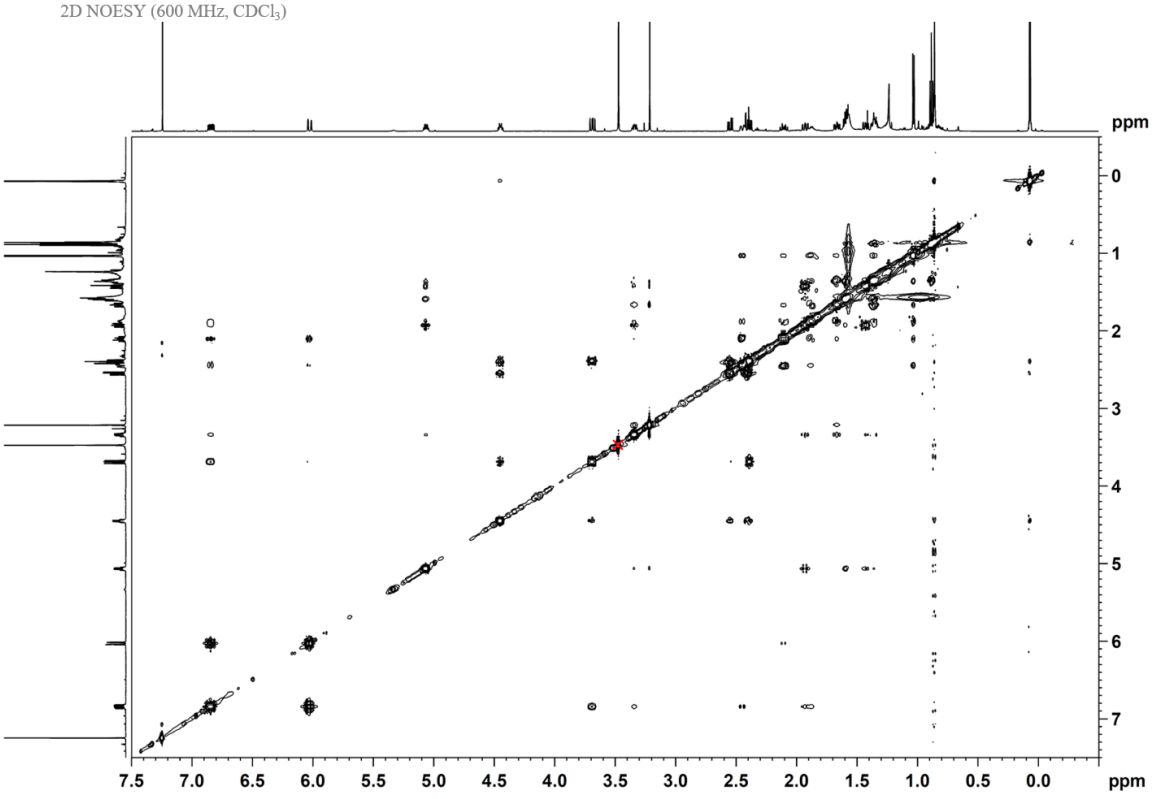

(3*S*,9*R*,11*S*,13*S*)-(*E*)-*3*-TBS-11-methoxy-9-methyl-13-propyloxacyclotetradec-6-ene-1,5-dione (3*S*-**4.56**)

^{1}H NMR (600 MHz, $CDCl_3$)

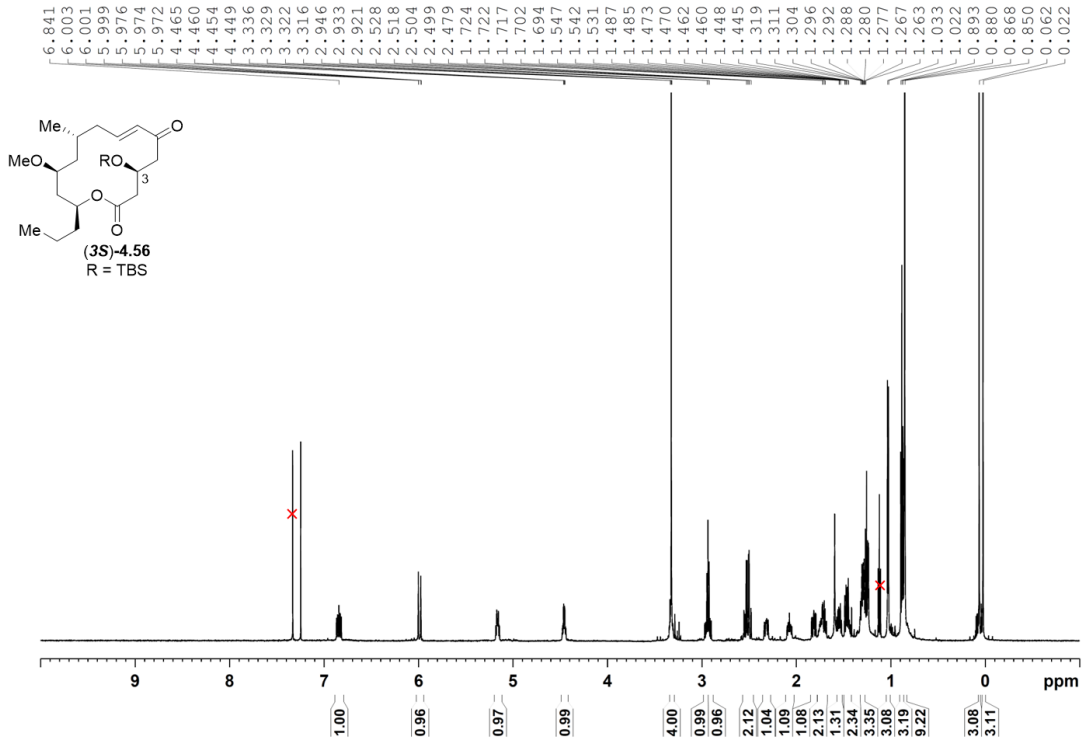

(3*S*,9*R*,11*S*,13*S*)-(*E*)-*3*-TBS-11-methoxy-9-methyl-13-propyloxacyclotetradec-6-ene-1,5-dione (3*S*-**4.56**)

^{13}C NMR (150 MHz, $CDCl_3$)

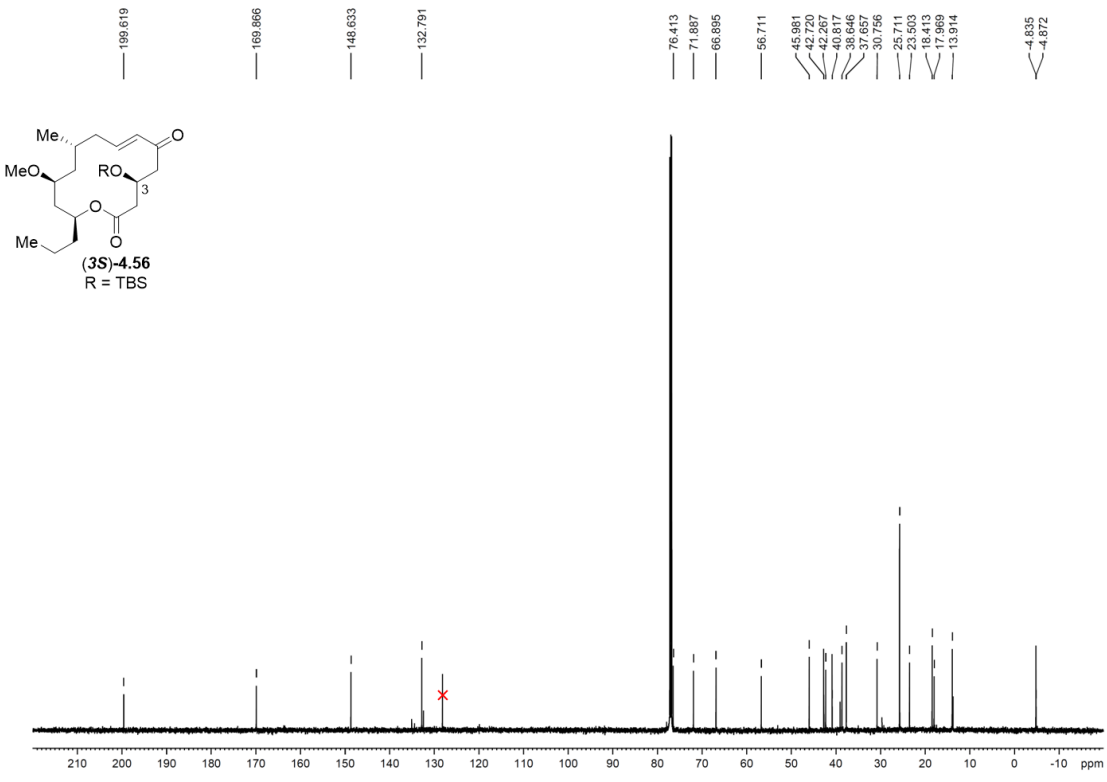

(3*S*,9*R*,11*S*,13*S*)-(*E*)-3-TBS-11-methoxy-9-methyl-13-propyloxacyclotetradec-6-ene-1,5-dione (3*S*-**4.56**)

COSY (600 MHz, $CDCl_3$)

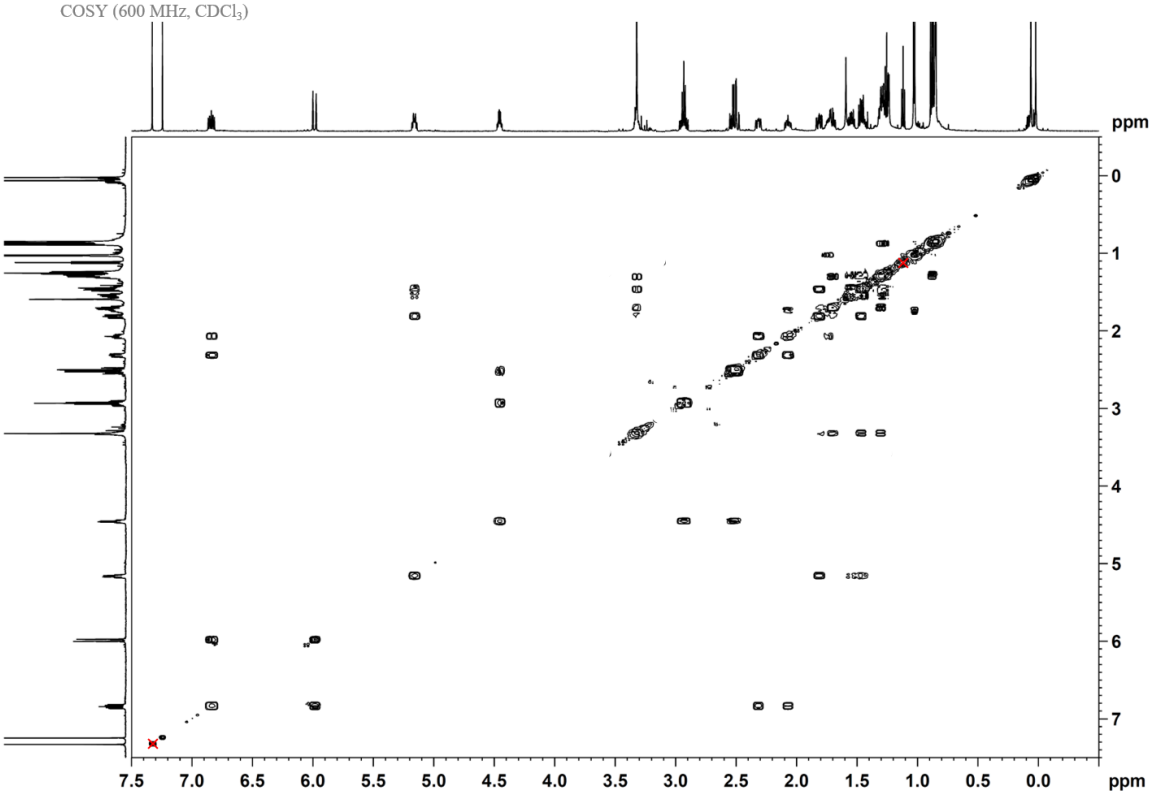

(3*S*,9*R*,11*S*,13*S*)-(*E*)-3-TBS-11-methoxy-9-methyl-13-propyloxacyclotetradec-6-ene-1,5-dione (3*S*-**4.56**)

HSQC (600 MHz, $CDCl_3$)

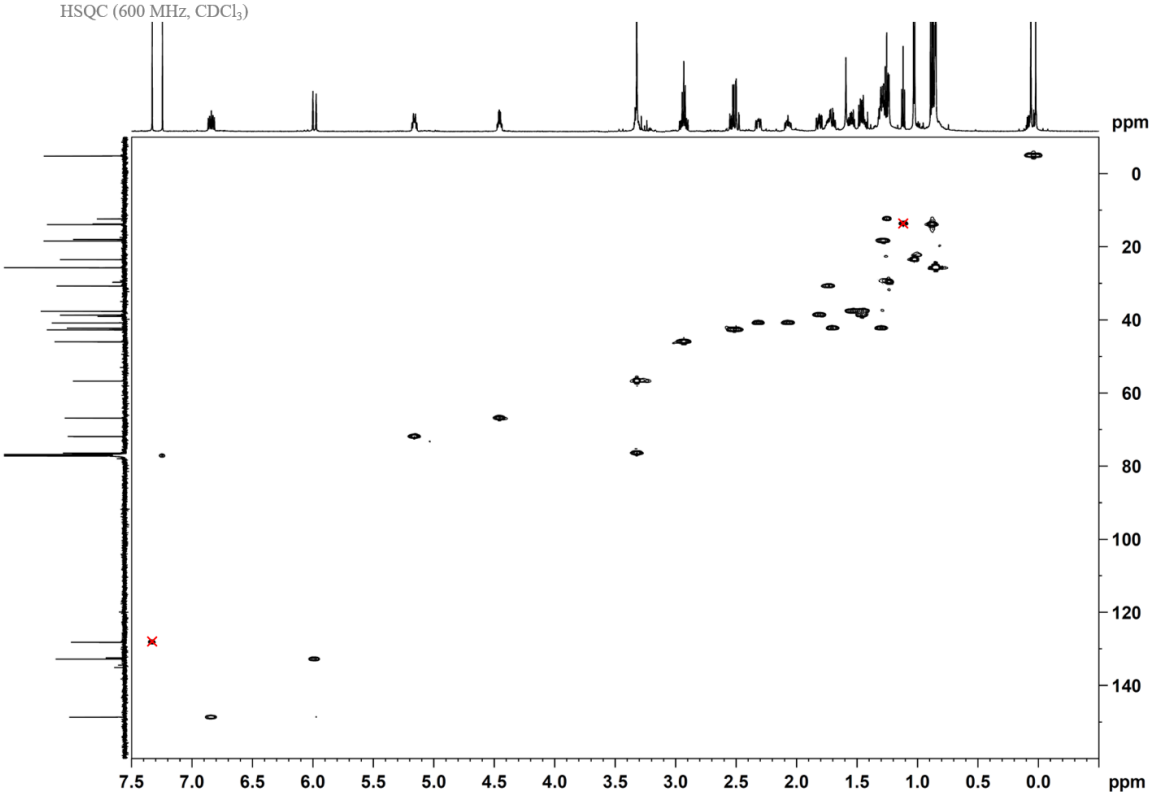

(3*S*,9*R*,11*S*,13*S*)-(*E*)-*3*-TBS-11-methoxy-9-methyl-13-propyloxacyclotetradec-6-ene-1,5-dione (3*S*-**4.56**)

2D NOESY (600 MHz, $CDCl_3$)

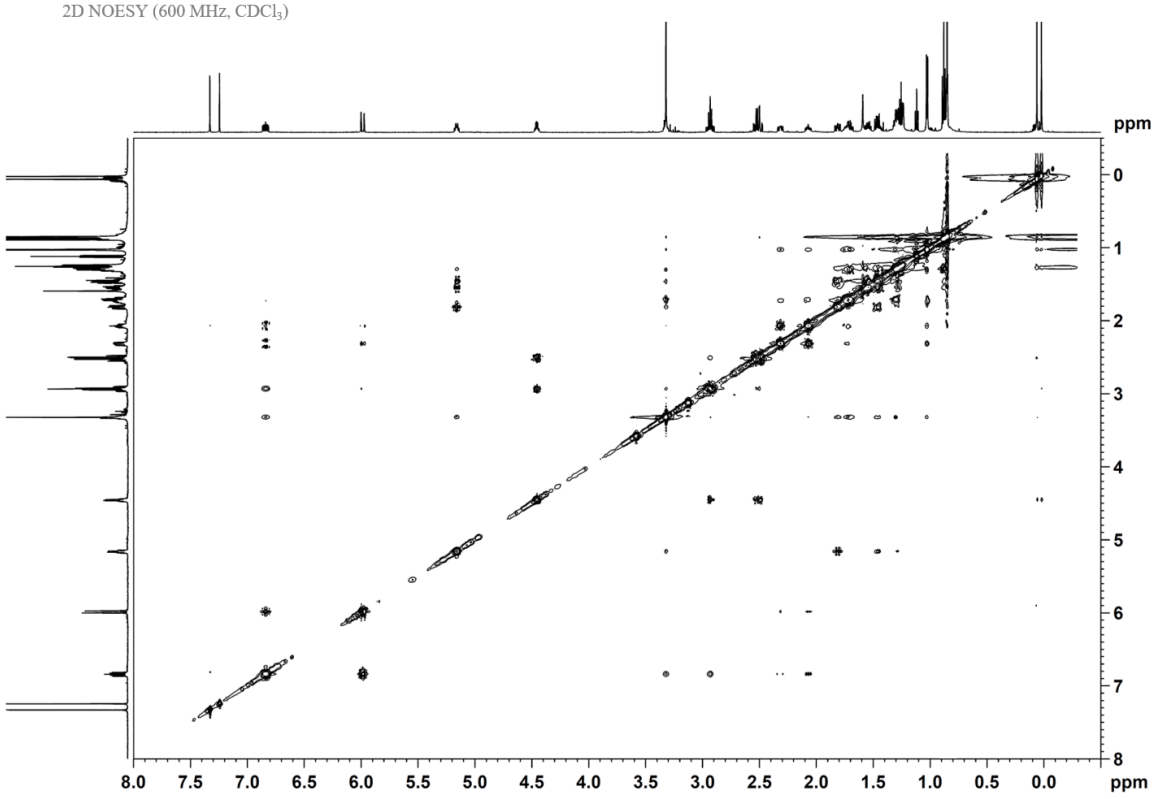

S1.3.8 Thermodynamic Transannular Oxa-Conjugate Assembly of cis-THP of Neopeltolide (§ 4.6.2)

Product Distrubtions from (*3R*)-**4.56**	***cis*-4.14**	***trans*-4.80**	***cis*-4.81**	***trans*-4.82**
Kinetic Conditions (MeCN, 22 ºC, 5 h)	**1.0**	**40**	**0.8**	**0.5**
Thermodynamic ($CDCl_3$, 80 ºC, 15 h)	**1.0**	*trace*	**0.54**	*trace*

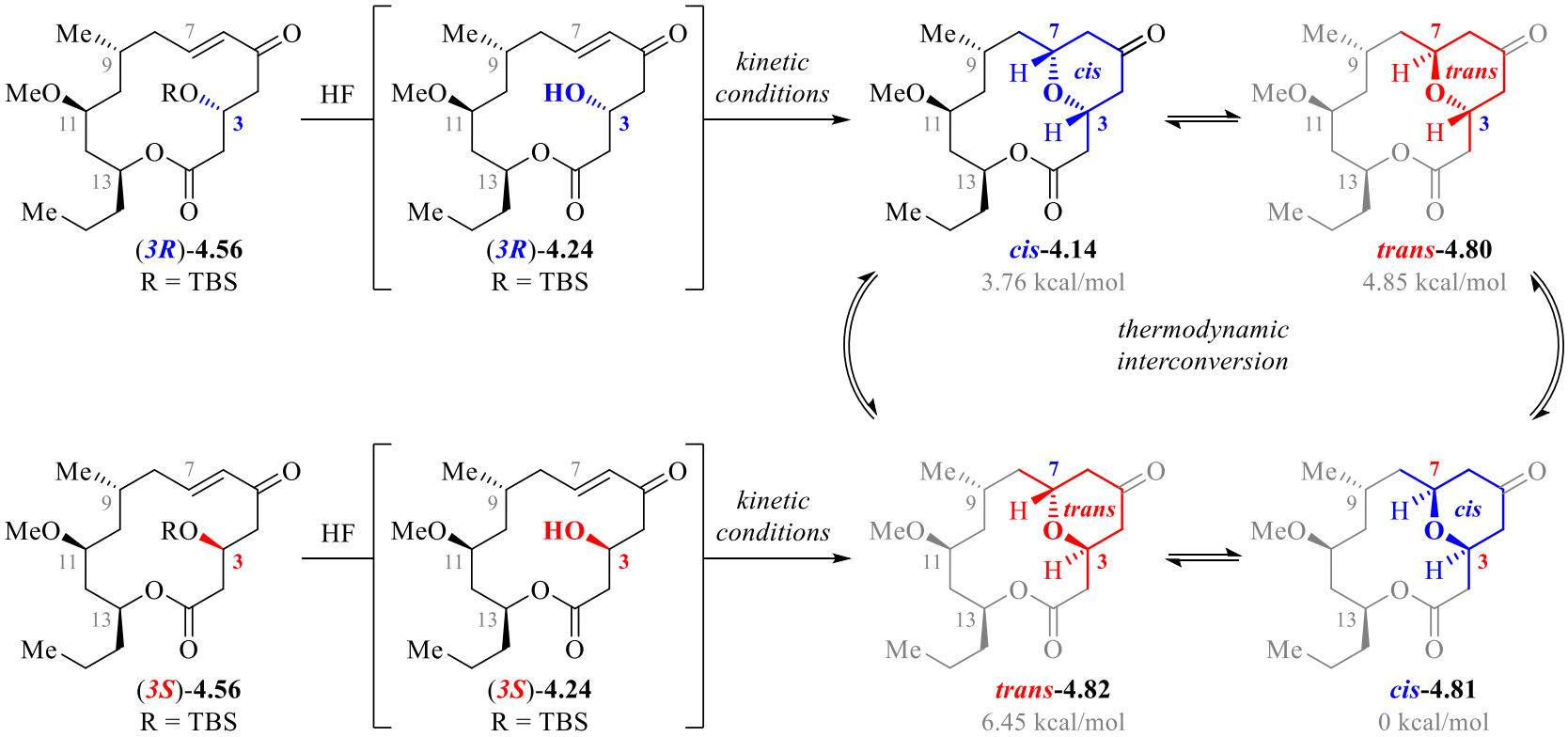

Product Distrubtions from (*3S*)-**4.56**	***cis*-4.14**	***trans*-4.80**	***cis*-4.81**	***trans*-4.82**
Kinetic Conditions (MeCN, 22 ºC, 5 h)	**-**	**-**	**1.0**	**1.8**
Thermodynamic ($CDCl_3$, 80 ºC, 15 h)	**0.18**	**-**	**1.0**	**0.15**

Kinetic Mixture *via* spontaneous cyclization of (3*R*-**4.24**), all 4 pyran isomers generated

^{1}H NMR (600 MHz, $CDCl_3$)

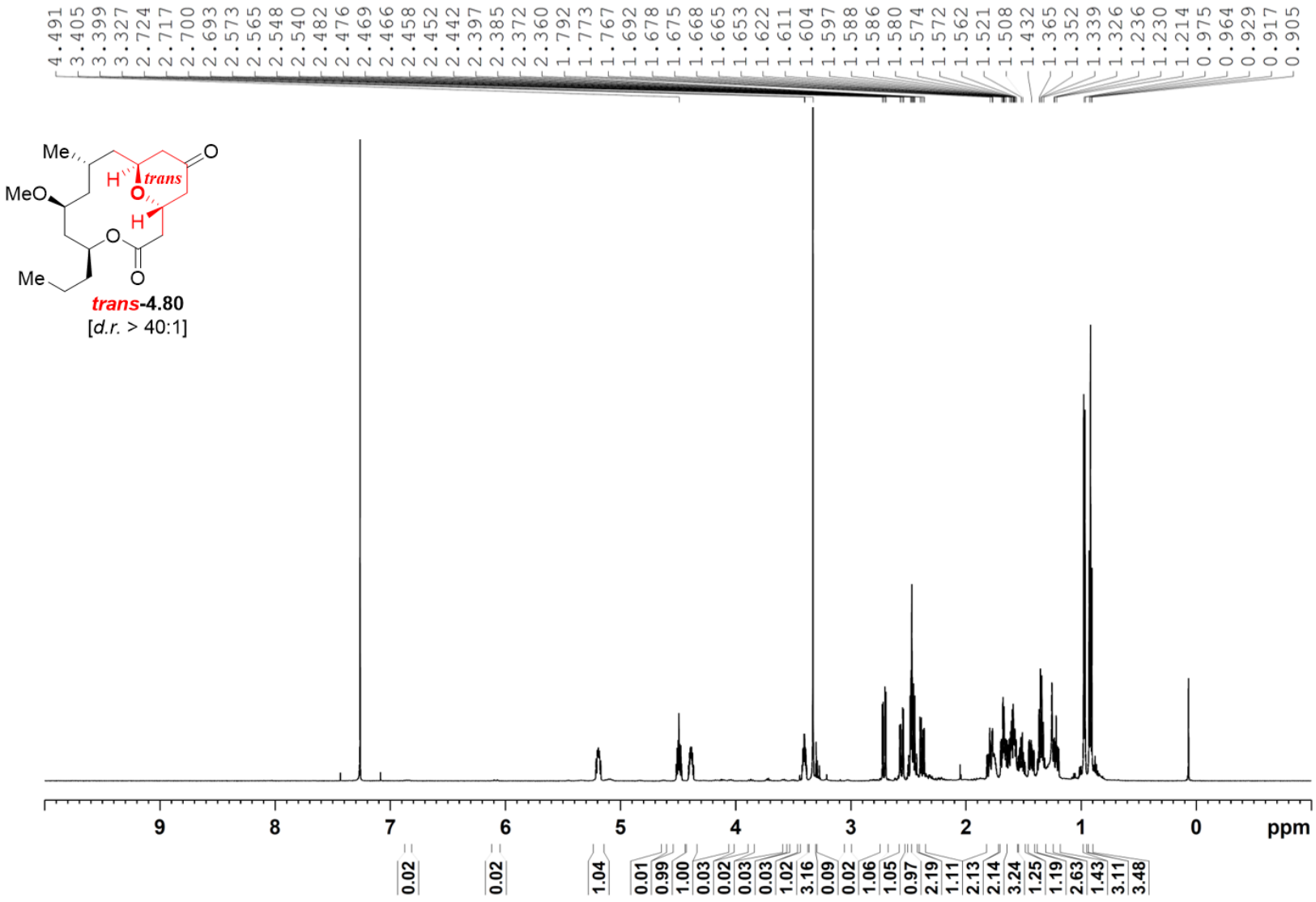

***trans*-4.80**
[*d.r.* > 40:1]

Kinetic Mixture *via* spontaneous cyclization of (3*R*-**4.24**): All 4 pyran isomers generated

^{1}H NMR (600 MHz, $CDCl_3$)

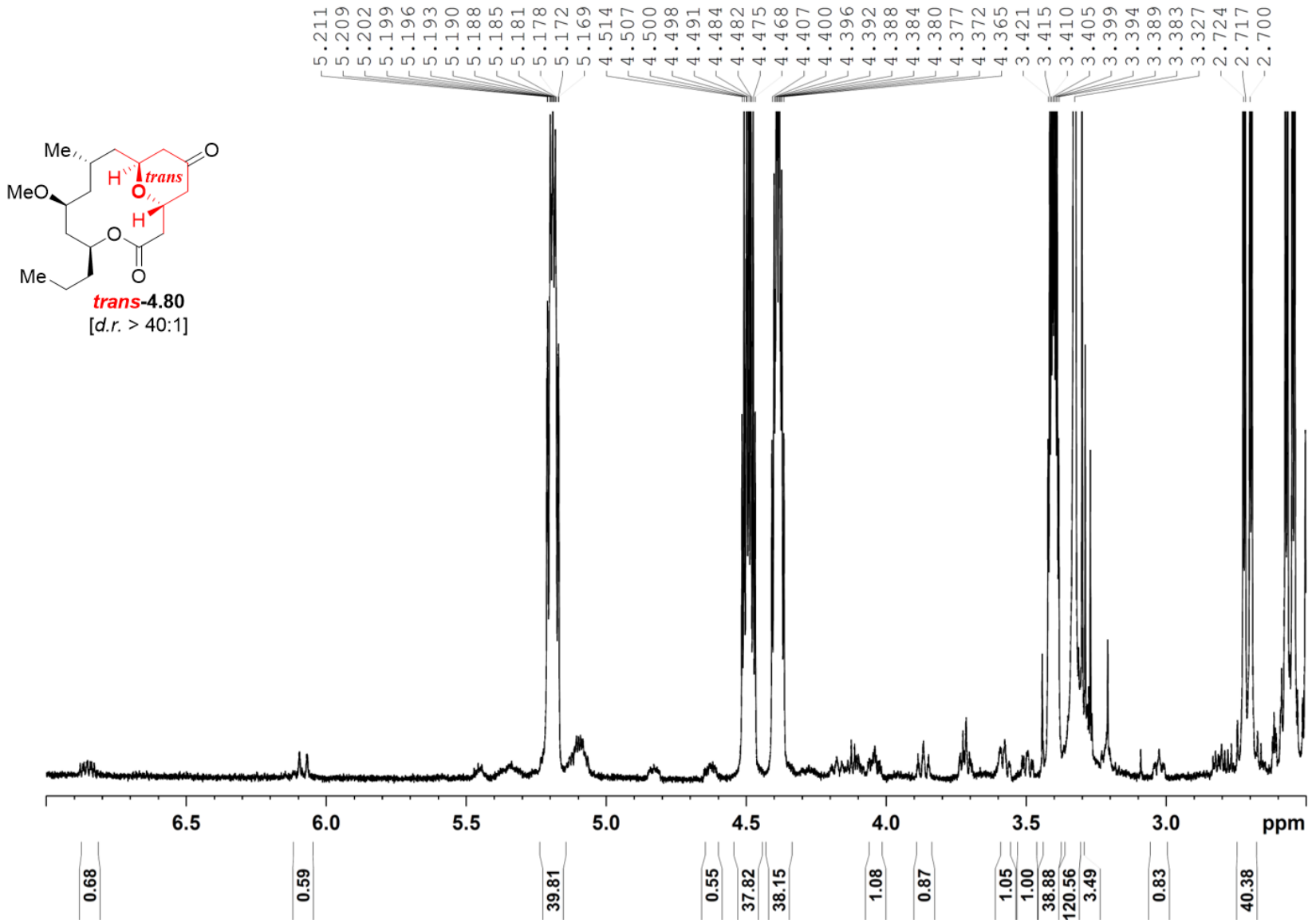

(3*R*,7*S*)-*trans*-$^{\Delta 7}$*epi*-neopeltolide macrocyclic core (*trans*-**4.80**)

^{13}C NMR (150 MHz, $CDCl_3$)

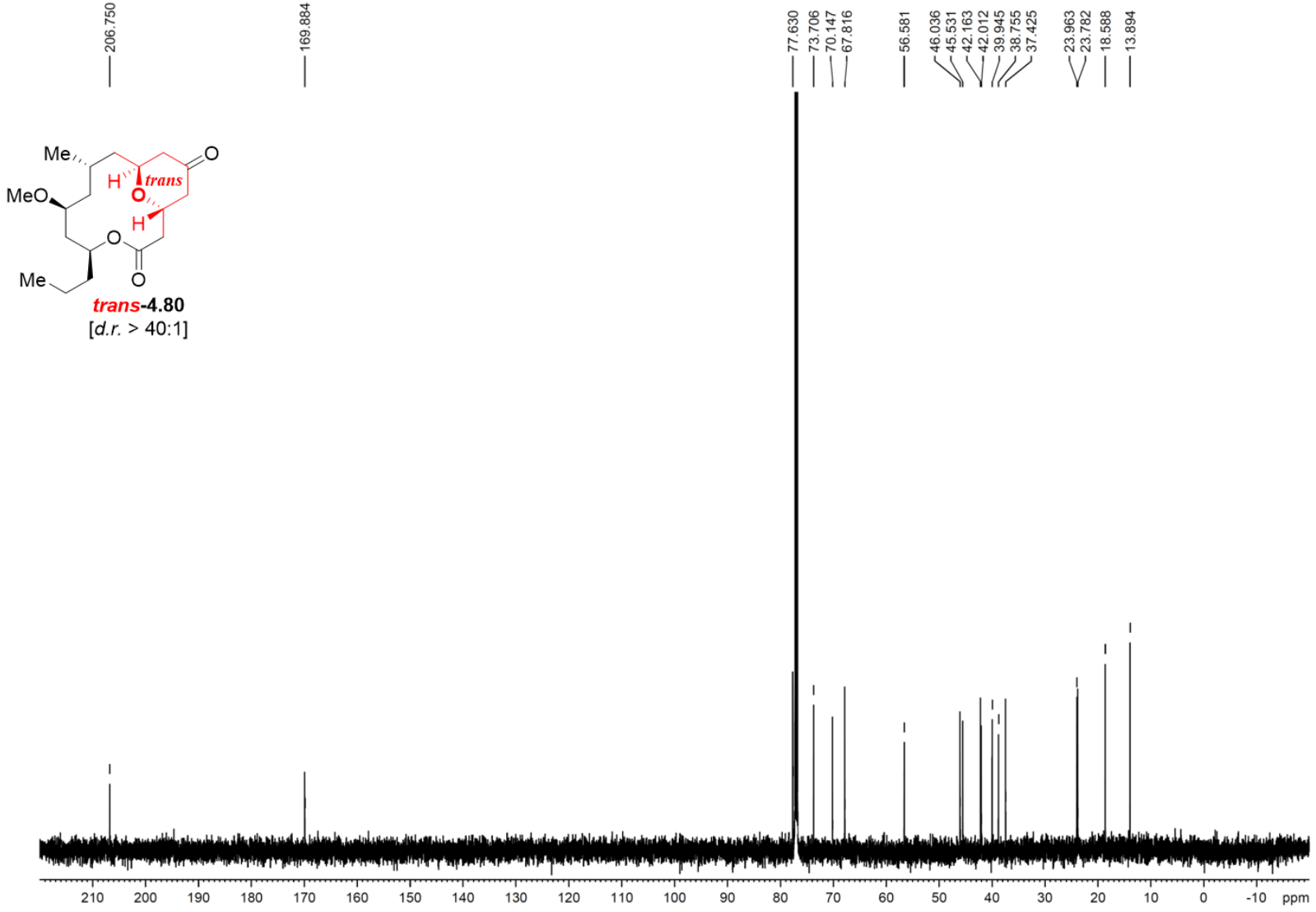

***trans*-4.80**
[*d.r.* > 40:1]

(3*R*,7*S*)-*trans*-$^{\Delta 7}$*epi*-neopeltolide macrocyclic core (*trans*-**4.80**)

COSY (600 MHz, $CDCl_3$)

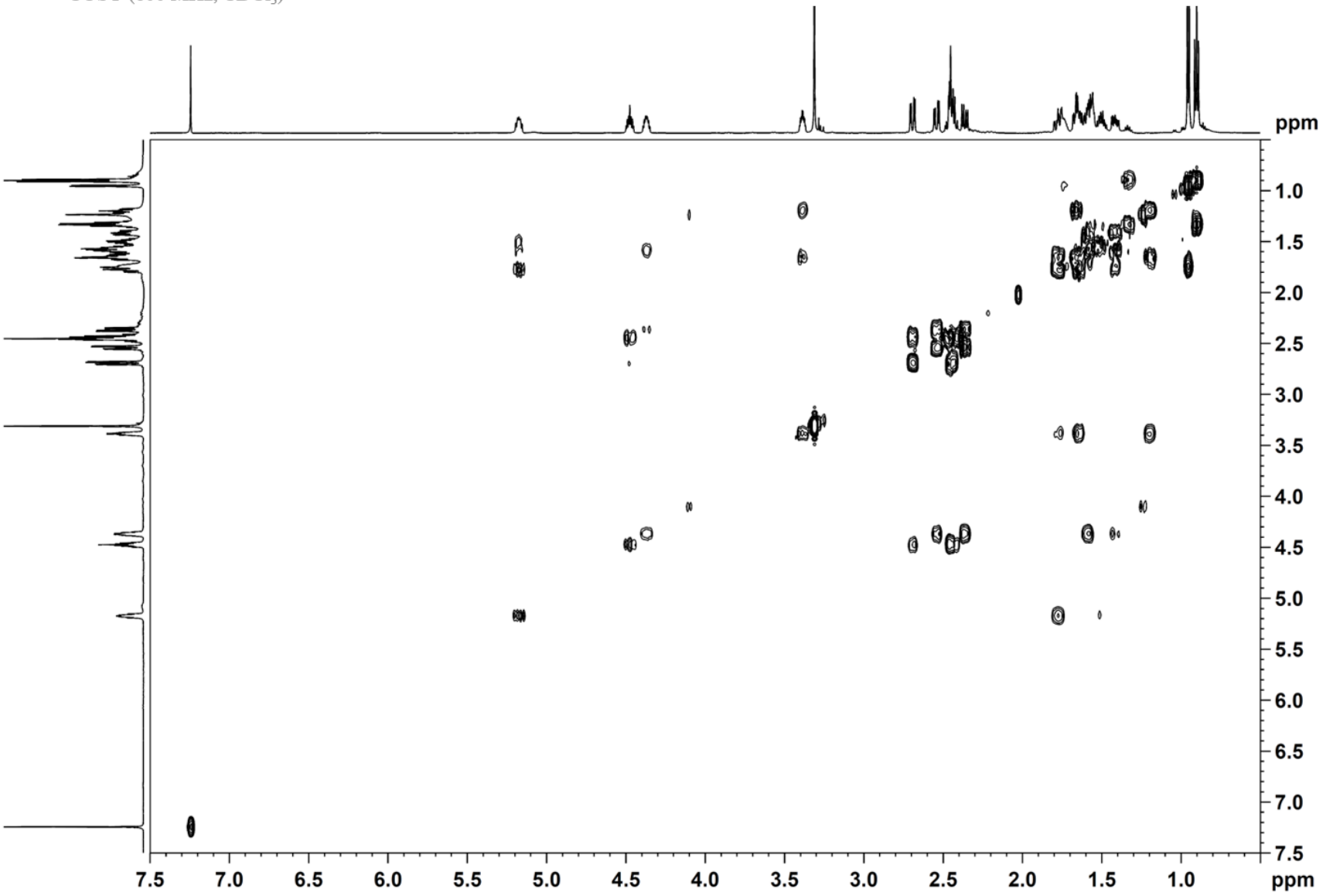

(3*R*,7*S*)-*trans*-$^{\Delta 7}$*epi*-neopeltolide macrocyclic core (*trans*-**4.80**)

HSQC (600 MHz, $CDCl_3$)

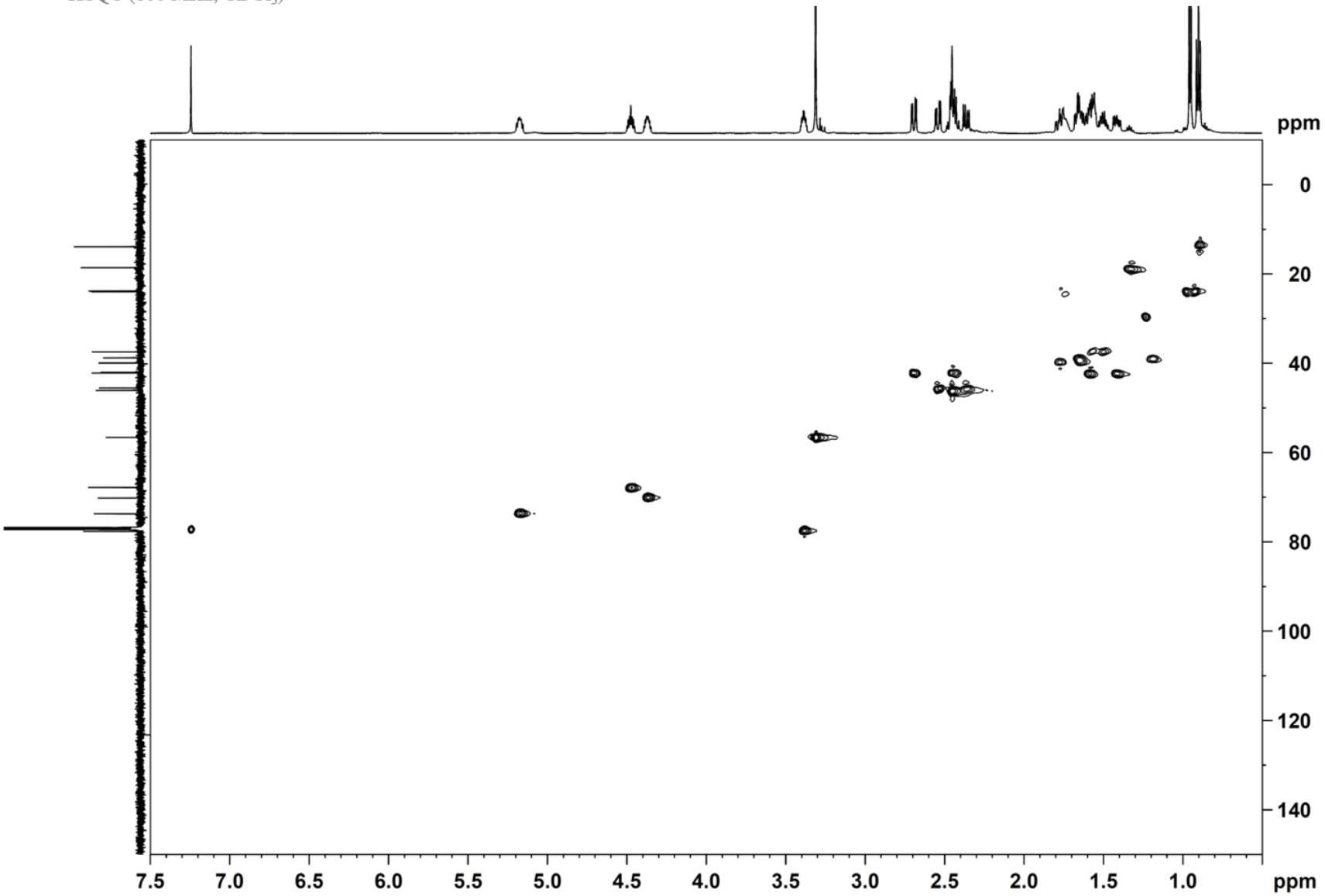

(3*R*,7*S*)-*trans*-$^{\Delta 7}$*epi*-neopeltolide macrocyclic core (*trans*-**4.80**)

1D Selective Gradient NOESY (600 MHz, $CDCl_3$)

δ 5.174 ppm (***H13***)

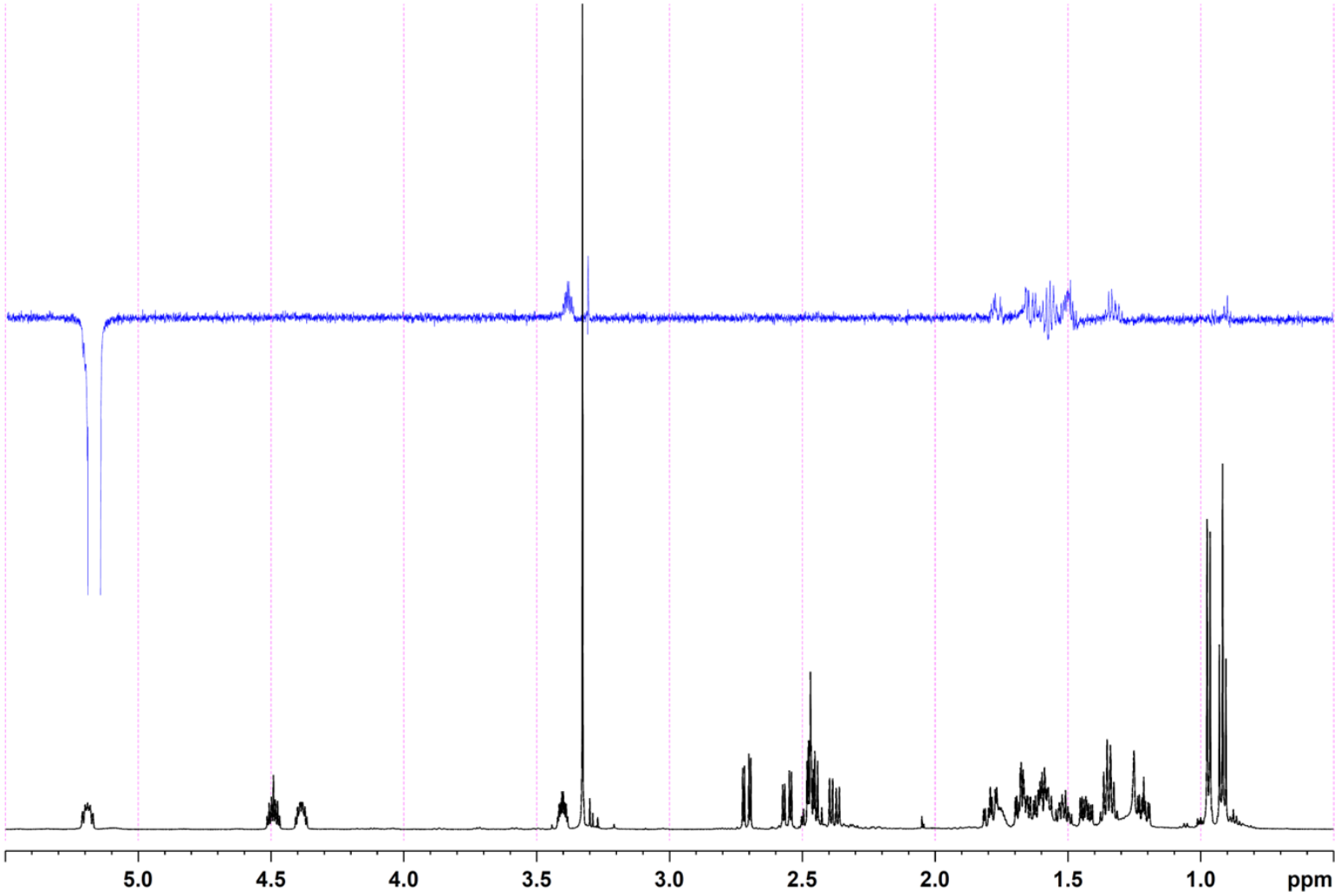

(3*R*,7*S*)-*trans*-$^{\Delta 7}$*epi*-neopeltolide macrocyclic core (*trans*-**4.80**)

1D Selective Gradient NOESY (600 MHz, $CDCl_3$)

δ 4.474 ppm (***H3***)

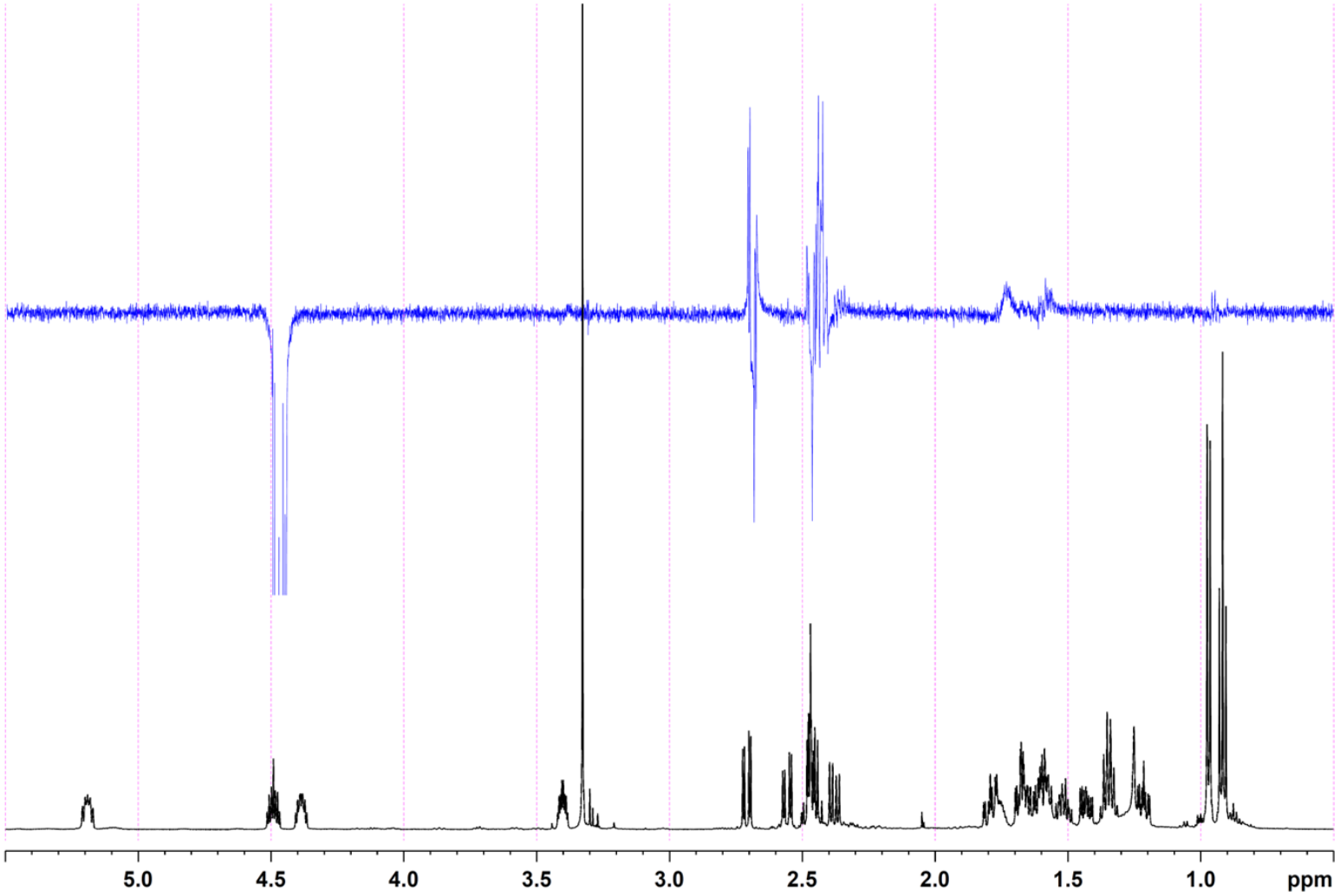

(3*R*,7*S*)-*trans*-$^{\Delta 7}$*epi*-neopeltolide macrocyclic core (*trans*-**4.80**)

1D Selective Gradient NOESY (600 MHz, $CDCl_3$)

δ 4.369 ppm (***H7***)

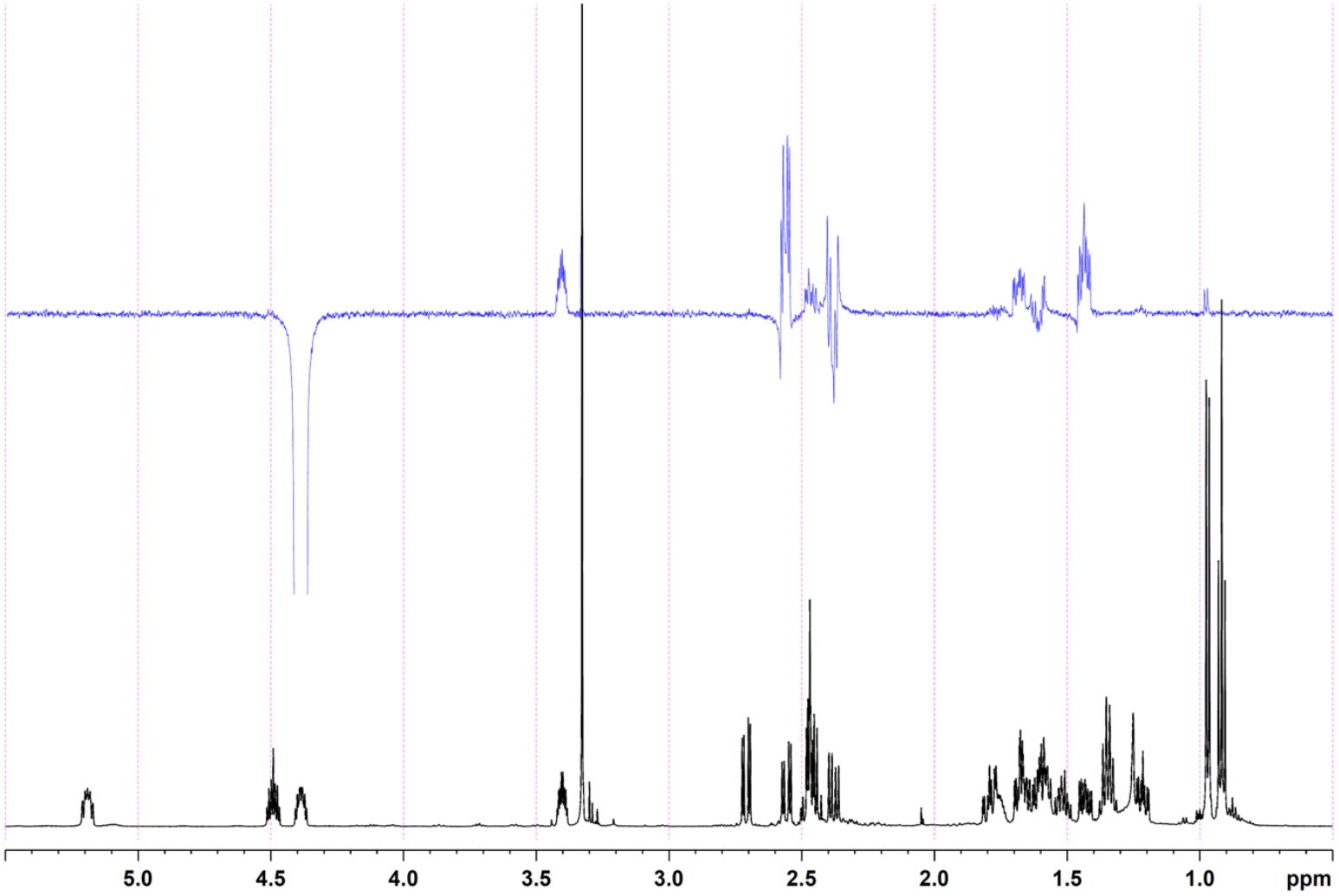

Thermodynamic Equilibration *via* (3*R*)-**4.24** (5 h reaction mixture): *cis*-**4.14** to *trans*-**4.80** to *cis*-**4.81** to *trans*-**4.82** [*d.r.* = 25 : 4 : 20 : 1]

^{1}H NMR (600 MHz, $CDCl_3$)

t = 5 h, T = 80 °C, H^+ = Amberlyst-15®

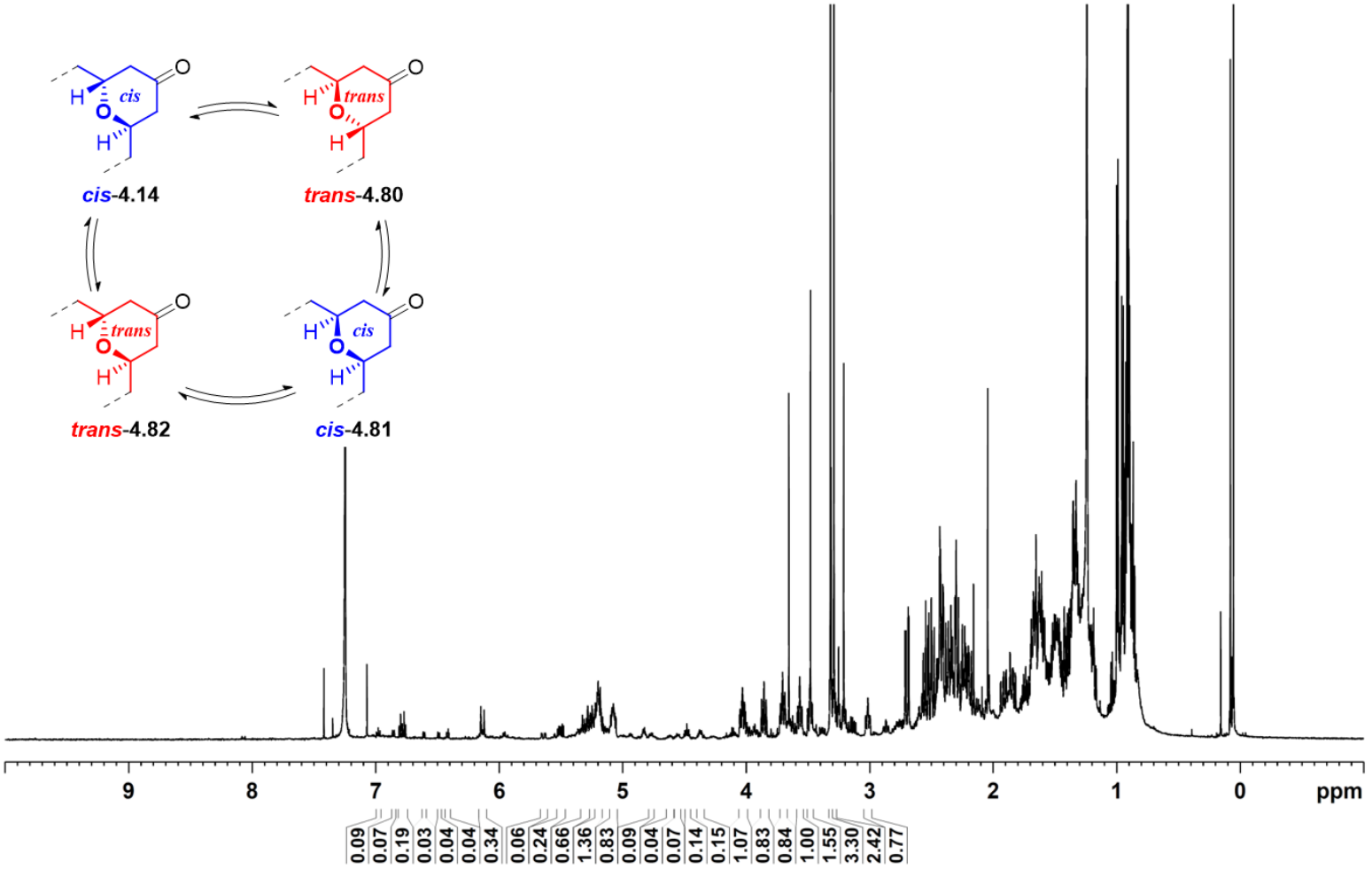

Thermodynamic Equilibration *via* (3*R*)-**4.24** (10 h reaction mixture): *cis*-**4.14** to *trans*-**4.80** to *cis*-**4.81** to *trans*-**4.82** [*d.r.* = 25 : 2.5 : 17.5 : 1]

^{1}H NMR (600 MHz, $CDCl_3$)

t = 10 h, T = 80 °C, H^+ = Amberlyst-15®

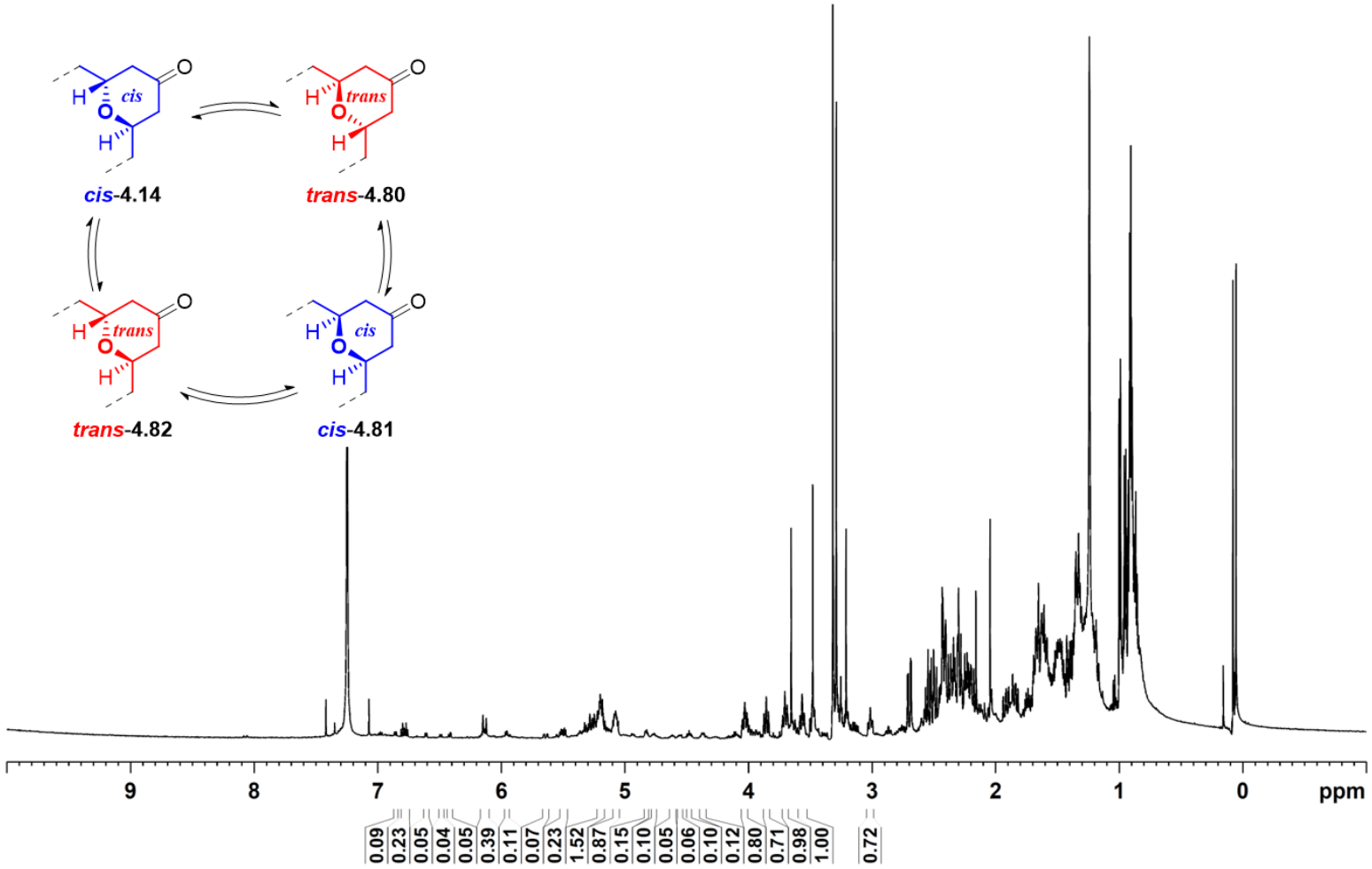

Thermodynamic Equilibration (3*R*, 10 h): *cis*-**4.14** to *cis*-**4.81** [*d.r.* ~ 10:7]

1D Selective Gradient NOESY (600 MHz, $CDCl_3$)

δ 4.028 ppm (***cis*-4.14 *H3***)

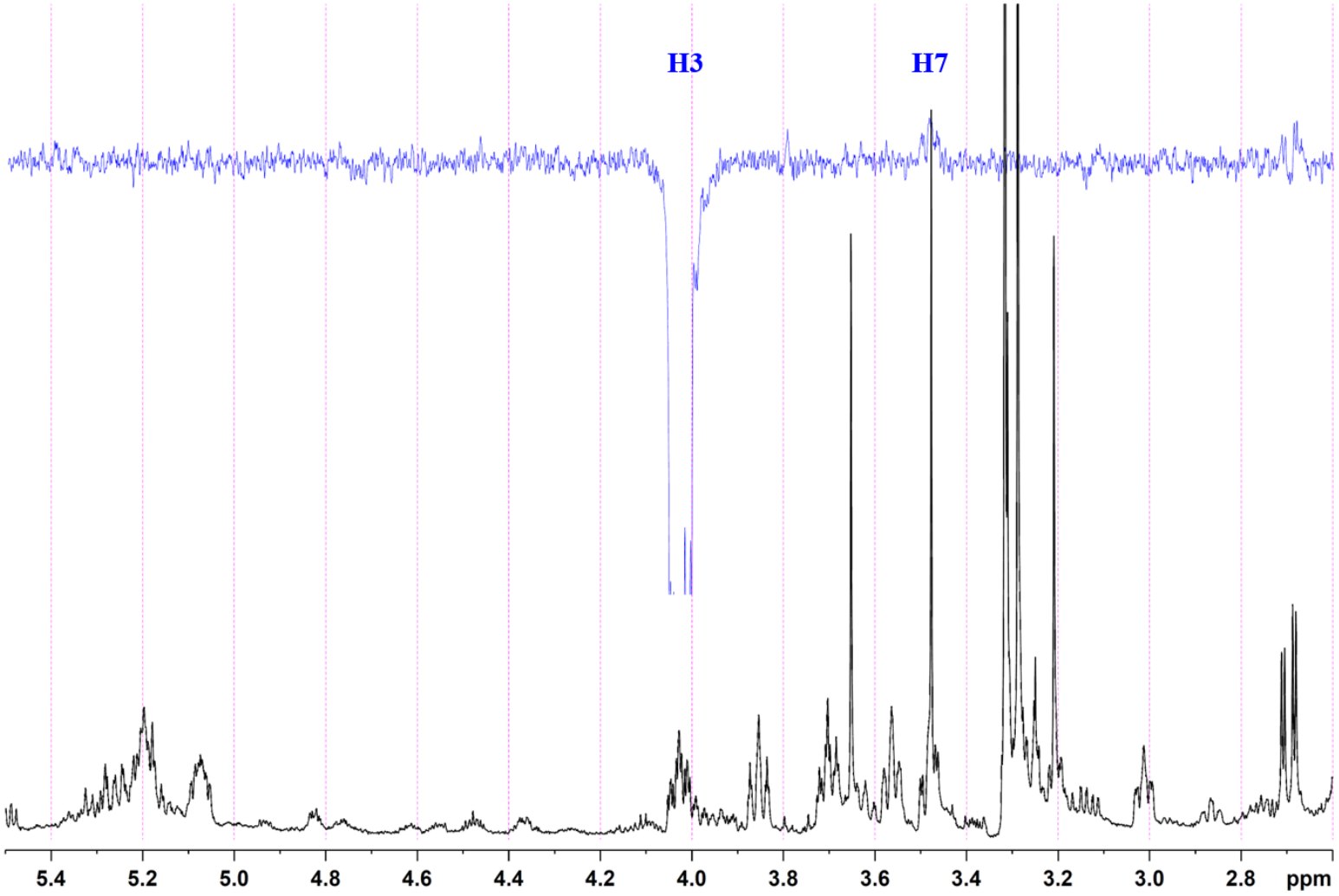

Thermodynamic Equilibration (3*R*, 15 h): *cis*-**4.14** to *cis*-**4.81** [*d.r.* ~ 5:3]

^{1}H NMR (600 MHz, $CDCl_3$)

t = 15 h, T = 80 °C, H^+ = Amberlyst-15®

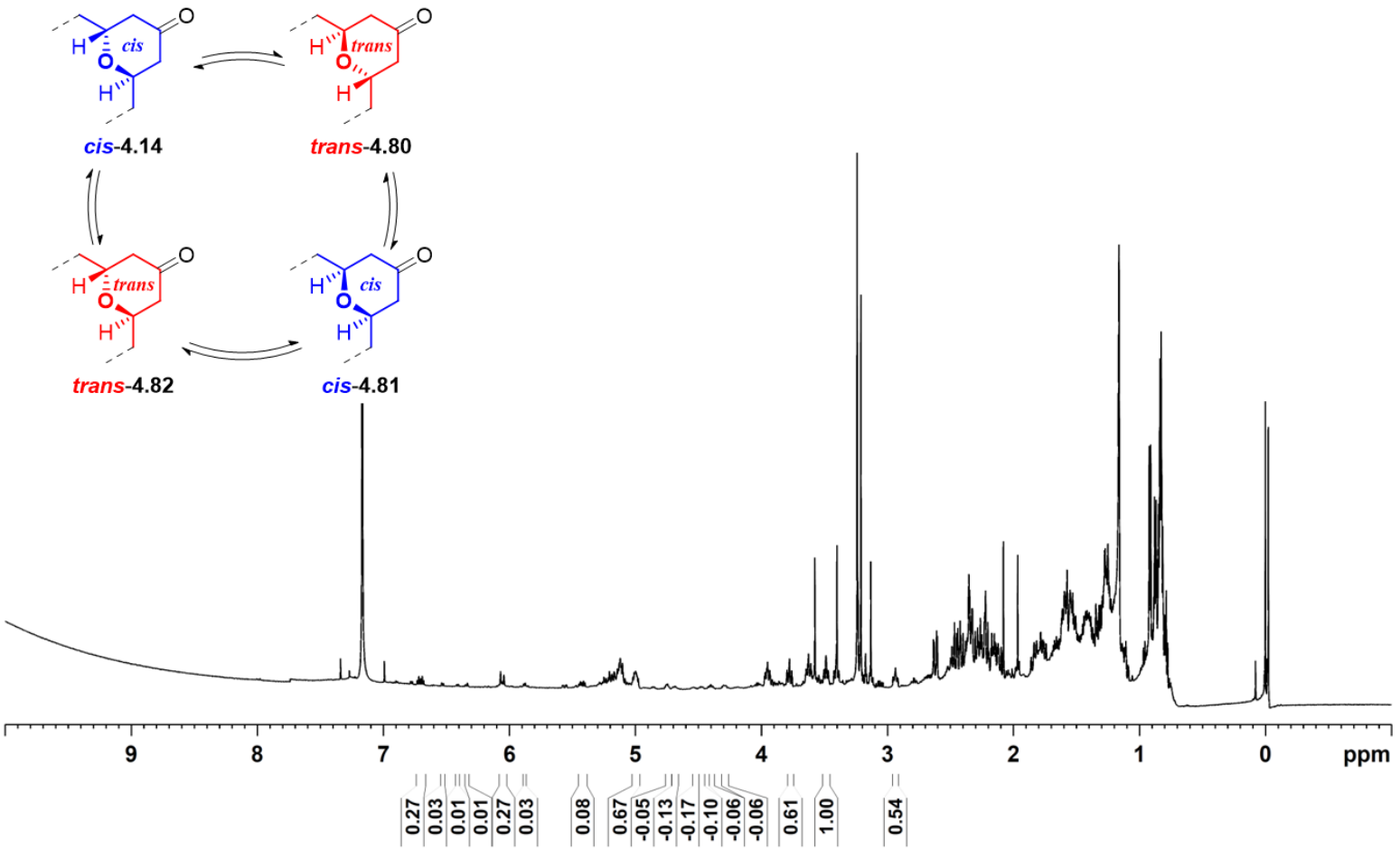

Kinetic Mixture *via* spontaneous cyclization of (3*S*-**4.24**): *cis*-**4.81** to *trans*-**4.82** [*d.r.* = 5:9]

^{1}H NMR (600 MHz, $CDCl_3$)

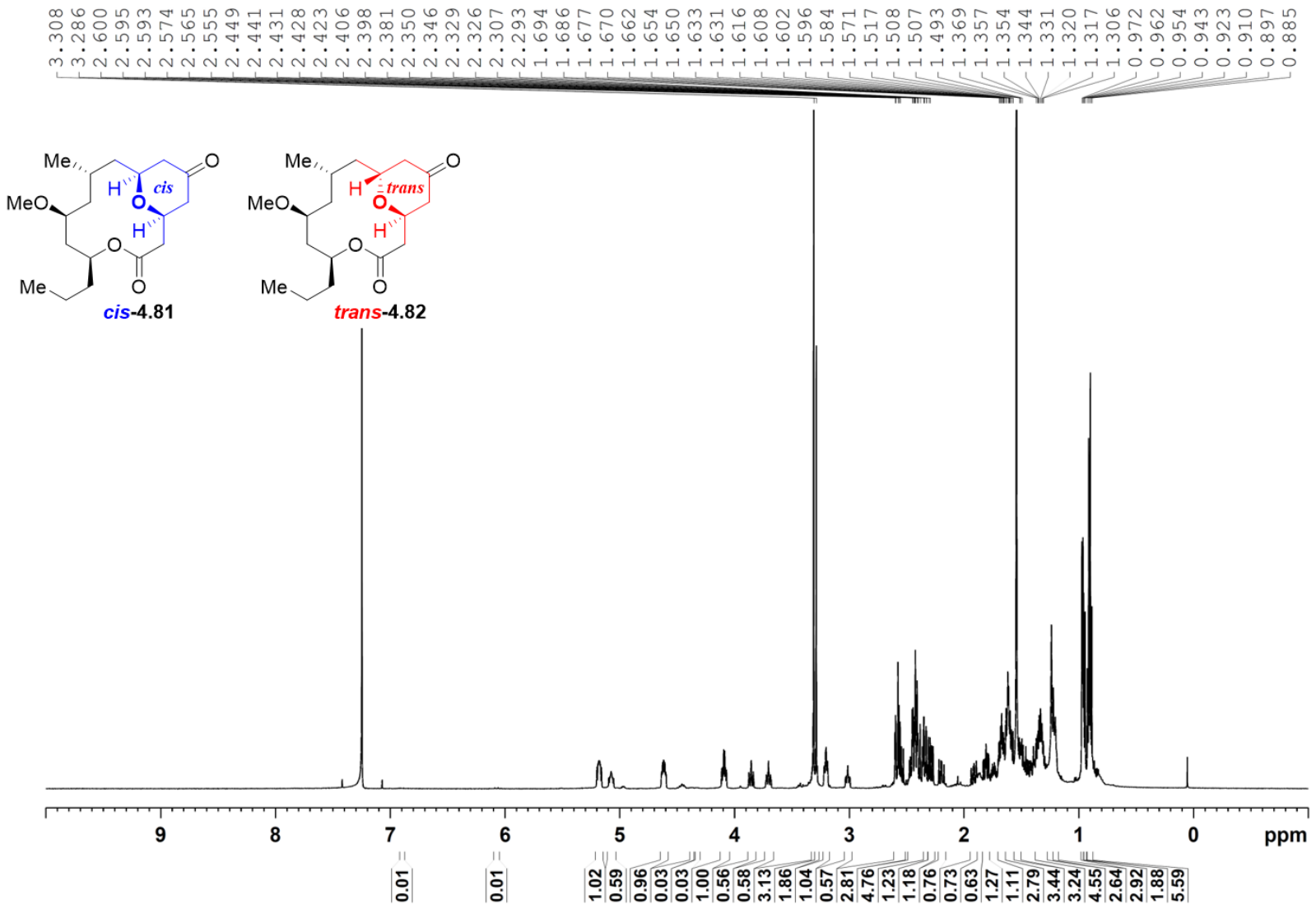

Kinetic Mixture *via* spontaneous cyclization of (3*S*-**4.24**): *cis*-**4.81** to *trans*-**4.82** [*d.r.* = 5:9]

^{1}H NMR (600 MHz, $CDCl_3$)

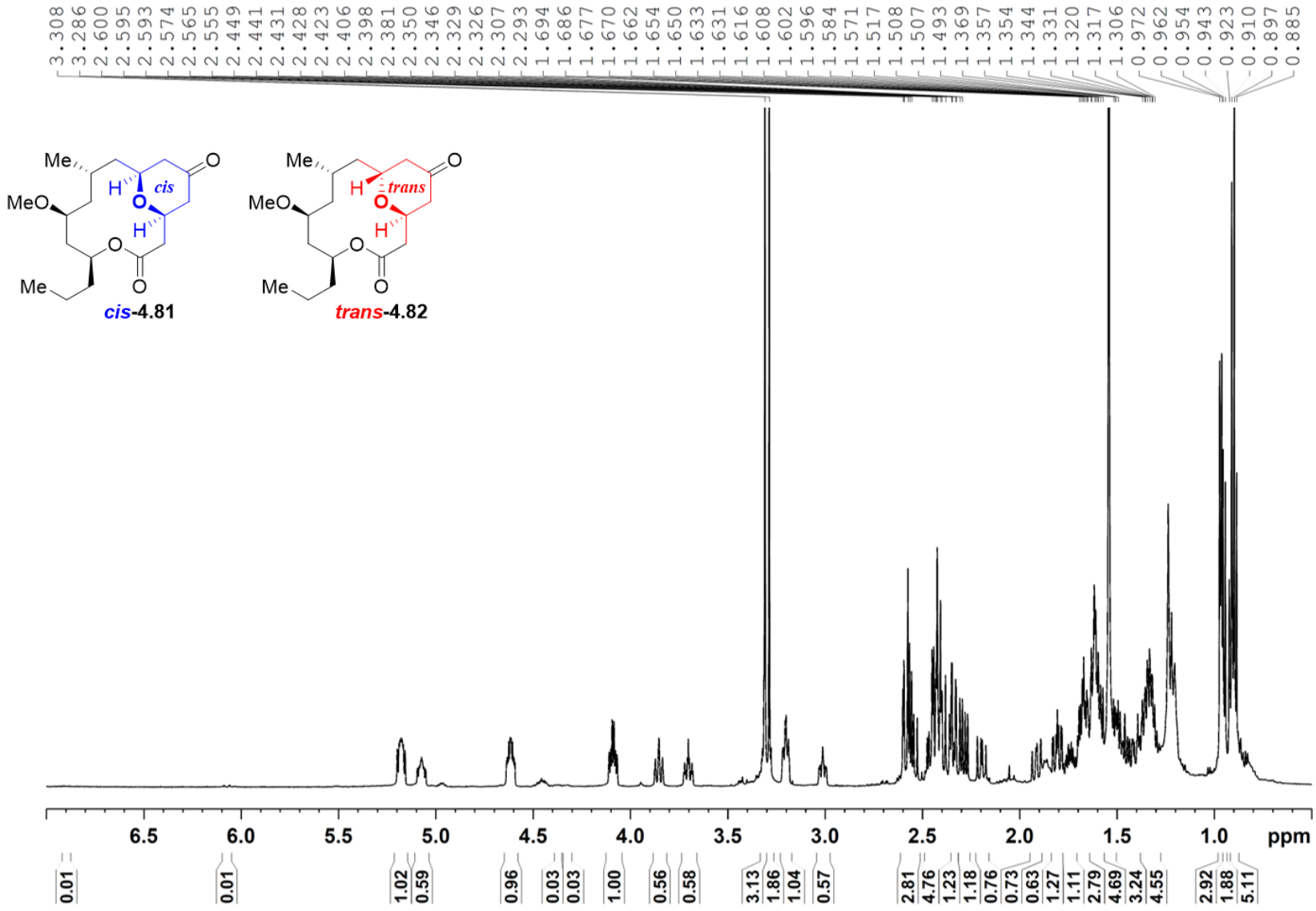

Kinetic Mixture *via* spontaneous cyclization of (3*S*-**4.24**): *cis*-**4.81** to *trans*-**4.82** [*d.r.* = 5:9]

^{13}C NMR (150 MHz, $CDCl_3$)

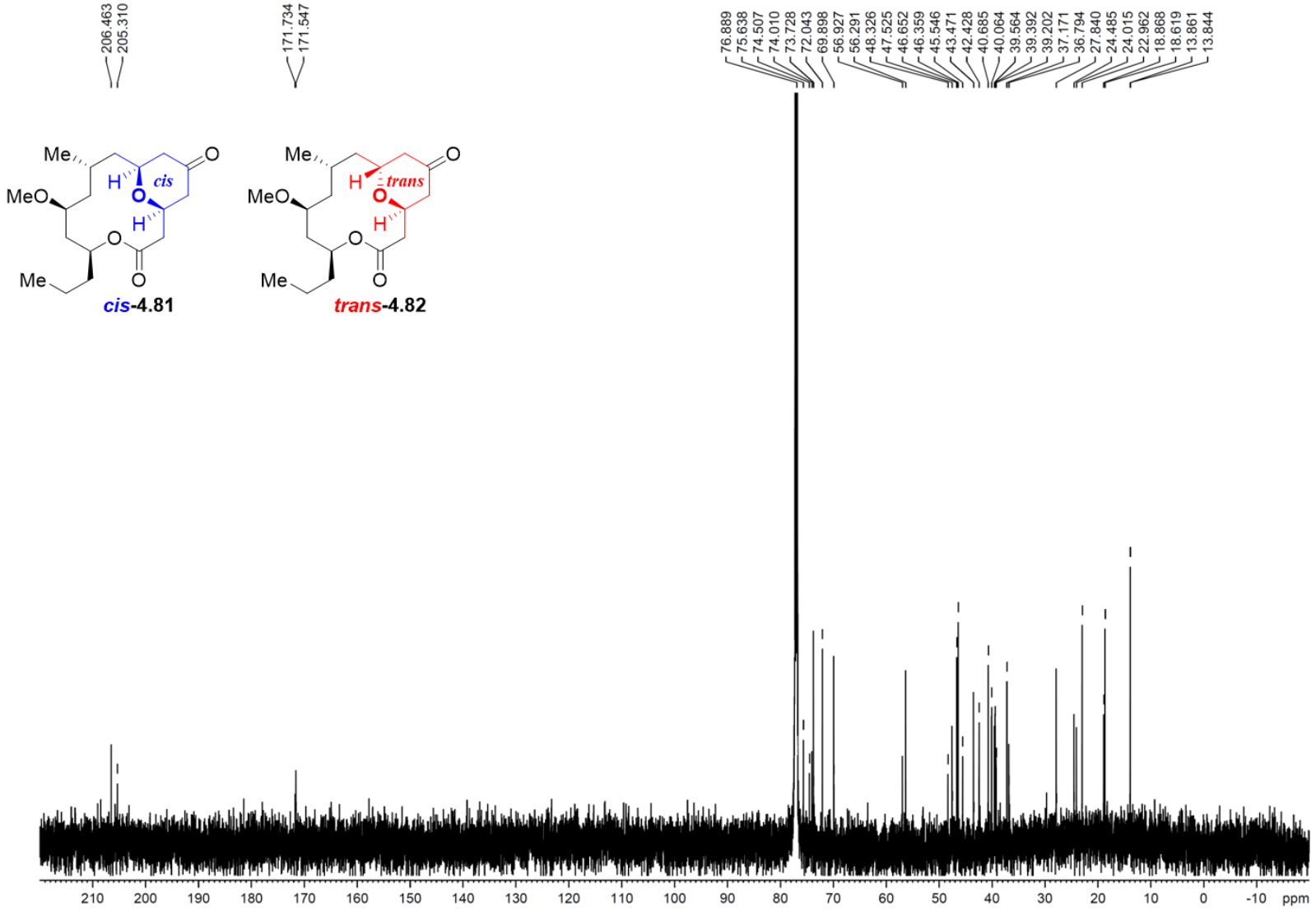

Kinetic Mixture *via* spontaneous cyclization of (3*S*-**4.24**): *cis*-**4.81** to *trans*-**4.82** [*d.r.* = 5:9]

COSY (600 MHz, $CDCl_3$)

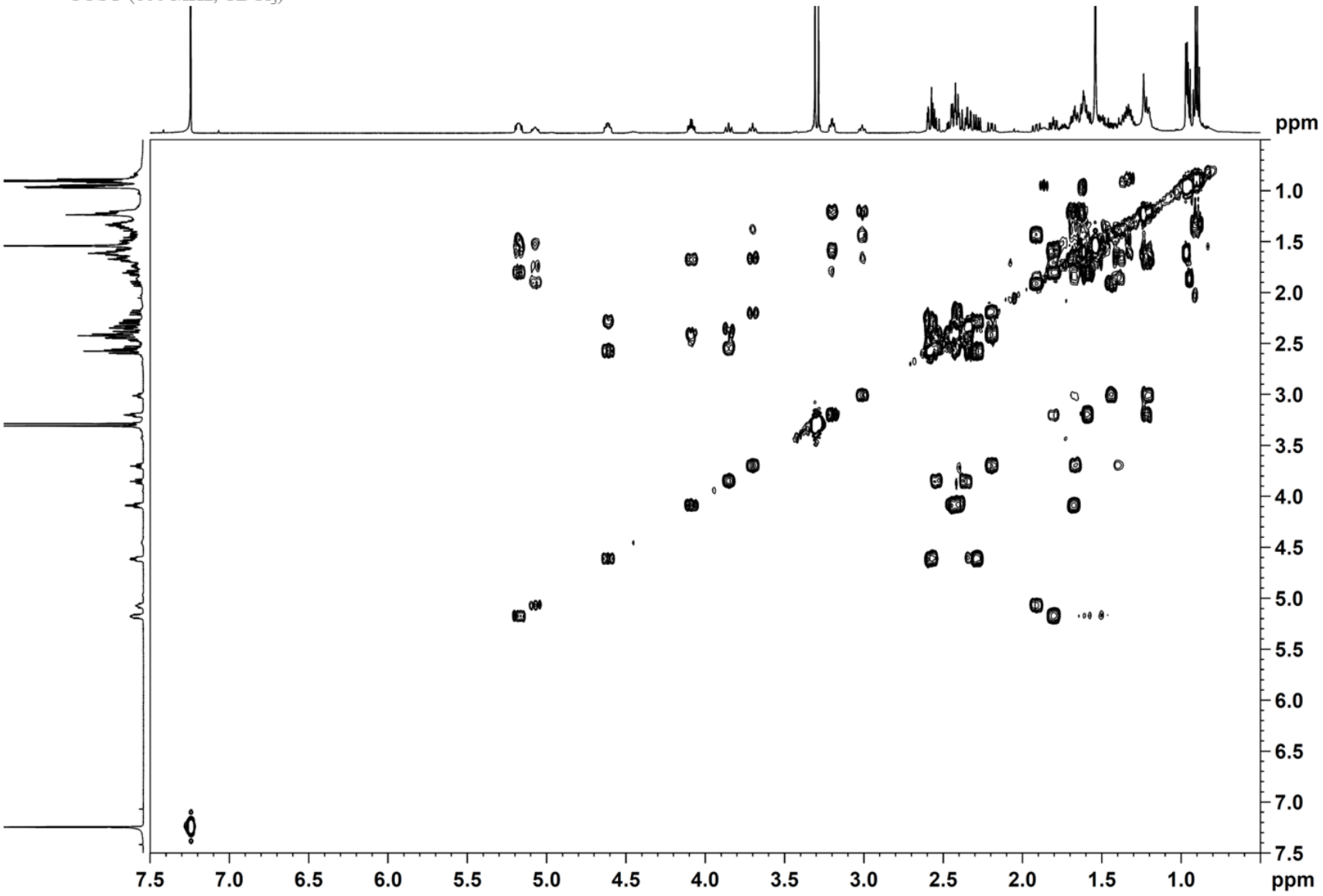

Kinetic Mixture *via* spontaneous cyclization of (3*S*-**4.24**): *cis*-**4.81** to *trans*-**4.82** [*d.r.* = 5:9]

HSQC (600 MHz, $CDCl_3$)

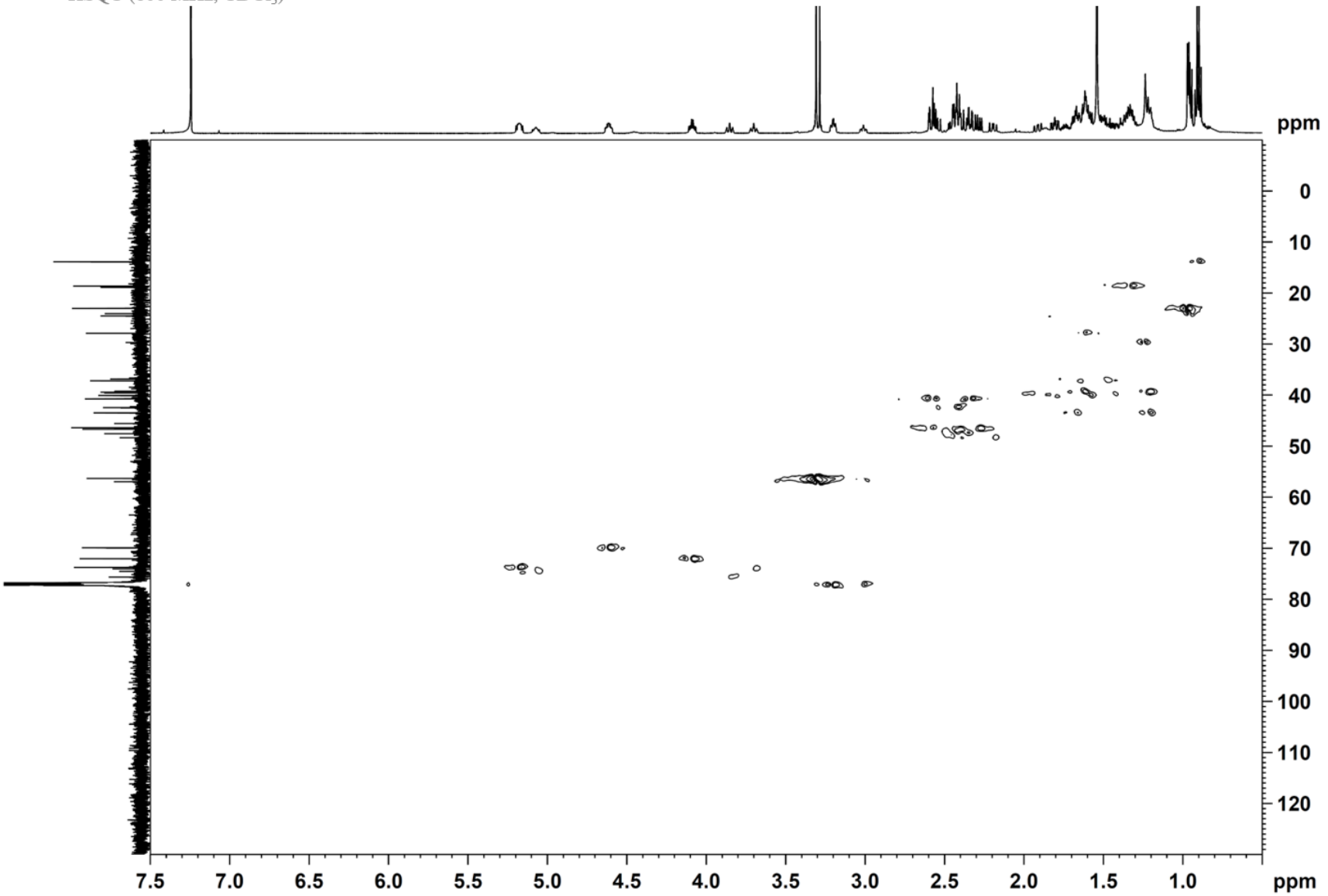

(3*S*,7*R*)-*trans*-$^{\Delta 3}$*epi*-neopeltolide macrocyclic core (*trans*-**4.82**)

1D Selective Gradient NOESY (600 MHz, $CDCl_3$)

δ 5.180 ppm (***H13***)

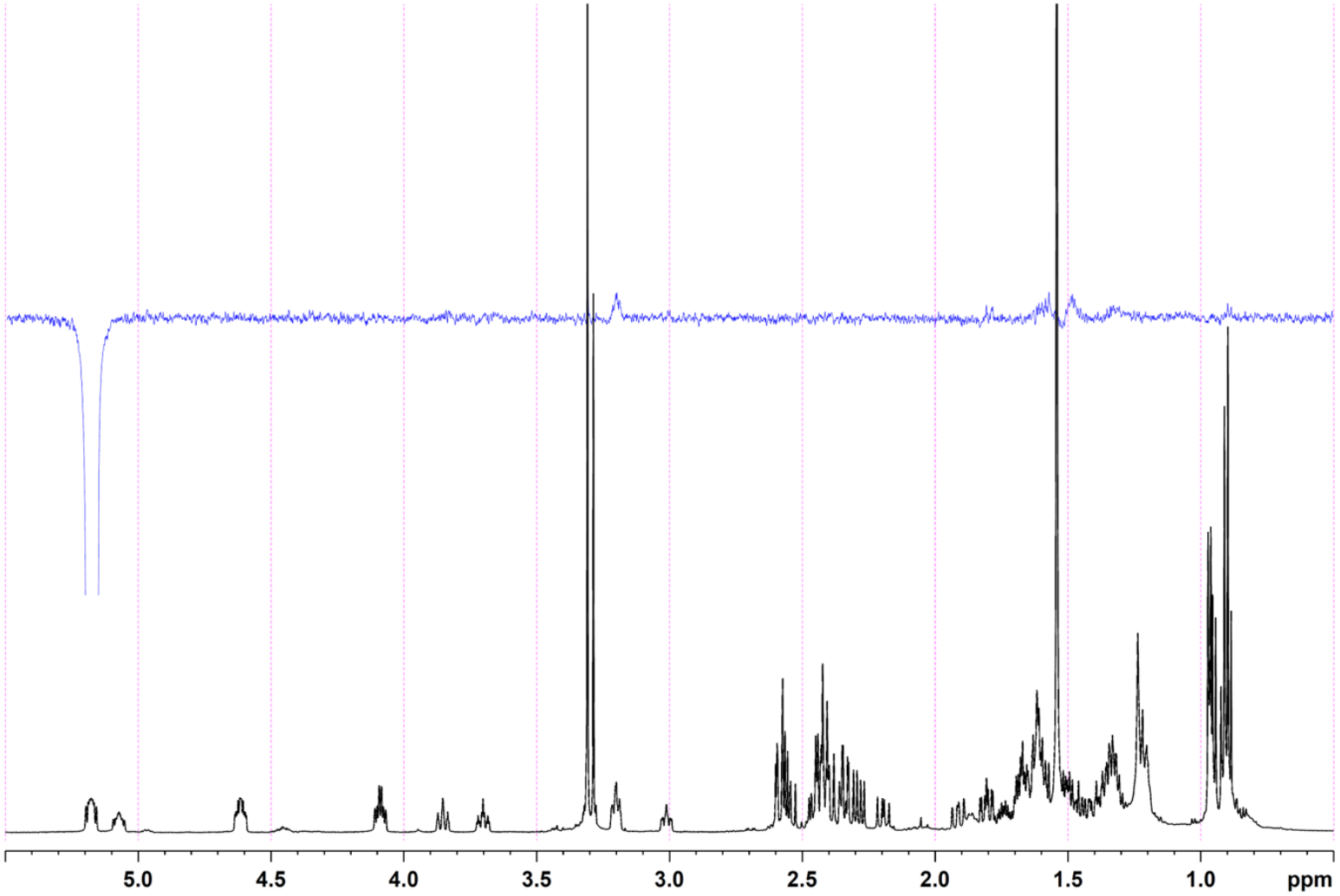

(3*S*,7*S*)-*cis*-$^{\Delta 3,7}$*epi*-neopeltolide macrocyclic core (*cis*-**4.81**)

1D Selective Gradient NOESY (600 MHz, $CDCl_3$)

δ 5.071 ppm (***H13***)

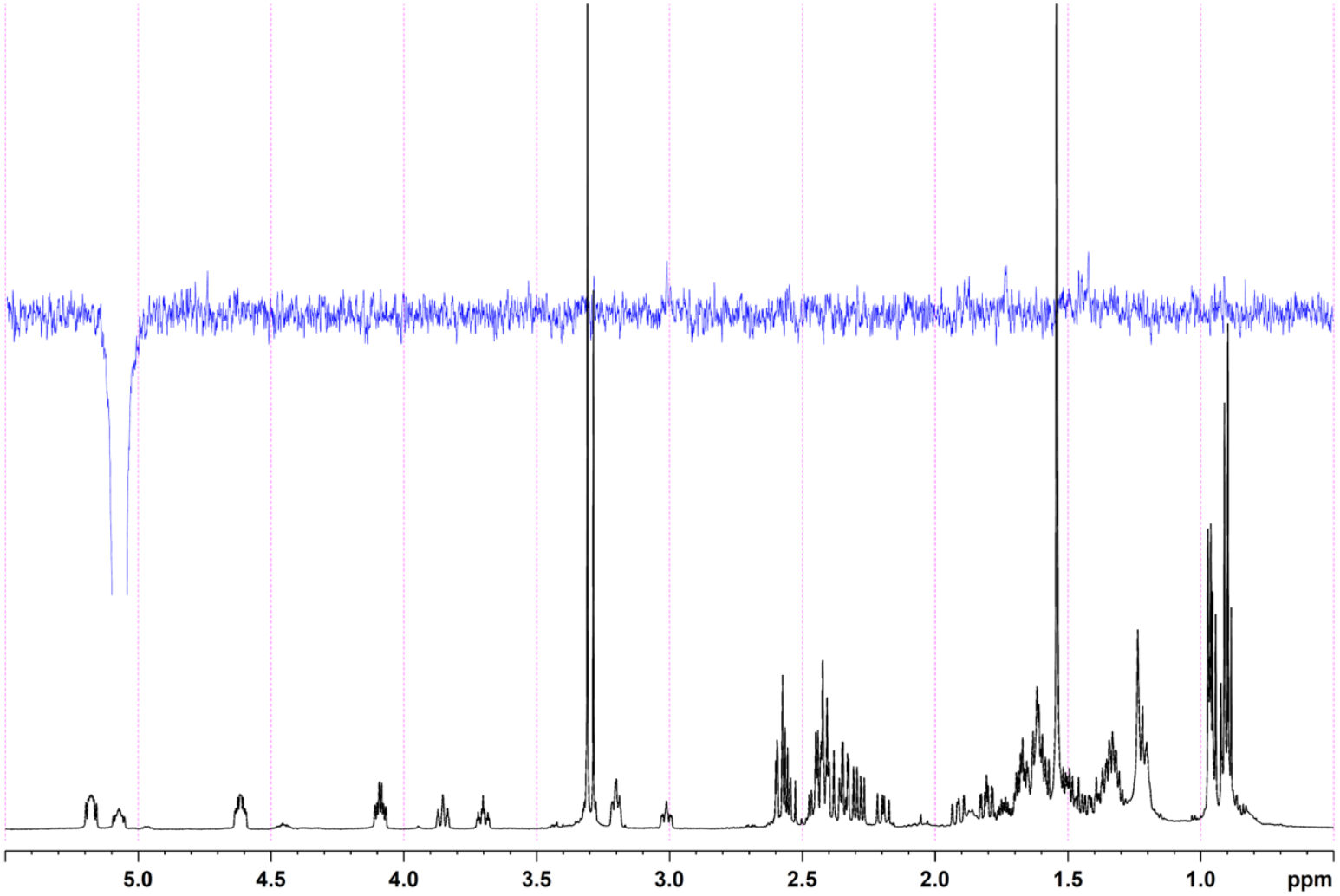

(3*S*,7*R*)-*trans*-$^{\Delta 3}$*epi*-neopeltolide macrocyclic core (*trans*-**4.82**)

1D Selective Gradient NOESY (600 MHz, $CDCl_3$)

δ 4.614 ppm (***H3***)

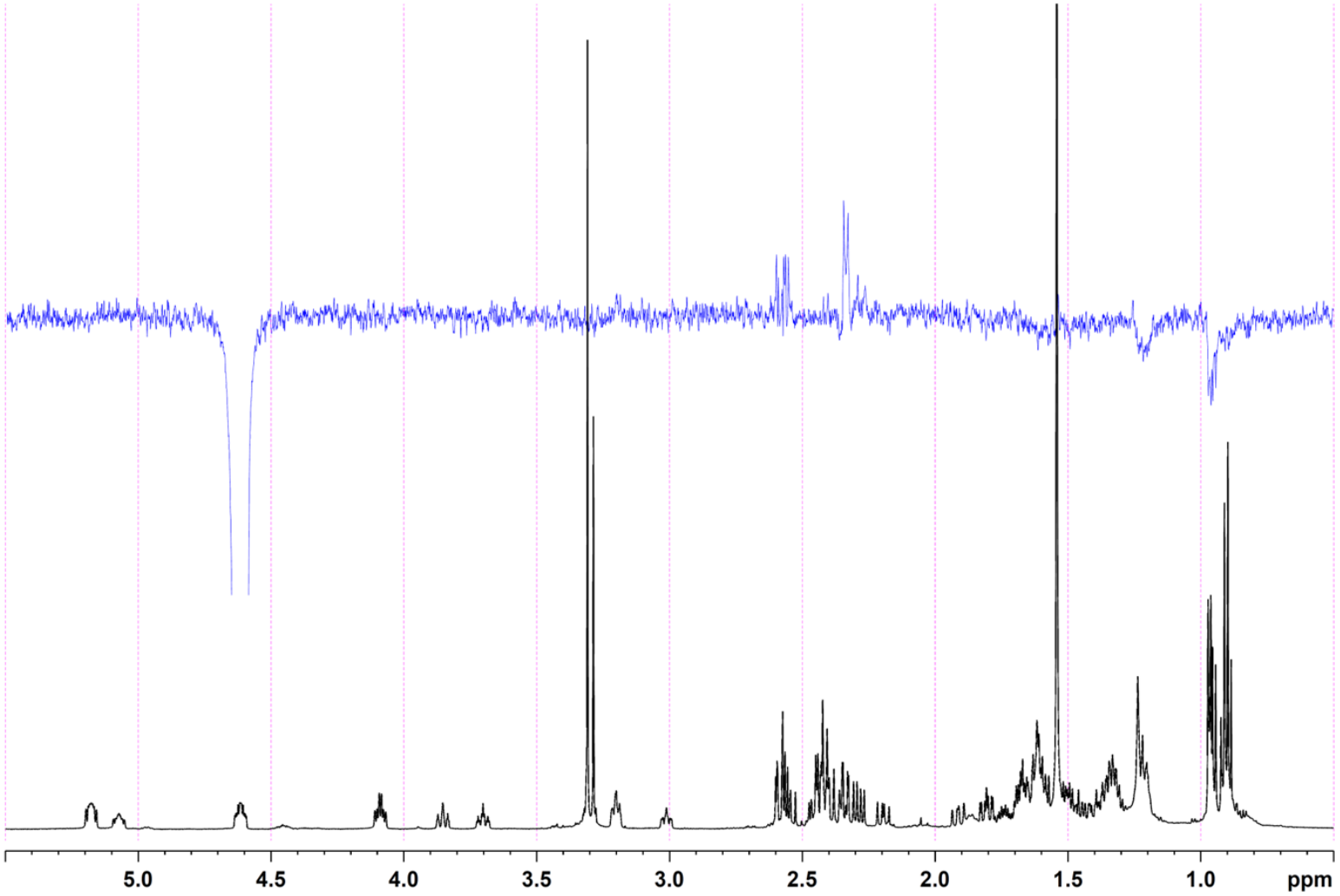

(3*S*,7*R*)-*trans*-$^{\Delta 3}$*epi*-neopeltolide macrocyclic core (*trans*-**4.82**)

1D Selective Gradient NOESY (600 MHz, $CDCl_3$)

δ 4.094 ppm (***H7***)

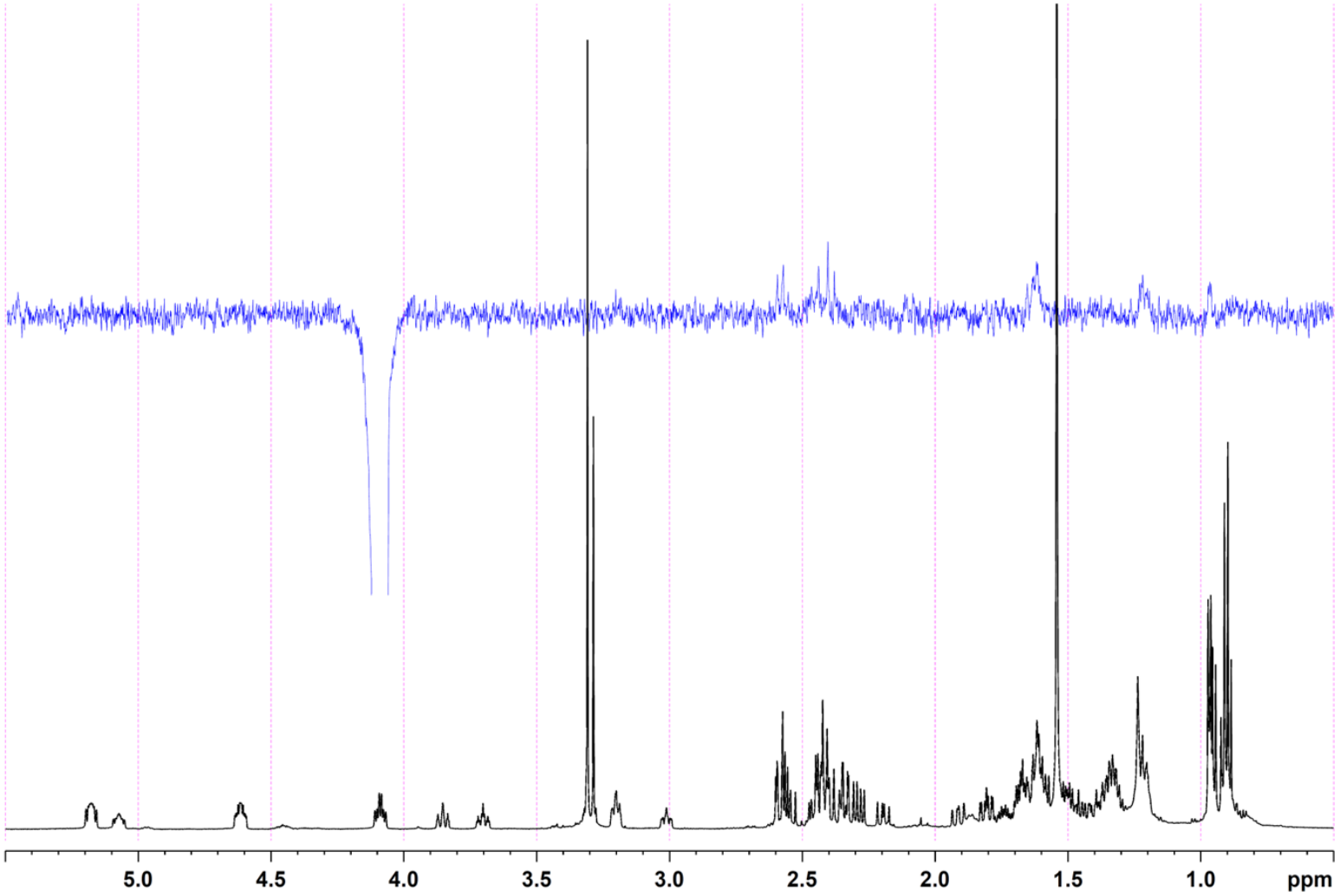

(3*S*,7*S*)-*cis*-$^{\Delta 3,7}$*epi*-neopeltolide macrocyclic core (*cis*-**4.81**)

1D Selective Gradient NOESY (600 MHz, $CDCl_3$)

δ 3.856 ppm (***H3***)

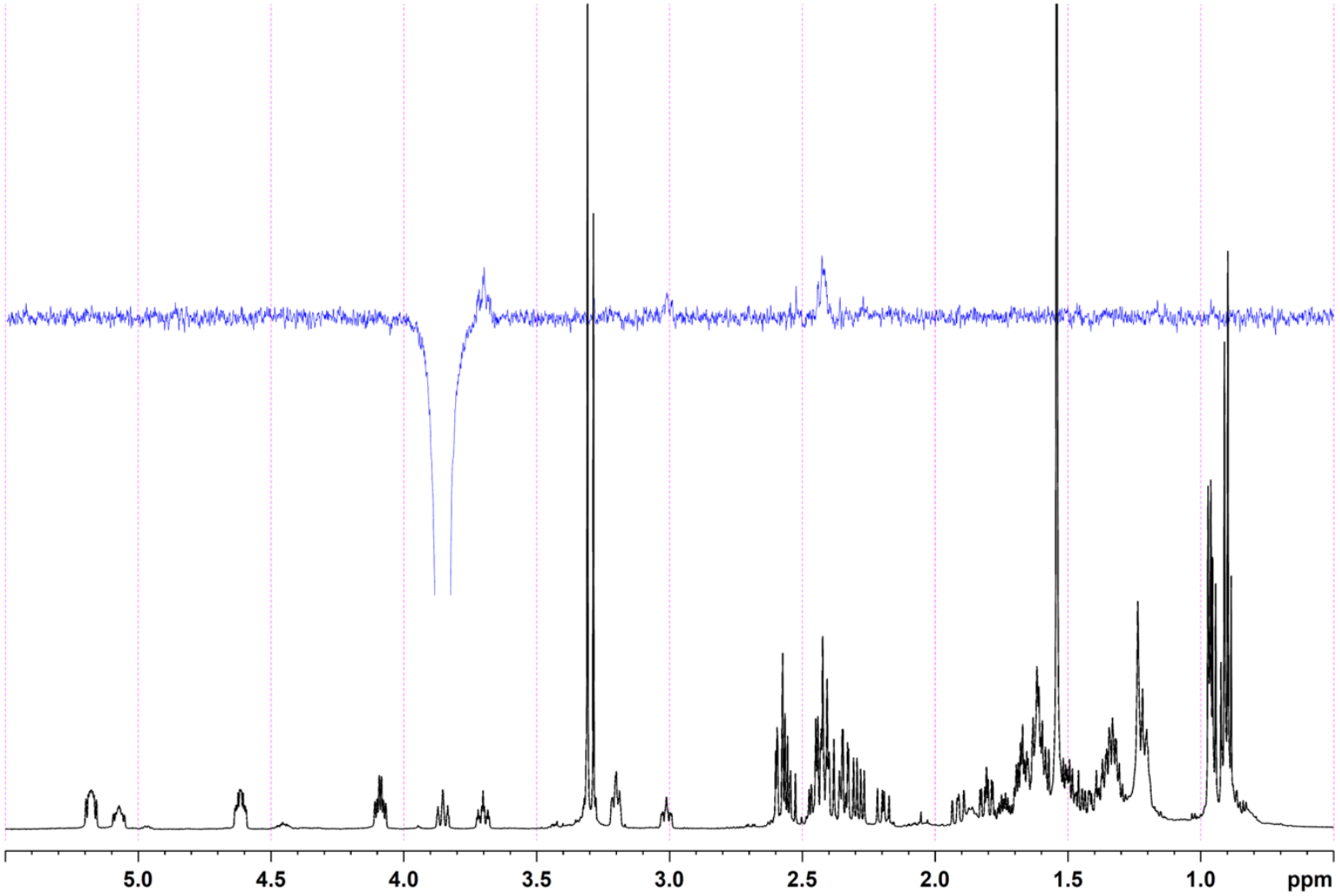

(3*S*,7*S*)-*cis*-$^{\Delta 3,7}$*epi*-neopeltolide macrocyclic core (*cis*-**4.81**)

1D Selective Gradient NOESY (600 MHz, $CDCl_3$)

δ 3.700 ppm (***H7***)

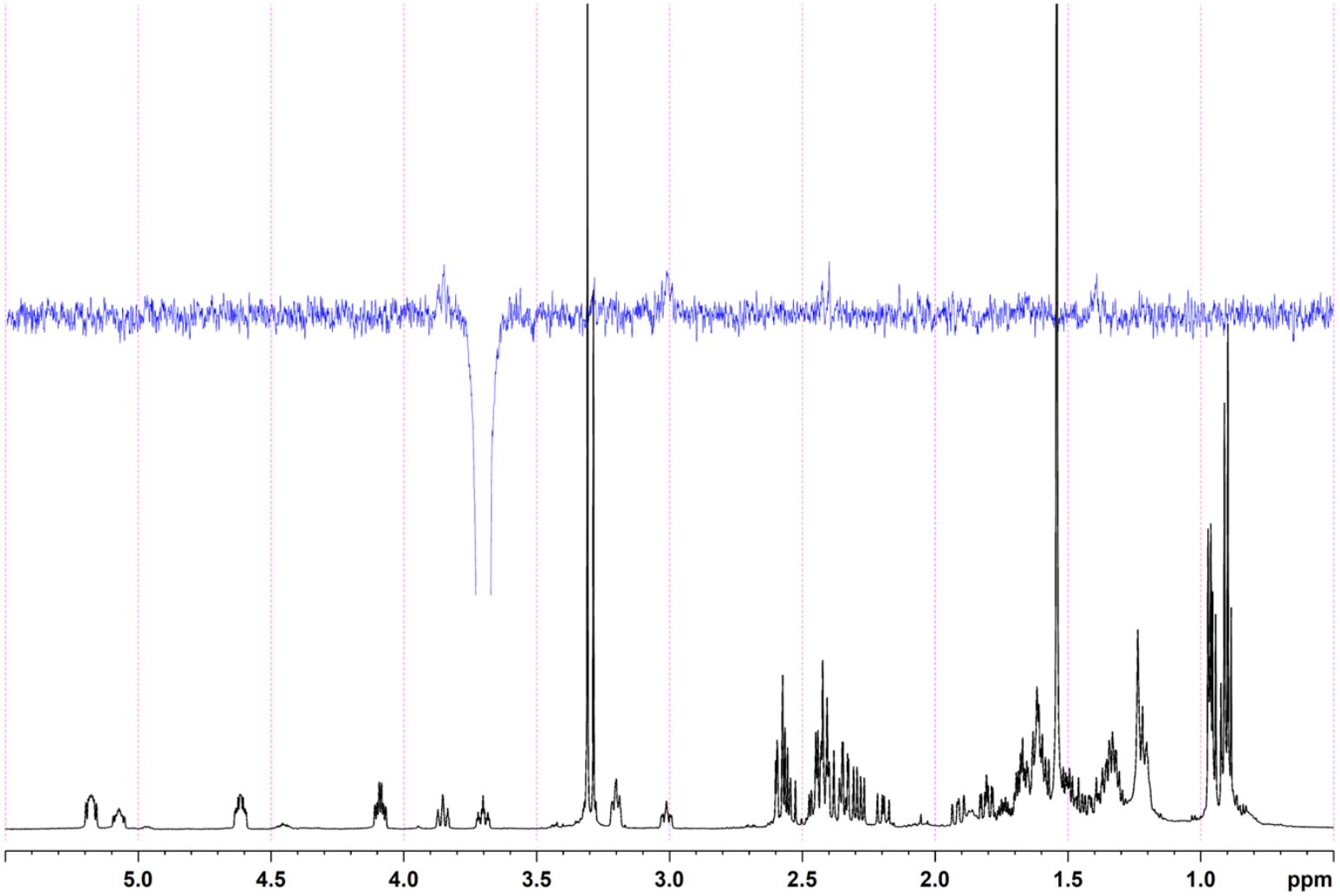

(3*S*,7*R*)-*trans*-$^{\Delta 3}$*epi*-neopeltolide macrocyclic core (*trans*-**4.82**)

1D Selective Gradient NOESY (600 MHz, $CDCl_3$)

δ 3.201 ppm (***H11***)

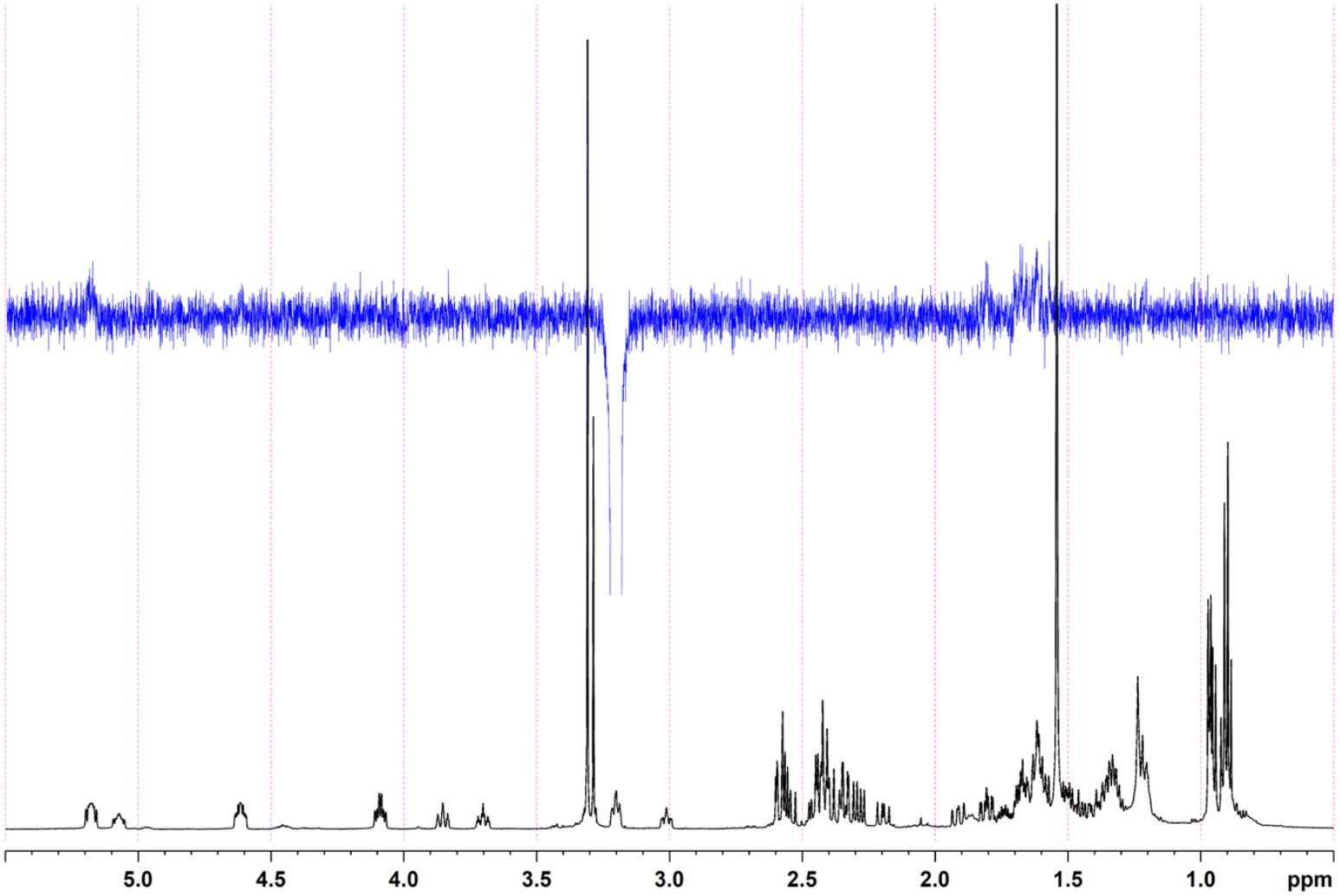

(3*S*,7*S*)-*cis*-$^{\Delta 3,7}$*epi*-neopeltolide macrocyclic core (*cis*-**4.81**)

1D Selective Gradient NOESY (600 MHz, $CDCl_3$)

δ 3.011 ppm (***H11***)

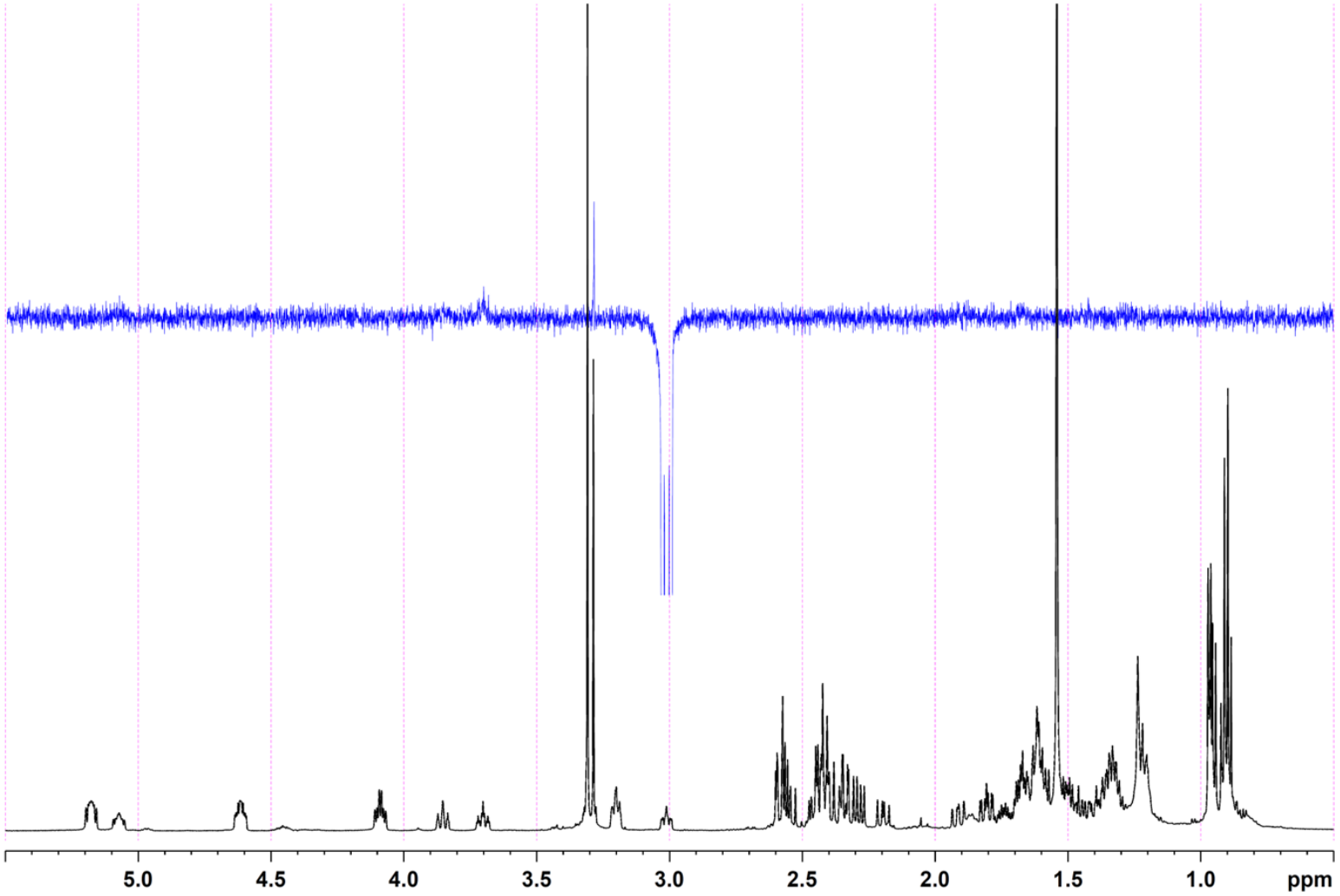

Thermodynamic Equilibration (3*S*, 5 h): *cis*-**4.14** to *cis*-**4.81** [*d.r.* ~ 1:5]

^{1}H NMR (600 MHz, $CDCl_3$)

t = 5 h, T = 80 °C, H^+ = Amberlyst-15®

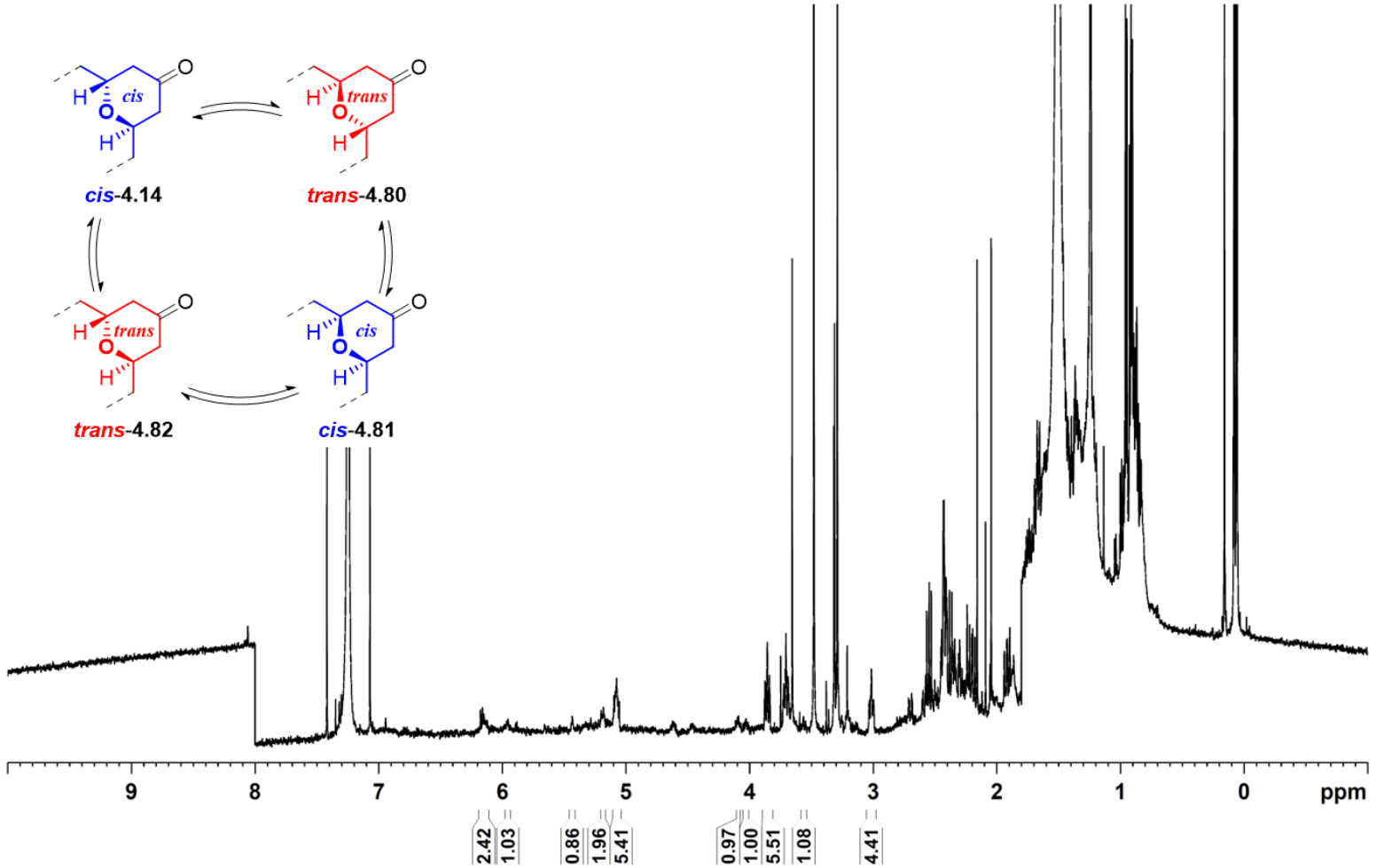

Thermodynamic Equilibration (3*S*, 15 h): *cis*-**4.14** to *cis*-**4.81** [*d.r.* ~ 7:32]

^{1}H NMR (600 MHz, $CDCl_3$)

t = 15 h, T = 80 °C, H^+ = Amberlyst-15®

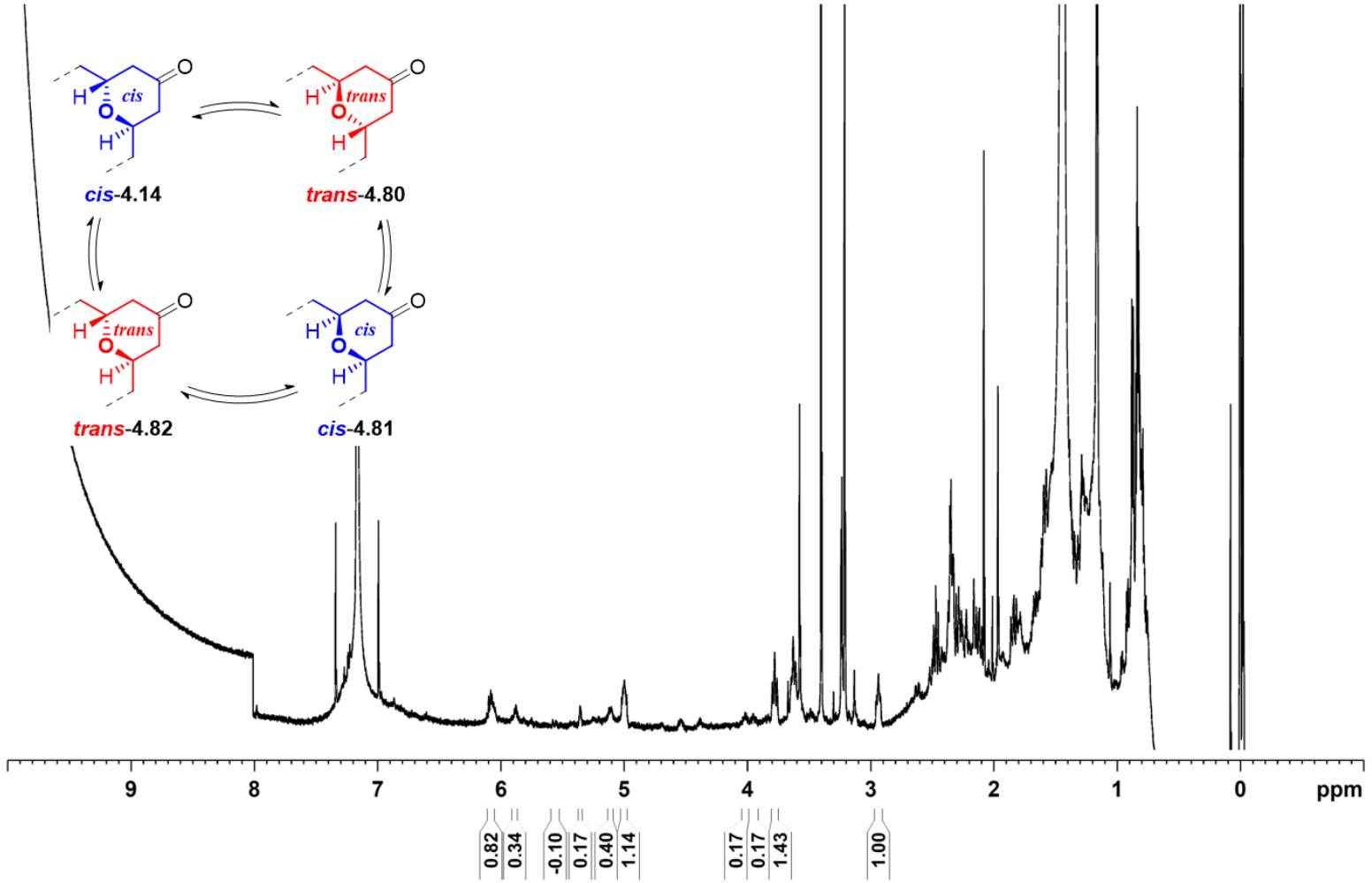

S1.4 Probing the Specificity of the DEBS Thioesterase (Chapter 6)

S1.4.1 Second-Generation NAC-Thioester Substrates: D-Configured Analogue Design & Evaluation (§ 6.4.1)

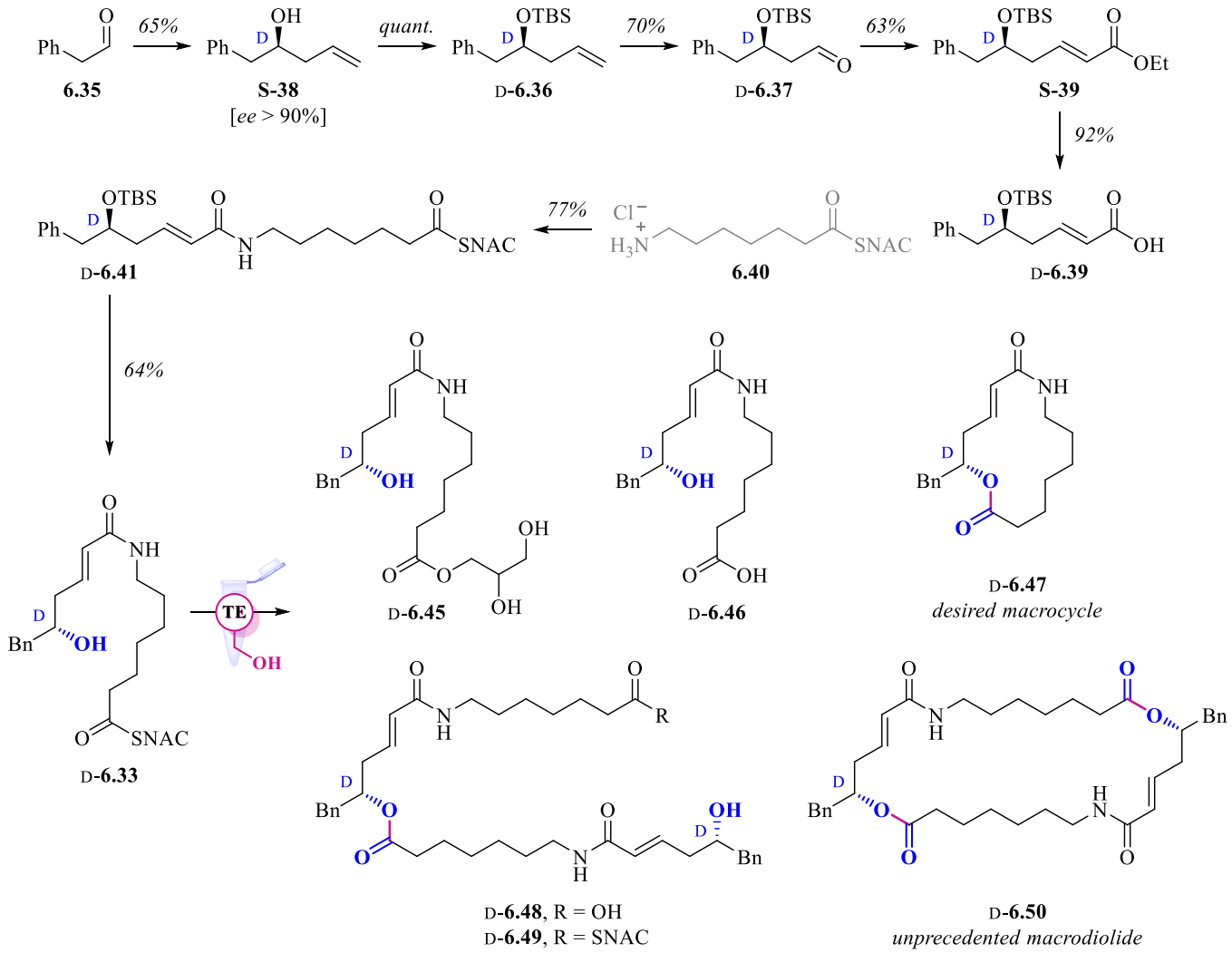

Figure S13 – Rapid development of D-configured second-generation NAC-thioester analogue to characterize substrate-specificity of DEBS TE.

7-*tert*-Butyloxycarbonylamino heptanoic acid (**S-36**)

^{1}H NMR (400 MHz, $CDCl_3$)

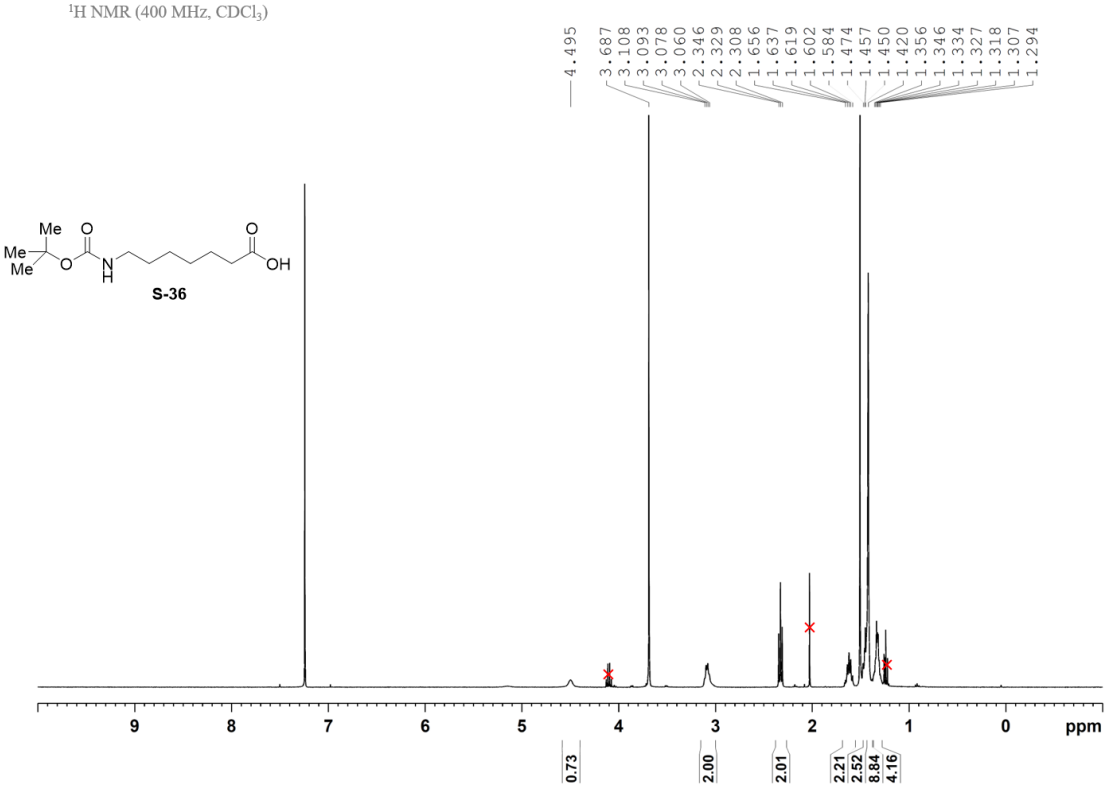

1-(2-Acetamidoethylthio)-7-(*tert*-butoxycarbonylamino)-heptanethioate (**S-37**)

^{1}H NMR (400 MHz, $CDCl_3$)

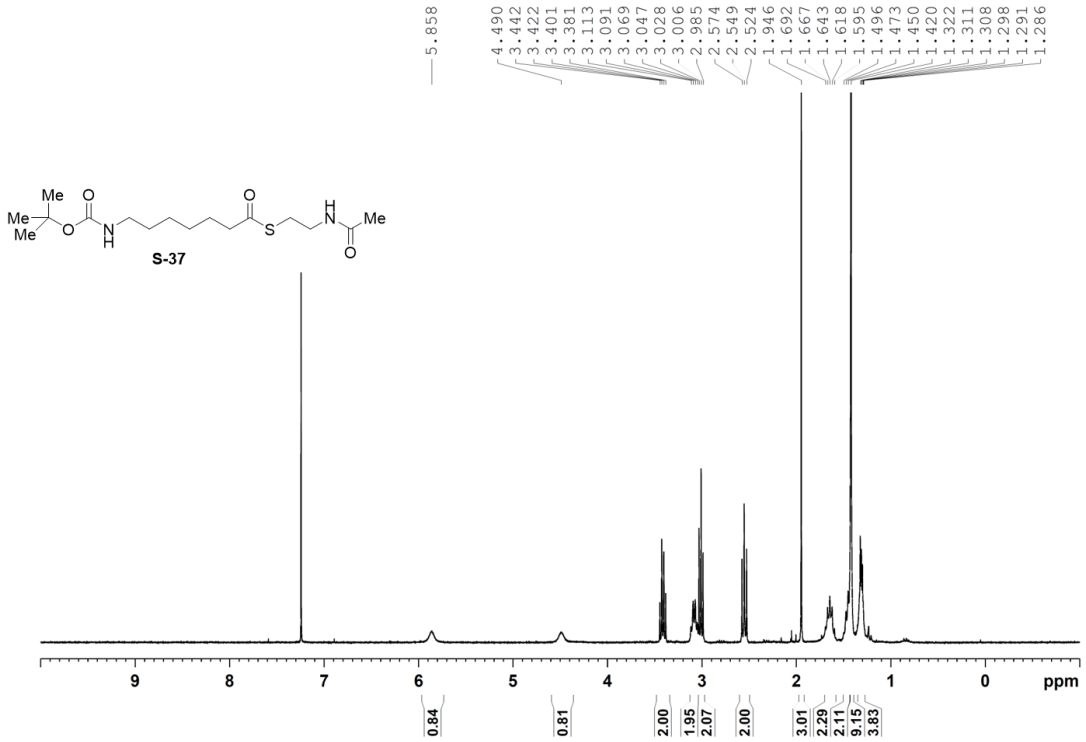

1-(2-Acetamidoethylthio)-7-(*tert*-butoxycarbonylamino)-heptanethioate (**S-37**)

^{13}C NMR (100 MHz, $CDCl_3$)

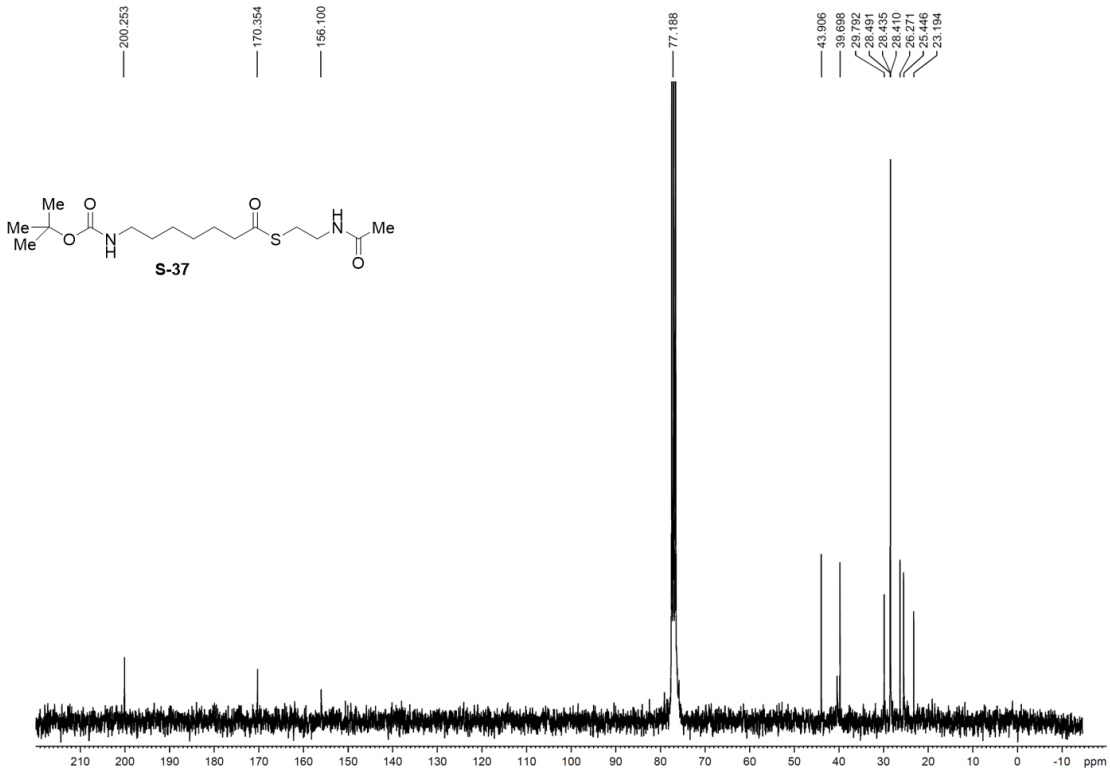

7-(2-Acetamidoethylthio)-7-oxoheptan-1-ammonium chloride (**6.40**)

^{1}H NMR (400 MHz, D_2O)

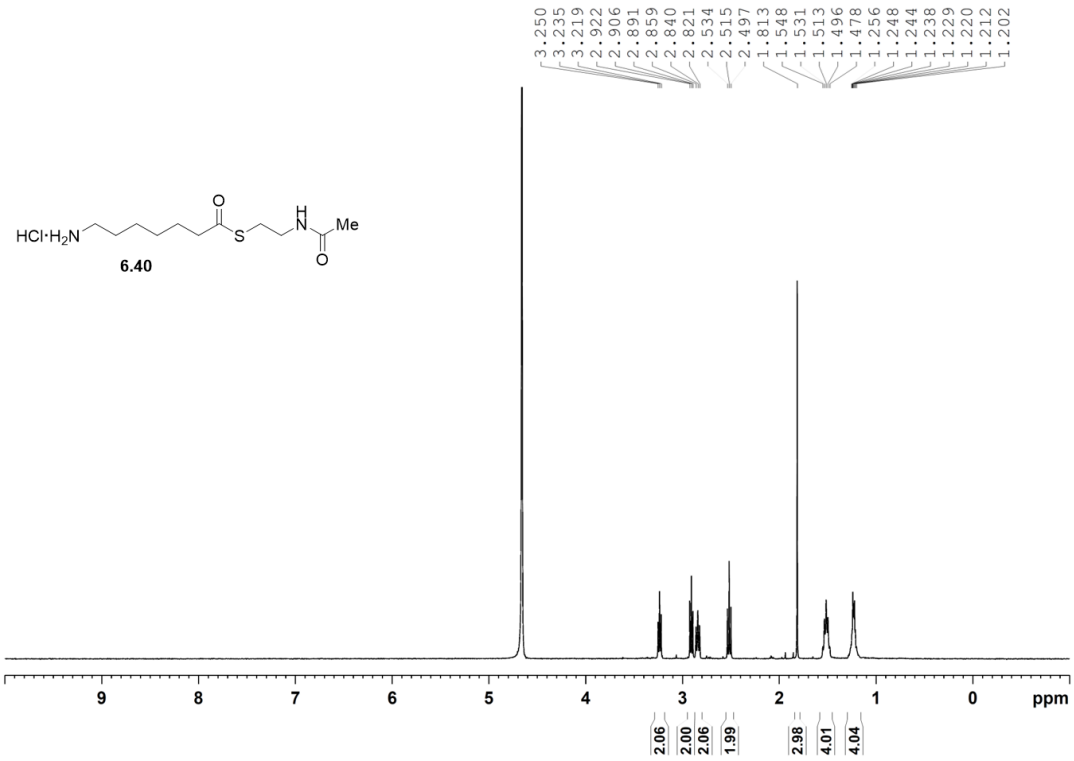

D-Phenylpent-4-en-2-ol (**S-38**)

^{1}H NMR (400 MHz, $CDCl_3$)

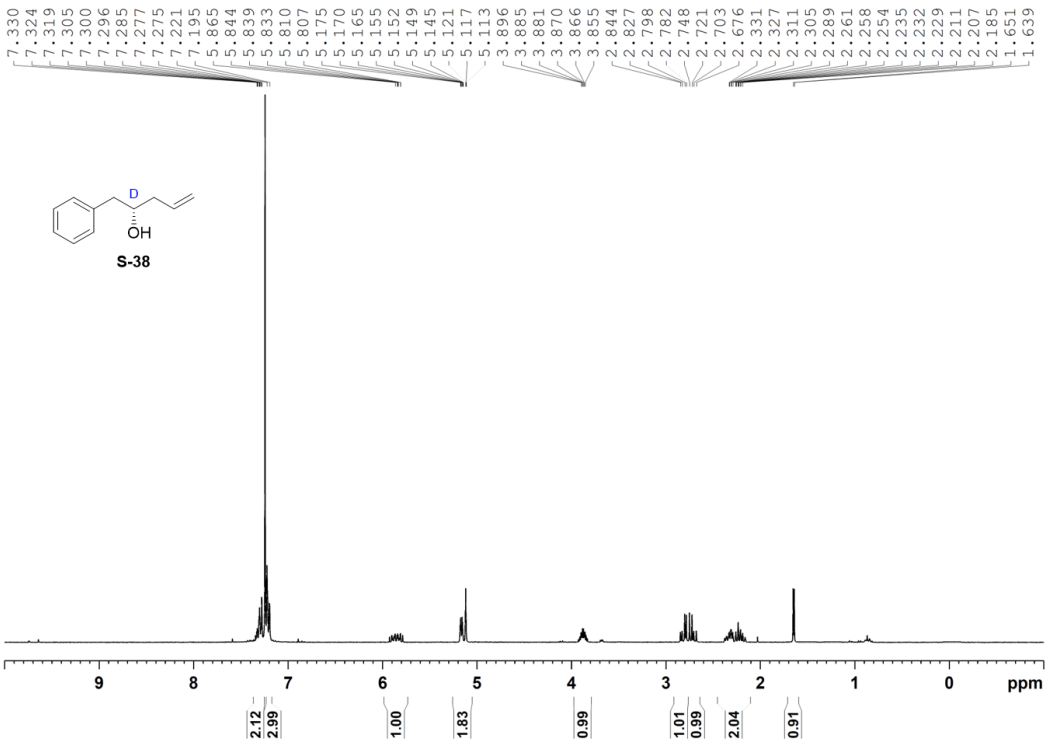

D-Phenylpent-4-en-2-ol (**S-38**)

^{13}C NMR (100 MHz, $CDCl_3$)

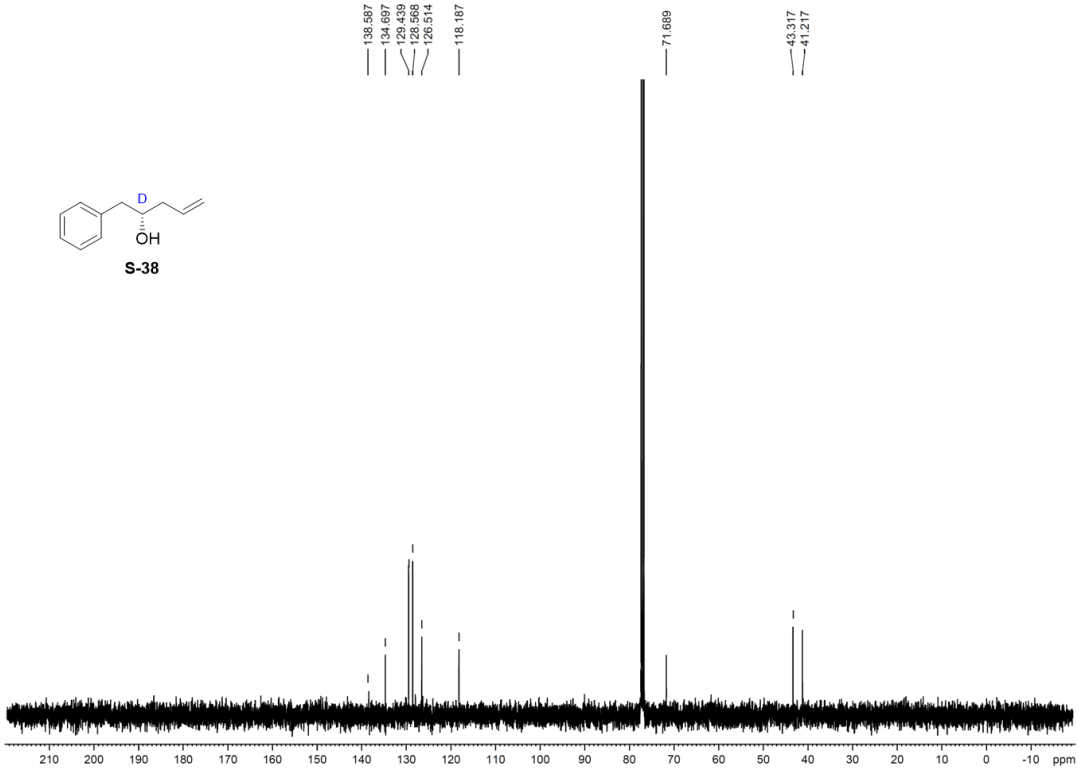

D-*tert*-Butyldimethyl-(1-phenylpent-4-en-2-yloxy)-silane (**6.36**)

^{1}H NMR (400 MHz, $CDCl_3$)

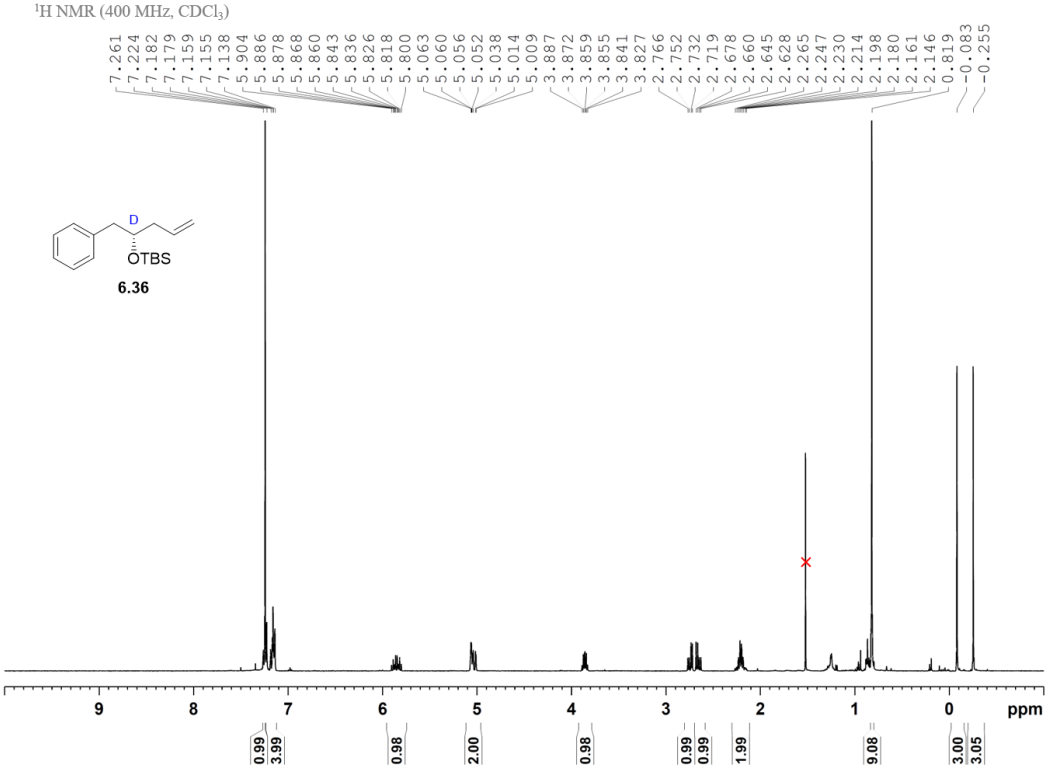

D-*tert*-Butyldimethyl-(1-phenylpent-4-en-2-yloxy)-silane (**6.36**)

^{13}C NMR (100 MHz, $CDCl_3$)

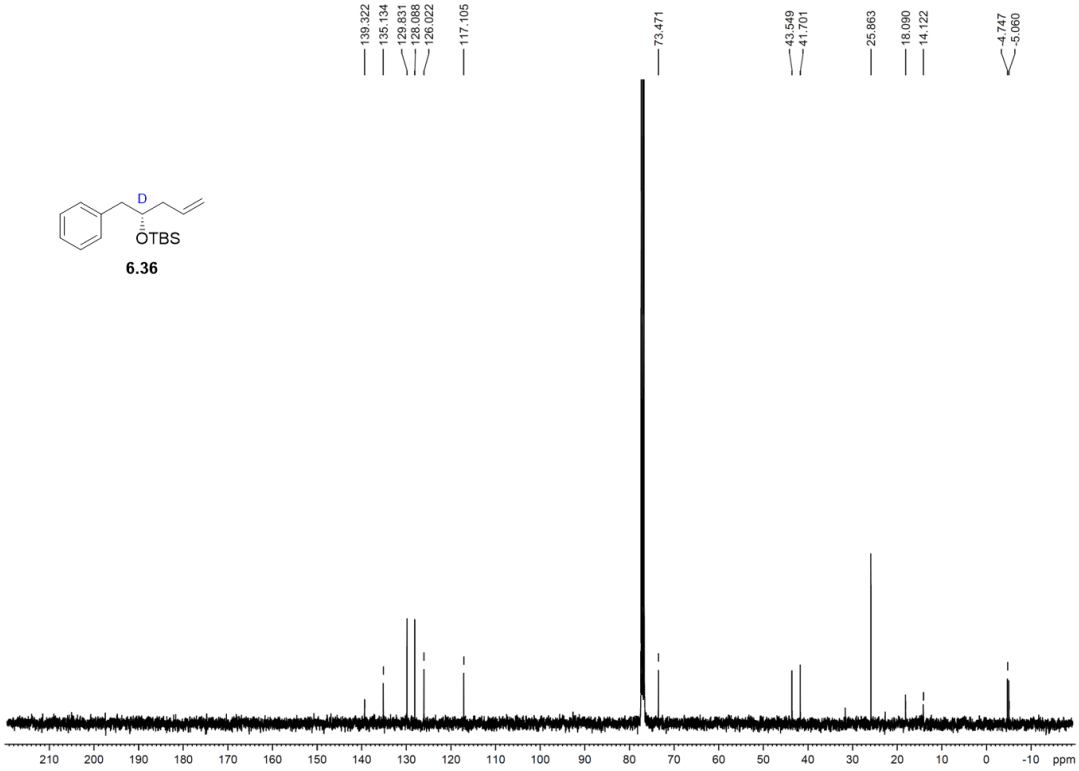

D-3-(*tert*-Butyldimethylsilyloxy)-4-phenylbutanal (**6.37**)

^{1}H NMR (400 MHz, $CDCl_3$)

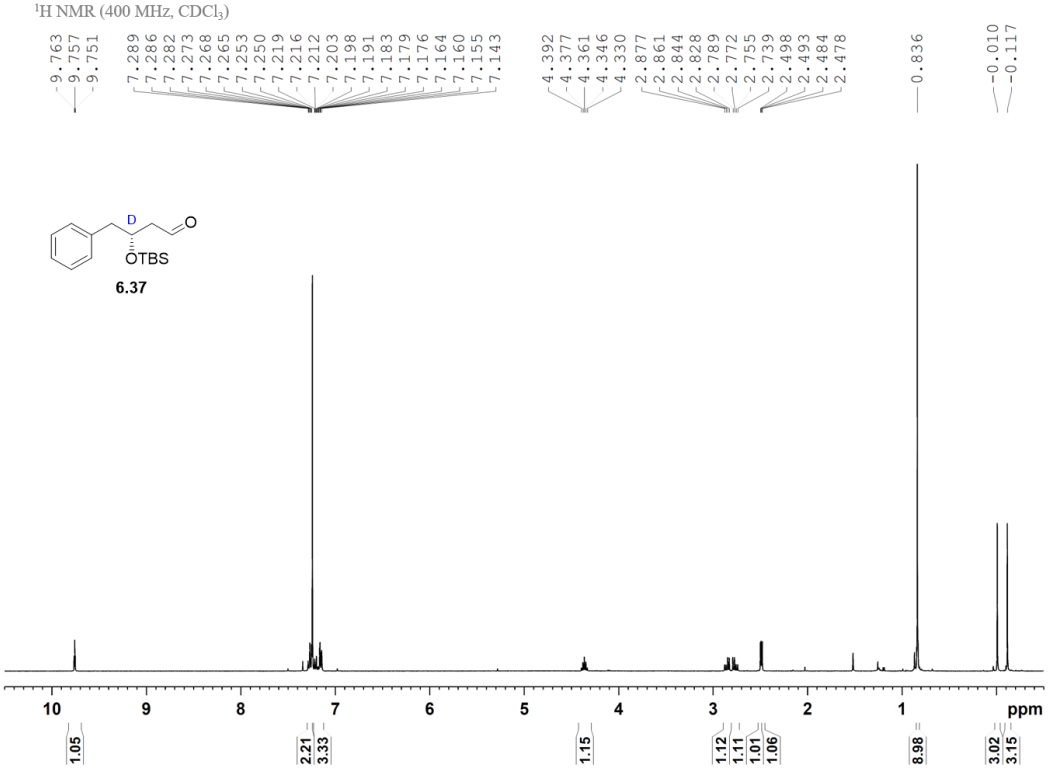

D-3-(*tert*-Butyldimethylsilyloxy)-4-phenylbutanal (**6.37**)

^{13}C NMR (100 MHz, $CDCl_3$)

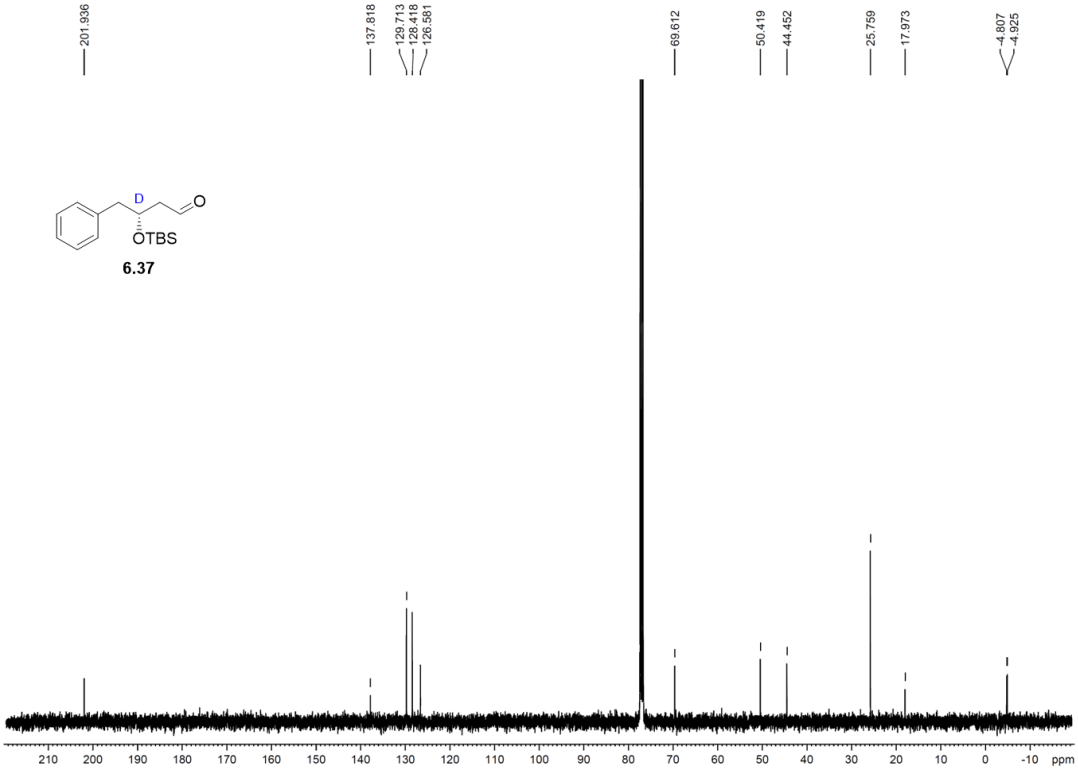

D-(*E*)-Ethyl 5-(*tert*-butyldimethylsilyloxy)-6-phenylhex-2-enoate (**S-39**)

^{1}H NMR (400 MHz, $CDCl_3$)

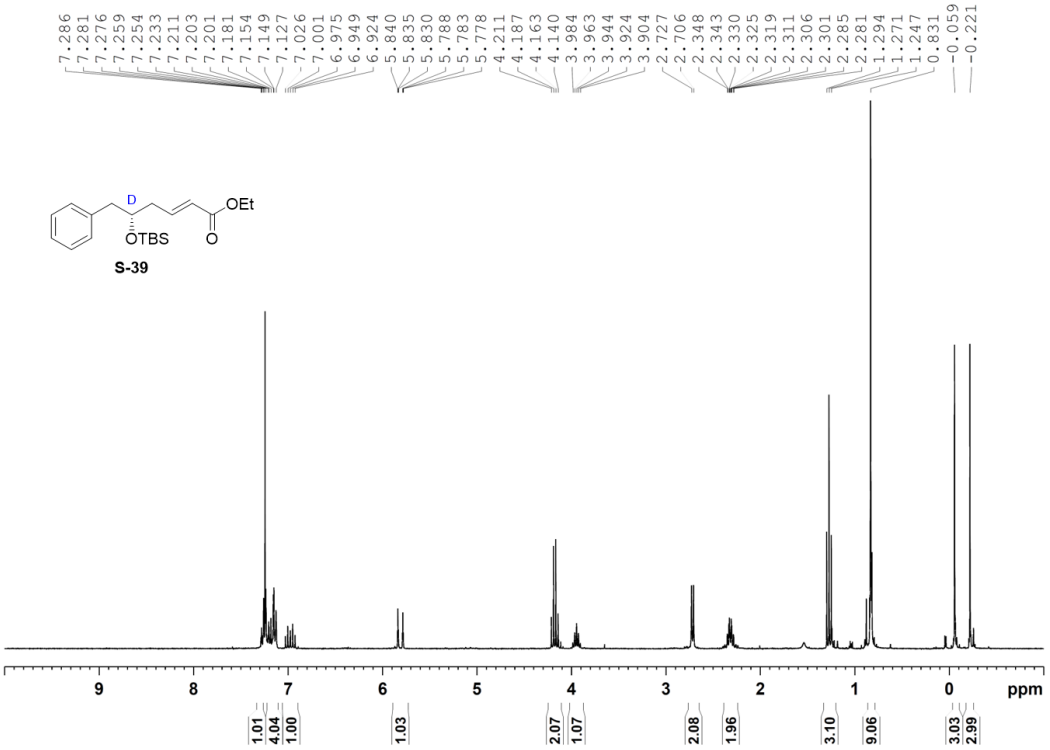

D-(*E*)-Ethyl 5-(*tert*-butyldimethylsilyloxy)-6-phenylhex-2-enoate (**S-39**)

^{13}C NMR (100 MHz, $CDCl_3$)

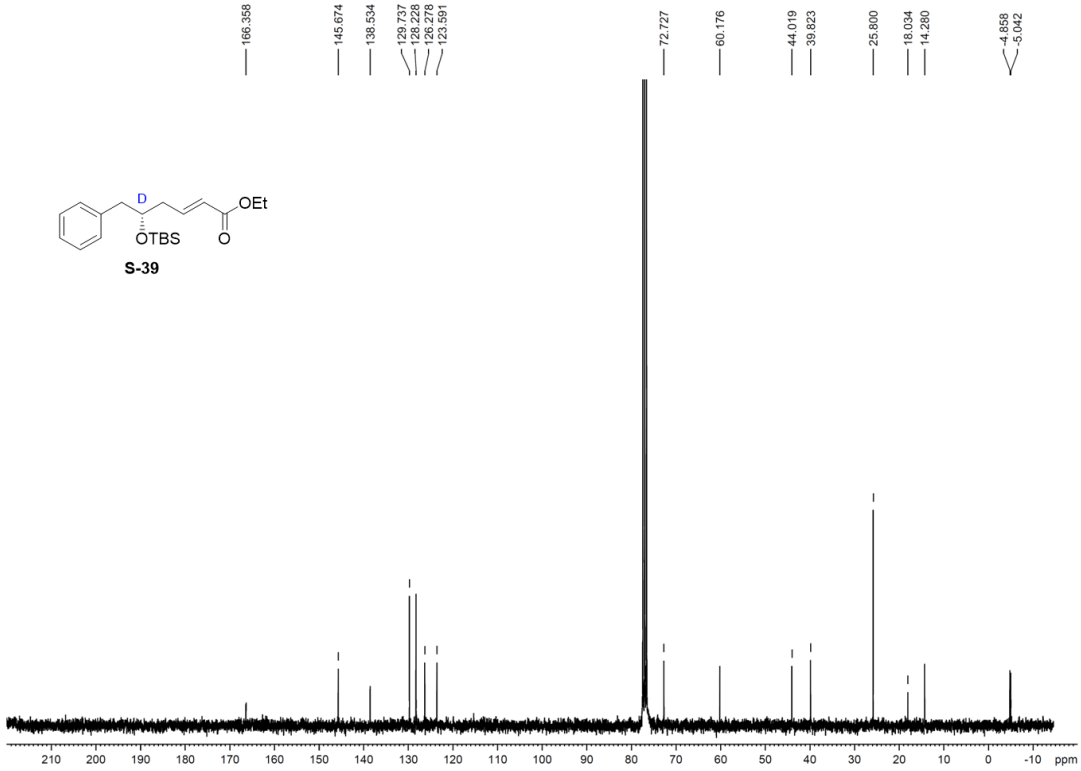

D-(*E*)-5-(*tert*-Butyldimethylsilyloxy)-6-phenylhex-2-enoic acid (**6.39**)

^{1}H NMR (400 MHz, $CDCl_3$)

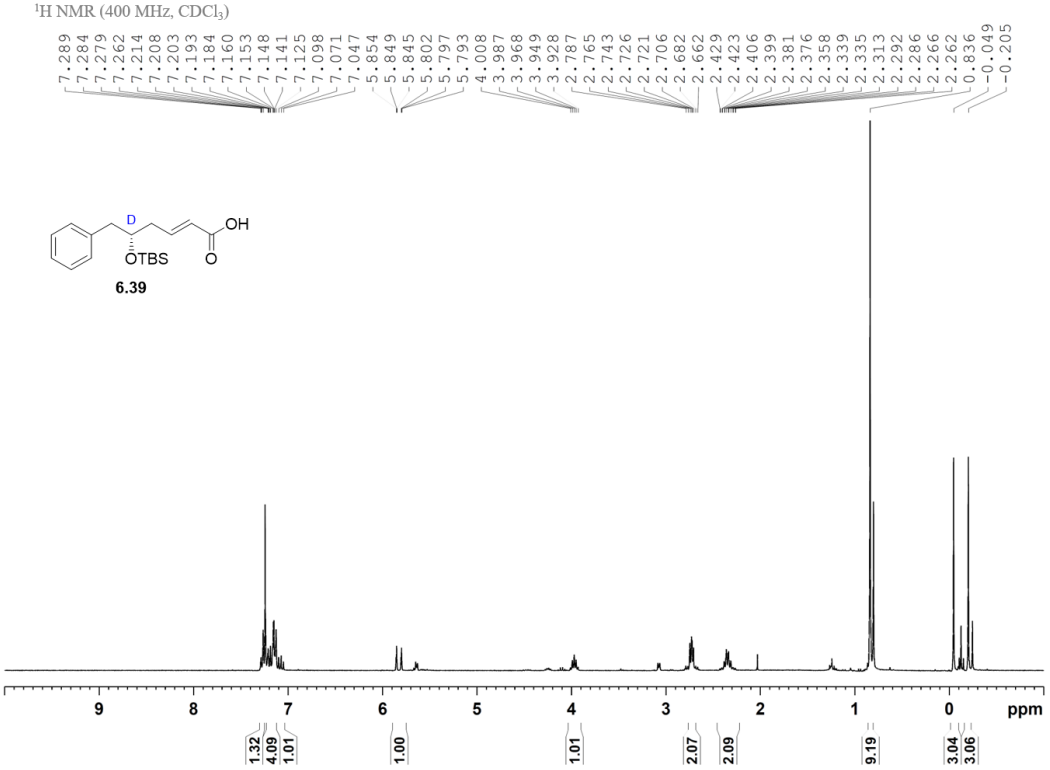

D-(*E*)-5-(*tert*-Butyldimethylsilyloxy)-6-phenylhex-2-enoic acid (**6.39**)

^{13}C NMR (100 MHz, $CDCl_3$)

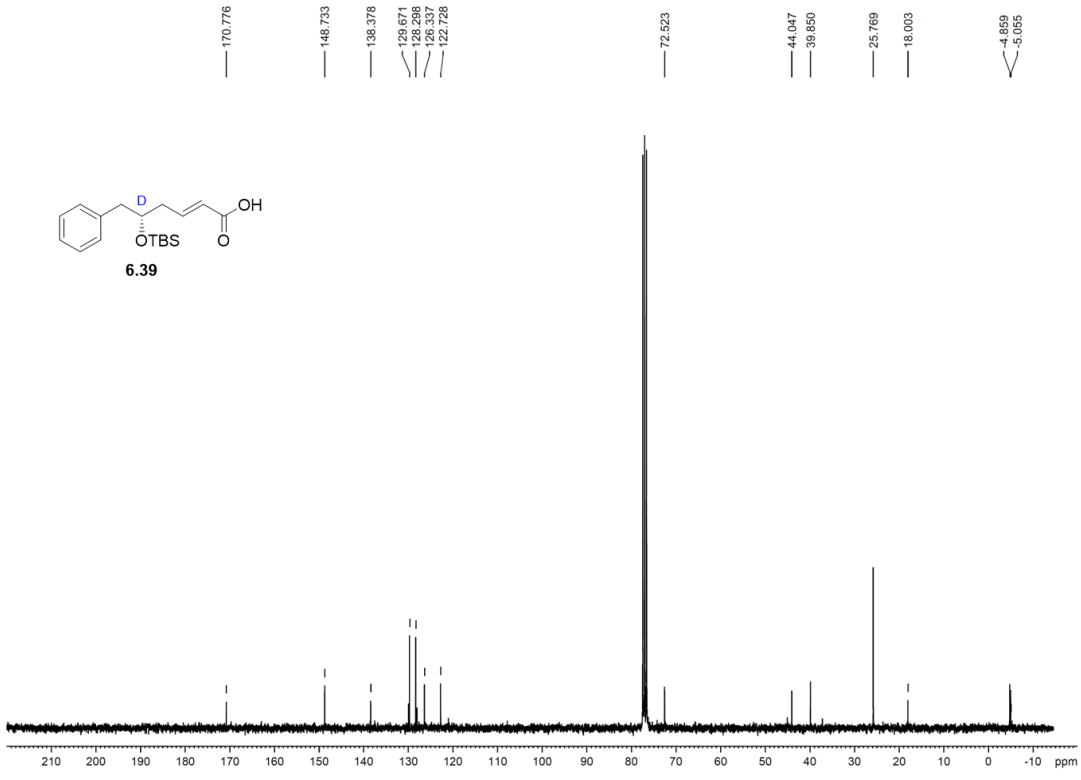

D-(*E*)-*S*-2-Acetamidoethyl-7-(5-*tert*-butyldimethylsilyloxy-6-phenylhex-2-enamido)-heptanethioate (**6.41**)

^{1}H NMR (400 MHz, $CDCl_3$)

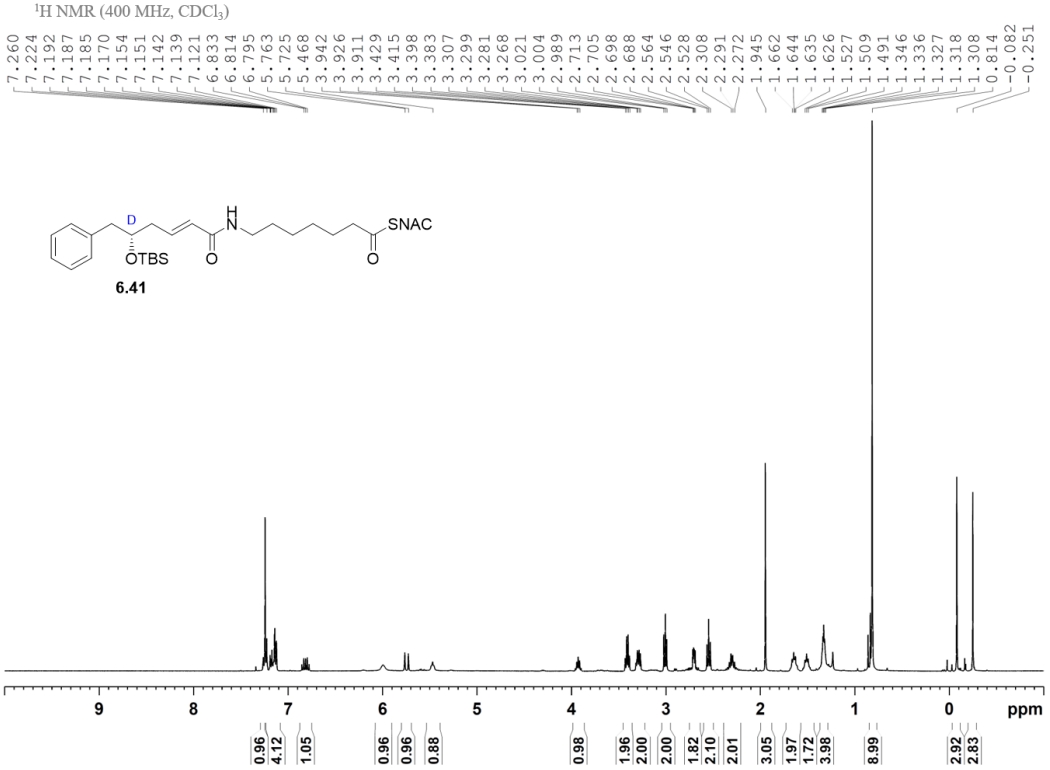

D-(*E*)-*S*-2-Acetamidoethyl-7-(5-*tert*-butyldimethylsilyloxy-6-phenylhex-2-enamido)-heptanethioate (**6.41**)

^{13}C NMR (100 MHz, $CDCl_3$)

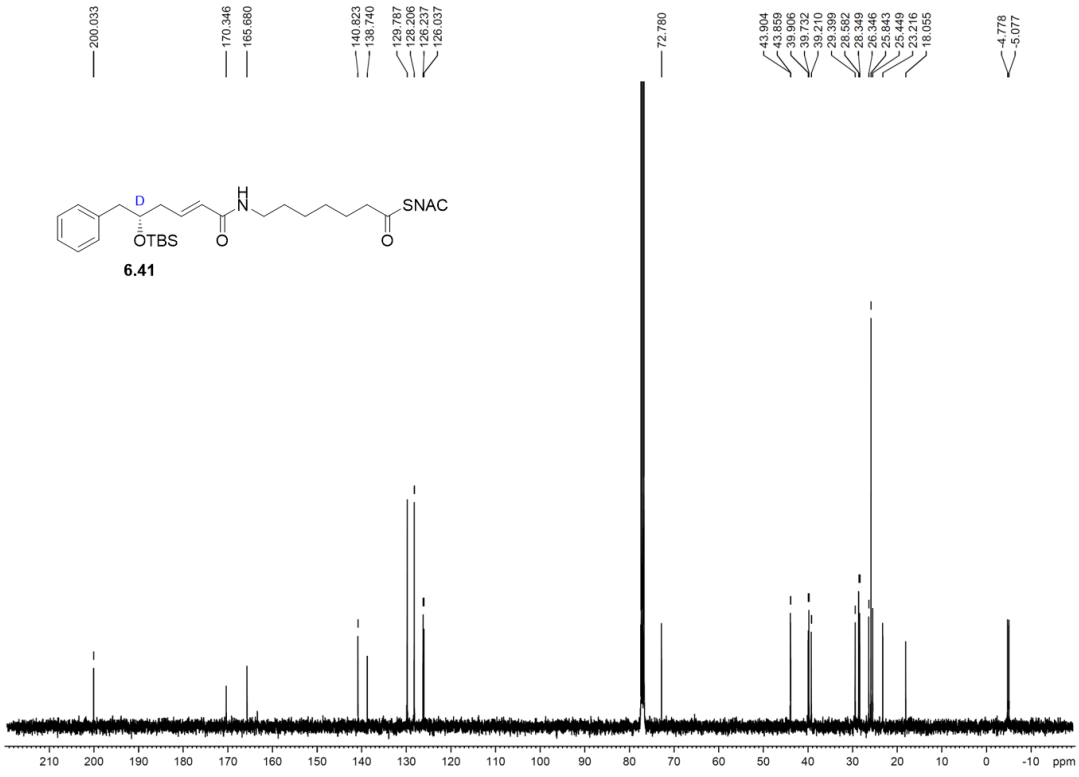

D-(*E*)-*S*-2-Acetamidoethyl-7-(5-*tert*-butyldimethylsilyloxy-6-phenylhex-2-enamido)-heptanethioate (**6.41**)

HSQC (400 MHz, $CDCl_3$)

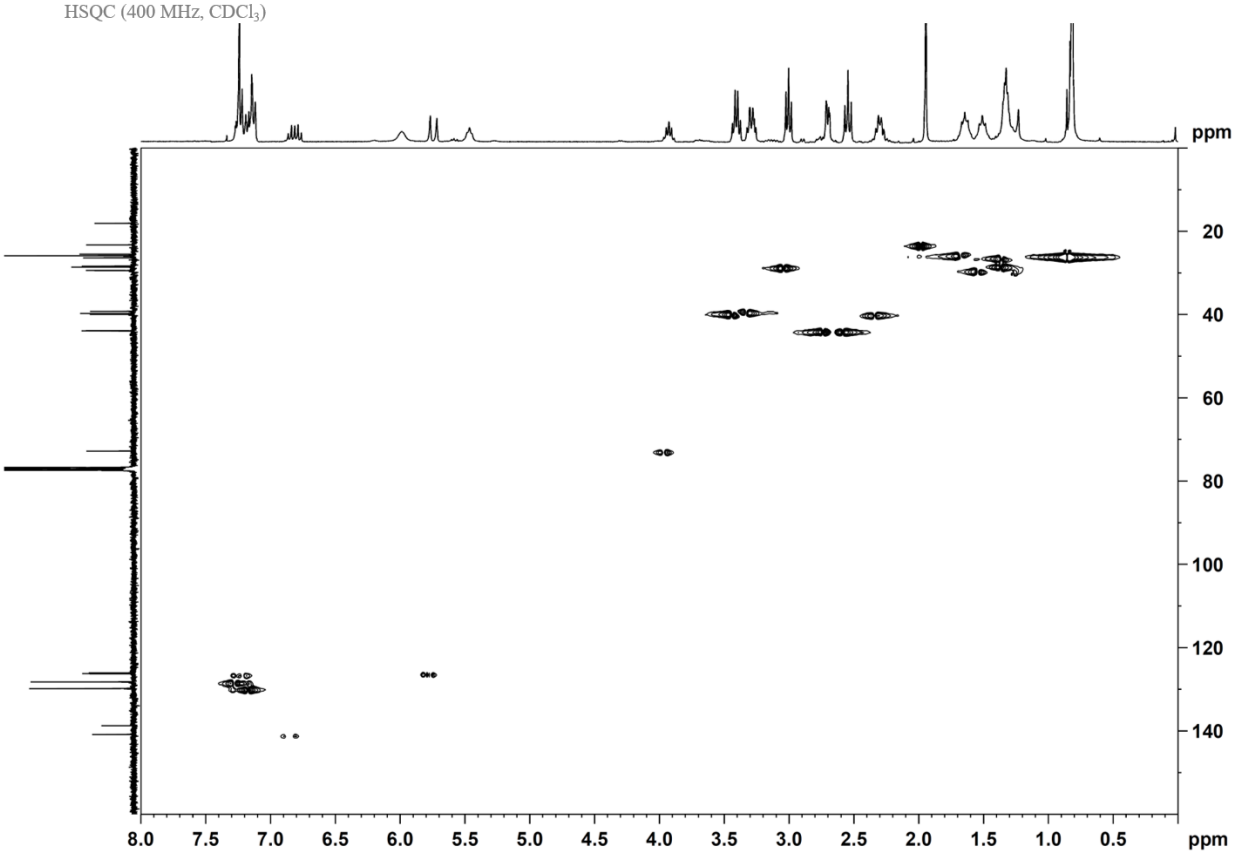

D-(*E*)-*S*-2-Acetamidoethyl-7-(5-hydroxy-6-phenylhex-2-enamido)-heptanethioate (D-**6.33**)

^{1}H NMR (400 MHz, $CDCl_3$)

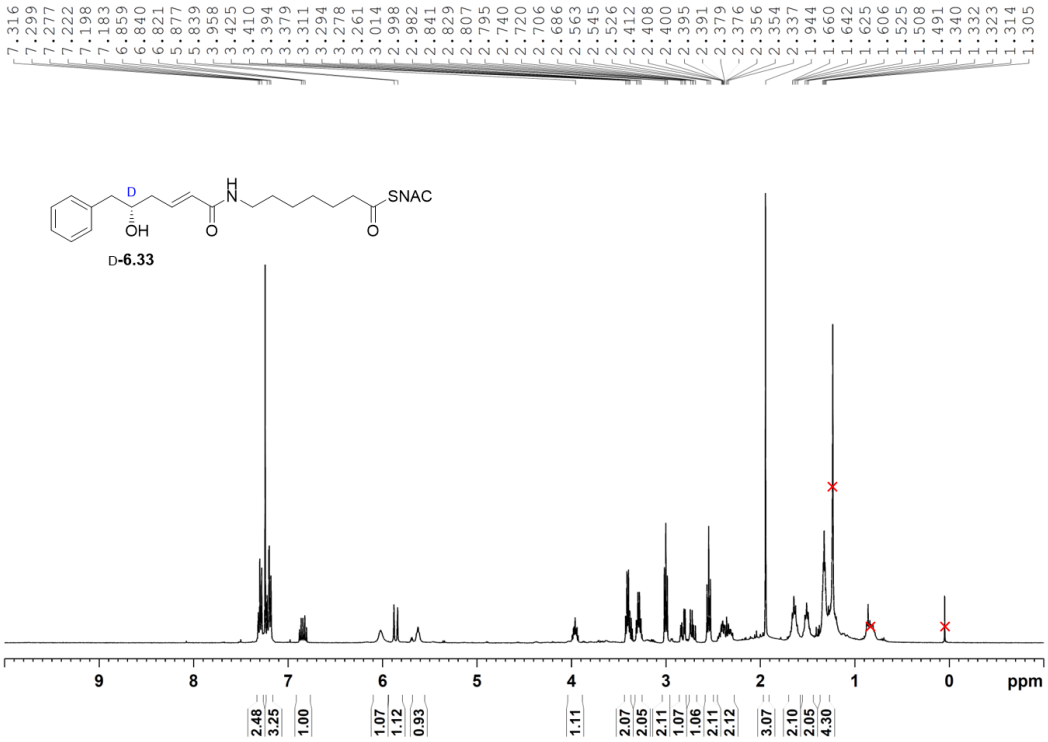

D-(*E*)-*S*-2-Acetamidoethyl-7-(5-hydroxy-6-phenylhex-2-enamido)-heptanethioate (D-**6.33**)

^{13}C NMR (100 MHz, $CDCl_3$)

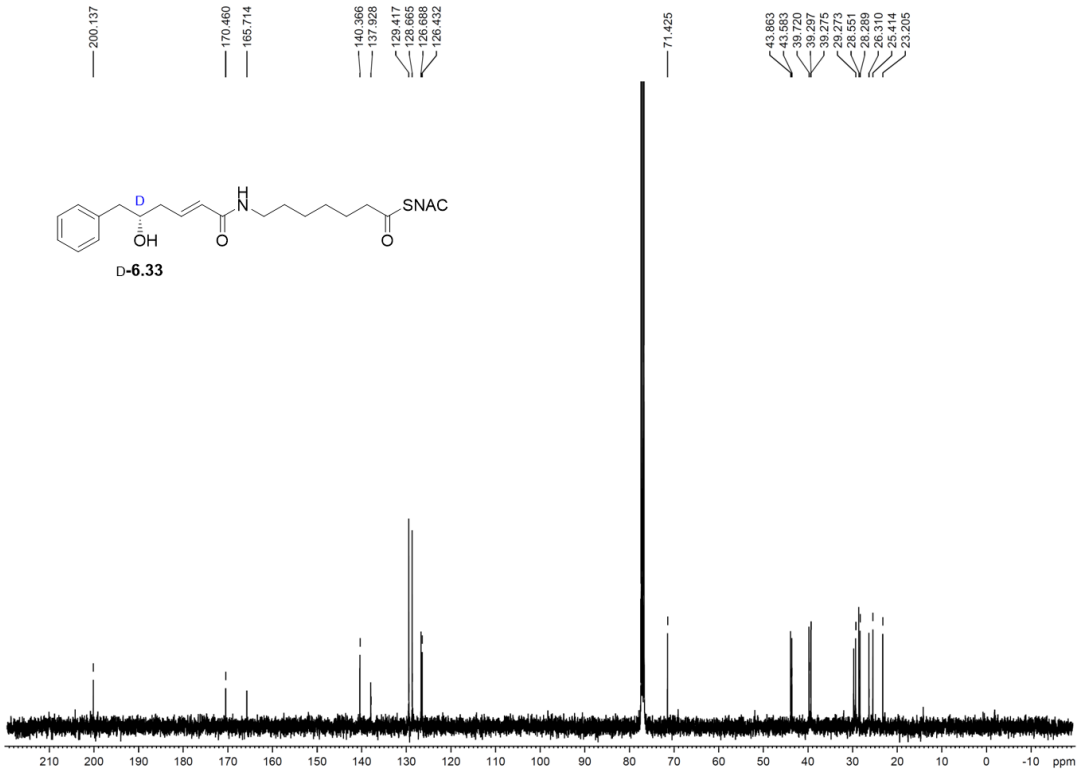

D-(*E*)-*S*-2-Acetamidoethyl-7-(5-hydroxy-6-phenylhex-2-enamido)-heptanethioate (D-**6.33**)

COSY (600 MHz, CD_3CN)

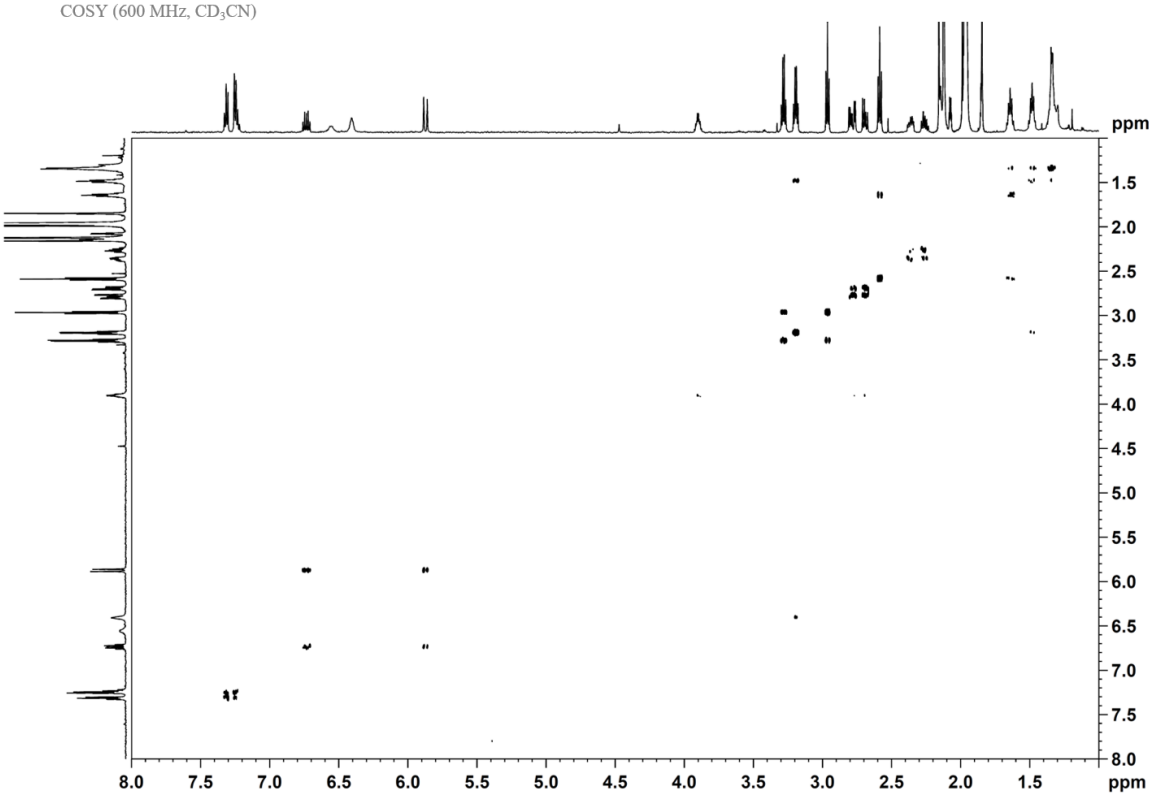

D-(*E*)-*S*-2-Acetamidoethyl-7-(5-hydroxy-6-phenylhex-2-enamido)-heptanethioate (D-**6.33**)

HSQC (400 MHz, $CDCl_3$)

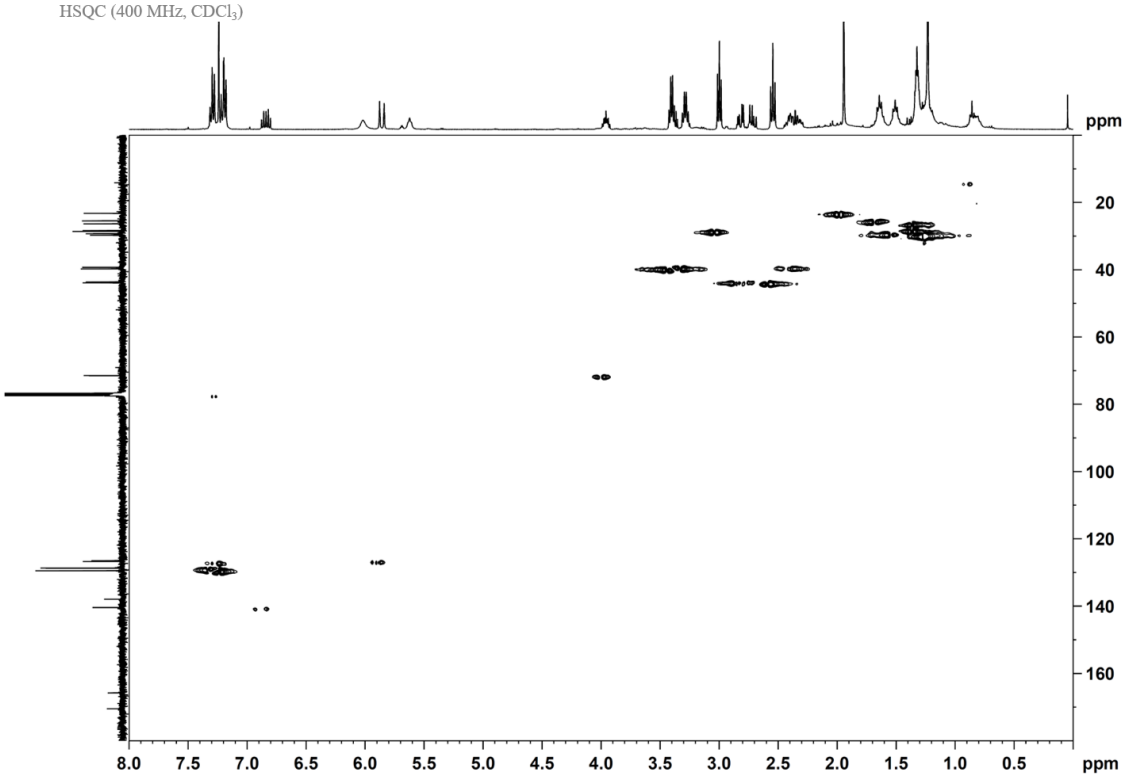

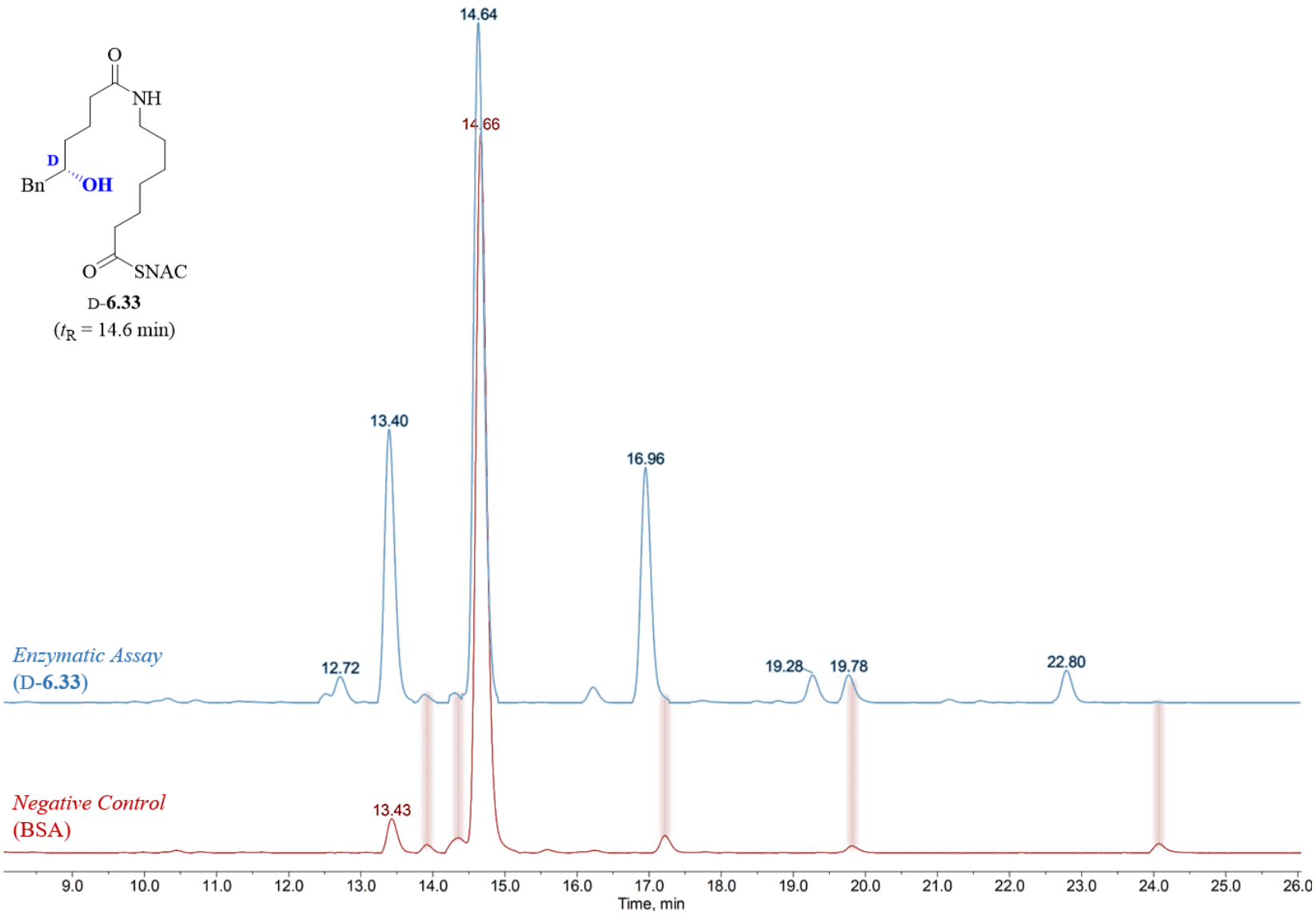

D-**6.33**
(t_R = 14.6 min)

Figure S14 – LCMS comparison of UV traces (254 nm) showing negative control (BSA, trace **1**) and enzymatic assay (trace **2**) for D-configured substrate **6.33**. Assay mixtures consists of 15 μM BSA (blank) or DEBS TE, 2.5 mM D-**6.33** in 50 mM phosphate buffer (pH 7.4) at 22 ºC, and DMSO (10% *v*/*v*) as a solubility additive.

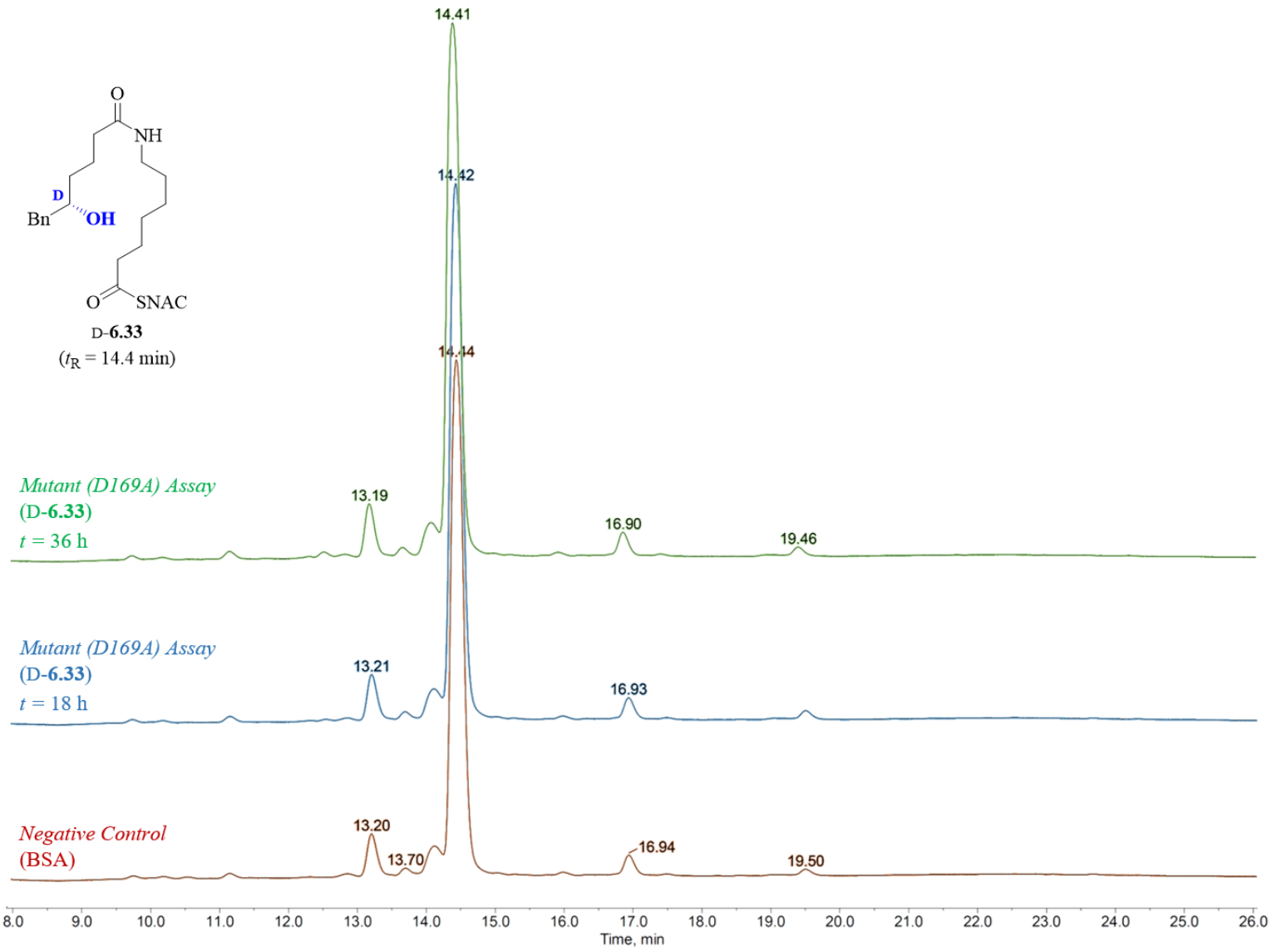

Figure S15 – LCMS comparison of UV traces (254 nm) showing negative control (BSA, trace **1**), and D169A mutant assay after 18 h (trace **2**) and 36 h (trace **3**) for D-configured substrate **6.33**. Assay mixtures consists of 15 µM BSA (blank) or DEBS D169A mutant TE, 2.5 mM D-**6.33** in 50 mM phosphate buffer (pH 7.4) at 22 ºC, and DMSO (10% *v*/*v*) as a solubility additive.

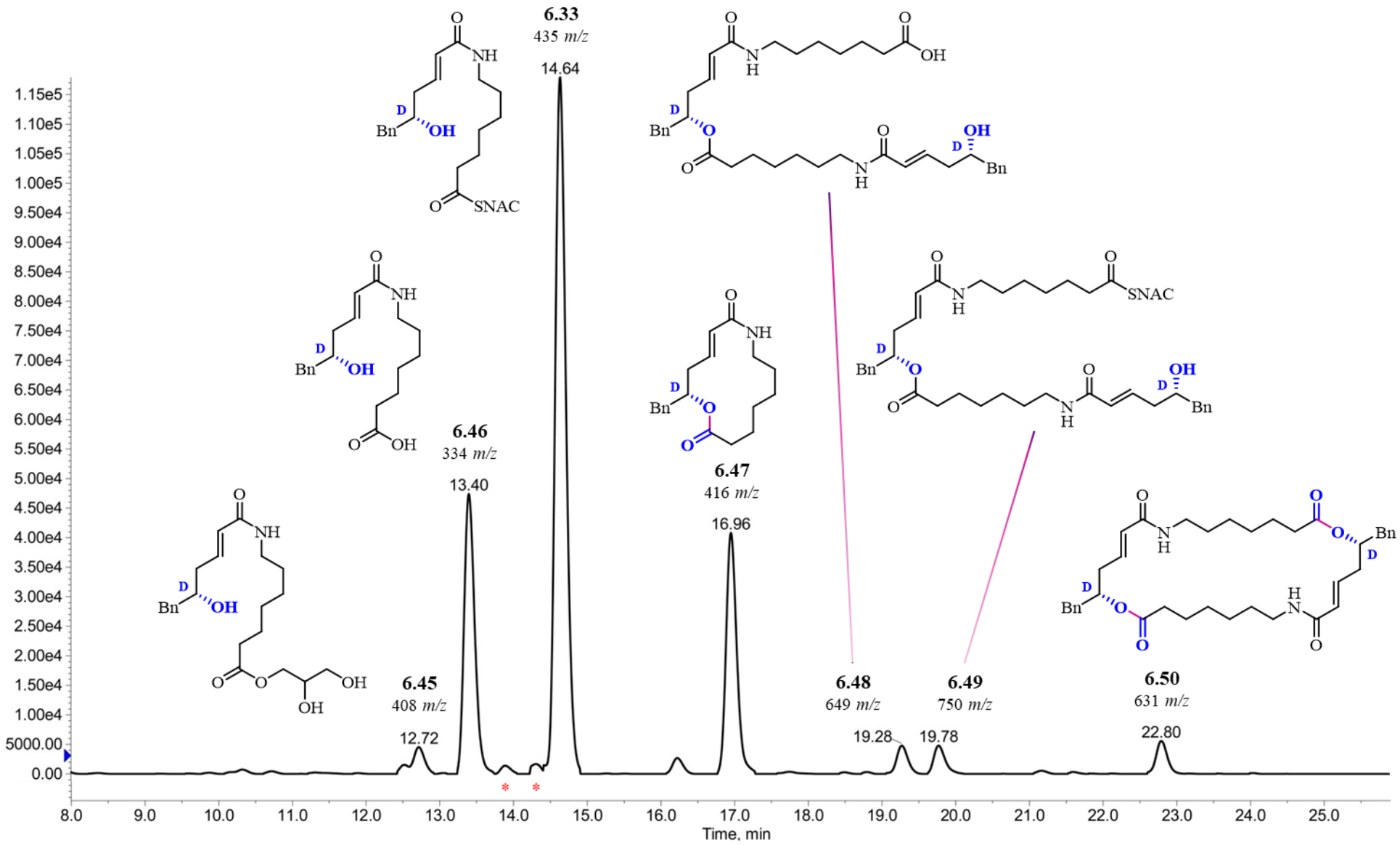

Figure S16 – LCMS analysis (254 nm) for *in vitro* enzymatic assay of D-configured NAC-thioester **6.33** with wild-type DEBS TE.

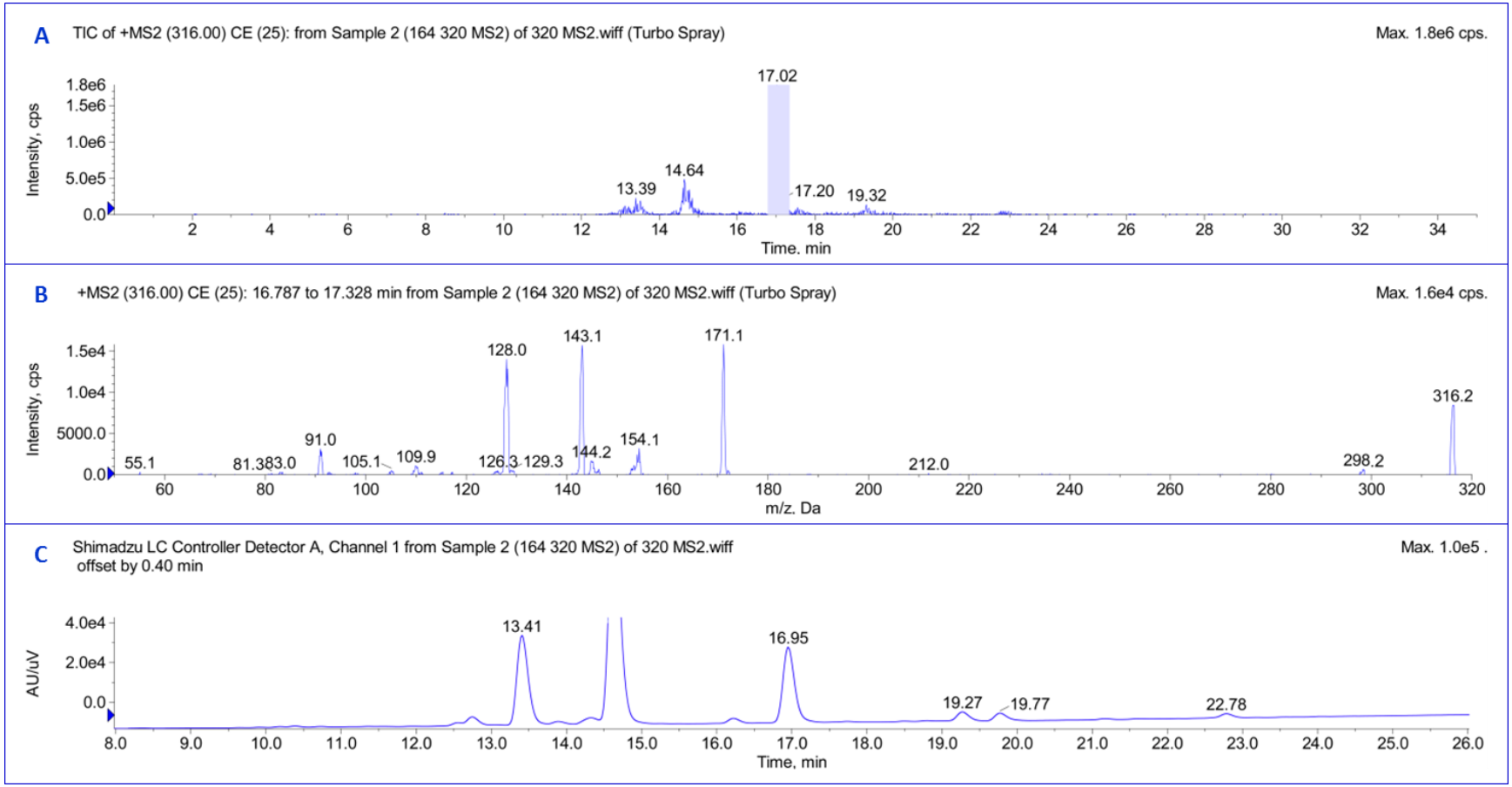

Figure S17 – LC-MS/MS analysis from *in vitro* enzymatic assays of D-**6.33** with wild-type DEBS TE. A) Total ion count (TIC) of MS2data collected for parent ion scan (316 Da); B) MS2 fragmentation pattern between 16.787 and 17.328 min over a mass range of 50-to-320 Da; C) UV trace (254 nm). Assay mixture consists of 15 µM DEBS TE, 2.5 mM D-**6.33** in 50 mM phosphate buffer (pH 7.4) at 22 ºC, and DMSO (10% *v*/*v*) as a solubility additive.

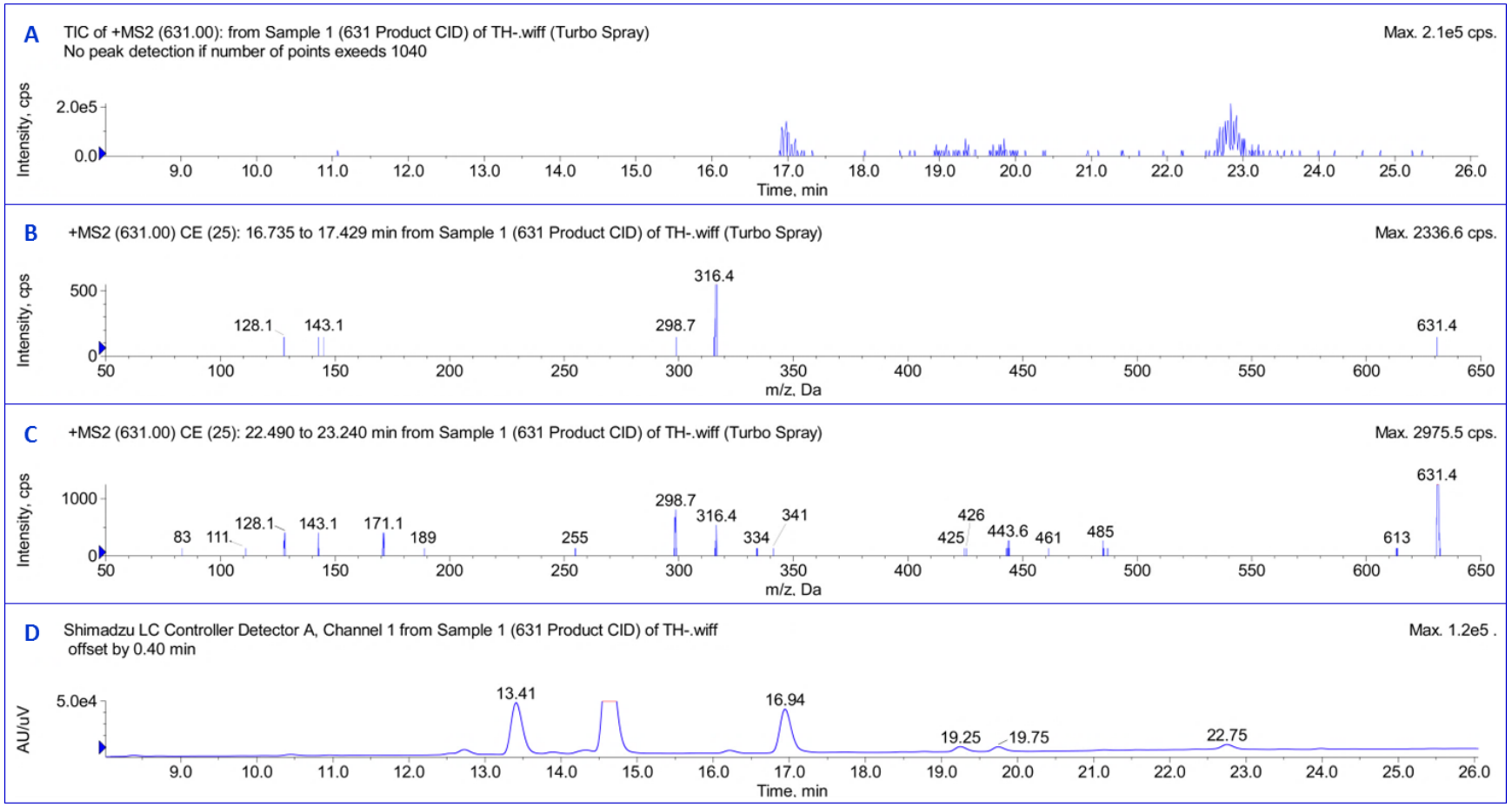

Figure S18 – LC-MS/MS analysis from *in vitro* enzymatic assays of D-**6.33** with wild-type DEBS TE. A) Total ion count (TIC) of MS2data collected for parent ion scan (631.4 Da); B) MS2 fragmentation pattern between 16.735 and 17.429 min, and C) 22.490 and 23.240 min over a mass range of 50-to-650 Da; D) UV trace (254 nm). Assay mixture consists of 15 µM DEBS TE, 2.5 mM D-**6.33** in 50 mM phosphate buffer (pH 7.4) at 22 ºC, and DMSO (10% *v*/*v*) as a solubility additive.

Glycerolysis product *via* enzymatic assay (**6.45**)

^{1}H NMR (600 MHz, CD_3CN)

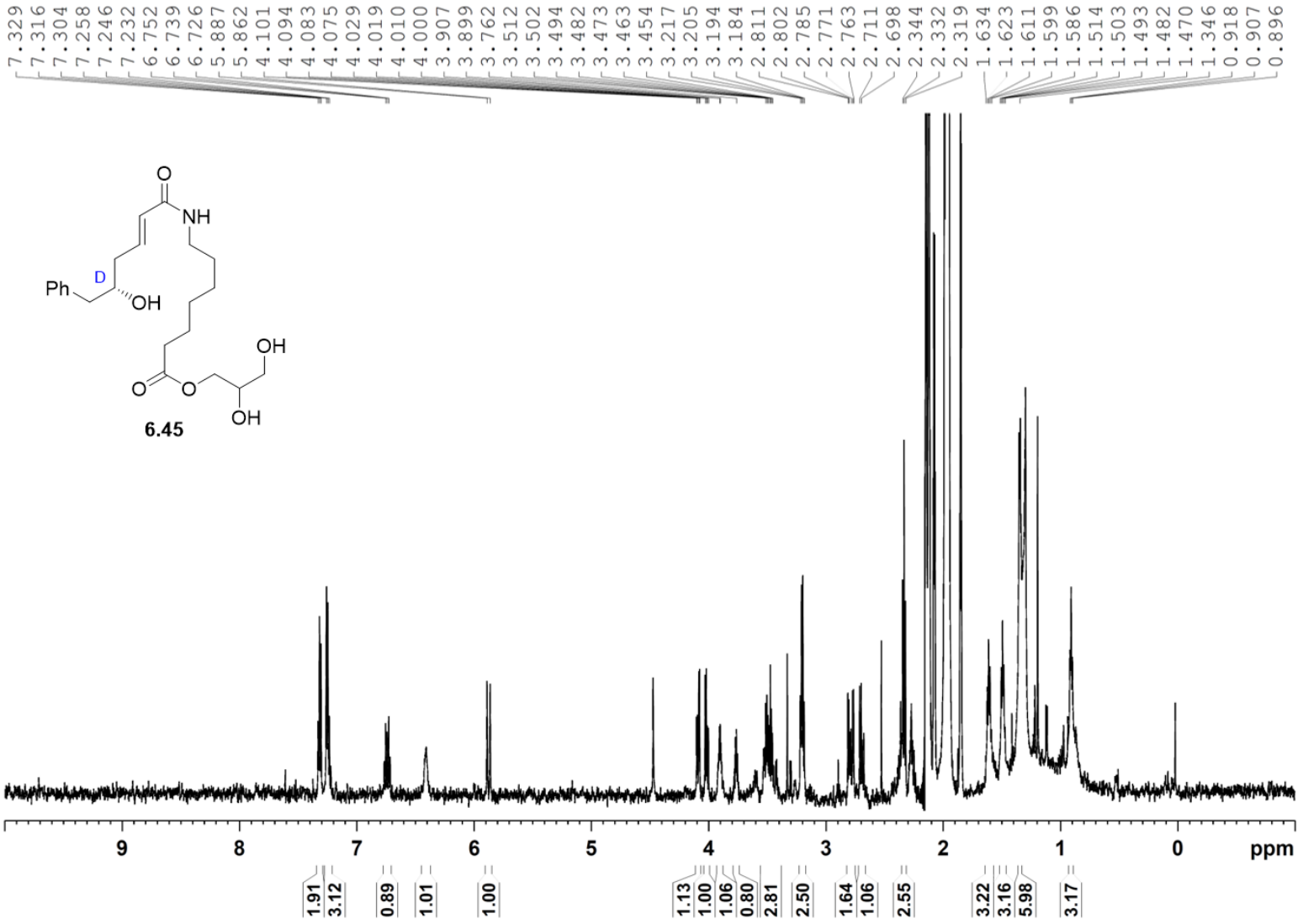

6.45

Hydrolysis product *via* enzymatic assay (**6.46**)

^{1}H NMR (600 MHz, CD_3CN)

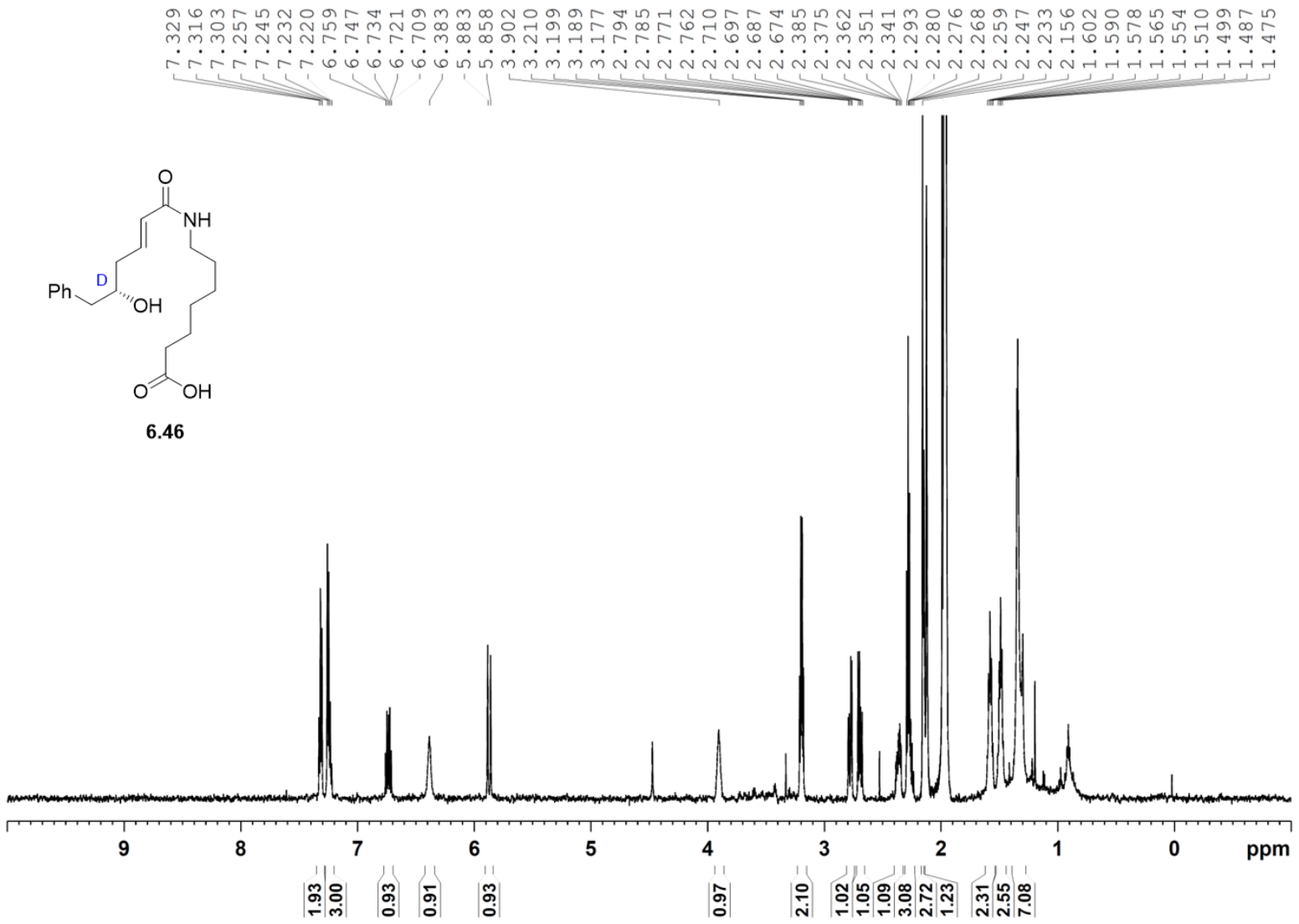

Hydrolysis product *via* enzymatic assay (**6.46**)

COSY (600 MHz, CD_3CN)

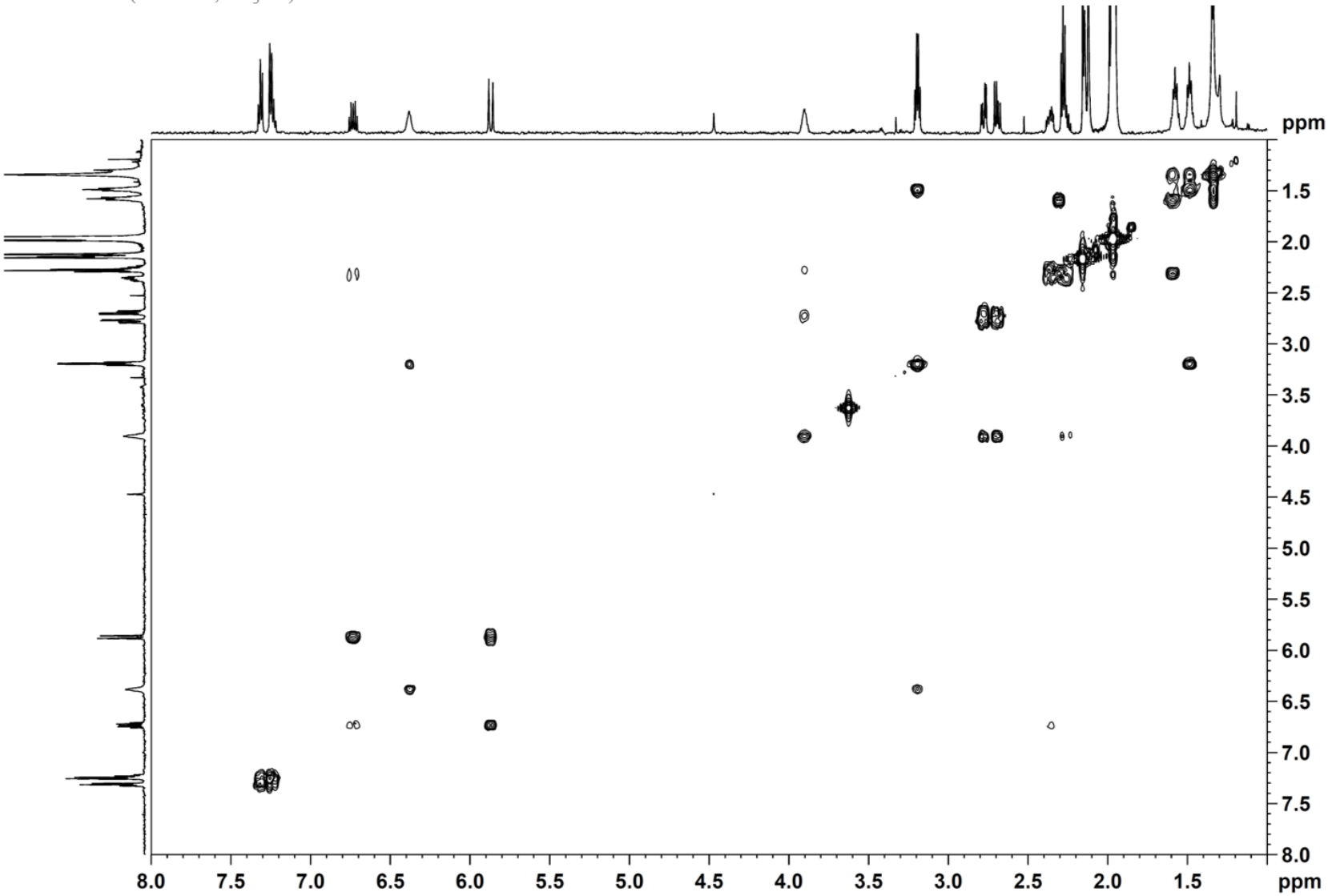

Macrocyclic product *via* enzymatic assay (**6.47**)

^{1}H NMR (600 MHz, CD_3CN)

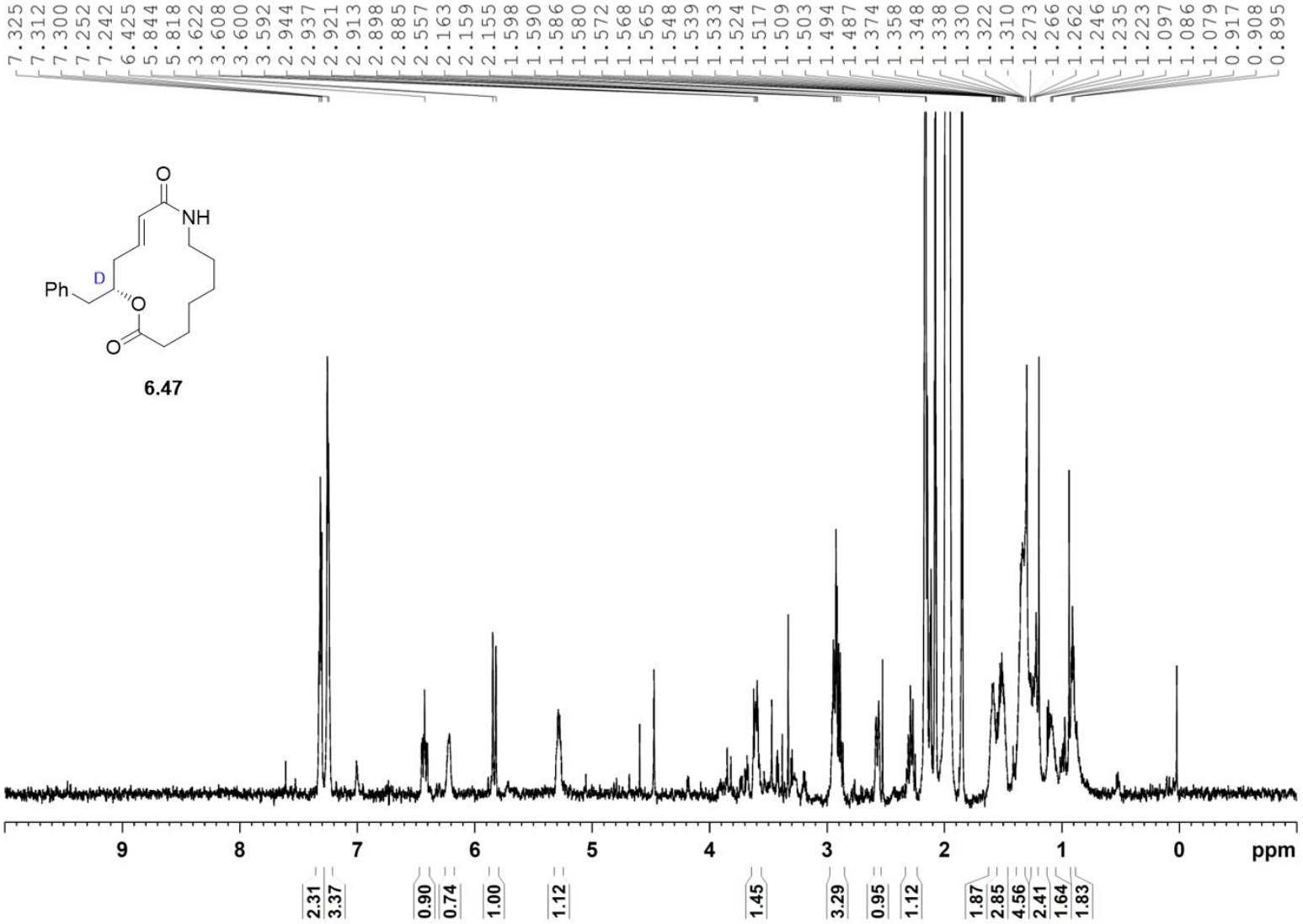

Macrocyclic product *via* enzymatic assay (**6.47**)

COSY (600 MHz, CD_3CN)

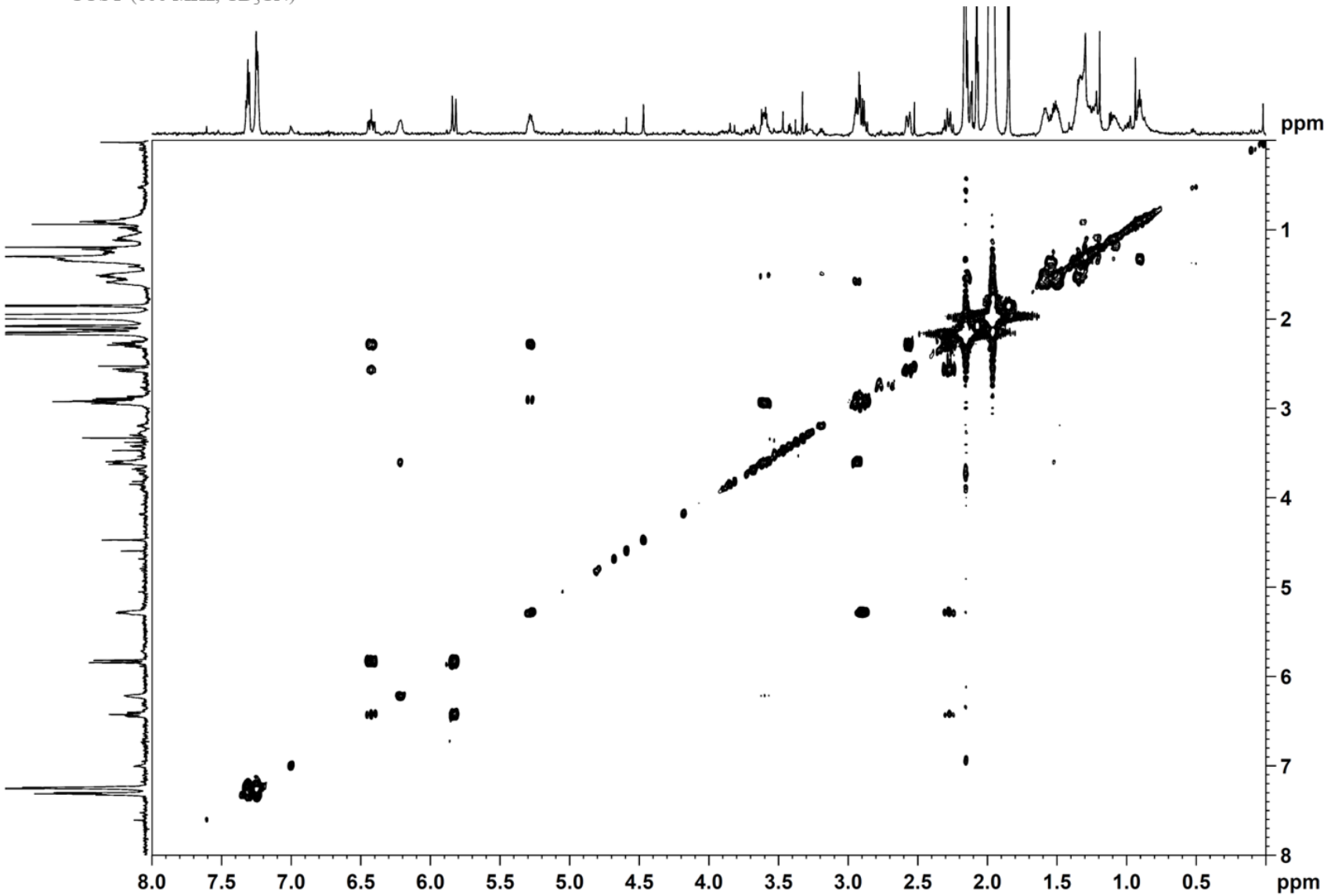

Linear Dimer Acid *via* enzymatic assay (**6.48**)

^{1}H NMR (600 MHz, CD_3CN)

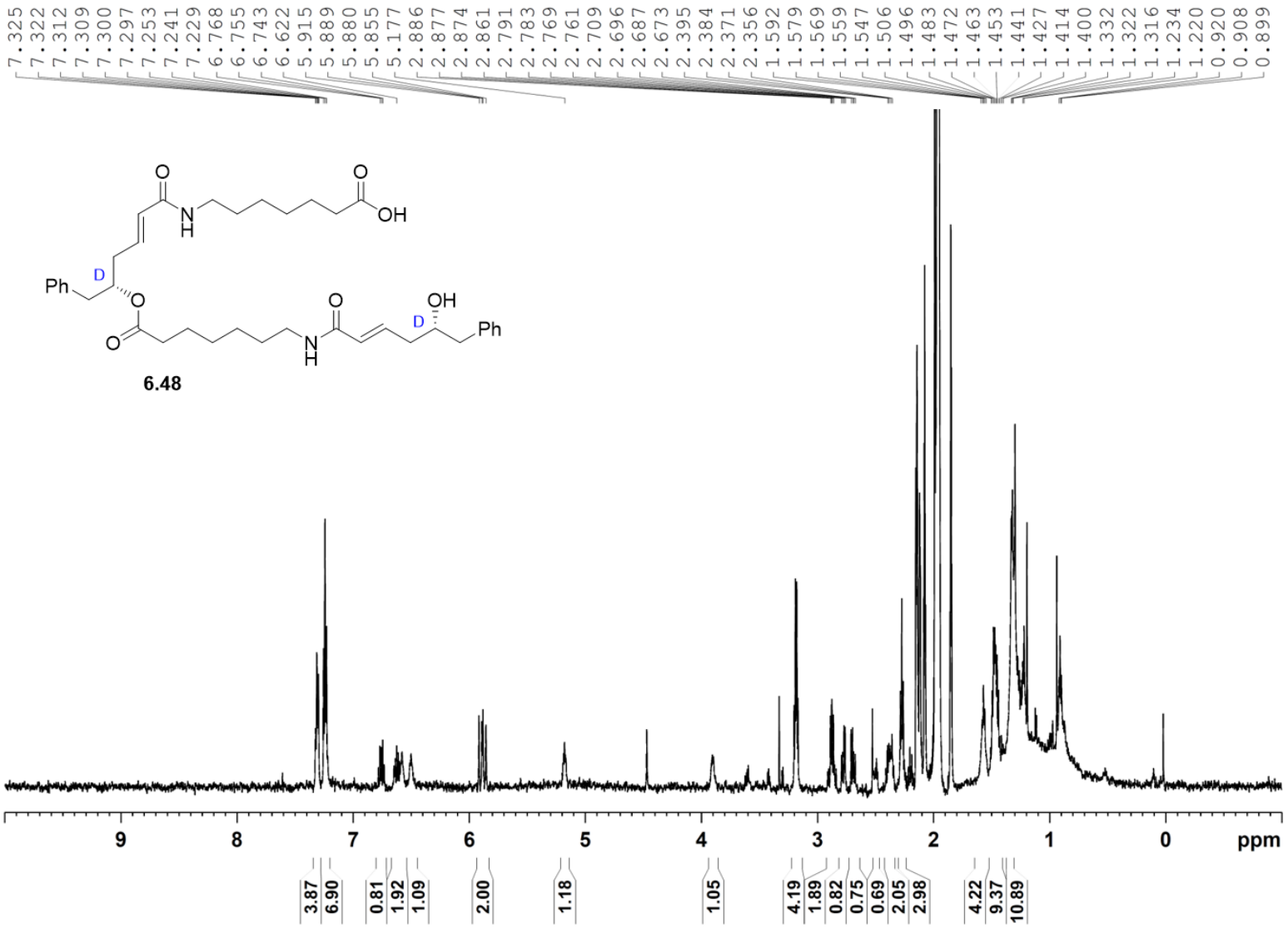

6.48

Linear Dimer Acid *via* enzymatic assay (**6.48**)

COSY (600 MHz, CD_3CN)

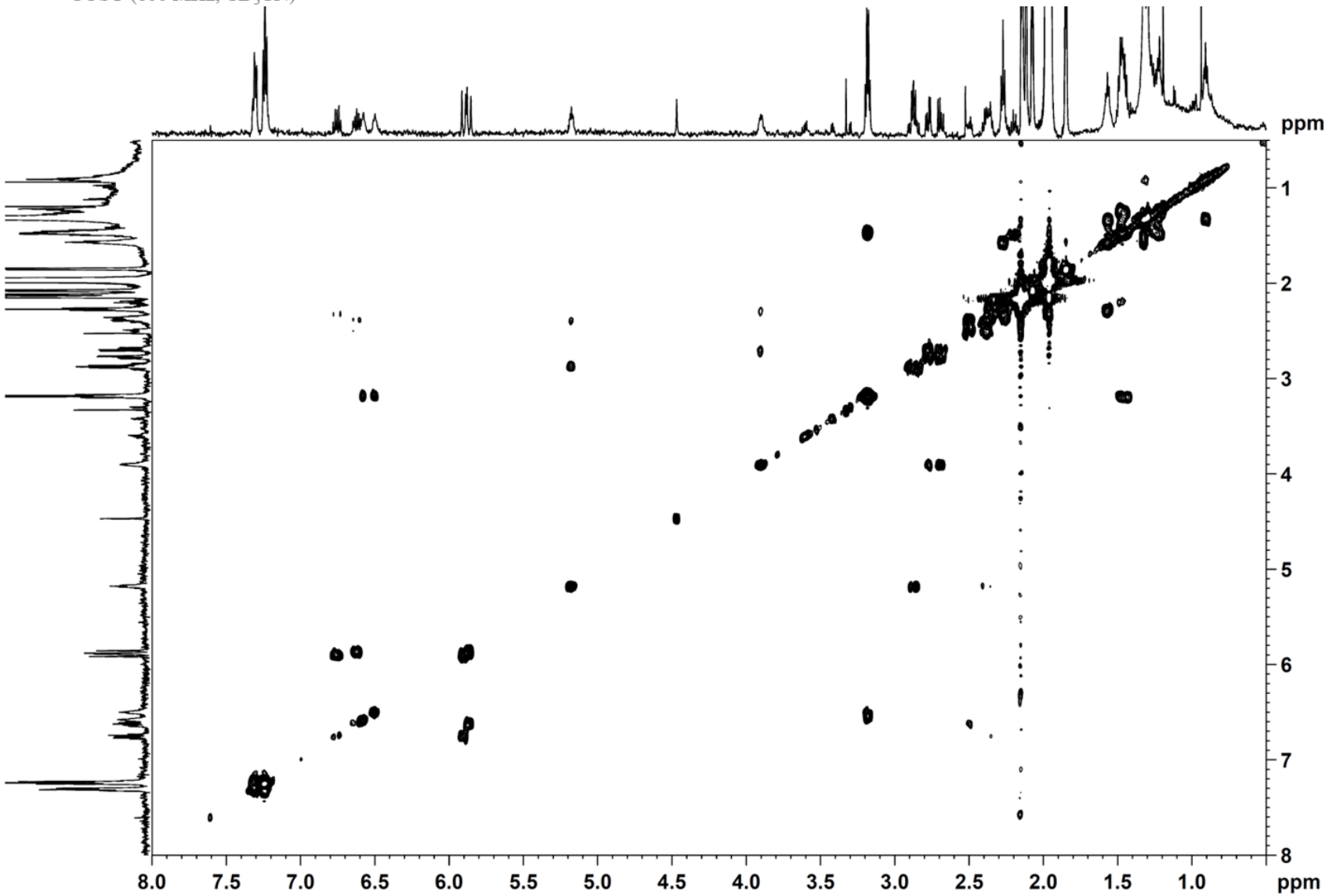

S1.4.2 Second-Generation NAC-Thioester Substrates: L-Configured Analogue Design & Evaluation

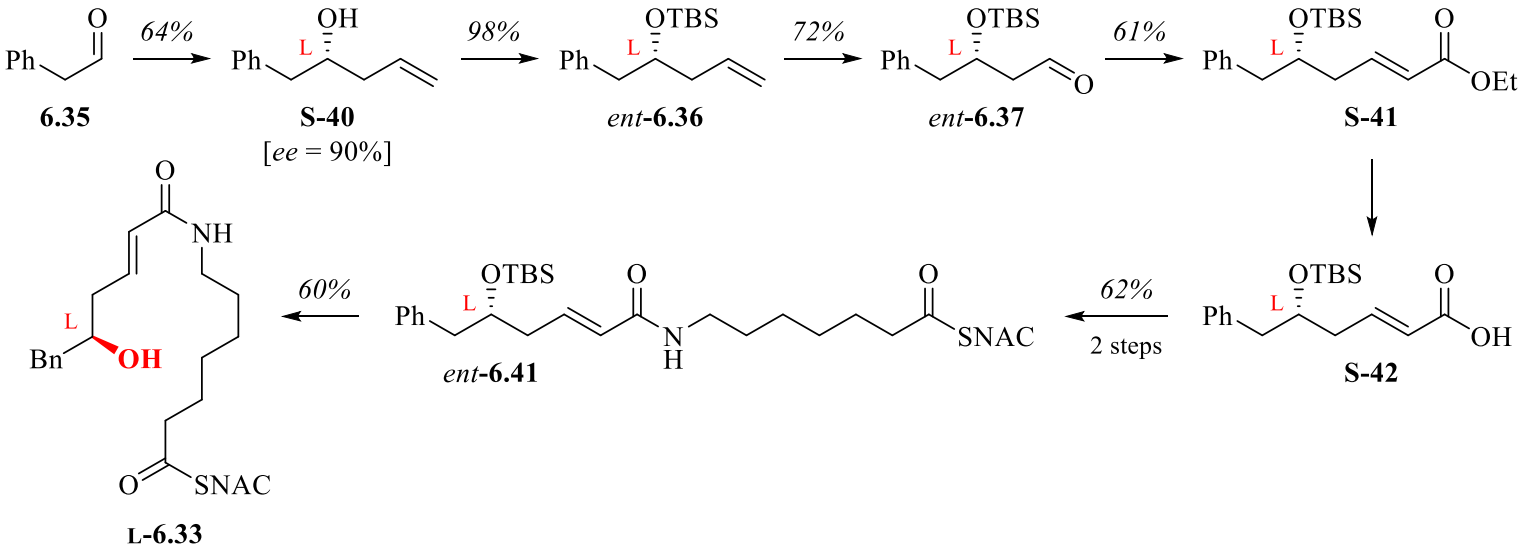

Figure S19 – Rapid development of L-configured second-generation NAC-thioester analogue to characterize substrate-specificity of DEBS TE.

L-Phenylpent-4-en-2-ol (**S-40**)

^{1}H NMR (400 MHz, $CDCl_3$)

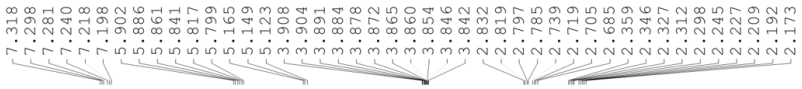

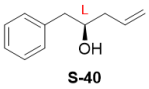

S-40

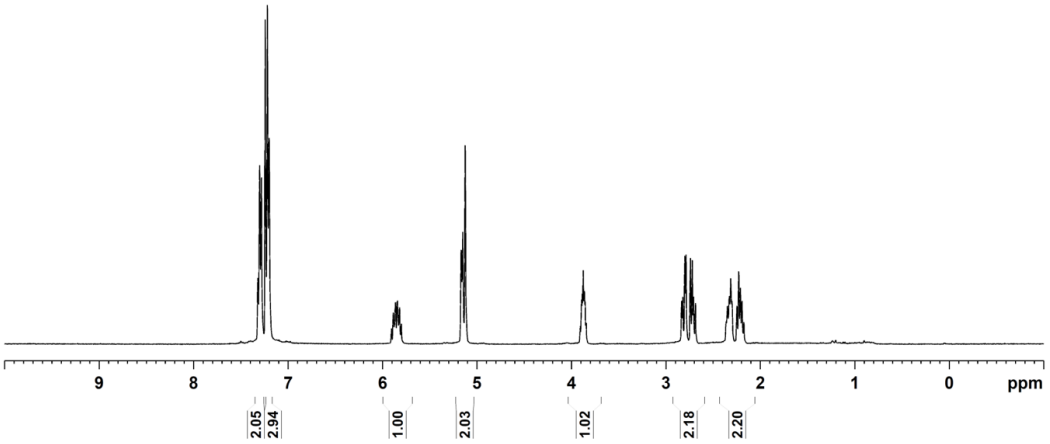

L-Phenylpent-4-en-2-ol (**S-40**)

^{13}C NMR (100 MHz, $CDCl_3$)

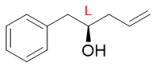

S-40

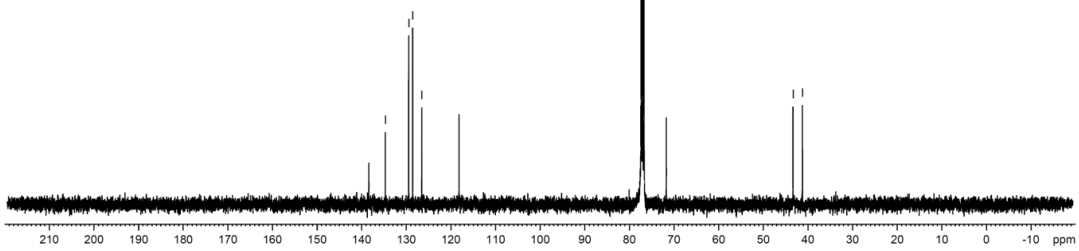

L-*tert*-Butyldimethyl-(1-phenylpent-4-en-2-yloxy)-silane (*ent*-**6.36**)

^{1}H NMR (400 MHz, $CDCl_3$)

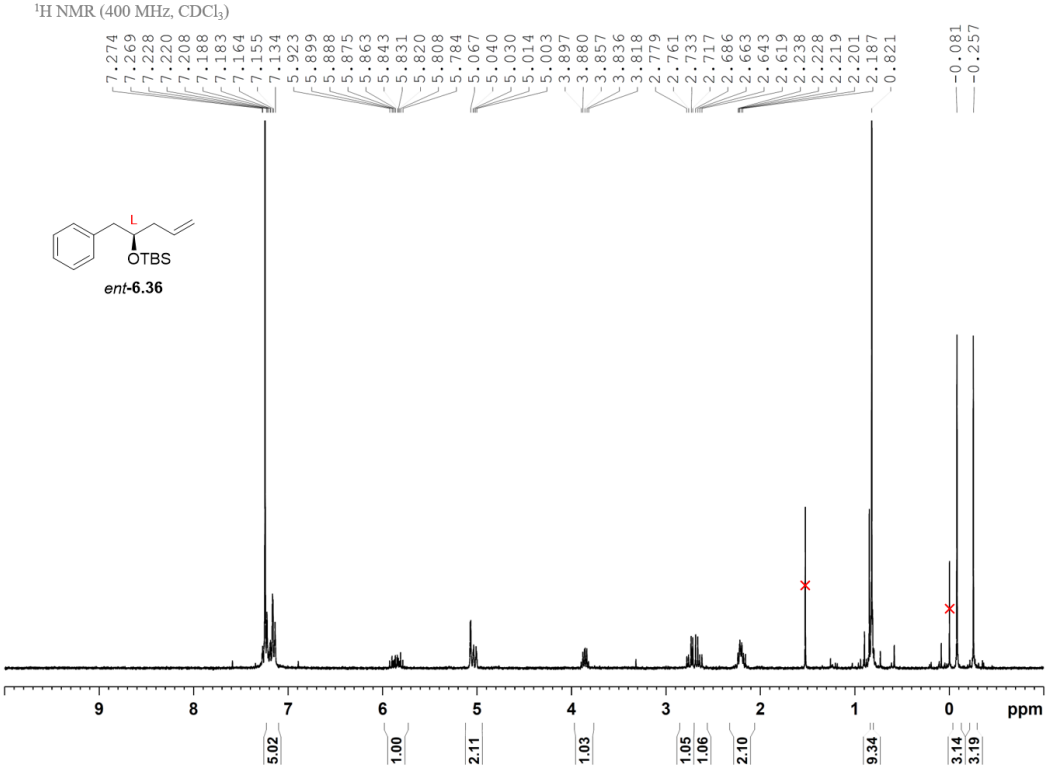

L-*tert*-Butyldimethyl-(1-phenylpent-4-en-2-yloxy)-silane (*ent*-**6.36**)

^{13}C NMR (100 MHz, $CDCl_3$)

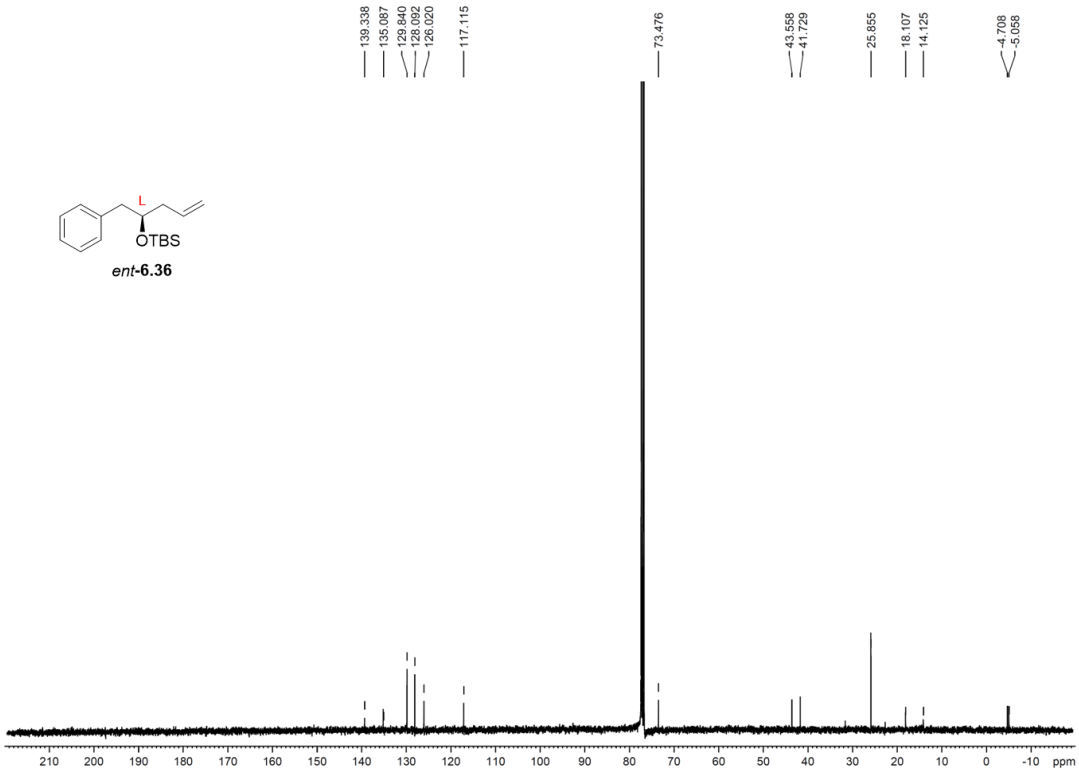

L-3-(*tert*-Butyldimethylsilyloxy)-4-phenylbutanal (*ent*-**6.37**)

^{1}H NMR (400 MHz, $CDCl_3$)

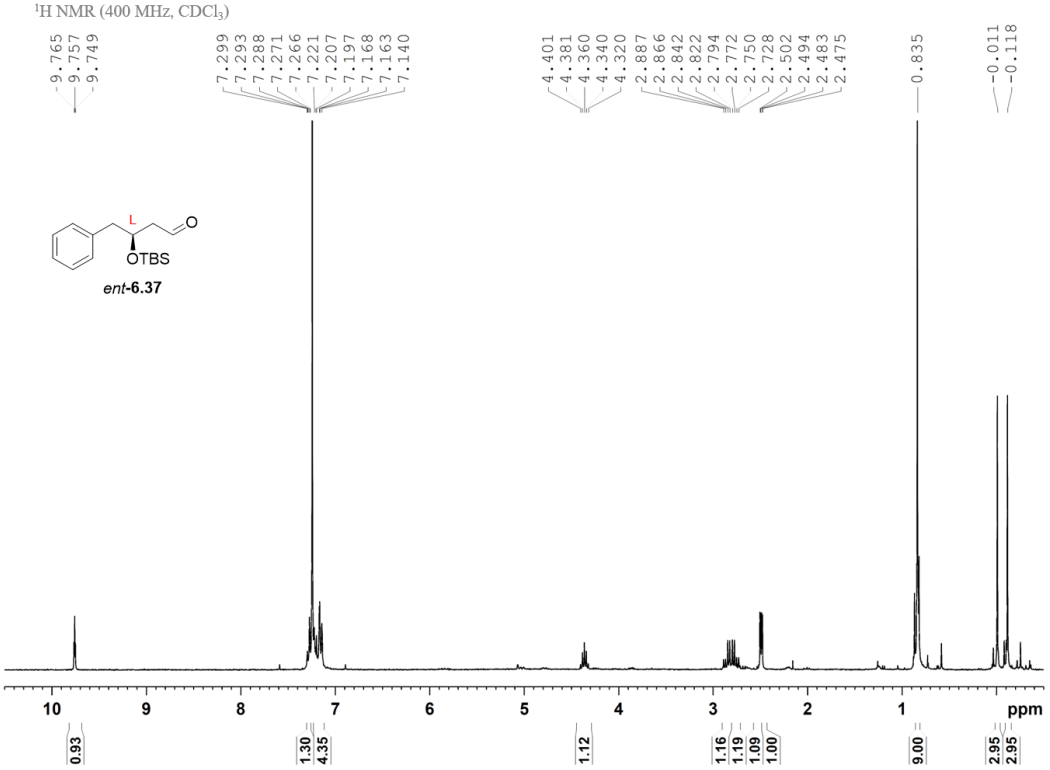

L-3-(*tert*-Butyldimethylsilyloxy)-4-phenylbutanal (*ent*-**6.37**)

^{13}C NMR (100 MHz, $CDCl_3$)

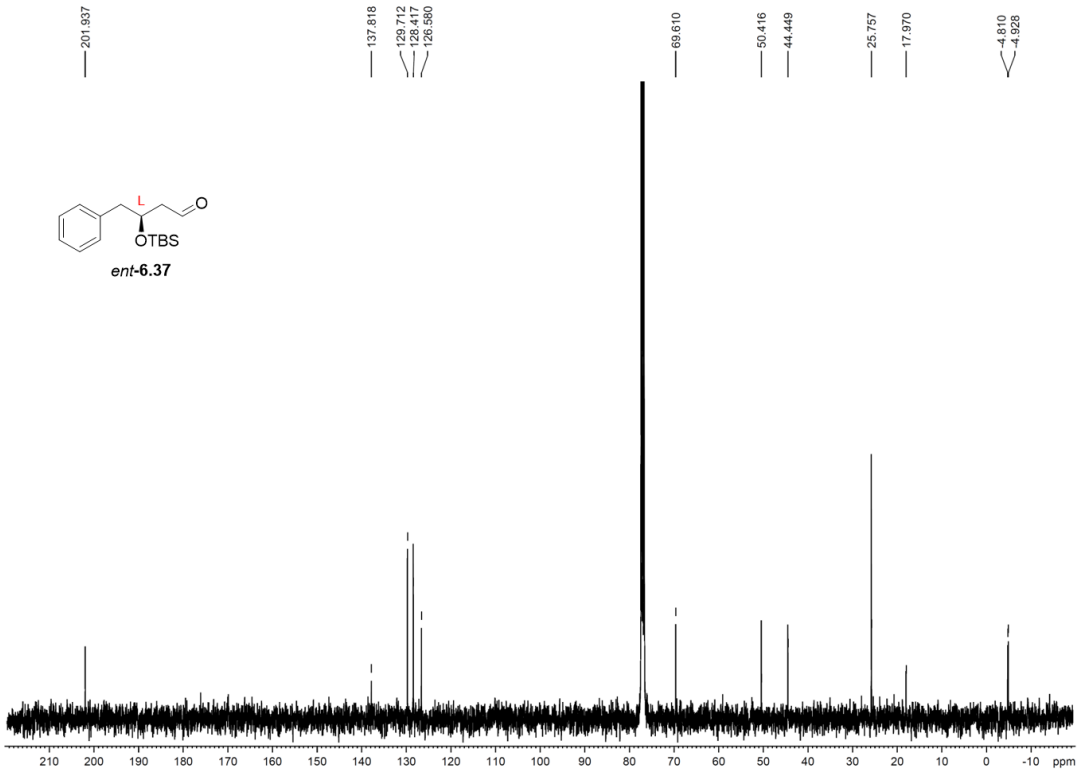

L-(*E*)-Ethyl 5-(*tert*-butyldimethylsilyloxy)-6-phenylhex-2-enoate (**S-41**)

^{1}H NMR (400 MHz, $CDCl_3$)

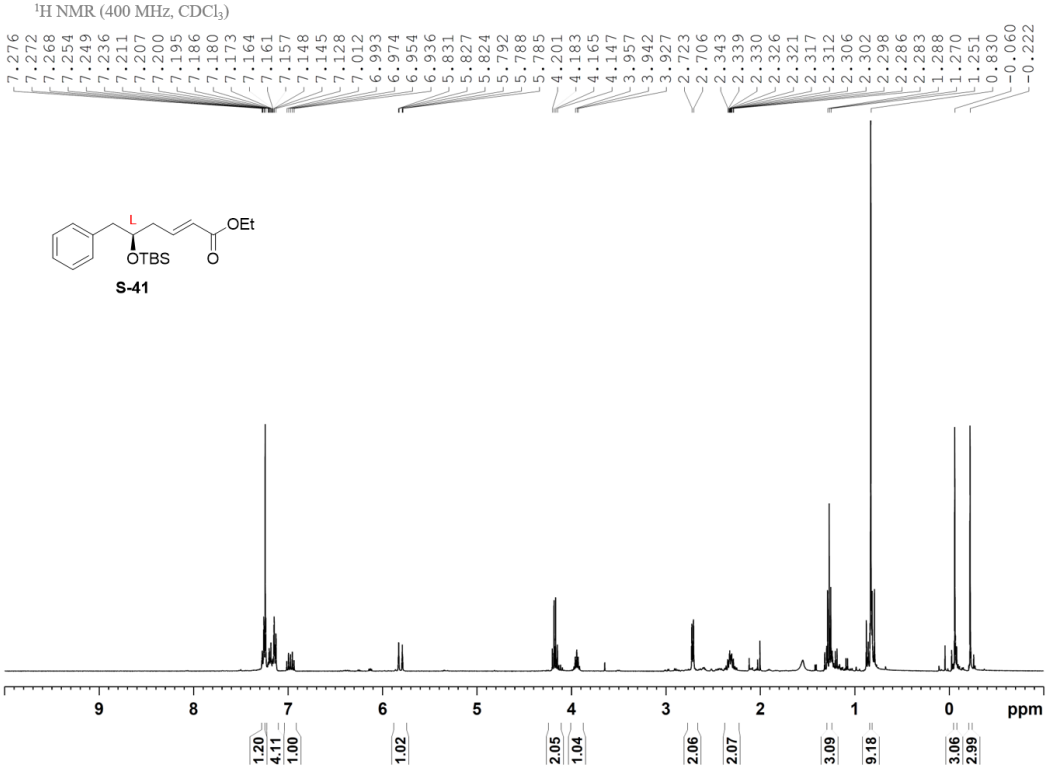

L-(*E*)-Ethyl 5-(*tert*-butyldimethylsilyloxy)-6-phenylhex-2-enoate (**S-41**)

^{13}C NMR (100 MHz, $CDCl_3$)

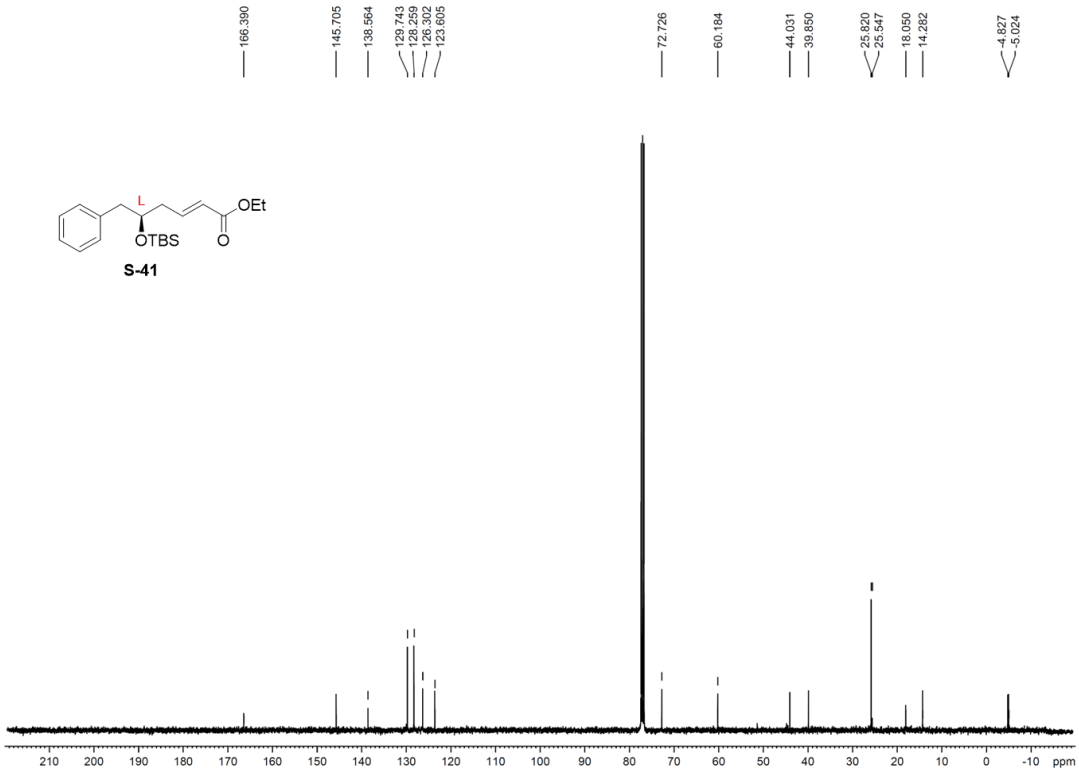

L-(*E*)-5-(*tert*-Butyldimethylsilyloxy)-6-phenylhex-2-enoic acid (**S-42**)

^{1}H NMR (400 MHz, $CDCl_3$)

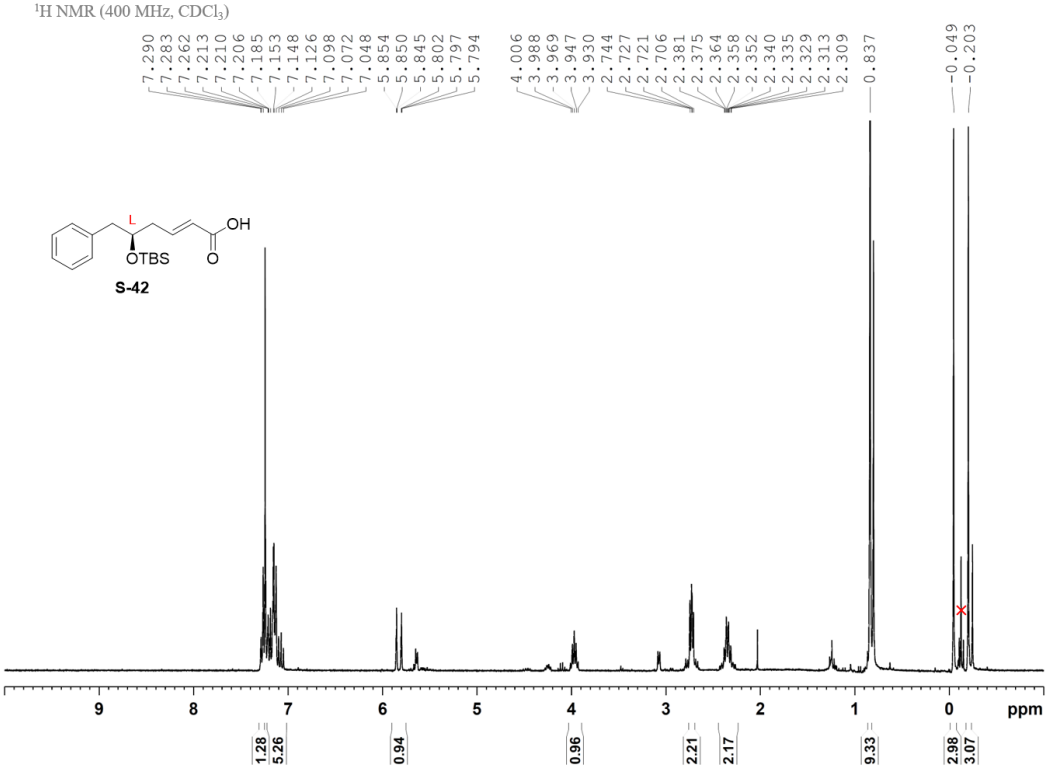

L-(*E*)-5-(*tert*-Butyldimethylsilyloxy)-6-phenylhex-2-enoic acid (**S-42**)

^{13}C NMR (100 MHz, $CDCl_3$)

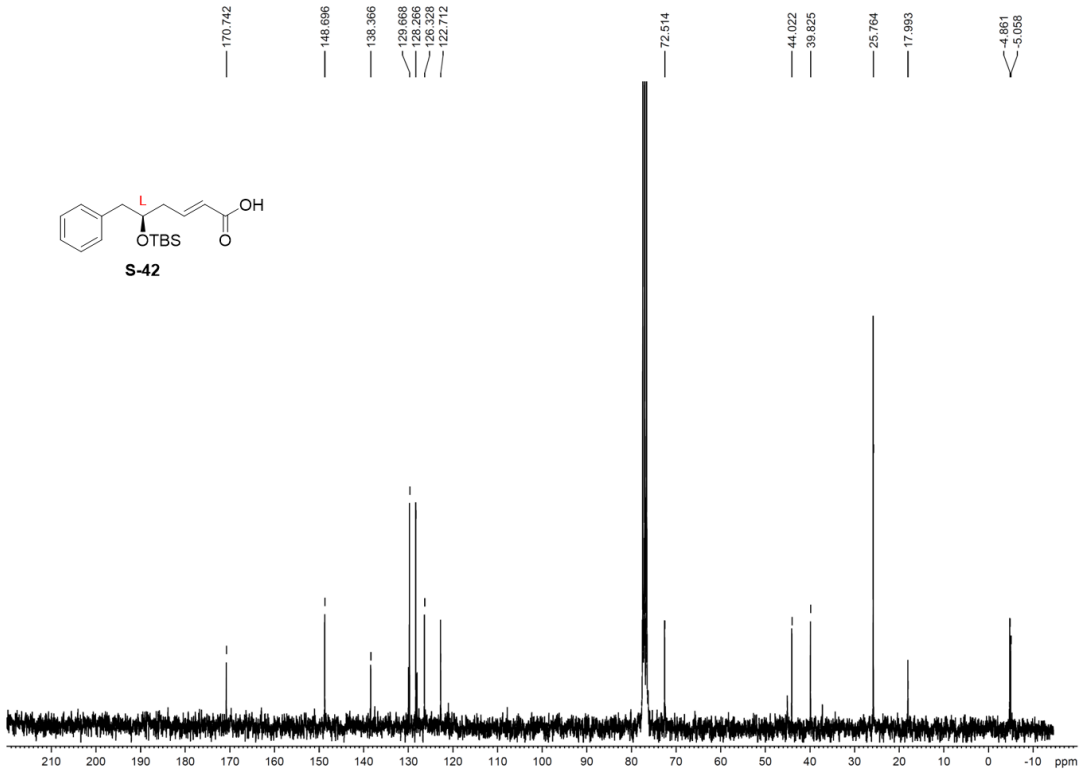

L-(*E*)-*S*-2-Acetamidoethyl-7-(5-*tert*-butyldimethylsilyloxy-6-phenylhex-2-enamido)-heptanethioate (*ent*-**6.41**)

^{1}H NMR (400 MHz, $CDCl_3$)

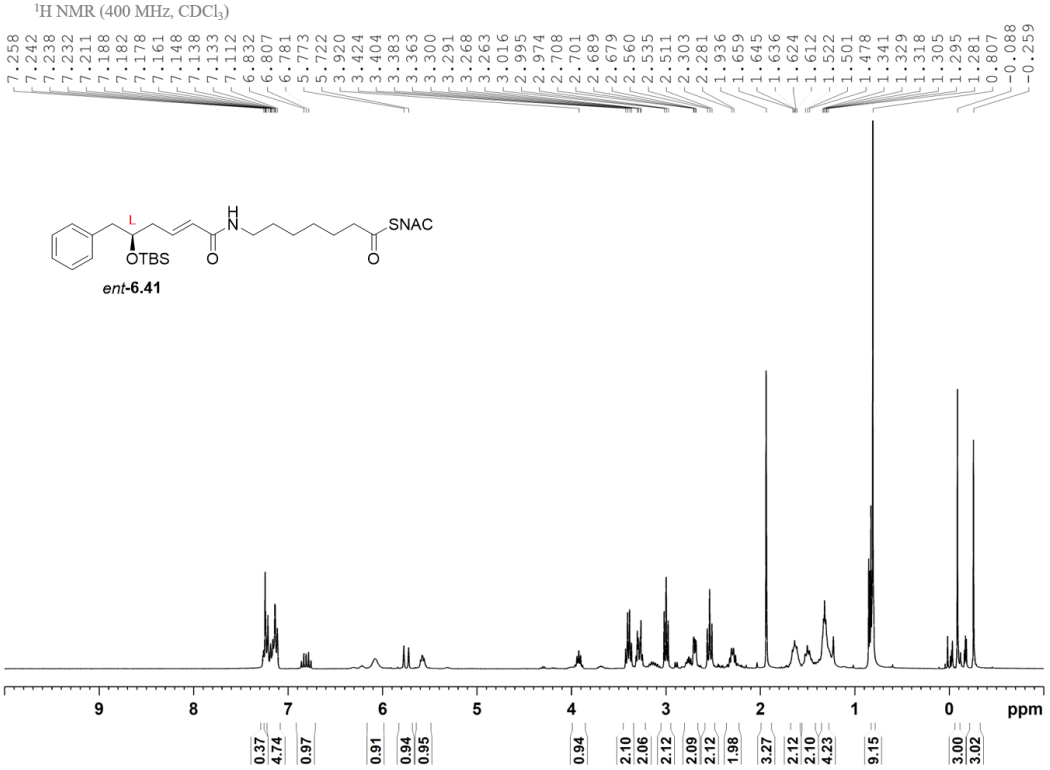

L-(*E*)-*S*-2-Acetamidoethyl-7-(5-*tert*-butyldimethylsilyloxy-6-phenylhex-2-enamido)-heptanethioate (*ent*-**6.41**)

^{1}H NMR (400 MHz, $CDCl_3$)

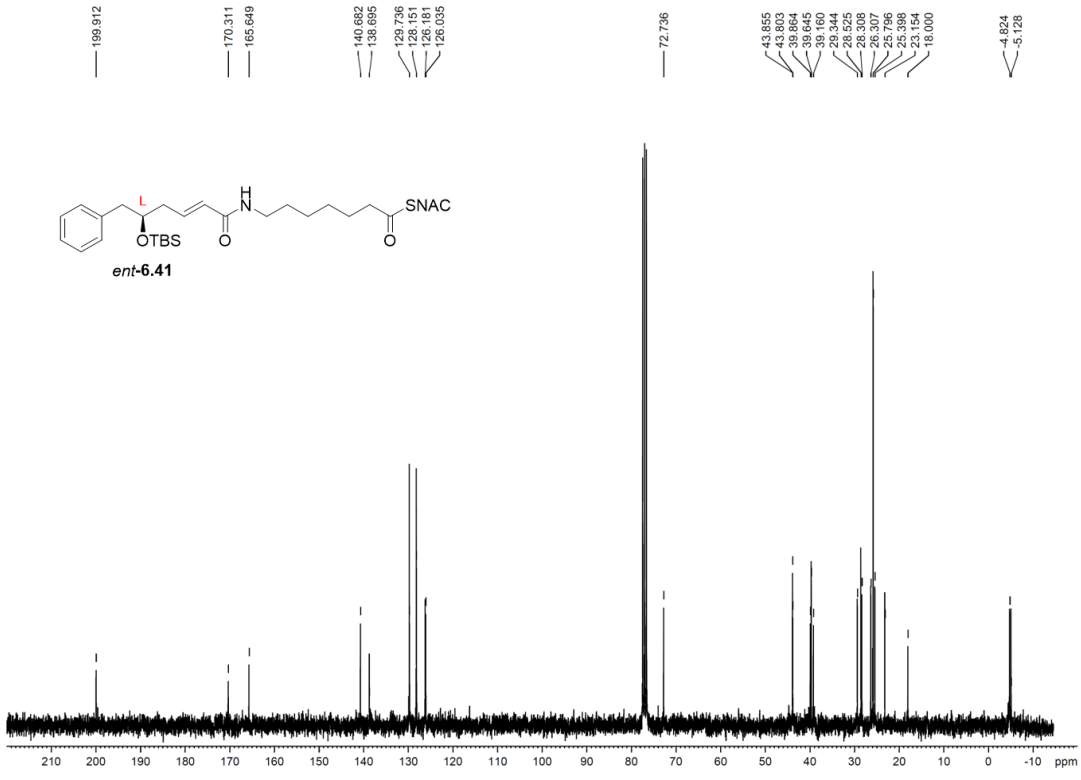

L-(*E*)-*S*-2-Acetamidoethyl-7-(5-hydroxy-6-phenylhex-2-enamido)-heptanethioate (L-**6.33**)

^{1}H NMR (400 MHz, $CDCl_3$)

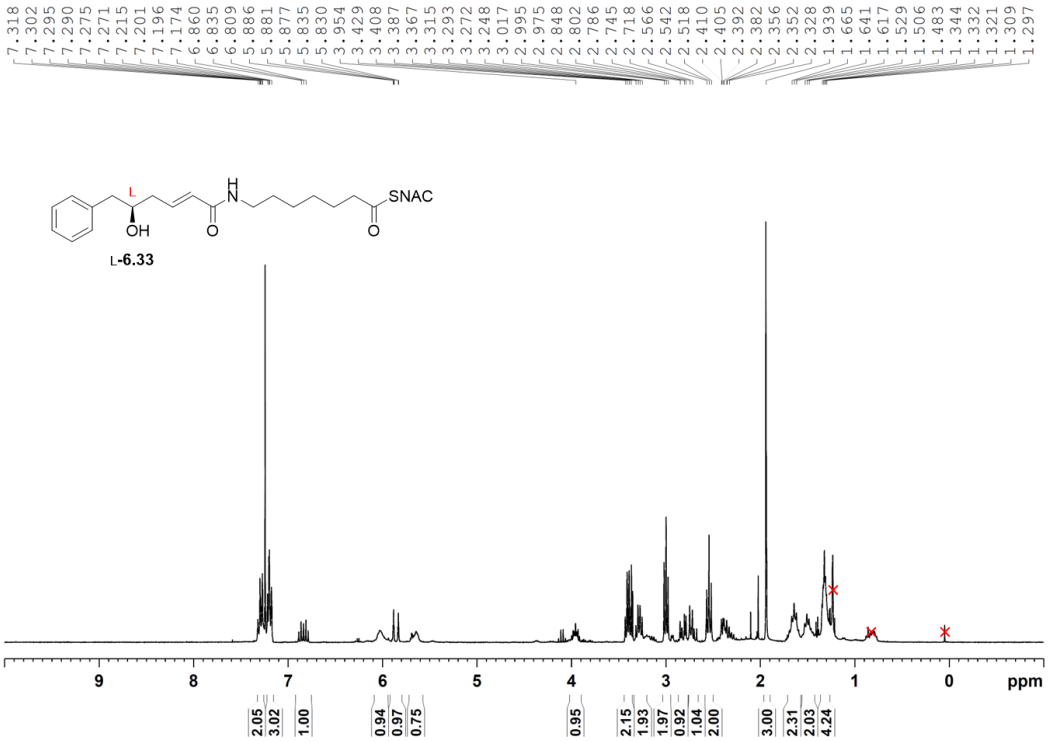

L-(*E*)-*S*-2-Acetamidoethyl-7-(5-hydroxy-6-phenylhex-2-enamido)-heptanethioate (L-**6.33**)

^{13}C NMR (100 MHz, $CDCl_3$)

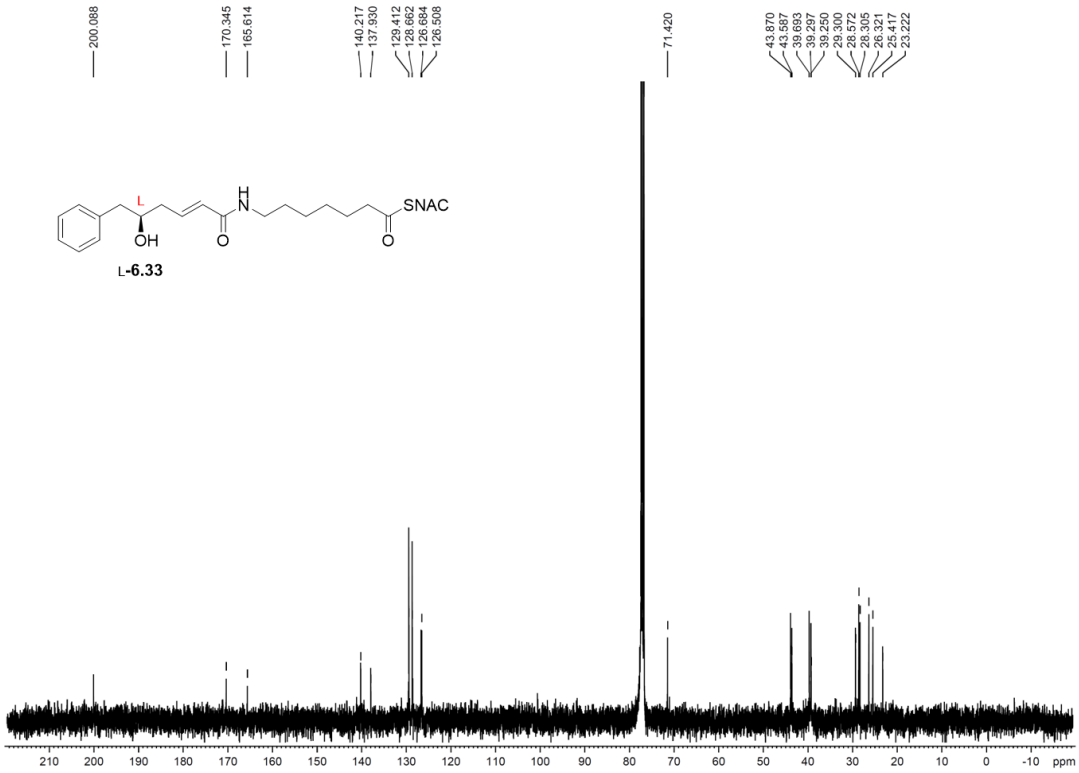

L-(*E*)-*S*-2-Acetamidoethyl-7-(5-hydroxy-6-phenylhex-2-enamido)-heptanethioate (L-**6.33**)

HSQC (400 MHz, $CDCl_3$)

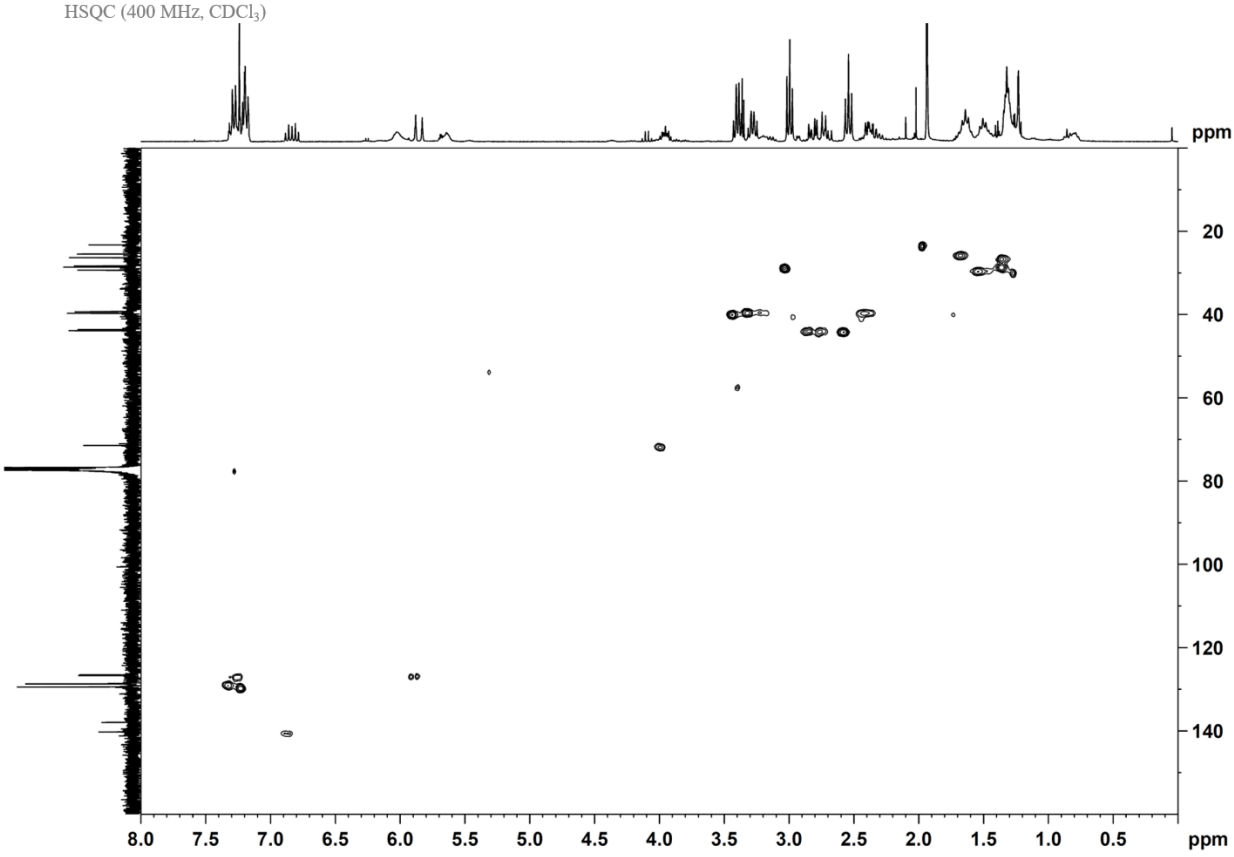

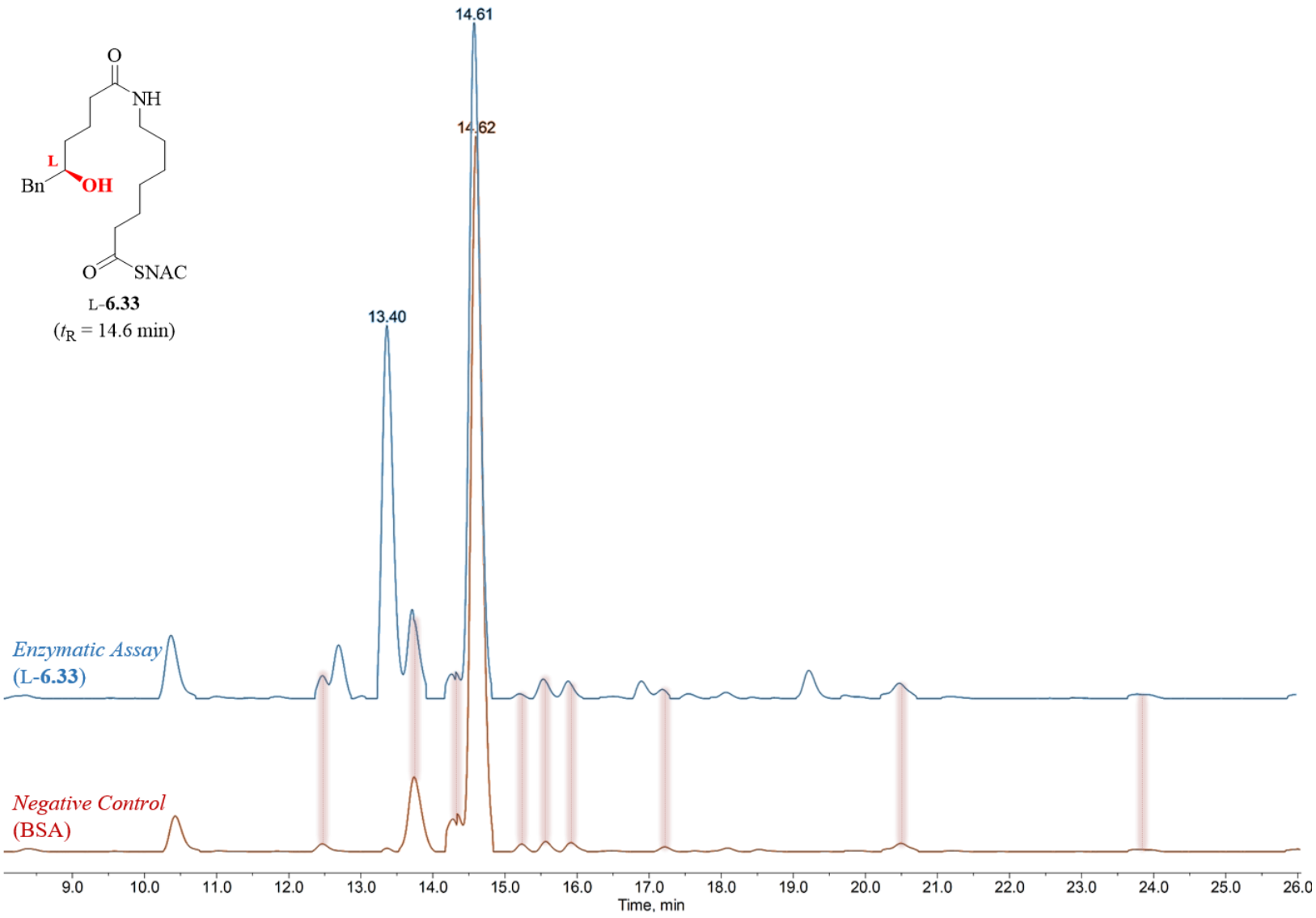

Figure S20 – LCMS comparison of UV traces (254 nm) showing negative control (BSA, trace **1**) and enzymatic assay (trace **2**) for L-configured substrate **6.33**. Assay mixtures consists of 15 μM BSA (blank) or DEBS TE, 2.5 mM L-**6.33** in 50 mM phosphate buffer (pH 7.4) at 22 ºC, and DMSO (10% *v*/*v*) as a solubility additive.

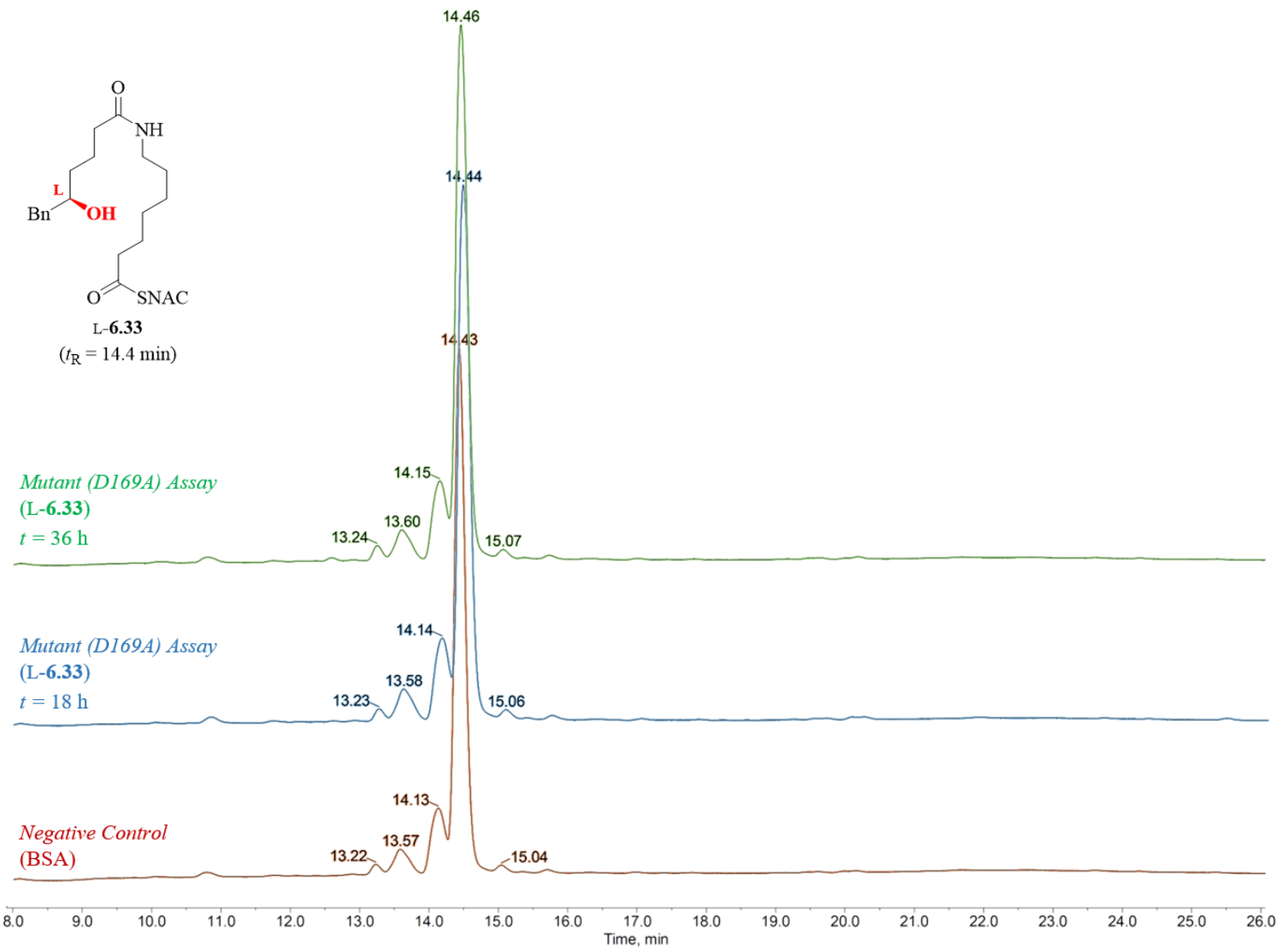

Figure S21 – LCMS comparison of UV traces (254 nm) showing negative control (BSA, trace **1**), and D169A mutant assay after 18 h (trace **2**) and 36 h (trace **3**) for L-configured substrate **6.33**. Assay mixtures consists of 15 µM BSA (blank) or DEBS D169A mutant TE, 2.5 mM L-**6.33** in 50 mM phosphate buffer (pH 7.4) at 22 ºC, and DMSO (10% *v*/*v*) as a solubility additive.

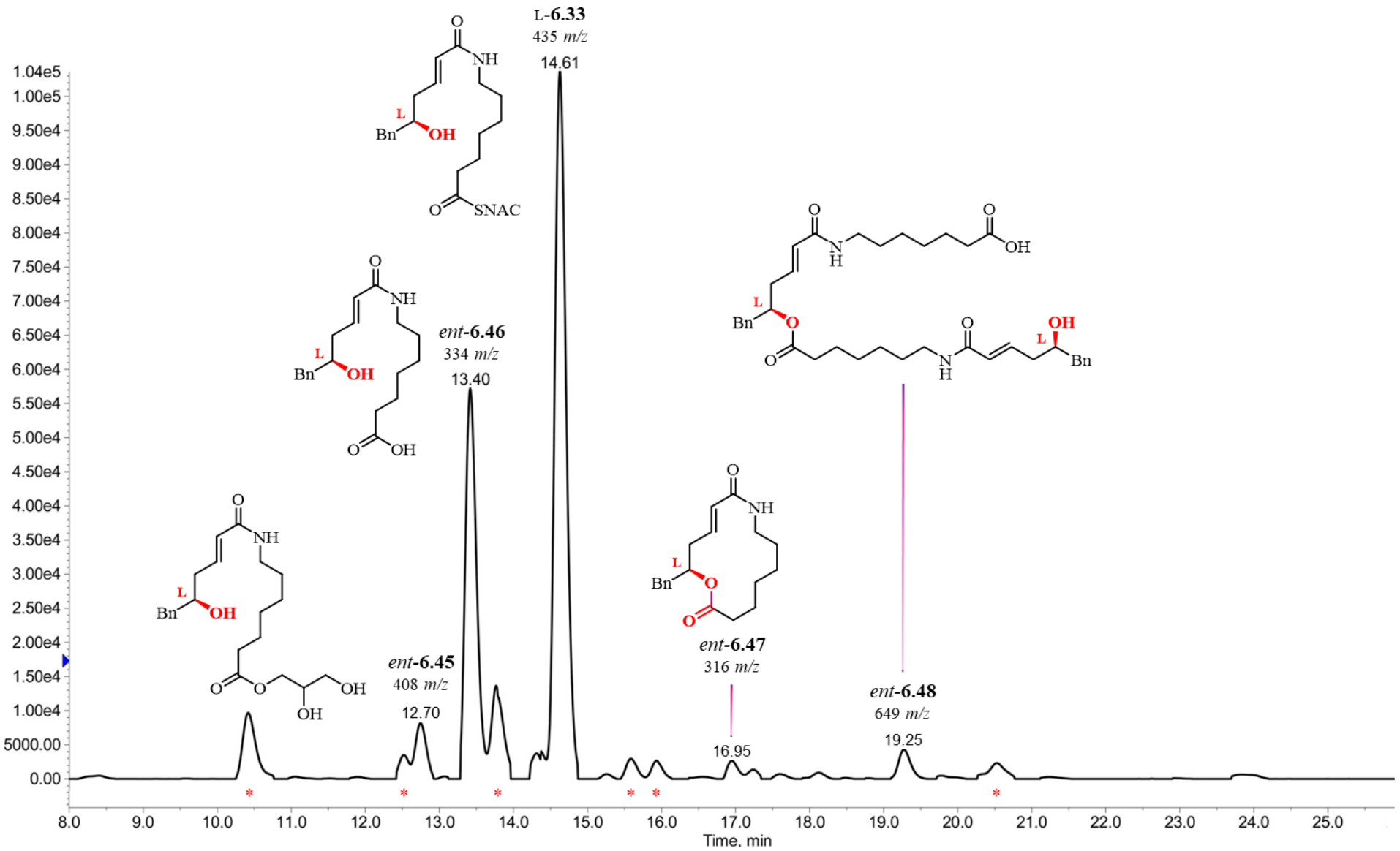

Figure S22 – LCMS analysis (254 nm) for *in vitro* enzymatic assay of L-configured NAC-thioester **6.33** with wild-type DEBS TE.

S1.4.3 Second-Generation NAC-Thioester Substrates: Racemic Methyl Derivative Design & Evaluation (§ 6.4.1)

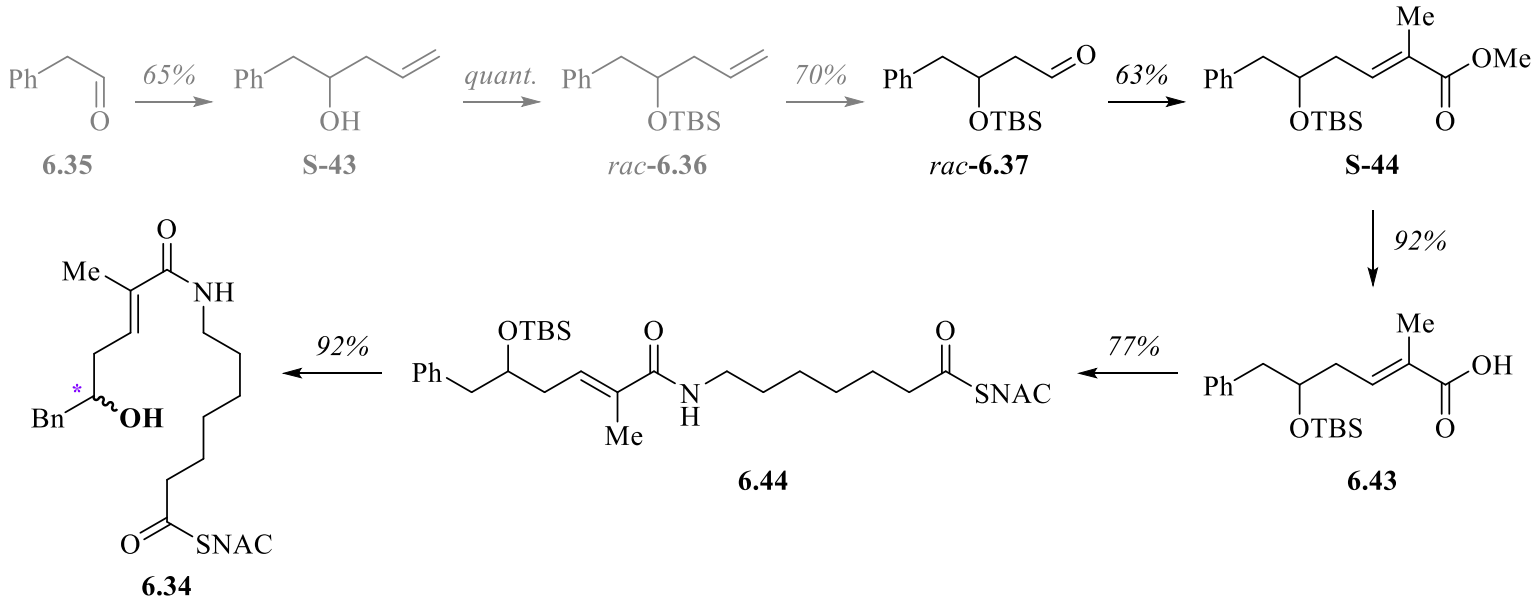

Figure S23 – Rapid development of racemic second-generation NAC-thioester methyl derivative for characterization of substrate-specificity for DEBS TE.

Methyl-(*E*)-5-(*tert*-butyldimethylsilyloxy)-2-methyl-6-phenylhex-2-enoate (**S-44**)

^{1}H NMR (400 MHz, $CDCl_3$)

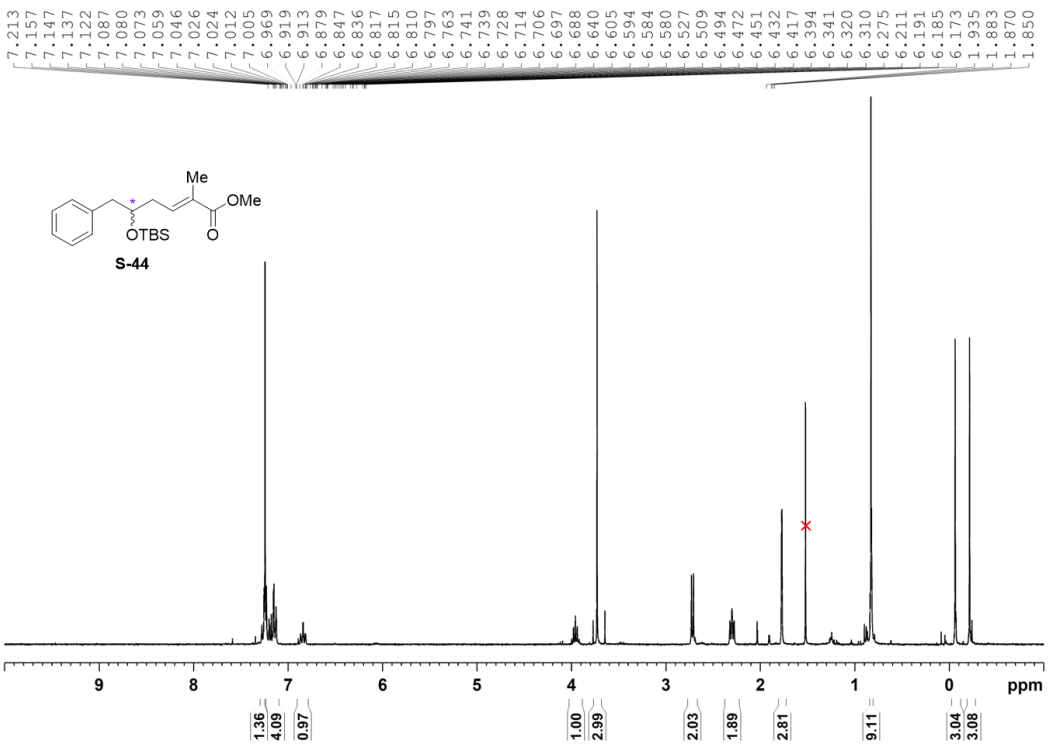

Methyl-(*E*)-5-(*tert*-butyldimethylsilyloxy)-2-methyl-6-phenylhex-2-enoate (**S-44**)

^{13}C NMR (100 MHz, $CDCl_3$)

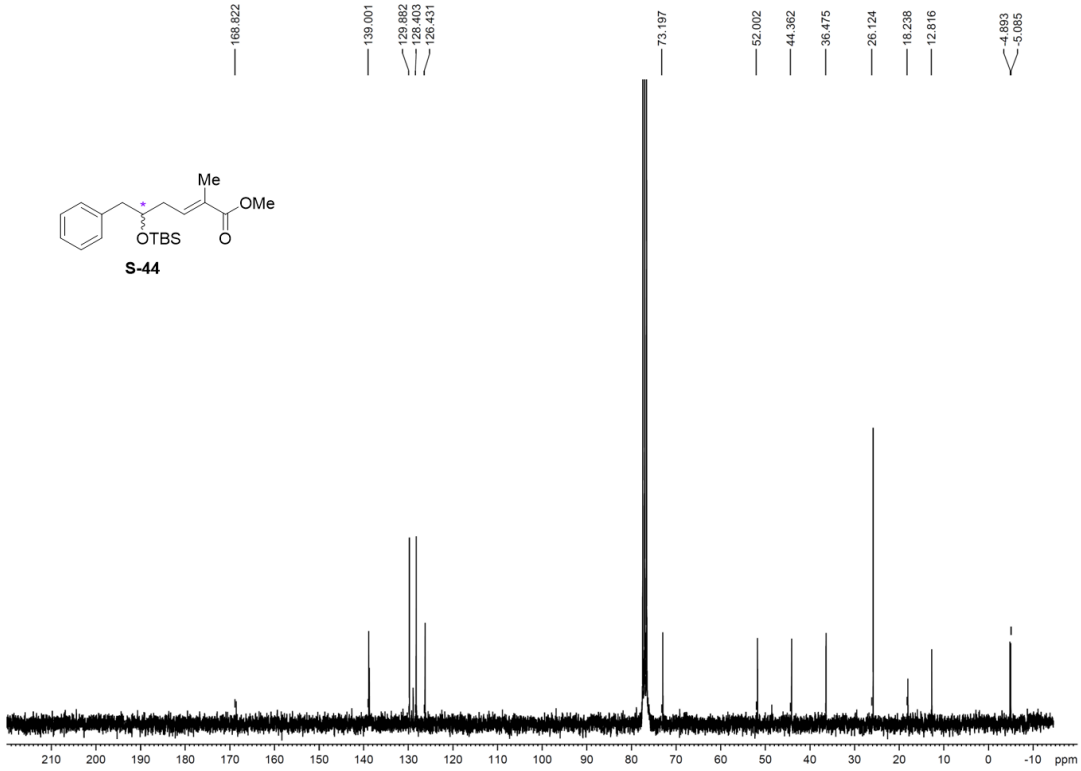

(*E*)-5-(*tert*-Butyldimethylsilyloxy)-2-methyl-6-phenylhex-2-enoic acid (**6.43**)

^{1}H NMR (400 MHz, $CDCl_3$)

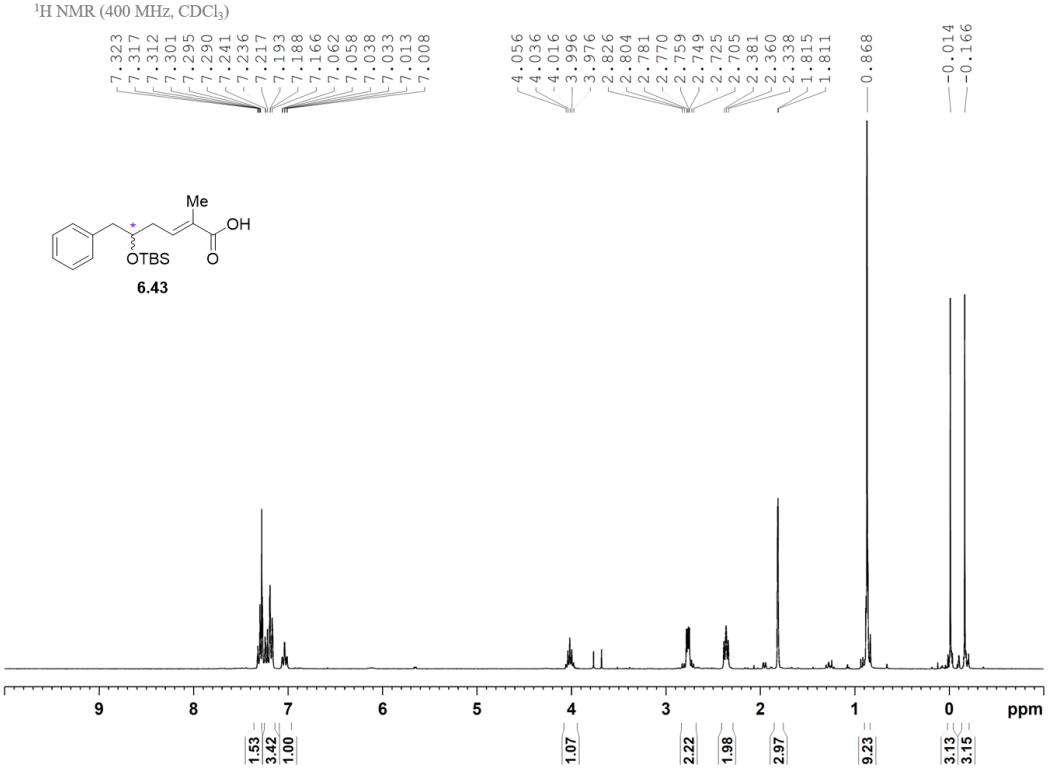

(*E*)-5-(*tert*-Butyldimethylsilyloxy)-2-methyl-6-phenylhex-2-enoic acid (**6.43**)

^{13}C NMR (100 MHz, $CDCl_3$)

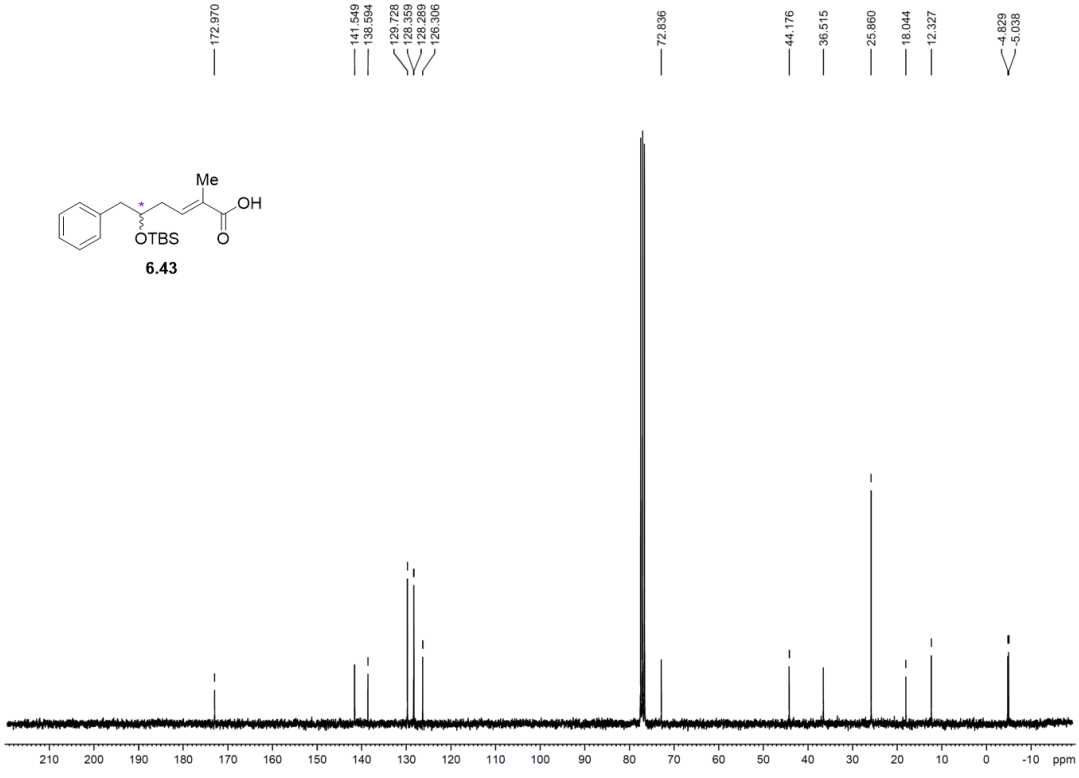

(*E*)-*S*-2-Acetamidoethyl-7-(5-(*tert*-butyldimethylsilyloxy)-2-methyl-6-phenylhex-2-enamido)-heptanethioate (**6.44**)

^{1}H NMR (400 MHz, $CDCl_3$)

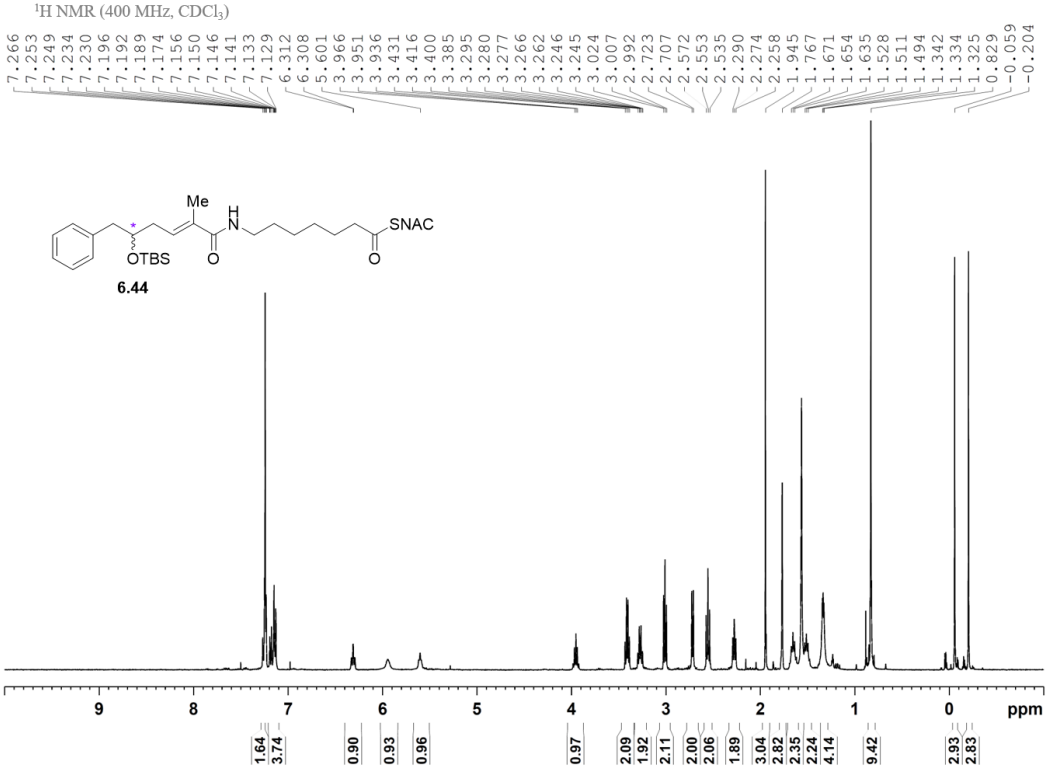

(*E*)-*S*-2-Acetamidoethyl-7-(5-(*tert*-butyldimethylsilyloxy)-2-methyl-6-phenylhex-2-enamido)-heptanethioate (**6.44**)

^{13}C NMR (100 MHz, $CDCl_3$)

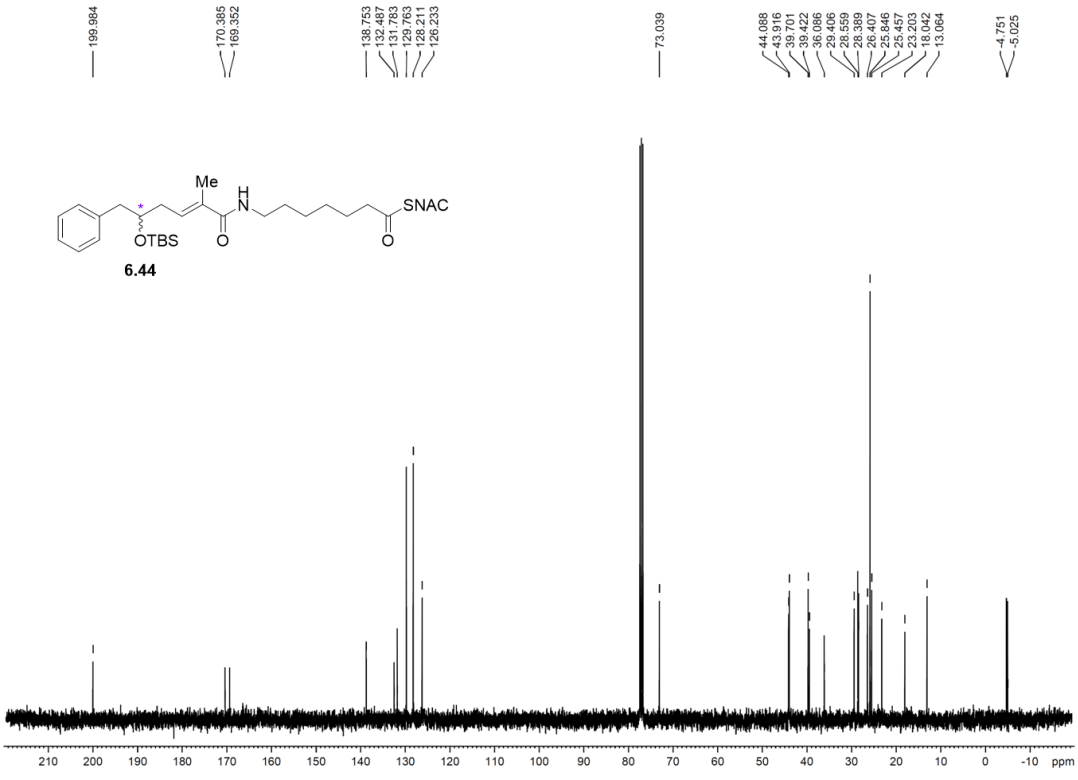

(*E*)-*S*-2-Acetamidoethyl-7-(5-hydroxy-2-methyl-6-phenylhex-2-enamido)-heptanethioate (**6.34**)

^{1}H NMR (400 MHz, $CDCl_3$)

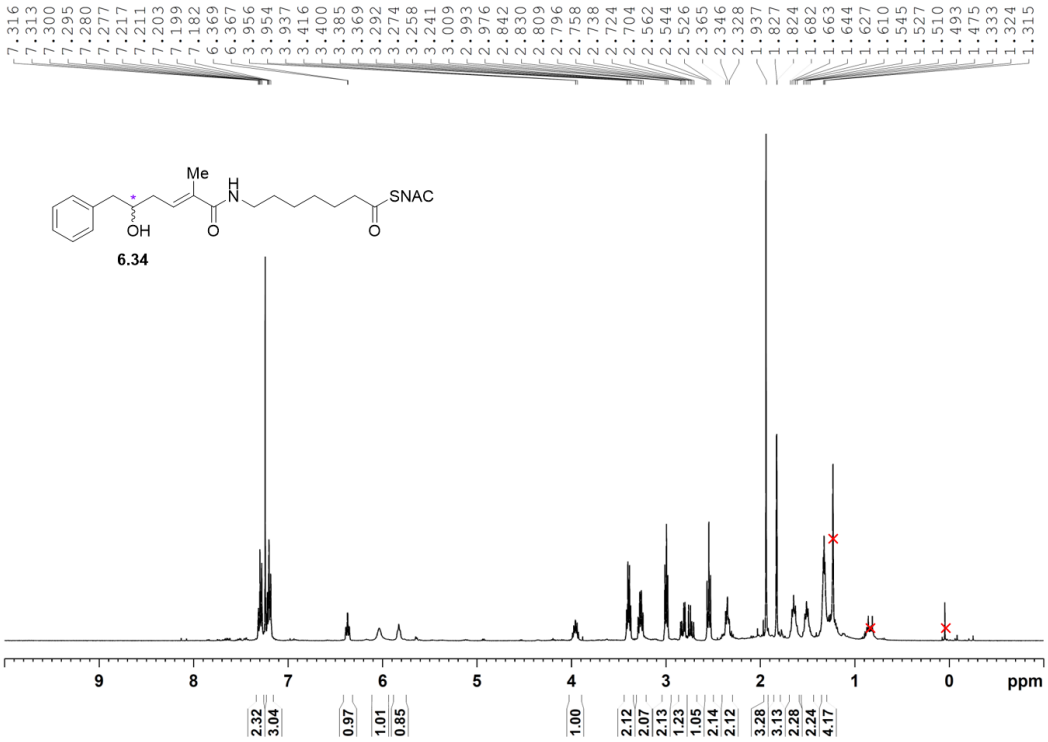

(*E*)-*S*-2-Acetamidoethyl-7-(5-hydroxy-2-methyl-6-phenylhex-2-enamido)-heptanethioate (**6.34**)

^{13}C NMR (100 MHz, $CDCl_3$)

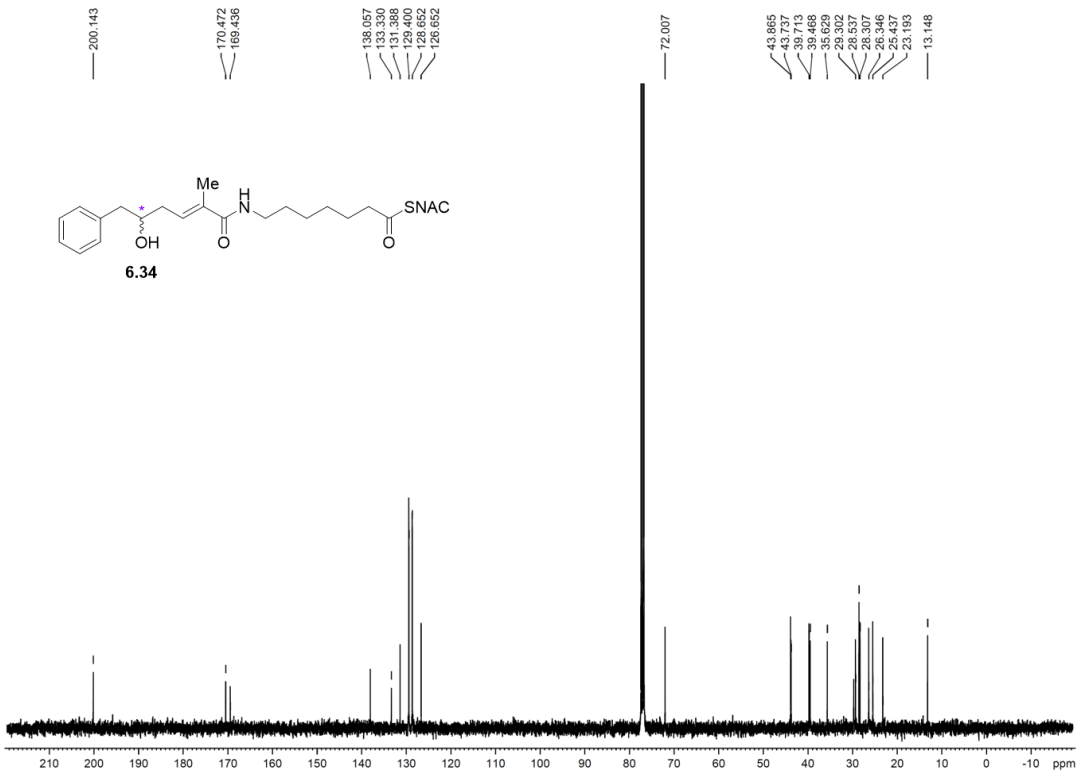

(*E*)-*S*-2-Acetamidoethyl-7-(5-hydroxy-2-methyl-6-phenylhex-2-enamido)-heptanethioate (**6.34**)

COSY (400 MHz, $CDCl_3$)

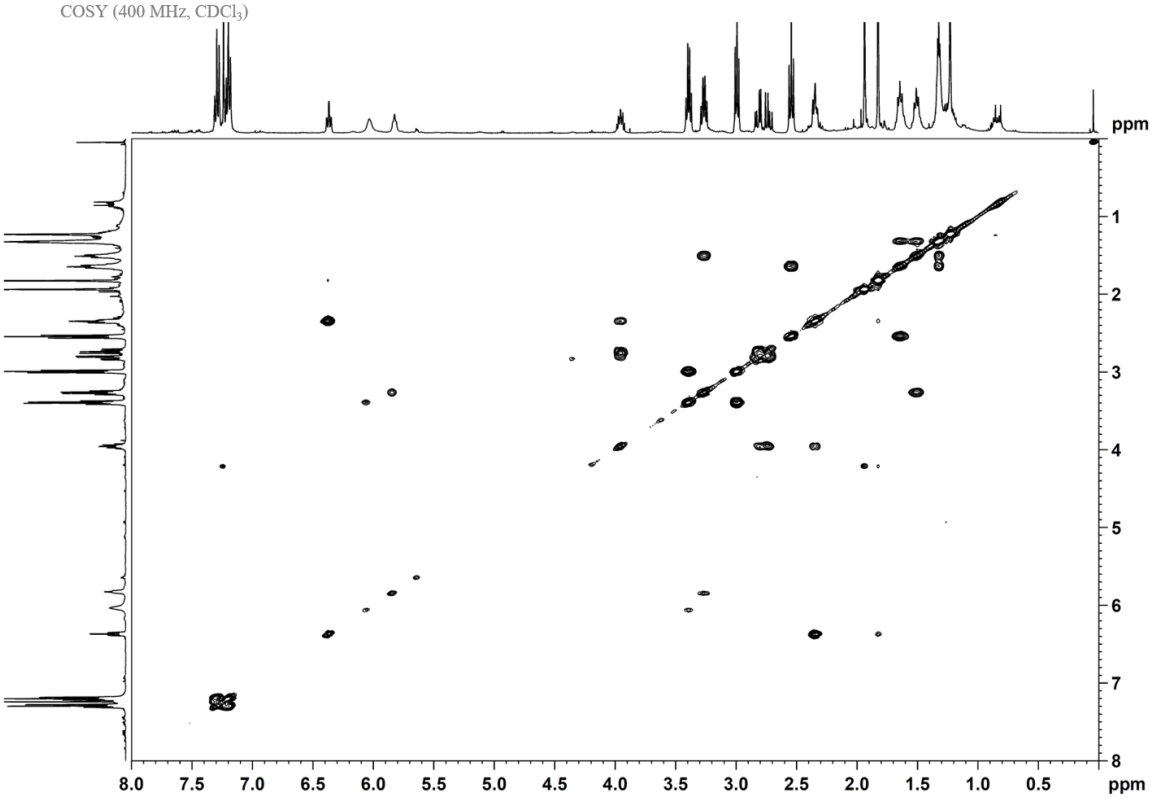

(*E*)-*S*-2-Acetamidoethyl-7-(5-hydroxy-2-methyl-6-phenylhex-2-enamido)-heptanethioate (**6.34**)

HSQC (400 MHz, $CDCl_3$)

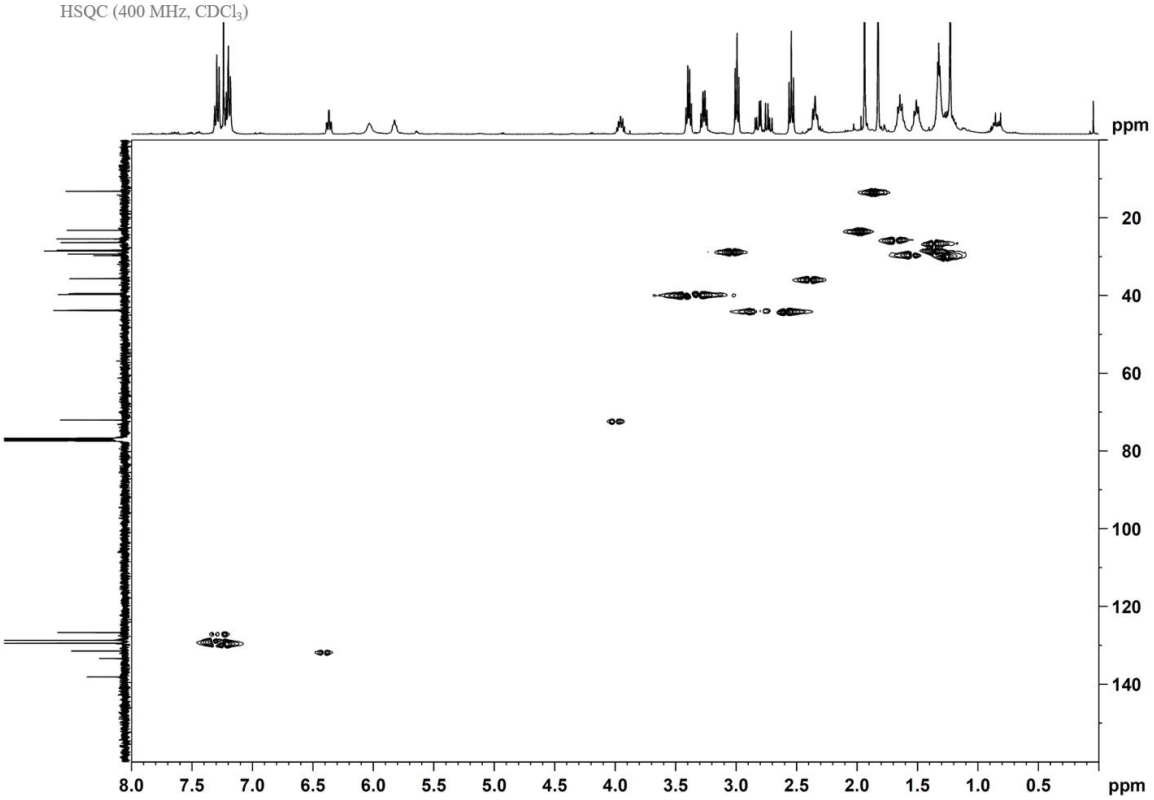

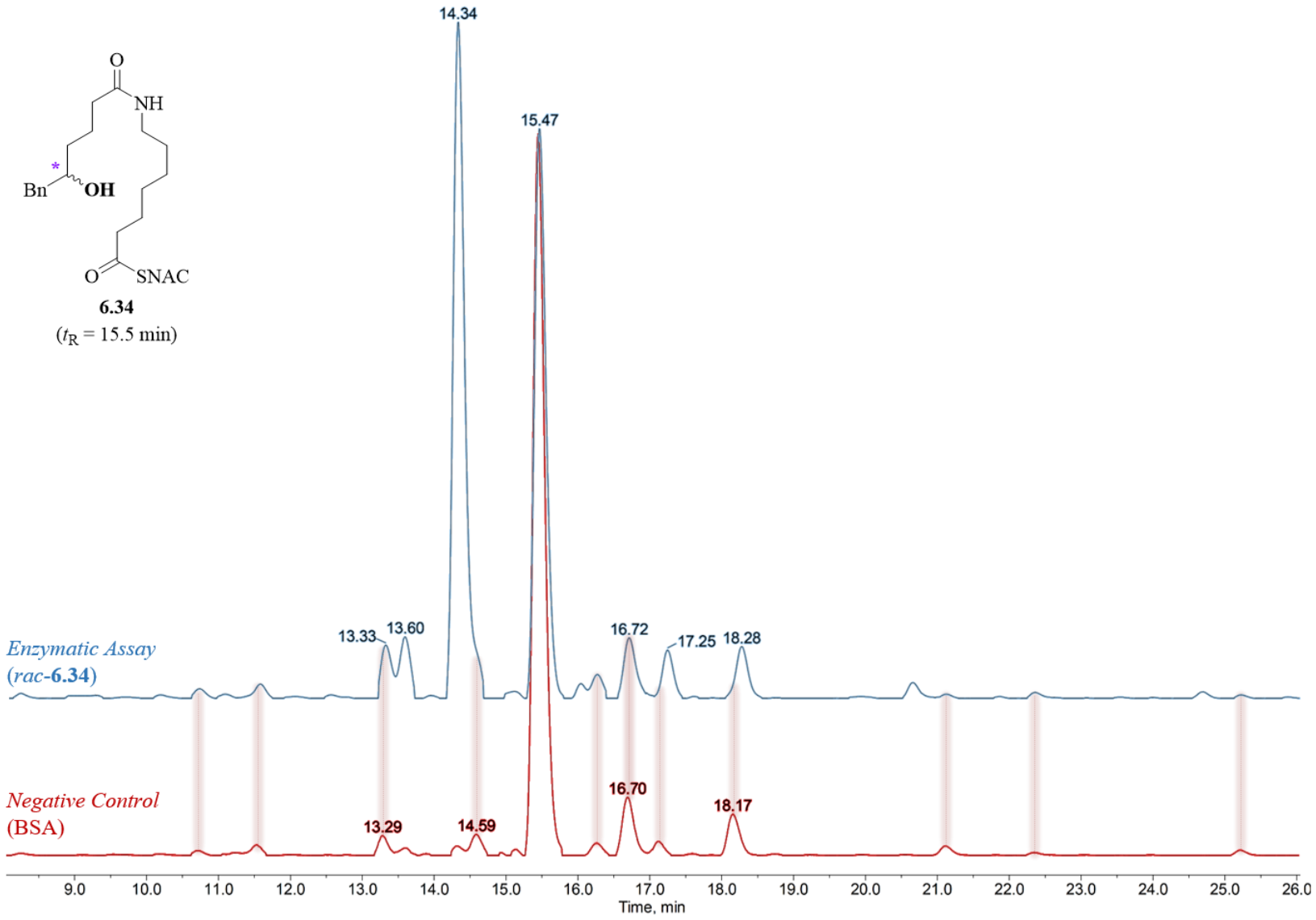

Figure S24 – LCMS comparison of UV traces (254 nm) showing negative control (BSA, trace **1**) and enzymatic assay (trace **2**) for racemic methyl derivative **6.34**. Assay mixtures consists of 15 µM BSA (blank) or DEBS TE, 2.5 mM *rac*-**6.34** in 50 mM phosphate buffer (pH 7.4) at 22 ºC, and DMSO (10% *v*/*v*) as a solubility additive.

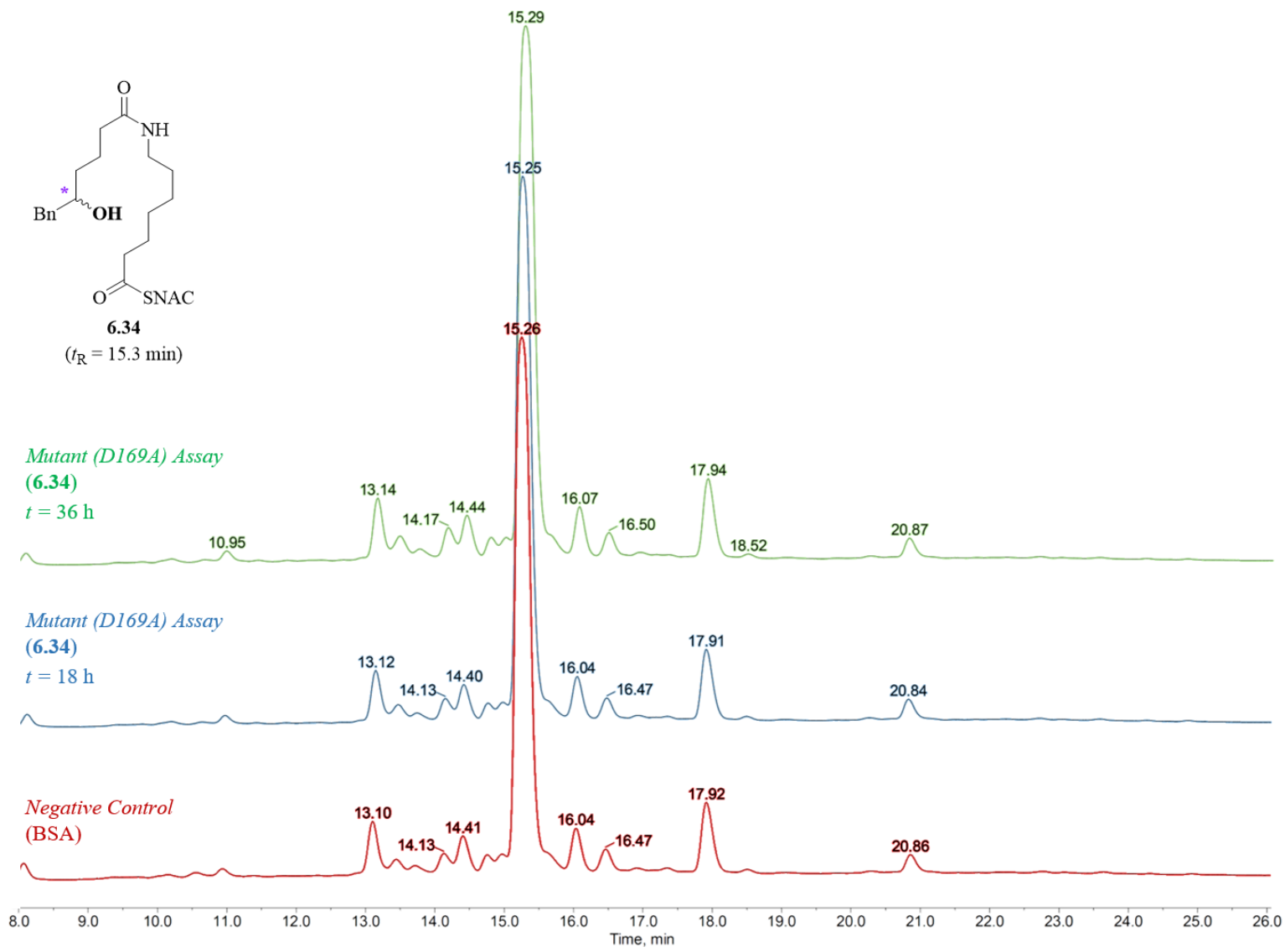

Figure S25 – LCMS comparison of UV traces (254 nm) showing negative control (BSA, trace **1**), and D169A mutant assay after 18 h (trace **2**) and 36 h (trace **3**) for racemic methyl derivative **6.34**. Assay mixtures consists of 15 μM BSA (blank) or DEBS D169A mutant TE, 2.5 mM *rac*-**6.34** in 50 mM phosphate buffer (pH 7.4) at 22 ºC, and DMSO (10% *v*/*v*) as a solubility additive.

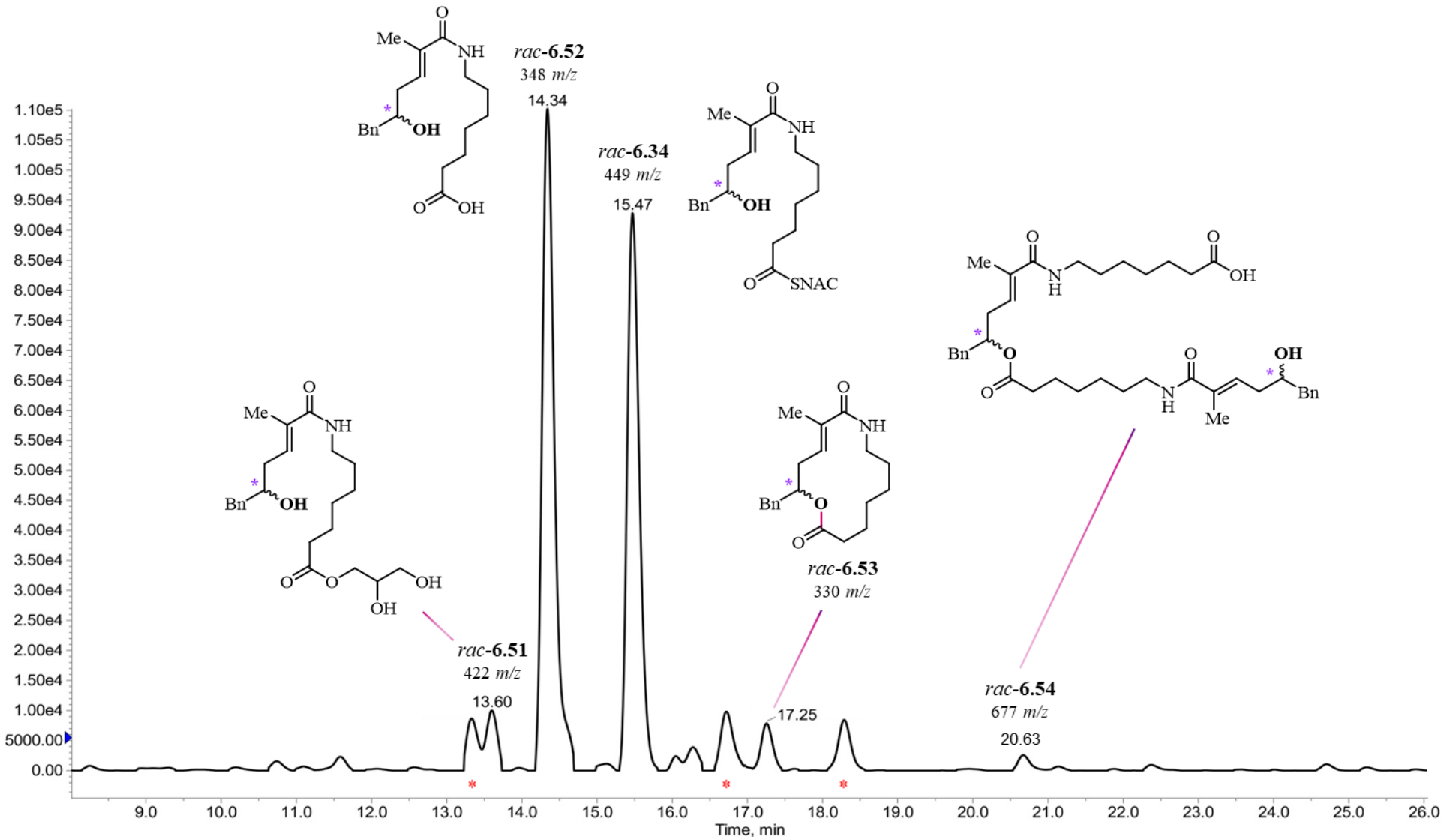

Figure S26 – LCMS analysis (254 nm) for *in vitro* enzymatic assay of racemic methyl-derivative NAC-thioester **6.34** with wild-type DEBS TE.

S1.4.4 Preliminary Development of Linear Analogues for In Vitro Generation of 12-Membered Rings

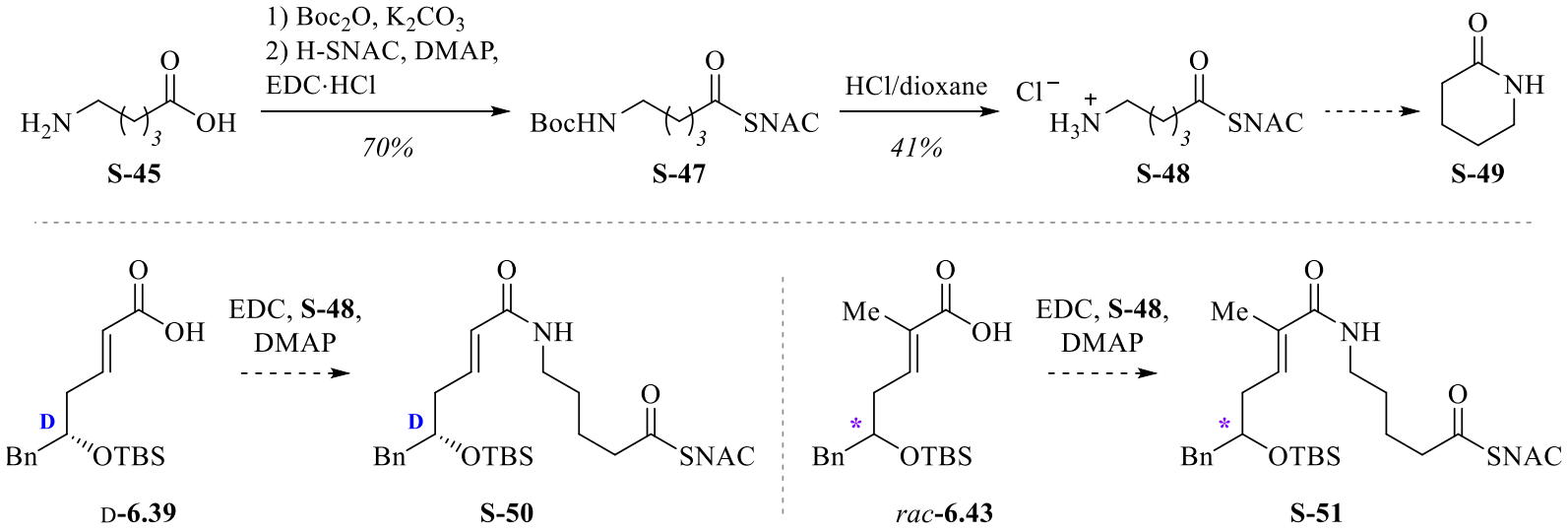

Figure S27 – Preliminary investigation of contracted 12-membered NAC-thioester precursors *via* preparation of truncated amine **S-48**.

5-*tert*-Butyloxycarbonylamino pentanoic acid (**S-46**)

^{1}H NMR (400 MHz, $CDCl_3$)

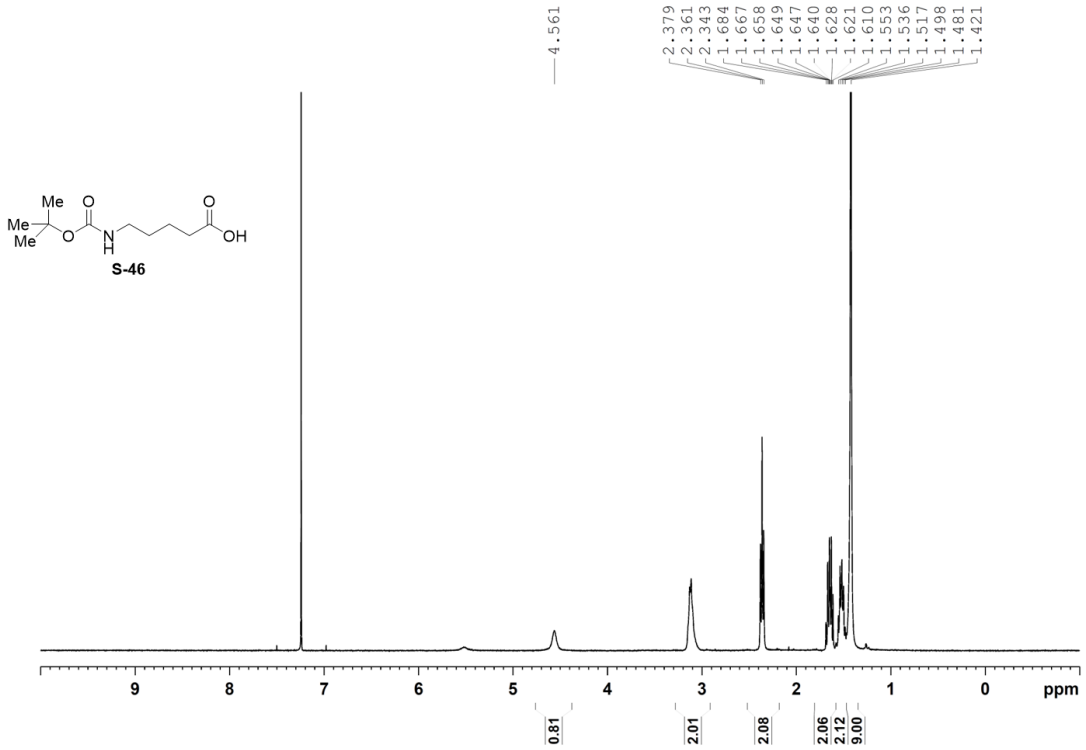

5-*tert*-Butyloxycarbonylamino pentanoic acid (**S-46**)

^{13}C NMR (100 MHz, $CDCl_3$)

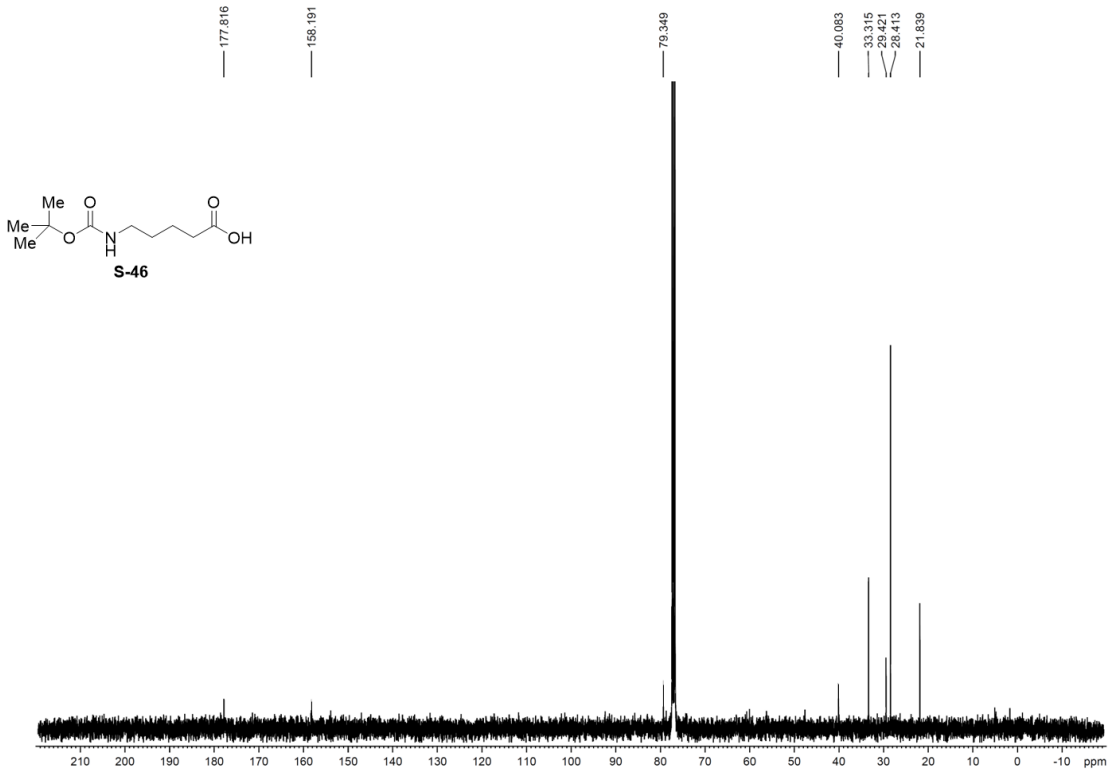

1-(2-Acetamidoethylthio)-5-(*tert*-butyloxycarbonylamino)-pentanethioate (*3 × HSNAC contamination*) (**S-47**)

^{1}H NMR (400 MHz, $CDCl_3$)

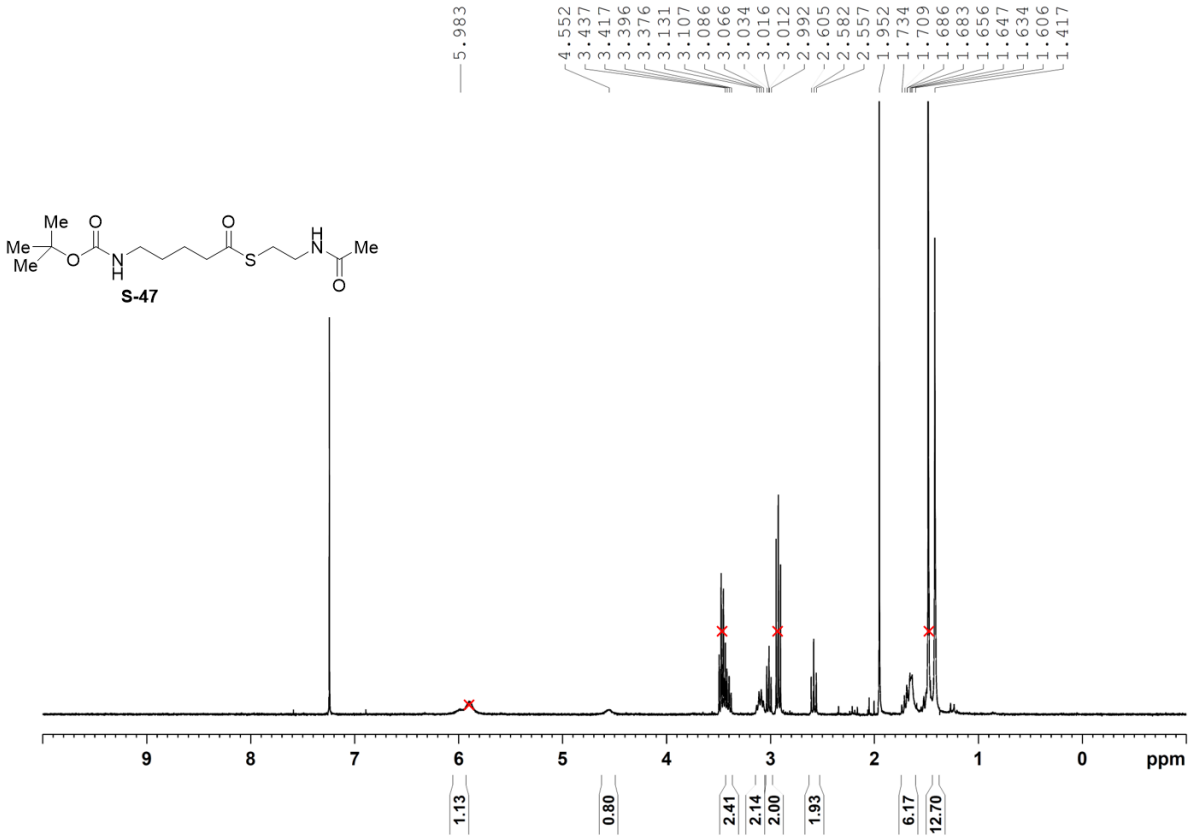

7-(2-Acetamidoethylthio)-7-oxoheptan-1-ammonium chloride (**S-48**)

^{1}H NMR (400 MHz, D_2O)

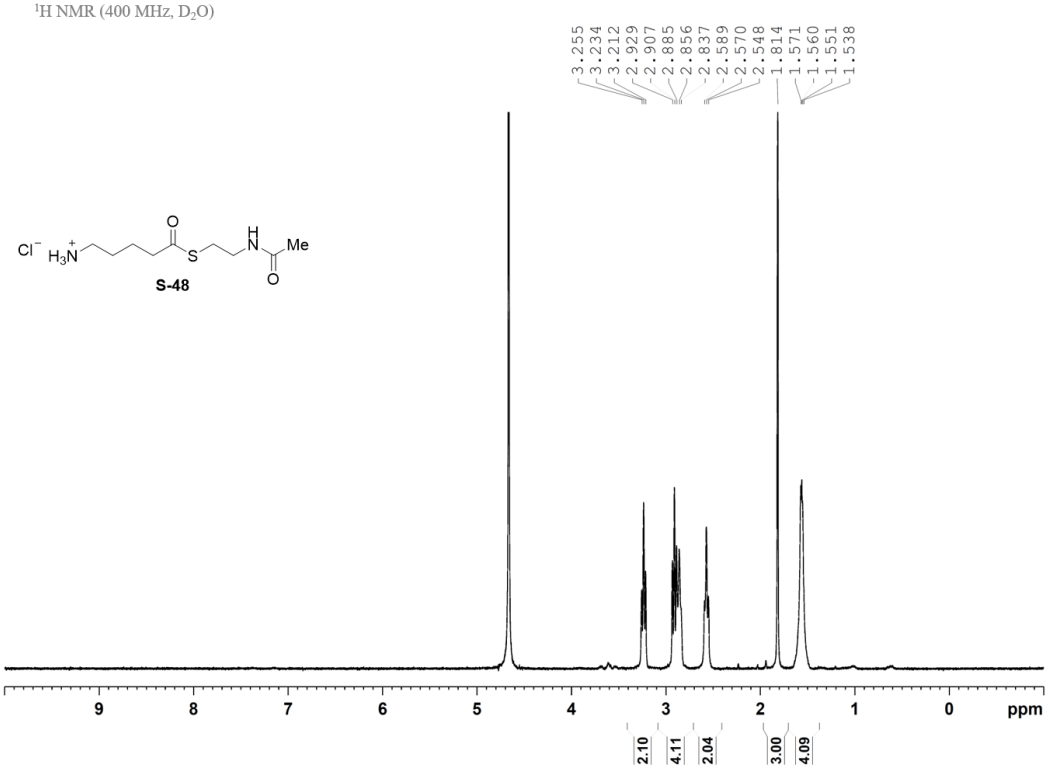

7-(2-Acetamidoethylthio)-7-oxoheptan-1-ammonium chloride (**S-48**)

^{13}C NMR (100 MHz, **$CDCl_3$**)

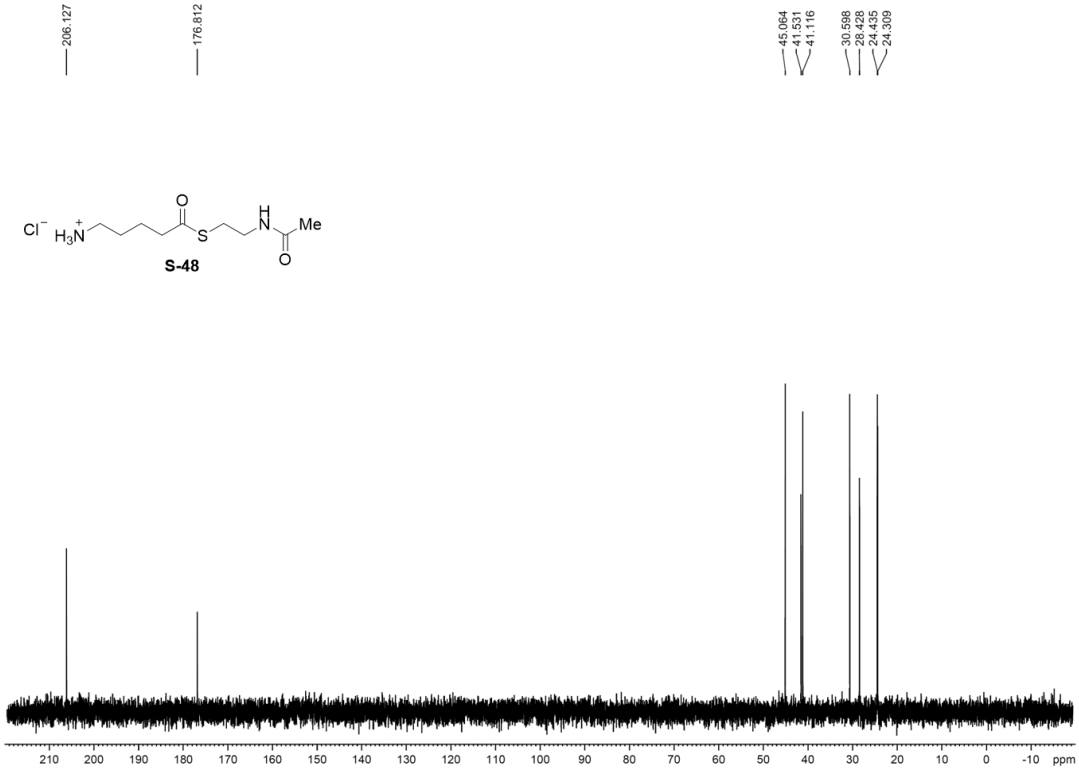

D-(*E*)-*S*-2-Acetamidoethyl-5-(3-(TBS)-6-phenylhex-2-enamido)-pentanethioate, *crude* (**S-50**)

^{1}H NMR (400 MHz, $CDCl_3$)

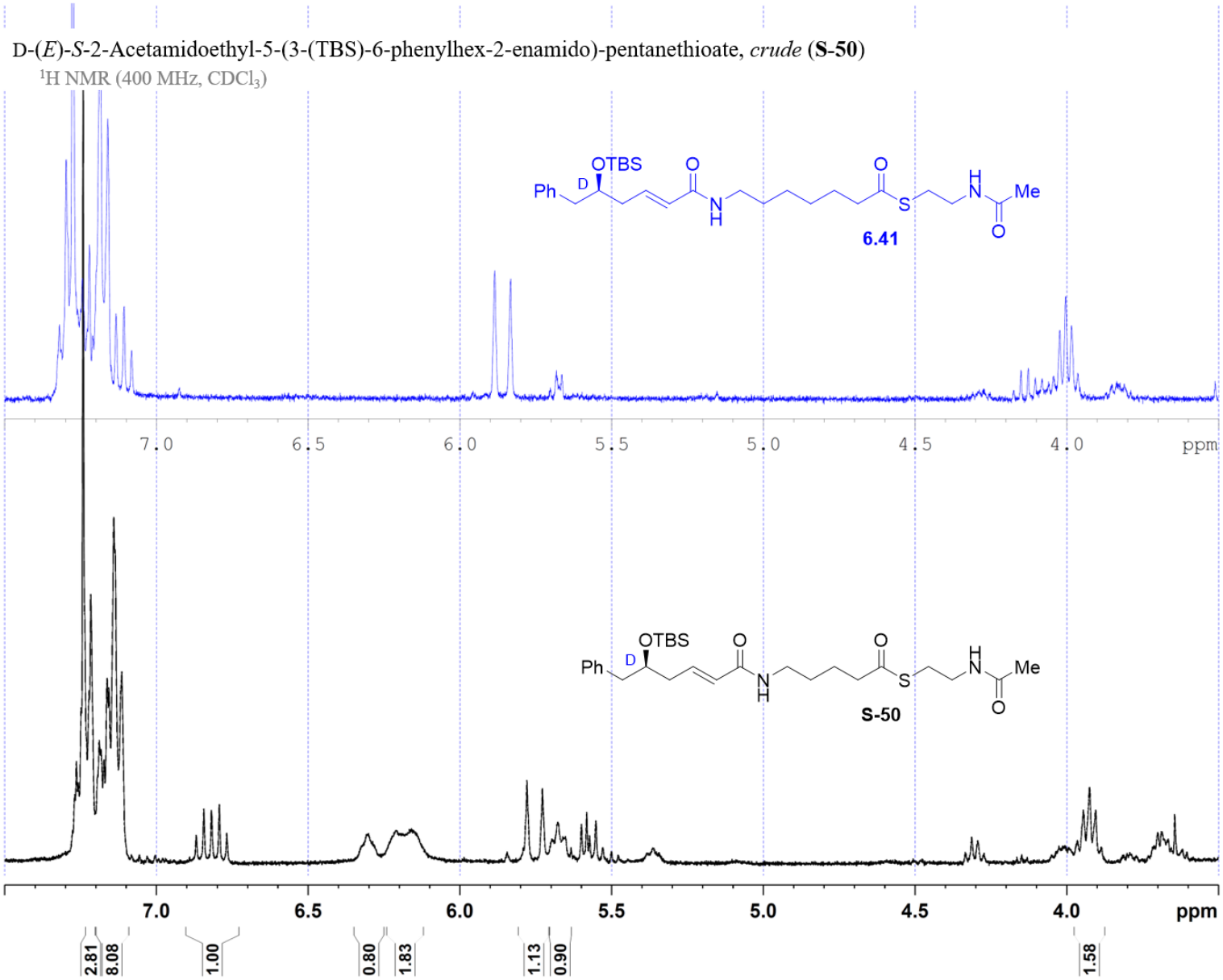

D-(*E*)-*S*-2-Acetamidoethyl-5-(3-(TBS)-6-phenylhex-2-enamido)-pentanethioate, *crude* (**S-50**)

^{1}H NMR (400 MHz, $CDCl_3$)

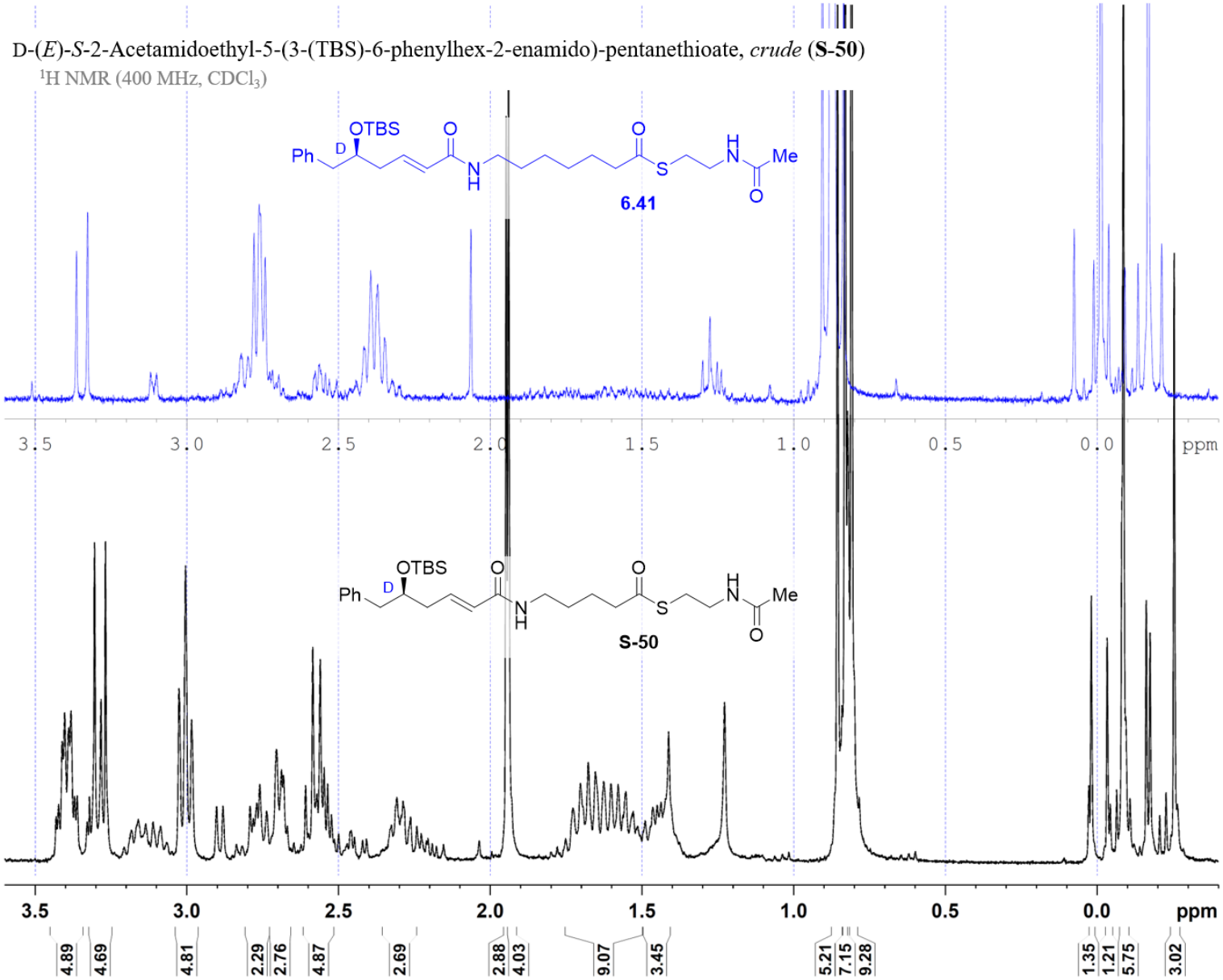

(*E*)-*S*-2-Acetamidoethyl-5-(3-(TBS)-2-methyl-6-phenylhex-2-enamido)-pentanethioate, *crude* (**S-51**)

^{1}H NMR (400 MHz, $CDCl_3$)

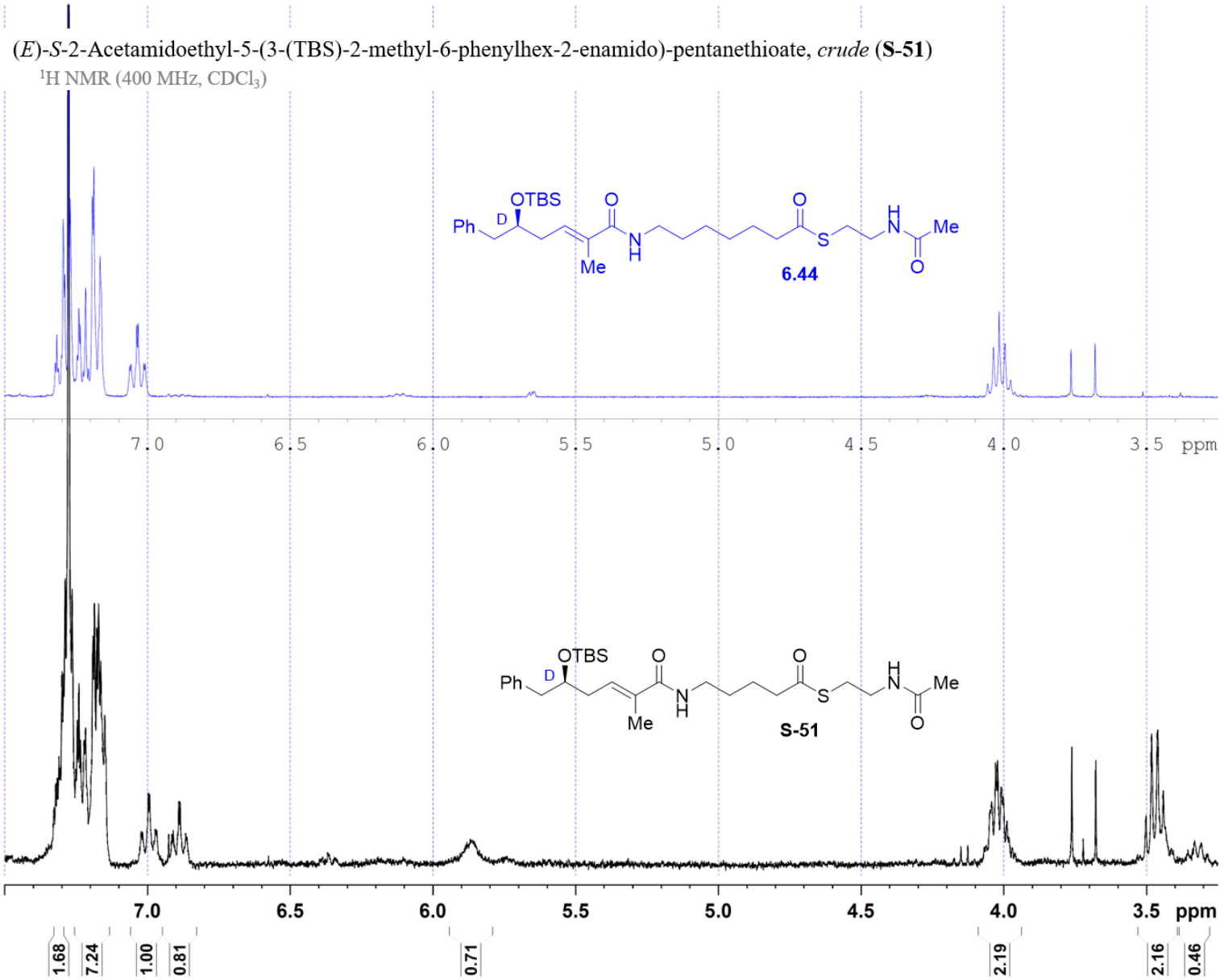

(*E*)-*S*-2-Acetamidoethyl-5-(3-(TBS)-2-methyl-6-phenylhex-2-enamido)-pentanethioate, *crude* (**S-51**)

^{1}H NMR (400 MHz, $CDCl_3$)

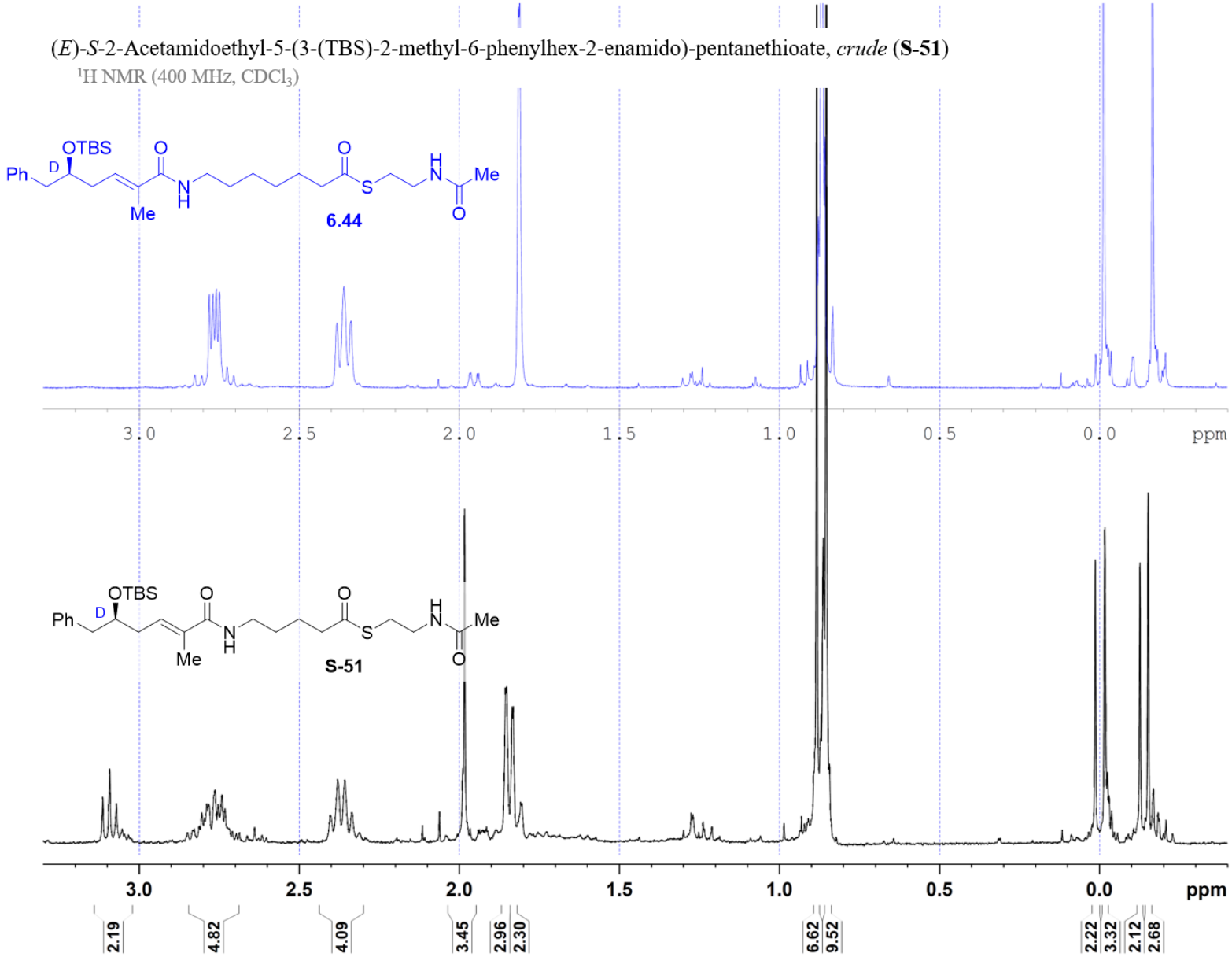

· Appendix II ·

Supplemental Information

S2.1 *cis*-Tetrahydropyran Assembly Strategies in Neopeltolide Synthesis (Chapter 2)

Table S1 – Summary of strategies used for the synthesis of neopeltolide (2007-2016).

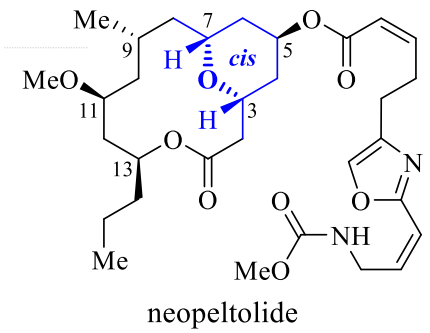

neopeltolide

Legend

AGh	A. Ghosh (*2013*)[1]	Mai	Maier (*2008*)[2,3]
Dai[a]	Dai (*2014*)[4]	Pat	Paterson (*2008*)[5]
Flo	Floreancig (*2009*)[6,7]	Pnk	Panek (*2007*)[8]
Fu1	Fuwa (*2008*)[9]	Rag	Raghavan (*2012*)[10]
Fu2	Fuwa (*2010*)[11]	Rou	Roulland (*2009*)[12]
Fu3	Fuwa (*2013*)[13]	Sht	Scheidt (*2008*)[14]
Hong	Hong (*2009*)[15]	SGh	S. Ghosh (*2012*)[16]
Hov	Hoveyda (*2014*)[17]	Shm	Sharma (*2012*)[18]
Jen[b]	Jennings (*2010*)[19]	She	She (*2011*)[20]
Koz	Kozmin (*2008*)[21]	Tay	Taylor (*2008*)[22]
Lee	Lee (*2008*)[23]	Ydv	Yadav (*2010*)[24]

C9 (*R*)-Methyl Installation

Asymmetric Reduction
Mai, Lee, Pat, Rag, Rou, SGh, Shm, Sht

Substrate-Controlled Hydrogenation
Flo, Fu2, Fu3, Hov, Jen[b], Koz, She

Pre-configured Chiral Pool
Fu1, Hong, Ydv

Enzymatic Desymmetrization
AGh (lipase), Pnk (esterase), Tay (esterase)

C11 (*S*)-Alcohol Installation

Evans-Tishchenko Reaction
Flo, Hong, Hov, Pnk, Rag, Rou, Sht, She, Tay

Asymmetric Allylation
AGh, Dai[a], Fu1, Fu2, Fu3, Jen[b], Lee, Mai, Pat

Epoxide-Opening
SGh, Shm

Oxonium-Ion Cyclization
Ydv

Asymmetric aldol / Mitsunobu
Koz

C13 (*S*)-Alcohol Installation

Asymmetric Reduction
Dai[a], Fu2, Hov, Koz, Mai, Pat, Rou, Sht, She, Shm

Asymmetric Allylation
AGh, Fu1, Jen[b], Lee, Rag

Pre-configured Chiral Pool
Fu3, Hong

Epoxide-Opening
Flo, Pnk, SGh, Tay

Oxonium-Ion Cyclization
Ydv

2,6-*cis*-Tetrahydropyran Assembly

Oxonium-Ion Cyclization
Flo, Jen, Koz, Lee, Mai, Pnk, Sht, Ydv

Oxa-Conjugate Addition
Fu2/3, Hong, Rou, SGh

Transition-Metal-Catalysis
Dai (Pd), Hov (Mo), Shm (Hg), She (Pd)

Asymmetric Hetero Diels-Alder
AGh, Pat, Rag

Radical Cyclization
Tay

Ring-Closing Metathesis
Fu1

Macrocyclization

Yamaguchi Esterification
AGh, Flo, Fu1, Hong, Jen, Koz, Mai, Pat, Pnk, Rag, Rou, SGh, Tay

Ring-Closing Metathesis
Fu2/3, Hov, She, Shm

Oxonium-Ion Cyclization
Lee, Sht, Ydv

Pd$^{(II)}$-Alkoxycarbonylative Cascade
Dai

Oxazole Side-Chain Installation

Mitsunobu Reaction
AGh, Dai, Flo, Fu1, Fu3, Hov, Koz, Lee, Mai, Pat, Rou, Sht

Still-Gennari Olefinination
Pnk

[a] – the Dai synthesis was of 9-*des*-methylneopeltolide analog; C7-C16 development followed procedures previously-reported by Fuwa.[25]
[b] – the Jennings synthesis was of enantiomeric (–)-neopeltolide; thus, 9*S*, 11*R*, and 13*R* stereocenters.

S2.2 A Transannular Oxa-Conjugate Addition Model of Neopeltolide (Chapter 3)

S2.2.1 Development of C1-C6 Fragment

Preparation of our C1-C6 coupling fragment proved to be a difficult task. Multiple variations of synthetic routes and structures were envisaged during the developmental process.

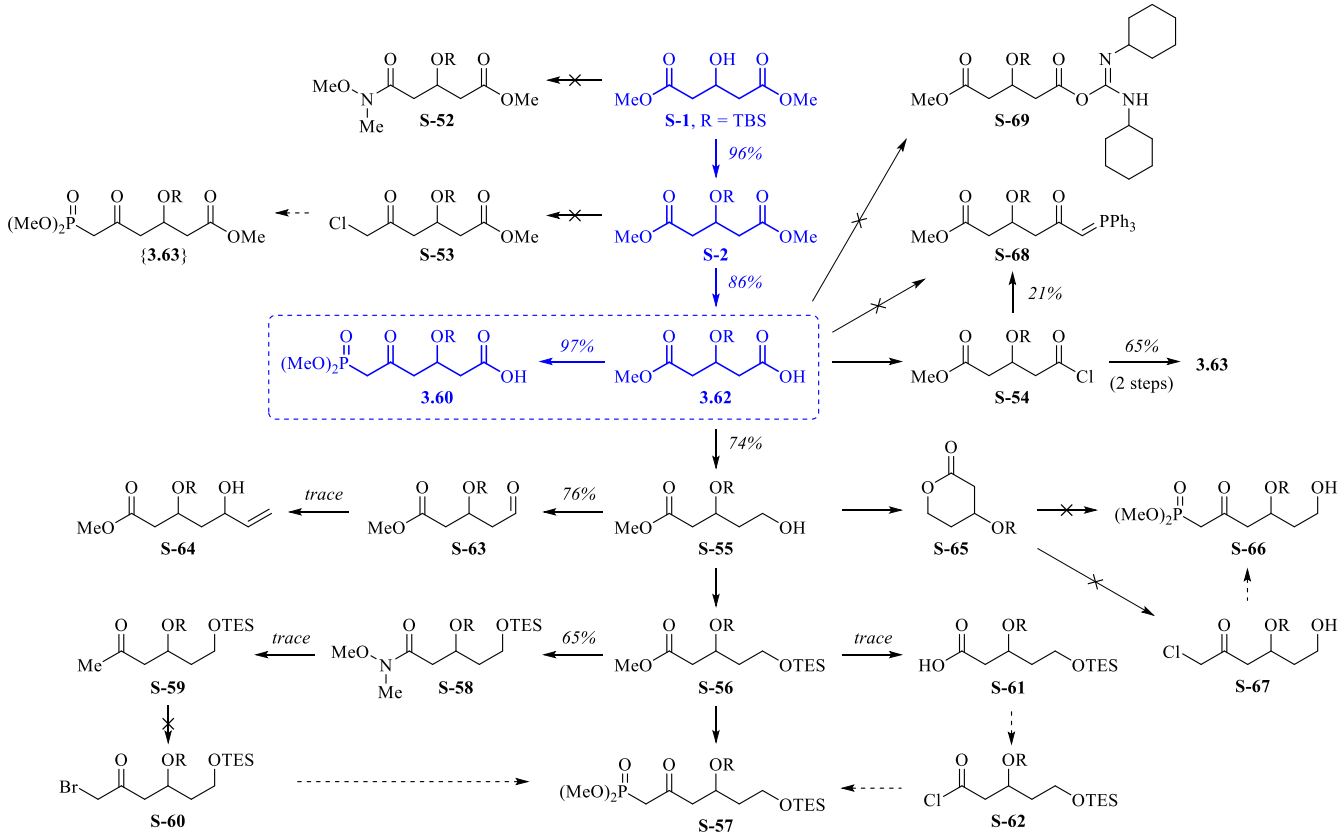

Figure S28 – Summary map of alternative routes and structures for C1-C6 fragment development. Reaction conditions are not included, and transformations may have only been performed as single attempts during this exploratory work.

S2.3.2 Alternative Ester Moieties Fail to Hydrolyze Cleanly (Ketone Model v2)

Preliminary investigations into coupling with bromo-aldehyde **3.59** were performed using methyl-**3.63** and benzyl ester phosphonates **S-3**. Olefination by HWE conditions[26] successfully afforded the complete carbon frameworks, however suffered similar beta-elimination fates during saponification attempts under a variety of standard and exotic conditions (Figure S29).

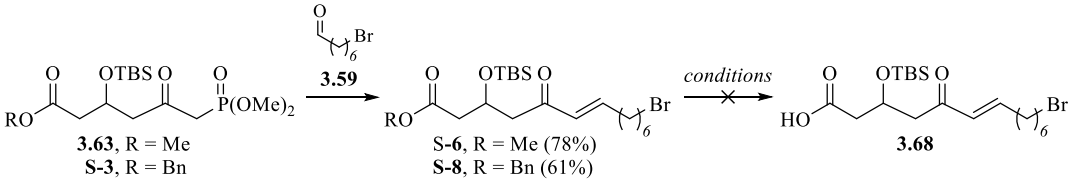

Figure S29 – Introduction of C13 bromide did not affect base-sensitivity, and failed to provide the desired *seco*-acid products under multiple saponification conditions.

To circumvent difficulties associated with *seco*-acid formation by cleavage of our coupled ester products, we explored direct esterification of diprotic phosphonate **3.60** with 7-bromoheptanol **S-4** (Figure S30). This would prove more step-economical, and potentially enhance the reactivity of ring-closing olefination by being intramolecular attack. Unfortunately, limited formation of desired phosphonate **S-70** were observed and proved to be very difficult to isolate.

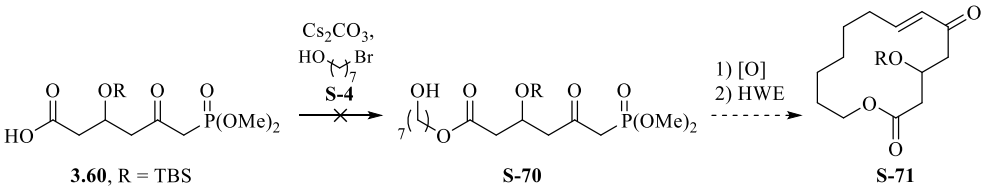

Figure S30 – Direct-esterification of **3.60** using 7-bromoheptanol **S-4** failed under the previously-successful conditions.

S2.3.3 Calculation Protocol & Computational Data to First-Generation Ketone Model

Input atomic coordinates for structures were generated using MOE.[27] A search of each structure's conformational space was performed by NVT molecular dynamics simulation (Nosé-Poincaré-Anderson equations of motion)[28] in a periodic boundary with a 10 Å cube of explicit solvent[29] using the MMFF94 force field.[30] Each molecular-dynamics simulation consisted of an initial 250 picosecond heating of the system and a further 750 picoseconds at constant temperature (300 K). Each molecular-dynamics trajectory was sampled at 1.0 picosecond intervals to generate a total of 1,000 structures. The list of structures was stripped of solvent and ranked per their MMFF94 energy. These lists were parsed to identify unique structures (exceeding 0.2 Å from all other structures) for further calculation. Each unique structure was subjected to a B3LYP/6-31++G** minimization.[31–33] Vibrational frequency calculations were performed on each optimized structure to ensure all structures occupy a local minimum on the potential energy surface. The potential energy, lowest vibrational frequency, and Cartesian coordinates for each optimized structure

are reported in the supplementary information. All calculations were performed in a gas using the Gaussian09 suite[34] as previously reported.[35] The set of unique B3LYP optimized structures generated from each molecular-dynamics trajectory revealed a single minimum energy conformation for all structures.

(*R*)-*β'*-Hydroxy Enone (3*R*)-3.36

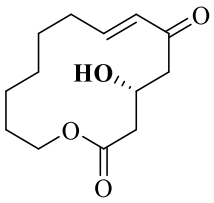

E_{rel} = 9.73 kcal/mol
E_{min} = −808.3686 Ha ν_{min} = 39.3298 cm^{-1} * first-generation computational data (Aug. 2015)

Atom No.	Element	Cartesian Coordinates (Å)			Atom No.	Element	Cartesian Coordinates (Å)		
		X	Y	Z			X	Y	Z
1	C	2.0549	-1.7637	-0.1619	31	H	-2.7592	3.5400	0.2033
2	C	0.7327	-2.5222	-0.1001	32	H	-1.9861	2.5678	1.4589
3	C	-0.4419	-1.6544	0.3740	33	H	-0.7572	3.4950	-1.1988
4	O	-0.3995	-1.4635	1.7942	34	H	-0.3223	3.9983	0.4273
5	O	2.0092	-0.6050	0.5551	35	H	-2.2572	-2.7008	0.8929
6	C	0.3919	2.0168	-0.1134	36	H	-1.8384	-2.8705	-0.8175
7	C	1.8372	2.4955	-0.3237	37	H	-2.2115	0.1811	1.3807
8	C	2.8682	1.3908	-0.6361					
9	C	3.1202	0.3298	0.4384					
10	C	-2.5749	1.4526	-0.2602					
11	C	-2.0562	2.7140	0.3740					
12	C	-0.6605	3.1373	-0.1648					
13	C	-1.8484	-2.1709	0.0228					
14	C	-2.7954	-1.0225	-0.3665					
15	C	-2.5744	0.2607	0.3580					
16	O	3.0268	-2.1271	-0.7870					
17	O	-3.6063	-1.1537	-1.2723					
18	H	0.5636	-2.9087	-1.1105					
19	H	0.8610	-3.3912	0.5572					
20	H	-0.3216	-0.6822	-0.1132					
21	H	0.4176	-0.9824	1.9909					
22	H	0.1490	1.2742	-0.8827					
23	H	0.3157	1.4913	0.8464					
24	H	2.1666	3.0624	0.5591					
25	H	1.8597	3.2061	-1.1613					
26	H	3.8381	1.8708	-0.8241					
27	H	2.6014	0.8801	-1.5704					
28	H	4.0216	-0.2428	0.2117					
29	H	3.2124	0.7761	1.4327					
30	H	-2.8717	1.4972	-1.3090					

(*R*)-*β'*-Hydroxy Enone (3*R*)-3.36

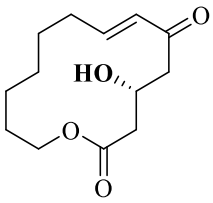

E_{rel} = 16.13 kcal/mol
E_{min} = −808.3682 Ha ν_{min} = 29.82 cm^{-1} * second-generation computational data (Oct. 2016)

Atom No.	Element	Cartesian Coordinates (Å)			Atom No.	Element	Cartesian Coordinates (Å)		
		X	Y	Z			X	Y	Z
1	C	-3.1301	-1.7833	-0.5555	31	H	2.9315	2.0343	0.8232
2	C	-2.2528	-2.9374	-1.0186	32	H	1.9503	1.6563	-0.5862
3	C	-0.7405	-2.7467	-0.8063	33	H	0.4089	2.4559	1.8938
4	O	0.0083	-3.7224	-1.5355	34	H	1.4332	3.7048	1.2267
5	O	-2.4312	-0.6304	-0.4457	35	H	-0.2928	-3.7590	1.0692
6	C	-0.1655	3.1613	-0.0879	36	H	-1.1551	-2.2417	1.2535
7	C	-1.1287	2.0553	-0.5565	37	H	1.0512	-0.6474	-0.6499
8	C	-2.1107	1.5584	0.5149					
9	C	-3.1386	0.5563	0.0041					
10	C	1.6824	0.3506	1.0920					
11	C	1.9301	1.7125	0.5089					
12	C	0.8950	2.7859	0.9672					
13	C	-0.3569	-2.7350	0.6818					
14	C	0.9132	-1.9960	1.1115					
15	C	1.2513	-0.7245	0.4151					
16	O	-4.3176	-1.8772	-0.3240					
17	O	1.5385	-2.3876	2.0882					
18	H	-2.6241	-3.8418	-0.5228					
19	H	-2.4367	-3.0709	-2.0918					
20	H	-0.4685	-1.8010	-1.2737					
21	H	-0.0861	-4.5847	-1.1072					
22	H	0.3588	3.5538	-0.9699					
23	H	-0.7570	3.9998	0.3063					
24	H	-0.5611	1.2058	-0.9509					
25	H	-1.7091	2.4499	-1.4023					
26	H	-2.6706	2.4114	0.9235					
27	H	-1.5713	1.1072	1.3564					
28	H	-3.8479	0.2647	0.7828					
29	H	-3.7076	0.9515	-0.8450					
30	H	1.8308	0.2474	2.1677					

(*S*)-*β'*-Hydroxy Enone (3*S*)-3.36

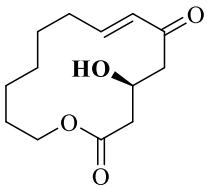

E_{rel} = 7.09 kcal/mol
E_{min} = −808.3728 Ha ν_{min} = 35.1132 cm^{-1} * first-generation computational data (Aug. 2015)

Atom No.	Element	Cartesian Coordinates (Å)			Atom No.	Element	Cartesian Coordinates (Å)		
		X	Y	Z			X	Y	Z
1	C	1.8744	1.7408	0.5022	31	H	-3.8486	-2.3596	-0.7923
2	C	2.8050	0.5830	0.1893	32	H	-3.5514	-1.8546	0.8746
3	C	2.1503	-0.7419	-0.1987	33	H	-2.7024	-0.1746	-1.5545
4	O	3.1555	-1.5404	-0.8144	34	H	-4.2732	-0.0165	-0.7813
5	O	0.6878	1.6677	-0.1509	35	H	1.0217	-0.7919	1.6817
6	C	-2.6444	0.6824	0.4489	36	H	2.3466	-1.9762	1.5638
7	C	-2.6538	2.1601	0.0108	37	H	-1.1252	-1.8562	1.7033
8	C	-1.4582	2.6316	-0.8418					
9	C	-0.1481	2.8584	-0.0802					
10	C	-1.7849	-2.3292	-0.2495					
11	C	-3.1763	-1.7753	-0.1535					
12	C	-3.2253	-0.2852	-0.5949					
13	C	1.5339	-1.4896	1.0123					
14	C	0.5645	-2.5225	0.4556					
15	C	-0.8694	-2.2753	0.7317					
16	O	2.1794	2.6738	1.2178					
17	O	0.9650	-3.3972	-0.3103					
18	H	3.4203	0.9047	-0.6612					
19	H	3.4842	0.4623	1.0378					
20	H	1.3537	-0.5287	-0.9237					
21	H	2.7647	-2.4172	-0.9707					
22	H	-1.6218	0.3864	0.7078					
23	H	-3.2372	0.5813	1.3682					
24	H	-2.7015	2.7983	0.9031					
25	H	-3.5800	2.3599	-0.5449					
26	H	-1.7287	3.5941	-1.2936					
27	H	-1.2700	1.9491	-1.6796					
28	H	0.4277	3.6784	-0.5195					
29	H	-0.3206	3.1050	0.9718					
30	H	-1.4605	-2.6932	-1.2246					

(*S*)-*β'*-Hydroxy Enone (3*S*)-3.36

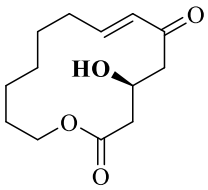

E_{rel} = 12.05 kcal/mol
E_{min} = −808.3747 Ha ν_{min} = 29.07 cm^{-1} * second-generation computational data (Oct. 2016)

Atom No.	Element	Cartesian Coordinates (Å)			Atom No.	Element	Cartesian Coordinates (Å)		
		X	Y	Z			X	Y	Z
1	C	-2.8860	0.1079	0.0152	31	H	3.7264	-0.1332	-0.6341
2	C	-3.0981	-1.2612	-0.6032	32	H	3.2413	1.0837	-1.8192
3	C	-1.8329	-2.1430	-0.6110	33	H	2.0125	0.8931	0.9771
4	O	-2.2763	-3.4925	-0.6457	34	H	3.4064	1.8921	0.6245
5	O	-1.9693	0.8401	-0.6681	35	H	-0.8132	-0.7753	-1.9576
6	C	1.5705	2.6346	-0.2639	36	H	-1.3303	-2.3010	-2.6982
7	C	0.5629	3.0787	0.8154	37	H	2.5418	-2.2782	-1.0019
8	C	-0.6144	2.0997	1.0032					
9	C	-1.6391	2.1559	-0.1461					
10	C	1.7260	-0.3522	-1.3563					
11	C	2.8922	0.5001	-0.9546					
12	C	2.4934	1.4763	0.1823					
13	C	-0.8882	-1.8494	-1.8025					
14	C	0.4584	-2.5054	-1.5415					
15	C	1.6706	-1.6956	-1.2964					
16	O	-3.4523	0.5175	1.0075					
17	O	0.5127	-3.7338	-1.4342					
18	H	-3.8574	-1.7677	-0.0052					
19	H	-3.4812	-1.1498	-1.6245					
20	H	-1.2853	-1.9628	0.3293					
21	H	-1.4968	-4.0471	-0.8260					
22	H	1.0166	2.3503	-1.1683					
23	H	2.1900	3.4893	-0.5615					
24	H	0.1690	4.0727	0.5640					
25	H	1.0877	3.1980	1.7720					
26	H	-1.1223	2.2976	1.9518					
27	H	-0.2316	1.0749	1.0735					
28	H	-2.5638	2.6469	0.1647					
29	H	-1.2357	2.6773	-1.0172					
30	H	0.8368	0.1924	-1.6641					

***trans*-Tetrahydropyran-5-one (3.73)**

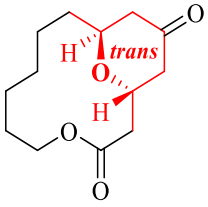

E_{rel} = 1.32 kcal/mol

E_{min} = −808.3820 Ha ν_{min} = 37.9243 cm^{-1} * first-generation computational data (Aug. 2015)

Atom No.	Element	Cartesian Coordinates (Å)			Atom No.	Element	Cartesian Coordinates (Å)		
		X	Y	Z			X	Y	Z
1	C	-1.3475	-1.7547	0.1271	31	H	-3.9762	-0.8306	-1.4912
2	C	0.0498	-2.0682	-0.3823	32	H	0.8235	2.0794	1.5355
3	C	1.1068	-1.0590	0.0898	33	H	1.5108	3.2832	0.4560
4	O	0.8605	0.1550	-0.6211	34	H	-0.7810	3.6959	0.0877
5	O	-2.1288	-1.2270	-0.8324	35	H	-0.5046	2.4984	-1.1685
6	C	-1.5630	1.7238	0.5577	36	H	2.5948	-1.9403	-1.2308
7	C	-2.8892	1.5881	-0.2060	37	H	2.8313	-2.3544	0.4673
8	C	-3.7142	0.3795	0.2916					
9	C	-3.5124	-0.9138	-0.5054					
10	C	1.6821	1.2991	-0.3026					
11	C	0.9003	2.3707	0.4784					
12	C	-0.5121	2.6454	-0.0805					
13	C	2.5312	-1.5443	-0.2097					
14	C	3.5519	-0.4177	-0.0919					
15	C	2.9930	0.9014	0.4083					
16	O	-1.7132	-1.9603	1.2694					
17	O	4.7268	-0.5799	-0.3669					
18	H	1.9356	1.7177	-1.2852					
19	H	2.8011	0.7767	1.4848					
20	H	3.7496	1.6820	0.2986					
21	H	0.3140	-3.0552	0.0103					
22	H	0.0587	-2.1004	-1.4747					
23	H	0.9823	-0.9023	1.1728					
24	H	-1.7715	2.0665	1.5815					
25	H	-1.1202	0.7334	0.6596					
26	H	-2.6845	1.4773	-1.2791					
27	H	-3.4760	2.5090	-0.0981					
28	H	-4.7890	0.5944	0.2266					
29	H	-3.4989	0.1950	1.3494					
30	H	-3.9436	-1.7663	0.0271					

***trans*-Tetrahydropyran-5-one (*ent*-3.73)**

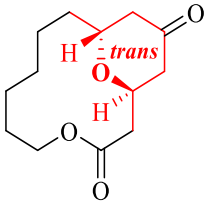

E_{rel} = 6.21 kcal/mol

E_{min} = −808.3840 Ha ν_{min} = 44.04 cm^{-1} * second-generation computational data (Oct. 2016)

Atom No.	Element	Cartesian Coordinates (Å)			Atom No.	Element	Cartesian Coordinates (Å)		
		X	Y	Z			X	Y	Z
1	C	0.7445	-1.8977	-0.2983	31	H	3.4167	-1.4817	1.4486
2	C	-0.7048	-1.9967	0.1351	32	H	-0.5702	2.8774	1.0846
3	C	-1.5439	-0.8182	-0.4018	33	H	-0.8543	2.3403	2.7349
4	O	-0.9770	0.4330	0.0004	34	H	1.4707	2.1067	2.6895
5	O	1.5392	-1.5031	0.7184	35	H	1.0331	0.5041	2.1153
6	C	1.7980	1.8315	0.5765	36	H	-3.1081	-1.5010	0.9612
7	C	3.2220	1.2266	0.5563	37	H	-3.6077	-1.5005	-0.7331
8	C	3.3913	-0.0938	-0.2244					
9	C	2.9653	-1.3923	0.4566					
10	C	-1.4326	0.9143	1.2729					
11	C	-0.4845	2.0114	1.7550					
12	C	0.9913	1.5693	1.8607					
13	C	-3.0321	-0.9478	0.0128					
14	C	-3.6948	0.4000	0.2615					
15	C	-2.8849	1.3802	1.1024					
16	O	1.1407	-2.1410	-1.4212					
17	O	-4.8077	0.6660	-0.1532					
18	H	-1.3907	0.0898	2.0035					
19	H	-2.9224	2.3542	0.6008					
20	H	-3.3895	1.4994	2.0707					
21	H	-1.1115	-2.9286	-0.2722					
22	H	-0.7656	-2.0379	1.2263					
23	H	-1.4720	-0.8091	-1.4934					
24	H	1.8723	2.9198	0.4481					
25	H	1.2316	1.4635	-0.2845					
26	H	3.5941	1.0989	1.5838					
27	H	3.8979	1.9521	0.0878					
28	H	4.4607	-0.2307	-0.4393					
29	H	2.8949	-0.0201	-1.1985					
30	H	3.2621	-2.2485	-0.1551					

cis-Tetrahydropyran-5-one (3.74)

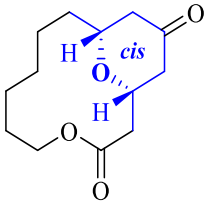

E_{rel} = 0 kcal/mol

E_{min} = −808.3841 Ha ν_{min} = 48.5413 cm^{-1} * first-generation computational data (Aug. 2015)

Atom No.	Element	Cartesian Coordinates (Å)			Atom No.	Element	Cartesian Coordinates (Å)		
		X	Y	Z			X	Y	Z
1	C	-1.3252	-1.8769	-0.0175	31	H	-3.9161	-0.5047	-1.3958
2	C	0.0750	-2.1325	-0.5687	32	H	1.5450	3.3361	-0.1131
3	C	1.0998	-1.1549	0.0303	33	H	0.9035	2.4506	-1.4947
4	O	0.8328	0.1199	-0.5371	34	H	-0.5281	3.1527	1.1287
5	O	-2.0986	-1.1804	-0.8711	35	H	-0.9614	3.6204	-0.5095
6	C	-1.4532	1.5542	-0.0054	36	H	2.6978	-1.6625	-1.3278
7	C	-2.9545	1.6775	0.2720	37	H	2.8878	-2.4247	0.2691
8	C	-3.5599	0.2953	0.6031					
9	C	-3.4502	-0.8118	-0.4558					
10	C	1.4996	1.1985	0.1245					
11	C	0.8881	2.5049	-0.3981					
12	C	-0.5562	2.7940	0.0899					
13	C	2.5715	-1.5131	-0.2459					
14	C	3.4931	-0.3698	0.1797					
15	C	3.0125	1.0467	-0.1276					
16	O	-1.6879	-2.2479	1.0831					
17	O	4.5592	-0.5811	0.7307					
18	H	1.3114	1.1174	1.2096					
19	H	3.6079	1.7498	0.4618					
20	H	3.2049	1.2418	-1.1926					
21	H	0.3487	-3.1534	-0.2859					
22	H	0.0864	-2.0415	-1.6581					
23	H	0.9417	-1.1128	1.1207					
24	H	-1.0607	0.8203	0.7039					
25	H	-1.3185	1.1014	-0.9886					
26	H	-3.4725	2.1304	-0.5852					
27	H	-3.1419	2.3371	1.1308					
28	H	-4.6378	0.4033	0.7888					
29	H	-3.1236	-0.0740	1.5372					
30	H	-3.9449	-1.7154	-0.0881					

cis-Tetrahydropyran-5-one (3.74)

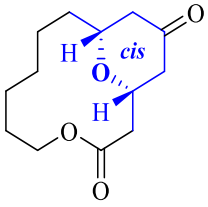

E_{rel} = 0 kcal/mol

E_{min} = −808.3939 Ha ν_{min} = 44.87 cm^{-1} * second-generation computational data (Oct. 2016)

Atom No.	Element	Cartesian Coordinates (Å)			Atom No.	Element	Cartesian Coordinates (Å)		
		X	Y	Z			X	Y	Z
1	C	0.8641	-1.9720	-1.1765	31	H	3.2927	-0.6251	0.4372
2	C	-0.3296	-2.7974	-0.7258	32	H	-2.9739	2.1692	-0.1154
3	C	-1.6185	-2.0210	-1.0164	33	H	-2.3633	1.2700	1.2691
4	O	-1.5341	-0.8213	-0.2543	34	H	-0.5356	1.7026	-1.1276
5	O	1.5407	-1.4443	-0.1383	35	H	-0.8019	3.0453	-0.0334
6	C	0.2659	1.4044	0.8777	36	H	-2.8314	-3.1243	0.3873
7	C	1.7151	1.6973	0.4456	37	H	-3.0654	-3.6519	-1.2972
8	C	2.2511	0.8774	-0.7459					
9	C	2.6594	-0.5676	-0.4522					
10	C	-2.5596	0.1271	-0.5482					
11	C	-2.2278	1.4251	0.1901					
12	C	-0.8019	1.9489	-0.0914					
13	C	-2.9071	-2.7815	-0.6543					
14	C	-4.1176	-1.8614	-0.7621					
15	C	-3.9328	-0.4695	-0.1752					
16	O	1.1514	-1.7890	-2.3442					
17	O	-5.1598	-2.2188	-1.2825					
18	H	-2.5421	0.3266	-1.6340					
19	H	-4.7587	0.1664	-0.5061					
20	H	-3.9822	-0.5584	0.9196					
21	H	-0.3316	-3.7315	-1.2953					
22	H	-0.2645	-3.0202	0.3423					
23	H	-1.6377	-1.7668	-2.0885					
24	H	0.1308	0.3286	1.0050					
25	H	0.0970	1.8619	1.8626					
26	H	2.3830	1.5394	1.3041					
27	H	1.8011	2.7637	0.1934					
28	H	3.1621	1.3651	-1.1198					
29	H	1.5460	0.8838	-1.5840					
30	H	3.1920	-0.9909	-1.3073					

S2.3 Synthesis of Neopeltolide by Transannular Oxa-Conjugate Addition (Chapter 4)

S2.3.1 Screening Conditions for HWE Coupling of Diprotic Phosphonate (§ 4.4.5)

Olefination reactions of aldehydes with phosphoranes (Wittig), or phosphonates (HWE) have produced a versatile range of products within synthetic chemistry. Classical conditions for these transformations utilize anhydrous organic solvents and inert atmospheres, however there has been extensive research into utilizing phase-transfer (PT) systems. The success of HWE coupling can be variable under PT conditions,[36] and is heavily influenced by factors such as the solvent, base, temperature, catalyst, carbanion (phosphonate) and carbonyl (aldehyde) compounds.[37] To identify optimal reaction conditions for our system, and to prevent additional loss of advanced material, we performed a thorough screen of these factors. Commercially-available octanal **4.57** was used with diprotic phosphonate **4.26** as our model system (Figure S31). In addition to the formation of desired *α*,*β*-unsaturated ketone **4.58**, literature precedence suggests the potential of common side-reactions under alkaline conditions. These potential reactions are summarized below, and include Cannizzaro-type disproportiation products **S-72** and **S-73**, aldolization **4.60** and subsequent dehydration **4.61** products, *β*,*γ*-unsaturated ketone **4.62**, or *β*-elim.by-products **4.63** (Figure S31).

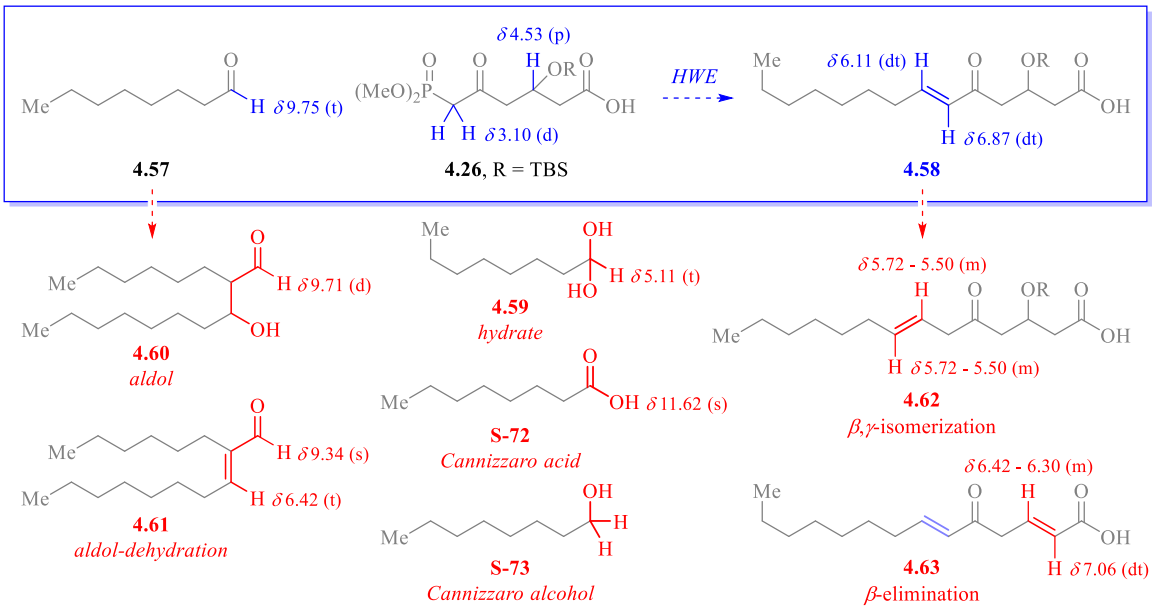

Figure S31 – Summary of the desired HWE coupling product (**blue**), and potential products of common undesired side-reactions in alkaline conditions (**red**).

The screening process for the HWE coupling of diprotic phosphonate **4.26** is detailed in the following section. Results have been tabulated and presented in a qualitative manner, where the potential formation of side-products is referenced. Herein summarizes those efforts.

Negative controls demonstrated barium hydroxide and cesium carbonate in polar solvents (DMF and *i*PrOH) facilitated formation of aldol and aldol-dehydration by-products, and this undesired by-product formation was suppressed with anhydrous THF and MeCN. In liquid-solid (LS) PT-HWE systems, THF is the most commonly used solvent,[36–41] but often is hydrated. Based on this observation, we explored these bases with hydrated forms of THF and MeCN (Table S2). Generally, the hydrated form benefits the low-solubility of bases like cesium carbonate and barium hydroxide by acting like a PT catalyst such as crown ethers. Aqueous media disrupts the reticular energies (lattice formation) of the bases and improves access to the basic sites, thus increasing the capability of the carbonate or hydroxide anions for the requisite deprotonation of phosphonate.[42] Likewise, in LS-PT the addition of water creates a thin film on the surface of the solid base, improving the dissociation and mass transport of organic anions. Conversely, addition of water is distributed to the organic phase, which can increase formation of hydrated or disproportiation side-products such as **S-72** and **S-73** (Figure S31). In this model system, addition of water negatively-affected results by facilitating undesired formation of elimination products. Though these products were not isolated and characterized, they were not consistent with *β*-elim.of the coupled product. It is believed that the hydrated solvent increased the basicity of solution and effectively eliminated the C3-TBS alcohol of **4.26**. Entries 14 and 17 indicated that heating the aqueous solution promoted formation of aldol-dehydration by-product. Anhydrous conditions suppressed side-reactions and generated trace amounts of desired **4.58**. Based on these results, use of anhydrous solvent was carried forward in the screening process.

Table S2 – Aqueous conditions increase basicity of the system and facilitated the formation of elimination by-products. Elevated temperatures promote aldol-dehydration side-reactions under aqueous conditions.

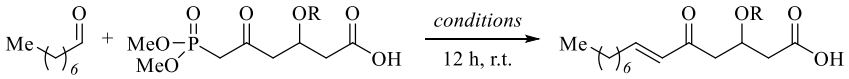

4.57 **4.26**, R = TBS **4.58**

Entry[a]	Solvent		Base	Yield[b]	Notes
9	THF	anhyd.	$Ba(OH)_2{\cdot}8H_2O$	n.r.	Trace formation of **4.58** and side-products
10	MeCN	anhyd.	$Ba(OH)_2{\cdot}8H_2O$	n.r.	Trace formation of **4.58** and side-products
11	THF	anhyd.	Cs_2CO_3	n.r.	Trace formation of **4.58** and side-products
12	MeCN	anhyd.	Cs_2CO_3	n.r.	Trace formation of **4.58** and side-products
13	$THF_{aq.}$	20:1	$Ba(OH)_2{\cdot}8H_2O$	–	*β*-elim.> **4.57** > hydrate > aldol
14[c]	$THF_{aq.}$	20:1	$Ba(OH)_2{\cdot}8H_2O$	–	*β*-elim.>> **4.57** ≥ aldol-dehydration >>> aldol
15	$THF_{aq.}$	20:1	Cs_2CO_3	–	*β*-elim.> **4.57** > hydrate > aldol / aldol-dehydration
16	$THF_{aq.}$	30:1	$Ba(OH)_2{\cdot}8H_2O$	–	*β*-elim.> **4.57** > aldol-dehydration > aldol
17[c]	$THF_{aq.}$	30:1	$Ba(OH)_2{\cdot}8H_2O$	–	aldol-dehydration > *β*-elim.>> **4.57** > aldol
18	$THF_{aq.}$	30:1	Cs_2CO_3	–	*β*-elim.> **4.57** > aldol-dehydration ≥ aldol
19	$THF_{aq.}$	40:1	$Ba(OH)_2{\cdot}8H_2O$	–	**4.57** > *β*-elim.>> aldol-dehydration >> aldol
20	$THF_{aq.}$	40:1	Cs_2CO_3	–	**4.57** > *β*-elim.> aldol

[a] – Conditions: base (1.9 equiv.) was added to phosphonate **4.26** (1.3 equiv.) in solvent (0.1 M) under argon, and incubated for 30 min at ambient temperature (22 ºC). Aldehyde (1.0 equiv.) added neat, and stirred for 12 h at 22 ºC.
[b] – Yield is presented as qualitative observation based on TLC and crude ^{1}HNMR analysis, indicating relative formation of product (+), no reaction (n.r.), or the erosion (–) of starting material(s).
[c] – Reactions were performed at 45 ºC.

Deprotonation of the weakly-acidic α-methylene could be better achieved with stronger bases, but the proven base-sensitivity of desired coupled product impeded our options (Table S3). With weakly-acidic systems, hydroxide bases have been reported as optimal choices for PT-HWE coupling. Activated forms of barium hydroxide are generated by heating commercial hydrate to temperatures indicated in the name (for example, C-200 was heated at 200 ºC), and are more active. Using C-100 and C-200 base catalysts, formation of desired coupling product was achieved. The increased basicity of these reagents promoted formation of β,γ-unsaturated ketone isomer. Likewise, microcrystallization of the base catalysts increased basicity and promoted formation of side-products (entry 21 v 22). Based on these results, activated C-200 was carried forward for additional screening.

Table S3 – Activated barium hydroxide facilitates the desired olefination reaction, and the microcrystalline surface of its powdered form improves the activity.

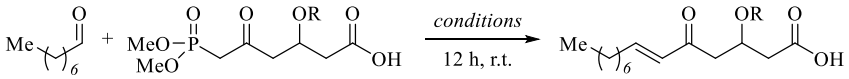

4.57 **4.26**, R = TBS **4.58**

Entry[a]	Solvent	Base		Yield[b]	Notes
21	THF	$Ba(OH)_2 \cdot 8H_2O$	whole	n.r.	Trace formation of **4.58** and side-products
22	THF	$Ba(OH)_2 \cdot 8H_2O$	powdered	–	**4.57** > aldol-dehydration > aldol > β-elim.= β,γ
23	THF	C-100	powdered	+	**4.58** ≥ **4.57** > aldol = aldol-dehydration > β,γ
24	THF	C-200	powdered	+	**4.58** >> **4.57** = β,γ > aldol > β-elimination

[a] – Conditions: base (1.9 equiv.) was added to phosphonate **4.26** (1.3 equiv.) in solvent (0.1 M) under argon, and incubated for 30 min at ambient temperature (22 ºC). Aldehyde (1.0 equiv.) added neat, and stirred for 12 h at 22 ºC.
[b] – Yield is presented as qualitative observation based on TLC and crude ^{1}HNMR analysis, indicating relative formation of product (+), no reaction (n.r.), or the erosion (–) of starting material(s).

Based on the positive results obtained with modification of reaction temperature with our first-generation model, the effect of kinetic and thermodynamic conditions was evaluated using C-200 as a base (Table S4). As expected, sub-zero temperatures effectively-suppressed reactivity within our system. Surprisingly, formation of **4.58** as the major product was achieved at 4 ºC (entry 27); however, relative formation of side-products was not improved at low temperatures. Conversely, elevated temperatures dramatically increased formation of undesired aldol-dehydration and elimination side-products. Ambient reaction temperatures furnished the best relative production of desired-to-undesired products. To improve

solubility, the results suggested temperatures can be increased by 10 ºC without significant detriment to desired coupling.

Table S4 – Heating the HWE olefination increased formation of side-products. Under cooled conditions, the desired reaction is limited, though does not eliminate undesired side-reactions.

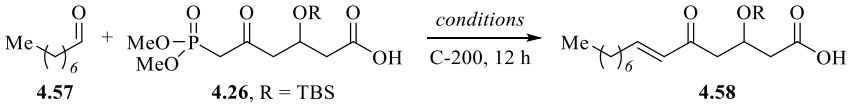

4.57 **4.26**, R = TBS **4.58**

Entry[a]	Solvent	Temp.	Yield[b]	Notes
25	THF	-60 ºC	n.r.	Negligible formation of any products
26	MeCN	-60 ºC	n.r.	Negligible formation of any products
27[c]	THF	4 ºC	+	**4.58** ≥ **4.57** >> hydrate > *β*,*γ* > aldol >>> Cannizzaro
28[c]	MeCN	4 ºC	+	**4.57** ≥ **4.58** >> *β*,*γ* > hydrate >> aldol
29	THF	30 ºC	+	**4.58** >> **4.57** > *β*,*γ* > aldol-dehydration > *β*-elim.> aldol
30	MeCN	30 ºC	+	**4.58** > **4.57** >> *β*,*γ* > *β*-elim.> aldol-dehydration
31	THF	45 ºC	–	aldol-dehydration ≥ *β*-elim.> **4.58** > *β*,*γ* ≥ aldol
32	MeCN	45 ºC	–	aldol-dehydration > *β*-elim.> **4.58** ≥ *β*,*γ* >>> aldol
33	THF	70 ºC	–	aldol-dehydration > *β*-elim.>>> **4.58** = *β*,*γ* > aldol
34	MeCN	88 ºC	–	aldol-dehydration > *β*-elim.>>> *β*,*γ* > **4.58** > aldol

[a] – Conditions: C-200 (1.9 equiv.) was added to **4.26** (1.3 equiv.) in solvent (0.1 M) under argon, and incubated for 30 min at indicated temperature. Aldehyde (1.0 equiv.) added neat, and stirred for 12 h at indicated temperature.
[b] – Yield is presented as qualitative observation based on TLC and crude ^{1}HNMR analysis, indicating relative formation of product (+), no reaction (n.r.), or the erosion (–) of starting material(s).
[c] – Reaction time was doubled (24 h) after poor conversion was achieved under the employed conditions.

Additional equivalents of base are required to promote ylide formation by deprotonation of the weakly-acidic *α*-methylene (Table S5). Using less than two equivalents facilitated nearly complete consumption of **4.57** *via* non-productive side-reactions. The complex mixture of side-products was believed to include elimination of **4.26** and erosion of any desired product that was generated. With two equivalents of base, the desired **4.58** is formed as a major product. Increasing basicity beyond 3.5 equivalents proved deleterious to our base-sensitive system.

Table S5 – Ylide formation of diprotic phosphonate **4.26** required at least two equivalents of base, otherwise erosion of starting materials is promoted.

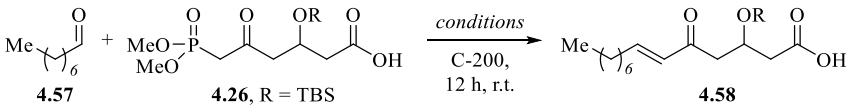

4.57 **4.26**, R = TBS **4.58**

Entry[a]	Solvent	Base		Yield[b]	Notes
35	THF	C-200	1.5 equiv.	–	**4.26** >> complex mixture of erosion products
36	THF	C-200	2.0 equiv.	+	**4.58** >> *β*,*γ* > **4.57** ≥ hydrate > aldol
37	THF	C-200	2.5 equiv.	+	**4.58** >> *β*,*γ* > *β*-elim.> **4.57** ≥ aldol-dehydration
38	THF	C-200	3.5 equiv.	+	**4.58** >>> *β*,*γ* > **4.57** > hydrate > aldol

39	THF	C-200	5.0 equiv.	+	**4.58** > *β*,*γ* >> **4.57** ≥ *β*-elim.> aldol

[a] – Conditions: C-200 was added to phosphonate **4.26** (1.3 equiv.) in solvent (0.1 M) under argon, and incubated for 30 min at ambient temperature (22 ºC). Aldehyde (1.0 equiv.) added neat, and stirred for 12 h at 22 ºC.
[b] – Yield is presented as qualitative observation based on TLC and crude ^{1}HNMR analysis, indicating relative formation of product (+), no reaction (n.r.), or the erosion (–) of starting material(s).

Aldolization and other side-reactions are reported to occur when aldehyde and phosphonate substrates are added separately (Table S6).[43] Because our 30-minute period proved successful, we evaluated the effect of our ylide-forming deprotonation step in 30-minute intervals and used an NMR time-course experiment to monitor for undesired product formation. Evaluation revealed our incubation period had no observable effect on formation of by-products, and best results were obtained with 30- and 60-minute entries.

Table S6 – Evaluation of ylide formation incubation period indicated no observable effect on the incidence of by-product formation.

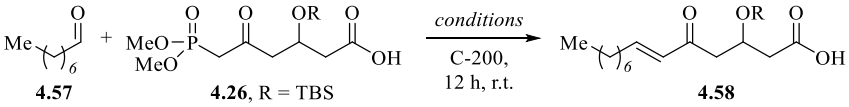

4.57 **4.26**, R = TBS **4.58**

Entry[a]	Solvent	Ylide Formation	Yield[b]	Notes
40	THF	simultaneous	+	**4.58** >> *β*,*γ* >> *β*-elim.>> aldol/aldol-dehydration
41	THF	30 min	+	**4.58** >> *β*,*γ* > *β*-elim.>> aldol-dehydration > aldol
42	THF	60 min	+	**4.58** >>> *β*,*γ* >> *β*-elim.>> aldol-dehydration
43	THF	90 min	+	**4.58** >> *β*,*γ* >> *β*-elim.>> aldol-dehydration ≥ Cannizzaro
44	THF	2 h	+	**4.58** >> *β*,*γ* > *β*-elim.> aldol-dehydration > Cannizzaro
45[c]	THF$_{d8}$	4 h	+	**4.58** >>> *β*,*γ* > hydrate >> aldol > Cannizzaro

[a] – Conditions: C-200 (3.5 equiv.) was added to phosphonate **4.26** (1.3 equiv.) in solvent (0.1 M) under argon, and incubated for the indicated time at ambient temperature (22 ºC). Aldehyde (1.0 equiv.) added neat, and stirred for 12 h.
[b] – Yield is presented as qualitative observation based on TLC and crude ^{1}HNMR analysis, indicating relative formation of product (+), no reaction (n.r.), or the erosion (–) of starting material(s).

HWE coupling reactions have demonstrated high success from nearly-instantaneous[44] to week-long[45] reaction times, and everywhere in between (Table S7).[46–49] Our results showed that product formation was observable upon addition of aldehyde, but conversion was rate-limiting. The highest percentage of conversion was realized between 9-and-18 hours following aldehyde addition, though formation of *β*,*γ*-isomer **4.62** dramatically increased thereafter. Based on these observations, we believed overnight conditions were optimal to allow appropriate monitoring of undesired product formation.

Table S7 – Coupling was very facile and favors desired product **4.58** within 60-minute reaction times. This observation confirmed ylide-formation to be the limiting-step of this transformation.

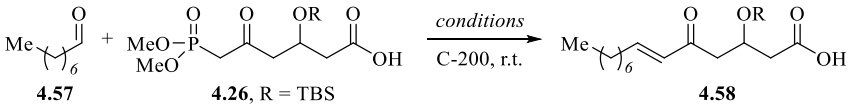

4.57 **4.26**, R = TBS **4.58**

Entry[a]	Solvent	Time	Yield[b]	Notes
46	THF	1 h	+	**4.58** > **4.57** >> *β*,*γ* > hydrate > aldol >> Cannizzaro
47	THF	6 h	+	**4.58** >> *β*,*γ* > hydrate > aldol >> aldol-dehydration = Cannizzaro
48	THF	9 h	+	**4.58** >>> *β*,*γ* >> hydrate >>> aldol >> aldol-dehydration > Cannizzaro
49	THF	18 h	+	**4.58** >>> *β*,*γ* >> hydrate >>> aldol >> aldol-dehydration > Cannizzaro
50	THF	24 h	+	**4.58** >> *β*,*γ* >>> aldol-dehydration = *β*-elim.= Cannizzaro
51[c]	THF_{d8}	4 d	+	**4.58** > *β*,*γ* >>> *β*-elim.> aldol-dehydration > Cannizzaro

[a] – Conditions: C-200 (3.5 equiv.) was added to phosphonate **4.26** (1.3 equiv.) in solvent (0.1 M) under argon, and incubated for 40 min at ambient temperature. Aldehyde (1.0 equiv.) added neat, and stirred for indicated times.
[b] – Yield is presented as qualitative observation based on TLC and crude ^{1}HNMR analysis, indicating relative formation of product (+), no reaction (n.r.), or the erosion (–) of starting material(s).
[c] – Reaction performed in NMR tube and monitored over course of 4 days.

Use of additives and promoters provide excellent improvements to HWE and PT coupling systems. These reagents are commonly used to form a chelate with a metal cation to increase the system acidity (Table S8). Masamune-Roush conditions[50] employ LiCl to provide mild olefination with base-sensitive aldehydes and phosphonates. We evaluated this strategy using readily-available salts with a different metal and/or counterion. Conditions failed to provide our desired **4.58**, and dramatically increased formation of aldol-dehydration and elimination side-products. Similar formation of side-reactions was realized with Helquist's zinc-promoted conditions for mild coupling of diprotic phosphonates.[51] Rather than investigating the potential causes of these observations, we moved forward with the positive results from preceding trials.

Table S8 – The use of additives or promoters did not benefit the HWE coupling, including the conditions used (entry 50) for mild coupling with diprotic phosphonates.[51]

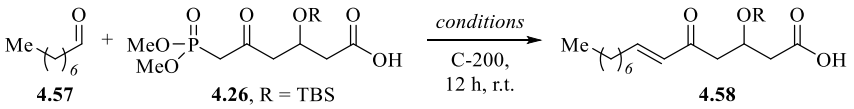

4.57 **4.26**, R = TBS **4.58**

Entry[a]	Solvent	Additive	Yield[b]	Notes
52	THF	KBr	–	Complex mixture
53	THF	LiBr	–	aldol-dehydration ≥ *β*-elim.
54	THF	LiCl	–	aldol-dehydration ≥ *β*-elimination
55[c]	THF	$Zn(OTf)_2$, TMEDA	–	aldol-dehydration >> *β*-elim./ unknown >>> **4.58**

56[d]	THF	$Zn(OTf)_2$, TMEDA	–	aldol-dehydration > β-elim.>>> **4.58**

[a] – Conditions: additives (2.0 equiv.) and C-200 (3.5 equiv.) was added to phosphonate **4.26** (1.3 equiv.) in solvent (0.1 M) under argon, and incubated for 40 min at ambient temperature. Aldehyde (1.0 equiv.) added neat, and stirred for 12 h.
[b] – Yield is presented as qualitative observation based on TLC and crude ^{1}HNMR analysis, indicating relative formation of product (+), no reaction (n.r.), or the erosion (–) of starting material(s).
[c] – Additives: $Zn(OTf)_2$ (2.2 equiv.), TMEDA (0.4 equiv.).
[d] – Conditions: **4.26** (1.0 equiv.), DBU (4 equiv.), $Zn(OTf)_2$ (2.2 equiv.), TMEDA (0.4 equiv.), **4.57** (1.1 equiv.), 12 h, rt.[51]

Isolation of **4.58** required a proton source to neutralize the carboxylate; conditions needed to be mild to suppress desilylation of our C3 alcohol (Table S9). Our small screen of quenching conditions indicated that strongly-acidic conditions facilitated isomerization of the unsaturated olefin. Concentrating reaction mixture *in vacuo* promoted formation of elimination product, likely due to increased alkalinity. The mild conditions of aqueous ammonium chloride suppressed non-productive pathways during product isolation, and were carried forward with our screening process.

Table S9 – Product isolation requires a proton source that is unreactive toward desilylation. Saturated ammonium chloride solution provides optimal conditions that suppress by-product formation *via* non-productive pathways.

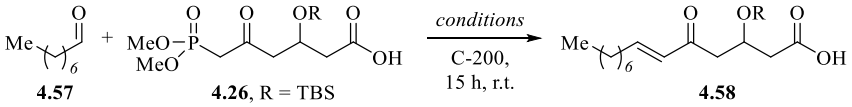

4.57 **4.26**, R = TBS **4.58**

Entry[a]	Solvent	Work-up	Yield[b]	Notes
57	THF	HCl (1 M)	+	**4.58** >> β,γ >> hydrate >>> aldol-dehydration > aldol > Cannizzaro
58	THF	HCl (5 M)	+	**4.58** >> β,γ > β-elim.>> hydrate > Cannizzaro
59	THF	sat. NH_4Cl	+	**4.58** >>> β,γ
60	THF	citric	+	**4.58** >> β,γ >> hydrate >> aldol-dehydration > Cannizzaro
61	THF	*in vacuo*	+	**4.58** > β-elim.> β,γ > aldol/aldol-dehydration

[a] – Conditions: C-200 (3.5 equiv.) was added to phosphonate **4.26** (1.3 equiv.) in solvent (0.1 M) under argon, and incubated for 40 min at ambient temperature. Aldehyde (1.0 equiv.) added neat, and stirred for 15 h.
[b] – Yield is presented as qualitative observation based on TLC and crude ^{1}HNMR analysis, indicating relative formation of product (+), no reaction (n.r.), or the erosion (–) of starting material(s).

The conditions that had been established to this point effectively provided desired olefination product with reliability (Table S10). We wished to screen the substrate concentration to monitor for suppression of undesired side-reactions or improved reaction rates. We observed that lower concentrations did not positively-suppress side-reactions, and simply decreased reactivity. Conversely, higher concentrations increased side-reactions. The originally-employed 0.10 M concentration was most efficient for desired product formation and to limit non-productive pathways.

Table S10 – The reaction concentration was evaluated for suppression of side-product formation *via* non-productive pathways, but indicated a linear relationship between concentration and product formations.

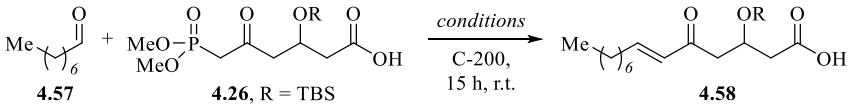

4.57 **4.26**, R = TBS **4.58**

Entry[a]	Solvent		Yield[b]	Notes
62	THF	0.05 M	+	**4.58** >> *β*,*γ* >> **4.57** >> aldol
63	THF	0.10 M	+	**4.58** >>> *β*,*γ* >>> hydrate
64	THF	0.25 M	+	**4.58** >> *β*,*γ* >> *β*-elimination
65	THF	0.5 M	+	**4.58** > *β*,*γ* > *β*-elimination

[a] – Conditions: C-200 (3.5 equiv.) was added to phosphonate **4.26** (1.3 equiv.) in solvent under argon, and incubated for 40 min at ambient temperature. Aldehyde (1.0 equiv.) added neat, and stirred for 15 h at ambient temperature.
[b] – Yield is presented as qualitative observation based on TLC and crude ^{1}HNMR analysis, indicating relative formation of product (+), no reaction (n.r.), or the erosion (–) of starting material(s).

Initial screening suggested that THF and acetonitrile provided similar results, however THF was employed throughout most of the screening process based on ease of access to anhydrous solvent delivery system (Table S11). The two solvents were evaluated under the optimized conditions and revealed acetonitrile was superior to THF. Each trial confirmed conditions could reliably generate our desired olefination product **4.58**, but a higher incidence of side-product was observed with THF. The reaction rate was slower with acetonitrile, but we believed we could quickly recycle our recovered aldehyde. Quantitative product ratios are indicated for these trials below.

Table S11 – Acetonitrile proved superior to THF for relative reaction efficiency, despite lower rates of conversion.

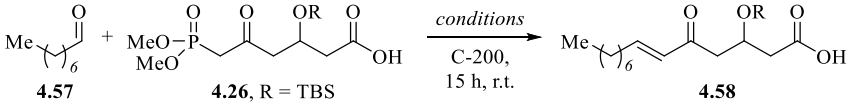

4.57 **4.26**, R = TBS **4.58**

Entry[a]	Solvent	Ylide Formation	Yield[b]
66	THF	simultaneous	**4.57** (0.05), **4.58** (1.00), *β*,*γ* (0.61), Hydrate (0.06), aldol (-), aldol-dehydration (0.03), *β*-elim.(0.31)
67	MeCN	simultaneous	**4.57** (0.43), **4.58** (1.00), *β*,*γ* (0.09), Hydrate (0.15), aldol (0.06), aldol-dehydration (-), *β*-elim.(-)
68	THF	40 min	**4.57** (0.13), **4.58** (1.00), *β*,*γ* (0.46), Hydrate (0.15), aldol (0.03), aldol-dehydration (0.17), *β*-elim.(0.20)
69	MeCN	40 min	**4.57** (0.33), **4.58** (1.00), *β*,*γ* (0.25), Hydrate (0.23), aldol (0.04), aldol-dehydration (0.03), *β*-elim.(-)

[a] – Conditions: C-200 (3.5 equiv.) was added to phosphonate **4.26** (1.3 equiv.) in solvent (0.1 M) under argon, and incubated for 40 min at ambient temperature. Aldehyde (1.0 equiv.) added neat, and stirred for 15 h.
[b] – Yield is presented based on relative integration ratios for single protons from crude reaction mixtures.

S2.3.2 Secondary HWE Screening & Serendipitous Discovery

Continued failure for HWE coupling of fully-functionalized neopeltolide fragments using diprotic phosphonate fragment **4.26** prompted deeper exploratory work with the octyl aldehyde model system (Figure S32). Alternative phosphonate fragments displayed no improvement. Thus, to identify suitable reaction conditions, an exhaustive screening process systematically-investigated the choice of solvent, base, and additives under various modifications including, but not limited to temperature, time, concentration, atmosphere, and reaction vessel.

General procedure for screening included preparing reactions conditions in duplicate, and running one at 4 ºC (fridge) and the other left at ambient temperature. Screening reactions were monitored on a qualitative basis using tandem TLC analysis (20% EtOAc in hexanes, and 5% MeOH in CH_2Cl_2) to monitor progression against authentic **4.58** standard. Reactions were monitored simultaneously at various time-points up to two weeks, or consumption of starting materials. Reactions that displayed unique characteristics such as unidentified product formation, were quenched (HCl) and mixtures were extracted by aqueous work-up. Hundreds of combinations were prepared, where most listed solvents were evaluated using most listed bases. Because most combinations that were evaluated exhibited poor reactivity, or facilitated the formation of by-products, it is fruitless to list all combinations. Eventually, the fortuitous discovery of successful, reproducible conditions was made when mildly-hydrated THF was used with cesium carbonate as the phase-transfer base-catalyst.

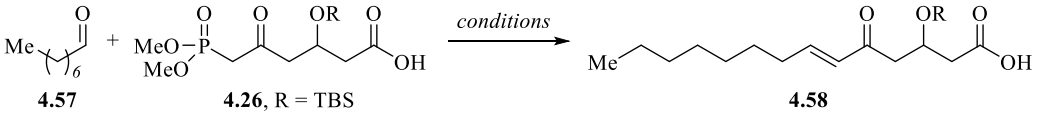

4.57 **4.26**, R = TBS **4.58**

solvent	base	additives	temperature	concentration	equiv. of acid
THF	Cs_2CO_3	LiBr	-78 ºC	0.05 M	0.7 equiv.
THF_{aq}	K_2CO_3	KBr	-20 ºC	0.5 M	1.0 equiv.
1,4-dioxane	NaH	LiCl	4 ºC	1.25 M	1.3 equiv.
MeCN	DBU	$Sn(OTf)_2$	22 ºC	5.0 M	3.0 equiv.
DMF	$Ba(OH)_2 \cdot 8H_2O$	$Zn(OTf)_2$	45 ºC		5.0 equiv.
MeOH	C-100	TMEDA	130 ºC		
DMSO	C-200				
1-pentane	Et_3N				
hexanes	DIPEA				
cyclohexane	*n*BuLi				
1-heptane	LDA				
acetone	LiHMDS				
chloroform	KO*t*Bu				
benzene					
toluene					

miscellaneous

- placing reaction vessel in sonication bath
- running reaction in microwave at elevated temperatures
- keeping reactions void of light
- use of various reaction atmospheres (N_2, Ar, ambient)

Figure S32 – An exhaustive screening process of solvent, base, additives, temperature, time, and patience; combinations were systematically-evaluated to identify HWE conditions for coupling fragments for neopeltolide synthesis.

2.3.3 Comparison of Energetic Profiles for Transannular Oxa-Conjugate Systems

Unexpectedly, we determined that native configuration of neopeltolide ***cis*-4.14** was energetically-*dis*favored by 3.76 kcal/mol to its diastereomeric pyran, which prompted an investigation into related transannular oxa-conjugate systems (Figure S33).

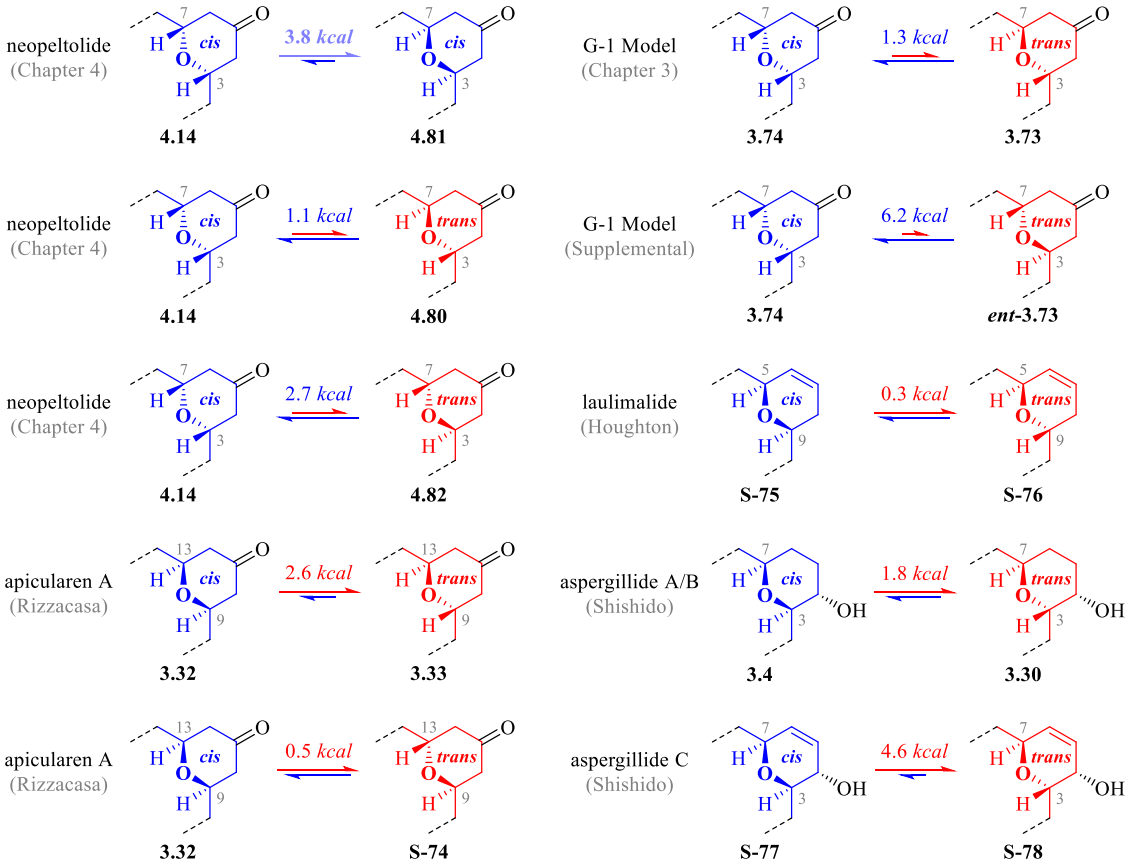

Figure S33 – Comparison of relative energy differences for *cis*- and *trans*-pyrans of select 2,6-disubstituted systems.[35,52–54] Data for the *trans*-isomers from our first-generation model was generated at two unique times, which may affect the calculated profiles.

2.3.4 Calculation Protocol & Computational Data for Neopeltolide Core

Computational data was performed in identical fashion to results obtained for preliminary work with ester and ketone models (*vide supra*).

(3*R*)-*β'*-Hydroxy Enone (3*R*)-4.24

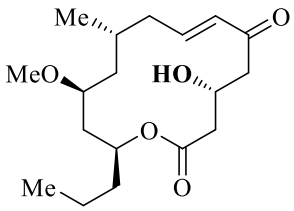

E_{rel} = 7.82 kcal/mol

E_{min} = −1080.1686 Ha ν_{min} = 23.40 cm^{-1}

Atom No.	Element	Cartesian Coordinates (Å)			Atom No.	Element	Cartesian Coordinates (Å)		
		X	Y	Z			X	Y	Z
1	C	0.3408	−2.0865	−1.2748	31	H	−4.5828	2.4226	−0.3664
2	C	1.4098	−2.2305	−0.2124	32	H	−4.2574	1.5296	−1.8706
3	C	2.8101	−1.9124	−0.7767	33	H	−3.5491	3.1517	−1.6258
4	O	3.2980	−3.0146	−1.5362	34	H	−0.7772	0.2052	−2.8405
5	O	−0.7890	−1.5683	−0.7665	35	H	−2.5095	0.3999	−2.9095
6	C	−0.3524	1.3546	−0.3098	36	H	−3.4307	−3.5134	−1.4659
7	C	−1.5542	1.4274	−1.2591	37	H	−5.6152	−2.7936	−0.4128
8	O	−2.7159	1.6436	−0.4498	38	H	−4.7895	−2.5708	1.1359
9	C	−3.8250	2.2116	−1.1245	39	H	−4.9232	−4.1873	0.4290
10	C	−1.6790	0.2148	−2.2161	40	H	−2.6130	−3.2917	0.0743
11	C	−1.8883	−1.2079	−1.6653	41	H	−4.0085	−1.0691	−1.5089
12	C	−3.1829	−1.4427	−0.8882	42	H	−3.1790	−0.8307	0.0196
13	C	−3.4376	−2.9163	−0.5433	43	H	−1.8396	−1.8948	−2.5171
14	C	−4.7652	−3.1297	0.1930	44	H	2.9489	2.3518	0.4327
15	C	2.3144	1.7488	1.0817	45	H	0.5670	1.6983	2.3078
16	C	1.0341	2.3612	1.5695	46	H	1.2589	3.3081	2.0802
17	C	0.0015	2.6572	0.4359	47	H	−0.9063	3.0102	0.9409
18	C	0.4907	3.7741	−0.5007	48	H	0.7740	4.6667	0.0683
19	C	3.8492	−1.6021	0.3259	49	H	−0.2885	4.0768	−1.2076
20	C	3.8943	−0.1059	0.6423	50	H	1.3618	3.4611	−1.0881
21	C	2.7091	0.4868	1.3228	51	H	4.8330	−1.8879	−0.0512
22	O	0.5033	−2.3760	−2.4497	52	H	3.6340	−2.1890	1.2284
23	O	4.8340	0.5817	0.2633	53	H	2.0991	−0.1659	1.9445
24	H	1.1494	−1.5893	0.6299					
25	H	1.4176	−3.2676	0.1468					
26	H	2.7373	−1.0334	−1.4347					
27	H	2.6737	−3.1482	−2.2676					
28	H	−0.5496	0.5666	0.4228					
29	H	0.5197	1.0281	−0.8894					
30	H	−1.4320	2.3039	−1.9176					

(3*S*)-*β'*-Hydroxy Enone (3*S*)-4.24

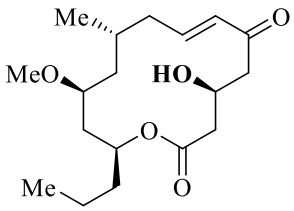

E_{rel} = 8.55 kcal/mol

E_{min} = −1080.1674 Ha ν_{min} = 24.38 cm^{-1}

Atom No.	Element	Cartesian Coordinates (Å)			Atom No.	Element	Cartesian Coordinates (Å)		
		X	Y	Z			X	Y	Z
1	C	0.3374	−1.4254	−1.2898	31	H	−1.9470	4.8433	−1.2610
2	C	1.7431	−1.8180	−0.8640	32	H	−2.7770	4.5927	0.2993
3	C	2.0013	−1.9068	0.6506	33	H	−3.1119	3.5031	−1.0670
4	O	1.5116	−3.1397	1.1916	34	H	−0.6168	1.0716	−2.5503
5	O	−0.2020	−0.5074	−0.4535	35	H	−2.1691	1.7063	−2.0715
6	C	0.8577	2.2922	−0.4023	36	H	−3.2332	−1.5937	0.4524
7	C	−0.4914	2.6108	−1.0523	37	H	−3.8159	−1.6562	2.8901
8	O	−1.2847	3.2726	−0.0576	38	H	−4.4641	−0.1843	2.1529
9	C	−2.3300	4.0865	−0.5595	39	H	−3.0007	−0.1061	3.1433
10	C	−1.1987	1.3825	−1.6738	40	H	−1.7823	−1.5223	1.4429
11	C	−1.4702	0.1262	−0.8263	41	H	−3.1666	0.9107	0.1933
12	C	−2.2659	0.3422	0.4600	42	H	−1.6999	0.9813	1.1454
13	C	−2.6806	−0.9596	1.1593	43	H	−1.9972	−0.5870	−1.4679
14	C	−3.5381	−0.7140	2.4061	44	H	4.2739	1.9689	−0.2859
15	C	3.6251	1.8983	0.5870	45	H	2.3434	2.9274	1.9425
16	C	2.8346	3.1111	0.9797	46	H	3.5103	3.9668	1.1163
17	C	1.7465	3.5080	−0.0694	47	H	1.1174	4.2619	0.4203
18	C	2.3696	4.1443	−1.3224	48	H	2.9737	5.0199	−1.0597
19	C	3.5010	−1.8547	0.9896	49	H	1.6009	4.4799	−2.0264
20	C	4.1501	−0.5249	0.6144	50	H	3.0166	3.4394	−1.8578
21	C	3.5203	0.6977	1.1816	51	H	4.0393	−2.6598	0.4823
22	O	−0.2120	−1.8394	−2.2910	52	H	3.5968	−2.0075	2.0726
23	O	5.0991	−0.4782	−0.1596	53	H	2.8611	0.5722	2.0391
24	H	1.9888	−2.7688	−1.3439					
25	H	2.4013	−1.0577	−1.3061					
26	H	1.4955	−1.0698	1.1430					
27	H	0.5474	−3.1555	1.1231					
28	H	0.6602	1.7250	0.5125					
29	H	1.4096	1.6149	−1.0637					
30	H	−0.3338	3.3179	−1.8843					

(7*R*)-*β'*-Hydroxy Enone (7*R*)-4.83

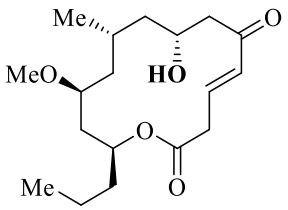

E_{rel} = –762.6 kcal/mol

E_{min} = −1081.3838 Ha ν_{min} = 17.42 cm^{-1}

Atom No.	Element	Cartesian Coordinates (Å)			Atom No.	Element	Cartesian Coordinates (Å)		
		X	Y	Z			X	Y	Z
1	C	−0.2578	−2.1133	−1.2983	31	H	2.4602	−2.5149	−2.1854
2	C	0.9668	−2.7076	−0.6309	32	H	0.1597	1.0435	0.5366
3	C	2.2601	−2.0737	−1.2034	33	H	1.0535	0.9319	−0.9678
4	O	−0.7615	−1.0945	−0.5597	34	H	−0.4578	2.7776	−1.8858
5	C	0.5007	1.6258	−0.3234	35	H	−3.0196	4.1608	0.0859
6	C	−0.7478	2.0629	−1.0975	36	H	−3.3156	3.0969	−1.3092
7	O	−1.5889	2.7515	−0.1652	37	H	−2.0585	4.3629	−1.4048
8	C	−2.5407	3.6300	−0.7400	38	H	−0.7999	0.5724	−2.6448
9	C	−1.4602	0.9014	−1.8323	39	H	−2.3509	1.3042	−2.3313
10	C	−1.9189	−0.3532	−1.0682	40	H	−3.9488	−1.9719	−0.0870
11	C	−2.8572	−0.1154	0.1156	41	H	−5.2709	−0.5384	1.5230
12	C	−3.4398	−1.4066	0.7059	42	H	−3.9311	−0.6045	2.6763
13	C	−4.4190	−1.1434	1.8557	43	H	−4.8154	−2.0799	2.2620
14	C	3.3629	1.0181	0.9585	44	H	−2.6212	−2.0431	1.0621
15	O	3.9695	0.9904	−0.3412	45	H	−3.6774	0.5228	−0.2395
16	C	2.4870	2.2715	1.2114	46	H	−2.3402	0.4602	0.8904
17	C	1.4373	2.7525	0.1610	47	H	−2.4087	−1.0072	−1.7966
18	C	2.0704	3.5423	−1.0036	48	H	1.9633	2.0995	2.1608
19	C	3.4959	−2.2510	−0.3106	49	H	3.1669	3.1133	1.3900
20	C	3.5107	−1.5418	1.0467	50	H	0.8092	3.4662	0.7093
21	C	2.6385	−0.3136	1.2898	51	H	2.8080	4.2603	−0.6312
22	O	−0.7042	−2.4645	−2.3727	52	H	1.3134	4.1089	−1.5550
23	O	4.2532	−1.9466	1.9274	53	H	2.5839	2.9042	−1.7334
24	H	4.2182	1.0773	1.6399	54	H	4.3725	−1.8574	−0.8432
25	H	3.3016	1.1830	−1.0096	55	H	3.7019	−3.3098	−0.1170
26	H	1.7025	−0.3886	0.7391					
27	H	2.4027	−0.3044	2.3590					
28	H	0.8990	−2.5435	0.4481					
29	H	0.9685	−3.7857	−0.8144					
30	H	2.0983	−1.0063	−1.3847					

(7*S*)-*β'*-Hydroxy Enone (7*S*)-4.83

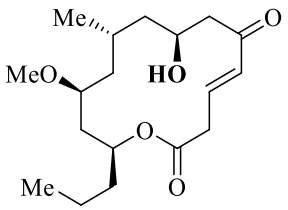

E_{rel} = –757.8 kcal/mol

E_{min} = −1081.3915 Ha ν_{min} = 26.20 cm^{-1}

Atom No.	Element	Cartesian Coordinates (Å)			Atom No.	Element	Cartesian Coordinates (Å)		
		X	Y	Z			X	Y	Z
1	C	−1.1141	−2.5509	−1.0566	31	H	2.0818	−3.8690	−0.9737
2	C	−0.0452	−3.5823	−0.7408	32	H	0.4113	0.7060	0.8663
3	C	1.3972	−3.0295	−0.8123	33	H	0.9991	0.3410	−0.7565
4	O	−1.1584	−1.5522	−0.1404	34	H	−0.4343	2.3110	−1.5688
5	C	0.6358	1.1465	−0.1113	35	H	−2.3982	4.1609	0.6747
6	C	−0.6787	1.6808	−0.6964	36	H	−3.0295	3.1450	−0.6429
7	O	−1.2598	2.5289	0.3057	37	H	−1.6012	4.1801	−0.9226
8	C	−2.1146	3.5465	−0.1832	38	H	−1.2307	0.1544	−2.1114
9	C	−1.6693	0.6181	−1.2199	39	H	−2.5601	1.1471	−1.5829
10	C	−2.1829	−0.5142	−0.3127	40	H	−4.2087	−1.6148	1.2416
11	C	−2.6573	−0.1157	1.0841	41	H	−4.5856	0.0127	3.1409
12	C	−3.3636	−1.2486	1.8411	42	H	−3.0409	−0.4689	3.8548
13	C	−3.8676	−0.8121	3.2216	43	H	−4.3658	−1.6367	3.7427
14	C	3.8035	1.0017	1.1852	44	H	−2.6756	−2.0951	1.9542
15	O	4.7441	1.2706	2.2462	45	H	−3.3458	0.7306	0.9671
16	C	2.6880	2.0674	1.2241	46	H	−1.8159	0.2658	1.6720
17	C	1.7141	2.2492	0.0311	47	H	−3.0065	−0.9935	−0.8508
18	C	2.4556	2.4960	−1.2954	48	H	2.1095	1.9241	2.1466
19	C	1.8213	−2.2523	0.4378	49	H	3.2029	3.0328	1.3413
20	C	2.9128	−1.2210	0.2109	50	H	1.1663	3.1673	0.2813
21	C	3.3549	−0.4420	1.4409	51	H	3.1727	3.3200	−1.1987
22	O	−1.8475	−2.6067	−2.0249	52	H	1.7575	2.7687	−2.0946
23	O	3.4181	−1.0315	−0.8847	53	H	3.0023	1.6070	−1.6258
24	H	4.3272	1.0311	0.2224	54	H	2.1561	−2.9291	1.2380
25	H	5.0725	2.1741	2.1477	55	H	0.9680	−1.7097	0.8611
26	H	2.5900	−0.4831	2.2244					
27	H	4.2290	−0.9792	1.8359					
28	H	−0.2408	−4.0014	0.2543					
29	H	−0.1771	−4.3813	−1.4733					
30	H	1.5067	−2.3883	−1.6931					

(3*R*,7*R*)-*cis*-neopeltolide macrocyclic core (4.14)

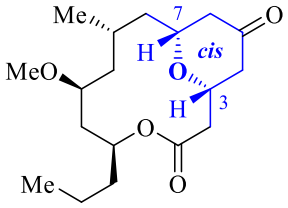

E_{rel} = 3.76 kcal/mol

E_{min} = −1080.1750 Ha ν_{min} = 28.36 cm^{-1}

Atom No.	Element	Cartesian Coordinates (Å)			Atom No.	Element	Cartesian Coordinates (Å)		
		X	Y	Z			X	Y	Z
1	C	0.4159	−2.3379	−1.1909	31	H	−3.4272	3.3075	−0.2242
2	C	1.8272	−2.6292	−0.7064	32	H	−3.0962	2.9356	1.4915
3	C	2.3825	−1.5751	0.2530	33	H	−0.6757	0.0876	−1.7101
4	O	2.0082	−0.2952	−0.2529	34	H	−2.4157	0.1405	−1.8994
5	O	−0.3974	−1.9051	−0.2085	35	H	−3.2393	−3.6832	−0.0227
6	C	−0.7727	1.2701	1.0078	36	H	−4.8456	−2.9740	1.7968
7	C	−1.7281	1.2319	−0.2194	37	H	−3.5058	−2.9102	2.9496
8	O	−3.1076	1.2891	0.1918	38	H	−3.9874	−4.4575	2.2389
9	C	−3.5791	2.5661	0.5752	39	H	−1.9081	−3.6193	1.1230
10	C	−1.6180	0.0171	−1.1576	40	H	−3.6357	−1.2171	0.2979
11	C	−1.7278	−1.4271	−0.6176	41	H	−2.3161	−1.1470	1.4425
12	C	−2.6745	−1.6768	0.5525	42	H	−2.0250	−2.0554	−1.4617
13	C	−2.8745	−3.1642	0.8745	43	H	1.9834	0.4806	1.6536
14	C	−3.8581	−3.3903	2.0287	44	H	2.2798	2.8889	0.2716
15	C	2.3386	0.7644	0.6480	45	H	1.3406	1.9234	−0.8574
16	C	1.5967	2.0329	0.2039	46	H	0.6916	2.3510	2.1005
17	C	0.3453	2.3517	1.0556	47	H	0.6419	4.5060	0.9767
18	C	−0.1511	3.7786	0.7708	48	H	−1.0075	4.0376	1.4016
19	C	3.9175	−1.6570	0.3950	49	H	−0.4516	3.9153	−0.2738
20	C	4.4922	−0.4376	1.1053	50	H	4.3548	−1.6831	−0.6133
21	C	3.8731	0.8957	0.7142	51	H	4.2333	−2.5588	0.9275
22	O	0.0746	−2.4872	−2.3481	52	H	4.2416	1.1809	−0.2811
23	O	5.3798	−0.5295	1.9355	53	H	4.1889	1.6561	1.4343
24	H	1.8388	−3.6093	−0.2137					
25	H	2.4458	−2.7042	−1.6045					
26	H	1.9178	−1.7049	1.2429					
27	H	−1.4065	1.4203	1.8897					
28	H	−0.3125	0.2868	1.1378					
29	H	−1.5400	2.1112	−0.8553					
30	H	−4.6502	2.4625	0.7653					

(3*R*,7*S*)-*trans*-$^{\Delta 7}$*epi*-neopeltolide macrocyclic core (4.80)

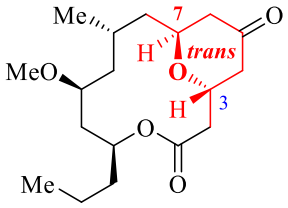

E_{rel} = 4.85 kcal/mol

E_{min} = −1080.1733 Ha ν_{min} = 26.74 cm^{-1}

Atom No.	Element	Cartesian Coordinates (Å)			Atom No.	Element	Cartesian Coordinates (Å)		
		X	Y	Z			X	Y	Z
1	C	−0.1437	−2.6036	−1.0165	31	H	−3.7637	1.0172	1.2349
2	C	1.2545	−2.7862	−0.4417	32	H	−3.0211	2.6262	1.0116
3	C	1.8780	−1.5241	0.1571	33	H	−2.3635	−0.4064	−2.2466
4	O	2.1829	−0.6588	−0.9440	34	H	−3.6626	−0.1335	−1.1080
5	O	−0.9187	−1.8799	−0.1808	35	H	−3.3983	−4.0227	0.5489
6	C	−0.4028	1.0050	−1.2885	36	H	−4.9052	−3.3148	2.4531
7	C	−1.8135	0.9438	−0.6778	37	H	−3.4822	−2.8992	3.4192
8	O	−1.7216	1.0158	0.7498	38	H	−3.7805	−4.5819	2.9615
9	C	−2.8458	1.6045	1.3809	39	H	−1.9861	−3.6132	1.5125
10	C	−2.5817	−0.3091	−1.1764	40	H	−4.1452	−1.6279	0.6307
11	C	−2.3299	−1.6755	−0.4968	41	H	−2.7113	−1.2084	1.5704
12	C	−3.0954	−1.8970	0.8108	42	H	−2.6097	−2.4531	−1.2146
13	C	−3.0321	−3.3402	1.3283	43	H	3.7687	0.5874	−1.1998
14	C	−3.8450	−3.5461	2.6117	44	H	2.6159	2.6849	−1.0450
15	C	2.8184	0.6073	−0.6476	45	H	1.9641	1.6590	−2.3096
16	C	2.0074	1.7863	−1.2194	46	H	0.5692	1.8977	0.4036
17	C	0.5762	2.0304	−0.6848	47	H	0.8189	4.1977	−0.4955
18	C	0.1451	3.4782	−0.9744	48	H	−0.8658	3.6795	−0.6048
19	C	3.1479	−1.8026	0.9649	49	H	0.1529	3.6816	−2.0532
20	C	3.8085	−0.5007	1.4061	50	H	3.8744	−2.3605	0.3587
21	C	3.1656	0.7567	0.8469	51	H	2.9407	−2.4060	1.8568
22	O	−0.5234	−3.0833	−2.0650	52	H	3.8402	1.6028	0.9997
23	O	4.7708	−0.4791	2.1518	53	H	2.2567	0.9491	1.4340
24	H	1.1766	−3.5462	0.3465					
25	H	1.8917	−3.1849	−1.2347					
26	H	1.1308	−1.0500	0.8075					
27	H	0.0560	0.0232	−1.2348					
28	H	−0.5262	1.2210	−2.3598					
29	H	−2.3802	1.8247	−1.0209					
30	H	−2.6255	1.6480	2.4504					

(3*S*,7*S*)-*cis*-$^{\Delta 3,7}$*epi*-neopeltolide macrocyclic core (4.81)

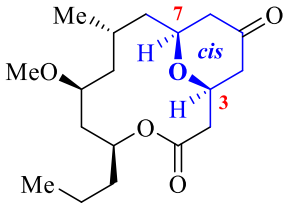

E_{rel} = 0 kcal/mol

E_{min} = −1080.1810 Ha ν_{min} = 31.80 cm^{-1}

Atom No.	Element	Cartesian Coordinates (Å)			Atom No.	Element	Cartesian Coordinates (Å)		
		X	Y	Z			X	Y	Z
1	C	−0.6958	−2.1839	−0.0769	31	H	−3.5058	3.2587	0.4987
2	C	0.6469	−2.5700	0.5196	32	H	−2.9302	4.4357	−0.7015
3	C	1.7571	−1.8107	−0.2193	33	H	−3.5475	1.1159	0.2473
4	O	1.3589	−0.4435	−0.2202	34	H	−2.5486	0.8632	1.6768
5	O	−1.3931	−1.3899	0.7616	35	H	−4.0678	−3.0978	−0.4158
6	C	−0.2758	1.8057	0.8140	36	H	−5.3070	−4.6460	1.1209
7	C	−1.4569	1.5006	−0.1251	37	H	−6.1334	−3.0835	1.0515
8	O	−1.9721	2.6632	−0.8061	38	H	−5.1341	−3.4942	2.4527
9	C	−2.6145	3.6482	−0.0128	39	H	−3.0844	−3.5152	0.9751
10	C	−2.5882	0.7131	0.5901	40	H	−4.7296	−0.9421	0.7052
11	C	−2.6419	−0.7891	0.2925	41	H	−3.7048	−1.3439	2.0794
12	C	−3.8154	−1.4784	0.9944	42	H	−2.6961	−0.9586	−0.7869
13	C	−3.9846	−2.9683	0.6703	43	H	2.3373	0.0171	−1.9756
14	C	−5.2075	−3.5824	1.3620	44	H	2.2814	2.4689	−1.5295
15	C	2.2189	0.4248	−0.9572	45	H	0.7292	1.7173	−1.8097
16	C	1.5411	1.7956	−1.0783	46	H	1.7760	2.3377	0.9946
17	C	1.0068	2.4547	0.2171	47	H	1.8170	4.4221	−0.2779
18	C	0.8531	3.9701	−0.0164	48	H	0.4885	4.4727	0.8866
19	C	3.1407	−1.9695	0.4405	49	H	0.1491	4.1768	−0.8278
20	C	4.1432	−0.9659	−0.1154	50	H	3.5395	−2.9797	0.3119
21	C	3.6126	0.4471	−0.2919	51	H	3.0380	−1.7721	1.5171
22	O	−1.0649	−2.5223	−1.1840	52	H	4.3318	1.0233	−0.8807
23	O	5.2864	−1.2795	−0.3981	53	H	3.5266	0.9079	0.7017
24	H	0.6697	−2.3241	1.5842					
25	H	0.7936	−3.6467	0.3927					
26	H	1.8015	−2.1688	−1.2600					
27	H	−0.6257	2.4435	1.6380					
28	H	−0.0045	0.8488	1.2651					
29	H	−1.0938	0.8873	−0.9545					
30	H	−1.9454	4.0883	0.7376					

(3*S*,7*R*)-*trans*-$^{\Delta 3}$*epi*-neopeltolide macrocyclic core (4.82)

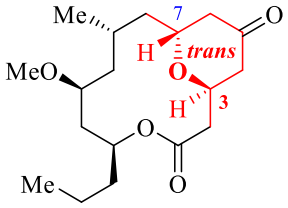

E_{rel} = 6.45 kcal/mol

E_{min} = −1080.1707 Ha ν_{min} = 24.62 cm^{-1}

Atom No.	Element	Cartesian Coordinates (Å)			Atom No.	Element	Cartesian Coordinates (Å)		
		X	Y	Z			X	Y	Z
1	C	0.4681	−2.4606	−0.8350	31	H	−3.7209	2.9397	−0.1216
2	C	1.7839	−2.3898	−0.0860	32	H	−3.4397	2.4562	1.5748
3	C	2.6120	−1.2307	−0.6757	33	H	−0.8009	−0.0695	−1.7476
4	O	1.8191	−0.0279	−0.6682	34	H	−2.5388	−0.0812	−1.9992
5	O	−0.5503	−1.9921	−0.0898	35	H	−4.5642	−1.0977	−0.8344
6	C	−0.9952	0.9379	1.0083	36	H	−5.4970	−1.9922	1.3234
7	C	−1.9418	0.9417	−0.2287	37	H	−5.2224	−3.6483	0.762
8	O	−3.3280	0.9113	0.1612	38	H	−6.3997	−2.6171	−0.0646
9	C	−3.8699	2.1359	0.6157	39	H	−4.2910	−2.7437	−1.4095
10	C	−1.7604	−0.2092	−1.2377	40	H	−2.9604	−1.4797	1.0500
11	C	−1.8110	−1.6798	−0.7750	41	H	−2.7031	−3.1351	0.4939
12	C	−2.9391	−2.1163	0.1595	42	H	−1.8334	−2.2977	−1.6772
13	C	−4.3213	−2.1143	−0.5090	43	H	2.1852	0.6129	1.2775
14	C	−5.4221	−2.6224	0.4296	44	H	1.6981	3.0902	0.2777
15	C	2.1982	1.0085	0.2481	45	H	0.7837	2.1519	−0.8882
16	C	1.1647	2.1409	0.1410	46	H	0.4829	1.9469	2.1506
17	C	0.0105	2.1095	1.1694	47	H	0.0683	4.2681	1.4754
18	C	−0.6664	3.4893	1.2423	48	H	−1.4323	3.5145	2.0240
19	C	3.9732	−1.0685	0.0256	49	H	−1.1445	3.7672	0.2963
20	C	4.5891	0.2998	−0.2189	50	H	4.6715	−1.8441	−0.2977
21	C	3.6205	1.4682	−0.0982	51	H	3.8488	−1.1699	1.1140
22	O	0.3729	−2.8348	−1.9883	52	H	3.6189	2.0002	−1.0586
23	O	5.7699	0.4543	−0.4707	53	H	4.0136	2.1666	0.6513
24	H	1.6115	−2.2349	0.9828					
25	H	2.3263	−3.3296	−0.2328					
26	H	2.7840	−1.4486	−1.7357					
27	H	−1.6364	0.9307	1.8985					
28	H	−0.4401	−0.0007	1.0317					
29	H	−1.7847	1.8685	−0.8049					
30	H	−4.9422	1.9747	0.7521					

α,β-unsaturated-*β',γ'* diene by-product (4.87)

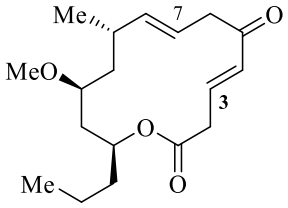

E_{min} = −1003.7037 Ha ν_{min} = 23.35 cm^{-1}

Atom No.	Element	Cartesian Coordinates (Å)			Atom No.	Element	Cartesian Coordinates (Å)		
		X	Y	Z			X	Y	Z
1	C	0.9956	−1.8604	−1.5810	31	H	−2.7353	2.5755	1.8702
2	C	2.4370	−2.0995	−1.1161	32	H	−0.8419	0.4144	−2.0660
3	C	2.7487	−1.8081	0.3231	33	H	−2.5479	0.0910	−1.8328
4	O	0.1623	−1.5064	−0.5864	34	H	−2.1676	−3.9295	−0.4824
5	C	−0.4341	1.4068	0.6402	35	H	−3.7911	−3.7862	1.4501
6	C	−1.6837	1.2368	−0.2558	36	H	−2.4413	−3.5056	2.5586
7	O	−2.8563	0.9668	0.5283	37	H	−2.5860	−5.0549	1.7164
8	C	−3.4207	2.1081	1.1480	38	H	−0.8269	−3.6532	0.6213
9	C	−1.5816	0.1211	−1.3143	39	H	−3.1114	−1.6669	0.1043
10	C	−1.2696	−1.3339	−0.9076	40	H	−1.7746	−1.3813	1.1916
11	C	−2.0544	−1.9050	0.2711	41	H	−1.4484	−1.9445	−1.7973
12	C	−1.8847	−3.4199	0.4492	42	H	1.2961	1.0226	2.5046
13	C	−2.7224	−3.9736	1.6079	43	H	2.7528	2.8449	0.5224
14	C	2.1259	1.5417	2.0290	44	H	0.1546	3.4814	0.4678
15	C	1.8995	2.3332	0.9735	45	H	1.6323	3.3079	−1.5081
16	C	0.5866	2.4965	0.2269	46	H	0.0196	2.7096	−1.8909
17	C	0.9089	2.5162	−1.2842	47	H	1.3445	1.5661	−1.6121
18	C	3.4310	−0.7301	0.7347	48	H	3.7677	0.0111	0.0117
19	C	3.5931	−0.3937	2.1789	49	H	4.2791	1.6622	1.9977
20	C	3.4869	1.1051	2.5143	50	H	3.6162	1.2136	3.5950
21	O	0.6660	−1.9901	−2.7435					
22	O	3.6892	−1.2435	3.0515					
23	H	2.6450	−3.1515	−1.3516					
24	H	3.0703	−1.5073	−1.7852					
25	H	2.3623	−2.4953	1.0732					
26	H	−0.7803	1.6315	1.6550					
27	H	0.0844	0.4482	0.6998					
28	H	−1.8704	2.1734	−0.8082					
29	H	−4.3126	1.7721	1.6817					
30	H	−3.7115	2.8638	0.4016					

S2.4 Probing the Specificity of the DEBS TE (Chapter 6)

S2.4.1 Tree Construction & Phylogenetic Analysis

Sequences were aligned using Muscle[55] in MEGA, version 5.00[56] with default parameters. Model-selection was performed with ProtTest based on the Akaike Information Criterion,[57] which identified WAG as the best substitution model.

Phylogenetic analysis was carried-out by Christopher Boddy using 138 type-I polyketide synthase TE domains, downloaded from the ClusterMine360 database (www.clustermine360.ca)[58] on May 10, 2014. Analysis was performed using PhyML with the sub-tree pruning and regrafting (SPR) tree-searching algorithm.[59] Branch support was estimated using approximate likelihood ratio test (aLRT).[60]

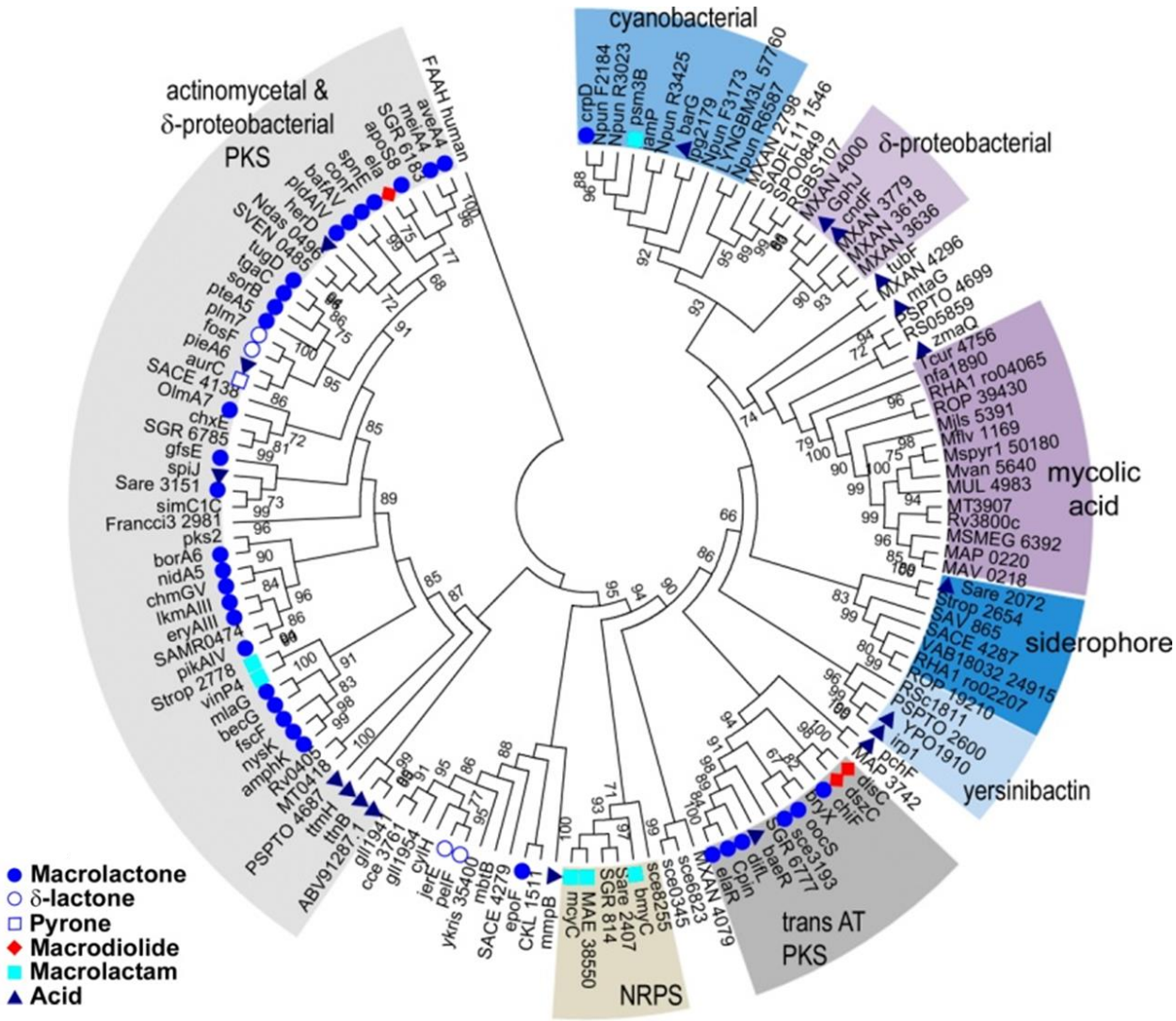

Figure S34 – Phylogenetic analysis of 138 thioesterase domains shows clustering is not based on substrate specificity or function. Pathway type and origin appear to be greater determinants for clustering of TEs.

Table S12 – Sequences used for phylogenetic analysis of type-I polyketide thioesterase domains.

name	accession number	start	stop	product type	compound	producing organism
aveA4	WP_010982381	4670	4858	macrolactone	avermectin	*Streptomyces avermitilis*
ela	EXU62911	1724	2092	macrodiolide	elaiophylin	*Streptomyces sp. DSM4137*
gphJ	AHA38203.1	1451	1809	acid	gephyronic acid	*Cystobacter violaceus Cb vi76*
dszC	AAY32966.1	3523	3794	macrodiolide	disorazole	*Sorangium cellulosum So ce12*
bryX	ABK51302.1	3391	3351	*unknown*	bryostatin	*Candidatus Endobugula sertula*
sorB	AAA79984.2	8596	8807	macrolactone	soraphen	*Sorangium cellulosum*
nysK	AAF71768	1849	2058	macrolactone	nystatin	*Streptomyces noursei*
cndF	CAQ43084.1	1113	1365	acid	chondrochlorens	*Chondromyces crocatus Cm c5*
spiJ	CAD43451.1	3373	3574	acid	spirangiene	*Sorangium cellulosum So ce90*
jamP	AAS98787.1	1552	1801	*unknown*	jamaicamides	*Lyngbya majuscula*
mcyC	WP_002742831.1	1030	1225	macrolactam	microcystin	*Microcystis aeruginosa PCC7806*
amphK	AAK73503.1	1817	2026	macrolactone	amphotericin	*Streptomyces nodosus*
lkmAIII	WP_011113114.1	3083	3291	macrolactone	lankamycin	*Streptomyces rochei*
eryAIII	AAU93805.2	2984	3192	macrolactone	erythromycin	*Saccharopolyspora erythraea*
aurC	CAE02606.1	1987	2197	pyrone	aureothin	*Streptomyces thioluteus HKI-227*
nidA5	CAE02606.1	1643	1856	macrolactone	niddamycin	*Streptomyces caelestis*
conF	AAZ94391.1	1832	2045	macrolactone	concanamycin A	*Streptomyces neyagawaensis*
crpD	ABM21572.1	3070	3330	macrolactone	cryptophycins	*Nostoc sp. ATCC 53789*
fscF	AAQ82566.1	1814	2049	macrolactone	FR-008	*Streptomyces sp. FR-008*
mtaG	AAF19815.1	1483	1726	acid	myxothiazol	*Stigmatella aurantiaca DW4-3/1*
herD	AEZ64503.1	1823	2026	acid	Herboxidiene	*Streptomyces chromofuscus*
bafAV	ADC79620.1	1881	2093	macrolactone	bafilomycin	*Streptomyces lohii*
borA6	CAE45672.1Q	1522	1730	macrolactone	borrelidin	*Streptomyces parvulus Tü4055*
jerE	ABK32291.1	2636	2867	lactone	jerangolid	*Sorangium cellulosum*
pldAIV	BAH02271.1	1589	1804	macrolactone	pladienolide	*Streptomyces platensis*
PSPTO_4687	WP_005894401.1	453	651	acid	coronafacic acid	*Pseudomonas syringae*
PSPTO_4699	WP_011105127.1	4269	4445	*unknown*	coronatine	*Pseudomonas syringae*

pikAIV	AAC69332.1	1121	1335	macrolactone	pikromycin	*Streptomyces venezuelae*
plm7	AAQ84147.1	1588	1799	lactone	phoslactomycin B	*Streptomyces sp. HK-803*
simC1C	AEU17898.1	1113	1327	*unknown*	simocyclinone	*Streptomyces antibioticus*
pks2	ADC45515.1	1735	1949	*unknown*		*Streptomyces nanchangensis*
meiA4	ADC45535.1	5066	5269	macrolactone	meilingmycin	*Streptomyces nanchangensis*
zmaQ	ACM79812.1	1919	2167	acid	zwittermicin	*Bacillus cereus*
ttmH	ABI94380.1	7384	7600	acid	tautomycetin	*Streptomyces griseochromogenes*
chmGV	AAS79463.1	1136	1347	macrolactone	Chalcomycin	*Streptomyces bikiniensis*
disC	CAI43934.1	3520	3791	macrodiolide	disorazol	*Polyangium cellulosum*
apoS8	AEP40932.1	1648	1861	macrolactone	Apoptolidin	*Nocardiopsis sp. FU40*
psm3B	WP_004162181.1	1146	1407	*unknown*		*Microcystis aeruginosa*
spnE	AAG23262.1	5363	5577	macrolactone	spinosad	*Saccharopolyspora spinosa*
vinP4	BAD08360.1	3577	3804	macrolactam	vicenistatin	*Streptomyces halstedii*
mlaG	ACO94498.1	1772	1988	macrolactam	ML-449	*Streptomyces sp. MP39-85*
becG	ACO94470.1	1776	1982	macrolactam	BE-14106	*Streptomyces sp. DSM 21069*
Strop_2778	ABP55220.1	3501	3709	macrolactam		*Salinispora tropica CNB-440*
irp1	CAA73127.1	2913	3150	acid	yersinibactin	*Y.enterocolitica*
ttnB	ABI94380.1	7385	7600	acid	tautomycetin	*Streptomyces griseochromogenes*
ABV91287.1	ABV91287.1	7341	7556	acid	tautomycetin	*Streptomyces griseochromogenes*
mmpB	AAM12911.1	1817	2058	acid	mupirocin	*Pseudomonas fluorescens*
bmyC	WP_023356939.1	2318	2529	macrolactam	bacillomycin	*Bacillus amyloliquefaciens*
difL	CAG23983.1	1756	2037	macrolactone	difficidin	*Bacillus amyloliquefaciens*
pieA6	AEZ54379.1	2195	2384	acid	Piericidin	*Streptomyces piomogenus*
chxE	AFO59866.1	6696	6888	*unknown*	cycloheximide	*Streptomyces sp. YIM 56141*
epoF	AAF62885.1	2200	2421	macrolactone	epothilone	*Sorangium cellulosum*
gfsE	BAJ16471.1	3583	3795	macrolactone	FD-891	*Streptomyces graminofaciens*
pelF	CCE88378.1	2220	2422	lactone	Pellasoren	*Sorangium cellulosum*
oocS	AFX60341.1	3773	4069	macrolactone	oocydin	*Serratia plymuthica*
baeR	AGZ56446.1	2180	2455	acid	bacillaene	*Bacillus amyloliquefaciens*
pksR	CAB13606.2	2235	2511	acid	bacillaene	*Bacillus amyloliquefaciens*
barG	AEE88297.1	2622	2874	acid	barbamide	*Lyngbya majuscula*

elaR	AEC04364.1	1600	1877	macrolactone	elansolid	*Chitinophaga pinensis*
Cpin_5289	ACU62720.1	1600	1877	macrolactone	elansolid	*Chitinophaga pinensis*
fosF	AEC13072.1	1708	1922	lactone	Fostriecin	*Streptomyces pulveraceus*
cylH	AFV96142.1	1994	2190	acid	Cylindrocyclophane	*Cylindrospermum licheniforme*
tubF	CAF05651.1	2554	2828	acid	tubulysin	*Cystobacter sp. SBCb004*
chiF	AAY89053.1	5557	5824	macrolactone	chivosazol	*Polyangium cellulosum*
MAV_0218	WP_023871500.1	144	297	*unknown*		*Mycobacterium avium*
MAP_0220	ETB47487.1	139	291	*unknown*		*Mycobacterium avium*
MAP_3742	ETB45250.1	200	486	*unknown*		*Mycobacterium avium*
Mjls_5391	ABO01155.1	1578	1818	*unknown*	mycolic acid	*Mycobacterium sp. JLS*
SAMR0474	CAJ88184.1	6118	6328	*unknown*		*Streptomyces ambofaciens*
cce_3761	ACB53109.1	1055	1277	*unknown*		*Cyanothece sp. ATCC 51142*
SPO0849	YP_166102.1	1879	2019	*unknown*		*Ruegeria pomeroyi DSS-3*
LYNGBM3L_57760	EGJ30011.1	613	865	*unknown*		*Moorea producens*
Francci3_2981	ABD12338.1	1845	2062	*unknown*		*Frankia sp. CcI3*
Mvan_5640	ABM16405.1	1581	1778	*unknown*	mycolic acid	*Mycobacterium vanbaalenii PYR-1*
SADFL11_1546	EEE44259.1	1873	2118	*unknown*		*Labrenzia alexandrii*
Mspyr1_50180	ADU01548.1	1521	1716	*unknown*	mycolic acid	*Mycobacterium gilvum Spyr1*
tugD	ADH04660.1	6394	6596	macrolactone	thuggacin	*Chondromyces crocatus Cm c5*
SACE_4138	CAM03407.1	1595	1797	*unknown*	pke gene cluster	*Saccharopolyspora erythraea NRRL 2338*
SACE_4279	EQD86806.1	815	1048	*unknown*	nrps7 gene cluster	*Saccharopolyspora erythraea NRRL 2338*
SACE_4287	CAM03556.1	3097	3323	*unknown*	nrps7 gene cluster	*Saccharopolyspora erythraea*
Tcur_4756	ACZ00277.1	1892	2077	*unknown*		*Thermomonospora curvata DSM 43183*
VAB18032_24915	AEB46081.1	4266	4511	*unknown*		*Verrucosispora maris AB-18-032*
tgaC	ADH04641.1	6442	6656	macrolactone	thuggacin	*Sorangium cellulosum So ce895*
RGBS107_09711	WP_014879188.1	1896	2130	*unknown*		*Phaeobacter gallaeciensis BS107*
Mflv_1169	ADU01548.1	1521	1716	*unknown*	mycolic acid	*Mycobacterium gilvum PYR-GCK*
MSMEG_6392	AFP42650.1	1579	1720	*unknown*		*Mycobacterium smegmatis str. MC2 155*
Rv3800c	EFP49159.1	479	646	*unknown*		*M. tuberculosis H37Rv*
Rv0405	KAK28653.1	426	652	*unknown*		*M. tuberculosis H37Rv*
ykris0001_35400	EEP93409.1	2151	2385	*unknown*		*Yersinia kristensenii*

SVEN_0485	CCA53772.1	1115	1322	*unknown*		*Streptomyces venezuelae ATCC 10712*
pchF	CCA53804.1	1531	1823	acid	pyochelin	*Pseudomonas aeruginosa*
MT0418	KBG03305.1	547	774	*unknown*	pks6 gene	*Mycobacterium tuberculosis CDC1551*
mbtB	EFD58999.1	574	798	*unknown*	Phenyloxazoline	*Mycobacterium tuberculosis CDC1551*
MT3907	WP_015575375.1	1014	1181	*unknown*	mycolic acid	*Mycobacterium tuberculosis CDC1551*
olmA7	WP_010984327.1	3404	3608	macrolactone	Oligomycin	*Streptomyces avermitilis*
pteA5	WP_010981852.1	3122	3333	macrolactone	polyene macrolide	*Streptomyces avermitilis*
SAV_865	WP_010982303.1	670	897	*unknown*		*Streptomyces avermitilis*
nfa1890	WP_011206718.1	1477	1724	*unknown*		*Nocardia farcinica IFM 10152*
MUL_4983	WP_020726972.1	1521	1716	*unknown*	mycolic acid	*Mycobacterium ulcerans*
Strop_2654	ABP55098.1	1945	2212	acid	sid2 gene cluster	*Salinispora tropica CNB-440*
SGR_6183	YP_001827695.1	3359	3570	*unknown*		*Streptomyces griseus*
SGR_6777	WP_012382207.1	1186	1467	*unknown*		*Streptomyces griseus*
SGR_6785	WP_012382213.1	6667	6878	*unknown*		*Streptomyces griseus*
SGR_814	WP_012378089.1	2941	3148	*unknown*		*Streptomyces griseus*
gll1941	WP_011141939.1	737	956	*unnkown*		*Gloeobacter violaceus*
gll1954	WP_011141952.1	1815	2042	*unnkown*		*Gloeobacter violaceus*
MAE_38550	WP_012266626.1	1076	1281	macrolactam	microcystin	*Microcystis aeruginosa*
Npun_R6587	WP_012412781.1	1171	1421	*unknown*		*Nostoc punctiforme*
Npun_F2184	WP_012408786.1	2236	2501	*unknown*		*Nostoc punctiforme*
Npun_R3023	WP_012409512.1	4187	4451	*unknown*		*Nostoc punctiforme*
Npun_F3173	WP_012409612.1	1146	1394	*unknown*		*Nostoc punctiforme*
Npun_R3425	WP_012409810.1	1549	1803	*unknown*		*Nostoc punctiforme*
CKL_1511	WP_012101903.1	1507	1790	*unknown*		*Clostridium kluyveri DSM 555*
Ndas_0496	WP_013151550.1	1873	2085	*unknown*		*Nocardiopsis dassonvillei*
RSc1811	WP_011001749.1	1728	1977	*unknown*		*Ralstonia solanacearum GMI1000*
RS05859	WP_011003940.1	5392	5654	*unknown*		*Ralstonia solanacearum GMI1000*
MXAN_4296	WP_011554299.1	1147	1307	*unknown*		*Myxococcus xanthus*
MXAN_2798	WP_011552865.1	1827	2069	*unknown*		*Myxococcus xanthus*
MXAN_3618	WP_011553636.1	4305	4556	*unknown*		*Myxococcus xanthus*
MXAN_3636	WP_011553654.1	11619	11937	*unknown*		*Myxococcus xanthus*

MXAN_3779	WP_011553792.1	14019	14269	*unknown*		*Myxococcus xanthus*
MXAN_4000	WP_011554010.1	4259	4511	*unknown*		*Myxococcus xanthus*
MXAN_4079	WP_020478335.1	4209	4470	*unknown*		*Myxococcus xanthus*
sce0345	WP_012232980.1	3591	3814	*unnkown*		*Sorangium cellulosum So ce56*
sce6823	WP_012239431.1	3415	3640	*unnkown*		*Sorangium cellulosum So ce56*
sce8255	WP_012240864.1	1053	1307	*unknown*		*Sorangium cellulosum So ce56*
sce3193	WP_012235824.1	5663	5946	macrolactone	etnangien	*Sorangium cellulosum So ce56*
ROP_19210	WP_012689124.1	3559	3799	*unknown*		*Rhodococcus opacus B4*
ROP_39430	WP_012691127.1	1401	1641	*unknown*		*Rhodococcus opacus B4*
lpg2179	WP_027265435.1	1197	1417	*unknown*		*Legionella pneumophila*
YPO1910	WP_016671762.1	496	733	acid	yersinibactin	*Yersinia pestis*
PSPTO_2600	WP_011104106.1	2927	3164	*unknown*		*Pseudomonas syringae*
RHA1_ro02207	WP_011595005.1	3588	3830	*unknown*		*Rhodococcus jostii RHA1*
RHA1_ro04065	WP_011596563.1	1424	1664	*unknown*		*Rhodococcus jostii RHA1*
Sare_3151	WP_018825763.1	1268	1480	macrolactone	*uncharacterized*	*Salinispora arenicola CNS-205*
Sare_2072	WP_026302140.1	1957	2224	acid	sid1 gene cluster	*Salinispora arenicola CNS-205*
Sare_2407	WP_019032802.1	2889	3096	*unknown*	pksnrps2 gene cluster	*Salinispora arenicola CNS-205*
FAAH human	NP_001432					

2.4.2 Expression & Purification of Thioesterase Proteins

Expression vector encoding wild-type DEBS TE (pRSG33) was transformed into chemical competent *E. coli* BL21(DE3) for protein expression. Luria-Bertani (LB, 400 mL) media supplemented with 50 µg/mL of ampicillin was inoculated with 0.5% *v/v* of a dense overnight culture of *E. coli* BL21(DE3) with pRSG33, and grown at 30 °C to OD600 of 0.6. Protein expression was introduced by adding isopropanol thiogalactoside (IPTG, Sigma-Aldrich) to a final concentration of 0.1 mM. Cultures were incubated at 30 °C, with shaking at 200 rpm, for 12 h.

Protein purification was performed at 4 °C. Cells were harvested by centrifugation at 4000 G, and resuspended in lysis buffer (10 mL, 100 mM sodium phosphate, 300 mM NaCl, 10% *v/v* glycerol, 1 mg/mL lysozyme, 1 µg/mL leupeptin, pH 8.0). The cells were disrupted by sonication on ice, and cell debris was removed by centrifugation at 15,000 G (4 °C). After adding imidazole to a final concentration of 10 mM, the cleared lysate was incubated for 1 h with nickel-nitrilotriacetic acid (Ni-NTA, 400 µL) resin (QIAGEN, Valencia, CA) and loaded onto a column. The resin was rinsed with wash buffer (100 mM Tris, 300 mM NaCl, 20 mM imidazole, pH 8.0), and protein was eluted with wash buffer supplemented with 250 mM imidazole. Purified protein was exchanged into dialysis buffer (100 mM Tris, 300 mM NaCl, 20% *v/v* glycerol, pH 7.43) and concentrated by centrifugation (Amicon 5000 MWCO). The concentrated proteins were flash-frozen in liquid nitrogen and placed in long-term storage (-80 °C). Protein concentration was determined by Bradford assay (Bio-rad). Approximately 5 mg of purified DEBS TE was obtained *per* liter of cell culture.

Expression and purification of DEBS TE mutant D169A was done as described by Dr. Meng Wang in his doctoral dissertation, and corresponding publication.[61]

S2.5 Future Directions: Combining Lessons from Both Studies (Chapter 7)

S2.5.1 A Proposed Biosynthetic Pathway to Neopeltolide

During the discovery of neopeltolide, the genome for the producing organism was not sequenced and re-isolation has not been realized to date. This suggests that neopeltolide may have been produced by symbiotic bacteria, and could make it impossible to harvest natural material again. Because of this, my presented research has been toward the design of an engineered *de novo* PKS pathway that could produce neopeltolide in a rapid, reliable, and sustainable fashion. Using sound knowledge based on type-I PKS architecture, it is possible to propose a plausible pathway that could be used in physiological producing conditions (Figure S35).

Methylation is well characterized at the α-position relative to the thioester carbonyl,[62] alkylation at the β-position – such as the C9-methyl group of neopeltolide – is less-commonly observed. The common understanding is that β-branching is introduced through an "HMGS cassette" of enzymes performing reactions akin to mevalonate biosynthesis.[63] This set of catalytic domains includes an HMGS homolog (HCS), a decarboxylative ketosynthase (KS^{Q}), and enoyl-CoA hydratase homologs responsible for dehydration (ECH1) and decarboxylation (ECH2) transformations.

Computational data for the macrocyclic core of neopeltolide indicated that the native *cis*-THP configuration was not energetically favored, and suggested this structural element was not generated spontaneously. It is hypothesized that a pyran synthase (PS) catalyzes intramolecular attack of an immature acyl-intermediate, prior to macrocyclization during off-loading from the PKS protein.

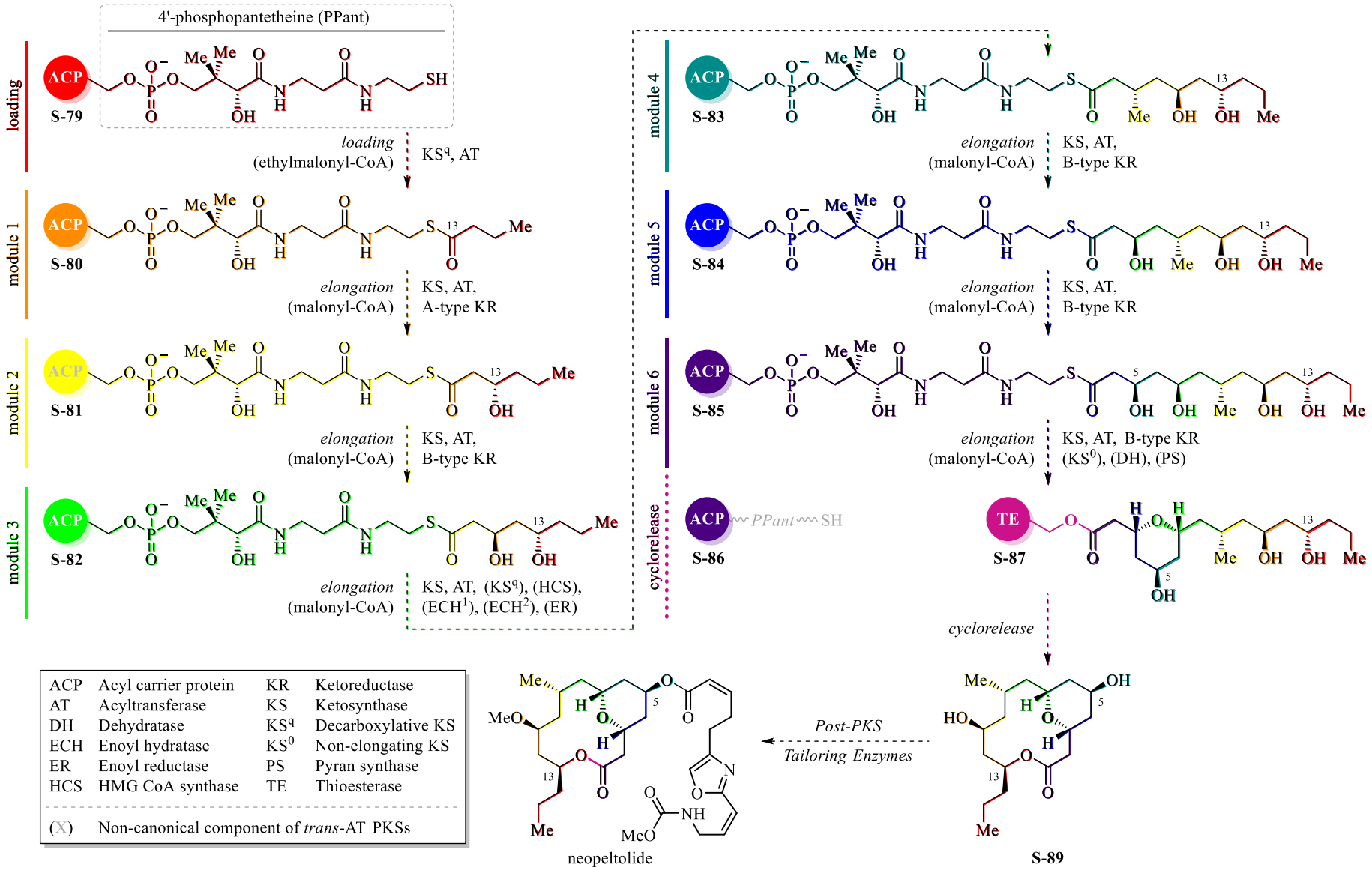

Figure S35 – Proposed biosynthetic pathway for neopeltolide. Generation of *cis*-THP is hypothesized to be an enzyme (PS)-mediated process, and not spontaneously once off-loaded from protein. Without re-isolation of the producing organism, elucidation of the true biosynthetic pathway will not be possible.

S2.5.2 Chemoenzymatic Development of Complete Diastereomeric Triketide Lactone Libraries

Córdova's amino-acid-catalyzed asymmetric synthesis was proposed as an efficient strategy to efficiently generate enantiopure triketide δ-lactones.[64] This methodology has potential to install four stereogenic centers with near-exclusive enantio- and diastereoselectivity using proline catalysts. Unfortunately, this method would only generate four of the potential 16 stereoisomers, and would require standard chemical catalysis such as Evans-type aldol reactions to complete the full diastereomeric library. Building these libraries would require extensive man-hours, but in addition to populating our library of precursors for the characterization of thioesterase domains, these chiral scaffolds could serve as desirable building blocks for other synthetic endeavours and drug-development.

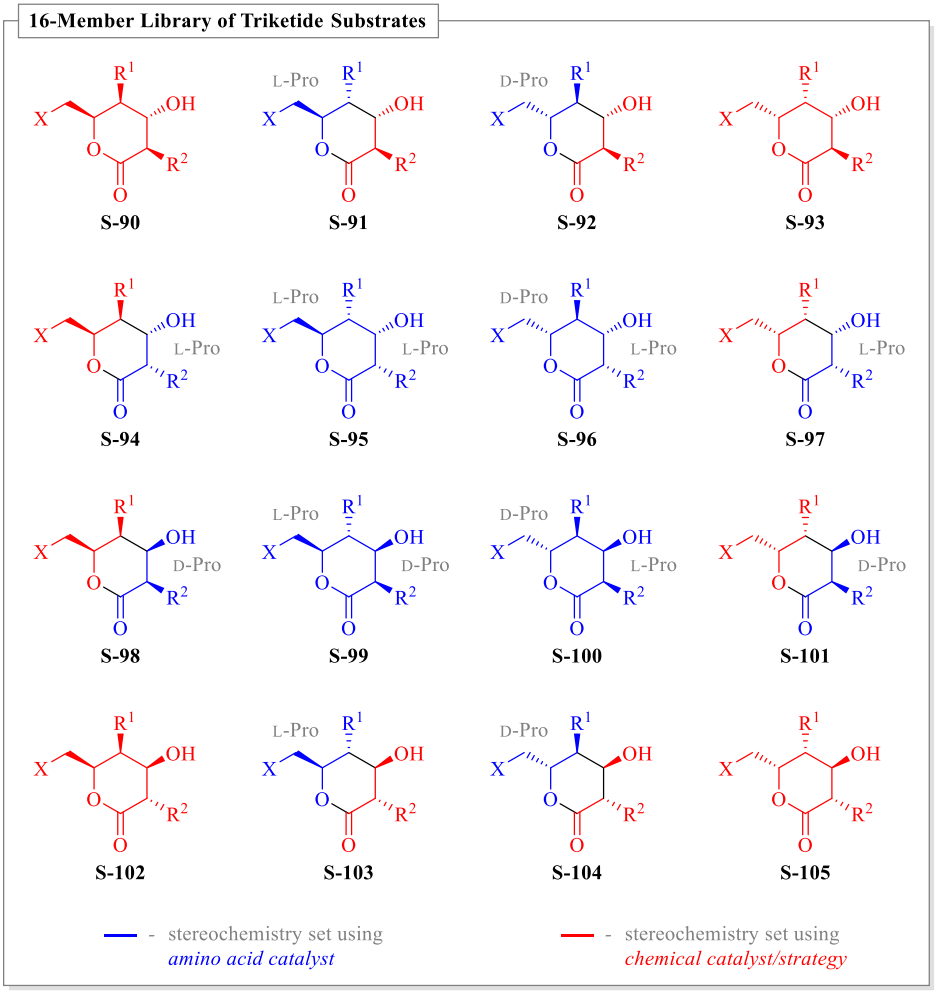

Figure S36 – Complete diastereomeric 16-membered library of triketide δ-lactone substrates. Assembly would require combination of Córdova's amino-acid-catalytic methodology and standard chemical catalytic strategies.

S2.5.3 Proposed Research Beyond the Scope of this Dissertation

The preliminary testing by Kozmin suggested the putative cellular target of neopeltolide is cytochrome bc_1 (complex III) of the electron-transport chain.[21] This transmembrane reducing protein is critical to oxidative phosphorylation and to maintain efflux of protons between the mitochondrial matrix and intermembrane space. Cancerous cells have increased dependency on glycolysis due to their rapid-division, which makes them particularly vulnerable to disruption of ATP synthesis. This is the basis for the suggested mechanism of action, though it remains uncertain how much of a role the inhibition of cytochrome bc_1 plays in the potent antiproliferative activity of neopeltolide, if at all. In fact, a report by Singh and coworkers suggests the activity of bc_1 is already reduced in cancer cell lines and that impairment of the complex contributes to their proliferation.[65]

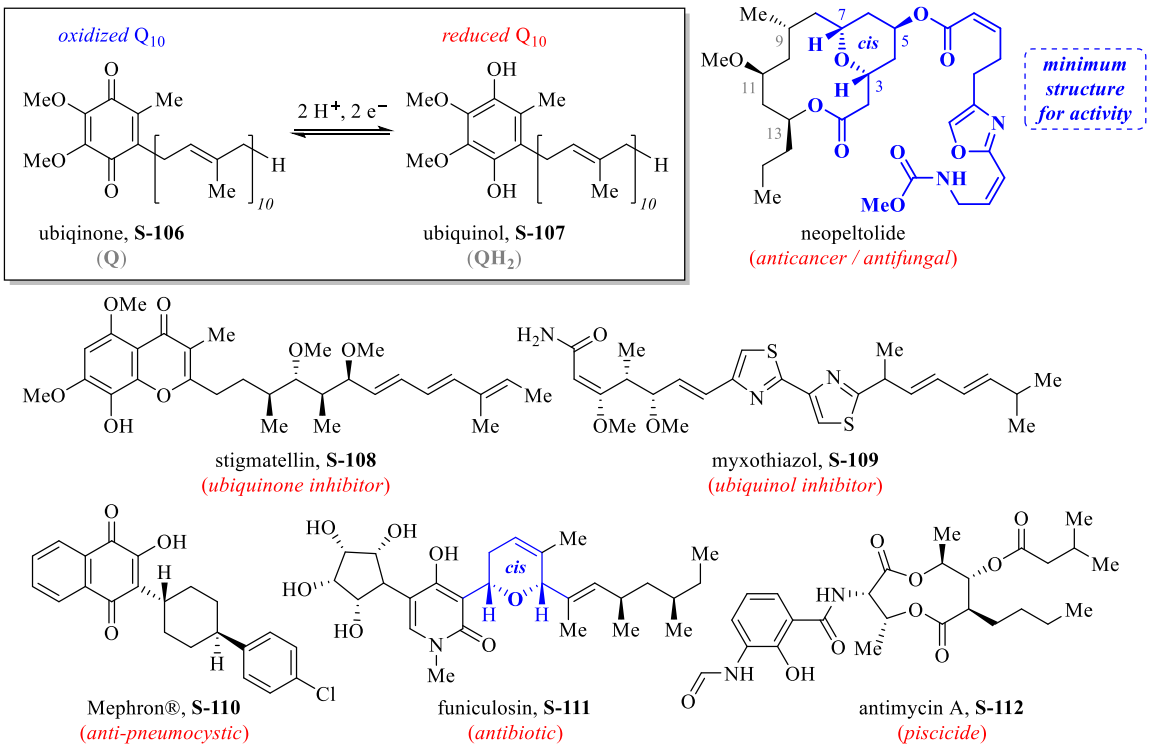

Figure S37 – The two forms of coenzyme Q_{10} are highlighted to illustrate the limited structural-homology with the macrocyclic core of neopeltolide. A selection of known cytochrome bc_1 inhibitors are included to emphasize the differences.

Interestingly, Kozmin's work indicates that neither neopeltolide or the synthetic congener of leucascandrolide A could inhibit other complexes of the electron-transport chain.[21] This is particularly important because complexes I, II and III all rely on coenzyme Q_{10}, which is a cofactor that functions as the electron carrier between complexes.[66] Coenzyme Q_{10} (Figure S37) is crucial since no other molecular can perform this function and the archetypical disruption point for the mechanism of inhibition. All bc_1

inhibitors act on either the ubiquinol oxidation or ubiquinone reduction site,[67] and primarily display fungicidal or antibiotic activities.

Aim S1: Controlled Re-Evaluation of Biological Activity

Neopeltolide is a potent inhibitor of the fungal pathogen *Candida albicans* (0.625 μg/mL),[68] and it was shown that the oxazole-bearing side chain was responsible for this activity.[69] As cytochrome bc_1 inhibitors often display antifungal activity, Kozmin's observations may not be the result of the antiproliferative activity. Unlike the biological evaluation of leucascandrolide A by D'Ambrosio,[69] the macrocyclic core and side-chain were not tested separately as controls. Moreover, Fuwa noted that the bioactivity of neopeltolide was strongly dose- and time-dependent in the commonly-used A549 (lung), MCF-7 (breast), and P388 (leukemia) cancer cell lines, emphasizing the benefit of thoroughly re-evaluating the bioactivity. This evaluation would rapidly provide insight into the structural elements that affect cytochrome bc_1, and to eliminate the potential of this target being a false-positive.

Aim S2: Determination of Protein Target *via* Activity-Based Proteomics

Independent of the results from Aim S1, the inconclusive role of cytochrome bc_1 in the antiproliferative bioactivity of neopeltolide warrants an investigation of its cellular target. The cellular effects of neopeltolide and its synthetic analogs remain largely-underexplored, and the biochemical mechanism-of-action (MOA) for its antiproliferative properties unknown. Though this knowledge is not required for clinical candidates,[70] it could better enable the use of neopeltolide as a tool for biological testing. Cytochrome bc_1 is well-studied, and if this putative target is confirmed, it could potentially reveal a novel mechanism or binding site from that of other known inhibitors (Figure S37). This result would benefit the investigation of eukaryotic energy metabolism and the treatment of energy metabolism-directed cancers.[71]

Derivatization of the macrocyclic core of neopeltolide as a bioorthogonal probe for activity-based protein profiling (ABPP[1]) can be used to identify its cellular target (Figure S38). ABPP is a powerful tool that can provide insights into active-site residues or sequences of the binding target, which can be used to refine the design of neopeltolide analogs *via* target-oriented synthesis. Design of the arbitrary 2-alkynyl-neopeltolide probe **S-113** could be realized by enolate addition of the macrocyclic core product of the transannular oxa-conjugate addition pyran-formation. This probe would allow Click-chemistry coupling with a cleavable azido tag **S-116** following *in situ* labelling of specific cell lines like A549, MCF-7, or

[1] The reader is encouraged to review the wealth of material available on ABPP for details on this methodology,[70,75–78] as it is beyond the scope of this thesis.

P388. The study could also employ human cancer cell line panels for anti-cancer drug screening, such as NCI-60[72] and JCFR39,[73] to broaden the scope of evaluation. Alternatively, use of a coumarin-based probe could be employed for fluorescent tagging and live-cell imaging.[74] This methodology was developed by an impressive cast of researchers who found that ethyl 7-dimethylaminocoumarin-4-acetate-based probes of macrocyclic polyketides did not see any adverse effects on bioactivity from its incorporation.

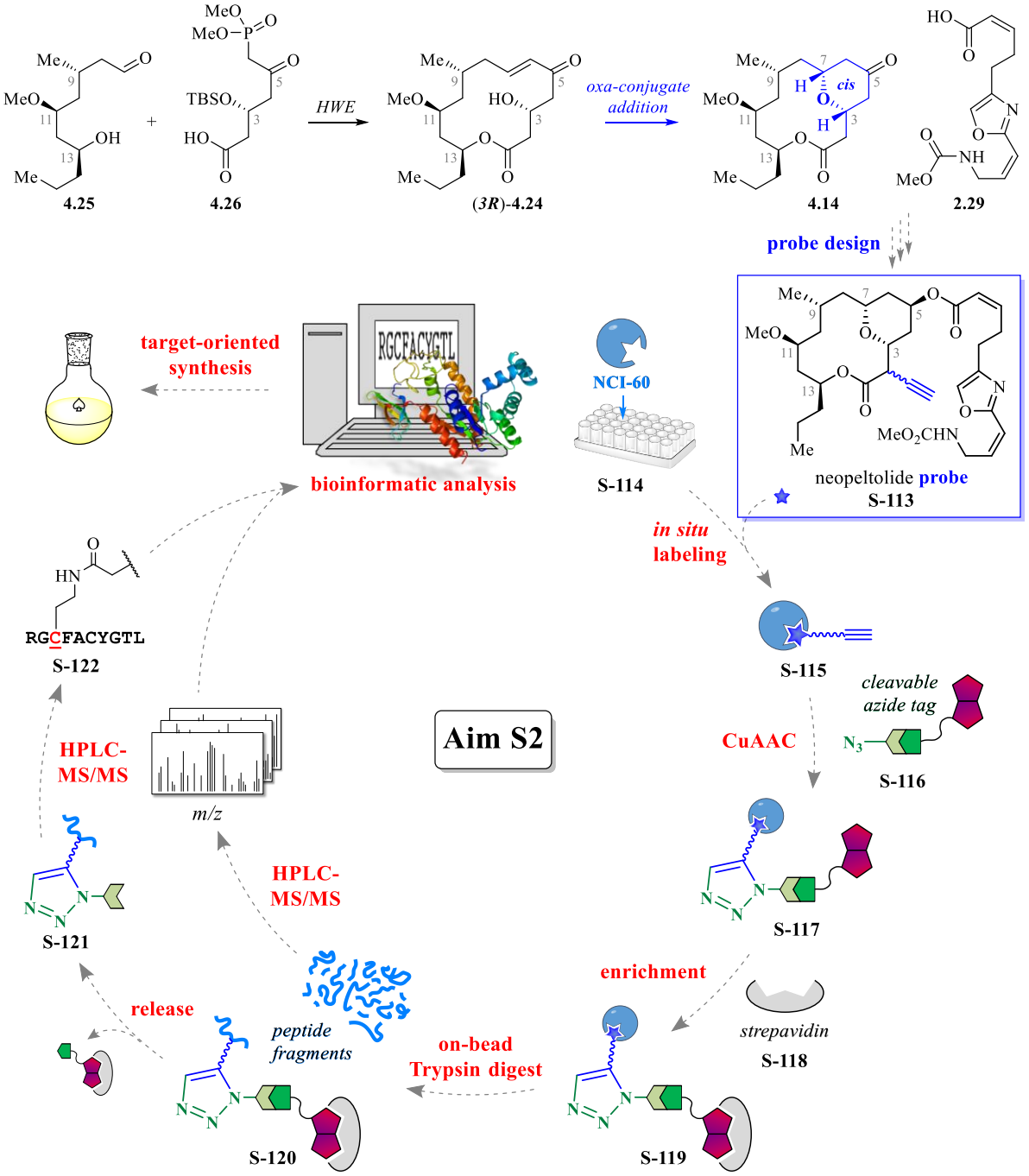

Figure S38 – Summary of experiments for proposed activity-based protein profiling to investigate the cellular target of neopeltolide. Probe- and tag-design are arbitrarily depicted as handles for Click-chemistry.

S2.6 References

(1) Ghosh, A. K.; Shurrush, K. A.; Dawson, Z. L. *Org. Biomol. Chem.* **2013**, *11* (44), 7768–7777.
(2) Vintonyak, V. V; Kunze, B.; Sasse, F.; Maier, M. E. *Chemistry*, **2008**, *14* (35), 11132–11140.
(3) Vintonyak, V. V; Maier, M. E. *Org. Lett.* **2008**, *10* (6), 1239–1242.
(4) Bai, Y.; Davis, D. C.; Dai, M. *Angew. Chem. Int. Ed.* **2014**, *53*, 6519–6522.
(5) Paterson, I.; Miller, N. *Chem. Commun.* **2008**, No. 39, 4708–4710.
(6) Tu, W.; Floreancig, P. E. *Angew. Chem. Int. Ed.* **2009**, *48* (25), 4567–4571.
(7) Cui, Y.; Tu, W.; Floreancig, P. E. *Tetrahedron* **2010**, *66* (26), 4867–4873.
(8) Youngsaye, W.; Lowe, J. T.; Pohlki, F.; Ralifo, P.; Panek, J. S. *Angew. Chem. Int. Ed.* **2007**, *46* (48), 9211–9214.
(9) Fuwa, H.; Naito, S.; Goto, T.; Sasaki, M. *Angew. Chem.* **2008**, *120* (25), 4815–4817.
(10) Raghavan, S.; Samanta, P. K. *Org. Lett.* **2012**, *14* (9), 2346–2349.
(11) Fuwa, H.; Saito, A.; Sasaki, M. *Angew. Chem.* **2010**, *122* (17), 3105–3108.
(12) Guinchard, X.; Roulland, E. *Org. Lett.* **2009**, *11* (20), 4700–4703.
(13) Fuwa, H.; Noto, K.; Kawakami, M.; Sasaki, M. *Chem. Lett.* **2013**, *42* (9), 1020–1022.
(14) Custar, D. W.; Zabawa, T. P.; Scheidt, K. A. *J. Am. Chem. Soc.* **2008**, *130* (3), 804–805.
(15) Kim, H.; Park, Y.; Hong, J. *Angew. Chem. Int. Ed.* **2009**, *48* (41), 7577–7581.
(16) Athe, S.; Chandrasekhar, B.; Roy, S.; Pradhan, T. K.; Ghosh, S. *J. Org. Chem.* **2012**, *77*, 9840–9845.
(17) Yu, M.; Schrock, R. R.; Hoveyda, A. H. *Angew. Chem. Int. Ed.* **2015**, *54* (1), 215–220.
(18) Sharma, G. V. M.; Reddy, S. V.; Ramakrishna, K. V. S. *Org. Biomol. Chem.* **2012**, *10* (18), 3689–3695.
(19) Martinez-Solorio, D.; Jennings, M. P. *J. Org. Chem.* **2010**, *75* (12), 4095–4104.
(20) Yang, Z.; Zhang, B.; Zhao, G.; Yang, J.; Xie, X.; She, X. *Org. Lett.* **2011**, *13* (21), 5916–5919.
(21) Ulanovskaya, O.; Janjic, J.; Suzuki, M.; Sabharwal, S. S.; Schumacker, P. T.; Kron, S. J.; Kozmin, S. *Nat. Chem. Biol.* **2008**, *4* (7), 418–424.
(22) Taylor, R. E.; Kartika, R.; Gruffi, T. R. *Org. Lett.* **2008**, *10* (21), 5047–5050.
(23) Woo, S. K.; Kwon, M. S.; Lee, E. *Angew. Chem. Int. Ed.* **2008**, *47* (17), 3242–3244.
(24) Yadav, J. S.; Krishana, G. G.; Kumar, S. N. *Tetrahedron* **2010**, *66* (2), 480–487.
(25) Fuwa, H.; Saito, A.; Naito, S.; Konoki, K.; Yotsu-Yamashita, M.; Sasaki, M. *Chem. Eur. J.* **2009**, *15*, 12807–12818.
(26) Wadsworth, W. S.; Emmons, W. D. *J. Am. Chem. Soc.* **1961**, *83* (7), 1733–1738.
(27) Molecular Operating Environment (MOE^{TM}), 2013.08; Chemical Computing Group Inc., 2017.
(28) Bond, S. D.; Leimkuhler, B. J.; Laird, B. B. *J. Comp. Phys.* **1998**, *151*, 1–17.
(29) Labute, P. *Proteins Struct. Funct. Bioinforma.* **2009**, *75* (1), 187–205.
(30) Halgren, T. *J. Comput. Chem.* **1996**, *17* (5–6), 490–519.
(31) Becke, A. D. *J. Chem. Phys.* **1993**, *98*, 5648–5652.
(32) Miehlich, B.; Savin, A.; Stoll, H.; Preuss, H. *Chem. Phys. Lett.* **1989**, *157* (3), 200–206.
(33) Lee, C.; Yang, W.; Parr, R. G. *Phys. Rev. B* **1988**, *37* (2), 785–789.
(34) Frisch, M.; Trucks, G.; Schlegel, H.; Scuseria, G.; Robb, M.; Cheeseman, J.; Scalmani, G.; Barone, V.; Mennucci, B.; Petersson, G.; Nakatsuji, H.; Caricato, M.; Li, X.; Hratchian, H.; Izmaylov, A.; Bloino, J.; Zheng, G.; Sonnenberg, J.; Hada, M.; Ehara, M.; Toyota, K.; Fukuda, R.; Hasegawa, J.; Ishida, M.; Nakajima, T.; Honda, Y.; Kitao, O.; Nakai, H.; Vreven, T.; Montgomery, J.; Peralta, J.; Ogliaro, F.; Bearpark, M.; Heyd, J.; Brothers, E.; Kudin, K.; Staroverov, V.; Kobayashi, R.; Normand, J.; Raghavachari, K.; Rendell, A.; Burant, J.; Iyengar, S.; Tomasi, J.; Cossi, M.; Rega, N.; Millam, J.; Klene, M.; Knox, J.; Cross, J.; Bakken, V.; Adamo, C.; Jaramillo, J.; Gomperts, R.; Stratmann, R.; Yazyev, O.; Austin, A.; Cammi, R.; Pomelli, C.; Ochterski, J.; Martin, R.; Morokuma, K.; Zakrzewski, V.; Voth, G.; Salvador, P.; Dannenberg, J.; Dapprich, S.; Daniels, A.; Farkas, Ö.; Foresman, J.; Ortiz, J.; Cioslowski, J.; Fox, D. Gaussian, Inc.: Wallingford, CT 2009.
(35) Hari, T. P. A.; Wilke, B. I.; Davey, J. A.; Boddy, C. N. *J. Org. Chem.* **2016**, *81*, 415–423.
(36) Sinisterra, J. V.; Barrios, J.; Mouloungui, Z. *Bull. Soc. Chim. Belg.* **1991**, *100* (3), 267–275.
(37) Pascariu, A.; Ilia, G.; Bora, A.; Iliescu, S.; Popa, A.; Dehelean, G.; Pacureanu, L. *Cent. Eur. J. Chem.* **2003**, *4*, 491–542.
(38) Barrios, J.; Marinas, J. M.; Sinisterra, J. V. *Bull. Chem. Soc. Belg.* **1986**, *95* (2), 107–117.
(39) Alvarez-lbarra, C.; Arias, S.; Baiion, G.; Fernandez, M. J.; Rodriguez, M.; Sinisterra, V. *J. Chem. Soc., Chem. Commun.* **1987**, 1509–1511.
(40) Ibarra, C. A.; Arias, S.; Fernandez, M. J.; Sinisterra, J. V. *J. Chem. Soc., Perkin Trans. II* **1989**, 503–508.

(41) Weber, W. P.; Gokel, G. W. *Phase Transfer Catalysis in Organic Synthesis*; Springer-Verlag, 1977; Vol. 4.
(42) Mouloungui, Z.; Delmas, M.; Gaset, A. *J. Org. Chem.* **1989**, *54* (16), 3936–3941.
(43) Piechucki, C. *Synthesis*, **1974**, No. December, 869–870.
(44) Heathcock, C. H.; Hadley, C. R.; Rosen, T.; Theisen, P. D.; Hecker, S. J. *J. Med. Chem.* **1987**, *30* (10), 1858–1873.
(45) Ianni, A.; Waldvogel, S. R. *Synthesis*, **2006**, No. 13, 2103–2112.
(46) Maloney, K. M.; Chung, J. Y. L. *J. Org. Chem.* **2009**, *74* (19), 7574–7576.
(47) Dakarapu, U. S.; Bokka, A.; Asgari, P.; Trog, G.; Hua, Y.; Nguyen, H. H.; Rahman, N.; Jeon, J. *Org. Lett.* **2015**, *17* (23), 5792–5795.
(48) Magnus, P.; Giles, M.; Bonnert, R.; Johnson, G.; McQuire, L.; Deluca, M.; Merritt, A.; Kim, C. S.; Vicker, N. *J. Am. Chem. Soc.* **1993**, *115* (18), 8116–8129.
(49) Kolb, H. C.; Ley, S. V; Slawin, A. M.; Williams, D. J. *J. Chem. Soc., Perkin Trans. 1* **1992**, No. January, 2735–2762.
(50) Blanchette, M. A.; Choy, W.; Davis, J. T.; Essenfeld, A. P.; Masamune, S.; Roush, W. R. *Tetrahedron Lett.* **1984**, *25* (21), 2183–2186.
(51) Schauer, D. J.; Helquist, P. *Synthesis*, **2006**, No. 21, 3654–3660.
(52) Houghton, S. R.; Furst, L.; Boddy, C. N. *J. Org. Chem.* **2009**, *74* (4), 1454–1463.
(53) Hilli, F.; White, J. M.; Rizzacasa, M. *Org. Lett.* **2004**, *6* (8), 1289–1292.
(54) Kanematsu, M.; Shishido, K. *J. Synth. Org. Chem. Jpn.* **2012**, *70* (11), 1196–1205.
(55) Edgar, R. C. *Nucleic Acids Res.* **2004**, *32* (5), 1792–1797.
(56) Tamura, K.; Peterson, D.; Peterson, N.; Stecher, G.; Nei, M.; Kumar, S. *Mol. Biol. Evol.* **2011**, *28* (10), 2731–2739.
(57) Abascal, F.; Zardoya, R.; Posada, D. *Bioinformatics* **2005**, *21* (9), 2104–2105.
(58) Conway, K. R.; Boddy, C. N. *Nucleic Acids Res.* **2013**, *41* (D1), 402–407.
(59) Guindon, S.; Dufayard, J.-F.; Lefort, V.; Anisimova, M.; Hordijk, W.; Gascuel, O. *Syst. Biol.* **2010**, *59* (3), 307–321.
(60) Anisimova, M.; Gascuel, O. *Syst. Biol.* **2006**, *55* (4), 539–552.
(61) Wang, M.; Boddy, C. N. *Biochemistry* **2008**, *47* (45), 11793–11803.
(62) Staunton, J.; Weissman, K. J. *Nat. Prod. Rep.* **2001**, *18* (4), 380–416.
(63) Calderone, C. T.; Iwig, D. F.; Dorrestein, P. C.; Kelleher, N. L.; Walsh, C. T. *J. Chem. Biol.* **2007**, *14*, 835–846.
(64) Casas, J.; Engqvist, M.; Ibrahem, I.; Kaynak, B.; Córdova, A. *Angew. Chem. Int. Ed.* **2005**, *44* (9), 1343–1345.
(65) Owens, K. M.; Kulawiec, M.; Desouki, M. M.; Vanniarajan, A.; Singh, K. K. *PLoS One* **2011**, *6* (8).
(66) Deichmann, R.; Lavie, C.; Andrews, S. *Ochsner J.* **2010**, *10*, 16–21.
(67) Xiao, Y. M.; Esser, L.; Zhou, F.; Li, C.; Zhou, Y. H.; Yu, C. A.; Qin, Z. H.; Xia, D. *PLoS One* **2014**, *9* (4), 1–12.
(68) Wright, A. E.; Botelho, J. C.; Guzmán, E.; Harmody, D.; Linley, P.; McCarthy, P. J.; Pitts, T. P.; Pomponi, S.; Reed, J. K. *J. Nat. Prod.* **2007**, *70* (3), 412–416.
(69) D'Ambrosio, M.; Guerriero, A.; Pietra, F.; Debitus, C. *Helv. Chim. Acta* **1996**, *79* (1), 51–60.
(70) Gregori-puigjané, E.; Setola, V.; Hert, J.; Crews, B. A.; Irwin, J. J.; Lounkine, E. *Proc. Natl. Acad. Sci.* **2012**, *109* (28), 11178–11183.
(71) Altmann, K.-H.; Carreira, E. M. *Nat. Chem. Biol.* **2008**, *4* (7), 388–389.
(72) Shoemaker, R. H. *Nat. Rev.* **2006**, *6* (10), 813–823.
(73) Kong, D.; Yamori, T. *Bioorg. Med. Chem. Lett.* **2012**, *20* (6), 1947–1951.
(74) Alexander, M. D.; Burkart, M. D.; Leonard, M. S.; Portonovo, P.; Liang, B.; Ding, X.; Joullié, M. M.; Gulledge, B. M.; Aggen, J. B.; Chamberlin, A. R.; Sandler, J.; Fenical, W.; Cui, J.; Gharpure, S. J.; Polosukhin, A.; Zhang, H. R.; Evans, P. A.; Richardson, A. D.; Harper, M. K.; Ireland, C. M.; Vong, B. G.; Brady, T. P.; Theodorakis, E. A.; La Clair, J. J. *ChemBioChem* **2006**, *7* (3), 409–416.
(75) Cravatt, B. F.; Wright, A. T.; Kozarich, J. W. *Annu. Rev. Biochem.* **2008**, *77* (1), 383–414.
(76) Thirumurugan, P.; Matosiuk, D.; Jozwiak, K. *Chem. Rev.* **2013**, *113*, 4905–4979.
(77) Sadaghiani, A. M.; Verhelst, S. H. L.; Bogyo, M. *Curr. Opin. Chem. Biol.* **2007**, *11*, 1–9.
(78) Rix, U.; Superti-furga, G. *Nat. Chem. Biol.* **2009**, *5* (9), 616–624.

S2.7 Re-Prints of Publications

NPR

RSC Publishing

REVIEW

View Article Online
View Journal | View Issue

Published on 24 September 2013. Downloaded by University of Ottawa on 04/11/2014 16:44:57.

Cite this: *Nat. Prod. Rep.*, 2013, **30**, 1391

The role of transcription in heterologous expression of polyketides in bacterial hosts

D. Cole Stevens,[ab] Taylor P. A. Hari[b] and Christopher N. Boddy*[b]

Received 29th June 2013

DOI: 10.1039/c3np70060g

www.rsc.org/npr

Heterologous expression of biosynthetic pathways is an indispensable tool in the discovery, production, engineering, and characterization of bacterial polyketides and the complex enzymology involved in their biosynthesis. Ensuring transcription of polyketide biosynthetic gene clusters in heterologous hosts is a pressing problem. This review evaluates the two strategies used to ensure transcription. The first is a promoter replacement approach where promoters known to function in the heterologous host are inserted into the biosynthetic gene cluster. The second is an approach that relies on the heterologous host recognizing and utilizing promoters native to the gene cluster. Both have been successful methodologies and have different strengths and weaknesses, which are highlighted and discussed.

1 Introduction
2 Challenges in heterologous expression of polyketides
3 Promoter replacement to ensure transcription
3.1 The actI/actIII promoter
3.2 The T7 promoter
3.3 The ermE promoter
3.4 The Pm promoter
3.5 The tet promoter
3.6 Other promoters
4 Transcription from native promoters
4.1 *Streptomyces* as heterologous hosts
4.2 Myxobacteria as heterologous hosts
4.3 *E. coli* as a heterologous host
5 Conclusion
6 References

1 Introduction

Heterologous expression of biosynthetic pathways has proven to be an indispensable tool in the discovery, production, engineering, and characterization of bacterial secondary metabolites and the complex enzymology involved in their biosynthesis.[1–4] The heterologous production of a secondary metabolite requires the necessary biosynthetic genes to be inserted into a non-native host (the heterologous host). The genes must then be transcribed, translated, and the subsequent enzymes correctly folded, and post-translationally modified to be functional. In many cases it is also essential that specific substrates required for the biosynthesis of the natural product be produced.[3–5] This multistep process places stringent requirements on the heterologous host, limiting the bacterial strains capable of acting as a heterologous host, and the natural product biosynthetic pathways that can be produced through heterologous expression.

Originally developed in the early 1980s, heterologous production of natural products has been instrumental in addressing a wide variety of research questions.[3,4] The expression and manipulation of biosynthetic pathways in heterologous hosts has dramatically increased our understanding of the mechanisms of natural product biosynthesis.[4] Heterologous expression of biosynthetic pathways has become a key tool for the combinatorial biosynthesis of libraries of natural product-like analogues, particularly when genetic modification of the biosynthetic pathways in the native producing strain is challenging.[4,6–8] Due to the biomedical and clinical applications intrinsic to natural products, substantial effort has been placed into development of heterologous production platforms capable of over-producing these compounds, enabling a decrease in production cost and production time.[4,9] Heterologous expression is also proving to be essential for characterizing the metabolites produced from cryptic or silent biosynthetic pathways, sequenced gene clusters with no known small molecule product.[4,6] Finally, one of the most exciting applications of heterologous expression is for the discovery of new natural products through bioprospecting of metagenomic or environmental DNA (eDNA) libraries.[10] This approach to natural product discovery will likely enable researchers to discover natural products from uncultivable bacterial strains, whose biosynthetic potential are

[a]*Department of Chemistry, University of Notre Dame, Notre Dame, USA*
[b]*Department of Chemistry and the Center for Advanced Research in Environmental Genomics, University of Ottawa, Ottawa, Canada. E-mail: cboddy@uottawa.ca; Fax: +613-562-5170; Tel: +613-562 5800 x8970*

This journal is © The Royal Society of Chemistry 2013

View Article Online

Published on 24 September 2013. Downloaded by University of Ottawa on 04/11/2014 16:44:57.

virtually untapped.[11–13] While tremendous efforts have been made in all these research areas, heterologous expression techniques have not evolved substantially since their inception.

The polyketides represent one of the first and most successful classes of secondary metabolites to be heterologously expressed in bacteria.[1,2] Polyketides are a large class of natural products possessing a wide range of chemical diversity and biological activities (Fig. 1). As these compounds function to improve bacterial fitness through selective and specific interactions with biological targets, many have been successfully developed into clinical drugs including tetracycline, epothilone, rapamycin, erythromycin, FK506, doxorubicin, and bleomycin.[1,14,15]

These complex molecules are produced by polyketide synthases (PKSs). PKS enzymes construct broad ranges of cyclic and linear carbon-based scaffolds using simple substrates from primary metabolism such as malonyl-CoA and methylmalonyl-CoA. The malonyl- or methylmalonyl-extender units

David Cole Stevens received his Bachelor of Science from Northwestern State University in 2006. He obtained his PhD in chemistry at the University of Ottawa in 2011 under the supervision of Christopher N. Boddy. He is currently a postdoctoral fellow in the Richard E. Taylor laboratory at the University of Notre Dame where he is investigating the biosynthesis and heterologous expression of polyketide inhibitors of eukaryotic protein synthesis. His research focuses on increasing the utility of heterologous expression towards the production, characterization, and discovery of microbial natural products.

Taylor P.A. Hari received his B.Sc. with Honours in Medicinal Chemistry (2009), and M.Sc. in Chemistry (2012) from the University of Ottawa, Canada. He is currently completing his Ph.D. research under the direction of Christopher N. Boddy at the University of Ottawa. In addition, Taylor will receive his Type II-MBA in Scientific Management and Leadership from the Telfer School of Management at the University of Ottawa. His research focuses on total synthesis and chemoenzymatic studies used to better understand biosynthetic details of tetrahydropyran formation, and macrocyclization in polyketide natural products.

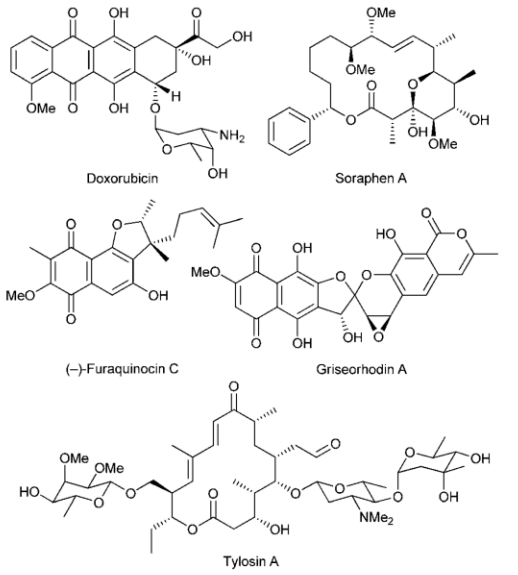

Fig. 1 Polyketides of diverse structure, biosynthetic origin, and biological function have been heterologously expressed.

are tethered as thioesters onto phosphopantetheinylated acyl carrier domains (ACPs). These extender units are attached to specific ACPs by highly substrate specific acyl-transferase (AT) domains. Tethered thioesters are then elongated through decarboxylative Claisen condensation with the extender units. This reaction is catalysed by a ketosynthase (KS).[14] The ACP, AT, and KS represent the minimal catalytic domains necessary to elongate polyketide thioester intermediates. Reduction of the β-ketothioesters produced by the KS domain is catalysed by

Christopher Boddy received a Bachelors of Science from the University of Alberta in 1995 and a PhD at The Scripps Research Institute in 2001 under the direction of K. C. Nicolaou. He was a Post-doctoral Fellow at Stanford University working with Chaitan Khosla from 2001–2004. In 2004 he joined the Department of Chemistry at Syracuse University and in 2008 moved to the University of Ottawa, Departments of Chemistry and Biology where he is currently an Associate Professor. His research program focuses on harnessing biosynthetic pathways to produce complex molecules. More information about his research program can be found at www.boddylab.ca.

This journal is © The Royal Society of Chemistry 2013

View Article Online

Published on 24 September 2013. Downloaded by University of Ottawa on 04/11/2014 16:44:57.

ketoreductase (KR), dehydratase (DH), and enoyl reductase (ER) domains, yielding β-hydroxy, α,β-unsaturated, and saturated thioesters, respectively. The completed polyketide chain is then off-loaded from the ACP often *via* thioesterase (TE) catalysed hydrolysis or macrocyclization. The free polyketide chain may then be tailored by a diverse set of enzymes, including cyclases (CYC), aromatases (ARO), oxidases, reductases, acylases, and glycosyl transferases. These tailoring steps dramatically increase the chemical diversity accessible from PKS biosynthesis.[14]

PKS pathways have a number of features that make them well suited for heterologous expression. For example, the vast majority of bacterial and many fungal PKS biosynthetic genes cluster together.[4] These clusters encode not only the required PKS biosynthetic enzymes but when necessary the resistance enzymes specific to the produced metabolite, enzymes required to produce unusual building blocks, and regulatory machinery to control transcription in the native host.[3,4] This clustering simplifies isolating the complete biosynthetic pathway from the genome of the producing organism, particularly when compared to, for example, plant biosynthetic pathways.[16] PKSs and their associated proteins are functional in the cytosol and have activity independent from intracellular substructure.[4] This allows successfully expressed enzymes to be functional in non-native cellular environments. The limited variety in acyl-CoA substrates used in polyketide biosynthesis and their wide distribution in the native metabolism of most bacteria also benefits the heterologous production of polyketides. Even with these advantages in mind, many challenges remain in order to successfully produce a polyketide in a heterologous host (Fig. 2).

2 Challenges in heterologous expression of polyketides

Many polyketides are produced by organisms with high GC content in their genomes, such as the *Actinomycetales* and the *Deltaproteobacteria*. Any heterologous expression host used to produce these compounds must be able to adapt to the GC-rich codons used in these pathways.[3,4] Transcripts with rare codons can be problematic for heterologous hosts as the rare codons can lead to stalling during translation, which can produce truncated proteins that are then degraded.[4,17] In addition to the codon bias, native producers, such as *Streptomyces*, often have unique rare codons, such as TTA, embedded in regulatory genes for polyketide biosynthetic pathways.[18] Presumably these rare codons serve as a mechanism to negatively regulate production for these pathways in the native host. While codon bias was identified as a key hurdle for heterologous expression, in practice it has not significantly limited heterologous expression systems.[4,19] For example *Escherichia coli* was a successful host for the heterologous expression of the *Saccharopolyspora erythraea* 6-deoxyerythronolide B biosynthetic pathway even though

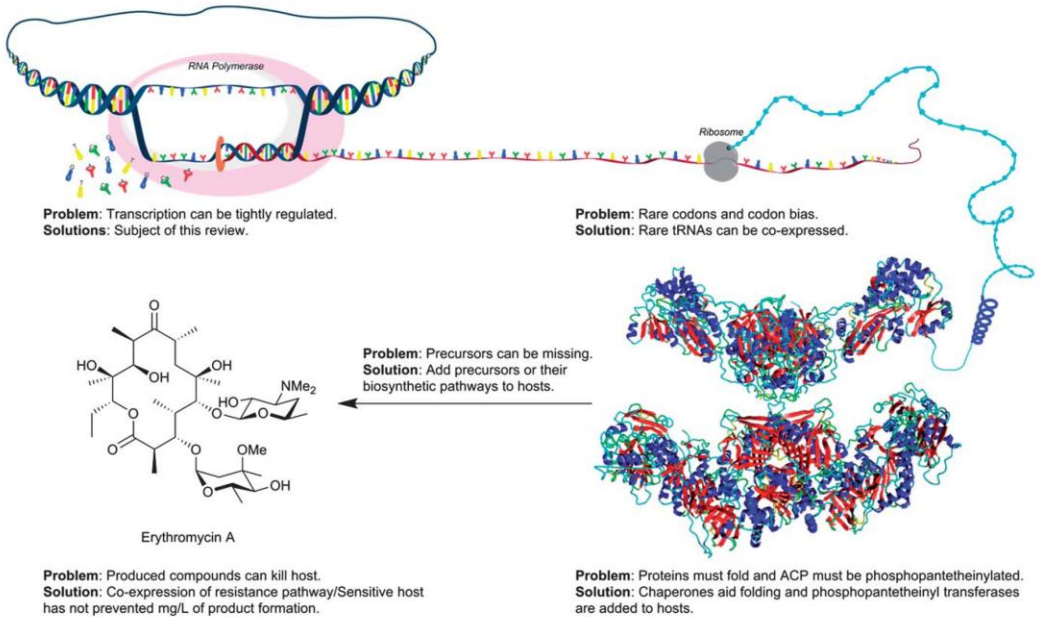

Fig. 2 Heterologous expression is a multistep process. Problems in any one of transcription, translation, protein folding, post-translational modification, precursor availability, or product toxicity can prevent successful heterologous expression of a polyketide biosynthetic pathway. This figure highlights some of the common problems and approaches to addressing them.

This journal is © The Royal Society of Chemistry 2013

View Article Online

Published on 24 September 2013. Downloaded by University of Ottawa on 04/11/2014 16:44:57.

17% of the codons in the *S. erythraea* gene cluster are rare codons in *E. coli*.[19–24]

Ensuring the correct folding of biosynthetic proteins to produce functional proteins has also been a major concern in the development of heterologous expression systems. However, novel strategies and techniques have been developed to provide efficient production of folded, soluble protein in a range of heterologous hosts.[25–27] In addition, most polyketide biosynthetic pathways have ACPs that must be post-translationally phosphopantetheinylated. While phosphopantetheinylation has not been problematic in hosts, such as *Streptomyces* that possess the broadly substrate tolerant Sfp-like phosphopantetheinyl transferase (PPTase), it has been problematic in hosts like *E. coli* that have only an AcpS-like PPTase.[28] The AcpS class of PPTases show restricted substrate specificity, primarily modifying carrier proteins from primary metabolism.[29,30] In order to address this problem in *E. coli*, the *Bacillus subtilis* PPTase encoding gene *sfp* was inserted into the *E. coli* genome to generate the strain BAP1, which is able to heterologously express the functional, post-translationally modified 6-deoxyerythronolide B pathway.[19,31,32]

While the majority of substrates used by polyketide biosynthetic pathways are primary metabolites and are present in most bacteria, some pathways require uncommon building blocks. The unavailability of necessary precursors has also been addressed in heterologous hosts by either the insertion of precursor biosynthesis enzymes or the removal of precursor degradation pathways.[19,33–41] For example to ensure sufficient methoxymalonyl-CoA for the efficient production of mid-ecamycin, *fkbG–K*, the genes encoding methoxymalonyl-CoA biosynthesis from *Streptomyces hygroscopicus*, were introduced into the chromosome of *Streptomyces fradiae*.[36]

As many polyketides possess antibiotic activity, protecting the heterologous host from the heterologously produced compound is clearly a concern. As the native producing organisms must also protect themselves from the antibiotic activities of the polyketides, the biosynthetic gene clusters generally encode a resistance mechanism as well. Successful heterologous expression of the gene cluster thus also produces the proteins needed for resistance. For example the albicidin efflux pump, AlbXIV, expressed in the heterologous host *Xanthomonas axonopodis* increased resistance and facilitated a six-fold increase in albicidin production.[42] In cases where the heterologous host is sensitive to the polyketide product and no resistance mechanism is present, low levels of the polyketide product can be produced.[43] Based on these results, it seems likely that while resistance mechanisms are required for high-level over-production of polyketides from heterologous hosts, low-level polyketide production can be successful even in organisms sensitive to the polyketide product.

The transcription of polyketide biosynthetic gene clusters is tightly regulated in native producing organisms.[44] Ensuring that the heterologous host is able to transcribe the complete pathway is a major challenge. Secondary metabolite biosynthetic pathways are often transcriptionally repressed in the native hosts and are only expressed during specific stages of the growth cycle, often the transition into stationary phase, or under specific metabolic or environmental conditions, such as starvation or change in pH. This is particularly true in light of the observation that many pathways are silent in the native host, presumably due to transcriptional repression. Two approaches have been used to tackle this problem. In the first approach, one or more of the native promoters present in a gene cluster are replaced with promoters known to function in the heterologous host. The use of directed promoter replacement has been successful and has relied primarily on the actI/actIII, T7, ermE, Pm, and Tet promoters (Fig. 3). The alternative approach is to use a host that is closely related to the native strain and rely on the native promoters from the gene cluster to be functional in the heterologous host. This has been especially successful for the heterologous expression of streptomycetal polyketide

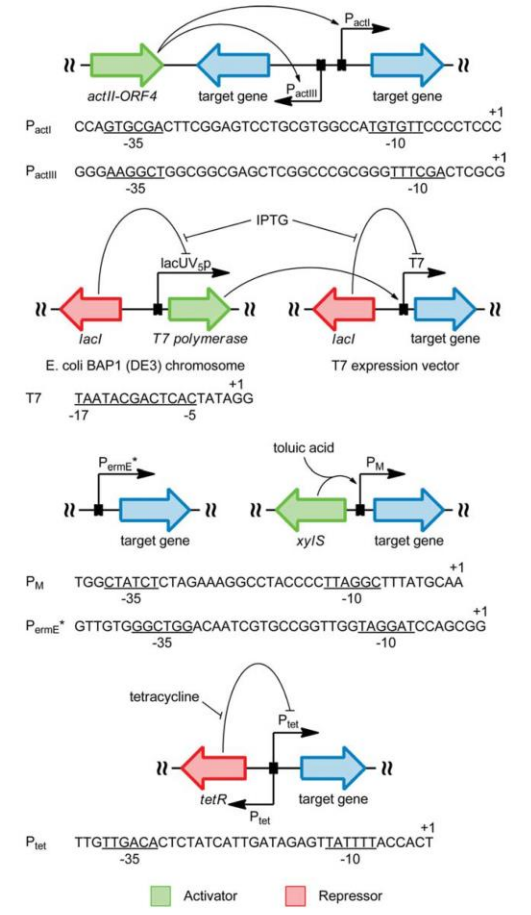

Fig. 3 The five most common promoter systems employed in promoter replacement strategies for heterologous production of polyketides.

This journal is © The Royal Society of Chemistry 2013

View Article Online

Published on 24 September 2013. Downloaded by University of Ottawa on 04/11/2014 16:44:57.

pathways in streptomycetal hosts, such as *Streptomyces coelicolor* and *Streptomyces lividans*.

This review is designed to provide an overview of the successful examples of heterologous polyketide production, focusing particularly on transcription of the biosynthetic pathway. We will critically evaluate the promoters currently used in promoter replacement strategies and look at heterologous hosts that have successfully transcribed pathways from non-native promoters. In advance, we apologize for any oversights or omissions.

3 Promoter replacement to ensure transcription

One of the most successful approaches towards ensuring the transcription of polyketide biosynthetic pathways involves the incorporation of promoters known to be functional in the heterologous host upstream of a transcriptional start site in the gene cluster (Table 1). This approach is essential if the heterologous host is unable to recognize or use the promoters or regulatory elements native to the pathway. In many cases only a single promoter need be added, especially when it is placed upstream of a pathway-specific transcriptional activator, or when the pathway is encoded on a single polycistronic operon. In the case of polycistronic operons, the promoter must be compatible with formation of the long transcripts seen in polyketide biosynthesis (>20 kb). Replacement of a single promoter is clearly advantageous as it limits the genetic manipulations required to generate a heterologous expression system. In some cases, however, multiple promoters must be added to the gene cluster to ensure transcription of all the biosynthetic genes.

A limited number of promoters have been successfully used for the heterologous expression of polyketide biosynthetic pathways (Fig. 3). All have proven capable of producing the long transcripts needed for polyketide production. Some of them are restricted to use in *Streptomyces*, including the actI/actIII promoter with its cognate transcriptional activator ActII-ORF4.[45] ActII-ORF4 is a member of the family of *Streptomyces* Antibiotic Regulatory Proteins (SARPs), which bind DNA between −15 and −40 from the transcriptional start site and recruit a sigma factor–RNA polymerase complex to the promoter at the start of transcription.[46] Additional *Streptomyces*-derived promoters that have been used successfully include the ermE promoter and the tipA promoter. The ermE promoter is the native promoter upstream of the erythromycin resistance gene *ermE* in *Sachropolyspora erythryae*. It is a powerful constitutive promoter in *Streptomyces*.[47]

In Gram negative bacteria the T7, Pm, and tet promoters have proven successful. The T7 promoter (P_{T7}), from the T7 bacteriophage, is located −17 to +6 from the transcriptional start site and is the only promoter to be recognized by an exogenous RNA polymerase (RNAP), the highly active T7 RNAP.[48] It should also be noted that the T7 promoter is perhaps the least compatible promoter with the production of the large transcripts needed in heterologous polyketide production, with transcript lengths limited to 20 kb. The inducible Pm promoter from the benzoate catabolism pathway in *Pseudomonas putida* requires approximately 80 bp of sequence extending upstream from the transcriptional start site. Holo-RNAP binds to the promoter sites at −10 and −35 and is activated by the transcriptional activator XylS, which binds directly upstream of the −35 site.[49] The Pm promoter is known to have broad utility across Gram negative bacteria.[49] The tet promoter (P_{tet}) is an inducible promoter based on the tetracycline resistance cassette from the transposon *Tn10*.[50] It is a bidirectional promoter which drives expression of a transcriptional repressor, TetR in one direction and the gene of interest in the other. In the absence of tetracycline, the repressor TetR binds to the promoter preventing the host RNAP from transcribing genes in either direction. The binding of tetracycline to TetR induces a conformational change in the repressor making it unable to bind DNA and alleviating the repression.[51] This promoter system has broad utility across bacterial strains, including Gram negative bacteria like *E. coli* and in Gram positive bacteria, such as *Bacillus subtilis* and *Mycobacterium smegmatis*.[52]

3.1 The actI/actIII promoter

In 1984 Malpartida and Hopwood successfully produced actinorhodin, a type II polyketide native to *S. coelicolor*, in the heterologous host *Streptomyces parvulus* by inserting an SCP2-based plasmid containing the actinorhodin biosynthetic pathway into their host strain.[93] Following this study the actinorhodin biosynthetic pathway was inserted into several other streptomycetal hosts, which resulted in the production of actinorhodin, an easily detected pigment, and several shunt products. The ability to produce actinorhodin across several strains of *Streptomyces* led to the investigation of regulatory mechanisms native to the actinorhodin biosynthetic pathway. The regulatory *actII-ORF4* gene was discovered in the biosynthetic pathway, and its ability to regulate transcription from the actI/actIII promoter and facilitate an increase in actinorhodin production in *S. coelicolor* when overexpressed was explored.[94–96] This established the actI/actIII-actII-ORF4 promoter–activator expression system as a successful technique for the heterologous production of polyketides in *Streptomyces*.

The Khosla group's use of the actI/actIII promoter in heterologous *Streptomyces* hosts provided some of the first examples of polyketides produced using promoter replacement.[53,54,97–99] They inserted type II polyketide pathways into a SCP2-based vector downstream of the actI/actIII promoter. The actII-ORF4 regulatory gene necessary for activation of the actI/actIII promoter was cloned into the vector pRM5 to activate transcription of the heterologous pathway.[97] Using this expression platform, the Khosla group explored polyketide production across several combinations of ACPs, KSs, and chain length factors (CLFs) from the actinorhodin pathway from *S. coelicolor*, the granatacin pathway from *Streptomyces violaceoruber*, the tetracenomycin pathway from *Streptomyces glaucescens*, and the frenolicin pathway from *Streptomyces roseofulvus* (Fig. 4).[98–100] Later experiments used the same expression systems and biosynthetic pathways to look at similar combinations

This journal is © The Royal Society of Chemistry 2013

View Article Online

Published on 24 September 2013. Downloaded by University of Ottawa on 04/11/2014 16:44:57.

Table 1 Polyketides produced using heterologous promoters to ensure transcription in the bacterial heterologous host

Product	Type	Native producer	Promoter	Heterologous host	Reference
Mutacin/SEKs	Type II PKS	*S. glaucescens*	actI	*S. coelicolor*	9,53,54
		S. coelicolor	actI	*S. lividans*	
		S. roseofulvus	T7	*E. coli*[a]	
Epothilones	Mixed PKS/NRPS	*S. cellulosum*	actI	*S. coelicolor*	55–58
			pikAI	*S. venezuelae*	
			T7	*E. coli*	
			Tn5	*M. xanthus*	
6-MSA	Fungal PKS	*P. patulum*	actI	*S. coelicolor*	59,60
			T7	*E. coli*	
6-DEB	Type I PKS	*S. erythraea*	actI	*S. lividans*	8,19
			T7	*E. coli*	
Tylosins	Type I PKS	*S. fradiae*	actI	*S. venezuelae*	61
			pikAI		
Narbonolides	Type I PKS	*S. venezuelae*	actI	*S. lividans*	62,63
		S. erythraea[b]	actI[b]	*S. lividans*	
		S. venezuelae[b]			
		S. antibioticus[b]			
Aloesoponarin II	Type II PKS	*S. roseofulvus*	actI	*S. coelicolor*	64
R1128	Type II PKS	*Streptomyces* sp. R1128	actI	*S. lividans*	65
Deoxyoleandolide	Type I PKS	*S. antibioticus*	actI	*S. lividans*	66
Frenolicins	Type II PKS	*S. roseofulvus*	actI	*S. coelicolor*	99
Macrotetrolides	Type III PKS	*S. griseus*	actI	*S. lividans*	67
Lankacidinol A	Mixed *trans*-AT PKS/NRPS	*S. rochei*	actI	*S. lividans*	68
Soraphen A	Type I PKS	*S. cellulosum*	tipA	*S. lividans*	69
Dechloroneocarzilin A	Type I PKS	*S. carzinostaticus*	tipA	*S. coelicolor*	70
Meridamycin	Mixed PKS/NRPS	*Streptomyces* sp. NRRL 30748	ermE	*S lividans*	71
Flavanols/Flavones	Type III PKS	*P. crispum*	ermE	*S. venezuelae*	72
		C. siensis			
		C. unshiu			
Phenylpropanoids	Type III PKS	*S. coelicolor*	ermE	*S. venezuelae*	73
		A. thaliana			
		M. sativa			
		A. hypgaea			
Napthoic acid	Type I PKS	*S. carzinostaticus*	ermE	*S. lividans*	74
				S. coelicolor	
Fredericamycin	Type II PKS	*S. griseus*	ermE	*S. albus*	75
Landomycin	Type II PKS	*S. cyanogenus*	ermE	*S. fradiae*	76
Flavones/Flavonols	Type III PKS	*P. crispum*	ermE	*S. venezuelae*	72
Erythromycins	Type I PKS	*S. erythrae*	T7	*E. coli*	77
P8_1-OG	Mixed PKS/NRPS	*A. mediterranei*	T7	*E. coli*	78
Yersiniabactin	Mixed PKS/NRPS	*Y. pestis*	T7	*E. coli*	79
SMA76/SMA93	Fungal PKS	*G. fujikuroi*	T7	*E. coli*	9
Midecamycin	Type I PKS	*S. hygroscopicus*	tylGI	*S. fradiae*	36
Chalcolactones	Type I PKS	*S. bikiniensis*	tylGI	*S. fradiae*	80
Tylactone	Type I PKS	*S. fradiae*	pikAI	*S. venezuelae*	61
4-*O*-demethylbarbamide	Mixed PKS/NRPS	*M. producens*	pikAI	*S. venezuelae*	81
Orsellinic acid	Iterative Type I PKS	*S. viridochromogenes*	tipA	*S. lividans*	82
				S. coelicolor	
Alkyl-*O*-dihydrogeranyl-methoxyhydroquinones	Mixed PKS/Isoprenoid	*A. missouriensis*	tipA	*S. lividans*	83
Myxothiazol	Mixed PKS/NRPS	*S. cellulosum*	Pm	*P. putida*	38,84
			Tn5		
Myxochromide S	Mixed PKS/NRPS	*S. aurantiaca*	Pm	*P. putida*	85–87
			Tn5	*M. xanthus*	
			aphII	*C. macrosporus*	
Flaviolins	Type III PKS	*S. cellulosum*	Pm	*P. putida*	88
				P. syringae	
				P. stutzeri	
Luminmycins	Mixed PKS/NRPS	*P. luminescens*	P_{tet}	*E. coli*	89,90
Syringolins	Mixed PKS/NRPS	*P. syringae*	P_{tet}	*E. coli*	91
Tubulysins	Mixed PKS/NRPS	*Cystobacter* sp. SBCb004	P_{tet}	*P. putida*	92
				M. xanthus	

[a] Produced when co-expressed with PKS4 from *G. fujikuroi*. [b] Expressed as chimeric PKS mixtures using the erythromycin, pimaricin, and oleandomycin pathways.

This journal is © The Royal Society of Chemistry 2013

View Article Online

Published on 24 September 2013. Downloaded by University of Ottawa on 04/11/2014 16:44:57.

of PKS elements including the introduction of various ketoreductases.[54]

Within one year of its introduction, the actI/actIII ActII-ORF4 promoter–activator expression system produced a myriad of previously uncharacterized molecules.[53,54,97–99] It increased our understanding of the cyclization mechanisms in type II polyketide biosynthesis, and established the ground work for the use of heterologous expression as a platform for combinatorial chemistry.[53,54,97–100] Use of the actI/actIII promoter has provided nearly a dozen different compounds from type I, II, III, fungal, and mixed PKS/NRPS pathways (Table 1).

While the actI/actIII promoter is one of the most successful non-native promoters for the production of heterologous polyketides, its activity has only been clearly demonstrated in two highly related heterologous hosts, *S. coelicolor* and *S. lividans*. A key limiting factor in its use is that the host must be capable of transcribing the activator, *actII-ORF4*, as no promoters have been engineered at the start of the gene.[101–103] As *actII-ORF4* is native to *S. coelicolor*, it is easily expressed in this organism. It also appears to be expressed in the closely related strain *S. lividans* from the *S. coelicolor* promoter.[8,53,62,63,65–67,104] There is a single report of *S. venezuelae* acting as the host of actI/actIII heterologous expression.[61] In this example the type I PKS tylosin was shown to be produced from an actI/actIII developed vector, however, the authors acknowledge that the strain was capable of transcribing the tylosin pathway in the absence of the actI/actIII promoter and conclude that a promoter intrinsic to the tylosin pathway may have been utilized instead.[61] Until the actI/actIII promoter system can be extended to additional hosts, including non-*Streptomyces*, the future applications of this promoter system will be limited.

3.2 The T7 promoter

One of the most successful heterologous protein expression systems has been the T7 promoter in *E. coli* hosts.[105] The vast majority of recombinant proteins are expressed using this system. It is thus not surprising that the T7 promoter with an *E. coli* host has been adapted for the heterologous expression of PKS gene clusters.[105,106] For a host to use the T7 promoter, it must also express the T7 polymerase, which is required for transcription from the T7 promoter.[48] In general for heterologous expression, the T7 promoters must be upstream of a gene or an operon to be expressed. Often transcription from T7 promoters is inducible *via* the *lac* operator. LacI, a transcriptional repressor binds DNA at a recognition site upstream of the T7 promoter, preventing transcription. Transcription is induced by the addition of lactose or the more stable isopropyl β-D-1-thiogalactopyranoside (IPTG), which binds LacI, relieving the repression and allowing transcription to begin.[106]

Heterologous expression in *E. coli* has several benefits, including fast growth rates, adaptable culture conditions, a vast genetic toolset, well-characterized primary metabolism, and the lack of any native PKS pathways.[105] The initial drawbacks associated with *E. coli*, the inability to post-translationally modify PKS ACP domains and the inability to produce methylmalonyl-CoA a common extender unit in PKS pathways, have been addressed. ACPs can be post-translationally modified by the broadly substrate tolerant *B. subtilis* phosphopantetheinyl transferase Sfp. The *E. coli* strain BAP1 has *sfp* inserted into its propionyl-CoA catabolism pathway.[19] To produce methylmalonyl-CoA, the propionyl-CoA carboxylase gene cluster has been utilized.[22,40,107,108]

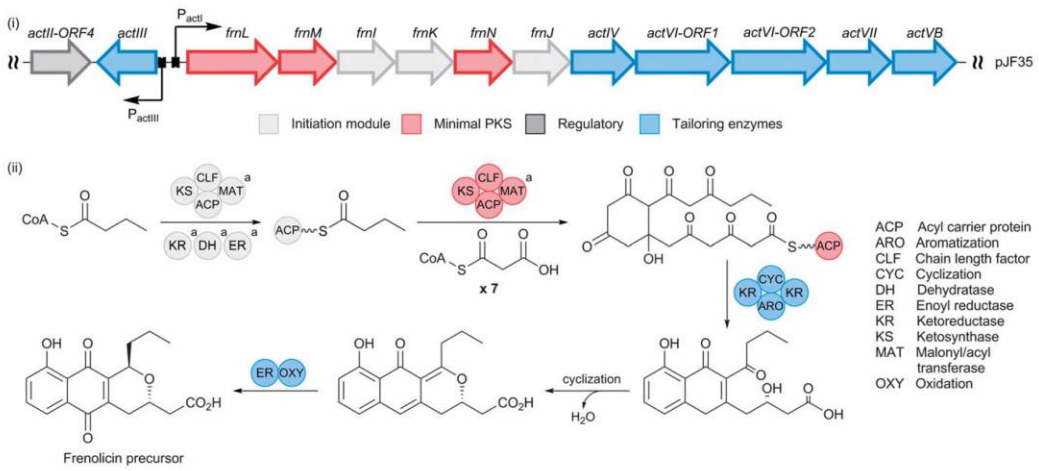

Fig. 4 Aromatic polyketides were produced by heterologous expression of the frenolicin biosynthetic pathway in *S. coelicolor* using a promoter replacement strategy. (i) shows the frenolicin gene cluster from pJF35. The actI/actIII promoter was placed upstream of *frnL*, which encodes a KS. Based on the direction of the genes in the pathway, it is possible that the entire pathway is transcribed from this promoter. (ii) shows the biochemical pathway for frenolicin formation in the heterologous host *S. coelicolor*. [a]These proteins are not encoded in the gene cluster and are likely from the host.

View Article Online

Published on 24 September 2013. Downloaded by University of Ottawa on 04/11/2014 16:44:57.

The first example of heterologous expression of a polyketide using the T7 promoter system in *E. coli* was the production of 6-deoxyerythronolide B.[19] This work successfully demonstrated that by placing a T7 promoter upstream of each PKS gene, it was possible to produce full length, active, greater than 200 kDa PKS proteins from GC rich genes in *E. coli*. Following this work several groups produced various 6-deoxyerythronolide B-based analogues by replacing, inactivating, or changing the available starter units of the DEBS promiscuous loading didomain.[19,24,34,35] In 2010 Zhang *et al.* successfully expressed the complete erythromycin biosynthetic pathway, including all tailoring enzymes, producing erythromycin A from *E. coli* by placing the T7 promoter in front of multiple operons throughout the entire pathway across multiple expression vectors and co-expressing the GroEL/ES chaperone system to ensure correct protein folding (Fig. 5).[77]

The successful production of P8_1-OG, a metabolite from the rifamycin hybrid PKS/NRPS pathway native to *Amycolatopsis mediterranei*, provides an excellent example of the versatility of the T7 promoter when used in *E. coli* BAP1.[78] The introduction of the seven genes needed to produce the 3-amino-5-hydroxybenzoic acid (AHBA) primer unit into *E. coli* resulted in poor expression of two of the required proteins. The genes encoding these proteins were replaced with the homologs present in the ansamycin biosynthetic pathway from *Actionsynnema pretiosum*. This enabled detectable levels of the starter unit AHBA though the authors do not address potential explanations for the poor expression of the AHBA pathway from *A. mediterranei*. The initial hybrid NRPS/PKS, RifA, represented another hurdle due to its size of ~530 kDa, which prevented soluble expression in *E. coli*. This was remedied by splitting the RifA protein into two fragments of similar size and introducing the terminal domains from the docking regions between DEBS modules 2 and 3 onto their respective C- and N- termini. Through this novel linkage, the successful production of P8_1-OG, a key intermediate from the rifamycin NRPS/PKS pathway, was observed.[78]

The use of the T7 promoter has enabled type I, fungal, and mixed PKS/NRPS pathways to be heterologously expressed in *E. coli* and remains a viable strategy for the production of polyketides in *E. coli*. One of the major drawbacks to this approach is the requirement to insert a T7 promoter at the start of each individual biosynthetic transcript to ensure proper transcription.[105] This requires each target biosynthetic gene cluster to undergo rigorous engineering to enable polyketide production and has seriously limited its application and prevented its routine use with gene clusters that possess a large number of genes or operons.[105] In addition to this limitation, no examples of type II polyketides have been heterologously expressed in *E. coli* using the T7 promoter. In fact it has been observed that type II PKS KS and CLF domains are not produced as soluble proteins when expressed under control of the T7 polymerase, suggesting that this approach will not be successful for type II polyketides.[105]

3.3 The ermE promoter

The ermE promoter from the *S. erythraea* erythromycin resistance gene *ermE* has proven to be a successful promoter for the production of type I, II, and III PKS products in *Streptomyces* hosts. The ermE promoter was first recognized as an asset due to its ability to express functional glycotransferases involved in polyketide tailoring enzymes in heterologous hosts.[109–111] The first use of the ermE promoter for transcription of an entire PKS pathway was for the production in *Streptomyces fradiae* of the highly glycosylated type II polyketide 5,6-anhydro-landomycin A from *Streptomyces cyanogenus*.[76] von Mulert *et al.* hypothesized that previous unsuccessful attempts to produce landomycins in *S. fradiae* were hampered by competition between native biosynthetic enzymes from the structurally similar urdamycin PKS pathway and the absence of regulatory enzymes necessary for the production of landomycin. The authors constructed a *S. fradiae* strain incapable of producing urdamycin and transformed it with the landomycin PKS gene cluster. Only when this strain was co-transformed with the regulatory gene, *lndI*, under the control of the ermE promoter was 5,6-anhydro-landomycin A produced.[76]

Lui *et al.* also demonstrated that transcription limited heterologous production of the mixed PKS/NRPS product meridamycin from *Streptomyces* sp. NRRL 30748 in *S. lividans* (Fig. 6).[71] The complete meridamycin pathway, identified from a BAC library, was transformed into *S. lividans*. The authors demonstrated that the transcript levels from the first gene in the biosynthetic pathway, *merP* which encodes a NRPS, were much lower when compared to the native producer. The replacement of the native *merP* promoter with the ermE promoter led to detectable levels of the *merP* transcript and detectable levels of meridamycin. This result represents one of the few examples in which the authors demonstrate unsuccessful transcription from native promoters and investigate promoter replacement strategies in a heterologous host.[71] Other applications of the ermE promoter include its success with the production of flavones and phenylpropanoids from type III PKS synthase pathways in the heterologous host *S. venezuelae*.[72,73,77] Recently the ermE promoter facilitated the discovery tetarimycin A from a screen of type II PKS library clones constructed from eDNA. Utilizing the ermE promoter and screening the library in *Streptomyces albus*, Brady *et al.* were able to characterize the tetarimycin A PKS pathway along with its regulatory SARP (Fig. 7).[12]

Although the ermE promoter has proven to be capable of ensuring the transcription of polyketide biosynthetic pathways in several strains of *Streptomyces*, the approach has afforded less success overall when compared to the actI/actIII expression system (Table 1). All reported examples of successful production of non-*Streptomyces* natural products using the ermE promoter have required the codon optimization of the inserted biosynthetic pathway.[72,73,77] Although a potential alternative to the use of the actI/actIII expression system, the ermE promoter has also only been capable of producing heterologous polyketides in *Streptomyces* hosts.

3.4 The Pm promoter

Gram negative bacteria, such as the *Pseudomonas*, have been excellent hosts for the heterologous expression of PKS gene

This journal is © The Royal Society of Chemistry 2013

View Article Online

Published on 24 September 2013. Downloaded by University of Ottawa on 04/11/2014 16:44:57.

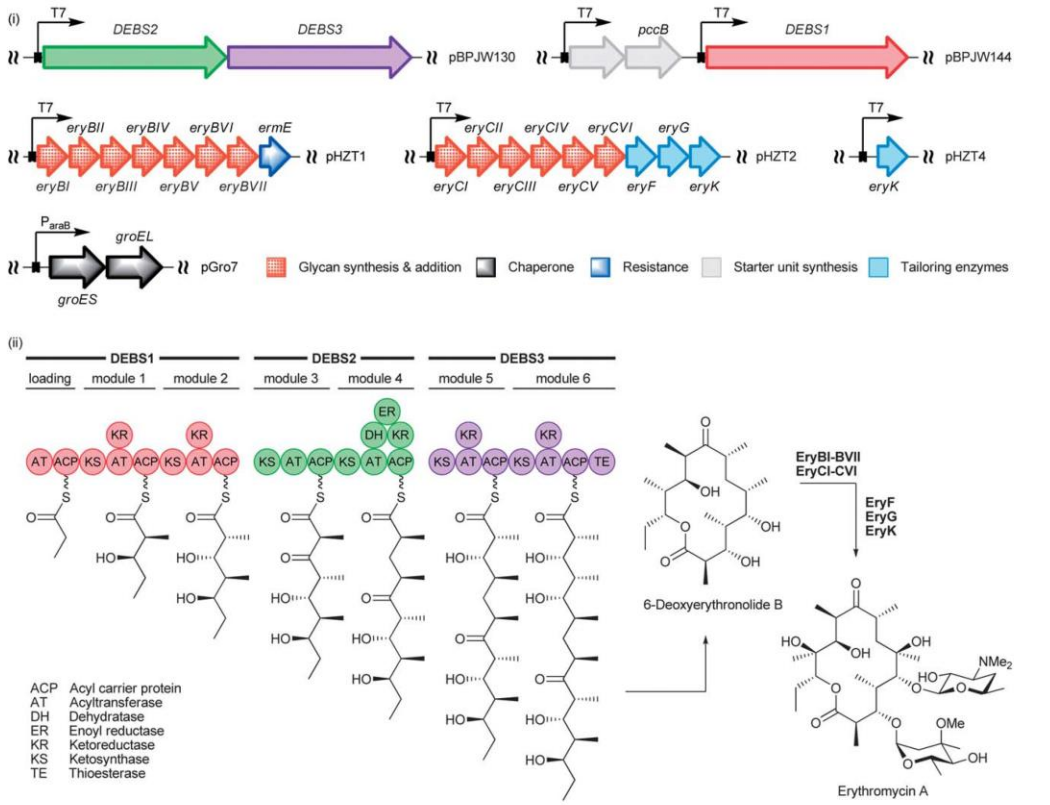

Fig. 5 Erythromycin A was heterologously produced in *E. coli* by using a 5 plasmid system and placing T7 promoters upstream of two PKS genes and upstream of two large polycistronic transcripts encoding the tailoring enzymes and carbohydrate biosynthesis pathways (i). The use of the chaperones GroEL aided in ensuring proper protein folding for erythromycin A production. (ii) shows the biochemical pathway for erythromycin A production. PKS protein colours in (ii) correspond to the PKS genes in (i).

clusters from Gram negative species, such as the myxobacteria. Much of this has been enabled by the use of the Pm promoter from *Pseudomonas putida*. The mixed polyketide non-ribosomal peptide myxochromide S, from the myxobacteria *Stigmatella aurantiaca*, was successfully produced when the Pm promoter was placed upstream of the three gene, single operon gene cluster.[85] Using *P. putida* as a heterologous host, the rate of myxochromide S production was doubled.

A key advance enabling *P. putida* to function as a broad heterologous host for PKS biosynthesis was the addition of the methylmalonyl-CoA biosynthetic pathway from *Sorangium cellulosum* So ce56, which enabled formation of sufficient pools of methylmalonyl-CoA from the primary metabolite succinyl-CoA.[38] Myxothiazol, a mixed PKS/NRPS product also from *S. aurantiaca*, was heterologously expressed in this *P. putida* strain when the Pm promoter was installed upstream of the first gene in this six gene, single operon gene cluster (Fig. 8).[38] Induction of the Pm promoter by addition of toluic acid increases the levels of the transcriptional activator XylS, which is natively transcribed by the transcription factors σ^H and σ^S in the *Pseudomonas* host.[112–114]

The production of metabolites from pathways that are cryptic or silent in their native hosts represents one of the attractive benefits of heterologous expression. Utilizing the Pm promoter, *P. putida*, *Pseudomonas syringae*, and *Pseudomonas stutzeri* were capable of producing flaviolins from a cryptic type III PKS native to the myxobacteria, *S. cellulosum*.[85,88] These examples clearly established the use of *Pseudomonas* in combination with the Pm promoter as attractive heterologous expression systems for the production of cryptic myxobacterial PKS pathways.

The use of the Pm promoter expression methodology remains the only reported approach towards the production of complex myxobacterial metabolites in *Pseudomonas*.[84,85,88] Despite its unique success, the Pm promoter has not been successfully implemented in a broader range of metabolites or in non-*Pseudomonas*.

View Article Online

Published on 24 September 2013. Downloaded by University of Ottawa on 04/11/2014 16:44:57.

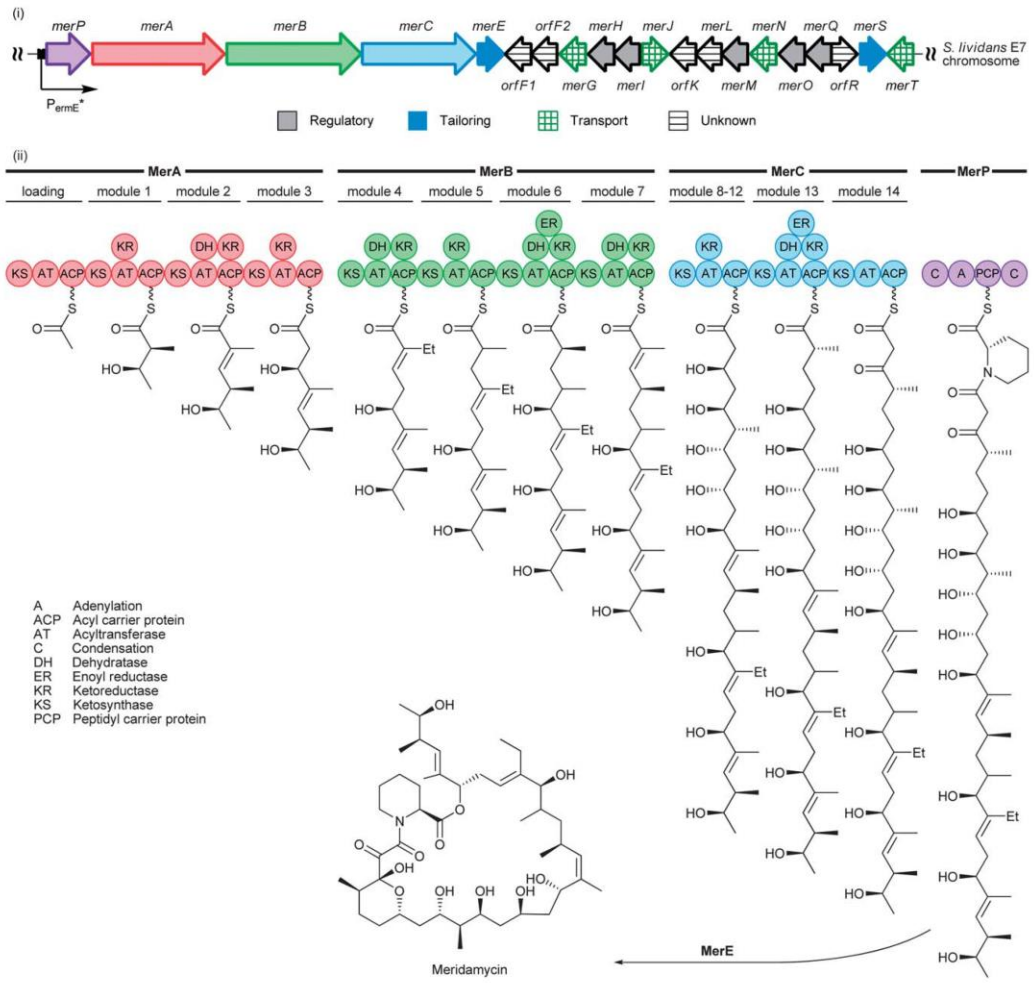

Fig. 6 The promoter replacement approach was used to heterologously express meridamycin in *S. lividans*. (i) shows the gene cluster for meridamycin biosynthesis where the native promoter upstream of *merP*, which encodes a transcriptional regulator, was replaced with the ermE promoter. The promoter replacement was necessary for heterologous expression. (ii) shows the biochemical pathway for meridamycin production. PKS/NRPS protein colours in (ii) correspond to the PKS/NRPS genes in (i).

3.5 The tet promoter

Recently a tetracycline inducible *tetR*-P_{tet} expression system has been introduced across a variety of heterologous hosts, including *E. coli*, *P. putida*, and *Myxococcus xanthus* to produce mixed PKS/NRPS products, including tubulysin, luminmycin, and syringolin (Fig. 9).[89–92] In one example the *tubCDEF* operon, which encodes all but the loading domain from the tubulysin biosynthetic pathway from the myxobacteria *Cystobacter* sp. SBCb004, was placed under control of P_{tet}.[92] When heterologously expressed in *P. putida*, low $\mu g\ L^{-1}$ of tubulysin could be produced and when placed into *M. xanthus*, a host much more closely related to the producing organism, sub-mg L^{-1} of tubulysin could be produced.[92] To increase yields of the cryptic mixed PKS/NRPS luminmycins natively produced by *Photorhabdus luminescens* in the heterologous host *E. coli*, Bian *et al.* installed P_{tet} lacking the repressor, *tetR*. This converted the promoter to a constitutive promoter and enabled them to increase the productivity of the heterologous expression system.[89]

The tet promoter has proven to be extremely versatile. No other promoter system has been shown to function in hosts as diverse as *E. coli*, *P. putida*, and *M. xanthus*. In addition P_{tet} has enabled production of mixed PKS/NRPS natural products in heterologous hosts, such as *E. coli* and *P. putida*, which are not closely related to

This journal is © The Royal Society of Chemistry 2013

View Article Online

Published on 24 September 2013. Downloaded by University of Ottawa on 04/11/2014 16:44:57.

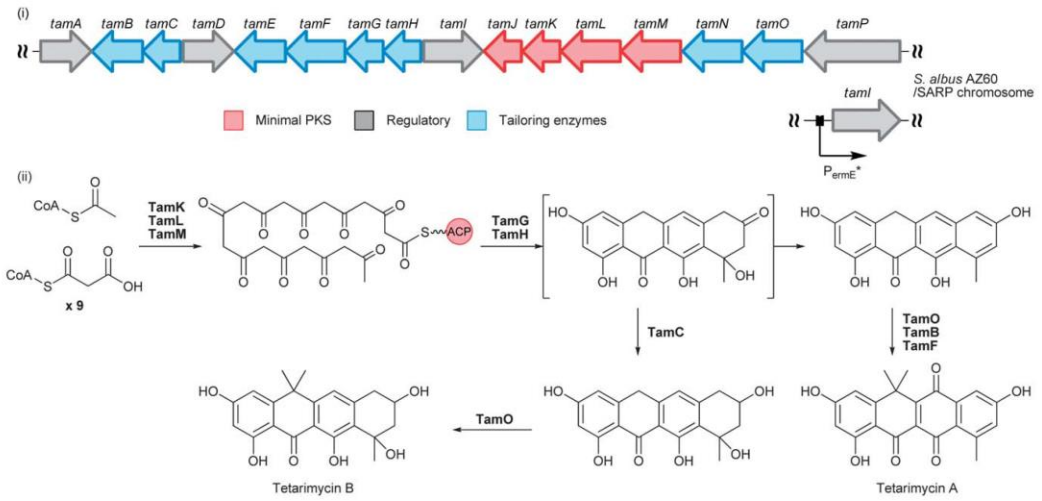

Fig. 7 The tetarimycin gene cluster was obtained from an environmental DNA library and tetarimycin B was heterologously expressed in *S. albus* by a promoter replacement strategy. (i) shows both the tetarimycin gene cluster and a second copy of *taml*, which encodes a transcriptional regulator and is under the control of the ermE promoter. (ii) shows the biochemical pathway for production of tetarimycin.

the native producing organisms.[89–92] A current limitation appears to be the low levels of heterologous production observed in many of the P_{tet} controlled systems. This potential limitation of the tet promoter system may also be attributed to the challenging nature of the pathways investigated.

3.6 Other promoters

Several additional promoters have also proven to be successful in the production of polyketides from heterologous hosts. Two of these are derived from promoters found in *Streptomyces* polyketide biosynthetic gene clusters, the pikAI and tylGI promoters. The pikAI promoter is native to the pikromycin biosynthetic pathway in *S. venezuelae* and transcription from this promoter is positively regulated by binding of the SARP PikD.[115] It has been used to heterologously express the mixed polyketide non-ribosomal peptide epothilone and the type I PKS product tylosin in *S. venezuelae*.[56,61] The pikAI promoter has also been recently used in *S. venezuelae* to produce the barbamide analogue 4-*O*-demethylbarbamide, natively produced by the marine cyanobacteria *Moorea producens*.[81] This represents the first reported heterologous production of a marine cyanobacterial polyketide non-ribosomal peptide in an actinobacterial heterologous host and highlights the potential of the pikAI promoter. The heterologous host range for the pikAI promoter, however, is currently limited to *S. venezuelae* due to the requirement for activation by native *S. venezuelae* PikD. The tylGI promoter regulates transcription from the first PKS gene in the tylosin biosynthetic pathway and is activated by the transcriptional activator TylR.[116] It has been used to heterologously express the type I PKS product midecamycin from *Streptomyces hygroscopicus* and chalcolactone intermediates from *Streptomyces bikiniensis*.[36,80] Due to the requirement for transcriptional activation by TylR, the use of the tylGI promoter has so far been limited to *S. venezuelae*.

The thiostrepton inducible tipA promoter from *S. lividans* has been used to heterologously express four polyketides in *Streptomyces*.[117] Thiostrepton induced transcription from the tipA promoter by binding to the transcriptional activator TipAL, increasing its affinity for the tipA promoter, and enabling transcription.[118] This promoter has been used to produce the type I PKS product soraphen A from *S. cellulosum* in *S. lividans*, dechloroneocarzilin A from *Streptomyces carzinostaticus* in *S. coelicolor*, and orsellinic acid from *Streptomyces viridochromogenes* in both *S. lividans* and *S. coelicolor*.[69,70,82] The tipA promoter has also been used in *S. lividans* to produce the unique polyketide/isoprenoid alkyl-*O*-dihydrogeranyl-methoxyhydroquinones from the rare actinobacteria *Actinoplanes missouriensis*.[83] The tipA promoter represents one of the few inducible promoters successfully applied to heterologous expression in *Streptomyces*, however, it is likely limited to highly related hosts *S. lividans* and *S. coelicolor*.

Other promoters have been used to heterologously express polyketide biosynthetic pathways. The Tn5 promoter has been used in *Myxococcus xanthus* and *P. putida* heterologous hosts and the aphII promoter in the thermophilic heterologous host *Corallococcus macroporus* GT-2.[84,86,87] However, these promoters have only been used to produce a small number of polyketide products in very specific heterologous hosts. Their utility and general use has yet to be determined.

4 Transcription from native promoters

Although promoter replacement approaches have been extremely successful in ensuring transcription of heterologous

View Article Online

Published on 24 September 2013. Downloaded by University of Ottawa on 04/11/2014 16:44:57.

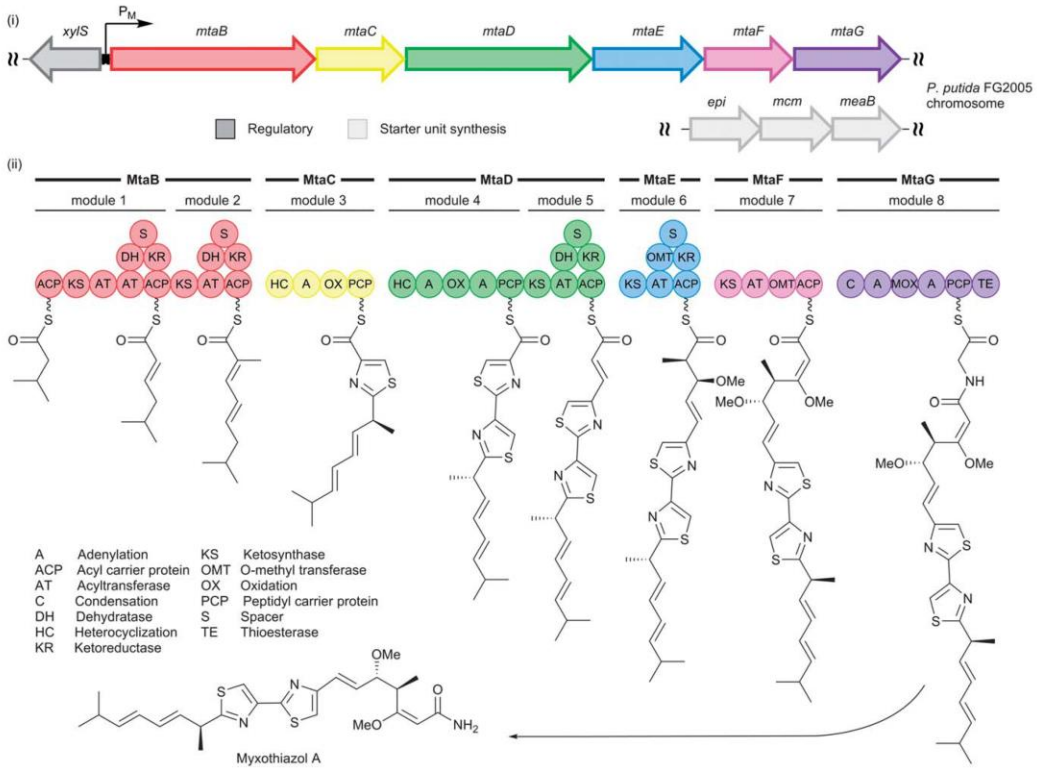

Fig. 8 Myxothiazol A was heterologously expressed in *P. putida*. (i) shows the myxothiazol biosynthetic gene cluster that was inserted into the genome of *P. putida*. Pm was placed upstream of the first gene in the six gene, polycistronic gene cluster. In addition a methylmalonyl-CoA biosynthetic gene cluster was also inserted into the genome of *P. putida* to ensure that the correct precursor was available. (ii) shows the biochemical pathway for formation of myxothiazol A. PKS/NRPS protein colours in (ii) correspond to the PKS/NRPS genes in (i).

polyketide biosynthetic gene clusters, there are a significant number of examples where gene clusters are efficiently transcribed from promoters native to the pathway (Table 2). The use of promoters native to the gene cluster is clearly advantageous since there is no need to genetically modify the gene cluster. This advantage is tempered by the unknown and unpredictable ability of heterologous hosts to recognize and use these promoters. Because of this unpredictability, a limited number of hosts that have proven effective at transcribing from non-native promoters have been predominantly used. These include representative members of major polyketide producing bacteria, such as *Streptomyces* for *Actinomycetales* and *M. xanthus* for *Deltaproteobacteria*.

4.1 *Streptomyces* as heterologous hosts

Throughout the 1980s several type II PKS pathways were isolated from various *Streptomyces* strains and inserted into closely related strains of *Streptomyces*.[93,119–122] These experiments, such as actinorhodin production from the heterologous host *S. parvulus*, provided the first examples of heterologous polyketide production from promoters native to the biosynthetic gene cluster and established *Streptomyces* as the bacterium of choice for the production of heterologous metabolites.

From the initial success of *S. parvulus* to the incredibly versatile *S. lividans*, the *Streptomyces* remain the powerhouse of heterologous hosts capable of utilizing non-native promoters systems and producing the encoded natural product. This success has led to the construction of several engineered strains of *Streptomyces* optimized for production and detection of heterologous polyketides. Engineered strains of *S. coelicolor*, *S. lividans*, and *S. albus* incapable of producing the majority of their native polyketides have been developed to eliminate background competition for metabolites and also to provide a much less complex matrix for the detection and isolation of produced metabolites.[4,5] These strains have proven to be capable of producing a broad range of polyketides, including those from type I, II, and mixed isoprenoid/PKS pathways, and utilizing the native promoters from approximately 20 various streptomycetal-derived biosynthetic

This journal is © The Royal Society of Chemistry 2013

View Article Online

Published on 24 September 2013. Downloaded by University of Ottawa on 04/11/2014 16:44:57.

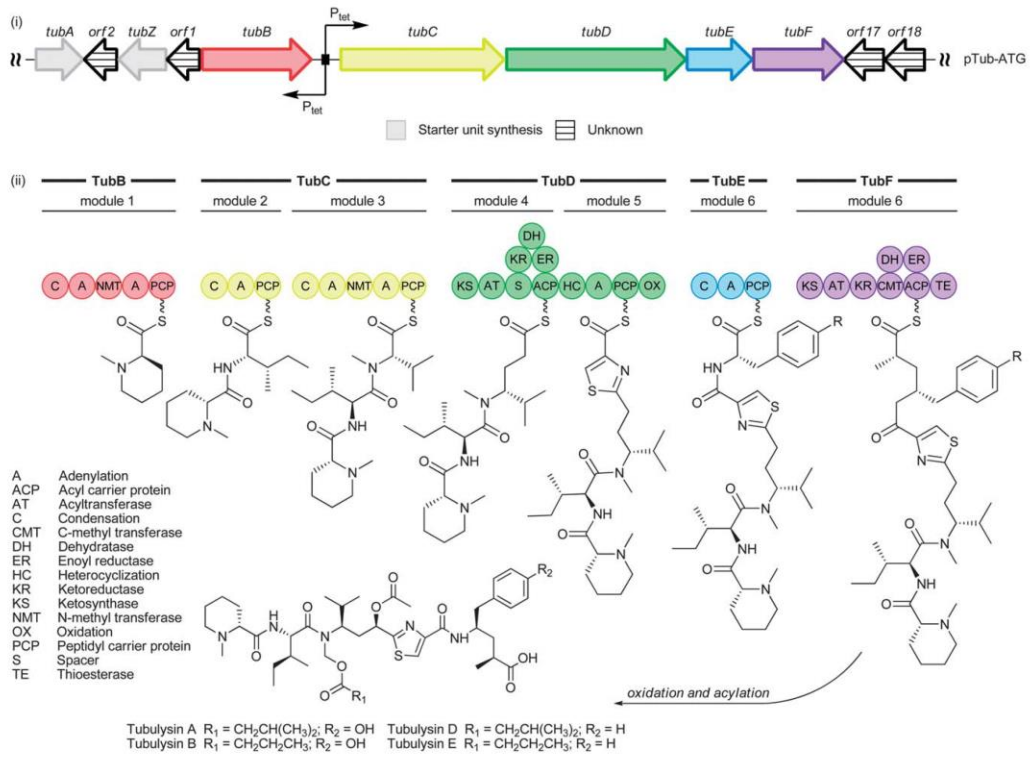

Fig. 9 The tet promoter was used to heterologously express tubulysin in *P. putida* and *M. xanthus*. (i) shows the tubulysin gene cluster. While bidirectional, the tet promoter was only used in one direction to drive transcription of the final four PKS genes in the tubulysin gene cluster. (ii) shows the biochemical pathway for tubulysin production. PKS/NRPS protein colours in (ii) correspond to the PKS/NRPS genes in (i). The low titer for tubulysin production may be attributable to the lack of an appropriate promoter upstream of *tubB*, the first PKS gene in the pathway.

pathways. No non-actinomycetal PKS pathway has yet been expressed from its native promoters in a *Streptomyces* host. These results suggest that the *Streptomyces* polyketide transcriptional regulatory mechanisms are conserved across *Streptomyces* but may not be conserved among non-actinomycetal polyketide producers.

S. lividans, the most successful engineered heterologous strain, has proven to be capable of recognizing the endogenous promoters from a variety of PKS pathways native to *Streptomyces.* Over 15 different polyketides have been produced in *S. lividans* since its development as a heterologous host. In 1999 Ziermann *et al.* developed the *S. lividans* strain T4-114 incapable of producing its native polyketide actinorhodin.[123] Similar work had been done by Kao *et al.* to construct the actinorhodin negative strain *S. coelicolor* CH999, however, this strain exhibits low transformation efficiencies.[4,5,124] Recently Zaleta-Rivera *et al.* transformed the newly discovered A-74528 type II PKS pathway from *Streptomyces* sp. SANK 61196 into *S. lividans* T4-114 to explore the exceptional sequence identity to the fredericamycin biosynthetic pathway from *Streptomyces rimosus*.[125] *S. lividans* T4-114 strains transformed with the entire A-74528 biosynthetic pathway were capable of producing the native metabolite, A-74528, and fredericamycin A. The authors hypothesized that the minimal difference between the two biosynthetic pathways could be attributed to the transference of fredericamycin PKS into *Streptomyces* sp. SANK 61196 or vice-versa followed by further recombination and rearrangements.[125] This homology also allows the observation that the evolution between the two pathways had minimal effect on the promoters of the two pathways and that both of the native hosts *S. rimosus* and *Streptomyces* sp. SANK 61196 share the ability to recognize promoters native to the two biosynthetic pathways. A further observation is that *S. lividans* T4-114 also has the ability to recognize the native promoters as no introduction of a non-native promoter into the pathway was necessary.

The heterologous production of the rare nitrophenyl-substituted polyketides aureothin and spectinabilin from *Streptomyces thioluteus* and *Streptomyces spectabilis*, respectively, in *S. lividans* represents another example of the production of two metabolites from evolutionary divergent PKS pathways (Fig. 10).[126,127] The heterologous production of aureothin from *S. lividans* provided the first strong evidence for

View Article Online

Published on 24 September 2013. Downloaded by University of Ottawa on 04/11/2014 16:44:57.

Table 2 Polyketides produced in heterologous hosts using promoters native to the biosynthetic clusters

Product	Type	Native Producer	Heterolgous Host	Reference
Oxytetracycline	Type II PKS	*S. rimosus*	*S. lividans* *S. albus* *M. xanthus* *E. coli*	43,122,130
Tetracenomycins	Type II PKS	*S. glacescens*	*S. cinnamonesis* *S. lividans*	131
Granaticin	Type II PKS	*S. violaceoruber*	*S. coelicolor* *S. lividans*	132,133
6-MSA	Type I PKS	*S. pactum*	*S. lividans*	134
3,5-dihydroxybenzoic acid	Type I PKS	*S. violaceoruber*	*S. coelicolor*	135
A-74528	Type II PKS	*Streptomyces* sp. SANK 61196	*S. lividans*	125
Fredericamycin	Type II PKS	*Streptomyces* sp. SANK 61196	*S. lividans*	125
Actinorhodin	Type II PKS	*S. coelicolor*	*S. parvulus*	93
Aloesaponarin II	Type II PKS	*S. coelicolor*	*S. parvulus* *S. lividans*	64
Aureothin	Type I PKS	*S. thioluteus*	*S. lividans*	126
Benastatin	Type II PKS	*Streptomyces* sp. A2991200	*S. albus* *S. lividans*	136
Cytosylglucuronic acid	Type I PKS	*S. griseochromogenes*	*S. lividans*	137
Dehydrorabelomycin	Type II PKS	*S. murayamaensis*	*S. lividans*	138
Epothilone	Mixed NRPS/PKS	*S. cellulosum*	*M. xanthus*	58,129,139
Fluorstatins	Type II PKS	Environmental DNA	*S. albus*	11
Landomycin	Type II PKS	Environmental DNA	*S. albus*	128
Furaquinocin	Mixed PKS/Isoprenoid	*Streptomyces* sp. strain KO-3988	*S. lividans*	140
Griseorhodin A	Type II PKS	*Streptomyces* sp. JP95	*S. lividans*	141
Lysolipin	Type II PKS	*S. tendae* Tu 4042	*S. albus*	142
Medermycin	Type II PKS	*Streptomyces* sp. AM-7161	*S. coelicolor*	143
PD116740	Type II PKS	*Streptomyces* sp. strain WP 4669	*S. lividans*	144
Fridamycin E	Type II PKS	*S. rimosus*	*S. lividans*	144
Ravidomycins	Type II PKS	*S. ravidus*	*S. lividans*	145
Spectinabilin	Type I PKS	*S. spectinabilis*	*S. lividans*	127
Steffimycin	Type II PKS	*S. steffisburgensis*	*S. albus*	146
Myxothiazol	Mixed PKS/NRPS	*S. aurantiaca*	*M. xanthus*	84
Albicidin	Mixed *trans*-AT PKS/NRPS	*X. albineaus*	*X. axonopodis*	42
Pladienolide B	Type I PKS	*S. platensis* Mer-117	*S. avermitilis*	147
Caerulomycin A	Mixed PKS/NRPS	*A. cyanogriseus*	*S. coelicolor*	148
Didesmethylmensacarcin	Type II PKS	*S. bottropensis*	*S. albus*	149
Rishirilide A/B	Type II PKS	*S. bottropensis*	*S. albus*	149
Glidobactin A	Mixed PKS/NRPS	*P. luminescens*	*P. putida*	150
Syringolins	Mixed PKS/NRPS	*P. syringae*	*P. putida*	151
Furaquinocins	Mixed PKS/NRPS	*Streptomyces* sp. strain KO-3988	*S. albus*	152
Merochlorins	Mixed PKS/terpenoid	*Streptomyces* sp. strain CNH-189	*S. coelicolor*	153
Nogalamycin	Type II PKS	*S. nogalater*	*S. albus*	154
Enterocins and Wailupemycins	Type II PKS	*S. maritimus*	*S. lividans*	155
Marinopyrroles	Mixed PKS/NRPS	*Streptomyces* sp. CNQ-418	*S. coelicolor*	156
Napyradiomycins	Mixed PKS/Isoprenoid	*Streptomyces* sp. CNQ-525	*S. albus*	157

iterative use of a module in a type I PKS pathway.[126] The heterologous production of spectinabilin further demonstrated the iterative ability of the conserved type I PKS module and also explored the high level of homology between the two PKS pathways. Zhao *et al.* hypothesized that this homology is due to the transfer of the PKS pathway between the two strains and the differences arise from further evolution within the respective native strains.[127] The ability to produce both metabolites aureothin and spectinabilin from the same *S. lividans* host without the introduction of non-native promoters into either pathway further exemplifies *S. lividans* ability to recognize a diverse range of streptomycetal promoters.

The production of novel compounds from libraries of environmental DNA in a universal host would provide access to the untapped chemical diversity produced by the 99% of bacterium that currently cannot be cultured under laboratory conditions.[10] The Brady lab has provided the only examples of the production of previously undiscovered polyketides from a BAC library constructed from eDNA.[11,12,128] The heterologous host *S. albus* was able to produce multiple fluorstatin compounds previously uncharacterized without need of an introduced promoter. This work provides the first successful example of a culture independent methodology for the production of metabolites from eDNA. However, the

This journal is © The Royal Society of Chemistry 2013

View Article Online

Published on 24 September 2013. Downloaded by University of Ottawa on 04/11/2014 16:44:57.

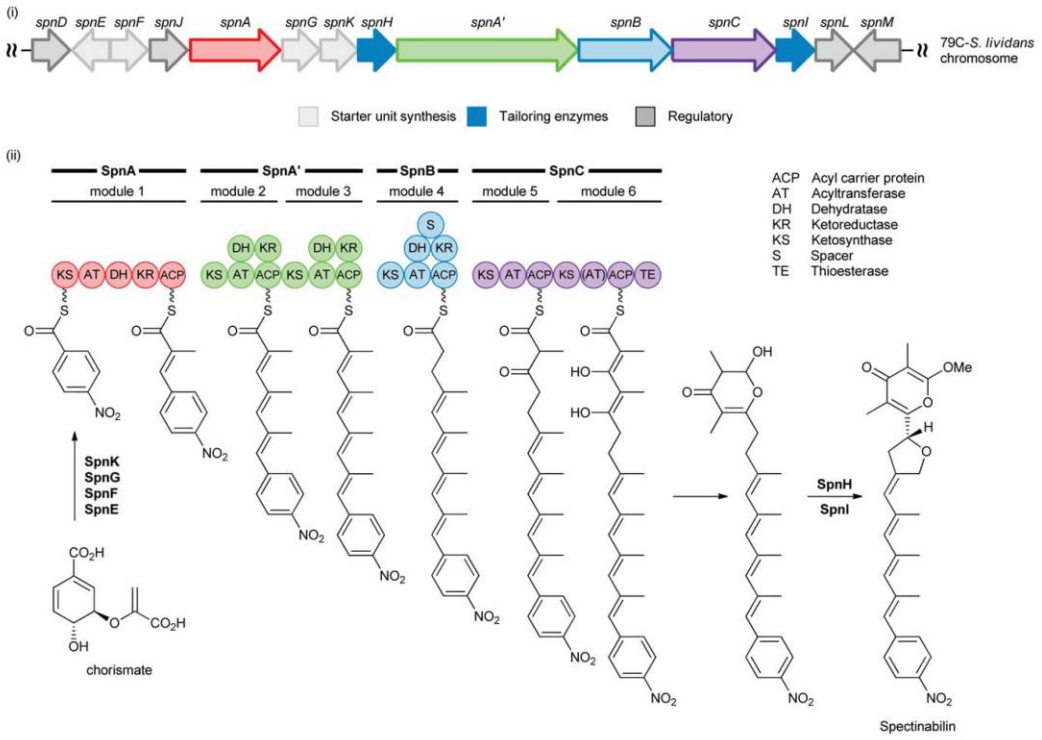

Fig. 10 The spectinabilin biosynthetic gene cluster (i) from *S. spectabilis* was heterologously expressed in *S. lividans* using the promoters native to the gene cluster. (ii) shows the biochemical pathway for spectinabilin formation. PKS protein colours in (ii) correspond to the PKS genes in (i).

fluorstatin compounds and their precursor metabolite rabelomycin are known to be produced from streptomycetal strains, such as *Streptomyces lavendulae* and *Streptomyces olivaceus*, and the authors do not report the production of any other isolated metabolites known to be produced by non-streptomycetal strains.[11] Recently, however, the Brady lab has demonstrated their culture independent methodology is capable of identifying previously uncharacterized aromatic polyketides, UT-X26, UT-V167, and tetarimycin A from eDNA (Fig. 7).[128] The exploration and exploitation of eDNA in a universal heterologous host remains a promising approach towards the discovery of new chemical diversity.

4.2 Myxobacteria as heterologous hosts

Despite the limited genetic toolset available when working with myxobacteria, much has been done towards the establishment of the myxobacteria as a viable heterologous host. When compared to heterologous expression in *Streptomyces*, far fewer pathways have been examined; however, the examples in the literature show a breadth that has not been reported from streptomycetal hosts. Initial work with the myxobacterial host *Myxococcus xanthus* demonstrated the ability to produce the mixed PKS/NRPS product epothilone from the related native strain *S. cellulosum* (Fig. 11).[129] This work along with the production of myxothiazol from the native myxobacteria, *Stigmatella aurantiaca* demonstrates the ability of *M. xanthus* to produce natural products from *Deltaproteobacteria* without the need to introduce heterologous promoters into the gene clusters and is similar in principle to the methodology observed from heterologous hosts of *Streptomyces*.[84]

Production of the type II PKS product oxytetracycline from native host *S. rimosus* in *M. xanthus* represents the first and only reported example of a myxobacterial host producing a polyketide native to a *Streptomyces* without the use of a promoter replacement stretegy.[130] The oxytetracycline biosynthetic pathway was inserted into the chromosome of *M. xanthus* through homologous recombination and mutants possessing the insertion were capable of producing oxytetracycline. This work established *M. xanthus* as the only strain capable of producing polyketides from phylogenetically distant native hosts without promoter replacement. This attribute makes *M. xanthus* an excellent candidate as a heterologous host when screening eDNA libraries that possess pathways from diverse bacterial lineages. To date unfamiliar and limited genetic

View Article Online

Published on 24 September 2013. Downloaded by University of Ottawa on 04/11/2014 16:44:57.

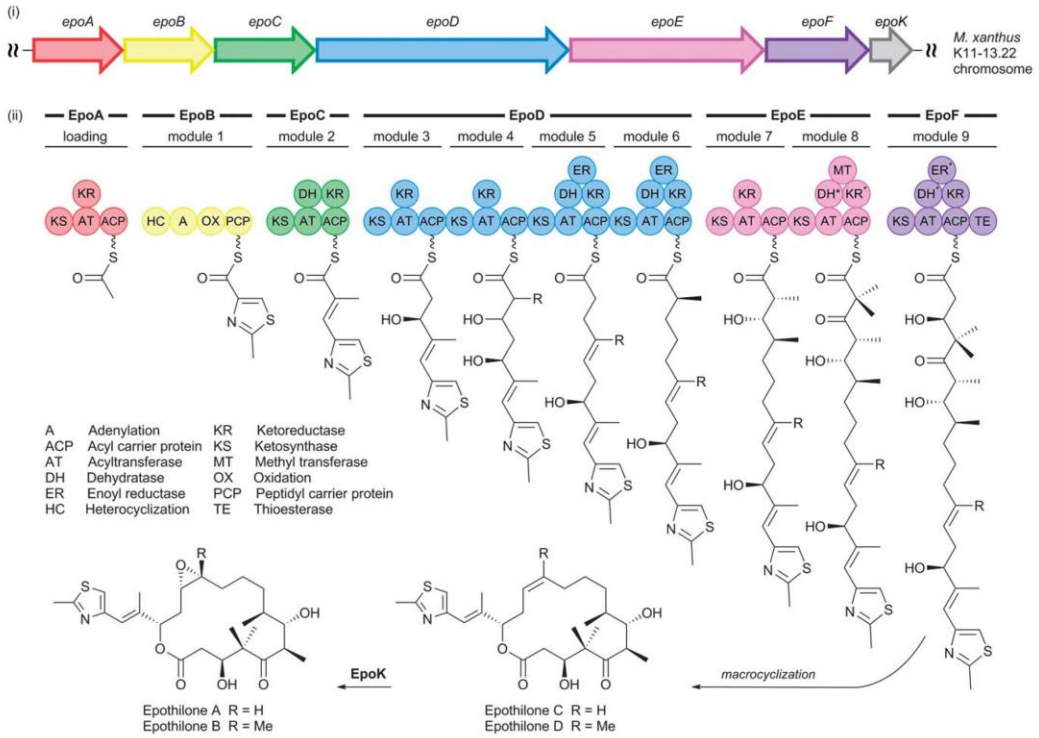

Fig. 11 The epothilones were heterologously produced in *M. xanthus* by introducing the epothilone biosynthetic gene cluster from *S. cellulosum* (i) into the genome of *M. xanthus*.(ii) shows the biochemical pathway for epothilone production. PKS/NRPS protein colours in (ii) correspond to the PKS/NRPS genes in (i).

techniques restrict the use of *M. xanthus* as a heterologous host.[130]

4.3 *E. coli* as a heterologous host

The use of *E. coli* as a heterologous host has many attractive advantages. These include the use of chaperone proteins and inclusion of rare tRNA synthases to ensure translation and folding of functional proteins, the ability to insert and produce all necessary starter metabolites, the superior genetic toolset, and the well characterized primary metabolism.[105] Though much work has been done in the heterologous host *E. coli* utilizing the T7 expression system, the range of the strain's abilities to recognize and transcribe promoters from foreign DNA has not been extensively reported.

The production oxytetracycline from the *S. rimosus* type II PKS gene cluster provided the first example of polyketide production in *E. coli* from promoters native to a PKS gene cluster (Fig. 12).[43] Under native culturing conditions it was observed that *E. coli* BAP1 was not capable of producing transcripts from the *oxyABCDE* operon. Contrastingly, transcripts for all other operons were detected. A native sequence consistent with a σ^{54} promoter was identified upstream of the *oxyABCDE* operon and upon over-expression of the *E. coli* alternative sigma factor σ^{54} the missing operon expressed in *E. coli*.

We hypothesized that a general mechanism for the transcription of PKS pathways should be present in bacteria and regulated by alternative transcription factors downstream of stringent response. Over-expression of any of the other five alternative sigma factors in *E. coli* did not lead to substantial levels of the *oxyABCDE* transcript. Furthermore only over-expression of σ^{54} led to detectable production of oxytetracycline in *E. coli*. This example represents only the second example of polyketide heterologous expression of a *Streptomyces* PKS gene cluster in a non-streptomycetal host utilizing intrinsic promoters; this suggests that adapted *E. coli* expression systems may serve to expand the diversity of pathway/host combinations.

Transcription can limit the ability of *E. coli* to heterologously express type II PKS gene clusters, and our work establishes that alternative sigma factor over-expression is a potential method to remedy this limitation. The application of alternative sigma factor over-expression to positively regulate PKS gene cluster heterologous expression in other bacterium is also an intriguing possibility that may strengthen the transcription

This journal is © The Royal Society of Chemistry 2013

View Article Online

Published on 24 September 2013. Downloaded by University of Ottawa on 04/11/2014 16:44:57.

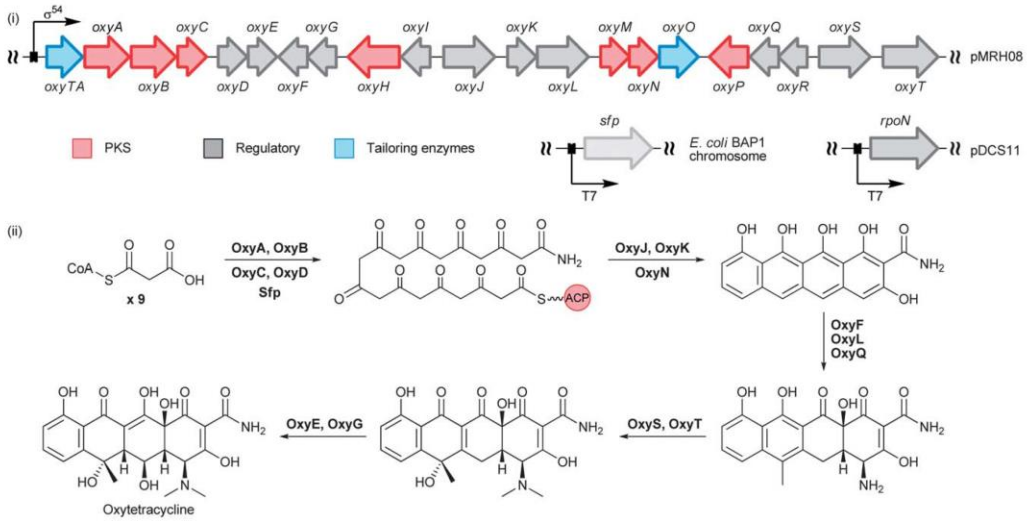

Fig. 12 The oxytetracycline gene cluster from *S. rimosus* (i) was heterologously expressed in *E. coli* using promoter elements native to the *S. rimosus* gene cluster by over-expressing the *E. coli* alternative sigma factor σ^{54}. This positively regulated transcription of the oxyABCDE operon from a native σ^{54} promoter site, leading to oxytetracycline production in *E. coli*. (ii) shows the biochemical pathway for oxytetracycline production.

ability of other heterologous hosts, such as *P. putida*, *M. xanthus* and perhaps *S. lividans*.

5 Conclusion

Heterologous expression of PKS gene clusters is a robust and essential tool in modern natural products chemistry. Current methodologies have proven to be successful with a wide variety of PKS pathways including type I, type II, and type III pathways. One exception appears to be *trans* AT PKS pathways. There have only been two reports of successful heterologous expression of these pathways. Additionally there are very limited examples of successful heterologous expression of PKS pathways from marine bacteria, particularly cyanobacteria.

Results from heterologous expression studies have had major impacts on chemistry, biochemistry, pharmacognosy, drug discovery, and molecular pharmacology. Heterologous expression is a complex, multifaceted problem, requiring transcription and translation for foreign genes, the correct folding and functioning of the encoded proteins, and the required metabolic building blocks. A problem with any one of these steps will prevent the final product from being produced. There is an excellent body of literature demonstrating individual gene cluster-based or heterologous host-based solutions to these problems.

Herein we have reviewed specifically the approaches that have been developed for ensuring transcription of the heterologous pathways. Researchers have relied primarily on two approaches. The first is a promoter replacement strategy where one or more of the native PKS promoters is replaced with promoters known to function in the heterologous host. The second strategy is to rely on the promoters intrinsic to the gene cluster functioning in the heterologous host. Both have advantages and disadvantages. The promoter replacement strategy enables a single heterologous host to be able to express polyketides from phylogenetically diverse organisms. However promoter replacement requires a significant amount of genetic manipulation of the gene cluster, something that can be both technically challenging and in the case of multiple promoter replacement, very time consuming. Relying on the native promoter has the advantage of minimizing the amount of genetic manipulation necessary. Its major limitation is the requirement for the heterologous host to be closely related to the native producing organism to ensure that the promoters are recognized. This is particularly problematic for applications to new polyketide discovery from eDNA libraries where gene clusters likely come from a diversity of *Actinomycetales*, *Deltaproteobacteria*, and other polyketide producers, such as *Gammaproteobacteria* and *Burkholderia*. The ideal heterologous expression system would be able to recognize promoters native to gene clusters from diverse bacteria without the need for promoter replacement.

While there are some promising steps towards a general heterologous host, such as the ability of the *Deltaproteobacteria M. xanthus* transcribe PKS pathway from streptomycetal promoters and the ability of *E. coli* to use alternative sigma factor over-expression to transcribe genes from a *Streptomyces* gene cluster, there is clearly much work to be done. On a technical front, development of rapid methods for promoter replacement would enable the insertion of powerful promoters systems like T7 or P_{tet} into gene clusters for heterologous expression in a diversity of hosts. At the basic research end of the spectrum, improving our understanding of the native

View Article Online

Published on 24 September 2013. Downloaded by University of Ottawa on 04/11/2014 16:44:57.

mechanisms of pathways specific regulation of PKS gene clusters in diverse organisms will provide key information for understanding the compatibility of heterologous hosts with native promoters and may reveal general mechanisms for the transcriptional regulation of these pathways that can be harnessed for a general heterologous host.

6 References

1 B. A. Pfeifer and C. Khosla, *Microbiol. Mol. Biol. Rev.*, 2001, **65**, 106–118.
2 S. R. Park, A. R. Han, Y. H. Ban, Y. J. Yoo, E. J. Kim and Y. J. Yoon, *Appl. Microbiol. Biotechnol.*, 2010, **85**, 1227–1239.
3 S. C. Wenzel and R. Müller, *Curr. Opin. Biotechnol.*, 2005, **16**, 594–606.
4 E. Rodriguez, H. G. Menzella and H. Gramajo, *Methods Enzymol.*, 2009, **459**, 339–365.
5 H. Zhang, Y. Wang and B. A. Pfeifer, *Mol. Pharmaceutics*, 2008, **5**, 212–225.
6 B. Wilkinson and J. Micklefield, *Nat. Chem. Biol.*, 2007, **3**, 379–386.
7 C. Khosla and R. J. Zawada, *Trends Biotechnol.*, 1996, **14**, 335–341.
8 Q. Xue, G. Ashley, C. R. Hutchinson and D. V. Santi, *Proc. Natl. Acad. Sci. U. S. A.*, 1999, **96**, 11740–11745.
9 W. Zhang, Y. Li and Y. Tang, *Proc. Natl. Acad. Sci. U. S. A.*, 2008, **105**, 20683–20688.
10 J. Handelsman, M. R. Rondon, S. F. Brady, J. Clardy and R. M. Goodman, *Chem. Biol.*, 1998, **5**, R245–249.
11 Z. Feng, J. H. Kim and S. F. Brady, *J. Am. Chem. Soc.*, 2010, **132**, 11902–11903.
12 D. Kallifidas, H. S. Kang and S. F. Brady, *J. Am. Chem. Soc.*, 2012, **134**, 19552–19555.
13 Z. Charlop-Powers, J. J. Banik, J. G. Owen, J. W. Craig and S. F. Brady, *ACS Chem. Biol.*, 2013, **8**, 138–143.
14 M. A. Fischbach and C. T. Walsh, *Chem. Rev.*, 2006, **106**, 3468–3496.
15 J. Clardy, M. A. Fischbach and C. T. Walsh, *Nat. Biotechnol.*, 2006, **24**, 1541–1550.
16 D. J. Kliebenstein and A. Osbourn, *Curr. Opin. Plant Biol.*, 2012, **15**, 415–423.
17 M. Marin, *Biotechnol. J.*, 2008, **3**, 1047–1057.
18 K. F. Chater, *Philos. Trans. R. Soc. London, Ser. B*, 2006, **361**, 761–768.
19 B. A. Pfeifer, S. J. Admiraal, H. Gramajo, D. E. Cane and C. Khosla, *Science*, 2001, **291**, 1790–1792.
20 G. A. Roberts, J. Staunton and P. F. Leadlay, *Eur. J. Biochem.*, 1993, **214**, 305–311.
21 S. Murli, J. Kennedy, L. C. Dayem, J. R. Carney and J. T. Kealey, *J. Ind. Microbiol. Biotechnol.*, 2003, **30**, 500–509.
22 J. Lau, C. Tran, P. Licari and J. Galazzo, *J. Biotechnol.*, 2004, **110**, 95–103.
23 Y. Wang and B. A. Pfeifer, *Metab. Eng.*, 2008, **10**, 33–38.
24 M. Pistorino and B. A. Pfeifer, *Biotechnol. Prog.*, 2009, **25**, 1364–1371.
25 J. Anne, B. Maldonado, J. Van Impe, L. Van Mellaert and K. Bernaerts, *J. Biotechnol.*, 2012, **158**, 159–167.
26 D. M. Francis and R. Page, *Current Protocols in Protein Science*, 2010, Unit 5 24, Ch. 5, pp. 21–29.
27 J. C. Samuelson, *Methods Mol. Biol.*, 2011, **705**, 195–209.
28 R. H. Lambalot, A. M. Gehring, R. S. Flugel, P. Zuber, M. LaCelle, M. A. Marahiel, R. Reid, C. Khosla and C. T. Walsh, *Chem. Biol.*, 1996, **3**, 923–936.
29 D. V. Debabov, M. P. Heaton, Q. Zhang, K. D. Stewart, R. H. Lambalot and F. C. Neuhaus, *J. Bacteriol.*, 1996, **178**, 3869–3876.
30 T. Ritsema, O. Geiger, P. van Dillewijn, B. J. Lugtenberg and H. P. Spaink, *J. Bacteriol.*, 1994, **176**, 7740–7743.
31 L. E. Quadri, P. H. Weinreb, M. Lei, M. M. Nakano, P. Zuber and C. T. Walsh, *Biochemistry*, 1998, **37**, 1585–1595.
32 M. R. Mofid, R. Finking and M. A. Marahiel, *J. Biol. Chem.*, 2002, **277**, 17023–17031.
33 F. Lombó, B. Pfeifer, T. Leaf, S. Ou, Y. S. Kim, D. E. Cane, P. Licari and C. Khosla, *Biotechnol. Prog.*, 2001, **17**, 612–617.
34 L. C. Dayem, J. R. Carney, D. V. Santi, B. A. Pfeifer, C. Khosla and J. T. Kealey, *Biochemistry*, 2002, **41**, 5193–5201.
35 J. Kennedy, S. Murli and J. T. Kealey, *Biochemistry*, 2003, **42**, 14342–14348.
36 E. Rodriguez, S. Ward, H. Fu, W. P. Revill, R. McDaniel and L. Katz, *Appl. Microbiol. Biotechnol.*, 2004, **66**, 85–91.
37 J. Kennedy and J. T. Kealey, *Anal. Biochem.*, 2004, **327**, 91–96.
38 F. Gross, M. W. Ring, O. Perlova, J. Fu, S. Schneider, K. Gerth, S. Kuhlmann, A. F. Stewart, Y. Zhang and R. Müller, *Chem. Biol.*, 2006, **13**, 1253–1264.
39 Y. Wang, B. A. Boghigian and B. A. Pfeifer, *Appl. Microbiol. Biotechnol.*, 2007, **77**, 367–373.
40 H. Zhang, B. A. Boghigian and B. A. Pfeifer, *Biotechnol. Bioeng.*, 2010, **105**, 567–573.
41 S. Maharjan, J. W. Park, Y. J. Yoon, H. C. Lee and J. K. Sohng, *Biotechnol. Lett.*, 2010, **32**, 277–282.
42 E. Vivien, D. Pitorre, S. Cociancich, I. Pieretti, D. W. Gabriel, P. C. Rott and M. Royer, *Antimicrob. Agents Chemother.*, 2007, **51**, 1549–1552.
43 D. C. Stevens, K. C. Conway, N. Pearce, L. R. Villegas-Peñaranda, A. G. Garza and C. N. Boddy, *PLoS One*, 2013, **8**, e64858.
44 M. J. Bibb, *Curr. Opin. Microbiol.*, 2005, **8**, 208–215.
45 P. Arias, M. A. Fernandez-Moreno and F. Malpartida, *J. Bacteriol.*, 1999, **181**, 6958–6968.
46 A. Tanaka, Y. Takano, Y. Ohnishi and S. Horinouchi, *J. Mol. Biol.*, 2007, **369**, 322–333.
47 M. J. Bibb, G. R. Janssen and J. M. Ward, *Gene*, 1985, **38**, 215–226.
48 M. Rong, B. He, W. T. McAllister and R. K. Durbin, *Proc. Natl. Acad. Sci. U. S. A.*, 1998, **95**, 515–519.
49 J. L. Ramos, S. Marques and K. N. Timmis, *Annu. Rev. Microbiol.*, 1997, **51**, 341–373.
50 M. Geissendorfer and W. Hillen, *Appl. Microbiol. Biotechnol.*, 1990, **33**, 657–663.
51 C. Berens and W. Hillen, *Eur. J. Biochem.*, 2003, **270**, 3109–3121.
52 P. Carroll, D. G. Muttucumaru and T. Parish, *Appl. Environ. Microbiol.*, 2005, **71**, 3077–3084.

This journal is © The Royal Society of Chemistry 2013

View Article Online

Published on 24 September 2013. Downloaded by University of Ottawa on 04/11/2014 16:44:57.

53 R. McDaniel, S. Ebert-Khosla, H. Fu, D. A. Hopwood and C. Khosla, *Proc. Natl. Acad. Sci. U. S. A.*, 1994, **91**, 11542–11546.

54 H. Fu, D. A. Hopwood and C. Khosla, *Chem. Biol.*, 1994, **1**, 205–210.

55 L. Tang, S. Shah, L. Chung, J. Carney, L. Katz, C. Khosla and B. Julien, *Science*, 2000, **287**, 640–642.

56 S. R. Park, J. W. Park, W. S. Jung, A. R. Han, Y. H. Ban, E. J. Kim, J. K. Sohng, S. J. Sim and Y. J. Yoon, *Appl. Microbiol. Biotechnol.*, 2008, **81**, 109–117.

57 S. C. Mutka, J. R. Carney, Y. Liu and J. Kennedy, *Biochemistry*, 2006, **45**, 1321–1330.

58 C. Osswald, G. Zipf, G. Schmidt, J. Maier, H. S. Bernauer, R. Muller and S. C. Wenzel, *ACS Synth. Biol.*, 2012, DOI: 10.1021/sb300080t.

59 D. J. Bedford, E. Schweizer, D. A. Hopwood and C. Khosla, *J. Bacteriol.*, 1995, **177**, 4544–4548.

60 J. T. Kealey, L. Liu, D. V. Santi, M. C. Betlach and P. J. Barr, *Proc. Natl. Acad. Sci. U. S. A.*, 1998, **95**, 505–509.

61 W. S. Jung, S. K. Lee, J. S. Hong, S. R. Park, S. J. Jeong, A. R. Han, J. K. Sohng, B. G. Kim, C. Y. Choi, D. H. Sherman and Y. J. Yoon, *Appl. Microbiol. Biotechnol.*, 2006, **72**, 763–769.

62 L. Tang, H. Fu, M. C. Betlach and R. McDaniel, *Chem. Biol.*, 1999, **6**, 553–558.

63 L. Tang, H. Fu and R. McDaniel, *Chem. Biol.*, 2000, **7**, 77–84.

64 E. S. Kim, K. D. Cramer, A. L. Shreve and D. H. Sherman, *J. Bacteriol.*, 1995, **177**, 1202–1207.

65 T. Marti, Z. Hu, N. L. Pohl, A. N. Shah and C. Khosla, *J. Biol. Chem.*, 2000, **275**, 33443–33448.

66 S. Shah, Q. Xue, L. Tang, J. R. Carney, M. Betlach and R. McDaniel, *J. Antibiot.*, 2000, **53**, 502–508.

67 H. J. Kwon, W. C. Smith, L. Xiang and B. Shen, *J. Am. Chem. Soc.*, 2001, **123**, 3385–3386.

68 S. Tatsuno, K. Arakawa and H. Kinashi, *J. Antibiot.*, 2007, **60**, 700–708.

69 R. Zirkle, J. M. Ligon and I. Molnár, *Microbiology*, 2004, **150**, 2761–2774.

70 M. Otsuka, K. Ichinose, I. Fujii and Y. Ebizuka, *Antimicrob. Agents Chemother.*, 2004, **48**, 3468–3476.

71 H. Liu, H. Jiang, B. Haltli, K. Kulowski, E. Muszynska, X. Feng, M. Summers, M. Young, E. Graziani, F. Koehn, G. T. Carter and M. He, *J. Nat. Prod.*, 2009, **72**, 389–395.

72 S. R. Park, J. H. Paik, M. S. Ahn, J. W. Park and Y. J. Yoon, *J. Microbiol. Biotechnol.*, 2010, **20**, 1295–1299.

73 S. R. Park, J. A. Yoon, J. H. Paik, J. W. Park, W. S. Jung, Y. H. Ban, E. J. Kim, Y. J. Yoo, A. R. Han and Y. J. Yoon, *J. Biotechnol.*, 2009, **141**, 181–188.

74 B. Sthapit, T. J. Oh, R. Lamichhane, K. Liou, H. C. Lee, C. G. Kim and J. K. Sohng, *FEBS Lett.*, 2004, **566**, 201–206.

75 E. Wendt-Pienkowski, Y. Huang, J. Zhang, B. Li, H. Jiang, H. Kwon, C. R. Hutchinson and B. Shen, *J. Am. Chem. Soc.*, 2005, **127**, 16442–16452.

76 U. von Mulert, A. Luzhetskyy, C. Hofmann, A. Mayer and A. Bechthold, *FEMS Microbiol. Lett.*, 2004, **230**, 91–97.

77 H. Zhang, Y. Wang, J. Wu, K. Skalina and B. A. Pfeifer, *Chem. Biol.*, 2010, **17**, 1232–1240.

78 K. Watanabe, M. A. Rude, C. T. Walsh and C. Khosla, *Proc. Natl. Acad. Sci. U. S. A.*, 2003, **100**, 9774–9778.

79 B. A. Pfeifer, C. C. Wang, C. T. Walsh and C. Khosla, *Appl. Environ. Microbiol.*, 2003, **69**, 6698–6702.

80 S. L. Ward, Z. Hu, A. Schirmer, R. Reid, W. P. Revill, C. D. Reeves, O. V. Petrakovsky, S. D. Dong and L. Katz, *Antimicrob. Agents Chemother.*, 2004, **48**, 4703–4712.

81 E. J. Kim, J. H. Lee, H. Choi, A. R. Pereira, Y. H. Ban, Y. J. Yoo, E. Kim, J. W. Park, D. H. Sherman, W. H. Gerwick and Y. J. Yoon, *Org. Lett.*, 2012, **14**, 5824–5827.

82 S. Gaisser, A. Trefzer, S. Stockert, A. Kirschning and A. Bechthold, *J. Bacteriol.*, 1997, **179**, 6271–6278.

83 T. Awakawa, N. Fujita, M. Hayakawa, Y. Ohnishi and S. Horinouchi, *ChemBioChem*, 2011, **12**, 439–448.

84 O. Perlova, J. Fu, S. Kuhlmann, D. Krug, A. F. Stewart, Y. Zhang and R. Müller, *Appl. Environ. Microbiol.*, 2006, **72**, 7485–7494.

85 S. C. Wenzel, F. Gross, Y. Zhang, J. Fu, A. F. Stewart and R. Müller, *Chem. Biol.*, 2005, **12**, 349–356.

86 J. Fu, S. C. Wenzel, O. Perlova, J. Wang, F. Gross, Z. Tang, Y. Yin, A. F. Stewart, R. Müller and Y. Zhang, *Nucleic Acids Res.*, 2008, **36**, e113.

87 O. Perlova, K. Gerth, S. Kuhlmann, Y. Zhang and R. Müller, *Microb. Cell Fact.*, 2009, **8**, 1.

88 F. Gross, N. Luniak, O. Perlova, N. Gaitatzis, H. Jenke-Kodama, K. Gerth, D. Gottschalk, E. Dittmann and R. Müller, *Arch. Microbiol.*, 2006, **185**, 28–38.

89 X. Bian, A. Plaza, Y. Zhang and R. Muller, *J. Nat. Prod.*, 2012, **75**, 1652–1655.

90 J. Fu, X. Bian, S. Hu, H. Wang, F. Huang, P. M. Seibert, A. Plaza, L. Xia, R. Muller, A. F. Stewart and Y. Zhang, *Nat. Biotechnol.*, 2012, **30**, 440–446.

91 X. Bian, F. Huang, F. A. Stewart, L. Xia, Y. Zhang and R. Muller, *ChemBioChem*, 2012, **13**, 1946–1952.

92 Y. Chai, S. Shan, K. J. Weissman, S. Hu, Y. Zhang and R. Muller, *Chem. Biol.*, 2012, **19**, 361–371.

93 F. Malpartida and D. A. Hopwood, *Nature*, 1984, **309**, 462–464.

94 E. Takano, H. C. Gramajo, E. Strauch, N. Andres, J. White and M. J. Bibb, *Mol. Microbiol.*, 1992, **6**, 2797–2804.

95 H. C. Gramajo, E. Takano and M. J. Bibb, *Mol. Microbiol.*, 1993, **7**, 837–845.

96 T. Fujii, H. C. Gramajo, E. Takano and M. J. Bibb, *J. Bacteriol.*, 1996, **178**, 3402–3405.

97 R. McDaniel, S. Ebert-Khosla, D. A. Hopwood and C. Khosla, *Science*, 1993, **262**, 1546–1550.

98 C. Khosla, R. McDaniel, S. Ebert-Khosla, R. Torres, D. H. Sherman, M. J. Bibb and D. A. Hopwood, *J. Bacteriol.*, 1993, **175**, 2197–2204.

99 H. Fu, R. McDaniel, D. A. Hopwood and C. Khosla, *Biochemistry*, 1994, **33**, 9321–9326.

100 J. T. Fitzgerald, C. P. Ridley and C. Khosla, *J. Antibiot.*, 2011, **64**, 759–762.

101 Z. Hu, D. A. Hopwood and C. R. Hutchinson, *J. Ind. Microbiol. Biotechnol.*, 2003, **30**, 516–522.

This journal is © The Royal Society of Chemistry 2013

View Article Online

Published on 24 September 2013. Downloaded by University of Ottawa on 04/11/2014 16:44:57.

102 M. Bierman, R. Logan, K. O'Brien, E. T. Seno, R. N. Rao and B. E. Schoner, *Gene*, 1992, **116**, 43–49.
103 C. J. Rowe, J. Cortés, S. Gaisser, J. Staunton and P. F. Leadlay, *Gene*, 1998, **216**, 215–223.
104 C. Hertweck, L. Xiang, J. A. Kalaitzis, Q. Cheng, M. Palzer and B. S. Moore, *Chem. Biol.*, 2004, **11**, 461–468.
105 X. Gao, P. Wang and Y. Tang, *Appl. Microbiol. Biotechnol.*, 2010, **88**, 1233–1242.
106 K. Terpe, *Appl. Microbiol. Biotechnol.*, 2006, **72**, 211–222.
107 E. Rodriguez and H. Gramajo, *Microbiology*, 1999, **145**(11), 3109–3119.
108 B. Pfeifer, Z. Hu, P. Licari and C. Khosla, *Appl. Environ. Microbiol.*, 2002, **68**, 3287–3292.
109 A. Trefzer, D. Hoffmeister, E. Künzel, S. Stockert, G. Weitnauer, L. Westrich, U. Rix, J. Fuchser, K. U. Bindseil, J. Rohr and A. Bechthold, *Chem. Biol.*, 2000, **7**, 133–142.
110 A. Trefzer, C. Fischer, S. Stockert, L. Westrich, E. Künzel, U. Girreser, J. Rohr and A. Bechthold, *Chem. Biol.*, 2001, **8**, 1239–1252.
111 D. Hoffmeister, B. Wilkinson, G. Foster, P. J. Sidebottom, K. Ichinose and A. Bechthold, *Chem. Biol.*, 2002, **9**, 287–295.
112 S. Marqués, M. T. Gallegos and J. L. Ramos, *Mol. Microbiol.*, 1995, **18**, 851–857.
113 S. Marqués, M. T. Gallegos, M. Manzanera, A. Holtel, K. N. Timmis and J. L. Ramos, *J Bacteriol*, 1998, **180**, 2889–2894.
114 S. Marqués, M. Manzanera, M. M. González-Pérez, M. T. Gallegos and J. L. Ramos, *Mol. Microbiol.*, 1999, **31**, 1105–1113.
115 D. J. Wilson, Y. Xue, K. A. Reynolds and D. H. Sherman, *J. Bacteriol.*, 2001, **183**, 3468–3475.
116 G. Stratigopoulos, N. Bate and E. Cundliffe, *Mol. Microbiol.*, 2004, **54**, 1326–1334.
117 T. Murakami, T. G. Holt and C. J. Thompson, *J. Bacteriol.*, 1989, **171**, 1459–1466.
118 D. J. Holmes, J. L. Caso and C. J. Thompson, *EMBO J.*, 1993, **12**, 3183–3191.
119 D. A. Hopwood, F. Malpartida, H. M. Kieser, H. Ikeda, J. Duncan, I. Fujii, B. A. Rudd, H. G. Floss and S. Omura, *Nature*, 1985, **314**, 642–644.
120 S. Omura, H. Ikeda, F. Malpartida, H. M. Kieser and D. A. Hopwood, *Antimicrob. Agents Chemother.*, 1986, **29**, 13–19.
121 D. H. Sherman, F. Malpartida, M. J. Bibb, H. M. Kieser and D. A. Hopwood, *EMBO J.*, 1989, **8**, 2717–2725.
122 C. Binnie, M. Warren and M. J. Butler, *J. Bacteriol.*, 1989, **171**, 887–895.
123 R. Ziermann and M. C. Betlach, *BioTechniques*, 1999, **26**, 106–110.
124 C. M. Kao, L. Katz and C. Khosla, *Science*, 1994, **265**, 509–512.
125 K. Zaleta-Rivera, L. K. Charkoudian, C. P. Ridley and C. Khosla, *J. Am. Chem. Soc.*, 2010, **132**, 9122–9128.
126 J. He and C. Hertweck, *Chem. Biol.*, 2003, **10**, 1225–1232.
127 Y. S. Choi, T. W. Johannes, M. Simurdiak, Z. Shao, H. Lu and H. Zhao, *Mol. BioSyst.*, 2010, **6**, 336–338.
128 Z. Feng, D. Kallifidas and S. F. Brady, *Proc. Natl. Acad. Sci. U. S. A.*, 2011, **108**, 12629–12634.
129 B. Julien and S. Shah, *Antimicrob. Agents Chemother.*, 2002, **46**, 2772–2778.
130 D. C. Stevens, M. R. Henry, K. A. Murphy and C. N. Boddy, *Appl. Environ. Microbiol.*, 2010, **76**, 2681–2683.
131 C. Li, C. Hazzard, G. Florova and K. A. Reynolds, *Metab. Eng.*, 2009, **11**, 319–327.
132 K. Ichinose, D. J. Bedford, D. Tornus, A. Bechthold, M. J. Bibb, W. P. Revill, H. G. Floss and D. A. Hopwood, *Chem. Biol.*, 1998, **5**, 647–659.
133 A. Martinez, S. J. Kolvek, C. L. Yip, J. Hopke, K. A. Brown, I. A. MacNeil and M. S. Osburne, *Appl. Environ. Microbiol.*, 2004, **70**, 2452–2463.
134 T. Ito, N. Roongsawang, N. Shirasaka, W. Lu, P. M. Flatt, N. Kasanah, C. Miranda and T. Mahmud, *ChemBioChem*, 2009, **10**, 2253–2265.
135 S. C. Wenzel, H. B. Bode, I. Kochems and R. Muller, *ChemBioChem*, 2008, **9**, 2711–2721.
136 Z. Xu, A. Schenk and C. Hertweck, *J. Am. Chem. Soc.*, 2007, **129**, 6022–6030.
137 M. C. Cone, A. K. Petrich, S. J. Gould and T. M. Zabriskie, *J. Antibiot.*, 1998, **51**, 570–578.
138 S. J. Gould, S. T. Hong and J. R. Carney, *J. Antibiot.*, 1998, **51**, 50–57.
139 R. L. Arslanian, C. D. Parker, P. K. Wang, J. R. McIntire, J. Lau, C. Starks and P. J. Licari, *J. Nat. Prod.*, 2002, **65**, 570–572.
140 T. Kawasaki, Y. Hayashi, T. Kuzuyama, K. Furihata, N. Itoh, H. Seto and T. Dairi, *J. Bacteriol.*, 2006, **188**, 1236–1244.
141 A. Li and J. Piel, *Chem. Biol.*, 2002, **9**, 1017–1026.
142 P. Lopez, A. Hornung, K. Welzel, C. Unsin, W. Wohlleben, T. Weber and S. Pelzer, *Gene*, 2010, **461**, 5–14.
143 K. Ichinose, M. Ozawa, K. Itou, K. Kunieda and Y. Ebizuka, *Microbiology*, 2003, **149**, 1633–1645.
144 S. T. Hong, J. R. Carney and S. J. Gould, *J. Bacteriol.*, 1997, **179**, 470–476.
145 M. K. Kharel, S. E. Nybo, M. D. Shepherd and J. Rohr, *ChemBioChem*, 2010, **11**, 523–532.
146 S. Gullón, C. Olano, M. S. Abdelfattah, A. F. Braña, J. Rohr, C. Méndez and J. A. Salas, *Appl. Environ. Microbiol.*, 2006, **72**, 4172–4183.
147 M. Komatsu, T. Uchiyama, S. Omura, D. E. Cane and H. Ikeda, *Proc. Natl. Acad. Sci. U. S. A.*, 2010, **107**, 2646–2651.
148 Y. Zhu, P. Fu, Q. Lin, G. Zhang, H. Zhang, S. Li, J. Ju, W. Zhu and C. Zhang, *Org. Lett.*, 2012, **14**, 2666–2669.
149 X. Yan, K. Probst, A. Linnenbrink, M. Arnold, T. Paululat, A. Zeeck and A. Bechthold, *ChemBioChem*, 2012, **13**, 224–230.
150 A. Dudnik, L. Bigler and R. Dudler, *Microbiol. Res.*, 2013, **168**, 73–76.
151 C. Ramel, M. Tobler, M. Meyer, L. Bigler, M. O. Ebert, B. Schellenberg and R. Dudler, *BMC Biochem.*, 2009, **10**, 26.
152 S. Isogai, M. Nishiyama and T. Kuzuyama, *Bioorg. Med. Chem. Lett.*, 2012, **22**, 5823–5826.

This journal is © The Royal Society of Chemistry 2013

View Article Online

153 L. Kaysser, P. Bernhardt, S. J. Nam, S. Loesgen, J. G. Ruby, P. Skewes-Cox, P. R. Jensen, W. Fenical and B. S. Moore, *J. Am. Chem. Soc.*, 2012, **134**, 11988–11991.

154 V. Siitonen, M. Claesson, P. Patrikainen, M. Aromaa, P. Mantsala, G. Schneider and M. Metsa-Ketela, *ChemBioChem*, 2012, **13**, 120–128.

155 J. Piel, C. Hertweck, P. R. Shipley, D. M. Hunt, M. S. Newman and B. S. Moore, *Chem. Biol.*, 2000, **7**, 943–955.

156 K. Yamanaka, K. S. Ryan, T. A. Gulder, C. C. Hughes and B. S. Moore, *J. Am. Chem. Soc.*, 2012, **134**, 12434–12437.

157 J. M. Winter, M. C. Moffitt, E. Zazopoulos, J. B. McAlpine, P. C. Dorrestein and B. S. Moore, *J. Biol. Chem.*, 2007, **282**, 16362–16368.

Published on 24 September 2013. Downloaded by University of Ottawa on 04/11/2014 16:44:57.

This journal is © The Royal Society of Chemistry 2013

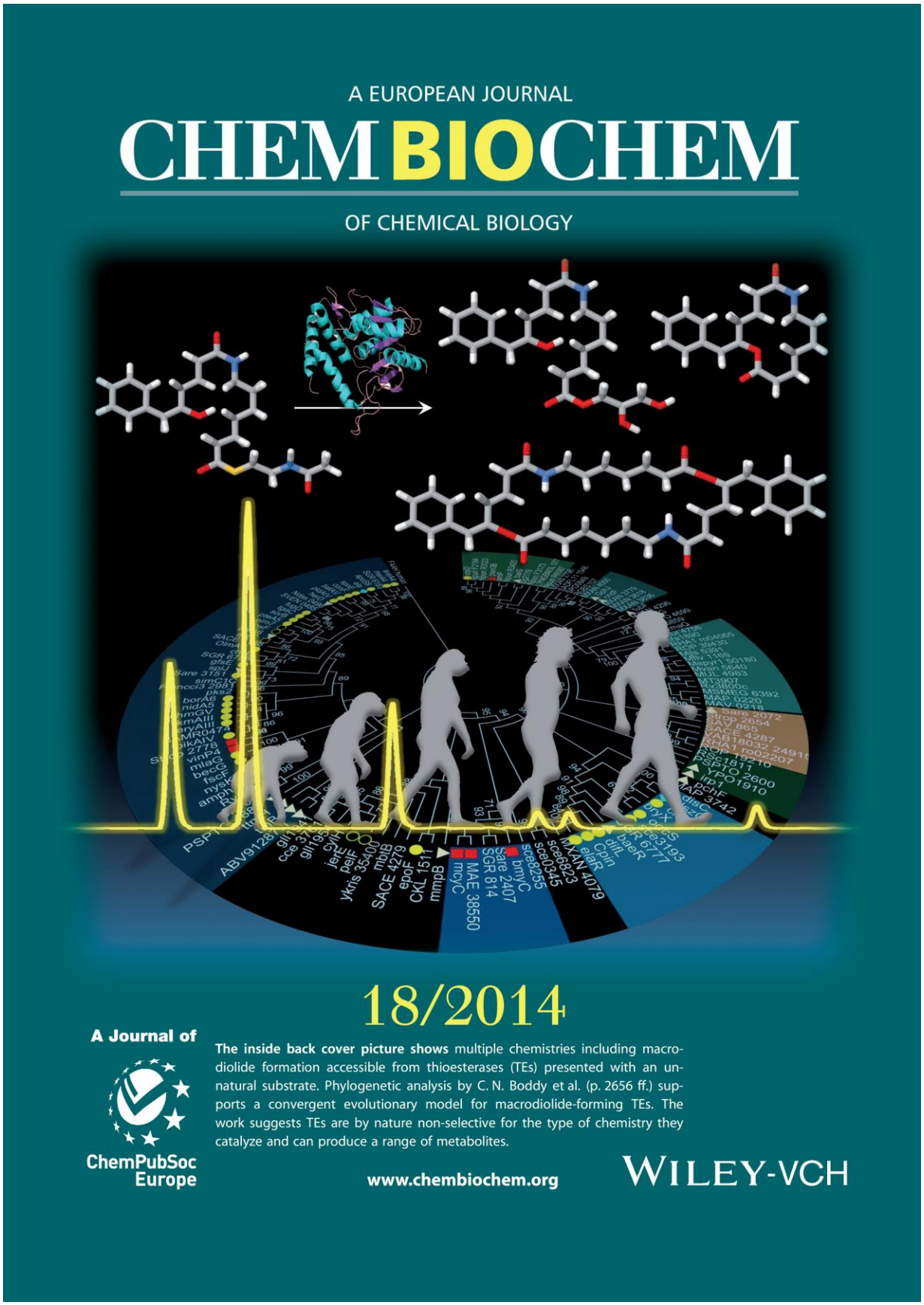
A EUROPEAN JOURNAL
CHEMBIOCHEM
OF CHEMICAL BIOLOGY
18/2014
A Journal of
ChemPubSoc Europe
The inside back cover picture shows multiple chemistries including macrodiolide formation accessible from thioesterases (TEs) presented with an unnatural substrate. Phylogenetic analysis by C. N. Boddy et al. (p. 2656 ff.) supports a convergent evolutionary model for macrodiolide-forming TEs. The work suggests TEs are by nature non-selective for the type of chemistry they catalyze and can produce a range of metabolites.
www.chembiochem.org
WILEY-VCH

CHEMBIOCHEM
COMMUNICATIONS

ChemPubSoc Europe

DOI: 10.1002/cbic.201402475

An Evolutionary Model Encompassing Substrate Specificity and Reactivity of Type I Polyketide Synthase Thioesterases

Taylor P. A. Hari, Puneet Labana, Meaghan Boileau, and Christopher N. Boddy*[a]

Bacterial polyketides are a rich source of chemical diversity and pharmaceutical agents. Understanding the biochemical basis for their biosynthesis and the evolutionary driving force leading to this diversity is essential to take advantage of the enzymes as biocatalysts and to access new chemical diversity for drug discovery. Biochemical characterization of the thioesterase (TE) responsible for 6-deoxyerythronolide macrocyclization shows that a small, evolutionarily accessible change to the substrate can increase the chemical diversity of products, including macrodiolide formation. We propose an evolutionary model in which TEs are by nature non-selective for the type of chemistry they catalyze, producing a range of metabolites. As one metabolite becomes essential for improving fitness in a particular environment, the TE evolves to enrich for that corresponding reactivity. This hypothesis is supported by our phylogenetic analysis, showing convergent evolution of macrodiolide-forming TEs.

Modular polyketides, produced by bacteria, represent some of the most chemically rich and biologically potent molecules known. This diverse family of compounds includes clinical antibiotics, anticancer agents, and immunosuppressants. Although highly diverse in structure and function, these compounds are unified by their mechanism of biosynthesis.[1,2] All are produced from simple building blocks in an assembly line-like fashion by multidomain proteins called type I polyketide synthases (PKS). Understanding the detailed mechanism of their biosynthesis is critical to the discovery of new polyketides and to harnessing PKSs to produce new and designer polyketide products.

Phylogenic analysis of type I PKS catalytic domains has shown that substrate specificity or reactivity of the domains often has a primary sequence determinant. For example, the acyltransferase (AT) domains cluster into malonyl-CoA- and methylmalonyl-CoA-specific clades.[3–6] β-ketosynthase (KS) domains from *trans* AT pathways cluster based on the substitution at the α and β carbons of the upstream polyketide intermediates.[7,8] Ketoreductase (KR) domains cluster into type A or type B, based on the facial selectivity for delivery of the hydride from NADPH.[9,10]

[a] *T. P. A. Hari, P. Labana, M. Boileau, Prof. C. N. Boddy*
Departments of Chemistry and Biology
Centre for Catalysis Research and Innovation, University of Ottawa
Ottawa, ON K1N 6N5 (Canada)
E-mail: cboddy@uottawa.ca

Supporting information for this article is available on the WWW under http://dx.doi.org/10.1002/cbic.201402475.

Unique among these PKS domains is the thioesterase (TE). Phylogenic analysis of TEs show that they do not cluster based on substrate specificity or reactivity (Figure 1). Thus, predicting and characterizing TE specificity and reactivity has relied on experimental characterization.[11–13] We characterized the in vitro substrate specificity and reactivity of the TE from the erythromycin biosynthetic pathway (DEBS TE), and herein we show that it is both highly substrate-specific and capable of catalyzing a high diversity of chemistries, including hydrolysis, esterification, macrocyclization, and macrodiolide formation. We propose an evolutionary model using the screening hypothesis[14,15] to account for these observations.

Type I PKS TEs play a key role in the biosynthesis of polyketides, catalyzing release of the completed polyketide chain from the PKS to which it is covalently linked.[16] This step is essential for turnover of the biosynthesis machinery and provides an opportunity to increase the chemical diversity and complexity of the polyketide product. Type I PKS TEs can catalyze hydrolysis of the acyl-PKS intermediate, generating free acids as seen in ambruticin[17] and gephyronic acid[18] biosynthesis, transesterification with an intermolecular alcohol to generate esters as has been observed in vitro,[19] macrocyclization with intramolecular alcohols to generate macrolactones as seen in erythromycin[20] and epothilone[21,22] biosynthesis, or dimerization with a second equivalent of acyl-PKS to generate macrodiolides as is predicted in elaiophylin[23] and disorazol[24] biosynthesis.

The best-studied type I PKS TE is the TE from the erythromycin biosynthetic pathway, DEBS TE. In vitro biochemical characterization of DEBS TE has shown that macrocyclization activity is highly substrate-selective, with hydrolytic activity predominating in virtually all substrates investigated. For example, a small change in oxidation state or stereochemistry of the two substrates known to undergo macrocyclization completely abolishes macrocycle formation.[11,25,26] The TE from the pikromycin biosynthetic pathway(PIK TE) demonstrates similarly high substrate specificity for macrocyclization, suggesting that this is a general phenomenon of type I PKS TEs.[13,26]

In our efforts to investigate the origin of substrate selectivity for macrocyclization, we synthesized substrates that were biosynthetically related to a known DEBS TE macrocyclization-competent substrate, **3** (Scheme 1). Compound **3** possessed key design features we wished to retain in the panel of substrates used for this study. These included the replacement of the ethyl group from **1** with a benzyl group, as this was known to be effectively processed by DEBS TE and provided an easily detectable chromophore,[25,27] the amide linkage, which facilitates synthesis, and the *N*-acetylcysteamine (NAC) activation of the carboxylate, which has been extensively used

 © 2014 Wiley-VCH Verlag GmbH & Co. KGaA, Weinheim

CHEMBIOCHEM
COMMUNICATIONS
www.chembiochem.org

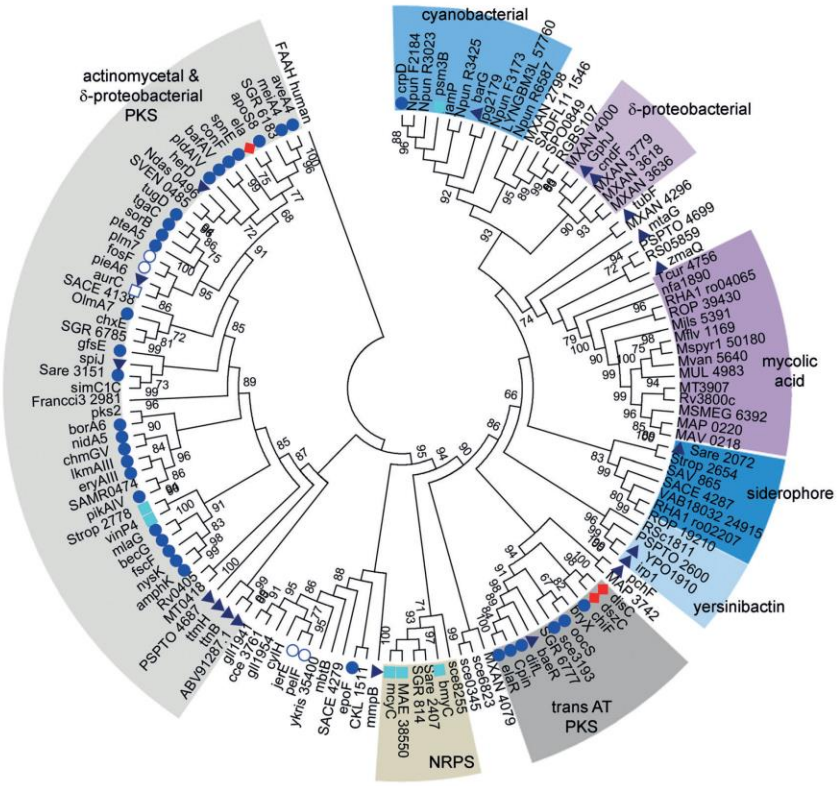

Figure 1. Phylogenetic analysis of 138 TE domains shows that they do not cluster based on substrate specificity or function. Pathway type and origin appear to be greater determinants for clustering of TEs. Sequences and phylogenetic methodology can be found in the Supporting Information. ●: macrolactone, ○: δ-lactone, □: pyrone, ◆: macrodiolide, ■: macrolactam, ▲: acid.

with DEBS TE[11,25,26,28–31] and mimics the cysteamine and C terminus of β-alanine from the native substrate's phosphopantetheinyl group.[30,32] Compound **4** could be envisaged as arising from a biosynthetic gain of dehydratase (DH) function, resulting in conversion of the β-hydroxy functionality of **3** into an α,β-unsaturated carbonyl. The relationship between **3** and **4** is similar to what is seen for 6-deoxyerythronolide B (**1**) and narbonolide (**2**), which are generated by the related TEs DEBS TE and PIK TE, respectively. The enantiomer, *ent*-**4**, was synthesized as a negative control compound, as no D-configured alcohol has been shown to be macrocyclized in vitro or in vivo by DEBS TE.[25,27,33–36] Substrate **5** was envisioned as being related to **4** through modulation of the specificity of the acyltransferase domain, from malonyl-CoA-specific to methylmalonyl-CoA-specific. This panel of substrates provided compounds that could be expected to arise through the evolution of PKS pathways, thus enabling us to provide some of the first insights into the relationship between substrate selectivity and PKS pathway evolution.

Synthesis of **4** and *ent*-**4** was accomplished in eight linear steps (Scheme 2). An asymmetric Brown allylation[37,38] of phenylacetaldehyde (**6**) set the configuration of the stereogenic carbon, furnishing the homoallylic alcohols **7** and *ent*-**7** in moderate yields. These were silylated, and the allylic double bonds were oxidized to yield aldehydes **8** and *ent*-**8**. Horner–Wadsworth–Emmons coupling between **8** and phosphonate **9** was accomplished in moderate yield, furnishing the *E*-α,β-unsaturated esters **10** and *ent*-**10**. Subsequent hydrolysis of the ethyl ester gave the carboxylic acid, which was treated with EDC and coupled with free amine **13** to yield the silylated NAC-thioester substrates **11** and *ent*-**11** in good yield. Deprotection in an acetonitrile solution of HF/pyridine[25] completed the synthesis of enantio-enriched substrates **4** and *ent*-**4** (Scheme 2 and Scheme S2 in the Supporting Information). Substrate **5** was generated in racemic form through an analogous route, starting with the racemic form of aldehyde **8** (Scheme S3). Wittig coupling with methyl 2-(triphenylphosphoranylidene)propionate, gave the methyl substituted α,β-un-

© 2014 Wiley-VCH Verlag GmbH & Co. KGaA, Weinheim

CHEMBIOCHEM
COMMUNICATIONS
www.chembiochem.org

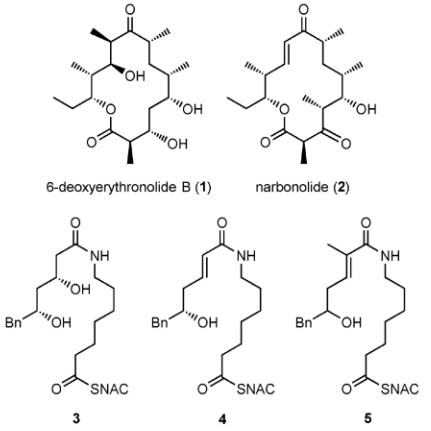

Scheme 1. Substrate **3** is known to undergo macrocyclization with DEBS TE. Substrates **4**, *ent*-**4**, and racemic **5** were designed based on the relationship between 6-deoxyerythronolide B (**1**) and narbonolide **2** to evaluate the effect of evolutionarily accessible substrate modifications on the function of the DEBS TE.

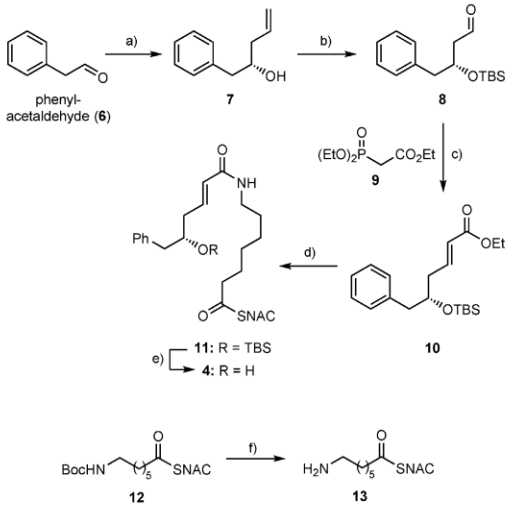

Scheme 2. Synthesis of L-enantio-enriched substrate **4**: a) (−)-Ipc$_2$BAllyl, −100 °C, 90% *ee*, 65%; b) TBSCl, imidazole; $K_3Fe(CN)_6$, K_2OsO_4; $Pb(OAc)_4$, 70% over three steps; c) **9**, KOH, 63%; d) NaOH; **13**, EDC, DMAP, Et_3N, 72% over two steps; e) HF, pyridine, 64%; f) HCl/Dioxane, 100%. The D-enantio-enriched substrate *ent*-**4** was prepared in identical fashion by using (+)-Ipc$_2$BAllyl.

saturated ester, which was converted into the NAC-thioester substrate following analogous chemistry to **4** and *ent*-**4**.

To evaluate the ability of DEBS TE to macrolactonize **4**, *ent*-**4**, and **5**, purified recombinant DEBS TE[30] (15 μM) was treated with each NAC-thioester substrate (2.5 mM) in 50 mM phosphate buffer (pH 7.4) with DMSO (10% *v*/*v*). After 18 h, the reactions were quenched and analyzed for product formation by LC/MS. The results obtained for **4** and *ent*-**4** were consistent with the stereochemical hypothesis indicating that L-config-

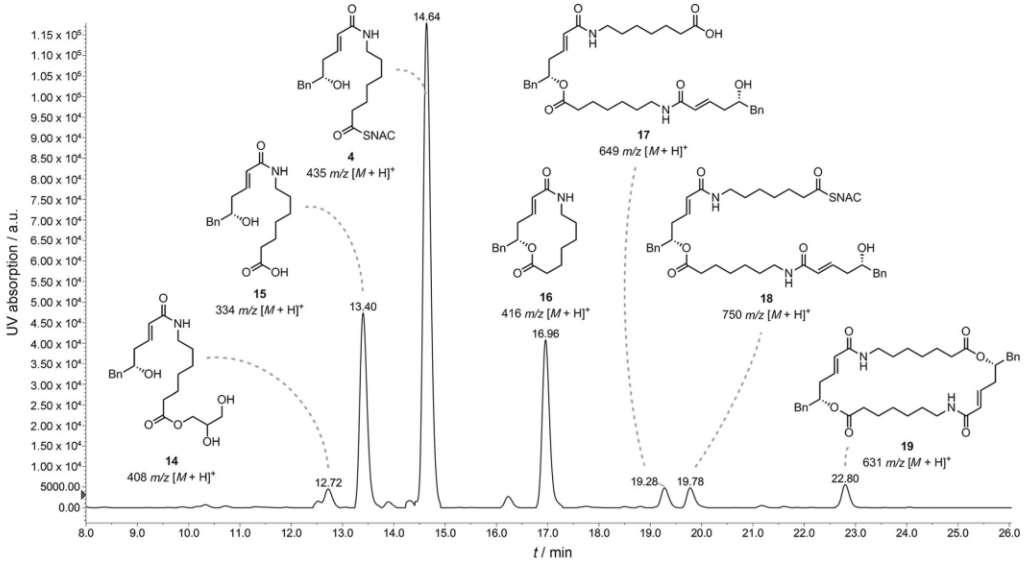

Figure 2. LCMS analysis of the enzymatic reaction of **4** with DEBS TE. The UV (254 nm) trace between 8 and 26 min is shown. Major and minor products are indicated on each trace with the observed *m*/*z* values.

© 2014 Wiley-VCH Verlag GmbH & Co. KGaA, Weinheim

CHEMBIOCHEM
COMMUNICATIONS
www.chembiochem.org

ured alcohols were necessary for macrocyclization (Figures 2 and S4). The L-configured alcohol **4** was clearly converted into the 14-member ring macrolactone **16**, whereas the D-configured alcohol *ent*-**4**, did not appear to be converted. Although trace **16** can be observed from prolonged incubation of *ent*-**4** with DEBS TE (Figure S4), the level of **16** formation was consistent with conversion of trace **4** found in *ent*-**4** into macrocycle (*ent*-**4** *ee* 90%, see the Supporting Information). Incubation of **4** and *ent*-**4** with DEBS TE D169A, which is folded but catalytically inactive,[30] showed no consumption of the substrates or product formation (Figures S7–S12). Macrolactone **16** obtained from the treatment of **4** with wild type DEBS TE was confirmed by MS and ^{1}H NMR analysis. Kinetic characterization of DEBS TE activity with **4** and *ent*-**4** displayed Michaelis–Menten kinetics with k_{cat} values of 0.228 ± 0.015 min^{-1} and 0.114 ± 0.008 min^{-1}, respectively, K_M values of 2.8 ± 0.4 mM and 1.3 ± 0.2 mM, respectively and k_{cat}/K_M values of 1.4 ± 0.3 M^{-1} s^{-1} and 1.5 ± 0.3 M^{-1} s^{-1}, respectively (Figures S13 and S14). These data are consistent with the observed catalytic efficiencies of in vitro characterized modular polyketide TEs.[11–13,25,26,28–31,39,40] For example DEBS TE processed **3** with a specificity constant of 1.2 ± 0.5 M^{-1} s^{-1}, which is in excellent agreement with our data.

Analysis of the reaction products for **4** also demonstrated that the C_2- symmetrical, head-to-tail dimerized macrodiolide product **19** ([*M*+H]$^+$ 631 *m/z*) was also formed. In addition, the glycerolysis adduct **14** ([*M*+H]$^+$ 408 *m/z*), hydrolysis product **15** ([*M*+H]$^+$ 334 *m/z*), the linear dimer *seco*-acid **17** ([*M*+H]$^+$ 648 *m/z*), and linear dimer NAC-thioester **18** ([*M*+H]$^+$ 750 *m/z*) were also observed (Figure 2). The structures of the dimeric compounds were consistent with ^{1}H NMR and MS/MS data collected on these compounds (Supporting Information). The formation of the macrodiolide and linear dimer structures is unprecedented for the DEBS TE, though TEs from the biosynthesis of elaiophylin[23] and disorazol[24] are proposed to catalyze this chemistry.

The mechanism for related non-ribosomal peptide synthetase TE-mediated dimer formation has been investigated in vitro.[41–43] Enterobactin TE, which trimerizes a 2,3-dihydroxybenzoyl-L-serinyl monomer and macrocyclizes it to generate a macrotriolide has been biochemically characterized. By using top-down mass spectrometry, a mutant of this TE was shown to accumulate monomeric and dimeric acyl-enzyme intermediates. It was postulated that the dimer was formed by the seryl side chain alcohol of the monomer-TE attacking an activated thioester of a second equivalent of monomer.[41] The formation of **18** in the current study strongly suggests that a second equivalent of monomer attacks the electrophilic monomeric TE acyl-enzyme intermediate, generating the dimeric NAC-thioester **18**. This type of mechanism was also proposed for the formation of the macrocyclic dimeric non-ribosomal peptide, gramicidin.[43] We thus propose that in our assay, formation of the macrodiolide **19** and the dimeric free acid **17** occurs by loading of **18** onto the TE to generate a dimeric acyl-enzyme intermediate, which can undergo macrocyclization and hydrolysis, respectively.

This mechanism requires an exogenous nucleophile (a second equivalent of monomer) to attack the TE acyl-enzyme intermediate, releasing a linear ester. This type of transesterification activity has been seen with glycerol and type I PKS TEs,[19] as well as with the TE for the fungal pathway responsible for zearalenone biosynthesis (Zea TE).[44] In the case of the Zea TE, a wide range of simple exogenous nucleophiles were shown to be capable of accessing the acyl-enzyme intermediate. We thus hypothesized that if dimer formation was occurring through exogenous nucleophile attack on the acyl-enzyme intermediate by a second equivalent of monomer, then other exogenous nucleophiles should also be able to attack the acyl-enzyme intermediate. We therefore investigated the ability of **4** to undergo DEBS TE-catalyzed transesterification with exogenous alcohols. A panel of alcohols were incubated with **4**, generating the corresponding ester adducts (Table 1). The formation of the ester products was consistent with our proposed mechanism for dimer formation, further supporting this mechanism. Comparison of the relative conversion to the transesterification product showed that primary alcohols were converted most effectively into esters as compared to secondary and tertiary alcohols. As was seen with the transesterification catalyzed by the fungal Zea TE, butan-1-ol was the most competent alcohol substrate for DEBS TE.[44] This similar substrate specificity in two diverse TEs suggests that transesterification could be a broadly conserved activity for PKS TEs; however, further examples are needed to test this hypothesis.

Table 1. Relative velocities for DEBS TE-mediated crosscoupling with exogenous *O*-nucleophiles.[a]

Nucleophile	Relative conversion	Nucleophile	Relative conversion	Nucleophile
butan-1-ol	1.00 ± 0.08	pentan-3-ol	0.26 ± 0.02	butan-1-ol
propan-1-ol	0.85 ± 0.16	pentan-1-ol	0.22 ± 0.08	propan-1-ol
methanol	0.38 ± 0.03	hexan-1-ol	0.17 ± 0.05	methanol
ethanol	0.36 ± 0.04	*t*-butanol	0.14 ± 0.01	ethanol
cyclohexanol	0.34 ± 0.02	propan-2-ol	0.12 ± 0.01	cyclohexanol

[a] For 15 μM DEBS TE with 2.5 mM **4** in 50 mM phosphate buffer (pH 7.4) at 23 °C, with DMSO (10%, *v/v*) and 100 μM nucleophile. Negative controls lacking DEBS TE showed no reactivity.

Incubation of DEBS TE with **5**, the methyl-substituted derivative, led to formation of the hydrolysis product with no detectable macrocycle. Kinetic characterization of the enzymatic activity fit the Michaelis–Menten model, providing a k_{cat} value of 0.20 ± 0.01 min^{-1} and a K_M value of 0.75 ± 0.13 mM (Figure S15), consistent with type I PKS TE-catalyzed chemistries.[11–13,25,26,28–31,39,40] The addition of the α-methyl group substantially increases the allylic 1,3-strain[45] across the amide bond, limiting access to the *S-trans* configuration required for macrocyclization. The observed lack of macrocyclization with **5** thus suggests that DEBS TE was unable to overcome intrinsic unfavorability of the reactive conformation of the substrate.

The screening hypothesis suggests that long-term evolutionary selection favors pathways that support chemical diversity and can be readily "screened" in the face of new environ-

© 2014 Wiley-VCH Verlag GmbH & Co. KGaA, Weinheim

CHEMBIOCHEM
COMMUNICATIONS
www.chembiochem.org

ments.[14,15] In part, the diversity in a multistep pathway is dependent on substrate tolerance of late-stage enzymes. This tolerance permits plasticity in the upstream components of the pathway and fitness-based screening of the newly released compounds. In addition, the off-loading enzymes should be able to process diverse substrates and introduce substantial new chemical diversity to amplify the new compounds accessible from upstream modifications.

Our results, in light of the screening hypothesis, suggest a model for the evolution of type I polyketide chemical diversity in the context of TE-mediated off-loading. We propose that ancestral TEs were able to catalyze a variety of chemistries including hydrolysis, esterification, amidation, macrocyclization, and macrodiolide formation. This range of reactivity expands the chemical diversity accessible from a PKS pathway. As one metabolite, such as a macrodiolide, becomes essential for improving fitness in a particular environment, the TE evolves under pressure to enrich for the corresponding reactivity. This is supported by the phylogenic analysis, which is consistent with convergent evolution of macrodiolide-forming activity. We hypothesize that the ability to access this diversity of reactivity is retained as TE evolves to become selective for a particular product. Based on this hypothesis, we predict that small changes to the substrate can unlock access to this ancestral activity. This has been observed in the in vitro characterization of the DEBS TE domain, where subtle structural changes lead to dramatic changes in reactivity, from hydrolysis, to macrocycle formation, to macrodiolide formation.

Our fitness-based model is sufficient to account for the observed experimental TE activity results in the literature. It can also be used predictively. For example, polyketide natural products have been isolated with functional groups derived from TE-mediated hydrolysis, macrolactonization, macrolactamization, and dimerization. However, no transesterification-derived polyketide products have been isolated. Having observed a butan-1-ol kinetic preference in two diverse TEs, we predict that a butan-1-ol ester would likely be natively produced by a yet unidentified PKS pathway. Furthermore, as the presence of butan-1-ol is required for this activity, we predict that it will be observed in a native producer of butanol, such as the genus *Clostridium*, when at least three of the forty sequenced genomes (*Clostridium kluyveri* DSM 555, *Clostridium botulinum* A2 BoNT, and *C. botulinum* H04402 065) encode a TE[46] and possess a butanol dehydrogenase A (*bdhA*) orthologue.[47]

In summary, we have used phylogenic analysis and in vitro biochemical characterization to develop and support an evolutionary model in which the plasticity of TEs increases long-term fitness through the retained ability to generate and access chemical diversity. We biochemically showed with recombinant DEBS TE that small, evolutionarily accessible changes to the substrate can lead to multiple different chemistries, including hydrolysis, macrocyclization, dimerization, macrodiolide formation, and transesterification.

Acknowledgements

This work was supported by the Natural Sciences and Engineering Research Council (NSERC) of Canada, the Canadian Foundation for Innovation, the Ministry for Research and Innovation, and the University of Ottawa.

Keywords: macrodiolide · macrolactone · screening hypothesis · substrate selectivity · thioesterase

[1] C. Khosla, D. Herschlag, D. E. Cane, C. T. Walsh, *Biochemistry* **2014**, *53*, 2875.
[2] T. A. M. Gulder, M. F. Freeman, J. Piel, *Top. Curr. Chem.* **2011**; DOI: 10.1007/128_2010_113.
[3] H. Jenke-Kodama, A. Sandmann, R. Müller, E. Dittmann, *Mol. Biol. Evol.* **2005**, *22*, 2027.
[4] C. P. Ridley, H. Y. Lee, C. Khosla, *Proc. Natl. Acad. Sci. USA* **2008**, *105*, 4595.
[5] G. Yadav, R. S. Gokhale, D. Mohanty, *J. Mol. Biol.* **2003**, *328*, 335.
[6] P. Hill, J. Piel, S. Aris-Brosou, V. Krištůfek, C. N. Boddy, L. Dijkhuizen, *J. Ind. Microbiol. Biotechnol.* **2014**, *41*, 75.
[7] T. Nguyen, K. Ishida, H. Jenke-Kodama, E. Dittmann, C. Gurgui, T. Hochmuth, S. Taudien, M. Platzer, C. Hertweck, J. Piel, *Nat. Biotechnol.* **2008**, *26*, 225.
[8] R. Teta, M. Gurgui, E. J. N. Helfrich, S. Künne, A. Schneider, G. Van Echten-Deckert, A. Mangoni, J. Piel, *ChemBioChem* **2010**, *11*, 2506.
[9] P. Caffrey, *ChemBioChem* **2003**, *4*, 654.
[10] R. Reid, M. Piagentini, E. Rodriguez, G. Ashley, N. Viswanathan, J. Carney, D. V. Santi, C. R. Hutchinson, R. McDaniel, *Biochemistry* **2003**, *42*, 72.
[11] R. S. Gokhale, D. Hunziker, D. E. Cane, C. Khosla, *Chem. Biol.* **1999**, *6*, 117.
[12] C. N. Boddy, T. L. Schneider, K. Hotta, C. T. Walsh, C. Khosla, *J. Am. Chem. Soc.* **2003**, *125*, 3428.
[13] C. C. Aldrich, L. Venkatraman, D. H. Sherman, R. A. Fecik, *J. Am. Chem. Soc.* **2005**, *127*, 8910.
[14] R. D. Firn, C. G. Jones, *Nat. Prod. Rep.* **2003**, *20*, 382.
[15] R. D. Firn, C. G. Jones, *J. Exp. Bot.* **2009**, *60*, 719.
[16] R. M. Kohli, C. T. Walsh, *Chem. Commun.* **2003**, 297.
[17] B. Julien, Z.-Q. Tian, R. Reid, C. D. Reeves, *Chem. Biol.* **2006**, *13*, 1277.
[18] J. Young, D. C. Stevens, R. Carmichael, J. Tan, S. Rachid, C. N. Boddy, R. Müller, R. E. Taylor, *J. Nat. Prod.* **2013**, *76*, 2269.
[19] A. J. Hughes, M. R. Tibby, D. T. Wagner, J. N. Brantley, A. T. Keatinge-Clay, *Chem. Commun.* **2014**, *50*, 5276 – 5278.
[20] S. Donadio, M. J. Staver, J. B. McAlpine, S. J. Swanson, L. Katz, *Science* **1991**, *252*, 675.
[21] L. Tang, S. Shah, L. Chung, J. Carney, L. Katz, C. Khosla, B. Julien, *Science* **2000**, *287*, 640.
[22] I. Molnár, T. Schupp, M. Ono, R. Zirkle, M. Milnamow, B. Nowak-Thompson, N. Engel, C. Toupet, A. Stratmann, D. D. Cyr, J. Gorlach, J. M. Mayo, A. Hu, S. Goff, J. Schmid, J. M. Ligon, *Chem. Biol.* **2000**, *7*, 97.
[23] M. Kopp, H. Irschik, S. Pradella, R. Müller, *ChemBioChem* **2005**, *6*, 1277.
[24] S. F. Haydock, T. Mironenko, H. I. Ghoorahoo, P. F. Leadlay, *J. Biotechnol.* **2004**, *113*, 55.
[25] A. Pinto, M. Wang, M. Horsman, C. N. Boddy, *Org. Lett.* **2012**, *14*, 2278.
[26] W. He, J. Wu, C. Khosla, D. E. Cane, *Bioorg. Med. Chem. Lett.* **2006**, *16*, 391.
[27] J. R. Jacobsen, C. R. Hutchinson, D. E. Cane, C. Khosla, *Science* **1997**, *277*, 367.
[28] H. Lu, S.-C. Tsai, C. Khosla, D. E. Cane, *Biochemistry* **2002**, *41*, 12590.
[29] K. K. Sharma, C. N. Boddy, *Bioorg. Med. Chem. Lett.* **2007**, *17*, 3034.
[30] M. Wang, C. N. Boddy, *Biochemistry* **2008**, *47*, 11793.
[31] M. Wang, P. Opare, C. N. Boddy, *Bioorg. Med. Chem. Lett.* **2009**, *19*, 1413.
[32] Y. Liu, T. Zheng, S. D. Bruner, *Chem. Biol.* **2011**, *18*, 1482.
[33] C. M. Kao, G. Luo, L. Katz, D. E. Cane, C. Khosla, *J. Am. Chem. Soc.* **1995**, *117*, 9105.
[34] C. M. Kao, M. McPherson, R. N. McDaniel, H. Fu, D. E. Cane, C. Khosla, *J. Am. Chem. Soc.* **1997**, *119*, 11339.
[35] Q. Xue, G. Ashley, C. R. Hutchinson, D. V. Santi, *Proc. Natl. Acad. Sci. USA* **1999**, *96*, 11740.

© 2014 Wiley-VCH Verlag GmbH & Co. KGaA, Weinheim

CHEMBIOCHEM
COMMUNICATIONS
www.chembiochem.org

[36] R. McDaniel, A. Thamchaipenet, C. Gustafsson, H. Fu, M. Betlach, G. Ashley, *Proc. Natl. Acad. Sci. USA* **1999**, *96*, 1846.
[37] H. C. Brown, P. K. Jadhav, *J. Am. Chem. Soc.* **1983**, *105*, 2092.
[38] P. K. Jadhav, K. S. Bhat, P. T. Perumal, H. C. Brown, *J. Org. Chem.* **1986**, *51*, 432.
[39] J. B. Scaglione, D. L. Akey, R. Sullivan, J. D. Kittendorf, C. M. Rath, E.-S. Kim, J. L. Smith, D. H. Sherman, *Angew. Chem. Int. Ed.* **2010**, *49*, 5726; *Angew. Chem.* **2010**, *122*, 5862.
[40] Z. Q. Beck, C. C. Aldrich, N. A. Magarvey, G. I. Georg, D. H. Sherman, *Biochemistry* **2005**, *44*, 13457.
[41] C. A. Shaw-Reid, N. L. Kelleher, H. C. Losey, A. M. Gehring, C. Berg, C. T. Walsh, *Chem. Biol.* **1999**, *6*, 385.
[42] J. W. Trauger, R. M. Kohli, H. D. Mootz, M. A. Marahiel, C. T. Walsh, *Nature* **2000**, *407*, 215.
[43] K. M. Hoyer, C. Mahlert, M. A. Marahiel, *Chem. Biol.* **2007**, *14*, 13.
[44] M. Wang, H. Zhou, M. Wirz, Y. Tang, C. N. Boddy, *Biochemistry* **2009**, *48*, 6288.
[45] R. W. Hoffmann, *Chem. Rev.* **1989**, *89*, 1841.
[46] A.-C. Letzel, S. J. Pidot, C. Hertweck, *Nat. Prod. Rep.* **2013**, *30*, 392.
[47] D. J. Petersen, R. W. Welch, F. B. Rudolph, G. N. Bennett, *J. Bacteriol.* **1991**, *173*, 1831.

Received: August 22, 2014
Published online on October 29, 2014

© 2014 Wiley-VCH Verlag GmbH & Co. KGaA, Weinheim

JOC The Journal of Organic Chemistry

Article

pubs.acs.org/joc

Diastereoseletive Transannular Oxa-Conjugate Addition Generates the 2,6-*cis*-Disubstituted Tetrahydropyran of Neopeltolide

Taylor P. A. Hari,[†] Burkardt I. Wilke,[‡] James A. Davey,[†] and Christopher N. Boddy*[,†]

[†]Department of Chemistry & Biomolecular Sciences, University of Ottawa, Ottawa, Ontario, Canada K1N 6N5

[‡]Department of Chemistry, Syracuse University, Syracuse, New York 13244, United States

Supporting Information

ABSTRACT: Transannular 2,6-disubstituted pyrans, like the one found in the cytotoxic marine natural product neopeltolide, are a key functional group in many polyketides. While oxa-conjugate additions have been shown to provide direct and rapid access to tetrahydropyrans in acyclic neopeltolide intermediates, a transannular strategy for construction of this ring system in a macrocyclic core has not been investigated. In this study, we demonstrate that a transannular oxa-conjugate addition strategy is a viable approach to the construction of the bicyclic core of neopeltolide. We show that transannular addition occurs readily with an α,β-unsaturated ketone as the Michael acceptor and does not occur when an α,β-unsaturated ester is the Michael acceptor. Our data indicates that oxa-conjugate addition is reversible and that the stereochemical outcome can be under thermodynamic control. Using computational chemistry, we show that the lowest energy diastereomer is the desired *cis*-pyran found in neopeltolide, and we experimentally demonstrate that the *trans* and *cis* diastereomers are interconvertible under reaction conditions with the *cis*-pyran product predominating. This oxa-conjugate addition strategy should provide a viable route to accessing the fully elaborated macrocyclic core of neopeltolide.

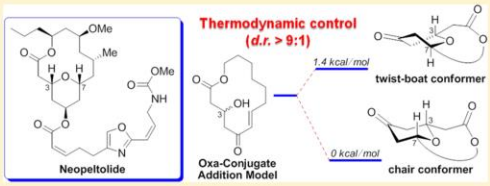

INTRODUCTION

2,6-Disubstituted pyrans are a common ring system found in polyketides, which add significant conformational rigidity to these natural products and can play a role in controlling the bioactive conformation of the molecule. While pyrans with varying oxidation states are observed in polyketides, a common and important motif is the tetrahydropyran (THP), as seen in the natural products neopeltolide[1] (**1**, Figure 1), leucascandrolide[2] (**2**), bryostatin[3] (**3**), and dactylolide[4] (**4**). In line with our efforts to develop bioinspired transannular oxa-conjugate addition strategies for the total synthesis and chemo-enzymatic syntheses of this class of natural products,[5] we present two strategies for accessing the neopeltolide macrocyclic core via a transannular oxa-conjugate addition.

Neopeltolide is a 14-membered macrolide natural product that was isolated from a deep-water sponge of the family Neopeltidae, collected off the northern coast of Jamaica by Wright and co-workers in 2007.[1] They established the planar structure and relative configuration of **1** through extensive NMR spectroscopic data. Subsequent reassignment of the relative stereochemistry and determination of the absolute configuration were independently reported by Panek[6] and Scheidt[7] through total syntheses. The key structural elements of **1** include a 14-membered macrocyclic backbone containing a 2,6-*cis*-tetrahydropyran ring with an oxazole-bearing side chain attached to the THP.

Initial biological evaluation revealed that neopeltolide exhibits potent cytotoxic activities against several cell lines

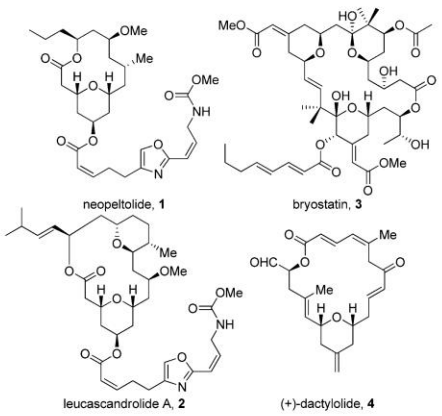

Figure 1. Selected polyketide natural products that possess a 2,6-disubstituted THP motif.

with nanomolar IC_{50} values.[1] Kozmin and co-workers reported that neopeltolide targets cytochrome bc_1 complex and may inhibit mitochondrial ATP synthesis.[8] Because of its promising

Received: August 28, 2015
Published: December 16, 2015

ACS Publications © 2015 American Chemical Society

DOI: 10.1021/acs.joc.5b02014
J. Org. Chem. 2016, 81, 415−423

biological activity and appealing architecture, several total syntheses,[6,7,9−14] formal total syntheses,[15−25] and analog syntheses[8,26−33] have been reported. In this paper, we report the synthesis of a neopeltolide model that exploits an acid-catalyzed transannular oxa-conjugate addition for the construction of the 2,6-*cis*-disubstituted tetrahydropyran ring.

While Michael additions using carbon or nitrogen nucleophiles are common and typically facile, Michael additions with oxygen nucleophiles are more challenging.[34,35] These oxa-conjugate additions are typically under thermodynamic control and are enthalpically unfavorable. In addition, the hard oxygen nucleophile is mismatched with the softer electrophilic β-carbon of the α,β-unsaturated carbonyl.

However, since oxa-conjugate additions provide direct and rapid access to THPs, this strategy has been applied to the construction of neopeltolide (Scheme 1). Both Hong in 2009[18]

Scheme 1. Literature Examples of Oxa-Conjugated Ester and Aldehyde/Ketone Michael Addition Strategies Used To Access the 2,6-Disubstituted THP Ring of Neopeltolide

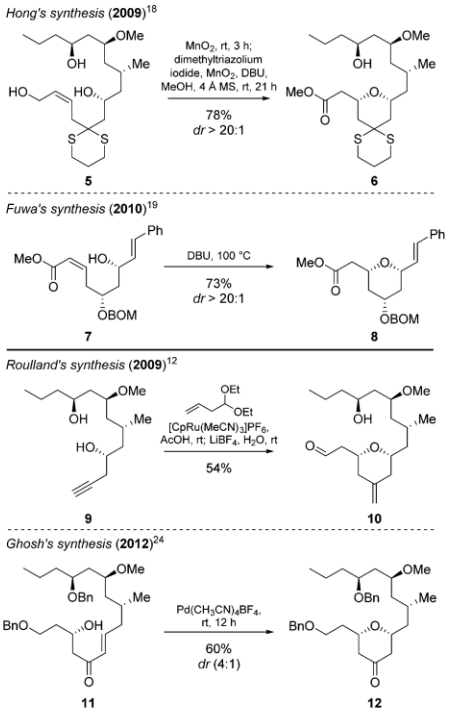

and Fuwa in 2010[19] used addition of a ζ-hydroxy into a linear α,β-unsaturated ester to generate the *cis*-THP found in neopeltolide (**6** and **8**, Scheme 1). Roulland (2009)[12] and Ghosh (2012)[24] both developed mild oxa-conjugate addition routes to the neopeltolide THP core. These two strategies relied on addition to α,β-unsaturated aldehydes and ketones respectively (**10** and **12**, Scheme 1). The lowest unoccupied molecular orbital (LUMO) energies for these electrophiles is significantly lower in energy as compared to the corresponding α,β-unsaturated esters, facilitating the addition reaction.

While both the ester and aldehyde/ketone strategies provide strong precedent for use of oxa-conjugate addition in the construction of the *cis*-THP from neopeltolide, they also highlight some of the challenges associated with this strategy. For example, Fuwa's system required moderately high temperatures for THP formation, and low diastereoselectivity was observed under the mild conditions employed by Ghosh. In this study, we investigate the effect of preorganizing the nucleophilic alcohol and the electrophilic α,β-unsaturated carbonyl for oxa-conjugate addition by constraining it in a 14-membered macrocycle. Like Hong's[18] use of the Thorpe−Ingold effect,[36] this preorganization is expected to lower the reaction energy barrier, thereby enabling milder reaction conditions. The macrocycle is also expected to exacerbate the energetic differences between the *cis*- and *trans*-THP, resulting in increased diastereoselectivity. Herein we validate this approach by demonstrating transannular addition to an α,β-unsaturated ketone is effective in accessing the neopeltolide macrocyclic core in both high yield and high diastereoselectivity.

■ RESULTS AND DISCUSSION

Two conjugated model substrates were designed to address the impact of the macrocycle on oxa-conjugate addition approaches to the neopeltolide core (**13**, Figure 2). In the first model

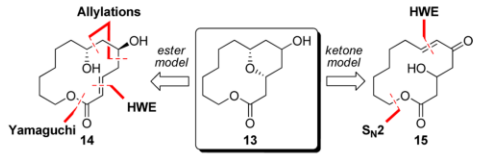

Figure 2. Unsaturated ester and ketone model systems for accessing the macrocyclic core of neopeltolide via transannular oxa-conjugate addition.

system, THP formation relies on the addition of a ζ-hydroxy group into an α,β-unsaturated ester (**14**). Ester **14** was envisioned to be readily accessible through sequential allylations with the macrocyclic core being synthesized by a Yamaguchi macrolactonization. In the second system THP formation relies on the addition of a β'-hydroxy into an α,β-unsaturated ketone (**15**). Ketone **15** was deigned to be accessed through a convergent route relying on a Horner−Wadsworth−Emmons olefination and an S_N2 lactonization.

***α,β*-Unsaturated Ester System.** Synthesis of the α,β-unsaturated ester system began by addition of allylmagnesium bromide to the known aldehyde **16**[37] (Scheme 2) to afford the corresponding homoallylic alcohol. The alcohol was protected with a *tert*-butyldimethylsilyl (TBS) group to yield the silyl ether, **17**, in 64% yield over two steps. The olefin was dihydroxylated and the diol was oxidatively cleaved to provide its aldehyde, which was used in a second nondiastereoselective allylation and subsequent TBS protection. Conversion of olefin **18** to its corresponding aldehyde allowed for a Horner−Wadsworth−Emmons (HWE)[38] coupling with triethylphosphonoacetate to give the desired *trans*-α,β-unsaturated ethyl ester **19** in 57% yield. Removal of the PMB ether and saponification of the ethyl ester yielded the *seco*-acid, which

DOI: 10.1021/acs.joc.5b02014
J. Org. Chem. 2016, 81, 415−423

Scheme 2. Synthesis of the α,β-Unsaturated Ester Model System of Neopeltolide

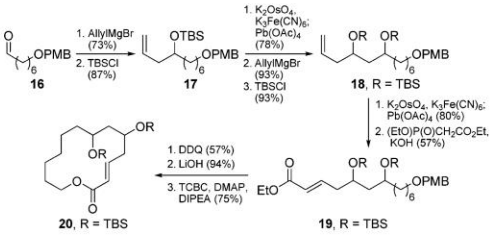

cleanly underwent Yamaguchi macrolactonization[39] to provide macrolactone **20** in 75% yield as an inseparable mixture of *syn* and *anti* diastereomers.

With macrolactone **20** in hand, desilylation was accomplished by treatment with HF to provide a 1:1 ratio of separable *syn*- (**14**) and *anti*-diols (**21**, Scheme 3) in high yield. The Rychnovsky acetal-based approach[40] was used to establish the relative stereochemistry of the diols in each diastereomer.[41]

Scheme 3. Transannular Oxa-Michael Addition Fails for Ester-Conjugated Model System of Neopeltolide

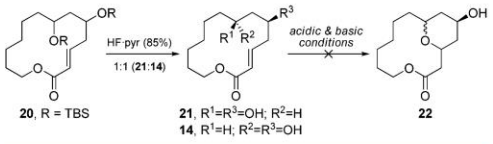

A stock solution of 0.1 M DBU in C_6D_6 was prepared and used as the reaction solvent for both diastereomers **21** and **14**. Contrary to the successful use of DBU in the oxa-conjugate additions observed for both linear and transannular systems by Fuwa[13] and Shishido,[42,43] respectively, **21** and **14** were unreactive at room temperature and completely consumed at reflux without observable formation of the desired THP product. Elimination, leading toward formation of sorbate containing compounds, predominated. Screening of a variety of alternative basic and acidic reaction conditions similarly failed to find conditions that accessed the THP from **14** and **21**.

***α,β*-Unsaturated Ketone System.** We hypothesized that the ability to access the THP system from either of diastereomers **14** and **21** was limited by the high energy of the α,β-unsaturated ester LUMO. Because α,β-unsaturated ketones possess markedly lower energy LUMOs as compared to their α,β-unsaturated esters homologues,[44] we redesigned the model system to incorporate this functional group as the Michael acceptor, **15**.

A key precedent for our ketone model system (**15**) was Rizzacasa and co-workers' study of apicularen A.[45,46] In their total synthesis of apicularen A, which possesses a *trans* dihydropyrone, they rely on a reversible acid-catalyzed transannular addition of a β'-hydroxy into an α,β-unsaturated ketone **23** (Figure 3). Their studies showed that they could access the kinetic *cis*-pyran **24**[45] and that, via E1cB elimination/oxa-conjugate addition mechanisms, they were able to equilibrate the products to the thermodynamically favored *trans* diastereomer **25** with a good diastereomeric ratio (>10:1).[46]

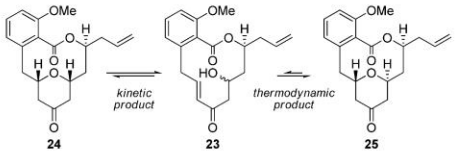

Figure 3. Rizzacasa and co-workers' study of apicularen A demonstrates the success of a reversible acid-catalyzed transannular addition of a β'-hydroxy into an α,β-unsaturated ketone.[45,46]

Based on this precedent, we undertook the synthesis of model system **15** to access the THP of neopeltolide (Scheme 4). The synthesis began with the HWE-coupling of the

Scheme 4. Synthesis of the α,β-Unsaturated Ketone System of Neopeltolide Model

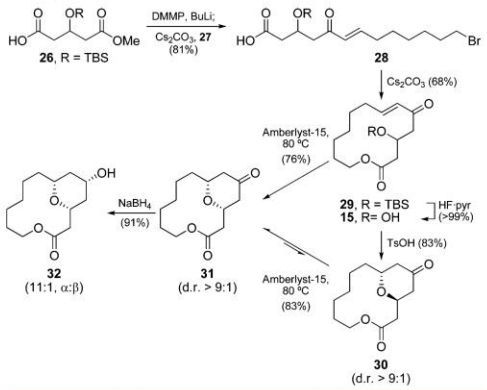

phosphonate, generated from addition of dimethyl methylphosphonate to the acid **26**,[47] and 7-bromoheptanal (**27**), to yield the bromo acid **28** in good yield. Base-mediated S_N2 macrolactonization generated macrocyclic enone **29**, which was desilylated with HF to yield the oxa-conjugate addition precursor **15**.

Oxa-conjugate addition precursor **15** failed to produce THP containing products under a wide variety of typical base-mediated conditions for oxa-conjugate addition, including DBU[13] and KOtBu,[48−50] at room temperature and elevated temperatures (up to 110 °C). Treatment with *p*-toluenesulfonic acid at room temperature however rapidly (<15 min) led to formation of the THP containing macrocycle **30** with high diastereoselectivity (d.r. > 9:1). Extensive 1D and 2D NMR analysis (HSQC, COSY, NOESY, Figure S1) confirmed that the major product was the 2,6-*trans*-THP.

A computational approach was used to evaluate the relative energies of the *cis* and *trans* diastereomers to determine if reversible oxa-conjugate addition under thermodynamic control could access the desired *cis* product. The structures of **30** and **31** were subjected to an initial PM6[51] optimization prior to a B3LYP/6-31++G** energy minimization.[52−54] Potential energies of the energy-minimized structures were computed. A vibrational analysis was performed and resulted in no imaginary frequencies, indicating the geometries of each compound occupy a local minimum. The *trans*-THP (**30**) was found to be in a twist boat conformation and was approximately 1.4 kcal/

DOI: 10.1021/acs.joc.5b02014
J. Org. Chem. 2016, 81, 415−423

mol higher in energy that the *cis*-THP (**31**), which was predicted to adopt a chair conformation.

Based on these computational results, we identified reaction conditions that led to thermodynamic control for the transannular oxa-conjugate addition. **15** was converted in high diastereoselectivity (>9:1 d.r.) to the thermodynamic product **31** by treatment with Amberlyst-15 (80 °C, 4 h). The observed *cis*-to-*trans* product ratio of 90:10 is in good agreement with the computationally predicted equilibrium ratio at 80 °C of 87.5:12.5 *cis*-to-*trans*. To confirm that formation of the *cis* product is occurring from the kinetic *trans* product, the *trans*-THP **30** was subjected to identical Amberlyst-15 conditions and the *cis* product was isolated in comparable yield with identical diastereoselectivity (>9:1 d.r.).

Under thermodynamic conditions, THP ring opening of **30** and **32** is expected to occur through elimination of the C3−*O* bond and C7−*O* bond as is seen for thermodynamically controlled oxa-conjugate additions of linear enantiopure β-hydroxy enones[54] and the transannular oxa-conjugate addition based synthesis of apicularen.[46] For linear enantiopure β-hydroxy enones, this dual elimination pathway is problematic as it leads to loss of stereochemical integrity.[55] However, in the context of transannular oxa-conjugate addition approaches, it enables remote stereochemical control of both stereogenic centers as was shown in the synthesis of **25** from **23**, where the configuration of the lactone stereocenter was sufficient to control both THP stereogeneic centers.[46] This remote stereocontrol may ultimately prove useful in the synthesis of neopeltolide by an oxa-conjugate addition approach.

Selective reduction of the ketone **31** was accomplished with $NaBH_4$ into key alcohol **32** (11:1, α:β). Under Mitsunobu conditions,[56] Scheidt[7] and others[8,9,11−14,26,29−31,33] have established that this configuration at C5 allows coupling with a suitable oxazole-bearing neopeltolide side chain.

■ CONCLUSIONS

In this study, we have demonstrated that a transannular oxa-conjugate addition strategy is a viable approach to the construction of the macrocyclic core of neopeltolide. We have shown that addition of an intramolecular alcohol to an α,β-unsaturated ketone embedded in a 14-membered macrolactone is superior to the strategy where the corresponding α,β-unsaturated ester acts as the Michael acceptor. Our experimental and computational data indicate that the addition is reversible and can be performed under kinetic control to access the *trans*-THP product or thermodynamic control to access the *cis*-THP. This oxa-conjugate addition strategy should provide a viable route to accessing the fully elaborated macrocyclic core of neopeltolide. Finally due to the strategic position of the functional groups required for oxa-conjugate addition, engineered polyketide synthase pathways can be designed to produce these oxa-conjugate addition substrates, opening the door to *in vivo*[57] or *in vitro*[58] chemoenzymatic production of THP precursors that can be chemically converted into THP containing compounds.[5]

■ EXPERIMENTAL SECTION

7-(*O*-*p*-Methoxybenzyloxy)heptanal (16). To an oven-dried round-bottom flask under N_2 containing a Teflon stir bar were added SO_3-pyridine (12.2 g, 76.6 mmol, 2.0 equiv), methylene chloride (75 mL), and DMSO (27.0 mL, 383 mmol, 10 equiv). The resulting suspension was cooled to 0 °C in an ice bath. To the vigorously stirred suspension was added triethylamine (27 mL, 192 mmol, 5 equiv) followed by stirring at 0 °C for 30 min. Known PMB alcohol[37] (9.67 g, 38.3 mmol, 1.0 equiv) was dissolved in methylene chloride (65 mL) in a separate flask and added to the vigorously stirred solution of the activated DMSO complex at 0 °C via cannula. An additional portion of methylene chloride (10 mL) was used to transfer via cannula any remaining starting material. The reaction was allowed to warm to rt and stirred for an additional 6 h. The reaction was quenched with saturated aqueous NH_4Cl (50 mL) followed by the addition of distilled water (50 mL). The organic layer was washed with a second portion of 1:1 v/v saturated aqueous NH_4Cl/distilled water (100 mL total volume) followed by saturated aqueous NH_4Cl (100 mL). The organic layer was washed with brine (100 mL), dried with $MgSO_4$, and concentrated *in vacuo* to give a clear oil. The residue was purified by flash chromatography (silica gel, 20% ethyl acetate in hexanes) to obtain 7.19 g of a colorless oil (28.7 mmol, 75% yield). R_f = 0.50 (silica gel, 40% ethyl acetate in hexanes); ^{1}H NMR (400 MHz, $CDCl_3$) δ 9.73 (t, J = 1.8 Hz, 1H), 7.24 (d, J = 8.6 Hz, 2H), 6.86 (d, J = 8.6 Hz, 2H), 4.40 (s, 2H), 3.78 (s, 3H), 3.41 (t, J = 6.5 Hz, 2H), 2.40 (td, J = 7.5, 1.8 Hz, 2H), 1.66−1.52 (m, 4H), 1.42−1.27 (m, 4H) ppm. NMR spectra consistent with those previously reported within literature.[37]

4-Hydroxy-10-(*O*-*p*-methoxybenzyloxy)dec-1-ene (S1). To an oven-dried round-bottom flask under N_2 charged with a Teflon stir bar and PMB aldehyde **16** (7.19 g, 28.7 mmol, 1 equiv) was added THF (250 mL). The resulting solution was cooled to 0 °C in an ice bath, and allylmagnesium bromide, 1.0 M in THF (30 mL, 30 mmol, 1.05 equiv), was added dropwise over 5 min. The reaction was stirred at 0 °C for 10 min. The reaction was quenched with saturated aqueous NH_4Cl (150 mL), and the organic layer was removed. The aqueous phase was extracted with ethyl acetate (3 × 75 mL). The combined organic layers were washed with brine (100 mL), dried with $MgSO_4$, and concentrated *in vacuo* to give a yellow oil. The residue was purified by flash chromatography on silica gel (60 g) with a 20% ethyl acetate in hexanes solvent system to obtain 6.10 g of colorless oil (20.9 mmol, 73% yield). R_f = 0.45 (silica gel, 40% ethyl acetate in hexanes); ^{1}H NMR (300 MHz, $CDCl_3$) δ 7.24 (d, J = 8.6 Hz, 2H), 6.86 (d, J = 8.6 Hz, 2H), 5.86−5.72 (m, 1H), 5.11−5.04 (m, 2H), 4.38 (s, 2H), 3.73 (s, 3H), 3.56 (br s, 1H), 3.39 (t, J = 6.6 Hz, 2H), 2.27−2.18 (m, 1H), 2.18−2.04 (m, 2H), 1.57 (p, J = 7.0 Hz, 2H), 1.40−1.26 (m, 8H) ppm; ^{13}C NMR (100 MHz, $CDCl_3$) δ 159.0, 135.0, 130.7, 129.2, 117.6, 113.7, 72.4, 70.6, 55.2, 41.9, 36.7, 29.6, 29.4, 26.1, 25.6 ppm. HRMS (ESI+ TOF) m/z: calculated for $C_{18}H_{28}O_3K$ [(M + K)$^+$] 331.1675, observed 331.1666 (Δ = 0.9 mmu).

4-(*O*-*tert*-Butyldimethylsilyloxy)-10-(*O*-*p*-methoxybenzyloxy)-dec-1-ene (17). To an oven-dried round-bottom flask under a N_2 atmosphere containing a Teflon stir bar and hydroxyalkene **S1** (6.1 g, 20.9 mmol, 1 equiv) were added *N*,*N*-dimethylformamide (50 mL) and imidazole (2.13 g, 31.4 mmol, 1.5 equiv), followed by *tert*-butyldimethylsilyl chloride (3.46 g, 22.9 mmol, 1.1 equiv). The resulting solution was stirred at rt overnight. The reaction was quenched with saturated aqueous NH_4Cl (100 mL), and the organics were extracted with ethyl acetate (3 × 150 mL). The combined organic layers were then washed with 1:1 v/v saturated aqueous NaCl/distilled water (2 × 100 mL) followed by brine (200 mL). The organic layer was then dried with $MgSO_4$ and concentrated *in vacuo* to give a clear oil. The residue was purified by flash chromatography on silica gel (50 g) with a stepwise ethyl acetate in a hexanes gradient (200 mL 10%; 200 mL 20%) to obtain 7.4 g of a colorless oil (18.2 mmol, 87% yield). R_f = 0.45 (silica gel, 10% ethyl acetate in hexanes); ^{1}H NMR (400 MHz, $CDCl_3$) δ 7.24 (d, J = 8.6 Hz, 2H), 6.86 (d, J = 8.6 Hz, 2H), 5.79 (ddt, J = 16.8, 10.6, 7.2 Hz, 1H), 5.03−4.98 (m, 2H), 4.41 (s, 2H), 3.78 (s, 3H), 3.65 (p, J = 5.6 Hz, 1H), 3.41 (t, J = 6.6 Hz, 2H), 2.23−2.12 (m, 2H), 1.61−1.54 (m, 2H), 1.43−1.19 (m, 8H), 0.86 (s, 9H), 0.022 (s, 3H), 0.017 (s, 3H) ppm; ^{13}C NMR (100 MHz, $CDCl_3$) δ 159.1, 135.5, 130.8, 129.2, 116.5, 113.8, 72.5, 72.0, 70.2, 55.3, 41.9, 36.8, 29.7, 29.6, 26.2, 25.9, 25.3, 18.2, −4.4, −4.5 ppm. HRMS (EI) m/z: calculated for $C_{24}H_{42}O_3Si$ [M] 406.2903, observed 406.2885 (Δ = 1.8 mmu).

4-Hydroxy-6-(*O*-*tert*-Butyldimethylsilyloxy)-12-(*O*-*p*-methoxy-benzyloxy)dodec-1-ene (S2). To an oven-dried round-bottom flask under N_2 containing alkene **17** (0.1477 g, 0.363 mmol, 1

DOI: 10.1021/acs.joc.5b02014
J. Org. Chem. 2016, 81, 415−423

equiv) was added a Teflon stir bar followed by methylene chloride (3 mL), *tert*-butanol (1.5 mL), distilled water (1.5 mL), potassium ferricyanate (0.359 g, 1.09 mmol, 3 equiv), and potassium carbonate (0.150 g, 1.09 mmol, 3 equiv). A solution of potassium osmate dihydrate (0.02 g, 0.54 mmol, 0.015 equiv) was prepared in 15% w/w NaOH (1.07 mL) and added to the vigorously stirred biphasic solution of alkene **17**, and then the reaction was sealed with a glass stopper and allowed to stir overnight at rt. The reaction was quenched with saturated aqueous NH_4Cl (10 mL), and the organics were extracted with methylene chloride (3 × 10 mL). The combined organic layers were then washed with brine (20 mL), dried with $MgSO_4$, and concentrated *in vacuo* to give a yellow oil. The crude diol was dissolved in methylene chloride (8 mL) and partitioned into two equal (4 mL) portions under N_2. A Teflon stir bar was added to the flask and then cooled to 0 °C in an ice bath. A portion of lead(IV) acetate (0.579 g, 0.13 mmol, 1.2 equiv) was added, and the resulting brown suspension was stirred at 0 °C for 30 min. The white solids were filtered on a plug of Celite (0.5 g) and then washed with methylene chloride (2 × 1 mL). The organic layers were pooled and concentrated *in vacuo* to give a black oil. The residue was purified by flash chromatography on silica gel (10 g) with a 30% ethyl acetate in hexanes solvent system to obtain 0.0584 g of a colorless oil (0.143 mmol, 78% yield). R_f = 0.69 (silica gel, 30% ethyl acetate in hexanes); ^{1}H NMR (400 MHz, $CDCl_3$) δ 9.77 (t, J = 2.4 Hz, 1H), 7.23 (d, J = 8.7 Hz, 2H), 6.85 (d, J = 8.7 Hz, 2H), 4.40 (s, 2H), 4.15 (t, J = 5.9 Hz, 1H), 3.78 (s, 3H), 3.41 (t, J = 6.6 Hz, 2H), 2.49−2.47 (m, 2H), 1.60−1.53 (m, 2H), 1.53−1.46 (m, 2H), 1.38−1.25 (m, 6H), 0.85 (s, 9H), 0.04 (s, 3H), 0.03 (s, 3H) ppm; ^{13}C NMR (100 MHz, $CDCl_3$) δ 201.8, 159.1, 130.7, 129.1, 113.7, 72.4, 70.0, 68.1, 55.0, 50.8, 37.7, 29.7, 29.4, 26.2, 25.8, 17.9, −4.4, −4.7 ppm. To an oven-dried round-bottom flask under N_2 charged with a Teflon stir bar and the obtained aldehyde (58.4 mg, 0.143 mmol, 1 equiv) was added THF (2 mL). The resulting solution was cooled to 0 °C in an ice bath, and allylmagnesium bromide, 1.0 M in THF (0.176 mL, 0.176 mmol, 1.2 equiv), was added dropwise. The reaction was stirred at 0 °C for 30 min. The reaction was quenched with saturated aqueous NH_4Cl (10 mL), and the organic layer was removed. The aqueous phase was extracted with ethyl acetate (3 × 10 mL). The combined organic layers were washed with brine (20 mL), dried with $MgSO_4$, and concentrated *in vacuo* to give a clear oil. The residue was purified by flash chromatography on silica gel (7 g) with a 20% ethyl acetate in hexanes solvent system to obtain 60.0 mg of a colorless oil (0.133 mmol, 93% yield). R_f = 0.26 (silica gel, 10% ethyl acetate in hexanes); ^{1}H NMR (400 MHz, $CDCl_3$) δ 7.19 (d, J = 8.7 Hz, 2H), 6.80 (d, J = 8.7 Hz, 2H), 5.87−5.69 (m, 1H), 5.1−4.97 (m, 2H), 4.36 (s, 3H), 3.94−3.72 (m, 2H), 3.70 (s, 3H), 3.37 (t, J = 6.7 Hz, 2H), 2.21−2.12 (m, 2H), 1.58−1.41 (m, 6H), 1.35−1.19 (m, 6H), 0.86 (d, J = 1.7 Hz, 9H), 0.06−0.03 (m, 6H) ppm; ^{13}C NMR (100 MHz, $CDCl_3$) δ 159.1, 135.02, 134.97, 130.7, 129.1, 117.3, 117.2, 113.7, 72.7, 72.5, 71.4, 70.0, 69.9, 67.6, 55.1, 42.5, 42.2, 41.2, 37.8, 36.4, 29.7, 29.7, 29.6, 26.22, 26.19, 25.9, 25.6, 24.6, 17.96, 17.94, −4.0, −4.5, −4.6, −4.7 ppm. HRMS (ESI+ TOF) m/z: calculated for $C_{26}H_{46}O_4SiK$ $[(M + K)^+]$ 489.2802, observed 489.2754 (Δ = 4.8 mmu).

4,6-(Di-*O*-*tert*-butyldimethylsilyloxy)-12-(*O*-*p*-methoxybenzyl-oxy)dodec-1-ene (18). To an oven-dried round-bottom flask under a N_2 atmosphere containing a Teflon stir bar and hydroxyalkene **S2** (0.4055 g, 0.90 mmol, 1 equiv) were added *N*,*N*-dimethylformamide (1 mL), imidazole (0.122 g, 1.8 mmol, 2 equiv), and *N*,*N*-dimethylpyridine (11 mg, 0.09 mmol, 0.1 equiv), followed by *tert*-butyldimethylsilyl chloride (0.203 g, 1.35 mmol, 1.5 equiv). The resulting solution was stirred at rt overnight. The reaction was quenched with saturated aqueous NH_4Cl (10 mL), and the organics were extracted with ethyl acetate (3 × 10 mL). The combined organic layers were then washed with 1:1 v/v saturated aqueous NaCl/distilled water (2 × 10 mL) followed by brine (10 mL). The organic layer was then dried with $MgSO_4$ and concentrated *in vacuo* to give a clear oil. The residue was purified by flash chromatography on silica gel (15 g) with a stepwise ethyl acetate in hexanes gradient (200 mL 5%; 200 mL 20%) to obtain 0.4747 g of colorless oil (0.84 mmol, 93% yield). R_f = 0.44 (silica gel, 10% ethyl acetate in hexanes); ^{1}H NMR (400 MHz, $CDCl_3$) δ 7.26 (d, J = 8.7 Hz, 2H), 6.87 (d, J = 8.7 Hz, 2H), 5.90−5.79 (m, 1H), 5.09−5.03 (m, 2H), 4.43 (s, 2H), 3.89−3.75 (m, 2H), 3.78 (s, 3H), 3.44 (t, J = 6.8 Hz, 2H), 2.34−2.15 (m, 2H), 1.69−1.54 (m, 4H), 1.50−1.30 (m, 8H), 0.93−0.92 (m, 18H), 0.10−0.08 (m, 12H) ppm; ^{13}C NMR (100 MHz, $CDCl_3$) δ 159.2, 135.04, 134.98, 130.8, 129.2, 116.93, 116.92, 113.7, 72.6, 70.1, 69.8, 69.5, 69.2, 55.1, 45.0, 44.6, 42.6, 42.0, 37.9, 37.3, 31.7, 29.8, 29.7, 26.34, 26.32, 26.01, 25.99, 25.98, 25.96, 25.1, 25.0, 22.7, 18.13, 18.11, 18.09, 14.2, −3.81, −3.89, −4.07, −4.22, −4.24, −4.34, −4.46 ppm. HRMS (EI) m/z: calculated for $C_{32}H_{60}O_4Si_2Na$ $[(M + Na)^+]$ 587.3928, observed 587.3946 (Δ = 1.8 mmu).

Ethyl (*E*)-5,7-(Di-*O*-*tert*-butyldimethylsilyloxy)-2,3-ene-13-(*O*-*p*-methoxybenzyloxy)tridecanoate (19). To an oven-dried round-bottom flask under N_2 containing alkene **18** (2.022 g, 3.58 mmol, 1 equiv) was added a Teflon stir bar, followed by *tert*-butanol (20 mL), deionized water (20 mL), potassium ferricyanate (3.52 g, 10.7 mmol, 3 equiv), and potassium carbonate (1.48 g, 10.7 mmol, 3 equiv). A solution of potassium osmate dihydrate (0.02 g, 0.054 mmol, 0.015 equiv) was prepared in 15% w/w NaOH (1.07 mL) and added to the vigorously stirred biphasic solution of alkene **18**, and then the reaction was sealed with a glass stopper and stirred at rt overnight. The reaction was quenched with saturated aqueous NH_4Cl (100 mL), and the organics were extracted with methylene chloride (3 × 75 mL). The combined organic layers were then washed with brine (200 mL), dried with $MgSO_4$, and concentrated *in vacuo* to give a yellow oil. The crude diol was dissolved in methylene chloride (50 mL), and a Teflon stir bar was added to the flask, followed by cooling to 0 °C in an ice bath. A portion of lead(IV) acetate (1.67 g, 3.76 mmol, 1.05 equiv) was added, and the resulting brown suspension was stirred at 0 °C for 30 min. The white solids were filtered on a plug of Celite (1 g) and then washed with two portions of methylene chloride (10 mL). The organic layers were pooled and concentrated *in vacuo* to give a black oil. The residue was purified by flash chromatography on silica gel (50 g) with a 30% ethyl acetate in hexanes solvent system to obtain 1.634 g of a colorless oil (2.88 mmol, 80% yield). ^{1}H NMR (400 MHz, $CDCl_3$) δ 9.78 (dt, J = 3.10, 1.9 Hz, 1H), 7.24 (d, J = 8.7 Hz, 2H), 6.86 (d, J = 8.7 Hz, 2H), 4.41 (s, 2H), 4.34−4.20 (m, 1H), 3.78 (s, 3H), 3.74−3.64 (m, 1H), 3.41 (t, J = 6.6 Hz, 2H), 2.62−2.42 (m, 2H), 1.79−1.67 (m, 1H), 1.64−1.53 (m, 3H), 1.50−1.35 (m, 2H), 1.35−1.23 (m, 4H), 0.87−0.83 (m, 18H), 0.07−0.01 (m, 12H) ppm. To an oven-dried round-bottom flask under N_2 containing the obtained aldehyde (0.809 g, 1.4 mmol, 1 equiv) were added a Teflon stir bar, THF (10 mL), and triethylphosphonoacetate (0.31 mL, 1.5 mmol, 1.1 equiv). Freshly powdered KOH (0.16 g, 2.8 mmol, 2 equiv) was added in one portion to the vigorously stirred solution. The resulting suspension was stirred at rt for 1 h. The reaction was quenched with saturated aqueous NH_4Cl (10 mL), and the organics were extracted with ethyl acetate (3 × 20 mL). The combined organic layers were then washed with brine (2 × 50 mL), dried with $MgSO_4$, and concentrated *in vacuo* to give a yellow oil. The residue was purified by flash chromatography on silica gel (20 g) with a stepwise gradient of ethyl acetate in hexanes (200 mL 2%; 100 mL 5%; 100 mL 100% ethyl acetate) to obtain 0.4976 g of a colorless oil (0.798 mmol, 57% yield). R_f = 0.30 (silica gel, 10% ethyl acetate in hexanes); ^{1}H NMR (400 MHz, $CDCl_3$) δ 7.24 (d, J = 8.7 Hz, 2H), 6.93 (dt, J = 15.6, 7.8 Hz, 1H), 6.85 (d, J = 8.7 Hz, 2H), 5.81 (ddt, J = 15.7, 5.3, 1.3 Hz, 1H), 4.41 (s, 2H), 4.16 (q, J = 7.1 Hz, 2H), 3.91−3.84 (m, 2H), 3.78 (s, 3H), 3.73−3.65 (m, 1H), 3.41 (t, J = 6.6 Hz, 2H), 2.43−2.21 (m, 2H), 1.66−1.48 (m, 4H), 1.46−1.35 (m, 2H), 1.34−1.31 (m, 2H), 1.29−1.22 (m, 4H), 1.26 (t, J = 7.1 Hz, 3H), 0.87−0.85 (m, 18H), 0.02−0.01 (m, 12H) ppm; ^{13}C NMR (100 MHz, $CDCl_3$) δ 167.3, 166.3, 159.1, 145.8, 144.8, 140.9, 130.8, 130.4, 129.2, 123.4, 119.6, 113.7, 72.5, 71.7, 70.1, 69.4, 68.6, 68.0, 60.2, 60.1, 55.2, 44.9, 40.9, 40.1, 37.4, 37.1, 29.74, 29.72, 29.6, 26.24, 26.20, 25.90, 25.86, 25.84, 25.6, 25.3, 25.0, 18.09, 18.04, 18.02, 14.31, 14.27, −4.2, −4.4, −4.5 ppm. HRMS (ESI+ TOF) m/z: calculated for $C_{35}H_{64}O_6Si_2Na$ $[(M + Na)^+]$ 659.4139, observed 659.4101 (Δ = 3.8 mmu).

Ethyl 5,7-(Di-*O*-*tert*-butyldimethylsilyloxy)-13-hydroxy-(*E*)-2,3-enetridecanoate (S3). To an oven-dried round-bottom flask under an Ar atmosphere containing a Teflon stir bar and PMB ether

DOI: 10.1021/acs.joc.5b02014
J. Org. Chem. 2016, 81, 415−423

19 (0.331 g, 0.53 mmol, 1 equiv) was added 9:1 v/v methylene chloride/deionized water (10 mL) and cooled to 0 °C in an ice bath. The septum was removed, and DDQ (0.1498 g, 0.66 mmol, 1.2 equiv) was added. The resulting dark green suspension was sealed with a glass stopper and then allowed to warm to rt. After 15 min, the green color had dissipated yielding a white precipitate and was stirred for an additional 30 min at rt. The resulting solids were filtered off through a plug of Celite (0.5 g), and the solids were washed with methylene chloride (3 × 10 mL). The organics were pooled and washed with 1:1 v/v thiosulfate/saturated $NaHCO_3$ (10 mL). The organics were removed, and the resulting aqueous layer was washed with methylene chloride (3 × 10 mL). The organic layers were combined and washed with brine (20 mL), dried with $MgSO_4$, and concentrated *in vacuo* to give an orange oil. The residue was purified by flash chromatography on silica gel (10 g) with a 15% ethyl acetate in a hexanes solvent system to obtain 0.1563 g of a colorless oil (0.302 mmol, 57% yield). R_f = 0.40 (silica gel, 30% ethyl acetate in hexanes); ^{1}H NMR (400 MHz, $CDCl_3$) δ 6.94 (dt, J = 15.7, 7.2 Hz, 1H), 5.81 (ddt, J = 15.7, 4.8, 1.2 Hz, 1H), 3.95−3.83 (m, 1H), 3.74−3.65 (m, 1H), 3.62 (dt, J = 1.2, 6.6 Hz, 2H), 2.48−2.26 (m, 2H), 1.72−1.48 (m, 4H), 1.46−1.36 (m, 2H), 1.36−1.25 (m, 6H), 1.86−1.85 (m, 18H), 0.05−0.00 (m, 12H) ppm; ^{13}C NMR (100 MHz, $CDCl_3$) δ 171.06, 170.96, 148.51, 148.47, 122.93, 122.85, 70.0, 69.3, 69.1, 68.4, 63.0, 45.3, 44.6, 41.0, 40.1, 37.8, 37.4, 32.65, 32.59, 29.62, 29.55, 25.91, 25.88, 25.83, 25.7, 24.9, 18.1, 18.03, 18.01, −3.9, −4.15, −4.18, −4.2, −4.3, −4.4, −4.50, −4.53 ppm. HRMS (ESI+ TOF) m/z: calculated for $C_{27}H_{56}O_5Si_2Na$ $[(M + Na)^+]$ 539.3564, observed 539.3566 (Δ = 0.2 mmu).

(*E*)-6,8-Bis(*tert*-butyldimethylsilyloxy)oxacyclotetradec-3-en-2-one (20). To an oven-dried round-bottom flask under an N_2 atmosphere containing a Teflon stir bar and ethyl ester **S3** (0.126 g, 0.24 mmol, 1 equiv) were added 95% ethanol (3 mL) and 1.0 M LiOH (0.5 mL, 0.5 mmol, 2.1 equiv). The resulting solution was stirred at rt overnight. The reaction was quenched with the addition of water (10 mL), and 1.0 M HCl was added dropwise until the aqueous phase was acidic indicated by pH paper. Ethyl acetate was added, the organics were removed, and the aqueous phase was washed with ethyl acetate (3 × 10 mL). The combined organic layers were washed with brine (30 mL), dried with $MgSO_4$, and concentrated *in vacuo* to give a clear oil. The residue was purified by flash chromatography on silica gel (6 g) with a 30% ethyl acetate in hexanes solvent system to obtain 0.1106 g of a colorless oil (0.226 mmol, 94% yield). R_f = 0.42 (silica gel, 50% ethyl acetate in hexanes); ^{1}H NMR (400 MHz, $CDCl_3$) δ 7.06 (dt, J = 15.6, 7.7 Hz, 1H), 5.83 (d, J = 15.5 Hz, 1H), 3.93−3.85 (m, 1H), 3.75−3.67 (m, 1H), 3.62 (t, J = 6.6 Hz, 2H), 2.47−2.26 (m, 2H), 1.61−1.47 (m, 4H), 1.46−1.36 (m, 2H), 1.36−1.24 (m, 6H), 0.86 (s, 9H), 0.85 (s, 9H), 0.05−0.03 (m, 12H) ppm. HRMS (ESI+ TOF) m/z: calculated for $C_{25}H_{52}O_5Si_2Na$ $[(M + Na)^+]$ 511.3251, observed 511.3254 (Δ = 0.3 mmu). To an oven-dried round-bottom flask under N_2 containing a Teflon stir bar and azeotropically dried (3 × 5 mL PhH) obtained hydroxy acid (0.1003 g, 0.205 mmol, 1 equiv) were added freshly distilled PhH (20 mL), diisopropylethylamine (0.36 mL, 2.07 mmol, 10 equiv), and 2,4,6-trichlorobenzoylyl chloride (0.32 mL, 2.07 mmol, 10 equiv). The resulting mixture was stirred at rt overnight. Powdered DMAP (0.375 g, 3.075 mmol, 15 equiv) was added, and the resulting suspension was stirred at rt for 2 h. The reaction was quenched with deionized water (50 mL) and was acidified by dropwise addition of 1 M HCl until pH = 2. The organics were extracted with ethyl acetate (20 mL), and the aqueous phase was washed with ethyl acetate (3 × 20 mL). The organic layers were combined, washed with saturated aqueous $NaHCO_3$ (50 mL), washed with brine (50 mL), dried with $MgSO_4$, and concentrated *in vacuo* to give a white solid. The residue was purified by flash chromatography on silica gel (9 g) with a 5% ethyl acetate in hexanes solvent system to obtain 72.8 mg of a colorless oil (0.15 mmol, 75% yield). R_f = 0.77 (silica gel, 40% ethyl acetate in hexanes); ^{1}H NMR (400 MHz, $CDCl_3$) δ 7.01−6.83 (m, 1H), 5.85−5.80 (m, 1H), 4.50−4.34 (m, 1H), 4.09−4.01 (m, 1H), 3.96−3.79 (m, 1H), 3.74−3.66 (m, 1H), 2.60−2.35 (m, 2H), 1.79−1.58 (m, 4H), 1.54−1.17 (m, 8H), 0.86 (d, J = 7.4 Hz, 9H), 0.86 (d, J = 7.4 Hz, 9H), 0.05−0.01 (m, 12H) ppm; ^{13}C NMR (100 MHz, $CDCl_3$) δ 166.1, 165.8, 145.8, 145.6, 124.5, 123.4, 69.7, 68.6, 68.4, 68.3, 65.5, 64.2, 48.4, 42.7, 42.5, 39.3, 36.8, 34.5, 29.0, 27.8, 26.9, 26.5, 26.3, 25.9, 25.79, 25.78, 24.6, 24.0, 23.5, 18.1, 18.03, 18.00, 17.98, −4.0, −4.1, −4.55, −4.61, −4.70, −4.73, −4.77, −4.8 ppm. HRMS (ESI+ TOF) m/z: calculated for $C_{25}H_{50}O_4Si_2Na$ $[(M + Na)^+]$ 493.3145, observed 493.3111 (Δ = 3.4 mmu).

(*E*)-6,8-Dihydroxyoxacyclotetradec-3-en-2-one (14 and 21). To a polypropylene Eppendorf tube charged with diTBS lactone **20** (27.8 mg, 59 μmol, 1 equiv) was added acetonitrile (600 μL) followed by 48% HF (41 μL, 1.2 mmol, 20 equiv) and the resulting solution was vortexed and allowed to sit at rt overnight with occasional vortexing. The reaction was quenched with the addition of saturated aqueous $NaHCO_3$ (2 mL), and the organics were removed with ethyl acetate (2 mL). The aqueous layer was washed with saturated aqueous $NaHCO_3$ (3 × 2 mL). The organic layers were pooled, washed with brine (5 mL), dried with $MgSO_4$, and concentrated *in vacuo* to give a pale yellow oil. The diastereomers were separated with preparative TLC using a 90% v/v ethyl acetate in hexanes solvent system to give a 1:1 mixture of diastereomers; 6.8 mg of the *anti* and 5.3 mg of the *syn* (50 mmol, 85% yield).

Syn ***(14)***. R_f = 0.22 (silica gel, 90% ethyl acetate in hexanes); ^{1}H NMR (400 MHz, $CDCl_3$) δ 6.87 (dt, J = 15.8, 7.8 Hz, 1H), 5.88 (dt, J = 15.7, 1.3 Hz, 1H), 4.30 (ddd, J = 11.1, 7.5, 3.7 Hz. 1H), 4.19 (ddd, J = 11.1, 7.0, 3.7 Hz, 1H), 4.07−3.99 (m, 1H), 3.71−3.62 (m, 1H), 2.68 (dddd, J = 13.3, 7.9, 4.4, 1.3 Hz, 1H), 2.35 (dtd, J = 13.3, 8.1, 1.3 Hz, 1H), 2.05 (br s, 1H), 1.85 (ddd, J = 14.3, 7.8, 2.6 Hz, 1H), 1.79−1.54 (m, 4H), 1.52−1.42 (m, 3H), 1.40−1.24 (m, 5H) ppm; ^{13}C NMR (100 MHz, $CDCl_3$) δ 166.0, 144.4, 124.9, 69.4, 69.2, 65.0, 43.3, 40.0, 36.6, 27.9, 26.9, 26.5, 24.4 ppm. HRMS (ESI+ TOF) m/z: calculated for $C_{13}H_{22}O_4Na$ $[(M + Na)^+]$ 265.1416, observed 265.1423 (Δ = 0.7 mmu).

Anti ***(21)***. R_f = 0.35 (silica gel, 90% ethyl acetate in hexanes); ^{1}H NMR (400 MHz, $CDCl_3$) δ 6.85 (ddd, J = 15.7, 9.4, 6.4 Hz, 1H), 5.89 (d, J = 15.7 Hz, 1H), 4.32−4.24 (m. 1H), 4.21−4.11 (m, 1H), 4.09−3.98 (m, 1H), 3.09 (br s, 1H), 2.70−2.61 (m, 1H), 2.45 (dt, J = 13.4, 9.2, Hz, 1H), 2.18 (br s, 1H), 1.75−1.69 (m, 2H), 1.68−1.18 (m, 10H) ppm; ^{13}C NMR (100 MHz, $CDCl_3$) δ 166.0, 144.8, 124.6, 68.83, 68.80, 65.2, 39.2, 38.5, 36.5, 28.2, 26.93, 26.87, 24.7 ppm. HRMS (ESI + TOF) m/z: calculated for $C_{13}H_{22}O_4Na$ $[(M + Na)^+]$ 265.1416, observed 265.1418 (Δ = 0.2 mmu).

3-(*tert*-Butyldimethylsilyloxy)-5-methoxy-5-oxopentanoic acid (26). R_f = 0.20 (silica gel, 20% ethyl acetate in hexanes); ^{1}H NMR (300 MHz, $CDCl_3$): δ 10.65 (br s, 1H), 4.53 (p, J = 6.0 Hz, 1H), 3.66 (s, 3H), 2.65−2.53 (m, 4H), 0.83 (s, 9H), 0.06 (m, 6H) ppm; ^{13}C NMR (100 MHz, $CDCl_3$): δ 175.5, 171.3, 66.1, 51.7, 42.1, 41.9, 25.6, 17.9, −5.0 ppm. NMR spectra were consistent with those previously reported within literature data.[59]

7-Bromoheptanal (27). To a round-bottom flask charged with 7-bromo-1-alkene (400 mg, 2.09 mmol, 1.0 equiv) in *tert*-butanol/deionized water (1:1, 20 mL) were added potassium ferricyanide (2.07 g, 6.27 mmol, 3.0 equiv) and potassium carbonate (867 mg, 6.27 mmol, 3.0 equiv). A solution of potassium osmate dihydrate (15 mg, 0.04 mmol, 2 mol %) was prepared in 15% w/w NaOH (0.5 mL) and added to the vigorously stirred biphasic solution of bromoalkene, sealed with a glass stopper and stirred at rt overnight. The reaction was quenched with saturated aqueous NH_4Cl (30 mL), and the organics were extracted with methylene chloride (3 × 20 mL). The combined organic layers were washed with brine, dried ($MgSO_4$), filtered, and concentrated *in vacuo* to yield a clear oil. The crude diol in methylene chloride (8.5 mL) was added a portion of lead tetraacetate (1.1 g, 2.50 mmol, 1.2 equiv) and left to stir at rt for 60 min under an Ar atmosphere. The reaction mixture was concentrated to 20% volume *in vacuo* and added directly to a pre-equilibrated column (silica gel, 10% ethyl acetate in hexanes) for isolation of 288.3 mg of **27** (1.5 mmol, 72%) as clear, colorless oil. R_f = 0.36 (silica gel, 10% ethyl acetate in hexanes); ^{1}H NMR (400 MHz, $CDCl_3$): δ 9.75 (t, J = 1.7 Hz, 1H), 3.39 (t, J = 6.7 Hz, 2H), 2.43 (dt, J = 1.7, 7.2 Hz, 2H), 1.89−1.80 (m, 2H), 1.63 (p, J = 7.5 Hz, 2H), 1.50−1.28 (m, 4H) ppm; ^{13}C NMR (100 MHz, $CDCl_3$): δ 202.5, 43.7, 33.7, 32.4, 28.2, 27.8, 21.8 ppm.

DOI: 10.1021/acs.joc.5b02014
J. Org. Chem. 2016, 81, 415−423

NMR spectra were consistent with those previously reported within literature.[60]

(*E*)-13-Bromo-3-(*tert*-butyldimethylsilyloxy)-5-oxotridec-6-enoic Acid (28). A stirring solution of dimethyl methylphosphonate (750 μL, 6.70 mmol, 3.7 equiv) in dry THF (8 mL) was cooled to −78 °C under an inert atmosphere. To this solution 2.5 M *n*BuLi (2.5 mL, 6.25 mmol, 3.5 equiv) was added dropwise to effect a yellow color, followed by stirring for 2 h. Addition of acid **26** (500 mg, 1.81 mmol, 1.0 equiv) in THF (4 mL) via cannula yielded a clear, orange solution. The solution was brought to rt, and product formation was observed via TLC (silica gel, 5% MeOH in methylene chloride), where the product was bright red under visualization with *p*-anisaldehyde stain. Upon completion, the reaction was quenched with 1.0 M HCl solution (3 × 3 mL), diluted in ethyl acetate (3 × 20 mL), and separated. The combined organic layers were washed with brine, dried ($MgSO_4$), filtered, and concentrated to afford 645.6 mg of crude phosphonate as a pale yellow oil, which was spectroscopically pure enough for use in the following step. R_f = 0.24 (silica gel, 5% MeOH in methylene chloride; *p*-anisaldehyde stain); ^{1}H NMR (300 MHz, $CDCl_3$): δ 4.54 (p, *J* = 5.8 Hz, 1H), 3.78 (d, *J* = 11.3 Hz, 3H), 3.77 (d, *J* = 11.3 Hz, 3H), 3.11 (d, *J* = 22.7 Hz, 2H), 2.89 (d, *J* = 6.1 Hz, 2H), 2.58 (dd, *J* = 5.9, 15.4 Hz, 1H), 2.49 (dd, *J* = 5.5, 15.4 Hz, 1H), 0.84 (s, 9H), 0.09 (s, 3H), 0.06 (s, 3H) ppm; ^{31}P NMR (121 MHz, $CDCl_3$): δ 19.6 ppm. HRMS (EI) *m*/*z*: calculated for $C_{10}H_{20}O_7PSi$ [M − *t*-Bu] 311.0716, observed 311.0705 (Δ = 1.1 mmu). A solution of the obtained phosphonate (230 mg, 0.62 mmol, 1.2 equiv) in isopropanol (4 mL, dried over 4 Å MS) was cooled to 0 °C. Cesium carbonate (390 mg, 1.2 mmol, 1.9 equiv) was added in one portion, and the mixture was stirred at 0 °C for 2 h. To the reaction mixture a solution of bromoaldehyde **27** (99 mg, 0.51 mmol, 1.0 equiv) in isopropanol (1 mL, dried over 4 Å MS, 0.1 M overall reaction mixture) was added dropwise. The reaction mixture was warmed to 30 °C and stirred overnight. The reaction was diluted with ethyl acetate (10 mL) and quenched by the addition of 1.0 M HCl solution (4 mL). The mixture was extracted with ethyl acetate (2 × 10 mL), and the combined organic layers were washed with brine, dried with $MgSO_4$, filtered, and concentrated *in vacuo*. Purification via column chromatography (20% ethyl acetate/hexanes) yielded 179.9 mg of **28** (0.413 mmol, 81%) as a clear, colorless oil. R_f = 0.29 (silica gel, 20% Ethyl acetate in hexanes); ^{1}H NMR (400 MHz, $CDCl_3$): δ = 9.70 (br s, 1H), 6.81 (dt, *J* = 15.9, 6.9 Hz, 1H), 6.08 (dt, *J* = 15.9, 1.5 Hz, 1H), 4.59 (p, *J* = 5.9 Hz, 1H), 3.38 (t, *J* = 6.7 Hz, 2H), 2.84 (dd, *J* = 15.9, 6.4 Hz, 1H), 2.72 (dd, *J* = 15.9, 6.0 Hz, 1H), 2.60 (dd, *J* = 15.1, 5.5 Hz, 1H), 2.49 (dd, *J* = 15.1, 6.0 Hz, 1H), 2.24−2.17 (m, 2H), 1.89−1.78 (m, 2H), 1.51−1.29 (m, 8H), 0.82 (s, 9H), 0.06 (s, 3H), 0.02 (s, 3H) ppm; ^{13}C NMR (100 MHz, $CDCl_3$): δ = 198.2, 176.5, 148.3, 131.0, 66.0, 46.9, 42.3, 33.7, 32.5, 32.3, 28.3, 27.8, 27.7, 25.7, 17.9, −4.8, −5.0 ppm. HRMS (EI) *m*/*z*: calculated for $C_{15}H_{26}BrO_4Si$ [(M − *t*-Bu)] 377.0784, observed 377.0789 (Δ = 0.5 mmu).

(*E*)-4-(*tert*-Butyldimethylsilyloxy)oxacyclotetradec-7-ene-2,6-dione (29). To a flask charged with bromoacid **28** (120 mg, 0.28 mmol, 1.0 equiv) in anhydrous DMF (28 mL, 0.01 M) was added cesium carbonate (162.1 mg, 0.50 mmol, 1.8 equiv) under an Ar atmosphere at 0 °C. The reaction was left to warm to room temperature as it was stirred overnight. The reaction mixture was then diluted with ethyl acetate (40 mL) and washed with brine. The aqueous layer was re-extracted with ethyl acetate, and the combined organic layers were washed with water (3 × 40 mL) and brine, dried ($MgSO_4$), filtered, and concentrated to dryness *in vacuo*. The residue was purified by column chromatography (silica gel, 10% ethyl acetate in hexanes) to afford 66.3 mg of macrolactone **29** (0.19 mmol, 68%) as a clear, pale yellow oil. R_f = 0.54 (silica gel, 10% ethyl acetate in hexanes); ^{1}H NMR (400 MHz, $CDCl_3$): δ 6.80 (ddd, *J* = 16.0, 8.1, 6.6 Hz, 1H), 6.05 (dt, *J* = 16.0, 1.4 Hz, 1H), 4.54 (ddt, *J* = 8.2, 4.3, 6.0 Hz, 1H), 4.15 (ddd, *J* = 11.1, 7.3, 3.1 Hz, 1H), 4.08−4.01 (m, 1H), 3.00 (dd, *J* = 13.8, 8.2 Hz, 1H), 2.70 (dd, *J* = 13.8, 6.0 Hz, 1H), 2.52 (dd, *J* = 14.7, 4.3 Hz, 1H), 2.47 (dd, *J* = 14.7, 6.1 Hz, 1H), 2.39−2.21 (m, 2H), 1.65−1.54 (m, 4H), 1.48−1.39 (m, 4H), 0.85 (s, 9H), 0.06 (s, 3H), 0.05 (s, 3H) ppm; ^{13}C NMR (100 MHz, $CDCl_3$): δ 198.8, 170.4, 149.5, 131.8, 67.3, 64.7, 47.0, 42.5, 32.2, 27.4, 27.2, 25.8, 25.7, 25.5, 18.0, −4.8, −4.8 ppm. HRMS (EI) *m*/*z*: calculated for $C_{15}H_{25}O_4Si$ [(M − *t*-Bu)] 297.1522, observed 297.1518 (Δ = 0.4 mmu).

(*E*)-4-Hydroxyoxacyclotetradec-7-ene-2,6-dione (15). To a 1.5 mL polypropylene Eppendorf tube charged with macrolactone **29** (16 mg, 0.045 mmol, 1.0 equiv) were added acetonitrile (450 μL, 0.1 M) and pyridine (18 μL, 0.225 mmol, 5.0 equiv). The reaction mixture was vortexed to homogeneity, upon which 48% HF (82 μL, 0.450 mmol, 50 equiv) was added. The reaction mixture was again vortexed, then centrifuged, and left for 5 h. The reaction was quenched with water (2 × 1 mL) and diluted with ethyl acetate (2 × 2 mL). The aqueous layer was re-extracted with ethyl acetate, and the combined organic layers were washed with brine, dried ($MgSO_4$), filtered, and concentrated to dryness *in vacuo*. The product was purified by column chromatography (silica gel, 20% ethyl acetate in hexanes) to afford 10.8 mg of **15** (0.045 mmol, > 99%) as a clear, colorless oil. R_f = 0.28 (silica gel, 40% ethyl acetate in hexanes); ^{1}H NMR (400 MHz, $CDCl_3$): δ 6.81 (dt, *J* = 16.0, 7.3 Hz, 1H), 6.07 (dt, *J* = 16.0, 1.4 Hz, 1H), 4.33−4.27 (m, 1H), 4.17 (t, *J* = 5.4 Hz, 2H), 3.73 (br s, 1H), 2.92 (d, *J* = 5.7 Hz, 2H), 2.62 (dd, *J* = 16.1, 3.6 Hz, 1H), 2.52 (dd, *J* = 16.1, 8.4 Hz, 1H), 2.36 (dd, *J* = 7.1, 1.6 Hz, 1H), 2.32 (dd, *J* = 7.1, 1.4 Hz, 1H), 1.66−1.57 (m, 4H), 1.44−1.31 (m, 4H) ppm; ^{13}C NMR (100 MHz, $CDCl_3$): δ 201.5, 171.8, 151.9, 132.5, 66.7, 64.4, 41.6, 39.6, 32.6, 27.8, 27.7, 25.9, 25.6 ppm. HRMS (EI) *m*/*z*: calculated for $C_{13}H_{20}O_4$ [M] 240.1362, observed 240.1348 (Δ = 1.4 mmu).

***trans*-4,15-Dioxabicyclo[9.3.1]pentadecane-3,13-dione (30).** To a 5 mm NMR tube charged with **15** (3.5 mg, 14.57 μmol, 1.0 equiv) in $CDCl_3$ (0.5 mL) was added *p*-toluenesulfonic acid monohydrate (1.6 mg), of which most did not go into solution. Instantaneous conversion of material was realized via ^{1}H NMR and TLC (silica gel, 20% ethyl acetate in hexanes) monitoring, at which point the mixture was filtered, concentrated, and purified by column chromatography (silica gel, 20% ethyl acetate in hexanes) to afford 2.9 mg of **30** (12.09 μmol, 83%) as a clear, colorless oil. R_f = 0.19 (silica gel, 20% ethyl acetate in hexanes); ^{1}H NMR (400 MHz, $CDCl_3$): δ 4.74 (ddt, *J* = 12.2, 6.3, 3.8 Hz, 1H), 4.47 (ddd, *J* = 11.2, 6.4, 2.4 Hz, 1H), 4.17 (dddd, *J* = 10.8, 8.7, 3.9, 1.9 Hz, 1H), 3.97 (ddd, *J* = 11.2, 9.4, 1.9 Hz, 1H), 2.71 (dd, *J* = 12.3, 1.4 Hz, 1H), 2.67 (ddd, *J* = 14.3, 6.2, 1.2 Hz, 1H), 2.42 (ddd, *J* = 14.1, 4.1, 1.7 Hz, 1H), 2.34 (dd, *J* = 13.7, 3.4 Hz, 1H), 2.32−2.26 (m, 1H), 2.24 (ddd, *J* = 14.4, 4.3, 1.7 Hz, 1H), 1.92−1.82 (m, 1H), 1.73−1.43 (m, 5H), 1.43−1.26 (m, 4H) ppm; ^{13}C NMR (100 MHz, $CDCl_3$): δ 206.5, 170.4, 70.8, 69.9, 66.7, 48.2, 46.1, 39.6, 33.4, 26.8, 25.4, 25.1, 22.1 ppm. HRMS (EI) *m*/*z*: calculated for $C_{13}H_{18}O_3$ [M − H_2O] 222.1256, observed 222.1270 (Δ = 1.4 mmu).

***cis*-4,15-Dioxabicyclo[9.3.1]pentadecane-3,13-dione (31).** To a 5 mm NMR tube charged with **15** (4.7 mg, 19.56 μmol, 1.0 equiv) in $CDCl_3$ (0.5 mL) was added Amberlyst 15 hydrogen form (5 mg), followed by heating to 80 °C for 4 h. The reaction was monitored by ^{1}H NMR and TLC, and upon consumption of starting material the mixture was filtered, concentrated, and purified by column chromatography (silica gel, 10% ethyl acetate in hexanes) to afford 3.6 mg of **31** (14.87 μmol, 76%) as a clear, colorless oil. R_f = 0.25 (silica gel, 20% ethyl acetate in hexanes); ^{1}H NMR (300 MHz, $CDCl_3$): δ 4.32 (ddd, *J* = 11.0, 10.1, 2.9 Hz, 1H), 4.18 (ddd, *J* = 11.0, 4.7, 4.0 Hz, 1H), 3.95 (dddd, *J* = 11.5, 7.7, 6.4, 2.7 Hz, 1H), 3.58 (m, 1H), 2.51 (d, *J* = 7.7 Hz, 1H), 2.50 (d, *J* = 6.4 Hz, 1H), 2.41 (ddd, *J* = 14.4, 2.7, 1.6 Hz, 1H), 2.32 (ddd, *J* = 14.4, 3.1, 1.6 Hz, 1H), 2.36−2.18 (m, 2H), 1.93−1.78 (m, 1H), 1.77−1.27 (m, 9H) ppm; ^{13}C NMR (100 MHz, $CDCl_3$): δ 206.1, 171.0, 77.2, 74.3, 64.4, 48.3, 47.1, 42.3, 33.6, 26.1, 25.2, 24.4, 24.2 ppm. HRMS (ESI+ TOF) *m*/*z*: calculated for $C_{13}H_{20}O_4Na$ [(M + Na)$^+$] 263.1259, observed 263.1276 (Δ = 1.7 mmu). Alternatively, to a 5 mm NMR tube charged with **30** (2.7 mg, 11.24 μmol, 1.0 equiv) in $CDCl_3$ (0.5 mL) was added Amberlyst 15 hydrogen form (5 mg) and heated to 80 °C for 4 h. The reaction was monitored by ^{1}H NMR, following key proton shifts in the range of δ 4.74−3.58 (H3, H7, H13A, H13B). Upon completion, the reaction mixture was filtered and purified by column chromatography (silica gel, 10% ethyl acetate in hexanes) to afford 2.2 mg of **31** (9.33 μmol, 83%) as a clear, colorless oil.

DOI: 10.1021/acs.joc.5b02014
J. Org. Chem. 2016, 81, 415−423

***α-cis*-13-Hydroxy-4,15-dioxabicyclo[9.3.1]pentadecan-3-one (32).** To a vial charged with *cis*-pyranone **31** (2.6 mg, 10.8 μmol, 1.0 equiv) in methanol (0.25 mL) at 0 °C was added $NaBH_4$ (1.2 mg, 32.5 μmol, 3.0 equiv) followed by stirring for 1 h. Upon completion, the reaction mixture was quenched with one drop of acetic acid and diluted with ethyl acetate and water. The layers were separated, and the aqueous later was re-extracted with ethyl acetate. The combined organic layers were washed with brine, dried ($MgSO_4$), filtered, and concentrated *in vacuo*. The residue was purified by column chromatography (silica gel, 20% ethyl acetate in hexanes) to afford 2.2 mg of the α-product **32** (9.16 μmol, 84%) and 0.2 mg of the β-product (0.83 μmol, 7%) as clear, colorless oil. R_f = 0.38 (silica gel, 50% ethyl acetate in hexanes); ^{1}H NMR (400 MHz, $CDCl_3$): δ 4.36 (dt, *J* = 3.2, 11.0 Hz, 1H), 4.06 (dt, *J* = 11.0, 4.6 Hz, 1H), 3.81 (dddd, *J* = 11.0, 11.0, 4.6, 4.6 1H), 3.66 (m, 1H), 3.27 (m, 1H), 2.43−2.41 (m, 2H), 1.96 (ddt, *J* = 12.0, 4.7, 1.9 Hz, 1H), 1.88−1.76 (m, 2H), 1.74−1.66 (m, 1H), 1.61−1.32 (m, 6H), 1.31−1.14 (m, 4H) ppm, hydroxyl proton absent (H/D exchange); ^{13}C NMR (100 MHz, $CDCl_3$): δ 172.1, 76.3, 73.4, 68.1, 63.9, 42.2, 41.7, 40.6, 33.2, 26.2, 25.5, 24.8, 23.7 ppm. HRMS (ESI+ TOF) *m*/*z*: calculated for $C_{13}H_{22}O_4Na$ [$(M + Na)^+$] 265.1410, observed 265.1408 (Δ = 0.2 mmu). NMR spectra were consistent with those previously reported within literature.[31]

■ ASSOCIATED CONTENT

Supporting Information

The Supporting Information is available free of charge on the ACS Publications website at DOI: 10.1021/acs.joc.5b02014.

^{1}H and ^{13}C NMR spectra of all new compounds, and NOESY, COSY, and HSQC for compounds **30**−**32** (PDF)

■ AUTHOR INFORMATION

Corresponding Author

*E-mail: cboddy@uottawa.ca.

Notes

The authors declare no competing financial interest.

■ ACKNOWLEDGMENTS

Thanks to the John L. Holmes Mass Spectrometry Facility, and Profs. Roberto A. Chica and Tom Woo of the University of Ottawa for access to computational resources. This work was supported by the Natural Sciences and Engineering Research Council (NSERC) of Canada, the Canadian Foundation for Innovation, the Ministry for Research and Innovation, and the University of Ottawa.

■ REFERENCES

(1) Wright, A. E.; Botelho, J. C.; Guzmán, E.; Harmody, D.; Linley, P.; McCarthy, P. J.; Pitts, T. P.; Pomponi, S. A.; Reed, J. K. *J. Nat. Prod.* **2007**, *70* (3), 412−416.

(2) D'Ambrosio, M.; Tatò, M.; Pocsfalvi, G.; Debitus, C.; Pietra, F. *Helv. Chim. Acta* **1999**, *82* (3), 347−353.

(3) Pettit, G. R.; Herald, C. L.; Doubek, D. L.; Herald, D. L.; Arnold, E.; Clardy, J. *J. Am. Chem. Soc.* **1982**, *104* (24), 6846−6848.

(4) Cutignano, A.; Bruno, I.; Bifulco, G.; Casapullo, A.; Debitus, C.; Gomez-Paloma, L.; Riccio, R. *Eur. J. Org. Chem.* **2001**, *2001*, 775−778.

(5) Houghton, S. R.; Furst, L.; Boddy, C. N. *J. Org. Chem.* **2009**, *74* (4), 1454−1463.

(6) Youngsaye, W.; Lowe, J. T.; Pohlki, F.; Ralifo, P.; Panek, J. S. *Angew. Chem., Int. Ed.* **2007**, *46*, 9211−9214.

(7) Custar, D. W.; Zabawa, T. P.; Scheidt, K. A. *J. Am. Chem. Soc.* **2008**, *130*, 804−805.

(8) Ulanovskaya, O. A.; Janjic, J.; Suzuki, M.; Sabharwal, S. S.; Schumacker, P. T.; Kron, S. J.; Kozmin, S. A. *Nat. Chem. Biol.* **2008**, *4*, 418−424.

(9) Woo, S. K.; Kwon, M. S.; Lee, E. *Angew. Chem., Int. Ed.* **2008**, *47*, 3242−3244.

(10) Paterson, I.; Miller, N. A. *Chem. Commun.* **2008**, 4708−4710.

(11) Fuwa, H.; Naito, S.; Goto, T.; Sasaki, M. *Angew. Chem., Int. Ed.* **2008**, *47*, 4737−4739.

(12) Guinchard, X.; Roulland, E. *Org. Lett.* **2009**, *11*, 4700−4703.

(13) Ghosh, A. K.; Shurrush, K. A.; Dawson, Z. L. *Org. Biomol. Chem.* **2013**, *11*, 7768−7777.

(14) Yu, M.; Schrock, R. R.; Hoveyda, A. H. *Angew. Chem., Int. Ed.* **2015**, *54*, 215−220.

(15) Vintonyak, V. V.; Maier, M. E. *Org. Lett.* **2008**, *10*, 1239−1242.

(16) Kartika, R.; Gruffi, T. R.; Taylor, R. E. *Org. Lett.* **2008**, *10*, 5047−5050.

(17) Tu, W.; Floreancig, P. E. *Angew. Chem., Int. Ed.* **2009**, *48*, 4567−4571.

(18) Kim, H.; Park, Y.; Hong, J. *Angew. Chem., Int. Ed.* **2009**, *48*, 7577−7581.

(19) Fuwa, H.; Saito, A.; Sasaki, M. *Angew. Chem., Int. Ed.* **2010**, *49*, 3041−3044.

(20) Martinez-Solorio, D.; Jennings, M. P. *J. Org. Chem.* **2010**, *75*, 4095−4104.

(21) Yadav, J. S.; Krishana, G. G.; Kumar, S. N. *Tetrahedron* **2010**, *66*, 480−487.

(22) Yang, Z.; Zhang, B.; Zhao, G.; Yang, J.; Xie, X.; She, X. *Org. Lett.* **2011**, *13*, 5916−5919.

(23) Sharma, G. V. M; Reddy, S. V.; Ramakrishna, K. V. S. *Org. Biomol. Chem.* **2012**, *10*, 3689−3695.

(24) Athe, S.; Chandrasekhar, B.; Roy, S.; Pradhan, T. K.; Ghosh, S. *J. Org. Chem.* **2012**, *77*, 9840−9845.

(25) Raghavan, S.; Samanta, P. K. *Org. Lett.* **2012**, *14*, 2346−2349.

(26) Vintonyak, V. V.; Kunze, B.; Sasse, F.; Maier, M. E. *Chem. - Eur. J.* **2008**, *14*, 11132−11140.

(27) Custar, D. W.; Zabawa, T. P.; Hines, J.; Crews, C. M.; Scheidt, K. A. *J. Am. Chem. Soc.* **2009**, *131*, 12406−12414.

(28) Fuwa, H.; Saito, A.; Naito, S.; Konoki, K.; Yotsu-Yamashita, M.; Sasaki, M. *Chem. - Eur. J.* **2009**, *15*, 12807−12818.

(29) Cui, Y.; Tu, W.; Floreancig, P. E. *Tetrahedron* **2010**, *66*, 4867−4873.

(30) Cui, Y.; Balachandran, R.; Day, B. W.; Floreancig, P. E. *J. Org. Chem.* **2012**, *77*, 2225−2235.

(31) Fuwa, H.; Kawakami, M.; Noto, K.; Muto, T.; Suga, Y.; Konoki, K.; Yotsu-Yamashita, M.; Sasaki, M. *Chem. - Eur. J.* **2013**, *19*, 8100−8110.

(32) Fuwa, H.; Noguchi, T.; Kawakami, M.; Sasaki, M. *Bioorg. Med. Chem. Lett.* **2014**, *24*, 2415−2419.

(33) Bai, Y.; Davis, D. C.; Dai, M. *Angew. Chem., Int. Ed.* **2014**, *53*, 6519−6522.

(34) Nising, C. F.; Bräse, S. *Chem. Soc. Rev.* **2008**, *37*, 1218−1228.

(35) Nising, C. F.; Bräse, S. *Chem. Soc. Rev.* **2012**, *41*, 988−999.

(36) Beesley, R. M.; Ingold, C. K.; Thorpe, J. F. *J. Chem. Soc., Trans.* **1915**, *107*, 1080−1106.

(37) Kobayashi, Y.; Fukuda, A.; Kimachi, T.; Ju-ichi, M.; Takemoto, Y. *Tetrahedron Lett.* **2004**, *45* (4), 677−680.

(38) Wadsworth, W. S.; Emmons, W. D. *J. Am. Chem. Soc.* **1961**, *83* (7), 1733−1738.

(39) Inanaga, J.; Hirata, K.; Saeki, H.; Katsuki, T.; Yamaguchi, M. *Bull. Chem. Soc. Jpn.* **1979**, *52*, 1989−1993.

(40) Rychnovsky, S. D. *Org. Lett.* **2006**, *8* (13), 2895−2898.

(41) Key ^{13}C peak assignments for the identification of the corresponding acetonide for *syn* diol **14** δ 97.7, 31.5, 19.6 ppm.

(42) Kanematsu, M.; Yoshida, M.; Shishido, K. *Angew. Chem., Int. Ed.* **2011**, *50*, 2618−2620.

(43) Kobayashi, H.; Kanematsu, M.; Yoshida, M.; Shishido, K. *Chem. Commun.* **2011**, *47*, 7440−7442.

(44) LoPachin, R. M.; Gavin, T.; DeCaprio, A.; Barber, D. S. *Chem. Res. Toxicol.* **2012**, *25* (2), 239−251.

(45) Hilli, F.; White, J. M.; Rizzacasa, M. *Tetrahedron Lett.* **2002**, *43*, 8507−8510.

DOI: 10.1021/acs.joc.5b02014
J. Org. Chem. 2016, 81, 415−423

(46) Hilli, F.; White, J. M.; Rizzacasa, M. *Org. Lett.* **2004**, *6*, 1289−1292.
(47) Heathcock, C. H.; Hadley, C. R.; Rosen, T.; Theisen, P. D.; Hecker, S. J. *J. Med. Chem.* **1987**, *30*, 1858−1873.
(48) Bhattacharjee, A.; Soltani, O.; De Brabander, J. K. *Org. Lett.* **2002**, *4* (4), 481−484.
(49) Frein, J. D.; Rovis, T. *Tetrahedron* **2006**, *62* (18), 4573−4583.
(50) Reddy, P. J.; Reddy, A. S.; Yadav, J. S.; Reddy, B. V. S. *Tetrahedron Lett.* **2012**, *53* (32), 4054−4055.
(51) Stewart, J. J. P. *J. Mol. Model.* **2007**, *13* (12), 1173−1213.
(52) Becke, A. D. *J. Chem. Phys.* **1993**, *98*, 5648−5652.
(53) Lee, C.; Yang, W.; Parr, R. G. *Phys. Rev. B: Condens. Matter Mater. Phys.* **1988**, *37*, 785−789.
(54) Miehlich, B.; Savin, A.; Stoll, H.; Preuss, H. *Chem. Phys. Lett.* **1989**, *157*, 200−206.
(55) Fuwa, H.; Mizunuma, K.; Matsukida, S.; Sasaki, M. *Tetrahedron* **2011**, *67*, 4995−4510.
(56) Mitsunobu, O. *Synthesis* **1981**, *1981*, 1−28.
(57) Boddy, C. N.; Hotta, K.; Tse, M. L.; Watts, R. E.; Khosla, C. *J. Am. Chem. Soc.* **2004**, *126* (24), 7436−7437.
(58) Hansen, D. A.; Rath, C. M.; Eisman, E. B.; Narayan, A. R.; Kittendorf, J. D.; Mortison, J. D.; Yoon, Y. J.; Sherman, D. H. *J. Am. Chem. Soc.* **2013**, *135* (30), 11232−11238.
(59) Wang, B.; Liu, J.; Tang, X.; Cheng, C.; Gu, J.; Dai, L.; Yu, H. *Tetrahedron Lett.* **2010**, *51*, 309−312.
(60) Kuwahara, S.; Morihiro, E.; Nemoto, A.; Hiramatsu, A. *Biosci., Biotechnol., Biochem.* **1992**, *56* (9), 1417−1419.

DOI: 10.1021/acs.joc.5b02014
J. Org. Chem. 2016, 81, 415−423

NPR

REVIEW

View Article Online
View Journal | View Issue

Published on 02 February 2015. Downloaded by University of Ottawa on 15/03/2016 18:33:08.

Cite this: *Nat. Prod. Rep.*, 2016, **33**, 183

Polyketide synthase and non-ribosomal peptide synthetase thioesterase selectivity: logic gate or a victim of fate?†

Mark E. Horsman, Taylor P. A. Hari and Christopher N. Boddy*

Covering: 1999 to 2014

Type 1, α/β hydrolase-like thioesterase (TE) domains are essential offloading enzymes, releasing covalently bound products from fatty acid, polyketide, and non-ribosomal peptide biosynthetic complexes. The release step can occur by attack of an exogenous nucleophile effecting hydrolysis or transesterification or by an intramolecular O-, N-, or C-nucleophile, effecting macrolactonization, macrolactamization or Claisen-like condensation of the product. Thus in addition to ensuring turnover of the pathway, TEs provide access to increased chemical diversity. We review the diversity, structure, and mechanism of PKS and NRPS TEs and discuss recent works that highlight the role of TEs as potential arbitrators in offloading. In particular, we examine cases where TEs act as logic gates that ask a particular question about the substrate and use this information to determine the substrate's fate. As the TE mechanism occurs *via* two steps, we analyze both the loading and release steps independently as logic gates. The use of logic gates provides an important perspective when evaluating the evolution of TEs within a pathway, as well as highlighting work towards the goal of predicting TE function in unknown and engineered pathways.

Received 12th November 2014

DOI: 10.1039/c4np00148f

www.rsc.org/npr

1. Introduction
1.1 TE structure
1.2 TE sequence diversity
1.3 Mechanism
1.4 Logic gates in natural product biosynthesis
2. The loading stage
2.1 Typical type I PKS and linear NRPS TEs have low selectivity for the loading stage
2.2 Stringent logic gates can occur if an acyl-CP intermediate must be processed
2.3 TEs from iterative pathways are likely to be stringent logic gates
3. The release step
3.1 Logic gate for NRPS macrocyclization can be controlled by substrate conformation
3.2 Modular type I PKS TEs are capable of ring-size tolerant, stereoselective macrocyclization
3.3 Macrocylization logic gate is relaxed in some fungal macrocyclizing TEs
3.4 Some fungal TEs restrict release to Claisen carbon–carbon bond formation
4. Summary and conclusions
4.1 TE logic that impacts loading and release decisions
4.2 TEs as senseless catalysts
4.3 The evolution of loading and release selectivity
5. Acknowledgements
6. Notes and references

Department of chemistry, Centre for Catalysis Research and Innovation, University of Ottawa, Canada. E-mail: cboddy@uottawa.ca

† Electronic supplementary information (ESI) available: The phylogenetic alignment used in Fig. 3 is available as "Thioesterase alignment.fas" and "Thioesterase alignment.meg". The resulting tree, including aLRT branch support stats are available as "Full Tree with PFAM Seed.nwk". The accompanying label key and statistics are included in "Thioesterase label table.xlsx". The CastP pore figure and analysis are included in "pore CASTp analysis.xlsx" and an exemplar pore is shown in "1kez pore measurement". Structures of late-stage pyochelin biosynthetic intermediates and other compounds discussed but not shown in this review are provided. See DOI: 10.1039/c4np00148f

1. Introduction

Type 1, α/β hydrolase-like thioesterase (TE) domains are essential offloading enzymes in fatty acid, polyketide, and non-ribosomal peptide biosynthesis. Common to the biosynthesis of these three families of compounds is the covalent attachment of the growing compound through a thioester bond to a carrier protein (CP). Expedient offloading of these acyl- and peptidyl-CP intermediates is required to prevent stalling and to enable

This journal is © The Royal Society of Chemistry 2016

View Article Online

Published on 02 February 2015. Downloaded by University of Ottawa on 15/03/2016 18:33:08.

turnover of the biosynthetic pathways. Cleavage of completed acyl or peptidyl chain from the terminal CP is catalyzed by a two-step TE-mediated mechanism (Fig. 1). The release step can occur by attack of an exogenous nucleophile effecting hydrolysis or transesterification or by an intramolecular O-, N-, or C-nucleophile, effecting macrolactonization, macrolactamization or Claisen-like condensation. Thus in addition to ensuring turnover of the pathway, TEs provide access to increased chemical diversity.

Because of the importance of TE-mediated offloading in polyketide and non-ribosomal peptide biosynthesis, TE function has been reviewed in a number of different contexts. At the primary sequence level, a number of reviews have catalogued TEs and examined their alignment[1,2] with the most recent being the ThYme database from 2010,[3] which sorts the TE clade into 23 families. In the context of all offloading mechanisms for polyketides and non-ribosomal peptides, Du and Lou[4] provided a comprehensive review that included TE-mediated offloading and effectively highlighted its breadth and importance in offloading. As macrocyclization is both chemically challenging and essential for the biological activity of many polyketide and non-ribosomal peptides, TE-mediated macrocyclization was reviewed by Kohli and Walsh[5] in 2003 and non-ribosomal pepitide TE-mediated macrolactamization by Kopp and Marahiel[6] in 2007. Because the CP is required to deliver the substrate to the TE, recent reviews have focused on molecular level interactions between CPs and TEs.[7,8] These reviews provide excellent companions to this article.

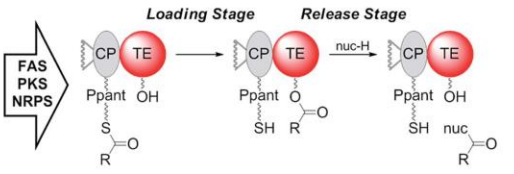

Fig. 1 TEs catalyze substrate offloading from CPs of fatty acid synthases, polyketide synthases and non-ribosomal peptide synthetases. Acyl and peptidyl chains bound to the Ppant arm of CPs are loaded onto the active site serine of a TE and then released *via* nucleophilic attack.

Type 1 TEs can be found at the terminus of *cis* acyl transferase (AT) type I polyketide synthase (T1 PKS)[9] modules, *trans* AT T1 PKS[10] modules, non-ribosomal peptide synthases (NRPS)[8] modules and fungal PKS[11] pathways. The cited reviews cover key points on the function and organisation of each of these pathway types. A second class of TE is also found in some pathways. These type II TEs,[12,13] along with proof-reading ATs,[14] catalyze release of incomplete acyl and peptidyl intermediates from CP and will not be discussed here. This review summarize

Mark Horsman received his B.Sc. with Specialization in Biochemistry and his B.A.Sc. with Specialization in Chemical Engineering in 2010. He is currently completing Ph.D. research in the Chemistry Department of the University of Ottawa under the direction of Christopher Boddy. Mark's research focuses on the substrate specificity of thioesterases isolated from trans *AT gene clusters with potential late-stage biosynthetic tailoring events. He is grateful for the opportunities NSERC, the University of Ottawa, and his supervisor have provided for international exchange through conferences and internships. These exposures and the collaborative spirit of the research community at large were vital in the development of this review.*

Taylor P.A. Hari received his BSc(Hons) in Medicinal Chemistry (2009), and MSc in Chemistry (2012) from the University of Ottawa, Canada. He recently returned from an NSERC Visiting Researcher position at the University of Notre Dame under the supervision of Prof. Richard E. Taylor, and is currently completing his PhD under the direction of Prof. Christopher N. Boddy at the University of Ottawa. In addition, Taylor will receive his Type II-MBA in Scientific Management and Leadership from the Telfer School of Management. His research focuses on total synthesis and chemoenzymatic studies used to better understand biosynthetic details of tetrahydropyran formation, and thioesterase-catalyzed macrocyclization in polyketide natural products.

Christopher Boddy received a Bachelors of Science from the University of Alberta in 1995 and a PhD at The Scripps Research Institute in 2001 under the direction of K. C. Nicolaou. He was a Post-doctoral Fellow at Stanford University working with Chaitan Khosla from 2001–2004. In 2004 he joined the Department of Chemistry at Syracuse University and in 2008, he moved to the University of Ottawa, Departments of Chemistry and Biology where he is currently an Associate Professor and Director of the undergraduate Biochemistry program. His research program focuses on harnessing biosynthetic pathways to produce complex molecules. More information about his research program can be found at http://www.boddylab.ca.

This journal is © The Royal Society of Chemistry 2016

View Article Online
Review NPR

Published on 02 February 2015. Downloaded by University of Ottawa on 15/03/2016 18:33:08.

Table 1 High-resolution structures of TEs

TE	PDB code
Aflatoxin pksA	3ILS[16]
Curacin	3QIT[18]
Deoxyerythronolide B	1KEZ,[17] 1MO2[19]
Enterobactin	2ROQ,[20] 3TEJ[21]
Fengycin	2CB9 (ref. 15), 2CBG[15]
Pikromycin	1MN6 (ref. 19), 1MNA,[19] 1MNQ,[19] 2H7X,[22] 2H7Y,[22] 2HFJ,[23] 2HFK[23]
Prodiginine	3QMV,[24] 3QMW[24]
Surfactin	1JMK,[25] 2VSQ,[26] 2K2Q[27]
Tautomycetin	3LCR[28]

the literature on type 1 TE structure, diversity and mechanism, and explore the role of type 1 TEs as logic gates that test for key properties at the loading and release steps.

1.1 TE structure

High-resolution structural data have been obtained for a number of TEs (Table 1). In general TEs consist of an N-terminal two helix dimerization region and a repeating β/α/β motif that forms a seven- or eight-stranded parallel β-sheet with a left-handed helical twist (Fig. 2). The protein topology diagram (Fig. 2A) depicts the TE from PksA involved in aflatoxin biosynthesis.[15] In this case the first N-terminal strand of the β-sheet, typical of most α/β hydrolases, is absent and the β-sheet has a single anti-parallel strand. The active-site serine is positioned between the C-terminus of β-strand 5 and the N-terminus of the subsequent α-helix. In general, the elements between β-strand 6 and 7 are often referred to as the lid region[5,6] and consist of two α-helices (L1 and L2). These helices line the perimeter of the substrate channel. In dimerizing TEs, this lid has been shown inserted between the core sheet and the N-terminal dimerization region.[17] Some TEs such the one from curacin biosynthesis,[18] have been crystallized with the lid in an open conformation, which forms an open-faced trough for the substrate and nucleophile. In others, including the TE from erythromycin biosynthesis (6-deoxyerythronolide B synthase TE, DEBS TE),[17,19] crystal structures show the lid helices spaced to form a channel through the enzyme that restricts substrate and nucleophile entry along the axis of the channel. Because the upstream CP domain delivers the substrate to the TE active site, its contact with its cognate TE is clearly of importance. CP domains are highly mobile by nature, as they must also deliver substrates to a number of other catalytic domains. They are small domains, typically ~100 residues or less, and are composed of two helices followed by smaller helical stretch at the C-terminus. To be functional all CPs are post-translationally modified by addition of a phosphopantetheinyl (Ppant) group that is covalently attached to a serine residue at the N-terminus of helix two.

Work by Liu, Zheng, and Bruner in 2011 captured a high resolution snapshot of an NRPS CP–TE didomain[21] by cross-linking the CP and TE using a modified Ppant analogue that reacted with the TE active site serine. The crystal structure showed helix three of the CP resting between the first β-strand of the TE's twisted β sheet (β2 in Fig. 2A) and the first inter-strand α-helix (αA), supporting a 2001 docking study prediction.[17] While the docking study proposed an interaction between N-terminal arginines of the TE (coined the Arg patch) and an electron rich patch on the CP, the crystal structure showed these regions were separated by 6 Å and that substantial hydrophobic contacts dominated the CP–TE binding interaction (Fig. 3). Interestingly the CP appears to use helix two rather than helix three to interact with other catalytic domains such as the phosphopantetheinyl transferase and upstream PKS modules.[7,20,26] Discrete hydrogen bonding interactions and hydrophobic packing between the CP Ppant group and the TE were also observed, presumably facilitating penetration of the substrate loaded Ppant arm into the active site binding cavity.[29]

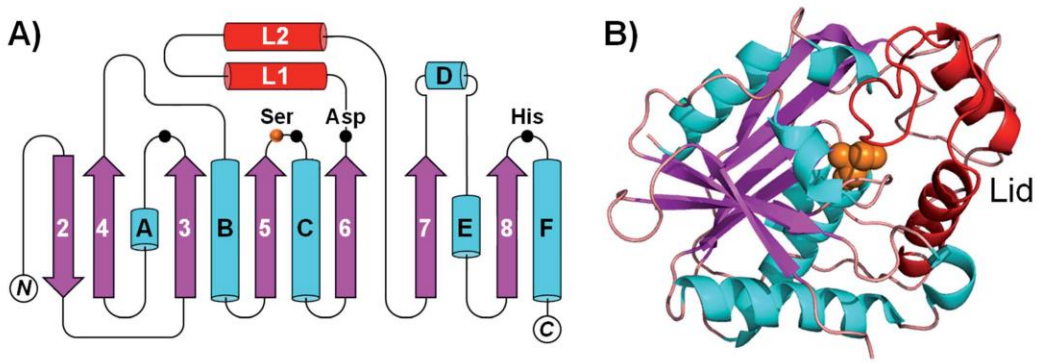

Fig. 2 Representative structure of a Type I TE (aflatoxin). (A) Topology diagram highlighting the active site triad (labelled residues) and oxyanion participants (shown in black), the lid domain (shown in red) and the overall β–α–β repeating pattern (pink and cyan). This adaptation of the aflatoxin TE is from Korman *et al.*[16] (B) 3D structure of the aflatoxin TE (pdb 3ILS) highlighting the left-handed twisted β-sheet core (pink), the lid region in red, and the active-site serine (orange) at the end of a β-strand and the start of the next α-helix. Substrates are predicted to access the active site by traversing from above the plane of the page.

View Article Online

Published on 02 February 2015. Downloaded by University of Ottawa on 15/03/2016 18:33:08.

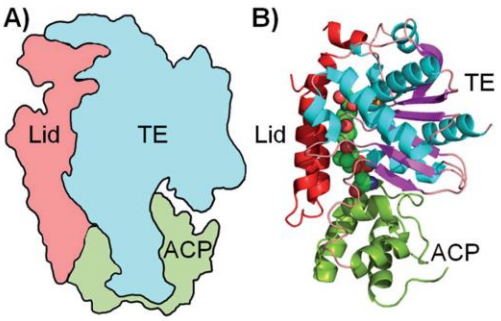

Fig. 3 Protein–protein interactions between terminal ACPs and their cognate TEs. (A) crystal cartoon model of the structure of cross-linked enterobactin CP–TE (B) A ribbon diagram of the enterobactin CP–TE. Liu *et al.*[21] linked enterobactin's ACP (green) and TE (lid red, outer helices teal, and core beta sheet pink) *via* a reactive phosphopantetheine linker (green and red), locking the didomain in a putative substrate transfer conformation.

Both biophysical characterization of CP–TE interactions and kinetic characterization of substrate transfer from CPs to TEs[29] support a common model. In this model, once the substrate is tethered to the CP upstream of the TE, essential CP–TE contact points are required for the delivery of the substrate into the TE channel.[29] Once transfer is initiated, little CP–TE contact is detected *via* NMR,[30,31] however discrete Ppant–TE contacts are required for the transfer of the substrate from Ppant thiol to TE active site serine.[21]

1.2 TE sequence diversity

TE sequences are highly diverse. Unlike many other catalytic domains involved in the biosynthesis of polyketides and non-ribosomal peptides, such as ketosynthase (KS),[32] condensation,[33] adenylation,[34–36] AT,[37] ketoreductase (KR),[38] and methyl transferases[39] for which hidden Markov models (HMMs) or conserved motifs can effectively predict selectivity, no model exists for predicting TE loading or release selectivity.[40]

Phylogenetic analysis of TE sequences show that they do not cluster based on type of offloading chemistry they catalyze. This observation is consistent with a convergent evolution model for reactivity types such as hydrolysis, macrolactone formation, macrolactam formation, and macrodiolide formation.[40] It appears the largest factor in their diversity is tied to the nature of the module directly upstream of the TE. For example, T1 PKS[9] and NRPS[8] associated TEs each generate major branches on a TE dendrogram (Fig. 4). In addition, the *trans* AT PKS[10] associated TEs also appear to cluster away from the bulk of PKS and NRPS TEs. While pathway type is an important determinant of sequence diversity, in some cases TE clustering is based on phylogeny. For example, fungal PKS TEs form a well-defined, tight branch on the dendrogram that clusters well away from other PKS TEs (Fig. 4).

Examination of the alignment of type 1 TEs highlights how diverse their sequences are. For example, a clustalW alignment of 300 predicted TEs extracted from clustermine360[41] shows there is no 50% consensus region larger than 5 amino acids throughout the entire sequence. As a result, regions of moderate diversity are not immediately isolatable to establish sequence property correlations. The largest source of sequence diversity is found in the inter-β6/β7 lid region, which ranges in length from approximately 80 amino acids in a TE from a *Myxococcus xanthus* isolate (|gb|NC_008095.1) to 25 amino acids from the coronatine TE in *Pseudomonas syringae* (PSPTO_4699|gb|NC_004578.1|). Curiously, both the open-pore DEBS TE and the shielded curacin TE have shorter than average lid regions. This suggests that lid-size alone cannot serve as a predictor of reactivity since DEBS TE generates a macrolactone and curacin TE produces a carboxylate that undergoes decarboxylative elimination to generate a terminal olefin.

PKS and NRPS TE diversity is not evenly distributed through the larger Pfam[42] TE family. When these TE sequences are compared with the Pfam training set (PF00975, shown as green circles in Fig. 4) used to generate the HMM for TE domain detection, five of the training set sequences cluster with the major PKS TE branch and only two of the training set sequences cluster with the major NRPS TE branch. The majority of the training set form new branches, many of which are sparsely populated by PKS and NRPS TEs. This suggests that a further refined HMM may better discriminate between pathway origins of TEs and an expanded HMM may better capture NRPS TEs. Bioinformatic detection of NRPS TE can be problematic. For example, a recent study used the powerful bioinformatics tool antiSMASH,[43] which relies on the Pfam TE HMM, to perform an *in silico* screen for NRPS pathways without annotated release mechanisms. This screen was unable to find TE domains in 15 NRPS pathways that after more rigorous analysis were confirmed to possess TEs.[44] Adapting the TE HMM to better detect NRPS TEs may thus improve the false negative rate of essential biosynthetic pathway analysis tools like antiSMASH.

1.3 Mechanism

TEs operate *via* a two-step mechanism, loading followed by release, which is consistent with known serine hydrolase mechanisms (Fig. 5).[48] The active site Ser side chain alcohol is activated by the conserved His-Asp dyad, increasing its nucleophilicity. The thioester substrate approaches the activated Ser from the N-terminal side of the substrate channel. The approach is mediated by the Ppant tether that links the substrate to the CP. It has been hypothesized that the lid region opens to accommodate the presentation of thioester substrates.[17,20] Once in the active site, the substrate thioester is attacked as the Ser is deprotonated by the His–Asp dyad, and the charged tetrahedral intermediate is stabilized in the oxyanion hole by hydrogen bonding from two backbone amide NH groups typically found at $i + 1$ from the active site Ser and in the β-turn after β strand 3 (Fig 2A).[16] This intermediate is resolved by loss of the Ppant thiolate, generating the acyl-TE intermediate.

The second step of the mechanism involves release of the acyl group and is often referred to as offloading. This step

This journal is © The Royal Society of Chemistry 2016

View Article Online

Published on 02 February 2015. Downloaded by University of Ottawa on 15/03/2016 18:33:08.

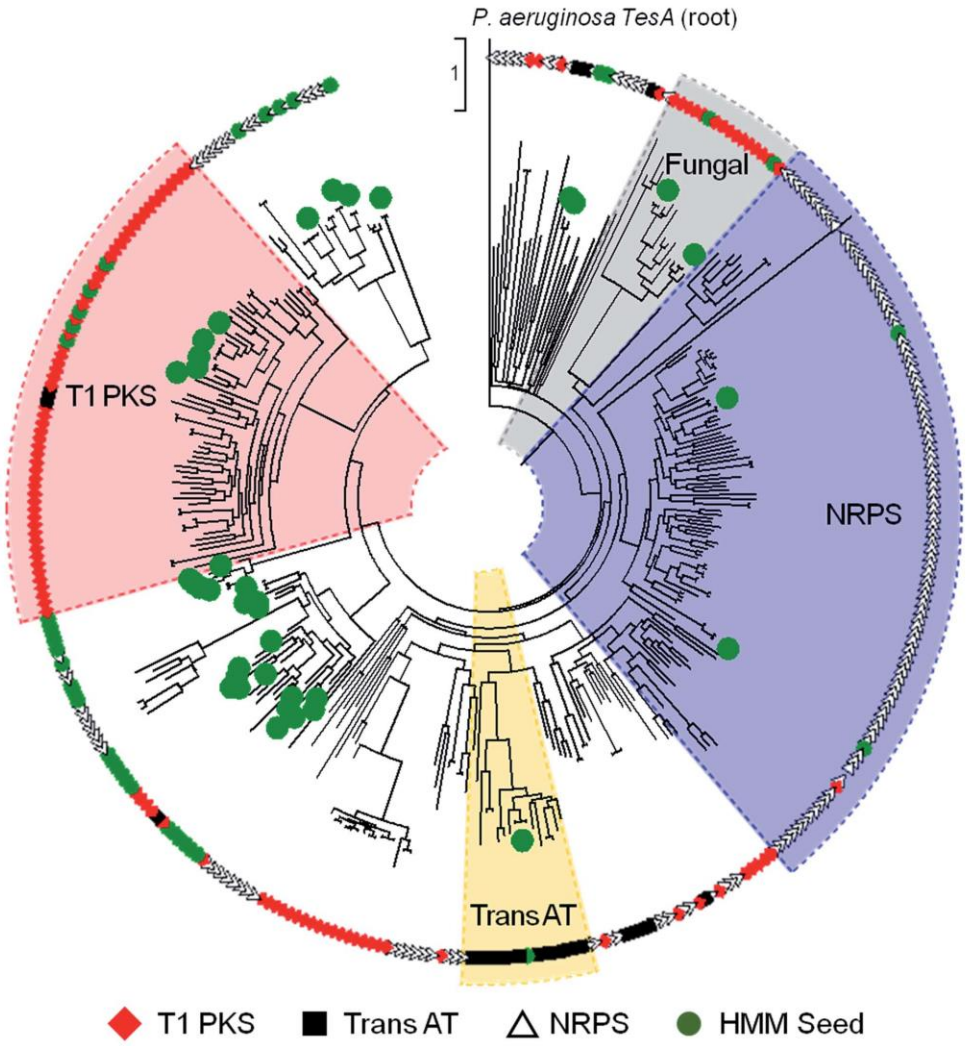

Fig. 4 Amino acid-level diversity of type I TE domains. Diversity of sequenced NRPS and PKS TEs at the amino acid level. 295 TEs were downloaded from clustermine360 *ca.*,[41] combined with the 38 sequence TE seed (http://pfam.xfam.org/family/PF00975/alignment/seed) for the current TE HMM, truncated to a clustalW[45]-aligned 268-amino acid core structure, phylogenetically analyzed using WAG,[46] and assessed for branch support using approximate likelihood ratio test (aLRT) *via* phylogeny.fr.[47] The multiple sequence clustalW alignment produced a phylogenetic tree reproducible *via* a Muscle multiple sequence alignment (data not shown). For sequences and branch strength see SI. Seed sequences are highlighted with green circles.

begins with the approach of an intramolecular or intermolecular nucleophile. Townsend has suggested that the active-site histidinium ion is deprotonated by the departing thiolate,[16,49] and thus capable of activating the incoming nucleophile. Alternatively, the histidinium may be retained since the thiolate leaving group is a weak base (as contrasted with ester hydrolysis) and thus may not participate in the release phase unless otherwise activated. The nucleophile adds into the carbonyl of the acyl-TE intermediate and the tetrahedral intermediate is once again stabilized by the oxyanion hole. Finally the seryl alkoxide is released with concerted protonation and the product leaves the active site.

Some TEs deviate from the canonical Ser-His-Asp triad (see alignment in ESI†) and contain a Cys in place of the Ser. For

This journal is © The Royal Society of Chemistry 2016

Published on 02 February 2015. Downloaded by University of Ottawa on 15/03/2016 18:33:08.

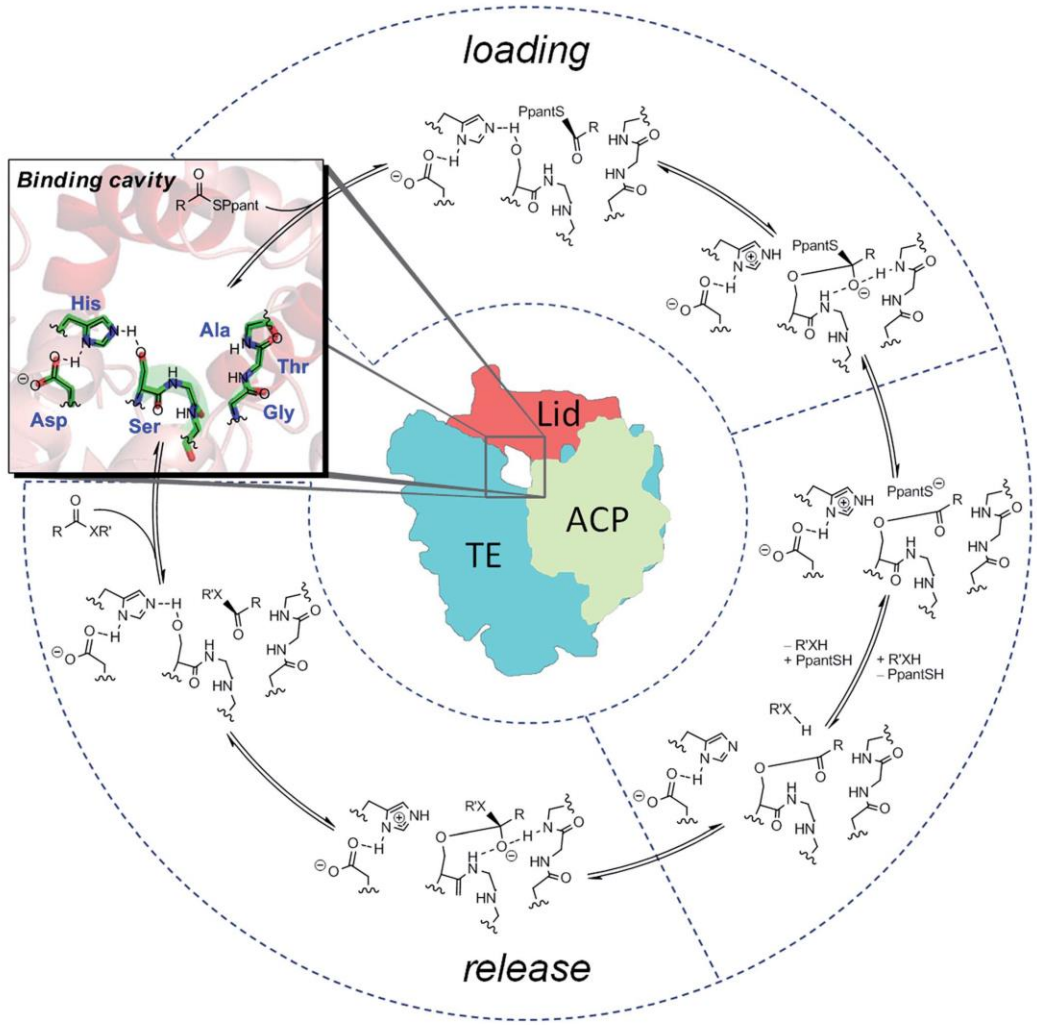

Fig. 5 Detailed TE mechanism for substrate loading and release. DEBS TE active site as viewed from a perspective where the substrate would enter the cavity from above the plane of the page. The Ppant-conjugated substrate enters the active site with the R-group leading and the Ppant lagging. In the loading stage, serine replaces the thioester bond, and in the release stage, a nucleophile replaces the seryl moiety and the active site is recovered.

example, the TE domain from pyochelin biosynthesis in *Pseudomonas aeruginosa*[50] and *Streptomyces venezuelae*[51] both contain a GXCXG motif rather than the canonical GXSXG motif. Mutation of the native Ser nucleophile to Cys in both myristoyl-ACP TE from *Vibrio harveyi*[52] and rat mammary gland TE II[53] generates catalytically active TEs, suggesting that native Cys containing TEs are likely active. Deacylation of the active site Cys in Ser to Cys mutants has been shown *in vitro* to be rate limiting.[52,53] The Ser to Cys and His to Arg double mutant has even slower rates of deacylation and has been used to trap the acyl-TE intermediate for the TE from the tautomycin biosynthetic pathway.[28] The catalytic His appears to be essential for activity of TEs and is invariant among the TEs with the exception of the TE from mycolactone biosynthesis. In this TE the catalytic His has been proposed to be replaced with a Pro, however there is no experimental evidence to support Pro in this role as of yet.[54] In the third position of the catalytic triad, the sample alignment demonstrates six examples of Glu replacing the Asp and ten examples of Ser replacing Asp. This follows the trends seen for general hydrolase active site as discussed by

 This journal is © The Royal Society of Chemistry 2016

Published on 02 February 2015. Downloaded by University of Ottawa on 15/03/2016 18:33:08.

Heikinheimo.[1] Holmquist covered variants of the catalytic triad in greater detail in 2000[2] and a comprehensive update to this work incorporating recent sequences data would be a welcome addition to the literature.

1.4 Logic gates in natural product biosynthesis

Enzymatic domains in natural product biosynthesis often intrinsically select for a substrate and stall until these selection criteria can be met. Enzymatic domains of this type have been termed gate-keepers,[55] decision gates,[56] and most recently, logic gates.[57] While these three terms are synonymous, we will use logic gate throughout as it highlights the programming and decision tree inherent in PKS and NRPS biosynthetic pathways. In the context of TE catalyzed chemistry, logic gates describe the test for key properties at the loading and release steps. Enzyme–substrate interactions probe shape, size, rigidity, and electronics of the substrate and a subset of these features can be used at either stage; however, these are only some of the conditions placed on the substrate. Factors external to the TE from the upstream pathway can also place restrictions on loading or release. Collectively, these TE-based and external factors are the logic gates that impact the decision to load and release the substrate. Understanding what question each logical gate "asks" of the substrate will enable us to predict substrate loading and release in natural and engineered *in vivo* pathways as well as *in vitro* pathways and chemoenzymatic situations.

Thus, herein, we discuss to what extent TEs are logic gates responsible for discriminating between thioester substrates and directing the route of release. We will highlight factors involved in the selectivity for the loading and release steps, discuss the implication of the differing levels of selectivity, and provide biosynthetic predictions that result from placing TEs with these patterns in selectivity in different metabolic environments.

2. The loading stage

The location of TEs at the end of PKS and NRPS biosynthetic pathways has important implications for the selectivity of these catalytic domains. The screening hypothesis suggests that there is an evolutionary cost associated with tying stringent substrate selectivity to late-stage components of multistep syntheses.[58,59] For T1 PKS and NRPS pathways, the substrate presented to the TE is tightly controlled by the modular configuration of the pathway. Thus, pathway evolution, which is required to access new chemical diversity and maintain long term evolutionary fitness, should be facilitated by low intrinsic selectivity of the TE. In certain cases however, the TE must be more stringent in its substrate selection. This includes instances of substantial processing of the terminal CP bound intermediate such as in nocardicin A biosynthesis[49] and in iterative extension pathways such as the radicicol biosynthetic pathway.[56]

2.1 Typical type I PKS and linear NRPS TEs have low selectivity for the loading stage

There is substantial *in vivo* and *in vitro* data on the ability of NRPS and PKS TEs to load diverse substrates. Reductive domain inactivation in full native T1 PKS pathways provided some of the first examples of TE loading substrate tolerance. For example, inactivation of individual KR domains from the complete biosynthetic pathways for erythromycin[60,61] and amphotericin[62] produced the corresponding keto polyketide products *in vivo* and inactivation of an ER domain from the erythromycin pathway produced the alkene containing natural product *in vivo*.[63] Both examples demonstrate the flexibility of the TE loading toward oxidation state changes. Similarly precursor directed biosynthesis experiments using synthetic substrates and blocked mutants of native pathways, such as the erythromycin pathway, also showed that analogues of the native polyketide natural product could be produced, confirming that TE loading was substrate tolerant.[64] Lastly, truncation of native pathways to produce fragments of natural products has also been successful, further demonstrating the flexibility of TE loading for substrates that are smaller and less complex than their native substrates.[65,66]

The construction of *de novo* designed PKS pathways has enabled diverse substrates to be presented to type I PKS TEs *in vivo*.[67–71] For example, Menzella *et al.* generated a small library of 6-member lactones by combining two different modules from the erythromycin, soraphen, epothilone, geldanamycin, leptomycin, rifamycin, rapamycin, and pikromycin biosynthetic pathways.[67,68] Fourteen of these combinations produced over 10 mg L^{-1} of the expected products. While this suggests the TE can load these diverse substrates, it is not possible to rule out spontaneous non-TE mediated offloading, particularly since non-TE mediated cyclization of 6-member lactones is kinetically and thermodynamically favoured[72] and known to occur.[73] Subsequent work where a third module was added to produce tetraketide 6-member lactones showed a similar results, with over twenty systems generating at least 1 mg L^{-1} of δ-lactone product when cultured.[69]

McDaniel *et al.* provided unambiguous data on the ability of a PKS TE to load diverse substrates.[68] In this study, over 60 different 14-member macrolactones were produced by swapping the AT domains and the reductive domains from modules 2, 5 and 6 of the erythromycin biosynthetic pathway with AT and reductive domains from the rapamycin biosynthetic pathway. As these 14-member rings cannot be generated from spontaneous non-TE mediated chemistry, their formation confirms that the TE used in this study (DEBS TE) must be able to load all of the macrocyclized substrates.

While the detection of a final product that cannot be offloaded spontaneously from *in vivo* experiments informs our understanding of the substrate tolerance of TEs, little can be deduced from *in vivo* systems that do not generate any observable products. McDaniel *et al.* indicate non-native intermediates may stall partway through the assembly line, fail to transfer downstream, or be cleaved by pathway editors.[68] Alternatively, the TE may fail to load or release the chain. In a state of protein cycling, cell growth, and asynchrony of substrate turn-over, it is impossible to establish which of these possibilities is responsible for the failure of the system to generate a product.

Much effort has thus been extended to isolate individual catalytic domains, including the TE, to be able to deconvolute

View Article Online
NPR Review

Published on 02 February 2015. Downloaded by University of Ottawa on 15/03/2016 18:33:08.

their activities and selectivities separate from the full PKS pathway. These types of *in vitro* assays are typically performed at elevated substrate and enzyme concentrations, often with synthetic non-native substrates. Typically, an excised TE domain is used; thus, the loading step is occurring intermolecularly, rather than intramolecularly, through transfer from the upstream, acylated CP. Pulse-chase experiments indicate that the rate limiting step *in vitro* for *Vibrio fisheri* TE LuxD is the loading of myristoyl-CoA.[52] This suggests that steady-state kinetic assays provide a quantitative rate constant that in cases of saturatable TEs with a rapid pre-equilibrium of substrate binding can define the disassociation equilibrium constant and turn over number for formation of the acyl-enzyme intermediate from the enzyme substrate complex.[74] This observation is useful for characterizing substrate loading and has major implications for characterization of the release step.

Kinetic characterization of DEBS TE,[74–77] and the TEs from pikromycin (PikTE)[78] and pimaricin biosynthesis[75] with simple substrates has demonstrated that all substrates are hydrolyzed at rates well above background. This suggests that all small substrates presented to the type I PKS TEs in the absence of other external selectivity filters load into the active site and the loading gate selectivity is limited. The substrates that match with the shape of the TE active-site react the fastest, while the poorly fitting substrates require extended exposure to the TE to be loaded. In these examples, the selectivity of the TE towards the simple substrates could not be predicted from comparison of the substitution pattern and oxidation state of the small substrate with that of the C-terminal portion of the native substrate. Often non-native like substrates were much more efficiently processed.[77]

Much like type I PKS TEs, NRPS TEs studied to date have shown remarkable tolerance for substrate loading. Work from 2000 suggested that the isolated tyrocidine TE was capable of loading activated esters of a diverse array of over 100 tyrocidine A analogues. Replacement of each of the ten residues, except the N-terminal D-Phe and penultimate residue, L-Orn, generated substrates that could be readily processed by the TE.[79,80] Of particular note is that the tyrocidine TE was able to release a large diversity of peptidyl substrates attached *via* an ester linkage to PEGA solid phase peptide synthesis resin, impressively demonstrating its application as a biocatalyst.[80,81] Thus, like type I PKS TEs, the NRPS TEs typically appear to have a limited role as a logic gate in substrate loading.

2.2 Stringent logic gates can occur if an acyl-CP intermediate must be processed

While NRPS TEs appear to have limited roles as logic gates in most cases, the nocardicin pathway highlights a situation where the TE is required to act as a logic gate. The core of nocardicin is a β-lactam containing tripeptide (Fig. 6, **3**). Recent work investigating β-lactam formation showed that the recombinant excised nocardicin TE was unable to catalyze hydrolysis of a model of the peptidyl-CP intermediate lacking the β-lactam ring. Neither the *N*-acetylcysteamine or Ppant thioester activated tripeptide lacking the β-lactam ring could be loaded to the nocardicin TE.[49] However, treatment of the TE with thioester substrates containing the β-lactam ring led to rapid hydrolysis of the thioester bond, releasing **3**. Intriguingly the TE proved to be bifunctional, also catalyzing isomerization of the α-carbon of the C-terminal L-4-hydroxyphenylglycinate (pHPG) residue. This unexpected result provides a potential origin for the D-pHPG found in norcardicin A.[49]

While β-lactam formation in this pathway has yet to be characterized, it is a reasonable hypothesis that β-lactam formation occurs *via* an *in trans* interaction of a yet to be identified enzyme acting on the ACP-bound serine containing linear peptide (Fig. 6, **1**).[49] Rapid processing of this intermediate by the TE would release a non-β-lactam containing product. Selective release of the β-lactam intermediate **2** however, ensures that the serine containing intermediate remains on the

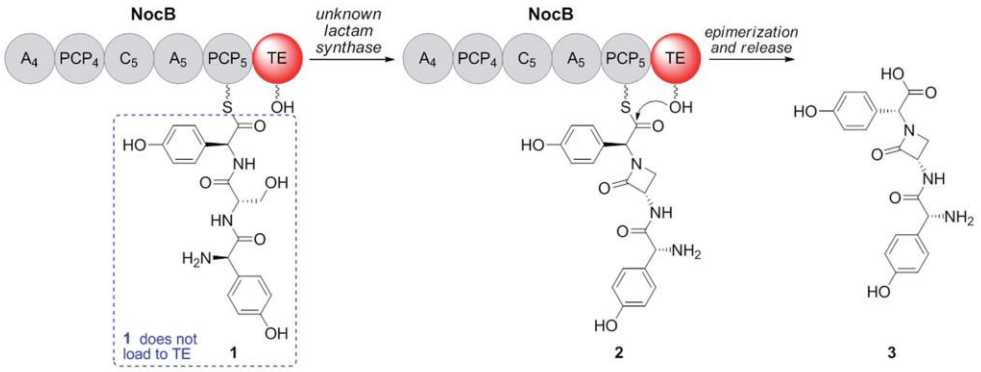

Fig. 6 The nocardicin TE selectively loads β-lactam containing substrates. *In vitro* assays of both *N*-acetylcysteamine and Ppant acrtivated nocardicin analogues[49] demonstrated that the nocardicin TE was only able to load β-lactam containing substrates. Linear seryl containing substrates did not undergo loading or hydrolysis. In addition the TE catalyzes epimerization of the C-terminal L-tyrosine to the D configuration seen in the final product.

This journal is © The Royal Society of Chemistry 2016

Published on 02 February 2015. Downloaded by University of Ottawa on 15/03/2016 18:33:08.

CP long enough to be processed into the β-lactam. This TE-mediated substrate pause may thus be a control element in nocardicin pathway fidelity.

A similar effect is observed in pyochelin biosynthesis, where the CP-bound intermediate must also be processed prior to release by the TE (Fig. S4†). In this case a linear C-terminal Cys containing peptidyl-CP intermediate must be cyclized to a thiazoline ring, reduced, and methylated to the *N*-methyl tetrahydrothiazole-CP intermediate prior to release.[82–84] Schneider *et al.* described this tetrahydrothiazole formation and the subsequent *N*-methylation as "prerequisites for pyochelin chain maturation and hydrolytic disconnection from PchF [*via* the terminal TE]."[85] In this system reduction of a CP-bound thiazoline intermediate is catalyzed by an *in trans* acting reductase.[84] In the absence of the reductase a thiazoline intermediate builds up on the CP[82] and is slowly released by the TE.[83] In the presence of the TE, the thiazoline is reduced and methylated, and released by the TE with a 40 fold increase in turnover.[83] These results suggest that the TE from pyochelin biosynthesis, like the TE in the nocardicin pathway, selectively loads certain substrates ensuring that complete processing of the CP bound intermediate by an *in trans* enzyme occurs.

2.3 TEs from iterative pathways are likely to be stringent logic gates

Unlike in modular polyketide biosynthesis, during iterative polyketide biosynthesis an ACP is acylated with a variety of different substrates. The majority of these substrates must be transferred back to the KS domain for additional elongation. If the pathway possesses an offloading TE, as is the case for some fungal polyketide biosynthetic pathways, the TE competes with the elongation process for each of these substrates. In order to ensure complete elongation, the TE must exhibit selective offloading of the substrate. Based on this concept, a TE from these pathways is expected to display higher chain-length related loading selectivity than their modular equivalents and has the capacity to act as a stringent logic gate, potentially controlling the fidelity of the pathway. The iterative pathways for the biosynthesis of radicicol and other related macrocyclic fungal natural products provide *in vivo* and *in vitro* evidence for the TE acting as a strict logic gate for substrate loading.

Radicicol biosynthesis is catalyzed by a highly-reducing PKS (hrPKS) and a non-reducing PKS (nrPKS). The hrPKS synthesizes the initial pentaketide acyl chain containing an alcohol and an olefin.[86] This residual oxygenation is a result of cryptically encoded incomplete reduction by the embedded reductive

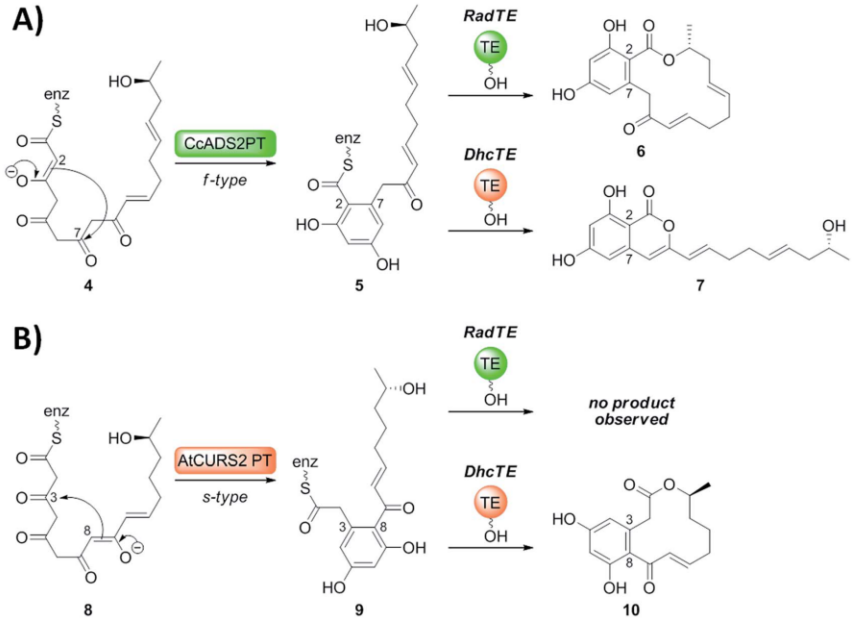

Fig. 7 Fungal macrocyclizing TEs selectively load substrates with aromatic rings generated by their cognate PT domains. (A) In radicicol biosynthesis the F-type PT domain (CcADS2, green) generates a resorcylate intermediate **5** from the poly-β-keto intermediate **4**. The native radicicol TE (Rad TE, green) loads the resorcylate substrate and macrocyclizes it whereas the dehdyrocurvularin TE (Dhc TE, orange) is unable to load the substrate, leading to spontaneous pyrone formation. (B) In dehydrocurvularin biosynthesis the poly-β-keto intermediate **8** is cyclized by the S-type PT domain (AtCURS2, orange) producing a phenylacetate intermediate, **9**. The native dehydrocurvularin TE (DhC TE, orange) effectively loads this substrate producing **10** wheras the rardicicol TE (Rad TE, green) cannot and produces no detectable product. Figure adapted from Xu *et al.*[87]

View Article Online

Published on 02 February 2015. Downloaded by University of Ottawa on 15/03/2016 18:33:08.

domains in the hrPKS. Interestingly in the related fungal polyketides dehydrocurvularin[87] and zearalenone,[88] the hrPKS generates a tetraketide and hexaketide chain respectively. The chain length control mechanism in this first round of iterative polyketide biosynthesis is still poorly understood.

In contrast, much is known about how the nrPKS regulates exposure of the growing acyl chain to the C-terminal TE. The nrPKS accepts the substrate from the hrPKS and elongates it into a poly-β-ketothioester substrate. During this elongation the ACP is loaded with β-ketothioesters of various lengths. For additional elongation to occur the substrate must be passed back to the KS rather than loaded onto the TE domain. Loading onto the TE would terminate chain elongation leading to alternative products. *In vitro* kinetic characterization of the TE from the zearalenone hrPKS shows that the TE has over a 100-fold lower specificity constant for hydrolysis of a β-ketothioester containing substrate over a benzoate thioester,[55] which is generated by cyclization and aromatization of the poly-β-ketothioester once elongation is complete.[87] This result suggests that the loading selectivity of the TE is matched to ensure that the KS can outcompete the TE for β-ketothioester substrates. Once the substrate is cyclized to generate a benzoate, the complete chain is rapidly offloaded.

Aromatic ring formation from the ACP-tethered poly-β-ketothioester substrate is catalyzed by the product-template (PT) domain, a domain unique to nrPKSs.[87,89] Because of the high reactivity and dense functionalization of the poly-β-ketothioester intermediate, a variety of aromatic rings can be accessed. In zearalenone and radicicol biosynthesis the intermediate adopts an "F-type" (for fungal)[90] fold that leads to formation of an aromatic ring between C2 and C7 (the resorcylate ring system) (Fig. 7A). In dehydrocurvularin biosynthesis the substrates adopts an "S-type" (for *Streptomyces*)[90] fold leading to aromatic ring formation between C3 and C8 (phenylacteate ring system) (Fig. 7B).

Recent *in vivo* work suggests that these TEs are selective for their native aromatic functional group, either resocylate or phenylacetate. For example, the radicicol pathway contains an F-type PT domain that generates an ACP-bound resorcylate thioester (Fig. 7A, **5**). In the native systems, this is loaded onto the TE and subsequently released as a 14-member ring macrolactone **6**. Replacement of the native TE with the TE from dehydrocurvularin biosynthesis leads to formation of pyrone **7**. The dehydrocurvularin TE is presented, in its native pathway, with a phenylacteate-ACP intermediate **9**. In this experiment, it is presented with a resorcylate-ACP intermediate **5**, which is not processed into a macrolactone. Instead the intermediate undergoes hydrolysis to the pyrone. This chemistry is observed in trace amounts in the absence of a TE[56] and pyrones are known spontaneous release product of other systems lacking TEs.[73] Interestingly, pyrone formation increases substantially when the dehydrocurvularin TE is added to the radicicol nrPKS *versus* the TE deletion. Whether the role of the dehydrocurvularin TE is structural and no formation of an acyl-TE intermediate is occurring or catalytic where TE-mediated hydrolysis releases the pyrone is not known. When the same linear radicicol precursor **4** is presented to the dehydrocurvularin PT, it generates a phenylacetate-ACP intermediate which is easily loaded onto the dehydrocurvularin TE and released as a 14-member ring macrocycle (Fig. 12, **27**).[56]

The native dehydrocurvularin pathway produces a phenylacetate-ACP intermediate (Fig. 7B, **9**). The dehydrocurvularin TE effectively loads this substrate and macrocyclizes it to generate the 12-member macrolactone natural product **10**. Replacing the TE with the radiciol TE does not yield any product from intermediate **9**. Presumably the radiciol TE is unable to load the phenylacetate substrate and the pathway stalls. Only trace products form misprimed dehydrocurvularin nrPKS are released, presumably by background hydrolysis of the acyl-ACP intermediate.[56]

Taken together, these data suggest that matching the PT and TE domains is required to enable efficient offloading. This data supports a model where loading of the TE is slow in cases where the PT domain and TE are mismatched, and faster in cases where the PT domain and TE are matched. However, confirmation of this hypothesis will require kinetic characterization of TE loading by both resorcylate and phenylacetate substrates.

3. The release step

Cleavage of the acyl-TE intermediate releases the untailored polyketide or non-ribosomal peptide from the core biosynthetic machinery. A stall in processing of the intermediate at this stage due to enzyme selectivity would impede flux through the pathway. Thus, the selectivity of the release step focuses on the type of release-chemistry catalyzed by the TE. This ranges from hydrolysis, macrocyclization, transesterification, dimerization, and trimerization among others. This diverse reactivity enables the TE to dramatically impact the chemical and functional diversity of the metabolites produced by a pathway.[5] It is in this context that the TE can act as a logic gate during release. The chemistry of release can be controlled by extrinsic factors, such as substrate pre-organization, which has been shown to facilitate macrocyclization in favour of hydrolysis in some NRPS TEs. Intrinsic TE selectivity for macrocyclization *versus* hydrolysis has been observed for PKS TEs when the acyl chains meet stringent functional group and stereochemical requirements. Fungal RAL TEs, on the other hand, have been shown to favour macrocyclization over hydrolysis for a much wider range of substrates. Fused-ring C–C bond forming Claisen-like condensation (CLC) fungal TEs shield their reactive intermediates from spontaneous 6-member ester formation through substrate restriction. The ability to toggle between these various release chemistries is likely an important evolutionary adaptation and thus, intrinsic release selectivity is predicted to be malleable and unpredictable.

3.1 Logic gate for NRPS macrocyclization can be controlled by substrate conformation

Macrocyclization is a key feature of many polyketides and non-ribosomal peptides. In the case of non-ribosomal peptides, it has been proposed to decrease the natural products susceptibility to proteases,[15,91] improve their membrane solubility, and

 This journal is © The Royal Society of Chemistry 2016

Published on 02 February 2015. Downloaded by University of Ottawa on 15/03/2016 18:33:08.

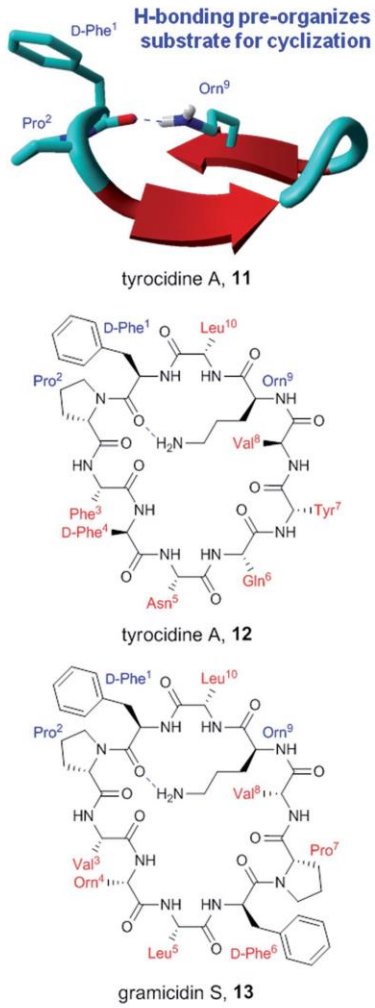

Fig. 8 General model of tyrocidin-type substrate-preorganization driven NRPS macrocyclization. Trauger *et al.*'s[99] model for the necessary elements for Tyrocidine TE mediated macrocyclization (shown in blue). Five peptide backbone hydrogen bonding partners are required as well as the L-ornithine side chain (key Orn-backbone carbonyl hydrogen bond is shown). The N-terminal amino acid must be an aromatic D-amino acid.

limit their conformational flexibility.[91,92] This may constrain a peptide to a target binding favoured conformation, limiting the entropic barrier for binding[91,92] (DeLorbe *et al.* has cautioned that this assumption should be tested[93]). Notably though, most of the known non-ribosomal peptides of greater than four residues are produced as macrocycles. It is thus not surprising that NRPS TEs are effective at producing macrocycles from a variety of substrates.[80,81,94–98]

In 2001, Trauger *et al.* established that the tyrocidine TE can macrocylize nona-, deca-, and undecapeptides, and could remarkably dimerize and then macrocyclize the related gramicidin pentapeptide.[99] Through an alanine scan, they established that only the N-terminal and penultimate C-terminal residues were essential for macrocyclization. To account for this substrate tolerance, they proposed a model where the peptidyl substrate backbone can effectively hydrogen bond and in addition form a key hydrogen bonding interaction between the Orn side chain amine and the carbonyl of the N-terminal residue to pre-organize the linear peptide for cyclization (Fig. 8).[99]

The TE also exerted intrinsic substrate selectivity for macrocyclization, limiting the N-terminal residue to D-amino acids. When these pre-organized substrates were loaded onto the TE active site, water was excluded from the active site through the bulk of the side chain of the oxyanion-hole residue Phe29 (found at the C-terminus of β3, see Fig 2A). Hydrolysis of the peptidyl-TE intermediate was favoured by mutation of Phe29 to a small nonpolar amino acid.[99] In 2002 this work was extended to show that a proline residue at the 4th position disrupted the pre-organisation, and macrocyclization did not occur.[80] Futhermore, the N-terminal D-Phe could be replaced with similar aromatic D-amino acids. However, this study did not comment on the rate of processing or macrocycle/free acid product release partition beyond stating that they acted as better substrates for cyclization.

A number of other NRPS TEs have been characterized *in vitro* and shown to be substrate tolerant macrocyclization catalysts. For example the cryptophycin TE was found to cyclize both homo and nor cryptophycin 3 (cryptophycins 51 and 24 respectively).[97,100] TEs from the lipopeptide antibiotic class, which includes daptomycin and A54145, have been shown to generate macrocycles with specific amino acid substitutions and tolerance for ring size, ranging from 8–11 amino acid residues.[95,101] However, insufficient data is available to propose a mechanism by which these TEs control macrocyclization over hydrolysis.

3.2 Modular type I PKS TEs are capable of ring-size tolerant, stereoselective macrocyclization

In their native pathways, modular type I PKS TEs are selective in the chemistry they catalyze. The vast majority of characterized, native pathways produce a metabolite corresponding either to macrocyclization, such as the epothilone pathway,[102] or hydrolysis, such as the gephyronic acid pathway.[103] There are no characterized examples of both macrocycles and free acids being generated *in vivo* from the same native pathway in appreciable amounts. However, we cannot rule out this absence being due to an isolation bias as most compounds are isolated by an activity guided fractionation approach.[104,105] In addition to being selective for the type of chemistry, macrocyclizing TEs typically are highly selective for a single intramolecular nucleophile. For example, the DEBS TE is highly selective for the C13 alcohol over the C11 and C5 alcohols. Only the native 14-member ring compound (Fig. 9, **17**) is obtained from

This journal is © The Royal Society of Chemistry 2016

Published on 02 February 2015. Downloaded by University of Ottawa on 15/03/2016 18:33:08.

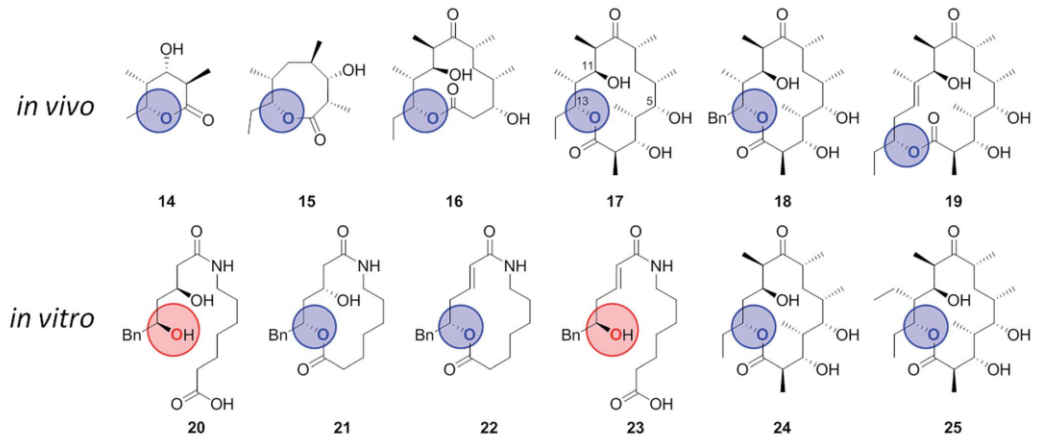

Fig. 9 Erythronolide analogs macrocyclized *via* DEBS TE *in vitro* and *in vivo*. 6-,[111] 8-,[110] 12-,[66] 14-, and 16-member[64] rings have been constructed heterologously *in vivo*, and diverse analogues have been constructed synthetically and from *in vitro* reconstituted pathways to incorporate amides,[40,112] benzyl[64] side chains, remove methyl side-chains,[109] and change the reduction state. Only the D-configuration of the ring-forming nucleophile is tolerated.

erythromycin producers,[106,107] even though the 6-member ring is enthalpically and entropically favoured.[72] Pikromycin biosynthesis is one of the few examples where multiple ring sizes are accessed, though in this case it is due to skipping the terminal polyketide synthase module rather than the TE selecting between two possible nucleophiles.[108]

By modifying native biosynthetic pathways, TEs can be exposed to a range of non-native substrates, however this substrate diversity is limited by the selectivity of the upstream biosynthetic enzymes. Once loaded, these non-native substrates are released through hydrolysis unless they meet the TE's intrinsic requirements for macrocyclization or transesterification. For example, erythronolide analogs lacking methyl substituents (*e.g.* Fig. 9, **24**)[109] have been generated by taking advantage of *trans* AT domains with malonyl-CoA selectivity, *versus* the native methylmalonyl-CoA selectivity. These compounds have been successfully macrocyclized.[109] Similarly, truncated pathways that generate shorter linear polyketide chains have been successfully cyclized to generate macrocycles of reduced ring size (*e.g.* Fig. 9, **14–16**).[66,110] Using tools such as precursor directed biosynthesis, larger ring sizes have also been accessed (Fig. 9, **19**).[64] A combinatorial biosynthesis experiment *in vivo* successfully generated over sixty 14-member ring macrocylic analogs of erythronolide by combining catalytic domains from the erythromycin and rapamycin biosynthetic pathways.[68] Conserved amongst all these examples was the D-configuration of the lactone alcohol and the presence of a carbonyl 1,5 to the lactone alcohol.

In vitro characterization of TE activity can provide for even broader probing of the substrate selectivity of TEs since synthetic substrates can be assayed. Isolated TEs can be treated with preloaded CPs or thioester substrates enabling selectivity to be studied independent of the upstream biosynthetic machinery. This dramatically increases the potential diversity that can be screened. In practice however, the challenge of synthesizing complex substrates for these enzymes has limited the probing of the TEs with non-biogenic substrates. In 2005, He *et al.* ring-opened 10-deoxymethynolide produced by *Streptomyces venezuelae* and reduced the ketone to a secondary alcohol.[113] While the ketone containing linear substrate was effectively macrocyclized by the excised recombinant PikTE, which is highly related to the DEBS TE, the reduced compound was only hydrolysed. This is consistent with the trends seen *in vivo*.

Work by Pinto *et al.* has demonstrated that for the DEBS TE the D-configuration of the nucleophilic C13 alcohol is required (Fig. 9, **21**) and that L-configured alcohols do not macrocyclize but rather generate the free acid (Fig. 9, **20**).[112] Interestingly, chemical macrocyclization of two diastereomeric substrates – one that undergoes TE-mediated macrocyclization and the other hydrolysis – occur with comparable efficiencies.[112] This result suggests that substrate preorganization is not a major factor in DEBS TE mediated macrocyclization, unlike with the tyrocidine TE.[79]

While TEs are generally selective in the chemistries they catalyze such as hydrolysis, macrocyclization, or transesterification, recent work by Hari *et al.* has shown that with some substrates, multiple offloaded products can be obtained.[40] For example, the DEBS TE was shown to generate macrocycle **22** (Fig. 9) from the linear *N*-aceylcystemaine activated thioester, and to catalyze transesterification and dimerizeation, generating a linear dimer and a macrodiolide product.[40] This result confirms that it is biochemically possible for pathways to produce substantial quantities of a diversity of offloaded products, even though no pathway has been identified with this phenotype.

Because DEBS TE was one of the first PKS TEs characterized, it has served as a model for TE activity in the PKS community.

This journal is © The Royal Society of Chemistry 2016

Published on 02 February 2015. Downloaded by University of Ottawa on 15/03/2016 18:33:08.

Consequently, there is a substantial amount of *in vivo* and *in vitro* data cataloguing its substrate selectivity.[40,64,66,68,109–112] Fig. 10 summarizes the current state of characterization for the substrate selectivity for macrocyclization of 14-member rings by DEBS TE. Unlike the tyrocidine TE, where substrate pre-organization appears to drive macrocyclization, it appears that specific enzyme substrate interactions are required for macrocyclization.

Recent work has begun to decipher the enzyme–substrate interactions governing loading and release of substrates.[22,23] Non-hydrolyzable acyl-enzyme intermediate models have been generated by treating the PikTE with diphenylphosphonate-based inhibitors. This leads to the formation of a phosophonate ester on the active site Ser. High-resolution crystal structure data from these covalently modified TEs has shown that the substrate interacts primarily through hydrophobic packing with the enzyme binding cavity, rather than hydrogen-bonding or dipole–dipole interactions.[22,23] This binding mode has been further supported by kinetic characterization of mutants of the highly-related DEBS TE.[74] However, the use of the phosphonate ester generates an acyl-enzyme mimic that most closely resembles the tetrahedral intermediate for substrate loading and may not accurately reflect the binding mode for macrocyclization. High-resolution structural data of TEs with substrate analogues arrested between the loading and release stages, akin to Dias *et al.*'s characterization of the type II TE FIK,[114] would likely give the most accurate measure of how the substrate interacts with the TE for release. NMR-based structural characterization of TEs could also provide exciting data on the detailed mechanism of catalysis.[115,116] In particular, it offers the exciting prospect of measuring dynamics of the lid region, which is thought to play a role in substrate loading and release.

Prediction of TE offloading chemistry has proven to be challenging.[40] Sequence-based approaches have not yet been able to distinguish hydrolyzing and macrocyclizing TEs. Using structural information, Jiang *et al.* proposed a model to distinguish α/β hydrolases with esterases activity from those with acyl transferase activity.[117] By examining over forty α/β hydrolase structures, they observed that the β-turn at the C-terminus of β-strand 3 (Fig 2A), which forms part of the oxyanion hole, adopted a type-II β-turn in hydrolases and a type-I β-turn in acyl transferases. They propose that the type-I β-turn deactivates water for attack by presenting the backbone NH bond, whereas the type-II β-turn presents a carbonyl that could potential activate water for attack (Fig. 11).

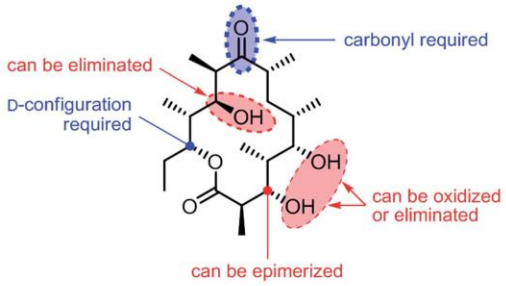

Fig. 10 DEBS TE substrate tolerance map for modifications to the erythronolide core. Some elements of the erythronolide core are nonessential for DEBS TE mediated macrocyclization. The C2, 4, 6, 8, 10, 12 and 13 alkyl side chains can be omitted, the C11 hydroxyl can be reduced to an alkane, and the C3 and C5 hydroxyls can be oxidized to ketones or reduced to alkanes. The epimer at C3 is tolerated. No experiment has showed ring formation beyond 10-member rings for any analogues lacking the C6 methyl, the C9 carbonyl, or the D-configuration of the C13 hydroxyl.

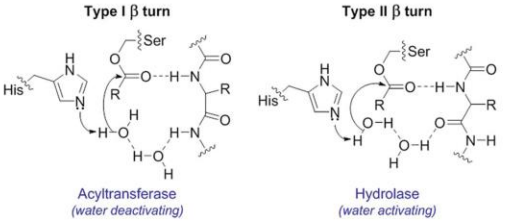

Fig. 11 Proposed β-turn dependent water activation in α/β hydrolase active-sites. Type II turns orient the *i* + 1 carbonyl into the active-site, whereas type I turns cannot activate water for hydrolysis.[117] While the model may hold for NRPS TEs, most T1 PKS TEs do not fit this model due to insertion of additional residues into the turn.

While this analysis appears to fit well with NRPS TEs, such as the surfactin[27] and fengycin[15] TEs, PKS TEs, like the DEBS TE[17] and pikTE,[19] contain two residue insertions into this loop. These insertions dramatically change its orientation, rendering them unsuitable for fitting to this model. Potentially, the use of structural conformation predictors such as Phyre2,[118] or β-turn analyzers such as NetTurnP[119] on the current set of TE sequences may enable analysis of the β3 loop to determine if its conformation tracks with the release mechanisms of known TEs. However, as PKS TEs vary substantially in this loop, activity prediction with this model may not be possible.

An alternate structure-based model for prediction of hydrolysis *versus* macrocyclization, could involve the overall binding pocket size and geometry. Several X-ray crystal structures are available for both hydrolytic and macrocyclic TEs. Assuming macrocyclizing TEs require a larger, more spherical pocket than the rod-like hydrolytic pocket, a reactivity prediction could be based on overall volume of the cavity or the surface area/volume ratio. Using the crystal structure topology program CASTp,[120] 2 hydrolytic (curacin,[18] tautomycenin[28]) and 4 macrocyclizing (2 DEBS TE[17,19] and 2 pikTE[19,23]) structures were compared, but no clear difference could be resolved (Fig. S1†). In part, the topology must be refined to better define the pore entrance and eliminate artefacts related to lid repositioning during crystallization. However, the lack of structural data for a substantial number of PKS TEs limits the ability to develop new structural-based models for reactivity prediction.[6]

3.3 Macrocylization logic gate is relaxed in some fungal macrocyclizing TEs

Recent work has shown fungal TEs to have a relaxed substrate selectivity for macrocyclization as compared to T1 PKS TEs. For

Published on 02 February 2015. Downloaded by University of Ottawa on 15/03/2016 18:33:08.

example, while T1 PKS TEs are highly stereoselective, *in vivo* and *in vitro* experiments have shown that TEs from resorcylic acid lactone (RAL) biosynthetic pathways can be highly stereotolerant for macrocyclization. In 2010, Zhou *et al.* used an *in vivo* precursor directed biosynthesis experiment where they fed both enantiomers of a synthetic substrate to the nrPKS module and TE from the radicicol biosynthetic pathway.[86] Both the D- and L-configured substrates were accepted and processed by the PKS domains and cyclized by the TE, generating the two enantiomeric macrocycles. This is in stark contrast to T1 PKS TEs, such as DEBS TE, which has shown very rigid stereoselectivity towards macrocyclization.[40,112]

In vitro kinetic characterization of the TEs from radicicol and zearalenone biosynthesis has shown that these TEs have little-to-no kinetic selectivity for the configuration of the alcohol involved in macrocyclization. Radicicol and zearalenone are highly related 14-member RALs. Radicicol has a L-configured macrolactone, whereas zearalenone has an D-configured macrolactone. The TE from radicicol biosynthesis showed virtually no kinetic preference for macrocyclization of synthetic substrates with the D- *versus* L-configured alcohol. The ratio of the specificity constants for the native configuration *versus* the enantiomer was 0.88.[121] The zearalenone TE displayed slightly greater selectivity with the ratio of specificity constants for the native configured substrate over its enantiomer of 0.17.[121] While this difference in specificity constants is small and insufficient to be used as a catalyst for resolution of racemates, both TEs show slightly enhanced activity for the non-native substrate nucleophile configuration.

In addition to the TEs from RAL pathways, a TE from the fungal phenylacetic acid lactone pathway for dehydrocurvularin has been characterized. Similar to the RAL TEs, the dehydrocurvularin TE was stereotolerant.[56] Dehydrocurvularin has a native 12-member L-configured lactone, **26** (Fig. 12). By combining the hrPKS from radicicol biosynthesis with the nrPKS from dehdyrocurvularin biosynthesis, it was possible to present the dehydrocurvularin TE with a D-configured substrate which was effectively macrocycled, generating the 14-member lactone **27**.

The TEs from RAL biosynthesis and phenylacetic acid lactone biosynthesis display similar trends (Fig. 12). Both appear to be stereotolerant, macrocyclizing both D- and L-configured substrates. In addition both RAL TEs and phenylacetic acid lactone TEs appear to be highly selective for the position of the aromatic ring. The RAL TEs macrocyclize compounds that have a resorcylated group, generated by their F-type PT domain, but are unable to macrocyclize phenylacetic acid containing substrates. Similarly, the dehydrocurvularin TE macrocyclizes substrates possessing a phenylacetic acid group, generated by its S-type PT domains, but is unable to macrocyclize resorcylate containing substrates. Based on these observations we predict that apralactone A, a macrolide isolated from a fungal genus Curvularia, which contains a D-configured phenylacetic acid lactone,[122] will be produced by a

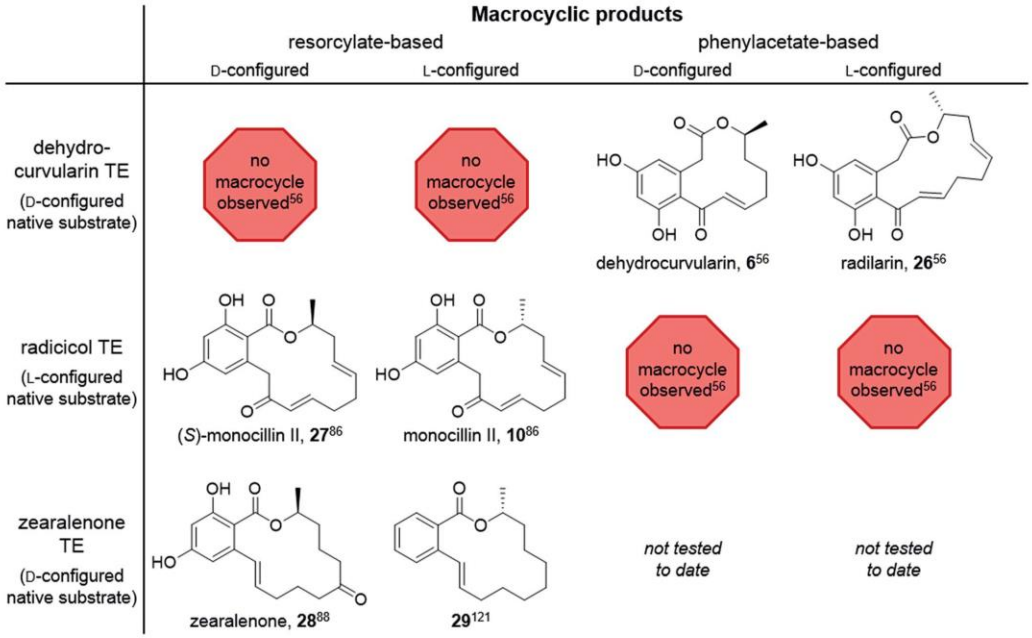

Fig. 12 Fungal TEs tolerate nucleophile inversion but are PT specific. Examination of macroyclizing TEs from fungal PKS pathways shows them to be stereotolerant for macrocyclization and highly selective for resorcylate or phenylacetate functional groups.

 This journal is © The Royal Society of Chemistry 2016

View Article Online
Review NPR

Published on 02 February 2015. Downloaded by University of Ottawa on 15/03/2016 18:33:08.

stereotolerant TE also able to macrocycle both D- and L-configured substrates. In addition, based on the trend seen with the RALs and dehydrocurvularin, we predict that the apralactone TE will not be able to macrocyclize RAL substrates.

The structural similarity between RAL natural products, such as radicicol, zearalenone, and hypothemycin, suggests their biosynthetic pathways diverged from a common genetic ancestor.[121] One of the stages in the divergence of these pathways was the change in stereochemistry of the macrolactone alcohol. This alcohol is introduced by the KR domain of the upstream hrPKS. The cryptic programing of RAL hrPKSs is challenging to decipher.[123] In the case of hypothemycin, the KR domain of the hrPKS reduces one intermediate β-ketothioester to produce a D-configured alcohol and reduces a subsequent β-ketothioester intermediate to produce an L-configured alcohol. Zhou *et al.* demonstrated that this hypothemycin KR D-selective reduction could be inverted by generating a chimeric KR domain with secondary structural elements from the radicicol hrPKS KR domain.[124] This study highlights the ease by which hrPKS systems can switch between D- and L-specific reductions and the capacity for diverse products. As the alcohol generated from this reduction is involved in macrocyclization, it is not unreasonable to assume the relaxed TE stereoselectivity is related to the ability of the KR domain to generate either stereogenic configuration. For example, if the TE was highly stereoselective as is seen in the type I PKS TEs, a change in the stereogenic outcome of the KR domain reduction could lead to a compound that does not cyclize, decreasing the likelihood that the compound would be bioactive. This outcome would likely not increase the producing organism's fitness and would be readily outcompeted by a pathway with a stereotolerant TE able to cyclize structures with either stereogenic configuration.

3.4 Some fungal TEs restrict release to Claisen carbon–carbon bond formation

TEs from some non-reducing iterative fungal pathways catalyze Claisen-like carbon–carbon bond formation to generate aromatic rings.[16] Here, the nucleophilic carbon is generated from tautomerization or deprotonation of a 1,3-diketone positioned such that attack on the acyl-enzyme intermediate carbonyl leads to 6-member ring formation. Subsequent tautomerization and release from the enzyme generates an aromactic ring. In these pathways, a key feature of the TE is to disfavour pyrone formation from the enol or enolate.[16,125]

One of the best studied of these TEs, often called Claisen-like cyclases (CLC), is from aflatoxin biosynthesis. Based on high-resolution structural data, molecular modelling studies, and mutational analyses, Korman *et al.* propose a detailed model for TE/CLC activity (Fig. 13).[16] They propose that the ACP-bound thioester substrate is loaded on to the active site Ser and the departing thiolate of the Ppant arm deprotonates the histidinium ion from the catalytic triad. Upon departure of the Ppant arm, the hexyl-β-diketo side chain of the substrate can undergo free rotation into the cavity previously occupied by the Ppant arm. The hexyl chain is buried between the lid and the TE core, bringing the α-carbon from the β-diketo group in close proximity to the acyl-enzyme carbonyl and catalytic His. Deprotonation of the α-carbon by the His, promotes substrate offloading *via* Claisen cyclization. Mutation of the catalytic His to Phe drastically reduced cyclase activity, leading to the vast majority of product being offloaded as the pyrone *via* C–O bond formation. Presumably pyrone formation is occurring on the acyl-ACP intermediate since in the absence of a TE, the acyl-ACP intermediate is spontaneously offloaded as the corresponding pyrone, suggesting that this is the favoured non-enzymatic pathway.[73]

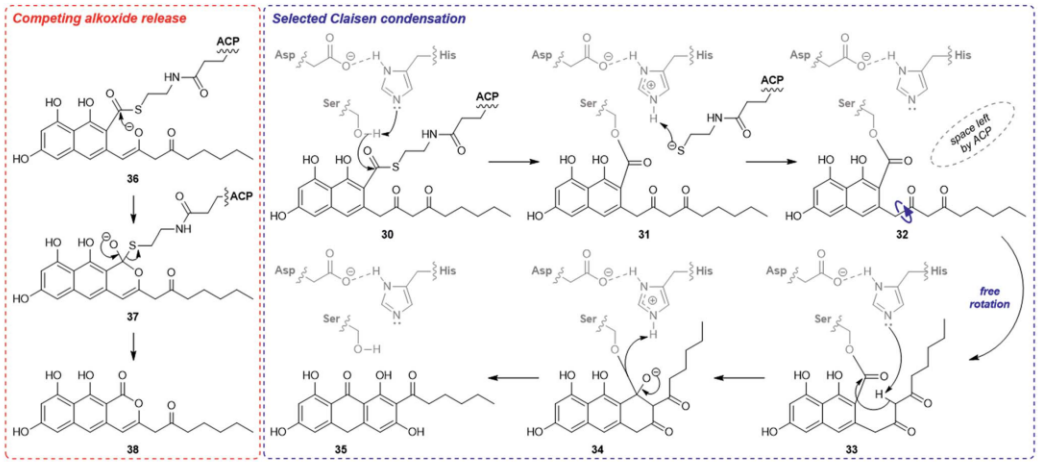

Fig. 13 Claisen-condensation type fungal TEs control substrate reorganisation during C–C bond forming release. In the presence of the aflatoxin TE,[16] the substrate loads *via* the standard mechanism, but after the ACP Ppant departs, the T promotes attack from C14 rather than the spontaneous attack of the proximal carbonyl oxygen in the alkoxide tautomer (alternate route shown in red).

Published on 02 February 2015. Downloaded by University of Ottawa on 15/03/2016 18:33:08.

This last example highlights the TE's role in regulating which release route is selected. This is similar to what is seen for DEBS TE where the TE drives release *via* macrocyclization in place of the more stable and kinetically favoured 6-member lactone. In aflatoxin biosynthesis, the presence of the TE attenuates the spontaneous release *via* pyrone formation, and facilitates C–C bond forming release in its place. Unlike the loading stage, substrate gating for elongation or tailoring is not observed at the release stage. It remains to be seen if TEs with permissive loading stages and highly selective release stages become kinetically defined by the rate of offloading.

4. Summary and conclusions

The seven examples presented here highlight the range of loading and release selectivity seen across PKS and NRPS TEs. In a number of cases TEs are seen to faithfully process the majority of substrates, as in the loading of type I PKS TEs or the macrocyclization of gramicidin analogues. In other cases TEs show a high degree of selectivity for specific structural feature of the substrates, as in the case of loading the nocardicin TE or macrocyclization of polyketides by TEs. Understanding and predicting this selectivity is a major challenge. Herein, we have summarized some of the key features of TEs and tried to correlate these features to selectivity predictions.

TEs are α/β hydrolases and their structures adopt a β sheet core that is twisted in a left-handed helix. The active site is accessible through a trough that is capped with a highly variable lid, the most diverse part of the TE sequence. The channel leading to the catalytic triad terminates at the nucleophilic elbow, the vertex of β-strand 5 and α-helix C (Fig. 2) where the active site Ser is found. The largest factor in sequence diversity associated with TEs appears to be the nature of the module directly upstream of the TE (Fig. 4), rather than the type of chemistry it catalyzes or the substrate selectivity it possesses. While phylogenetic analysis of the full sequence does not predict activity, it remains to be seen if a phylogenetic analysis of TE lids or specific structural units can produce a model capable of predicting channel geometry or release route.

With the large number of TE sequences in the literature, there are well developed HMM for the detection of this family of proteins. Our phylogenetic analysis shows that the seed sequences for the Pfam TE HMM (http://pfam.xfam.org/family/PF00975/alignment/seed) appear to be somewhat biased with few examples from NRPS TEs (Fig. 4). This bias can lead to false negatives in the detection of TEs by bioinformatic tools that rely on this model, such as antiSMASH.[43] Re-examining the cut-off scores for the current TE Pfam model or refining the TE HMM is likely to incrementally improve the effectiveness of bioinformatic TE screens. It should be noted however that this diversity discussion is based on the assumption that newly discovered TEs will be sufficiently similar in sequence to those that are already characterized, such that they will be recognized by the model. Identifying outliers and incorporating them into the model is essential to maintaining a useful predictive tools as well as providing insight in to TE structure–function relationships.

TE chemistry prediction substantially lags behind other PKS and NRPS domains.[40] The activity and selectivities of many PKS and NRPS domains can be effectively predicted and are incorporated into bioinformatic tools like anitSMASH. This enables researchers to rapidly and accurately annotate PKS and NRPS biosynthetic pathways. While in many cases these tools can predict meaningful structural aspects of the final product, the lack of ability to predict release chemistry continues to limit overall structure prediction. Advances in this area will greatly impact natural product discovery approaches based on genome mining.[126]

Examples in this review show that CPs interact with TEs through helix three of CP, and this helix is not used to mediate other CP–protein interactions. While CP and TE conformations do not appear to change significantly during interaction, there are discrete interaction between the Ppant arm and the TE that mediate substrate loading. Of note, while non-native substrates activated as *N*-acetylcysteamine derivatives lack some of these key Ppant–TE interactions, they have proven to be extremely useful in characterizing TE activity, providing data that is essential for deciphering the role of TEs in different pathways.

4.1 TE logic that impacts loading and release decisions

Several examples in this review show that some TEs differentially process substrates during loading and release based on localized substrate properties. Importantly, in each example a different structural property of the substrate was tested for by the TE. In addition, properties tested for by one TE were typically ignored by other TEs. While PKS and NRPS TEs appear to be highly general in their ability to load different substrates some key exceptions emerged. The Nocardicin TE shows strong selectivity for β-lactone containing substrates.[49] The TE thus appears to be acting as a checkpoint for the yet unidentified β-lactam forming enzyme which must interact *in trans* with the ACP-bound substrate, prior to TE loading (Fig. 6). It also appears that iterative fungal TEs are functionally linked to the activity of their cognate PT, which do not offload substrates that are precursors to the PT domain,[55] nor structures generated from alternative ring type processing by the PT (Fig. 7).[56] Current evidence supports this being a loading step selectivity, though additional *in vitro* evidence is required to fully confirm this. Conserved among these examples of TEs acting as logic gates and restricting loading of a substrate is the requirement for ACP-bound intermediates to be extensively processed, either by the as yet uncharacterized β-lactam forming enzyme in nocardicin biosynthesis or the PT domain in fungal macrocyclic polyketide formation. We thus hypothesize that in systems where processing of terminal ACP-bound intermediate is required, the TE will exhibit substantial substrate selectivity for loading, acting as logic gates to control the fidelity of the pathway.

Release strategies show some TEs to be highly selective in the chemistry they catalyze to offload acyl-TE intermediates. The model bacterial type I PKS macrocyclizing DEBS TE is lenient with regard to a number of structural changes to the substrate, such as removal of the methyl side chains, oxidation or

 This journal is © The Royal Society of Chemistry 2016

Published on 02 February 2015. Downloaded by University of Ottawa on 15/03/2016 18:33:08.

elimination of many of the alcohols, and alterations in ring-size, but as with other characterized type I macrocyclizing TEs, macrocycle forming activity is highly selective for the absolute configuration of the nucleophilic alcohol (Fig. 10). Fungal TE/CLCs which catalyze carbon-centered nucleophile attack on the acyl-TE intermediate also demonstrated high selectivity for offloading chemistry principally however by limiting access of oxygen-centered nucleophiles to the acyl-TE bond (Fig. 13).

4.2 TEs as senseless catalysts

In some cases, TEs are victims of fate and will process all substrates presented to them. For example, when exposed to a potential substrate bound to the immediately upstream CP, most type I PKS and NRPS TEs load the acyl or peptidyl substrate without fail. Similarly, the TE from the tyrocidine NRPS pathway was able to effect macrocyclization of all substrates that pre-organized in the absence of the TE to place the intramolecular nucleophile in close proximity to the electrophilic activated ester (Fig. 8). In this case, it is the substrates themselves, rather than the TE that determines if the compounds are release *via* hydrolysis or macrocyclization thus the TE is exerting no selectivity.

In contrast to the tight regulation of nucleophile stereochemistry seen in macrocyclizing bacterial type I PKS TEs, fungal macrocyclizing TEs are indiscriminate of nucleophile absolute stereochemistry (Fig. 12). This observation suggests that there is something fundamentally different about how the fungal TEs gate the release stage with regards to nucleophile stereochemistry. Understanding the discrete enzyme–substrate interactions that govern the selectivity in bacterial type I PKS TEs and facilitate the lack of selectivity in fungal macrocyclizing TEs is thus a key question moving forward. Insights in this area will be particularly useful for the development of new biocatalysts from TEs.

Historically, TEs as well as many other biosynthetic domains have been characterized by perturbing their pathways though deletion mutants or formation of chimeric pathways and observing the resulting products or by steady-state kinetic characterization of isolated catalytic domains. Higher resolution analysis is becoming needed to answer further questions about these processes. For example, in the context of the TE what is the role of movement of the clearly dynamic lid region? Are motions of the lid region on the same time scale as the rate constant for TE chemistry? Does the lids motion facilitate entry of the loaded Ppant arm into the active site cavity? Is it required for release of the Ppant arm after transfer of the substrate or for product release? Insight into these questions will enable the community to better understand offloading and its overall impact on pathway flux and fidelity.

4.3 The evolution of loading and release selectivity

Evolution provides a useful lens for interpreting and rationalizing the function and selectivities of biosynthetic pathways. For example, the evolution of two sequentially acting catalytic domains from a pathway can be linked. If variation in one domain varies the structure of the intermediate such that the next domain cannot process it, the pathway yields no product. If the second domain is sufficiently tolerant to accommodate the substrate change, the new pathway can produce a new compound, which may or may not increase the fitness of the producing organism.

In light of the screening hypothesis[58,59] that starts with the premise that potent biological activity is a rare property of a natural product and predicts that evolution will favour organisms that can generate diversity at a low cost, we can examine the selectivity of TEs. As a late acting enzyme in a pathway, the loading step is predicted to occur with minimal substrate selectivity, ensuring that the intermediates are processed into natural products that can be screened for biological activity. Similarly we can predict that the release step should occur with limited selectivity for the type of chemistry catalyzed as this will maximize the chemical diversity accessible from the pathway, increasing the chances of identifying an active compound.

Both of these predictions suggest that the TE should not act as a logic gate for PKS and NRPS biosynthetic pathways but rather, it should behave as a victim of fate, processing all substrates it is supplied with. Herein, however, we have highlighted examples where the TE clearly has a role in controlling fidelity of the pathway through substrate selectivity. We thus hypothesize that these examples of selectivity emerge from selection pressures to retain biological activity for the natural product produced by the pathway or a natural product produced by an ancestral pathway. For example, in the context of loading selectivity, only nocardicins containing the β-lactam ring are antibiotic[127] and only intermediates possessing this functional group are effectively loaded onto the nocardicin TE to be released from the biosynthetic pathway.[49] In this case, we propose the selective pressure for generation of the active natural product led to the evolution of TE selectivity ensuring release of the active compound.

The stereoselectivity of macrocyclizing TEs also provides an intriguing case study for this hypothesis. The RAL TEs show the predicted lack of stereoselectivtiy for late stage enzymes and both D- and L-configured lactone natural products, such as radicicol[128] and zearalenone,[129] exhibit potent though different biological activity. This is consistent with the screening hypothesis. The bacterial type I PKS TE, DEBS TE, which macrocyclizes an erythromycin precursor, shows high stereoselectivity, macrocyclizing only D-configured alcohols. Erythromycin binds to the ribosome[130] inhibiting protein synthesis. Examination of the high-resolution structural model for erythromycin binding shows interaction between the C13 ethyl substituent and the ribosome suggesting that the 13-*epi*-erythromycin A would be unable to bind, and thus inactive. If this is the case, than the stereoselectivity of the DEBS TE may have arisen to ensure that the active diastereomer of the natural product is produced.

Fungal macrocyclizing TEs are selective for type of aromatic system present in the substrate, either resorcylate or phenylacatete. In these systems, the PT domain and the TE need to be matched to effect macrocyclization. The radicicol TE requires a resocylate substrate such as the one generated by its cognate PT. The dehydrocurvularin TE requires a phenylacetate substrate,

Published on 02 February 2015. Downloaded by University of Ottawa on 15/03/2016 18:33:08.

as generated by its PT, for effective macrocyclization to occur. Based on our above analyses we predict that the substrate selectivity of these TEs indicates that the resorcylate and phenylacatete structures are required for biological activity. Intriguingly both of these structural scaffolds give rise to active fungal polyktide natural products. Thus why are the TEs selective for one scaffold over the other?

Examining the hypothetical product of a non-selective TE from one of these systems can be insightful in answering this question. The compound radilarin (**26**), which is formed by swapping the PT and TE domains from the radicicol biosynthetic pathway with those from dehydrocurvularin biosynthesis,[56] approximates mutation of the PT domain from F- to S-type in the presence of a TE that tolerates both rings. Radilarin shows minimal cyctotoxicity activity,[131] suggesting that a compound from a pathways with a tolerant TE would still be active and thus be able to impact the producing organisms fitness. This observation in conjunction with the above analyses suggests that the TE should not be selective for the type of aromatic substrate. However radilarin is much less active than radicicol in HSP90 inhibition, the most potent known activity for radicicol. If HSP90 inhibition is required to improve the fitness of the producing organism, the selectivity of the TE would be expected and consistent with our interpretation of the screening hypothesis. Ultimately resolving this question requires identifying the role polyketide products play in the biology of producing organisms. What is clear is that control of the aromatic ring position is a crucial aspect in determining the fitness of the resorcylate and phenylacate lactone pathways and their producing organisms.

5. Acknowledgements

The authors gratefully acknowledge helpful discussion with Dr Fabien Bergeret, Graham Heberlig, Dr Ata Pinto, Dr Cole Stevens, and Luis Villegas during the writing of this manuscript, and Jessamyn Horsman for cartoon mock-ups for Fig. 3.

6. Notes and references

1 P. Heikinheimo, A. Goldman, C. Jeffries and D. L. Ollis, *Structure*, 1999, **7**, R141–R146.
2 M. Holmquist, *Curr. Protein Pept. Sci.*, 2000, **1**, 209–235.
3 D. C. Cantu, Y. F. Chen and P. J. Reilly, *Protein Sci.*, 2010, **19**, 1281–1295.
4 L. C. Du and L. L. Lou, *Nat. Prod. Rep.*, 2010, **27**, 255–278.
5 R. M. Kohli and C. T. Walsh, *Chem. Commun.*, 2003, 297–307.
6 F. Kopp and M. A. Marahiel, *Nat. Prod. Rep.*, 2007, **24**, 735–749.
7 W. Xu, K. Qiao and Y. Tang, *Crit. Rev. Biochem. Mol. Biol.*, 2013, **48**, 98–122.
8 A. Koglin and C. T. Walsh, *Nat. Prod. Rep.*, 2009, **26**, 987–1000.
9 A. T. Keatinge-Clay, *Nat. Prod. Rep.*, 2012, **29**, 1050–1073.
10 Y. Q. Cheng, J. M. Coughlin, S. K. Lim and B. Shen, in *Complex Enzymes in Microbial Natural Product Biosynthesis, Part B: Polyketides, Aminocoumarins and Carbohydrates*, ed. D. A. Hopwood, Elsevier Academic Press Inc, San Diego, 2009, vol. 459, pp. 165–186.
11 N. P. Keller, G. Turner and J. W. Bennett, *Nat. Rev. Microbiol.*, 2005, **3**, 937–947.
12 M. L. Heathcole, J. Staunton and P. F. Leadlay, *Chem. Biol.*, 2001, **8**, 207–220.
13 D. Schwarzer, H. D. Mootz, U. Linne and M. A. Marahiel, *Proc. Natl. Acad. Sci. U. S. A.*, 2002, **99**, 14083–14088.
14 K. Jensen, H. Niederkruger, K. Zimmermann, A. L. Vagstad, J. Moldenhauer, N. Brendel, S. Frank, P. Poplau, C. Kohlhaas, C. A. Townsend, M. Oldiges, C. Hertweck and J. Piel, *Chem. Biol.*, 2012, **19**, 329–339.
15 S. A. Samel, B. Wagner, M. A. Marahiel and L.-O. Essen, *J. Mol. Biol.*, 2006, **359**, 876–889.
16 T. P. Korman, J. M. Crawford, J. W. Labonte, A. G. Newman, J. Wong, C. A. Townsend and S. C. Tsai, *Proc. Natl. Acad. Sci. U. S. A.*, 2010, **107**, 6246–6251.
17 S. C. Tsai, L. J. W. Miercke, J. Krucinski, R. Gokhale, J. C. H. Chen, P. G. Foster, D. E. Cane, C. Khosla and R. M. Stroud, *Proc. Natl. Acad. Sci. U. S. A.*, 2001, **98**, 14808–14813.
18 J. J. Gehret, L. Gu, W. H. Gerwick, P. Wipf, D. H. Sherman and J. L. Smith, *J. Biol. Chem.*, 2011, **286**, 14445–14454.
19 S. C. Tsai, H. Lu, D. E. Cane, C. Khosla and R. M. Stroud, *Biochemistry*, 2002, **41**, 12598–12606.
20 D. P. Frueh, H. Arthanari, A. Koglin, D. A. Vosburg, A. E. Bennett, C. T. Walsh and G. Wagner, *Nature*, 2008, **454**, 903–906.
21 Y. Liu, T. Zheng and S. D. Bruner, *Chem. Biol.*, 2011, **18**, 1482–1488.
22 J. W. Giraldes, D. L. Akey, J. D. Kittendorf, D. H. Sherman, J. L. Smith and R. A. Fecik, *Nat. Chem. Biol.*, 2006, **2**, 531–536.
23 D. L. Akey, J. D. Kittendorf, J. W. Giraldes, R. A. Fecik, D. H. Sherman and J. L. Smith, *Nat. Chem. Biol.*, 2006, **2**, 537–542.
24 J. R. Whicher, G. Florova, P. K. Sydor, R. Singh, M. Alhamadsheh, G. L. Challis, K. A. Reynolds and J. L. Smith, *J. Biol. Chem.*, 2011, **286**, 22558–22569.
25 S. D. Bruner, T. Weber, R. M. Kohli, D. Schwarzer, M. A. Marahiel, C. T. Walsh and M. T. Stubbs, *Structure*, 2002, **10**, 301–310.
26 A. Tanovic, S. A. Samel, L. O. Essen and M. A. Marahiel, *Science*, 2008, **321**, 659–663.
27 A. Koglin, F. Lohr, F. Bernhard, V. V. Rogov, D. P. Frueh, E. R. Strieter, M. R. Mofid, P. Guntert, G. Wagner, C. T. Walsh, M. A. Marahiel and V. Dotsch, *Nature*, 2008, **454**, 907–911.
28 J. B. Scaglione, D. L. Akey, R. Sullivan, J. D. Kittendorf, C. M. Rath, E. S. Kim, J. L. Smith and D. H. Sherman, *Angew. Chem.*, 2010, **49**, 5726–5730.
29 Z. Zhou, J. R. Lai and C. T. Walsh, *Chem. Biol.*, 2006, **13**, 869–879.
30 L. Tran, M. Tosin, J. B. Spencer, P. F. Leadlay and K. J. Weissman, *ChemBioChem*, 2008, **9**, 905–915.

 This journal is © The Royal Society of Chemistry 2016

Published on 02 February 2015. Downloaded by University of Ottawa on 15/03/2016 18:33:08.

31 L. Tran, R. W. Broadhurst, M. Tosin, A. Cavalli and K. J. Weissman, *Chem. Biol.*, 2010, **17**, 705–716.
32 G. Yadav, R. S. Gokhale and D. Mohanty, *PLoS Comput. Biol.*, 2009, **5**, e1000351.
33 C. Rausch, I. Hoof, T. Weber, W. Wohlleben and D. H. Huson, *BMC Evol. Biol.*, 2007, **7**, 78.
34 M. Roettig, M. H. Medema, K. Blin, T. Weber, C. Rausch and O. Kohlbacher, *Nucleic Acids Res.*, 2011, **39**, W362–W367.
35 T. Stachelhaus, H. D. Mootz and M. A. Marahiel, *Chem. Biol.*, 1999, **6**, 493–505.
36 G. L. Challis, J. Ravel and C. A. Townsend, *Chem. Biol.*, 2000, **7**, 211–224.
37 G. Yadav, R. S. Gokhale and D. Mohanty, *J. Mol. Biol.*, 2003, **328**, 335–363.
38 P. Caffrey, *ChemBioChem*, 2003, **4**, 654–657.
39 M. Z. Ansari, J. Sharma, R. S. Gokhale and D. Mohanty, *BMC Bioinf.*, 2008, **9**.
40 T. P. A. Hari, P. Labana, M. Boileau and C. N. Boddy, *ChemBioChem*, 2014, **15**, 2656–2661.
41 K. R. Conway and C. N. Boddy, *Nucleic Acids Res.*, 2013, **41**, D402–D407.
42 R. D. Finn, A. Bateman, J. Clements, P. Coggill, R. Y. Eberhardt, S. R. Eddy, A. Heger, K. Hetherington, L. Holm, J. Mistry, E. L. Sonnhammer, J. Tate and M. Punta, *Nucleic Acids Res.*, 2014, **42**, D222–D230.
43 K. Blin, M. H. Medema, D. Kazempour, M. A. Fischbach, R. Breitling, E. Takano and T. Weber, *Nucleic Acids Res.*, 2013, **41**, W204–W212.
44 S. Müller, S. Rachid, T. Hoffmann, F. Surup, C. Volz, N. Zaburannyi and R. Müller, *Chem. Biol.*, 2014, **21**, 855–865.
45 J. D. Thompson, D. G. Higgins and T. J. Gibson, *Nucleic Acids Res.*, 1994, **22**, 4673–4680.
46 S. Whelan and N. Goldman, *Mol. Biol. Evol.*, 2001, **18**, 691–699.
47 A. Dereeper, V. Guignon, G. Blanc, S. Audic, S. Buffet, F. Chevenet, J. F. Dufayard, S. Guindon, V. Lefort, M. Lescot, J. M. Claverie and O. Gascuel, *Nucleic Acids Res.*, 2008, **36**, W465–W469.
48 A. Ferscht, *Enzyme structure and mechanism*, W. H. Freeman and Company, New York, 1985.
49 N. M. Gaudelli and C. A. Townsend, *Nat. Chem. Biol.*, 2014, **10**, 251–258.
50 L. Serino, C. Reimann, P. Visca, M. Beyeler, V. DellaChiesa and D. Haas, *J. Bacteriol.*, 1997, **179**, 248–257.
51 S. T. Pullan, G. Chandra, M. J. Bibb and M. Merrick, *BMC Genomics*, 2011, **12**, 175.
52 J. Li, R. Szittner, Z. S. Derewenda and E. A. Meighen, *Biochemistry*, 1996, **35**, 9967–9973.
53 A. Witkowski, H. E. Witkowska and S. Smith, *J. Biol. Chem.*, 1994, **269**, 379–383.
54 J. L. Meier, T. Barrows-Yano, T. L. Foley, C. L. Wike and M. D. Burkart, *Mol. BioSyst.*, 2008, **4**, 663–671.
55 M. Wang, H. Zhou, M. Wirz, Y. Tang and C. N. Boddy, *Biochemistry*, 2009, **48**, 6288–6290.
56 Y. Q. Xu, T. Zhou, S. W. Zhang, L. J. Xuan, J. X. Zhan and I. Molnar, *J. Am. Chem. Soc.*, 2013, **135**, 10783–10791.
57 A. O. Zabala, Y.-H. Chooi, M. S. Choi, H.-C. Lin and Y. Tang, *ACS Chem. Biol.*, 2014, **9**, 1576–1586.
58 R. D. Firn and C. G. Jones, in *Phytochemical Diversity and Redundancy in Ecological Interactions*, ed. J. T. Romeo, J. A. Saunders and P. Barbosa, 1996, vol. 30, pp. 295–312.
59 R. D. Firn and C. G. Jones, *Nat. Prod. Rep.*, 2003, **20**, 382–391.
60 R. Reid, M. Piagentini, E. Rodriguez, G. Ashley, N. Viswanathan, J. Carney, D. V. Santi, C. R. Hutchinson and R. McDaniel, *Biochemistry*, 2003, **42**, 72–79.
61 S. Donadio, M. J. Staver, J. B. McAlpine, S. J. Swanson and L. Katz, *Science*, 1991, **252**, 675–679.
62 P. Power, T. Dunne, B. Murphy, L. Nic Lochlainn, D. Rai, C. Borissow, B. Rawlings and P. Caffrey, *Chem. Biol.*, 2008, **15**, 78–86.
63 S. Donadio, J. B. McAlpine, P. J. Sheldon, M. Jackson and L. Katz, *Proc. Natl. Acad. Sci. U. S. A.*, 1993, **90**, 7119–7123.
64 J. R. Jacobsen, C. R. Hutchinson, D. E. Cane and C. Khosla, *Science*, 1997, **277**, 367–369.
65 J. Cortes, K. E. Wiesmann, G. A. Roberts, M. J. Brown, J. Staunton and P. F. Leadlay, *Science*, 1995, **268**, 1487–1489.
66 C. M. Kao, G. L. Luo, L. Katz, D. E. Cane and C. Khosla, *J. Am. Chem. Soc.*, 1995, **117**, 9105–9106.
67 H. G. Menzella, R. Reid, J. R. Carney, S. S. Chandran, S. J. Reisinger, K. G. Patel, D. A. Hopwood and D. V. Santi, *Nat. Biotechnol.*, 2005, **23**, 1171–1176.
68 R. McDaniel, A. Thamchaipenet, C. Gustafsson, H. Fu, M. Betlach and G. Ashley, *Proc. Natl. Acad. Sci. U. S. A.*, 1999, **96**, 1846–1851.
69 H. G. Menzella, J. R. Carney and D. V. Santi, *Chem. Biol.*, 2007, **14**, 143–151.
70 L. Kellenberger, I. S. Galloway, G. Sauter, G. Bohm, U. Hanefeld, J. Cortes, J. Staunton and P. F. Leadlay, *ChemBioChem*, 2008, **9**, 2740–2749.
71 R. McDaniel, S. Ebertkhosla, D. A. Hopwood and C. Khosla, *Science*, 1993, **262**, 1546–1550.
72 G. Illuminati and L. Mandolini, *Acc. Chem. Res.*, 1981, **14**, 95–102.
73 A. J. Hughes, J. F. Detelich and A. T. Keatinge-Clay, *MedChemComm*, 2012, **3**, 956–959.
74 M. Wang and C. N. Boddy, *Biochemistry*, 2008, **47**, 11793–11803.
75 K. K. Sharma and C. N. Boddy, *Bioorg. Med. Chem. Lett.*, 2007, **17**, 3034–3037.
76 R. S. Gokhale, D. Hunziker, D. E. Cane and C. Khosla, *Chem. Biol.*, 1999, **6**, 117–125.
77 M. Wang, P. Opare and C. N. Boddy, *Bioorg. Med. Chem. Lett.*, 2009, **19**, 1413–1415.
78 H. X. Lu, S. C. Tsai, C. Khosla and D. E. Cane, *Biochemistry*, 2002, **41**, 12590–12597.
79 J. W. Trauger, R. M. Kohli, H. D. Mootz, M. A. Marahiel and C. T. Walsh, *Nature*, 2000, **407**, 215–218.
80 R. M. Kohli, C. T. Walsh and M. D. Burkart, *Nature*, 2002, **418**, 658–661.
81 T. A. Mukhtar, K. P. Koteva and G. D. Wright, *Chem. Biol.*, 2005, **12**, 229–235.

This journal is © The Royal Society of Chemistry 2016

Published on 02 February 2015. Downloaded by University of Ottawa on 15/03/2016 18:33:08.

82 L. E. Quadri, T. A. Keating, H. M. Patel and C. T. Walsh, *Biochemistry*, 1999, **38**, 14941–14954.
83 H. M. Patel and C. T. Walsh, *Biochemistry*, 2001, **40**, 9023–9031.
84 C. Reimmann, H. M. Patel, L. Serino, M. Barone, C. T. Walsh and D. Haas, *J. Bacteriol.*, 2001, **183**, 813–820.
85 T. L. Schneider and C. T. Walsh, *Biochemistry*, 2004, **43**, 15946–15955.
86 H. Zhou, K. J. Qiao, Z. Z. Gao, J. C. Vederas and Y. Tang, *J. Biol. Chem.*, 2010, **285**, 41412–41421.
87 Y. Q. Xu, P. Espinosa-Artiles, V. Schubert, Y. M. Xu, W. Zhang, M. Lin, A. A. L. Gunatilaka, R. Sussmuth and I. Molnar, *Appl. Environ. Microbiol.*, 2013, **79**, 2038–2047.
88 I. Gaffoor and F. Trail, *Appl. Environ. Microbiol.*, 2006, **72**, 1793–1799.
89 D. W. Udwary, M. Merski and C. A. Townsend, *J. Mol. Biol.*, 2002, **323**, 585–598.
90 R. Thomas, *ChemBioChem*, 2001, **2**, 612–627.
91 T. W. Giessen and M. A. Marahiel, *FEBS Lett.*, 2012, **586**, 2065–2075.
92 J. Rizo and L. M. Gierasch, *Annu. Rev. Biochem.*, 1992, **61**, 387–418.
93 J. E. DeLorbe, J. H. Clements, B. B. Whiddon and S. F. Martin, *ACS Med. Chem. Lett.*, 2010, **1**, 448–452.
94 J. Grunewald, S. A. Sieber, C. Mahlert, U. Linne and M. A. Marahiel, *J. Am. Chem. Soc.*, 2004, **126**, 17025–17031.
95 V. Miao, M. F. Coeffet-Le Gal, K. Nguyen, P. Brian, J. Penn, A. Whiting, J. Steele, D. Kau, S. Martin, R. Ford, T. Gibson, M. Bouchard, S. K. Wrigley and R. H. Baltz, *Chem. Biol.*, 2006, **13**, 269–276.
96 G. Christiansen, W. Y. Yoshida, J. F. Blom, C. Portmann, K. Gademann, T. Hemscheidt and R. Kurmayer, *J. Nat. Prod.*, 2008, **71**, 1881–1886.
97 N. A. Magarvey, Z. Q. Beck, T. Golakoti, Y. Ding, U. Huber, T. K. Hemscheidt, D. Abelson, R. E. Moore and D. H. Sherman, *ACS Chem. Biol.*, 2006, **1**, 766–779.
98 C. Mahlert, S. A. Sieber, J. Gruenewald and M. A. Marahiel, *J. Am. Chem. Soc.*, 2005, **127**, 9571–9580.
99 J. W. Trauger, R. M. Kohli and C. T. Walsh, *Biochemistry*, 2001, **40**, 7092–7098.
100 Y. Ding, C. M. Rath, K. L. Bolduc, K. Hakansson and D. H. Sherman, *J. Am. Chem. Soc.*, 2011, **133**, 14492–14495.
101 F. Kopp, J. Grunewald, C. Mahlert and M. A. Marahiel, *Biochemistry*, 2006, **45**, 10474–10481.
102 I. Molnar, T. Schupp, M. Ono, R. E. Zirkle, M. Milnamow, B. Nowak-Thompson, N. Engel, C. Toupet, A. Stratmann, D. D. Cyr, J. Gorlach, J. M. Mayo, A. Hu, S. Goff, J. Schmid and J. M. Ligon, *Chem. Biol.*, 2000, **7**, 97–109.
103 F. Sasse, H. Steinmetz, G. Hofle and H. Reichenbach, *J. Antibiot.*, 1995, **48**, 21–25.
104 W. H. Gerwick, P. J. Proteau, D. G. Nagle, E. Hamel, A. Blokhin and D. L. Slate, *J. Org. Chem.*, 1994, **59**, 1243–1245.
105 T. J. Turbyville, E. M. K. Wijeratne, M. X. Liu, A. M. Burns, C. J. Seliga, L. A. Luevano, C. L. David, S. H. Faeth, L. Whitesell and A. A. L. Gunatilaka, *J. Nat. Prod.*, 2006, **69**, 178–184.
106 C. M. Kao, L. Katz and C. Khosla, *Science*, 1994, **265**, 509–512.
107 B. A. Pfeifer, S. J. Admiraal, H. Gramajo, D. E. Cane and C. Khosla, *Science*, 2001, **291**, 1790–1792.
108 B. J. Beck, Y. J. Yoon, K. A. Reynolds and D. H. Sherman, *Chem. Biol.*, 2002, **9**, 575–583.
109 B. J. Dunn, K. R. Watts, T. Robbins, D. E. Cane and C. Khosla, *Biochemistry*, 2014, **53**, 3796–3806.
110 C. M. Kao, M. McPherson, R. N. McDaniel, H. Fu, D. E. Cane and C. Khosla, *J. Am. Chem. Soc.*, 1997, **119**, 11339–11340.
111 C. M. Kao, G. L. Luo, L. Katz, D. E. Cane and C. Khosla, *J. Am. Chem. Soc.*, 1996, **118**, 9184–9185.
112 A. Pinto, M. Wang, M. Horsman and C. N. Boddy, *Org. Lett.*, 2012, **14**, 2278–2281.
113 J. He and C. Hertweck, *Chem. Biol.*, 2003, **10**, 1225–1232.
114 M. V. B. Dias, F. Huang, D. Y. Chirgadze, M. Tosin, D. Spiteller, E. F. V. Dry, P. F. Leadlay, J. B. Spencer and T. L. Blundell, *J. Biol. Chem.*, 2010, **285**, 22495–22504.
115 A. J. Baldwin and L. E. Kay, *Nat. Chem. Biol.*, 2009, **5**, 808–814.
116 S. Hammes-Schiffer, *Biochemistry*, 2013, **52**, 2012–2020.
117 Y. Jiang, K. L. Morley, J. D. Schrag and R. J. Kazlauskas, *ChemBioChem*, 2011, **12**, 768–776.
118 L. A. Kelley and M. J. Sternberg, *Nat. Protoc.*, 2009, **4**, 363–371.
119 B. Petersen, C. Lundegaard and T. N. Petersen, *PLoS One*, 2010, **5**, e15079.
120 J. Dundas, Z. Ouyang, J. Tseng, A. Binkowski, Y. Turpaz and J. Liang, *Nucleic Acids Res.*, 2006, **34**, W116–W118.
121 G. W. Heberlig, M. Wirz, M. Wang and C. N. Boddy, *Org. Lett.*, 2014, **16**, 5858–5861.
122 H. Greve, P. J. Schupp, E. Eguereva, S. Kehraus, G. Kelter, A. Maier, H.-H. Fiebig and G. M. Koenig, *Eur. J. Inorg. Chem.*, 2008, 5085–5092.
123 Y. Xu, T. Zhou, P. Espinosa-Artiles, Y. Tang, J. Zhan and I. Molnar, *ACS Chem. Biol.*, 2014, **9**, 1119–1127.
124 H. Zhou, Z. Z. Gao, K. J. Qiao, J. J. Wang, J. C. Vederas and Y. Tang, *Nat. Chem. Biol.*, 2012, **8**, 331–333.
125 A. L. Vagstad, E. A. Hill, J. W. Labonte and C. A. Townsend, *Chem. Biol.*, 2012, **19**, 1525–1534.
126 C. N. Boddy, *J. Ind. Microbiol. Biotechnol.*, 2014, **41**, 443–450.
127 H. Kojo, Y. Mine, M. Nishida, S. Goto and S. Kuwahara, *Microbiol. Immunol.*, 1988, **32**, 119–130.
128 N. Winssinger, J. G. Fontaine and S. Barluenga, *Curr. Top. Med. Chem.*, 2009, **9**, 1419–1435.
129 G. G. Kuiper, J. G. Lemmen, B. Carlsson, J. C. Corton, S. H. Safe, P. T. van der Saag, B. van der Burg and J. A. Gustafsson, *Endocrinology*, 1998, **139**, 4252–4263.
130 F. Schlunzen, R. Zarivach, J. Harms, A. Bashan, A. Tocilj, R. Albrecht, A. Yonath and F. Franceschi, *Nature*, 2001, **413**, 814–821.
131 Y. Xu, T. Zhou, S. Zhang, P. Espinosa-Artiles, L. Wang, W. Zhang, M. Lin, A. A. L. Gunatilaka, J. Zhan and I. Molnár, *Proc. Natl. Acad. Sci. U. S. A.*, 2014, **111**, 12354–12359.

 This journal is © The Royal Society of Chemistry 2016